Anonyme. The Journal of physical chemistry. Published at Cornell university [puis Published under the auspices of the American chemical society, the Chemical society and the Faraday society]. 1896 [I]-. 1938 . May-dec..

1/ Les contenus accessibles sur le site Gallica sont pour la plupart des reproductions numériques d'oeuvres tombées dans le domaine public provenant des collections de la BnF.Leur réutilisation s'inscrit dans le cadre de la loi n°78-753 du 17 juillet 1978 :
*La réutilisation non commerciale de ces contenus est libre et gratuite dans le respect de la législation en vigueur et notamment du maintien de la mention de source.
*La réutilisation commerciale de ces contenus est payante et fait l'objet d'une licence. Est entendue par réutilisation commerciale la revente de contenus sous forme de produits élaborés ou de fourniture de service.

Cliquer ici pour accéder aux tarifs et à la licence

2/ Les contenus de Gallica sont la propriété de la BnF au sens de l'article L.2112-1 du code général de la propriété des personnes publiques.

3/ Quelques contenus sont soumis à un régime de réutilisation particulier. Il s'agit :

*des reproductions de documents protégés par un droit d'auteur appartenant à un tiers. Ces documents ne peuvent être réutilisés sauf dans le cadre de la copie privée sans l'autorisation préalable du titulaire des droits.
*des reproductions de documents conservés dans les bibliothèques ou autres institutions partenaires. Ceux-ci sont signalés par la mention Source Gallica.BnF.fr / Bibliothèque municipale de ... (ou autre partenaire). L'utilisateur est invité à s'informer auprès de ces bibliothèques de leurs conditions de réutilisation.

4/ Gallica constitue une base de données, dont la BnF est producteur, protégée au sens des articles L341-1 et suivants du code la propriété intellectuelle.

5/ Les présentes conditions d'utilisation des contenus de Gallica sont régies par la loi française. En cas de réutilisation prévue par un autre pays, il appartient à chaque utilisateur de vérifier la conformité de son projet avec le droit de ce pays.

6/ L'utilisateur s'engage à respecter les présentes conditions d'utilisation ainsi que la législation en vigueur, notamment en matière de propriété intellectuelle. En cas de non respect de ces dispositions, il est notamment passible d'une amende prévue par la loi du 17 juillet 1978.

7/ Pour obtenir un document de Gallica en haute définition, contacter reutilisation@bnf.fr.

Journal of physical chemistry

Tome 42

Volume 56

Washington 1938

TITANUM OXIDE HYDROSOLS. SOME RELATIONSHIPS TO OXIDE HYDROSOLS OF ZIRCONIUM AND THORIUM

HARRY S. OWENS AND ROBERT MORRIS
Department of Chemistry, University of Idaho, Moscow, Idaho

Received January 15, 1938

Thomas and his coworkers have made numerous contributions to the literature of hydrous oxide hydrosols, explaining their reactions on the basis of polyolated structures. Since their work has been reviewed (10) recently it is unnecessary to discuss in this paper evidence in favor of the Thomas complex compound theory. However, two papers on basic thorium chloride (4) and basic zirconium chloride (6) hydrosols illustrate striking differences in the chemical reactions of these hydrosols when aged or when heated and then allowed to age; it seems advisable to mention these before giving the purpose of this investigation.

Basic thorium chloride hydrosols age rapidly and come to equilibrium in two months. Boiling the freshly prepared sols increases the acidity to a relatively high degree, with equilibrium being reached in 10 hours. When such heated sols are cooled and allowed to stand at room temperatures, there is a tendency for the acid produced to reverse the reaction so that the degree of acidity approaches the same values as those of the unheated sols aging at room temperature. Basic zirconium chloride sols, on the other hand, age slowly but continuously for periods as long as eight months, if not longer. On boiling, the pH values decrease rapidly for a short time, then more slowly for at least 240 hours. The heated sols, when cooled and allowed to stand, remain at the pH values attained with no tendency to become less acid.

These differences were ascribed to the less metallic nature of zirconium, which ionizes to only a small extent as the quadrivalent ion and tends to form basic radicals. The oxygen bridges in these radicals are very resistant to the action of acids like hydrochloric acid, which contain anions having low penetrating power. Consequently there is little or no tendency for the chloride ion to penetrate the complex, thus breaking the oxo bridges, or for the hydrogen ion to unite with oxo bridges to form ol groups.[1]

Titanium, occurring in a still lower position of the periodic table, is even

---

[1] Schmid (1) has found that in very concentrated solutions of hydrochloric acid some oxonium salts are formed with zirconium oxychloride, but he found little or no evidence for the formation of zirconium tetrachloride.

THE JOURNAL OF PHYSICAL CHEMISTRY, VOL. 42, NO. 5

less basic than zirconium. Therefore it seemed that it would form oxide hydrosols in which the micelles would contain mainly oxo bridges. The purpose of this paper is to submit evidence in support of this postulation.

TABLE 1

Composition of hydrosols

SOL	pH VALUE	Ti	Cl	EQUIVALENT RATIO Ti/Cl
		milliequivalents	*milliequivalents*	
T1	2.7	120	9	13.4
T2	2.7	88	8	11.0
T3	2.0	400	23	17.4

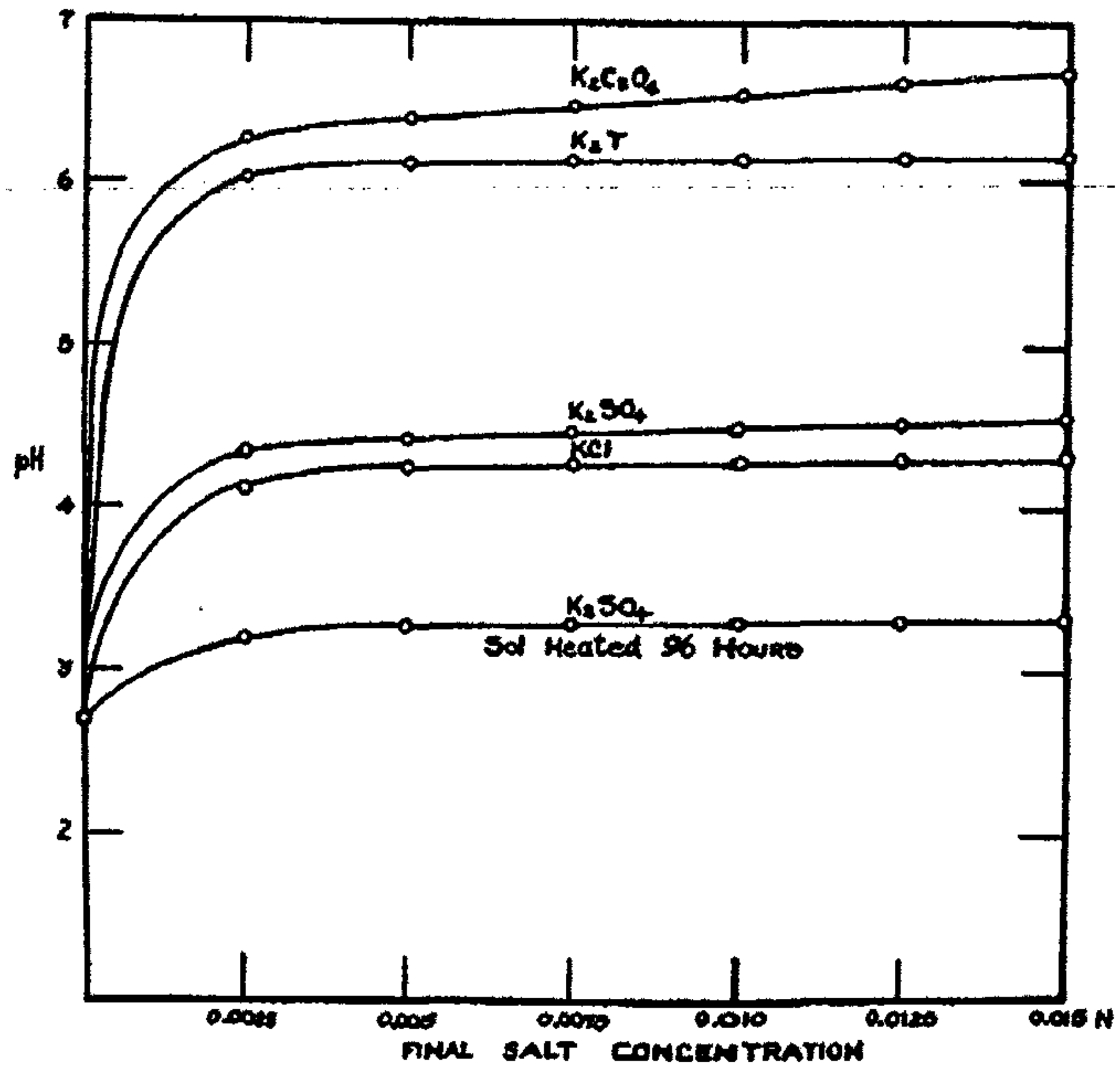

FIG. 1. Effect of potassium salts on sol T2

EXPERIMENTAL

Preparation and composition of the hydrosols

Hydrated titanium oxide was precipitated from titanium chloride solutions by addition of a slight excess of ammonium hydroxide. Centrifugal washings and decantations were used until the oxide was free from chloride. A portion of this material was peptized in boiling dilute hydrochloric acid to prepare sol T2. Another portion was peptized in dilute hydrochloric acid at room temperature to prepare sol T3.

Sol T1 was prepared by adding dilute ammonium hydroxide dropwise to a dilute solution of titanium tetrachloride until half the possible acid was neutralized. This sol was dialyzed for 148 hours.

Table 1 shows the composition of these three sols, which are typical of the eight run during the course of the investigation.

Action of neutral salts

The method used to study the effect of added neutral salts on the pH values of the hydrosols is essentially the same as that previously described (4). Figure 1 illustrates the results obtained with sol T2, which is typical of all those run. The order of effectiveness of the added anions to raise the pH value is oxalate > tartrate > sulfate > chloride. This order, while less complete, is the same as that obtained by Stewart (2).

TABLE 2

Effect of heating titanium oxide hydrosols

(a) sol T2		(b) sol T3	
TIME OF HEATING	pH	TIME OF HEATING	pH
hours		*hours*	
0	2.7	0	2.0
1	2.7	24	2.0
10	2.7	48	2.0
24	2.7	96	1.9
48	2.7		
96	2.7		

Effect of heating

The effect of heating was studied in the same manner as with the basic zirconium chloride sols (6). The results are given in table 2. The effect of heating on the action of the sol with potassium sulfate is shown in figure 1.

DISCUSSION

Titanium oxide sols react in some ways like basic zirconium chloride and basic thorium chloride hydrosols. For example, the order of effectiveness of anions in raising the pH values of the sols is the same for the few salts run. Also the tartrate, if allowed to remain in contact with the precipitate originally produced on addition to the sol, will peptize the precipitate to form a titanate hydrosol. But there the similarities seem to end and differences are the rule.

The effectiveness of the anions might be in the same order, but the magnitude of the effect is not nearly so great. If the increases in the pH values are compared with the results obtained by von Wicklen (8) with dilute hydrochloric acid and neutral salt solutions, one finds that there must be little displacement of hydroxo groups and most of the pH change comes from simple buffer action. This is borne out by experiments on heating in which the pH values of the sols remain practically constant even after 96 hours heating. If there were many hydroxo or ol groups present, there should have been some tendency for the formation of oxo bridges through ordinary oxolation with the concomitant increase in acidity. The absence of any increase in acidity on heating, accompanied by a decrease in reactivity of the sol with neutral salts, indicates that oxo bridges are formed through the following reaction.

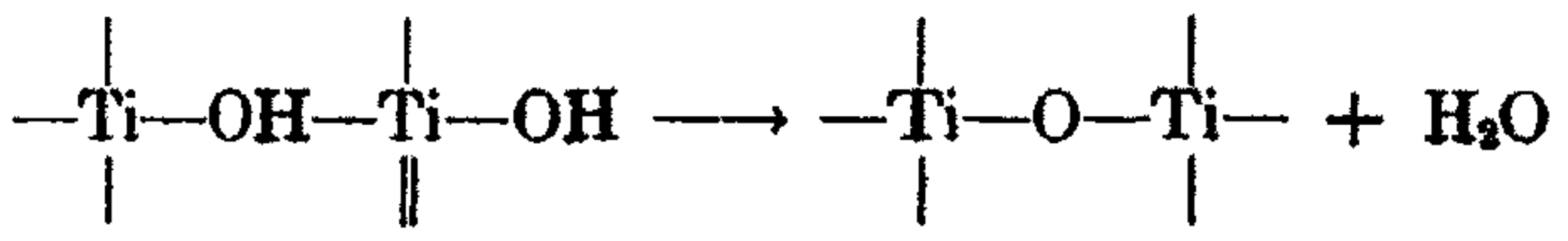

$$-\mathrm{Ti}-\mathrm{OH}-\mathrm{Ti}-\mathrm{OH} \longrightarrow -\mathrm{Ti}-\mathrm{O}-\mathrm{Ti}- + \mathrm{H_2O}$$

From the facts presented it seems logical to conclude that the micelles in these titanium oxide hydrosols are composed mainly of titanium oxide.[2] This conclusion agrees with the findings of Weiser and Milligan (9).

However, even with these, the simplest of the oxide hydrosols yet studied from this point of view, the conclusion should not be drawn that chemical reactions are completely obviated. There is to be explained, besides the displacement of hydroxo groups, the reaction with tartrate forming negatively charged micelles. This is done nicely by assuming chelation, such as occurred with basic zirconium chloride (7), basic thorium chloride (5), and basic beryllium salt hydrosols (3). Stewart (2) in his investigation of titanium oxide hydrosols agrees with this explanation.

SUMMARY

Micelles in titanium oxide hydrosols are mainly titanium oxide with few hydroxo or ol groups in the complex. This conclusion is drawn from the small change in pH values obtained on adding neutral salts or heating titanium oxide hydrosols. The result is entirely in accordance with the Thomas theory of colloidal oxides when the position of titanium in the periodic table is considered.

REFERENCES

(1) SCHMID: Z. anorg. allgem. Chem. **167**, 369 (1927).
(2) STEWART: Dissertation, Columbia University, 1937.
(3) THOMAS AND MILLER: J. Am. Chem. Soc. **58**, 2526 (1936).
(4) THOMAS AND KREMER: J. Am. Chem. Soc. **57**, 1821 (1935).
(5) THOMAS AND KREMER: J. Am. Chem. Soc. **57**, 2538 (1935).
(6) THOMAS AND OWENS: J. Am. Chem. Soc. **57**, 1825 (1935).
(7) THOMAS AND OWENS: J. Am. Chem. Soc. **57**, 2131 (1935).
(8) VON WICKLEN: J. Am. Leather Chem. Assoc. **29**, 194 (1934).
(9) WEISER AND MILLIGAN: J. Phys. Chem. **40**, 1095 (1936).
(10) WHITEHEAD: Chem. Rev. **21**, 113 (1937).

---

[2] Water of hydration has not been considered, although it must be present to allow irregular series formation with potassium tartrate.

NEUTRONS BY ALPHA-PARTICLE BOMBARDMENT OF LIGHT ELEMENTS[1]

C. S. COPELAND[2] AND S. C. LIND

School of Chemistry, University of Minnesota, Minneapolis, Minnesota

Received February 5, 1938

In view of the widespread interest in neutrons, it was felt that it might be of interest to examine the light elements under the same experimental conditions with respect to their neutron emission under α-particle bombardment, using radon as the source of α-particles.

For detection of the neutrons, it was decided to use the radioactivity induced in iodine. This element is one which is strongly activated by neutrons, and forms a single radioactive isotope, I^{128}, with a very convenient half-period of 25 minutes. By the use of ethyl iodide and the method of Szilard and Chalmers (5), the activity induced in a very large quantity of iodine can be concentrated and easily measured.

It must be admitted that the activity so obtained is not an absolute measure of the number of neutrons emitted by a given source, nor is the ratio of two activities produced by two different sources necessarily the ratio of the numbers of neutrons emitted by the two sources. This is because iodine (or any detector element) is not activated to the same extent by neutrons of different energies, and the energy spectrum of the neutrons emitted by different elements may vary widely. For a discussion of the difficulty of determining the absolute number of neutrons emitted by a given source, the reader is referred to the paper by Amaldi, Hafstad, and Tuve (1).

EXPERIMENTAL

The element, or compound of the element, to be examined was sealed, except where otherwise stated, with radon in a soft-glass bulb approximately 7 mm. in diameter. This bulb was kept in a soft-glass tube, sealed at one end, which could be dipped into ethyl iodide.

The radioiodine was prepared by placing the neutron source at the

---

[1] This paper was abstracted from a thesis submitted by C. S. Copeland to the Graduate Faculty of the University of Minnesota in partial fulfillment of the requirements for the degree of Doctor of Philosophy, June, 1937.

[2] Present address: Department of Chemistry, University of Southern California, Los Angeles, California.

center of a 500-ml. volumetric flask which contained 490 ml. of ethyl iodide plus approximately 27 mg. of free iodine. To increase the amount of radioiodine produced, the flask was cast in paraffin in a 4-liter beaker.

After a measured time of irradiation the neutron source was removed and the free iodine was extracted with 30 ml. of water containing a little sodium bisulfite. The iodide so formed was precipitated as silver iodide, filtered, washed, dried with alcohol and ether, and then examined for radioactivity.

The radioactivity of the silver iodide was measured by means of an ionization chamber connected to a linear amplifier. The ionization chamber consisted of a brass cylinder 13 cm. long and 7.7 cm. in diameter fitted at one end with an aluminum window 0.1 mm. thick and 5.2 cm. in diameter. The central electrode was a brass wire 1 mm. in diameter and approximately 9 cm. long. A brass rod mounted in an amber plug in the side of the chamber served to support the central electrode and also to connect the electrode with the amplifier circuit. To prevent any electrical leakage from the case to the central electrode across the amber, the amber plug was mounted in a grounded brass tube which was in turn mounted in hard rubber. By means of six 45-volt B-batteries, the case was kept at +270 volts with respect to the central electrode. The ionization chamber was filled with carbon dioxide at pressures ranging from 1 to 3 atmospheres. The chamber was mounted with the aluminum window face down so that

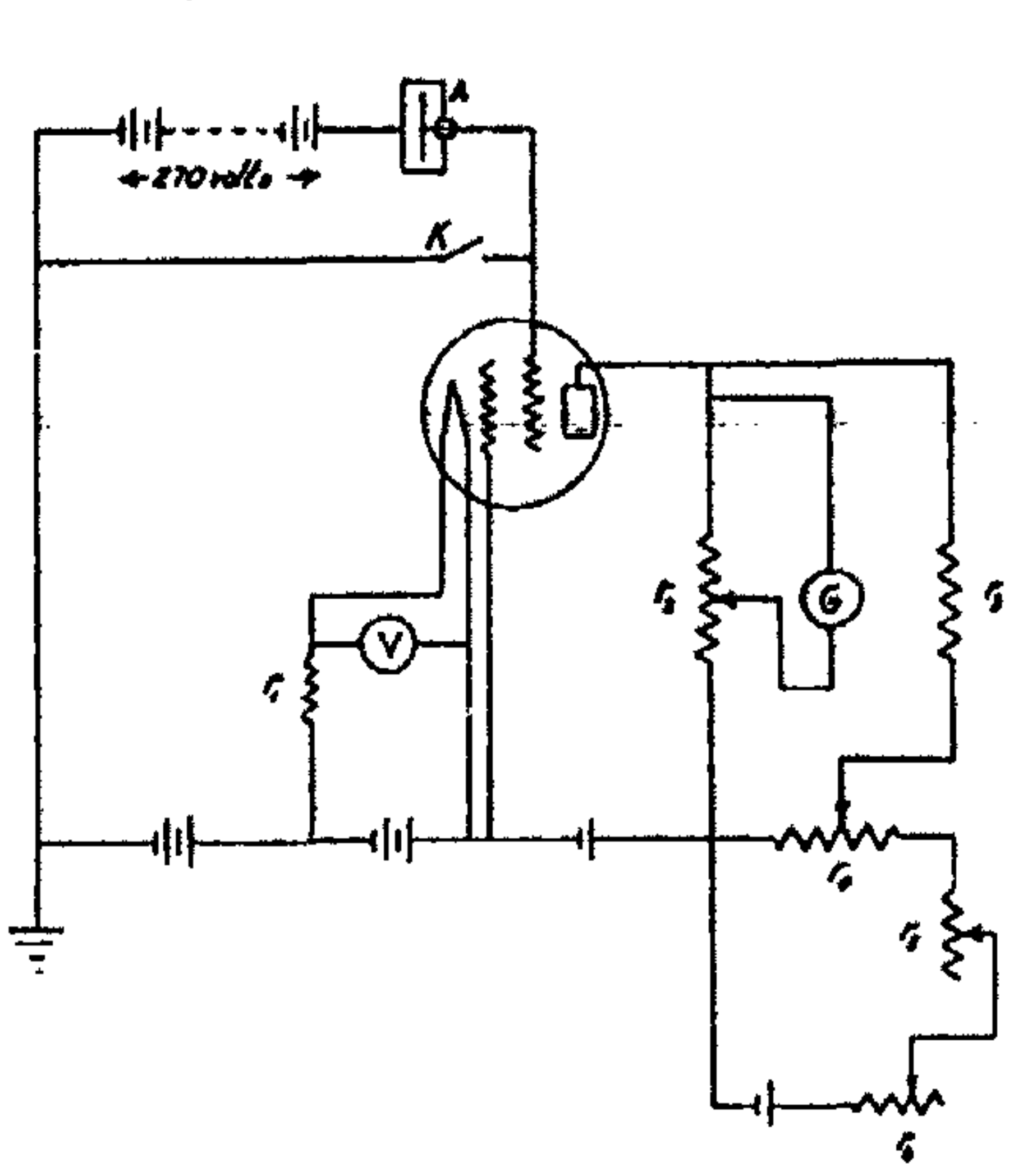

FIG. 1. Diagram of the circuit. r_1, resistance of such value that the potential drop across the filament is 2.5 volts; r_2, r_4, 10,000-ohm potentiometers; r_3, fixed resistance, 30,000 ohms; r_5, 500-ohm rheostat; r_6, 100-ohm rheostat; A, ionization chamber; G, galvanometer, 10^{-9} to 10^{-10} amperes per millimeter, 1500 ohms resistance; V, 0 to 10 voltmeter.

the filter paper holding the silver iodide could be placed directly under the window.

The linear amplifier circuit was a standard circuit using the General Electric FP 54 Pliotron tube. The circuit is shown in figure 1. The circuit was shielded and the Pliotron tube was mounted in a brass case which could be evacuated. This case was equipped with a contact key (K in figure 1), so that the control grid of the tube could be grounded or floated at will. The floating grid method of measurement was used.

The radioactivity of the radioiodine was measured with respect to the activity of a standard radium tube (0.0036 mg. of radium) taken as unity. The radium standard was used in order to eliminate error arising either from variations in the sensitivity of the circuit or from variations in the pressure in the ionization chamber. It was proved experimentally that the relative activity of the radioiodine was independent of the pressure in the ionization chamber over the range of pressure used.

The value of the relative activity of the radioiodine, α_0, at the time of removal of the neutron source was obtained by graphical extrapolation. The half-period was taken as 25 minutes. From α_0, a quantity κ, proportional to the neutron emission per millicurie per second, was calculated by means of the equation

$$\kappa = \frac{\alpha_0(\lambda_1 - \lambda)}{M_0(e^{-\lambda t} - e^{-\lambda_1 t})}$$

where t is the time of irradiation of the ethyl iodide and M_0 is the number of millicuries of radon present at the start of the irradiation. λ_1 and λ are the decay constants of radioiodine and radon, respectively.

Since in most cases compounds and not pure elements were used as neutron sources, it was necessary to calculate the neutron emission which would have been observed if the pure emitting element, and not its compound, had been used. The appropriate conversion factor, μ, to make this calculation was obtained from the equation

$$\mu = \frac{\sum n_i Z_i^{2/3}}{n_e Z_e^{2/3}}$$

where n_i is the subscript of the i^{th} element in the formula of the compound and n_e is the subscript of the emitting element. Z is the atomic number.

DISCUSSION OF RESULTS

The results obtained for a number of substances are shown in table 1. In the column headed "neutron source" are given the elements or compounds which were sealed in glass bulbs with radon. In the case of compounds, the neutron emission given is for the compound as a whole. The last column gives the neutron emission on the basis that the emission for

TABLE 1

Neutron emission by various substances when bombarded by α-particles from radon

NEUTRON SOURCE	TIME OF IRRADIATION OF ETHYL IODIDE	M_0	α_0	κ	$\bar{\kappa}$	$\bar{\kappa}$ (Be=100)
	minutes					
Beryllium	218	34.6	30.0	157	157	100
	22	32.2	12.2	150		
	55	23.5	17.0	164		
Lithium carbonate	196	60.0	2.74	8.28	8.4	5.4
	223	47.7	1.82	8.36		
	83	46.3	2.04	8.75		
	137	40.6	2.13	8.04		
Boron (amorphous)	154	63.0	5.20	15.0	14.8	9.43
	235	49.4	4.13	15.1		
	93	47.9	3.54	14.2		
Calcium fluoride	224	79.8	8.70	19.8	19.5	12.4
	271	55.7	6.35	20.7		
	2912	53.7	3.80	17.9		
Sodium carbonate	397	104.3	4.35	7.69	6.9	4.4
	426	88.9	2.96	6.18		
	164	83.4	3.15	6.85		
Magnesium oxide	227	80.6	1.33	2.99	2.8	1.8
	315	76.8	1.18	2.81		
	266	37.3	0.51	2.5		
	256	31.2	0.48	2.8		
Aluminum (100-mesh filings)	293	69.1	2.55	6.71	6.8	4.3
	100	66.6	2.50	7.12		
	164	64.7	2.45	6.86		
	400	56.9	2.00	6.48		
Phosphorus (red)	370	59.1	0.49	1.6	1.6	1.0
	354	48.4	0.40	1.5		
Potassium chloride	324	59.1	0.56	1.9	1.7	1.1
	200	39.2	0.26	1.4		
Potassium carbonate	281	73.3	0.12	0.3	0.4	0.3
	179	70.1	0.16	0.4		
Calcium carbonate	316	79.6	0.17	0.4	0.4	0.3
	138	66.2	0.15	0.4		

M_0 is the initial number of millicuries of radon in the neutron source.

α_0 is the radioactivity of the silver iodide at the time of removal of the neutron source.

κ is proportional to the neutron emission per unit time per millicurie of radon.

$\bar{\kappa}$ is the average value of κ.

beryllium is 100. In addition to the substances listed in table 1, silica, sulfur, zinc, carbon, and paracyanogen were examined.

Silica was examined by sealing about 30 millicuries of radon in a fused quartz bulb. A very weak emission was observed. As nearly as could be judged, after allowing for the amount of radon used, the emission was of the same order of magnitude as the emission observed with the potassium and calcium carbonate sources.

Sulfur and zinc were examined under conditions somewhat different from those used for the other substances investigated. Flowers of sulfur and zinc dust were sealed with radon in Pyrex bulbs, and the ethyl iodide was irradiated in a 500-ml. round-bottom flask. The results so obtained were compared with the result observed when a Pyrex bulb containing aluminum and radon was employed.

Both the sulfur and zinc bulbs showed a weak emission of about the same order of magnitude. The emission was certainly less than one-tenth that obtained with an aluminum bulb.

The paracyanogen and carbon were both sealed in fused quartz bulbs. The ethyl iodide was irradiated according to the standard procedure, but the activity of the radioiodine was measured with a Geiger tube counter. This activity was compared with that produced by a Pyrex bulb filled with beryllium and radon. Taking the neutron emission for beryllium as 100, the emission for paracyanogen was approximately 0.9 and the value for carbon was approximately 0.4.

The above value for the neutron emission of paracyanogen is certainly too low. It was discovered after the radon had been introduced that insufficient paracyanogen had been used to fill the bulb, and, furthermore, a globule of mercury was accidentally introduced at the time the radon was collected.

Since an emission of about the same order of magnitude was obtained with calcium carbonate, potassium carbonate, sulfur, and zinc sealed in glass, carbon sealed in quartz, and an empty quartz bulb, it seems rather difficult to ascribe any significance to this emission from the standpoint of any particular element involved. Indeed, in those cases where glass bulbs were used, a weak residual emission might be expected, since an empty soft-glass bulb filled with radon shows a neutron emission of about 1.5 (beryllium = 100).

On the whole, in view of the results obtained, it would seem best to consider that there is a general background, and that all definitely positive results should be corrected for this background. Table 2 gives the values for the substances listed in table 1 after this correction has been made. In addition, in table 2 the corrected values of the neutron emission for the compounds listed have been converted into values for the active element involved. These results are shown graphically in figure 2.

TABLE 2

Corrected values of the neutron emission for the substances listed in table 1

NEUTRON SOURCE	κ	ACTIVE ELEMENT	μ	κ'
Lithium carbonate	5.1	Li	4.68	24
Beryllium	100	Be		100
Boron	9.1	B		9.1
Paracyanogen	0.5	N	1.90	1
Calcium fluoride	12.1	F	1.85	22.4
Sodium carbonate	4.1	Na	2.55	11
Magnesium oxide	1.5	Mg	1.76	2.6
Aluminum	4.0	Al		4.0
Phosphorus	0.7	P		0.7
Potassium chloride	0.8	Cl	1.93	1.5

κ is proportional to the neutron emission per second per millicurie of radon.

μ is the conversion factor by which the value of the neutron emission for a compound is multiplied to obtain the neutron emission of the active element in the compound.

$\kappa' = \mu\kappa$.

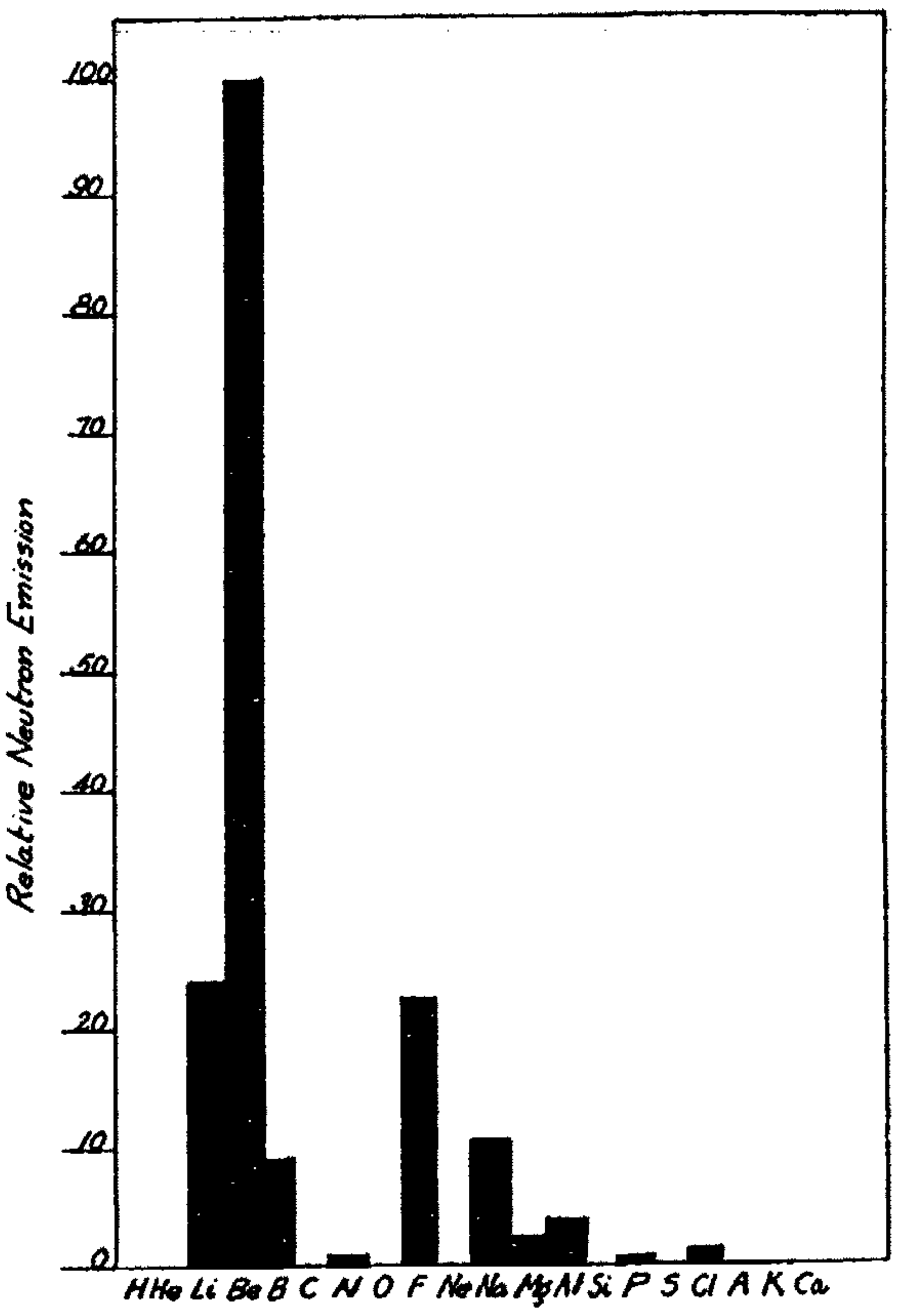

FIG. 2. Neutron yields from certain light elements (rare gases not investigated)

In the case of the oxides and carbonates listed in table 2, the neutron emission is ascribed to the metal involved, because of the weak neutron emission observed with potassium carbonate, calcium carbonate, and silica.

The neutron emission observed with paracyanogen is due to the nitrogen, since a similar carbon-filled bulb is a decidedly poorer neutron emitter. This is in agreement with the observation of Wertenstein (7) that nitrogen under RaC′ α-particle bombardment produces radiofluorine.

In the case of potassium chloride, the active element is undoubtedly chlorine, because of the appreciable difference in neutron emission shown by potassium chloride and potassium carbonate. If potassium were the active element, we should expect the two compounds to show about the same neutron emission, since the conversion factor to potassium is 1.93 for potassium chloride and 2.07 for potassium carbonate.

The choice of chlorine as the neutron emitter in potassium chloride is given added weight by the recent work of Pollard, Schultz, and Brubaker (3), who showed that both argon and chlorine emit neutrons under ThC′ and RaC′ α-particle bombardment. The chlorine disintegration has been further studied by Hurst and Walke (2) and by Ridenour and Henderson (4), using artificially accelerated 11 Mev. and 9 Mev. α-particles, respectively.

With regard to a neutron emission from potassium, Zwy (8) has shown, by studying the radioactivity induced in potassium chloride, that potassium must disintegrate with neutron emission under RaC′ α-particle bombardment. Walke (6) has also investigated this reaction, using 11 Mev. α-particles, and has shown that both K^{39} and K^{41} disintegrate with neutron emission.

Our experiments would seem to show that the neutron emission from potassium under RaC′ α-particle bombardment must be slight, since we were unable to detect any difference between potassium and calcium carbonates. Even if we assign all of the emission observed with potassium carbonate to potassium, the emission for potassium would only be approximately 0.5 per cent of that observed for beryllium.

SUMMARY

All of the elements from lithium through calcium, with the exception of the rare gases, have been investigated for neutron emission under α-particle bombardment. The α-particle source used was radon, and in each case the neutron yield was determined by measurement of the radioactivity induced in iodine. Positive neutron emission was observed for lithium, beryllium, boron, nitrogen, fluorine, sodium, magnesium, aluminum, phosphorus, and chlorine. The neutron emission from carbon, silica, sulfur, potassium carbonate, calcium carbonate, and zinc is less than 0.5 per cent of the emission from beryllium.

REFERENCES

(1) Amaldi, Hafstad, and Tuve: Phys. Rev. **51**, 896 (1937).
(2) Hurst and Walke: Phys. Rev. **51**, 1033 (1937).
(3) Pollard, Schultz, and Brubaker: Phys. Rev. **51**, 140 (1937).
(4) Ridenour and Henderson: Phys. Rev. **52**, 889 (1937).
(5) Szilard and Chalmers: Nature **134**, 462 (1934).
(6) Walke: Phys. Rev. **52**, 400 (1937).
(7) Wertenstein: Nature **133**, 564 (1934).
(8) Zwy: Nature **134**, 64 (1934).

STUDIES ON SILICA JELLIES. I

GELATION TIME AND CHANGE IN pH VALUE AS FUNCTIONS OF CONCENTRATION, INITIAL pH VALUE, AND TEMPERATURE[1]

HAROLD W. BATCHELOR

Ohio Agricultural Experiment Station, Wooster, Ohio

Received August 25, 1937

INTRODUCTION

An extensive literature on the properties of gels has accumulated since Pott (cited by Walden (14)) first prepared silica jellies in 1746, yet a diversity of opinion still exists regarding several important factors involved in their formation. A number of investigations have been conducted on sol-concentration (or dilution), hydrogen-ion concentration, and temperature as affecting the gelation time of inorganic sols, as well as on various factors affecting the gelation times of organic sols.

The general conclusions from such studies on silica sols may be summarized as follows: (*1*) Increasing concentration of sols reduces gelation time. (*2*) In solutions whose hydrogen-ion concentrations varied from pH 4.2 to pH 5.5, Hurd, Raymond, and Miller (5) found the log of the gelation time to be a lineal function of the initial pH value. Considerable confusion still exists regarding the hydrogen-ion concentration at which gelation takes place in minimum time. It may take place at neutrality or at slightly alkaline reactions. Apparently no observations on minimum time for gelation of slightly acid sols have been reported. (*3*) The change in pH undergone by a sol during and subsequent to gel formation is not well understood, since numerous conflicting and contradictory views have been expressed. The general opinion appears to be that gelation of acid silica sols is attended by little or no change in hydrogen-ion concentration, but in neutral and alkaline sols there is an increase in pH value. (*4*) Increasing temperature is generally regarded as reducing gelation time. (*5*) No single systematic study has yet been made of all these factors to determine their interrelations.

Silica gels, first proposed by Kuhne (7) as a base for bacteriological media, possess some characteristics which make them superior to other solid media. If prepared by mixing sufficiently dilute alkali silicates and

---

[1] A second paper dealing with the bacteriological phases of the work will be submitted for publication in the Journal of Bacteriology.

acid solutions to obviate the dialysis of excess salts, their ease of preparation and suitability for use are important in practical applications. The close regulation of pH desirable in the preparation of media and the importance of details essential to a uniform product with the desired characteristics are believed sufficient justification for a careful study of the factors involved. The present study has been concerned with gelation time and shift in pH value as affected by concentration (or dilution), initial pH value of the sol, and temperature during gelation. The data obtained permit a reconciliation of contradictory opinions regarding the behavior of silica sols and gels.

EXPERIMENTAL AND DISCUSSION

During the seven years that silica jellies have been used as bacteriological media in this laboratory, five brands of sodium silicate and two brands of potassium silicate have been studied. Potassium silicates are more satisfactory for the preparation of jellies that are not to be dialyzed, because the potassium ion induces gelation at lower concentrations than the sodium ion. For a given strength of jelly, therefore, potassium jellies may be prepared at a lower salt concentration than sodium jellies,—a matter of considerable importance in the use of bacteriological media. For this and other reasons to be noted elsewhere, potassium silicates have been studied more in this laboratory than sodium silicates. The work here reported has been confined to one brand of silicate, known as "Potassium Silicate Solution Bé30°", manufactured by the Grasselli Chemical Company. Although stock solutions of silicates are usually prepared on the basis of specific gravity or of molarity of the solution, as a matter of convenience the solutions used in these studies were based on titrable alkalinity. As supplied by the manufacturer the potassium silicate is somewhat stronger than a 2 N alkali solution. The solutions were, therefore, diluted with an equal volume of freshly distilled water before attempting the standardization. To 10 ml. of this solution were added 100 ml. of distilled water and several drops of a 0.16 per cent solution of bromothymol blue. The silicate solution was then titrated with normal hydrochloric acid. From this titration the amount of water necessary to make the stock solution equivalent to normal hydrochloric acid was calculated and added. A second titration was then made and the solution further corrected if necessary. Manifestly, such a procedure could not be used for work in which absolute values were expected, since Weiser (15) has shown that titrations of colloids made in the usual stepwise manner require an appreciable lapse of time before equilibrium is reached. The method suffices, however, if only approximations are required. A 12-liter stock solution thus prepared was allowed to stand several weeks in a tightly stoppered bottle before being used. Aside from a slight brownish sediment which probably consists of iron compounds, no changes in stored stock potassium silicates have been noted. Sodium silicates, on the contrary, tend to lose their silica by flocculation.

In the preparation of bacteriological media the use of several acids has been necessary to obtain an optimum ratio of anions for the growth of any particular organism. In the work here reported a mixture of 50 parts of normal sulfuric acid, 40 parts of normal hydrochloric acid, and 10 parts of 1.5 *N* orthophosphoric acid has been used. The proper compositions of the silicate-acid mixtures to give the desired initial pH values have been determined in the following manner. Sufficient distilled water was added to each of sixty-six 135-ml. screw-cap bottles to bring the total volume in each bottle to 100 ml. after the silicate and acid solutions had been added. As each solution was prepared it was thoroughly rotated by hand, and its pH value was determined by means of the Coleman glass electrode electrometer within 1 minute after the solution was prepared. The term "initial pH value" as used in this paper refers to the hydrogen-ion concentration of the sols determined under these conditions. The compositions of the solutions giving the desired initial pH values were derived from the titration curve thus obtained, and are given in table 1. The sols thus prepared to have initial pH values between 5.5 and 9.4 were found to be sufficiently well buffered for reproduction with considerable accuracy; the more acid sols presented greater difficulties in pH control. This may account for some of the inconsistencies in the data.

TABLE 1

Volumes of acid mixture per 10 ml. of potassium silicate to give initial pH value indicated

Initial pH value....	3.5	4.0	5.0	5.5	6.0	6.5	7.0	7.5	8.0	8.5	9.0
Volumes of acid mixture (ml.).........	10.6	10.5	10.45	10.3	10.0	9.5	9.0	8.4	7.6	6.4	5.4

GELATION TIME AS A FUNCTION OF CONCENTRATION, INITIAL pH VALUE, AND TEMPERATURE

The precise point at which a sol passes into a gel cannot be defined, but an approximate determination by one of the numerous tests which are available may nevertheless be useful. In the absence of equipment required for the more precise optical methods, for the present study a device suggested by Sommer (11) has been employed. It consists of a mechanism by which several bottles are rotated at a slow uniform speed at an angle of about 30 degrees from the horizontal with a suitable provision for counting the number of revolutions of each bottle. The gelation time can be calculated from this number. Disturbance of the solutionin validates

Smoluchowski's derivations (12, 13), but Flemming (2), Jabłczyński (6), and others have found slight disturbances to have little or no effect. Under the conditions of these studies Sommer's device permitted an easy and, for the purpose at hand, a sufficiently accurate means of determining the gelation times.

The following procedure was strictly adhered to. At room temperature sufficient distilled water was added to each bottle to bring the solutions to the desired volumes after the silicate and the acid were added. The bottles were then placed in the water bath and allowed to come to the proper temperature. The stock solutions of silicate and acids were kept in the same water bath and were used only when the temperatures of the solutions were within the temperature limits allowed. After the addition of the silicate and of the acid mixture (added in that order) the bottle was rotated by hand to mix the solutions. It was then placed in the machine and the revolution counter was started. In each case record was kept of the time which elapsed from the moment the acid began to mix with the silicate until the automatic counter was engaged. All containers were kept tightly stoppered except when intentionally opened. For the 60° and 80°C. temperatures, the acid and alkali pipets were standardized to deliver a volume of solution equivalent to that delivered at room temperature (27°–28°C.), the temperature on which the initial pH values were based. In the absence of an accurate thermoregulator, the water bath was maintained within only ±2°C. of the desired temperature. Variations within the water bath were prevented by the use of an efficient stirring device.

Provision was made to determine the gelation times at temperatures of 20°, 40°, 60°, and 80°C., at initial pH values of 5.0, 5.5, 6.0, 6.5, 7.0, 7.5, 8.0, 8.5, and 9.0, and at total solution volumes of 50, 60, 70, 80, 90, and 100 ml. The ultimate concentrations of the solutions, estimated from the original stock normal silicate solution, therefore varied from 0.1 to 0.2 *N*, calculated as potassium. The actual pH values at which the jellies were formed at the higher temperatures are unknown, because the hydrogen-ion concentration is a function of temperature. In all probability they were more acid or less alkaline, as the case may be, than is indicated by the initial pH values determined at room temperature. Buchanan and Fulmer (1) have summarized the relations involved. Were water alone concerned in these studies, one might reasonably calculate the actual reactions of the solutions when raised to the higher temperatures, but one would scarcely be justified in making these calculations for solutions containing appreciable concentrations of electrolytes and of colloids. For the purpose at hand, this relation may be omitted from the remainder of the discussion. The data are shown graphically in figure 1.

If a three-dimensional figure, similar to that in figure 1, were pictured as a typical isometric or dimetric drawing, an incorrect interpretation of the data might result. To prevent this, some deviations from usual conventions of drawing have been made. One may imagine that he is viewing this drawing from a point almost directly above and slightly to the right

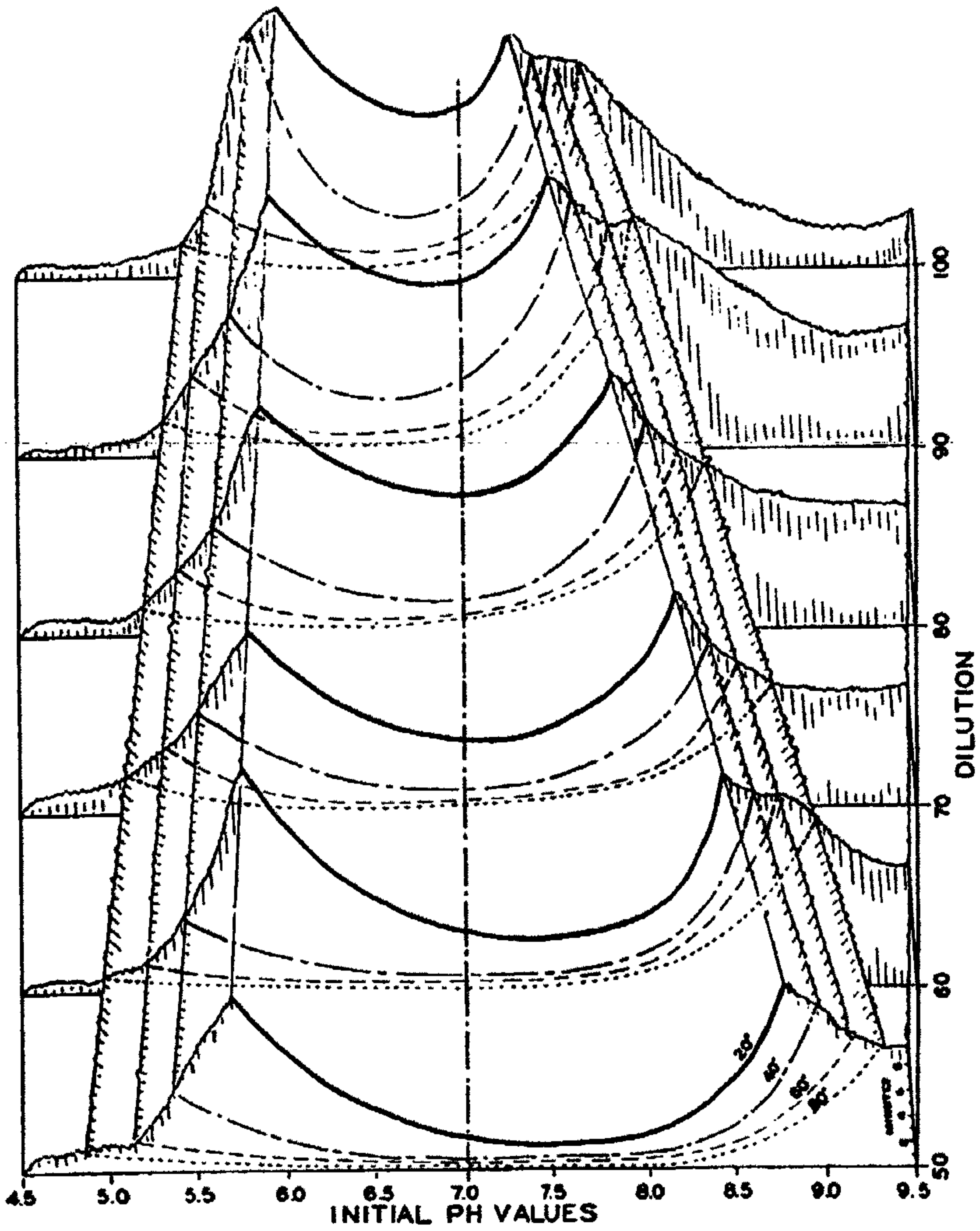

Fig. 1. Gelation time as a function of pH, dilution, and temperature

of the figure. Across the front of the unshaded base, which is indicated by the lowest horizontal line in the figure, the different initial reactions of the solutions are shown in terms of pH values. At the extreme right, along the right-hand side of the base, are given the total volumes of the solutions in terms of milliliters; they are labeled by the rather inapt term "dilution". The least dilute solution is indicated at the front of the base by the figure "50", and the most dilute solution is indicated at the rear by the figure "100". At each dilution there rises a vertical plane upon which are plotted the data for the time interval (gelation time) elapsed before the jellies formed. It should be noted that the time scale should be imagined on the other vertical planes, each starting at zero time at the intersection of the respective vertical planes with the base. These latter intersection lines theoretically extend entirely across the figure, but for the sake of legibility are not shown in those areas where they are "hidden" by the warped surfaces. The gelation times at any single temperature, including all the pH values and dilutions at that temperature, assume the form of a concave warped surface whose intersections with the vertical planes are indicated by a series of curved lines; each temperature is indicated on the front vertical plane. The upper portions of the vertical planes and of the concave surfaces have been "torn off", and the resulting serrated edges are indicated by wavy lines. To emphasize the position of neutrality at all concentrations and temperatures, a dot-dash line has been drawn through the entire figure.

In the first complete series, the two hundred sixteen determinations were made singly. As a result of inconsistencies with the extremely alkaline and especially the extremely acid sols, thirty-eight of these determinations were repeated in duplicate. In some cases these determinations were made three or four times, each time in duplicate. Three points on the extremely acid side and one on the extremely alkaline side of the 20°C. surface were persistently inconsistent with the remaining data for that temperature. In the interest of legibility this surface was therefore idealized by slightly lowering each of these points. The figure conforms accurately to the data obtained, with these and one additional exception, that several of the lines on the extreme margins of the surfaces were extrapolated slightly beyond the actual limits at which they were determined. Except for the strongly acid and strongly alkaline sols at 60° and 80°C., whose gelation times showed a maximum error of ±10 per cent, the maximum errors involved (2.4 to 3.5 per cent) are considered not unreasonable for this type of determination.

In some of the more concentrated solutions at least, and particularly at the higher temperatures, the data require that the conception "minimum gelation point" be expanded to what may be termed the "minimum gelation range". The mid-point of this minimum gelation range may then be compared either with the minimum gelation point of the more dilute solutions or with the minimum gelation point of the lower temperatures. Considering only the upper 20°C. surface indicated by the heavy solid lines, with attention to the lowest point of each line, it is observed that at dilution "50" the minimum point lies near pH 7.5, at dilution "70" it lies near pH 7.0, and at dilution "100" it approaches pH 6.5. At this temperature, therefore, the minimum gelation time shifts from the alkaline, through the neutral, and toward the acid reaction as gelation takes place in progressively more dilute solutions. This relation also obtains at the higher temperatures but is less evident, since the minimum gelation time is expanded and the surfaces for the higher temperatures have not been fully extended in the acid region. This relation harmonizes several conflicting statements in the literature regarding the pH values at which gelation of silica sols takes place in minimum time. Another relation in minimum gelation time is best shown at the "100" dilution. It may be stated thus: *at constant concentration, the minimum gelation time shifts from the acid reactions toward neutrality as the temperature is progressively lowered.* This relation remains consistent at dilutions "80" and "90". If the conception with regard to minimum gelation range mentioned above is applied, the same tendency holds for the other dilutions. Had data been obtained at greater dilutions or lower temperatures, it is conceivable that the minimum gelation time might have shifted into the alkaline range. This assumption is supported by the data at dilution "50". This relation between minimum gelation times at constant concentration but varying temperatures appears not to have been noted previously. Parenthetically, it may be noted that the use of the minimum gelation time as an index of the position of the isoelectric point of the jellies would be questionable under the conditions obtaining in these studies.

Thus far, the use of silica jellies for bacteriological media has been necessarily confined to approximately neutral reactions since, except for the recent work by Ray and Ganguly (10), no means have been available by which jellies could be prepared at reactions deviating much from neutrality. It is evident from these data, however, that they may be prepared both at fairly acid and alkaline reactions, the range of reactions being limited by at least two factors,—concentration and temperature. The organisms studied grow less vigorously at concentrations of "50" and "60" than at greater dilutions. However, with jellies prepared at dilutions greater than "100", the bacterial colonies tend to coalesce. Accordingly, the undialyzed jellies employed for bacteriological studies in this laboratory have been employed at concentrations of "70" to "100" inclusive. In routine practice the "100" dilution has been used.

THE SHIFT IN pH VALUE DURING GELATION

Shift in pH value during gelation also limits the pH values of undialyzed jellies usable in bacteriological media. The shift has been studied as a function of concentration (dilution), initial pH value, and temperature. The technique followed was similar to that given previously. The bottles

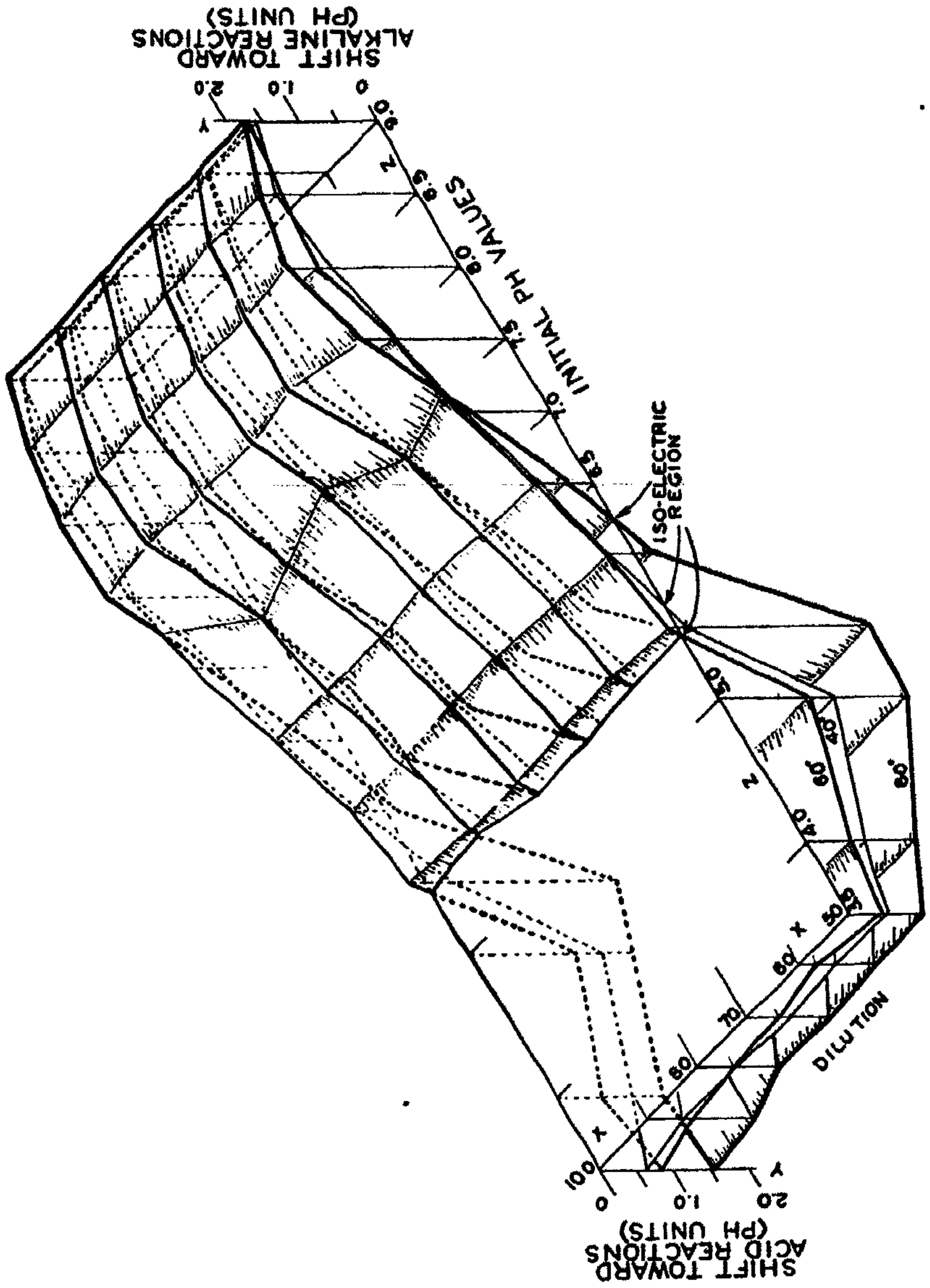

FIG. 2. Shift in pH value as a function of initial pH, dilution, and temperature

were not rotated, however, and all of the sixty-six bottles for a given temperature were placed in the water bath at one time. The temperature of the water bath was maintained at the desired point for 2 hours after the solutions were prepared and was then allowed to return to room temperature. The pH values of the sols and jellies were determined after 24 hours, again after three or four days, and finally after one week. The samples, after being stirred, were pipetted into the electrometer cup with an inverted 10-ml. pipet. Care was taken not to dilute the sample, since previous studies have shown that in strongly acid and strongly alkaline solutions even a twofold dilution may vary the reaction by as much as three-tenths of a pH unit. In strongly acid solutions the shift is toward less acid reactions, and in strongly alkaline solutions toward less alkaline reactions. The data for this study are shown graphically in figure 2. The dilutions and initial pH values are plotted along the ends and sides, respectively, of the X–Z plane. Variations in reaction from the initial pH values are plotted in terms of pH units on the Y-axis; the shifts toward more alkaline reactions are plotted above and the shifts toward more acid reactions below the X–Z plane. The shifts in pH value at any given temperature, including all the initial pH values and "dilutions" for that temperature, take the form of an S-shaped warped surface lying above the X–Z plane at neutral and alkaline reactions and below this plane at acid reactions. For the sake of legibility, the data obtained at 20°C. have not been included. Within the limits of the data, the relations found may be expressed as follows:

1. The pH values of silica sols and jellies having neutral and alkaline initial pH values shifted toward the alkaline side.
2. The pH values of slightly acid sols and jellies remained stable.
3. The pH values of more strongly acid sols and jellies shifted toward more acid reactions.
4. The shifts in pH value were greater at the higher temperatures.
5. At extremely acid and extremely alkaline initial pH values the shifts in reaction were less marked than at moderately acid and moderately alkaline reactions.
6. The shifts in pH value were largely independent of variations in concentration.
7. The shifts in pH value were independent of gel formation.
8. The positions of the hypothetical isoelectric points of these sols and jellies probably lie within the region formed by the intersections of the warped surfaces with the X–Z plane and appear to be a function of temperature.

The regions of minimum or no shift in pH value conform roughly to the region between pH values 4.64 and 5.92, in which Hurd and Griffith (4) found no shift in reaction during gelation. A similar agreement is found with the results of Prasad and Hattiangadi (9), who found no appreciable shifts between reactions of pH 5.2 and 6.1. Had they determined the reactions of their alkaline solutions after a greater lapse of time, it is possible that the shifts in reaction which they noted would have conformed more closely to the results obtained in the study here reported. The data for the shifts in reaction from pH 7.0 are given in detail in table 2. These results agree surprisingly well with the shift in reaction (equivalent to 1.1 pH unit) which Hanks and Weintraub (3) found at initial reactions from pH 6.3 to 7.1. On the basis of this single value these authors proposed a method for preparing silica jellies at "any pH desired". In the light of the results here reported the value of the method proposed by them appears to be questionable. In connection with their work on undialyzed jellies they stated, "Observations on diluted acid-silicate mixtures suggest that the rapid pH drift does not occur until gelation is initiated; the hydrogen-ion exchange seems to be intimately related to the process of gel formation". The validity of this statement has not been verified in the present study, since shifts in pH value developed in solutions which failed to produce any evidence of gelation even after one week.

TABLE 2

The shift in pH value from pH 7.0 toward alkaline reactions

DILUTION	TEMPERATURE			
	20°C.	40°C.	60°C.	80°C.
	pH units	*pH units*	*pH units*	*pH units*
50	1.22	1.10	1.19	1.02
60	1.30	1.16	1.06	1.15
70	1.31	1.08	1.37	1.20
80	1.31	1.16	1.43	1.42
90	1.31	1.19	1.42	1.15
100	1.35	1.06	1.45	1.21

The accumulation of data which might have led to explanations of the physical-chemical factors involved in these studies was beyond the scope of the project under investigation. For this reason the author is content to follow McBain's advice (8) ". . . the phenomena of colloidal behavior should be described in terms of the directly observed facts rather than of theories or influences".

SUMMARY

1. Studies have been made of gelation times and of shifts in pH value of silica sols and jellies as functions of concentration, initial pH value, and

temperature. The data are expressed in the form of three-dimensional figures.

2. The data permit a reconciliation of a number of conflicting statements in the literature regarding the influence of the factors mentioned.

3. Minimum gelation time at constant concentration but at progressively lower temperatures appears to shift from acid through neutral and toward alkaline reactions.

4. Several relations have been pointed out between the factors studied and the shift in hydrogen-ion concentration of silica sols during gelation.

It is a pleasure to acknowledge the author's indebtedness to Professor R. M. Salter and Mr. C. J. Schollenberger for their interest and criticisms of the manuscript and to Dr. A. A. Hendrickson, Albert Dickinson Fellow in Soil Biology, for his assistance during the preliminary work in these studies.

REFERENCES

(1) Buchanan, R. E., and Fulmer, E. I.: Physiology and Biochemistry of Bacteria, Vol. 1, pp. 231-5 (1928).
(2) Flemming, W.: Z. physik. Chem. **41**, 427 (1903).
(3) Hanks, J. H., and Weintraub, R. L.: J. Phys. Chem. **41**, 583 (1937).
(4) Hurd, C. B., and Griffith, R. L.: J. Phys. Chem. **39**, 1155 (1935).
(5) Hurd, C. B., Raymond, C. L., and Miller, P. S.: J. Phys. Chem. **38**, 663 (1934).
(6) Jablczyński, C. K.: Bull. soc. chim. [4] **35**, 1277 (1924).
(7) Kuhne, M. W.: Z. Biol. IX, 173.
(8) McBain, J. W.: Colloid Symposium Monograph, Vol. IV, p. 18.
(9) Prasad, M., and Hattiangadi, R. R.: J. Indian Chem. Soc. **6**, 653 (1929).
(10) Ray, R. C., and Ganguly, P. B.: J. Phys. Chem. **34**, 352 (1930).
(11) Sommer, H. H., and Matsen, H.: J. Dairy Sci. **18**, 741 (1935).
(12) von Smoluchowski, M.: Z. physik. Chem. **92**, 129 (1917).
(13) von Smoluchowski, M.: Physik. Z. **17**, 357 (1916).
(14) Walden, O.: Kolloid Z. **9**, 145 (1911).
(15) Weiser, H. B.: J. Phys. Chem. **35**, 1 (1931).

EQUILIBRIA IN THE SYSTEM POTASSIUM SULFATE–MAGNESIUM SULFATE–CALCIUM SULFATE–WATER AT 100°C.[1]

J. E. CONLEY,[2] ALTON GABRIEL,[3] AND EVERETT P. PARTRIDGE[4]

Bureau of Mines, Eastern Experiment Station, College Park, Maryland

47-74

Received January 22, 1938

Among the processes proposed for the recovery of potassium sulfate from polyhalite is the extraction of the calcined complex salt with hot water. Since better results have been attained at 100°C. than at lower temperatures (4), a knowledge of the equilibria, both stable and metastable, in the system potassium sulfate–magnesium sulfate–calcium sulfate–water at this temperature is essential to an adequate understanding of the phenomena observed during these extractions. The information available concerning this four-component system is, however, fragmentary. From the data of Geiger (6) and van't Hoff (13) it has been possible to obtain an idea of the phase diagram at 83°C., and largely from the work of van Klooster (12), Basch (2), and van't Hoff a fairly complete picture of the system at 25°C. may be visualized. Data at intermediate temperatures and at temperatures above 83°C. are entirely lacking for the four-component system, although the three-component systems potassium sulfate–calcium sulfate–water and potassium sulfate–magnesium sulfate–water have been thoroughly studied at 100°C. by Hill (8) and by Starrs and Clarke (11), respectively. The present paper describes a detailed study of part of the four-component system at 100°C.

The portion of the four-component system with special bearing on the extraction of calcined polyhalite is that involving the solid phases, polyhalite ($K_2SO_4 \cdot MgSO_4 \cdot 2CaSO_4 \cdot 2H_2O$), syngenite ($K_2SO_4 \cdot CaSO_4 \cdot H_2O$), pentasalt ($K_2SO_4 \cdot 5CaSO_4 \cdot H_2O$), anhydrite ($CaSO_4$), gypsum ($CaSO_4 \cdot 2H_2O$), and hemihydrate ($CaSO_4 \cdot 0.5H_2O$). Gypsum and hemihydrate

---

[1] Published by permission of the Director, Bureau of Mines. (Not subject to copyright.)

[2] Associate chemical engineer, Bureau of Mines Eastern Experiment Station, College Park, Maryland.

[3] Associate chemist-petrographer, Bureau of Mines Eastern Experiment Station, College Park, Maryland.

[4] Formerly supervising engineer, Bureau of Mines Non-metallic Experiment Station, New Brunswick, New Jersey. Now with Hall Laboratories, Inc., Pittsburgh, Pennsylvania.

appear only as metastable solid phases which are in process of replacement by anhydrite, which is the stable form of calcium sulfate at 100°C.

The concentrations of the liquid phases covered in these studies were from 0 to 17.0 g. of potassium sulfate per 100 grams of water and from 0 to approximately 14.0 g. of magnesium sulfate per 100 grams of water. This range is sufficient to include all compositions of extract solutions that are likely to be obtained by the extraction of calcined polyhalite with water at 100°C.

The investigation has included not only the stable but also some of the more frequent metastable relations through which the system passed in attaining final equilibrium. From the standpoint of the chemical engineer these metastable equilibria are of the greatest importance, especially since the stable equilibria which involve pentasalt or anhydrite as a solid phase are approached only at an extremely slow rate at 100°C. This slow establishment of equilibrium with anhydrite was noted at temperatures below 100°C. by D'Ans (5), who concluded that the difference in calcium sulfate concentration between equilibria involving gypsum and anhydrite, respectively, would not be important. That this difference in calcium sulfate has a profound effect upon the system is shown by the work reported in the present paper.

Even where a form of calcium sulfate is not involved as a solid phase, the rate of approach to equilibrium in the system is in general very slow, owing to the fact that in the decomposition of one double salt and the formation of another, all of the calcium sulfate must pass through the solution phase where the concentration is of the order of 0.2 g. of calcium sulfate per 100 grams of water.

Particular emphasis has been given to the location of the isothermally invariant polyhalite-syngenite-pentasalt and polyhalite-pentasalt-anhydrite equilibria. A few experiments have been made in an effort to locate the pentasalt-syngenite and pentasalt-anhydrite invariant points in the system potassium sulfate-calcium sulfate-water at 100°C. In addition to the experiments made in the search for stable equilibrium a number of shorter-time tests in which metastable conditions were encountered have been made by taking samples of the reaction mixtures at relatively short intervals. In the study of both stable and metastable equilibria the progress of the reaction has been followed by the change in the composition of liquid phase as determined by chemical analyses and the change in the nature of the solid phases as disclosed by examination with the petrographic microscope. The attainment of stable equilibrium has been seriously retarded in many instances, owing to the inability of the natural anhydrite to enter into the reaction. In certain instances supersaturation of the liquid phase with calcium sulfate as a result of the decomposition of polyhalite and pentasalt effectively prevents any dissolution of the anhydrite. Also, the limited solubility of anhydrite, even under favorable conditions, and a well-known slow rate of solution are contributing factors.

The metastable equilibrium studies conducted in this system consisted of time-concentration extractions of certain solid phases by means of solutions in contact with which these solid phases were not stable. These tests comprise a time-concentration extraction of polyhalite from an initial point in the pentasalt stability field, the decomposition of polyhalite by magnesium sulfate solutions in the anhydrite field, and the addition of gypsum to solutions in the stable pentasalt and polyhalite fields. The latter tests were made in an attempt to fix the limits of metastable pentasalt-gypsum equilibrium and to follow the changes occurring as the gypsum, which appeared as a decomposition product, was slowly transformed to the stable form, anhydrite. One unsuccessful attempt was made to realize the metastable invariant point for pentasalt, gypsum, and polyhalite at 100°C.

EXPERIMENTAL PROCEDURE

Long-time tests

The first experiments represented an attempt to attain the polyhalite-syngenite-pentasalt invariant point. The preliminary time-concentration tests starting with the necessary liquid and solid phases indicated that the rate of approach to equilibrium was extremely slow. It was soon realized that the mixtures would require days instead of hours to accomplish the necessary changes. Accordingly, provision was made to permit the reactions to proceed for a number of days at a carefully controlled temperature. Agitation was accomplished by attaching a number of the tubes to circular brass discs rotated vertically within the bath to impart an end-over-end motion to the tube and contents. Crisco was used as the heating bath. Temperature was automatically maintained at 100°C. ± 0.2° by a mercury-in-glass thermoregulator.

The method of placing the charges in the bath was as follows: The Pyrex tubes of sufficient size to hold 110 to 115 g. of solution, together with about 20 to 30 g. of solid material, were provided with a smaller tube for sealing and after being attached to the circular vertical disc were lowered into the Crisco bath. After the tubes had attained the temperature of the bath the desired weights of the mixture of the solid phases were introduced. The liquid phase was then heated to boiling in a small Erlenmeyer flask provided with a reflux condenser. When sufficiently hot, the solution was quickly poured into the tube and onto the solid mixture. Usually from 10 to 15 cc. of vapor space remained after the charge had been added. The small inlet tube was then quickly sealed off with an oxygen-gas torch. As soon as all tubes had been sealed the disc and tubes were turned over by hand and care taken to see that none of the solids remained caked on the bottoms of the sample tubes. Mechanical agitation was then begun and continued as long as the samples remained in the bath. This time ranged from 15 to 50 days, 30 days being the most commonly selected time.

Considerable care was exercised in opening the tubes at the end of each experiment. The sealed tips were broken with a pair of pliers and a sampling tube consisting of a bent glass tube inserted through the straight run of a glass T-tube was attached to the reaction bulb by means of a rubber connection. Pressure applied to the horizontal outlet of the tube by the use of a rubber aspirator bulb forced the solution out of the tube onto a rapid filter paper. A few of the samples were filtered through a small cotton plug placed on the end of the glass tube used for removal of the sample. This scheme was tried both with and without the addition of a coarse filter paper around the cotton plug, and was discarded in favor of the outside rapid filter. The clear filtrate was caught in a tared glass-stoppered bottle and reserved for chemical analysis. An attempt was usually made to collect samples ranging from 50 to 60 cc. The remainder of the mixture was then thrown upon a suction filter after the tube had been removed from the bath. The solid residue was always washed, first with 95 per cent ethyl alcohol diluted with an equal volume of water, then with a small amount of 95 per cent alcohol. The washed residue was then air-dried and reserved for microscopic examination.

The solutions were analyzed for potassium by the modified chloroplatinate method of Hicks (7). The calcium content was obtained by separation in small volume as the oxalate with a double precipitation, and after solution in dilute sulfuric acid was determined volumetrically by titration with $N/50$ or $N/100$ standard permanganate, depending upon the size of sample used. After separation of the calcium oxalate, the magnesium was precipitated as magnesium ammonium phosphate and weighed as pyrophosphate after ignition. The equivalent sulfate was then calculated for each constituent.

Time-concentration studies

While in many cases metastable equilibrium was encountered in mixtures in the sealed tubes agitated in the thermostat, a different technique was generally used on the short-time tests involving metastable conditions. The apparatus used in the latter tests consisted of a three-necked Pyrex flask provided with a reflux condenser, a sampling outlet tube, and a mechanical stirring device. Heating was accomplished by means of an electric heater. Mixtures containing from 750 to 800 g. of water were commonly used with varying amounts of solid phases. In general, the quantity of solids added was limited to the amount that could be readily kept in suspension. In certain instances, large amounts were necessary to attain the proper concentration changes desired. Samples of the liquid phases were obtained by applying pressure to the top of the reflux condenser so as to force a portion onto a rapid filter. The filtered and tared samples were analyzed as previously indicated, and the solid residues remaining on the filter paper were washed with 1:1 alcohol-water and 95 per cent alcohol, and then air-dried.

Materials used

Only materials of selected purity were used in preparing the mixtures of liquid and solid phases. Baker's c.p. chemicals of tested purity were used as the source of the dehydrated calcium sulfate and the potassium and magnesium sulfates.

TABLE 1

Composition of synthetic solid phases used

LOT NO.	COMPOSITION		
	K_2SO_4	$MgSO_4$	$CaSO_4$
	per cent	*per cent*	*per cent*
Syngenite ($K_2SO_4 \cdot CaSO_4 \cdot H_2O$)			
Theoretical	53.07		41.45
P16	52.78		
P17	51.85		
P18	51.98	Nil	41.70
P20	52.35	Nil	42.70
Pentasalt ($K_2SO_4 \cdot 5CaSO_4 \cdot H_2O$)			
Theoretical	19.96		77.98
P19	18.99	Nil	77.97
P30	21.08	Nil	77.44
Polyhalite ($K_2SO_4 \cdot MgSO_4 \cdot 2CaSO_4 \cdot 2H_2O$)			
Theoretical	28.9	20.00	45.10
P21	29.48	19.17	45.81
P31	29.53	19.30	46.07

The natural anhydrite used was a sample of high purity obtained from Midland, California. This product was ground to minus 100-mesh and later to a much finer size by pulverizing in a pebble mill for several days. The finer material was used in all experiments involving anhydrite except experiment 8.

The double salts—pentasalt, syngenite, and polyhalite—were prepared from gypsum and solutions of potassium and magnesium sulfates by the usual methods, which consisted of choosing a solution composition and temperature for the reaction definitely known from available literature or from previous experience to be in the stable field for the synthesis of the desired solid phase. For instance, room temperatures were used for prep-

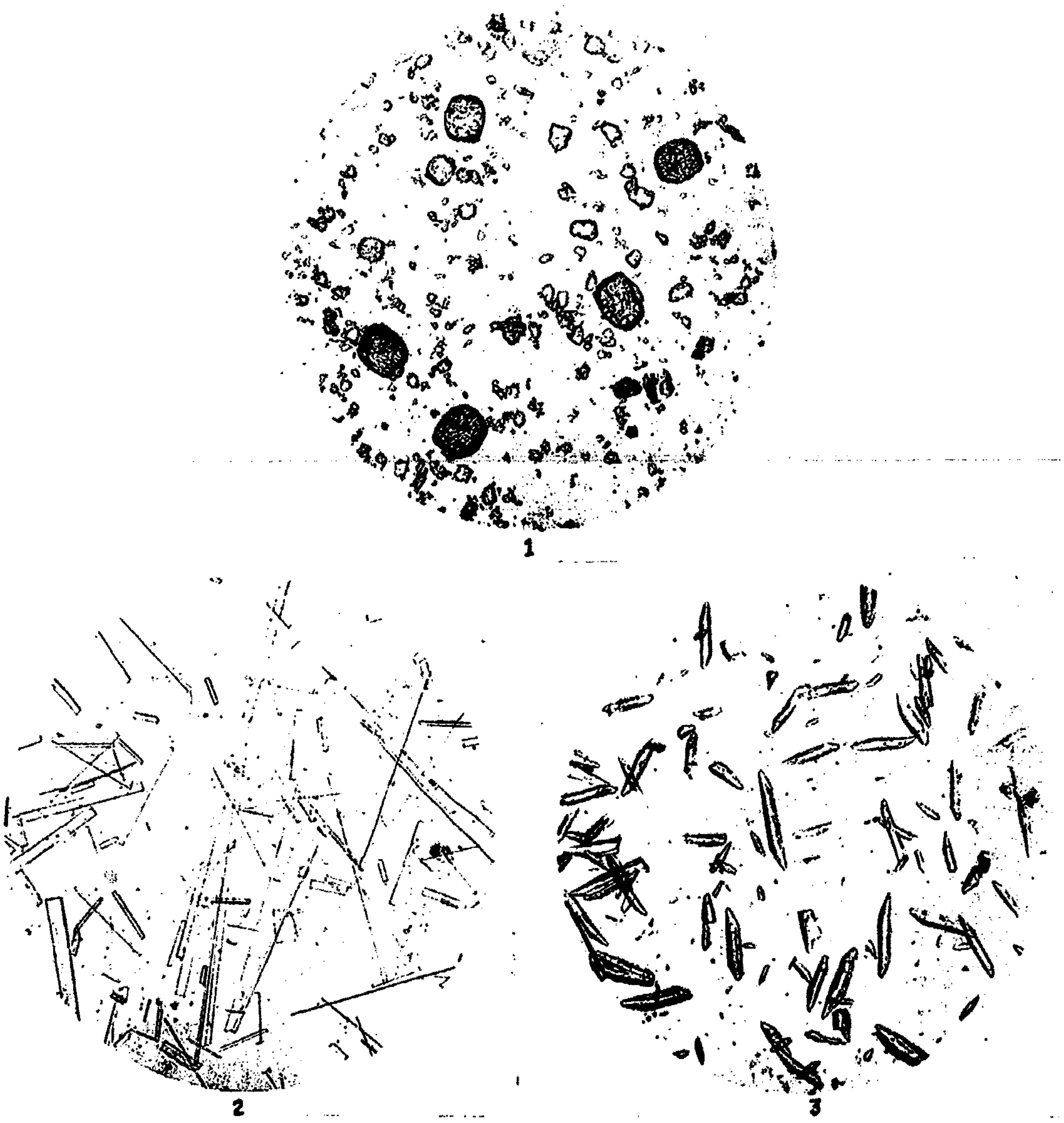

FIG. 1. Photomicrographs of double salts encountered in the system potassium sulfate–magnesium sulfate–calcium sulfate–water. (1) Polyhalite, $K_2SO_4 \cdot MgSO_4 \cdot 2CaSO_4 \cdot 2H_2O$, × 75. (2) Syngenite, $K_2SO_4 \cdot CaSO_4 \cdot H_2O$, × 75. (3) Pentasalt, $K_2SO_4 \cdot 5CaSO_4 \cdot H_2O$, × 75.

aration of syngenite and the temperatures of the boiling solutions for pentasalt and polyhalite. The reacting mixtures were agitated by mechanical stirrers, and in the case of the higher temperatures were heated under reflux condensers. The double salts were refined by filtering from the first solution and treating with fresh solutions of either potassium sulfate or potassium sulfate and magnesium sulfate, depending upon whether syngenite and pentasalt or polyhalite were being produced. Any excess of gypsum, which was the form of calcium sulfate used, was eliminated by the refining treatment. The earlier lots of these synthetic salts were subjected to chemical analysis and also examined under the petrographic microscope. Typical analyses of some of the products used are given in table 1. Figure 1 illustrates the distinctive crystal habits of the double salts, which served as a guide in microscopic examination, although identification was always based on actual measurement of optical properties.

EXPERIMENTAL RESULTS

As previously indicated, the usual procedure in the studies aimed at the determination of stable equilibrium was to seal a mixture of the necessary liquid and solid phases in a Pyrex tube and to agitate the charge within a thermostat for periods of 20 to 40 days. A few of the samples in the first experiments, in which only occasional manual agitation was used, were held in the bath for 69 days.

The usual practice was to add two solid phases to the mixture when it was desired to secure a point in the equilibrium diagram on the boundary line between these two solid phases. These equilibria of course are isothermally univariant with respect to the four-component system potassium sulfate–magnesium sulfate–calcium sulfate–water and isothermally univariant with respect to the three-component system potassium sulfate–calcium sulfate–water. When it was desired to approach the invariant points in the four-component system, that is, equilibria involving three solid phases, all three solid phases were added to the initial reaction mixture. The extremely slow rate of decomposition of many of the solid phases containing calcium sulfate very seriously handicapped the attainment of equilibrium conditions in a reasonable time. For this reason, initial starting mixtures were usually selected so as to take advantage of the more active reaction rates of certain solid phases. This plan partly explains the comparatively large number of mixtures originally started with a solution phase corresponding to concentrations in the polyhalite field.

Methods of representation

A space model is desirable in the interpretation of the data for the four-component system. It is possible, however, to analyze the results

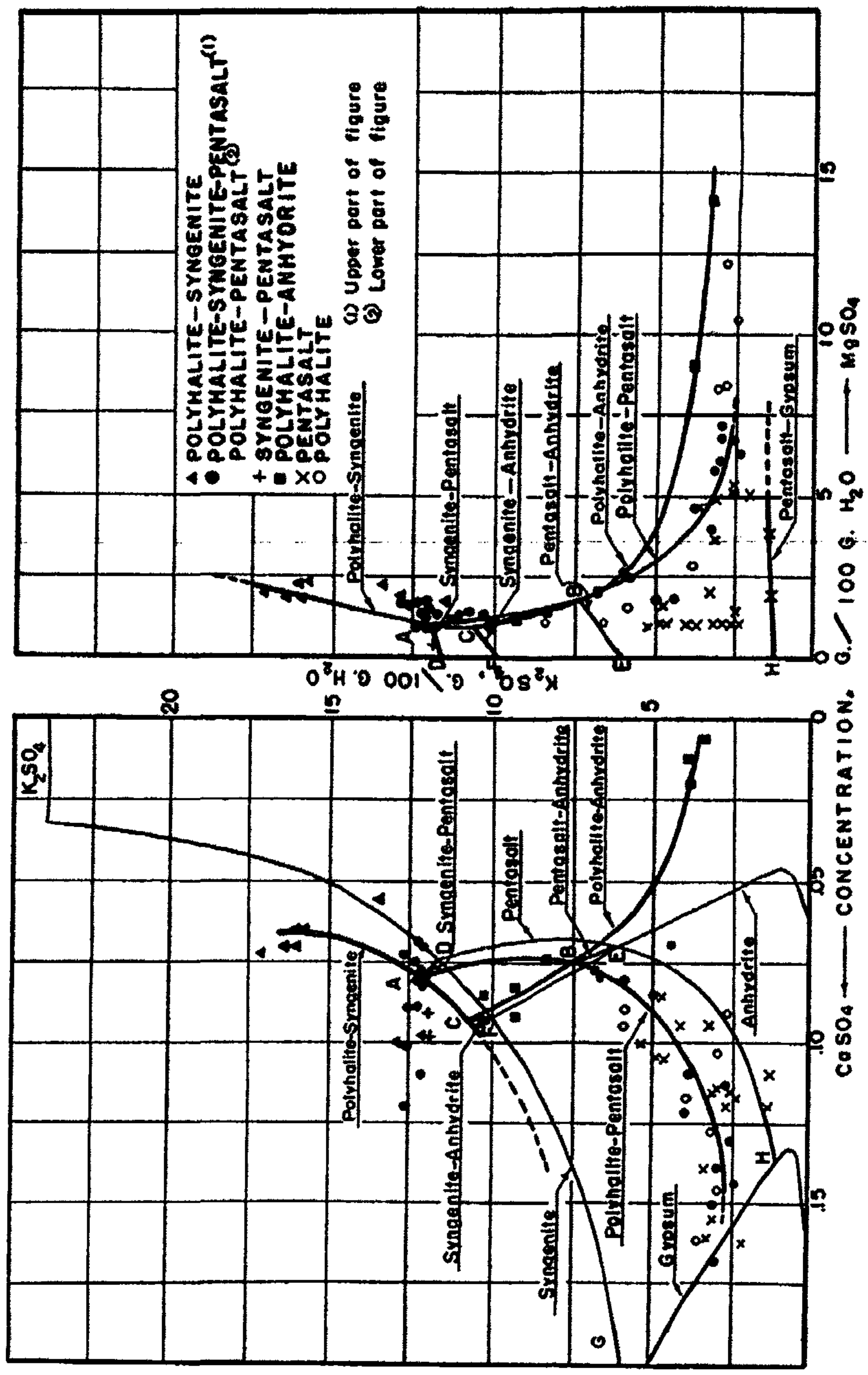

FIG. 2. Plot of experimental data in the system potassium sulfate-magnesium sulfate-calcium sulfate-water at 100°C, on potassium sulfate-calcium sulfate and potassium sulfate-magnesium sulfate planes.

in terms of projections on the potassium sulfate–calcium sulfate, calcium sulfate-magnesium sulfate, and potassium sulfate–magnesium sulfate planes. Figures 2 to 5, inclusive, show the experimental values in this manner. Figure 6 represents a projection of the space model, the positions of the various equilibria being derived from the preceding figures.

Polyhalite–syngenite boundary line

The experiments to determine the location of the syngenite–polyhalite boundary line up to approximately 17.0 g. of potassium sulfate per 100 grams of water are shown in table 2 and represented graphically in figures 2 and 3. Table 2 gives the results obtained in several experiments by adding a mixture of syngenite and polyhalite to a solution of potassium and magnesium sulfates and allowing the reaction to proceed for 19, 27, or 30 days as indicated in the specific instances. All of these samples, except No. 7, showed a decrease in magnesium sulfate and an increase in potassium sulfate. This change indicates the formation of a solid phase containing magnesium sulfate and the decomposition of an original solid containing potassium sulfate. Examination by the microscope showed the syngenite to be badly corroded with well-formed polyhalite appearing from solution. These facts, together with additional data to be presented later, permit tentative location of the syngenite–polyhalite boundary line. This represents a considerable change from the line determined by Geiger (6) and van't Hoff (13) at 83°C. The chemical reaction involved in these tests is as follows:

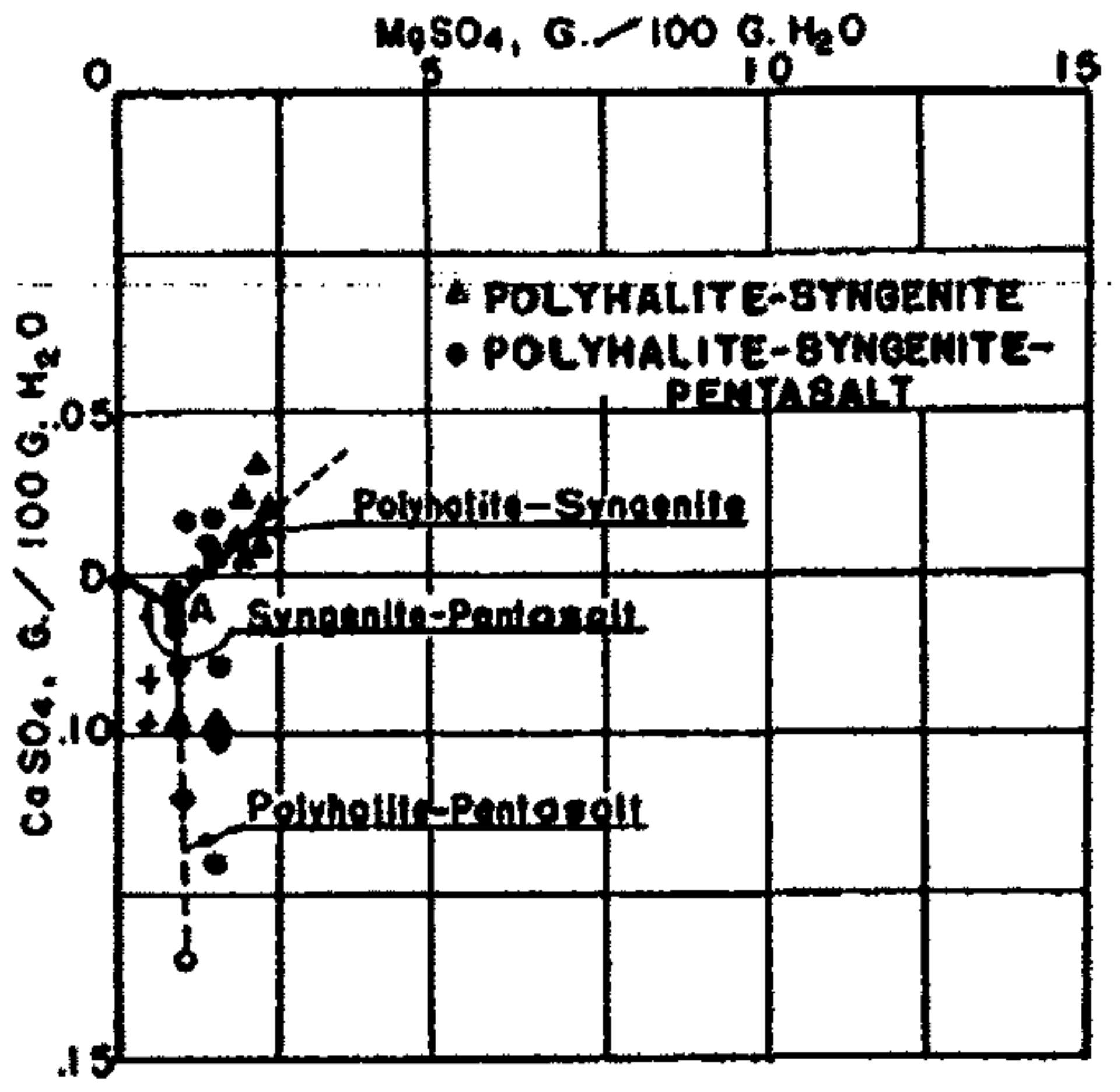

FIG. 3. Plot of experimental data on magnesium sulfate–calcium sulfate plane to determine the polyhalite–syngenite boundary line at 100°C.

$$\underset{\text{solid syngenite}}{2(K_2SO_4\cdot CaSO_4\cdot H_2O)} + \underset{\text{solution}}{MgSO_4} \rightleftharpoons \underset{\text{solid polyhalite}}{K_2SO_4\cdot MgSO_4\cdot 2CaSO_4\cdot 2H_2O} + \underset{\text{solution}}{K_2SO_4} \quad (1)$$

Obviously the reaction proceeds from left to right when syngenite is decomposing in the polyhalite field, and in the reverse direction when polyhalite is decomposing in the syngenite field.

TABLE 2

Equilibrium in the system K_2SO_4–$MgSO_4$–$CaSO_4$–H_2O *at 100°C.*

Syngenite–polyhalite boundary line

SAMPLE NO.	TIME IN THERMOSTAT	PROPORTIONS OF ORIGINAL MIXTURE					CONCENTRATION OF LIQUID PHASE IN GRAMS PER 100 GRAMS OF WATER					PETROGRAPHIC DATA ON SOLIDS	
		Weight of solids		Weight of solution components			Initial		Final			F = Forming D = Dissolving	
		P.H.*	S.†	K_2SO_4	$MgSO_4$	H_2O	K_2SO_4	$MgSO_4$	K_2SO_4	$MgSO_4$	$CaSO_4$	P.H.	S.
	days	*grams*	*grams*	*grams*	*grams*	*grams*	*grams*	*grams*	*grams*	*grams*	*grams*		
1	27	1.0	15.0	9.22	4.61	82.2	11.1	2.8	12.84	1.59	0.100	F	D
2	19	2.0	15.0	9.70	2.7	77.5	12.5	3.5	13.45	2.17	0.058	F	D
3	30	10.0	10.0	14.0	3.0	100.0	14.0	3.0	15.79	2.26	0.066	F	D
4	19	20.0	2.0	9.75	1.3	65.0	15.0	2.0	16.03	1.76	0.065	D	F
5	30	10.0	10.0	15.10	2.5	99.9	15.0	2.5	16.07	2.19	0.071	F	D
6	30	10.0	10.0	15.99	2.0	100.1	16.0	2.0	16.55	1.96	0.071	F	D
7	30	10.0	10.0	17.0	1.5	100.0	17.0	1.5	17.15	1.88	0.073	F	D
8	27	15.0	1.0	15.1	1.0	99.7	15.0	1.0	12.11	0.99	0.098	D	F

* P.H. = polyhalite. † S. = syngenite.

Syngenite–pentasalt equilibria

The few tests made to determine a point on the pentasalt–syngenite boundary line are given in table 3. Owing to the apparent shortness of this line only a limited number of tests were deemed necessary. The results obtained on samples 17 and 18 represent duplicate runs in every respect except for the time during which the mixture was allowed to react. The final concentrations attained in both these experiments were practically identical. The reaction involved in these tests is as follows:

$$\underset{\text{solid syngenite}}{5(K_2SO_4 \cdot CaSO_4 \cdot H_2O)} \leftrightarrows \underset{\text{solid pentasalt}}{K_2SO_4 \cdot 5CaSO_4 \cdot H_2O} + \underset{\text{solution}}{4H_2O + 4K_2SO_4} \quad (2)$$

The reaction is from left to right when syngenite is decomposing in the pentasalt field, and from right to left when pentasalt is decomposing in the syngenite stability region.

Several experiments were made to determine the pentasalt–syngenite invariant point in the three-component system at 100°C. These data are given in table 3 and also plotted in figures 2 and 3. Syngenite was added to potassium sulfate solutions of various concentrations considered to be below the invariant point, and pentasalt was added to solutions of concentrations higher than that point. The chemical reactions are the same as given by equation 2. Some of the tests, as illustrated by samples 10 and 12, showed little, if any, change even in 69 days. Later tests based upon the decomposition of syngenite yielded larger changes. The values secured on samples 12, 14, 15, and 16 are believed to represent the best results. The average of these four figures corresponds to 11.7 g. of potassium sulfate and 0.075 g. of calcium sulfate per 100 grams of water as the equilibrium point. This value, which is higher than the corresponding point for 83°C. as determined by van't Hoff and Geiger, and also higher than the figure 8.7 g. of potassium sulfate per 100 grams of water proposed for 100°C. by Anderson and Nestell (1), checks closely the results of Hill (8) at the latter temperature. Additional investigation by Clarke and Partridge (3) at more elvated temperatures would also tend to substantiate the higher concentrations found in the present work. In the light of the decided tendency for metastable equilibrium and the relatively short reaction periods used by the earlier investigators, it is likely that they failed to reach stable equilibrium.

TABLE 3

Equilibrium in the system K_2SO_4–$MgSO_4$–$CaSO_4$–H_2O *at 100°C.*

Syngenite–pentasalt boundary line

SAMPLE NO.	TIME IN THERMOSTAT	PROPORTIONS OF ORIGINAL MIXTURE					CONCENTRATION OF LIQUID PHASE, IN GRAMS PER 100 GRAMS OF WATER					PETROGRAPHIC DATA ON SOLIDS	
		Weight of solids		Weight of solution components			Initial		Final			F = Forming D = Dissolving	
		P.S.*	S.†	K_2SO_4	$MgSO_4$	H_2O	K_2SO_4	$MgSO_4$	K_2SO_4	$MgSO_4$	$CaSO_4$	P.S.	S
	days	*grams*	*grams*	*grams*	*grams*	*grams*	*grams*	*grams*	*grams*	*grams*	*grams*		
9	40	2.5	2.5	2.85	0	25	11.42	0	11.41	0		F	D
10	69	2.5	2.5	2.85	0	25	11.42	0	11.48	0			
11	40	5.0	0	3.0	0	25	12.04	0	12.03	0			
12	69	5.0	0	3.0	0	25	12.04	0	11.84	0			
13	40	0	5.0	2.7	0	25	10.80	0	11.20	0			
14	69	0	5.0	2.7	0	25	10.80	0	11.77	0			
15	18	12.0	8.0	10.38	0	83.0	12.50	0	11.67	0	0.075	D	F
16	18	8.0	12.0	8.74	0	76.0	11.50	0	11.52	0	0.075	F	D
17	20	10.0	15.0	9.89	0.45	89.0	11.0	0.50	12.00	0.46	0.098	F	D
18	26	10.0	15.0	9.80	0.45	88.2	11.0	0.50	12.01	0.47	0.091	F	D

* P.S. = pentasalt. † S. = syngenite.

Polyhalite–pentasalt–syngenite invariant point at 100°C.

A considerable number of reaction mixtures of varying initial compositions have been used to determine the equilibrium point at which syngenite, pentasalt, and polyhalite may coexist at 100°C. This point has been approached from initial starting compositions in both the polyhalite and the syngenite stability fields. Many of the tests indicated that pentasalt can exist as a metastable phase for prolonged periods, so that only a few experiments have been made in which the decomposition of pentasalt was expected to effect relatively large changes. The data on the various samples used, including information on the proportions of the solid phases

TABLE 4

Equilibrium in the system K_2SO_4-$MgSO_4$-$CaSO_4$-H_2O *at 100°C.*

Polyhalite-pentasalt-syngenite invariant point

SAMPLE NO.	TIME IN THERMOSTAT	PROPORTIONS OF ORIGINAL MIXTURE						CONCENTRATION OF LIQUID PHASE, IN GRAMS PER 100 GRAMS OF WATER					PETROGRAPHIC DATA ON SOLIDS		
		Weight of solids			Weight of solution components			Initial		Final			F = Forming D = Dissolving U = Unaltered		
		P.H.*	P.S.†	S.‡	K_2SO_4	$MgSO_4$	H_2O	K_2SO_4	$MgSO_4$	K_2SO_4	$MgSO_4$	$CaSO_4$	P.H.	P.S.	S.
	days	*gms.*	*gms.*	*grams*	*grams*	*gms.*	*grams*	*grams*	*gms.*	*grams*	*gms.*	*grams*			
19	40	1.0	2.5	2.5	2.23	0.64	25.0	8.92	2.56	11.80	1.36				
20	69	1.0	2.5	2.5	2.23	0.64	25.0	8.92	2.56	12.17	1.20				
21	40	1.0	2.5	2.5	2.23	0.64	25.0	8.92	2.56	11.78	1.27				
22	69	1.0	2.5	2.5	2.23	0.64	25.0	8.92	2.56	12.06	1.11				
23	45	10.0	10.0	10.0	14.65	2.40	142.95	10.25	1.68	12.10	1.10	0.110			
24	20	10.5	15.0	9.0	9.65	0.37	73.4	13.14	0.50	12.25	0.94	0.089	D	D	F
25	26	7.0	10.0	6.0	13.00	0.50	99.45	13.10	0.50	12.24	0.94	0.089	D	D	F
26	19	1.5	9.0	10.0	13.00	2.00	101.1	12.86	1.98	12.49	1.61	0.089	F	D	D
27	27	1.5	9.0	10.0	13.00	2.00	101.1	12.86	1.98	12.61	1.56	0.120	F	D	D
28	19	1.5	7.5	12.0	10.74	1.80	91.3	11.76	1.98	12.54	1.59	0.101	F	U	D
29	26	1.5	7.5	12.0	12.00	2.00	101.1	11.87	1.98	12.58	1.57	0.073	F	F(?)	D
30	10	8.0	8.0	8.0	10.65	0.90	88.0	12.10	1.00	11.90	0.91	0.082	D	D	F
31	19	8.0	8.0	8.0	9.98	0.82	82.5	12.10	1.00	11.86	0.89	0.080	D	D	F
32	10	8.0	8.0	8.0	10.71	1.28	85.0	12.60	1.50	12.21	1.23	0.075	U	D	F
33	19	8.0	8.0	8.0	11.09	1.32	88.0	12.60	1.50	12.13	1.20	0.069	U	D	D
34	10	5.0	8.0	12.0	11.10	1.93	96.5	11.50	2.00	12.08	1.52	0.069	F	F	D
35	19	5.0	8.0	12.0	10.64	1.85	92.5	11.50	2.00	12.10	1.42	0.070	F	D	D
36	10	12.0	8.0	5.0	11.83	0.90	91.0	13.00	1.00	11.96	0.93	0.081	F	F	D
37	19	12.0	8.0	5.0	11.05	0.85	85.0	13.00	1.00	12.09	0.92	0.078	D	D	F

* P.H. = polyhalite. † P.S. = pentasalt. ‡ S. = syngenite.

added to the initial starting solution, the initial and final compositions of the liquid phases, and data on the solid phases from microscopic examination are given in table 4. These data are also represented graphically in figures 2 and 3.

Reference to the tabulated results will show that all three solid phases (polyhalite, pentasalt, and syngenite) were added to the initial mixtures.

As most of these samples were originally in the polyhalite field, a smaller proportion of that salt was usually present in the sample. Obviously the chemical reactions representing the changes occurring when pentasalt and syngenite are present as unstable phases in the polyhalite field may be represented by the following equation:

$$\underset{\text{solid syngenite}}{3(K_2SO_4 \cdot CaSO_4 \cdot H_2O)} + \underset{\text{pentasalt}}{K_2SO_4 \cdot 5CaSO_4 \cdot H_2O} + \underset{\text{solution}}{4MgSO_4 + 4H_2O} = \underset{\text{solid polyhalite}}{4(K_2SO_4 \cdot MgSO_4 \cdot 2CaSO_4 \cdot 2H_2O)} \qquad (4)$$

The paths of liquid-phase changes would therefore depend upon the relative rates of decomposition of the two unstable phases. The net changes attained in the various samples definitely indicate a rapid rate of decomposition for syngenite, with a much slower rate for pentasalt. In fact, it may be shown by stoichiometric calculations based on concentration changes and also by microscopic data that the greater portion of the total changes was due to the decomposition of the syngenite with simultaneous conversion to polyhalite. Similarly pentasalt is fairly stable in the syngenite field, while polyhalite decomposes to form syngenite at a much more rapid rate. This latter condition would require the reaction as indicated by equation 4 to proceed from right to left.

It may be seen from the data in table 4 and figures 2 and 3 that many of the reaction mixtures had failed to reach equilibrium in the allotted time, although the solution composition changes were tending to approach the desired point. The average of the ten samples comprising tests 20, 22, 23, 24, 25, 28, 30, 31, 32, and 33 yields values of 12.10 g. of potassium sulfate, 1.05 g. of magnesium sulfate, and 0.084 g. of calcium sulfate per 100 grams of water. However, from inspection of figures 2 and 3, samples 30, 31, 36 and 37 are believed to represent the best approach to equilibrium, which has accordingly been taken as 12.1 g. of potassium sulfate, 0.9 g. of magnesium sulfate, and 0.08 g. of calcium sulfate per 100 grams of water. It seems quite possible that the higher values for magnesium sulfate may represent points in the polyhalite surface not yet in equilibrium with the other solid phases.

Polyhalite–pentasalt boundary line

Data obtained in the experiments made to determine the polyhalite–pentasalt boundary line at 100°C. are presented in table 5 and plotted in figures 2 and 4. Since pentasalt was found to persist as a metastable form, under some conditions, for as long as 60 days, attempts made to approach the line from points in the polyhalite stability region had but slight success. Polyhalite was found to decompose fairly readily to produce pentasalt, but pentasalt was converted to polyhalite at an extremely slow rate.

TABLE 5

Equilibrium in the system K_2SO_4-$MgSO_4$-$CaSO_4$-H_2O *at 100°C.*

Polyhalite-pentasalt boundary line

SAMPLE NO.	TIME IN THERMOSTAT	PROPORTIONS OF ORIGINAL MIXTURE						CONCENTRATION OF LIQUID PHASE, IN GRAMS PER 100 GRAMS OF WATER					PETROGRAPHIC DATA ON SOLIDS		
		Weight of solids			Weight of solution components			Initial		Final			F = Forming D = Dissolving U = Unaltered		
		P.H.*	P.S.†	S.‡ or A.§	K_2SO_4	$MgSO_4$	H_2O	K_2SO_4	$MgSO_4$	K_2SO_4	$MgSO_4$	$CaSO_4$	P.H.	P.S.	A.
	days	*gms.*	*gms.*	*grams*	*gms.*	*gms.*	*grams*	*gms.*	*gms.*	*grams*	*gms.*	*grams*			
38	40	2.0	2.0	2.0 S	2.08	0.53	25.0	8.30	2.10	11.14	1.32				
39	69	2.0	2.0	2.0	2.08	0.53	25.0	8.30	2.10	11.04	1.25				
40	40	2.0	2.0	2.0	2.08	0.53	25.0	8.30	2.10	11.06	1.22				
41	69	2.0	2.0	2.0	2.08	0.53	25.0	8.30	2.10	10.94	1.15				
42	40	1.0	2.5	2.5	1.93	0.61	25.0	7.72	2.53	10.93	1.43				
43	69	1.0	2.5	2.5	1.93	0.61	25.0	7.72	2.53	10.84	1.35				
44	40	2.5	2.5	1.0	2.21	0.39	25.0	8.83	1.54	10.43	1.30				
45	69	2.5	2.5	1.0	2.21	0.39	25.0	8.83	1.54	10.39	1.26				
46	40	2.5	2.5	1.0	2.21	0.39	25.0	8.83	1.54	10.34	1.23				
47	69	2.5	2.5	1.0	2.21	0.39	25.0	8.83	1.54	10.30	1.17				
48	40	2.5	1.0	2.5	1.91	0.38	25.0	7.64	1.53	11.32	1.13				
49	69	2.5	1.0	2.5	1.91	0.38	25.0	7.64	1.53	11.51	1.06				
50	40	2.5	1.0	2.5	1.91	0.38	25.0	7.64	1.53	11.37	1.09				
51	69	2.5	1.0	2.5	1.91	0.38	25.0	7.64	1.53	11.41	0.98				
52	40	1.0	15.0		4.80	2.40	80.0	6.00	3.00	5.88	2.63	0.081	F	D	
53	39	1.0	15.0		4.00	5.00	100.0	4.00	5.00	3.84	4.63	0.109	F	D	
54	40	8.0	8.0	8.0 A	2.45	6.37	98.0	2.50	6.50	2.73	6.47	0.113	F	D	F
55	38	5.0	10.0	10.0	1.25	4.82	63.0	2.00	8.00	3.05	6.81	0.168	D(?)	D	F
56	38	10.0	10.0	2.0	0.67	4.02	67.0	1.00	6.00	2.38	6.29	0.144	D	F(?)	F(?)
57	38	0	1.0	20.0	3.40	0.85	85.0	4.00	1.00	4.78	1.60	0.085			
58	30	10.0	10.0	0	3.32	2.90	83.0	4.00	3.50	4.00	3.26	0.122	F	D	
59	32	20.0	0	0	4.30	1.15	72.0	6.00	1.60	5.86	1.58	0.095	U		
60	33	20.0	0	0	5.67	0	81.0	7.00	0	8.43	1.06	0.134	D	F	
61	33	20.0	0	0	3.15	2.50	83.0	3.80	3.00	3.89	2.77	0.117	U		
62	30	25.0	0	0	6.30	0	90.0	7.00	0	6.62	1.10	0.080	F(?)	D(?)	
63	30	1.0	20.0	0	7.20	4.00	90.0	8.00	4.44	5.82	2.39	0.090	F	D	
64	26	18.0	1.0	15.0	4.50	1.80	90.0	5.00	2.00	4.44	1.79	0.070	D	F	D

* P.H. = polyhalite. † P.S. = pentasalt. ‡ S. = syngenite. § A. = anhydrite.

Experiments 38 to 52 were made to locate the polyhalite-pentasalt-syngenite invariant point and originally contained all three solid phases. Owing to the large change in concentrations needed to reach this point, practically all of the syngenite present in the various samples dissolved and was replaced by polyhalite, the stable solid phase. Chemical analyses and stoichiometric calculations showed but a very small residual quantity of syngenite in the final solids in samples 38 to 46 and none in samples 47 to 51. These latter tests therefore tended to approach the polyhalite–pentasalt boundary line rather than the polyhalite-pentasalt–syngenite point.

The grouping of the several end solution concentrations fixes the directional trend of the boundary line. Tests 60 and 62 were made in an attempt to reach the polyhalite-pentasalt boundary line by decomposing polyhalite by means of a solution of potassium sulfate. Well-formed pentasalt was produced, probably metastable, and the compositions of the end solutions failed to reach the boundary line as desired.

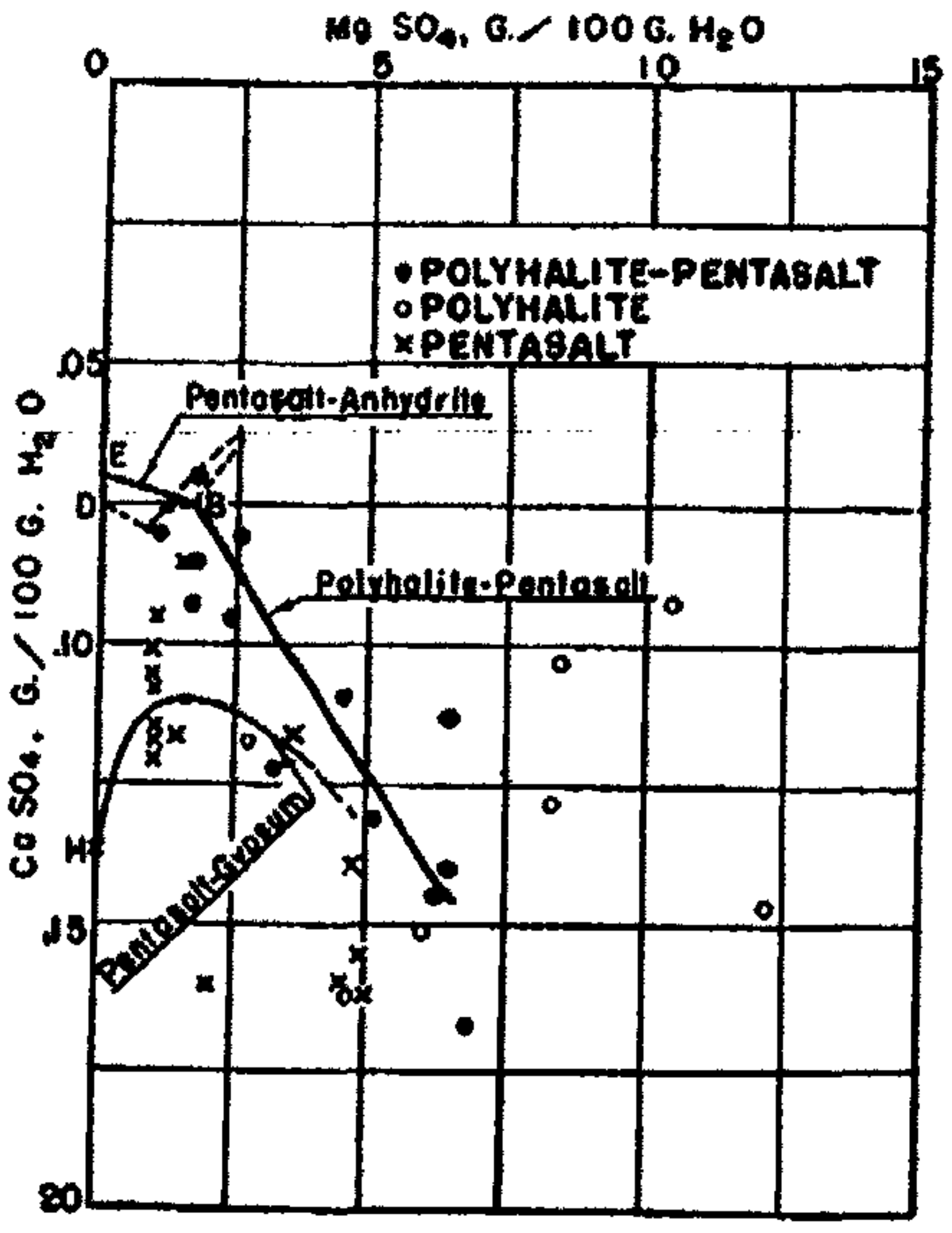

FIG. 4

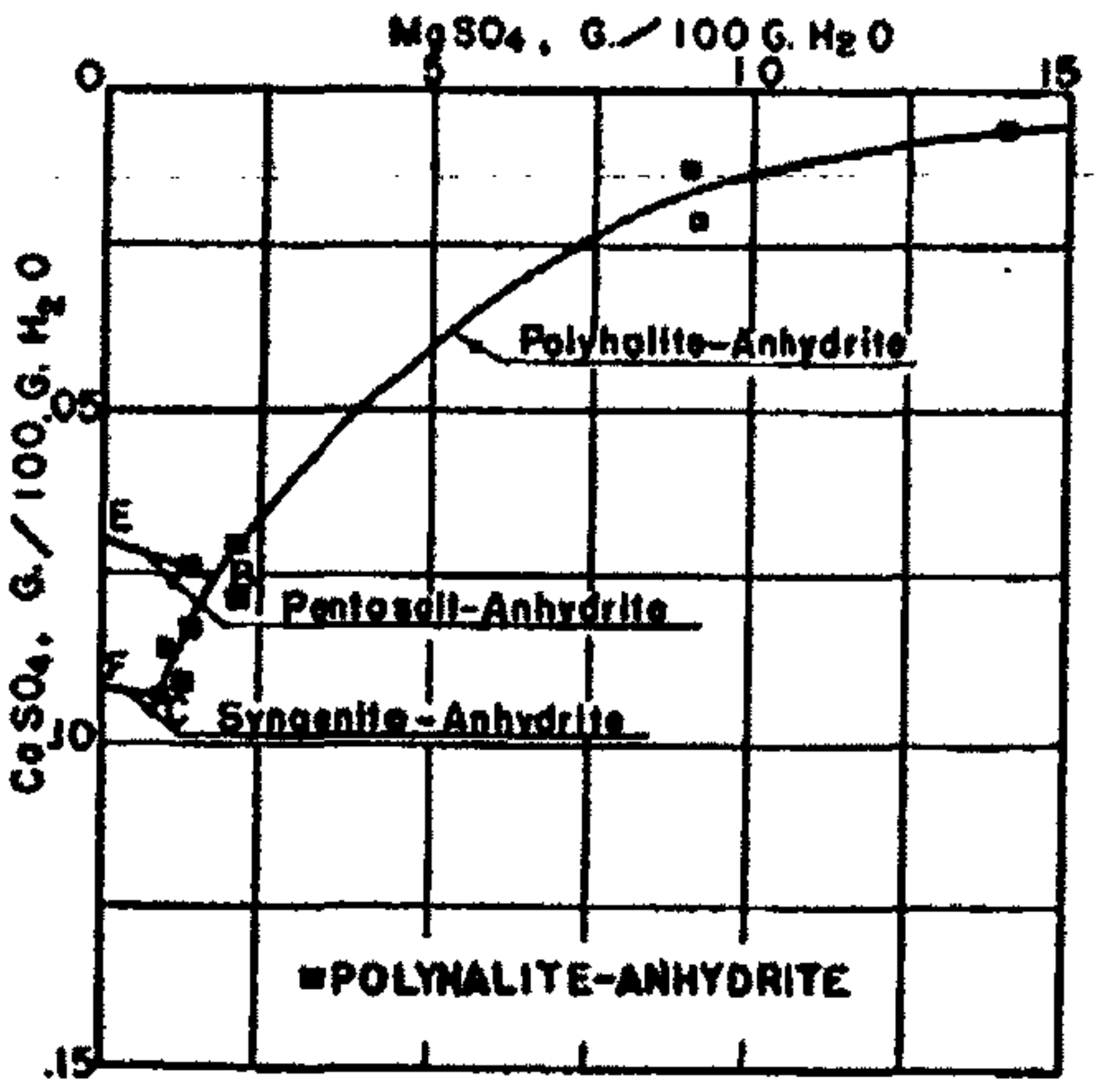

FIG. 5

FIG. 4. Plot of experimental data on magnesium sulfate–calcium sulfate plane to determine the polyhalite–pentasalt boundary line at 100°C.

FIG. 5. Plot of experimental data on magnesium sulfate–calcium sulfate plane to determine the polyhalite–anhydrite boundary line at 100°C.

Pentasalt–anhydrite equilibria

The stable equilibria between pentasalt and anhydrite encountered in the system potassium sulfate–magnesium sulfate–calcium sulfate–water consist of the invariant point, pentasalt–anhydrite, in the magnesium sulfate-free system, and the invariant equilibria which constitute the

TABLE 6

Equilibrium in the system K_2SO_4–$MgSO_4$–$CaSO_4$–H_2O *at 100°C.*

Pentasalt–anhydrite boundary line

		PROPORTIONS OF ORIGINAL MIXTURE						CONCENTRATION OF LIQUID PHASE, IN GRAMS PER 100 GRAMS OF WATER					PETROGRAPHIC DATA ON SOLIDS		
		Weight of solids			Weight of solution components			Initial		Final			F = Forming D = Dissolving U = Unaltered		
SAMPLE NO.	TIME IN THERMOSTAT	P.H.*	P.S.†	A.‡	K_2SO_4	$MgSO_4$	H_2O	K_2SO_4	$MgSO_4$	K_2SO_4	$MgSO_4$	$CaSO_4$	P.H.	P.S.	A.
	days	*gms.*	*gms.*	*gms.*	*grams*	*grams*	*grams*	*gms.*	*grams*	*gms.*	*grams*	*grams*			
53	39	1.0	15.0	0	4.0	5.0	100.0	4.00	5.00	3.84	4.63	0.109	F	D	Nil
54	40	8.0	8.0	8.0	2.45	6.37	98.0	2.50	6.50	2.73	6.47	0.113	F	D	F
55	38	5.0	10.0	10.0	1.25	4.82	63.0	2.00	8.00	3.05	6.81	0.168	D	D	F
56	38	10.0	10.0	2.0	0.67	4.02	67.0	1.00	6.00	2.38	6.29	0.144	D	F	F
58	30	10.0	10.0	0	3.32	2.90	83.0	4.00	3.50	4.00	3.26	0.122	F	D	Nil
61	33	20.0	0	0	2.74	8.43	98.0	2.80	8.50	2.96	8.45	0.103	U	Nil	Nil
64	26	18.0	1.0	15.0	4.50	1.80	90.0	5.00	2.00	4.44	1.79	0.070	D	F	D
65	40	0	8.0	12.0	2.0	1.5	100.0	2.00	1.50	2.55	1.39	0.116		D	F
66	40	0	8.0	12.0	1.8	2.7	90.0	2.00	3.00	3.13	4.17	0.124		D	F
67	40	15.0	10.0	0	1.7	4.3	85.0	2.00	5.00	2.14	5.05	0.162		D	F
~~68~~	~~38~~	~~0~~	~~1.0~~	~~20.0~~	~~3.4~~	~~0~~	~~85.0~~	~~4.00~~	~~0~~	~~4.16~~	~~0~~	~~0.079~~		~~D~~	~~F~~
69	30	0	2.0	20.0	4.15	0	69.0	6.00	0	5.60		0.104		F	D
70	30	0	2.0	20.0	1.98	1.32	66.0	3.00	2.00	3.35	2.05	0.161		D	F
71	32	0	15.0	0	1.64	0.82	82.0	2.00	1.00	2.40	1.06	0.117		D	F
72	32	0	15.0	0	1.97	0.82	82.0	2.40	1.00	2.72	1.06	0.120		D	F
73	32	0	15.0	0	2.04	0.73	73.0	2.80	1.00	2.98	1.06	0.114		D	F
74	32	0	15.0	0	2.53	0.79	79.0	3.20	1.00	3.29	1.07	0.095		D	F
75	32	0	15.0	0	2.92	0.81	81.0	3.60	1.00	3.78	1.03	0.107		D	F
76	32	0	15.0	0	4.00	0.99	99.0	4.00	1.00	4.12	1.05	0.095		D	F
77	32	0	15.0	0	4.09	0.93	93.0	4.40	1.00	4.70	1.01	0.105		D	F
78	32	0	15.0	0	4.80	0.99	99.0	4.80	1.00	4.90	1.06	0.105		D	F
79	32	0	20.0	0	2.58	4.60	92.0	2.80	5.00	3.18	4.91	0.155		D	F
80	33	0	0	20.0	4.48	0	80.0	5.60	0	5.67	0				U
81	33	0	15.0	0	4.68	0.90	90.0	5.20	1.00	5.27	0.97	0.101		D	F
82	33	0	0	20.0	5.30	0.98	98.0	5.40	1.00	5.21	0.93				U
83	33	0	15.0	0	3.06	4.50	90.0	3.40	5.00	3.46	4.77	0.139		D	F
84	29	0	25.0	0	0	0	90.0	0	0	1.08	0	0.11		D	F(?)
85	25	0	2.0	20.0	2.70	0	90.0	3.00	0	3.15	0	0.06		D	F(?)
86	29	0	25.0	0	0.90	1.80	90.0	1.00	2.00	1.24	1.79	0.11		D	Trace§
87	29	0	25.0	0	0.90	3.60	90.0	1.00	4.00	1.36	3.84	0.12		D	F
88	7	0	75.0	0			800.0	2.84	5.13	3.18	5.33			U	
89	40	10.0	10.0	2.0	3.68	0.92	92.0	4.00	1.00	4.91	1.75	0.085	D	F	D
90	40	20.0	1.0	0	1.80	2.70	90.0	2.00	3.00	3.21	3.68	0.116	D	D	F
91	40	5.0	5.0	10.0	1.53	5.85	90.0	1.70	6.50	2.97	6.42	0.139	D	D	F
92	38	15.0	10.0	0	1.20	3.00	60.0	2.00	5.00	2.61	5.13	0.131	D	F	F
93	30	2.0	0	20.0	1.74	6.96	58.0	3.00	12.00	2.88	12.15	0.146	F		D
94	30	2.0	0	20.0	1.46	7.30	73.0	2.00	10.00	2.59	10.45	0.092	D		F
95	30	8.0	8.0	8.0	2.56	6.05	93.0	2.75	6.50	3.09	6.10	0.151	D-F	D	F
96	33	20.0	0	0	3.53	4.90	98.0	3.60	5.00	3.63	4.68	0.162	D	Nil	F
97	33	0	0	20.0	2.86	7.56	84.0	3.40	9.00	3.18	8.29	0.128	Nil	Nil	U
98	33	20.0	0	0	3.15	2.50	83.0	3.80	3.00	3.89	2.77	0.117	U	Nil	Nil
99	6	75.0	0	0	23.00	40.00	800.0	2.87	5.04	3.27	5.76		D	F	D

* P.H. = polyhalite. † P.S. = pentasalt. ‡ A. = anhydrite. § Gypsum instead of anhydrite.

boundary line between the pentasalt and anhydrite fields when magnesium sulfate is present in the system. Hill (8) has placed the pentasalt-anhydrite equilibrium at 5.78 g. of potassium sulfate per 100 grams of water. The data of experiments 69 and 80 in table 6 in which the equilibrium was approached from the pentasalt and anhydrite fields, respectively, gave an average of 5.64 g. of potassium sulfate per 100 grams of water. The concentration of the calcium sulfate, like the values found by Hill, was higher than 0.071, the figure Hill obtained by graphic interpolation.

Tests 71 to 78 and 81 to 82 are the result of an effort to discover the pentasalt-anhydrite boundary line at a concentration of 1.0 g. of magnesium sulfate per 100 grams of water. The extremely small concentration changes occurring in 32 to 33 days in these tests are additional proof of the slow rate of dissolution of pentasalt in a metastable region. Based solely on these data, the obvious conclusion would indicate this region as the stable pentasalt field; however, additional data prove this area to be the anhydrite field, as shown by figure 2. Experimental results prove that the pentasalt-anhydrite boundary line is very short and may therefore be determined with reasonable accuracy by a line connecting the pentasalt-anhydrite invariant point in the three-component system with the polyhalite-pentasalt-anhydrite invariant point in the four-component system.

Polyhalite-pentasalt-anhydrite invariant point

Several attempts were made to realize the polyhalite-pentasalt-anhydrite invariant point, but the slow rate of approach to equilibrium with both anhydrite and pentasalt as solid phases defeated such efforts. Innumberable compositions might easily be mistaken for the polyhalite-pentasalt-anhydrite equilibrium, since all three phases can exist for prolonged periods with little or no dissolution. This was apparently not fully appreciated by many previous investigators and resulted in errors in the location of equilibrium points and boundary lines. However, the intersection of the polyhalite-pentasalt and polyhalite-anhydrite curves defined by the present work, as indicated by the projections on the potassium sulfate-calcium sulfate and potassium sulfate-magnesium sulfate planes of figure 2, indicate values for the invariant point of 7.5 g. of potassium sulfate, 1.75 g. of magnesium sulfate, and 0.075 g. of calcium sulfate per 100 grams of water.

Polyhalite-anhydrite boundary line

The data collected to determine the polyhalite-anhydrite boundary line, given in table 7, are plotted in figures 2 and 5.

TABLE 7

Equilibrium in the system K_2SO_4-$MgSO_4$-$CaSO_4$-H_2O *at 100°C.*

Polyhalite–anhydrite boundary line

SAMPLE NO.	TIME IN THERMOSTAT	WEIGHT OF SOLIDS IN ORIGINAL MIXTURE			COMPOSITION OF LIQUID PHASE, IN GRAMS PER 100 GRAMS OF WATER					PETROGRAPHIC DATA ON SOLIDS		
					Initial		Final			F = Forming D = Dissolving		
		P.H.*	P.S.†	A.‡	K_2SO_4	$MgSO_4$	K_2SO_4	$MgSO_4$	$CaSO_4$	P.H.	P.S.	A.
	days	*grams*	*grams*	*grams*	*grams*	*grams*	*grams*	*grams*	*grams*			
100	45	10.0		5.0	13.05	2.66	10.30	1.08	0.086	F		D
101	60	10.0		5.0	13.05	2.66	10.23	1.02	0.093	F		D
102	45	10.0		5.0	10.30	2.13	9.37	1.27	0.083	F		D
103	60	10.0		5.0	10.30	2.13	9.28	1.27	0.092	F		D
104	60	10.0	5.0	5.0	11.96	2.37	8.35	1.43	0.074	F	D	D
105	45	10.0		5.0	8.91	3.59	6.77	2.11	0.078	F		D
106	60	10.0		5.0	8.91	3.59	6.69	2.08	0.070	F		D
107	45	10.0		5.0	4.72	9.53	3.94	9.03	0.012	F		D
108	60	10.0		5.0	4.72	9.53	3.89	9.16	0.020	F		D
109	60	10.0		5.0	4.00	14.06	3.47	14.06	0.006	F		D

* P.H. = polyhalite. † P.S. = pentasalt. ‡ A. = anhydrite.

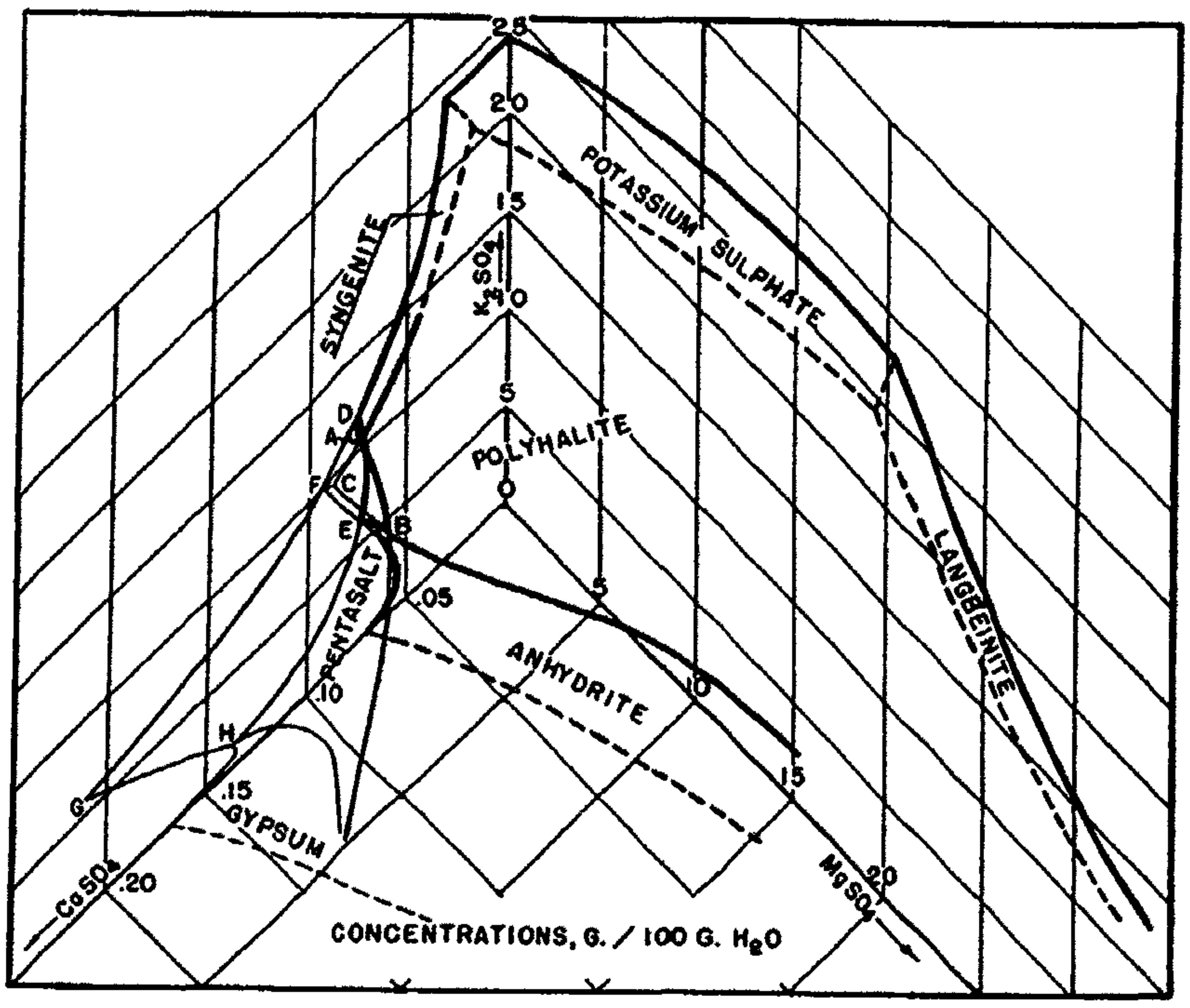

FIG. 6. Projection of space model representation of available data on the system potassium sulfate–magnesium sulfate–calcium sulfate–water at 100°C.

Space model of the system potassium sulfate–magnesium sulfate–calcium sulfate–water at 100°C.

In figures 2 to 5 the equilibrium data have been plotted on rectangular coördinates and liquid phase composition indicated in grams per 100 grams of water for pairs of components. In figure 6, the data have been utilized to represent a space model by isometric projection. Actual experimental points have, of course, been omitted. The 100°C. isotherm of Hill (8) has been used in constructing the potassium sulfate–calcium sulfate face of the figure and the corresponding isotherm of Starrs (12) for the potassium sulfate–magnesium sulfate face. An attempt has been made to indicate the curvature of the surfaces where evidence for such curvature existed. It is evident that a much clearer conception of both the stable and the metastable equilibria may be had by reference to such a diagram.

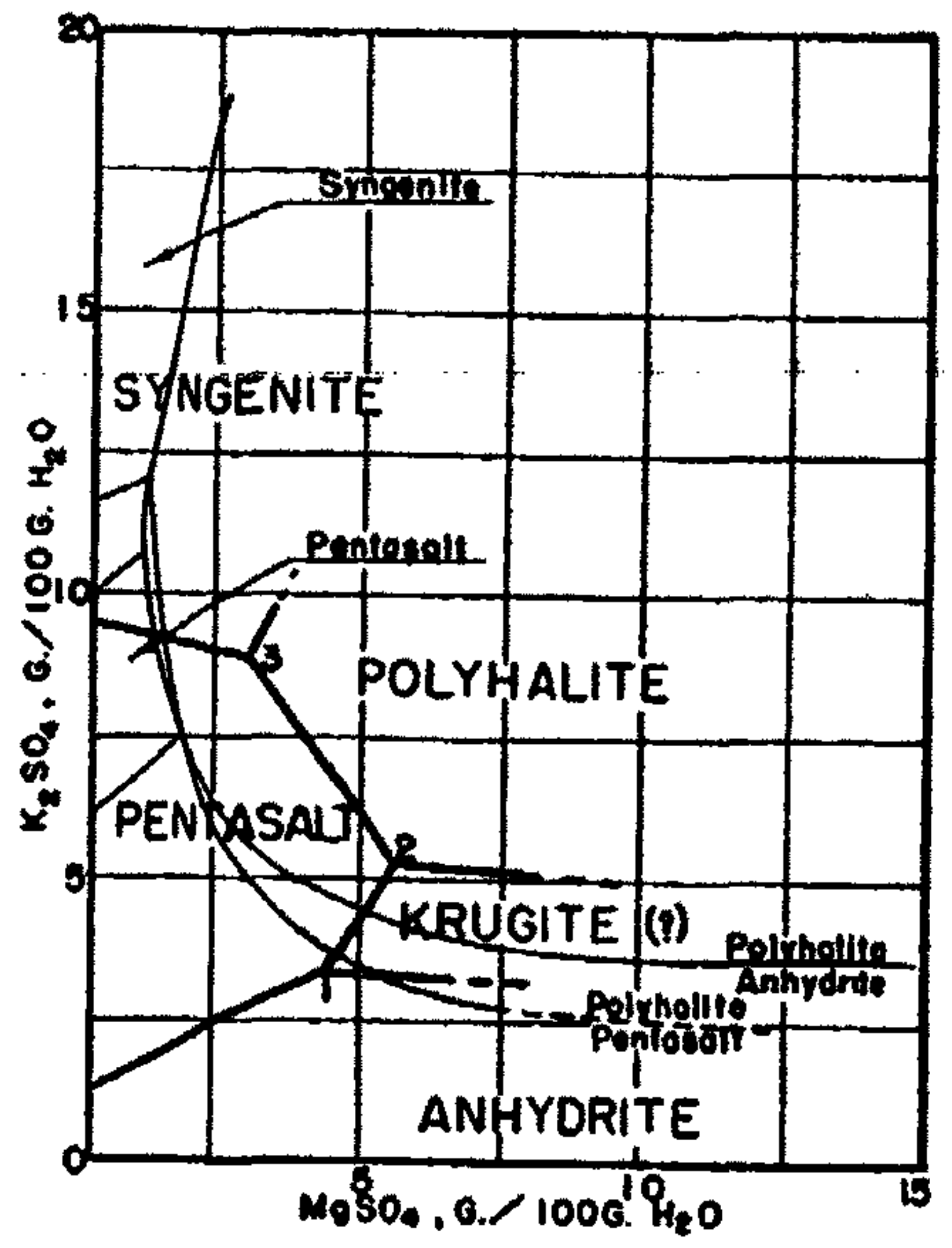

FIG. 7. Comparison of equilibria data of Geiger at 83°C. (heavy lines) and present work (light lines) at 100°C. by projection on the potassium sulfate–magnesium sulfate plane.

Comparison of system at 100°C. with prior data for system at 83°C.

In figure 7 the stability field for pentasalt according to Geiger (6) at 83°C. has been superimposed on the potassium sulfate–magnesium sulfate plane on the equilibrium curves shown in figure 2 for 100°C. This field for pentasalt is considerably larger than that occurring at 100°C., a condition difficult to justify in that, according to Hill (8), the pentasalt field in the system potassium sulfate–calcium sulfate–water increases with increasing temperature. Furthermore, it is evident that the boundary line 1–2 (figure 7) exactly represents the change in liquid-phase composition which would result from the dissolution of a solid phase such as polyhalite containing potassium sulfate and magnesium sulfate in equimolar proportions. If a mixture containing anhydrite, polyhalite, and pentasalt and a liquid phase corresponding to point 1 were permitted to react for a short period, the line or path 1–2 could be obtained from the following reaction:

$$\underset{\text{polyhalite}}{K_2SO_4\cdot MgSO_4\cdot 2CaSO_4\cdot 2H_2O} + \underset{\text{pentasalt}}{K_2SO_4\cdot 5CaSO_4\cdot H_2O} + \underset{\text{anhydrite}}{CaSO_4} =$$

$$\underset{\text{solution}}{(1 + x)K_2SO_4 + MgSO_4} + (3 + 5x)CaSO_4 + (1 - x)K_2SO_4\cdot 5CaSO_4\cdot H_2O + (2 + x)H_2O \qquad (5)$$

where x represents an extremely small fraction of the pentasalt originally present. The stable phase being produced would be calcium sulfate in the form of anhydrite. This explanation agrees with observed facts, in that pentasalt may exist as a metastable phase under a wide range of conditions and that the polyhalite stability field expands with increase in temperature.

According to Geiger, krugite ($K_2SO_4\cdot MgSO_4\cdot 4CaSO_4\cdot 2H_2O$), may exist at 83°C. as a stable phase. Other occurrences of this complex substance as a natural mineral have been reported by Schmidt (10) and van't Hoff (13). No such compound as krugite was encountered in any of the present tests made at 100°C. All attempts even under supposedly favorable conditions at 83°C. likewise failed to produce any krugite. Microscopic examination invariably disclosed the presence of polyhalite, but Ide (9) has shown recently from x-ray studies that "krugite" is a mixture of polyhalite and anhydrite. Chemical analysis, which has supplied the only suggestion of the existence of krugite, is applicable only in case the pure compound may be segregated. Obviously, a heterogeneous mixture of polyhalite, pentasalt, and anhydrite in the proper proportions might easily correspond to the composition of krugite.

Similarly it is found that the proposed boundary line 2–3 (figure 7), according to Geiger, separating the pentasalt and polyhalite fields has the exact slope corresponding to the decomposition of syngenite and formation of polyhalite. Similar paths are easily obtained at 100°C. by starting with mixtures of syngenite, polyhalite, and pentasalt in the region adjacent to the line 2–3. These facts would tend to condemn the practice of locating boundary lines by allowing an unstable mixture to react at a previously determined equilibrium point and fixing the resulting liquid phase composition change as an equilibrium boundary line. The path followed would invariably depend upon the relative rates of formation and decomposition of the stable and unstable phases respectively.

METASTABLE EQUILIBRIUM STUDIES AT 101–102°C.

A number of time-concentration experiments were made to obtain some information on the relative rate of approach to equilibrium in various regions. Owing to the exceptionally slow rate at which this system attains final stable equilibrium, most of these tests involved intermediate metastable phenomena tending toward stable equilibrium. From the results obtained in some of these experiments it has been possible to explain logically the behavior of certain of the long-time tests in which gypsum was added as the initial form of calcium sulfate. It has also been possible to interpret intelligently many of the phenomena encountered in the extraction of calcined polyhalite. The results of this class of experiments are given in table 8. These data have also been represented graphically in figure 8. As previously described, these tests represent the change in liquid and solid phases with lapse of time ranging in specific instances from intervals of a few hours up to several days. It should be noted that the temperatures at which all of these experiments were conducted were slightly above 100°C. All tests were made at the boiling point of the solution, which ranged from 101°C. to 102°C.

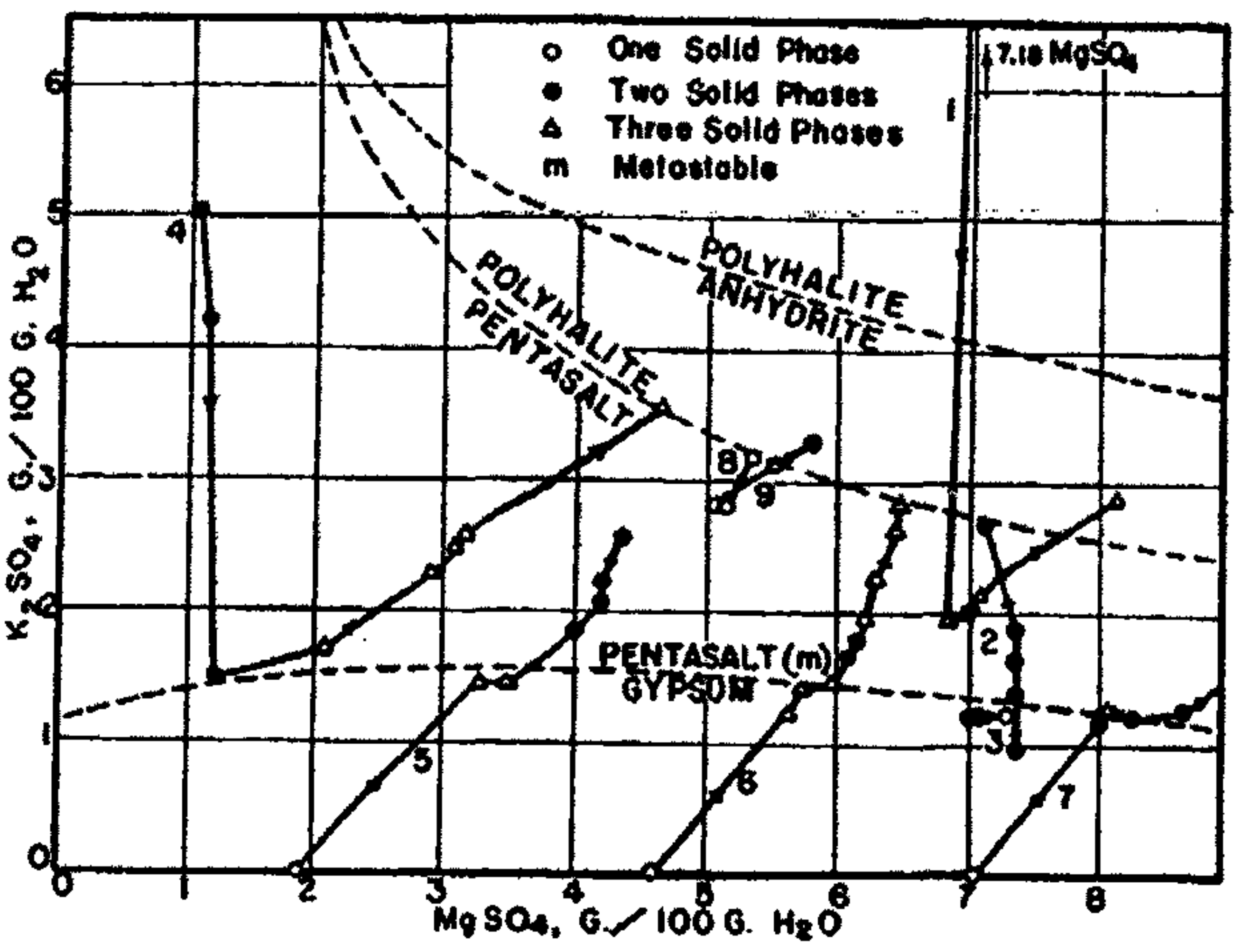

FIG. 8. Plotted data summarizing short-time tests made on the system potassium sulfate–magnesium sulfate–calcium sulfate–water at atmospheric boiling points of the respective solutions.

TABLE 8

Metastable equilibrium studies in the system K_2SO_4-$MgSO_4$-$CaSO_4$-H_2O *at 101-102°C.*

EXPERIMENT NO. AND COMPOSITION OF ORIGINAL MIXTURE	SAMPLE NO.	TIME FROM START	CONCENTRATION OF LIQUID PHASE, IN GRAMS PER 100 GRAMS OF WATER		PETROGRAPHIC DATA						REMARKS
			K_2SO_4	$MgSO_4$‡	Poly-halite	Penta-salt	Hemi-hy-drate	Gyp-sum	Anhy-drite	Syn-genite	
		days									
Experiment 1:											
500.0 g. H_2O	1	0.0	7.18	6.94							
62.5 g. pentasalt	2	0.5*	1.97	6.82							Predominantly pentasalt; about 1 per cent each of gypsum and polyhalite. Gypsum corroded
20. g. polyhalite											
100.0 g. gypsum											
	3	1.0*	1.98	6.94							Little change apparent
	4	2.0*	2.06	7.00							Trace of polyhalite remaining
	5	4.0*	2.13	7.06							Little change
	6	8.0*	2.35	7.26							Same as No. 5
	7	1.0	2.88	8.15							Same as No. 5
	8	2.0	2.94	8.13							Same as No. 5
Experiment 2:											
800.0 g. H_2O	1	0.0	2.67	7.08							
80.0 g. gypsum	2	2.0*	1.90	7.35		1-2		98-99			Gypsum corroding; pentasalt small well-formed crystals
	3	5.0*	1.65	7.36		35±		65±			
	4	12.0*	1.38	7.37		35±		65±			
	5	22.5*	0.95	7.38		40		60			
Experiment 3:											
800.0 g. H_2O	1	0	1.22	6.99							
50.0 g. $MgSO_4$	2	1.0	1.21	7.26							Corroded gypsum predominant; a few small crystals of hemihydrate
9.8 g. K_2SO_4											
50.0 g. gypsum	3	3.0	1.26								Hemihydrate predominating; gypsum corroded

	4	5.0	1.22	7.04							Hemihydrate increasing as poorly formed crystals; gypsum badly corroded
	5	7.0	1.23	7.05							Same as No. 4
	6	9.0	1.24	7.11							Hemihydrate is only solid phase
	7	12.0	1.23	7.08							Increase in refractive index indicates transformation to anhydrite
Experiment 4:											
750.0 g. H_2O	1	0	5.04	1.03							
37.5 g. K_2SO_4	2	0.5*	4.20	1.15		10		90			Well-formed pentasalt
150.0 g. gypsum	3	1.5*	1.49	1.21		80		20			Pentasalt forming
75.0 g. polyhalite	4	2.5*	1.73	2.09	5-10	85-90		5			Pentasalt still forming
added after No. 3	5	7.0*	2.30	2.92				99+			Solid phase nearly pure pentasalt
sample was taken	6	14.0*	2.48	3.08				99+			Same as No. 5
	7	1.0	2.61	3.18				99+			Same as No. 5
	8	2.0	3.55	4.61				99+			Same as No. 5
Experiment 5:											
800.0 g. H_2O	1	0	0	1.87							
80.0 g. polyhalite	2	3.0*	1.43	3.28	65±	15±	20±	1			Hemihydrate in long well-formed needles; polyhalite corroded
20.0 g. pentasalt	3	12.0*	1.46	3.50	60±	40±	Nil	Nil			Pentasalt forming; hemihydrate disappearing
	4	1.0	1.62†		50±	50±	Nil	Nil			
	5	2.0	1.86	3.99	20±	80±	Nil	Nil			Pentasalt forming; polyhalite dissolving
	6	3.0	1.88†		5±	95±	Nil	Nil			
	7	5.0	2.08	4.19	1±	99±	Nil	Nil			Few fragments of polyhalite left
	8	7.0	2.18	4.22							
	9	9.0	2.23	4.18							
	10	12.0	2.35	4.26							
	11	15.0	2.57	4.33							

---

* Time in hours.

† Expressed in percentage instead of grams per 100 grams of water.

‡ Also contains the $CaSO_4$ present in solution.

TABLE 8—*Concluded*

EXPERIMENT NO. AND COMPOSITION OF ORIGINAL MIXTURE	SAMPLE NO.	TIME FROM START	CONCENTRATION OF LIQUID PHASE, IN GRAMS PER 100 GRAMS OF WATER		PETROGRAPHIC DATA						REMARKS
			K_2SO_4	$MgSO_4$‡	Poly-halite	Penta-salt	Hemi-hy-drate	Gyp-sum	Anhy-drite	Syn-genite	
		days									
Experiment 6: 800.0 g. H_2O 80.0 g. polyhalite 20.0 g. pentasalt 10.0 g. polyhalite added after sample 9	1	0	0	4.60							
	2	2.5*	1.25	5.62	50±	25±		25			Polyhalite corroded; gypsum present in large crystals
	3	11.5*	1.41	5.70	45±	25±	30±				Gypsum has changed to hemihydrate; trace remaining
	4	1.0	1.48	5.97	40±	50±	10±				Hemihydrate is disappearing
	5	2.0	1.66	6.08	30±	70±					
	6	3.0	1.79	6.12	20-25	75-80					
	7	5.0	1.96	6.20	15±	85±			Trace		
	8	7.0	2.07	6.25	10±	90±			Trace		Anhydrite increasing
	9	9.0	2.26	6.26							Pentasalt corroding; anhydrite still increasing
	10	12.0	2.62	6.41	25+	65+			10+		
	11	15.0	2.84	6.39	25±	25±			50±		Anhydrite appears as imperfect fragments, some roughly serrated; a fine-grained precipitate visible on the surface of polyhalite fragments
Experiment 7: 800.0 g. H_2O 80.0 g. polyhalite	1	0	0.02	7.04							
	2	4.0*	1.17	8.01	70±			30±			
	3	12.0*	1.27	8.09							Polyhalite and gypsum decomposing; hemihydrate forming
	4	21.0*	1.22	8.29	65±		35±				Gypsum now all converted to hemihydrate
	5	2.0	1.26	8.69							Same as No. 4

	6	4.0	1.92	10.06							Polyhalite corroded; hemihydrate corroding; anhydrite forming
	7	6.0	2.44	11.90							Same as No. 6
	8	8.0	3.11	14.68							Same as No. 6
Experiment 8: 800.0 g. H_2O 75.0 g. pentasalt	1	0	2.84	5.13							
	2	0.5	2.89	5.12							Solid phase is all pentasalt
	3	1.0	3.01	5.22							Same as No. 2
	4	2.0	2.98	5.24							Same as No. 2
	5	3.0	3.02	5.24							Same as No. 2
	6	5.0	3.09	5.25							Same as No. 2
	7	7.0	3.18	5.33							Little if any change apparent under the microscope
Experiment 9: 800.0 g. H_2O 75.0 g. polyhalite	1	0	2.87	5.04							
	2	1.0	3.17	5.52							Polyhalite unchanged
	3	2.0	3.07	5.56							Same as No. 2
	4	3.0	3.19	5.55							Same as No. 2
	5	5.0	3.27	5.72							A few crystals of pentasalt have appeared
	6	6.0	3.27	5.76							Slight increase in amount of pentasalt
Experiment 10: 800.0 g. H_2O 75.0 g. polyhalite	1	0	5.95	0							
	2	1.0*	6.09	0.30	60					40	Syngenite showing evidence of solution
	3	4.0*	6.06	0.39	70	15				15	Pentasalt forming; syngenite decomposing
	4	0.5	6.44	0.58	55	45					Occasional crystal of pentasalt
	5	1.0	6.52	0.70							Pentasalt increasing
	6	2.0	8.62	1.12	50	50					
	7	4.0	10.16	1.80							Same as No. 6
	8	6.0	10.22	1.91							Same as No. 6

Gypsum-pentasalt metastable equilibrium

Experiment 1 was made to explain the relatively large change in liquid-phase composition encountered in an experiment in which solid gypsum, together with pentasalt and a few polyhalite "seeds," had been added to a solution of potassium and magnesium sulfates containing 6.0 g. of each per 100 g. of water. The results obtained in this test showed that the gypsum added to the original mixture reacted rapidly with the potassium sulfate to precipitate pentasalt. This reaction proceeded so rapidly that the liquid phase was altered to a composition probably outside the boundaries of the polyhalite field. The subsequent disappearance of practically all of the polyhalite present, together with the increase in the magnesium sulfate in the liquid phase, confirms this belief. Subsequent experiments indicated the metastable gypsum-pentasalt equilibrium to be at a lower concentration than was reached in this test, and therefore likely to represent the state which the system was tending to approach. This assumption was checked further by experiments 2 and 3. In the former test 80.0 g. of gypsum was added to the solution containing 2.67 g. of potassium sulfate and 7.08 g. of magnesium sulfate per 100 g. of water. A decrease in potassium sulfate occurred, owing to the formation of pentasalt as disclosed by the petrographic microscope. Obviously this test comprises an approach from supersaturation with respect to potassium sulfate. Experiment 3 shows the results of an attempt at approach from undersaturation with respect to potassium and calcium sulfates. As may be seen by reference to the data given in table 8, the solution composition showed no apparent change in composition in 12 days, but the gypsum was partly converted to hemihydrate. Microscopic examination usually showed a rapid transformation of the gypsum to hemihydrate and evidence of a subsequent slow change to anhydrite in many experiments made in this region. This fact is evidence to show that this liquid-phase composition is in the metastable gypsum, or hemihydrate fields. These two experiments fix the limits of the gypsum-pentasalt boundary as being between 1.22 and 1.38 g. of potassium sulfate per 100 g. of water in this portion of the diagram.

Experiment 4 is an experiment similar to No. 1 of this series, except that the initial starting composition is in a different region and a larger quantity of polyhalite was added to the reaction mixture after 1½ hours. From the behavior of the liquid phase and from the nature and appearance of the solid phases the changes taking place can be followed. During the first 1½ hours pentasalt was formed rapidly, thereby removing potassium sulfate from solution. As soon as the polyhalite was added it began to decompose, but pentasalt continued to form for the next 5 or 6 hours. This test would tend to prove that polyhalite was unstable in this region and pentasalt was the stable phase. However, between samples 5 and 7 the liquid-phase composition corresponds to the simple decomposition of polyhalite without any apparent formation of pentasalt. This is of special significance, since it gives a clue to whether pentasalt is the final stable phase in this region. Stoichiometric calculations indicate that all of the polyhalite added to the initial mixture would have to decompose to effect the liquid-phase concentration represented by sample 6. The petrographic microscope fails to disclose the presence of any polyhalite at this point. Unfortunately, subsequent solution changes are only explainable as due to evaporation losses. It may be concluded, therefore, that as we are able to produce pentasalt up to a point falling somewhere between sample 4 and sample 5, this region is possibly the stable field for pentasalt or at least a metastable region for the salt. Other data on this region would lend credence to the latter assumption.

Experiments 5, 6, and 7 show the results obtained when mixtures of polyhalite and pentasalt or polyhalite alone (experiment 7) are decomposed with solutions containing the indicated amounts of magnesium sulfate but no potassium sulfate. These tests were made to see if it would be possible to realize the gypsum-pentasalt or the gypsum-pentasalt-polyhalite metastable equilibria. No conclusive evidence of attaining the latter point was obtained, but every test showed an indication of passing through the former metastable boundary. The various reactions that occur can be explained from consideration of the concentration changes of the liquid phase and from the nature of the solid phase. The following reactions express the changes:

$$\underset{\text{polyhalite}}{K_2SO_4\cdot MgSO_4\cdot 2CaSO_4\cdot 2H_2O} + 2H_2O = \underset{\text{gypsum}}{2CaSO_4\cdot 2H_2O} + \underset{\text{(solution)}}{K_2SO_4 + MgSO_4} \tag{6}$$

$$5(\underset{\text{polyhalite}}{K_2SO_4\cdot MgSO_4\cdot 2CaSO_4\cdot 2H_2O}) = 2(\underset{\text{pentasalt}}{K_2SO_4\cdot 5CaSO_4\cdot H_2O}) + \underset{\text{(solution)}}{5MgSO_4 + 3K_2SO_4} \tag{7}$$

$$\underset{\text{gypsum}}{CaSO_4\cdot 2H_2O} \rightarrow \underset{\text{hemihydrate}}{CaSO_4\cdot 0.5\,H_2O} \rightarrow \underset{\text{anhydrite}}{CaSO_4} \tag{8}$$

$$\underset{\text{pentasalt}}{K_2SO_4\cdot 5CaSO_4\cdot H_2O} + XH_2O = K_2SO_4 + 5CaSO_4\cdot (X + 1)H_2O \tag{9}$$

$$X = (-1 \text{ to } 9)$$

Apparently in all three experiments the reaction expressed by equation 6 takes place until the potassium sulfate in solution is increased to approximately 1.35 g. per 100 grams of water. This concentration is reached in from 3 to 4 hours. Each curve then shows a slight break, which has been interpreted as indicating that the reactions as given by equations 7 and 8 enter the picture. Microscopic evidence shows that the gypsum rapidly disappears by replacement with hemihydrate, which in turn is much more slowly replaced by anhydrite. These breaks are at, or probably very near, the gypsum-pentasalt equilibrium. Pentasalt apparently forms for several days at the expense of the polyhalite until the latter disappears. This reaction is more pronounced in test 5 than in test 6 or 7. As the polyhalite is exhausted the pentasalt formed by equation 7 decomposes in turn, according to equation 9. The actual attainment of a form of calcium sulfate which completely satisfies the physical constants for natural anhydrite has proved difficult to realize in these short-time experiments, since anhydrite forms at an extremely slow rate. However, all of the evidence points toward this region as representing the stability field for anhydrite.

Experiments 8 and 9 were made in an effort to define the limits of the pentasalt (or anhydrite) field and of the polyhalite field. A quantity of synthetic pentasalt was extracted in experiment 8 for a total of 7 days with a potassium sulfate-magnesium sulfate solution, while polyhalite was similarly extracted for a 6-day period. Data from previous experiments indicate that 6 or 7 days is too short a time to permit intelligent conclusions in regard to the final stable phases. Both of the initial solid phases gave evidence of decomposition, although of a small order. The behavior of the pentasalt in experiment 8 agrees with the behavior of pentasalt over a large area in this region in many of the 30-day tests, in that a very slight decomposition occurs, accompanied by a slight increase in potassium sulfate in solution. The small amount of calcium sulfate that should appear in the solid phase would be easily overlooked, particularly if present as hemihydrate in process of conversion to anhydrite. The results of experiment 9 show that polyhalite is the unstable phase, and the appearance of a few crystals of pentasalt would indicate this region as probably metastable with respect to pentasalt. However, hemihydrate in process of change to anhydrite has been identified at lower potassium sulfate concentrations and may also be present here. This inherent difficulty was probably the reason why Geiger concluded that he had produced "krugite" as a new solid phase at about this composition but at 83°C.

The next experiment (No. 10) is an excellent example which illustrates the danger of fixing the last solid phase obtained in periods ranging from 1 to 8 days as the final stable phase. In the test polyhalite decomposed, forming first syngenite and finally pentasalt. Data presented elsewhere have proved that pentasalt is not the final stable phase in the region of sample 3 but that anhydrite is, and that both syngenite and pentasalt are able to exist for more or less prolonged periods as metastable phases.

SUMMARY AND CONCLUSIONS

As the result of a considerable number of tests in the system potassium sulfate-magnesium sulfate-calcium sulfate-water the tentative stability fields for syngenite, pentasalt, polyhalite, and anhydrite have been defined within the limits of 17.0 g. of potassium sulfate and 14.0 g. of magnesium sulfate per 100 grams of water at 100°C.

The actual attainment of the final equilibria was found to be extremely slow, and in some instances was incomplete after 60 and 69 days. Metastable equilibria were encountered in nearly every portion of the area explored, and in certain cases were distinguished from stable equilibria only by the utmost precautions. Invariably, the short-time tests of a few hours or even several days resulted in metastable conditions. Pentasalt ($K_2SO_4 \cdot 5CaSO_4 \cdot H_2O$) was found to persist in a large portion of the area studied and particularly when initially placed in the anhydrite field. Natural anhydrite reacted at a very slow rate also, but the limited solubility and the fact that all of the calcium sulfate must pass through the solution phase to be available for subsequent reaction explains this phenomenon.

TABLE 9

Summarized data on important equilibrium points in the system K_2SO_4-$MgSO_4$-$CaSO_4$-H_2O at 100°C.

POINT	SOLID PHASES	LIQUID PHASE COMPOSITION IN GRAMS PER 100 GRAMS OF WATER		
		K_2SO_4	$MgSO_4$	$CaSO_4$
		grams	*grams*	*grams*
A	Polyhalite-syngenite-pentasalt	12.1	0.9	0.08
B	Polyhalite-pentasalt-anhydrite	7.5	1.7	0.075
C (m)	Polyhalite-syngenite-anhydrite	10.7	0.8	0.093
D	Syngenite-pentasalt	11.7	0	0.075
E	Pentasalt-anhydrite	6.0	0	0.07
F (m)	Syngenite-anhydrite	10.0	0	0.092
G (m)	Syngenite-gypsum	5.7	0	0.21
H (m)	Pentasalt-gypsum	1.1	0	0.137

Note: Points to which the suffix "(m)" is added are metastable.

The form in which the calcium sulfate is added to the mixtures used in the study of this system is extremely important. The stable form is, of course, anhydrite. If gypsum is used, metastable equilibria are obtained and the gypsum slowly alters to hemihydrate and finally anhydrite. Mixtures having optical properties intermediate between hemihydrate and anhydrite were frequently noted.

From the data collected during this investigation many of the results obtained during the extraction of calcined polyhalite at 100°C. are easily explained, and a much clearer conception of reactions taking place within the specified region is possible.

To facilitate the determination of the various equilibria involving some form of calcium sulfate either as such, or as a component of the solid phase in the three- and four-component systems, table 9 has been prepared. The location of the various points tabulated may be clearly understood by referring to figure 6.

REFERENCES

(1) ANDERSON, E., AND NESTELL, R. J.: Ind. Eng. Chem. **12**, 243-6 (1920).
(2) BASCH, E. E.: Sitzber. preuss. Akad. Wiss., pp. 1084-5 (1900).
(3) CLARKE, L., AND PARTRIDGE, E. P.: Ind. Eng. Chem. **26**, 897 (1934).
(4) CONLEY, J. E., AND FRAAS, F.: Ind. Eng. Chem. **25**, 1007 (1933).
(5) D'ANS, J., AND SCHREINER, O.: Z. anorg. Chem. **62**, 129-67 (1909).
(6) GEIGER, A.: Dissertation, Berlin, 1904.
(7) HICKS: Ind. Eng. Chem. **5**, 650 (1913).
(8) HILL, A. E.: J. Am. Chem. Soc. **56**, 1071-5 (1934).
(9) IDE, KARL H.: Kali **29**, 83-6, 93-6, 103-5 (1935).
(10) SCHMIDT, L. F.: Ges. Naturw. **53**, 504 (1880).
(11) STARRS, B. A., AND CLARKE, LOYAL: J. Phys. Chem. **34**, 1058-63 (1930).
(12) VAN KLOOSTER, H. S.: J. Phys. Chem. **21**, 513-18 (1917).
(13) VAN'T HOFF, I. H.: Z. anorg. Chem. **47**, 244-80 (1905).

DECOMPOSITION AND SYNTHESIS OF HYDROGEN IODIDE BY ALPHA PARTICLES[1]

KEREN GILMORE BRATTAIN[2]

School of Chemistry, University of Minnesota, Minneapolis, Minnesota

Received August 14, 1937

The radiochemical decomposition and synthesis of hydrogen iodide have been studied by Vandamme (15) at 20°C. and 100°C., respectively. He used comparatively small amounts of radon. The author also studied these reactions under somewhat different conditions. The decomposition of hydrogen iodide by alpha particles was determined by two methods: (*1*) the rate of reaction was followed by pressure measurements, which were made at 25°C.; (*2*) closed-system experiments were performed at 27°, 100°, and 200°C., and the amount of reaction determined by chemical analysis at the end of the experiment. Similar closed-system experiments on synthesis were made at temperatures ranging from 25°C. to 200°C.

EXPERIMENTAL PROCEDURE

In the first set of decomposition experiments the radon and hydrogen iodide were enclosed in a small bulb connected to a mercury manometer. The apparatus and procedure were the same as those employed by Lind and Bardwell (11). There was practically no contamination of the mercury until the experiment was well along. A phosphoric acid lubricant (13) was used on the stopcocks in all systems in which hydrogen iodide was present. The closed-system decomposition experiments were performed in reaction bulbs, with two capillary tubes connected along one diameter. These bulbs, which had an approximate volume of 60 cc., have been described by Truesdale and Lind (14). The experimental procedure was as follows: Small fragile glass ampoules filled with radon were sealed into the reaction bulb. The bulb was then connected to a high-vacuum system and pumped for several hours. During this time it was washed with small volumes of hydrogen iodide. An approximate amount of hydrogen iodide was then frozen in the reaction bulb and the bulb was sealed off. Extreme care was taken to obtain a capillary tip that could be broken readily later. The ampoule containing the radon was broken,

---

[1] This article is based upon a thesis submitted by Keren Gilmore to the Graduate School of the University of Minnesota in partial fulfillment of the requirements for the degree of Doctor of Philosophy, August, 1932.

[2] Present address: 270 West 11th Street, New York City.

and the reaction bulb placed in a constant-temperature apparatus at once. A small electrically heated oven, constant to within ±1°C., was used for all experiments with the exception of those run at 25°C. and 27°C. In these cases the bulbs were placed in a constant-temperature water bath. At the end of the experiment the bulbs were quickly cooled to room temperature, and one of the tips was broken off under a solution of potassium iodide. A sufficient amount of the solution entered the bulb to dissolve the iodine. The second tip was broken, and the bulb rinsed with small amounts of potassium iodide. The resulting solution was used for the determination of both the iodine and the remaining hydrogen iodide. First the amount of iodine present was determined by titration with sodium thiosulfate to a water-white solution. The acid was then titrated with sodium hydroxide, bromothymol blue being used as the indicator. A blank run containing no radon accompanied each experiment. From this the amount of thermal reaction was obtained.

The procedure used for the synthesis experiments was very similar to that of the closed-system decomposition experiments described above. A fragile glass ampoule containing iodine and one containing radon were introduced into the reaction bulb before it was sealed onto the vacuum line. The bulb was pumped and washed with hydrogen. A known volume of hydrogen was introduced in the reaction bulb from a Ramsay buret, and the bulb sealed off. The experiment was then performed in the manner given above.

The following method was used for preparing the hydrogen iodide used in the decomposition experiments: First, a fuming solution of hydriodic acid was prepared, in an all-glass system, by dropping water on phosphorus and iodine. The resulting gas was passed through four traps cooled with an ice–salt mixture, and then into an absorption bulb containing distilled water. This bulb was also cooled by an ice-salt mixture. The solution thus prepared was stored in a refrigerator. The hydrogen iodide was prepared from the stock solution as it was needed by the following series of vacuum distillations. Twenty cubic centimeters of the hydriodic acid was placed in a distilling flask, and the flask was sealed onto a high-vacuum line. The pumps were well protected with liquid air. The solution was frozen with carbon dioxide snow. The air was thoroughly pumped out of the system, and then the solution was allowed to warm up slowly. The resulting gas was passed through a trap cooled with solid carbon tetrachloride, which removed most of the water vapor, then dried over phosphorus pentoxide. The hydrogen iodide was frozen down with liquid air and the system well pumped. The gas was then distilled through two traps cooled with carbon dioxide snow, and finally frozen in the reaction bulb with liquid air. For the decomposition experiments the hydrogen was prepared by the electrolytic decomposition of a potassium hydroxide solution. The gas from the generator was passed over palladinized asbestos, heated to 300°C., dried over phosphorus pentoxide, and stored in a 2-liter bulb. This bulb had been pumped and flushed with hydrogen several times previous to the storage. The iodine was purified by three consecutive sublimations (9) of chemically pure iodine obtained from the Mallinckrodt Company. The resublimed iodine was dried over calcium chloride in an ungreased desiccator and stored in a dark glass-stoppered bottle. For experimental use small quantities of the iodine were placed in fragile glass ampoules, pumped for an hour, and then sealed off.

TABLE 1

Pressure decomposition experiments

TIME	TOTAL P	P_{HI}	P_{H_2}	$N_{HI} \times 10^{-19}$	$N_{H_2} \times 10^{-19}$	M_{HI} DECOMPOSED $\times 10^{-19}$	$\frac{M_{HI}}{N_{HI}}$
Expt. No. I. Volume = 3.99 cm.³; T = 25°C.; R = 0.984 cm.; E_0 = 125.9 mc.							
hours	*mm.*	*mm.*	*mm.*				
0	597	597					
1.0	558	520	38	0.161	0.000	1.00	6.21
2.0	514	431	83	0.295	0.000	2.16	7.32
3.0	482	367	115	0.405	0.003	3.00	7.42
4.0	453	309	144	0.496	0.007	3.74	7.54
8.0	405	213	192	0.764	0.030	4.99	6.54
12.	390	182	208	0.965	0.052	5.39	5.58
18.	370	143	227	1.20	0.088	5.90	4.90
24.	356	115	241	1.38	0.123	6.27	4.54
36.	327	57	270	1.57	0.208	7.02	4.47
Expt. No. II. Volume = 11.50 cm.³; T = 25°C.; R = 1.40 cm.; E_0 = 103.8 mc.							
0	676	676					
1.0	657	638	19	0.228	0.006	1.44	6.31
5.3	587	498	89	1.03	0.020	6.67	6.48
9.0	540	403	136	1.69	0.041	10.3	6.08
18.	467	258	209	2.54	0.106	15.7	6.20
25.	425	174	251	2.94	0.160	18.9	6.43
45.	370	64	306	3.41	0.371	23.0	6.73
69.	359	42	317	3.64	0.533	23.2	6.37

The sodium thiosulfate used in the titrations was resublimed, and the solution standardized against a weighed amount of resublimed iodine. A water-white solution was used as the end point. The normality of the solution was redetermined at various intervals. The sodium hydroxide solution was standardized against Mallinckrodt's reagent quality oxalic acid with phenolphthalein as the indicator.

EXPERIMENTAL RESULTS

The experimental results are given in tables 1, 2, and 3. The last four columns in table 1 will be discussed later. In tables 2 and 3 the pressure of hydrogen iodide was calculated from the chemical analysis. The pressure of hydrogen in table 2 was calculated from the iodine analysis, since equal amounts of hydrogen and iodine are formed by the decomposition of hydrogen iodide. In table 3 the hydrogen pressure was calculated from the Ramsay buret measurements. The vapor pressure of solid iodine was computed by the method of Giauque (4), and that of liquid iodine was obtained from the data of Ramsay and Young (12). In all the synthesis experiments performed at temperatures below 150°C. a sufficient amount of iodine was present to maintain a constant pressure. In the experiment performed at 150°C. the pressure of iodine was constant only during the first part of the run. The vapor pressure of iodine at this temperature is 294 mm. The amount of iodine introduced was sufficient to give a pres-

TABLE 2

Closed-system decomposition experiments

EXPT. NO.	REACTION TEMPERATURE	TIME	BULB VOLUME	INITIAL RADON	P°_{HI}	P_{H_2} FINAL	P_{I_2} FINAL
	°C.	*hours*	*cm.³*	*millicuries*	*mm.*	*mm.*	*mm.*
1..........	27.5	53.0	54.9	41.2	383.	49.7	0.3
2..........	27.5	53.2	57.2	31.7	806.	87.8	0.3
3..........	100.	88.9	57.2	30.1	252.	28.4	28.4
4..........	203.	63.8	54.9	13.9	215.	12.5	12.5
5..........	203.	63.5	57.2	15.1	212.	11.2	11.2

TABLE 3

Synthesis experiments

EXPT. NO.	REACTION TEMPERATURE	TIME	BULB VOLUME	INITIAL RADON	$P^\circ_{H_2}$	$P^\circ_{I_2}$	P_{HI} FINAL
	°C.	*hours*	*cm.³*	*millicuries*	*mm.*	*mm.*	*mm.*
1.........	200	58.9	58.3	64.4	323.	285.	26.8
2.........	200	59.0	57.0	60.3	320.	287.	27.3
3.........	174	211.	58.4	118.9	368.	358.	80.6
4.........	225	213.	58.5	103.3	346.	317.	81.6
5.........	120	209.	56.9	31.6	506.	109.	27.9
6.........	150	186.	58.4	112.0	530.	294.	99.4
7.........	200	183.	57.1	126.1	581.	353.	129.
8.........	121	196.	56.9	93.9	570.	115.	74.0
9.........	100	213.	56.4	103.5	397.	45.9	51.5
10.........	174	165.	56.9	108.6	676.	70.3	63.0
11.........	100	208.	56.4	94.2	543.	45.9	59.6
12.........	81.0	208.	57.0	100.0	687.	15.9	52.7
13.........	54.7	192.	57.0	100.2	537.	3.0	22.0
14.........	25.0	216.	58.5	117.2	520.	0.3	4.5
15.........	25.0	238.	58.4	110.9	535.	0.3	9.4

sure of 309 mm. The final pressure of iodine was 259 mm. The initial pressure of iodine for all the synthesis experiments above 150°C. was obtained by adding one-half the calculated pressure of hydrogen iodide to the final pressure of iodine obtained from analysis. The number of molecules of hydrogen iodide where given as yields has been corrected for thermal reaction. These corrections were small.

CALCULATIONS AND RESULTS

In order to analyze the data it is necessary to determine some measure of the excitation produced by the alpha particles in each of the gases present. The accepted method for doing this is to calculate the number of ion pairs formed. The total number of ion pairs formed in the gaseous mixture was obtained from the following equation.

$$N_t = N_0 E g F' k(r)^{\frac{2}{3}}$$

where N_t = total number of ion pairs formed,
N_0 = number of alpha particles per curie of radon (1.764×10^{16}) (6),
E = number of curies of radon decomposed (corrected for non-equilibrium decomposition) (14),
g = specific ionization in gaseous mixture (7),
F' = efficiency factor (6), and
$k(r)^{\frac{2}{3}}$ = number of ion pairs produced by an alpha particle in its range in air (N.T.P.) (1.55×10^5) (6).

A slight modification of this equation was used for the calculation of the pressure experiments. An average F' was calculated for each interval. This value was then used in calculating the number of ion pairs formed during each interval. The total number of ion pairs at any time was then obtained by addition.

The number of ion pairs formed in each component of the system was calculated from the following equation,

$$N_a = N_t \frac{s_a g_a p_a}{\Sigma s g p} \tag{2}$$

where s = stopping power and p = partial pressure of the component. The summation is over all components present.

In the closed-system experiments the arithmetical mean of the initial and final pressures was used in all calculations. The stopping power of iodine was taken as 3.70 (5) and that of hydrogen iodide as 1.97, computed as an additive property from values of stopping powers of hydrogen and iodine. The values 1.31 (8) and 1.29 (10) were used for the specific ionization of iodine and hydrogen, respectively.

The results of the calculations for the decomposition of hydrogen iodide are given in tables 1 and 4. In figure 1 the number of molecules of hydrogen iodide decomposed is plotted against the number of hydrogen iodide ion pairs. It is seen that on the whole the amount of decomposition is proportional to the hydrogen iodide ion pairs, and that for each

TABLE 4

Decomposition results

EXPT. NO.	RADON DECOMPOSED	$N'_{HI} \times 10^{-19}$	$N'_{H_2} \times 10^{-19}$	$N_{I_2} \times 10^{-19}$	$M_{HI} \times 10^{-19}$	$\frac{M_{HI}}{N_{HI}}$
	millicuries					
1	13.5	3.28	0.02	0.005	17.7	5.38
2	10.4	5.38	0.03	0.004	32.5	6.04
3	14.6	1.84	0.01	0.22	8.37	4.55
4	5.28	0.450	0.001	0.027	2.52	5.60
5	5.71	0.490	0.001	0.026	2.32	4.74
1*	13.1	5.06	0.02	0.009	36.9	7.28
2*	12.4	6.26	0.03	0.008	46.0	7.33
3*	10.4	6.10	0.03	0.006	59.1	9.69
1*	7.98	4.62	0.01	0.004	30.8	6.67
2*	7.95	3.26	0.01	0.005	26.6	8.16
3*	8.22	3.62	0.01	0.005	20.9	5.78
4*	8.25	1.20	0.004	0.004	10.8	9.03

* Calculated from Vandamme's data.

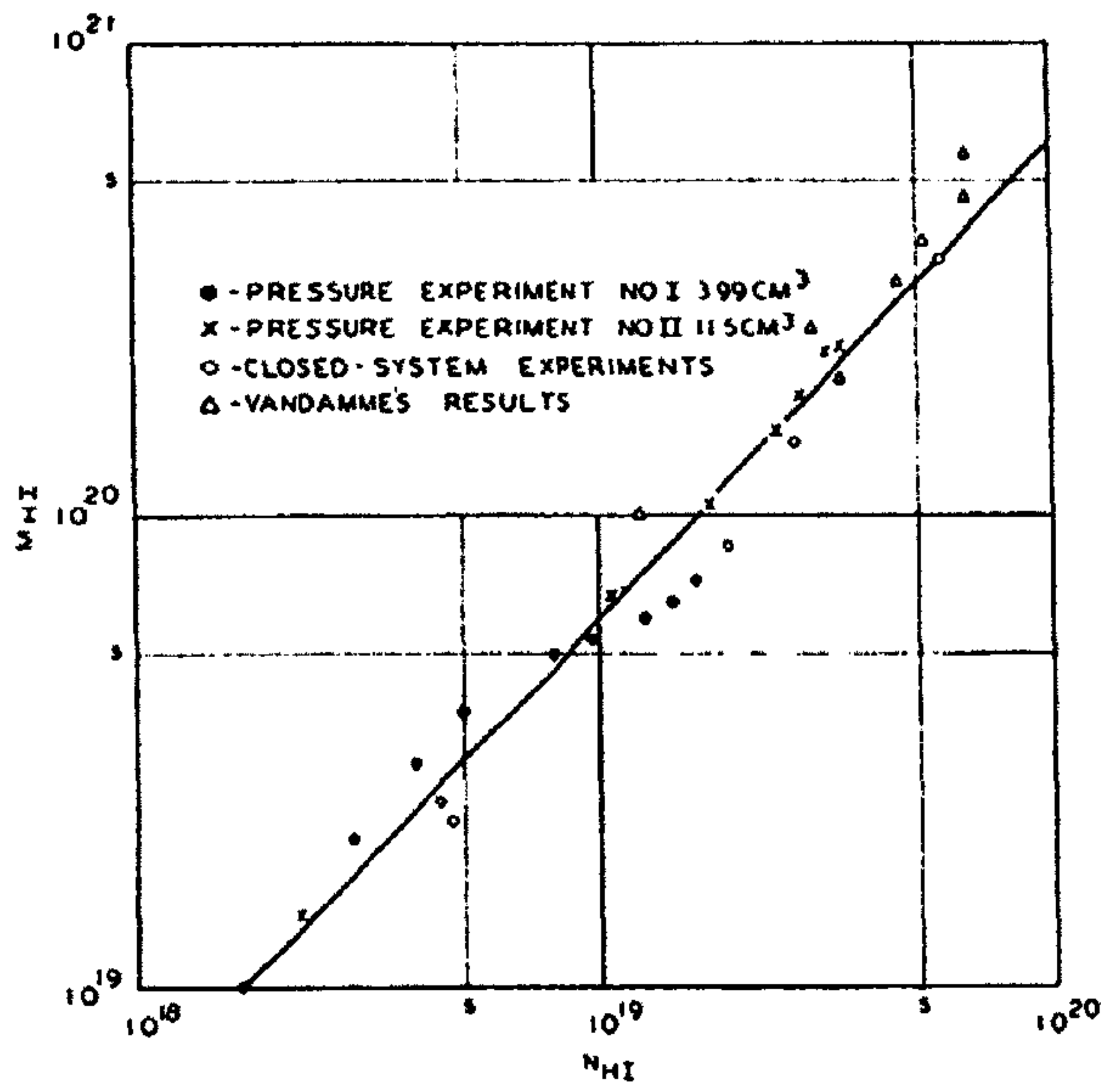

FIG. 1. Decomposition of hydrogen iodide

ion pair 6+ molecules of hydrogen iodide are decomposed. The various points scatter to some extent, and Vandamme's results are on the average a little higher than the author's. This last fact could be caused by differences in radon standards. The simplest explanation of the reaction is that, on an average, for each hydrogen iodide ion pair produced by an alpha particle two activated hydrogen iodide molecules are also produced.

TABLE 5

Synthesis results

EXPT. NO.	$N_{H_2} \times 10^{-19}$	$N_{HI} \times 10^{-19}$	$N_{I_2} \times 10^{-19}$	$M_{I_2} \times 10^{-19}$	$M_{HI} \times 10^{-19}$	$\frac{M_{HI}}{M_{I_2}}$ OBSD.	$\frac{M_{HI}}{M_{I_2}}$ CALCD.
1.........	0.333	0.149	5.92	33.2	2.71	0.082	0.094
2.........	0.312	0.145	5.64	32.7	2.69	0.083	0.090
3.........	1.64	2.02	32.4	42.7	10.1	0.235	0.261
4.........	1.19	1.59	22.0	33.6	8.11	0.241	0.217
5.........	0.626	0.187	2.78	15.4	3.79	0.246	0.260
6.........	2.26	2.35	25.3	37.5	12.9	0.343	0.322
7.........	2.44	3.04	28.8	37.8	13.9	0.367	0.298
8.........	2.04	1.45	8.60	16.1	10.3	0.640	0.597
9.........	1.64	1.16	3.98	6.75	6.95	1.03	1.03
10.........	2.24	1.13	3.72	6.74	7.80	1.16	1.61
11.........	2.02	1.20	3.54	6.75	8.32	1.23	1.35
12.........	2.88	1.20	1.38	2.49	8.23	3.30	5.65
13.........	2.37	0.518	0.266	0.503	3.71	7.39	25.9
14.........	3.16	0.147	0.038	0.059	0.83	14.1	332.
15.........	3.18	0.298	0.036	0.059	0.89	15.0	325.
1*.........	0.206	0.031	1.29	20.8	1.88	0.090	0.074
2*.........	0.218	0.029	1.18	20.6	1.94	0.094	0.078
3*.........	0.414	0.056	1.24	19.0	3.27	0.172	0.145
1*.........	0.036	0.005	0.614	23.4	0.787	0.034	0.017
2*.........	0.171	0.012	0.625	20.1	1.51	0.075	0.060
3*.........	0.245	0.013	0.556	18.4	1.64	0.089	0.090

* Calculated from Vandamme's data.

Each of these three reacts with a neutral hydrogen iodide molecule, thus giving a net result of six molecules decomposed.

$$HI + \alpha \rightarrow HI^+ + \alpha + e$$
$$2[HI + \alpha \rightarrow HI' + \alpha]$$
$$HI^+ + HI \rightarrow H_2 + I^+$$
$$2[HI' + HI \rightarrow H_2 + I_2]$$

The reaction, of course, may be much more complicated, but this mechanism is sufficient to explain the facts.

In these decomposition experiments the number of hydrogen ion pairs was always so small as to be negligible, except possibly in the last two or three points of the pressure runs. Consequently no conclusions can be drawn from these data as to the effect of the hydrogen ion pairs on the reaction. The highest pressure of iodine occurred in the closed-system experiment No. 3. In this experiment the average iodine pressure was one-fifteenth that of the average hydrogen iodide pressure. An iodine pressure of this relative magnitude appears to have no effect on the yield, provided one considers only the ion pairs formed in hydrogen iodide.

The calculated results for the synthesis of hydrogen iodide are given in table 5. These data are not so easy to analyze. The reasons for this are obvious. One has a complicated mixture of three components and the ion pairs due to each component. In a general way one can say that the amount of synthesis should be some function of the various types of ion pairs present.

$$M_{\mathrm{HI}} = F(N_{\mathrm{H_2}}, N_{\mathrm{HI}}, N_{\mathrm{I_2}}) \tag{3}$$

where M_{HI} is the yield. In analyzing these data the author found it a distinct advantage to consider ratios instead of absolute magnitudes. The particular ratios that were found useful were the various magnitudes divided by the average number of molecules of iodine present ($M_{\mathrm{I_2}}$). The synthesis results consist of the measurements of the yield at the end of a long run. Since the number of ion pairs of the components varies throughout the run, and since back reaction is always possible, the yield is probably given accurately only in terms of a complicated integral. However, an attempt was made to analyze the data using average values. From the results of this analysis the author has come to the conclusion that this procedure is justified where these data are concerned.

As a first trial the author made the assumption that only the hydrogen ion pairs were effective in the synthesis of hydrogen iodide, and that the ion pairs of iodine and hydrogen iodide could be neglected. Figure 2 is a plot of $M_{\mathrm{HI}}/M_{\mathrm{I_2}}$ versus $N_{\mathrm{H_2}}/M_{\mathrm{I_2}}$. The data of Vandamme and of the author give results which follow a straight line. This relationship can be approximately represented by the following equation.

$$\frac{M_{\mathrm{HI}}}{M_{\mathrm{I_2}}} = k\left(\frac{N_{\mathrm{H_2}}}{M_{\mathrm{I_2}}}\right)^{\frac{5}{4}} \tag{4}$$

where k is a constant. Since the yield is not proportional to the hydrogen ion pairs, it would appear that there were other factors involved in the reaction. Therefore the assumptions were too simple. The relationship does indicate, however, that there is no large discrepancy between the results of Vandamme and those of the author. An attempt was made to see if a reasonable amount of back reaction would account for the fact that the yield is not proportional to the hydrogen ion pairs. Farkas and Bonhoeffer (3) report that in equal mixtures of hydrogen iodide and iodine a hydrogen atom combines one hundred times more readily with an iodine molecule than with a hydrogen iodide molecule. It was found that a back reaction based on the probability of a hydrogen atom reacting fifty to one hundred times more readily with iodine than with hydrogen iodide would affect only the last few points for large values of $M_{\mathrm{HI}}/M_{\mathrm{I}_2}$. These points are seen to deviate from the straight line anyway, and in a direction which could be accounted for by a back reaction. No assumed value of the relative probability of these two reactions would make the yield proportional to the hydrogen ion pairs over any appreciable range.

The next logical assumption which might be made is that the hydrogen iodide ion pairs as well as those of the hydrogen affect the yield. An examination of the possible reactions of an excited hydrogen iodide molecule indicates that the products of ionization or activation of hydrogen iodide could at most react with hydrogen or iodine in such a way that the net hydrogen iodide formed or decomposed is zero. Therefore the only effect of the hydrogen iodide ion pairs would be the decomposition of neutral molecules of hydrogen iodide. The simplest way of considering the effect of both the hydrogen and hydrogen iodide ion pairs is to assume that it is proportional to the number of ion pairs of each gas present.

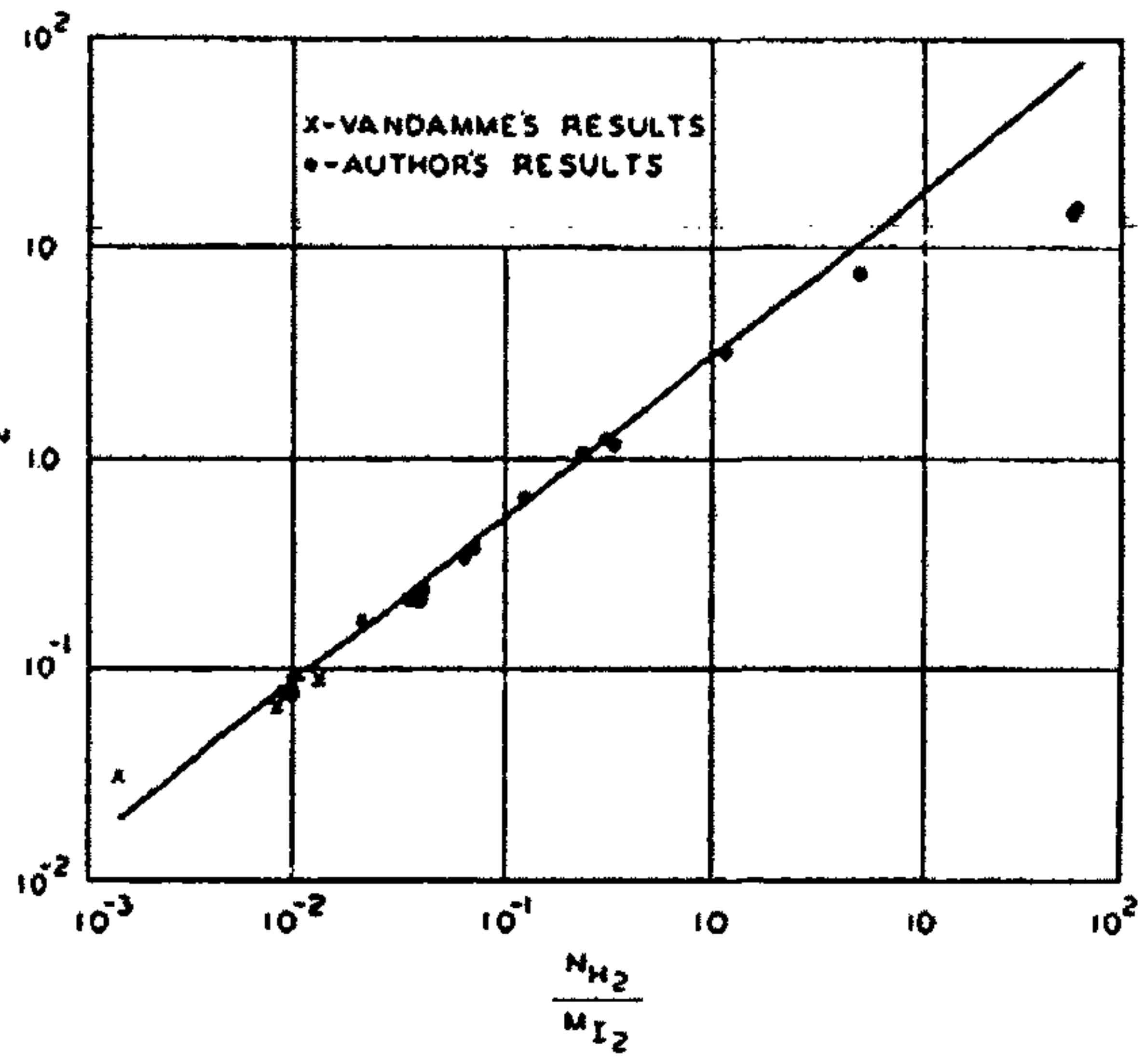

FIG. 2. Synthesis of hydrogen iodide. $M_{\mathrm{HI}}/M_{\mathrm{I}_2}$ plotted against $N_{\mathrm{H}_2}/M_{\mathrm{I}_2}$

$$\frac{M_{\mathrm{HI}}}{M_{\mathrm{I}_2}} = a\frac{N_{\mathrm{H}_2}}{M_{\mathrm{I}_2}} + b\frac{N_{\mathrm{HI}}}{M_{\mathrm{I}_2}} \tag{5}$$

where a and b are constants. The values of the constants which gave the best correlation were $a = 10$ and $b = -4$. However, the correlation at best was very poor. Work by Eyring, Hirschfelder, and Taylor (1, 2) would indicate that six molecules of hydrogen iodide should be formed per hydrogen ion pair instead of ten. An examination of the data on the basis of the above correlation made it appear that the reaction was also dependent upon the number of ion pairs formed in iodine.

An assumption was then made that each of the different ion pairs present affected the synthesis according to the following relationship.

$$\frac{M_{\mathrm{HI}}}{M_{\mathrm{I_2}}} = a\frac{N_{\mathrm{H_2}}}{M_{\mathrm{I_2}}} + b\frac{N_{\mathrm{HI}}}{M_{\mathrm{I_2}}} + c\frac{N_{\mathrm{I_2}}}{M_{\mathrm{I_2}}} \tag{6}$$

It was found that the data of Vandamme and of the author could be well represented by equation 6, when the constants *a*, *b*, and *c* have the values 6.4, − 4.0, and 0.27, respectively (table 5, column 8). A plot of this relationship using these constants is given in figure 3. The relationship indicates that 6.4 molecules of hydrogen iodide are formed per hydrogen ion pair. The value of the constant *b* is surprisingly high. However, it is possible that for every hydrogen iodide ion pair an average of two ionized or activated hydrogen iodide molecules will react with neutral hydrogen iodide molecules, thus causing a counter reaction. If the assumptions underlying equation 6 are correct, the data indicate that a small fraction of the iodine ion pairs react with hydrogen to form hydrogen iodide. There are two possible reactions which might explain this effect. First, a neutral hydrogen molecule may cluster with an I_2^+ ion. The reaction of an electron with this cluster could give two molecules of hydrogen

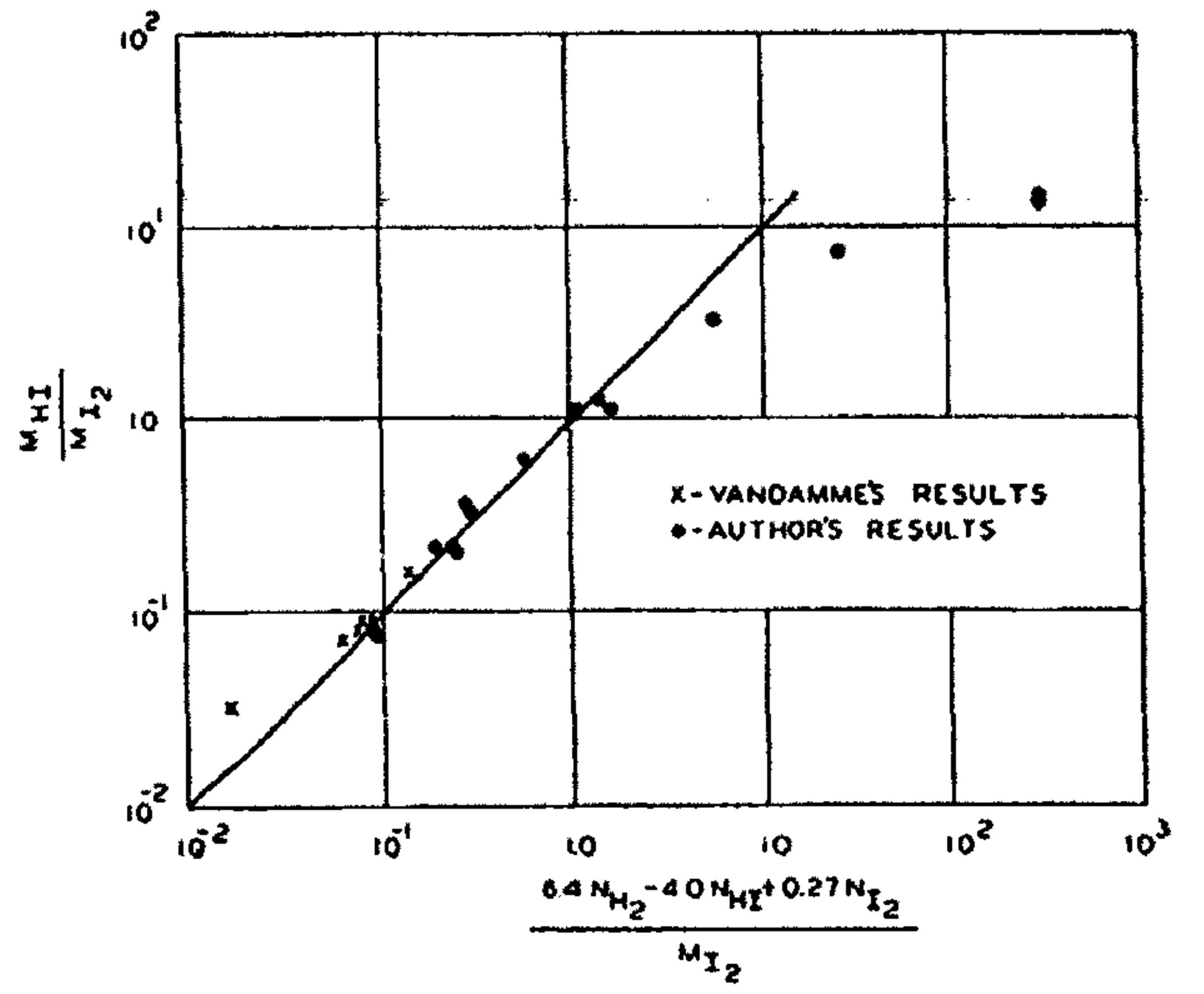

FIG. 3. Synthesis of hydrogen iodide

iodide and excess energy. Second, it is also possible for an excited iodine molecule to react with a hydrogen molecule to form hydrogen iodide and excess energy. The explanation of the data by equation 6 requires only that one excited or ionized iodine molecule react for every seven ion pairs formed in iodine.

We see in figure 3 that the last few points, for large values of M_{HI}/M_{I_2}, still deviate from the straight line. This is probably the effect of the back reaction, which has been discussed in the first attempt to analyze these data. The deviation of these points could also be caused by the fact that in these experiments the pressure of the iodine is so low that a large portion of the excited hydrogen may become deactivated without coming in contact with iodine molecules. The number of the points and the accuracy of the data in this region are probably not sufficient to decide definitely between these two possibilities. The data, however, are not inconsistent with the probability that the activated hydrogen reacts one hundred times more readily with iodine than with hydrogen iodide.

The author has also attempted to analyze these data on assumptions similar to those used by Eyring, Hirschfelder, and Taylor (2) to explain both the radiochemical synthesis and back reaction of hydrogen bromide, but arrived at the conclusion that these results can not be explained on this basis.

The constants used for the stopping power of iodine and hydrogen iodide and for the specific ionization of iodine are more or less assumed values, because they have never been experimentally determined. Some experimentation with changes in these values indicated that the results were of the same general character, regardless of the exact values assumed for these constants. From such results it does not appear probable that the explanation of the synthesis reaction could be simplified by assuming different values for the specific ionization of iodine and the stopping power of iodine and hydrogen iodide.

SUMMARY

It has been found that the work of Vandamme and of the author, on the decomposition of hydrogen iodide by alpha particles, can be explained on the basis that 6+ molecules of hydrogen iodide decompose per hydrogen iodide ion pair.

The experiments of Vandamme and of the author on the synthesis of hydrogen iodide give data for this reaction over a range of iodine pressure from 0.3 to 350 mm. All the data can be explained on the following basis: (*1*) for every hydrogen ion pair 6+ molecules of hydrogen iodide are formed; (*2*) for every seven iodine ion pairs 1 molecule of hydrogen iodide is formed; (*3*) for every hydrogen iodide ion pair 4 molecules of hydrogen iodide decompose. There is a further indication, from a few of the

author's runs at very low iodine pressure, that either an appreciable back reaction takes place, or not all the hydrogen ion pairs are used up in syntheses.

The author wishes to express her thanks and appreciation to Professor S. C. Lind under whose direction this research was done, and to Professors R. S. Livingston and George Glockler for their aid and criticism in the calculation of the experimental results.

REFERENCES

(1) Eyring, Hirschfelder, and Taylor: J. Chem. Phys. **4**, 479 (1936).
(2) Eyring, Hirschfelder, and Taylor: J. Chem. Phys. **4**, 570 (1936).
(3) Farkas and Bonhoeffer: Z. physik. Chem. **132**, 235 (1928).
(4) Giauque: J. Am. Chem. Soc. **53**, 507 (1931).
(5) Glasson: Phil. Mag. [6] **43**, 477 (1922).
(6) Glockler and Heisig: J. Phys. Chem. **36**, 769 (1932).
(7) Glockler and Livingston: J. Phys. Chem. **38**, 655 (1934).
(8) Kleeman: Proc. Roy. Soc. (London) **A79**, 220 (1907).
(9) Kolthoff and Furman: Volumetric Analysis, Vol. II, Practical Principles, p. 357. John Wiley and Sons, New York (1929).
(10) Lind: The Chemical Effects of Alpha Particles and Electrons, revised edition. The Chemical Catalog Co., Inc., New York (1927).
(11) Lind and Bardwell: J. Am. Chem. Soc. **47**, 2679 (1925).
(12) Ramsay and Young: J. Chem. Soc. **49**, 453 (1886).
(13) Stephens, H. N.: J. Am. Chem. Soc. **52**, 625 (1930).
(14) Truesdale and Lind: J. Am. Chem. Soc. **54**, 516 (1932).
(15) Vandamme: Bull. soc. chim. Belg. **41**, 597 (1932).

THE IRREVERSIBILITY OF PHOTOGRAPHIC DEVELOPMENT IN ELON SOLUTIONS CONTAINING SODIUM SULFITE[1]

ANGUS E. CAMERON

Kodak Research Laboratories, Rochester, New York

96-497

Received February 18, 1938

In a preceding publication in this Journal (2) the writer has presented evidence that the platinum electrode potentials which R. M. Evans and W. T. Hanson, Jr., (3) of these Laboratories measured in photographic developer solutions were not oxidation–reduction potentials but were functions of the partial pressure of oxygen with which the solutions were more or less in equilibrium. The explanation given by them for the existence of an oxidation–reduction potential in the presence of sodium sulfite, which can remove the oxidized forms of photographic developer chemicals by converting them into the reduced form of the monosulfonates, was that this sulfonation process was reversible and that there was thus maintained a small and essentially constant concentration of the oxidized form of the developing agent.

Sheppard (6) and, more precisely, Beukers (1) and Reinders (5) have shown that a reversible oxidation–reduction system, such as mixtures of ferric and ferrous ions in the form of organic complexes, could act either as a reducer or as an oxidizer upon a predeveloped photographic image. Evans and Hanson have attempted to show that this is also true for organic developers in the presence of sulfite.

Within the limits of stability of the oxidized forms, some, at least, of the developer chemicals give rise to reversible oxidation–reduction systems. Thus it was shown by Evans and Hanson that in solutions of amidol and oxidized amidol there was a definite reduction in density upon the high potential side of the equivalence point. However, in the presence of sodium sulfite the existence of any reversible oxidation–reduction system must be questioned. The data given by Evans and Hanson for amidol with slightly less than 1 mole of sodium sulfite per mole of reducing agent and in the presence of 8 g. of potassium bromide per liter would appear to indicate that a marked discontinuity occurred in the density–potential curve at the "equivalence" point and that the reduction in density occurring in solutions showing more positive potentials is, at best, very small.

[1] Communication No. 656 from the Kodak Research Laboratories.

Elon[2] was selected as the developer for the investigation reported here in order to avoid troubles caused by staining of the emulsion layer. The oxidation-reduction potential of the compound was known, as well as its "oxygen" electrode potential behavior in the presence of sodium sulfite.

EXPERIMENTAL

Motion picture positive film, No. 1301, was used for the experiments. Strips of 35-mm. film were exposed on a model 2B sensitometer, giving a series of twenty-one increasing exposures on each strip. These strips were developed for 5 minutes in D-16 (Eastman Kodak formula) at 18°C. with air agitation, rinsed in 1 per cent acetic acid, and thoroughly washed and dried in the dark. These strips were then numbered and slit lengthwise; one half of each strip was fixed in non-hardening alkaline sodium thiosulfate solution, washed, and dried. The fixed, or control strips, were then read with a Capstaff densitometer and the corresponding fixed and unfixed strips were immersed in the developer solutions for 15.5 hours with air or nitrogen agitation at 20°C. in the dark.

The glass developing tubes of half-liter capacity were jacketed and water from a 20°C. thermostat was pumped through the jackets. The film strips were suspended from the rubber stopper closing the top of the tube. Purified nitrogen or air was introduced through a perforated glass agitator tube at the bottom. A water-sealed trap permitted escape of gas from the tube. When nitrogen agitation was used, the solutions were swept out with nitrogen for an hour before the film was immersed. The nitrogen was purified by burning out the oxygen present with ammonia over a heated platinum catalyst. Ammonia was introduced by passing the gas over solid ammonium carbonate. Carbon dioxide was removed with soda lime before the gas entered the furnace tube. Excess ammonia was removed with a sulfuric acid wash.

After 15.5 hours in the developer solutions the strips were removed, washed briefly, immersed in an acid fixing and hardening bath for 5 minutes, washed thoroughly, and dried; the densities were then read on both strips. The results have been recorded as changes in density and have been plotted as a function of pH of the developer solutions. It is apparent that this is equivalent to plotting the *first* derivative of the density, and that an equivalence point of development will be shown by the reversal of sign of the change in density.

The solutions were read both before and after development with a glass electrode and platinum electrodes in atmospheres of controlled oxygen content. In many cases readings were taken with a silver electrode. The glass electrode was standardized against the hydrogen elec-

---

[2] Elon is a trade name for *p*-methylaminophenol.

trode in solutions of the same sodium-ion concentration, 1.5 *N* in all cases, in which sodium sulfite had been replaced with sodium sulfate. The buffer salt employed was, in most cases, potassium hydrogen phthalate.

TABLE 1

Results obtained with the first series of strips with nitrogen agitation

8 g. of elon, 8 g. of potassium bromide, and 6.25 g. of sodium sulfite per liter

pH	ΔD STEP 12	ΔD STEP 16	ΔD FOG	E_{air} BEFORE	E_{air} AFTER	E_{Ag}
				volts	*volts*	*volts*
3.63	−0.01	−0.01	−0.01	−0.046	−0.047	−0.080
4.18	0.01	0.00	−0.01	−0.002	−0.008	−0.082
5.20	0.05	0.04	0.01	−0.065	−0.087	−0.099
5.68	0.27	0.10	0.03	−0.092	−0.100	−0.138
6.12	0.53	0.40	0.13	−0.120	−0.144	−0.171
6.12	0.55	0.39	0.13	−0.113	−0.120	−0.180

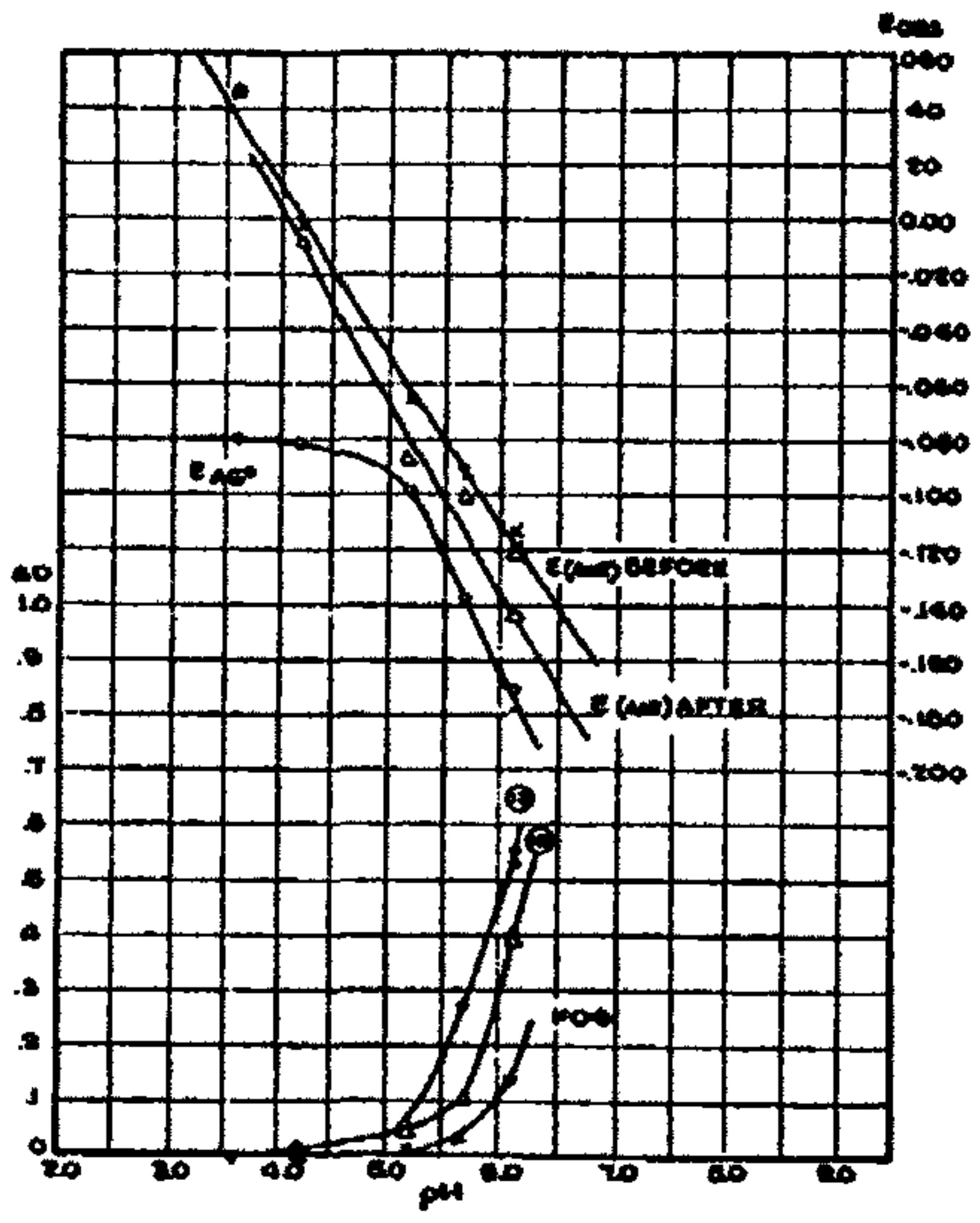

FIG. 1

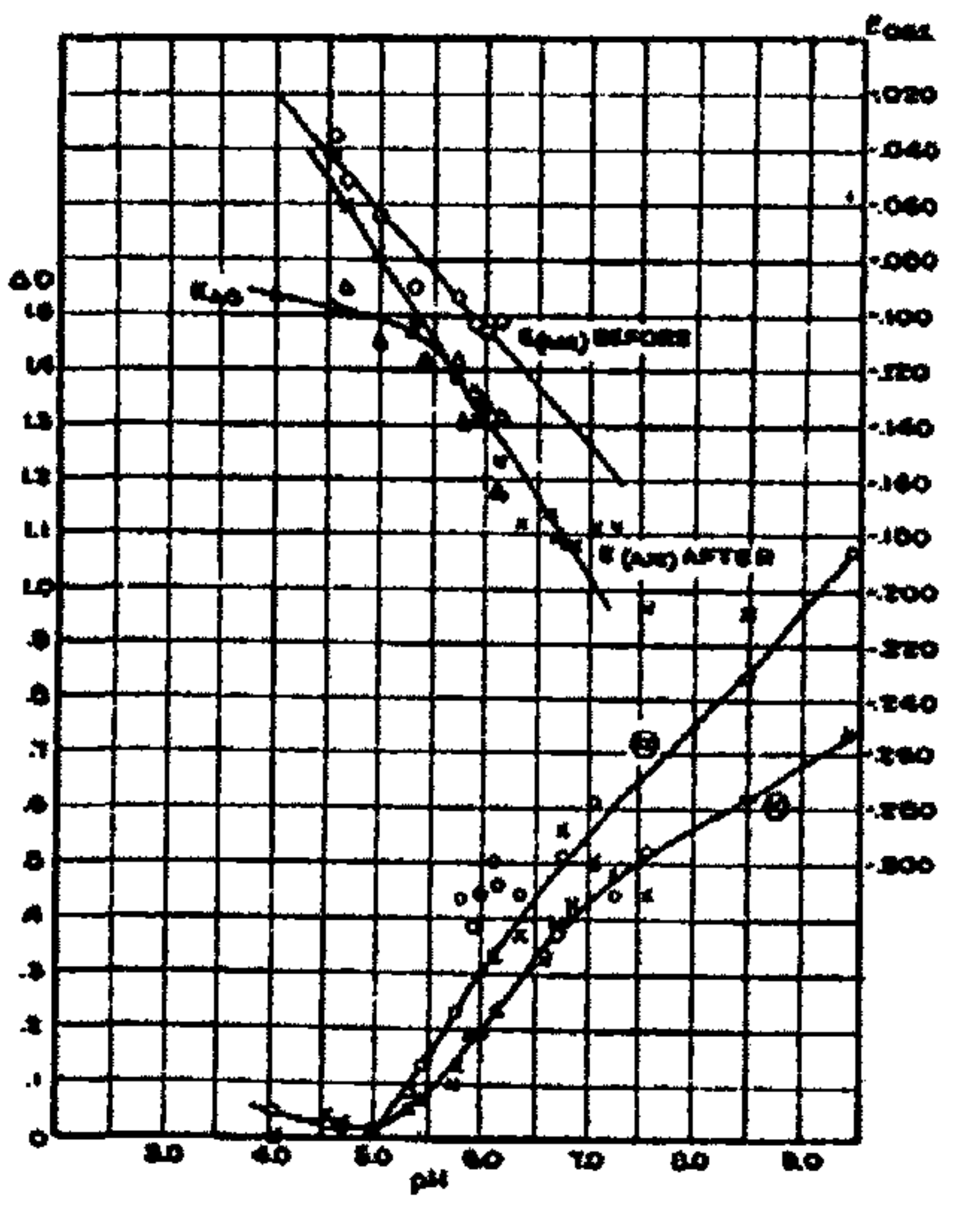

FIG. 2

FIG. 1. Change in density of predeveloped strips, and platinum and silver electrode potentials in air, as functions of the pH of the developer solution; 8 g. of elon, 8 g. of potassium bromide, and 6.25 g. of sodium sulfite per liter.

FIG. 2. Change in density of predeveloped strips, and platinum and silver electrode potentials in air, as functions of the pH of the developer solution; 8 g. of elon, 8 g. of potassium bromide, and 64 g. of sodium sulfite per liter.

Sulfuric acid was added when necessary to overcome the buffering effect of sodium sulfite in adjusting the pH to the desired value.

The 3.5 *N* calomel half-cell and bridge were used as a reference half-cell.

This combination was assigned a value of 0.2502 volt against the normal hydrogen electrode at 20°C. For convenience in comparing the results obtained and reported by Evans and Hanson, these potentials have been recorded as "observed potentials" and have not been converted to the hydrogen scale. The saturated calomel half-cell employed by Evans and Hanson is assigned a value of 0.2488 volt at 20°C.

TABLE 2

Measurements similar to those of table 1, but made with a tenfold greater concentration of sodium sulfite

8 g. of elon, 8 g. of potassium bromide, and 64 g. of sodium sulfite per liter

pH	ΔD STEP 12	ΔD STEP 16	ΔD FOG	E_{air} BEFORE	E_{air} AFTER	E_{Ag}
				volts	*volts*	*volts*
4.01	0.04	−0.01	−0.01	0.006	0.002	−0.093
4.57	0.02	0.04	0.01	−0.035	−0.041	−0.097
4.67*	0.01	0.02	−0.02	−0.052	−0.060	−0.090
5.00	0.01	0.01	0.01	−0.064	−0.077	−0.110
5.32*	0.08	0.05	0.00	−0.090	−0.102	−0.106
5.43	0.13	0.07	0.01		−0.117	−0.117
5.75	0.23	0.10	0.01	−0.094	−0.124	−0.117
5.80	0.43	0.13	0.02		−0.140	−0.139
5.93*	0.38	0.19	0.03	−0.104	−0.138	−0.129
6.00	0.44	0.19	0.03	−0.106	−0.135	−0.134
6.10	0.50	0.33	0.14		−0.165	−0.166
6.14	0.46	0.23	0.02	−0.112	−0.154	−0.138
6.35	0.44	0.37	0.35		−0.177	
6.60†	0.34	0.32	0.92		−0.173	
6.70†	0.37	0.39	1.00		−0.182	
6.75	0.51	0.56	0.50		−0.184	
6.85†	0.41	0.42	1.13		−0.184	
7.05†	0.61	0.50	2.39		−0.178	
7.25†	0.44	0.48	1.44		−0.177	
7.56	0.52	0.44	0.70		−0.207	
5.50	0.84	0.62	0.75		−0.208	−0.291
9.40	1.07	0.74	0.67		−0.240	−0.325

* Air agitation.

† Potassium dihydrogen phosphate buffer.

The first series of strips was developed in solutions of the following composition, sulfuric acid or sodium hydroxide being added as necessary to adjust the pH to the desired value: 8 g. of elon, 8 g. of potassium bromide, 6.25 g. of sodium sulfite (anhydrous), 20.2 g. of potassium acid phthalate, 106.5 g. of sodium sulfate (anhydrous), and water to make 1 liter. The results of this series with nitrogen agitation are given in table 1. These data appear graphically in figure 1, where the change in density and the potentials are plotted as functions of the pH of the solutions. Similar measurements with a tenfold greater concentration of sodium sulfite are

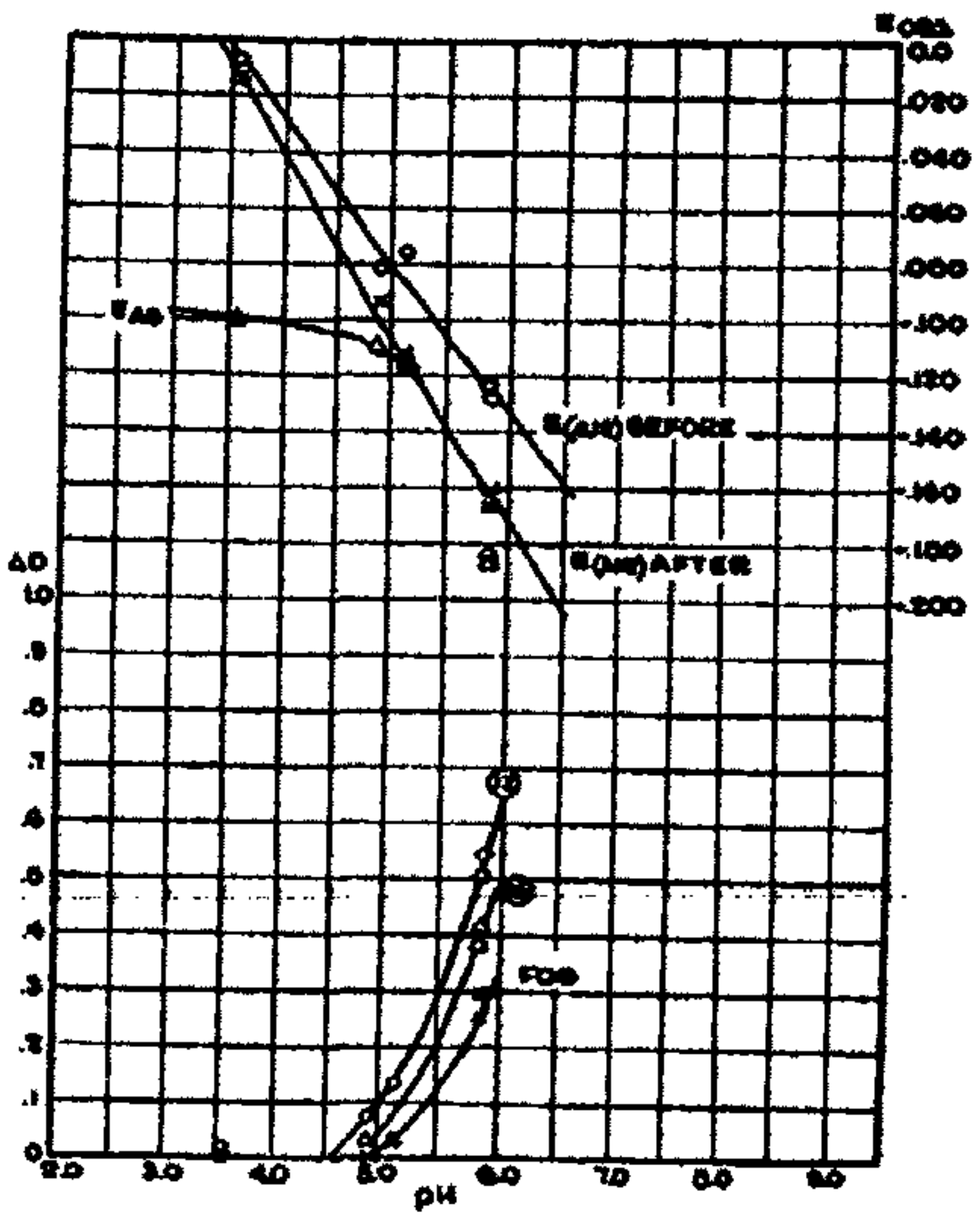

Fig. 3

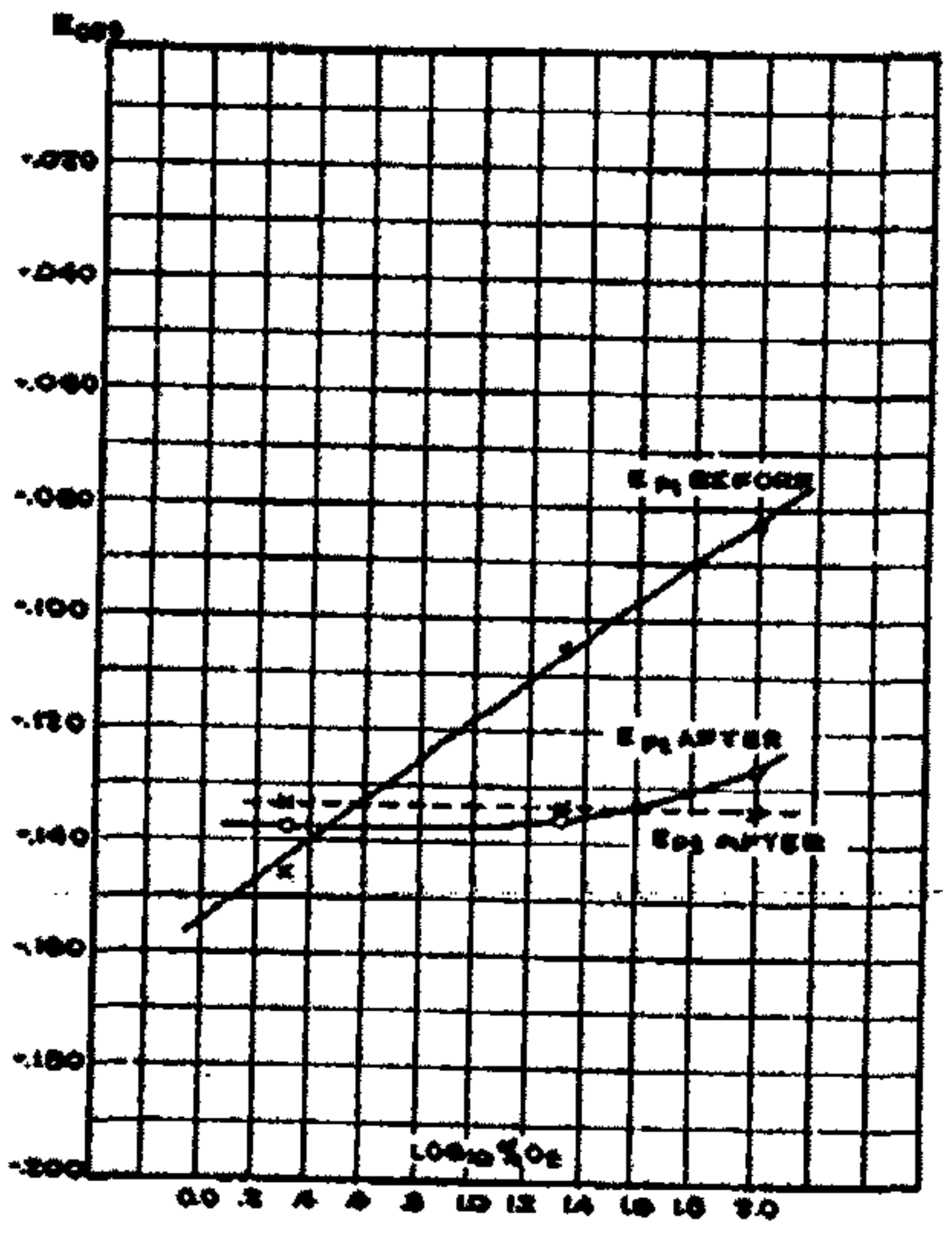

Fig. 4

Fig. 3. Change in density of predeveloped strips, and platinum and silver electrode potentials in air, as functions of the pH of the developer solution; 40 g. of elon, 8 g. of potassium bromide, and 29.2 g. of sodium sulfite per liter.

Fig. 4. Potentials of platinum and silver electrodes in air as functions of the partial pressure of oxygen at pH 6.0 in a developer containing 8 g. of elon, 8 g. of potassium bromide, and 64 g. of sodium sulfite per liter.

TABLE 3

Measurements in solutions containing five times the concentration of elon but with the ratio of elon to sodium sulfite the same as in table 1

40 g. of elon, 8 g. of potassium bromide, and 29.2 g. of sodium sulfite per liter

pH	ΔD STEP 12	ΔD STEP 16	ΔD FOG	E_{air} BEFORE	E_{air} AFTER	E_{Ag}
				volts	*volts*	*volts*
3.60	0.01	0.01	0.00	−0.007	−0.012	−0.100
4.93	0.07	0.03	−0.01	−0.081	−0.093	−0.108
5.15	0.13	0.03	0.03	−0.076	−0.112	−0.115
5.87	0.54	0.41	0.29	−0.128	−0.167	−0.184
5.87	0.50	0.38	0.25	−0.123	−0.161	−0.185

given in table 2. The change in fog density has been omitted from the plot of these data in figure 2 to avoid undue complication.

A third series of strips was run in solutions containing five times the concentration of elon but with the ratio of elon to sodium sulfite mole to mole as in the data of table 1. These data are shown graphically in figure 3.

DISCUSSION

From an examination of the plotted data it is apparent that on the acid side of the pH at which development continues there is no reduction in density. Estimating this point from the plotted data and reading the potentials of the "air" electrode at the same value of pH, the data in table 4 result. None of the potentials recorded is found to be in agreement with the value of –0.150 volt given by Evans and Hanson for amidol at this bromide concentration.

The point of continuation of development is not markedly influenced by a tenfold increase in the concentration of sulfite, but a fivefold increase in the elon concentration appears to cause a shift to a lower value of pH. The measurements made with air agitation show good agreement with those made with purified nitrogen. The control strips showed slight variations in density when read for the second time. Below pH 5 there were small decreases in the second densities. The first set of readings was used in determining the change of density in the predeveloped but unfixed strips.

TABLE 4

GRAMS OF ELON AND OF SODIUM SULFITE PER LITER	pH	E_{air} BEFORE	E_{air} AFTER
		volts	*volts*
8 g. of elon; 6.25 g. of sodium sulfite	5.0	–0.050	–0.062
8 g. of elon; 64 g. of sodium sulfite	5.0	–0.064	–0.081
40 g. of elon; 29.2 g. of sodium sulfite	4.8	–0.067	–0.084

Considerable variation appeared in the potentials of the same solution before and after development. This variation was not due to change in pH, because in every case the agreement between solutions before and after development was perfect or was within 0.05 pH unit. Figure 4 shows the behavior of the potentials before and after development as a function of the percentage of oxygen in the saturating atmosphere. The potential behavior of the platinum electrode after the film has been immersed in the solution for 15.5 hours is very much like that of a silver electrode. Kolthoff and Wang (4) have shown that gold and platinum electrodes in silver-ion concentrations greater than 0.01 M behave like silver electrodes and are independent of the hydrogen-ion concentration or the presence of oxygen. In low concentrations of silver ion, such as might exist in a developer solution of low reducing power in which silver has been dissolved by the sodium sulfite, platinum electrodes show this same behavior. Solutions in which colloidal silver is present after development show a shift in the dependence of the platinum electrode potentials upon the partial pressure of oxygen. This shift to lower values of the potentials can be produced by addition of colloidal silver to a solution which has not been in contact with photographic emulsion and appears to be the result of the catalytic effect of the metal upon the rate of autoxidation of the elon. The potential dependence upon the logarithm of the partial pressure of oxygen remains a straight line.

Examination of the plots of the silver electrode potentials as functions of pH shows that the silver-ion concentration decreases above the pH at which development is found to continue. It is perhaps not surprising that such is the case, for development in solutions of such low pH, compared to those usually used in photographic development, appears to be largely, if not entirely, due to reduction of silver ion present in solution with deposition of the finely divided silver upon the nuclei present in the predeveloped image.

SUMMARY

1. Attempts have been made to determine a reversal point of photographic development in solutions of elon containing sodium sulfite.

2. A point of "continuation" of development is found which is not markedly shifted by a tenfold increase in sulfite concentration and which shows a slight shift toward lower values of pH with a fivefold increase in elon concentration.

3. The "air" electrode potential of solutions at the pH of "continuation" of development does not agree with the potential reported by Evans and Hanson for the reversal point of development in amidol solutions containing sodium sulfite.

4. It is concluded that no reversible oxidation–reduction system exists in elon solutions containing sodium sulfite.

REFERENCES

(1) Beukers, M. F. C.: Fotografische Ontwikkelaars, Thesis, Delft, 1934.
(2) Cameron, A. E.: J. Phys. Chem. **42**, 521 (1938).
(3) Evans, R. M., and Hanson, Jr., W. T.: J. Phys. Chem. **41**, 509–34 (1937).
(4) Kolthoff, I. M., and Wang, Chin: J. Phys. Chem. **41**, 539–44 (1937).
(5) Reinders, W.: J. Phys. Chem. **38**, 783–96 (1934); IXth International Congress of Photography, pp. 345-6, Paris (1935).
(6) Sheppard, S. E.: J. Chem. Soc. **87**, 1311 (1905).

MEASUREMENTS OF THE IONIZATION CONSTANT OF BENZOIC ACID USING SILVER CHLORIDE ELECTRODES[1]

H. T. BRISCOE AND JOHN S. PEAKE

Department of Chemistry, Indiana University, Bloomington, Indiana

Received February 19, 1938

A method has been described by Harned and his coworkers for determining the ionization constants of weak acids and weak bases. In the present investigation this method has been applied to the determination of the ionization constant of benzoic acid.

Briefly, the method consists in measuring the electromotive forces of cells containing benzoic acid, sodium benzoate, and sodium chloride. These cells may be conventionally represented by

$$H_2 \mid HB(m_1), NaB(m_2), NaCl(m_3) \mid AgCl \mid Ag$$

The ionization constant, K, is calculated by means of the equation:

$$E - E_0 + \frac{RT}{F} \ln \frac{m_{Cl} m_{HB}}{m_B} = -\frac{RT}{F} \ln K' = -RT \ln \frac{\gamma_{Cl} \gamma_{HB}}{\gamma_B} \frac{-RT}{F} \ln K$$

At zero ionic strength ($\mu = 0$), $\ln \frac{\gamma_{Cl}\, \gamma_{HB}}{\gamma_B}$ becomes equal to zero, so that K' then equals K. Since E, E_0, and the molalities are measurable, K' can be determined for a number of solutions and its value at zero ionic strength be determined by extrapolation. The values of the electromotive forces of our cells and the corresponding values of the terms of the above equation are assembled in tables 1 and 2.

EXPERIMENTAL PROCEDURE

The solutions were prepared from recrystallized benzoic acid, sodium benzoate, and sodium chloride by weighing out the thoroughly dried solid reagents and adding them to weighed quantities of water.

Crystals of electrolytically deposited silver and metathetically precipitated silver chloride were used in the preparation of the silver–silver chloride electrodes. The hydrogen electrodes were prepared by the

---

[1] This paper is abstracted from the thesis presented by John S. Peake to the Faculty of the Graduate School of Indiana University in partial fulfillment of the requirements for the degree of Doctor of Philosophy.

method of Hammett and Lorch. The water and hydrogen were purified in the usual manner.

TABLE 1

Composition of solutions and electromotive forces of cells

SOLUTION	^{m}HB	$^{m}NaCl$	^{m}NaB	μ	E
I	0.01636	0.01197	0.01240	0.02445	0.5785
II	0.01385	0.02637	0.00670	0.03320	0.5472
III	0.02338	0.01009	0.00480	0.03381	0.5514
IV	0.01858	0.02877	0.00462	0.03363	0.5294
V	0.01734	0.02668	0.00516	0.03204	0.5354
VI	0.01879	0.06823	0.00900	0.07736	0.5229

TABLE 2

Calculation of ionization constant

SOLUTION	^{m}H	$\frac{E - E_0}{0.05916}$	$\log \frac{^{m}H b^{m}Cl}{^{m}B}$	$\log K'$	$K' \times 10^5$
I	0.00008	5.0243	−1.8065	−4.2178	6.056
II	0.00013	5.4953	−1.2760	−4.2193	6.035
III	0.00029	5.5662	−1.3394	−4.2268	5.932
IV	0.00024	5.1944	−0.9643	−4.2301	5.387
V	0.00020	5.2958	−1.0690	−4.2268	5.932
VI	0.00013	5.0845	−0.8556	−4.2289	5.903

Extrapolated value of $K' = K = 6.05 \times 10^{-5}$

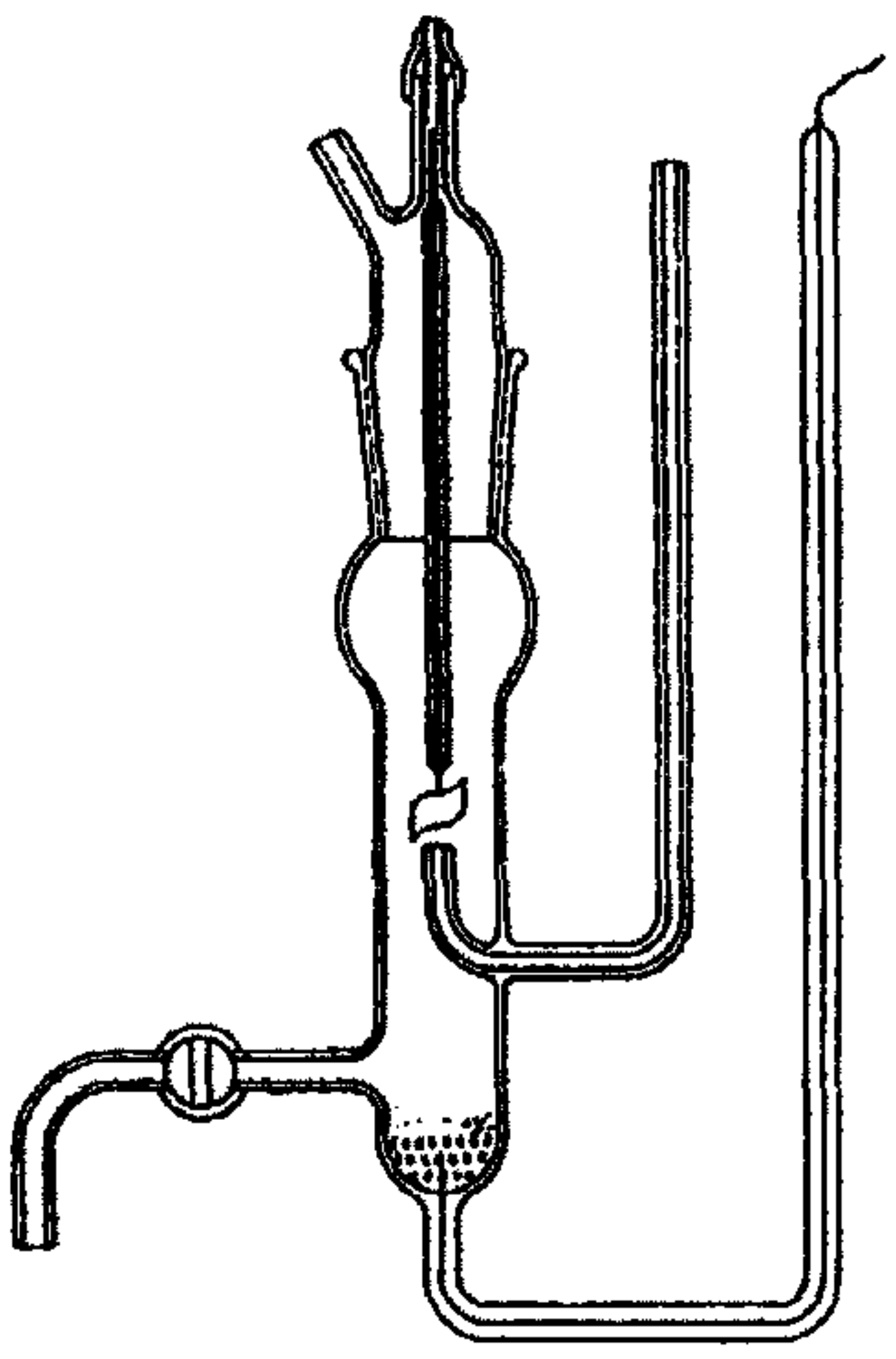

FIG. 1. The cell

The cells used in this investigation were contained in the glass vessel shown in the figure. The silver-silver chloride electrodes were placed in the bottom of the vessel as shown, and the vessel was filled with enough solution so that the platinum foil of the hydrogen electrode was covered. The electrodes were washed repeatedly by decantation with fresh solution. This solution was first saturated with hydrogen by bubbling it through the solution before it was used for washing the electrodes or filling the cell.

During measurements the cells were kept at 25°C. ± 0.02° by means of a thermostat, and readings were taken at 15-minute intervals until equilibrium was reached. Readings were made by means of a Leeds and Northrup Type K potentiometer and Type R reflecting galvanometer.

EXPERIMENTAL RESULTS

The values obtained for the electromotive force of cells using six solutions of benzoic acid, sodium benzoate, and sodium chloride have been listed in tables 1 and 2. Each E.M.F. value listed was obtained by comparing the values from six or more different cells containing the same solution. The molalities of the constituents of the solutions and the values of all terms of the equation for each solution are also listed in the tables. The value of E_0 is taken as 0.2221 volt.

Because of the extreme difficulty encountered in obtaining reproducible results with aqueous benzoic acid solutions in these cells, the accuracy is not claimed to be as high as that claimed by Brockman and Kilpatrick and by Saxton and Meier, who used the conductivity method. The electromotive forces were not reproducible to more than 0.1 millivolt. The difficulty in reproducibility was due chiefly to the fact that the range of acid concentrations that can be used is necessarily very small, and the activity of the hydrogen ion is limited to very low values in aqueous solutions owing to the low solubility of the acid.

This method for determining ionization constants has been found by Harned and his coworkers to yield very accurate results with acids of comparatively high solubility. The results of this investigation show that the method will also yield reasonably accurate results with the slightly soluble benzoic acid.

The value of 6.05×10^{-5} for K is slightly higher than the value of 5.9×10^{-5} obtained by Larsson from solubility measurements and lower than the values of 6.312×10^{-5} obtained by Brockman and Kilpatrick and of 6.295×10^{-5} obtained by Saxton and Meier, both from conductivity measurements. It is much lower than the value of 6.7×10^{-5} which was obtained by Kilpatrick and Chase from measurements with a quinhydrone electrode.

SUMMARY

Measurements of cells containing benzoic acid, sodium benzoate, and sodium chloride using silver-silver chloride electrodes gave a value of

6.05×10^{-5} for the ionization constant of benzoic acid in aqueous solutions.

REFERENCES

(1) Brockman and Kilpatrick: J. Am. Chem. Soc. **56**, 1483 (1934).
(2) Hammett and Lorch: J. Am. Chem. Soc. **55**, 70 (1933).
(3) Harned and Ehlers: J. Am. Chem. Soc. **54**, 1350 (1932).
(4) Harned and Owne: J. Am. Chem. Soc. **52**, 5079 (1930).
(5) Kilpatrick and Chase: J. Am. Chem. Soc. **53**, 1732 (1931).
(6) Larsson: Z. physik. Chem. **A148**, 148 (1930).
(7) Saxton and Meier: J. Am. Chem. Soc. **56**, 1918 (1934).

ELECTROKINETICS. XX. INTERFACIAL ENERGY AND THE MOLECULAR STRUCTURE OF ORGANIC COMPOUNDS. VI

THE ELECTRIC MOMENT OF ALIPHATIC ALCOHOLS, ACIDS, AND ESTERS AT CELLULOSE AND ALUMINUM OXIDE INTERFACES[1]

MAX A. LAUFFER AND ROSS AIKEN GORTNER

Division of Agricultural Biochemistry, University of Minnesota, St. Paul, Minnesota

Received February 19, 1938

INTRODUCTION

In previous papers in this series (3, 5) the electrokinetic properties of various solid-organic liquid interfaces were presented and discussed. In these papers, as in this one, it was assumed that the theory of Helmholtz is applicable to the electrical phenomena observed at such interfaces. The justification of this position will be presented in a subsequent paper. Using cellulose diaphragms and the streaming potential method, Martin and Gortner (5) studied the electrokinetics of a homologous series of aliphatic alcohols and of some of the substituted benzenes. Striking regularities were observed; for instance, the introduction of a methyl group into the main chain of an aliphatic alcohol changed the value of the zeta-potential by about 36 millivolts. Benzene gave no potential, and substituents in the ring influenced the zeta-potential in the order $NO_2 > NH_2 > Br > Cl > CH_3$. Jensen and Gortner (3), using the same method, studied normal fatty acids and esters at an aluminum oxide interface. Again regularities were observed within homologous series, together with an alternating effect of odd and even number of carbon atoms in the chain on electrokinetic functions. From the electric moment of the double layer and the moments of individual molecules, they calculated a function called "the percentage of 'unbalanced' orientation in the interface."

In view of the interesting relationships between electrokinetic functions and the molecular structure of organic compounds that were observed in these studies, it seemed to be desirable to extend the investigation. In-

---

[1] Paper No. 1594, Journal Series, Minnesota Agricultural Experiment Station. This paper is greatly condensed from a thesis presented by Max A. Lauffer, Jr., to the Graduate School of the University of Minnesota in partial fulfillment of the requirements for the degree of Doctor of Philosophy, June, 1937. The thesis containing detailed tabular data is on file in the library of the University of Minnesota.

asmuch as Martin and Gortner studied alcohols at cellulose interfaces, and Jensen and Gortner studied acids and esters at aluminum oxide interfaces, it seemed desirable to study alcohols at aluminum oxide interfaces and acids and esters at cellulose interfaces, in order to decide whether the regularities observed are fundamentally a property of the solid or of the liquid phase. This study was devoted to that task. As in the earlier studies, the streaming potential technic was used. In order to gain some insight into the mechanism of the electrical conductivity of organic liquids in diaphragms, the variations of the conductivity of methyl acetate in a cellulose diaphragm were studied with respect to temperature changes. In addition, the relationships of certain electrokinetic functions to temperature changes were also studied.

EXPERIMENTAL

Functions calculated

The electrokinetic function calculated in this study is the function introduced by Bull and Gortner (2), i.e., the electric moment of the double layer per square centimeter of surface (*qd*). This function imparts as much knowledge concerning the electrical properties of the interface as does the conventional zeta-potential, and it has the advantage of being free of a specific inductive capacity term and, therefore, of the hazardous assumptions concerning the magnitude of this effect in the region of the double layer. The equation presented by Bull and Gortner is,

$$qd = 2.262 \times 10^5 \frac{\eta H \kappa_s}{P} \tag{1}$$

where qd = electric moment per square centimeter expressed in electrostatic units,

η = the coefficient of viscosity,

H = the streaming potential in volts,

κ_s = the specific conductivity of the liquid in the diaphragm, and

P = the pressure in centimeters of mercury.

The values for viscosity at 30°C. used in the calculations are shown in table 1. Most of the values are interpolated from data found in the International Critical Tables. Those for *n*-butyl and *n*-amyl acetates are taken from Jensen and Gortner (3). The viscosities of *n*-amyl, *n*-hexyl, and *n*-heptyl alcohols, and of ethyl *n*-valerate, ethyl *n*-caproate, and ethyl *n*-heptylate were determined with an Ostwald viscometer.

Apparatus

The apparatus used to evaluate H/P and κ_s is a modification of the general type used in the earlier studies. In order to surmount the difficulty of finding suitable gaskets for the earlier type of streaming potential cell, a Pyrex streaming potential cell was designed which has ground-glass joints. Figure 1 shows the new cell in detail. The compartment in which the diaphragm is packed is made by fusing together the outside parts of two 15/30 ground-glass tapers. The electrodes are made of 80-mesh platinum gauze welded onto a platinum grid, and are permanently mounted on the ends of the inside parts of the two standard tapers. Each is held in place by the tension on the platinum wire which connects it to the tungsten seal in the end of the cell.

The general apparatus was so designed that streaming potential values up to about 165 volts could be measured. This was accomplished by using a battery consisting of a variable number of dry cells in series with the potentiometer. These cells were standardized from time to time by shorting their terminals through a megohm resistor and bucking a known fraction of the potential drop with a potentiometer. The E.M.F. values of the cells did not change appreciably with time.

TABLE 1

Showing the viscosity values used for the liquids studied

ORGANIC LIQUID	$(\eta) \times 1000$	ORGANIC LIQUID	$(\eta) \times 1000$
Methanol	5.2	*n*-Caproic acid	25.6
Ethanol	10.0	Methyl acetate	3.44
n-Propanol	17.6	Ethyl acetate	4.01
Isopropanol	18.0	*n*-Propyl acetate	5.13
n-Butanol	23.0	*n*-Butyl acetate	6.58
Isobutanol	11.37	*n*-Amyl acetate	7.57
n-Amyl alcohol	27.9	Ethyl formate	3.75
n-Hexanol (1-hexanol)	37.6	Ethyl propionate	4.73
n-Heptanol (1-heptanol)	38.4	Ethyl *n*-butyrate	6.04
Acetic acid	10.4	Methyl formate	3.17
Propionic acid	9.63	Ethyl *n*-valerate	7.35
n-Butyric acid	13.4	Ethyl *n*-caproate	9.12
n-Valeric acid	18.6	Ethyl *n*-heptylate	10.7

Conductivity measurements may be made using alternating current, or, for systems of very low conductivity, using direct current. The high-resistance end of the circuit was carefully insulated with all points of contact to supports made of sulfur.

Materials

Diaphragm materials used in these studies were cellulose and aluminum oxide. The cellulose was prepared from Schleicher and Schüll filter paper No. 589, as previously described (5). Immediately before use, it was again dried in a vacuum oven at 94°C. for at least 8 hours. The aluminum oxide was a part of the supply used by Jensen and Gortner (3). Immediately before using, it was dried in a vacuum at 94°C. for at least 8 hours. The organic liquids studied were chemicals of high quality (generally Eastman C.P. chemicals), and they were further purified by fractional distillation, end fractions being discarded and only that portion being retained which boiled in a narrow correct range.

Preparation of diaphragms

In the preparation of the cellulose diaphragms, one end of the diaphragm compartment of the streaming cell was placed over an inside taper fitted with a perforated gold disk on its end and permanently mounted over a heavy suction flask. Cellulose fibers, which had been soaked for at least 24 hours in the organic liquid to be studied, were then packed into the compartment, compressing with the flattened end of a stirring rod to obtain uniform packing. Excess liquid was drawn off by suction. The cell was then ready to be assembled.

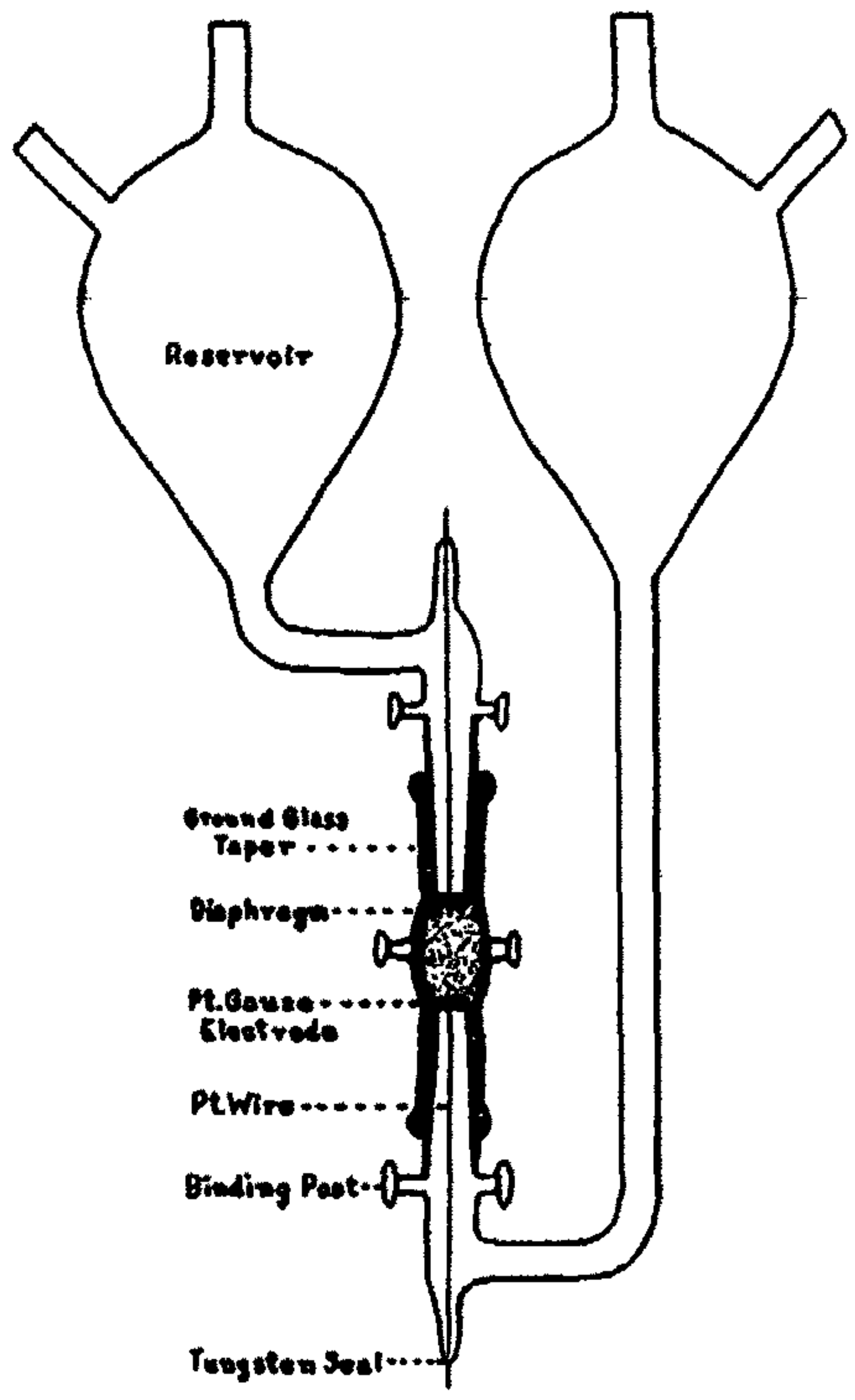

FIG. 1. Design of streaming potential cell

A somewhat different technic was necessary in preparing the aluminum oxide diaphragms. Since the particles of aluminum oxide were small enough to pass through the pores of the electrodes, a small cap of percale was fitted over each electrode. This cloth disk was cut with a slightly larger diameter than that of the electrode, allowing the margins to fold over the perimeter of the circular electrodes and to fit into a cylindrical groove 0.3 mm. deep and 5 mm. long, ground from the inside taper just adjacent to the electrode. Hence the cloth cap was held in place between the ground-glass walls of the inside and outside tapers, but did not prevent a tight fit of the glass joint. After one end of the diaphragm compartment was fitted to its half of the streaming cell, aluminum oxide, which had been suspended for at least 24 hours in the liquid to be studied, was packed as tightly as possible into the compartment, using suction and the flattened end of a stirring rod. The assembly of the cell was now completed. The cloth over the electrodes did not cause any appreciable error in the streaming potential, because the pressure gradient through the cloth was negligible as compared to that across the diaphragm.

Measurement of streaming potential

After the diaphragm had been packed and the streaming cell assembled, it was filled with the liquid to be studied and placed in a constant-temperature cabinet where it was allowed to remain for at least an hour before any measurements were made. Electrical contacts were made through mercury wells. The details of measurement are similar to those described in the previous papers.

In the measurement of the streaming potentials of systems with very high resistances (order of magnitude of 1000 megohms or more) the electrodes of the streaming cell were short-circuited through a high resistance (usually an 11-megohm resistor). From a practical point of view this operation lowers the probability of electrical leaks in the high-resistance end of the circuit and lowers the streaming potential which must be measured. The theoretical justification and significance of this operation will be discussed in a subsequent publication.

Measurement of specific conductivity of liquid in diaphragm

In order to determine the specific conductivity of organic liquids in the diaphragm, the conductivity in the diaphragm and the cell constant must be measured. For measurement of extremely low conductivities, the direct current circuit described by Jensen and Gortner (3) was used. The higher values of conductivity found in some systems were measured by the Wheatstone bridge principle, using an alternating current galvanometer and a 60-cycle 6-volt alternating current.

The cell constant was determined after displacing the liquid in the diaphragm by streaming 75 cc. of 95 per cent ethyl alcohol, 300 cc. of water, and finally about 100 cc. of $N/10$ potassium chloride through the diaphragm, and then measuring the conductivity with $N/10$ potassium chloride by the Wheatstone bridge principle. Specific conductivities of $N/10$ potassium chloride at various temperatures are taken from Reilly, Rae, and Wheeler (6). In this work the cell constant is defined as the specific conductivity of $N/10$ potassium chloride divided by the conductivity of the solution in the diaphragm. Hence the specific conductivity of the organic liquid in the diaphragm becomes its conductivity in the diaphragm multiplied by the cell constant.

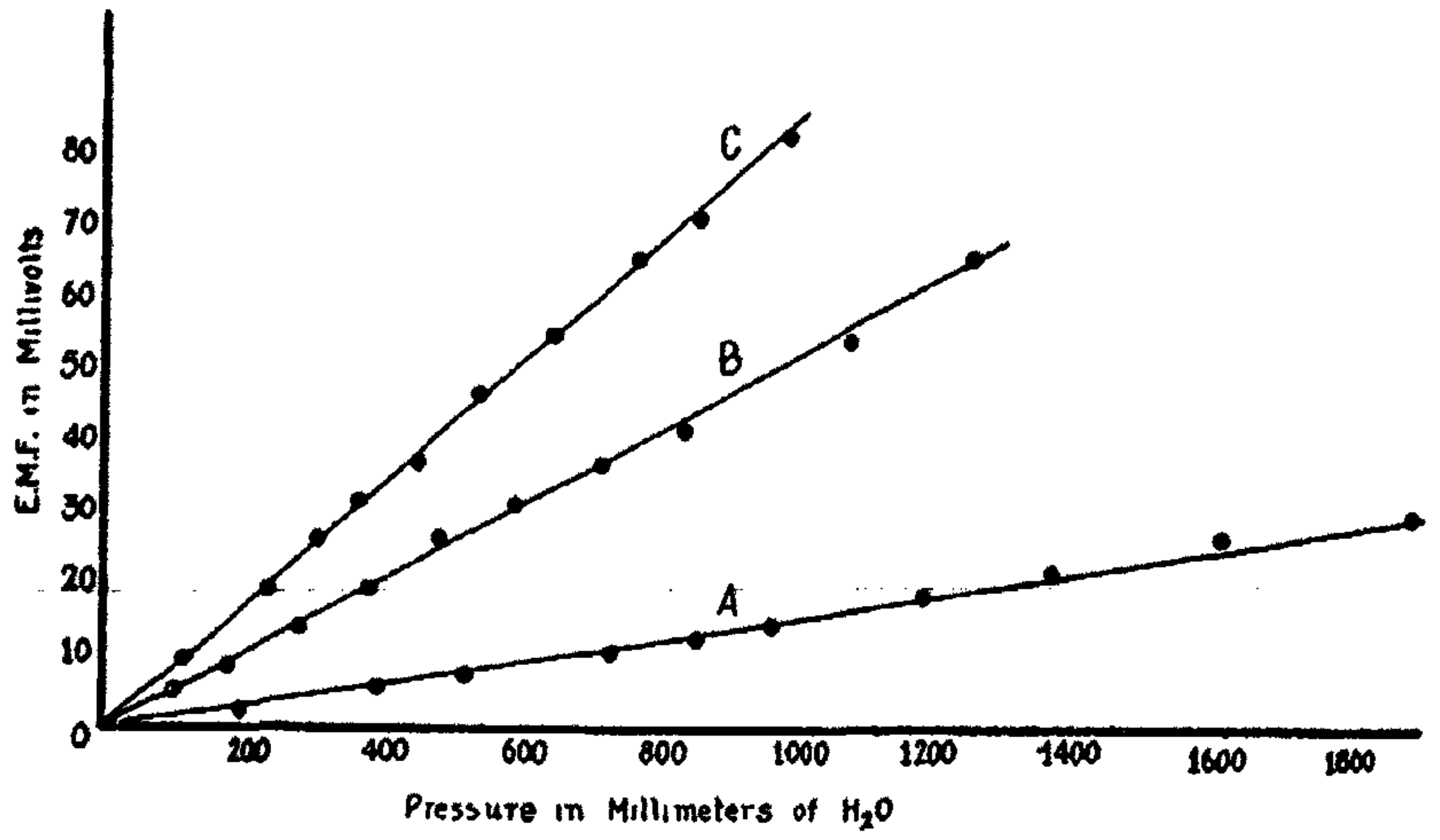

FIG. 2. Showing direct proportionality between streaming potential and hydrostatic pressure. Curve A = *n*-propionic acid at cellulose interface. Curve B = *n*-propanol at aluminum oxide interface. Curve C = ethyl *n*-propionate at cellulose interface.

TABLE 2

Summary of data on aliphatic alcohols at aluminum oxide interfaces at 30°C.

ALCOHOL	SIGN OF CHARGE ON Al_2O_3 SURFACE	H/P	κ_s	qd
		mv. per cm. Hg	*mhos*	*e.s.u. per cm.* $\times 10^5$
Methanol	−	6.82	2.73×10^{-5}	21.8
Ethanol	−	13.19	3.17×10^{-6}	9.42
n-Propanol	−	6.99	2.32×10^{-6}	6.47
Isopropanol	+	35.2	5.15×10^{-7}	7.36
n-Butanol	−	15.43	2.22×10^{-7}	1.78
Isobutanol	+	26.65	1.492×10^{-7}	1.02
n-Amyl alcohol	+	75.3	7.67×10^{-8}	3.68
n-Hexanol	+	123.7	1.162×10^{-7}	12.24
n-Heptanol	+	219.5	1.364×10^{-8}	2.60

The experimental data

In each system investigated from ten to fourteen independent determinations were made of the streaming potential which developed under different hydrostatic pressures. The pressures used ranged from less than 100 mm. of water to 1500–2000 mm. of water except in the cases of *n*-butyric acid, *n*-valeric acid, and *n*-caproic acid, where pressures ranging from 40 to 850 mm. of mercury were employed. Typical series of data are shown in figure 2, where the E.M.F. developed is plotted against the pressure of streaming. Curve A is for *n*-propionic acid and curve C for ethyl propionate at cellulose interfaces. Curve B is for *n*-propanol at an aluminum oxide interface. In all cases the data could be fitted to a straight line

TABLE 3

Summary of data on aliphatic acids at cellulose interfaces at 30°C.

ACID	SIGN OF CHARGE ON CELLULOSE SURFACE	H/P	ϵ_s'	qd
		mv. per cm. Hg	*mhos* × 10^6	*e.s.u. per cm.* × 10^6
Acetic acid	+	21.4	1.732	8.74
Propionic acid	+	2.10	2.43	1.12
n-Butyric acid	–	0.457	2.49	0.345
n-Valeric acid	–	0.780	2.365	0.773
n-Caproic acid	–	0.996	2.42	1.40

TABLE 4

Summary of data on aliphatic esters at cellulose interfaces at 30°C., using an 11-megohm shunt

ESTER	SIGN OF CHARGE ON CELLULOSE SURFACE	H/P	ϵ_s'	qd
		mv. per cm. Hg	*mhos* × 10^7	*e.s.u. per cm.* × 10^4
Methyl acetate	–	56.9	3.07	13.65
Ethyl acetate	–	24.3	2.595	5.72
n-Propyl acetate	–	11.05	2.45	3.13
n-Butyl acetate	–	10.7	2.30	3.67
n-Amyl acetate	–	5.17	2.385	2.105
Ethyl formate	–	48.7	2.855	11.80
Ethyl propionate	–	11.51	2.445	3.02
Ethyl *n*-butyrate	–	8.80	2.365	2.85
Methyl formate	–	113.8	2.72	22.3
Ethyl *n*-valerate	–	9.60	2.95	4.71
Ethyl *n*-caproate	–	7.05	3.66	5.33
Ethyl *n*-heptylate	–	5.69	3.00	4.14

passing through the point of origin. Accordingly H was found to be proportional to P for all studies reported in this paper. This agrees with the earlier studies and is an essential requirement if the theory of Helmholtz is to be applied to organic liquids at interfaces.

Since the ratio H/P was found to be a constant, the individual measurements are not presented in detail; summaries are given in tables 2, 3, 4, and 5. In these tables the value H/P is taken to be the slope of the line which best fits the points obtained by plotting H against P, as is illustrated in figure 2. In some instances the function κ_s' is reported instead of κ_s. This function is defined as the conductivity of the system, diaphragm in parallel with shunt, multiplied by the cell constant of the diaphragm.

TABLE 5

Summary of data on effect of temperature on a methyl acetate-cellulose interface

TEMPERATURE	H/P	κ_s	$H\kappa_s/P$
°C.	*mv. per cm.* Hg	*mhos* × 10^6	× 10^6
40	522	3.82	20.0
35	498	3.67	18.27
30	488	3.41	16.67
26.8	492	3.245	16.0
21	501	2.905	14.58

DISCUSSION

We have noted that for all of our series of data the plot of H/P was essentially a straight line passing through the point of origin. Martin and Gortner (5) and Martin (4) found a change of the function, zeta, with pressure for certain alcohols at cellulose interfaces. In their studies a value of zeta was calculated for every observation of pressure and potential, using the equation,

$$\zeta = \frac{4\pi H\kappa_s\eta}{P\epsilon} \tag{2}$$

In the cases of methanol and isopropanol (2-propanol) zeta changed rapidly when pressure was varied in the low pressure range, while little or no change of zeta took place with changes of pressure at higher values of P. In the ethanol-water-cellulose system, a reversal in the sign of zeta was reported for low values of P. (The system described as ethanol-water-cellulose was a system the liquid phase of which was water, the solid phase being cellulose which had been in contact with ethanol before water was introduced into the cell.) Isobutanol (2-methyl-1-propanol) at a cellulose interface showed this effect to a smaller degree than did isopropanol or methanol. Ethanol, 1-propanol, and 1-butanol showed the effect to only a very slight degree.

In figure 3, *H* is plotted against *P* for Martin's data on (A) methyl alcohol, (B) ethanol, (C) ethanol water, (D) *n*-propanol (1-propanol), (E) isopropanol, (F) *n*-butanol (1-butanol), and (G) isobutanol at cellulose interfaces. An inspection of this figure shows that the data for all of these systems fall on essentially straight lines. The curves fail to pass through the origin by a considerable margin in the cases of methanol, isopropanol, and ethanol-water, fail by a small margin in the case of isobutanol, and practically pass through it in the cases of ethanol, *n*-propanol, and *n*-butanol. It is seen, then, that the zeta-pressure effect that he reports parallels the extent to which the *H*/*P* curves fail to pass through the origin of coördinates. It is possible to explain this failure of some of the curves to pass through the origin by assuming that an erroneous value

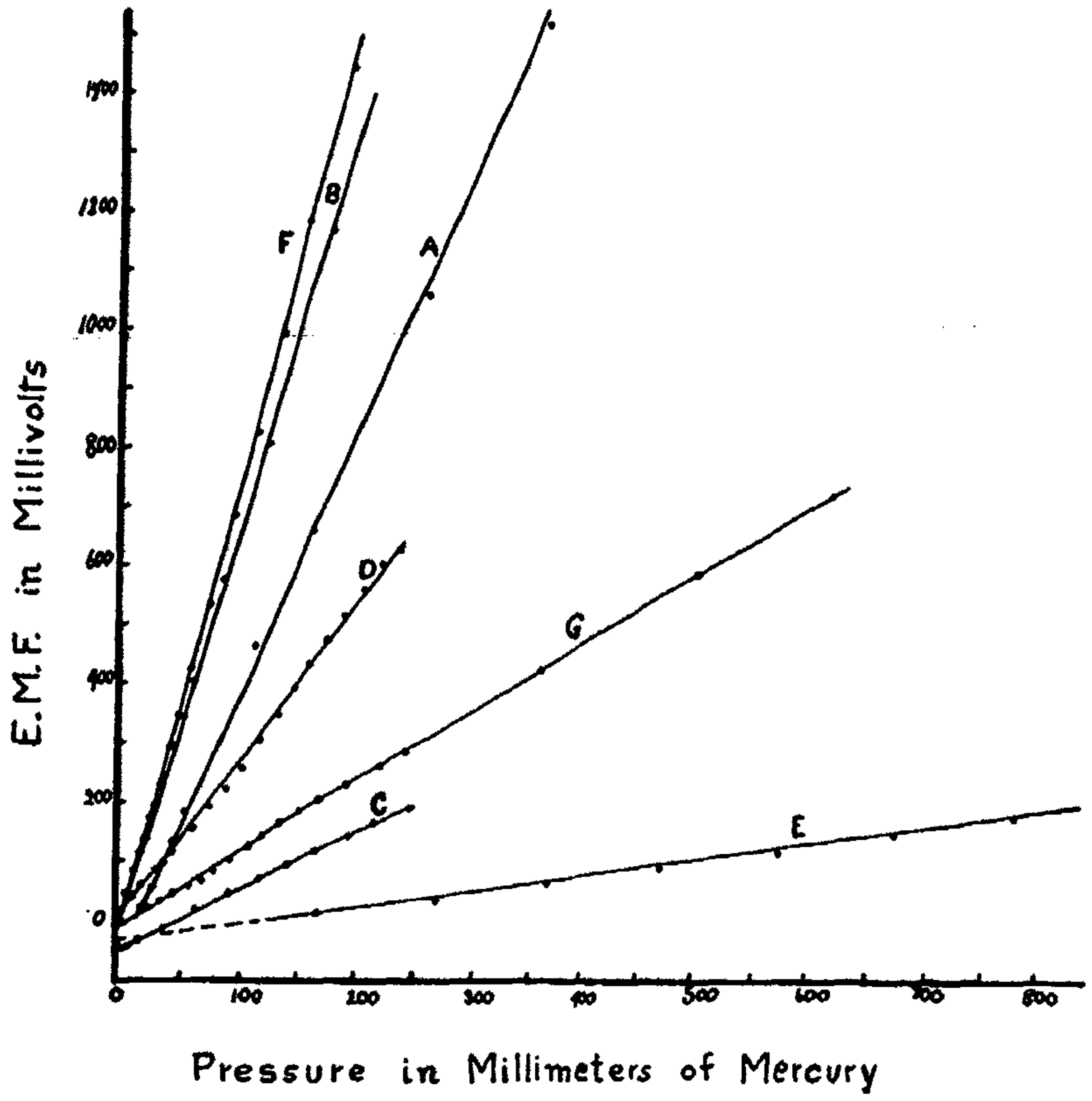

FIG. 3. Data of Martin and of Martin and Gortner for a variety of alcohols at a cellulose interface (for description see text).

for the zero point of the electrometer had been used. Such a mistake could easily be made if the zero point were taken to be the position of the electrometer needle when the circuit is open.

The behavior of organic liquids at interfaces

Figure 4 shows the way in which the electric moment of the double layer at aluminum oxide interfaces varies from alcohol to alcohol as one builds up the length of the carbon chain. Figure 5 contains the data of Martin and Gortner (5) for the same alcohols recalculated to show the same relationship at a cellulose interface. They considered their data for n-pentanol of doubtful value, since n-pentanol of unquestioned purity was not available at the time they made their determinations. The magnitudes of the electric moments are about twice as great for alcohols at cellulose interfaces as they are for alcohols at aluminum oxide interfaces.

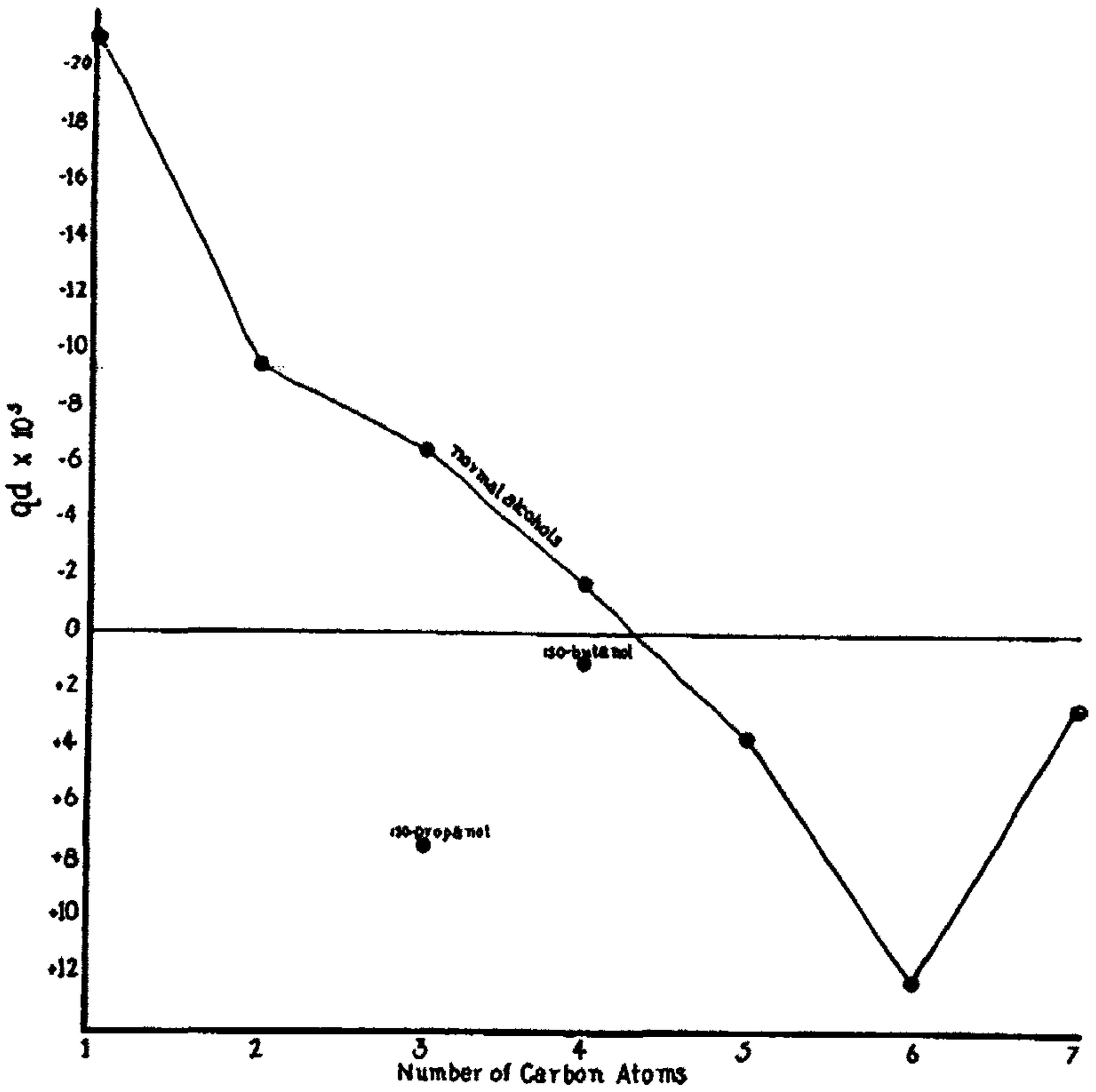

FIG. 4. The variation in the electric moment at an alcohol-aluminum oxide interface plotted as a function of the number of carbon atoms in the alcohol molecule.

Figure 6 shows the variation of the electric moment of the double layer at cellulose-fatty acid interfaces as one increases the number of carbons in the chains of the simple fatty acids. The relationship is quite regular. It will be noticed that there is a reversal of the sign of the charge on the

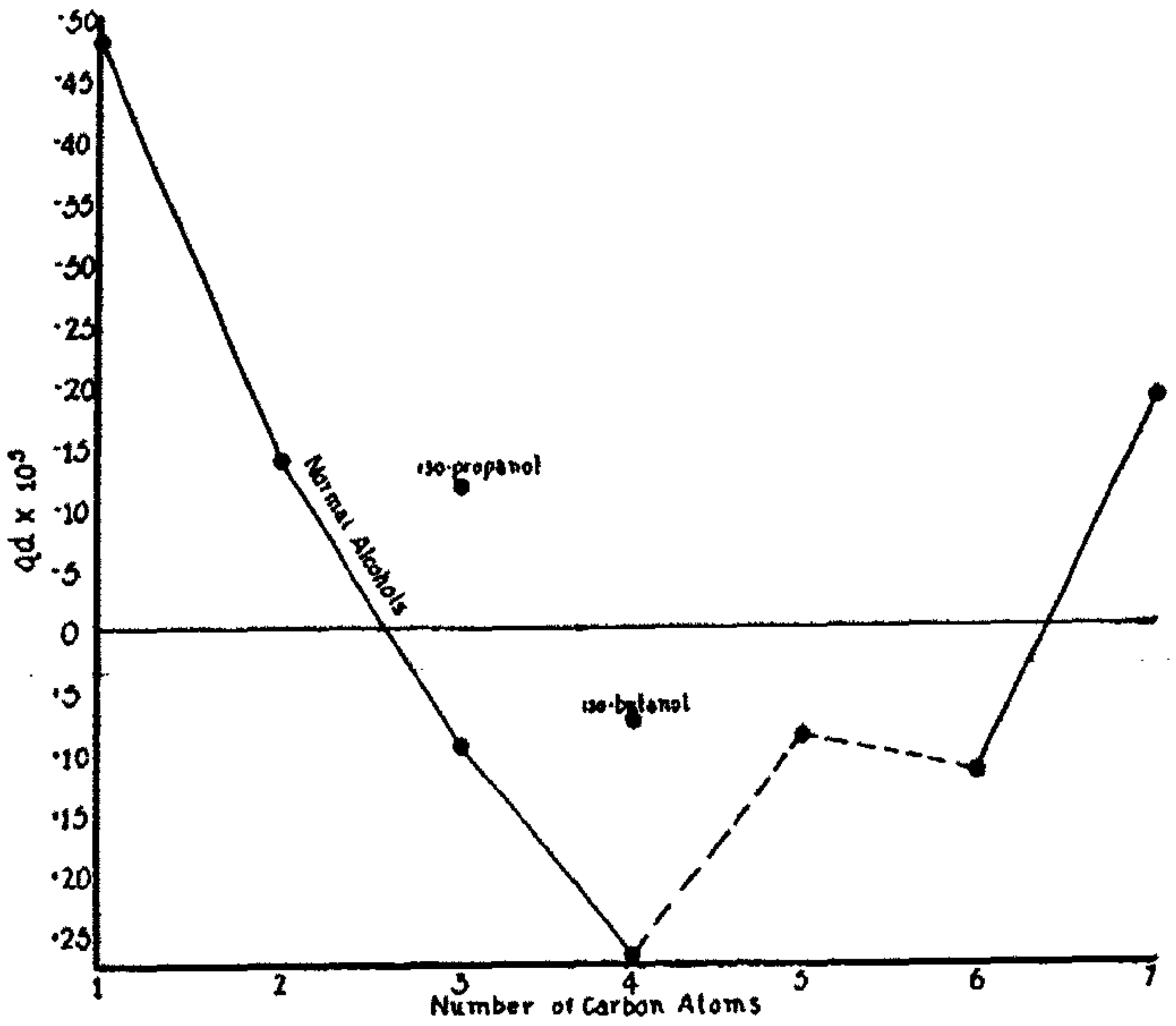

FIG. 5. Data similar to those in figure 4 except for an alcohol-cellulose interface (plotted from recalculated data of Martin and Gortner).

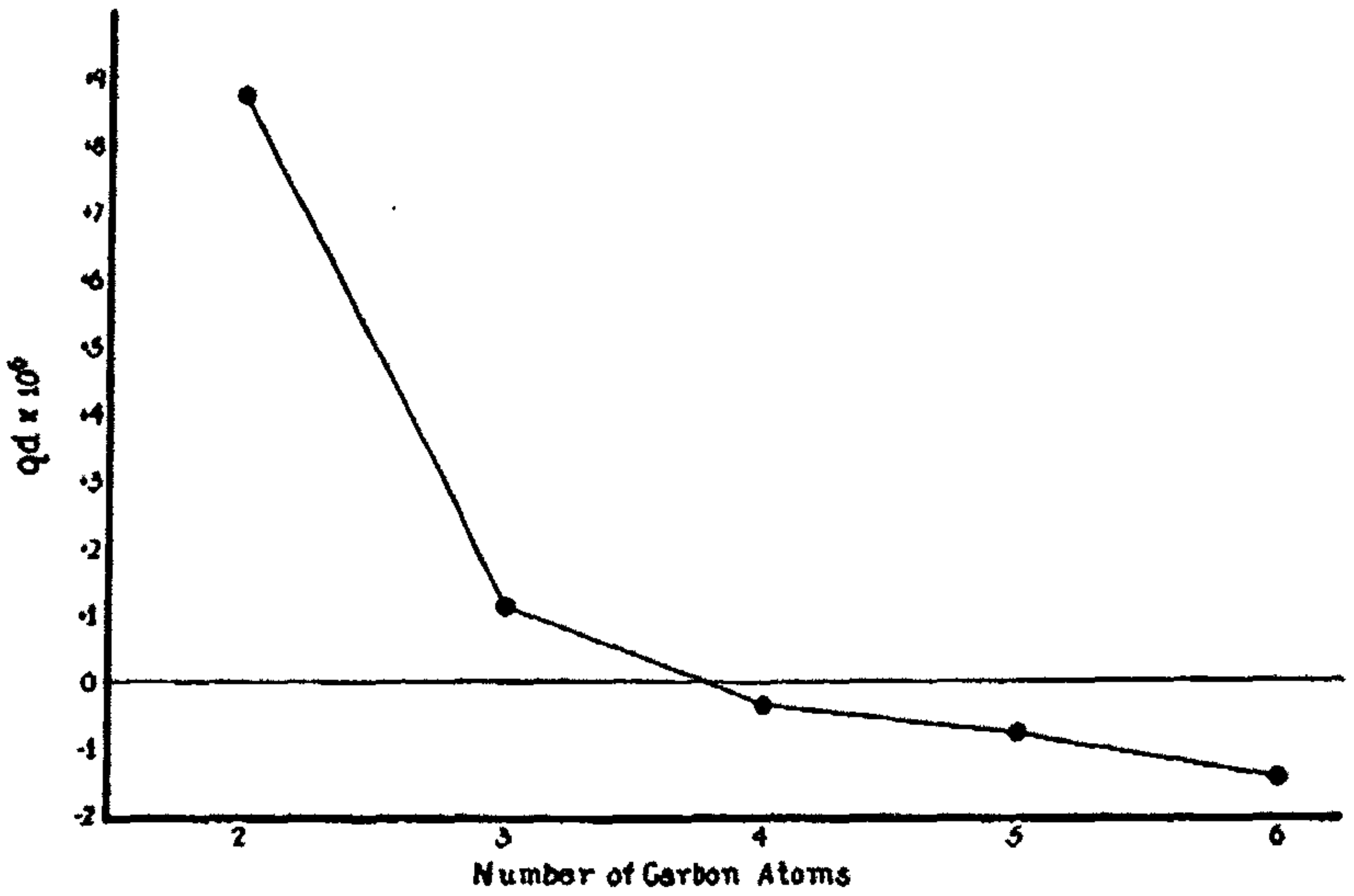

FIG. 6. The electric moment at a fatty acid-cellulose interface plotted as a function of the number of carbon atoms in the normal acid.

surface when one goes from three to four carbon atoms in the chain of the acids. Jensen and Gortner (3) found values for *qd* for the same acids at aluminum oxide interfaces that are about ten times as large as these values at a cellulose interface. Furthermore, in all of their studies with acids the sign of the charge on the surface of the solid was found to be positive.

In figure 7 we find the electric moments of esters at cellulose interfaces shown in relation to the number of carbon atoms in the chain of the ester. The unbroken line (*A*) connects points which represent the electric moments of double layers of the esters of acetic acid at the cellulose interface, whereas the broken line (*B*) connects points which represent the electric moments of the esters of ethyl alcohol. Point *D* is the moment for methyl formate at a cellulose interface. In a crude way the electrical properties of esters at cellulose interfaces seem to be related to the number of carbon atoms in the chain of the esters. The broken line (*C*) was copied from the line joining the points in figure 6 with the sign ignored, displaced the distance of one carbon atom to the right on the horizontal axis, and displaced somewhat along the vertical axis. However, no distortion of the shape of the curve was made. This curve was drawn in figure 7 in order to show the striking similarity between the actual magni-

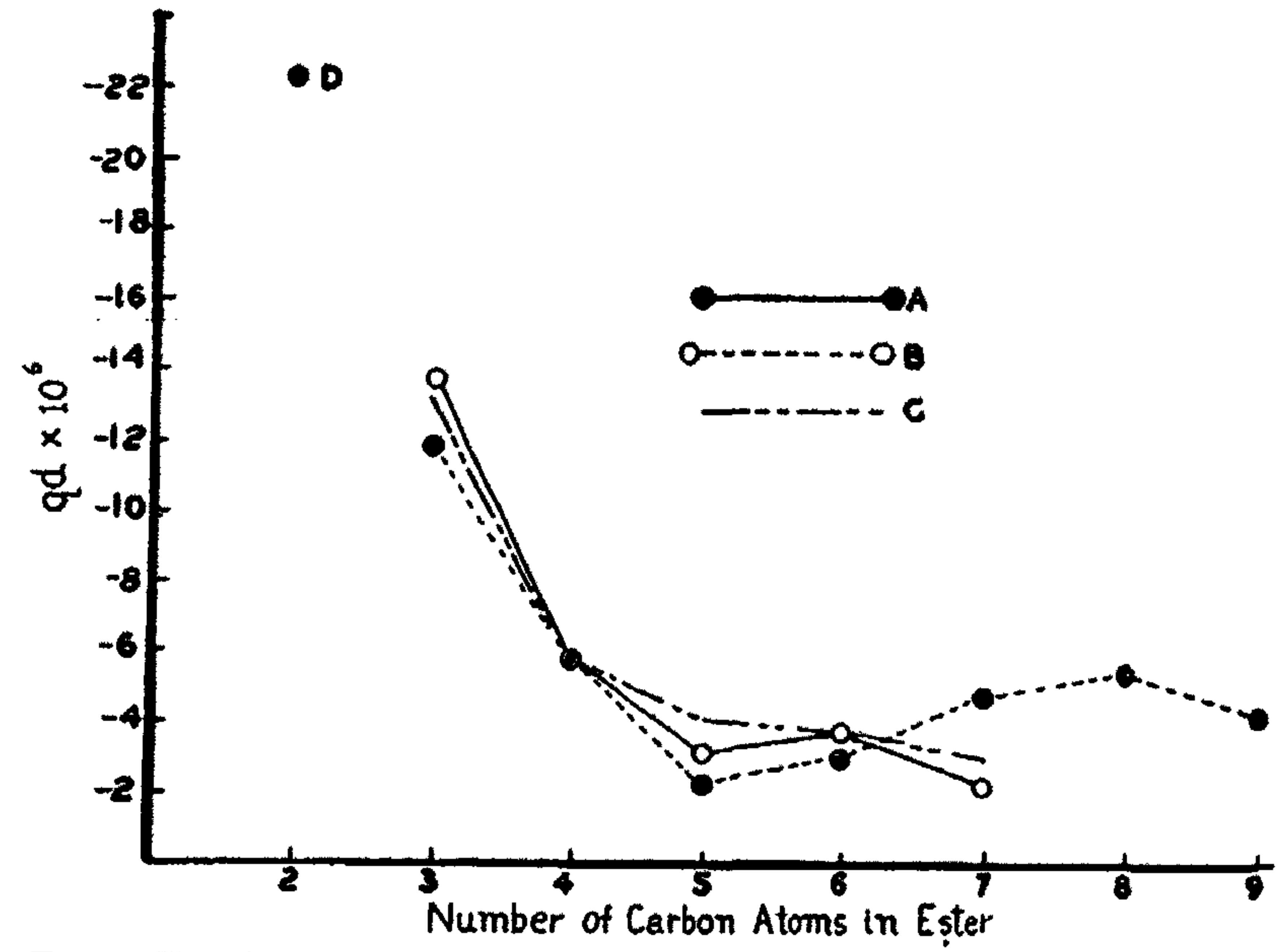

FIG. 7. The electric moment of a series of aliphatic esters at a cellulose interface plotted as a function of the number of carbon atoms in the ester. A = esters of acetic acid; B = esters of ethyl alcohol; C = the curve in figure 6 somewhat displaced with reference to coördinates to indicate similarity (see text); D = electric moment of methyl formate.

tude of the variations in electric moment of the double layer at cellulose interfaces as one ascends homologous series of acids on the one hand, and esters on the other hand. The data of Jensen and Gortner (3) for the same esters at aluminum oxide interfaces show negative surfaces, with the exception of ethyl formate, which is positive. Methyl formate, ethyl valerate, ethyl caproate, and ethyl heptylate were not included in their study. The values of the moments for the systems which they studied are about three times as great as are the ones reported for esters in this study. Their data show no similarities between the ethyl alcohol series of esters and the acetic acid series.

Figure 8 shows the way in which the conductivity of methyl acetate in a cellulose diaphragm and the electrokinetic function, $H\kappa_s/P$, measured for that system, vary with temperature. The values shown are plotted as the percentage of the values at 40°C. The variation of the specific conductivity of $N/10$ potassium chloride with temperature is included in the figure in order to point out the similarity between the temperature coefficient for the conductivity of potassium chloride and that for the conductivity of methyl acetate in the diaphragm.

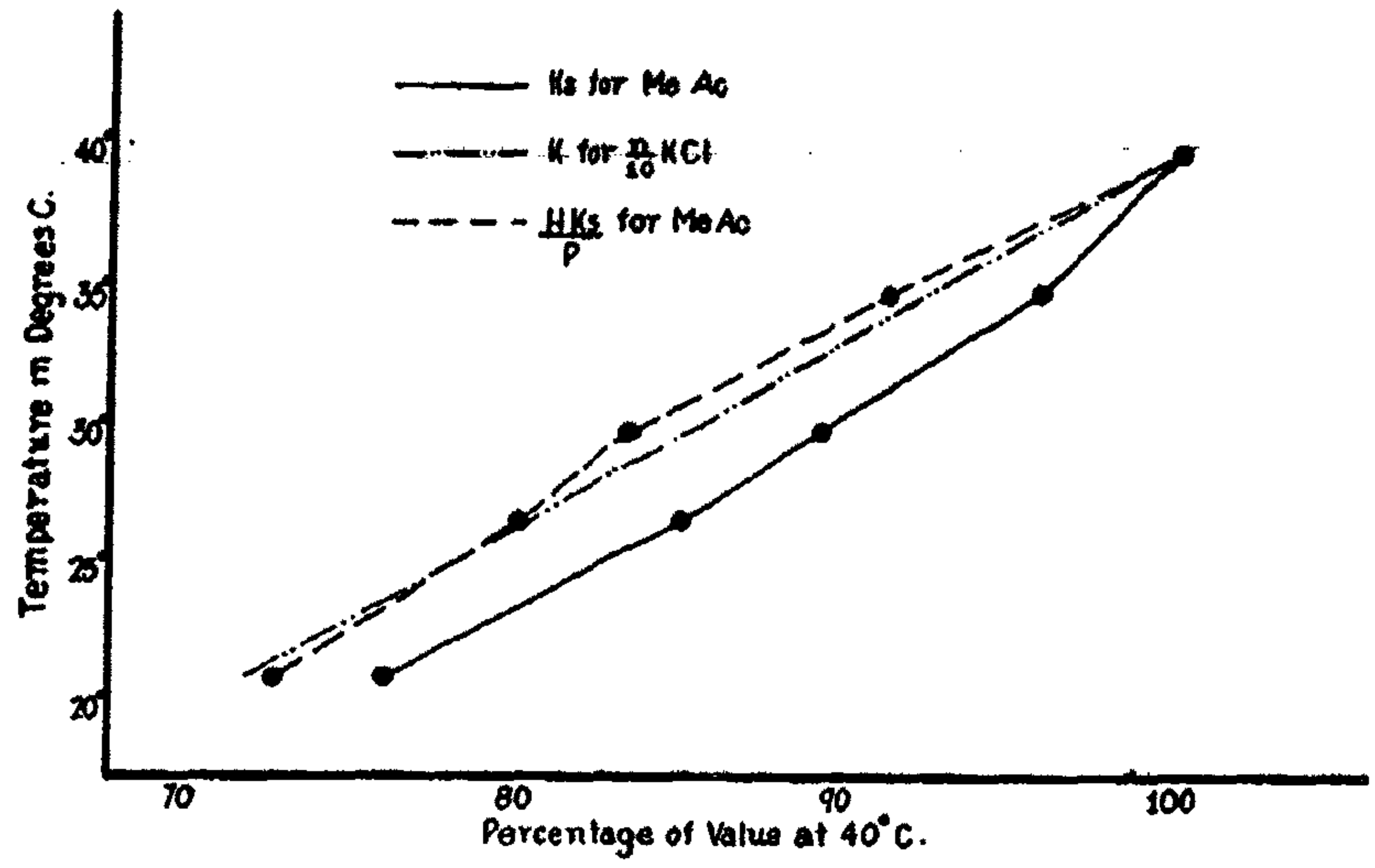

Fig. 8. Showing temperature effects upon the conductivity and electrokinetic functions in a methyl acetate-cellulose diaphragm.

These temperature coefficient studies were made in order to obtain some idea of the means by which electric currents are conducted by organic liquids in diaphragms. Conductivity can be either ionic or electronic. The former has a positive temperature coefficient, while the latter has a negative temperature coefficient. The behavior of the conductivity of methyl acetate with changing temperature, as well as the results of the similar study made by Bull and Gortner (1) on the system ethyl alcohol-cellulose, points strongly to the conclusion that ions are responsible for the conductivities shown by organic liquids in the diaphragms under consideration. The possible origin of the ions is problematical. It is possible that when a molecule of an organic compound orients itself in the region of an electrical center on the surface of the solid, an inductive effect takes place within either the oriented molecule or the configuration of atoms constituting the surface. This might cause a valence bond holding a proton, in one case, or a hydroxyl group, in the other, to be weakened, permitting a slight ionization at the interface. This could account for the presence of a charge on the surface, which is negative for some systems, and positive for others. It would also afford the ions necessary for the conductivity measured, and would give us some reasonable mechanism for the building up of the streaming potentials observed in these systems.

An alternative hypothesis would be the presence in the organic liquid (e.g., alcohols) of both "alcoholate" and "alcoholonium" ions. If the "alcoholate" ion is more strongly adsorbed than is the "alcoholonium" ion, then the solid will be negatively charged with respect to the streaming liquid, with a reversal in charge resulting whenever the adsorption of the "alcoholonium" ion exceeds that of the "alcoholate" ion. This appears to us to be the more probable mechanism. It is, however, difficult to explain why cellulose adsorbs preferentially the alcoholonium ion of *n*-propanol and the alcoholate ion of isopropanol and why these adsorption affinities are reversed when the cellulose is replaced by aluminum oxide. In the case of cellulose both *n*-butanol and isobutanol induce the same sign of charge at the interface, whereas opposite charges are induced at an aluminum oxide interface. Furthermore the physicochemical constants of the aliphatic acids afford no clue as to why a reversal in interfacial sign occurs as we pass from *n*-propionic acid to *n*-butyric acid at a cellulose-acid interface, whereas no similar reversal occurs at an aluminum oxide-acid interface. In some way these electric moments at the interface appear to be reflecting not only the interatomic structure of the organic liquids but also the interatomic, or at least the surface-atomic structure of the solid which is bathed by the organic liquid. Since the data obtained are easily reproducible, and since they cannot be predicted *a priori* from any existing physicochemical data, they afford an independent method for the study of the relationships which exist between organic structure and surface behavior.

SUMMARY

The electric moment of the double layer per square centimeter (qd) was determined for an homologous series of the aliphatic alcohols at aluminum oxide interfaces and for similar series of the fatty acids and esters at cellulose interfaces, using the streaming potential method. A new streaming cell with ground-glass joints was designed and used throughout these studies. This cell markedly increases the ease with which measurements can be made. In order to obviate the difficulties encountered in dealing with diaphragms of extremely high resistance and with the measurement of streaming potentials of excessively large magnitude, the electrodes of such diaphragms were shunted through an 11-megohm resistor, thus adding a new technic to electrokinetic methods. The data lead to the following conclusions:

1. The streaming potential was strictly proportional to pressure for all of the systems investigated.

2. At aluminum oxide interfaces alcohols, within an homologous series, show variations of electrokinetic functions which resemble to a considerable extent the variations at cellulose interfaces. The electric moment (*qd*) of alcohols at aluminum oxide interfaces are in general about half as large as are those at cellulose interfaces.

3. A reversal from (−) to (+) occurs between *n*-butanol and *n*-pentanol at an aluminum oxide interface and between ethanol and *n*-propanol at a cellulose interface. In both series isopropanol yields a sign opposite to that yielded by *n*-propanol.

4. Fatty acids at cellulose interfaces show a reversal of sign of surface charge between *n*-propionic acid and *n*-butyric acid. No such reversal is shown at an aluminum oxide interface. The magnitudes of *qd* are about one-tenth of those of acids at aluminum oxide interfaces.

5. Within an homologous series of esters the variations in electric moments at cellulose-ester interfaces seem to be closely associated with the number of carbon atoms in the ester. The variations, though opposite in direction, are of approximately the same magnitudes as the variations at cellulose interfaces encountered in ascending the homologous series of fatty acids. Furthermore, the behavior of an ester is analogous to that of the fatty acid containing one less carbon atom. Moments for esters at cellulose interfaces are about one-third as great as are those for esters at aluminum oxide interfaces.

6. Specific effects of surfaces on the electrical behavior of types of compounds must be postulated in order to rationalize the findings of this study with the earlier data of Martin and Gortner and of Jensen and Gortner.

7. Positive temperature coefficients of the conductivity of methyl acetate in the diaphragm and of $H\kappa_s/P$ for the same system were observed. It is postulated that the electrokinetic effects observed are the resultant of the interaction of ions derived from the organic molecules of the liquids and the solid with which the liquid is in contact.

8. Since the electrokinetic behavior of a solid–organic liquid interface cannot be predicted *a priori* from existing physicochemical data, it is sug-

gested that electrokinetic studies afford an independent technic for studying problems of organic structure.

REFERENCES

(1) Bull, H. B., and Gortner, R. A.: J. Phys. Chem. **35**, 456-66 (1931).
(2) Bull, H. B., and Gortner, R. A.: Physics **2**, 21-32 (1932).
(3) Jensen, O. G., and Gortner, R. A.: J. Phys. Chem. **36**, 3138-51 (1932).
(4) Martin, William McK.: Interfacial Energy and the Molecular Structure of Organic Compounds. Ph.D. Thesis, University of Minnesota, 1929.
(5) Martin, William McK., and Gortner, R. A.: J. Phys. Chem. **34**, 1509-30 (1930).
(6) Reilly, J., Rae, T., and Wheeler, T.: Physico-Chemical Methods, p. 598. D. Van Nostrand Co., New York (1925).

A PHYSICOCHEMICAL STUDY OF BLOOD SERA. III

Colloid Osmotic Pressure. An Analysis of One Hundred Cases

JOSÉ ZOZAYA

Gladwyne Research Laboratories, Gladwyne, Pennsylvania

Received February 5, 1938

The importance of the colloid osmotic pressure of the blood proteins in the interchange of fluids in the body is generally recognized. Since the work of Starling (14) a great many investigators have studied the colloid osmotic pressure of blood serum or plasma. These investigators have used different techniques, with variations in the conditions observed, such as temperature, concentration of serum, pH, different bathing fluids, and many kinds of membranes, all of which influence the final result. Few of these workers have used a theoretical colloid osmotic pressure value which could be calculated from the molecular weight of the serum proteins by the formula RTC/M, where C is the protein concentration and M the molecular weight of the protein.

The literature on the determination of the colloid osmotic pressure of human serum is large. For our present consideration we are interested mainly in the actual values obtained by different workers, so we have used the table given by Drinker and Field (4) and have determined the average values from the list given by them. These will be discussed later. The bibliography is given by Drinker.

Colloid osmotic pressure measurements were used in the first determinations of the molecular weight of serum albumin in a well-defined composition by Sörensen (13), who obtained the value of 45,000. By a similar method Adair (2) found the value to be 62,000, but he made some modifications in the calculations. Svedberg and Sjögren (15), using the ultracentrifuge, found the molecular weight of serum albumin to be 68,000 and that of globulin 169,000. In further work with the colloid osmotic pressure method, Adair (3) found the new values 72,000 for serum albumin and 170,000 for globulin. These last figures are the ones used in our calculations. It is of interest to note the close agreement between the values obtained by the different methods.

There are many factors which influence the colloid osmotic pressure of protein systems, such as the Donnan effect, the pressure due to the diffusible ion, etc., but they become of greater interest in academic studies with perfectly controlled systems. The important physiological consideration is the constant and accurate measurement of the colloid osmotic pressure of the blood serum as is, for it is in this form that the important physiological effect is obtained. In this work we shall not discuss the probable factors influencing our determinations other than those mentioned, for they already take into consideration the optimum conditions for eliminating some of the effects.

Adair (3) studied the serum albumin and globulin separately and in the whole serum, and he concluded that their behavior, so far as colloid osmotic pressure is concerned, follows Dalton's law of partial pressures and that it appears that serum protein is not a compound of albumin and globulins. He further believes that the state of aggregation of the proteins in the untreated serum appears to be the same as their state of aggregation in the purified proteins. With these experimental facts, we studied one hundred samples of human serum (from mental and nervous cases), only one showing a marked alteration. (This was sample No. 88, from a case with granuloma inguinale, which had a total protein of 10.75 and an A/G of 0.77.) The colloid osmotic pressures determined experimentally were compared with the theoretical values calculated on the basis of the added effects which the amount of serum albumin and globulin produced, their molecular weights in an ideal solution being considered.

METHODS

The general technique which we followed is essentially that described by Adair (1) in his studies on the molecular weight of hemoglobulin. A detailed description of the method is given below.

Collodion membranes

A 2 per cent parlodion (Pyroxylin Purified, Mallinckrodt) solution was made with equal parts of ether (distilled over sodium) and absolute alcohol. To this solution was added sufficient ethylene glycol to make a final concentration of 2 per cent. The percentage of ethylene glycol affects the permeability of the membrane, which increases with the percentage of the glycol. In our experience we found that a 2 per cent concentration gave the ideal permeability. It is best to let the solution of collodion rest for at least two weeks before using it. On a revolving glass tube, 1.1 cm. in diameter, arranged in a rotary mechanical device, the collodion was poured on at least 4 cm. of the length of the tube, including the end. After 1.5 minutes a second coating of collodion was applied. This procedure was repeated four times with 1.5-minute intervals between each pouring. After the fourth coating, 6 minutes were allowed to pass before shutting off the motion of the tube and the heat. Then the tube was allowed to dry overnight before the membrane was removed. An important provision is to have a heater two feet in front of the tube, while the collodion is being poured, to hasten drying. Before use all membranes were submitted to a pressure of 2.5 atmospheres with a mercury pump, to test their permeability and strength.

Osmometer

A heavy glass tube with a thin capillary opening graduated in millimeters was used as the osmometer (Westergren sedimentation tube). The details of the arrangement are best seen in figure 1, where A is the vacuum of a thermos bottle, B the collodion sac of 2-cc. capacity, which is fitted tightly to a rubber stopper D by means of a fine rubber thread C. Inserted through the stopper is a thin glass tube E, which by means of a rubber tube G connects the osmometer I with the collodion bag. The bag containing the serum is immersed in a large test tube through a stopper, which has a small glass tube inserted on the side to enable it to touch the surface of the bathing liquid. Both should be at the level of the zero reading of the osmometer. The tube prevents pressure on the liquid when the stopper is tightly fitted to the tube. The whole apparatus is immersed in a thermos bottle which has previously been filled with finely cracked ice, a space being formed in the ice for the tube to fit into it. To keep a constant temperature of 0°C. the bottle was refilled with ice every other day, for low temperature is the most important factor in insuring chemical stability.

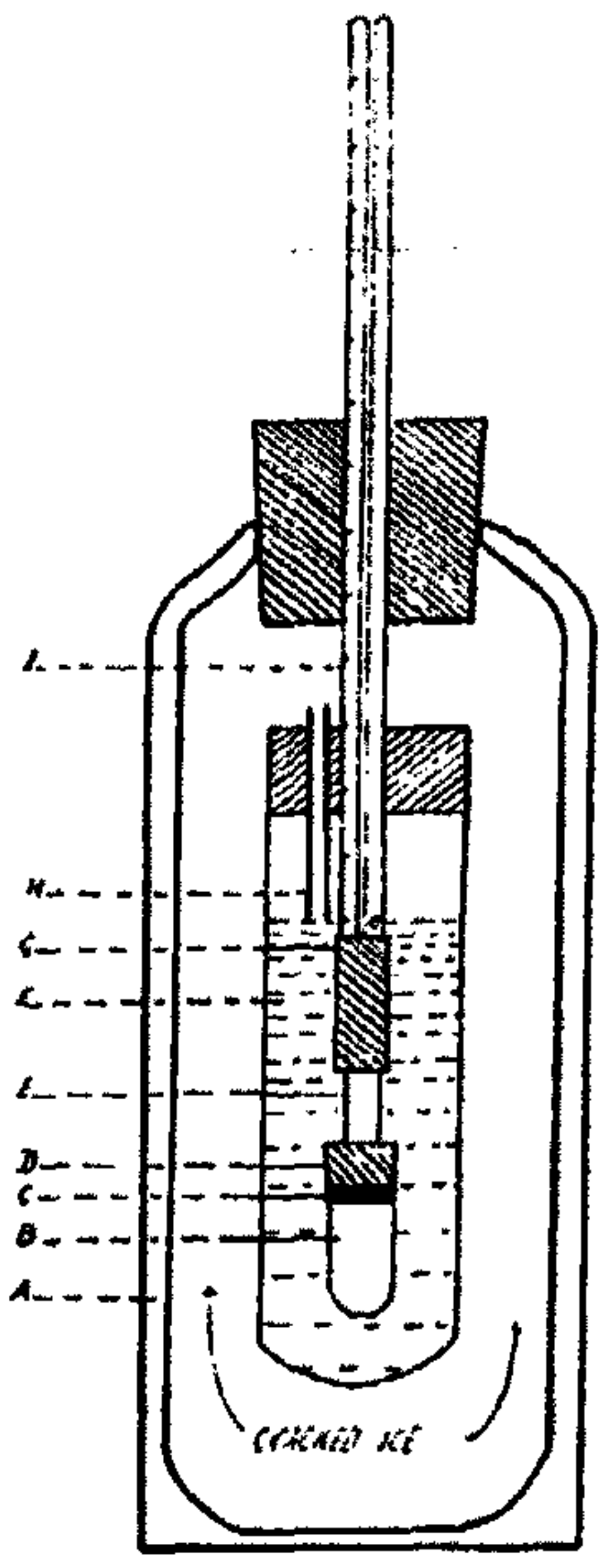

FIG. 1. Osmometer apparatus in thermos

Bathing fluid

The bathing fluid used in these experiments was an equal mixture of Sörensen's disodium hydrogen phosphate and potassium dihydrogen phosphate in $M/30$ concentration. With the use of this low concentration of salts, the Donnan effect is negligible and no correction is made in our calculations. Further experiments are being made to measure the partial osmotic pressure of the protein ions. The pH at room temperature (18°C.) was 6.81 and at 0°C. was 6.91. The solution in the tube was changed daily at the time of the reading of the manometer. A constant pH of the fluid in colloid osmotic pressure determinations is of importance, for we know that it has an effect on the colloid osmotic pressure of proteins.

Calculations

$$p = R_1 - (R_2 - R_3)\frac{\text{Sp. G.}}{13.6}$$

R_1 = the scale reading of the meniscus on the osmometer,
$R_2 - R_3$ = the difference in the meniscus reading when the tube is dipped in the tube of the inner liquid (capillarity), and
Sp.G. = the specific gravity of the serum.

Readings of the manometer were made every day until an identical reading was observed for two or three consecutive days, when it was thought that equilibrium had been reached. All results are expressed in millimeters of mercury and at 0°C.

The theoretical calculation of colloid osmotic pressure was determined by the formula

$$p = \frac{RT(10C_a)}{M_a} + \frac{RT(10C_g)}{M_g}$$

where $RT = 760 \times 22.412 = 17{,}033$ at 0°C.,
M_a = molecular weight of serum albumin (72,000),
M_g = molecular weight of serum globulin (170,000),
C_a = concentration of albumin in the serum (per cent), and
C_g = concentration of globulin in the serum (per cent).

The concentration of the proteins is multiplied by 10 to make the relation in terms of parts per thousand.

The theoretical colloid osmotic pressure per gram of protein is denoted by n_0 in comparison to n, which is the relation of the colloid osmotic pressure determined per gram of protein. The value of n_0 was experimentally determined by Adair (3) as 2.36 for albumin and 1.00 for globulin. He also determined it in unfractionated serum and found it to be 1.90 ± 0.2. Using the data published by Verney (16), Mayrs (10), and Marrack and Hewitt (9), and recalculating their values to millimeters of mercury and for 0°C., Adair found 1.8 ± 0.2, 1.89 ± 0.2, and 1.9 ± 0.2, respectively.

The determined value for n_0 in the serum studied by Adair was 1.94, which agrees with the theoretical one within the limits of experimental error. From the values obtained for albumin and globulin one can calculate the theoretical value for n_0 for any given serum by taking into consideration the relative percentages of each fraction in the whole serum.

The ratio $p/RTCp$ is the relation of the observed colloid osmotic pressure and the calculated one.

Other measurements

The determination of the specific gravity and the relative viscosity as well as the fractionation of the proteins have already been described in a previous paper (18).

Time of observation

In the present series the average time for a serum to come to equilibrium was 10 days, the shortest time being 6 days, and the longest 32 days. (This extreme was a serum with a total protein of 10.75 and an A/G of 0.77.)

RESULTS

For lack of space the complete data on the one hundred cases cannot be published, so they have been tabulated in the form of general averages (table 1), showing the maximum and the minimum in each measurement to give an idea of the range of variation.

Our first consideration was to compare the theoretical and observed colloid osmotic pressures. In the total averages we find a difference of 1.24 mm. of mercury (1.78 cm. of water), or a difference of 9.4 per cent. Besides this discrepancy the colloid osmotic pressure reading has to account for the corrections in the probable error in the determination of the protein fractions, etc. We made only one determination of each one of the sera. One must consider also the correction of the volume occupied by the proteins, ion-pressure differences in non-ideal solutions, the volume occupied by the protein molecules, that is, the b in van der Waals equation, and other technical corrections, which were not taken into consideration. So we consider that the agreement between these two values is very good.

The ratio $p/RTCp$ in the general average is 0.906. The minimum 0.70 was from a serum with a total protein of 10.75 and an A/G of 0.77, a specific gravity of 1.0352, and a viscosity of 2.59, a definitely abnormal serum. The maximum, which should be 1.00, was found to be 1.07 in a serum with a total protein of 6.04 per cent and an A/G of 2.45, probably opposite to the one above. It may be suggested that probably the general average would be higher if some of these abnormal sera had been eliminated from our general consideration. But it is of importance to know how these kinds of sera behave.

The literature on colloid osmotic pressure determinations on human serum is very extensive, as has already been noted in the introduction, so the results of our averages were determined from Drinker's table. The colloid osmotic pressure was 33.25 cm. of water or 24.44 mm. of mercury. No correction was made for the temperature. The total protein in the average was 7.76 per cent, and the number of cases studied was three hundred and ninety-four. The value of n would be 3.02 mm. of mercury, compared to 1.702 in our cases. We are not able to explain these differences, the figures given by Drinker and Field being so much higher, nor can we correlate their findings with the theoretical expectation when taking into consideration the molecular weights of serum albumin and globulin.

These high values for the colloid osmotic pressure of human serum as found by other investigators have made the understanding of the water interchange rather difficult, and several hypotheses have been advanced to explain this fact, mainly those of Krogh (7), Schade (12), and Landis (8). Krogh and his coworkers could not detect any accumulation of fluid in the tissues until the obstructing pressure exceeded 15 mm. of mercury. They concluded that this represented a critical pressure below which there was no gross disturbance of the fluid balance between blood and tissues. It is of interest to note that our highest colloid osmotic pressure observed was 13.54 mm. of mercury, which is below the critical pressure observed by them. In another paper we shall discuss this point further.

TABLE I

Total average with maxima and minima of the various calculations on one hundred sera

	SPECIFIC GRAVITY	VISCOSITY	TOTAL PROTEIN	ALBUMIN	GLOBULIN	ALBUMIN / GLOBULIN	p*	$RTCp$	n	n_0	$p/RTCp$
Maximum....	1.0358	2.59	10.75	5.64	6.06	3.76	13.53	16.98	2.11	2.07	1.070
Average......	1.02717	1.776	7.037	4.525	2.512	1.801	11.96	13.201	1.702	1.876	0.906
Minimum....	1.0240	1.61	5.50	2.93	1.48	0.71	8.51	9.46	1.04	1.56	0.695

* p = observed colloid osmotic pressure in millimeters of mercury.
$RTCp$ = calculated colloid osmotic pressure from formula 1.
n = colloid osmotic pressure per gram of protein (determined).
n_0 = colloid osmotic pressure per gram of protein (theoretical).

Govaerts (6), who studied the colloid osmotic pressure of human serum extensively and whose results are generally quoted in the literature, found that 1 g. of serum albumin exerted a pressure of 5.5 mm. of mercury and 1 g. of globulin a pressure of 1.4 mm. of mercury. From these findings he suggested the calculation of the colloid osmotic pressure of a serum from the A/G, and he thinks that there is an approximation of within 10 per cent. We have plotted the A/G and our value n in figure 2. We can see the wide distribution of our findings away from the theoretical line. So it is difficult to imagine any close agreement by calculating colloid osmotic pressure from these data. At the same time it would be inadvisable to calculate any colloid osmotic pressure of any serum from standardized formulas, for one would not be able to detect those sera which behave differently owing to radical changes in the behavior of the molecules because of some disease condition.

TABLE 2

Group of cases showing the same values of A/G and n_0, with different values of n and $p/RTCp$

CASE NO.	SPECIFIC GRAVITY	VISCOSITY	TOTAL PROTEIN	ALBUMIN / GLOBULIN	n	n_0	$p/RTCp$
3	1.0274	1.75	7.58	2.05	1.68	1.91	0.88
4	1.0254	1.65	6.81	2.02	1.80	1.91	0.94
19	1.0277	1.79	7.03	2.00	1.92	1.91	1.00
20	1.0273	1.75	7.03	2.00	1.80	1.91	0.94
25	1.0258	1.61	6.59	2.03	1.85	1.91	0.97
31	1.0246	1.64	5.83	2.00	1.72	1.91	0.90
39	1.0265	1.69	6.16	2.05	1.73	1.91	0.91
62	1.0271	1.73	6.59	2.03	1.56	1.91	0.94
73	1.0261	1.68	6.37	2.05	1.92	1.91	1.00
84	1.0289	1.90	8.23	2.02	1.51	1.91	0.79

TABLE 3

Group of cases showing a value for n of 1.80

CASE NO.	SPECIFIC GRAVITY	VISCOSITY	TOTAL PROTEIN	ALBUMIN / GLOBULIN	n_0	$p/RTCp$
4	1.0254	1.65	6.81	2.02	1.91	0.94
20	1.0273	1.75	7.03	2.00	1.91	0.94
34	1.0247	1.64	6.59	1.71	1.85	0.97
47	1.0251	1.69	6.59	1.31	1.79	1.01
48	1.0273	1.74	6.92	2.54	1.97	0.91
70	1.0260	1.68	6.70	1.78	1.87	0.96
72	1.0248	1.65	6.05	2.71	1.99	0.81
81	1.0260	1.69	6.92	2.10	1.92	0.94

To study further differences in sera besides the A/G, we selected a group of cases which had the same total protein per cent (table 4) and observed the variations in the other measurements. The value of A/G ranged from 1.31 to 2.46, the value of n from 1.56 to 1.96, and the ratio $p/RTCp$ from 0.85 to 1.01, showing that the concentration of the protein in itself had no direct effect on the value of n.

We then studied the group of cases with a $p/RTCp$ of less than 0.85 (table 5), and noticed that the total concentration of the protein ranged from 6.05 per cent to 10.75 per cent, the A/G from 0.77 to 2.81, and the value of n from 1.09 to 1.67, with nothing characteristic to explain the low ratio. Then we selected a group of cases which showed a value for $p/RTCp$ of 1.00 or higher (table 6), and here again we noticed the variation in the total protein from 6.04 to 7.47, in the A/G from 1.31 to 2.45, and in the value of n from 1.76 to 2.11. The value of 1.07 is not explained by us, except as an error in the determination of the total protein.

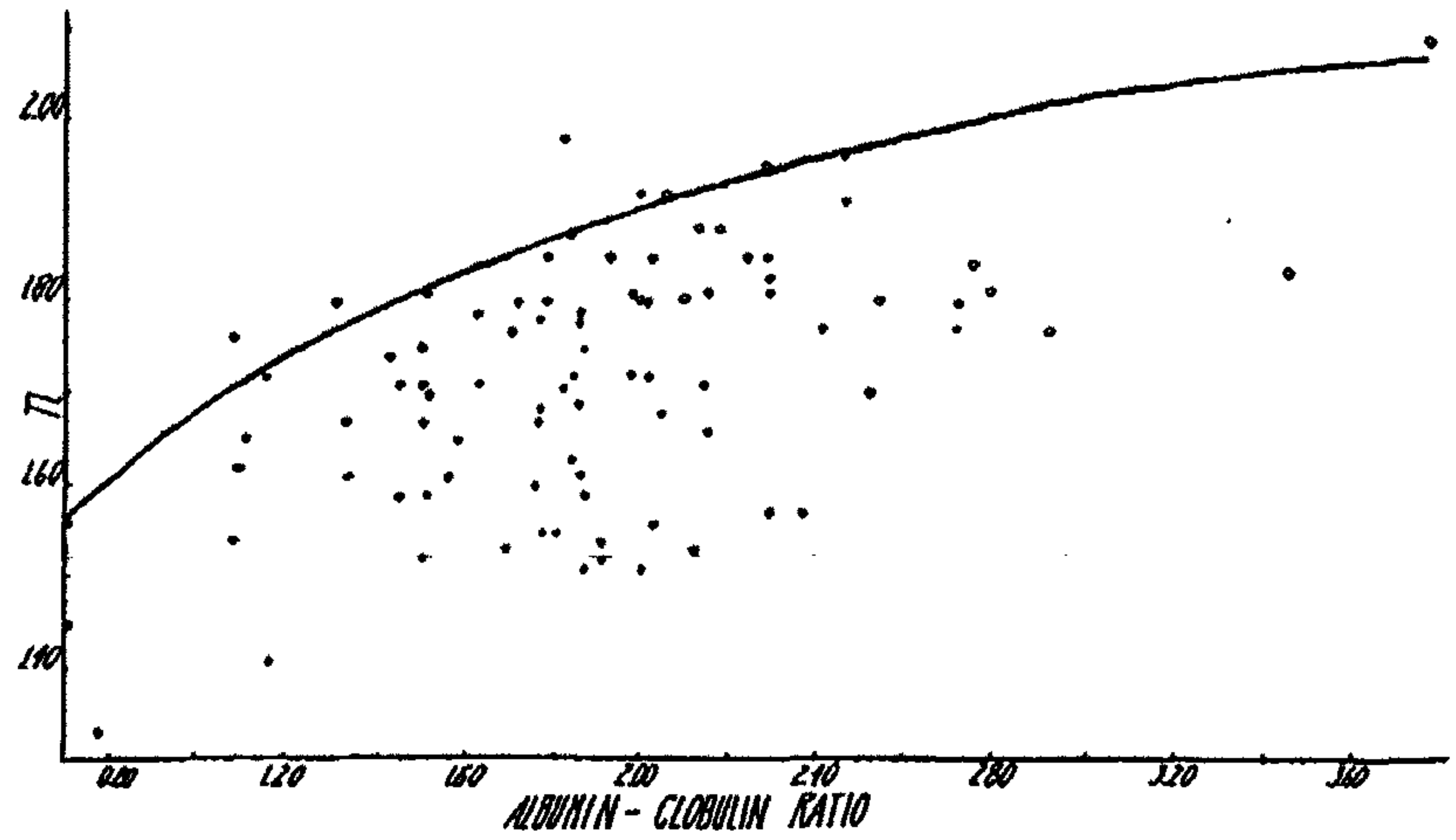

Fig. 2. Relation of albumin-globulin ratio to osmotic pressure per gram of protein

TABLE 4

Group of cases showing the same total protein and different values of n and p/RTCp

CASE NO.	SPECIFIC GRAVITY	VISCOSITY	TOTAL PROTEIN	$\frac{\text{ALBUMIN}}{\text{GLOBULIN}}$	n	n_0	$p/RTCp$
47	1.0251	1.69	6.59	1.31	1.80	1.79	1.01
43	1.0255	1.62	6.59	1.43	1.74	1.80	0.96
21	1.0255	1.67	6.59	1.86	1.69	1.88	0.90
6	1.0277	1.72	6.59	1.86	1.61	1.88	0.85
28	1.0261	1.68	6.59	1.86	1.79	1.88	0.95
11	1.0264	1.73	6.59	1.86	1.88	1.88	1.00
80	1.0271	1.77	6.59	1.86	1.78	1.88	0.95
62	1.0271	1.73	6.59	2.03	1.56	1.91	0.94
25	1.0258	1.61	6.59	2.03	1.85	1.91	0.97
45	1.0262	1.67	6.59	2.24	1.85	1.94	0.95
91	1.0275	1.78	6.59	2.46	1.91	1.96	0.97
41	1.0260	1.68	6.59	2.46	1.96	1.96	1.00

Pauli (11) discusses the relation between viscosity and colloid osmotic

TABLE 5

Group of cases with a value for p/RTCp of less than 0.85

CASE NO.	SPECIFIC GRAVITY	VISCOSITY	TOTAL PROTEIN	ALBUMIN / GLOBULIN	n	n_0	$p/RTCp$
1	1.0268	1.74	8.34	1.80	1.55	1.87	0.81
13	1.0270	1.72	7.69	1.17	1.41	1.73	0.81
16	1.0263	1.68	6.70	2.58	1.65	1.98	0.84
40	1.0287	1.85	7.91	2.29	1.57	1.94	0.81
66	1.0267	1.71	6.37	1.91	1.54	1.88	0.82
72	1.0248	1.65	6.05	2.71	1.80	1.99	0.81
77	1.0270	1.74	7.14	1.50	1.52	1.81	0.84
79	1.0271	1.78	7.14	1.91	1.52	1.89	0.80
84	1.0289	1.90	8.23	2.02	1.51	1.91	0.79
85	1.0325	2.32	9.11	0.78	1.33	1.60	0.83
88	1.0352	2.59	10.75	0.77	1.09	1.58	0.69
95	1.0272	1.82	6.92	1.00	1.23	1.68	0.74
98	1.0290	1.93	8.02	1.51	1.43	1.81	0.79
105	1.0298	1.96	7.47	2.81	1.67	2.00	0.83

TABLE 6

Group of cases showing values for p/RTCp of 1.00 or over

CASE NO.	SPECIFIC GRAVITY	VISCOSITY	TOTAL PROTEIN	ALBUMIN / GLOBULIN	n	n_0	$p/RTCp$
11	1.0264	1.73	6.59	1.86	1.88	1.88	1.00
19	1.0277	1.79	7.03	2.00	1.91	1.91	1.00
22	1.0275	1.72	7.47	1.16	1.72	1.73	1.00
26	1.0258	1.64	6.70	1.78	1.85	1.87	1.00
33	1.0263	1.71	6.37	2.26	1.94	1.94	1.00
38	1.0282	1.82	7.69	1.09	1.76	1.71	1.03
47	1.0251	1.69	6.59	1.31	1.80	1.79	1.01
55	1.0268	1.81	6.04	2.45	2.11	1.96	1.07
73	1.0261	1.68	6.37	2.06	1.92	1.91	1.00
59	1.0286	1.83	7.36	1.50	1.81	1.81	1.00

TABLE 7

Cases showing viscosity of 1.64 to 1.65

CASE NO.	SPECIFIC GRAVITY	VISCOSITY	TOTAL PROTEIN	ALBUMIN / GLOBULIN	n_0	$p/RTCp$
4	1.0254	6.81	2.02	1.80	1.91	0.94
15	1.0257	7.02	2.02	1.72	1.89	0.89
17	1.0255	6.70	2.33	1.83	1.95	0.93
21	1.0255	6.59	1.86	1.69	1.88	0.90
26	1.0258	6.70	1.78	1.85	1.87	1.00
34	1.0247	6.59	1.71	1.80	1.85	0.97
35	1.0257	7.03	1.84	1.72	1.88	0.92
72	1.0248	6.05	2.71	1.80	1.99	0.81
102	1.0253	7.14	1.76	1.78	1.86	0.95

pressure in albumin solutions, showing the parallelism between them. In table 7 we selected a group of cases with a viscosity of 1.64 to 1.65. We noted that the protein concentration varied between 6.05 and 7.14, the *A/G* between 1.71 and 2.71, the value of n between 1.69 and 1.85, and the value of $p/RTCp$ between 0.81 and 1.00. If viscosity has any direct relation to colloid osmotic pressure we are not able to show it in our cases. It may well be that there are too many other factors which work in different directions to be able to show it here.

Finally we studied a group of cases with a specific gravity of 1.0272 to 1.0273 (table 8), and we noted that the protein concentration varied between 6.70 and 7.36, the *A/G* between 1.50 and 2.54, the value of n between 1.51 and 1.88, and the $p/RTCp$ between 0.79 and 0.97, showing that there is no general effect.

TABLE 8

Cases showing specific gravity of 1.0272 to 1.0273

CASE NO.	VISCOSITY	TOTAL PROTEIN	$\frac{\text{ALBUMIN}}{\text{GLOBULIN}}$	n	n_0	$p/RTCp$
8..........	1.78	7.14	1.87	1.51	1.88	0.79
20..........	1.75	7.03	2.00	1.80	1.91	0.94
23..........	1.75	7.25	2.37	1.57	1.95	0.91
24..........	1.72	6.70	2.13	1.88	1.92	0.97
27..........	1.74	7.03	2.41	1.77	1.96	0.90
48..........	1.74	6.92	2.54	1.80	1.97	0.91
53..........	1.74	6.93	1.63	1.79	1.84	0.97
58..........	1.74	6.70	1.50	1.71	1.81	0.94
82..........	1.87	7.36	1.11	1.65	1.71	0.97

From these observations we can come to the general conclusion that the colloid osmotic pressure of human serum can not be predicted from a generalized formula, for there are too many factors which influence it besides the *A/G*, the protein concentration, the specific gravity or the viscosity. There is no doubt an intrinsic individuality in the physicochemical conditions that are found in each serum, besides the many effects such as the electrolytic antagonism of ions, Na, K against Ca, Mg, as well as the cholesterol-phospholipin equilibrium which von Farkas (17) has shown affects the colloid osmotic pressure of sera. Fishberg (5) finds that the colloid osmotic pressure per gram of protein is higher in lipaemic bloods.

The comparison of the measured with the theoretical colloid osmotic pressure is an important criterion by which to judge the results obtained as well as the deviation from the expected value which pathological sera may have. It will also help to direct further research to elucidate other factors that affect the measurement. We can at the same time mistrust obtained values which deviate very far from the theoretical expectation.

I wish to acknowledge to Prof. G. S. Adair the kindness and personal instruction as to the use of this method and to thank Dr. S. DeW. Ludlum for the interest and facilities given by him for the accomplishment of this work.

REFERENCES

(1) Adair, G. S.: Proc. Roy. Soc. (London) **A108**, 627 (1925).
(2) Adair, G. S.: Skand. Arch. Physiol. **49**, 76 (1926).
(3) Adair, G. S., and Robinson, M. E.: Biochem. J. **24**, 1864 (1930).
(4) Drinker, C. K., and Field, M. E.: Lymphatics, Lymph and Tissue Fluid. Williams & Wilkins Co., Baltimore (1933).
(5) Fishberg, E. H.: J. Biol. Chem. **81**, 205 (1929).
(6) Govaerts, P.: Compt. rend. soc. biol. **89**, 678 (1923); **93**, 441 (1925); **95**, 724 (1926); Bull. acad. roy. méd. Belg. **7**, 356 (1927).
(7) Krogh, A., Landis, E. M., and Turner, A. H.: J. Clin. Investigation **11**, 63 (1932).
(8) Landis, E. M.: Heart **15**, 209 (1929-30); Am. J. Physiol. **93**, 353 (1930).
(9) Marrack, J., and Hewitt, L. F.: Biochem. J. **21**, 1129 (1927).
(10) Mayrs, E. B.: Quart. J. Med. **19**, 273 (1926).
(11) Pauli, W.: in Colloid Chemistry, edited by J. Alexander, Vol. II, p. 223. The Chemical Catalog Co., Inc., New York (1928).
(12) Schade, H., and Claussen, F.: Z. klin. Med. **100**, 363 (1924).
(13) Sörensen, S.: The Proteins. The Fleischmann Co., New York (1925); Compt. rend. lab. Carlsberg **13**, 1 (1917).
(14) Starling, E. H.: J. Physiol. **19**, 312 (1895-96).
(15) Svedberg, T., and Sjögren, B.: J. Am. Chem. Soc. **50**, 3318 (1928); **52**, 2855 (1930).
(16) Verney, E. B.: J. Physiol. **61**, 319 (1926).
(17) von Farkas, G.: Z. ges. exptl. Med. **53**, 666 (1926).
(18) Zozaya, J.: J. Biol. Chem. **110**, 599 (1935).

X-RAY STUDIES ON THE HYDROUS OXIDES. IX

Scandium Oxide Monohydrate[1]

HARRY B. WEISER AND W. O. MILLIGAN

Department of Chemistry, The Rice Institute, Houston, Texas

Received March 21, 1938

The addition of alkalis to solutions of scandium salts gives a white hydrous precipitate. Crookes (2) represented the composition of the air-dried gel by the formula $Sc_2O_3 \cdot 3H_2O$, and Böhm and Niclassen (1) found that the gel gave an x-ray diffraction pattern different from that of the anhydrous oxide. More recently Štěrba-Böhm and Melichar (3) added freshly precipitated scandium oxide to boiling potassium hydroxide solutions and obtained from this mixture definite crystals which, after washing with alcohol, had a composition represented by the formula $K_2[Sc(OH)_5 \cdot H_2O] \cdot 3H_2O$. This compound was hydrolyzed on washing with water, giving a product which was formulated as $[2Sc(OH)_3] \cdot H_2O$ ($= Sc_2O_3 \cdot 4H_2O$).

The preparations analyzed by Crookes and by Štěrba-Böhm and Melichar were not dried under equilibrium conditions, and therefore their analysis of the products is insufficient to establish the existence of the alleged hydrates of hydrous scandium oxide. The x-ray data of Böhm and Niclassen indicate that the precipitated oxide is either some definite hydrate or a second modification of the oxide. This paper gives the isobaric dehydration and x-ray diffraction analysis of four samples of precipitated scandia.

EXPERIMENTAL

Preparation of samples

Sample A. To 100 cc. of a 0.1 *M* solution of scandium chloride at 25°C. was added a slight excess of ammonium hydroxide solution. The resulting white gelatinous precipitate was similar to hydrous alumina prepared in the same manner.

Sample B was prepared like sample A except that the scandium chloride solution was at 100°C. This precipitate was somewhat less gelatinous in appearance and settled more rapidly than sample A.

---

[1] A preliminary report was presented at the Ninety-first Meeting of the American Chemical Society, held in Kansas City, Missouri, April, 1936.

Sample C was prepared in the same manner as sample A, but from a different supply of scandium chloride.

Sample D. Scandium oxide gel precipitated at 25°C. (*cf.* sample A) was washed rapidly, using the centrifuge, and added at once to a boiling solution of potassium hydroxide. Part of the gel dissolved and part was peptized, giving a cloudy sol. After centrifuging the mixture at 2500 R.P.M. for 5 minutes to remove suspended material, it was allowed to stand 2 days until a considerable amount of a powdery precipitate had formed on the bottom and sides of the flask.

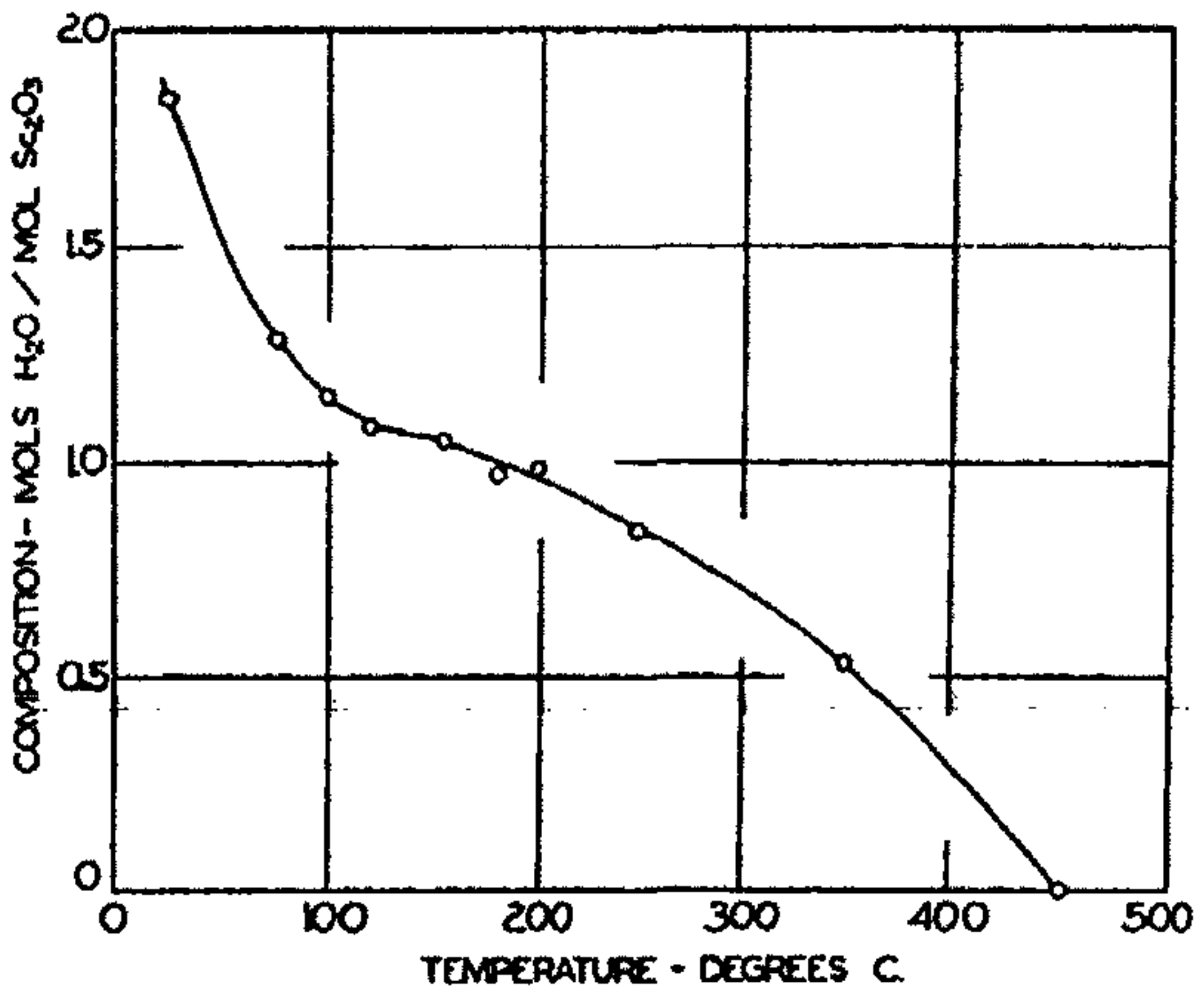

FIG. 1. Dehydration isobar for hydrous $Sc_2O_3 \cdot H_2O$(sample A)

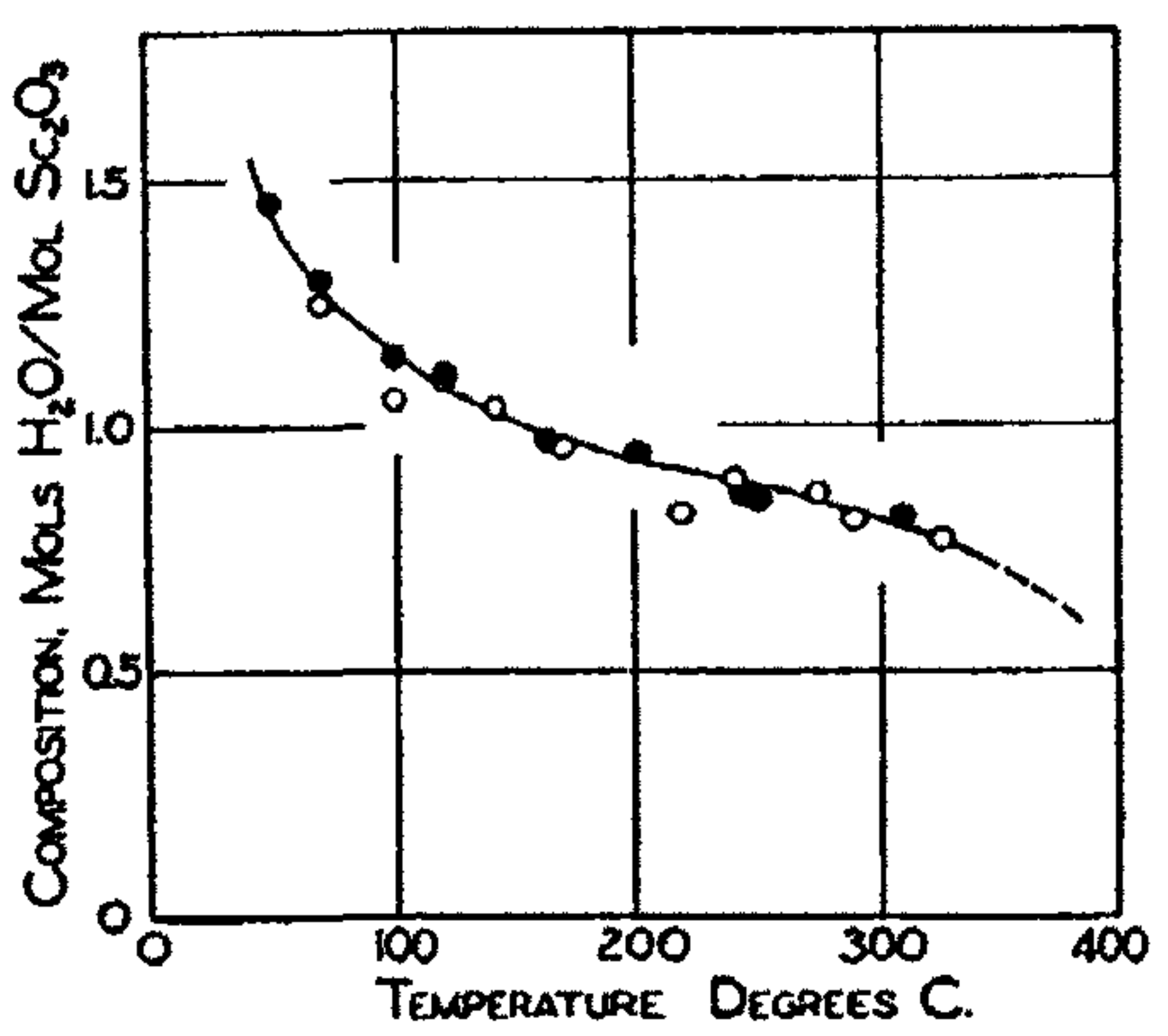

FIG. 2

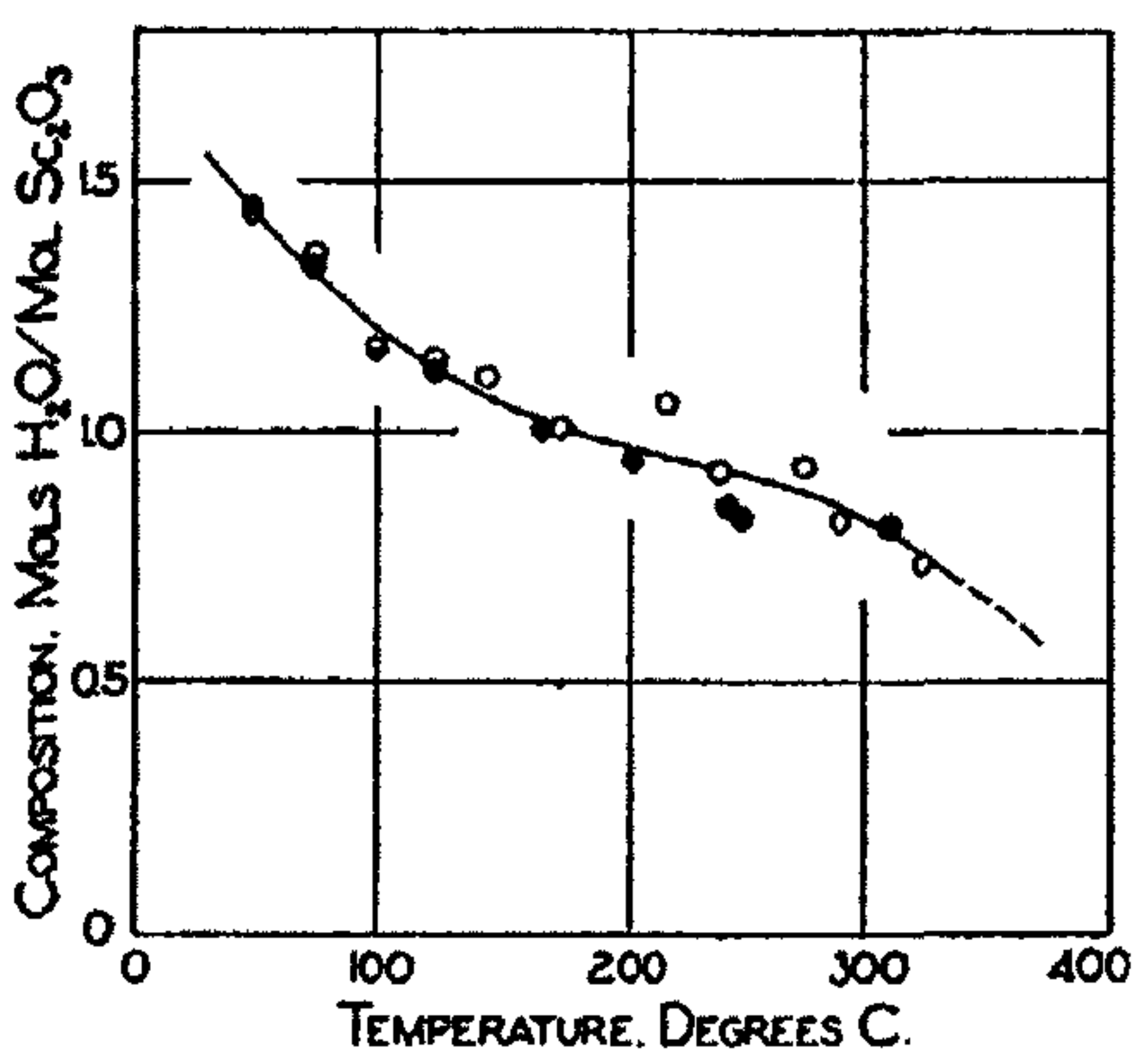

FIG. 3

FIG. 2. Dehydration isobar for hydrous $Sc_2O_3 \cdot H_2O$(sample B)
FIG. 3. Dehydration isobar for hydrous $Sc_2O_3 \cdot H_2O$(sample C)

Each of the above four samples was washed with 50-cc. portions of water by the aid of a centrifuge until the wash water gave no test for chloride (hydroxide in the case of sample D), after which they were air-dried at room temperature.

Dehydration isobars

Samples A, B, and C were dehydrated in an apparatus already described (4, 6) at an aqueous vapor pressure of 23.6 mm. The resulting isobars are given in figures 1 to 3. It is obvious from these curves that scandia precipitated at 25°C. and at 100°C. is the monohydrate $Sc_2O_3 \cdot H_2O$, corresponding to precipitated alumina, which is γ-$Al_2O_3 \cdot H_2O$.

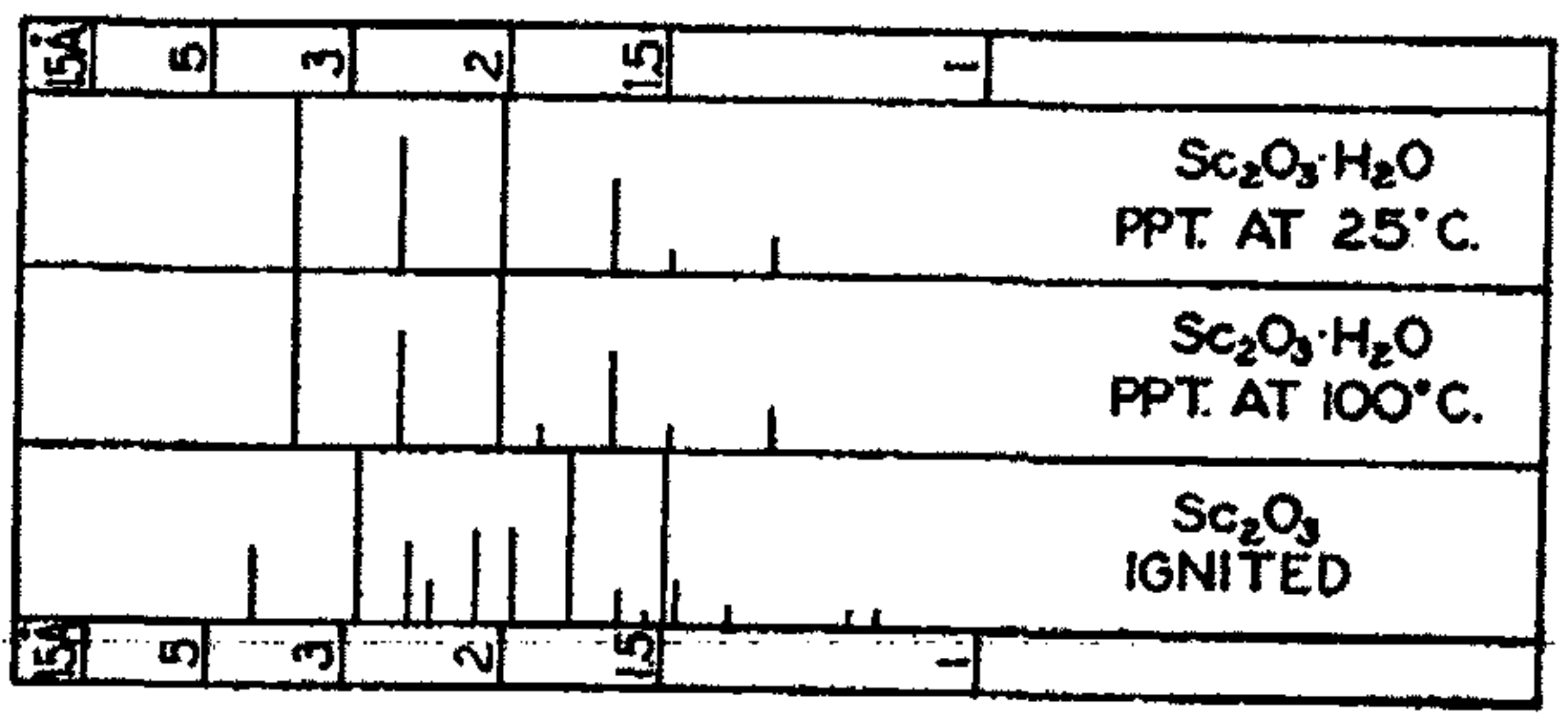

FIG. 4. X-ray diffraction patterns

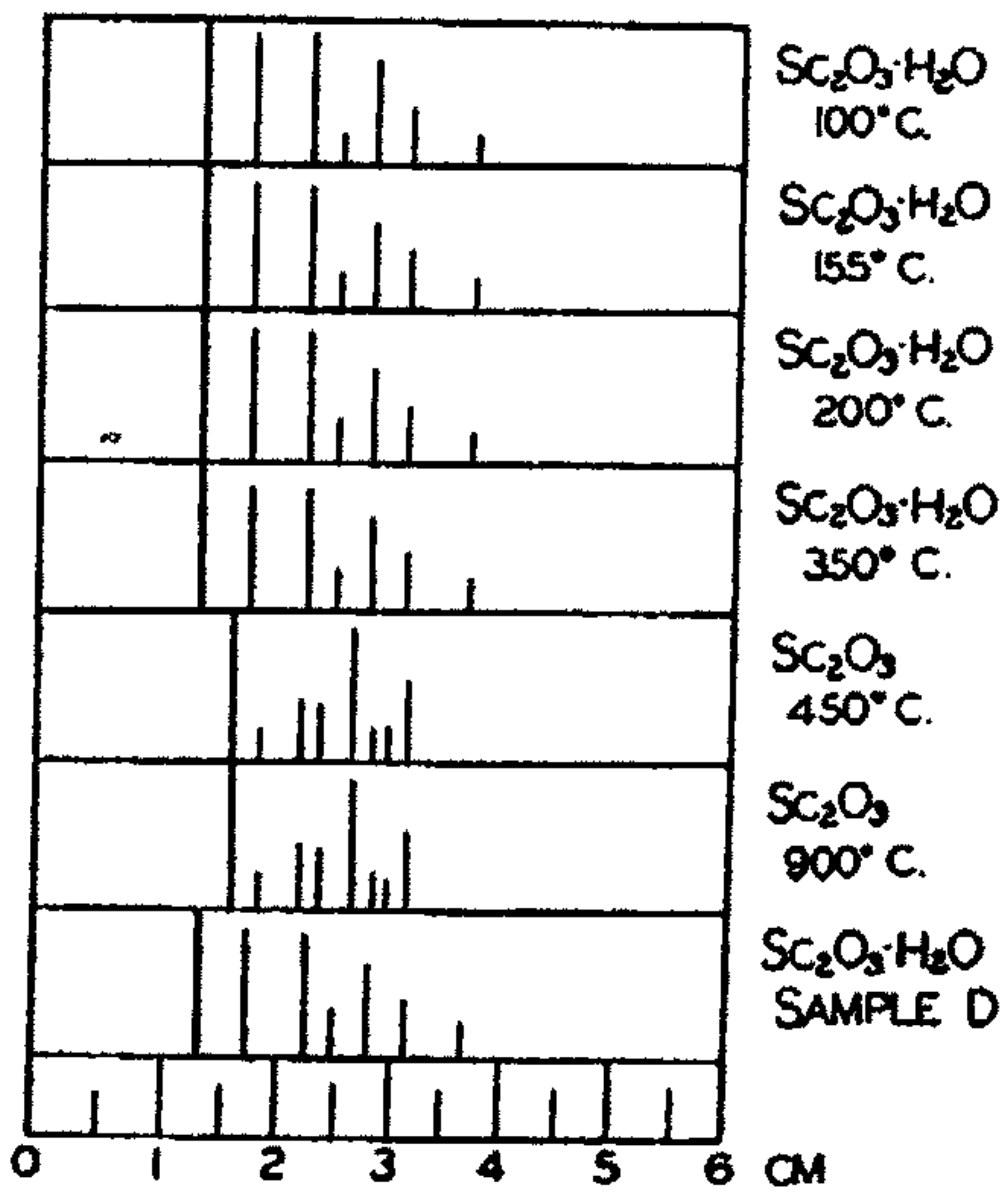

FIG. 5. X-ray diffraction patterns

X-ray examination

X-ray diffraction patterns were obtained for samples A and B with the General Electric apparatus. The samples in "nonex" glass tubes were examined with Mo K_α x-radiation; the exposure time was about 30 hours.

The films were standardized against pure sodium chloride in the usual way. The positions and intensities of the diffraction lines are represented in chart form in figure 4. The close resemblance between the diffraction patterns of $Sc_2O_3 \cdot H_2O$ and the corresponding γ-$Al_2O_3 \cdot H_2O$ (5) indicates a similarity in crystal structure.

Portions of sample C which had been dehydrated at temperatures of 100°, 155°, 200°, 350°, 450°, and 900°C., and of sample D were examined using Cu K_α x-radiation; the camera diameter was 57.6 mm. and the exposure time 30 to 60 minutes. To prevent gain or loss of water during examination, the samples were sealed in tubes of Lindemann glass following the procedure previously described (4, 6). The several patterns are represented diagrammatically in figure 5. They show (*a*) that the monohydrate lattice persists until the samples are almost anhydrous and (*b*) that but one modification of the anhydrous oxide exists between 450° and 900°C.

Sample D, prepared by a procedure similar to that of Štěrba-Böhm and Melichar, gave the same x-ray diffraction as the precipitated gel, $Sc_2O_3 \cdot H_2O$. It is probable, therefore, that the alleged compound, $[2Sc(OH)_3] \cdot H_2O$ or $Sc_2O_3 \cdot 4H_2O$, of Štěrba-Böhm and Melichar is hydrous $Sc_2O_3 \cdot H_2O$.

SUMMARY

The following is a brief summary of the results of this investigation:

1. The addition of alkalis to solutions of scandium salts at 25°C. or 100°C. throws down a white, highly hydrous precipitate.
2. Isobaric dehydration studies show that the precipitated gel is hydrous $Sc_2O_3 \cdot H_2O$.
3. X-ray diffraction examination shows scandium oxide monohydrate to have a crystalline structure distinct from that of the anhydrous oxide, but similar to that of γ-$Al_2O_3 \cdot H_2O$.
4. There is no indication of a second modification of anhydrous Sc_2O_3 between temperatures of 450°C. and 900°C.
5. The alleged compound $[2Sc(OH)_3] \cdot H_2O$ of Štěrba-Böhm and Melichar is probably hydrous $Sc_2O_3 \cdot H_2O$.

REFERENCES

(1) Böhm and Niclassen: Z. anorg. allgem. Chem. **132**, 1 (1924).
(2) Crookes: Phil. Trans. **209A**, 15 (1908).
(3) Štěrba-Böhm and Melichar: Collection Czechoslov. Chem. Commun. **7**, 131 (1935).
(4) Weiser and Milligan: J. Phys. Chem. **38**, 513, 1175 (1934); J. Am. Chem. Soc. **59**, 1457 (1937).
(5) Weiser and Milligan: J. Phys. Chem. **42**, 673 (1938).
(6) Weiser, Milligan, and Ekholm: J. Am. Chem. Soc. **58**, 1262 (1936).

THE HYDROUS OXIDES OF SOME RARER ELEMENTS[1]

HARRY B. WEISER AND W. O. MILLIGAN

Department of Chemistry, The Rice Institute, Houston, Texas

March 21, 1938

The composition of the precipitated oxides of aluminum (5, 10), gallium (8), indium (8), thallium (8), and scandium (14) has been established as a result of x-ray diffraction and isobaric dehydration studies on the several compounds. This paper is concerned with the application of similar methods of investigation to the remaining oxides of Group III, about which little authentic information was available. For the purpose of this summarizing report, the oxides of the metals under consideration will be classified into (*a*) the aluminum family (gallium, indium, thallium), (*b*) the scandium family (scandium, yttrium), and (*c*) the rare earths (neodymium, praseodymium, samarium).

EXPERIMENTAL

Following procedures already described (11, 12, 13, 15), dehydration isobars of the several preparations were obtained, taking care to allow sufficient time (days or weeks) for equilibrium to be established at each temperature point on the isobar.

Samples for x-ray diffraction analysis were taken at various temperatures from separate portions which had been heated in the same way and at the same time as the weighed samples for dehydration isobars. After sealing (9, 13, 15) in thin tubes of Lindemann glass, the samples were exposed to filtered Cu K_α x-radiation in a camera 57.6 mm. in diameter.

THE ALUMINUM FAMILY

Previous investigations (8) have shown that precipitated gallium oxide consists of hydrous particles of α-Ga_2O_3 when precipitated rapidly and unaged. The oxide prepared by slow precipitation from ammonium hydroxide solution or after aging may consist of hydrous $Ga_2O_3 \cdot H_2O$. Precipitated indium oxide is hydrous $In_2O_3 \cdot 3H_2O$ or $In(OH)_3$. Hydrous thallic oxide prepared by precipitation (6) or by Carnegie's (2) method (which was said to give a definite trihydrate) shows no indication of

---

[1] Presented at the Second Annual Symposium of the Division of Physical and Inorganic Chemistry,—A Symposium on the Less Familiar Elements,—held at Cleveland, Ohio, December 27-29, 1937.

hydrate formation. Dehydration isobars for the various samples are collected in figure 1. The isobar for hydrous thallic oxide is taken from the work of Hüttig and Mytyzek (6). X-ray diffraction patterns showing the chemical individuality of the several hydrous oxides and hydrates are given in figures 4, 5, and 6, respectively.

THE SCANDIUM FAMILY

In the preceding paper (14) it was shown that precipitated scandia is the monohydrate $Sc_2O_3 \cdot H_2O$, corresponding to precipitated alumina, which is γ-$Al_2O_3 \cdot H_2O$. In figure 4 is given a diagram of the x-ray diffraction patterns of $Ga_2O_3 \cdot H_2O$, $Sc_2O_3 \cdot H_2O$, and γ-$Al_2O_3 \cdot H_2O$. It will be noted that the patterns of the alumina and scandia monohydrates are very similar except for a uniform displacement of the lines. This furnishes additional evidence in support of the chemical individuality of γ-$Al_2O_3 \cdot H_2O$, even though the dehydration isobar for precipitated alumina is not a step curve (5, 12) corresponding to a monohydrate like that of $Sc_2O_3 \cdot H_2O$ (figure 2).

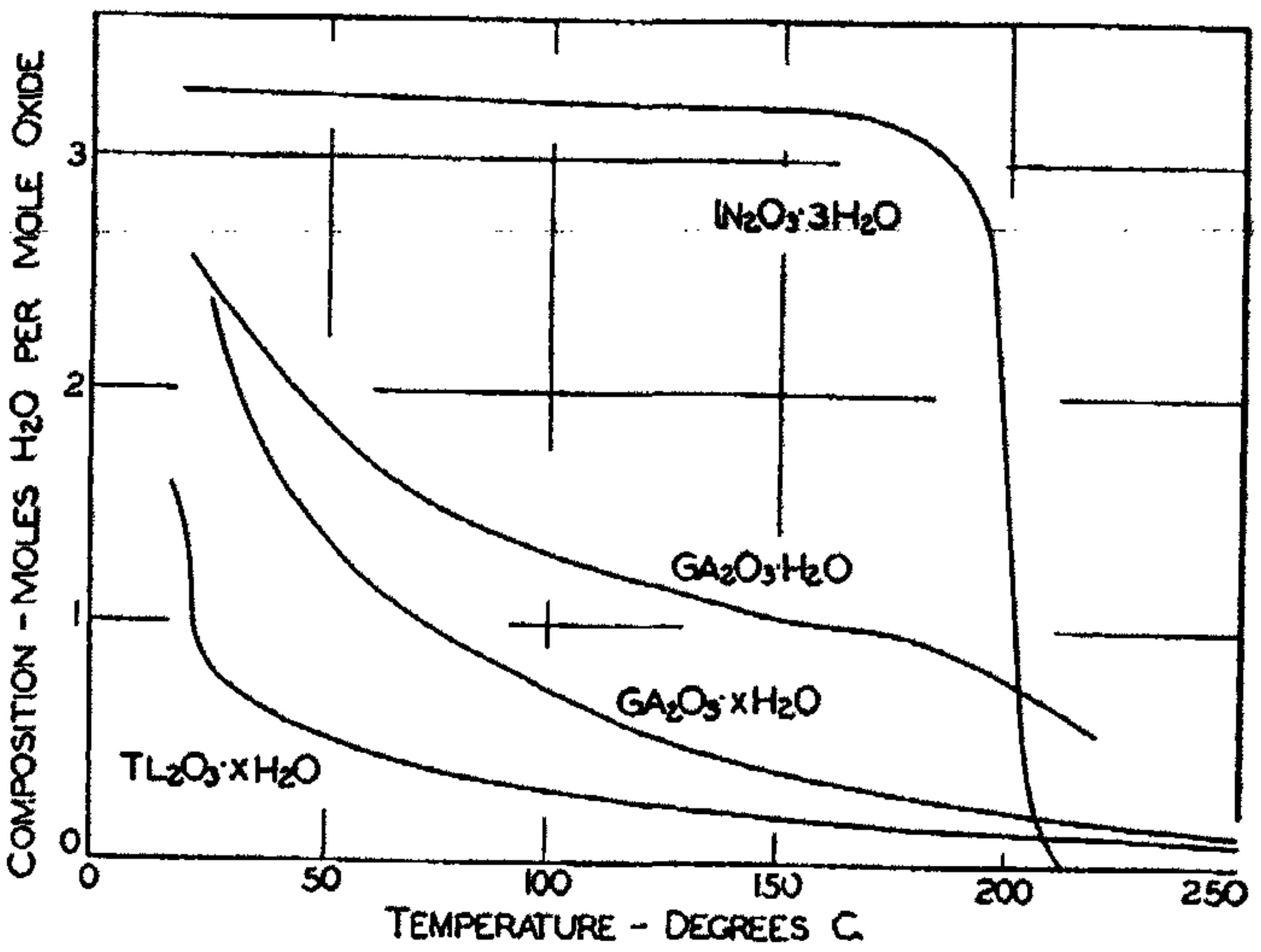

FIG. 1. Dehydration isobars for the hydrous oxides and hydrates of gallium, indium, and thallium.

No evidence is available concerning the constitution of precipitated yttria, except the observation of Böhm and Niclassen (1) that the freshly precipitated gel is amorphous to x-rays, becoming microcrystalline after prolonged aging. A sample of yttria was prepared by the interaction of solutions of yttrium chloride and ammonium hydroxide at 25°C., followed by washing with the aid of a centrifuge and air drying. The isobar for this preparation is a continuous curve (figure 2) with no indication of hydrate formation. In agreement with the results of Böhm and Niclassen, the x-ray diffraction pattern of the freshly formed product consists of two broad diffuse bands (figure 6). Aging experiments have not yet been carried out.

THE RARE EARTHS

Damiens (4) claimed that the composition of the precipitated oxides of neodymium, praseodymium, and samarium was represented by the respective formulas $Nd_2O_3 \cdot 3H_2O$, $Pr_2O_3 \cdot 3H_2O$, and $Sm_2O_3 \cdot 3H_2O$. Joye and Garnier (7) found that precipitated neodymium oxide retained 3.0, 1.5, and 1.0 moles of water per mole of oxide when the samples were dried at room temperature, 320°C., and 520°C., respectively. The evidence of Damiens and of Joye and Garnier is not conclusive, since (*a*) it is not known whether the analyzed products were in equilibrium with a fixed pressure of aqueous vapor at the temperature of drying, and (*b*) there are not enough data to establish an isobar.

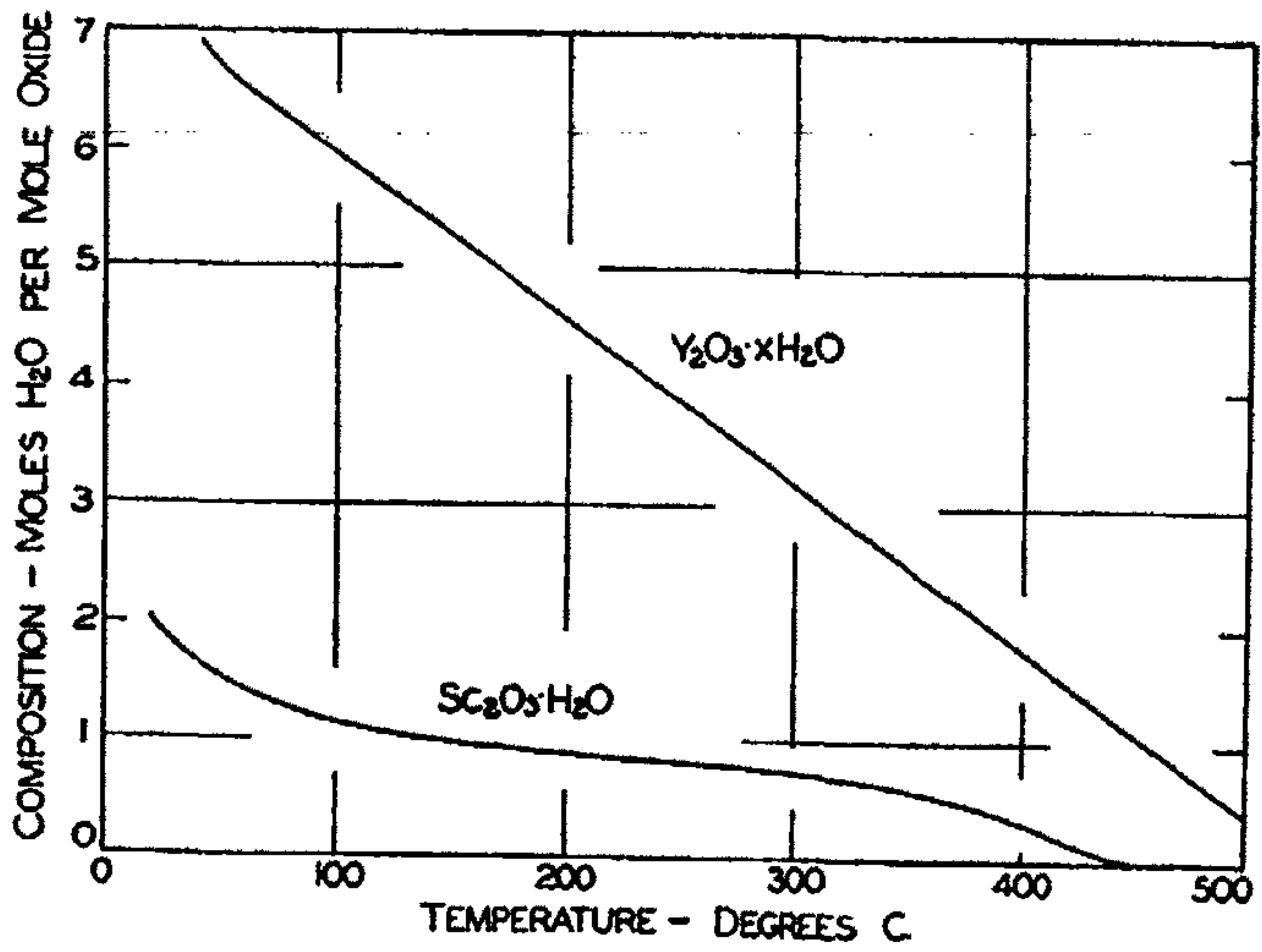

FIG. 2. Dehydration isobars for hydrous scandium oxide monohydrate and yttrium oxide.

In this investigation samples of precipitated neodymium, praseodymium, and samarium oxides were prepared as described above for yttrium oxide. The dehydration isobars for samples precipitated at 100°C. are given in figure 3. It is apparent that precipitated neodymium and praseodymium oxides consist of the hydrous trihydrate or hydroxide. There is only the slightest indication of a break in the samarium oxide isobar at the composition corresponding to the trihydrate. The neodymium isobar shows some

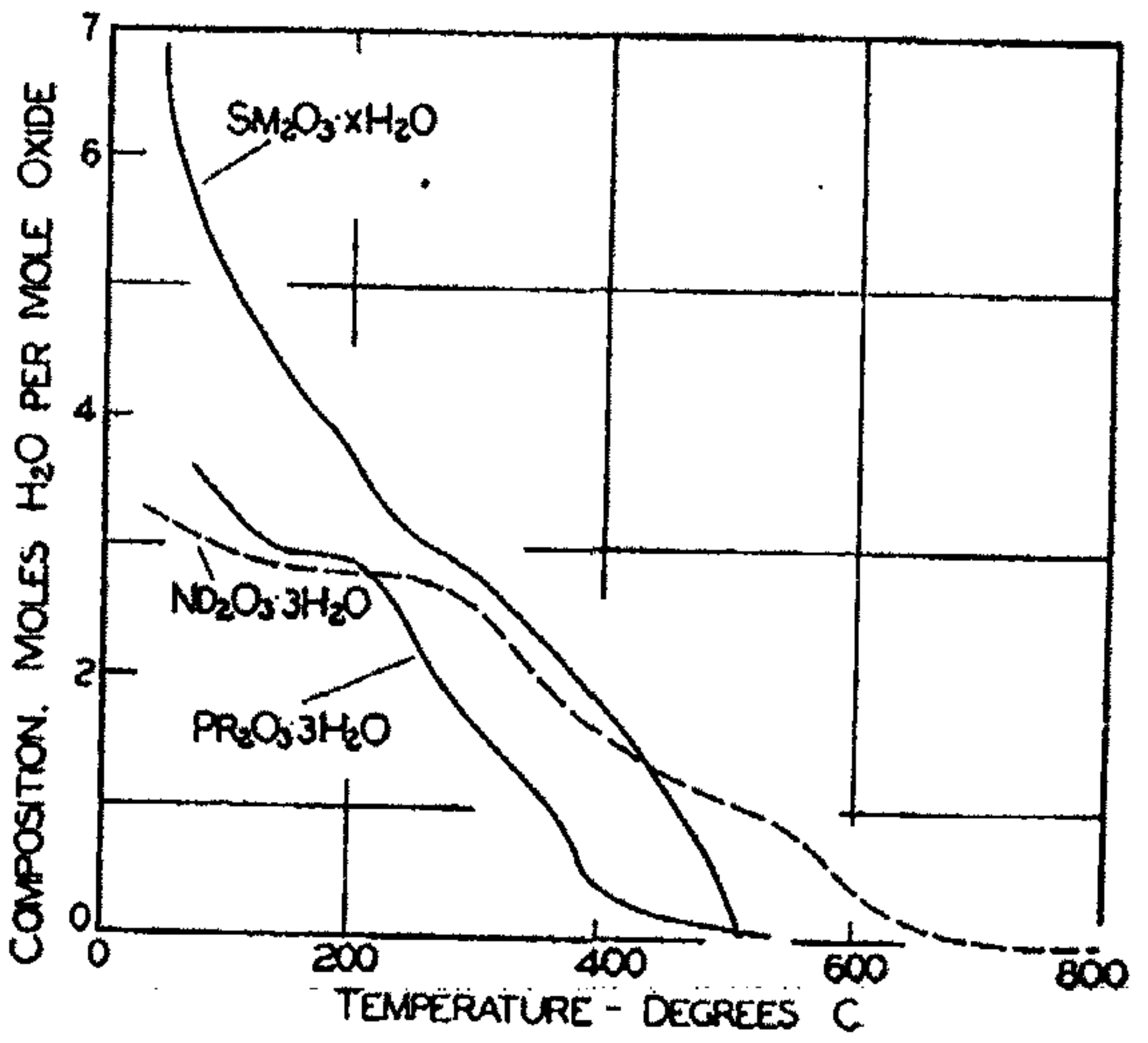

FIG. 3. Dehydration isobars for the hydrous oxides and hydrates of neodymium, praseodymium, and samarium.

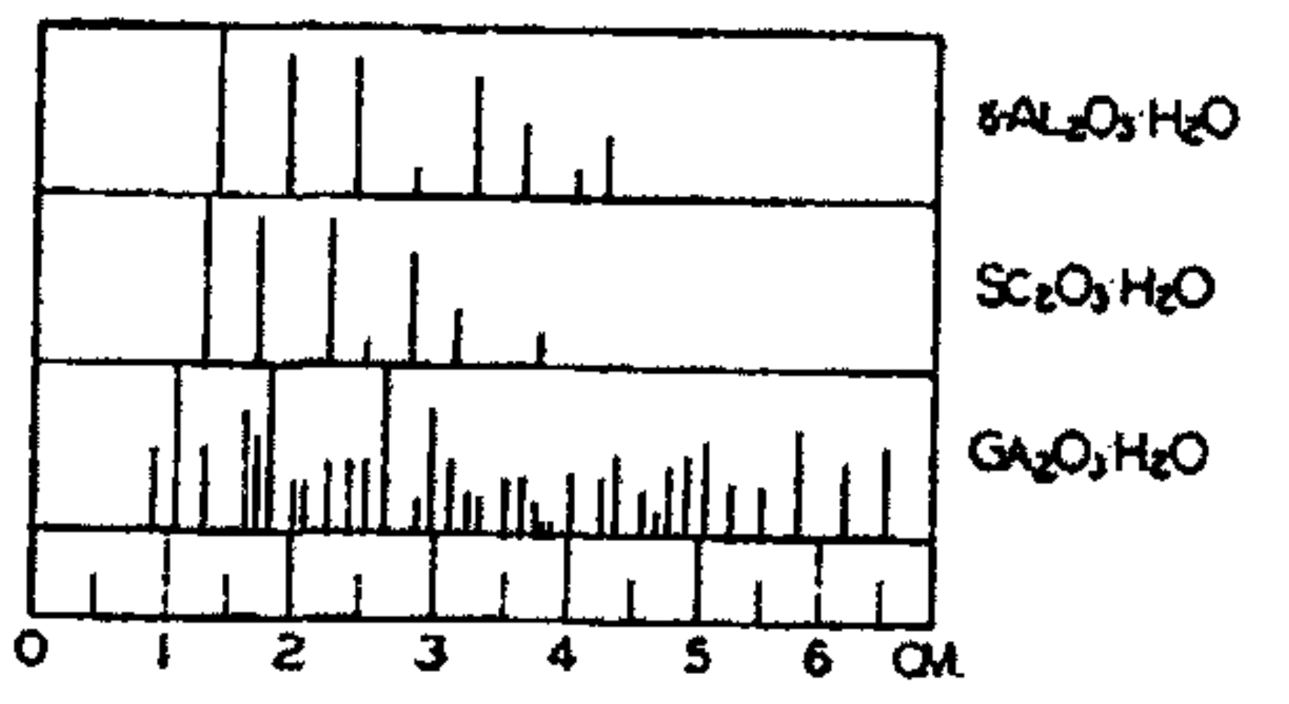

FIG. 4

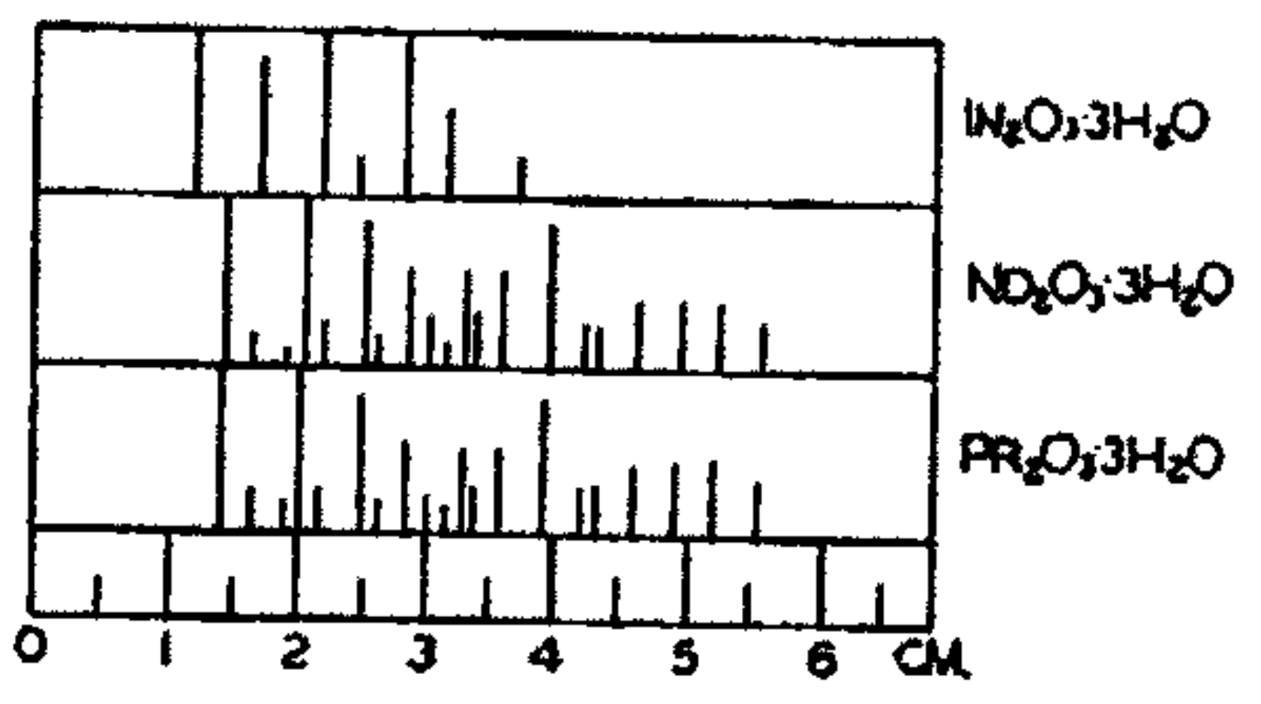

FIG. 5

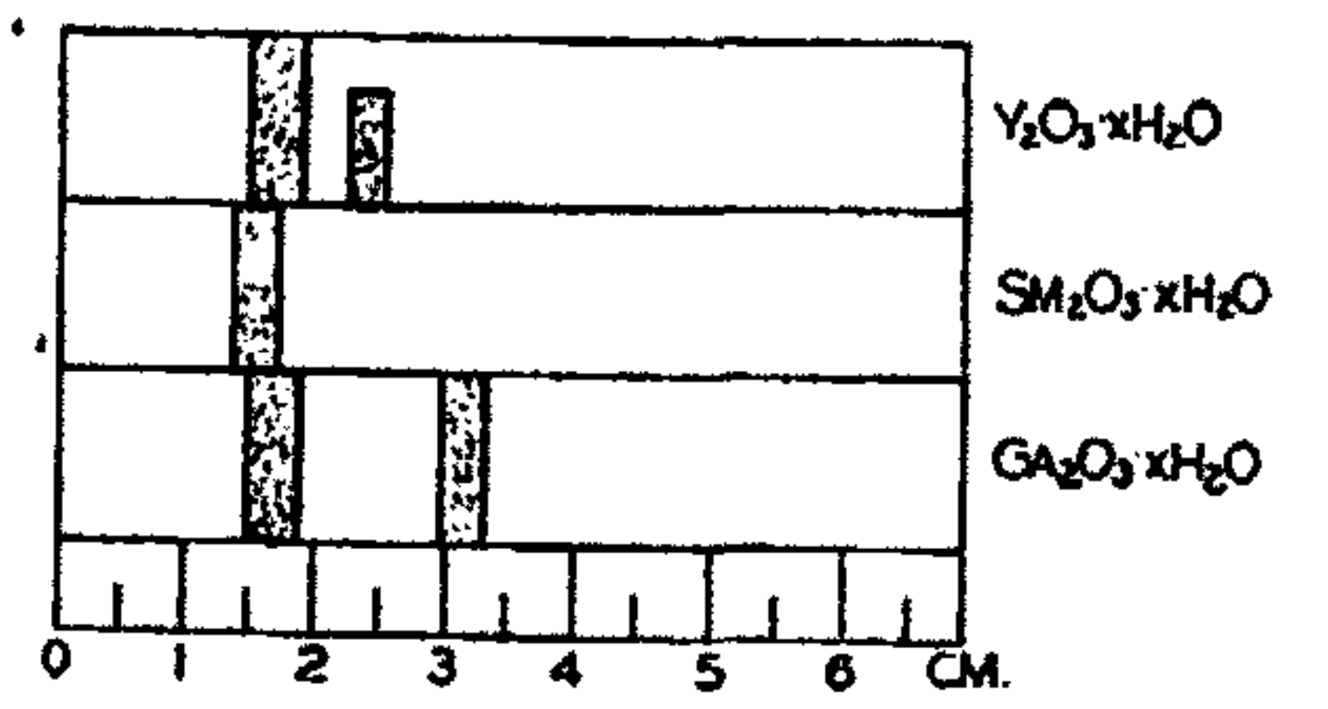

FIG. 6

FIG. 4. X-ray diffraction patterns for the trihydrates of the oxides of indium, neodymium, and praseodymium.

FIG. 5. X-ray diffraction patterns for the hydrous monohydrates of the oxides of aluminum, scandium, and gallium.

FIG. 6. X-ray diffraction patterns for the hydrous oxides of yttrium, samarium, and gallium.

indication and the praseodymium isobar a slight indication of the formation of monohydrate at temperatures around 400°C.

X-ray diffraction patterns of $Nd_2O_3 \cdot 3H_2O$ are given in figure 5. These patterns are distinct from the patterns of the respective anhydrous oxides. There is some indication of a new crystalline phase in the x-radiograms of samples of neodymium oxide dehydrated at temperatures around 400° to 500°C. These new diffraction lines are distinct from the lines of the trihydrate or anhydrous oxide. This evidence supports the suggestion that a monohydrate of neodymium oxide may exist.

The x-ray diffraction pattern of precipitated samarium oxide consists of one, or possibly two, very broad, diffuse bands. In the absence of a definite break in the dehydration isobar and a well-defined x-radiogram, the present authors prefer to consider this material to be hydrous samarium oxide, and not a definite hydrate or hydroxide.

SUMMARY

The following is a brief summary of the results of this paper:

1. But few early studies have been made of the hydrous oxides and hydrous hydrates of the Group III metals other than aluminum. In this report the composition of the hydrous oxides and hydrous hydrates of gallium, indium, thallium, scandium, yttrium, neodymium, praseodymium, and samarium have been investigated from the standpoint of their dehydration isobars and x-ray diffraction patterns.

2. The dehydration isobars have been obtained under conditions that ensure the establishment of equilibrium at each point of the isobar.

3. Samples for x-ray diffraction examination were removed and sealed in thin tubes of Lindemann glass under conditions that ensure neither loss nor gain of water vapor.

4. The precipitated oxides of indium, neodymium, and praseodymium consist of the hydrous trihydrates or hydroxides.

5. The precipitated oxides of gallium (when formed slowly or aged) and of scandium are hydrous monohydrates.

6. The precipitated oxides of thallium, gallium (when formed rapidly or unaged), yttrium, and samarium show no indication of hydrate formation. These precipitated gels should be considered as hydrous oxides of the respective metals.

REFERENCES

(1) Böhm and Niclassen: Z. anorg. allgem. Chem. **132**, 1 (1924).
(2) Carnegie: Chem. News **60**, 113 (1889).
(3) Crookes: Phil. Trans. **209A**, 15 (1908).
(4) Damiens: Ann. chim. [9] **10**, 181 (1918).
(5) Fricke and Hüttig: in Handbuch der allgemeinen Chemie, Vol. IX, pp. 57-106. Akademische Verlagsgesellschaft, Leipzig (1937).

(6) Hüttig and Mytyzek: Z. anorg. allgem. Chem. **192,** 187 (1930).
(7) Joye and Garnier: Compt. rend. **154,** 510 (1912).
(8) Milligan and Weiser: J. Am. Chem. Soc. **59,** 1670 (1937).
(9) Milligan and Weiser: J. Phys. Chem. **41,** 1029 (1937).
(10) Weiser: Inorganic Colloid Chemistry, Vol. II, pp. 90–100. John Wiley and Sons, Inc., New York City (1935).
(11) Weiser and Milligan: J. Phys. Chem. **38,** 513 (1934).
(12) Weiser and Milligan: J. Phys. Chem. **38,** 1175 (1934).
(13) Weiser and Milligan: J. Am. Chem. Soc. **59,** 1457 (1937).
(14) Weiser and Milligan: J. Phys. Chem. **42,** 669 (1938).
(15) Weiser, Milligan, and Ekholm: J. Am. Chem. Soc. **58,** 1262 (1936).

THE SORPTION OF CHLORINE BY ACTIVATED CHARCOAL[1]

L. H. REYERSON AND A. W. WISHART

School of Chemistry, University of Minnesota, Minneapolis, Minnesota

Received March 16, 1938

In a previous communication (5) the authors described a method for determining the sorption of chlorine by porous sorbents, which was a modification of the method given earlier by Cameron and Reyerson (1), and presented the results of a series of measurements on the sorption of chlorine by silica gel. The results of a similar series of measurements on the sorption of chlorine by activated charcoal are given at this time. The charcoal used in this study was a part of the material prepared by Cameron for use in the work reported by Reyerson and Cameron (3, 4). It was steam-activated at 850°C. and allowed to cool to room temperature before air was admitted. The steam-activated charcoal was then placed in a silica bulb and heated to 700°C. under high vacuum for 24 hours. Upon cooling to room temperature, oxygen was admitted. After standing several hours in oxygen the charcoal was heated once more, pumped out for 48 hours, and finally cooled in an atmosphere of nitrogen. Weighed amounts of this charcoal were placed in the glass bucket of the McBain-Bakr balance. The quantities of chlorine sorbed by this charcoal were determined at 35.5°, 51°, 73.5°, and 91.5°C. over a pressure ranging from zero to about atmospheric pressure. The chlorine was purified, introduced into the system, and maintained at the various vapor pressures as previously described (5). The results are given in table 1 and presented graphically in figure 1. As shown in figure 1 a slight hysteresis exists in the desorption points near 100 mm. pressure. Slightly more chlorine was retained during desorption than was taken up during adsorption. Since the establishment of equilibrium was slow, as shown in table 1, it may well be that the observed differences were due to the fact that equilibrium was not quite attained. However, similar results were observed in the sorption of bromine by the same activated charcoal (3).

It was found impossible to remove all of the sorbed chlorine under prolonged evacuation at elevated temperatures. The final desorption points reached by two methods of drastic treatment are shown in the figure.

---

[1] The material here presented formed a part of a thesis submitted to the Graduate Faculty of the University of Minnesota by Arthur W. Wishart in partial fulfillment of the requirements for the degree of Doctor of Philosophy, August, 1937.

Curves of the type here obtained are typical of a Langmuir type of sorption. This was further borne out by plotting values against the X/M $P/(X/M)$. A straight line is demanded by the Langmuir theory, and this was found when the values in table 2 were plotted as shown in figure 2. It appeared from these results that we were dealing with a monomolecular type of sorption. Since equilibria were established slowly, it seemed likely that the sorptions were of an activated type. Calculations of differential heats of sorption tended to confirm this idea. An average of nine of these values gave 8860 calories per mole as the differential heat of sorp-

TABLE 1

Sorption of chlorine by activated charcoal

PRESSURE (CORRECTED)	GAS (CHLORINE) SORBED PER GRAM OF CHARCOAL	X/M PER GRAM OF SORBENT	TIME FOR READING	PRESSURE (CORRECTED)	GAS (CHLORINE) SORBED PER GRAM OF CHARCOAL	X/M PER GRAM OF SORBENT	TIME FOR READING
Isothermal at 35.5°C.				Isothermal at 73.5°C.			
mm.		*millimoles*	*hours*	*mm.*		*millimoles*	*hours*
0.0*	0.0	0.0		0.0*	0.0	0.0	
81.6	0.3559	5.0192	24	25.2	0.2750	3.8781	20
227.3	0.3799	5.3579	18	260.2	0.3438	4.8481	20
348.7	0.3869	5.4552	16	586.5	0.3634	5.1245	18
526.0	0.3962	5.5873	12	720.3	0.3738	5.2714	12
672.3	0.3997	5.6360	12	610.5	0.3645‡	5.1406‡	12
409.1	0.3938‡	5.5526‡	15	303.0	0.3504‡	4.9411‡	14
103.6	0.3688‡	5.2000‡	15	127.1	0.3305‡	4.6612‡	18
24.0	0.3433‡	4.8405‡	18	24.2	0.2869‡	4.0454‡	20
6.9	0.3092‡	4.3600‡	24	18.2	0.2730‡	3.8495‡	20
0.00†	0.2327‡	3.2815‡	48	Isothermal at 91.5°C.			
Isothermal at 51.0°C.				0.0*	0.0	0.0	
0.0*	0.0	0.0		25.7	0.2663	3.7552	20
15.3	0.2903	4.0935	24	142.5	0.3101	4.3731	18
136.7	0.3503	4.9399	20	248.0	0.3294	4.6455	15
324.3	0.3703	5.2220	16	566.3	0.3543	4.9966	15
474.8	0.3775	5.3229	16	721.8	0.3587	5.0584	12
682.0	0.3892	5.4888	12	591.3	0.3554‡	5.0113‡	16
399.9	0.3735‡	5.2673‡	16	330.4	0.3426‡	4.8309‡	18
67.1	0.3404‡	4.8006‡	20	138.9	0.3211‡	4.5282‡	18
6.8	0.2853‡	4.0238‡	24	31.9	0.2813‡	3.9672‡	20
				10.5	0.2432‡	3.4294‡	20
				0.00†	0.1799‡	2.5369‡	36

* Readings in rows indicated in this manner were taken with the system evacuated and before admission of the halogen.

† Chlorine frozen down by liquid oxygen.

‡ Desorption readings.

tion. This is significantly larger than the heat of vaporization at the boiling point, 4778 calories, and indicates strong forces of attraction between the chlorine atoms and sorption centers on the carbon surface.

The type of sorption curve for chlorine on charcoal is fundamentally different from that of chlorine on silica gel (1), but it is almost exactly like that of bromine on activated charcoal (3). Furthermore, the quantity in millimoles of chlorine sorbed at a given temperature is about the same as the amount of bromine taken up at a like temperature above its boiling point. In figure 3 the isotherms of the sorption of chlorine, bromine, and iodine by charcoal are given. A similar comparison for the sorption of these halogens by silica gel is shown in figure 4. These two figures show the differences in the type of sorption exhibited by charcoal and silica gel for the halogens. Figure 3 shows that the sorptive capacity of charcoal for bromine and chlorine is about the same, while it is more than tenfold greater than for iodine. Since the sorptions of all of these halogens fit the Langmuir expression for a monomolecular layer of sorbed molecules, it may well be that the iodine molecules are enough larger than the bromine molecules so that steric hindrance prevents the iodine molecules from being sorbed on most of the active centers of the carbon surface. Weaker forces existing between the carbon and the iodine may account for some of the difference, but it does not seem probable that a shorter average life of

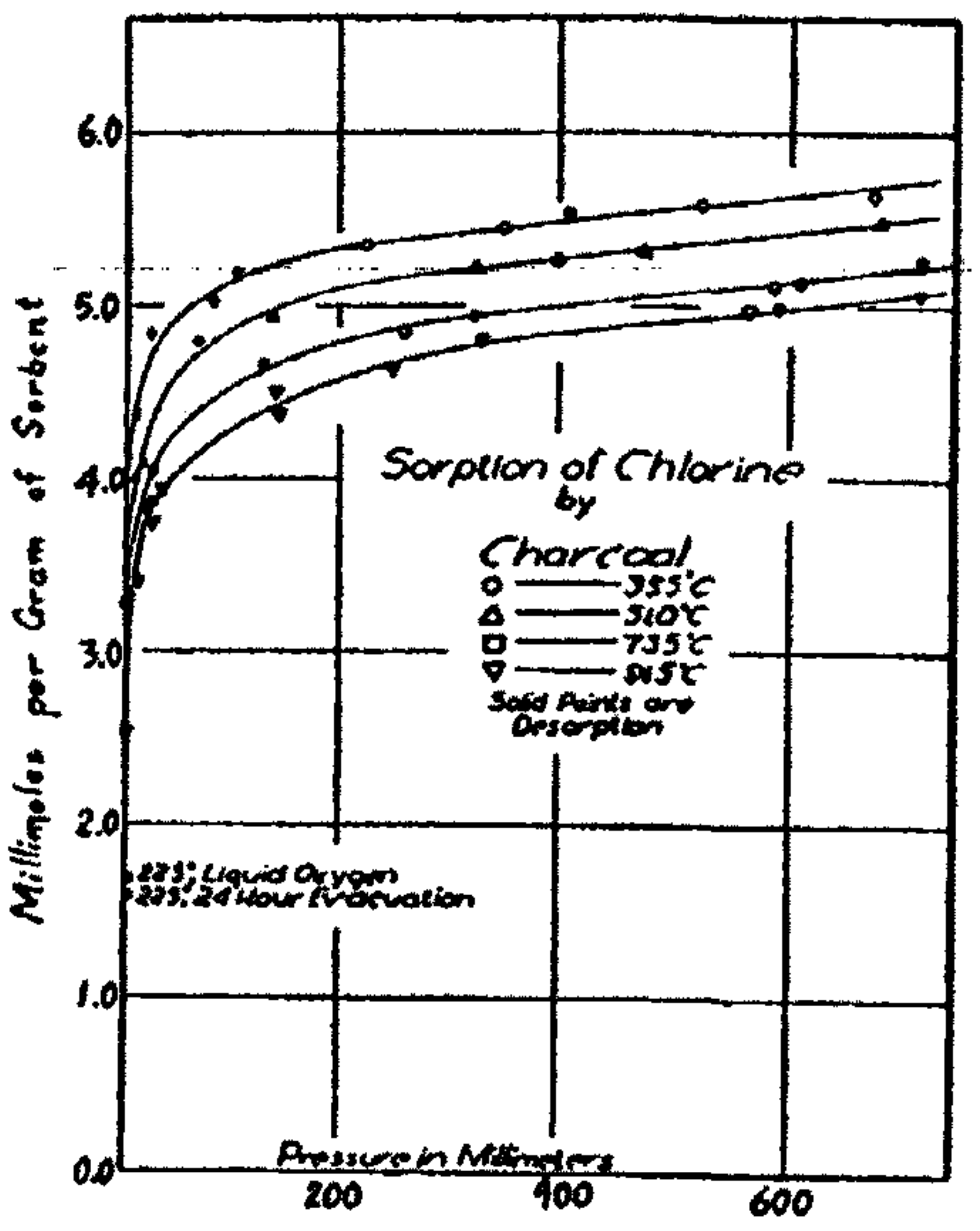

FIG. 1. Sorption of chlorine by steam-activated charcoal at different temperatures and pressures

TABLE 2

Sorption values used in Langmuir equation

P Pressure	X/M PER GRAM OF CHARCOAL	$\frac{P}{X/M}$	P PRESSURE	X/M PER GRAM OF CHARCOAL	$\frac{P}{X/M}$
Isothermal at 35.5°C.			Isothermal at 73.5°C.		
mm.	*millimoles*		*mm.*	*millimoles*	
6.9	4.3600	1.582	18.2	3.8495	4.728
24.0	4.8405	4.958	24.2	4.0454	5.982
81.6	5.0192	16.257	25.2	3.8781	6.498
103.6	5.2000	19.923	127.1	4.6612	27.268
227.3	5.3579	42.423	260.3	4.8481	53.691
348.7	5.4552	63.920	303.0	4.9411	61.322
409.1	5.5526	73.677	586.5	5.1245	114.450
526.0	5.5826	94.221	610.5	5.1406	118.760
672.3	5.6360	119.286	720.3	5.2714	136.643
Isothermal at 51.0°C.			Isothermal at 91.5°C.		
6.8	4.0238	1.690	10.5	3.4294	3.062
15.3	4.0935	3.738	25.7	3.7552	6.844
67.1	4.8006	13.977	31.9	3.9672	8.041
136.7	4.9399	27.672	138.9	4.5282	30.674
324.3	5.2220	62.103	142.5	4.3731	32.585
399.9	5.2673	75.921	248.0	4.6455	53.385
474.8	5.3229	89.199	330.4	4.8309	68.393
682.0	5.4885	124.253	566.3	4.9966	113.337
			591.3	5.0113	117.993
			721.8	5.0584	142.693

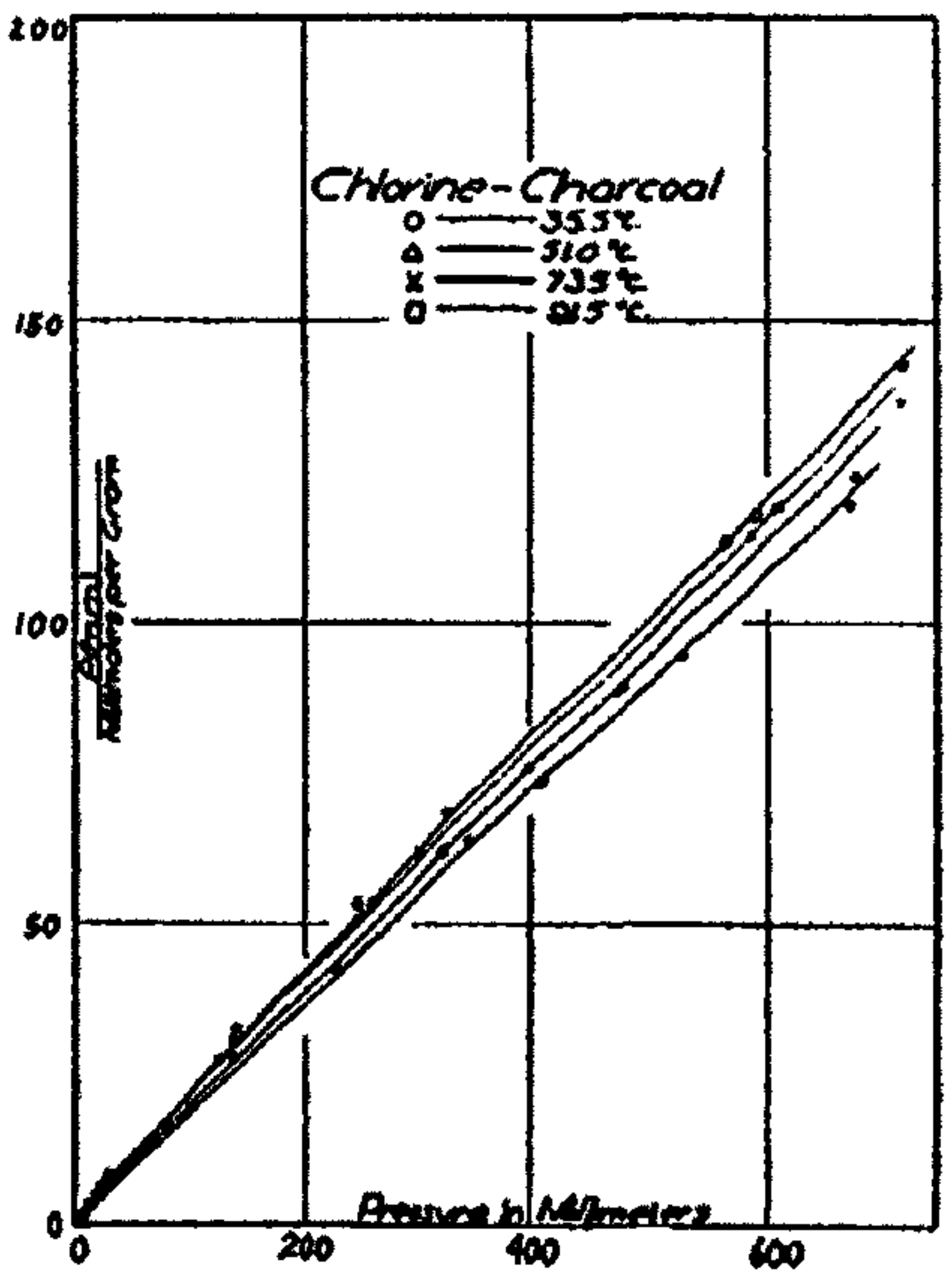

FIG. 2. Sorption isotherms obtained by use of the Langmuir equation

iodine on the carbon surface could be responsible for the tenfold decrease in sorption.

If steric hindrance prevents many of the active centers from taking up iodine but not chlorine or bromine, then it should be possible to obtain some idea concerning the spacing of active centers on activated charcoal. From viscosity measurements the radii of the halogen molecules are given as follows: chlorine, 1.85 Å.; bromine, 2.02 Å.; and iodine, 2.23 Å. Recent x-ray studies on solid bromine (6) and solid iodine (2) give the following distances between the halogen atoms of the molecules in the crystal lattice: Br—Br = 2.27 Å. and I—I = 2.70 Å. However, the absence of a like value for chlorine led us to use the values from viscosity data for comparison. If, for convenience, we assume the cross sections of the molecules to be circles, then the area covered will be 1.07×10^{-15} cm.^{2} by a chlorine molecule, 1.28×10^{-15} cm.^{2} by a bromine molecule, and 1.56×10^{-15} cm.^{2} by an iodine molecule. If the effective area is the same as this cross section, then the critical area from the steric hindrance point of view must lie between 1.28 and 1.56×10^{-15} cm.^{2} The real areas occupied by these molecules are probably somewhat greater than this, in view of the results of the x-ray studies and the knowledge of the probable shape of the molecules. Even so, the minimum spacing of the active centers on the charcoal surface must be somewhere between 2.5 Å and 3.2 Å. If the chlorine and bromine molecules occupy all of the active centers in a checkerboard arrangement, then the minimum area of charcoal covered by chlorine

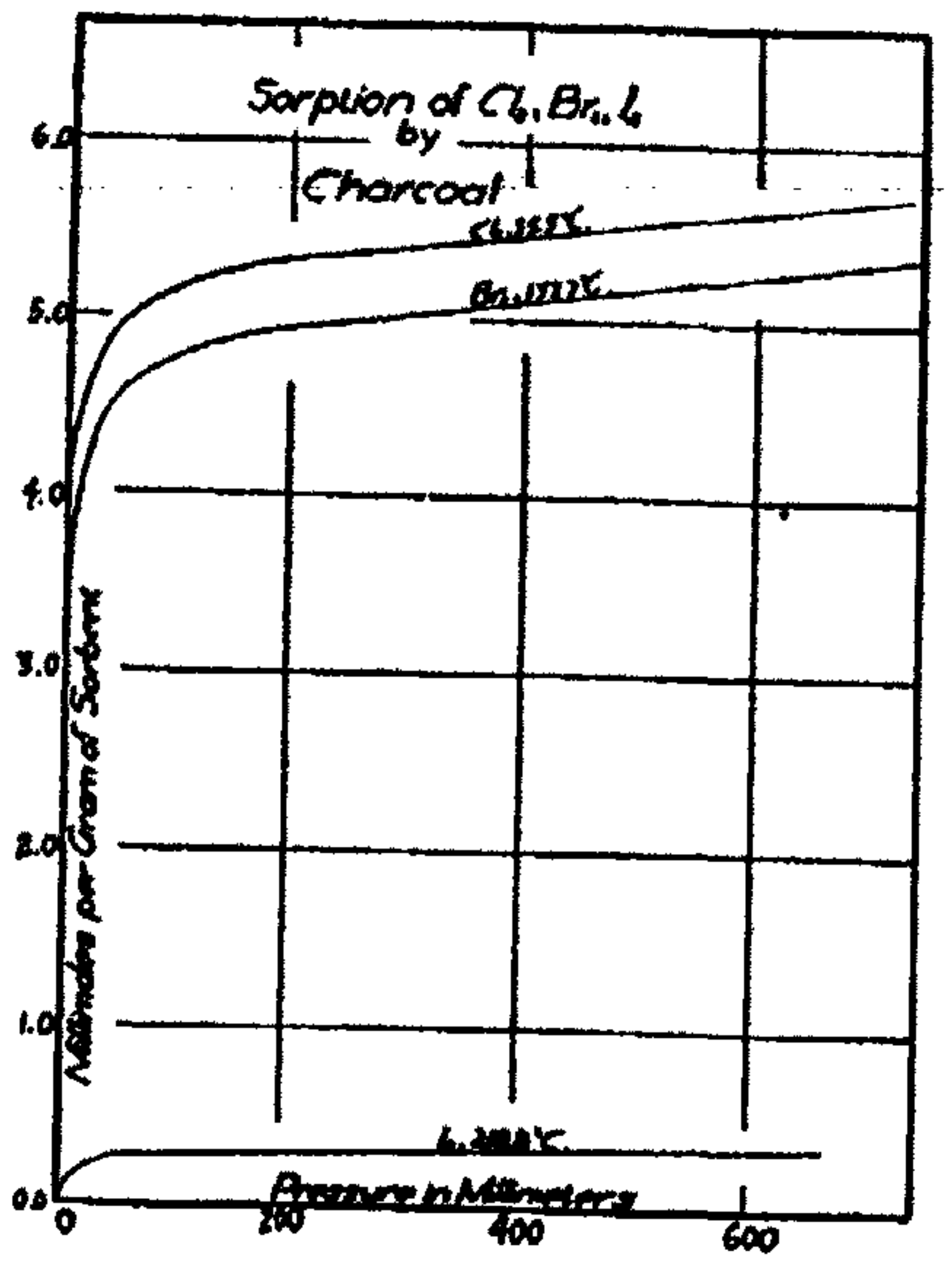

FIG. 3. Sorption of chlorine, bromine, and iodine by charcoal

molecules comes out to be 4.31 × 10^6 cm.^{2} per gram of charcoal. A similar calculation for bromine gives a minimum area of 5.54 × 10^6 cm.^{2} per gram. It is more than likely that the surface area of the charcoal used in these investigations is somewhat larger than these values. It is also possible that each atom of the halogen molecule is held by the carbon surface. If so, the spacing of the active centers may be such that they are able to hold the chlorine and bromine atoms without too much strain but not the iodine atoms.

These studies prove the very great difference that exists between the character of sorption on silica gel and charcoal. The surfaces of these two sorbents are of about the same magnitude, yet the whole character of the sorption is different. It should also be noted that the three halogens differ among themselves in the manner in which they are sorbed by silica gel. Further work will be needed to explain these differences. It is also suggested that the temperature of the sorbent surface plays a distinct rôle in the sorption process. The energy of the surface may be such that the amount of sorption is greatly reduced in spite of the fact that the sorbate at the temperature studied is below the critical temperature or even near the boiling point. Further study is in progress in the hope that additional light may be thrown on the problem.

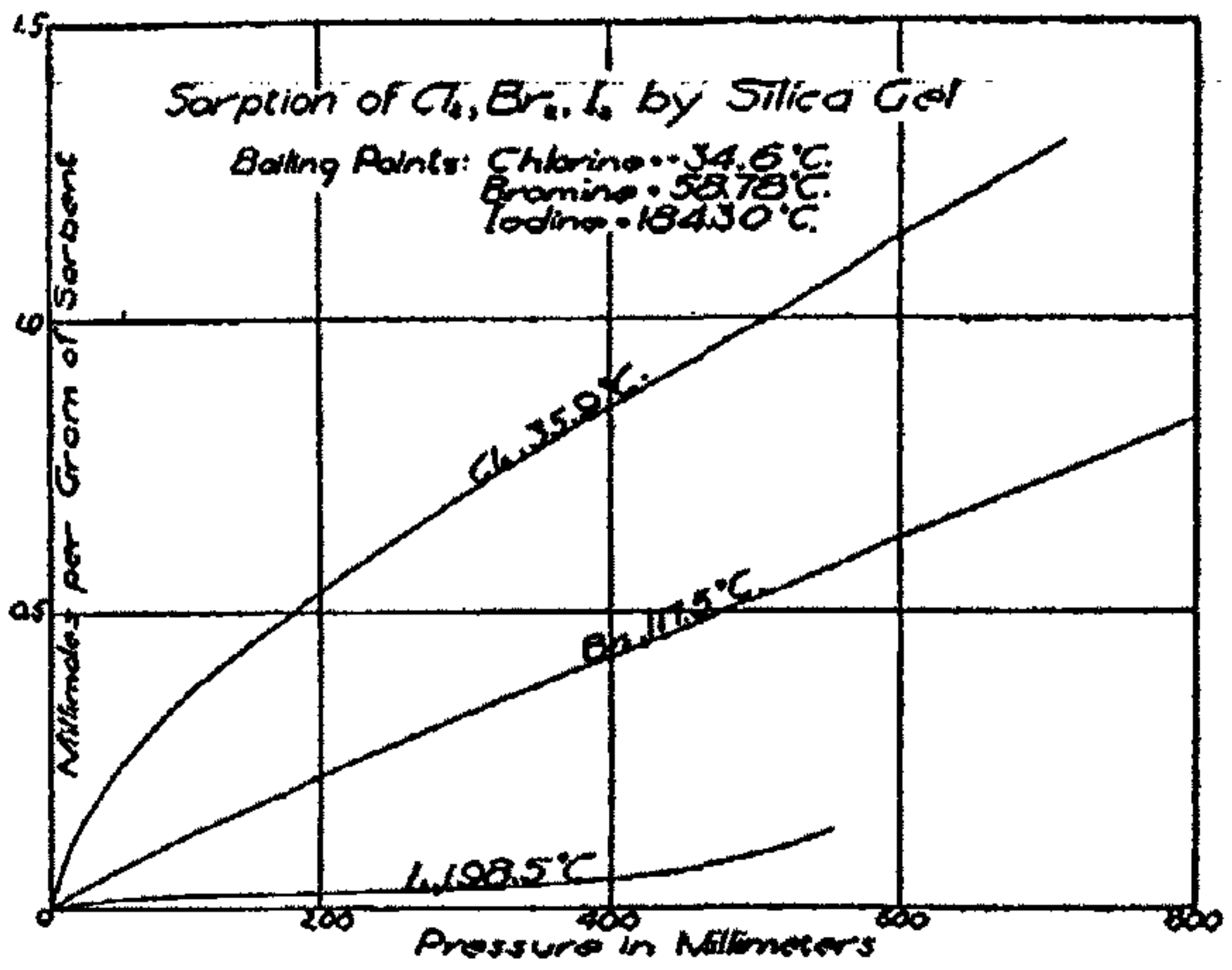

FIG. 4. Sorption of chlorine, bromine, and iodine by silica gel

SUMMARY

1. Sorption isotherms for chlorine on activated charcoal were obtained at 35.5°, 51.0°, 73.5°, and 91.5°C.
2. Comparison of these results with those of bromine and iodine is made.

3. Calculations show the minimum surface area of the activated charcoal to be 5.54×10^6 cm^2.

REFERENCES

(1) Cameron and Reyerson: J. Phys. Chem. **39**, 169 (1935).
(2) Harris, Mack, and Blake: J. Am. Chem. Soc. **50**, 1583 (1928).
(3) Reyerson and Cameron: J. Phys. Chem. **39**, 181 (1935).
(4) Reyerson and Cameron: J. Phys. Chem. **40**, 233 (1936).
(5) Reyerson and Wishart: J. Phys. Chem. **41**, 943 (1937).
(6) Vonnegut and Warren: J. Am. Chem. Soc. **58**, 2459 (1936).

HELMHOLTZ AND NERNST

WILDER D. BANCROFT
Cornell University, Ithaca, New York

Received March 21, 1938

About sixty years ago Helmholtz (4) worked out an equation for the electromotive forces of concentration cells with diffusion. For a cell of the type

$$\mathrm{Zn} \mid c_1\mathrm{ZnSO_4} \mid c_2\mathrm{ZnSO_4} \mid \mathrm{Zn}$$

Helmholtz wrote an equation which is equivalent to:

$$E = RT \frac{u}{u + v} \int_{h_2}^{h_1} h \frac{\partial \ln p}{\partial h} \mathrm{d}h \tag{1}$$

Here h is the dilution, or grams of water per gram of salt, instead of the concentration, which is the term we usually use nowadays. Helmholtz wrote $1 - n$, but I have changed that to conform with the modern custom. This equation can be right only when the transference number for the anion is independent of the concentration or dilution. This is usually not the case, and Helmholtz (3) discusses the matter very briefly in a later paper. The assumption is made throughout that water vapor follows the simple gas law $PV = RT$.

A few years later Helmholtz (5) discussed the case of concentration cells without diffusion. As typical he took reversed calomel cells

$$\mathrm{Zn} \mid c_1\mathrm{ZnCl_2}\ \underline{\mathrm{Hg_2Cl_2}} \mid \mathrm{Hg} \mid \underline{\mathrm{Hg_2Cl_2}}\ c_2\mathrm{ZnCl_2} \mid \mathrm{Zn}$$

The formula, as written by Helmholtz, is equivalent to:

$$E = RT \int_{h_2}^{h_1} h \frac{\partial \ln p}{\partial h} \mathrm{d}h \tag{2}$$

From Moser's data on the vapor pressures of zinc chloride solutions, Helmholtz calculated two interpolation formulas, which differ only slightly and which he called "a" and "b". For cells in which the two values of h are 0.8 and 9.1992 the observed and calculated values at temperatures varying between 17.7°C. and 21°C. were as given in table 1.

Helmholtz considered that his standard calomel cell had an electromotive force of about 1.043 volts, but he felt that the determinations of the ohm were so uncertain at that time that it was safer to give his observations in terms of his standard calomel cell. That means that the values in table 1 should be increased by approximately 4 per cent to give them in what he considered to be millivolts. The important thing is that he was able to calculate the electromotive force with surprising accuracy even though one of his solutions contained less than 1 gram of water per gram of zinc chloride.

In 1889 Nernst (6) applied the van't Hoff theory of osmotic pressure and the Arrhenius theory of electrolytic dissociation to the case of concentration cells. For a cell of the type

$$\mathrm{Ag} \mid 0.01\ \mathrm{AgNO_3} \mid 0.1\ \mathrm{AgNO_3} \mid \mathrm{Ag}$$

Nernst deduces the equation:

$$E = 0.860T\,\frac{2v}{u+v}\,\ln\frac{P_2}{P_1} \times 10^{-4}\ \text{volt} \tag{3}$$

where P_1 and P_2 are the osmotic pressures of the silver ions in the two solutions, respectively. Complete dissociation is assumed, and it is postulated tacitly that the transference number for the anion does not change with the concentration. On the same postulation with regard to change of transference number with dilution, Helmholtz (2) derived an approximately correct expression for the electromotive force which is essentially identical with the Nernst equation, since in it the electromotive force is proportional to the logarithm of the concentrations of the salt in the two solutions.

TABLE 1

Electromotive force in terms of calomel cell

Observed	Maximum	0.11648
	Minimum	0.11428
Mean for 13 days		0.11541
Calculated	(a)	0.11579
	(b)	0.11455

Nernst (reference 5, p. 163) rewrote the Helmholtz formula for a silver nitrate concentration cell with diffusion, making it read:

$$E = \frac{\pi_0 - \pi}{\pi_0}\cdot\frac{MS}{\mathrm{H_2O}}\cdot 0.000933\,\pi_0 V_0\,\frac{v}{u+v}\,\ln\frac{C_2}{C_1} \times 10^{-8}\ \text{volt} \tag{4}$$

π_0 is the vapor pressure of liquid water at the temperature of the experiment; π that of a solution containing S grams of water per gram of salt; V_0 the volume of 1 gram of water vapor at the temperature in question and the pressure π_0; 0.000933 the amount of water in grams decomposed by the electromagnetic unit of the quantity of electricity; and M/H_2O, finally, the amount of the salt decomposed by a quantity of electricity which decomposes 18 g. of water. When we compare this equation with equation 3 we see that at high dilutions osmotic pressure, P, and concentration, c (weight of salt per weight of water), are proportional one to the other, and consequently

$$\ln \frac{P_2}{P_1} = \ln \frac{c_2}{c_1}$$

If we are applying equation 4 to an electrolyte composed of univalent radicals, then $M = 2m$, where m is the molecular weight of the latter. The factor $2 \times 0.000933 \times \pi_0 V_0$ works out, in conjunction with Regnault's data, to 0.02542×10^{-8} in absolute C.G.S. units at 20°C. If we notice that V_0 is proportional to the absolute temperature and introduce this into equation 4, we get:

$$E = \frac{\pi_0 - \pi}{\pi_0} \cdot \frac{MS}{18} \cdot 0.867\ T \frac{u}{u + v} \ln \frac{P_2}{P_1} \times 10^{-4} \text{ volt} \tag{5}$$

For equation 3 and equation 5 to be compatible, we must have

$$\frac{\pi_0 - \pi}{\pi_0} \cdot \frac{MS}{18} = 2 \tag{6}$$

The constants of the two formulas, 0.860 and 0.867, would be equal if water vapor at this temperature, as assumed by Helmholtz, and hydrogen ion, as assumed by Nernst, really behaved like ideal gases.

If we replace $MS/18$ by ν_2/ν_1, where $\nu_2 = S/18$, the number of molecules of the solvent (water), and $\nu_1 = 1/m$, the corresponding value for the solute, we then have

$$(\pi_0 - \pi)/\pi_0 = 2\nu_1/\nu_2$$

The factor 2 arises from the fact that each molecule of a uni-univalent electrolyte gives two ions.

This is a case where the hand is quicker than the eye. In the Helmholtz equation we had the change of the partial pressure with the change of dilution. That does not integrate to $\ln \frac{P_2}{P_1}$ or $\ln \frac{c_2}{c_1}$ unless the dissolved substance behaves like an ideal gas of constant molecular weight. There cannot be any change of dissociation or any heat of dilution. Since the undissociated salt, if any, affects the vapor pressure, the Helmholtz and the Nernst formulas are identical only for infinitely dilute solutions. Since the Helmholtz equation is applicable at all concentrations, the Nernst equation must be in error to some extent at all finite concentrations.

Dolezalek (1) has applied a simplified form of Helmholtz's equation to reversed lead storage cells,

$$\mathrm{Pb} \mid c_2\mathrm{H_2SO_4}\ \underline{\mathrm{PbO_2}} \mid \mathrm{Pb} \mid \underline{\mathrm{PbO_2}}\ c_1\mathrm{H_2SO_4} \mid \mathrm{Pb}$$

For a change from 50.73 per cent to 35.82 per cent sulfuric acid the E.M.F. was 0.13 volt (calculated) and 0.13 volt (observed). For a change from 35.82 per cent to 19.07 per cent sulfuric acid the calculated value was 0.12 volt and the observed value 0.11 volt. When larger jumps were made, the results were poorer. Dolezalek made no attempt to apply exact theory and was rather pleased with the results he obtained.

Since the vapor pressures of sulfuric acid are thoroughly abnormal, owing to the high heat of dilution, and since nobody will claim 100 per cent dissociation for 50 per cent sulfuric acid, let alone 70 per cent acid, it is evident that the ion concentration is not the sole factor in determining the electromotive force. The lead storage cell should be studied with care over as wide a range of concentrations as possible and then compared with the most accurate formula obtainable.

One can also do a hydrogen-lead peroxide cell up to the concentration at which the solubility of lead sulfate becomes a serious factor. If a satisfactory equation can be developed for the change of the transference number with the concentration it would be possible to study the cell

$$\mathrm{H_2} \mid c_1\mathrm{H_2SO_4} \mid c_2\mathrm{H_2SO_4} \mid \mathrm{H_2}$$

up to the concentration at which the hydrogen reduces sulfuric acid.

If the transference problem can be solved, hydrogen electrodes with hydrochloric acid and with acetic acid will show the applicability of the Helmholtz equation to strong acids and weak acids. Since the undissociated part of an acid affects the electromotive force of a hydrogen concentration cell, and since the nature of the anion affects the dissociation, the nature of the anion will affect the apparent concentration quite apart from any effect due to the displacement of the water equilibrium.

One would also like to see experiments with cadmium and cadmium iodide concentration cells in methyl alcohol where the transference number is negative over quite a range of concentrations. Cadmium and cadmium chloride in water will give an extreme case of abnormally small dissociations. All cases of this type can be calculated by means of the Helmholtz formula once one has the data. There are some cases, however, to which the Helmholtz formula is certainly not applicable at present and perhaps may never be.

If we take a cell,

$$\mathrm{Ag} \mid x\mathrm{KCN} + y\mathrm{KAg(CN)_2} \mid x\mathrm{KCN} + y\mathrm{KAg(CN)_2} \mid \mathrm{Ag}$$

and add a little silver cyanide to one solution, there should be practically no change in partial pressure because one is merely replacing a cyanide ion by a silver cyanide ion. Consequently no accurate equation for this type of cell can be formulated in the present state of our knowledge.

The general results of this paper are as follows:

1. The Helmholtz equations for concentration cells coincide with the corresponding equations deduced by Nernst only at infinite dilution.
2. Since the Helmholtz equations are sound thermodynamically, it follows that the Nernst equations are accurate only at infinite dilution. It is not surprising, therefore, that one cannot run up even to moderate concentrations.
3. Since the Helmholtz equations involve the change of the vapor pressure with the concentration, the electromotive force depends also on the concentrations of the undissociated salt, base, or acid.
4. Dolezalek's rather crude application of the Helmholtz theory to the lead storage cell gives pretty good results for the change of electromotive force with change of sulfuric acid concentration. If the work were done well, the agreement would undoubtedly be excellent.
5. For reversed zinc–calomel concentration cells Helmholtz was able to get results to within 1 millivolt, even with a solution containing more than 1 gram of zinc chloride per gram of water.
6. It should be possible to calculate accurately the electromotive forces of hydrogen–sulfuric acid cells with diffusion up to concentrations at which hydrogen reduces sulfuric acid in a reasonable period of time.
7. Apparently no determination of pH in biological systems can be considered even approximately accurate, though we do not yet know the magnitude of the error.
8. At present nobody knows how to handle adequately the problem of electromotive forces in systems involving complex salts.

REFERENCES

(1) DOLEZALEK: Wied. Ann. **65**, 894 (1898).
(2) HELMHOLTZ: Monatsber. preuss. Akad. Wiss. **1877**, 720, 721.
(3) HELMHOLTZ: Wied. Ann. **3**, 201 (1878).
(4) HELMHOLTZ: Monatsber. preuss. Akad. Wiss Berlin **1877**, 713; Wiss. Abh. **1**, 840 (1882).
(5) HELMHOLTZ: Sitzungsber. preuss. Akad. Wiss. Berlin **1882**, II, 825; Wiss. Abh. **2**, 979 (1883).
(6) NERNST: Z. physik. Chem. **4**, 129 (1889).

NEW BOOKS

The Newer Alchemy. By Lord Rutherford. 67 pp. London: Cambridge University Press, 1937. New York: The Macmillan Company, 1937. Price: $1.50.

It is a long contrast from ancient to modern alchemy which Rutherford makes in this little volume based on the Henry Sidgwick lecture which he gave at Newnham College, Cambridge, in November, 1936. No one was better equipped for this span than he who, together with Soddy, first proposed atomic disintegration as the explanation of radioactivity; also he who observed the first transmutation by bombarding nitrogen with alpha particles and in whose laboratory Cockcroft and Walton made the first transmutation by purely artificial means.

The various counting methods are described, the cloud chamber, the Van der Graaf and Lawrence high voltage machine, and the discovery of neutrons and positrons. The mass-energy transformation of Einstein is accepted as the basis of mass-energy relations in the nuclear reactions.

Although a net energy gain results from some nuclear reactions, the prediction is made that they will not prove an energy source of practical importance.

The bombarding reagents and the various types of nuclear reactions are briefly reviewed. X-rays of high energy have also been found effective in bringing about nuclear changes as Rutherford predicted a number of years ago.

S. C. Lind.

A Hundred Years of Chemistry. by Alexander Findlay. 352 pp. New York: The MacMillan Company, 1937. Price: $3.75.

The author needs no introduction to American chemists. His previous works in the field of physical and general chemistry are well known to our readers.

The present book might be regarded as a series of essays or chapters on the history of development in about a dozen different fields of chemistry more or less unrelated. His style is, as usual, clear and vivid. The choice of material is representative. Of course, it is a rather large undertaking to give an adequate survey of the hundred years of chemistry which covers nine-tenths or more of the whole, and yet do equal justice to all the fields. Naturally, a specialist in one of the various fields may be disappointed to find neglect of an important part of his subject. The reviewer, for example, thinks it unfortunate not to have included in the chapter on radioactivity something of the newer nuclear chemistry. By the use of the expression "excess positive charge of the nucleus" the author seems to believe still that there are free electrons in the nucleus. The conception of the neutron, of course, renders this assumption unnecessary, or even untenable.

A very welcome and unusual feature of the book is an appendix of twenty pages containing biographical notes regarding about sixty chemists mentioned in the text. A combined subject and author index is also provided.

S. C. Lind.

Glossary of Physics. By LeRoy D. Weld. 255 pp. New York: The McGraw-Hill Book Company, 1937. Price: $2.50.

This glossary contains some 2500 to 3000 definitions of terms, equipment, principles, equations, etc., used in the science of physics. The definitions are clear, concise and up-to-date. Literature references are frequently given which greatly enhance its value. The arrangement is alphabetical. It is a valuable book of ready reference.

S. C. LIND.

Katalyse und Determinismus. Ein Betrag zur Philosophie der Chemie. By ALWIN MITTASCH. 14.5 x 22 cm.; ix + 203 pp. Berlin: Julius Springer, 1938. Price: 9.60 RM.

In this book Dr. Mittasch, who has in recent years written several very interesting books on the history of catalysis and on the rôle of catalytic phenomena in chemistry and biology, now enters the field of philosophy or, more correctly expressed, that of the philosophy of science. Starting with a discussion of the part played by catalysis in the "causation" of chemical phenomena (including especially the action of biocatalysts), the author soon proceeds to attack the wider general problems of determinism, causality, holism, and finalism in relation to all science. It would not be unfair to say that the main attack centers round the phenomena presented by living organisms.

From the hundreds of brief quotations interspersed throughout the text and the extensive bibliography, it is clear that Dr. Mittasch has read very widely in philosophical and biological literature and that his intention is to deal fairly with all shades of opinion. This embarrassment of riches, however, combined with a rather heavy literary style, makes the reading of the book somewhat difficult. One gathers that the author follows Planck and Einstein in holding to the principle of a "strict" causality. He adopts the "holistic" point of view so closely associated with the names of General Smuts and the late Professor Haldane, and sees in every "whole" (*Ganzheit*) a hierarchy of causes ("causalisms"), each of which possesses a determinate rank in the *Rangordnung* (order of ranking) of the whole, and all of which contribute to the causality of the whole." Thus, when we have to deal with living organisms, a place can be found for the "entelechial causalisms" postulated by Driesch, and especially for "psychical causalisms." That these causal factors cannot be pictured in time and space is no drawback, for, as the author points out, the same thing applies to the concepts of modern atomic physics. Moreover, as Bohr has so clearly indicated, the progressive advance of science must prepare us for a continuous development and widening of our concepts. Thus when we view the hierarchy of a living whole from "above downwards" or from "below upwards," the psychical-entelechial and the physicochemical descriptions may be regarded, not as contradictory, but as "complementary" in the sense of Bohr's principle of complementarity.

It would not be possible in a short review to do justice to Dr. Mittasch's learned discussion. Mathematicians, physicists, astronomers, and biologists have freely ventured to discuss the philosophy of science. It was time, as the author says, that a chemist took a hand in this game. With that opinion all chemists will surely agree, and we may certainly congratulate Dr. Mittasch on being led from meditations concerning the phenomena of catalysis to a brave attack on the dragons of philosophical doubt. Although the reviewer believes that progress in this direction is most likely to come from an application of the methods of mathematical analysis and symbolic logic to the statement of the problems, that is no reason why Dr. Mittasch should not follow the more usual method. Wisely perhaps, he nowhere attempts to define and distinguish what he means by causality, determinism, finalism, etc. But the results are somewhat disconcerting. Thus his "determinism" seems to involve "Plan" and "Ziel," whereas determinism as usually defined involves nothing more than a determinate functional relation between the "before" and the "after," as measured or observed.

One final remark on the subject of causality. Has Dr. Mittasch ever read the sound criticism of David Hume?

F. G. DONNAN.

Abridged Scientific Publication from the Kodak Research Laboratories. Volume XVIII (1936). Rochester, N. Y.: The Eastman Kodak Company, 1937.

The eighteenth volume contains about sixty abridged papers condensed from the form in which they appeared in 1936 in about a dozen and a half different scientific periodicals. These papers are principally in the field of photography, optics, and spectroscopy, with some contribution to analytical and organic chemistry and to radiography.

S. C. LIND.

The Retardation of Chemical Reactions. By KENNETH C. BAILEY. 479 pp. New York: Longmans, Green and Company, 1937. Price: $8.00.

For the past two decades the chemist has been learning that it is often as important to prevent reactions as to cause them. The discovery of chain mechanism, which put the subject on a scientific basis, has stimulated research and applications.

The author has covered the entire field mostly from the experimental viewpoint. After a brief historical survey he takes up the subject of oxidation, chain reactions, antioxidants, and oxidation of organic and inorganic substances in the gaseous, liquid, and solid states, to which more than half of the book is devoted.

Among applications he discusses the protection of rubber, the prevention of metallic corrosion, the setting of cement and plaster of Paris, antiknock action, the stabilization of hydrogen peroxide, decompositions of various types, the hydrogen-chlorine reactions, polymeric and isomeric changes, and a number of unclassified reactions. This subject cannot fail to be of interest both practically and theoretically to a wide circle of chemists. The author has made an excellent selection of experimental material, and has picked his way carefully through the maze of kinetic fact and fancy which fills the literature.

An extensive bibliography of 1630 references, which occupies nearly 100 pages and takes the place of an author index, doubtless has added materially to the cost of the book.

S. C. LIND.

The Fine Structure of Matter: Part I. X-rays and the Structure of Matter. By C. H. DOUGLAS CLARK. 216 pp. New York: John Wiley and Sons, 1937. Price: $4.25.

This book is Part I of Volume II of *A Comprehensive Treatise on Atomic and Molecular Structure* being prepared by the author in a fashion somewhat similar to Mellor's monumental work in the field of inorganic chemistry. Works of this type are a great boon to the teacher and to the research investigator, and are very welcome additions to our scientific literature. It is not a book from which to study the subject in detail, but attempts to give a general outline of the field together with many references to the original literature. More than a thousand references, chiefly from the period 1928-1934, are given. For earlier references the reader is expected to consult Ewald and Hermann's *Strukturbericht.*

In the general preface the author points out his purpose to save space by frequent reference to summarizing works, and thereby to avoid repetition of the original references quoted in them. It is surprising then to find only three additional books on the subject listed among the references. Such excellent books as Wyckoff's *Structure of Crystals* and its 1930–1934 *Supplement* might well have been mentioned for their important summaries of crystal structure results.

It is not quite clear why the references could not have been brought up to a later date than the end of 1934 in a book which did not appear off the press until late in 1937.

The common symbols of crystallography and crystal structure have been largely omitted from the list of symbols in the front of the book, but they have been used freely throughout the book. The first chapter, on crystal geometry and the methods of analysis, cannot be considered to have been adequately treated, but the rest of the material seems reasonably complete. For example, the atomic structure factor in the appendix has a list of 120 references. There are a few important omissions. The Weissenberg method is not mentioned, and the only reference to molecular rotation in solids is on page 103.

The book contains many excellent drawings of structures, but figures XI, XVII, and XXXV might well have been replaced with simpler diagrams. The reviewer doubts that much advantage was gained by the adoption of the symbols suggested on page 71. In fact, the author has not been wholly consistent in the use of his symbols, as is seen on pages 55, 56, and 86.

Errors of one kind or another inevitably creep into a work of this kind. Some of them noted by the reviewer are on pages 10, 15, 37, 71, and 119. A few simple typographical errors were also noted.

In conclusion, it is the reviewer's opinion that the book will serve a very useful purpose as a quick reference to the results of crystal analysis.

HAROLD P. KLUG.

Textbook of Thermodynamics. By PAUL EPSTEIN, Professor of Theoretical Physics, California Institute of Technology. xii + 406 pp.; 64 figs.; 14½ x 23 cm. New York: John Wiley and Sons, Inc., 1937. Price: cloth, $5.00.

The author treats thermodynamics from the point of view of the physicist. He has designed his book to be used partly as a basic course for seniors and younger graduate students, and partly for reference or for courses given to more advanced students. The arrangement of the material is along the lines of the classical treatment. The book contains, however, much modern material and much that is of interest to the chemist. The author has departed from the notation which has become more or less standardized in this country. He deals with the fundamental concepts in a detailed and careful manner, and makes numerous applications in the realm of physics and chemistry. His concept of entropy is based upon the cyclical processes. Chapters are included dealing with electron and ion clouds, equilibrium involving radiation, magnetic and electric phenomena, and the limitations of thermodynamics, including the theory of fluctuations. The historical development of the first law is interestingly discussed in seven pages. The author follows the Nernst tradition and omits references to important American contributions to the field.

MERLE RANDALL.

Gmelins Handbuch der anorganischen Chemie. 8 Auflage. Herausgegeben von der Deutschen Chemischen Gesellschaft. System-Nummer 22: Kalium. Lieferung 4. Verbindungen bis Kaliumacetat. 26 x 18 cm.; pp. xxv + 805-932. Berlin: Verlag Chemie, 1937. Price: 15 RM.

The present section includes compounds of potassium with boron and carbon.

The boron compounds include borates, perborates, and borofluorides; the carbon compounds include carbides, carbonyls, carbonates (with their manufacture), carbamate, percarbonates, cyanide (with its manufacture), cyanate, thiocyanate, formate, and acetate. The perborates are treated as true per-salts. The carbonate is now largely made by the Engel-Precht process, depending on the decomposition of potassium chloride solution with magnesium carbonate, full details of the various modifications of which are given, but it is also produced by the action of carbon dioxide on electrolytic caustic potash. Full details of the properties of all the compounds are given, the recent literature being well covered, but the solubility of potassium thiocyanate in alcohol is omitted.

J. R. PARTINGTON.

Gmelins Handbuch der anorganischen Chemie. 8 Auflage. Herausgegeben von der Deutschen Chemischen Gesellschaft. System-Nummer 24: Rubidium. 26 x 18 cm.; pp. x + 250. Berlin: Verlag Chemie, 1937. Price: 31.50 RM.

The present volume constitutes a complete monograph on rubidium and its compounds. The compounds of rubidium are prepared from carnallite, and rubidium and cesium compounds from lepidolite. A method of preparation depends on the precipitation of cesium, but not rubidium, by antimony trichloride from solutions of the chlorides in hydrochloric acid. There has been a considerable fall in price of rubidium and cesium compounds since 1930. Pure rubidium is obtained by thermal decomposition of the azide. There is a section on analytical chemistry.

J. R. PARTINGTON.

Gmelins Handbuch der anorganischen Chemie. 8 Auflage. Herausgegeben von der Deutschen Chemischen Gesellschaft. System-Nummer 27: Magnesium. Teil B. Lieferung 1. Verbindungen bis Magnesium und Jod. 28 x 18 cm.; pp. vii + 200. Berlin: Verlag Chemie, 1937. Price: 23.25 RM.

Compounds of magnesium with hydrogen (MgH detected in band spectra only), oxygen, nitrogen (including oxy-compounds), and halogens (including oxy-salts) are described in a very thorough manner. The nitride is prepared by heating magnesium filings for 4 to 5 hours at 800-850°C. in pure nitrogen. The use of magnesium perchlorate as a drying agent for gases is described. The descriptions of the solubilities are accompanied by phase rule diagrams, and there are extensive tables of numerical data. Some of the sections are of considerable technical interest. The general feature of the whole treatise, viz., a full description of the physical chemistry of the materials described, is evident in the present volume, which will be of considerable interest to physical chemists.

J. R. PARTINGTON.

Legierungen der Platinmetalle. Patentsammlung. By G. A. GRÜTZNER AND C. GÖTZE. Anhang zu den System-Nummern 63 bis 68, Gmelins Handbuch der anorganischen Chemie. 8 Auflage. Herausgegeben von der Deutschen Chemischen Gesellschaft. 26 x 18 cm.; 536 pp. Berlin: Verlag Chemie, 1937. Price: 40.50 RM.

The uses of the platinum metals and their alloys have recently become increasingly important and there is a large patent literature. The present volume brings this together in a very convenient tabular form, the compositions and properties of the alloys being given briefly in a systematic order, with references to the patents. The treatment is very complete, and the book is therefore of considerable value and importance.

J. R. PARTINGTON.

Reports on Progress in Physics. Volume IV. Published by the Physical Society. 26 x 18 cm.; vi + 389 pp. Cambridge: The University Press, 1937. Price: 20s.

The present volume contains eighteen articles, those of particular interest to physical chemists being on the adsorption of gases on solids, surface tension, supersonics, thermodynamics, the electronic charge, electrolytes, spectroscopy and some aspects of atomic physics, although nearly all the remaining articles contain more or less of general interest from the point of view of physical chemistry. The sections usually present enough background to make them intelligible and interesting, the abstract style being notably avoided in the better articles. In some cases, as in the section on electrolytes, the detailed presentation of well-known material, which can be found in textbooks, seems to the reviewer to have been overdone, to the exclusion of more recent developments, no mention at all of which is to be found. No modern presentation of the theory of electrolytes can be based on the simple theory of Debye and Hückel, as is done here, at least if the interests of physical chemists are to be considered. As in previous reports, there is a welcome tendency to include quantitative data, so that these volumes will, during the period of their youth, form useful supplements to tables of data. The paper, printing, and binding are of high quality.

J. R. PARTINGTON.

Thermodynamics. By E. FERMI. 23 x 16 cm.; x + 160 pp. London and Glasgow: Blackie and Son, Ltd., 1938. Price: 12s.6d.net.

This book is characterized by a very clear treatment of fundamental principles and their application to a restricted field of problems, especially chemical equilibria in gases and dilute solutions. Ideal systems only are considered. The two laws are treated in a very clear and satisfactory manner, the second law being developed in relation to Carnot's cycle through the efficiency of a reversible engine in the classical manner. This treatment can hardly be evaded if a real understanding of the matter is desired. The entropy and thermodynamic potentials are then carefully dealt with, irreversible changes being included. The chapter on thermodynamic potentials gives one of the very few deductions of the maximum work equation (called by the author the isochore equation) to be found in treatises on thermodynamics. The same remark may also be made about the deduction of the maximum work of a gas reaction in the following chapter, in which the external work term is correctly retained. In the chapter on dilute solutions Planck's treatment is essentially followed. The last chapter, on Nernst's theorem, contains a brief but valuable sketch of its relation to statistical methods, and, in view of recent criticisms of the theorem and the undoubted competence of the author in the field of statistics, it is interesting to note his conclusion that the theorem is generally valid. There are problems for exercise but no answers to them. Prof. Fermi's book would form a very useful supplement to some recent treatises in which the fundamentals of thermodynamics are dealt with in a sketchy manner, or entirely omitted, so that the real meaning of the subject is obscured and its applications become largely exercises in algebra or elementary calculus, a treatment which the author expressly avoids. The book may be recommended as a very clear and accurate introduction to the subject of thermodynamics.

J. R. PARTINGTON.

THIRD REPORT OF THE COMMITTEE ON PHOTOCHEMISTRY,[1] NATIONAL RESEARCH COUNCIL

INTRODUCTION

HUGH S. TAYLOR

Department of Chemistry, Princeton University, Princeton, New Jersey

Received May 25, 1938

The First Report of the Committee on Photochemistry presented six papers dealing with the quantitative technique of photoreactions, the classical point of view with respect to these processes, and the relation between the physical concept of quantized absorption and the chemical processes which succeed such absorption. The Second Report summarized the researches of the physicist with respect to the absorption process and their implications in the primary absorption process in photochemistry, and gave some examples of the secondary processes consequent upon such initial processes of absorption. The discussion was necessarily confined to gaseous systems since, at that time, knowledge of the nature of the individual steps in condensed systems was less certain.

In the seven years that have elapsed since the previous report there have been a large number of contributions to the subject and the technique of photochemistry. These have served to broaden the bases upon which the science rests, to add to our techniques, to increase the quantitative nature of our knowledge, to permit an extension of our investigations to the more complex condensed systems, and to make possible a more scientific presentation of important problems in the field of applied photochemistry. Some phases of this activity are summarized in the present report, in which some eleven papers dealing with various topics are assembled. Professor Daniels reviews some of the contributions to experimental technique (page 701) and has prepared with the assistance of the Committee a critical table of quantum yields (page 713). Professor Rollefson has summarized the more recent aspects of the primary absorption process (page 733). In the analysis of reactions subsequent to the primary process, Professor Dickin-

---

[1] This Committee of the National Research Council, Division of Chemistry and Chemical Technology, is composed (1937-38) of the following members: Hugh S. Taylor, *Chairman*, Wilder D. Bancroft, Farrington Daniels, Roscoe G. Dickinson, Philip A. Leighton, Samuel C. Lind, George K. Rollefson. Contributions to this report have also been kindly prepared by Gertrud Kornfeld and Winston M. Manning.

son has discussed the correlation of photoprocesses in the gaseous phase with those in solutions (page 739). Recent researches into a variety of photoprocesses have considerably increased our knowledge of the secondary processes in which free radicals are produced in the primary process. From this standpoint Professor Leighton has summarized the researches on aldehyde and ketone photolysis (page 749), and the writer has dealt with the reactions in alkyl iodides, metal alkyls, mercury-photosensitized hydrogenations and decompositions of hydrocarbons, and the photolysis of azo compounds (page 763). Professor Rollefson has dealt generally with the problem of the evaluation of specific reaction rate constants (page 773), and the writer has summarized present knowledge in the case of ammonia decomposition (page 783) and the reactions involving the photochlorination of hydrogen and of carbon monoxide (page 789). Two final contributions in the domain of applied photochemistry, that of Dr. Gertrud Kornfeld on "The Action of Optical Sensitizers on the Photographic Plate" (page 795) and of Dr. W. M. Manning on "Photosynthesis" (page 815), complete the series of contributions.

It is not intended that this report shall represent an exhaustive summary of the photochemical work which has accumulated since the issue of the preceding report. Many publications in the field have not been covered, even though the papers here reviewed exceed six hundred. Other topics undoubtedly merit attention equal to that given to the subjects here discussed. That this is so indicates both a healthy state of photochemical science and a continuing task for the Committee.

EXPERIMENTAL TECHNIQUE IN PHOTOCHEMISTRY[1]

FARRINGTON DANIELS

Department of Chemistry, University of Wisconsin, Madison, Wisconsin

Received May 25, 1938

Ten years ago, when G. S. Forbes (12) wrote the first report of the Committee on Photochemistry of the National Research Council, most of the principles of experimental photochemistry had been enunciated, but quantitative photochemical measurements had just begun. Since that time a few new techniques have been invented and old ones have been improved; over a hundred quantitative researches have given us the amount of chemical action produced and the amount of radiation of restricted wave length used. It is gratifying that workers in different laboratories are now able to check each other's results when the working conditions are the same.

The production of monochromatic light, the measurement of the energy absorbed and the chemical reaction produced, and the determination of the nature of the spectrum are the chief problems of the experimental photochemist. Because the monochromatic light is of reduced intensity, the first problem has led to the development of semi-micro methods of analysis.

It is not the purpose of this report to give a complete description of the methods used in photochemical investigations, for they may be found in the first report of this Committee (12) and elsewhere (10, 11, 15), or to include a bibliography of researches that have been published on this subject. It is planned merely to build on the first report giving trends of the past decade in experimental photochemistry, to record advances in technique, and to refer to a few selected researches where further details and additional references may be found.

LIGHT SOURCES

Arcs

The quartz mercury-vapor arc lamp is the almost universal standard for photochemical investigations when monochromatic light is necessary. It can be used, however, for only a few selected wave lengths extending from 2000 Å to 10,000 Å. Several types of arc lamps are commercially available.

---

[1] Contribution No. 1 to the Third Report of the Committee on Photochemistry, National Research Council.

A small 80-watt lamp which operates on alternating current with a transformer has been put on the market recently at a low price. It is about 4 mm. by 20 mm. and is suitable for many photochemical experiments.

Intense light, for illuminating monochromator slits or small cells, is best supplied by capillary lamps (9, 21), in which the light is concentrated in a small region. These lamps are so inexpensive that one can afford to run them at a heavy overload, even though their life is short. At these overloads, up to a kilowatt in 10 cubic millimeters of space, the lamps must be water-cooled.

For the line at 2537 Å. a high-voltage lamp filled with mercury vapor and argon and neon is particularly suitable (32, 45). It operates on alternating current at about 6000 volts. Eighty-eight per cent of all the radiation is given off at this wave length, all the other lines being quite weak.

Arc lamps of other metals comparable in intensity and practicality with the mercury lamp have long been needed. Sodium arc lamps in glass are now available ("Sodium Lab-arc") and are useful for many purposes, but the demands for high intensities in photochemical work are hardly met by them.

Neon lamps are also available in convenient form for producing red light, but it is difficult to obtain a highly concentrated radiation from a small area of these lamps.

Quartz capillary lamps of cadmium, zinc, thallium, bismuth, and lead can be made to give light at several different lines which is practically as intense as that of the capillary mercury lamp. These lamps (25) are troublesome to make and operate, however, and the intensity falls off because of the formation of an inner coating of silicate; moreover they break when the current is turned off.

Tungsten filament lamps are used when continuous light is needed in the red or throughout the visible spectrum. Concentrated filaments are preferred. The intensity of the lamps may be increased considerably by operating them for short times at voltages considerably above their rated voltage.

Steadiness of a lamp can be achieved through the use of storage batteries, storage batteries floated across a dynamo, an isolated dynamo, or a dynamo operated by a synchronous motor. Voltage regulators are available operating with electron tubes or with a ballast coil of iron wire in series with the lamp.

Sparks

For the shorter ultraviolet in the region of 2000 Å. and below, spark discharges between electrodes of aluminum, magnesium, and zinc are used (13, 26). Several types have been described. It is possible, though troublesome, to obtain from them intensities equal to those of the mercury lamp. Large transformers up to 10,000 volts and 5 kilowatts have been used together with large condensers. A blast of cooling air is directed against the spark. The noise and oxide dust are seriously annoying. Large discs of metal rotating at right angles may be used to confine the arc to one position and yet give constantly replaced surfaces (50).

PRODUCTION OF MONOCHROMATIC LIGHT

Filters

Filters are the cheapest and most convenient means for restricting the radiation to a narrow range of frequencies. A complete assortment of glass filters is available with which the various lines of mercury, helium, or hydrogen can be isolated (19).

A filter of chlorine and bromine gas in quartz is used for filtering out the longer ultraviolet and leaving the 2536 Å. line of mercury. Acetic acid cuts off all radiation below 2300 Å. Additional filters for specific purposes can be made from solids, liquids, and solutions, the absorption characteristics of which can be found in the literature (11, 18, 27).

An excellent set of laboratory filters for the mercury lamp has been assembled by Bowen (5).

The infrared radiation is practically completely absorbed by 4 cm. or more of a 1 per cent aqueous solution of copper sulfate (6).

The Christiansen filter (11) consists of a mass of particles of glass or quartz in a bath of liquid having the same refractive index at a given wave length, but a different dispersion. Particles of crown glass (1 to 2 mm. in size) are immersed in a mixture of carbon disulfide and benzene of such a composition that it will have the same refractive index at 5000 Å., for example. A beam of light of this wave length will pass through, but light of all other wave lengths will be dispersed. A different composition will pass light of a different wave length. Close temperature control is essential and the range of wave lengths transmitted is not as narrow as might be desired, but the filter can be adjusted to any wave length and the loss of energy in the transmitted light is not great.

Monochromators

Monochromators, their requirements, and their limitations, have been described by Forbes (12). Large aperture and short focus are desirable for photochemical work (16, 22) in order to conserve as much energy as possible. Glass and quartz prisms are commonly used, but large hollow prisms filled with a liquid are satisfactory. Ethyl cinnamate is an excellent liquid for this purpose on account of its high refractive index and its ability to withstand photochemical decomposition. Water is used sometimes, but its refractive index is comparatively low. These liquid prisms give lines which are slightly distorted unless the prisms are thermostated with great care, but they are satisfactory for most photochemical work and they are comparatively inexpensive. A large monochromator using a water prism has been described by Harrison (20).

A double monochromator, in which the light from the exit slit of the first one passes into the entrance slit of the second, is much more effective than a single one in giving monochromatic light of great purity. Obviously the intensity is decreased. A double monochromator making use of ethyl cinnamate prisms is on the market.

In the focal isolation method the light of different wave lengths is separated by refraction with a lens instead of a prism. The light of short wave length is brought to a focus closer to the lens and passes through a small hole in a plate, while the longer rays are stopped. The apparatus is simpler to construct and in the short ultraviolet it is probably more effective. It has been used in several investigations making use of spark emission in the ultraviolet (23, 50). This method has been compared critically with the monochromator method (23).

When mirrors are used, as with the Wadsworth mounting for a monochromator, the sputtering of a clean glass surface with aluminum or other vapor in a vacuum is found to be superior to the ordinary silvering process.

MEASUREMENT OF RADIATION

Thermopiles are usually the simplest and best instruments for measuring the intensity of radiation. Bismuth-silver, copper-constantan, and tellurium-platinum are among the combinations of metals which have been used, each being soldered to a thin, blackened metal receiver.

High sensitivity is not a very important characteristic of a thermopile, because the limiting factor in photochemical measurement is more likely to be the accuracy of the chemical analysis. The thermopile should be absolutely reproducible, with little drifting of the zero point. The theory and practice of thermopile construction have been discussed critically by Leighton and Leighton (32). The construction of a small thermopile has been described by Beckmann and Dickinson (1). The ordinary linear thermopile is smaller than the chemical reaction cell behind which it is placed, and it is necessary to move the thermopile over the whole area in order to obtain an average value. Large-area thermopiles which do their own integrating are simpler for photochemical investigations. The thermocouples, thoroughly protected with glyptal lacquer, are attached with de Khotinsky cement to the back of a blackened receiver 10 by 40 mm. in area.

High sensitivity galvanometers of the d'Arsonval type, giving deflections at 1 meter of 5 to 10 mm. per microvolt, are sufficiently sensitive. Galvanometers of the Paaschen type are more sensitive but more troublesome. If necessary the sensitivity can be pushed to the theoretical limit of 10^{-10} volt imposed by the Brownian motion of the electrons (28), by amplification with two galvanometers. A beam of light from the first galvanometer hits a thermopile or photoelectric cell connected to a second galvanometer, and the system is so arranged that the deflection of the second galvanometer is directly proportional to that of the first (36).

Calibration

The energy of radiation is now determined in nearly all photochemical investigations by means of the standard carbon-filament lamps obtainable from the U. S. Bureau of Standards (7, 10). Calibration of a thermopile and galvanometer is quickly and easily accomplished, and absolute values are reliable to within about 2 per cent.

As secondary standard, the uranyl oxalate actinometer (30) is widely used. It is desirable to cross check all photochemical measurements with this simple actinometer. A solution 0.05 molar in oxalic acid and 0.01 molar in uranyl sulfate is titrated with potassium permanganate. The following quantum yields (molecules reacting per quantum) apply at 25°C.:

Wave length (Å.).....	2550	2650	3000	3130	3660	4060	4350
Quantum yield.......	0.60	0.58	0.57	0.56	0.49	0.56	0.58

When the light is feeble the length of exposure may become impractically long, but more sensitive actinometers such as the mercuric oxalate actinometer, which depend on chain reactions, are not sufficiently reproducible or reliable for quantitative measurements.

Photoelectric cells

Photoelectric cells and electron tube amplifiers are easy to use and are much more sensitive than thermopiles, but they are selective and one must be sure that they give responses which are directly proportional to the intensity at the particular wave length used. They should be calibrated against a thermopile at each wave length.

In the study of ultraviolet radiation of extremely low intensity, Geiger counters are used in which a photoelectric surface emits electrons into a gas space between charged electrodes. A system of electron tubes amplifies greatly the ionization current produced each time that a photoelectron is shot out.

REACTION CELLS

A satisfactory photochemical cell should have clear windows with no distortion of light, and the light should fill practically the whole cell. Practices vary, but when a good thermopile is placed immediately behind the cell it is usually preferable to have the depth of the cell and the concentration such that a measurable part of the light is transmitted past the cell. When all the light is absorbed within the cell the calculations are somewhat simplified, but then the intensity at the front and back of the cell varies from full intensity to zero, a fact which may cause uncertainties if the intensity of the light affects the quantum yield. When a dark reaction is involved the correction factor may become too large if there is such a large excess of material as to absorb all the light.

Glass or quartz cells are conveniently made by fusing polished discs into tubing of just the right size. Both windows should be at right angles to the path of the light. Flasks or tubes can be used for approximate work when the light energy is measured with an actinometer in the cell.

The cell should be so designed that nearly all of the contents of the cell are in the path of the light. Rectangular or trapezoidal cells are preferred, and they can be made to order either in quartz or in Pyrex.

Stirring is usually unnecessary in gaseous reactions, but it may be necessary for liquid reactions, particularly if a dark reaction is involved or if the reaction is influenced by intensity of light or concentration of material. Stirring should be omitted only in case experiments show that it is not necessary under the conditions of the experiment.

CHEMICAL ANALYSIS

The requirements for monochromatic light reduce the energy intensity to such an extent that micro or semi-micro methods of analysis are often necessary. One of the most successful micromethods for gas analysis has been developed by Blacet and Leighton (2, 3, 4), using a small bead of solid absorbent,—phosphorus for oxygen, phosphorus pentoxide for water, silver oxide for carbon monoxide, and copper oxide and potassium hydroxide for hydrogen, and other absorbents. Only 0.25 to 1 cc. of gas is needed for a complete determination.

More micromethods are needed, particularly for complex organic compounds.

The removal of gas for analysis offers a problem, particularly when the gas is at reduced pressure. Toepler pumps, which utilize the filling and emptying of a mercury reservoir, are often used (43). Sometimes the gas is pumped out and frozen in a small tube surrounded with liquid air. Boiling points and freezing points are always useful in identification. Titration methods of precision such as iodimetry find frequent use. Electrotitrations have been developed to a point which makes possible increased accuracy in the study of some photochemical reactions. Conductance methods are applicable sometimes (47).

In gaseous reactions pressure change has been the most common method for following the course of a reaction. Obviously the method is applicable only when there is a change in the number of molecules and when the stoichiometrical reaction is known to be fairly simple. The pressure is usually followed in a constant-volume cell through a flexible diaphragm of glass or quartz. Many different types are available (8, 42).

The application of Beer's law to the determination of the chemical change is receiving increasing application. The absorption of light constitutes one of the simplest methods of analysis and is particularly desirable because it does not disturb the reacting system nor demand the removal of samples. Frequently the same thermopile measurements may be used for the determination of both energy absorption and chemical change. If Beer's law applies, the concentration at any time can be calculated directly from the absorption coefficient, or interpolation may be made on a logarithmic graph. Even when Beer's law does not apply, graphical interpolation on an experimentally determined logarithmic graph will give the concentration.

Thermopile-galvanometer readings may be summed up over long periods of time to give both energy absorbed and chemical change produced (24).

The analysis by absorption of light may be applied not only in the case of the light used in the photochemical reaction but to any other wave length. For example, the production of iodine or chlorine in a photolysis by ultraviolet light can be followed by the absorption of light in the visible. It must be proved experimentally that the materials actually absorbing the light are directly involved in the reaction. For example, Vesper and Rollefson (48) showed that earlier calculations involving the chlorination of monobromotrichloromethane were erroneous because it had been assumed that chlorine was the only substance absorbing the light, whereas in reality it was being absorbed by a bromine-chlorine compound having an entirely different absorption spectrum. Analysis by infrared absorption has been very accurate and successful in the case of the nitrogen oxides (49) and carbon dioxide (34).

Direct analysis with a colorimeter is often possible, and the increasing use of the photoelectric colorimeter will certainly find further application in photochemical investigations.

HIGH AND LOW TEMPERATURES

Most photochemical investigations have been limited to temperatures in the neighborhood of room temperature. Data over a wide range of temperature are needed. Particularly with the new interest in free-radical chain reactions it is desirable to obtain quantum yields and chain lengths at high temperatures,—at 300° to 400°C., for example (29, 35). Special techniques have been developed. It is a good plan to have the thermopile back of the heated reaction chamber completely immersed in water to prevent radiations from the heated walls striking the thermopile.

Low temperature halogenations have been carried out in "freon" surrounded by dry ice (14).

ABSORPTION SPECTRA

Intelligent planning of a photochemical investigation demands first a full knowledge of the regions in which light is absorbed. Spectrograms are essential for this purpose.

Much can be learned from absorption spectra concerning the primary photoprocess. The existence or non-existence of fine structure in the spectrum is often sufficient to decide between different photochemical mechanisms. Grating spectrographs give the greatest dispersion, but prism spectrographs of the best type are often adequate. The fine structure of the spectrum of acetone vapor offers an illustration (38, 39).

The more complex organic compounds and substances in the liquid phase are not likely to show fine structure, but a complete knowledge of the various absorption bands is helpful. Sometimes the finer details of the spectrum can be brought out by lowering the temperature of the absorbing substances with dry ice or liquid air.

Absorption spectra can be mapped in the usual way by splitting the beam of light into two paths, passing one through the absorbing material and reducing the intensity of the other until the two become equal. On a photographic plate the two are matched. Again the amount of absorption can be determined by the density of the lines or regions on the photographic plate as measured with a photoelectric cell or thermopile. Excellent recording apparatus is available for giving in full detail the intensity of absorption throughout the spectrum.

An important new development is the adaptation of the photoelectric cell to the direct determination of the percentage absorption in the different parts of the spectrum (53). Quantitative absorption measurements on chlorophyll have been obtained by this means (52) without the uncertainty of the photographic plate. In some ways this method is less expensive and more direct than the photographic method.

The emission spectra of fluorescent materials may give information regarding the photomechanisms. Since the light is weak, large apertures and long exposures are necessary with a photographic plate. Quantitative measurements of the energy emitted in fluorescence may be made with the photoelectric cell (53).

For the light needed in making absorption spectra tungsten filaments are suitable down to about 3600 Å., but the intensity is low at the shorter wave lengths. Quartz windows may be attached to the glass bulbs surrounding the filament. The iron arc gives many lines throughout the whole spectrum and is widely used in absorption spectra, but it is obviously unsuited for studying fine structure.

Improvements have been made in continuous sources of light in the ultraviolet. The spectrum of molecular hydrogen is most commonly used. Vessels are so arranged that an intense electrical discharge is passed through hydrogen at a low pressure in a tube which allows recombination of the atoms by collision with a metallic surface. An efficient tube of simple design has been described by Munch (37).

Isotopic tracers

The new techniques by which atoms can be traced through chemical reactions by means of radioactivity or abnormal (isotopic) atomic weights are destined to settle many problems of photochemistry. To date only a few experiments of this type are on record.

Taylor and Jungers (46) mixed deuterium with ammonia and mercury vapor and subjected the mixture to illumination with the resonance radiation at 2536 Å. Deuterium entered the ammonia under the influence of the radiation, and the results showed that the low quantum yield obtained in the photolysis of ammonia is due to the recombination of hydrogen atoms and the NH_2 radicals formed by the photochemical reaction.

Leighton and Mortensen (33) used radioactive lead in their study of the mechanism of the photolysis of lead tetramethyl.

Free radicals

Many photochemical reactions are now believed to involve the production of free radicals as a first step. There is a great deal of indirect evidence and some direct evidence for this theory. A test has been applied, for example, in the photolysis of acetone, in which removal of a lead or antimony mirror is used to support the view that free methyl radicals are produced in the photolysis (40, 44).

The existence of OH and other free radicals in the electrical discharge has been proved by characteristic absorption bands (17).

One of the most complete researches on absorption has given experimental proof of the production of iodine atoms when iodine molecules are illuminated. Rabinowitch (41) has described a delicately balanced colorimeter, with an amplifying circuit of electron tubes, which measures with great accuracy the change in absorption produced by a photochemical reaction.

The conversion of ortho–para hydrogen has been used also as a test for the independent existence of free radicals containing an odd number of electrons (51).

REMARKS

Quantitative methods for measuring photochemical reactions are now well established, but more intense sources of monochromatic light are needed. Also, the further development of the spectroscopy of polyatomic molecules will lead to advances in photochemistry. Improvements are needed in methods for the analysis of the complex products of photochemical reactions. Special care must be exercised in certain reactions to remove impurities such as oxygen and moisture, which sometimes affect the reaction. Interesting developments are to be expected in photochemical studies at high and low temperatures, and at low gas pressures.

Greater accuracy in determining quantum yields is useless unless the conditions of temperature, pressure or concentration, and light intensity are clearly defined.

REFERENCES

(1) Beckmann and Dickinson: J. Am. Chem. Soc. **52**, 126 (1930).
(2) Blacet and Leighton: Ind. Eng. Chem., Anal. Ed. **3**, 266 (1931).
(3) Blacet and MacDonald: Ind. Eng. Chem., Anal. Ed. **6**, 334 (1934).
(4) Blacet, MacDonald, and Leighton: Ind. Eng. Chem., Anal. Ed. **5**, 272 (1933).
(5) Bowen: J. Chem. Soc. **1935**, 76.
(6) Coblentz: Bur. Standards Bull. **9**, 110 (1913).
(7) Coblentz: Bur. Standards Bull. **11**, 87 (1915).
(8) Daniels: J. Am. Chem. Soc. **50**, 1115 (1928).
(9) Daniels and Heidt: J. Am. Chem. Soc. **54**, 2381 (1932).
(10) Daniels, Mathews, and Williams: Experimental Physical Chemistry, Chap. XXX. McGraw-Hill Book Co., Inc., New York (1934).
(11) Duggar: Biological Effects of Radiation, Chaps. IV and VII. McGraw-Hill Book Co., Inc., New York (1936).
(12) Forbes: J. Phys. Chem. **32**, 485 (1928).
(13) Forbes and Brackett: J. Am. Chem. Soc. **53**, 3973 (1931).
(14) Forbes and Nelson: J. Am. Chem. Soc. **58**, 182 (1936).
(15) Forsythe: Measurement of Radiant Energy. McGraw-Hill Book Co., Inc., New York (1937).
(16) Forsythe and Barnes: Rev. Sci. Instruments **4**, 289 (1933).
(17) Frost and Oldenberg: J. Chem. Phys. **4**, 642 (1936).
(18) Gibson: J. Optical Soc. Am. **13**, 267 (1926).
(19) Glass Color Filters, Corning Glass Works, Corning, New York.
(20) Harrison: Rev. Sci. Instruments **5**, 149 (1933).
(21) Harrison and Forbes: J. Am. Chem. Soc. **47**, 2449 (1925).
(22) Heidt and Daniels: J. Am. Chem. Soc. **54**, 2384 (1932).
(23) Heidt and Forbes: Rev. Sci. Instruments **5**, 253 (1934).
(24) Hoffman: J. Am. Chem. Soc. **56**, 1894 (1934).
(25) Hoffman and Daniels: J. Am. Chem. Soc. **54**, 4226 (1932).
(26) Howe and Noyes: J. Am. Chem. Soc. **58**, 1405 (1936).
(27) International Critical Tables, Vol. V, p. 271; Vol. VII, p. 160. McGraw-Hill Book Co., Inc., New York (1929 and 1930).
(28) Ising: Phil. Mag. **1**, 827 (1926).
(29) Leermakers: J. Am. Chem. Soc. **56**, 1537 (1934).
(30) Leighton and Forbes: J. Am. Chem. Soc. **52**, 3139 (1930).
(31) Leighton and Leighton: J. Phys. Chem. **36**, 1882 (1932).
(32) Leighton and Leighton: J. Chem. Education **12**, 139 (1935).
(33) Leighton and Mortensen: J. Am. Chem. Soc. **58**, 448 (1936).

(34) McAllister: Plant Physiol. **12**, 213 (1937).

(35) Mitchell and Hinshelwood: Proc. Roy. Soc. (London) **A159**, 32 (1937).

(36) Moll: Z. Physik **34**, 3 (1925).

(37) Munch: J. Am. Chem. Soc. **57**, 1863 (1935).

(38) Norrish, Crone, and Saltmarsh: J. Chem. Soc. **1934**, 1456.

(39) Noyes, Duncan, and Manning: J. Chem. Phys. **2**, 717 (1934).

(40) Paneth and Hofeditz: Ber. **62**, 1335 (1929).

(41) Rabinowitch: Trans. Faraday Soc. **32**, 547 (1936).

(42) Ramsperger and Tolman: J. Am. Chem. Soc. **46**, 6 (1930).

(43) Reilly and Rae: Physico-Chemical Methods, p. 72. D. Van Nostrand Co., New York (1933).

(44) Rice and Rice: The Aliphatic Free Radicals. The Johns Hopkins Press, Baltimore (1935).

(45) Taylor: J. Chem. Phys. **2**, 377 (1934).

(46) Taylor and Jungers: J. Chem. Phys. **2**, 452 (1934).

(47) Vaidja: Proc. Roy. Soc. (London) **A129**, 299 (1930).

(48) Vesper and Rollefson: J. Am. Chem. Soc. **56**, 620, 1455 (1934).

(49) Warburg and Leithauser: Ann. Physik **28**, 313 (1909).

(50) Wiig and Kistiakowsky: J. Am. Chem. Soc. **54**, 1807 (1932).

(51) West: J. Am. Chem. Soc. **57**, 1931 (1935).

(52) Zscheile: J. Phys. Chem. **38**, 95 (1934).

(53) Zscheile, Hogness, and Young: J. Phys. Chem. **38**, 1 (1934).

A TABLE OF QUANTUM YIELDS IN EXPERIMENTAL PHOTOCHEMISTRY[1]

FARRINGTON DANIELS

Department of Chemistry, University of Wisconsin, Madison, Wisconsin

Received May 26, 1938

In the early development of quantitative photochemistry it was believed by some that the Einstein relation would apply in many cases not only to the primary process of photoexcitations but to the overall reaction as well. Quantum yields were summarized with the purpose of testing this hypothesis. Any hope of simplicity in chemical kinetics disappeared long ago, and the present table has been assembled not to emphasize the almost universal occurrence of secondary effects which follow the primary process of quantum absorption, but to record the experimental facts of photochemistry in the simplest possible manner. The primary excitation is usually followed by rearrangements and degradation of the energy as heat, by reverse or competing reactions which make the overall quantum yield less than unity, or by continuing reactions which produce a chain and give a value greater than unity. Sometimes it is possible to study these factors from the magnitude of the quantum yield and its response to influences such as temperature, wave length, concentration, and chemical reagents.

The amount of chemical reaction produced by the absorption of radiation will change with the duration of exposure, the intensity of the light, the thickness and condition of the absorbing material, and other factors. The fundamental simple relation between light and chemical action, however, is the quantum yield Φ, i.e., the number of molecules of substance reacting for each quantum of radiation, or photon, absorbed. When this is known the extent of the chemical reaction produced by the absorption of a given amount of light is easily calculated.

In table 1 are summarized the findings of most of the quantitative photochemical researches in which the results are expressed in terms of quantum yields. Many excellent researches are not included, simply because the results were not given in these terms. Photochemistry has been greatly stimulated by hypotheses in chemical kinetics, and the testing of these hypotheses has been the chief aim in many cases. For

---

[1] Contribution No. 2 to the Third Report of the Committee on Photochemistry, National Research Council.

TABLE 1

Table of quantum yields in photochemistry

REACTION AND PRODUCTS	SOLVENT	ABSORBER	WAVE LENGTH	TEMPERATURE	QUANTUM YIELD	REMARKS AND REFERENCES*
			Å	°C.		
Acetaldehyde decomposition → CH_4; CO	Gas	CH_3CHO	2537	30	0.9	Polymerization accompanies reaction; Φ changes with pressure; some hydrogen produced (12, 71)
			2804	30	0.5	
			3130	30	0.2	
			3130	310	300	(69)
Acetaldehyde decomposition → CH_4; C_2H_6; CO		CH_3CHO		300	103$^{(1)}$	$^{(1)}$ at 100 mm.;
					409$^{(2)}$	$^{(2)}$at 700 mm.;
				350	196$^{(1)}$	Φ decreased by addition of NO
					710$^{(2)}$	
				400	338$^{(1)}$	
					1374$^{(2)}$	
				450	589$^{(1)}$	†
					2278$^{(2)}$	(84)
Acetic acid decomposition → CH_4; CO_2	H_2O	CH_3COOH	1850–2300		0.5	0.1 *M* solution (38)
Acetone decomposition → C_2H_6; CO	Gas	$(CH_3)_2CO$	3130–2650	56	0.17	680–760 mm. (27)
			3130	60	0.2	10 per cent CH_4
			2480–2770	60	0.4	(89)
			2200–3300	60–100	0.2–1	(135)
				160–400	1	
			1900	25	0.66	At 0.2 mm.
					0.46	At 52.3 mm. (58)

Acetone decomposition → alcohol, etc.	n-C_6H_{14}	$(CH_3)_2CO$	2480–3135		0.27	10 per cent solution (21)
Acetone hydrolysis → CH_3COOH; CH_4	H_2O	$(CH_3)_2CO$	Hg arc	30	(0.12)	In 0.05 molar solution; decreases in more concentrated solutions (97)
				40	(0.17)	
Acetylene polymerization						
→ $(C_2H_2)_n$	Gas	C_2H_2	2150	25	9.2	(77)
→ $(C_2H_2)_n$		Hg	2636	25	6.5	Mercury-sensitized; pressure 1–40 mm. (61)
→ $(C_2D_2)_n$		Hg			5	
Acraldehyde decomposition → CO; C_2H_2	Gas	C_3H_4O	3130	17	0.15	
			3660		0.01	(115)
Acraldehyde polymerization → $(C_3H_4O)_n$		C_3H_4O	2537–3660	30	<0.04	Banded absorption 3130–3660; continuous absorption below 2804
			2537	30	19	
			2654		19	
			2804		10	
			3020		1	
			3130		0.5	
			3660		0.3	(10)
			3130	17	2.3	
			3660		0.4	(115)
Allene polymerization → $(H_2C{:}C{:}CH_2)_n$	Gas	$H_2C{:}C{:}CH_2$	Hg arc	25–29	2.5	(78)
Amino acids deamination → NH_3; RC(OH)HCOOH	H_2O	Alanine	Hg arc	30	1.0	
		Betaine			0.5	
		Glycine			0.9	(129)

* A reference, given in parentheses in the last column, applies to all the material between it and the preceding reference.

TABLE 1—*Continued*

REACTION AND PRODUCTS	SOLVENT	ABSORBER	WAVE LENGTH	TEMPERATURE	QUANTUM YIELD	REMARKS AND REFERENCES
			Å	°C.		
Ammonia decomposition → N_2; H_2	Gas	NH_3	2099–2194	20	0.14	Pressure 1–8 atm.
				400	0.6	(95)
			2000–2200	19–400	0.25	Followed by ortho-para hydrogen conversion (39)
			2026–2138	21–31	0.10	At 0.1 mm.
					0.30	At 65 to 120 mm.
					0.18	At 760 mm. (133)
	Liquid	NH_3			<0.02	(94)
	Gas	Hg	1990		0.87	Mercury-sensitized; Φ approaches zero at low pressures (126)
			2537		0.12	
Anthracene polymerization → $(C_{14}H_{10})_2$	C_6H_6	$C_{14}H_{10}$	3130–3665	80	1 to 0 (0.5)	Reaction reverses in dark (128)
Arsine decomposition → As; H_2	Gas	Hg	2537	24–27	1.03	Mercury-sensitized (107)
Azomethane decomposition → C_2H_6; N_2	Gas	$(CH_3)_2N_2$	3665	20–226	1.0	At 181 mm.
					0.77	At 684 mm.
			2540		0.25	Primary products CH_3 and N_2; products complex (43, 28)
			2080		0.24	
Bromination of acetylene → $C_2H_2Br_2$	Gas	Br_2	4358–5791	20	3000	
				150	500	(19)

Bromination of acetylene dichloride → CHClBr·CHClBr	Gas CCl_4	Br_2 Br_2	4060–5460 4060–5460	30–40 30–40	(100) (1.8–3.0)	(47)
Bromination of benzene → $C_6H_6Br_6$	Liquid	Br_2	3000–5500	17–50	0.4–0.9	(98)
Bromination of cinnamic acid → $C_6H_5CHBr\cdot CHBrCOOH$	CCl_4	Br_2	4060–5460	0–30	1–30	Saturated with air; increases with concentration of bromine; in absence of oxygen Φ is large (5)
Bromination of hydrogen → HBr	Gas	Br_2	5000–5780	<150 >150	0 1–2	Several factors involved (16, 60)
Bromination of tetrachloroethylene → $C_2Cl_4Br_2$	Liquid	Br_2	4360	25–135	0.1 to 24	Depends on concentration of products and on oxygen (134)
Bromophosgene decomposition → CO; Br_2	Gas	$COBr_2$	<3200	10–40	1	(103)
Chlorination of benzene → $C_6H_6Cl_6$	Gas	Cl_2	3660 and 3130	25	12–46	Depends on pressures; Cl_2, 95–126 mm.; C_6H_6, 8–40 mm. (110)
Chlorination of formic acid → HCl; CO_2	Gas	Cl_2	3660	20–30	2000	HCOOH, 65–100 mm.; Cl_2, 200–300 mm. (131)
Chlorination of chlorom for → CCl_4; HCl	Gas	Cl_2	4358	60	300	Cl_2, 77 mm.; $CHCl_3$, 32–128 mm. (105)

TABLE 1—*Continued*

REACTION AND PRODUCTS	SOLVENT	ABSORBER	WAVE LENGTH	TEMPERATURE	QUANTUM YIELD	REMARKS AND REFERENCES
			Å	°C.		
Chlorination of cinnamic acid → $C_6H_5CHCl \cdot CHClCOOH$	CCl_4	Cl_2	3660	25	2.4	Depends on Cl_2 concentration. Probably oxygen-inhibited (9)
Chlorination of dichlorobenzenes → C_6Cl_6; HCl	Gas	Cl_2	3660	20	0.39	Depends on dichlorobenzene pressure (40)
Chlorination of dichloroethylene → $CHCl_2 \cdot CHCl_2$	Gas	Cl_2	4360	85–95	7000	Cl_2, 100 mm. (86)
Chlorination of hydrogen → HCl	Gas	Cl_2	3660		$(<10^4)$	Depends on many factors; inhibited by O_2 and HCl (99)
			3030–4360	17–27		(25)
			4300–5000	30	4×10^6	Silver walls. Oxygen removed (17)
Chlorination of methane → CH_xCl_{4-x}	Gas	Cl_2	2537 4360		(100,000)	(24)
Chlorination of pentane → $C_5H_{11}Cl$; HCl	Gas	Cl_2	3660	25	(190)	Oxygen excluded (114)
Chlorination of sulfur dioxide → SO_2Cl_2	Gas	Cl_2	4200		(1)	(18)
Chlorination of tetrachloroethylene → C_2Cl_6	Gas CCl_4	Cl_2 Cl_2	4360	40	300–500 300–500	In absence of oxygen (31)

Chlorination of toluene → $C_6H_5CH_2Cl$	Liquid	Cl_2	4050	−80	(27)	(20)
Chlorination of trichlorobromomethane → CCl_4; Br_2	Gas	Cl_2	3660	28	30	(119)
Chlorine monoxide decomposition						
→ Cl_2; O_2	Gas	Cl_2O	2350–2750	20	4.5	(104)
		Cl_2O or Cl_2	4030–4360	10–40	2	(14)
	CCl_4		4360		>1.8	ClO_2 formed also (32)
Chlorine dioxide decomposition						
→ Cl_2; O_2	Gas	ClO_2	3660	18	3.1	Addition of water vapor gives reproducible results (112)
			4360	31	2.7	
→ Cl_2; O_2		Br_2	5460	15	3	Bromine-sensitized (112)
Cinnamic acid isomerization	H_2O	C_6H_5CH $\|$ $HCCOOH$	3130	28	0.6	0.003 *M* solution (117)
Isocinnamic acid isomerization	H_2O	C_6H_5CH $\|$ $HOOCCH$	3130	28	0.2	0.003 *M* solution (117)
Citraconic acid isomerization	H_2O	CH_3CCOOH $\|$ $HCCOOH$	3130	18	0.2	0.01 *M* solution (117)
Crotonaldehyde decomposition → RH; R_2; H_2; CO	Gas	Crotonaldehyde	2400 and 3660	30	<0.02	(11)

TABLE 1—*Continued*

REACTION AND PRODUCTS	SOLVENT	ABSORBER	WAVE LENGTH	TEMPERATURE	QUANTUM YIELD	REMARKS AND REFERENCES
			Å	°C.		
Cobalt potassium oxalate → CO_2; CO; H_2O	H_2O	$K_3Co(C_2O_4)_3$	3660	10–22	(1.5)	
			4050		(0.9)	
			4360		(0.6)	(121)
Diazomethane decomposition → CH_4; N_2	Gas	CH_2N_2	3650 and 4360	25	4	(62)
Dibromotetrachloroethane decomposition → C_2Cl_4; Br_2	Gas	Br_2	4360	100	0.5	Bromine-sensitized 5–43 mm.
				125	3.2	Products decrease Φ (22)
				150	15.2	
Dimethyl ether decomposition with acetone → CH_4 CO; H_2	Gas	$(CH_3)_2CO$	3130	200–400	5–230	Depending on pressure and light intensity (70)
Ethyl iodide decompositions → C_4H_{10}; I_2	Liquid	C_2H_5I	2537	5–58	0.41	Independent of temperature
			2654		0.38	
			3130		0.31	(92)
	Gas		2610	25	0.01	At 90 mm.
			2026		0.1	
			2026		0.03	At 0.1 mm.
			2610		0.6	(130)
	C_6H_{14}		2026		0.1	At 95 mm. (132)
			2026		0.24	
			2610		0.6	(130)
Ethylene iodide decomposition → C_2H_4; I_2	CCl_4	$C_2H_4I_2$	3030 and 3130	25	0.76	0.036 *M* solution. With correction for retarding effect of iodine produced Φ = 1 (29)

Formaldehyde decomposition → H_2; CO	Gas	HCHO	2540–2640		0.9	
			3030–3130		1.1	
			3340–3650		0.7	(91)
			Hg arc	350	100	(1)
Formic acid decomposition → CO_2; H_2		$(HCOOH)_2$	1900–2540	23–134	1	Independent of temperature and pressure
→ CO_2; CO; H_2; H_2O		HCOOH			1	$(CO + H_2O)/(CO_2 + H_2)$ varies with wave length (51)
Fumaric-maleic acid transformation	H_2O	HCCOOH ‖	2070–2820		(0.1)	0.01 *M* (123)
		HOOCCH	3130	18	0.1	0.01 *M* (117)
Hydrazine decomposition → NH_3; N_2; H_2	Gas	N_2H_4	1990	25	1.0	At 2 mm.
					1.7	At 14 mm. (127)
		Hg	2547	15–45	(13)	Hg-sensitized (36)
Hydrogen azide decomposition → NH_3; N_2; H_2	Gas	N_3H	1990	22–27	1.74–3.89	Pressure 0.3–131 mm. (7)
Hydrogen azide decomposition → NH_3; N_2; H_2	Gas	Hg	2537	20–23	2.86	Hg-sensitized (83)
Hydrogen bromide decomposition → H_2; Br_2	Gas	HBr	2070		2	
			2530		2	(122)
Hydrogen iodide decomposition → H_2; I_2	Gas	HI	2070–2820	27	2.0	Simple photochemical reaction (76)
	Liquid C_6H_{14}				1.84	(15)
					2.0	(125)

TABLE 1—*Continued*

REACTION AND PRODUCTS	SOLVENT	ABSORBER	WAVE LENGTH	TEMPERATURE	QUANTUM YIELD	REMARKS AND REFERENCES
			Å	°C.		
Hydrogen peroxide decomposition → H_2O; O_2	H_2O	H_2O_2	2750–3660	2–26	20–500	Depending on concentration and pH (3)
			3130	28	(1)	At infinite dilution (55)
Hydrogen sulfide decomposition → H_2; S	Gas	H_2S	2050		2	At 250 mm. (113)
Hypochlorous acid decomposition → HCl; $HClO_3$; O_2	H_2O	HClO	3660 4360		(2) (2)	0.03–0.05 *M* solution (2)
Iodine with $N_2CHCOOC_2H_5$ → N_2; $I_2CHCOOC_2H_5$	CCl_4	I_2	5460 and 5780	18	<2	Proportional to I_2 in dilute solutions (87)
Iodine with ferricyanide ion → $Fe(CN)_6^{---}$; I^-	H_2O	I_3^-	5000–6300	0	1.0	(34)
Iodine with ferrous ion → Fe^{+++}; I^-	H_2O	I_3^-	3660–5790		1	(63)
Iodine with formate → CO	H_2O	I_3^-	3450–3500	15–25	(26–64)	(30)
Iodoform decomposition	C_6H_6	CHI_3	3130 and 3660	16–25	(1)	Increases with oxygen (50)
Ketene decomposition → C_2H_4; CO	Gas	CH_2CO	3130 3660		1 0.4	(100) (90)

Lead tetramethyl decomposition → Pb; C_2H_6	Gas	$Pb(CH_3)_4$	2537	25–29	1.11	Radioactive lead used; 22–31 mm. pressure.
	$(CH_3)_3C_3H_7$	$Pb(CH_3)_4$	2537		0.37 0.42	0.00067 *M* 0.0028 *M* (74)
Lead tetraphenyl decomposition → Pb; $C_{12}H_{10}$	C_6H_{14}	$Pb(C_6H_5)_4$	2537		0.37	Radioactive lead used (74)
Malachite green leucocyanide	C_2H_5OH	Malachite green	2537–3130	26–29	1.0	Colorless to colored compound (54)
Maleic-fumaric acid isomerization	H_2O	HCCOOH ‖ HCCOOH	2070–2820	18	(0.03)	0.01 *M* (117, 123)
			3130	18	0.05	0.01 *M* (117)
Maleic-fumaric ester isomerization	CCl_4	Br_2	4360 5460	20	300 150	Bromine-sensitized reaction accompanied by addition of bromine (35)
Mercury dimethyl decomposition → Hg; C_2H_6; CH_4	Gas	$Hg(CH_3)_2$	2537	20 189	1.0 2.2	20 mm. pressure; no inhibition by nitric oxide (116)
Methane decomposition → C_2H_4; H_2	Gas	CH_4	1400–1600 1295–1469	25	(1) (1.3)	Calculated from hydrogen produced (53, 75)
Methanol decomposition → H_2; H_2CO	Gas	CH_3OH	1800–2000		(1)	(96)

TABLE 1—*Continued*

REACTION AND PRODUCTS	SOLVENT	ABSORBER	WAVE LENGTH	TEMPERATURE	QUANTUM YIELD	REMARKS AND REFERENCES
			Å	°C.		
Methylamine decomposition → NH_3; H_2; CH_3NCH_2	Gas	CH_3NH_2	Hg arc	100–105	<0.7	(37)
Methyl butyl ketone decomposition → $(CH_3)_2CO$; C_3H_6	Gas	$CH_3COC_4H_9$	2480–2770	127	0.27	1 atm. pressure
Methyl butyl ketone polymerization	Gas	$CH_3COC_4H_9$	2480–2770	127	0.03	(13)
Methyl iodide decomposition → CH_4; C_2H_6; I_2	Gas	CH_3I	Hg arc 2026	25	(0.06) <0.01	H_2 and N_2O without effect (111) At 140 mm. (132)
Methyl iodide with hydriodic acid → CH_4; I_2	Gas	CH_3I	Hg arc		(2)	Independent of composition (59)
Methylacetylene polymerization → $(CH{\equiv}CCH_3)_n$	Gas	$CH{\equiv}CCH_3$	Hg arc	25	3.5	(78)
Monobromoacetic acid hydrolysis → $HOCH_2COOH$; Br^-; H^+	H_2O	$CH_2BrCOOH$	2537		0.3	0.01 *M* (101)
Monochloroacetic acid hydrolysis → $HOCH_2COOH$; Cl^-; H^+	H_2O	$CH_2ClCOOH$	2537 1850–2300		1 0.9	Affected by pH (101) (38)

Nitrate ion decomposition → NO_2^-; O_2	H_2O	NO_3^-	2536 3130 2536	25	0.3 0.01 0.05	At pH = 10 At pH = 10 At pH = 6 (120)
Nitric oxide → $N_2 + O_2$	Gas	NO	1832		0.75	(81)
o-Nitrobenzaldehyde rearrangement → $C_6H_4(NO)COOH$	Liquid	$C_6H_4(NO_2)CHO$	2540–3660	45–75	0.5	(136)
	Gas		3500	120 120	0.8 0.5	5 mm. pressure; with N_2 = 1 atm. (68)
	$(CH_3)_2CO$ Solid		3130–4360		0.5 0.5	(73)
Nitrogen dioxide decomposition → NO; O_2	Gas	NO_2	4050 3660 3130	0	0.5 1.83 1.93	Decreases regularly with increasing pressure of inert foreign gas (6, 57, 88)
	CCl_4	NO_2	3660–4050	0	<0.05	(57)
Nitrogen tetroxide decomposition → NO; O_2	Gas	N_2O_4	2800 2650	0	0.2 0.4	(57)
Nitrogen pentoxide decomposition → NO_2; O_2	Gas	N_2O_5	2800 2650	0	0.6 0.6	(57)
	CCl_4		2650–2800	0	<0.05	
Nitrogen pentoxide with dioxide → NO_2; O_2	Gas	NO_2	3130–4050	0		Results same as given under NO_2 decomposition (57)
Nitrous oxide decomposition → N_2; O_2; NO	Gas	N_2O	Al spark		1	(93)
β-Nitroso-β,ε-dimethylhexane decomposition → $H_2N_2O_2$, etc.	C_6H_6		6850		(1)	(4)

TABLE 1—*Continued*

REACTION AND PRODUCTS	SOLVENT	ABSORBER	WAVE LENGTH	TEMPERATURE	QUANTUM YIELD	REMARKS AND REFERENCES
			Å	°C.		
Nitrosoisopropylacetone decomposition → $H_2N_2O_2$, etc.	C_6H_6	$(CH_3)_2C(NO)$-CH_2COCH_3	6850		(1)	(4)
Nitrosyl chloride decomposition → NO; Cl_2	Gas	NOCl	3650–6300	22	2	(64)
Oxalic acid decomposition → H_2O; CO; CO_2	H_2O	Complex ion UO_2^{++} with $H_2C_2O_4$	2550 3130 3660 4350	25	0.60 0.56 0.49 0.58	Accurately known. This reaction is the universal standard for actinometry (72)
Oxalyl chloride decomposition → $COCl_2$; CO	Gas	$(COCl)_2$	2537 3660	25	0.8 1.8	(67)
Oxidation of acetone → CO_2; H_2O; CH_3COOH	Gas	$(CH_3)_2CO$	3130	25	0.24	Φ same as for decomposition (45)
Oxidation of carbon monoxide → CO_2	Gas	$COCl_2$	Hg arc		87–110	Sensitized by phosgene. Each of three gases at 200 mm. (85)
	Gas	Cl_2	4050–4360		(1000)	Sensitized by Cl_2 (102)
Oxidation of carbon tetrachloride → $COCl_2$; Cl_2	Liquid	CCl_4	2537	25	1	(79)
Oxidation of chloroform → $COCl_2$; HCl; Cl_2	Gas	Cl_2	4360	25 65	(100) 260	Sensitized by Cl_2 (23) (106)

Oxidation of hydrogen → H_2O_2; H_2O; O_3 → H_2O_2; H_2O; O_3	Gas	O_2 Hg	1719–1725 2537	20	1 2.6	Varies with pressure (109) Sensitized by Hg. Corrected value of Φ (80)
Oxidation of hydrogen → H_2O_2; H_2O	Gas	Hg	2537	50–200	1.2	Hg-sensitized. Light intensity 100 times that of Marshall (44, 80)
Oxidation of mandelic acid	H_2O	Br_2 UO_2^{++} UO_2^{++}	3660–5460 2560–3130 2547–4360	31 27	(12.5) (31.7) (1)	Under certain conditions (46) Under certain conditions (49) For low concentration UO_2^{++}. Methylene blue present (48)
Oxidation of methylene iodide → HCOOH; CO; H^+; I^-	Liquid	CH_2I_2	3100	21	1.4	With respect to iodine (52)
Oxidation of phosgene → CO_2; Cl_2	Gas	$COCl_2$	Hg arc		1.8	$COCl_2$, 63 mm.; O_2, 68 mm. (85)
Oxidation of phosphine → H_2O; P_2O_5	Gas	PH_3	Zn spark	18	200	At 0.05 mm. (82)
Oxidation of quinine and its derivatives by dichromic acid	H_2O	Alkaloid	3130 3660 4050	5–24	0.065 0.070 0.027	Hydroquinone and ten other derivatives of quinine given also. Φ's all range from 0.002 to 0.07 (41)
Oxidation of rubrene → $C_{42}H_{28}O_2$	C_6H_6 C_5H_5N	$C_{42}H_{28}$	4360	0–18	1	For large concentrations of rubrene and O_2 (65)

TABLE 1—*Concluded*

REACTION AND PRODUCTS	SOLVENT	ABSORBER	WAVE LENGTH	TEMPERATURE	QUANTUM YIELD	REMARKS AND REFERENCES
			Å	°C.		
Oxidation of sulfur dioxide → SO_3	Gas	SO_2	1860 2070		3.1 2.0	(66)
Oxidation of tetrachloroethylene → $COCl_2$; CCl_3COCl	CCl_4	Cl_2	4360	20	1	At low concentrations (33)
Ozone formation $O_2 \rightarrow O_3$	Gas	O_2	<2000 <1750		1.3-2.0 2.0	Depending on pressure (124) (118)
Ozone decomposition → O_2	Gas	O_3	2080-3130	0-60	1.8-6.2	Dry ozone at 177 and 390 mm. Varies with pressure (56)
			2100-2800	2-20	1.6-130	In presence of moisture. Depends on pressure (42)
Persulfate ion → SO_4^{--}; O_2; H^+	H_2O	$S_2O_8^{--}$	2536-3020		1.0	(26)
Phosphine decomposition → P_4; H_2	Gas	PH_3	2300	20-300	0.56 0.49	For 7 cm. bulb For 2 cm. bulb (82)
Propionaldehyde decomposition → C_2H_6; CO; H_2	Gas	C_2H_5CHO	3130	300	3 6 8	At 100 mm. At 200 mm. At 300 mm. (84)
Propionic acid → C_2H_6; CO_2	H_2O	C_2H_5COOH	1850-2300		(1)	(38)
n-Propyl iodide → I_2, etc.	Gas	*n*-C_3H_7I	2026-2610	25	0.01	At 35 mm. (131)

Isopropyl iodide → I_2, etc.	Gas	iso-C_3H_7I	2026 2610	25	0.43 0.17	At 56 mm. At 26 mm. (131)
Silver oxalate decomposition → Ag; CO_2	Solid	$Ag_2C_2O_4$	3600–5200	100	0.12	Inhibited by O_2 (8)
trans-Stilbene transformation → *cis*-stilbene	C_6H_{14}	$C_6H_5HC{=}CHC_6H_5$	1930 2260 2650 3020 3130		0.36 0.41 0.73 0.73 1.01	(108)

these purposes it is often unnecessary to express the results in absolute units (quantum yields).

In many cases the quantum yield varies with temperature, concentration, and intensity. Particularly in chain reactions the quantum yield may vary considerably with slight changes in the reacting system and with traces of impurities. Special conditions, such as concentration, are given in the last column of table 1. When the temperature is not given it may usually be taken as room temperature (about 20°C.). Parentheses around a quantum yield indicate a lesser degree of accuracy. When there is uncertainty regarding Φ, the original article should be consulted. The references are given in parentheses in the last column and include references to earlier investigations.

REFERENCES

(1) Akeroyd and Norrish: J. Chem. Soc. **1936**, 890.
(2) Allmand, Cunliffe, and Maddison: J. Chem. Soc. **131**, 655 (1927).
(3) Allmand and Style: J. Chem. Soc. **1930**, 596, 606.
(4) Anderson, Crumpler, and Hammick: J. Chem. Soc. **1935**, 1679.
(5) Bauer and Daniels: J. Am. Chem. Soc. **56**, 378, 2014 (1934).
(6) Baxter and Dickinson: J. Am. Chem. Soc. **51**, 109 (1929).
(7) Beckman and Dickinson: J. Am. Chem. Soc. **52**, 124 (1930).
(8) Benton and Cunningham: J. Am. Chem. Soc. **35**, 2227 (1935).
(9) Berthoud and Porret: Helv. Chim. Acta **17**, 237 (1934).
(10) Blacet, Fielding, and Roof: J. Am. Chem. Soc. **59**, 2375 (1937).
(11) Blacet and Roof: J. Am. Chem. Soc. **58**, 73 (1936).
(12) Blacet and Roof: J. Am. Chem. Soc. **58**, 278 (1936).
(13) Bloch and Norrish: J. Chem. Soc. **1935**, 1638.
(14) Bodenstein and Kistiakowsky: Z. physik. Chem. **116**, 371 (1925).
(15) Bodenstein and Lieneweg: Z. physik. Chem. **119**, 123 (1926).
(16) Bodenstein and Lütkemeyer: Z. physik. Chem. **114**, 208 (1925); Lewis and Rideal: J. Am. Chem. Soc. **48**, 2555 (1926).
(17) Bodenstein and Winter: Sitzber. preuss. Akad. Wiss., p. 2 (1936).
(18) Bonhoeffer: Z. Physik **13**, 94 (1923).
(19) Booher and Rollefson: J. Am. Chem. Soc. **56**, 2288 (1934).
(20) Book and Eggert: Z. Elektrochem. **29**, 521 (1923).
(21) Bowen and Horton: J. Chem. Soc. **1936**, 1685.
(22) Carrico and Dickinson: J. Am. Chem. Soc. **57**, 1343 (1935).
(23) Chapman: J. Am. Chem. Soc. **57**, 416 (1935).
(24) Coehn and Cordes: Z. physik. Chem. **B9**, 1 (1930).
(25) Craggs and Allmand: J. Chem. Soc. **1936**, 241.
(26) Crist: J. Am. Chem. Soc. **54**, 3939 (1932).
(27) Damon and Daniels: J. Am. Chem. Soc. **55**, 2363 (1933).
(28) Davis, Jahn, and Burton: J. Am. Chem. Soc. **60**, 10 (1938).
(29) DeRight and Wiig: J. Am. Chem. Soc. **57**, 2411 (1935).
(30) Dhar and Bhargava: J. Phys. Chem. **39**, 1231 (1935).
(31) Dickinson and Carrico: J. Am. Chem. Soc. **56**, 1473 (1934).
(32) Dickinson and Jeffreys: J. Am. Chem. Soc. **52**, 4288 (1930).
(33) Dickinson and Leermakers: J. Am. Chem. Soc. **54**, 3852 (1932).
(34) Dickinson and Ravitz: J. Am. Chem. Soc. **52**, 4770 (1930).

(35) Eggert and Borinski: Z. Physik **26**, 865 (1925).
(36) Elgin and Taylor: J. Am. Chem. Soc. **51**, 2059 (1929).
(37) Emeleus and Jolley: J. Chem. Soc. **1935**, 1612.
(38) Farkas: Z. physik. Chem. **B23**, 89 (1933).
(39) Farkas and Harteck: Z. physik. Chem. **B25**, 257 (1934).
(40) Fisk and Noyes: J. Am. Chem. Soc. **58**, 1707 (1936).
(41) Forbes and Heidt: J. Am. Chem. Soc. **55**, 2407 (1933).
(42) Forbes and Heidt: J. Am. Chem. Soc. **56**, 1671 (1934).
(43) Forbes, Heidt, and Sickman: J. Am. Chem. Soc. **57**, 1935, 2331 (1935).
(44) Frankenburger and Klinkhardt: Z. physik. Chem. **B15**, 421 (1932).
(45) Fugassi: J. Am. Chem. Soc. **59**, 2092 (1937).
(46) Ghosh and Bhattacharyya: Z. physik. Chem. **B31**, 420 (1936).
(47) Ghosh, Bhattacharyya, and Bhattacharyya: Z. physik. Chem. **B32**, 145 (1936).
(48) Ghosh, Narayanmurti, and Ray: Z. physik. Chem. **B29**, 236 (1935).
(49) Ghosh and Ray: Z. physik. Chem. **B32**, 158 (1936).
(50) Gibson and Iredale: Trans. Faraday Soc. **32**, 571 (1936).
(51) Gorin and Taylor: J. Am. Chem. Soc. **56**, 2042 (1934).
(52) Gregory and Style: Trans. Faraday Soc. **32**, 724 (1936).
(53) Groth: Z. physik. Chem. **B38**, 366 (1937).
(54) Harris and Kamisky: J. Am. Chem. Soc. **57**, 1154 (1935).
(55) Heidt: J. Am. Chem. Soc. **54**, 2840 (1932).
(56) Heidt: J. Am. Chem. Soc. **57**, 1710 (1935).
(57) Holmes and Daniels: J. Am. Chem. Soc. **56**, 630 (1934).
(58) Howe and Noyes: J. Am. Chem. Soc. **58**, 1404 (1936).
(59) Iredale and Stephen: Trans. Faraday Soc. **33**, 800 (1937).
(60) Jost: Z. physik. Chem. **134**, 92 (1928).
(61) Jungers and Taylor: J. Chem. Phys. **3**, 338 (1935).
(62) Kirkbride and Norrish: J. Chem. Soc. **1933**, 119.
(63) Kistiakowsky: J. Am. Chem. Soc. **49**, 976 (1927).
(64) Kistiakowsky: J. Am. Chem. Soc. **52**, 102 (1930).
(65) Koblitz and Schumacher: Z. physik. Chem. **B35**, 11 (1937).
(66) Kornfeld and Weegmann: Z. Elektrochem. **36**, 789 (1930).
(67) Krauskopf and Rollefson: J. Am. Chem. Soc. **58**, 443 (1936).
(68) Küchler and Patat: Monatsh. **68**, 275 (1936).
(69) Leermakers: J. Am. Chem. Soc. **56**, 1537 (1934).
(70) Leermakers: J. Am. Chem. Soc. **56**, 1899 (1934).
(71) Leighton and Blacet: J. Am. Chem. Soc. **55**, 1766 (1933).
(72) Leighton, W. G., and Forbes: J. Am. Chem. Soc. **52**, 3139 (1930).
(73) Leighton and Lucy: J. Chem. Phys. **2**, 756 (1934).
(74) Leighton and Mortenson: J. Am. Chem. Soc. **58**, 448 (1936).
(75) Leighton and Steiner: J. Am. Chem. Soc. **58**, 1823 (1936).
(76) Lewis: J. Phys. Chem. **32**, 270 (1928).
(77) Lind and Livingston: J. Am. Chem. Soc. **54**, 94 (1932).
(78) Lind and Livingston: J. Am. Chem. Soc. **55**, 1036 (1933).
(79) Lyons and Dickinson: J. Am. Chem. Soc. **57**, 443 (1935).
(80) Marshall: J. Phys. Chem. **30**, 1078 (1926); J. Am. Chem. Soc. **54**, 4460 (1932).
(81) McDonald: J. Chem. Soc. **1928**, 1.
(82) Melville: Proc. Roy. Soc. (London) **A139**, 541 (1933).
(83) Meyers and Beckman: J. Am. Chem. Soc. **57**, 89 (1935).
(84) Mitchell and Hinshelwood: Proc. Roy. Soc. (London) **A159**, 32 (1937).
(85) Montgomery and Rollefson: J. Am. Chem. Soc. **55**, 4025 (1933).

(86) Müller and Schumacher: Z. physik. Chem. **B35**, 285 (1937).
(87) Newling, Stavely, and Moelwyn-Hughes: Trans. Faraday Soc. **29**, 1155 (1933).
(88) Norrish: J. Chem. Soc. **1927**, 761; **1929**, 1158, 1611.
(89) Norrish, Crone, and Saltmarsh: J. Chem. Soc. **1934**, 1456 (1934).
(90) Norrish, Crone, and Saltmarsh: J. Chem. Soc., **1933**, 1533.
(91) Norrish and Kirkbride: J. Chem. Soc. **1932**, 1518.
(92) Norton: J. Am. Chem. Soc. **56**, 2294 (1934).
(93) Noyes: J. Chem. Phys. **5**, 807 (1937).
(94) Ogg, Leighton, and Bergstrom: J. Am. Chem. Soc. **55**, 1754 (1933).
(95) Ogg, Leighton, and Bergstrom: J. Am. Chem. Soc. **56**, 318 (1934).
(96) Patat and Koch: Z. Elektrochem. **41**, 494 (1935).
(97) Qureshi and Takir: J. Phys. Chem. **36**, 2670 (1932).
(98) Rabinowitsch: Z. physik. Chem. **B19**, 190 (1932).
(99) Ritchie and Norrish: Proc. Roy. Soc. (London) **A140**, 99 (1933).
(100) Ross and Kistiakowsky: J. Am. Chem. Soc. **56**, 1112 (1934).
(101) Rudberg: Z. Physik **24**, 247 (1924).
(102) Schumacher: Z. physik. Chem. **129**, 261 (1927).
(103) Schumacher and Bergmann: Z. physik. Chem. **B13**, 269 (1931).
(104) Schumacher and Townsend: Z. physik. Chem. **B20**, 375 (1933).
(105) Schumacher and Wolff: Z. physik. Chem. **B25**, 161 (1934).
(106) Schumacher and Wolff: Z. physik. Chem. **B26**, 453 (1934).
(107) Simmons and Beckman: J. Am. Chem. Soc. **58**, 454 (1936).
(108) Smakula: Z. physik. Chem. **B25**, 90 (1934).
(109) Smith and Kistiakowsky: J. Am. Chem. Soc. **57**, 835 (1935).
(110) Smith, Noyes, and Hart: J. Am. Chem. Soc. **55**, 4444 (1933).
(111) Spence and Wild: Proc. Leeds Phil. Lit. Soc., Sci. Sect. **3**, 141 (1936).
(112) Spinks and Porter: J. Am. Chem. Soc. **56**, 264 (1934).
(113) Stein: Trans. Faraday Soc. **29**, 583 (1933).
(114) Stewart and Wiedenbaum: J. Am. Chem. Soc. **57**, 1702 (1935).
(115) Thompson and Linnett: J. Chem. Soc. **1935**, 1452.
(116) Thompson and Linnett: Trans. Faraday Soc. **33**, 874 (1937).
(117) Vaidya: Proc. Roy. Soc. (London) **A129**, 299 (1930).
(118) Vaughn and Noyes: J. Am. Chem. Soc. **52**, 559 (1930).
(119) Vesper and Rollefson: J. Am. Chem. Soc. **56**, 1455 (1934).
(120) Villars: J. Am. Chem. Soc. **49**, 326 (1927).
(121) Vraneck: Z. Elektrochem. **23**, 336 (1917).
(122) Warburg: Sitzber. preuss. Akad. Wiss., p. 314 (1916).
(123) Warburg: Sitzber. preuss. Akad. Wiss. **50**, 960 (1919).
(124) Warburg: Z. Elektrochem. **27**, 133 (1921).
(125) Warburg and Rump: Z. Physik **47**, 305 (1928).
(126) Welge and Beckman: J. Am. Chem. Soc. **58**, 2462 (1936).
(127) Wenner and Beckman: J. Am. Chem. Soc. **54**, 2787 (1932).
(128) Weigert: Naturwissenschaften **15**, 124 (1927).
(129) Weizmann, Bergmann, and Hirshberg: J. Am. Chem. Soc. **58**, 1675 (1936).
(130) West and Ginsburg: J. Am. Chem. Soc. **56**, 2626 (1934).
(131) West and Rollefson: J. Am. Chem. Soc. **58**, 2140 (1936).
(132) West and Schlesinger: J. Am. Chem. Soc. **60**, 961 (1938).
(133) Wiig: J. Am. Chem. Soc. **57**, 1559 (1935).
(134) Willard and Daniels: J. Am. Chem. Soc. **57**, 2240 (1935).
(135) Winkler: Trans. Faraday Soc. **31**, 761 (1935).
(136) Zimmer: Z. physik. Chem. **B23**, 239 (1933).

THE NATURE OF THE PRIMARY PROCESS IN PHOTOCHEMICAL REACTIONS[1]

G. K. ROLLEFSON

Department of Chemistry, University of California, Berkeley, California

Received May 26, 1938

In the previous reports the nature of the primary action of light in photochemical reactions has been discussed in some detail. The principal developments since that time have been concerned with the determination of the products of the photodissociation processes and with the process known as predissociation. The term "predissociation" was introduced by Henri (4) in describing certain diffuse bands discovered by himself and his associates. Their choice of this name was based on their idea that these diffuse bands corresponded to excitation of the molecule to a loosely bound state in which it could dissociate readily. The present-day views are based on the picture, offered by Bonhoeffer and Farkas (2) and by Kronig (11), that the molecule in the activated state produced by the absorption of these diffuse bands undergoes a radiationless transfer to another electronic state and dissociates in a time which is short compared to the period of rotation. Such changes have been expressed graphically by Herzberg (6) by means of potential energy diagrams (figure 1). The transition from one state to another by this predissociation process must occur without any appreciable change in the separation of the atomic nuclei or in the energy of the system. From the standpoint of the diagrams, this means that we have radiationless transitions occurring only at the intersection of two curves. In our diagram (figure 1), if the excitation by light takes the molecule from the normal state, n, to a state represented by a point on the curve a above the level of the intersection of that curve with a', then as the molecule vibrates in the excited state we have the possibility of a transfer from a to a' occurring. If this intersection point is above the level corresponding to the dissociation of the state represented by a', the molecule will dissociate within the next vibration.

The diagrams (figure 1) must be looked upon as schematic only, since, actually, we cannot specify the positions and energies of the atoms with the precision indicated by the curves. According to Heisenberg's Uncertainty Principle, the product of the uncertainties of position and mo-

---

[1] Contribution No. 3 to the Third Report of the Committee on Photochemistry, National Research Council.

mentum is $h/2\pi$. A more convenient form for us to use in the discussion of predissociation is that the uncertainty in the energy multiplied by the uncertainty of the time is $h/2\pi$. Our curves therefore should be looked upon as representing mean values only. Furthermore the intersections of two curves must be considered not as points but rather as regions within which the molecule may be thought of as being in an indeterminate state. The probability of a transfer occurring will depend upon the time that the molecule is in this indeterminate condition. This time will depend on the kinetic energy of vibration and the range over which the transition may occur. Thus in figure 1a we should expect the transition to occur only if the condition of the molecule corresponds to a point rather close to the intersection. On the other hand, in figure 1b, where the two curves cross at a small angle, when we take into consideration the blurring called for by the Uncertainty Principle, we see that there will be a long region along the curve *a* which is in the indeterminate area. Hence we should expect, other things being equal, that molecules represented by diagrams similar to figure 1b will show predissociation over a wider range and more frequently than those corresponding to the other diagrams. At the present time we do not know enough about these potential curves to make any quantitative calculations concerning predissociation. Furthermore, these curves must be considered as only schematic for polyatomic molecules, as they are far from simple vibrators.

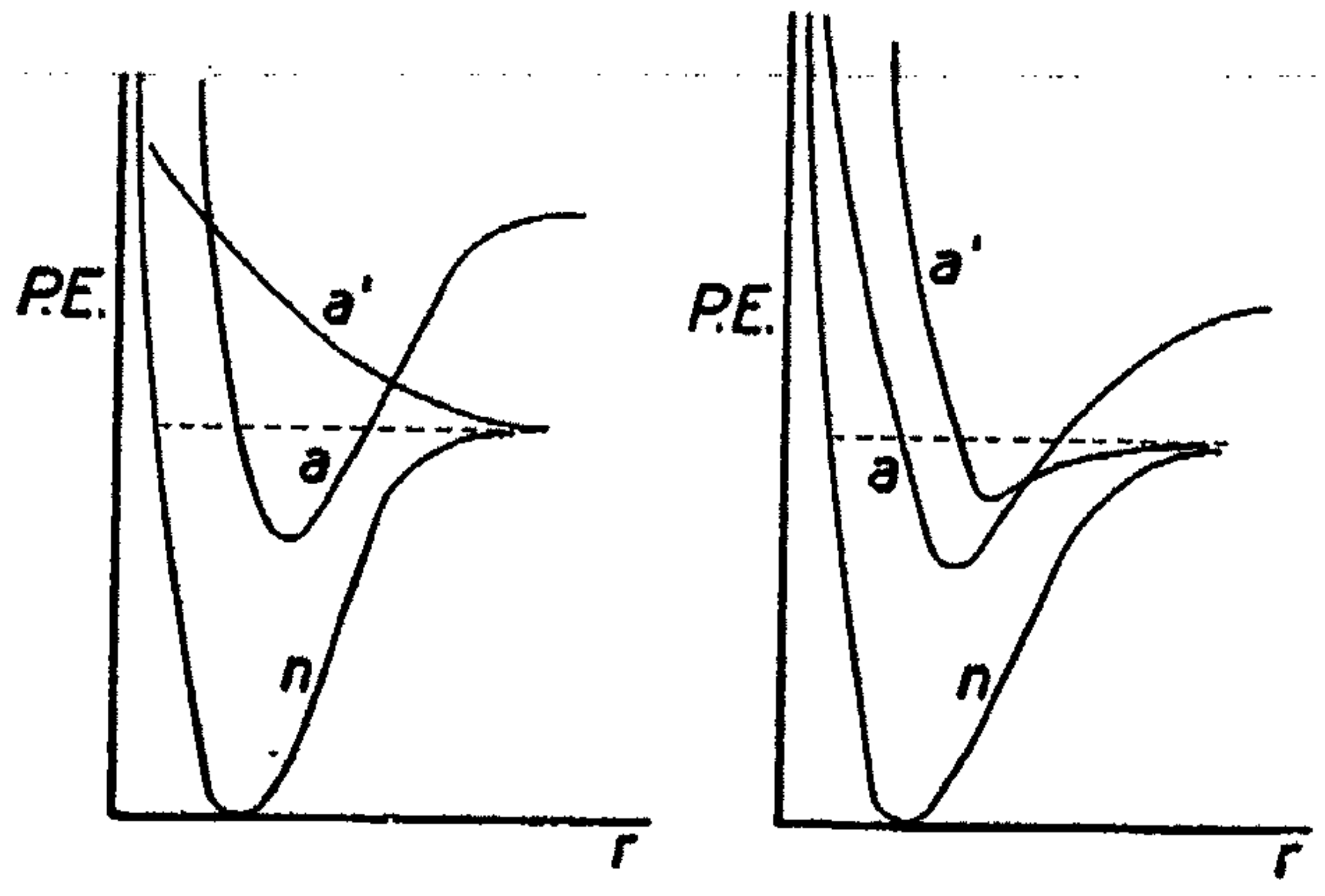

1a 1b

FIG. 1. Potential energy diagrams

The Uncertainty Principle also accounts for the appearance of a diffuse spectrum. If the excited state dissociates within a time τ the width, w, of the spectrum line which put the molecule into that state will be given by

$w\tau = h/2\pi$ or, if we express w in cm.$^{-1}$, $w\tau = h/2\pi c$. In any ordinary spectrum which shows a fine line structure, the broadening due to the Doppler effect is ten to one hundred times the natural width of the line; therefore the predissociation process must shorten the life of the excited state by a factor of this magnitude for the effect to be noticeable. It is to be expected therefore that, whenever we find a diffuse absorption spectrum, fluorescence will either be very weak or absent. If we consider the competition between fluorescence and decomposition as represented by

$$AB^* \xrightarrow{k_1} AB + h\nu$$

$$AB^* \xrightarrow{k_2} A + B + \text{k.e.}$$

the fraction of the activated molecules which radiate will be given by $\frac{1}{1 + k_2/k_1}$. Hence, the greater k_2 is relative to k_1, i.e., the shorter the life period, the weaker will be the fluorescence. As k_2 usually must be ten to one hundred times k_1 for a diffuseness to be observed, it follows that a marked weakening of fluorescence is a more sensitive indicator of predissociation than a diffuse spectrum.

It is by no means universally true that we have transitions from one state to another occurring whenever we have a crossing of the potential energy curves for those states. Kronig (11) has set up the following selection rules for diatomic molecules: *(1)* There shall be no change in the total angular momentum. *(2)* Transitions occur only between states of the same multiplicity. (Invalid for large multiplet separations.) *(3)* The quantum number Λ changes by 0 or ± 1. *(4)* Transitions occur from a positive to a positive state or from a negative to a negative. *(5)* If both atoms are the same, the states involved in a transition are either both symmetrical or both antisymmetrical. The interpretation of the spectra of polyatomic molecules has not progressed to the point where we can say whether an analogous set of rules applies or not. However, we may say that we can expect to find the probabilities of radiationless transfers occurring ranging from practically every time the molecule reaches the state represented by the intersection of the potential energy curves to practically complete prohibition of the change.

The probability of a radiationless transfer occurring is modified considerably by a magnetic field or collisions with other molecules. This gives rise to the phenomenon known as induced predissociation. Experimental evidence for the occurrence of this process was obtained by Loomis and Fuller (12) and by Kondratjew and Polak (10) in the study of the absorption spectrum of iodine. They found that the addition of inert gases increased the absorption coefficient of iodine in the vapor state for those bands involving values of v', the vibrational quantum number in the upper state, greater than 12. Turner (15) found that, if iodine vapor were illuminated with light absorbed in the band region in the presence of a magnetic field or inert gases, there was a marked absorption of the spectrum lines characteristic of iodine atoms. More recently, Rabinowitch and Wood (13) have made a more quantitative study of the effect of inert gases. In their experiments, the dissociation of the iodine was determined by measuring the light absorbed by the remaining iodine molecules. They concluded that argon, nitrogen, and oxygen caused the dissociation of the activated molecule at every "gas-kinetic" collision. Helium was somewhat less effective but, with a pressure of 500 mm. of that gas, all of the molecules absorbing light were dissociated.

In the case of bromine we have some evidence that dissociation occurs in the band region even without the aid of collisions. Urmston and Badger (16) found in their experiments on the photochemical reaction of bromine with platinum that the rate of the reaction was independent of the distance between the platinum and the illuminated zone. Their experiments were performed at low pressures, so that induced predissociation did not need to be considered. Neither could their results be accounted for on the basis of active molecules, as they were able to demonstrate that fluorescence was confined to the illuminated zone. It is possible that the reaction was due to a continuum underlying the band absorption, a situation analogous to that in the hydrogen-chlorine reaction which has been discussed recently by Bayliss (1). However, no appreciable difference was noted in rates whether blue or yellow light was used. Other reactions in which no effect was noted on comparing the rates using blue and yellow light are the bromination of acetylene (3) and the formation of hydrogen bromide (8). The effect of inert gases on the latter reaction has been studied in considerable detail. Instead of finding an accelerating effect, which could be attributed to induced predissociation, a retarding effect was noted, due to an increased rate of recombination of bromine atoms (7, 8, 14). This is understandable if we assume that with bromine, as has been found with iodine, every collision of an activated molecule results in dissociation. Under such conditions, no effect assignable to induced predissociation would be detectable above about 10 mm. pressure.

A quite different result has been reported for the hydrogen-chlorine reaction by Hertel (5). He found that, if the light absorption occurred in the banded region of the spectrum, this reaction was accelerated by the addition of inert gases. This effect was believed to be due to the activated molecules being dissociated by collisions. The mechanism of such a dissociation is probably induced predissociation.

The examples which we have just discussed show no sign of predissociation in their absorption spectra, indicating that the life of the undisturbed activated molecule is at least of the order of 10^{-9} sec.; with iodine, studies of the fluorescence indicate a life of 10^{-7} sec. It is apparent, therefore, that spontaneous or induced predissociation may occur with any kind of light absorption. Hence, the possibility of dissociation in the primary step of a photochemical reaction cannot be excluded on the basis of well-defined lines in the absorption bands nor even on the basis of fluorescence observations.

Another interesting example is furnished by tellurium vapor, Te_2. In this case the limits of the natural and induced predissociation do not coincide. The difference must be due to the induced effect involving a lower lying level than the spontaneous process (9).

If the light is absorbed by a complex molecule it is much more difficult to demonstrate an effect due to induced predissociation on account of the complexities introduced by secondary reactions. Usually, the photochemical experiments are carried out at such high pressures that the induced predissociation is a maximum if it is anything like that with simple molecules. Any effects of this type must therefore be sought for at low pressures, particularly in systems for which the quantum yield of the primary process is less than 1.

REFERENCES

(1) Bayliss: Trans. Faraday Soc. **33**, 1339 (1937).
(2) Bonhoeffer and Farkas: Z. physik. Chem. **134**, 337 (1928).
(3) Booher and Rollefson: J. Am. Chem. Soc. **56**, 2288 (1934).
(4) Henri and Teves: Nature **114**, 894 (1924); Compt. rend. **179**, 1156 (1924).
(5) Hertel: Z. physik. Chem. **B15**, 325 (1932).
(6) Herzberg: Z. Physik **61**, 604 (1930).
(7) Hilferding and Steiner: Z. physik. Chem. **B30**, 399 (1935).
(8) Jost and Jung: Z. physik. Chem. **B3**, 83 (1929).
(9) Kondratjew and Lauris: Z. Physik **92**, 741 (1934).
(10) Kondratjew and Polak: Physik. Z. Sowjetunion **4**, 764 (1933).
(11) Kronig: Z. Physik **50**, 347 (1928); **62**, 300 (1930).
(12) Loomis and Fuller: Phys. Rev. **39**, 180 (1932).
(13) Rabinowitch and Wood: Trans. Faraday Soc. **32**, 547 (1936).
(14) Ritchie: Proc. Roy. Soc. (London) **A146**, 828 (1934).
(15) Turner: Phys. Rev. **41**, 627 (1932).
(16) Urmston and Badger: J. Am. Chem. Soc. **56**, 343 (1934).

SOME COMPARISONS BETWEEN PHOTOCHEMICAL PROCESSES IN GASES AND SOLUTIONS[1, 2]

ROSCOE G. DICKINSON

Department of Chemistry, California Institute of Technology, Pasadena, California

Received May 25, 1938

The chief purpose of the present section of this report is a comparison of photochemical reactions in the gaseous state with those in solution or in the liquid state. It is not proposed to enter into a detailed discussion of photochemical processes in solution but rather to indicate the relation of such processes, when possible, to those occurring in the gaseous state. This section accordingly contains a brief statement of viewpoints involved in comparing gaseous and solution or liquid reaction, together with some discussion of pertinent experimental results.

In recent years theories of the liquid state and of various phenomena occurring in liquids have undergone active development; this may, for example, be seen in the general discussion of the liquid state published by the Faraday Society (43) as well as in other papers to which specific reference will be made. Theoretical approaches to the liquid state have sometimes started with the gaseous state and have sometimes started with the crystalline state; Bernal (4), however, has given reasons for believing that liquid structure, while having points of close resemblance to the crystalline, is of a character that can not be reached by continuous transition from the crystalline state.

Current views are that a liquid, at not too high a temperature, aside from differing from a gas in the matter of coherence, possesses a somewhat quasi-crystalline structure. This does not necessarily show itself in any large regions with crystalline regularity but appears rather in the character of the distribution function $p(r)$, where $4\pi r^2 p(r)dr$ gives the probability of finding a second molecule within the distance range r to $r + dr$ of a chosen molecule. This distribution function has been investigated by x-ray diffraction methods (25, 42, 5, 11, 29) and by experiments with models (30). The function does not show the monotonic character expected for a dilute gas, but rather exhibits maxima and minima which

---

[1] Contribution No. 4 to the Third Report of the Committee on Photochemistry, National Research Council.

[2] Contribution No. 643 from the Gates and Crellin Laboratories of Chemistry, California Institute of Technology.

become less pronounced with increasing r but are evident for a distance of several molecular diameters. The structure, at least in the case of simple non-polar liquids, may be thought of as such that a chosen molecule has immediately coördinated about it a number of other molecules at a distance corresponding to the first maximum of $p(r)$, others more loosely coördinated at a distance corresponding to the next maximum, and so on. The chosen molecule is accordingly closely confined in a "cage" of surrounding molecules, so that its motion becomes in part a pseudo-oscillatory one within this cage. (One estimate (8) places the mean displacement between the extremes of oscillation at about 0.5 Å.) This suggests that, for diffusion to occur, the molecule must acquire sufficient energy to break through the wall of immediately surrounding molecules (8), i.e., to move to the center of a new coördination complex (33).

In calculating numbers of collisions of solute molecules with each other, the custom has been to treat the solute as if it were gaseous with solvent absent; in the calculation the molecules have been ordinarily regarded as rigid. In recent theories the occurrence of collisions has been modified both as to distribution in time and as to average number per unit time. In view of the cage effect of the solvent molecules, once two solute molecules have made collision there is a greater probability of further collision between the same pair than would be the case in a gas. Thus a given solute molecule undergoes collisions with other solute molecules in sets. The occurrence of such collision sets has been found in experiments with models (35). For thermal bimolecular reactions between solutes, the number of sets per unit time is important when there is high probability of reaction at any collision, but the total number of collisions per unit time rather than the number of sets becomes important when any considerable activation energy is required (8, 33, 46). Present estimates of the total collisions per unit time between solute molecules give values rather higher (five to twenty times) than those from a gas calculation. In view of the present state of flux in these ideas, it would be premature to recommend any one mode of calculating collision numbers.

Specific information concerning primary absorption processes is considerably more abundant and certain for gaseous substances than for substances in the liquid state or in solution. This arises partly from the relative simplicity of the phenomenon in the gaseous state, where the absorption is by fairly isolated molecules, and partly from the related fact that in condensed states the fine structure of absorption spectra is lost, together with the detailed information derivable from such structure. Aside from the smoothing out of fine structure into a continuum in solution, dissolved substances frequently show spectra differing from those of the same substances in the gaseous state, both as to magnitude of absorption coefficient and as to position of absorption maxima. This is not surprising, since solution may be accompanied by such processes as solvation, dissociation, or ionization producing essentially new absorbing molecules. However, when interactions between molecules in the solution are not too great, the solution absorption spectrum becomes essentially a blurred copy of that of the gas. For example, the absorption coefficients of the halogens in non-polar solvents such as carbon tetrachloride differ little from values for the gases. In cases where this close similarity exists, it is usual to presume that absorption is accompanied by the same electronic transition in both cases, and to draw inferences concerning the primary process in solution from a knowledge of that in the gas.

When a molecule in solution absorbs a quantum of radiation, there is initially produced an excited molecule for which there exists a variety of conceivable fates. Among these are the following: The molecule may (*a*) immediately lose its excitation energy through collision of the second kind with solvent molecules, whereby the absorbed energy becomes ineffectively distributed through the solution, or it may (*b*) retain its excitation (in part at least) in spite of collisions with the solvent molecules and later fluoresce or enter into reaction; again, (*c*) the absorbing molecule may immediately enter into chemical reaction with an adjacent solvent molecule; and finally, (*d*) the molecule, after a lapse of time possibly dependent on whether a true continuous or a predissociation spectrum is involved, may dissociate.

Since molecules in solution are practically continuously in the process of collision with solvent, the effect of collisions of the second kind in degrading activation energy from light absorption may be expected to be of greater importance in solution than in the gaseous state. Indeed, the ability of a molecule to retain its excitation in solution sufficiently to fluoresce or to react with a second molecule of solute implies a considerable insensitiveness toward collisions of the second kind. Among inorganic substances only a few, such as the uranyl salts and compounds of the rare earths, are known to fluoresce in solution; among organic substances the phenomenon is largely confined to various ring compounds. The view has been that, in substances showing fluorescence in solution, the electronic transition was one protected from outside influences either because of occurring in the interior of an atom or because of occurring in a protected part of a complicated molecule. Frank and Levi (17) have remarked that this view is incomplete and does not explain how some substances may fluoresce yet have their fluorescence strongly suppressed by the addition of various substances to the solution. Using the idea that the electronic excitation energy of the absorbing molecule can be easily transformed only when it is approximately equal to that of a new electronic state (of the absorbing molecule, the collision partner, or both), Franck and Levi have discussed the conditions for fluorescence, quenching, and reaction in terms of potential energy curves. The retention of electronic excitation permitting reaction with a second molecule of solute is probably somewhat exceptional, most photochemical reactions occurring as a result of reaction with the solvent or of the formation of atoms or free radicals. In connection with these considerations, attention should be given to cases where sensitization of solute reaction by the solvent occurs. In the conversion of *o*-nitrobenzaldehyde into *o*-nitrosobenzoic acid in acetone solution (45), the gross quantum yield (molecules transformed per quantum absorbed by the system) for 3130 Å. remains near 0.5 for acetone solutions containing from 2 per cent to 0.02 per cent of aldehyde, although, at the lower concentration, 96 per cent of the absorption is due to the acetone. Again, the decomposition of ethyl iodide at a mean wave length of 2610 Å. gives a quantum yield (48) in 0.03 molar solution in benzene of 0.52, although only 1/180 of the absorption is due to the ethyl iodide; moreover in hexane solution, where the absorption is all due to the ethyl iodide, the yield is substantially the same. The mechanisms of these sensitizations are not known.

If, in the gaseous state, an induced predissociation occurs in competition with fluorescence, then, in solution, the dissociation may evidently be favored. However, even if the molecule does dissociate, there exists a possibility that the dissociating partners, in view of the fact that they are closely hemmed in by solvent molecules, will frequently immediately recombine. The greatly increased probability of this occurrence in solution has been emphasized by Franck and Rabinowitsch (18); they have called the process "primary recombination" to distinguish it from the "normal" recombination process which involves the uniting of atoms or radicals which were not previously partners. It has long been recognized that the Einstein photochemical equivalence law does not, in general, apply to the overall photochemical reaction, but frequently only to the primary process. The effect of a dissipation accompanying the absorption, or of primary recombination, would operate to prevent the occurrence of an integral relationship between the number of quanta absorbed and the number of *primary* products of the absorption process.

Existing experimental evidence which might be expected to have a bearing on the question of primary recombination may for the most part be divided into three classes: (*1*) experiments in which the stationary concentration of the primary products of dissociation is estimated by measurement of the light transmission of the solution while under irradiation; (*2*) photochemical experiments in which a reaction proceeds by a chain, with the rate of reaction interpreted as depending on the stationary concentration of transient substances resulting from the absorption process; and (*3*) photochemical experiments in which no chain is presumed to be involved and in which the stationary concentrations of transients are of secondary interest.

Extensive experiments of the first type have been carried out by Rabinowitsch, Wood, and Lehmann. In these the stationary decrease in concentration of halogen molecules under a measured strong irradiation was determined. With iodine in carbon tetrachloride or hexane solution (34), the processes apparently involved were only the photodissociation of the molecules and recombination of the atoms. If the fraction β of absorbed photons gives dissociation

$$I_2 + h\nu \rightarrow 2I$$

so that the rate of production of atoms by dissociation is $2\beta(I_{\text{abs.}})$, and if the atoms disappear only by recombination $2I \rightarrow I_2$ with a rate $2k(I)^2$, the value of β is evidently given by

$$\beta = k(I)^2/(I_{\text{abs.}})$$

at the steady state. Corresponding values of (I) and $(I_{\text{abs.}})$ have been measured experimentally; the value derived for β then depends on what is assumed concerning k. If a pair of normally diffusing iodine atoms are assumed to combine on their first collision, and if it be assumed that the specific rate, Z, of such collisions may be calculated with the gas kinetic expression

$$Z = 2\sqrt{\pi}d^2\sqrt{RT/M}$$

then this specific collision rate may be set equal to k and β may be obtained. Taking $d = 5.0 \times 10^{-8}$ cm., the data lead to average values of β of 0.7 ± 0.3 for I_2 in carbon tetrachloride and 1.0 ± 0.3 in hexane. However, if in the absence of combination, collisions between normally diffusing iodine atoms were to occur in sets of, on the average, n collisions each, then, with combination at the first collision, k becomes Z/n and the calculated values of β become the former values multiplied by $1/n$. Again if, in accord with ideas mentioned earlier, the total number of collisions between solute molecules is somewhat greater than the value given by the gas formula, say m times that value, then the calculated values of β become m/n times the values given above. Thus, while values of β of the order of magnitude of unity are compatible with the experimental results, more definite independent knowledge of the recombination rate is necessary in order to make a definite determination of β from the stationary concentrations.

The assumption that two particles just leaving a photodissociation have the same probability of immediate collision as two particles leaving an ordinary collision is doubtful when (as is usually the case) the dissociating partners have considerable excess kinetic energy. Rollefson and Libby (36) have urged that "such atoms have an excellent chance of forcing their way between the solvent molecules" so that the two probabilities would not be equal. Rabinowitsch and Wood (35) had considered such a dyssymmetry of cage effect possible when the molecules of the solvent were smaller in mass than the dissociation products but not when the solvent was greater since, from conservation of momentum, the dissociating products would be brought to rest by their first collision with the heavier particle irrespective of their kinetic energy. However, this consideration applies primarily to head-on collisions and may not seriously affect the contentions of Rollefson and Libby. In this connection it may be remarked that activation energies for diffusion of 3000 cal. and less have been calculated (8); at least this excess is often possessed by dissociating partners in photochemical experiments.

If it be admitted that the probability of separation is greater for a pair of photodissociating atoms than for a pair in normal collision, then an effect of wave length on stationary concentrations becomes possible. Such an effect was sought (34) but not certainly found.

Turning now to photochemical evidence concerning primary recombination, there are various photochemical chain reactions to which mechanisms have been assigned which are such that the rate of reaction is proportional to the steady concentration of transients produced immediately or indirectly by the light absorption process. Simple examples are the sensitized decomposition of ethylene iodide and the iodine-sensitized transformations of geometrical isomers. Attempts to draw inferences concerning primary recombination from the rates of such reactions encounter the same ambiguities, *inter alia*, as discussed above in connection with the experiments of Rabinowitsch and Wood. However, here again, if the solvent effect is not the same for primary and secondary recombination, a wave length effect is possible; for, whereas the secondary recombination is presumably unaffected by wave length, the kinetic energy of the dissociating partners will be smaller at longer wave lengths with possibly more primary recombination and a smaller rate of reaction. Reactions of the type under discussion often proceed at rates proportional to the square root of the intensity of illumination. In such cases the total material reacting per unit time depends not only on the rate of absorption of radiation but on the distribution of absorption through the reacting medium (1); this point has, unfortunately, been frequently ignored. A rather small wave length effect has been reported (14) for the iodine-sensitized ethylene iodide decomposition; the primary quantum yields for the wave lengths 4358, 5461, and 5780 Å. were found to stand in the ratios 1:0.87:0.75. Other halogen chain reactions in which yields somewhat smaller at longer wave lengths than at shorter have been reported are the following: the bromination of cinnamic acid in carbon tetrachloride solution (2); the bromination of liquid benzene (32); the bromination of maleic ester and its sensitized rearrangement to fumaric ester (15); the iodination of various olefins in chloroform solution at −55°C. (16). It is to be noted that similar wave length effects have been reported absent in the following *gaseous* reactions: the formation of hydrogen bromide (22); the bromination of acetylene (6); the bromination of cyclohexane (23); the bromine-sensitized decomposition of chlorine dioxide (40, 41). Considerable wave length effects in the same sense are often found in aqueous solution reactions, but caution must be exercised in attributing them to varying primary recombinations as opposed, for example, to reaction with solvent or to the occurrence of different electronic transitions on absorption.

The situation can be somewhat different in the case of certain reaction mechanisms not involving a chain. If conditions are such that the atoms or radicals formed in the primary process always react with some solute to give products without the intervention of a chain, then the gross quantum yield may be used to give indications of the primary quantum yield. A necessary experimental condition is evidently a constancy of gross quantum yield over a range of concentrations of reactant. Reactions which may be of this type have not been very thoroughly examined. The decomposition of ozone in carbon tetrachloride solution sensitized by chlorine has been reported (7) to occur with a quantum yield of $2O_3$ decomposed per quantum absorbed at the wave length 3660 Å. If the mechanism be such as the following (38),

$$Cl_2 + h\nu \rightarrow 2Cl$$

$$Cl + O_3 \rightarrow ClO + O_2$$

$$2ClO \rightarrow Cl_2 + O_2$$

the observed quantum yield would indicate absence of primary recombination. The gaseous reaction is complicated (21). Again the chlorination of trichlorobromomethane in carbon tetrachloride was reported (20) to proceed with a yield of 0.9 mole of bromine per quantum absorbed (wave lengths); if the mechanism is the following (38),

$$Cl_2 + h\nu \rightarrow 2\,Cl$$

$$Cl + CCl_3Br \rightarrow CCl_4 + Br$$

$$2Br \rightarrow Br_2$$

the quantum yield indicates little primary recombination. However, the compound BrCl was not known and its formation not considered in these experiments. In the gaseous reaction, chains have been found (44). The oxidation of carbon tetrachloride to phosgene by dissolved oxygen brought about by radiation (2537 Å.) absorbed by the carbon tetrachloride has been reported (28) to occur with a yield of 1 mole of carbon tetrachloride oxidized per quantum absorbed. But in the absence of dissolved oxygen the quantum yield of decomposition of carbon tetrachloride was found to be less than 0.01. Taken together, these results could mean either (*1*) no primary recombination but a low specific rate for the reaction $2CCl_3 \rightarrow C_2Cl_6$ as compared with reactions leading to reformation of carbon tetrachloride or (*2*) large primary recombination with a long chain oxidation. The second possibility would make the apparently simple yield of oxidation fortuitous. A similar result has been obtained (48) in the oxidation of ethyl iodide by oxygen in solution under the influence of radiation absorbed by the ethyl iodide. In the presence of oxygen a 1.38 molar solution of ethyl iodide in hexane irradiated with a wave length of 2610 Å. yielded "exactly 2 atoms of iodine for every quantum absorbed." In the absence of oxygen the yield was only 0.58. Franck and Rabinowitsch (18) pointed out how primary recombination might fail to operate through reaction of the dissociating molecule with the solvent. With the aid of radioactive chlorine Rollefson and Libby (36) have shown that, when chlorine absorbs visible radiation in carbon tetrachloride solution, little if any reaction with the solvent occurs.

A possibility of obtaining further information concerning primary recombination, that does not seem to have been exploited, is offered by the photochemical intermittency effect. To illustrate this possibility, suppose a photochemical solution reaction to proceed with the mechanism:

$$I_2 + h\nu \rightarrow 2I \qquad (1)$$

$$I + A \rightarrow I + B \qquad (2)$$

$$2I \rightarrow I_2 \qquad (3)$$

This mechanism involves the same processes as those occurring in the experiments of Rabinowitsch and Wood (34), and, in addition, an iodine atom catalysis of the conversion of A into B. The steady-state rate of this process is evidently $k_2\sqrt{\beta(I_{\text{abs.}})/k}$, where β and k have their former significance. If, however, the illumination is not steady but is carried out in regularly spaced periods of light and dark of measured duration, then it can be shown[3] that for the measurable reaction A → B, the ratio of the

---

[3] Complete details are too lengthy to be given here. However, the considerations are simply as follows: that in the light

$$\frac{d(I)}{dt} = 2\beta(I_{\text{abs.}}) - 2k(I)^2$$

that in the dark

$$\frac{d(I)}{dt} = -2k(I)^2$$

and that at all times

$$\frac{d(A)}{dt} = -k_2(I)(A)$$

rate under steady illumination to that under intermittent illumination is given by a complicated but known function of the measurable quantities ($I_{\text{abs.}}$), τ_{light} and τ_{dark} (the periods of light and dark in the intermittency experiment) and the unknown quantity βk. The points of importance are that, in the theory of the intermittency effect, the product of β and k occurs and may be rendered measurable by absolute measurements of ($I_{\text{abs.}}$), whereas steady-state experiments involve the ratio of β to k; combination of results from both types of experiment may thus give β and k separately.

The idea of primary recombination has been employed (31) to account for some of the special complications arising in the decomposition of ketones in hydrocarbon solvents where reaction with the solvent occurs. It has also been employed in the discussion (47) of the decomposition of ethyl iodide, which occurs with a larger quantum yield in the liquid state than in the gaseous, and in a discussion (12) of the decomposition of ethylene iodide in carbon tetrachloride solution.

When a comparison of gaseous and solution photochemical reactions with respect to processes subsequent to the primary one is undertaken, the ordinary problems of chemical kinetics of thermal reactions are encountered. The literature on the effect of solvent on thermal reaction rate is, of course, large (see, for example, the symposium on the kinetics of reaction (10)). There are, however, two very simple ways in which the kinetics may undergo large apparent alteration in passing from the gas to even an inert solvent. If the gaseous reaction involves some wall reaction (for example, a chain-breaking step) this process will hardly occur in solution; the kinetics (including, for example, the dependence on light intensity) may then be considerably altered. If the gaseous reaction involves a three-body combination of two atoms or simple radicals, this process can be strongly favored in solution, owing to the abundant supply of third bodies by the solvent; if the combining bodies are sufficiently complicated, however, a third body is of little advantage (24).

In 1935, a collection was made (13) of photochemical reactions which had been examined in both the gaseous and the liquid or solution states. It was found that when the same reaction occurred in the gaseous state as in the liquid or in an inert solvent, the reaction was usually as fast or faster in the gaseous state. Additional cases for which this is true are the bromination of dichloroethylene (19), the chlorination of chloroform (9, 37, 39, 3), and the conversion of *o*-nitrobenzaldehyde into *o*-nitrosobenzoic acid (45, 26, 27).

REFERENCES

(1) Allmand, A. J.: J. Chem. Soc. **1929**, 1557.
(2) Bauer, W. H., and Daniels, F.: J. Am. Chem. Soc. **56**, 384 (1934).
(3) Beezhold, W. F., and Ornstein, L. S.: Physica **3**, 154 (1936).

(4) Bernal, J. D.: Trans. Faraday Soc. **33**, 27 (1937).
(5) Bernal, J. D., and Fowler, R. H.: J. Chem. Phys. **1**, 515 (1933).
(6) Booher, J. E., and Rollefson, G. K.: J. Am. Chem. Soc. **56**, 2288 (1934).
(7) Bowen, E. J., Moelwyn-Hughes, E. A., and Hinshelwood, C. N.: Proc. Roy. Soc. (London) **A134**, 211 (1931).
(8) Bradley, R. S.: Trans. Faraday Soc. **33**, 1185 (1937).
(9) Chapman, A. T.: J. Am. Chem. Soc. **56**, 818 (1934); **57**, 416 (1935).
(10) Chem. Rev. **17**, 43-137 (1935).
(11) Debye, P., and Mecke, H.: Physik. Z. **31**, 797 (1930); **33**, 593 (1932).
(12) DeRight, R. E., and Wiig, E. O.: J. Am. Chem. Soc. **57**, 2411 (1935).
(13) Dickinson, R. G.: Chem. Rev. **17**, 413 (1935).
(14) Dickinson, R. G., and Nies, N. P.: J. Am. Chem. Soc. **52**, 2382 (1935).
(15) Eggert, J., and Borinski, W.: Z. Physik **26**, 865 (1925).
(16) Forbes, G. S., and Nelson, A. F.: J. Am. Chem. Soc. **59**, 693 (1937).
(17) Franck, J., and Levi, Hilde: Z. physik. Chem. **B27**, 409 (1934).
(18) Franck, J., and Rabinowitsch, E.: Trans. Faraday Soc. **30**, 125 (1934).
(19) Ghosh, J. C., and Bhattacharyya, S. K., and Bhattacharyya, S. Ch.: Z. physik. Chem. **B32**, 145 (1936).
(20) Grüss, H.: Z. Elektrochem. **29**, 144 (1923).
(21) Heidt, L. J., Kistiakowsky, G. B., and Forbes, G. S.: J. Am. Chem. Soc. **55**, 223 (1933).
(22) Jost, W.: Z. physik. Chem. **134**, 92 (1928).
(23) Jost, W.: Z. physik. Chem., Bodenstein Festband, p. 291 (1931).
(24) Kassel, L. S.: J. Am. Chem. Soc. **53**, 2143 (1931).
(25) Keesom, W. D., and deSmedt, J.: Proc. Acad. Sci. Amsterdam **25**, 118 (1922); **26**, 112 (1923).
(26) Küchler, L., and Patat, F.: Monatsh. **68**, 275 (1936).
(27) Leighton, P. A., and Lucy, F. A.: J. Chem. Phys. **2**, 756, 760 (1934).
(28) Lyons, E. H., Jr., and Dickinson, R. G.: J. Am. Chem. Soc. **56**, 443 (1935).
(29) Mencke, H.: Physik. Z. **33**, 593 (1932).
(30) Morrell, W. E., and Hildebrand, J. H.: J. Chem. Phys. **4**, 224 (1936).
(31) Norrish, R. G. W.: Trans. Faraday Soc. **33**, 1521 (1937).
(32) Rabinowitsch, E.: Z. physik. Chem. **B19**, 190 (1932).
(33) Rabinowitsch, E.: Trans. Faraday Soc. **33**, 1225 (1937).
(34) Rabinowitsch, E., and Wood, W. C.: Trans. Faraday Soc. **32**, 547 (1936).
(35) Rabinowitsch, E., and Wood, W. C.: Trans. Faraday Soc. **32**, 1381 (1936).
(36) Rollefson, G. K., and Libby, W. F.: J. Chem. Phys. **5**, 569 (1937).
(37) Schwab, G. M., and Heyde, U.: Z. physik. Chem. **B8**, 147 (1930).
(38) Schumacher, H. J., and Wagner, C.: Z. physik. Chem. **B5**, 205 (1929).
(39) Schumacher, H. J., and Wolff, K.: Z. physik. Chem. **B25**, 161 (1934).
(40) Spinks, J. W. T.: J. Am. Chem. Soc. **55**, 428 (1933).
(41) Spinks, J. W. T., and Porter, J. M.: J. Am. Chem. Soc. **56**, 264 (1934).
(42) Stewart, G. W.: Rev. Modern Phys. **2**, 116 (1930).
(43) Trans. Faraday Soc. **33**, 1 (1937).
(44) Vesper, H. G., and Rollefson, G. K.: J. Am. Chem. Soc. **56**, 1455 (1934).
(45) Weigert, F., and Pruckner, F.: Z. physik. Chem., Bodenstein Festband, p. 775 (1931).
(46) Weiss, J.: Naturwissenschaften **23**, 229 (1935).
(47) West, W., and Ginsburg, E.: J. Am. Chem. Soc. **56**, 2626 (1934).
(48) West, W., and Paul, B.: Trans. Faraday Soc. **28**, 688 (1932).

THE MECHANISM OF ALDEHYDE AND KETONE PHOTOLYSIS[1]

PHILIP A. LEIGHTON

Department of Chemistry, Stanford University, California

Received May 25, 1938

I. ABSORPTION SPECTRA

All aldehydes and ketones show an absorption band in the near ultraviolet, extending roughly from about 3500 Å. to below 2500Å., absorption in which probably produces transitions in non-bonding electrons of the carbonyl group (27, 45). The band shows, in general, the common phenomenon of structure at longer wave lengths, changing to a continuum at shorter wave lengths (9, 12, 13, 14, 16, 17, 18, 19, 25, 33, 53). Only in the case of formaldehyde has rotational structure been definitely observed and, except for formaldehyde, the transition from structure to continuum is very gradual. In the lighter aldehydes there appears to be a region of diffuse bands or predissociation preceding the continuum and, in addition, the bands themselves appear to be underlaid with a continuum which gradually becomes stronger as wave length is decreased.

Fluorescence, where observed, is most intense for absorption in the long wave length part of the band, but the observed limits of fluorescence do not necessarily agree with the observed limits of structure in absorption (14, 18, 19, 53). The structure becomes less marked with increase in magnitude of the hydrocarbon residue, while among the three classes, ketones, saturated aldehydes, and unsaturated aldehydes, it is interesting to note that ketones show the least structure but the most fluorescence, while the unsaturated aldehydes show the most structure and the least fluorescence.

A second and much stronger region of absorption begins at about 2000 Å. (2300 Å. for unsaturated aldehydes). In those cases which have been investigated this is found to consist of series of either diffuse or discrete bands (49, 53), some of which fit a Rydberg formula (36). The bands are underlaid with faint continuous absorption and are followed at still shorter wave lengths (<1500 Å.) by a strong continuum (14). Photochemical investigations have been confined almost entirely to the near ultraviolet

---

[1] Contribution No. 5 to the Third Report of the Committee on Photochemistry, National Research Council.

region, absorption in which produces two reactions,—decomposition and polymerization.

II. THE PRIMARY PROCESS IN DECOMPOSITION

Discrete bands together with fluorescence indicate the production of a relatively long-lived molecule on absorption at longer wave lengths, while the appearance of diffuse bands and continua indicate a dissociation process at shorter wave lengths, although, as the different types of absorption overlap, the resulting processes must also overlap.

The observation that the gaseous products of photolysis in the case of the lighter aldehydes and ketones consist chiefly of carbon monoxide and hydrocarbons or hydrogen has led to the conclusion that the bond or bonds adjacent to the carbonyl group are dissociated as the result of absorption. Supporting this are energetic considerations (51) and the demonstration by Pearson and his collaborators of the production of free methyl radicals during the photolysis of acetone and, to a lesser extent, of acetaldehyde (43) as well as of ethyl, propyl, and butyl radicals during the photolyses of diethyl and higher ketones (42, 44).

Referring to photolysis through the breaking of bonds adjacent to the carbonyl group as type I, three primary processes appear energetically possible (28):

(*A*) A dissociation into hydrocarbon (or hydrogen in the case of formaldehyde) and carbon monoxide molecules in one step:

$$R_1R_2CO + h\nu \rightarrow R_1R_2 + CO(^1\Sigma \text{ or } ^3\Sigma)$$

where R_1, R_2 = an alkyl radical or a hydrogen atom.

(*B*) The dissociation of a single R—C bond to produce an alkyl and an acyl radical:

$$R_1R_2CO + h\nu \rightarrow R_1 + R_2CO$$

(*C*) The dissociation of both R—C bonds simultaneously to give the corresponding radicals and normal ($^1\Sigma$) carbon monoxide:

$$R_1R_2CO + h\nu \rightarrow R_1 + R_2 + CO(^1\Sigma)$$

The decision as to the relative importance of these different dissociation processes constitutes one of the present problems in the photochemistry of aldehydes and ketones. The fact that aldehydes, RCHO, give predominantly a single hydrocarbon of composition RH, while mixed ketones give a mixture of three hydrocarbons R_1R_1, R_1R_2, and R_2R_2, led Norrish and Kirkbride (34) to the conclusion that the primary process is represented by process A for aldehydes and process C for ketones. More recent observations, however, necessitate the modification of both of these suggestions.

The isolation of diacetyl by Barak and Style (4), the demonstration by

Spence and Wild (50) that, for absorption in the continuum, the C_2H_6/CO ratio in the product gas is considerably greater than unity, and that the difference is quantitatively accounted for by diacetyl formation, and the detection by Glazebrook and Pearson (15) of acetyl radicals in concentration comparable to that of methyl radicals, all resulting from the photolysis of acetone at room temperatures, is convincing evidence that process B, rather than process C, must be concerned in ketone photolysis, at least in the case of acetone. The production of hydrogen (7, 24, 26), as well as of alkyl radicals (41, 42, 43, 44), and the existence of a chain at higher temperatures (1, 21, 26) all indicate that process B or process C must be concerned to some extent in aldehyde photolysis. The low stationary concentration of atomic hydrogen compared to that of methyl radicals (11, 40) is an indication that this dissociation occurs by process B, with the splitting of the C—C rather than the H—C bond, but the existing evidence is inconclusive in this regard.

The quantum yield of decomposition of the aldehydes at temperatures below 100°C. has been found to increase with decreasing wave length in all cases studied except that of formaldehyde (24, 25, 26, 35). Accompanying the increase in quantum yield is a marked increase in the yield of hydrogen (7, 24, 26). These facts have been explained by Rollefson (48) on the basis of a competition, following absorption, between four possible paths which determine the fate of the activated molecule: (*1*) deactivation by fluorescence or collision, (*2*) dissociation into hydrocarbon and carbon monoxide by process A, (*3*) dissociation into radicals by process B or process C, and (*4*) reaction with another molecule or molecules to form a polymer. At longer wave lengths, or in the region of banded absorption, processes 1 and 4 are predominant; with decreasing wave length, in agreement with the disappearance of structure and fluorescence, processes 2 and 3 become the more important, with 3 increasing more rapidly than 2. Rollefson estimates in the case of acetaldehyde that, at 3130 Å., 90 per cent of the molecules dissociating do so by process 2 and 10 per cent by process 3, while at 2537 Å. 75 per cent dissociate by process 2 and 25 per cent by process 3. The probability of dissociation into finished molecules compared to that of dissociation into radicals is thus 9:1 at 3130 Å., decreasing to 3:1 at 2537 Å. Although the magnitude of these ratios depends upon arbitrary assumptions as to the rates of the secondary reactions (26), the predominance of the dissociation into finished molecules, particularly at longer wave lengths, is in accordance with the smaller number of methyl radicals produced in acetaldehyde as compared with acetone (43), the small number of hydrogen atoms produced by absorption in the predissociation region as compared with the continuum in formaldehyde (39), and with the observation of Norrish and Bamford (30, 32) that, except as there is a reaction with the solvent, for dipropyl ketone type I photolysis is almost completely inhibited in solution (owing presumably to primary recombination of the radicals produced), while for isovaleraldehyde the solvent has relatively little effect. On the other hand, the report of Bowen and de la Praudiere (10) that the photolysis of acetaldehyde to yield gaseous products is virtually completely inhibited in the pure liquid would indicate a dissociation into radicals as predominant, while the statement of Akeroyd and Norrish (1) that, in the chain photolysis of acetaldehyde in the presence of acetone, it makes little difference which of these substances absorbs the light, suggests that dissociation into radicals is as efficient a process for acetaldehyde as for acetone.

Little evidence is available as to whether A and B are distinct processes (48), or whether process A results from a rapid secondary reaction following process B (7), *viz.*,

$$\mathrm{RCHO} + h\nu \rightarrow \mathrm{R} + \mathrm{CHO} \rightarrow \mathrm{RH} + \mathrm{CO}$$

In the former case the increase in B with decreasing wave length would arise from the changing potential energy of the excited molecule and the resultant change in relative probability of transition into different unstable states; in the latter case, it would arise from a more rapid separation of the radicals with increasing energy absorbed, with resultant change in the secondary reactions. By extending the latter point of view the data thus far discussed are capable of explanation entirely on the basis of a primary dissociation into free radicals, followed by appropriate secondary reactions (8, 20). Thus, while the production of some carbon monoxide and a hydrocarbon in the initial act more readily accounts for certain features of these reactions, there appears to be no fact which definitely requires such an act as a separate primary process.

When studying the photolysis of methyl butyl ketone, Norrish and Appleyard (31) found that an entirely different type of decomposition occurred, which can best be described as a species of cracking the hydrocarbon chain:

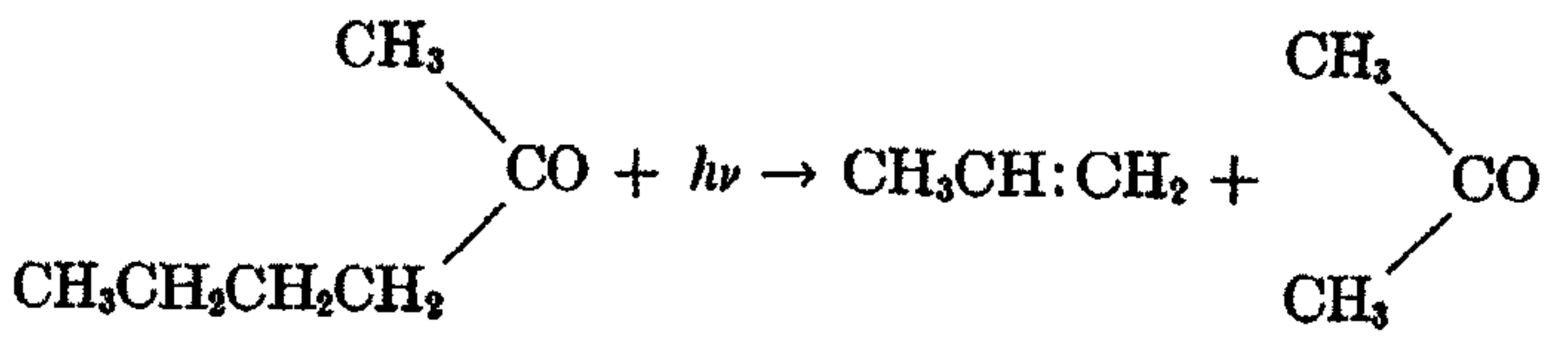

$$\begin{matrix}\mathrm{CH_3} \\ \mathrm{CH_3CH_2CH_2CH_2}\end{matrix}\!\!>\mathrm{CO} + h\nu \rightarrow \mathrm{CH_3CH{:}CH_2} + \begin{matrix}\mathrm{CH_3} \\ \mathrm{CH_3}\end{matrix}\!\!>\mathrm{CO}$$

Similar reactions, as judged from the decomposition products, have since been observed for a number of aldehydes and ketones containing an alkyl chain of three or more carbon atoms (3, 26, 29). In each case the bond between the carbon atoms α and β to the carbonyl group is broken, and a hydrogen atom or proton migrates to the α-carbon atom, leaving an olefin hydrocarbon and forming acetaldehyde or a methyl ketone. Following a suggestion of Norrish, this mode of decomposition may be referred to as type II. Judging from the data in table 1, type II decreases in importance with decreasing wave length, but increases in importance with increasing length of the hydrocarbon chain.

Evidence that type II dissociation results in finished molecules is furnished by the observation of Glazebrook and Pearson (15) that free radicals are apparently produced only by type I decomposition, and by the fact that, in all cases, type II decomposition occurs without modification in solution (29, 32). As suggested by Norrish, it appears that this is a true primary process involving some type of resonance between the excited carbonyl group and the α, β C—C bond.

TABLE 1

Relative numbers of molecules decomposing by type I and type II photolyses, as determined by the composition of the products

COMPOUND	CONDITIONS	TYPE I	TYPE II
		per cent	*per cent*
n-Butyraldehyde	3130 Å.; 30°C.	90	10
	2654 Å.; 30°C.	97	3
	2537 Å.; 30°C.	100	0
Isovaleraldehyde	Full radiation of Hg arc; approximately room temperature	47	53
Dipropyl ketone	Full radiation of Hg arc; approximately room temperature	37	63
Methyl butyl ketone	2770–2480 Å.; 127°C.	13	87

III. SECONDARY REACTIONS IN DECOMPOSITION

That a chain reaction follows the photodissociation of acetaldehyde was demonstrated by Leermakers (21), who found that the quantum yield increases from less than unity at room temperature to values of 100 or more at temperatures around 300°C. A similar increase has been observed for formaldehyde (1); it is less marked for the butyraldehydes (26) and absent for valeraldehyde (21, 23).

For acetaldehyde, in the temperature region of long chains, the variation in yield with pressure and intensity is given by the equation, after Leermakers,

$$-\frac{d(CH_3CHO)}{dt} = k_1 I_{abs.} + k_2 I_{abs.}^{1/2}\,(CH_3CHO) \qquad (1)$$

Taking into account the demonstration by Allen and Sickman (2) that methyl radicals initiate a chain decomposition of acetaldehyde, Leermakers proposed a mechanism for the photolysis similar to that of Rice and Herzfeld (46) for the thermal decomposition (table 2).

Reaction a2 was divided into steps

$$HCO \rightarrow H + CO$$

and

$$H + CH_3CHO \rightarrow H_2 + CH_3CO$$

by Leermakers and by Akeroyd and Norrish (1). The lack of a carbon monoxide deficiency in the products favors this division; the low atomic hydrogen concentration during the reaction and the greater energetic stability of formyl radicals as compared with acetyl radicals do not. Reaction a7 was included by Leermakers to explain certain differences between his work and that of Allen and Sickman, but Akeroyd and Norrish prefer to eliminate this step. In any case, a rate law in agreement with equation 1 is obtained. Eliminating reaction a7, temperature coefficients of the photolyses of formaldehyde and acetaldehyde assign activation energies of 16 Cal. to reaction a2 and 10 Cal. to reaction a3 (1).

TABLE 2

Reactions following dissociation into free radicals of acetaldehyde and acetone

<table>
<tr><th></th><th>a. ACETALDEHYDE</th><th>b. ACETONE</th><th></th></tr>
<tr><td>(a1)</td><td>$CH_3CHO + h\nu \rightarrow CH_3 + HCO$</td><td>$(CH_3)_2CO + h\nu \rightarrow CH_3 + CH_3CO$</td><td>(b1)</td></tr>
<tr><td>(a2)</td><td>$HCO + CH_3CHO \rightarrow H_2 + CO + CH_3CO$</td><td></td><td></td></tr>
<tr><td>(a3)</td><td>$CH_3 + CH_3CHO \rightarrow CH_4 + CH_3CO$</td><td>$CH_3 + (CH_3)_2CO \rightarrow CH_4 + CH_3COCH_2$</td><td>(b3)</td></tr>
<tr><td>(a4)</td><td colspan="2">$CH_3CO + M \rightarrow CH_3 + CO + M$</td><td>(b4)</td></tr>
<tr><td>(a5)</td><td colspan="2">$2CH_3CO \rightarrow (CH_3CO)_2$</td><td>(b5)</td></tr>
<tr><td>(a6)</td><td colspan="2">$2CH_3 \rightarrow C_2H_6$</td><td>(b6)</td></tr>
<tr><td>(a7)</td><td>$HCO + CH_3CHO \rightarrow CH_4 + CO + HCO$</td><td></td><td></td></tr>
<tr><td>(a8)</td><td>$CH_3 + HCO \rightarrow CH_4 + CO$</td><td>$CH_3 + CH_3CO \rightarrow C_2H_6 + CO$</td><td>(b8)</td></tr>
</table>

Recent analyses of Blacet and Volman (8) show that at room temperatures the gaseous products of acetaldehyde photolysis consist entirely of hydrogen, methane, and carbon monoxide, with no ethane or ethylene. The H_2/CO ratio decreases toward zero with increasing wave length and increasing temperature above 30°C. and with decreasing temperature below 30°C.; it decreases but slightly with increasing pressure. These results are in accordance with the Leermakers mechanism provided that reaction a5 serves as the chief chain-breaking step at low temperatures, and indicate that, contrary to Leermakers' conclusion, reaction a3 is still effective even at room temperature.

Contrasting sharply with the aldehydes, the quantum yield of acetone decomposition remains at unity or less even up to 400°C. (1, 22). At room temperature the sole products in quantity, as demonstrated by Spence and Wild (50), are diacetyl, ethane, and carbon monoxide. With increasing temperature the yield of diacetyl decreases, disappearing entirely above 60°C., although diacetyl itself is stable at this temperature, while in the gaseous products the C_2H_6/CO ratio approaches unity and considerable quantities of methane appear. For absorption in the continuum ($<$ 2900 Å.) at room temperature, the C_2H_6/CO ratio increases with acetone pressure and with light intensity, approaching a constant value at high intensities. At 60°C., also for absorption in the continuum, the yield of methane increases with increasing acetone pressure and with decreasing intensity. These data may be accounted for on the basis of Rice and Herzfeld's thermal decomposition scheme (46, 47), as later applied by Leermakers (22) and Patat (38) to the high-temperature photolysis of acetone (table 2).

The analytical data of Spence and Wild are explained by an increase in importance of reactions b3 and b4 with increasing temperature. At 20°C. reaction b3 is negligible, while the observed C_2H_6/CO ratio of 1.6 to 2.5 means that from 50 to 75 per cent of the acetyl radicals are reacting by reaction b5 to form diacetyl. At 60°C. absence of diacetyl indicates that the acetyl radicals are reacting entirely by reaction b4, while the amount of methane produced shows that from 15 to 40 per cent (depending on light intensity and pressure) of the methyl radicals are reacting by reaction b3. The thermal stability at room temperature and the instability at slightly higher temperatures, which are thus indicated for acetyl radicals, are verified by the report of Glazebrook and Pearson (15) that these radicals may be detected during the photolysis at room temperature but not at 60°C.

The absence of a chain in acetone photolysis signifies that the CH_2COCH_3 radicals produced by reaction b3 are incapable of further reaction with the acetone. Their ultimate fate is unknown. This mechanism is in harmony with Glazebrook and Pearson's observation that methyl radicals yield no diacetyl with acetone, and with the observation of Akeroyd and Norrish that, in acetone–acetaldehyde mixtures, there is neither inhibition or sensitization of the photodecomposition of one substance by the other, and that it makes little difference which compound absorbs the light.

The importance of reaction b5 at room temperatures in the acetone decomposition justifies its inclusion as the chain-breaking step in the low-temperature aldehyde photolysis. With the increase in rate of reaction 4 at higher temperatures, reaction 5 disappears and reaction 6 presumably becomes the chain-breaking step. Reaction b8 was considered necessary by Spence and Wild to account for the approach to a constant C_2H_6/CO ratio at high intensities. The absence of ethane in the decomposition products of acetaldehyde (8) shows that reaction b8 is negligible in acetaldehyde photolysis.

In the discussion thus far, no means have been provided to account for the low quantum yields, particularly of acetone and of the unsaturated aldehydes. The decomposition yields of crotonaldehyde and of acrolein are below 0.04 at room temperature (5, 6). Although no direct measurements appear to have been made of the quantum yield of acetone photolysis below 56°C., at this temperature, with an incident intensity of $\sim 10^4$ ergs cm.$^{-2}$ sec.$^{-1}$ of 3130 Å., it varies from 0.17 at atmospheric pressure to 0.04 at 50 to 80 mm. of acetone (12). These values were calculated on the basis of pressure change with the assumption of two molecules of gas per molecule decomposed. That the yield is much lower at room temperature is indicated by the observation of Taylor and Jungers (52) that the rate of carbon monoxide evolution from acetone at $\sim$ 80 mm. in the presence of ethylene at 150 mm. and exposed to the full radiation of a hot mercury arc is only one-tenth as great at 25°C. as at 80°C.

Four means of accounting for these low yields have been proposed: (*a*) The primary yield is unity, but the overall yield is reduced by a recombination of radicals (6, 20, 24), e.g.,

$$R_1 + R_2CO \rightarrow R_1R_2CO$$

where R_2 = a hydrogen atom or an alkyl group. (*b*) A reorganization or distribution of the absorbed energy occurs over many internal degrees of freedom, with the result that the life of the activated molecule is greatly increased and the chance for dissociation before ultimate collisional stabilization occurs is correspondingly decreased (29, 33, 48). An observed continuous absorption would in this case be "experimentally continuous", owing to the overlapping of a large number of closely spaced transitions. (*c*) In the majority of cases quantum yields have been based on rate of carbon monoxide evolution. In these cases any condensation reactions (5, 12) would reduce the apparent yield. (*d*) Deactivation by collision or fluorescence may be a contributing factor following absorption at longer wave lengths (e.g., acetone at 3130 Å.) (12).

Since theory b accounts for the low overall yield on the basis of a low primary yield, the question of chain length in the secondary reactions immediately becomes concerned. If the acetaldehyde photolysis at high temperatures proceeds entirely by reactions a1, a2, a3, a4, and a6, the rate of decomposition will be

$$-\frac{d(CH_3CHO)}{dt} = 2\phi I_{abs.} + \frac{k_3\phi^{1/2} I_{abs.}^{1/2}}{k_6^{1/2}} CH_3CHO \qquad (2)$$

where ϕ is the primary quantum yield (reaction a1). The chain length, which will then be given by

$$\frac{k_3(CH_3CHO)}{2k_6^{1/2}\phi^{1/2}I_{abs.}^{1/2}} \qquad (3)$$

is inversely proportional to the square root of the primary yield. It follows that the absence of a chain in the high-temperature acetone photolysis cannot be inferred on the basis of the low quantum yield alone. The yield shows a high temperature coefficient from room temperature at least to 160°C., and the observed values may be due to a very inefficient primary process. The fact, however, that methyl radicals from other sources fail to initiate a chain in acetone is confirming evidence that no chain is concerned in the photolysis.

The observation of Norrish and Kirkbride (35) that formaldehyde vapor at 110°C. is decomposed by absorption of 3650 Å., which lies in the region of definite rotational structure, with a quantum yield almost as great as that for absorption in the continuum (0.7 versus 1.0) led these authors to the postulation that activated molecules may be dissociated by collision. Absence of atomic hydrogen (37) and the low energy of the absorbed quantum would both indicate a dissociation into finished molecules,

$$H_2CO + h\nu\ (> 3000\ \text{Å.}) \rightarrow H_2CO^*$$

$$H_2CO^* + M \rightarrow H_2 + CO + M$$

The increase in quantum yield with pressure for absorption in the banded region (3130 Å.) for both acetone (12, 19) and the butyraldehydes (26) has likewise been interpreted as indicating a dissociation induced by collisions. That such a phenomenon is not general is shown by the decrease in yield with increasing pressure for acetaldehyde at 3130Å. Independence between yield and pressure at shorter wave lengths indicates that these effects are related to the production of activated molecules. The decrease in yield with increasing pressure for acetaldehyde may be interpreted as indicating collisional deactivation or the removal of activated molecules by polymerization. The high decomposition quantum yield for acetaldehyde at 3342 Å., which falls in the weak continuum between two bands, as compared with the low yield at 3130 Å., which falls directly on a band, is additional evidence in support of this view (25). In the case of acetone, data as to the nature of the process at 3130 Å. are conflicting. The C_2H_6/CO ratio of unity indicates a dissociation into finished molecules (50), while the known production of methyl radicals at this wave length indicates a dissociation into radicals. The change in quantum yield with intensity (12, 25) is difficult to reconcile with collisional dissociation. The data are best explained on the basis of a coexistence of two primary processes due to the overlapping of two types of absorption,—discrete absorption, with the production of activated molecules which are either deactivated or dissociated into finished molecules by collision, and continuous absorption, with direct dissociation into radicals.

IV. POLYMERIZATION

Relatively little attention has been given to the photopolymerization of aldehydes and ketones, but the data available indicate that two distinct processes are concerned. With change in wave length from the region of structure and fluorescence to the region of continuous absorption, the quantum yield of apparent polymerization uniformly decreases for acetaldehyde (25), first decreases (3130 to 3020 Å.) then increases (3020 to 2537 Å.) for propionaldehyde (24) and *n*-butyraldehyde (26), and uniformly increases for isobutyraldehyde. At 3130 Å. the yield increases at least with the first power of the pressure, while at 2654 and 2537 Å. it may either increase (propionaldehyde) or be independent (acetaldehyde) of the pressure. The two processes thus suggested are (*a*) polymerization involving activated molecules and (*b*) polymerization induced by the radicals resulting from photodissociation by absorption in the continuum. Process a becomes successively less important and process b more important in the series from acetaldehyde to isobutyraldehyde.

A remarkable increase in the rate of polymerization with decreasing wave length has been observed by Blacet, Fielding, and Roof (5) for acrolein, the quantum yield at $P = 200$ mm. and $T = 30°$C. changing from 0.3 at 3660 Å. (structure) to ~ 20 at 2654–2537 Å. (continuum). Blacet, Fielding, and Roof suggest a mechanism for the polymerization involving reaction of either CH_2CH, HCO, H, or more complex radicals with acrolein molecules, probably at the C═C bond. The process concerned is probably to be compared with the polymerization of ethylene by methyl radicals (52).

REFERENCES

(1) Akeroyd and Norrish: J. Chem. Soc. **1936**, 890.
(2) Allen and Sickman: J. Am. Chem. Soc. **56**, 1251 (1934).
(3) Bamford and Norrish: J. Chem. Soc. **1935**, 1504.
(4) Barak and Style: Nature **135**, 307 (1935).
(5) Blacet, Fielding, and Roof: J. Am. Chem. Soc. **59**, 2375 (1937).
(6) Blacet and Roof: J. Am. Chem. Soc. **58**, 73 (1936).
(7) Blacet and Roof: J. Am. Chem. Soc. **58**, 278 (1936).
(8) Blacet and Volman: J. Am. Chem. Soc. **60**, 1243 (1938).
(9) Blacet, Young, and Roof: J. Am. Chem. Soc. **59**, 608 (1937).
(10) Bowen and de la Praudiere: J. Chem. Soc. **1934**, 1503.
(11) Burton: J. Am. Chem. Soc. **58**, 1645, 1655 (1936); J. Phys. Chem. **41**, 322 (1937).
(12) Damon and Daniels: J. Am. Chem. Soc. **55**, 2363 (1933).
(13) Dieke and Kistiakowsky: Proc. Natl. Acad. Sci. U. S. **18**, 367 (1932); Phys. Rev. **45**, 4 (1934).
(14) Duncan, Ells, and Noyes: J. Am. Chem. Soc. **58**, 1454 (1936).
(15) Glazebrook and Pearson: J. Chem. Soc. **1937**, 567.
(16) Henri and Schou: Z. Physik **49**, 774 (1928).
(17) Herzberg: Trans. Faraday Soc. **27**, 378 (1931).
(18) Herzberg and Franz: Z. Physik **76**, 720 (1932).

(19) Howe and Noyes: J. Am. Chem. Soc. **58**, 1404 (1936).
(20) Kistiakowsky: Cold Spring Harbor Symposia Quant. Biol. **3**, **44** (1935).
(21) Leermakers: J. Am. Chem. Soc. **56**, 1537 (1934).
(22) Leermakers: J. Am. Chem. Soc. **56**, 1899 (1934).
(23) Leermakers: Cold Spring Harbor Symposia Quant. Biol. **3**, 49 (1935).
(24) Leighton and Blacet: J. Am. Chem. Soc. **54**, 3165 (1932).
(25) Leighton and Blacet: J. Am. Chem. Soc. **55**, 1766 (1933).
(26) Leighton, Levanas, Blacet, and Rowe: J. Am. Chem. Soc. **59**, 1843 (1937).
(27) Mulliken: J. Chem. Phys. **3**, 564 (1935).
(28) Norrish: Trans. Faraday Soc. **30**, 107 (1934).
(29) Norrish: Acta Physicochim. U.R.S.S. **3**, 171 (1935).
(30) Norrish: Trans. Faraday Soc. **33**, 1521 (1937).
(31) Norrish and Appleyard: J. Chem. Soc. **1933**, 874.
(32) Norrish and Bamford: Nature **138**, 1016 (1936).
(33) Norrish, Crone and Saltmarsh: J. Chem. Soc. **1934**, 1456.
(34) Norrish and Kirkbride: Trans. Faraday Soc. **27**, 404 (1931).
(35) Norrish and Kirkbride: J. Chem. Soc. **1932**, 1518.
(36) Noyes, Duncan, and Manning: J. Chem. Phys. **2**, 717 (1934).
(37) Patat: Z. physik. Chem. **B25**, 208 (1934).
(38) Patat: Z. physik. Chem. **B31**, 105 (1935).
(39) Patat and Löcker: Z. physik. Chem. **B27**, 431 (1935).
(40) Patat and Sachsse: Naturwissenschaften **23**, 247 (1935).
(41) Pearson: Nature **136**, 221 (1935).
(42) Pearson and Glazebrook: J. Chem. Soc. **1936**, 1777.
(43) Pearson and Purcell: J. Chem. Soc. **1935**, 1151.
(44) Pearson and Purcell: J. Chem. Soc. **1936**, 253.
(45) Price: Phys. Rev. **46**, 529 (1934); **47**, 444 (1935); J. Chem. Phys. **3**, 256 (1935).
(46) Rice and Herzfeld: J. Am. Chem. Soc. **56**, 284 (1934).
(47) Rice, Rodowskas, and Lewis: J. Am. Chem. Soc. **56**, 2457 (1934).
(48) Rollefson: J. Phys. Chem. **41**, 259 (1937).
(49) Scheibe, Povenz, and Linstrom: Z. physik. Chem. **B20**, 292 (1933).
(50) Spence and Wild: Nature **138**, 206 (1936); J. Chem. Soc. **1937**, 352.
(51) Taylor: J. Phys. Chem. **34**, 2049 (1930).
(52) Taylor and Jungers: Trans. Faraday Soc. **33**, 1356 (1937).
(53) Thompson and Linnett: J. Chem. Soc. **1935**, 1452.

Addendum[2]

Since the completion of the preceding discussion the results of some unpublished work carried out by E. Gorin in Moscow, U.S.S.R., have been communicated privately to the Committee. The newer data may modify some of the preceding conclusions on the problem of mechanism in such photolyses.

Gorin has studied the photolysis of acetaldehyde, acetone, formaldehyde, and methyl ethyl ketone in the presence of iodine vapor. It has been shown that a few tenths of a millimeter pressure of iodine molecules is sufficient to react with all the free radicals formed in the primary process.

[2] Contributed by Hugh S. Taylor.

From analyses for the products RI and HI so produced, the number of radicals produced by the action of the light can be deduced.

With acetaldehyde-iodine systems Gorin finds methane and carbon monoxide in addition to methyl iodide. At a given wave length the ratio $CH_4:CH_3I$ is constant, independent of the temperature and of the pressure of iodine and aldehyde. There are, therefore, on this evidence, two primary processes

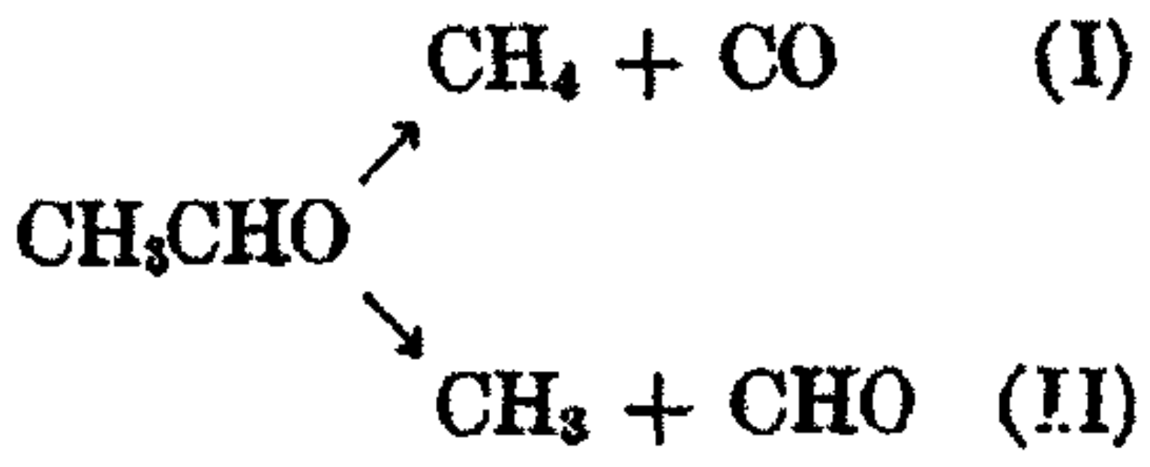

$$CH_3CHO \nearrow CH_4 + CO \quad (I)$$
$$CH_3CHO \searrow CH_3 + CHO \quad (II)$$

Gorin concludes that at 3130 Å. reaction II is 2.6 times as probable as I, but that at 2537 Å. reaction I is 2.9 times more probable. The quantum yield is unity for the formation of $CH_4 + CH_3I$ at both wave lengths. Gorin finds that HCO radicals do not react with iodine molecules below 100°C., but do react to give $H_2CO + CO$. The formaldehyde formed was equal to half the methyl iodide formed, and equal to the excess of carbon monoxide over methane formed by reaction I. Above 100°C. hydrogen iodide begins to be formed, suggesting that formyl radicals decompose at these temperatures. This gives a minimum value of 26 kg-cal. for the activation energy of the reaction $HCO = H + CO$.

The evidence as to the influence of wave length on the alternative modes of decomposition is not in accord with other evidence on the relative amounts obtained from other studies (see page 751).

In the photolysis of acetone in presence of traces of molecular iodine no appreciable carbon monoxide formation was observed by Gorin below 60°C. Methyl iodide is formed, with a quantum yield of unity, at all wave lengths. Acetyl iodide in small amounts and diacetyl were qualitatively detected. This supports the conclusion that the primary process is represented entirely by process B of the preceding paper (page 750). The quantum yield of unity would appear to eliminate theories b and d (page 756) of the discussion by Leighton.

With formaldehyde and iodine, at all wave lengths below 3650 Å., only carbon monoxide and hydrogen iodide are formed in the ratio 2HI:CO. The primary process should therefore be, exclusively,

$$H_2CO + h\nu = H + HCO \qquad (I)$$

At 3650 Å. hydrogen is also found, indicating the additional process

$$H_2CO + h\nu_{(3650)} = H_2 + CO \qquad (II)$$

The relative probabilities are 2.5 for reaction I to 1 for reaction II. The ratio is not changed by replacing iodine with mercuric iodide as acceptor.

With methyl ethyl ketone and iodine, Gorin's results indicate that not more than a few per cent of the total primary process produces saturated hydrocarbon and carbon monoxide; the radical-producing processes are therefore overwhelmingly predominant. With acetaldehyde and iodine no polymerization was found by Gorin, indicating that it is the free radicals which are largely responsible for the polymerization observed during photolysis in the absence of iodine.

HYDROCARBON FREE RADICALS IN PHOTOPROCESSES[1]

HUGH S. TAYLOR

Department of Chemistry, Princeton University, Princeton, New Jersey

Received May 26, 1938

The communication by Leighton (10) on the mechanism of aldehyde and ketone photolysis has discussed in detail one group of photoreactions in which the primary process leads, at least in part, to the production of hydrocarbon free radicals. In the present communication will be reviewed a group of other photoprocesses in which the absorption of light also gives rise to the production of hydrocarbon free radicals, from the secondary reactions of which further data on the properties of such radicals and their reactivities with various atomic and molecular species can be deduced. From such studies are slowly accumulating a series of data, first qualitative and later quantitative, with the aid of which a more certain interpretation of secondary reaction paths can be deduced.

The photoprocesses leading, in the primary process of absorption, to the production of free radicals include the photolysis of alkyl iodides, the photodecomposition of metal alkyls, the mercury-photosensitized hydrogenations of unsaturated hydrocarbons, and the mercury-photosensitized decompositions of saturated hydrocarbons. As yet, the majority of the studies are confined to the simpler homologs of the several series of compounds, and the radicals for which the studies are least equivocal are the methyl and ethyl radicals.

THE PRIMARY PROCESSES

With the lighter alkyl iodides, which show regions of continuous absorption in the ultraviolet with well-developed band spectra of greater intensity than the continua, beginning near 2000 Å. and extending into the Schumann region, it is quite generally postulated (2, 7, 8, 22, 24) that the primary process leads to dissociation into a free radical and an iodine atom. Thus, with methyl iodide we assume the formation of $CH_3 + I$, and with ethyl iodide the formation of $C_2H_5 + I$. There are no data which conflict with this point of view. Differences in reaction product arising from such photolyses are, as we shall see, to be ascribed to secondary processes rather than to any other products of the primary absorption.

---

[1] Contribution No. 6 to the Third Report of the Committee on Photochemistry, National Research Council.

Of the metal alkyls the best investigated are those of lead and mercury. The spectrum of mercury dimethyl shows diffuse bands below 2150 Å., with an overlapping continuum which extends to about 2600 Å. (12). Terenin and Prileshajeva (20) interpreted this absorption as leading to primary dissociation into free radicals and detected such by their action in removing metallic mirrors. Linnett and Thompson (12), after first assuming that the major primary process was decomposition to mercury and ethane, finally decided that the facts could be best interpreted by the two possible free-radical decompositions

$$Hg(CH_3)_2 + h\nu = Hg(CH_3) + CH_3$$

$$Hg(CH_3)_2 + h\nu = Hg + 2CH_3$$

Leighton and Mortensen (11) confirmed the observations of Terenin (19) and of Duncan and Murray (5), that the absorption spectra of lead tetramethyl, tetraethyl, and tetraphenyl were all continuous, the long wave length limits of absorption by the vapors being 2800 Å. for the methyl and 3500 Å. for the ethyl compound. Lead tetraphenyl in solution in trimethylpentane gave an absorption limit around 2800 Å. These continuous spectra point to dissociation in the primary absorption act, with radicals or saturated molecules as possible products in addition to the metal atoms or metal radical complexes.

In the mercury-photosensitized hydrogenation of unsaturated hydrocarbons, when hydrogen is present in any marked amount, the primary process occurs between excited mercury and molecular hydrogen generating atomic hydrogen. The free radical arises as a secondary reaction between the atomic hydrogen and the unsaturated hydrocarbon. The simplest radical so produced is the ethyl radical from ethylene. All the recent evidence indicates that this is a process of good efficiency and that the presence of ethylene serves to reduce the stationary state concentration of atomic hydrogen to small values.

For the saturated hydrocarbons Bates (1) has shown that the quenching efficiency of methane for excited mercury is very small, but that with the higher homologs there is an increased quenching efficiency. The data of Morikawa, Benedict, and Taylor (13) suggest that quenching of methane even at room temperatures gives rise to $CH_3 + H$ either directly or by collision with metastable mercury atoms. Indirect evidence suggests that the dissociation process may require an activation energy of $\sim$4.5 kg-cal. The efficiency increases with temperature.

A recent study of Steacie and Phillips (17) is concerned with the interaction, in a circulatory process, of excited mercury and ethane. They reached the conclusion that the products of the primary interaction between excited mercury and ethane are two methyl groups. The reaction

$$C_2H_6 + Hg' = C_2H_5 + H + Hg$$

was ruled out because of the absence of molecular hydrogen in the reaction products. In the corresponding experiments with butane, Steacie and Phillips found abundant production of hydrogen. More recent experiments by these authors, not yet published, indicate that, in single-pass experiments in place of a circulatory process, the formation of hydrogen from ethane definitely occurs. This means that, with circulation, the hydrogen formed is converted into atomic hydrogen by photosensitization and is consumed in further reaction processes the nature of which will later be discussed.

THE QUANTUM YIELD

The alkyl iodides show remarkably low quantum yields, especially in the vapor state. Methyl iodide has a yield of 0.02 in terms of iodine atoms per absorbed quantum in the gaseous state (2), and 0.05 in hexane solution in the region of continuous absorption (25). With ethyl iodide, the yield is of the order of 0.01 at 2600 Å., increasing to 0.1 at 2026 Å. In the continuous region, liquid ethyl iodide and its solution in hexane show yields of about 0.6, whereas at 2026 Å. the yield has decreased to 0.24 (24).

The low yield in the continuum points to dissociation followed by recombination. This view is supported by recent experiments of West (23), in which photolysis in the presence of silver foil as a trap for iodine atoms increased decomposition fortyfold, with a marked change in the composition of reaction products (see later discussion). The solvent molecules, in the experiments in the continuum, also should repress dissociation, according to the Franck–Rabinowitch principle, so that the large influence of solvent on quantum yield needs special consideration. In the short wave banded region, West and Ginsburg assume the production of optically excited molecules and their interaction with normal iodide molecules.

With lead tetramethyl vapor Leighton and Mortensen (11) found quantum yields at 25°C. somewhat more in excess of unity (1.01–1.13) than could be attributed to experimental error. The authors therefore suspected the existence of short chains. Linnett and Thompson (12), with mercury dimethyl, found a quantum yield of unity at room temperature, but at higher temperatures the yield increased gradually to 2.2 at 190°C. Cunningham (4) found a more than threefold increase in mercury dimethyl vapor decomposed between 50° and 300°C. These results point to the better propagation of chains with increase in temperature.

In the mercury-photosensitized hydrogenation processes the quantitative extinction of mercury fluorescence by hydrogen is well known, and hence the quantum yield of the total process is dependent on the efficiency of the secondary processes. In the hydrogenation of ethylene the evidence points to a 100 per cent utilization of the primary products in these secondary processes. In the mercury-sensitized decomposition of ethane, Steacie and Phillips found a quantum yield of approximately 0.2 in terms of ethane disappearing. This they ascribed, at least in part, to the inefficiency of the primary process of quenching by ethane. With butane a higher quantum yield, 0.55, was obtained.

THE SECONDARY PROCESSES

The primary processes in the photolysis of methyl iodide, lead tetramethyl, mercury dimethyl and, according to Steacie and Phillips, in the photosensitized decomposition of ethane, all lead to the production of methyl radicals. There are, however, conspicuous differences in the products finally obtained.

In the case of methyl iodide, methane comprises 80 per cent of the product at room temperatures with from 4 to 12 per cent each of ethylene and ethane, for reactions in quartz vessels, packed or unpacked. With silver foil present, the methane yield fell to 28 per cent, while the ethylene and ethane yields rose to 18 and 54 per cent, respectively, ethane becoming in this case the major product. As much as 36 per cent of the methyl iodide disappearing is recoverable as CH_2I_2. Ethane predominates almost to the exclusion of other products in the photolyses of lead tetramethyl and mercury dimethyl. Linnett and Thompson found from 7 to 10 per cent of methane and 0 to 5 per cent of ethylene with about 90 per cent of ethane. They do not record any variation in product with temperature change. Cunningham found ethane with negligible amounts of methane and ethylene from room temperatures to 160°C. Beyond this temperature the methane yield increased to about 20 per cent of the hydrocarbon product at 300°C. In the photolysis of acetone similar results obtain. At 70° and 160°C. the hydrocarbon is more than 90 per cent ethane; at 300°C. equal volumes of ethane and methane are formed. In the Steacie–Phillips experiments with excited mercury any methyl radicals are formed in the presence of excess ethane. Hence no conclusion as to the amount of ethane which is regenerated can be given. Of the other hydrocarbons, nearly 60 per cent is methane, 23 per cent propane, and nearly 20 per cent butane. The butane undoubtedly arises from recombination of two ethyl radicals, since this gas is the predominant product in the mercury-photosensitized hydrogenation of ethylene (9).

The low quantum yield and the abnormal products in the methyl iodide decomposition are accounted for by West with the following sequence of reactions:

$$CH_3I + h\nu = CH_3 + I \tag{1}$$

$$CH_3 + I = CH_3I \tag{2}$$

$$CH_3 + CH_3I = CH_4 + CH_2I \tag{3}$$

$$CH_2I + I = CH_2I_2 \qquad (4)$$

$$CH_2I + CH_3 = C_2H_5I \qquad (4a)$$

$$CH_2I + CH_3I = CH_2I_2 + CH_3 \qquad (5)$$

$$CH_2I_2 + h\nu = CH_2 + I_2 \qquad (6)$$

$$CH_2 + CH_2 = C_2H_4 \qquad (7)$$

$$CH_2 + CH_3I = C_2H_5I \qquad (8)$$

$$CH_3 + CH_3 = C_2H_6 \qquad (9)$$

$$I + I + X = I_2 + X \qquad (10)$$

It is evident that the recombination reaction (reaction 2) must be exceedingly efficient to account for the low quantum yield. All other processes are minor in comparison with processes 3, 4, and 5, the most important to account for the products found. West estimates that an activation energy of 10 kg-cal. for reaction 3 in competition with reaction 2 would account for the observed quantum yield. In agreement with this estimate are some measurements of Ginsburg (6), indicating an increase of quantum yield with temperature in the case of ethyl iodide photodecomposition.

Reaction 2 must also be rapid in comparison with reaction 9 which forms ethane. A steric factor of the order of 10^{-4} or 10^{-5} has been ascribed to the association of two methyls by Bawn (3). When, however, the iodine atoms are trapped by silver foil, reaction 9 appears to compete favorably with the methane-producing reaction (reaction 4).

A sequence of reactions to account for the photolyses of mercury and lead methyls is suggested by the following scheme of Thompson and Linnett:

$$Hg(CH_3)_2 + h\nu = Hg(CH_3) + CH_3 \qquad (1)$$

$$Hg(CH_3) + X = Hg + CH_3 + X \qquad (2)$$

$$Hg(CH_3) + Hg(CH_3)_2 = Hg + Hg(CH_3) + C_2H_6 \qquad (3)$$

$$CH_3 + Hg(CH_3)_2 = Hg(CH_3) + C_2H_6 \qquad (4)$$

$$CH_3 + Hg(CH_3)_2 = Hg + CH_3 + C_2H_6 \qquad (5)$$

$$CH_3 + CH_3 = C_2H_6 \qquad (6)$$

$$Hg(CH_3) + Hg(CH_3) = 2Hg + C_2H_6 \qquad (7)$$

In these cases the recombination process

$$HgCH_3 + CH_3 = Hg(CH_3)_2$$

must be of lower probability than in the case of the iodide in view of the quantum yield of ~ 1. That it occurs to some extent is known from work of Paneth and others on the removal of mirrors by methyl radicals. Taking this into account, the quantum yield of unity at room temperatures signifies that some chain propagation is already occurring at these temperatures. Reactions 3, 4, and 5 are chain-propagating stages. They must possess an activation energy, otherwise a quantum yield of $\sim 10^6$ might be expected. Thompson and Linnett calculate that an activation energy of ~ 11 kg-cal. for the chain-propagating reactions is in accord with the quantum yield of unity at ordinary temperatures and of 2.2 at 200°C. The presence of only traces of methane in the room temperature product indicates that, owing to the weakness of the Hg—C bond, this is broken in preference to the C—H bond in the mercury alkyls struck by methyl radicals. Since about 20 per cent of the hydrocarbon is found as methane at 300°C. this suggests that the breaking of the C—H bond must have an activation energy some 2 kg-cal. higher than that required for the breaking of the Hg—C bond.

Molecular hydrogen does not readily react with methyl radicals until temperatures of 160°C. and upwards are reached (13, 18, 21). The activation energy of the process has a value of 9 ± 2 kg-cal. The interaction of atomic hydrogen with methane is to be assigned a somewhat higher value (16, 21) of 13 ± 2 kg-cal. and is insignificant below 250°C. Interaction with ethane is much more easily obtained, some interaction occurring at room temperatures. Trenner, Morikawa, and Taylor (21) ascribed this to a reaction

$$H + C_2H_6 = CH_4 + CH_3 \tag{1}$$

The argument developed by them to exclude a reaction sequence

$$H + C_2H_6 = C_2H_5 + H_2 \tag{2}$$

$$C_2H_5 + H = 2CH_3 \tag{3}$$

is not entirely compelling. It is well known that F. O. Rice's free-radical mechanism (15) is incompatible with the ready occurrence of the first of these interactions.

The absence of methane, in the photosensitized hydrogenation of ethylene, until all the ethylene is hydrogenated, even though ethyl radicals and ethane are present, may be due to the low stationary state concentration of atomic hydrogen in presence of ethylene. Careful test by Jungers and Taylor (9) failed to reveal any significant amounts of methane with reaction in vessels kept carefully free from hydrocarbon deposits of higher molecular weight. Under these conditions also, the predominant product is butane, obviously by combination of ethyl radicals. The low relative production of ethane or propane is additional evidence of low hydrogen atom and methyl radical concentrations in such systems.

In the photosensitized decomposition of ethane, Steacie and Phillips now favor the C—H bond split by a reaction

$$Hg' + C_2H_6 = C_2H_5 + H + Hg \qquad (1)$$

They favor the reaction

$$C_2H_6 + H = CH_3 + CH_4 \qquad (2)$$

to account for their observed methane formation. For the reasons just discussed one is forced also to consider the possibility

$$C_2H_5 + H = 2CH_3 \qquad (3)$$

as the source of methyl radicals, subsequently converted to methane and propane by the recombination processes,

$$CH_3 + H = CH_4 \qquad (4)$$

$$CH_3 + C_2H_5 = C_3H_8 \qquad (5)$$

The recombination of ethyl radicals would produce the observed butane as in the photosensitized hydrogenation of ethylene. Unless one accepts reaction 3 as the mode of production of methyl radicals one is forced to conclude, as Steacie has called to the attention of the writer, that reaction 2 must be at least four times faster than

$$H + C_2H_6 = C_2H_5 + H_2 \qquad (6)$$

Otherwise hydrogen would not be *consumed* in the photosensitized interaction of hydrogen-ethane mixtures. The difficulties of the F. O. Rice chain mechanisms (15) would once more be acute. Rice and Teller, from a theoretical analysis, also strongly favor the mechanism. It is quite evident that there is need for further study in this field.

Contrasting with the relatively large butane formation in the photosensitization experiments are the products from the photolysis of ethyl iodide vapor. Here, as West has shown, the products are predominantly ethane and ethylene, with no butane and with minor amounts of hydrogen and methane. As in the case of the methyl radicals from methyl iodide it is the secondary processes which must account for the non-formation of butane.

The sequence of reactions suggested by West is:

$$C_2H_5I + h\nu = C_2H_5 + I \qquad (1)$$

$$C_2H_5 + I = C_2H_5I \qquad (2)$$

$$C_2H_5 + C_2H_5I = C_2H_6 + C_2H_4I \qquad (3)$$

$$C_2H_4I + I = C_2H_4I_2 \qquad (4)$$

$$C_2H_4I = C_2H_4 + I \qquad (4a)$$

$$C_2H_4I + C_2H_5I = C_2H_4I_2 + C_2H_5 \tag{5}$$

$$C_2H_4I_2 + h\nu = C_2H_4 + I_2 \tag{6}$$

$$I + I = I_2 \tag{7}$$

Of these reactions 3, 4, 4a, and 6 are the essential secondary reactions which account for the decomposition. The reactions must occur more readily than the methyl reactions, since even in presence of silver foil no butane was observed.

The increased yield in the photolyses of the alkyl iodides in the liquid or dissolved state over that in the gaseous state is ascribed by West, at any rate in part, to the action of the solvent molecules in providing third bodies for the yield-increasing radical associations. This influence must be exercised preferentially on the atom reaction I + I which certainly requires a third body, whereas the radical recombinations and $CH_3 + I$ and $C_2H_5 + I$ probably occur, at least in part, as association reactions. The interactions of the radical-iodine atom systems must be more efficient than the radical recombinations as the quantum yield is so low. West has shown that an inert gas such as carbon dioxide at a pressure of 10 to 40 atm. exercises an influence similar to solvent molecules in raising the quantum yield, a pressure of 40 atm. exercising an effect approximately 13.5 per cent of that obtaining in hexane solution.

In addition to the influence of solvent as third body in recombination processes there is a possible influence due to secondary reaction with the radicals. Recent work of Norrish and Bamford (14) has shown that radicals from the photolysis of ketones may remove hydrogen atoms from saturated hydrocarbon solvent molecules, becoming saturated thereby and producing, ultimately, unsaturation in the solvent. This possible effect has not yet been studied in alkyl iodide systems.

REFERENCES

(1) Bates: J. Am. Chem. Soc. **52**, 3825 (1930); **54**, 569 (1932).
(2) Bates and Spence: J. Am. Chem. Soc. **53**, 1689 (1931).
(3) Bawn: Trans. Faraday Soc. **31**, 1536 (1935).
(4) Cunningham: Ph.D. Thesis, Princeton University.
(5) Duncan and Murray: J. Chem. Phys. **2**, 640 (1934).
(6) Ginsburg: Thesis, New York University, 1934.
(7) Goodeve and Porret: Trans. Faraday Soc. **33**, 690 (1937).
(8) Iredale: J. Phys. Chem. **33**, 690 (1929).
(9) Jungers and Taylor: J. Chem. Phys. **6**, 325 (1938).
(10) Leighton: J. Phys. Chem. **42**, 749 (1938).
(11) Leighton and Mortensen: J. Am. Chem. Soc. **58**, 448 (1936).
(12) Linnett and Thompson: J. Chem. Soc. **1934**, 790; Proc. Roy. Soc. (London) **A150**, 603 (1935); **156**, 108 (1936); Trans. Faraday Soc. **33**, 501, 874 (1937).
(13) Morikawa, Benedict, and Taylor: J. Chem. Phys. **5**, 212 (1937).

(14) NORRISH AND BAMFORD: Trans. Faraday Soc. **33**, 1521 (1937).
(15) RICE, F. O., AND RICE, K. K.: The Aliphatic Free Radicals, p. 191. The Johns Hopkins Press, Baltimore (1935).
(16) STEACIE: Can. J. Research **15**, 264 (1937).
(17) STEACIE AND PHILLIPS: J. Chem. Phys. **6**, 179 (1938).
(18) TAYLOR AND ROSENBLUM: J. Chem. Phys. **6**, 119 (1938).
(19) TERENIN: J. Chem. Phys. **2**, 441 (1934).
(20) TERENIN AND PRILESHAJEVA: Trans. Faraday Soc. **31**, 1483 (1935).
(21) TRENNER, MORIKAWA, AND TAYLOR: J. Chem. Phys. **5**, 203 (1937).
(22) WEST: J. Am. Chem. Soc. **57**, 1931 (1935).
(23) WEST: J. Am. Chem. Soc. **60**, 961 (1938).
(24) WEST AND GINSBURG: J. Am. Chem. Soc. **56**, 2626 (1934).
(25) WEST AND PAUL: Trans. Faraday Soc. **28**, 688 (1932).

Addendum

The previous discussion might also have included the recent work from the New York University laboratories on the photolysis of azomethane as the source of free methyl radicals (Burton, Davis, and H. A. Taylor: J. Am. Chem. Soc. **59**, 1038, 1989 (1937); Davis, Jahn, and Burton: J. Am. Chem. Soc. **60**, 10 (1938)). The quantum yield of this photolysis has been carefully studied by Forbes, Heidt, and Sickman (J. Am. Chem. Soc. **57**, 1935 (1935)) with six monochromatic radiations at four pressures from 180 to 665 mm. The quantum yield approached unity as its upper limit for initial decomposition and a temperature increase from 20° to 226°C. had no effect on the quantum yield. The latter fell with increasing pressure. These results led the authors to the conclusion that the photolysis was not a chain reaction.

Burton, Davis, and Taylor have made a careful analytical study of products of the photolysis in the temperature range $-22.5°$ to 223°C. In every case there is an excess of nitrogen formed, about 55 per cent at room temperatures rising to a maximum of 69 per cent at about 220°C. Methane in the hydrocarbon product is about 7 per cent by volume at room temperature and increases to 70 per cent by volume at 220°C. Ethane, which represents more than 90 per cent at room temperature, decreases to 15 per cent at 220°C. In the higher temperature range propane and possibly butane, in small amounts, are increasingly produced. Hydrogen and unsaturated hydrocarbons are not formed in measurable amounts.

There is no doubt that the majority of these results are consistent with a primary act producing free methyl radicals with minor, if any, intramolecular rearrangement to form stable molecules. The change in the character of the hydrocarbon products with temperature is consistent with the data on the reactions already discussed. In the case of the azomethane photolysis, however, there is quite evidently a more marked interaction between the free radicals and the azomethane, presumably to yield hydrazines, than is the case in several of the other substances described. The overall reaction becomes correspondingly more complex, the authors being of the opinion that the ethane formed results, not from the recombination of the methyl radicals, but from decomposition of the more complex radicals and molecules. In view of the preceding discussion this conclusion should be accepted with great reserve.

THE EVALUATION OF SPECIFIC REACTION RATES IN CHAIN REACTIONS[1]

G. K. ROLLEFSON

Department of Chemistry, University of California, Berkeley, California

Received May 25, 1938

One task involving photochemical chain reactions which has been undertaken by many investigators is that of evaluating the specific reaction rates (or rate constants) for the various steps which occur. The problems which arise with each reaction studied are so similar that the discussion will be simplified if we consider the three main types of processes: (*1*) chain starting, (*2*) chain terminating, (*3*) chain continuing.

I. CHAIN-STARTING REACTIONS

A consideration of the mechanisms which have appeared in the literature leads to the conclusion that chains are started by some kind of an odd molecule, either an atom or a free radical, and are propagated by the alternate formation and disappearance of such molecules. Therefore, in this discussion, we are concerned with the rate of formation of odd molecules as a result of light absorption. In the simple cases, such as the absorption of light by diatomic molecules in the gaseous state in a continuous absorption band, it has been quite well established that dissociation occurs for every light quantum absorbed. The same may be said for the truly continuous absorption by more complex molecules, although, in such cases, it may be difficult to decide whether the spectrum is really continuous or only appears to be so because of inadequate resolution. Very often, however, we must consider a competition between the dissociation process and other processes such as fluorescence, deactivation by collision, or some reaction of the photoactivated molecule, either by itself or with other molecules, which does not involve the formation of odd molecules. For example, the photodecomposition of acetaldehyde at high temperatures is a chain reaction probably involving methyl radicals (15). From the work on this reaction at lower temperatures we know that, in the first stage, we have competition between fluorescence, a polymerization reaction, and probably a direct decomposition into methane and carbon monoxide as well as the dissociation to give methyl radicals (16, 27). It is appar-

---

[1] Contribution No. 7 to the Third Report of the Committee on Photochemistry, National Research Council.

ent, therefore, that in this case it would be definitely inaccurate to set the number of chains started equal to the number of quanta of light absorbed. This uncertainty is involved in every reaction in which the radicals are produced by a predissociation process. A similar uncertainty is introduced if we have two overlapping absorption bands corresponding to transitions to two different excited states. Even with such a simple molecule as chlorine, Aickin and Bayliss (1) have shown that the continuous absorption is complex and there is a continuum underlying the sharp line bands. In this case Bayliss (3) has shown that the observed facts concerning the combination of hydrogen and chlorine caused by light absorbed in the banded region of the spectrum can be accounted for by assuming that only the continuous absorption starts the reaction chains.

Another source of uncertainty as to the efficiency of the dissociation process was suggested by Franck and Rabinowitch (11). They expressed the view that the quantum yield of a primary dissociation process in solution must be very low, as the surrounding molecules will prevent the separation of the parts. Rollefson and Libby (28) pointed out that such an effect should be observed if the speed of the separating parts is small, but most experiments have been performed with such energies that the parts would be separating with relatively large kinetic energies and thus be able to break through the surrounding cordon of solvent molecules, making the dissociation practically as efficient as in the gas phase. Dickinson (8) has discussed a number of reactions in solution and shown that they could be most readily explained by assuming that the first step was a dissociation of the light-absorbing molecule. Rabinowitch (22) has objected to such arguments on the grounds that the rate considerations used by Dickinson and others depend on the steady state concentrations of radicals or atoms rather than on their rates of formation, and these steady state values could be unchanged if the rates of dissociation and recombination were affected equally by the solvent. Rollefson and Libby pointed out that such a symmetrical modification was unlikely. Furthermore, it must be said that it is difficult to conceive of chains which are unaffected by dilution having a length such that the quantum yield of the overall reaction would be 2; yet such an assumption is necessary for ClO_2 in carbon tetrachloride solution if we do not assume a high efficiency for the primary step.

II. CHAIN-TERMINATING REACTIONS

The best known of the chain-terminating reactions are those involving the recombination of atoms. Many studies with atomic hydrogen have shown that the recombination occurs at every collision during which a third body is present to remove some of the energy (2, 10, 32). Similarly, a comparison of the thermal and photochemical rates of formation of hydrogen bromide has led to the conclusion that bromine atoms recombine by a triple collision mechanism (5, 14). Ritchie (23) and Hilferding and Steiner (13) have studied the relative efficiencies of different molecules as the third body. Some idea of the range encountered is given by rate constants for the reaction

$$Br + Br + M = Br_2 + M + \text{k.e.}$$

taken from the paper by Hilferding and Steiner (see table 1). The variation is very similar to that found for the quenching of fluorescence by these gases. On the basis of these observations it seems reasonable to assume that any atom recombination process occurs at approximately every triple collision if the reaction is homogeneous.

The heterogeneous recombination of atoms depends quite markedly on the nature of the surface involved. It was found in the very first experiments with hydrogen atoms that dry glass or quartz surfaces are very much more effective in causing the recombination than ones which had not been dried (33). Metallic surfaces were also found to be very effective in causing recombination. Experiments with the hydrogen-bromine reaction at such pressures that the bromine atoms recombine on the wall show that the rate depends on the previous treatment of the walls (13). Another example is found in the hydrogen-chlorine reaction in which Bodenstein and Winter (6) calculated that only one collision in six thousand on a silver chloride surface resulted in removal of the chlorine atom. A comparison of their quantum yields with values obtained in the presence of glass surfaces indicates that glass is about ten times as effective. The failure of the atoms to react at every collision with the surface does not seem to be due to the requirement of any heat of activation, but rather to a low value of the accommodation coefficient. This idea is supported by a comparison of the photochemical temperature coefficients for the hydrogen-chlorine reaction as obtained by Hertel (12) and by Potts and Rollefson (21) with the value obtained by Rodebush and Klingelhoefer (24) for the reaction of chlorine atoms with hydrogen molecules, which shows that the latter reaction is capable of accounting for the entire temperature coefficient of the former. The principal difficulties in the way of securing exact values for the rate constant of such a chain-terminating reaction are the determination of the accommodation coefficient and the rate of approach to the wall. The latter rate is complicated by the fact that, usually, the heat of reaction sets up convection currents which make it

TABLE 1

Rate constants for $Br + Br + M$

M	H_2	He	A	N_2	Br_2	HBr	HCl	CO
$k \times 10^{-16}$	1.25	0.47	0.11	0.82	2.6	2.1	4.7	6.3

virtually impossible to decide on an average path length. On the whole, the error in the estimation of the rate of a chain-terminating process involving atoms is probably not greater than a factor of one hundred, whether it is a homogeneous or a heterogeneous reaction.

If the chain-terminating reaction involves more complex groups, more varieties of reaction are introduced. The surface reactions and the triple collision mechanism for association reactions are possible here as well as with atoms. However, it cannot be said with certainty that the association reactions do not involve heats of activation. Furthermore, it is possible for two radicals to combine to form a single molecule by a process which is the reverse of predissociation without having a third body present. In such a case, the quasi-molecule formed would have a sufficiently long life to lose some of its energy in a collision and become a stable molecule. Finally we have the possibility of two radicals reacting to form normal molecules. Some examples of these types of reaction which have been assumed are

$$COCl + Cl \rightarrow CO + Cl_2 \tag{1}$$

$$CH_3 + CH_3 \rightarrow C_2H_6 \tag{2}$$

$$C_2H_5 + C_2H_5 \rightarrow C_2H_4 + C_2H_6^* \tag{3}$$

* As the concentrations of these radicals are always very low, trimolecular processes involving them must be considered improbable.

The evidence for these reactions is not very conclusive, as the experiments have been such that other possibilities have been present. In support of reaction 2 we may cite the formation of ethane in the photolyses of lead tetramethyl (17), acetone (18), or methyl ethyl ketone (19). Reaction 3 has been assumed frequently, but probably the best evidence for it is the formation of ethane and ethylene in the photolysis of ethyl iodide (9). The magnitudes of the activation energies for these reactions are at present unknown. They are probably not large, but even a small activation energy would introduce a rather large uncertainty into the specific reaction rate. Until further data are available, we must conclude that the constants for reactions between two radicals are not sufficiently well known to be used in calculating rates of photochemical chain reactions.

III. CHAIN-CONTINUING REACTIONS

The direct measurement of the rate constants for reactions of the type involved in the propagation of chains has been limited to a very few cases involving atoms. Most of these reactions involve hydrogen or one of the halogen atoms. The specific rate of the reaction

$$Br + H_2 \rightarrow HBr + H$$

can be obtained from the thermal rate of formation of hydrogen bromide if we assume that bromine atoms and molecules are in equilibrium in the reaction mixture. On the basis of data obtained from the experimental study of both the thermal and photochemical formation of hydrogen bromide, Bodenstein and Lütkemeyer (5) give for the rate constant

$$\log k = -\frac{3859}{T} + 13.862$$

which corresponds to an activation energy of 17,640 cal. The reaction is endothermic to the extent of 14,500 cal., so the activation energy is only slightly greater than the energy required to offset the endothermicity of the reaction. The study of the rate of formation of hydrogen bromide also tells us that the ratio of the rate constants for the reactions

$$H + Br_2 \rightarrow HBr + Br$$

and

$$H + HBr \rightarrow H_2 + Br$$

is 8.6 over a very wide temperature range. This fact suggests that the heats of activation for these reactions are zero, the only difference being in the so-called "steric factor".

The rate of the reaction

$$Cl + H_2 \rightarrow HCl + H$$

was measured directly by Rodebush and Klingelhoefer (24), who used a known concentration of chlorine atoms produced by an electric discharge in chlorine gas. They found that the rate was given essentially by the number of collisions multiplied by $e^{-6000/RT}$ with the uncertainty in the numerator of the exponent being approximately 1000 cal. A similar value was obtained from the measurements by Hertel (12) and by Potts and Rollefson (21) of the temperature coefficient of the photochemical reaction of oxygen-free mixtures of hydrogen and chlorine, if it was assumed that the chain-terminating step involved no heat of activation.

A number of reactions of hydrogen atoms have been studied by preparing a measurable concentration of the atoms by means of an electrical discharge and passing these atoms into some other gas. The most important reaction studied by this method is the transformation of para-hydrogen into ortho-hydrogen. The fraction of the collisions between hydrogen atoms and hydrogen molecules which result in reaction is 2×10^{-6} and the heat of activation is approximately 7000 cal. Other reactions which have been tried include those with oxygen, water, the halogens, the hydrogen halides, some hydrocarbons, hydrogen sulfide, and methyl halides. Under these conditions most of these reactions proceed too fast to obtain accurate measurements, so the only conclusion which can be drawn is that the hydrogen atoms are destroyed in less than one hundredth of a second, which means that at least one collision in 10^4 is effective. The activation energy is therefore either zero or very small.

Other methods which have been used to obtain estimates of the rates of the steps in a chain process are (*1*) studies of the overall rate with appropriate assumptions concerning the chain-starting and chain-terminating reactions, and (*2*) studies of systems in which two reactions compete for the same reactive intermediate. The validity of both of these methods depends on the assumption that the mechanism used in the calculation is correct. It is essential therefore that any other mechanisms be excluded on the basis of the experimental evidence before rate constants obtained by these methods may be considered valid. We may illustrate the first method by referring to the formation of hydrogen chloride from the elements. The mechanism which seems to explain the behavior of oxygen-free mixtures of hydrogen and chlorine is expressed by the following equations:

$$k_3 \quad Cl_2 + h\nu \rightarrow 2Cl \qquad (1)$$

$$k_2 \quad Cl + H_2 \rightarrow HCl + H \qquad (2)$$

$$k_3 \quad H + Cl_2 \rightarrow HCl + Cl \qquad (3)$$

$$k_4 \quad Cl \rightarrow 1/2\ Cl_2 \text{ (on the walls of the reaction vessel)} \qquad (4)$$

This leads to the rate expression

$$\frac{d(HCl)}{dt} = \frac{k_1 k_2}{k_4} I_{abs.}(H_2)$$

If the light absorbed corresponds to the continuum in the chlorine spectrum, there is plenty of evidence to support the assumption that $k_1 = 2$. The constant k_4 is subject to much greater uncertainty. Usually, it is assumed that every collision of an atom with a surface is effective in causing recombination, but recently Bodenstein and Winter (6) have presented data which indicate that only one collision in six thousand of chlorine atoms with a silver chloride surface leads to the formation of molecules. This effect does not seem to be due to a heat of activation but rather is an accommodation coefficient analogous to the steric factor for bimolecular reactions. Collisions with glass or quartz surfaces are much more effective, but it is probable that the erratic rates of formation of hydrogen chloride that have been reported are at least partially due to the variation of this k_4 in different experiments. If we assume that reaction 4 has no heat of activation, then the entire heat of activation for the overall reaction is due to reaction 2. The value of k_2 may be calculated approximately by multiplying the collision number by $e^{-Q/T}$, where Q is the heat of activation. The efficiency factor for collisions between molecules possessing the necessary energy cannot be determined any more exactly than we know k_4. Usually in systems of this type the uncertainty in the heat of activation is sufficient to mask any uncertainty in the collision number or efficiency factor.

This type of calculation may be applied, with the same degree of approximation, to any other chain reaction involving atoms in the initial and final steps and having the rate determined by one step in the chain process. If radicals are involved in the initial or final steps, both of the uncertainties become much greater particularly on account of the activation energy of the chain-terminating step. Thus a reaction such as

$$2CCl_3 + Cl_2 \rightarrow 2CCl_4$$

which Schumacher and Wolf (31) assumed to be the chain-terminating step in the chlorination of chloroform probably requires some heat of activation, but the magnitude of this heat is not even approximately known. The same statement can be made about the other processes which we have discussed in the section on chain-terminating processes.

A further complication arises frequently owing to the complexity of the assumed mechanism. Thus, instead of having the overall rate constant expressed in terms of the constants for initial and final steps and one step of the chain (k_2 in the case of the formation of hydrogen chloride) we find that the constants of two or more steps of the chain appear in the rate equation. Such constants are indeterminate from rate measurements alone, and up to the present time no one has determined the constants for any system of this type from experimental data.[2]

The second method for evaluating the constants of steps in a chain, the use of competitive reactions, has not been used very extensively as yet. We have already cited the competition between hydrogen bromide and bromine for hydrogen atoms in the formation of hydrogen bromide. Other examples which have been studied quantitatively include the competition of carbon monoxide and hydrogen for chlorine atoms (4, 26), of oxygen and chlorine for COCl (25, 29), and of ozone and oxygen for oxygen atoms (30). The experiments determine only the ratio of the two rate constants but if one rate constant, as, for example, that for the reaction between atomic chlorine and hydrogen, is known from other studies, then the other can be calculated. We have already seen that the rate constant for the reaction

$$Cl + H_2 \rightarrow HCl + H$$

---

[2] Bodenstein and his students claim to have made such determinations for the formation of phosgene, but the details of their calculations have not been published. It may be remarked here that in their published work they have neither proven their mechanism to the exclusion of others nor listed enough independent equations based on experimental data to determine all of the constants involved in their rate equations. See, however, contribution No. 9 to this Report.

is pretty well known, therefore we may use this reaction as a means of measuring chlorine-atom concentrations in reaction mixtures and thus the specific rates of other reactions. Naturally this method is limited to those systems in which the chlorine atoms react at a rate comparable with that with hydrogen. Thus, the observation that in mixtures of ethylene, hydrogen, and chlorine the halogen adds to the ethylene with no appreciable formation of hydrogen chloride tells us that the first step in the addition reaction is very fast but does not permit an exact calculation of its specific rate.

Many reactions of hydrogen atoms have been studied by determining the concentration of the atoms by the rate of the conversion of para-hydrogen to ortho-hydrogen. This is essentially the method of competing rates, except that the atoms are not destroyed by the test reaction. The rate constant for this conversion has been given as $2 \times 10^9 T e^{-7000/RT}$, which indicates the order of magnitude of the rates which may be studied by this method. One point which has been overlooked in some investigations is that if the hydrogen atoms react very rapidly with other substances in the reaction mixture the concentration of the atoms may not be great enough to cause appreciable conversion of para-hydrogen to ortho-hydrogen. This method has been applied by Cremer, Curry, and Polanyi (7) to the study of reactions of atomic hydrogen with alkyl halides. Their results were only semiquantitative and their experimental method limited them to reactions for which the activation energy was in the range $2800 < Q < 7200$ cal. Farkas and Sachsse (10) studied $H + O_2 \rightarrow HO_2$ and $H + CO \rightarrow HCO$. They concluded that the former occurred once in seven hundred fifty triple collisions and the latter once in ten triple collisions. Patat (20) has also used this method to determine the concentrations of hydrogen atoms present during the decompositions of a number of organic compounds. On account of the complexity of such systems only qualitative results concerning rate constants were obtained.

In conclusion, it must be stressed that the great need at present is the determination, by methods free from assumptions, of a few rate constants for reactions of the type we have discussed. No matter how reasonable assumptions may seem, any rate constants based on them are little better than guesses. This is especially true in complex systems as, under such conditions, usually several mechanisms are capable of describing the facts, and hence there is no certainty that we are dealing with the right set of reactions. The constants which have been calculated for such systems in the literature must be looked upon as reasonable interpretations rather than as established facts.

REFERENCES

(1) Aickin and Bayliss: Trans. Faraday Soc. **33**, 1333 (1937).
(2) Amdur and Robinson: J. Am. Chem. Soc. **55**, 1395, 2616 (1933).
(3) Bayliss: Trans. Faraday Soc. **33**, 1339 (1937).
(4) Bodenstein, Brenschede, and Schumacher: Z. physik. Chem. **B28**, 81 (1935).
(5) Bodenstein and Lutkemeyer: Z. physik. Chem. **114**, 208 (1925).
(6) Bodenstein and Winter: Sitzber. preuss. Akad. Wiss., Physik.-math. Klasse **I** (1936).
(7) Cremer, Curry, and Polanyi: Z. physik. Chem. **B23**, 445 (1933).
(8) Dickinson: Chem. Rev. **17**, 413 (1935).
(9) Emschwiller: Ann. chim. **17**, 413 (1932).
(10) Farkas and Sachsse: Z. physik. Chem. **B27**, 111 (1934).
(11) Franck and Rabinowitch: Trans. Faraday Soc. **30**, 125 (1934).
(12) Hertel: Z. physik. Chem. **B15**, 325 (1931).
(13) Hilferding and Steiner: Z. physik. Chem. **B30**, 399 (1935).
(14) Jost and Jung: Z. physik. Chem. **B3**, 83 (1929).
(15) Leermakers: J. Am. Chem. Soc. **56**, 1537 (1934).
(16) Leighton and Blacet: J. Am. Chem. Soc. **54**, 3165 (1932); **55**, 1766 (1933).
(17) Leighton and Mortenson: J. Am. Chem. Soc. **58**, 448 (1936).
(18) Norrish and Appleyard: J. Chem. Soc. **1934**, 874.
(19) Norrish and Kirkbride: Trans. Faraday Soc. **30**, 103 (1934).
(20) Patat: Z. physik. Chem. **B32**, 274, 294 (1936).
(21) Potts and Rollefson: J. Am. Chem. Soc. **57**, 1027 (1935).
(22) Rabinowitch and Wood: Trans. Faraday Soc. **32**, 547 (1936).
(23) Ritchie: Proc. Roy. Soc. (London) **A146**, 828 (1934).
(24) Rodebush and Klingelhoefer: J. Am. Chem. Soc. **55**, 130 (1933).
(25) Rollefson: J. Am. Chem. Soc. **55**, 148 (1933).
(26) Rollefson: J. Am. Chem. Soc. **56**, 579 (1934).
(27) Rollefson: J. Phys. Chem. **41**, 259 (1937).
(28) Rollefson and Libby: J. Chem. Phys. **5**, 569 (1937).
(29) Rollefson and Montgomery: J. Am. Chem. Soc. **55**, 142 (1933).
(30) Schumacher: Z. physik. Chem. **B17**, 405 (1932).
(31) Schumacher and Wolff: Z. physik. Chem. **B25**, 161 (1934).
(32) Smallwood: J. Am. Chem. Soc. **51**, 1985 (1929).
(33) Wood: Phil. Mag. **42**, 729 (1921); **44**, 538 (1922).

THE SECONDARY PROCESSES IN THE PHOTODECOMPOSITION OF AMMONIA AND HYDRAZINE[1]

HUGH S. TAYLOR

Department of Chemistry, Princeton University, Princeton, New Jersey

Received May 25, 1938

Since the diffuse bands of the ammonia spectrum were interpreted by Bonhoeffer and Farkas (1) as due to a dissociation of the molecule, the direction of further research on the photodissociation process has been towards an elucidation of the secondary processes in such a manner that the low quantum yield (~ 0.2) might be satisfactorily explained. For the primary process, it has been generally assumed that

$$NH_3 + h\nu = NH_2 + H \qquad (1)$$

though the reaction,

$$NH_3 + h\nu = NH + H_2 \qquad (1a)$$

cannot be excluded on energetic grounds. It would, however, suggest an influence of molecular hydrogen which is not found experimentally in the photoreaction, although there is an effect in the reaction initiated by α-particles and ions, in which case, at higher pressures, NH^+ is certainly formed by secondary processes. The first reaction accounts for the presence of atomic hydrogen, made certain by the measurements of Geib and Harteck (6) and of Farkas and Harteck (4) on para-hydrogen conversion in ammonia undergoing decomposition.

Gedye and Rideal (5), using a streaming system, obtained yields of hydrazine from the photodecomposition of ammonia of as high as 57 per cent of the stoichiometric yield by the equation

$$2NH_3 \rightarrow N_2H_4 + H_2$$

The hydrazine yield decreased rapidly as the temperature of the system was increased. Koenig and Brings (7), and more recently Welge and Beckman (16), have obtained positive confirmation of the formation of hydrazine by photolysis of ammonia in a static system. The amounts obtained, however, were very small.

Indirect evidence of the production of amine radicals may be obtained from the photodecomposition of solutions of alkali metals in liquid am-

---

[1] Contribution No. 8 to the Third Report of the Committee on Photochemistry, National Research Council.

monia (13). Liquid ammonia does not photodecompose when pure, but does decompose on the addition of alkali metals. The sole products are hydrogen and amide ion, NH_2^-, in equivalent amounts, and the quantum yield is well under unity. Alkali metals virtually completely dissociate in liquid ammonia into positive metal ions and free electrons which become strongly solvated with the ammonia. It would appear, therefore, that in pure liquid ammonia deactivation or primary recombination effectively retards the decomposition, while in the presence of solvated electrons the NH_2 radicals are stabilized by the formation of amide ion, thus permitting the decomposition to proceed. The mechanism, according to this hypothesis, would be

$$NH_3 + h\nu \rightarrow NH_2 + H$$

$$NH_2 + H + M \rightarrow NH_3 + M \quad \text{(primary recombination)}$$

$$NH_2 + (-) \rightarrow NH_2^-$$

$$H + H + M \rightarrow H_2 + M$$

The majority of workers have accounted for the low quantum yield in ammonia decomposition by a recombination process,

$$NH_2 + H = NH_3 \tag{3}$$

though Farkas and Harteck (4) pointed out certain difficulties in accepting this, due to the low stationary state concentration of atomic hydrogen, especially if reaction 3 requires a third body. That ammonia is regenerated during the secondary processes was made definite by Taylor and Jungers (15), who showed the formation of deuteroammonias in mixtures of decomposing NH_3 and deuterium atoms produced from deuterium molecules by excited mercury. No exchange occurred unless the ammonia was undergoing photodecomposition. By investigating the photochemical decomposition in the region of very small decompositions Welge and Beckmann (16) found that the quantum yield measured by hydrogen produced approached unity; hence they concluded that the recombination reaction (reaction 3) does not play an important rôle. The products in such circumstances would be substantially hydrogen and hydrazine. They further assumed the secondary processes to be substantially heterogeneous, with a little of the hydrazine reacting with the atomic hydrogen to give ammonia, as shown by Dixon (2). With larger amounts of products this effect would be exaggerated and the non-condensable products would approach the stoichiometric ratio due to hydrazine decomposition.

In experiments of Elgin and Taylor (3) it was shown that the total process in both the photochemical and photosensitized decomposition of hydrazine can be with fair accuracy expressed by the stoichiometric equation

$$2N_2H_4 = 2NH_3 + N_2 + H_2 \tag{4}$$

With hydrazine in the presence of ammonia, even when only a small fraction of the light was absorbed by the hydrazine, it was shown, by Ogg, Leighton, and Bergstrom (14), that hydrazine was the compound which disappeared, with a quantum yield of 1.28 on total quanta absorbed. Such facts provide considerable support for their conclusion, recently restated by Mund and van Tiggelen (12), that the process which regenerates ammonia and causes the low quantum yield is not reaction 3 but the reaction

$$N_2H_4 + H = NH_3 + NH_2 \qquad (5)$$

a reaction which would also explain the work of Taylor and Jungers with deuterium atoms.

The nitrogen which is formed ultimately in the photodecomposition of ammonia must arise, therefore, from further decomposition of the hydrazine or NH_2 radicals or both. The assumption of Ogg, Leighton, and Bergstrom that this occurs by the reaction

$$N_2H_4 + 2NH_2 = 2NH_3 + N_2 + H_2 \qquad (6)$$

has been modified by Mund and van Tiggelen in a sequence of secondary processes which more satisfactorily than any alternatives, it would appear, accounts for the kinetics of the reaction and its quantum yield. The sequence is:

$$\begin{array}{rcll}
20(NH_3 + h\nu & = & NH_2 + H) & (1)\\
17(2NH_2 + M & = & N_2H_4) & (2)\\
16(N_2H_4 + H & = & NH_3 + NH_2) & (5)\\
1(N_2H_4 + 2NH_2 & = & 2N_2 + 4H_2) & (6a)\\
2(H + H + M & = & H_2) & (7)\\
\hline
20h\nu + 4NH_3 & = & 2N_2 + 6H_2 &
\end{array}$$

This sequence is based on a quantum yield of 0.2 at 1 atm. pressure, and the numerical coefficients by which the equations are multiplied must evidently be proportional to the velocities of the corresponding reactions. It leads to the following expression of Mund and van Tiggelen for the quantum yield

$$\Phi = \frac{1}{0.875 + \sqrt{0.0156 + K\sqrt{P/v}}}$$

where v ($\alpha I_{\text{abs.}}$) is the velocity of reaction expressed as the number of molecules of ammonia decomposed to nitrogen and hydrogen per cubic centimeter per second, P is the total pressure, and Φ the quantum yield equal to Q/v, where Q is the number of ammonia molecules per cubic centimeter per second primarily decomposed.

This equation reproduces the tendency of Φ to vary with the pressure. With $\Phi = 0.2$ at 1 atm. one calculates a value of $\Phi = 0.314$ at 0.1 atm. and 0.126 at 8.5 atm. The former is in agreement with the data of Wiig (18) and the latter with the measurements of Ogg, Leighton, and Bergstrom. At low pressures the influence of the walls begins to predominate and will assist especially reactions 2 and 7. Its effect on the quantum yield will be equivalent to that of high pressures in the gas phase, i.e., will lower the quantum yield as Wiig observed. The influence of the intensity or the velocity of decomposition, *v*, on the quantum yield is of the same order of magnitude as the equation suggests, as elucidated in a recent research by Mund, Brenard, and Kaertkemeyer (11), and as suggested by the work of Ogg, Leighton, and Bergstrom, by Wiig and Kistiakowsky (20), and by more recent measurements of Wiig (19). The Mund–van Tiggelen numerical values for the relative rates of the several reactions do not constitute a unique solution, as is evident from an analysis by Leighton (8). For the ratios 20:17:16:1:2 of the above sequence, Leighton substitutes the sequence

$$10(NH_3 + h\nu = NH_2 + H)$$

$$7(2NH_2 + M = N_2H_4 + M)$$

$$6(H + N_2H_4 = NH_3 + NH_2)$$

$$2(2NH_2 + N_2H_4 = 2NH_3 + N_2 + H_2)$$

$$2(H + H + M = H_2 + M)$$

It will be noted that in this sequence the nitrogen-producing mechanism simultaneously regenerates ammonia, whereas the Mund–van Tiggelen reaction does not. Both yield similar expressions for the relation between quantum yield, pressure, and intensity. Leighton believes his reaction producing nitrogen to be superior, because it accounts for the 1:1 N_2:H_2 ratio observed in the ammonia-sensitized decomposition of hydrazine (see later).

It has been known since Warburg's original researches on this reaction that neither molecular nitrogen nor hydrogen influenced the quantum yield. The above mechanism is in accord with such inertness except in so far as it might influence the total pressure, *P*; this influence is small, as seen. On the other hand, atomic hydrogen was shown by Melville (9) to inhibit strongly the photodecomposition of ammonia and the same is true of the photosensitized decomposition (10). This effect, which Melville attributed to the recombination reaction (reaction 3), is rather to be ascribed to the ammonia regenerative reaction with hydrazine (reaction 5), the velocity of which, as is to be seen from the magnitude of the molecular coefficient, 16, is very high. Analysis shows that in addition to the effect of atomic hydrogen concentration there is also an effect due to the diminution in v, the total decomposition. The cumulative effect of these two factors is evident in the data both of Mitchell and Dickinson and of Melville.

Farkas and Harteck found a sharp maximum in the atomic hydrogen concentration from the photodecomposition of ammonia in the presence of hydrogen when the ammonia was only 10 mm. in a total pressure of 30 to 70 cm. This led these authors to the assumption of NH_4 radicals in equilibrium with $NH_3 + H$. The maximum should bear some relation to the maximum observed in the quantum yield but this latter, though similar in form, is displaced to higher ammonia pressures. This discrepancy is not yet elucidated.

The objection that might be raised to the Mund-van Tiggelen development, namely, that nitrogen only results from the termolecular process (from $2NH_2 + N_2H_4$, reaction 6) and not from such a process as suggested, among others, by Wiig,

$$NH_2 + NH_2 = N_2 + 2H_2 \tag{8}$$

is discussed in the original communication of Mund and van Tiggelen and more recently by them in a comment on the newer work of Wiig. They point out that reaction 8 always leads to kinetic expressions from which the observed increase of quantum yield with velocity of decomposition cannot be deduced, and, further, it fails to account for the small variation of yield between 1 and 8.5 atm. found by Ogg, Leighton, and Bergstrom. One might expect that other molecules than N_2H_4 could act each with a particular efficiency in the recombination–decomposition process (reaction 6) of the Mund-van Tiggelen scheme. To introduce such possibilities into the kinetic scheme would further complicate the equation derived, and the experimental data at present are not accurate enough to justify, such further refinements.

In the ammonia-sensitized hydrazine decomposition experiments of Ogg, Leighton, and Bergstrom, the two initial stages are quite clear, namely, reactions 1 and 5 of the ammonia scheme above.

$$NH_3 + h\nu = NH_2 + H \tag{1}$$

$$H + N_2H_4 = NH_3 + NH_2 \tag{5}$$

The Mund-van Tiggelen mechanism would then give

$$N_2H_4 + 2NH_2 = 2N_2 + 4H_2 \tag{6a}$$

which would mean a quantum yield of 2 at a maximum diminished by the recombination process,

$$2NH_2 + M = 2N_2H_4 \tag{2}$$

The product gas should be 33 per cent nitrogen and 66 per cent hydrogen. The Ogg, Leighton, and Bergstrom mechanism would give

$$N_2H_4 + 2NH_2 = 2NH_3 + N_2 + H_2 \qquad (6)$$

again a maximum quantum yield of 2 on the hydrazine disappearing but a 1:1 ratio of nitrogen and hydrogen. This ratio was actually found by these authors and also by Elgin and Taylor. Wenner and Beckmann (17) found quantum yields ranging from 1 at low pressures to 1.7 at higher pressures and hydrogen concentrations ranging from 58 to 64 per cent in the same pressure range of 2 to 14 mm., decreasing toward 50 per cent with increasing pressure.

The primary mechanism in hydrazine decomposition is still uncertain. If it be

$$N_2H_4 + h\nu = 2NH_2$$

then it would be necessary to fall back on reaction 6 to explain the ammonia formation observed. On the other hand, a primary mechanism

$$N_2H_4 + h\nu = N_2H_3 + H$$

could by reaction 5 regenerate one-half the observed ammonia with the atomic hydrogen. The NH_2 and the N_2H_3 thus produced could, by several alternative mechanisms already proposed, but for which there is as yet no experimental test, yield $NH_3 + N_2 + H_2$ in approximate accord with the observations. The para-hydrogen conversion reaction might be employed to test these two alternative mechanisms for the primary photoprocess.

REFERENCES

(1) Bonhoeffer and Farkas: Z. physik. Chem. **136**, 337 (1928).
(2) Dixon: J. Am. Chem. Soc. **54**, 4262 (1932).
(3) Elgin and Taylor: J. Am. Chem. Soc. **51**, 2059 (1929).
(4) Farkas and Harteck: Z. physik. Chem. **B25**, 257 (1934).
(5) Gedye and Rideal: J. Chem. Soc. **1932**, 1160.
(6) Geib and Harteck: Z. physik. Chem., Bodenstein Festband, p. 849 (1931).
(7) Koenig and Brings: Z. physik. Chem., Bodenstein Festband, p. 595 (1931).
(8) Leighton: Actualités Scientifiques. Hermann et Cie, Paris (1938). In press.
(9) Melville: Trans. Faraday Soc. **28**, 885 (1932); Proc. Roy. Soc. (London) **A152**, 323 (1935).
(10) Mitchell and Dickinson: J. Am. Chem. Soc. **49**, 1478 (1927).
(11) Mund, Brenard, and Kaertkemeyer: Bull. soc. chim. Belg. **46**, 211 (1937).
(12) Mund and van Tiggelen: Bull. soc. chim. Belg. **46**, 104 (1937).
(13) Ogg, Leighton, and Bergstrom: J. Am. Chem. Soc. **55**, 1754 (1933).
(14) Ogg, Leighton, and Bergstrom: J. Am. Chem. Soc. **56**, 318 (1934).
(15) Taylor and Jungers: J. Chem. Phys. **2**, 373, 452 (1934).
(16) Welge and Beckmann: J. Am. Chem. Soc. **58**, 2462 (1936).
(17) Wenner and Beckmann: J. Am. Chem. Soc. **54**, 2787 (1932).
(18) Wiig: J. Am. Chem. Soc. **57**, 1559 (1935).
(19) Wiig: J. Am. Chem. Soc. **59**, 827 (1937).
(20) Wiig and Kistiakowsky: J. Am. Chem. Soc. **54**, 1806 (1932).

SECONDARY PROCESSES IN THE PHOTOCHLORINATION OF CARBON MONOXIDE AND HYDROGEN[1]

HUGH S. TAYLOR

Department of Chemistry, Princeton University, Princeton, New Jersey

Received May 25, 1938

Since the publication of the Second Report of the Committee on Photochemistry considerable progress has been made towards a final and quantitative formulation of the secondary processes both in the hydrogen-chlorine combination and in the reactions, thermal and photochemical, of phosgene synthesis and decomposition. These several reactions have been the principal objective of the researches of Bodenstein and his school. At the present time Bodenstein (6) is occupied with the publication of the definitive conclusions of this long series of investigations and is attempting to incorporate within the framework of those conclusions, or reject for reasons ascertained, the auxiliary data that have accumulated from the investigations of other workers, notably Rollefson (15, 19, 20, 21), Ritchie (17, 18), Norrish (16), Allmand (1), and others. A discussion of the earlier work (3, 7, 8, 9, 10, 15, 22, 23, 24, 26) was included in the Second Report.

I. THE PHOSGENE REACTIONS

For the photoreaction at room temperatures and pressures over 100 mm. the kinetic expression is

$$\frac{d[COCl_2]}{dt} = \kappa_1 I_{\text{abs.}}^{1/2} [Cl_2][CO]^{1/2}$$

This equation is derivable from the Bodenstein reaction scheme:

$$Cl_2 + E = 2Cl \tag{1}$$

$$Cl + CO + M = COCl + M \tag{2}$$

$$COCl + M = CO + Cl + M \tag{3}$$

$$COCl + Cl_2 = COCl_2 + Cl \tag{4}$$

$$COCl + Cl = CO + Cl_2 \tag{5}$$

$$Cl + \text{wall} = 1/2\ Cl_2 \tag{5'}$$

---

[1] Contribution No. 9 to the Third Report of the Committee on Photochemistry, National Research Council.

Equations 2 and 3 lead, on the Bodenstein interpretation, to an equilibrium expressed by the equation:

$$K_{\mathrm{COCl}} = [\mathrm{Cl}][\mathrm{CO}]/[\mathrm{COCl}]$$

The first five reactions, with the assumed equilibrium, yield the kinetic expression for κ_1, which is obeyed by experimental results, under the given conditions, except in the beginning of the reaction and towards the end when reaction 5′ becomes important with low concentration of COCl. The same chain-ending process (5′) becomes important also at higher temperatures and lower concentrations (< 90 mm.). At high temperatures the kinetic expression then becomes

$$\mathrm{d}[\mathrm{COCl_2}]/\mathrm{d}t = \kappa_2 I_{\mathrm{abs.}} [\mathrm{Cl_2}][\mathrm{CO}]$$

The reaction constants κ_1 and κ_2 are related by the following equations to the several constants of the individual reaction steps:

$$\kappa_1 = \frac{k_4}{k_5^{1/2} K_{\mathrm{COCl}}}; \qquad \kappa_2 = \frac{k_4}{k_{5'} K_{\mathrm{COCl}}}$$

By reason of the additional investigations of Bodenstein, Brenschede, and Schumacher (4, 5), Bodenstein (6) has rejected the interpretation by Rollefson (19, 20), which makes use of $\mathrm{Cl_3}$ as an intermediate, and maintains his contention that the COCl equilibrium exists in spite of reaction 4 in which this intermediate is steadily consumed.

The thermal formation and decomposition between 350° and 450°C. yield the kinetic expression

$$\mathrm{d}[\mathrm{COCl_2}]/\mathrm{d}t = \kappa_{\mathrm{th}} [\mathrm{Cl_2}]^{3/2}[\mathrm{CO}] - \kappa'_{\mathrm{th}}[\mathrm{Cl_2}]^{1/2}[\mathrm{COCl_2}]$$

The reaction scheme pertaining to this is

$$\mathrm{Cl_2} \rightleftarrows 2\mathrm{Cl} \text{ (equilibrium; } K_{\mathrm{Cl_2}} = [\mathrm{Cl}]^2/[\mathrm{Cl_2}]) \qquad (1)$$

$$\mathrm{Cl} + \mathrm{CO} \rightleftarrows \mathrm{COCl} \text{ (equilibrium; } K_{\mathrm{COCl_2}} = [\mathrm{Cl}][\mathrm{CO}]/[\mathrm{COCl}]) \qquad (2, 3)$$

$$\mathrm{COCl} + \mathrm{Cl_2} = \mathrm{COCl_2} + \mathrm{Cl} \text{ (formation)} \qquad (4)$$

$$\mathrm{COCl_2} + \mathrm{Cl} = \mathrm{COCl} + \mathrm{Cl_2} \text{ (decomposition)} \qquad (4')$$

The reaction constants κ_{th} and κ'_{th} are then given by the equations

$$\kappa_{\mathrm{th}} = \frac{k_4 K_{\mathrm{Cl_2}}^{1/2}}{K_{\mathrm{COCl}}} \quad \text{and} \quad \kappa'_{\mathrm{th}} = k_{4'} \cdot K_{\mathrm{Cl_2}}^{1/2}$$

The numerical data for the equilibrium and reaction constants

Bodenstein, Brenschede, and Schumacher (6) have recently completed a calculation of the numerical data for the several individual reactions and for the equilibria involved. Their results are summarized in the following.

For the equilibrium between chlorine molecules and atoms the accurate data of Giauque and Overstreet (13) are available

$$\log K_{Cl_2} = \frac{57156}{4.571T} + 3.820$$

For the equilibrium

$$COCl \rightleftarrows CO + Cl$$

both the heat of reaction and the constant must be so chosen that

$$\log K_{COCl} = \log k_3 - \log k_2$$

Further, $\log k_3$ must be sufficiently greater than $\log k_4$ so that the assumption of practical equilibrium in spite of reaction 4 can be maintained. By trial, the equation obtained was

$$\log K_{COCl} = -\frac{5676}{4.571T} + 1.770$$

For reactions 4 and 5 the data are given in the form of equations

$$\log k = -\frac{E}{4.571T} + \log Z_1 + 1/2 \log T - \log f$$

where E is the activation energy, Z_1 the collision yield for $T = 1°K.$, and f is the steric factor. In these equations E and f are both adjustable.

$$\log k_4 = -\frac{2612}{4.571T} + 1/2 \log T + 10.101 - 3.871$$

$$\log k_5 = -\frac{1940}{4.571T} + 1/2 \log T + 10.106 - 0.976$$

The equilibrium constant K_{COCl} yields the value 5676 cal. for the heat of formation of COCl. The heat of formation of phosgene from $CO + Cl_2$ is 26,100 cal. With these two data and the value of 2612 cal. from $\log k_4$ the expression for $k_{4'}$ becomes

$$\log k_{4'} = -\frac{23036}{4.571T} + 1/2 \log T + 10.110 - 0.171$$

With these several equations the calculated values for the overall reactions, photochemical and thermal, from room temperatures to 450°C. agree excellently with the measured values. Bodenstein sees in this concordance the best and most convincing support for the reaction schemes assumed and for the equilibrium,

$$CO + Cl = COCl$$

which Rollefson (19) especially has questioned. The heat of formation of COCl, 5676 cal., is materially lower than the value of 10 kg-cal. originally estimated, the higher figure justifying the objection of Rollefson. With the newer numerical data, Bodenstein is of the opinion that the several reactions are described very satisfactorily and, he believes, in final and definitive form.

II. THE HYDROGEN-CHLORINE PHOTOREACTION

The reaction sequence in the hydrogen-chlorine combination is, it is quite generally agreed, the Nernst chain mechanism, with the chains normally terminated by interaction of atomic hydrogen with oxygen impurities. The reaction scheme thus becomes

$$Cl_2 + E = 2Cl \tag{1}$$

$$Cl + H_2 = HCl + H - 800\text{ cal.} \tag{2}$$

$$H + HCl = H_2 + Cl + 800\text{ cal.} \tag{2'}$$

$$H + Cl_2 = HCl + Cl \tag{3}$$

$$H + O_2 + M = HO_2 + M \tag{4}$$

The numerical data for the several reactions are still subject to final revision but, according to Bodenstein, the most reliable data now available are obtained from the following equations for velocities, the units being in moles per liter per second.

$$\log k_2 = \frac{5750}{4.571T} + 1/2 \log T + 10.47 - 0.92 = 6.40 \text{ at } 288°\text{K.}$$

$$\log k_{2'} = \frac{4950}{4.571T} + 1/2 \log T + 10.48 - 1.39 = 6.55 \text{ at } 288°\text{K.}$$

$$\log k_3 = -\frac{2550}{4.571T} + 1/2 \log T + 10.50 - 0.78 = 9.01 \text{ at } 288°\text{K.}$$

$$\log k_4 = -\frac{500}{4.571T} + 1/2 \log T + 10.42 - 1.60 - \log f$$

In the last expression the datum -1.60 represents the logarithm of the number of three-body collisions (moles per liter). The value of $\log f$ varies with M according to the best evidence. Bodenstein assigns the following values: $\log f = -1.37$ for $M = Cl_2, H_2, O_2$; $\log f = -0.77$ for $M = HCl$; and $\log f \sim -1.07$ for $M = H_2 + Cl_2$ mixture.

The value $E_2 = 5750$ cal. is obtained from Hertel's value for the temperature coefficient for 10° = 1.37. Hence, since $E_2 - E_{2'} = 800$ cal.,

$E_{2'}$ becomes 4950 cal. From a comparison of

$$H + HCl = H_2 + Cl$$

with

$$H + Cl_2 = HCl + Cl$$

(in para-hydrogen) and the variation of $k_{2'}/k_3$ with temperature, $E_{2'} - E_3 = 2400$ cal. and so $E_3 = 2550$ cal. From Hertel's data (14) it follows also that E_3 would be 2060 cal. if $H + O_2 + M$ were temperature-independent. To reconcile the two data for E_3 we therefore can set E_4 equal to 500 cal.

The absolute value of $\log k_2 = 6.40$ at 288°K. comes from a comparison, by Brenschede and Schumacher (4, 5), of

$$CO + Cl + Cl_2 = COCl_2 + Cl$$

with

$$Cl + H_2 = HCl + H$$

Hence $\log f = -0.92$. The absolute value of $\log k_4 = 8.60$, in the mean, was obtained by Bodenstein from analysis of data by Frankenburger and Klinckhardt (12) and by Bates (2) on peroxide formation from atomic hydrogen. From data of Ritchie (18), with experiments in which both water and hydrogen chloride were formed, $\log k_3 - \log k_4 = 0.41$ and hence $\log k_3 = 9.01$. The steric factor corresponding is then $\log f_3 = -0.78$. From Hertel's data already discussed $\log k_3 - \log k_{2'} = 2.46$. Hence $\log k_{2'}$ at 288°K. is 6.55 and $\log f_{2'} = -1.39$. The uncertainty in the values for $\log k$ is estimated by Bodenstein to be not greater than 0.3.

REFERENCES

(1) ALLMAND: J. Chem. Soc. **1937**, 1878, and earlier papers.
(2) BATES: J. Chem. Phys. **1**, 457 (1933).
(3) BODENSTEIN: Z. physik. Chem. **130**, 422 (1927).
(4) BODENSTEIN, BRENSCHEDE, AND SCHUMACHER: Z. physik. Chem. **B28**, 81 (1935).
(5) BODENSTEIN, BRENSCHEDE, AND SCHUMACHER: Z. physik. Chem. **B35**, 382 (1937).
(6) BODENSTEIN, BRENSCHEDE, AND SCHUMACHER: Z. physik. Chem., in press (1938).
(7) BODENSTEIN, LENHER, AND WAGNER: Z. physik. Chem. **B3**, 459 (1929).
(8) BODENSTEIN AND ONODA: Z. physik. Chem. **131**, 153 (1927).
(9) BODENSTEIN AND PLAUT: Z. physik. Chem. **110**, 399 (1924).
(10) BODENSTEIN AND SCHENK: Z. physik. Chem. **B20**, 435 (1933).
(11) BODENSTEIN AND WINTER: Sitzber. preuss. Akad. Wiss., Physik.-math. Klasse **1936**, 2-18.
(12) FRANCKENBURGER AND KLINCKHARDT: Z. physik. Chem. **B15**, 421 (1932).
(13) GIAUQUE AND OVERSTREET: J. Am. Chem. Soc. **54**, 1731 (1932).
(14) HERTEL: Z. physik. Chem. **B15**, 325 (1932).

(15) **Lenher and Rollefson**: J. Am. Chem. Soc. **52**, 500 (1930).
(16) **Norrish and Ritchie**: Proc. Roy. Soc. (London) **A140**, 713 (1933).
(17) **Ritchie and Norrish**: Proc. Roy. Soc. (London) **A140**, 99, 112 (1933).
(18) **Ritchie**: J. Chem. Soc. **1937**, 857.
(19) **Rollefson**: Trans. Faraday Soc. **27**, 465 (1931).
(20) **Rollefson**: J. Am. Chem. Soc. **56**, 579 (1934).
(21) **Rollefson**: Z. physik. Chem. **B27**, 472 (1937).
(22) **Schultze**: Z. physik. Chem. **B5**, 368 (1929).
(23) **Schumacher**: Z. physik. Chem. **129**, 253 (1927).
(24) **Schumacher**: J. Am. Chem. Soc. **52**, 3132 (1930).
(25) **Schumacher**: Z. angew. Chem. **40**, 613 (1936).
(26) **Schumacher and Stieger**: Z. physik. Chem. **B13**, 157, 169 (1931).

THE ACTION OF OPTICAL SENSITIZERS ON THE PHOTOGRAPHIC PLATE[1]

9/b - 59

G. KORNFELD

Kodak Research Laboratories, Rochester, New York

Received May 25, 1938

In this paper a survey is given of the published work dealing with the mechanism of optical sensitizing of photographic emulsions, the connection between sensitizing and other properties, and the mechanism of desensitizing. There are some facts available concerning the first point, and a close connection has been established between light absorption and sensitizing power. Up to the present time, however, only fragmentary information has been published on the relation between sensitizing power and other properties and on the nature of desensitizing.

I. INTRODUCTION

The spectral range of photographic action

Since photochemical action in any system is necessarily connected with its light absorption, the light absorption in silver halide emulsions is of fundamental importance for determining the spectral range of photographic action.

The absorption of pure silver bromide in a microcrystalline state was measured by Slade and Toy (1) in 1920. They found absorption beginning at about 450 mμ which strongly increased towards the violet and ultraviolet regions. Eggert and Noddack (2), in 1923, found the limit towards the long wave length region at 465 mμ. In 1928 Eggert and Schmidt (3) undertook a very careful investigation of thin layers of microcrystalline silver bromide and silver chloride, for which they found the absorption limits towards the longer wave lengths, at 480 mμ and 400 mμ, respectively. There is no limit towards the shorter wave lengths in pure silver bromide. Absorption and photochemical action occur throughout the whole ultraviolet region and beyond it. It is well known that the photographic plate was instrumental in Roentgen's discovery of x-rays. Photographic action, however, in this region of very large quanta is essentially different from that in visible and ultraviolet light. Glocker and Traub (4) found that, with x-rays, there was no threshold of sensitivity for small intensities,

---

[1] Contribution No. 10 to the Third Report of the Committee on Photochemistry, National Research Council.

and Bunsen's reciprocity law was found to be valid over a long range. It is not to be expected that the law of photochemical equivalence will hold in the region of x-rays, where the photochemical action corresponds to the amount of energy transferred to secondary electrons. This was the conclusion from Glocker's (5) investigation in 1927. Eggert and Noddack (6) some time before had found that one quantum of x-rays absorbed corresponds to about 10^3 silver atoms released. That the law of equivalence does not hold in the x-ray region was also confirmed by Günther and Tittel (7). Between 0.245 Å. and 1.54 Å. the number of silver atoms per quantum absorbed changed from 920 to 148, but the ratio between the energy of the secondary electrons and the amount of reduced silver was found to be fairly constant.

The absorption of gelatin is negligible in the x-ray region, but, in the visible and ultraviolet regions, the presence of gelatin in the photographic emulsion distorts the close correlation between absorption and photographic action which can be observed in pure silver halides. Eggert and Noddack (2) determined the absorption of emulsion-coated plates in the region of the longer wave lengths and found more than 20 per cent absorption, even at 615 mμ. This absorption is of no use in photography, however, since gelatin can not act as a sensitizer. In the far ultraviolet region gelatin actually impedes photographic action by its own strong absorption. For the region below 200 mμ, therefore, Schumann plates, which do not contain any gelatin, are used.

Absorption is not so well defined in a photographic emulsion as it is in pure silver bromide. It is dependent, to some extent, on the mode of preparation. In an investigation with Frankenburger, Fajans (8) was the first to point out the deforming influence of adsorbed ions on the crystal forces which naturally must result in a spectral shift. In several succeeding investigations this spectral shift was thoroughly examined by him and his coworkers (9, 10, 11, 12, 13). Recently de Boer (14) has quantitatively connected the spectral shift with the heat of adsorption in the normal and excited state.

There is another factor which influences the absorption even more during exposure, that is, photolytically developed silver in colloidal form. The phenomenon was discovered as early as 1840 by E. Becquerel (15, 16) with a Daguerreotype plate (silver iodide on silver) which could be made sensitive to the yellow and even to the red region by long exposure. He observed the same effect with silver bromide and silver chloride papers. He therefore called the blue end of the spectrum "exciting radiation" and the yellow and red regions "continuing radiation". Lüppo-Cramer (17) and Eder (18), in 1909, explained the phenomenon as optical sensitizing by colloidal silver, and Lüppo-Cramer was able to reproduce the phenomenon by adding colloidal silver to silver chloride. The great extension of the absorption region pointed clearly to the absorption of light by the colloidal silver and to its sensitizing property. This sensitizing property of colloidal silver, as well as of colloidal silver sulfide, in analogy to the organic sensitizing dyes was extensively considered by Sheppard (19).

In 1873 H. W. Vogel (20) discovered that some of the strongly absorbing organic dyes could be used as sensitizers for the photographic plate. Corallin was the first dye used by him to sensitize the plate for the yellow and green regions. He saw at once the significant correspondence between the absorption of the dye in solution and the sensitized region, although both regions do not coincide exactly, and he foresaw its practical importance. The value of this discovery can hardly be overemphasized, since panchromatic and orthochromatic plates were developed as a result, and the extension of photography during recent years far into the infrared region can be traced to its influence.

Most of the dyes which were employed as sensitizers in the beginning are now rarely used. At present nearly all the sensitizers used belong to the polymethine group, many of them being cyanine dyes. It is not intended here to describe in detail all the work that has been done on this subject. It ought to be mentioned, however, that close connections were found between the constitution of the dyes and their spectral range of absorption in solution. Once these connections were established, sensitizing dyes were synthesized for the whole visible region of the spectrum and through the infrared as far as 1356 mμ (21).

The systematic connection, however, has been confined so far to the constitution of a dye, on the one hand, and the intensity as well as the region of its absorption, on the other. As yet no evidence has been found to connect its sensitizing property with its chemical constitution or with any other quality.

A great number of empirical facts on optical sensitizers have been found, but it seems hardly possible to fit them into a consistent picture. The conflicting results of earlier experiments can be explained partly by the fact that the sensitizers used were often not chemically pure and in some cases were even combined with various admixtures, but, even with pure materials, the complex nature of the phenomena makes it difficult to arrive at simple laws. Desensitizing was frequently regarded as optical sensitizing with a negative sign, and the difference in constitution was connected with this antagonistic behavior. It is only recently that desensitizing has been recognized as a property common to all sensitizers. It has been fairly well established, moreover, that sensitizing and desensitizing belong to different stages in the formation of the latent image and probably take place at different spots on the silver bromide grain. As early as 1907 Sheppard and Mees (22) made a very clear statement regarding the different stages for the action of sensitizers and desensitizers in the primary process, but it seems generally to have been overlooked by other investigators. Then, in 1925, Sheppard (23) emphasized the fact that desensitizing does not produce any detectable shift in the spectral sensitivity. One year later von Hübl (24) stated quite clearly that, for a special spectral region, a desensitizer might as well be considered also an optical sensitizer, since both actions were not connected with each other, optical sensitizing depending on color, whereas desensitizing as a chemical reaction can be produced by colorless substances. In 1931, writing on "Sensitizing by Desensitizers", Lüppo-Cramer (25) stated that it seemed futile to divide the dyes into sensitizers and desensitizers, since the same dye might belong to either class, according to the conditions under which it was used. He supported this statement by several facts: (*1*) Many dyes known as optical sensitizers in silver bromide emulsions act as desensitizers in silver iodide emulsions. (*2*) If an acceptor for halogen is added to a silver bromide emulsion, many dyes known as desensitizers then act only as sensitizers. (*3*) To unripened emulsions some desensitizing dyes (Capri blue, Janus green) act as sensitizers when used in low concentrations.

A very cogent argument in favor of the above statement is the existence of optimum conditions for the sensitizing baths regarding concentration and time of bathing. This fact was discovered by Sheppard (57) as early as 1908 with a solution of an isocyanine dye. In 1933 Heisenberg (26) showed for three dyes, namely, pinacyanol, thiocarbocyanine, and selenocarbocyanine, that there is an optimal concentration for the adsorption of a sensitizing dye, at which nearly all the dye is adsorbed. With concentrations increasing beyond this optimal concentration, desensitizing sets in, and Heisenberg proved that this desensitizing effect is real, since it is much too large to be accounted for merely by the increased light absorption of the dye. This desensitizing effect of sensitizing dyes when used in larger concentrations seems to be of a general nature. A very extensive and careful recent investigation by Leermakers, Carroll, and Staud (27) showed invariably the same result.

The desensitizing action, then, is to be considered a property common to all optical sensitizers and, although this statement is not reversible, because desensitizing is not exclusively a property of optical sensitizers, a study of desensitizing should contribute something to the knowledge of optical sensitizers. The connection, however, between the specific character of a sensitizer and its desensitizing property if used in excess is a little more remote than that with optical sensitizing which will, therefore, be dealt with first.

II. SENSITIZING ACTION

A. The sensitizing process

The sensitizing action has always been believed to be closely connected with the primary act of absorption, and quite recently Leermakers (28) has confirmed very accurately the close correspondence between sensitivity and absorption in a sensitized emulsion. The conclusion thus seems inevitable that sensitizing is connected with the primary act of light absorption. Now, according to the present state of the theory of the latent image, into which Webb (29) has introduced quantum mechanics, absorption in unsensitized silver bromide results first in the raising of an electron to a higher level. In this level its mobility is not blocked by other electrons and, accordingly, photoconductance results. This photoconductance was measured by Toy and Harrison (30) and was found within 0.07 sec. to reach a stationary state which was proportional to the intensity. This would be expected if the majority of the electrons left the upper level again and dropped to a lower level. It has been assumed that such lower levels are produced by impurities and that in catching the electrons they give rise to the color centers, which are called F centers, in Pohl's terminology. Hilsch and Pohl (31) found in crystals of alkali halides that these F color centers are characterized by sharp absorption bands; in silver halide crystals, the absorption bands are more diffuse and broader, overlapping the proper absorption of the silver halides. Hilsch and Pohl assume that it consists of various bands belonging to different states of aggregation, since there is evidence that, in the silver halides, the photoproduct collects into specks of varying dispersity immediately after it is formed. In this connection it is perhaps of some interest to point to the results of Wagner and Beyer (32). They found that the lattice defect in silver bromide crystals is produced by interstitial silver ions which have left their normal places in the lattice, whereas in alkali halides the ions which have left their places are not present in the lattice any more. For the photographic emulsion Sheppard (23) stressed the necessity of dividing the formation of the latent image into two stages: (*1*) the primary act of absorption and (*2*) the formation of concentration specks around the sensitivity specks. He was able to show that the relative spectral sensitivity was scarcely affected by the formation of sensitivity nuclei (such as from thiocarbamide), which greatly increased the absolute sensitivity to any wave length, and Carroll and Hubbard (33) confirmed this statement. Webb has pointed out that the results obtained by Pohl and his school, in crystals, fit very well into the concentration-speck hypothesis suggested by Sheppard, Trivelli, and Loveland (34) for the photographic emulsion. Recently experimental evidence has been found for the existence of such concentration centers in photographic emulsions. Van Kreveld and Jürriens (35) devised an extremely sensitive method for measuring the absorption of a photographic plate after exposure. They found that the characteristic absorption between 5900 Å. and 7000 Å. was proportional to the time of exposure (36). The intensity of absorption taken as a function of the time of exposure gave a straight line passing through zero. Moreover, the method was so sensitive that they could include very short exposures in their measurements. The first point was produced by an energy of 9 × 10^{11} quanta per $cm.^2$ on an Ilford Process plate. This point actually lies at the beginning of the overexposure region of the H. and D. curve, but is still so near to the region of the latent image that there is a high probability that the latent image is characterized by the same absorption.[2] Now the same absorption, only increased in intensity, has also been found for the print-out region, in which Eggert and Noddack (37) found the amount of photolytically produced silver to be that required by the law of photochemical equivalence. They also extrapolated their results to the region of the latent image, and the investigations of van Kreveld and Jürriens confirmed their statement. It can be assumed, therefore, with a probability very near to certainty, that the latent image consists of silver which has been produced by light according to the law of photochemical equivalence, so that, for each electron released, one atom of silver is formed.

In a sensitized emulsion the same primary process is supposed to take place, but with one exception. The original level from which the electron is raised is higher than the original level in the unsensitized emulsion and, accordingly, the energy required for raising it is less. Sheppard and Crouch (38) attributed this electron level to the sensitizing dye, and this assumption seems amply justified by the close resemblance between the absorption spectrum of the sensitized emulsion and that of the sensitizing dye itself. Thus, in the sensitized region, the electron should originate from the adsorbed dye, whereas, in the absorption region of silver bromide, it should originate from the bromide ion in the lattice. One more fact should be mentioned as an argument in favor of this theory, i.e., the photoconductance of sensitizing dyes. As early as 1905 Joly (40) pointed out the parallelism between photoconductance and absorption in sensitizing dyes, and in 1923 Zchodro (41), in comparing the photoconductance of three sensitizing dyes (cyanine, pinaverdol, and pinachrome) in dry collodion, with their absorption, found complete correlation. This result, however, is not conclusive. The photoconductance of the dyes should be investigated in the same specific molecular state in which they are adsorbed in the silver bromide emulsions.

From the theory just outlined it should be concluded that not more than one silver atom could be produced by the light-action of one dye molecule unless this molecule could be restored to its former state, rather than be decomposed after the release of an electron. This assumption seems far-fetched, although one fact points in this direction,—the strong fluorescence which is found in sensitizing dyes. It is to be regarded, however, as one of the possible solutions for a puzzling experimental result

---

[2] It must be borne in mind, however, that it would hardly be possible to discover a slight deviation of the straight line in the region of the latent image.

obtained by Leszynski (42), by Tollert (43), and recently by Bokinik and Iljina (44).

All these authors found that, in a sensitized emulsion, the number of silver atoms present after exposure was many times greater than the number of dye molecules. Leszynski found that, after the exposure of an emulsion sensitized by erythrosin, the ratio of silver atoms to dye molecules was of the order of 20. Tollert repeated Leszynski's investigation with a very fine-grained emulsion, taking care to consider only those dye molecules which had actually been adsorbed to the silver bromide, and arrived at the same result. With the dye concentrations and exposure times which were used in his experiments, a ratio of 64 was actually found. Both authors used the same analytical methods and there is a possibility, of course, that a systematic error could have been made which is responsible for the anomaly. The method used was the same as that of Eggert and Noddack (37), i.e., first dissolving the silver bromide in thiosulfate and then determining the amount of silver in the precipitate. The thiosulfate might have given rise to some silver sulfide which would increase the amount of silver in the precipitate. There is always a tendency for thiosulfate to give silver sulfide, especially in the presence of gelatin, and this might be increased by the presence of the dye.

There is, however, additional evidence for a high, although not equally high, efficiency of the sensitizing dyes, namely, the work of Bokinik and Iljina (44). These authors investigated the sensitizing action of erythrosin in silver bromide sols without gelatin and with an excess of bromide ions, with the result that the ratio of silver atoms to adsorbed dye molecules was found to lie between 4 and 15, rising with increasing alkalinity. It appears, however, that some other spectral region than the green light of the sensitizing region enhanced the effect on the silver bromide sol, for, if their curves (amount of silver against adsorbed dye) are extrapolated to a dye concentration of zero, a large and varying amount of silver seems to have been formed in every case.

Thus, although the results of all three experiments are not quite conclusive, still they are not to be considered wrong.[3] Accordingly an explanation for the results should be sought. Three different explanations have been offered, one of which has already been given, i.e., that the dye molecule is restored after the release of an electron. This restoration of the molecule could easily occur if the remaining part did not decompose in the meantime. In this connection, a study of phosphorescence in adsorbed dyes would be of interest.

Another explanation is the possibility that the absorbing dye molecule

[3] These results were strongly supported by an experiment recently reported by Dr. Sheppard at the September, 1937, Meeting of the American Chemical Society, which will be referred to later in this paper.

imparts its energy somehow to the crystal lattice, so that an electron is released from the lattice and the dye molecule is not affected at all. This is the explanation preferred by Leermakers (28), but it does not explain why the energy required to release an electron in the silver halide lattice should be reduced to such an unusual degree by the adsorbed dye, nor why this energy should correspond so closely to the absorption of the dye itself. Recently Scheibe (44a) has tried to find a solution for this question by assuming that the dye in an aggregated state should be able to absorb more than one quantum in one elementary act.

There is a third explanation connecting the excess of silver atoms over dye molecules with a chemical reaction of these latter molecules. Sheppard and Crouch (38) suggested an explosion of the dye molecule after the release of an electron, and they produced experimental evidence for the occurring of a chemical reaction between cyanine dyes and silver halide in the presence of light. Other contributions to this question have recently been made by Semerano (45, 46) and by Mecke and Semerano (47). The most recent results of Sheppard, Lambert, and Walker (46a), however, referred to already in this paper, rule out this explanation, for these authors were able to show that in the presence of an acceptor for halogen the sensitizing action proceeds without any decomposition of the dye. Thus the decomposition of the sensitizing dye can not be connected with the actual sensitizing. The part played by the sensitizing dyes in the photographic process seems, on the whole, to be fairly well established, although some questions remain still to be answered.

The main problem, however, concerns the properties which are required to make a sensitizer out of a dye, and unfortunately very little is known about them. In the following sections a survey will be given of the attempts which have been made to correlate the various properties of dyes with their sensitizing characteristics.

B. Adsorption of sensitizers

The fact that adsorption is a necessary though not a sufficient condition for sensitizing has been known for some time (22). As early as 1904 Kieser (48) studied a great number of sensitizing dyes in their relations to the surface of silver halide grains, and found that saturation was reached at very low concentrations of the dye, but it was only recently that quantitative measurements were started of the adsorption of sensitizing dyes by silver halide emulsions.

In 1925 Sheppard and Crouch (38) measured the adsorption of Orthochrome T, dissolved in water, on a silver bromide emulsion with only 1 per cent gelatin at 50°C. The adsorption was measured in two ways: (*1*) by extracting the aqueous solution of the remaining dye with chloroform and determining the dye concentration with a spectrophotometer, and (*2*) by determining directly the amount of dye adsorbed at the silver bromide grains after dissolving them in thiosulfate. The results of both methods agreed fairly well. The adsorption curves at first showed increasing adsorption with increasing concentration. Then, over a large part, the curves were parallel to the concentration axis until finally they rose steeply again with further increase in concentration. The parallel parts of the curves were interpreted by the authors as representing saturation in a single layer, and the steep rise afterwards was assumed to be due to the agglomeration of multilayers. The size-frequency of the silver bromide grains was measured, and the surface area was calculated and compared with the amount of adsorbed dye in a saturated single layer. This latter value varies according to the alkalinity. For a pH of 5.5 there were found 5×10^{-10} gram-moles of dye per square centimeter of surface area. According to a statement of Trivelli and Sheppard (49), the authors assumed the surface area to consist mainly of bromide ions, since excess bromide was present. By calculating the number of bromide ions in the surface, they were able to establish the ratio of bromide ions to dye molecules as 2.3. In connection with the adsorption at bromide ions, the increase of adsorption in alkaline solutions presented some difficulty. For, although it would have seemed natural to assume that the dye cations were adsorbed at the bromide ions, the increase in adsorption in alkaline solution pointed to the adsorption of the molecular form. There were two forms of the dye found in a solution in water, a dissociated uncolored form which was soluble in water, and an undissociated colored form which tended to be dispersed in colloidal solution in water (50), whereas, in alcohol and other organic polar solvents, the colored form was more soluble. The equilibrium between these two forms in water depended on the acidity. The dissociated colorless form prevailed in acid solution and the colored form in alkaline solution. Thus it seemed certain that the colored form, although not actually dissociated, was still exclusively adsorbed at the bromide ions. A parallel may be drawn, perhaps, to the statement of Franck and Eucken (51), according to which energy exchange is facilitated between molecules which can react with each other, even though they can not react under the special conditions under consideration.

The connection between the basic or acid nature of a dye and the place of adsorption in silver bromide was confirmed in an investigation by Sheppard, Lambert, and Keenan (52). The acid dye dichlorofluorescein was found to be adsorbed only in the presence of an excess of silver ions, whereas, in alkaline solution, the basic dye pinacyanol was adsorbed only at the bromide ions. It should be mentioned here that the experimenters of Leermakers, Carroll, and Staud (39) gave the same results. All the basic cyanine dyes were adsorbed exclusively by the bromide ions. An investigation of the adsorption of pinacyanol (52), carried out parallel with the investigation of the adsorption of Orthochrome T, yielded a value between 1.69 and 2.78 for the ratio of bromide ions to dye molecules. (The range of variation depends on the assumption of octahedral or of cubic faces at the surface.) This value was found to be roughly in agreement with the results of other investigations, on dye adsorption at silver bromide surfaces, which had been carried on in the meantime. Having found eight bromide ions for one molecule of adsorbed methylene blue, Wulff and Seidel (53) collected other data on adsorption at the surface of salts of heavy metals. They gave the ratio 3 as the result of an experiment on the adsorption of erythrosin at silver bromide surfaces carried out by O. J. Walker and K. Fajans.

Since that time other investigators have very definitely confirmed the ratio $\frac{\text{Br}^-}{\text{dye}} > 1$. Bokinik (54) gave the ratio 10 for pinacyanol, and Leermakers, Carroll, and Staud (27) found the ratio 10 for two different thiocarbocyanines and 20 for a thiodicarbocyanine. Their saturation value was defined as the amount of dye adsorbed at optimal sensitization, whereas saturation in Sheppard's experiment was defined by the parallel part of the adsorption curves. Since both methods yielded different results (the ratios being 2 and 10, respectively), the authors concluded that there exists a difference between saturation considered from the point of view of adsorption, and saturation considered from the point of view of sensitizing. Their investigation was a systematic study of the correlation between the optimal concentration of a sensitizer and the available grain area, and it was carried out with three different dyes and seven emulsions. The curves obtained by plotting the sensitivity in various spectral regions against the logarithm of the dye concentration show a great increase in sensitivity towards the optimal concentration in the red region, a slighter increase in the green part of the spectrum, and no change in the blue part. At higher concentrations a decrease in sensitivity occurs throughout the whole spectrum. At the optimal concentration, practically the whole amount, i.e., 99 per cent, of the dye was found to be adsorbed. For concentrations beyond this the percentage of unadsorbed dye increased rapidly. (For pinacyanol, thiocarbococyanine, and selenocarbocyanine, Heisenberg (26) obtained exactly the same results.) The surface area for each emulsion was determined from the projective area of the average grain, the number of grains per cm.^{3}, and the volume of the average grain (obtained by finding the silver content of the emulsion, the density of silver bromide, and the number of grains). The results are shown in table 1 (taken from the paper by Leermakers, Carroll, and Staud (27)).

The fifth column shows a remarkably constant value for each dye. This constant ratio of adsorbed dye to available surface is especially remarkable, since the emulsions were prepared in various ways, both from neutral silver nitrate and from ammoniacal silver oxide. Discussing the difference in the ratio, dye to surface, for dye I and dye II, on the one hand, and dye III, on the other, Leermakers, Carroll, and Staud point out that the deviation is in the right direction, since dye III as a thiodicarbocyanine has a larger area than dye I or dye II, both of which are thiocarbocyanines. They point out at the same time, however, that the deviation is greater than could be accounted for by the difference in size. The data of table 1 are used to estimate the amount of surface saturation at the optimal concentration. For dye II, an 8-alkylthiocarbocyanine, the surface is assumed to be 150 Å., according to the values given recently for atomic radii. If the molecules are assumed to lie flat on the crystal surface, they will then cover $11.5 \times 10^{-11} \times 6 \times 10^{23} \times 150 \times 10^{-16}$ cm.^{2} per square centimeter of surface, or 1 cm.^{2} per square centimeter, i.e., they will form a unimolecular layer.

TABLE 1

Optimal surface concentration of sensitizing dyes

(From Leermakers, Carroll, and Staud (27))

EMULSION	SURFACE	DYE	OPTIMAL CONCENTRATION	MOLES OF DYE PER CM.^{2} OF SURFACE $\times 10^{11}$
	cm.^{2} per cm.^{3}		*moles per cm.^{3} of emulsion $\times 10^8$*	
1	400	I	3.6	9.0
2	480		3.8	7.9
3	580		5.2	9.0
4	660		6.0	9.1
5	840		7.2	8.6
6	950		9.0	9.4
7	1080		12.0	11.1
1	400	II	4.4	11.0
3	580		6.3	10.9
4	660		8.0	12.1
6	950		11.2	11.8
7	1080		12.6	11.6
1	400	III	1.9	4.8
3	580		2.3	4.0
4	660		2.9	4.4
6	950		4.8	5.0
7	1080		4.8	4.4

This result seems fairly convincing, although the authors themselves are willing to assume that it may be a coincidence, because there are other facts (39) which seem to require the assumption of an agglomeration of the adsorbed dye. These data are connected with some spectral characteristics which will be reported later in the present paper.

Two more investigations should be mentioned in connection with adsorption measurements,—one by Bagdassarjan and Rabinovitch (55), and the other by Ščetinkina (56), which was reported by Rabinovitch. Bagdassarjan and Rabinovitch, studying the adsorption isotherms of silver bromide suspended in water, of erythrosin, eosin, rhodamine B, pyronine G, phloxine, acid rhodamine, and Bordeaux B, and their sensitizing power in silver bromide emulsions, found again that adsorption was necessary for sensitizing. In addition, they discovered that dyes (pyronine G) with adsorption isotherms which do not show any flat portions pointing to saturation are extremely weak sensitizers. Ščetinkina (56) measured the dependence of sensitizing action on the concentration of the sensitizer, and found a maximum for erythrosin and phloxine at relatively low concentrations. At very high concentrations the sensitivity decreases. These results are in good agreement with the results of the other investigators.

C. *Some special spectroscopic properties of sensitizers*

That the absorption spectra of dyes vary according to the solvent has been known for a long time. In 1908 Sheppard (57) investigated the absorption of some sensitizing dyes in alcoholic solutions and in water and found a very marked difference between them. The sensitivity curves of emulsions sensitized by these dyes resembled to some extent the absorption curves in water. In another investigation Sheppard (50) obtained some ultramicroscopic evidence of the colloidal state of the dyes dissolved in water. Recent investigations of this were carried on by Scheibe (58), by Scheibe, Kandler, and Ecker (59), by Scheibe, Mareis, and Ecker (60), by Jelley (61, 62), and by Leermakers, Carroll, and Staud (39).

A peculiar spectroscopic phenomenon, discovered by Jelley for a special cyanine dye (1, 1′-diethylpseudocyanine chloride), was observed when the dye was changing from true solution in alcohol or a similar solvent to the crystallized state. During the change it passed through a transitory state characterized by a sharp absorption band at about 575 mμ. This absorption band was associated with a strong resonance fluorescence, an unusual phenomenon in the liquid or solid state. This transitory state of the crystal was found to be relatively stable in solutions of some salts and in the case of adsorption of the dye on various substances (59).

In investigating silver bromide emulsions sensitized by cyanine dyes, Leermakers, Carroll, and Staud found similar sharp characteristic absorption bands for many adsorbed dyes. It was this fact which made them doubtful of the unimolecular layer, since Scheibe, Kandler, and Ecker attributed these spectral characteristics to a polymerized state, and Scheibe, Marcis, and Ecker confirmed this statement. Jelley, however, assumed a nematic state, i.e., a liquid crystal with orientation along one axis only, and the question of the "aggregated" state was left open.[4] Whatever this state be called, it will still be tempting to link it with the sensitizing power. But some of the results of Leermakers, Carroll, and Staud are not in agreement with the assumption that the sensitizing action is exclusively a property of this "aggregated" state. They found parallelism between sensitivity and absorption in all spectral regions, not merely for the bands belonging to the nematic state, but also for bands in other spectral regions which were obtained in emulsions dyed from alcoholic solutions. The sensitivity, however, was always proportional to the absorption.

Another connection seems worth investigating, namely, that between fluorescence and sensitizing, especially with regard to the possibility (mentioned in the discussion of the sensitizing process) that the dye molecule could be quickly restored after the release of an electron. Fluorescence in solutions is known to occur very frequently in cyanine dyes (63), but it is important to know whether the dyes adsorbed to silver bromide will show fluorescence. An investigation of the fluorescence of sensitized emulsions would be especially interesting in view of some remarkable results obtained with isomers by Brooker and Keyes (64) and by Leermakers, Carroll, and Staud (39). These isomers have the following constitution:

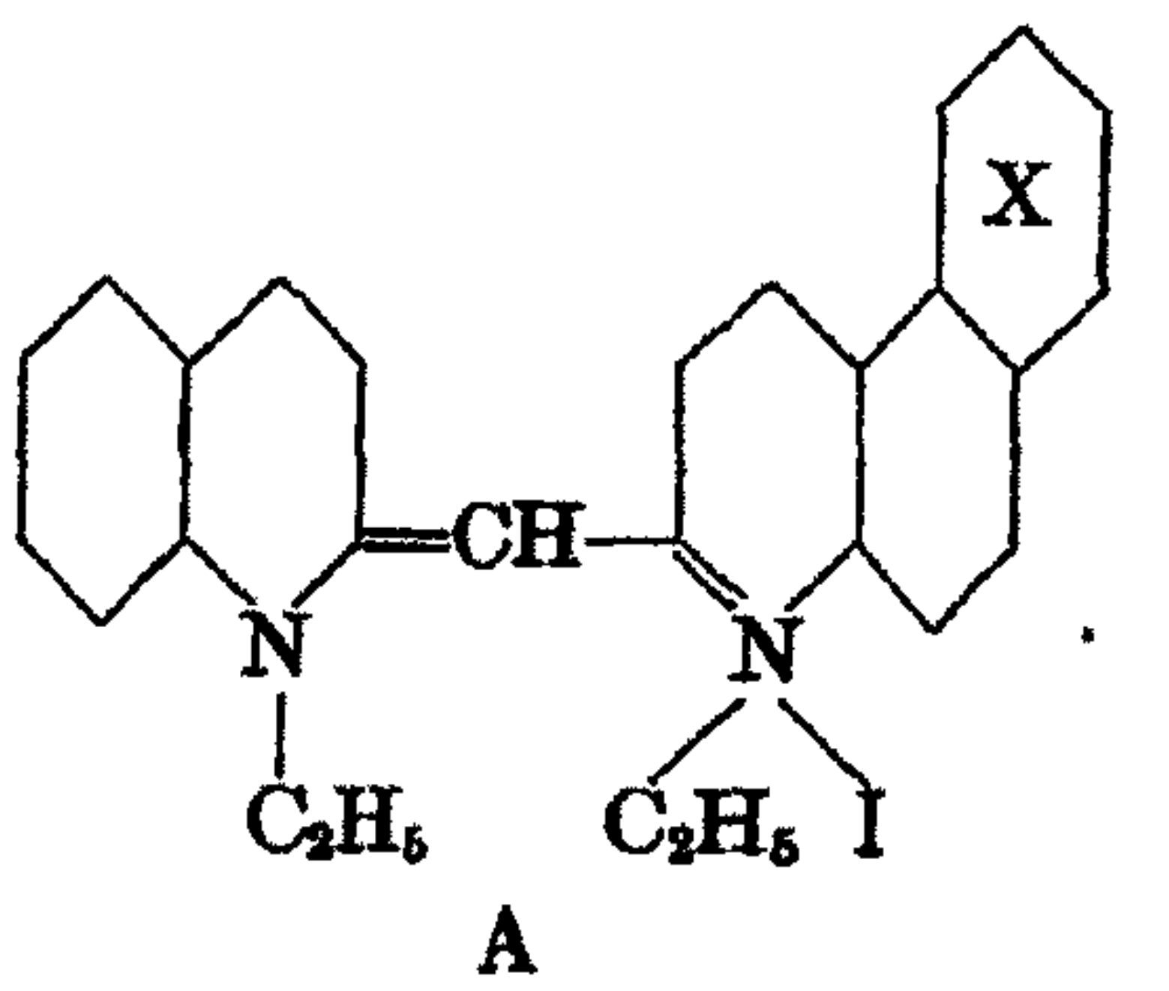

A

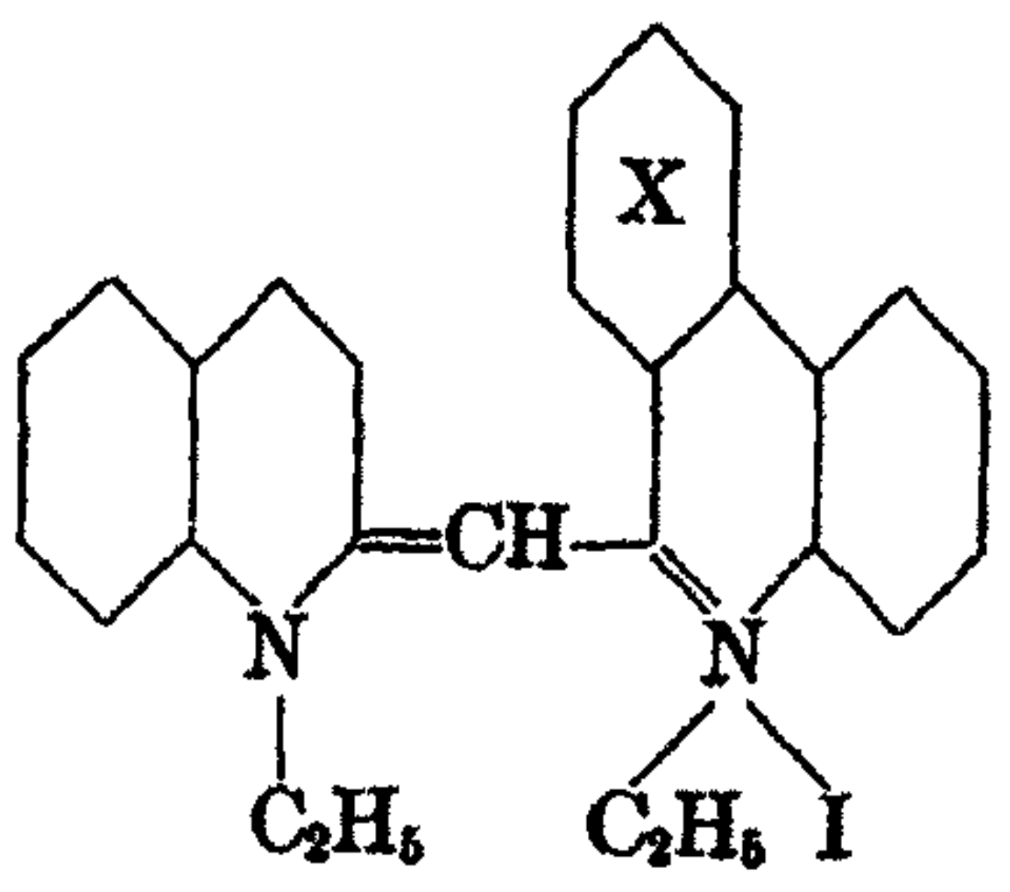

B

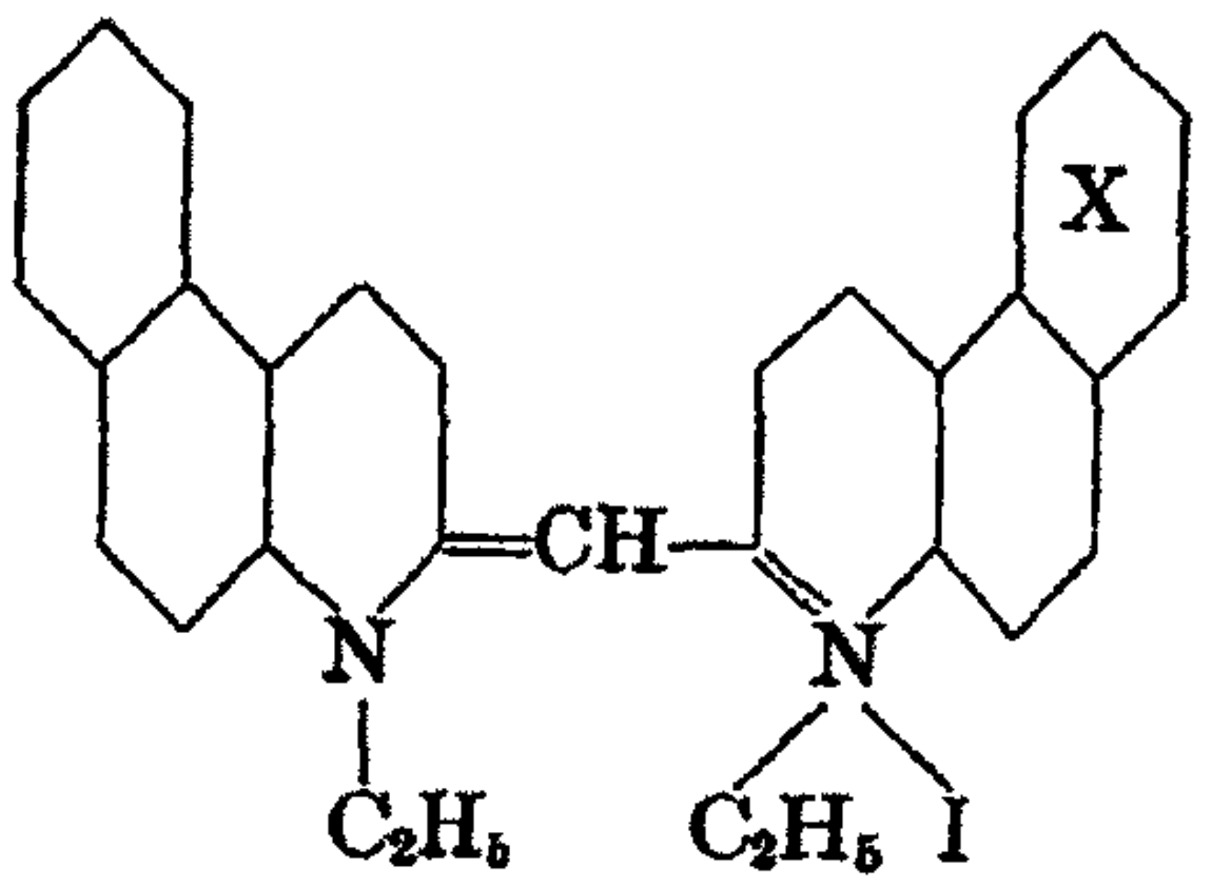

C

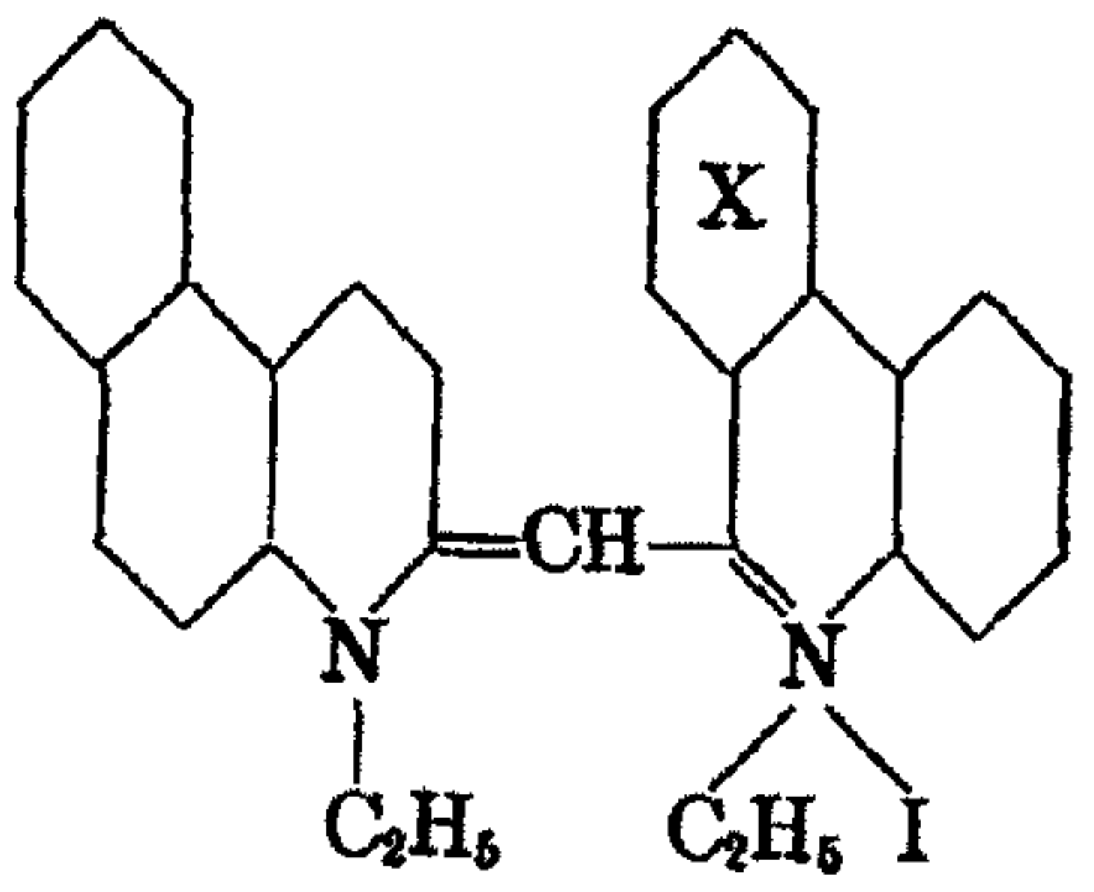

D

---

[4] At a recent meeting (September, 1937) of the American Chemical Society Dr. Sheppard suggested a unimolecular layer in which the molecules are standing on edge, so that aggregation could take place in one dimension.

The only difference between A and B, or between C and D, lies in the position of the benzene ring marked X. Each of the dyes showed strong adsorption to silver bromide emulsions and a sharp absorption band, but only A and C were found capable of sensitizing the emulsions; B and D did not act as sensitizers. It would be interesting in this connection to know whether the isomers show any differences in fluorescence or photoconductance.

There are at present very few data which can be attributed to the sensitizing property. Bokinik (65) points out, in discussing the various explanations offered for the sensitizing action, that, of all the existing dyes, only those related to the phthalein or the cyanine groups were found to be sensitizers, but this statement is more applicable to the properties desirable for a practically useful sensitizer than to the sensitizing property itself.

Chibisoff (66), on the other hand, calls attention to some secondary effects of optical sensitizers whereby they act simultaneously as chemical sensitizers. These effects are especially marked when the dyes are added to the emulsions before ripening. They can then influence the growth of the crystal and the ripening process. Bancroft, Ackerman, and Gallagher (67) have connected the sensitizing power of a dye with its reducing action as an acceptor for halogen, and accordingly define an optical sensitizer as a dye which absorbs light in a special region and which is capable of reducing silver salts.

III. DESENSITIZING ACTION

The desensitizing action, as a property common to all sensitizers at high concentrations, should reveal some information on their characteristics. Unfortunately, the phenomenon itself seems complex, and the variation of terminology with author and time has helped to confuse the picture still more. There is, however, one fact which seems to be fairly well established: namely, that desensitizing takes place at the developing centers and not at the places of primary absorption (68). In addition to many facts which lead to this conclusion, there is an experiment reported by Lüppo-Cramer that definitely proves this point. Pinakryptol yellow is a very strong desensitizer and is even capable of dissolving the silver of the print-out image (70, 71). Accordingly, no darkening was observed in developing a plate which had been desensitized with pinakryptol yellow before exposure, but after dissolving the silver bromide in thiosulfate, the plate could be developed physically. This demonstrates clearly that the primary act of absorption during exposure was not impeded by the desensitizer adsorbed at the surface.

According to this result Weber's theory (72, 73) can be rejected, in so far as optical sensitizers are concerned. His theory assumed that desensitizing has only an indirect influence on silver bromide by removing the optical and chemical sensitizers. This was supported by the following facts: Lüppo-Cramer (74) showed with many examples that emulsions of silver bromide in collodion were not susceptible to the action of desensitizers unless they contained a sensitizer. Mudrovčić observed that cyanine dyes and the desensitizer methylene blue reacted with each other. In water and in collodion the cyanine dye was bleached out in the presence of methylene blue. (Since, however, in gelatin the process was reversed, the methylene blue being destroyed, this effect could as well be used as an argument against Weber's theory.) Finally, Weber himself observed that, in a sensitized plate, desensitizing showed more strongly in the sensitized spectral region than the absorption region of silver bromide. Blau and Wambacher (76) strongly objected to accepting this as a general statement and pointed out that, wherever this secondary effect was found, it could be easily explained by preferential absorption of the desensitizer.

It would indeed be difficult to explain by this theory the desensitizing effect of optical sensitizers at high concentrations. With regard to the assumed effect of desensitizers on chemical sensitizers contained in gelatin, by which Weber explained the difference between gelatin and collodion in regard to the susceptibility to desensitizing, Blau and Wambacher pointed out that this explanation could not be valid. For, in the meantime, Ollendorff and Rhodius (77) had succeeded in coating plates with a silver bromide emulsion without any protective colloid which could be desensitized with methylene blue. Lüppo-Cramer confirmed (78) this result, although he did find that the number of dyes capable of acting as desensitizers is much more limited in such colloid-free emulsions. Even pinakryptol yellow, one of the strongest desensitizers, is ineffective with them. The exceptional susceptibility to desensitizing was explained for the gelatin emulsion by Lüppo-Cramer as being related to the high degree of dispersion of the latent image in gelatin.

In a special case there would, of course, always be the possibility of a complication by some of the secondary effects which have just been discussed, but desensitizing as a general phenomenon can safely be taken as a direct action on the developing centers. Even so, the range of possible reactions is still very wide and many questions remain to be answered.

There is the Herschel effect, i.e., the simple regression phenomenon produced by infrared radiation (the name, "Herschel effect," is used here for the direct regression, as it was used originally, i.e., the "visible" Herschel effect, as named by Trivelli (80)). Does desensitizing mean sensitizing of the Herschel effect? Or is it merely an oxidation of the silver in the latent image? Is it essentially an isolation of the developing nuclei (68)? Does it merely prevent the formation of the latent image, or does it also destroy it? Is the desensitizing action merely a "narcosis" (81) of the centers lasting through development? And are these reactions influenced by light absorption?

Some of these questions can be answered from the results of various investigators. Some significant results have been obtained by Sheppard (82) concerning the mechanism of reaction on the silver bromide grain. By measuring the electromotive force in concentration cells with silver salts, he found a strong tendency to form complex silver salts in several compounds used in photography either as sensitizers, desensitizers, or antifogging agents.

It is conceivable that complexes are formed with silver either *in statu nascendi* or in the very fine dispersion of the latent image when oxygen is present. In experiments by Blau and Wambacher it was found that, for desensitizing at least, oxygen was necessary, unless there was an excess of chloride ions (83, 84, 85). Pinakryptol yellow, induline scarlet, antilumine, and phenosafranine did not act as desensitizers when oxygen was completely removed, either by evacuation or by substituting nitrogen.

The strong influence of halide ions on the desensitizing action had previously been observed by Carroll and Kretchman (86) With safranine either the sensitizing or the desensitizing effect was found, depending upon the concentration of bromide ions. The investigation of Carroll and Kretchman rendered quantitative results on the influence of light on desensitizing, and they were able to show the good correlation between reversal and energy absorption. This reversal phenomenon is, of course, not related in any way to the well-known photographic reversal, the beginning of solarization. The reversal by desensitizers can be identified with the "latent Herschel effect" as Trivelli named it, contrasting it to the "visible Herschel effect", which is a direct regression of the print-out image and which was, in fact, the effect actually discovered by Herschel. Where the regions of absorption by silver bromide and the dye were sufficiently separated in wave length, maxima were found corresponding to each region. Desensitizing can, therefore, be considered as a reaction in the developing centers which can be photosensitized by the light absorbed either by silver bromide or by the desensitizing dye. The photosensitizing is not the only reaction produced by a desensitizer. Loss of developability occurs also in the dark, but at a much lower rate. This was demonstrated by Carroll (87) and confirmed by Mauz (88).

There still remains the question of whether desensitizing involves destroying the silver centers or merely making them unfit for development. Or rather, it should be asked whether there are any desensitizing dyes which impede the development of the silver centers without destroying them. For, quite aside from the dyes (such as methylene blue, Janus green, etc.) which are known to be capable of dissolving silver (89), there is pinakryptol yellow, which was found by Hübl (90) to be capable of preventing the formation of a print-out image. Lüppo-Cramer had shown that the dye can even destroy the print-out image (70). Tollert observed that a plate desensitized with pinakryptol yellow yielded a smaller amount of photolytically formed silver than a plate which had not been desensitized. If this experiment were repeated with other desensitizers, the question mentioned above could be answered. With a colorless desensitizer it could even be done in a region much nearer that of the latent image, since van Kreveld and Jürriens (35) have developed a method of determining the latent image by measuring the absorption in the red region of the spectrum.

The author wishes to express her indebtedness to Dr. B. H. Carroll, Dr. W. Clark, Dr. R. H. Lambert, Dr. J. A. Leermakers, Dr. S. E. Sheppard, Dr. C. J. Staud, Mr. R. D. Walker, and Dr. J. H. Webb for many helpful discussions.

REFERENCES

(1) Slade, R. E., and Toy, F. C.: Proc. Roy. Soc. (London) **97**, 181 (1920).
(2) Eggert, J., and Noddack, W.: Z. Physik **20**, 299 (1923).
(3) Eggert, J., and Schmidt, R.: Z. Physik **48**, 541 (1928).
(4) Glocker, R., and Traub, W.: Physik. Z. **22**, 345 (1921).
(5) Glocker, R.: Z. Physik **43**, 827 (1927).
(6) Eggert, J., and Noddack, W.: Z. Physik **43**, 222 (1927).
(7) Günther, P., and Tittel, H.: Z. Elektrochem. **30**, 646 (1933).
(8) Fajans, K.: Z. Elektrochem. **28**, 499 (1922).
(9) Frankenburger, W.: Z. physik. Chem. **105**, 273 (1923).
(10) Fajans, K., Fromberg, H., and Karagunis, G.: Z. Elektrochem. **33**, 548 (1927).
(11) Fromberg, H.: Z. physik. Chem. **1B**, 324 (1928).
(12) Fromberg, H., and Karagunis, G.: Z. physik. Chem. **1B**, 346 (1928).
(13) Fajans, K., and Karagunis, G.: Z. physik. Chem. **5B**, 385 (1929).
(14) de Boer, J. H.: Z. physik. Chem. **18B**, 49 (1932).
(15) Becquerel, E.: Compt. rend. **11**, 702 (1840).
(16) Becquerel, E.: La Lumière, Ses Causes et Ses Effets, Vol. II, pp. 76, 77, 176, 867. Firmin Didot Frères, Fils et Cie., Paris (1867).
(17) Lüppo-Cramer: Phot. Korr. **46**, 269 (1909).
(18) Eder, J. M.: Phot. Korr. **46**, 277 (1909).
(19) Sheppard, S. E.: J. Franklin Inst. **210**, 587 (1930).
(20) Vogel, H. W.: Photochemie und Beschreibung der photographischen Chemikalien, 5th Edition (D. E. König). Gustav Schmidt, Berlin (1906).
(21) Brooker, L. G. S., Hamer, F. M., and Mees, C. E. K.: J. Optical Soc. Am. **23**, 216 (1933).
(22) Sheppard, S. E., and Mees, C. E. K.: Investigations on the Theory of the Photographic Process, pp. 273–5. Longmans, Green and Co., London (1907).
(23) Sheppard, S. E.: Colloid Symposium Monograph **3**, 76 (1925).
(24) von Hübl, A.: Z. wiss. Phot. **24**, 133 (1936).
(25) Lüppo-Cramer: Z. wiss. Phot. **30**, 1 (1931).
(26) Heisenberg, E.: Veröffentlich. wiss. zentral-Lab. phot. Abt. Agfa **3**, 115 (1933).
(27) Leermakers, J. A., Carroll, B. H., and Staud, C. J.: J. Chem. Phys. **5**, 893 (1937).

(28) Leermakers, J. A.: J. Chem. Phys. **5**, 889 (1937).

(29) Webb, J. H.: J. Optical Soc. Am. **26**, 367 (1936).

(30) Toy, F. C., and Harrison, G. B.: Proc. Roy. Soc. (London) **A127**, 613, 629 (1930).

(31) Hilsch, R., and Pohl, R. W.: Z. Physik **77**, 421 (1932).

(32) Wagner, C., and Beyer, J.: Z. physik. Chem. **B32**, 113 (1936).

(33) Carroll, B. H., and Hubbard, D.: Bur. Standards J. Research **9**, 529 (1932).

(34) Sheppard, S. E., Trivelli, A. P. H., and Loveland, R. P.: J. Franklin Inst. **200**, 51 (1925).

(35) van Kreveld, A., and Jürriens, H. J.: Physica [IV] **4**, 297 (1937).

(36) van Kreveld, A., and Jürriens, H. J.: Physica [IV] **4**, 285 (1937).

(37) Eggert, J., and Noddack, W.: Z. Physik **31**, 922 (1925).

(38) Sheppard, S. E., and Crouch, H.: J. Phys. Chem. **32**, 751 (1928).

(39) Leermakers, J. A., Carroll, B. H., and Staud, C. J.: J. Chem. Phys. **5**, 878 (1937).

(40) Joly, J.: Brit. J. Phot. **52**, 551 (1905).

(41) Zchodro, N.: J. chim. phys. **26**, 59 (1929).

(42) Leszynski, W.: Z. wiss. Phot. **24**, 261 (1926).

~~(43) Tollert, H.: Z. physik. Chem. **140A**, 355 (1929).~~

(44) Bokinik, J. I., and Iljina, Z. A.: Acta Physicochim. U.R.S.S. **3**, 383 (1935).

(44a) Scheibe, G.: Naturwissenschaften **25**, 795 (1937).

(45) Semerano, G.: Ann. chim. applicata **25**, 473 (1935).

(46) Semerano, G.: Gazz. chim. ital. **66**, 154 (1936).

(47) Mecke, R., and Semerano, G.: Z. wiss. Phot. **36**, 25 (1937).

(47a) Sheppard, S. E., Lambert, R. H., and Walker, R. D.: Nature **140**, 1096 (1937).

(48) Kieser, K.: Dissertation, Freiburg, i/B, 1904.

(49) Trivelli, A. P. H., and Sheppard, S. E.: Monographs on the Theory of Photography, No. 1. Eastman Kodak Co., Rochester (1921).

(50) Sheppard, S. E.: Proc. Roy. Soc. (London) **A82**, 256 (1909).

(51) Franck, J., and Eucken, A.: Z. physik. Chem. **20B**, 460 (1933).

(52) Sheppard, S. E., Lambert, R. H., and Keenan, R. A.: J. Phys. Chem. **36**, 174 (1932).

(53) Wulff, P., and Seidel, K.: Z. wiss. Phot. **28**, 239 (1930).

(54) Bokinik, J. I.: Trans. Kino-Photo Research Inst. (Moscow) **3**, 14 (1935).

(55) Bagdassarjan, K. S., and Rabinovitch, A. J.: Trans. Kino-Photo Research Inst. (Moscow) **3**, 5 (1935).

(56) Rabinovitch, A. J.: Acta Physicochim. U.R.S.S. **3**, 359 (1935).

(57) Sheppard, S. E.: Phot. J. **32**, 300 (1908).

(58) Scheibe, G.: Z. angew. Chem. **49**, 563 (1936).

(59) Scheibe, G., Kandler, L., and Ecker, H.: Naturwissenschaften **25**, 75 (1937).

(60) Scheibe, G., Mareis, A., and Ecker, H.: Naturwissenschaften **25**, 474 (1937).

(61) Jelley, E. E.: Nature **138**, 1009 (1936).

(62) Jelley, E. E.: Nature **139**, 631 (1937).

(63) Fisher, N. I., and Hamer, F. M.: Proc. Roy. Soc. (London) **A154**, 703 (1936).

(64) Brooker, L. G. S., and Keyes, G. H.: J. Am. Chem. Soc. **58**, 659 (1936).

(65) Bokinik, J. I.: Kino-Photo Ind. **3**, 84 (1933).

(66) Chibisoff, K. V.: Kino-Photo Ind. **3**, 90 (1933).

(67) Bancroft, W. D., Ackerman, J. W., and Gallagher, C.: Proc. Natl. Acad. Sci. U. S. **17**, 407 (1931).

(68) Lüppo-Cramer: Neue Beitrage zur Kenntnis der Desensibilizierung, Eders Handbuch III, 3 (1932).

(69) Lüppo-Cramer: Phot. Ind. **25**, 93 (1927).
(70) Lüppo-Cramer: Phot. Ind. **24**, 1118 (1926).
(71) Lüppo-Cramer: Phot. Ind. **28**, 365 (1930).
(72) Weber, K.: Z. wiss. Phot. **35**, 124 (1936).
(73) Weber, K.: Z. wiss. Phot. **36**, 1 (1937).
(74) Lüppo-Cramer: Phot. Korr. **68**, 197 (1932).
(75) Mudrovčič, M.: Phot. Korr. **70**, 23 (1934).
(76) Blau, M., and Wambacher, H.: Z. wiss. Phot. **35**, 211 (1936).
(77) Ollendorff, G., and Rhodius, R.: Z. wiss. Phot. **35**, 119 (1936).
(78) Lüppo-Cramer: Z. wiss. Phot. **36**, 156 (1937).
(79) Lüppo-Cramer: Z. wiss. Phot. **35**, 197 (1936).
(80) Trivelli, A. P. H.: J. Franklin Inst. **207**, 765 (1929).
(81) Lüppo-Cramer: Phot. Korr. **61**, 12 (1925).
(82) Sheppard, S. E.: Phot. J. **70**, 439 (1930).
(83) Blau, M., and Wambacher, H.: Z. wiss. Phot. **33**, 191 (1934).
(84) Blau, M., and Wambacher, H.: Sitzber. Akad. Wiss. Wien, Math.-naturw. Klasse **II**, **144**, 403 (1935).
(85) Blau, M., and Wambacher, H.: Z. wiss. Phot. **34**, 253 (1935).
(86) Carroll, B. H., and Kretchman, C. N.: Bur. Standards J. Research **10**, 449 (1932).
(87) Carroll, B. H.: J. Phys. Chem. **29**, 693 (1925).
(88) Mauz, E.: Z. wiss. Phot. **27**, 49 (1929).
(89) Lüppo-Cramer: Z. wiss. Phot. **35**, 197 (1936).
(90) Hübl, A.: Phot. Rundschau **62**, 171 (1925).

PHOTOSYNTHESIS[1]

WINSTON M. MANNING

Wisconsin Geological and Natural History Survey, Madison, Wisconsin

Received May 25, 1938

I. INTRODUCTION

In this review major emphasis will be placed on the photochemical and kinetic aspects of photosynthesis. The influence of the various physiological factors is more fully discussed in other recent reviews of photosynthesis (23, 24, 58, 72).

Except for studies of the physical and chemical properties of extracted plant pigments, investigations of photosynthesis are practically limited to a study of living plants. This limitation introduces complications not found in non-biological photochemical studies. In the first place, other chemical reactions, thermal as well as photochemical, undoubtedly occur during a period of photosynthesis. Unless proper allowance is made, these reactions may be of sufficient magnitude to obscure the significance of the photosynthesis measurements. In the second place, variations in factors influencing photosynthesis must be limited to those which will not kill or seriously injure the plant during the time when measurements are being made. In many cases, moreover, a variation in a particular environmental (external) factor may influence photosynthesis indirectly through its effect in the plant on internal factors other than those directly connected with the photosynthetic mechanism. This is particularly true for experiments with the higher plants.

Emerson (23) has discussed more fully some of the limitations involved in photosynthesis research.

II. THE MEASUREMENT OF PHOTOSYNTHESIS

Only a brief outline of experimental procedure will be given here. More extensive descriptions of the earlier methods which have been employed may be found in the monographs of Spoehr (70) and Stiles (74). Details of later procedures may be obtained from the original papers.

Photosynthesis is usually measured by determining either the amount of carbon dioxide consumed or the amount of oxygen liberated, or both.

---

[1] Contribution No. 11 to the Third Report of the Committee on Photochemistry, National Research Council.

Less direct methods may also be used, such as the measurement of the change in dry weight or sugar content of the plant material under investigation. However, results so obtained may involve factors other than the photosynthetic process.

The measurement of photosynthesis in land plants

With land plants photosynthesis may be measured by using either an entire plant or only part of the plant (often a single leaf). When a single leaf is studied, it is often detached from the rest of the plant, although many recent investigators have worked with attached leaves (41, 59, 60). In either case the material to be investigated is usually enclosed in a light-transmitting chamber.[2] The change in carbon dioxide or oxygen composition during a period of illumination or darkness may then be determined. In practice a flow method is often employed in order to maintain a nearly constant carbon dioxide concentration in the reaction chamber.

The change in gas composition during a period of darkness gives a measure of respiration. It is usually assumed that, for a given temperature, this process proceeds at the same rate in light as in darkness. A correction for respiration is therefore made in calculating absolute photosynthetic rates.

The change in oxygen and carbon dioxide may be determined by gas analysis (17), but other methods, in which only carbon dioxide is determined, are more frequently used.

In the conductivity method (43, 59, 60, 71, 76), the carbon dioxide is absorbed by a solution of alkali at constant temperature (± 0.01°C.). The conductivity of the hydroxide–carbonate mixture gives an accurate measure of the amount of carbon dioxide absorbed. With this method a continuous record of photosynthetic (or respiratory) rate may be obtained. Thomas and Hill (76) constructed a chamber large enough to enclose a field plot of wheat or alfalfa plants 6 feet square, and used the conductivity method to obtain a continuous record of photosynthesis and respiration, the measurements sometimes extending over a period of several weeks.

Instead of measuring the conductivity of the hydroxide–carbonate mixture, some investigators have titrated the mixture with standard acid (41). This method requires less apparatus than the conductivity method, but it is not as suitable for continuous measurements.

McAlister (53) has recently developed a very sensitive spectrometric method for determining carbon dioxide. This method is well adapted for continuous measurements of photosynthesis in land plants. A closed

---

[2] In single leaf studies the chamber may be attached to the under side of the leaf, with the leaf forming part of the chamber wall (41, 60). This permits nearly normal air circulation and transpiration.

system is used, with the gas rapidly circulating through the plant chamber and through an optical absorption tube. The absorption by the 4.2–4.3μ band of carbon dioxide is determined with a rock salt spectrograph and a vacuum thermocouple. A notable characteristic of this method is its rapid response to changes in photosynthetic rate.

Photosynthesis measurements in algae and other aquatic plants

Photosynthesis measurements in aquatic plants are usually carried out with the plant material suspended in water. However, both van den Honert (77) and van der Paauw (78) have worked with moist films of *Hormidium* (a very small filamentous blue-green alga) attached to glass plates. The rate of oxygen evolution by the suspended plant material is usually used as the criterion of photosynthetic rate.

The manometric method of Warburg (84) has been widely used for measuring changes in oxygen concentration in experiments with aquatic plants. In this method the plant material is suspended in a carbonate–bicarbonate buffer mixture (usually about 0.1 molar), and placed in a closed glass vessel connected to a manometer. The buffer concentration is high enough to maintain a practically constant carbon dioxide partial pressure in the gas phase, so that the increase in gas volume due to oxygen evolution can be read directly on the manometer. Vigorous shaking is necessary to maintain equilibrium between gas and liquid phases. With some modifications the manometric method can be applied to measurements carried out with an unbuffered nutrient solution (9, 85). This modification requires the use of two vessels and depends upon the difference in solubility of carbon dioxide and oxygen in the nutrient solution. With this differential type of manometer both oxygen and carbon dioxide changes can be measured.

Another method frequently employed, especially in ecological studies, is the determination of dissolved oxygen in closed vessels by titration (Winkler method). This method avoids the use of the somewhat non-physiological buffer mixture and is much simpler than the differential manometric method. However, it does not permit a series of measurements on a single sample.

Petering and Daniels (62) have recently applied the dropping-mercury electrode to a determination of dissolved oxygen changes in photosynthesis. As in the manometric method, repeated measurements may be made on a single sample of plant suspension. In at least two respects, this method is superior to the usual manometric method. It does not necessitate the use of buffer mixtures and it does not involve an equilibrium between gas and liquid phases. In speed of response it compares favorably with the spectrometric method of McAlister (53).

III. GENERAL DESCRIPTION OF THE PHOTOSYNTHETIC PROCESS

The equation for the reaction involved in photosynthesis in green plants is often written as follows:

$$CO_2 + H_2O \rightarrow 1/6\ (C_6H_{12}O_6) + O_2 \qquad \Delta H = 112{,}000\ \text{cal.} \qquad (I)$$

This equation, when reversed, becomes the one usually used to represent the normal respiratory process.

It is usually assumed that formaldehyde is the first product of photosynthesis, and that subsequent polymerization is responsible for the formation of glucose or other carbohydrates. If formaldehyde is the first product, then ΔH for equation I becomes 134,000 cal. The subsequent polymerization reaction will then be exothermic. The necessary energy for photosynthesis is assumed to come from light absorbed by the two chlorophyll pigments in the plant, although it is possible that energy absorbed by other pigments, such as carotene and xanthophyll, may sometimes be utilized.[3] It is rather remarkable that light of wave length as long as 7000 Å. (see figure 2), for which $Nh\nu$ is equal to 40,500 cal., will bring about a reaction for which ΔH is 112,000 cal. Evidently photosynthesis involves a more complex series of endothermic reactions than has been observed for any non-biological photoreaction.

Photosynthesis at different wave lengths

Figures 1 and 2 show a rather close correlation between relative rates of photosynthesis at different wave lengths (Hoover (42)) and the absorption spectra (in ether solution) of chlorophylls *a* and *b* (93). Hoover's results were obtained with young wheat plants, using equal incident light intensities (less than 300 foot-candles) at the various wave lengths. A wheat leaf contains enough chlorophyll to absorb a considerable fraction of the incident radiation, even in the region between 5000 and 6000 Å.; this accounts for the relatively high minimum in the photosynthesis curve (figure 2). Chlorophyll absorbs more strongly at 3660 Å. than in the region between 5000 and 6000 Å. (90). Consequently the low rate of

---

[3] Except in the *Myxophyceae* (blue-green algae) the chlorophyll pigments are found only in restricted regions of the plant cell, known as chloroplasts. These regions also contain the yellow pigments carotene and xanthophyll. Frequently a large number of the cells in a green leaf contain no chloroplasts, while in the remaining cells the number may vary from one to many. Consequently only a small fraction of the total leaf volume consists of chloroplasts and hence is able to carry on photosynthesis. In many of the algae, however, the chloroplasts constitute a much larger fraction of the total plant material. For example, the single chloroplast in the unicellular green alga *Chlorella* probably occupies half of the cell volume.

This large proportion of photosynthetically active plant material constitutes one reason for the widespread use of *Chlorella* in photosynthesis investigations.

photosynthesis at 3660 Å. (figure 2) indicates a much lower quantum efficiency for the process than in the region from 4000 to 7000 Å. Below 3000 Å. ultraviolet radiation is distinctly injurious (57, 4).

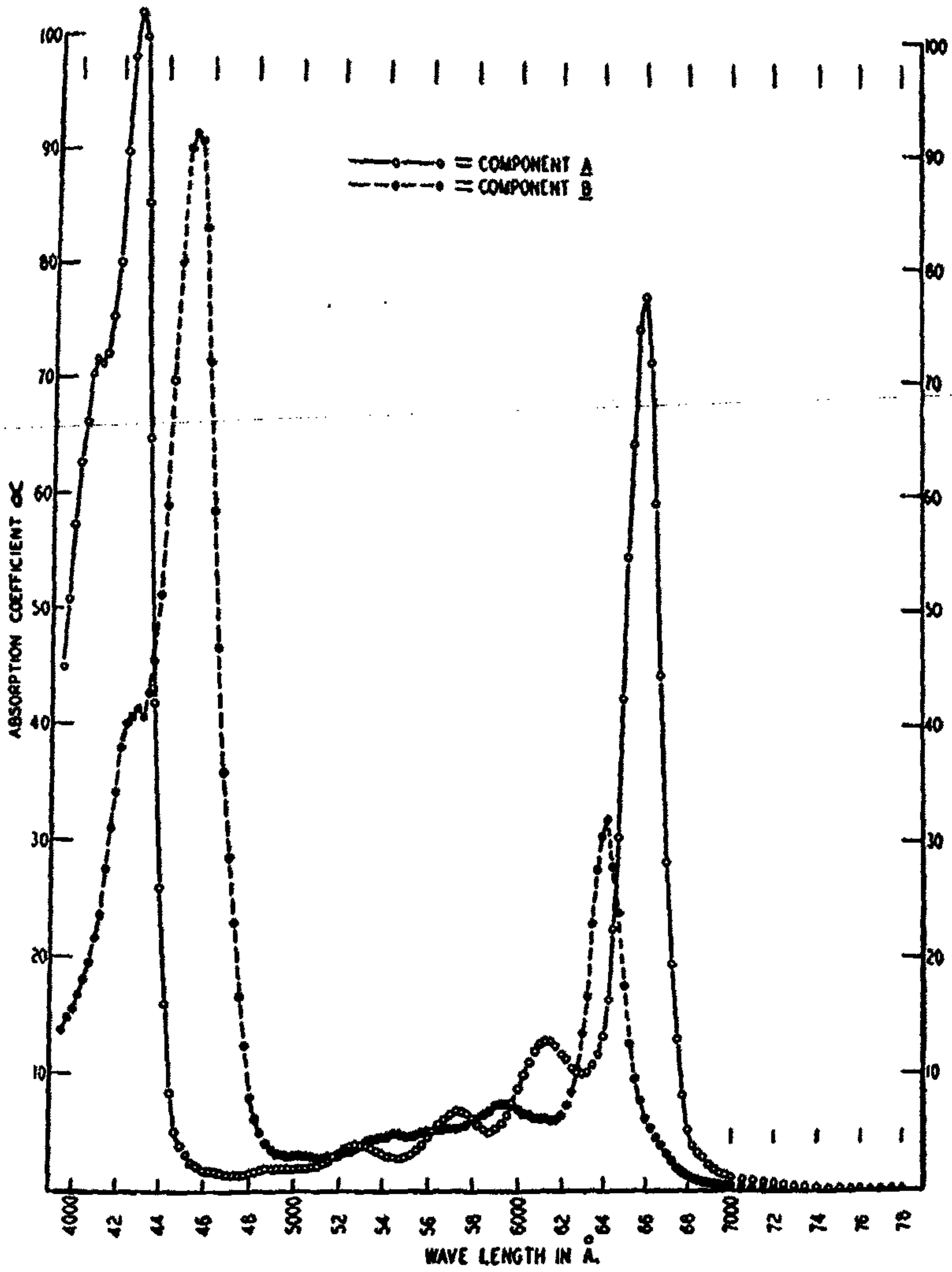

Fig. 1. The absorption spectra of chlorophylls *a* and *b* in ether (Zscheile (93))

The formaldehyde hypothesis

The occurrence of formaldehyde as an intermediate product of photosynthesis has been neither proved nor disproved (58). In any event its concentration must be very low, even during rapid photosynthesis, since concentrations higher than a few hundredths of a per cent are distinctly toxic. The presence of small amounts of formaldehyde in green leaves has been reported by a number of investigators. Others have found that plants in the dark can utilize low concentrations of formaldehyde to form carbohydrates. These observations add plausibility to the hypothesis that formaldehyde is an intermediate product in the photosynthetic process, but do not constitute proof of the hypothesis, since formaldehyde may be produced by other metabolic processes. Also, formaldehyde is only one of several organic compounds which may be utilized by plants in the formation of carbohydrates (58).

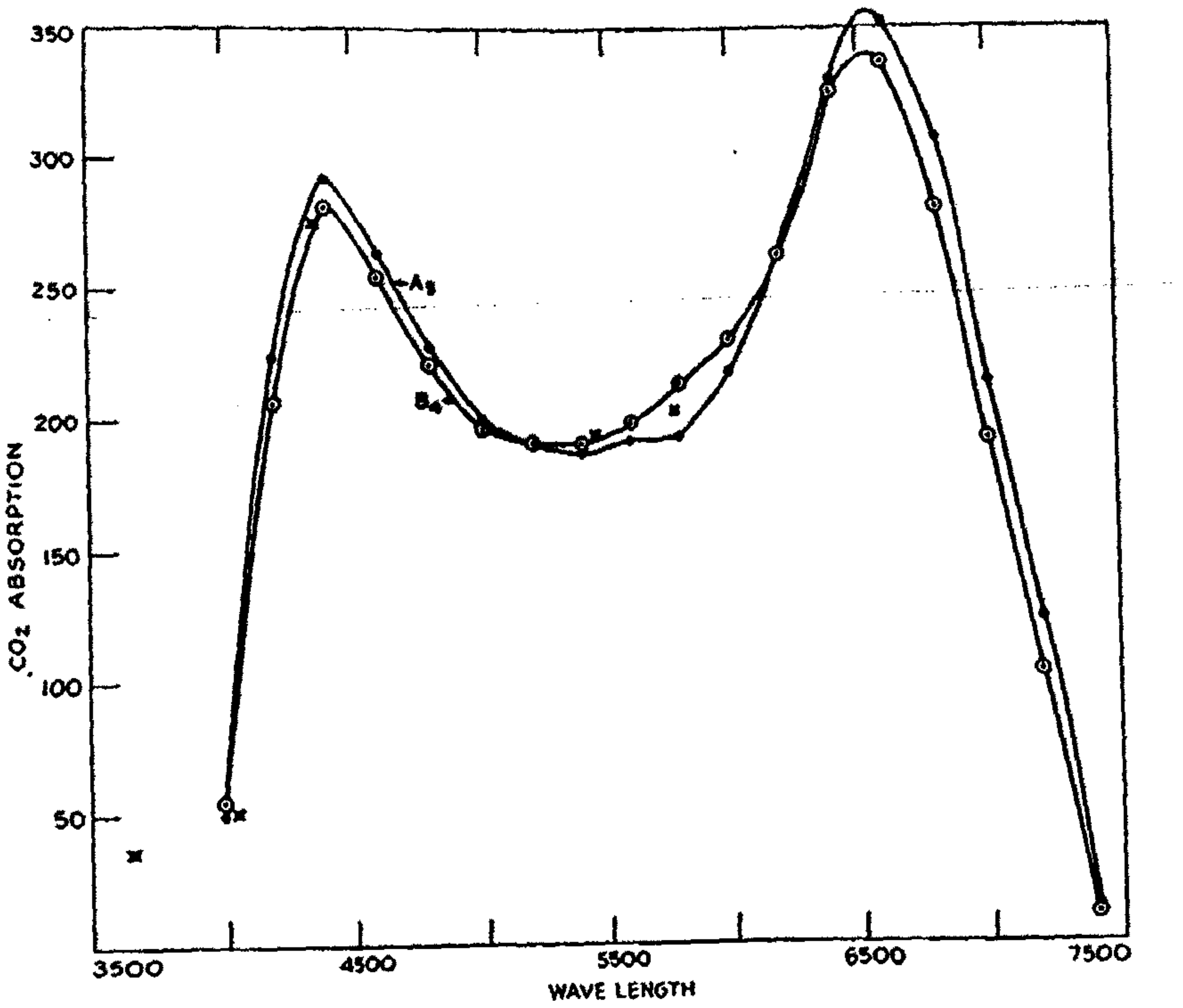

FIG. 2. Rate of photosynthesis as a function of wave length (low light intensity). A_3, the corrected form of the curve obtained with large Christianson filters; B_4, the corrected form of the curve obtained with small Christianson filters. Points marked × are the results obtained with line filters and quartz mercury arc. (Hoover (42)).

The photosynthetic quotient

The ratio of the number of moles of carbon dioxide absorbed to the number of moles of oxygen produced, $\Delta CO_2/\Delta O_2$, is called the photosynthetic quotient.[4] If glucose or some other carbohydrate is the final product of photosynthesis, the photosynthetic quotient should have a value of 1, as in equation I. Maquenne and Demoussy (56) and Willstätter and Stoll (89) investigated a large number of different plants and found a quotient very close to unity. Apparent values markedly different from unity are sometimes obtained, but these may often be attributed to the effects of abnormal respiration or other processes.

The value of the photosynthetic quotient constitutes the principal proof that a carbohydrate is the first product of photosynthesis. Many investigators have attempted to identify this carbohydrate product. From present evidence it may be considered probable that a hexose is the first product formed, though the prior formation of sucrose remains as a possibility.[5]

In diatoms (and also in some other plants) the products of photosynthesis are stored principally in the form of oils rather than as carbohydrates. Barker (10) has measured the photosynthetic quotient in two species of diatoms in an effort to determine whether the oils are formed as primary products of photosynthesis or whether they are secondary metabolic products. For complete conversion of the carbon dioxide to oils, the quotient should be approximately 0.70 instead of 1.00. For both species of diatoms Barker found a quotient close to 0.95, with a tendency for the value to increase slightly with increasing light intensity. He concluded that 10 per cent or less of the photosynthetic products appeared as stored fat and that this fat production was probably the result of a secondary reaction.[6]

The effect of light intensity and temperature on the rate of photosynthesis

Figure 3 shows diagrammatically the relation between the rate of photosynthesis and light intensity at high carbon dioxide concentration. Curve A represents the behavior at a relatively low temperature, perhaps 10°C.; curve B is for a higher temperature, such as 20°C.

While the type of behavior shown in figure 3 is characteristic of most

---

[4] Some writers apply the term "photosynthetic quotient" to the reciprocal of this ratio, i.e., $\Delta O_2/\Delta CO_2$.

[5] More complete discussions of this problem are given by Spoehr (reference 70, page 215) and Stiles (reference 74, page 151).

[6] When a simple alga, such as *Chlorella*, is grown under long-continued constant conditions, including constant illumination, it is probable that an equilibrium is reached between the rate (per unit of plant material) at which food is manufactured by photosynthesis and the rate at which it is used in growth. Under these conditions the *apparent* photosynthetic quotient (i.e., uncorrected for respiration) should give a measure of the average state of oxidation of the entire cell material. The oxygen eliminated during the reduction of nitrates to protein material should contribute noticeably to a lowering of the apparent quotient.

plants which have been studied, the exact numerical behavior may vary widely. Thus, in many land plants the maximum photosynthetic rate may not be reached until the light intensity approaches that of sunlight, while in other plants, particularly some of the algae, one-tenth of this intensity may produce the maximum rate.[7]

The shape of a rate-light intensity curve will depend on the fraction of light absorbed by the plant material under investigation. With a thick leaf containing an abundance of chlorophyll, or with a dense suspension of algae, different portions of the plant material will be exposed to widely different light intensities. A very high incident intensity will then be necessary to produce a maximum photosynthetic rate in the chloroplasts farthest removed from the incident surface.

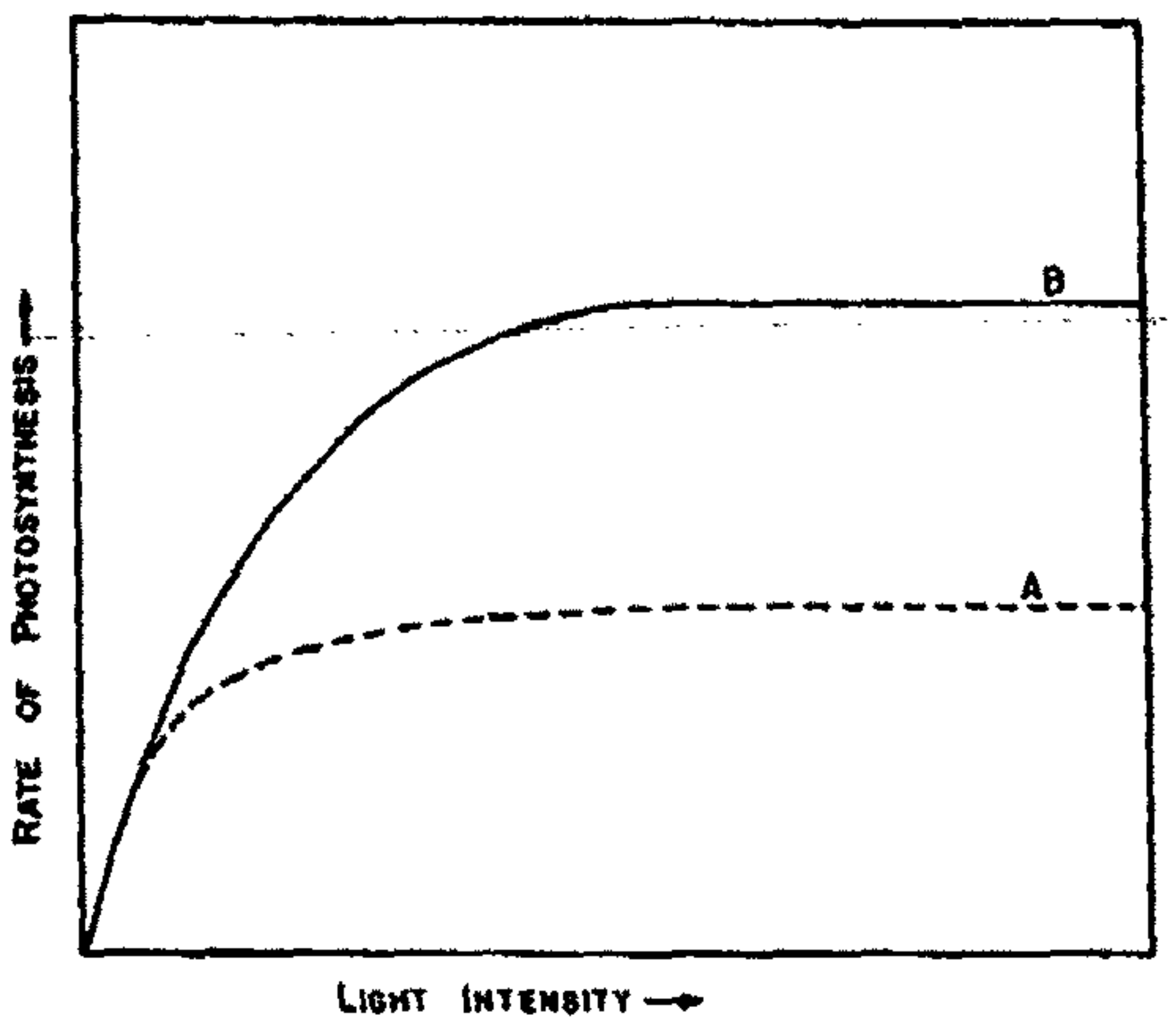

FIG. 3

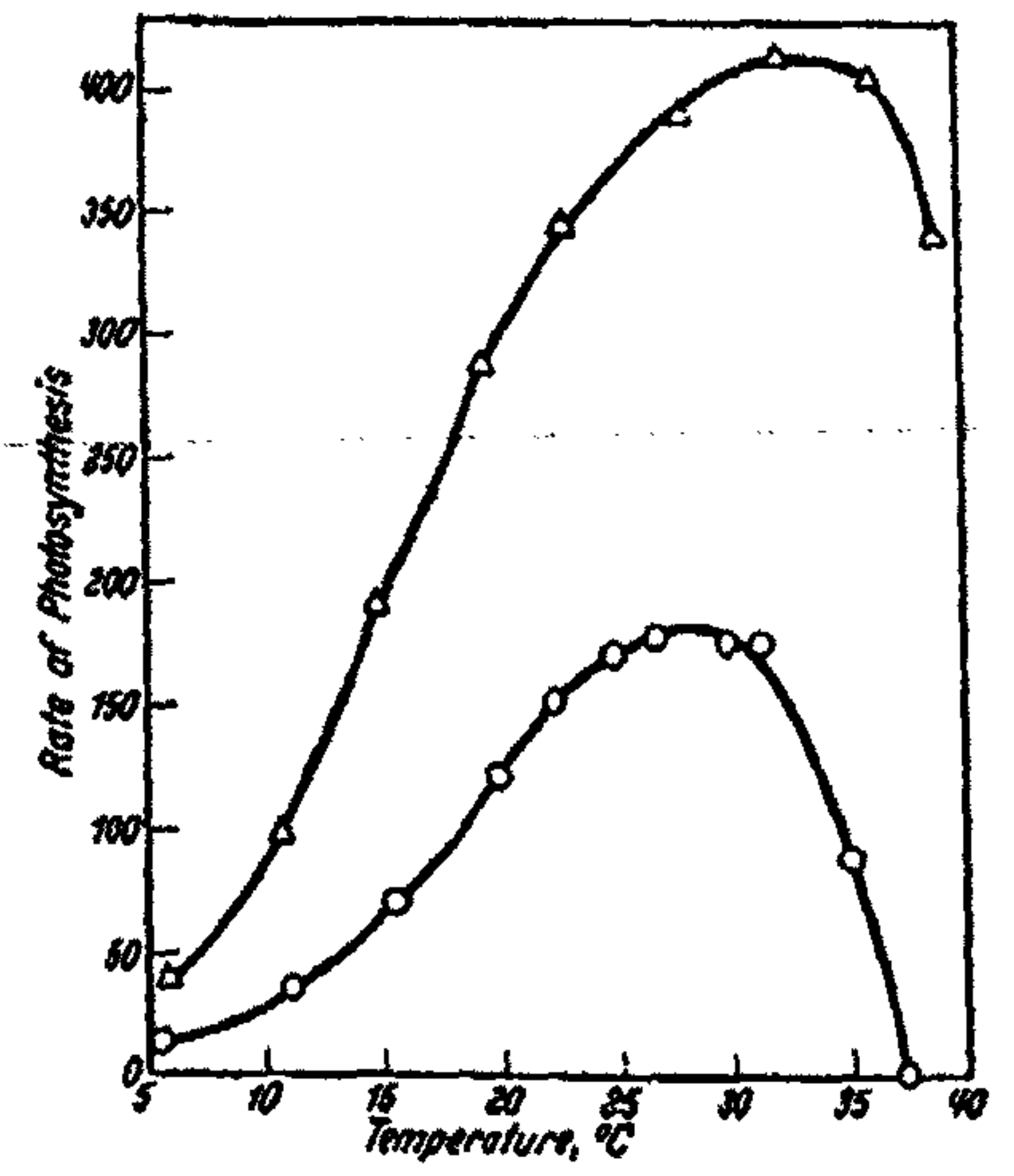

FIG. 4

FIG. 3. Rate of photosynthesis as a function of light intensity. A, low temperature curve; B, high temperature curve.

FIG. 4. Variation in rate of photosynthesis with temperature at high light intensities for *Nitzschia closterium* (O) and *Nitzschia palea* (Δ). Photosynthesis is expressed in cubic millimeters of evolved oxygen per hour per 10 cmm. of cells. (Barker (10)).

As shown in figure 3, the rate of photosynthesis is nearly independent of temperature at low light intensities, but becomes temperature-dependent at higher intensities. Thus, for *Chlorella* Warburg (82) found a temperature coefficient (Q_{10}) of unity at approximately 6 × 10^3 ergs per

---

[7] In some plants the rate of photosynthesis may increase to a maximum and then decrease again as the light intensity is increased (48, 54, 72). The reason for a decrease in rate at high intensities is not definitely known. It may be caused by some form of injury, or it may be caused by the simultaneous occurrence of photoöxidation processes.

cm.^{2} per second,[8] but a coefficient of from 2 to 5 (depending upon the temperature) at an intensity of approximately 100 × 10^3 ergs per cm.^{2} per second.

From the type of behavior shown in figure 3, as well as from other evidence to be discussed below, it must be concluded that photosynthesis is a complex cyclic reaction, involving at least one thermal reaction, usually known as the Blackman reaction,[9] in addition to whatever photoreactions are necessary. According to this view, at low light intensities, where the rate of photosynthesis is approximately proportional to the intensity, the time between the absorption of successive photons, by that portion of the mechanism involved in the reduction of a single carbon dioxide molecule, will be sufficient to permit the Blackman reaction to be completed. Light is then said to be the limiting factor. But at high intensities, where the rate has practically reached its maximum value (so-called light saturation), the rate will presumably be limited only by the rate of the Blackman reaction.[10] This implies that photons are absorbed so rapidly by the mechanism that the average time between the completion of the Blackman reaction and the next light absorption will be very short compared with the average time required for the Blackman reaction. An increase in temperature will increase the rate of the Blackman reaction without appreciably altering the rate of the light reaction.[11]

---

[8] In this research Warburg made only approximate estimates of absolute intensities.

[9] The term "Blackman reaction" as used in this paper refers to any reaction or reactions which contribute to the temperature dependence of the photosynthetic process. It is named for F. F. Blackman, who, in 1905 (12), formulated his principle of limiting factors in the following words: "When a process is conditioned as to its rapidity by a number of separate factors, the rate of the process is limited by the pace of the 'slowest' factor." Application of this principle did much to clarify the contradictory results of earlier research on photosynthesis.

Many subsequent investigators appear to have interpreted this principle too literally, i.e., they have assumed that for measurements under ideal conditions only a single factor could influence the rate of photosynthesis at any one time. According to this view, an increase in the intensity of a particular variable should result in an abrupt transition from direct dependence of the rate on this variable to complete independence. Such a transition is contrary to any reasonable kinetic formulation of the process.

[10] According to a recent mechanism of Franck and Herzfeld (34), the rate of the Blackman reaction is not limiting at high light intensity (see page 850).

[11] Warburg and Uyesugi (87) and Yabusoe (92) found some similarities between the Blackman reaction and the rate of decomposition of hydrogen peroxide by the enzyme catalase. There has therefore been a widespread belief that the Blackman reaction consists of a reaction between catalase and a peroxide. Hence many postulated mechanisms have included hydrogen peroxide or organic peroxides as intermediate products in photosynthesis. However, Emerson and Green (28) have recently made further comparisons of the two reactions without finding any significant similarity.

Figures 4 and 5 illustrate the effect of temperature on the rate of photosynthesis at high light intensity and high carbon dioxide concentration. Figure 4 gives the results obtained by Barker (10) with two species of diatoms; figure 5 gives the results obtained by Craig and Trelease (21) with *Chlorella vulgaris*. The lower curves in figure 5 are for rate measurements in 99.9 per cent heavy water. (The heavy water experiments will be discussed below, page 828.) The decrease in photosynthetic rate at high temperatures is probably due to injury to the plant material. Further evidence of injury is found in the fact that the photosynthetic rate at high temperatures is not constant, but decreases with time. Injury may be due to deactivation of enzymes (or of an enzyme-producing mechanism) connected with the Blackman reaction, or it may be due to a change in the physical condition of the chloroplasts.

The Arrhenius equation may be used to calculate apparent activation energies for the temperature-sensitive reaction in photosynthesis. However, in view of the complex system involved, the significance of the figures so obtained is doubtful. The apparent activation energy varies for different species and decreases with increasing temperature. The low temperature value for *Chlorella pyrenoidosa* and *Hormidium flaccidum* has been reported as being approximately 20,000 cal. (27, 78). Barker (10) found a value of about 30,000 cal. for the diatoms *Nitzschia closterium* and *Nitzschia palea* (see figure 4). Emerson and Green (27) found a value of approximately 50,000 cal. for *Chlorella vulgaris* and for the marine alga *Gigartina harveyana*.

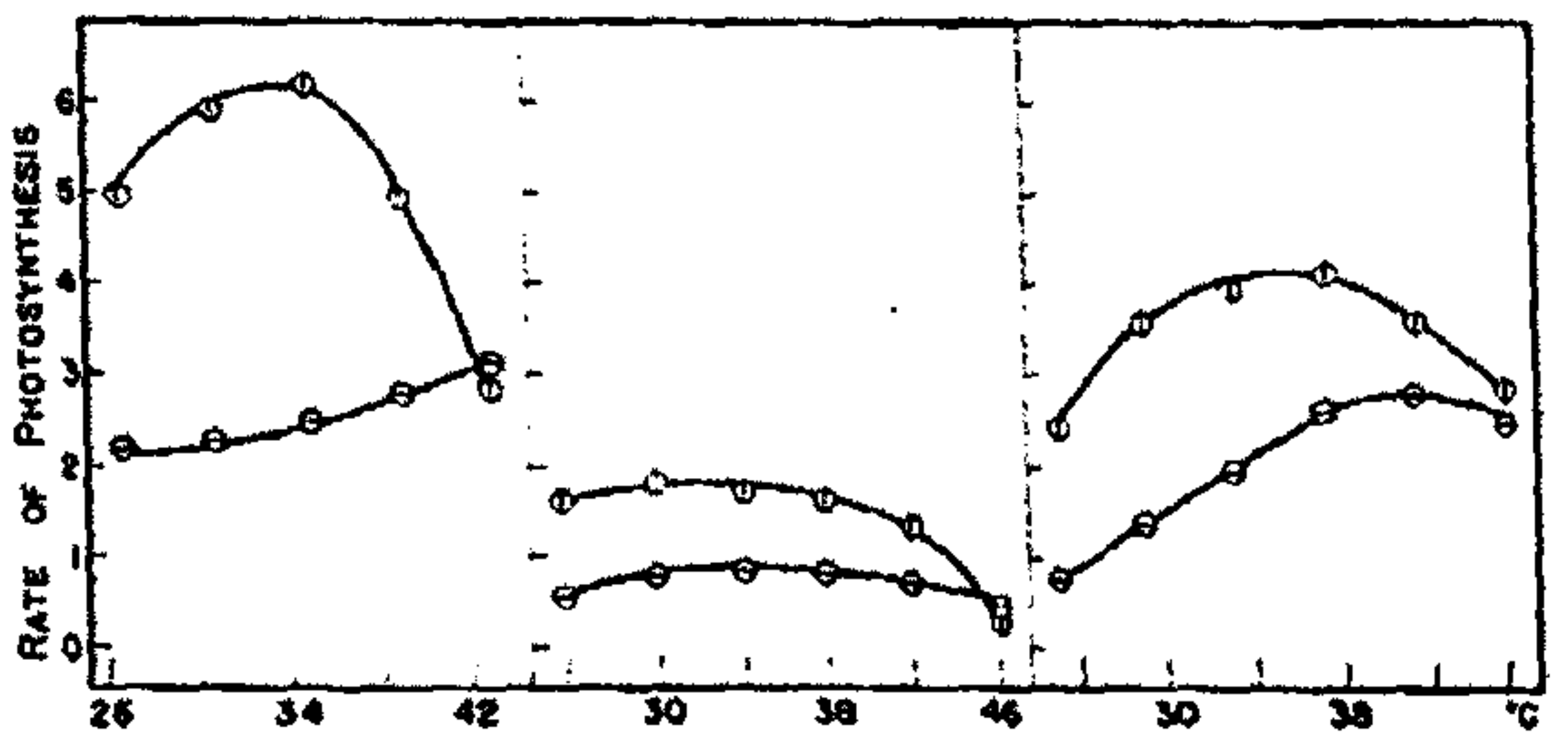

FIG. 5. Rate of photosynthesis as a function of temperature. For H_2O shown by circles with vertical bars, and for D_2O shown by circles with horizontal bars. (Craig and Trelease (21)).

The effect of carbon dioxide concentration on the rate of photosynthesis

Variation in carbon dioxide concentration apparently affects the rate of photosynthesis in a manner similar to variation in light intensity. Van den Honert (reference 77, page 225), working with moist films of *Hormid-*

ium at 12° and 20°C., and using high light intensity, obtained curves essentially like those of figure 3 (with light intensity replaced by carbon dioxide concentration). In both curves the rate of photosynthesis reached its maximum value at a carbon dioxide concentration of about 0.04 per cent by volume. (Normal carbon dioxide concentration in air is approximately 0.03 per cent.) For young wheat plants Hoover, Johnston, and Brackett (43) found that a higher carbon dioxide concentration, approximately 0.15 per cent, was necessary for a maximum rate of photosynthesis (light intensity one-fourth of that of sunlight). Light saturation was not reached in this work; at higher light intensities still higher carbon dioxide concentrations would have been required. In general, the diffusion of carbon dioxide into a chloroplast will encounter more resistance in a leaf, where most of the chloroplast-containing cells are usually some distance from the leaf surface, than in a small unicellular or filamentous alga, where every vegetative cell is photosynthetically active and not surrounded by other cells. A higher carbon dioxide concentration will then be necessary for leaves in order to overcome this diffusion resistance.[12]

For *Chlorella* in liquid suspension Emerson and Green (29) found that a carbon dioxide concentration of 10 or 15 × 10^{-6} moles per liter was sufficient for maximum photosynthesis.

Smith (68), using the water plant *Cabomba*, has studied the effect of light intensity and carbon dioxide concentration on the photosynthetic rate. He found that both variables affected the rate in the same way.

However, there is disagreement concerning the effect of temperature at low carbon dioxide concentrations. According to van den Honert's curves (reference 77, page 225), temperature is without effect on the rate at low concentrations, but Warburg (82) and Emerson (23) found a high temperature coefficient for *Chlorella* at low carbon dioxide concentrations. Both Warburg and Emerson used the manometric method in their measurements; the *Chlorella* was suspended in carbonate-bicarbonate buffer mixtures and the concentration of free carbon dioxide was varied by varying the ratio of carbonate to bicarbonate. At least three possible objections may be raised to the use of these buffers for regulating carbon dioxide concentration: (*1*) In varying the carbon dioxide concentration, the pH is also varied. The high pH necessary to obtain limiting carbon dioxide concentrations may influence the photosynthetic rate. (*2*) A high concentration of carbonate or bicarbonate ions may inhibit photosynthesis. (*3*) It is possible that water plants may be able to use carbonate or bicarbonate in the photosynthetic process (3). Emerson and Green (29), working with phosphate buffers, found that within the range from pH 4.6 to 8.9, neither bicarbonate nor hydrogen ion influenced the rate of photo-

---

[12] The problem of diffusion resistance has been discussed by James (47).

synthesis at saturating concentrations of carbon dioxide. They concluded, however, that in carbonate mixtures at a higher pH, other factors, probably carbonate and bicarbonate concentrations as well as free carbon dioxide concentration, were influencing the rate of photosynthesis. Moreover, with the phosphate buffers, their measurements of photosynthesis in *Chlorella* as a function of carbon dioxide concentration more closely resembled van den Honert's results for *Hormidium* than Warburg's results for *Chlorella* in carbonate-bicarbonate buffers. On the basis of the results of Emerson and Green, it may be considered probable that van den Honert's curves (77), showing little or no temperature effect at low carbon dioxide concentration, are valid for *Chlorella* as well as for *Hormidium*.

Since a knowledge of the temperature effect at low carbon dioxide concentrations is of importance in choosing a mechanism for the photosynthetic process (see page 841), it appears desirable that a further study should be made of this effect in both algae and higher plants.

The influence of intermittent light on photosynthesis

Warburg (82), Emerson and Arnold (25), and Pratt and Trelease (64) have studied the effect of intermittent light on photosynthesis in *Chlorella*.

Warburg used a rotating sector which cut out half of the incident light. He found that at high light intensity and abundant carbon dioxide concentration a given amount of light produced more photosynthesis when absorbed intermittently by the *Chlorella* than when it was absorbed continuously. Moreover, the improvement in yield depended upon the frequency of the flashing. At low light intensities, intermittent light produced no improvement in yield.

The effect of intermittent light can be explained on the basis of the cyclic mechanism discussed above (page 823). Thus, after a sufficiently long period of intense illumination, most of the chlorophyll molecules would be activated (or combined in an unstable compound) and waiting to undergo the so-called Blackman reaction. Photons absorbed by these molecules would presumably be without effect on the photosynthetic rate. But, if this period of intense illumination were followed by a sufficiently long period of darkness, the Blackman or thermal reaction should continue until completed. Then, at the beginning of the next light flash, all of the photons would presumably be absorbed by chlorophyll molecules ready to undergo the next photosynthetic cycle. By combining very short light flashes with long dark periods it should be possible, according to this picture, to have a plant utilize intermittent light of high intensity as efficiently as it can utilize continuous light of low intensity.

Emerson and Arnold (25) have extended considerably the observations of Warburg. They used a neon tube as a light source, with an electrical circuit which gave very short light flashes. The circuit was constructed so that the length of the dark periods could be varied without appreciable effect on the light flashes. The *Chlorella* was suspended in a buffer mixture and photosynthesis was measured manometrically.

Figure 6 shows the results obtained by Emerson and Arnold in their study of the effect of dark time on the yield of photosynthesis per flash. The lower curve was obtained at 1.1°C., while the two upper series were obtained at 25°C. All of the measurements shown in figure 6 were made with *Chlorella* cells from the same culture. It appears that at 25°C. a dark period of 0.04 sec. is sufficient for practical completion of the thermal or Blackman reaction, while at 1.1°C. a period of 0.2 or 0.3 sec. is required for practical completion. In these experiments of Emerson and Arnold, the duration of each light flash was less than 2×10^{-5} sec., a period which is short compared with the average duration of the thermal reaction, at least at 1.1°C.

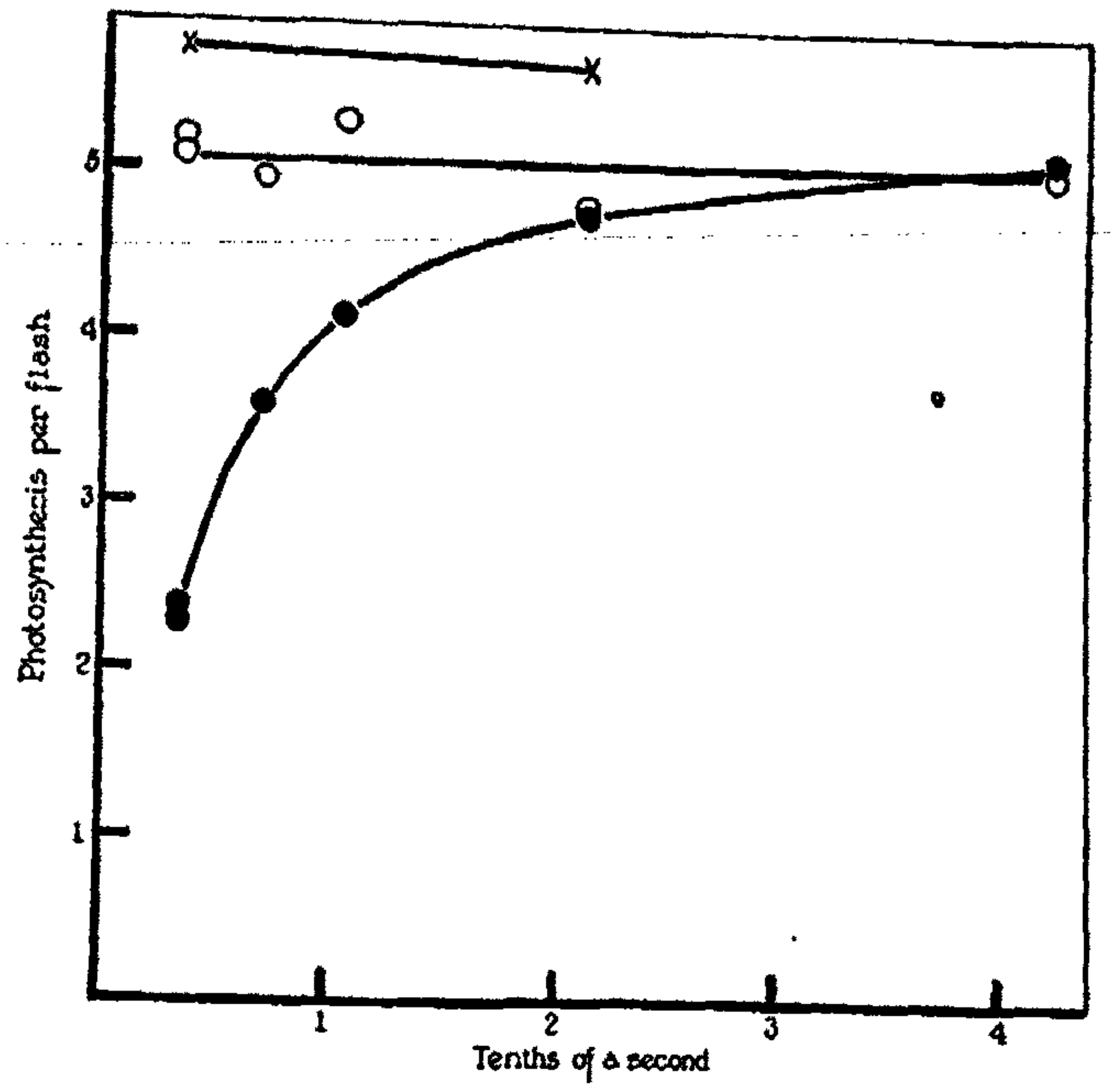

FIG. 6. The effect of dark time on the yield of photosynthesis per flash of light. Open circles are points made at 25°C.; solid circles at 1.1°C. The crosses are a check made at 25°C. (Emerson and Arnold (25)).

Figure 7 shows the results obtained with *Chlorella* at high light intensity and at 23.9°C. by Pratt and Trelease (64). Using *Chlorella* cells suspended in heavy water as well as in ordinary water, they studied the effect of flashing light on the rate of photosynthesis. Each light flash in these experiments lasted about 0.0045 sec. This period was much longer than that used by Emerson and Arnold. Consequently a considerable fraction of the chlorophyll molecules probably went through the reaction cycle more than once for each flash.

The point corresponding to a dark period of 0.0122 sec. on the upper curve in figure 7 is apparently slightly lower than the maximum, suggesting that the Blackman reaction is not quite completed in 0.01 sec. at 24°C. This is in approximate accord with indirect calculations of Emerson and Arnold (26) which indicated an *average* time of 0.012 sec. for the completion of a cycle (photochemical + Blackman reactions) in *Chlorella* at 25°C.

The lower curve in figure 7 was obtained from experiments in which the algae were suspended in heavy water. Evidently deuterium oxide retards the Blackman reaction without appreciably affecting the photochemical reaction, since, with a long dark period, the amount of photosynthesis per flash is the same in heavy water as in ordinary water.[13] These observations indicate that the specific effect of deuterium oxide is manifested in the Blackman reaction. Possibly the replacement of water by deuterium oxide may reduce the rate of the Blackman reaction by affecting a specific enzyme system.

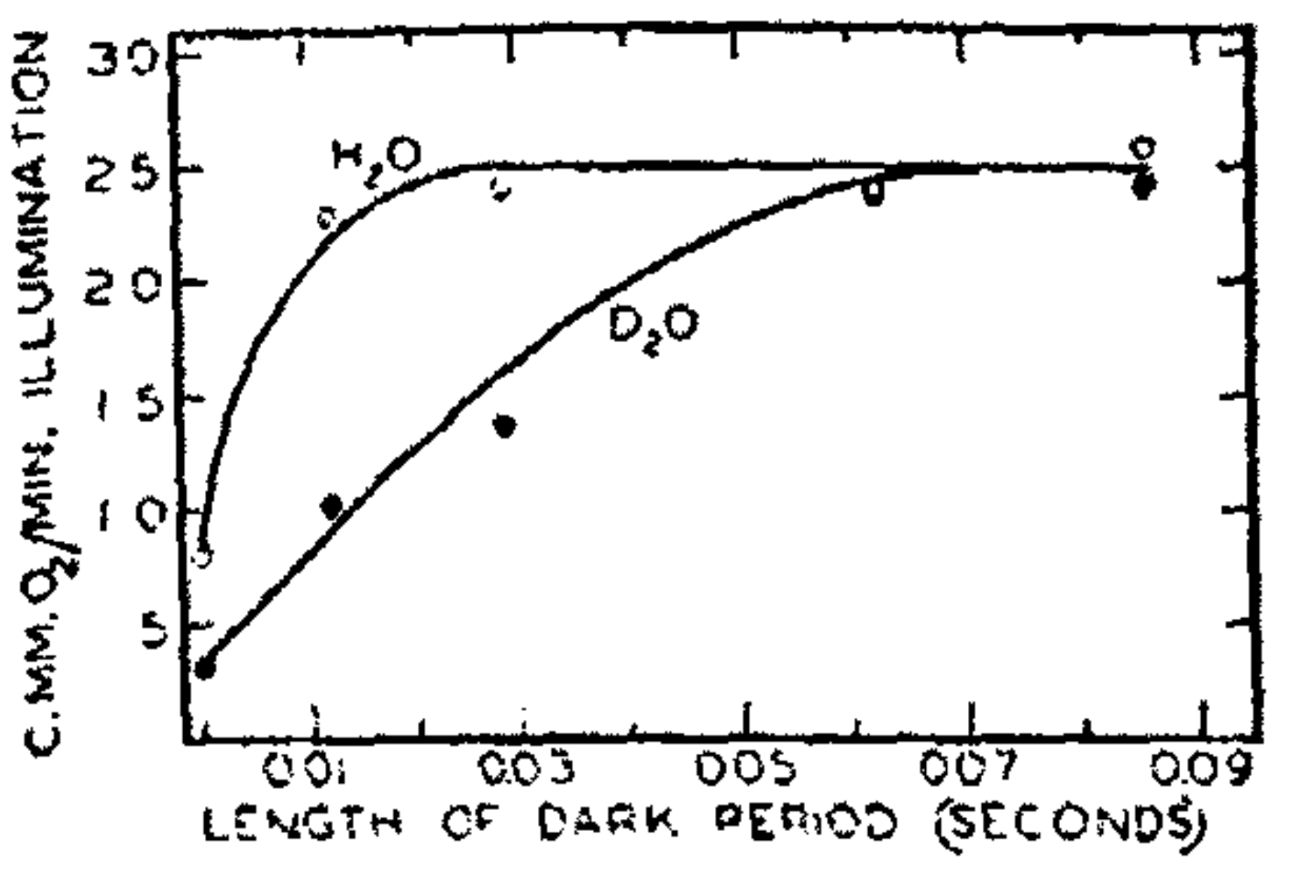

FIG. 7. Rate of photosynthesis in *Chlorella vulgaris* per minute of actual illumination as a function of the length of the dark period. The values are proportional to the photosynthesis per flash. (Pratt and Trelease (64)).

Emerson and Arnold (25) have studied the effect of low concentrations of hydrogen cyanide on photosynthesis in *Chlorella* in flashing light. With a hydrogen cyanide concentration of 1.14×10^{-4} moles per liter, the effect was very similar to that of 99.9 per cent deuterium oxide, as reported by

---

[13] With continuous light of high intensity, according to the measurements of Craig and Trelease (21), the rate of photosynthesis in D_2O is about 40 per cent of the rate in H_2O, except at very high temperatures (see figure 5), where the rate in H_2O falls more rapidly than the rate in D_2O. At low light intensities the rates in D_2O and H_2O become nearly equal. These observations are in agreement with the conclusions indicated by the flashing light experiments.

Pratt and Trelease (64) (see figure 7). The Blackman reaction was retarded but the maximum yield per flash was unchanged. But, if the hydrogen cyanide was replaced by a low concentration of phenylurethan or thymol, the maximum yield of photosynthesis per flash was decreased, with only a slight retardation of the Blackman reaction.[14]

Figure 8 shows the observations of Emerson and Arnold concerning the influence of carbon dioxide concentration on the yield of photosynthesis per flash. As before, the flash duration was less than 2×10^{-5} sec. They concluded from these experiments that carbon dioxide enters the process of photosynthesis either before or (less likely) coincident with the photochemical reaction. If chlorophyll alone were involved in the light reaction, then, according to their argument, a lower carbon dioxide concentration would not decrease the yield per flash but would necessitate longer dark periods for full utilization of the light. Since the opposite effect was actually found, Emerson and Arnold concluded that both chlorophyll and carbon dioxide (perhaps in combination) are required for the light reaction.

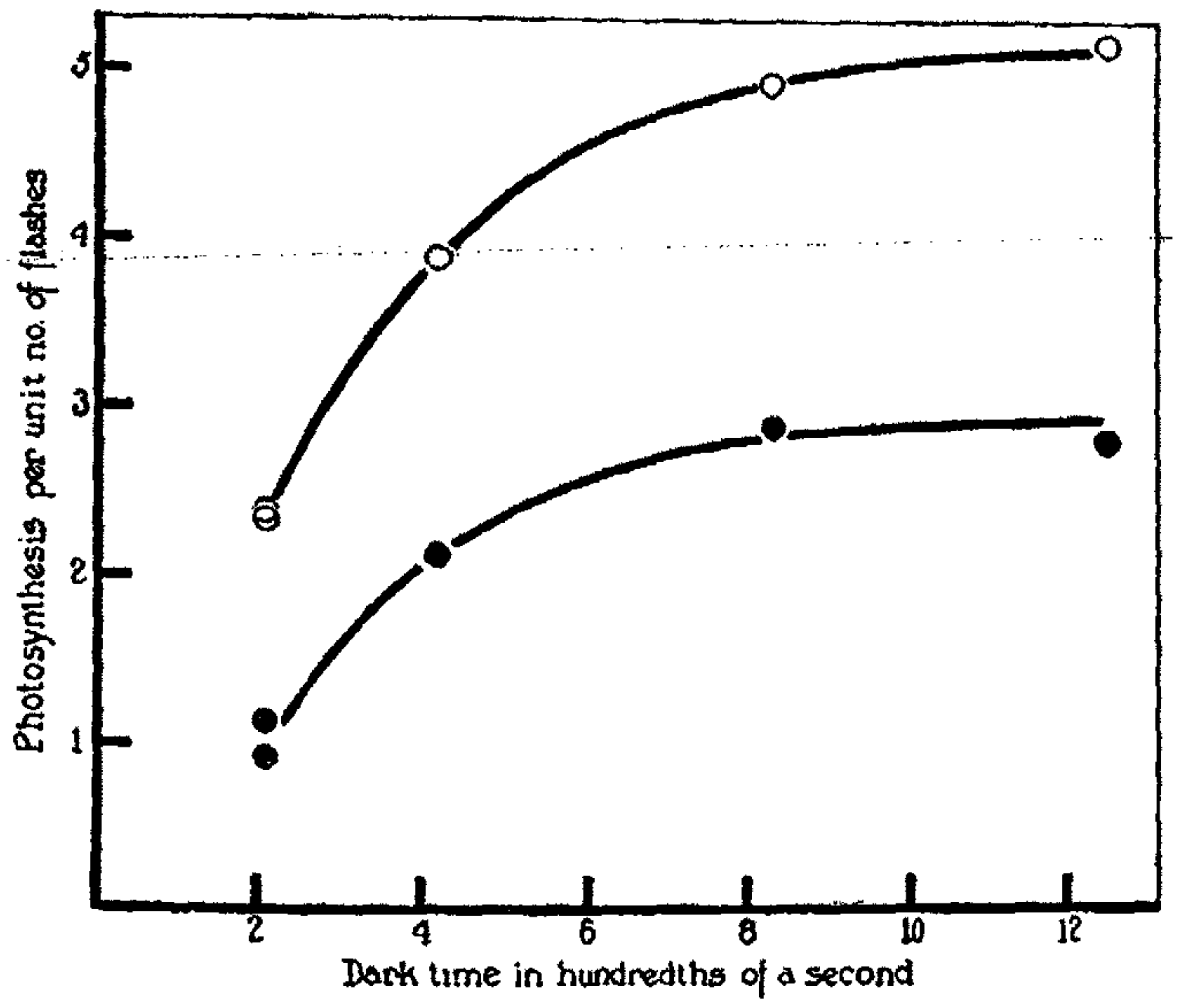

FIG. 8. The course of the dark reaction at two different concentrations of carbon dioxide. Open circles, carbon dioxide concentration = 71×10^{-6} moles per liter; solid circles, carbon dioxide concentration = 4.1×10^{-6} moles per liter. (Emerson and Arnold (25)).

[14] In continuous light, narcotics such as phenylurethan and thymol inhibit photosynthesis at both high and low light intensities, in contrast to hydrogen cyanide, which inhibits only at high intensities (83).

However, it appears that this conclusion is open to question from two points of view. In the first place, carbon dioxide concentration was varied by changing the proportion of carbonate to bicarbonate in the buffer mixtures. Later experiments of Emerson and Green (29) have thrown doubt on the validity of this method of obtaining low carbon dioxide concentrations (see page 825). Secondly, it appears that the argument of Emerson and Arnold (given in the preceding paragraph) would be strictly valid only if the average lifetime of an activated chlorophyll molecule were much longer than the average time required for the Blackman reaction. Otherwise, the lower curve in figure 8 could be interpreted as the resultant of two curves, one a slowly rising curve, like the lower curve in figure 7, and the other a falling curve representing a decrease in concentration of activated chlorophyll.

Although the behavior illustrated in figure 8 may not give very definite evidence concerning the order in which certain steps in the reaction cycle may occur, it probably indicates, as Emerson has pointed out (reference 23, page 319), that carbon dioxide enters into a reaction in the photosynthetic cycle other than the Blackman reaction, since, if the latter reaction alone were affected by carbon dioxide concentration, the maximum yield of photosynthesis per flash should remain constant. However, this last conclusion is still subject to the uncertainty concerning the influence of carbonate-bicarbonate buffers.

Other experiments involving the use of intermittent light will be discussed below (see pages 831 and 845).

The induction period in photosynthesis

A number of investigators have observed an induction period in photosynthesis, but the characteristics of this period appear to vary widely in different plant species. In the marine alga *Ulva*, Osterhout and Haas (61) found that about 2 hr. were necessary for attainment of a steady rate at high light intensity. In the moss *Mnium*, Briggs (14) found an induction period of nearly an hour. Emerson and Green (27) found a period of about 20 min. for the marine alga *Gigartina*. A period of 3 min. or less has been found in *Chlorella* (83), *Hormidium* (78), *Cabomba* (69), and wheat (53). After a 10-hr. period of darkness, however, McAlister found a longer induction period for wheat, about 12 min. Warburg found an induction period in *Chlorella* only at high light intensities, but for *Cabomba*, Smith observed an induction period at both high and low intensities. However, Warburg's measurements extended to lower intensity values than did those of Smith.

This wide diversity of characteristics suggests that the induction period may be caused by different mechanisms in different plants. Smith (69) has derived an equation for the induction period, relating the relative rate of photosynthesis to the duration of illumination, which satisfactorily describes his own data and also data obtained by several other investigators. However, the application of this equation to a particular series of data depends upon the evaluation of a constant which determines the time scale.

Most methods for measuring photosynthesis have too great a time lag to permit a satisfactory direct study of an induction period as short as 3 min. Warburg, van der Paauw, and Smith measured photosynthesis manometrically in their experiments, and resorted to an indirect integration method for studying the short induction periods which they encountered. Smith, for example, determined respiration for a 30-min. period and then exposed the plant (*Cabomba*) to light for 1 min. The manometer was not read until after a further 5- or 10-min. dark period. The rate so determined was, in effect, the resultant of 1 min. of photosynthesis superimposed on a 6- or 11-min. period of respiration. The procedure was then repeated for the same or for successively longer light exposures. The methods of Warburg and van der Paauw were similar to this. A potential source of error in this type of procedure is the possible stimulation of respiration by light. With a short light period such as 1 min., even a slight increase in respiratory rate during the subsequent 5- or 10-min. dark period would greatly reduce the apparent yield of photosynthesis.

Because of the very small time lag in his apparatus (see page 816), McAlister (53) was able to determine the induction period in wheat from continuous measurements of the photosynthetic rate. Considering the amount of carbon dioxide lost to photosynthesis as a measure of the induction period, he found that, in wheat, this quantity decreased with decreasing light intensity, apparently approaching zero at zero intensity. This result is in qualitative agreement with the behavior in *Chlorella* (83) and in *Cabomba* (69). McAlister also found the induction period in wheat to be nearly twice as long at 12°C. as at 31°C. Van der Paauw (78) observed a similar temperature effect in *Hormidium*.

In intermittent light, with equal light and dark periods, the rate of photosynthesis in wheat passes through a minimum for light and dark periods of about 1 min. (53). With longer intervals a smaller percentage of total illumination time is taken up by the induction periods, while at shorter intervals it is probable that two factors contribute to an increase in rate. One is the occurrence of the Blackman reaction during the dark periods (see page 826); the other is the probability that, after a short dark interval, the induction period is less pronounced than after a longer interval.

No very convincing mechanism has so far been advanced for the induction process in photosynthesis. Since three or more quanta of red light are necessary to supply energy for the reduction of one molecule of carbon dioxide to carbohydrate, it is often assumed that the process occurs through a series of three or more intermediate photochemical reactions (however, see page 851). On this basis it would appear probable that, after a long dark period, each reaction unit in the chloroplast would have to undergo some or all of this series of reactions before evolving oxygen or absorbing additional carbon dioxide. This should produce an induction period lasting until the establishment of equilibrium between the concentration of the various intermediates. Furthermore, the magnitude of the induction effect after a dark interval should give a measure of the extent to which the various intermediate compounds were decomposed during the dark interval.

According to this picture the induction period should last much longer at low light intensities than at high intensities. This is contrary to the observed facts. Consequently, it is evident that processes other than those considered in the preceding paragraph must play a part in the induction period.

According to the mechanism of Franck and Herzfeld (34), oxygen is evolved after the first photochemical step in the series of reduction reactions. They suggested that the induction period is the result of photo-oxidation processes (see page 850).

It appears that further data concerning the influence on the induction period of various external and internal factors are greatly to be desired.

Quantum efficiency of photosynthesis

A knowledge of the quantum efficiency of the photochemical process in photosynthesis is essential to any detailed consideration of the kinetics of the process. Unfortunately, the actual measurement of this quantity is accompanied by difficulties not encountered in quantum efficiency measurements carried out in non-living systems. Some of these difficulties will be considered in the following paragraphs.

Because of the complexity of the photosynthetic process, many factors other than the efficiency of the photoprocess may influence quantum efficiency values determined from a measurement of the overall reaction. To a certain extent, the influence of these other factors may be minimized by using low light intensities, high carbon dioxide concentration, and a relatively high temperature. In this range, since the rate of photosynthesis is nearly proportional to light intensity, the quantum efficiency should be nearly constant and relatively independent of other external variables. Under these conditions, however, the necessary correction for respiration becomes relatively very large. If it were definitely established that the respiratory and photosynthetic processes are independent and unaffected by each other, and that the rate of respiration is not influenced by light, then respiration corrections, even when large, would not seriously reduce the accuracy of photosynthesis measurements. However, van der Paauw (78) found that, in *Hormidium*, respiration was more than twice as rapid immediately after an hour of strong illumination as it had been before the photosynthetic period. Two hours after exposure, the respiration had dropped to its normal rate. In an atmosphere devoid of carbon dioxide, van der Paauw found that the respiratory rate was actually increased during illumination. However, it is possible that, in the absence of carbon dioxide, light may have produced an abnormal effect. Petering and Daniels (62) have observed a temporary increase in the rate of respiration for *Chlorella* after exposure to light, the extent of the increase depending on the previous treatment. On the other hand, McAlister (53) failed to find any stimulation in wheat plants after illumination at high light intensities, despite the fact that a very sensitive method was used. The difference between the response of wheat on the one hand, and *Hormidium* and *Chlorella* on the other, may be partially due to the much larger fraction of total cell volume occupied by the chloroplasts in the case of the algae.

The measurement of light absorption in plant material is difficult. Pigments are irregularly distributed and much light is lost by refraction and scattering. From this point of view, a small unicellular alga, such as *Chlorella*, is more satisfactory than a leaf of a higher plant. *Chlorella* in suspension settles only slowly, making it easy to maintain even distribution. Moreover, by varying the concentration of the suspension, the fraction of incident light absorbed can be varied at will.

Not all of the absorbed light is absorbed by chlorophyll. The amount absorbed by other substances can be estimated from measurements made with extracted pigments, but such an estimate is uncertain, since the optical properties and distribution of the various pigments are altered by the extraction process. Moreover, it is not known whether light absorbed by chloroplast pigments other than chlorophyll can contribute to photosynthesis. At wave lengths longer than 5500 Å., the uncertainty due to these other pigments is minimized, since their absorption is very slight at longer wave lengths.

Another difficulty is found in the fact that, in some plant material, a large part of the chlorophyll may be inactive so far as ability to produce photosynthesis is concerned. After reaching maturity a leaf usually decreases in photosynthetic activity, even though the amount of chlorophyll may remain constant or increase. Because of this, it is advisable to use only young or actively growing material for quantum efficiency measurements.

Finally, there is a possibility that the mechanism of photosynthesis is not the same for all plants. In this case the overall efficiency would probably vary in different plants, even if all measurements were made under ideal conditions. However, the apparently identical nature of the pigments in many different plant species, as well as other similarities in the photosynthetic process, suggest that the photochemical reactions are the same, at least throughout the green algae (*Chlorophyceae*) and the higher divisions of the plant kingdom (mosses, ferns, and seed plants).

The first measurements of the quantum efficiency of photosynthesis were made by Warburg and Negelein (85, 86), with the alga *Chlorella* as plant material. A differential manometer was used for the photosynthesis measurements. A mercury arc with filters served as a source of monochromatic light except in the red, where a filament lamp with filters was used to obtain the region 6100–6900 Å. To avoid the necessity of measuring transmitted light, Warburg and Negelein used very heavy suspensions of the algae. Except for a small amount of reflection, practically all of the incident light was absorbed. At any one time most of the *Chlorella* cells were thus receiving only a small fraction of the incident light intensity. To reduce the value of the respiration correction, these investigators carried out their measurements at a temperature of 10°C., where respiration is much slower than at 20° or 25°C.

At wave lengths of 6600, 5780, and 5461 Å. Warburg and Negelein found a quantum efficiency of approximately 0.25 molecule of carbon dioxide per quantum. The observed value at 4360 Å. was lower, about 0.20, but an approximate correction for light absorbed by the carotene and xanthophyll pigments increased the 4360 Å. value to 0.25 or slightly higher. The incident light intensity in these experiments varied from 575 to 3500 ergs per cm.^{2} per second. Within this range the quantum efficiency appeared to be independent of light intensity.

At 6600 Å. $Nh\nu = 43{,}000$ cal., so that a quantum efficiency of 0.25 corresponds to an energy efficiency of 65 per cent on the basis of equation I. If formaldehyde is the first product of photosynthesis, then ΔH for equation I becomes 134,000 cal. and the corresponding energy efficiency is 78 per cent. In either case the energy efficiency is surprisingly large, particularly since one or more of the intermediate reactions in photosynthesis is probably exothermic.

The quantum efficiency of photosynthesis in *Chlorella* has recently been investigated by Manning, Stauffer, Duggar, and Daniels (55). These investigators found quantum efficiencies much lower than those reported by Warburg and Negelein. Most of the experiments were carried out at 25°C., with high carbon dioxide concentrations. Light intensities varied from 830 to 24,000 ergs per cm.^{2} per second. A mercury arc was used with a monochromator to give monochromatic light of wave lengths 5461 and 4360 Å. Other measurements were made with polychromatic light from the mercury arc, and still others with light from a tungsten filament lamp.

In some experiments a gas stream was bubbled through the algal suspension and photosynthesis measured by gas analysis, while in other experiments a closed system was used, oxygen being determined by the Winkler method. In all cases the algal suspensions were less concentrated than those of Warburg and Negelein, since from 10 to 50 per cent of the incident light was transmitted through the back of the reaction vessel.

The quantum efficiency values obtained by Manning, Stauffer, Duggar, and Daniels were quite variable, but the maximum value of approximately 0.06 is so far below the figure obtained by Warburg and Negelein that it is difficult to attribute the discrepancy to differences in experimental procedure.[15] Different strains of *Chlorella* (possibly different species) may have been used in the two investigations (reference 55, page 272), but it is unlikely that such minor differences would cause any fundamental difference in the photosynthetic mechanism.

Quantum efficiency measurements, in *Chlorella* exposed to various intensities of sunlight below the surface of a lake, have been made by Manning, Juday, and Wolf (54). The maximum value approached at low light intensities was approximately 0.05.

Burns (18) has calculated quantum efficiencies from measurements of photosynthesis in white pine trees. In his experiments the top of a young tree was enclosed in a bell jar containing 1 per cent of carbon dioxide. The decrease in carbon dioxide concentration after 2 hr. of illumination was determined by gas analysis. Light sources were the 5890 Å. line of sodium, the 5780 Å. line of mercury, and polychromatic light with filters. The quantum efficiency for the yellow lines of sodium and mercury was approximately 0.13; for the polychromatic light the value was approximately 0.11. The light intensities used were apparently greater than 10,000 ergs per cm.^{2} per second.

In Burns' experiments it was necessary to estimate the amount of absorbed light by determining the absorption of an acetone solution of the extracted pigments. This procedure is subject to some uncertainty, since the pigment distribution is of course very different in the two cases. Such an approximation is apparently unavoidable when working with a light-absorbing system as complex as this.

---

[15] In both investigations it was evident that the previous conditions of growth played an important part in determining quantum efficiency values. Warburg and Negelein found that a week of growth at high light intensity, followed by a week of growth at low light intensity, gave the most favorable results for their strain of *Chlorella*. It is especially necessary to avoid using old cultures which have passed the period of most active growth. *Chlorella* cells from such cultures often contain a high chlorophyll concentration, but nevertheless show a low photosynthetic efficiency. It is possible that much of the chlorophyll in such cells is unable to transfer absorbed energy to the photosynthetic mechanism.

Briggs (13) has determined the energy utilization for photosynthesis in the leaves of the bean (*Phaseolus vulgaris*), the elder (*Sambucus nigra*), and the elm. Most of the light intensities were in the neighborhood of 5000 ergs per cm.^{2} per second. The higher quantum efficiencies estimated from Briggs' data are in approximate agreement with those determined by Burns.

The present data concerning the problem of the quantum efficiency of photosynthesis are in serious disagreement. Evidently a further study of the problem is greatly to be desired. It appears probable that accurate and extensive data on the variation of the quantum efficiency as a function of wave length in different species may help to dispel the uncertainty concerning the photosynthetic activity of pigments other than chlorophyll, and also serve to provide a more secure basis for the postulation of chemical and kinetic mechanisms for the process.

Photosynthesis in bacteria

The problem of photosynthesis in bacteria is a very interesting one, and may have an important bearing on the problem of photosynthesis in green plants. An adequate discussion of bacterial photosynthesis would require many pages; only a few aspects of the problem will be considered here. More complete information may be obtained from recent publications of van Niel (79, 80), whose researches have contributed a large portion of our present knowledge concerning bacterial photosynthesis.

In the presence of light, hydrogen sulfide, and carbon dioxide, the green and purple sulfur bacteria are able to develop in entirely inorganic media. These bacteria grow only under anaerobic conditions, and no oxygen is given off during their development. Instead, sulfur or sulfuric acid is produced.

Assuming that formaldehyde is the first product, the equation for the process in the green sulfur bacteria may be written:

$$CO_2 + 2H_2S \xrightarrow{\text{light}} (CH_2O) + H_2O + 2S \qquad \Delta H \cong 22{,}000 \text{ cal.} \qquad \text{(II)}$$

and in the purple bacteria:

$$2CO_2 + H_2S + 2H_2O \xrightarrow{\text{light}} 2(CH_2O) + H_2SO_4 \qquad \Delta H \cong 72{,}000 \text{ cal.} \qquad \text{(III)}$$

Apparently the green sulfur bacteria can utilize only hydrogen sulfide as a hydrogen donor for the reduction of carbon dioxide, but the purple sulfur bacteria can carry on photosynthesis in the presence of a number of substances other than hydrogen sulfide. Among these are sodium sulfite, sodium thiosulfate, sulfur, hydrogen, and various organic substances

(79).[16] For the reaction with hydrogen (37), the probable equation is

$$CO_2 + 2H_2 \xrightarrow{\text{light}} (CH_2O) + H_2O \qquad \Delta H \cong 2000 \text{ cal.} \qquad \text{(IV)}$$

As Spoehr and Smith have pointed out (72), it is questionable whether the processes represented by equations II and IV can, strictly speaking, be called photosynthesis, at least if the word is used to denote an accumulation of light energy in the form of chemical energy. As in the higher plants, the formaldehyde or other intermediate product is presumably polymerized almost immediately to carbohydrates. If equations II and IV are written with glucose instead of formaldehyde as the reduction product, ΔH becomes approximately zero for equation II and negative for equation IV.

Bacterio-chlorophyll, a pigment closely related to the chlorophyll found in green plants (32), occurs in both of these groups of bacteria. The purple bacteria also contain one or more red pigments, probably related to the carotenoid pigments of green plants. Bacterio-chlorophyll shows a strong absorption in the region between 8000 and 9000 Å., in addition to its visible absorption bands. Consequently the sulfur bacteria are able to utilize infrared radiation in the reduction of carbon dioxide.

French (38) has studied the effect of different wave lengths on the rate of carbon dioxide assimilation by one of the purple bacteria (*Spirillum rubrum*). Using very thin suspensions of the bacteria, he found that the reaction rate corresponded closely to the absorption spectrum of the green pigment, even in regions where the red pigment absorbed strongly. Consequently he concluded that the red pigment is photochemically inactive in photosynthesis.

Van Niel has suggested that the various equations for photosynthesis (I to IV) should be considered as special cases of a general type reaction:

$$CO_2 + 2H_2A + nh\nu \rightarrow (CH_2O) + H_2O + 2A \qquad \text{(V)}$$

where H_2A represents a substance able to furnish hydrogen for the reduction of carbon dioxide.

Quantum efficiency of photosynthesis in bacteria

Roelefson (66) has made some measurements of the quantum efficiency of photosynthesis in the purple sulfur bacteria. After making corrections for light absorbed by red pigments, he concluded that the maximum quantum efficiency is approximately 0.25 molecule of carbon dioxide per

[16] The purple bacteria referred to here are members of the *Thiorhodaceae*. Another group of photosynthetically active purple bacteria, the *Athiorhodaceae*, apparently require organic compounds instead of sulfur compounds as reducing agents.

quantum absorbed, in agreement with the measurements of Warburg and Negelein (86) for the alga *Chlorella*.

French (37), using the purple bacterium *Streptococcus varians*, has made quantum efficiency measurements in which infrared radiation (wave lengths 8520 + 8940 Å., from a cesium lamp) was used as the energy source. The red pigments do not absorb appreciably in this wave length region. The bacterial suspension was in equilibrium with an atmosphere of 5 per cent carbon dioxide and 95 per cent hydrogen. Consequently the overall reaction presumably corresponded to that of equation IV.

French's measurements were complicated by the fact that he found a sigmoid curve for the variation in reaction rate as a function of light intensity. Thus, at low intensities the rate was proportional to a higher power of intensity than the first power. Quantum efficiencies were calculated from the maximum slopes observed for his rate versus light intensity curves. The maximum slope occurred at various light intensities, depending upon the type of pretreatment of the bacteria. By extrapolation French found that as the position of the maximum slope approached zero light intensity, the quantum efficiency appeared to approach a value of 0.25 (or 0.5 on the basis of hydrogen), in agreement with the estimates of Roelefson. As Emerson has pointed out (24), there is some doubt concerning the validity of this indirect method of calculating quantum efficiencies, particularly since it yields higher efficiency values than those actually prevailing in French's experiments.

French agrees with van Niel (79) in believing that the agreement between the quantum efficiencies observed for purple bacteria and those observed for *Chlorella* by Warburg and Negelein (86) indicate that a similar sequence of photoreactions is involved, despite the great difference in energy requirements. However, recent experiments with *Chlorella* (54, 55) have created some doubt concerning the correctness of the quantum efficiency values obtained by Warburg and Negelein (see page 835).

IV. THE RÔLE OF CHLOROPHYLL IN THE PHOTOSYNTHETIC PROCESS

Chlorophyll production

The manner in which chlorophyll is manufactured by green plants is a problem of fundamental physiological importance. It will be mentioned only briefly in this review, since it probably is not a direct part of the problem of photosynthesis. Further information on chlorophyll production may be obtained from articles by Spoehr and Smith (72), Inman, Rothemund, and Kettering (46), and Rothemund (67).

In most of the higher plants light is necessary for chlorophyll production. However, other plants, particularly some of the algae, can apparently produce chlorophyll in the dark. Etiolated plants, although usually containing no chlorophyll, have been found to contain a very small amount of another green pigment which is usually called protochlorophyll. It differs spectroscopically from chlorophyll. When an etiolated plant is exposed to light, most of this green pigment disappears and is perhaps transformed into chlorophyll (67).

Most plants develop a higher chlorophyll concentration when grown in light of relatively low intensity than when grown in very bright light. Consequently several investigators have suggested that, in addition to its rôle in chlorophyll formation, light may also produce chlorophyll decomposition. According to this view, the chlorophyll concentration in a plant under given conditions can be regarded as a steady state concentration, with the rate of chlorophyll formation being approximately balanced by its rate of decomposition.

The production of chlorophyll is, of course, also dependent upon the proper supply of mineral nutrients; perhaps the most conspicuous of these are magnesium, which enters into the chlorophyll molecule, and iron, which apparently acts as a catalyst in some step in the formation process.

Chemical properties of chlorophyll

The structure and chemical properties of extracted chlorophyll are now known rather completely, largely as a result of the investigations of Willstätter, Stoll, Fischer, and Conant. The subject has recently been reviewed by Fischer (30) and by Steele (73). Figure 9 shows the probable formula for chlorophyll *a* (30). Fischer's formula for chlorophyll *b* is identical with the formula for *a*, except that the methyl group in the 3-position is replaced by a formyl group.

Willstätter and Stoll (89) have found that the *a*:*b* ratio for chlorophyll in leaves is approximately 3. They found that this ratio was practically constant for many different species and for different environmental conditions. However, other investigators have found evidence that the ratio depends somewhat upon external conditions.

Working with etiolated corn seedlings, Inman (45) found that, shortly after exposure to light, the chlorophyll *a*:*b* ratio was very high, approximately 22:1. After an additional 90 min. of light exposure the ratio dropped to 17:1. Similar behavior has been observed in oat seedlings by Burr and Miller (19). The simplest explanation for this behavior would be that chlorophyll *a* is produced first, and that chlorophyll *b* is an oxidation product of chlorophyll *a*. However, this type of oxidation would be very difficult to bring about *in vitro*.

In some of the earlier theories concerning the photosynthetic mechanism, it was assumed that the *a* and *b* components formed a photo-activated oxidation-reduction system, so that the coöperation of both components would be necessary to carry on photosynthesis. Aside from the difficulty involved in the methyl-formyl oxidation, further evidence that the *a* and *b* components do not function as an oxidation-reduction system is found in the observation of Fischer and Breitner (31) that chlorophyll *b* does not occur in several of the red algae (*Porphyra tenera*, *Bangia fuscopurpurea*, and *Polysiphonia nigrescens*). On the other hand, Beber and Burr (11) observed no photosynthesis in etiolated oat seedlings until long after a perceptible amount of chlorophyll *a* was formed. Their experiments suggested that chlorophyll *b* is necessary for photosynthesis in oat seedlings. Further evidence concerning the degree of interdependence of the two chlorophylls might be obtained from quantum efficiency measurements with wave lengths chosen to correspond to the respective absorption maxima of the two pigments.

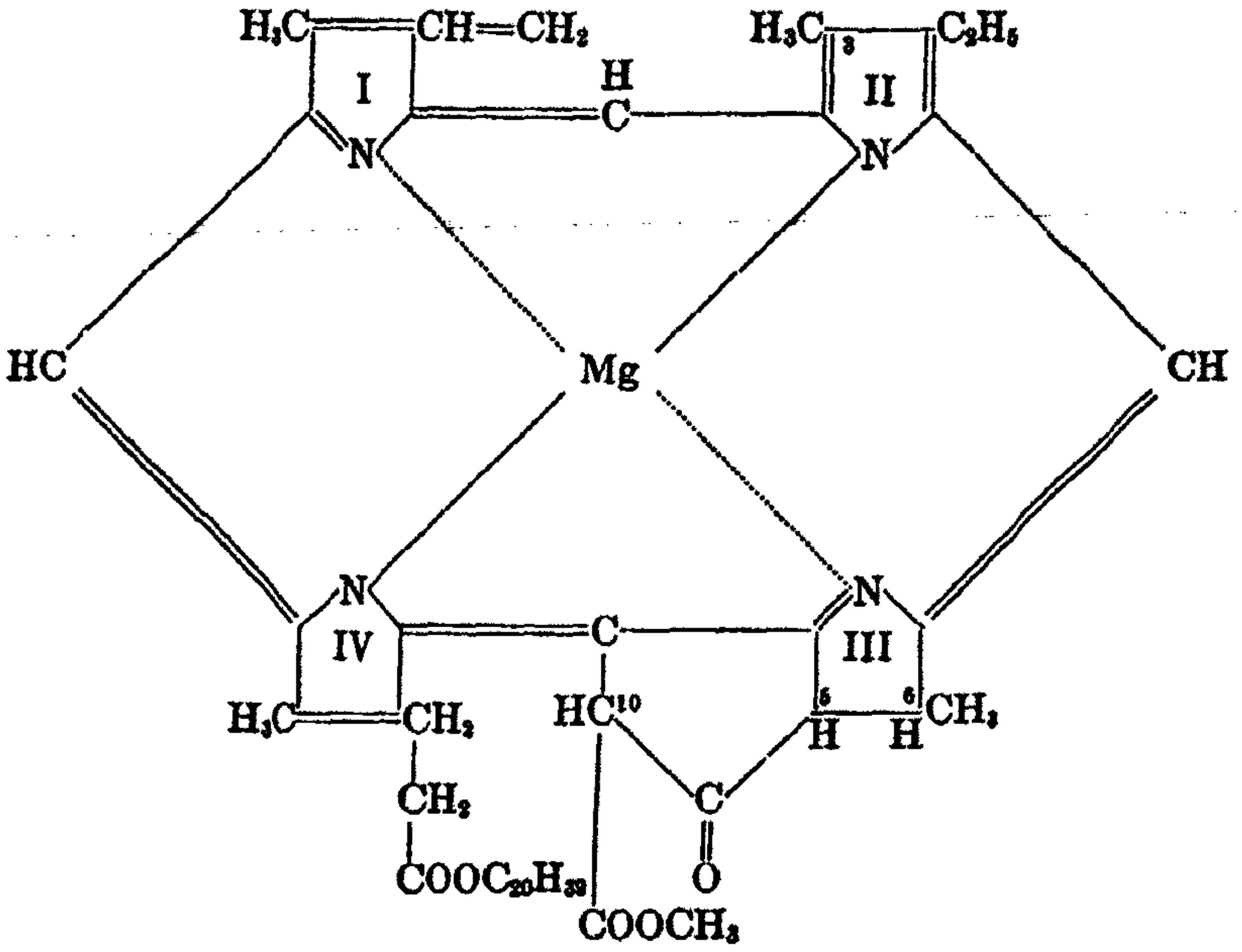

FIG. 9. Fischer's formula for chlorophyll *a* (Steele (73))

Stoll (75), on the basis of his own and other investigations, has concluded that the action of both chlorophylls in the photosynthetic process is in large part due to the labile hydrogen atom attached to the carbon atom in the 10-position (figure 9). According to his point of view, the existence of two chlorophyll components may be advantageous to a plant because of the increased range of wave lengths which can thus be absorbed (see figure 1). This might be particularly useful to a plant growing in dim light.

In the chloroplast the position of the absorption maxima for the two chlorophylls is shifted approximately 200 Å. to the red as compared to the position for the extracted pigments in ether solution. This shift is usually ascribed to differences in the optical properties of the solvents. Albers and Knorr (2) have recently studied the absorption spectra of single chloroplasts in the region from 6640 to 7040 Å. They found evidence for several maxima in the absorption band usually attributed to chlorophyll *a*. They suggested that the several maxima may be due to the presence of compounds between chlorophyll *a* and various intermediates in the photosynthetic process.

The phytyl group in the chlorophyll molecule has little influence on the optical properties. Replacement of the phytyl group by a methyl group produces only a slight change in the chlorophyll absorption spectrum. The optical properties are due principally to the ring of conjugated double bonds surrounding the central magnesium atom. The phytyl group, according to Stoll (75), may serve to make chlorophyll lipoid-soluble, thus permitting proper distribution in or on the plastid.

Stoll suggests that, in addition to maintaining the conjugated bond system, magnesium is important in maintaining the proper degree of reactivity with carbonic acid. Chlorophyll forms a complex with carbonic acid *in vitro*, and Stoll, as well as many other investigators, suggests that a similar complex is formed in the plant. As mentioned above (page 825), earlier evidence indicated that the rate of photosynthesis is temperature-dependent even at very low carbon dioxide concentrations. This was regarded as additional evidence for the formation of a carbonic acid (or carbon dioxide) complex with chlorophyll during the photosynthetic process. But the experiments of van den Honert (77) and of Emerson and Green (29) have indicated that the temperature dependence at low carbon dioxide concentrations may be only apparent, and due to complications resulting from the use of buffer mixtures. These observations weaken somewhat the evidence for participation of a carbonic acid–chlorophyll complex in photosynthesis.

It has frequently been observed that chlorophyll in solution is decomposed by the action of light. Albers and Knorr (1, 51) have followed this decomposition in the presence of various gases, by observing changes in the fluorescence spectra of chlorophylls *a* and *b*. Porret and Rabinowitch (63) have studied the bleaching of chlorophyll dissolved in methanol. In the presence of oxygen the quantum yield was approximately 10^{-6}. This value was independent of oxygen concentration over a wide range, but the bleaching disappeared on complete removal of oxygen.

In the absence of oxygen Porret and Rabinowitch (63) found that intense light caused a reversible bleaching of the red absorption band of chlorophyll. Using a 10^{-6} molar solution of chlorophyll in methanol, and a light intensity such that each chlorophyll molecule absorbed about 10 quanta per second, the bleaching of the red band amounted to about

1 per cent. Therefore, assuming the quantum efficiency of the bleaching process to be 1, they estimated an average lifetime for the bleached state of about 10^{-3} sec. The degree of bleaching was approximately proportional to the square root of light intensity. Porret and Rabinowitch suggested that the bleaching was probably due to a dissociation into "dehydrochlorophyll" and a hydrogen atom (perhaps from carbon atom No. 10; see figure 9). In the presence of formic acid the reversible bleaching was increased to 10 per cent. With a dissolved oxygen concentration of 10^{-5} molar, the bleaching with formic acid was reduced about 50 per cent. Apparently the oxygen either formed a complex with chlorophyll or removed the chlorophyll excitation before dissociation could occur.

Rabinowitch and Weiss (65) have found that chlorophyll in methyl alcohol solution is transformed by certain oxidizing agents, particularly ferric chloride, into a yellow product. The chlorophyll could be restored to its original condition by the action of ferrous chloride. The oxidation process was accelerated by light. In the yellow oxidation product the red absorption bands were virtually eliminated, and the blue bands shifted toward shorter wave lengths. A rather peculiar feature of the oxidation process was that the blue band of chlorophyll *b* was changed much more slowly than the red band of *b*, and also more slowly than either the red or blue bands of the *a* component. This suggests that the blue absorption band of *b* may be produced by a chromophoric group different from those responsible for the other absorption bands of chlorophyll. Rabinowitch and Weiss consider it probable that the oxidation of a chlorophyll molecule results in the formation of a positively charged chlorophyll ion, which perhaps then breaks down into a hydrogen ion and dehydrochlorophyll.

It is probable that, in the process of extraction from plant cells, the chlorophyll pigments undergo some sort of chemical change. Some investigators (e.g., Stoll (75) and Franck and Herzfeld (34)) have suggested that, in the chloroplast, chlorophyll may be combined with a protein. Its specific effectiveness in photosynthesis would thus depend upon its attachment to a particular colloidal carrier. In any event, attempts to bring about carbon dioxide reduction by extracted chlorophyll have thus far been unsuccessful.[17] Whether this failure is due principally to changes

---

[17] Baly, Stephen, and Hood (8) have reported the formation of carbohydrates from carbon dioxide and water, with visible light as the energy source. The light-absorbing agent in their experiments was not chlorophyll, but an aqueous suspension of nickel or cobalt carbonate. However, a number of other investigators have tried, without success, to repeat the experiment of Baly, Stephen, and Hood. It may be that these other investigators have failed to duplicate with sufficient exactness the procedure described by Baly *et al.*, but, as Emerson (23) has suggested, it seems reasonable to require that the production of photosynthesis *in vitro* should be capable of repetition before it can be regarded as an established fact.

in the chlorophyll, or to changes in the environment, or both, is as yet an unanswered problem.

Chlorophyll fluorescence

Solutions of chlorophyll emit a bright red fluorescence when illuminated with visible or near ultraviolet radiation. It has been estimated that, under favorable conditions, about 10 per cent of the absorbed radiation may be recovered as fluorescence (36). Chlorophyll in living cells also fluoresces, but much less strongly than solutions of the extracted pigment. The maximum yield for chlorophyll fluorescence in living material is of the order of 0.01 per cent (81). Colloidal solutions of chlorophyll do not fluoresce. The fact that fluorescence occurs in the living cell is often regarded as an indication that chlorophyll is in a dissolved state in the chloroplast. However, the very low intensity of fluorescence in the chloroplast lessens the force of this argument.

Zscheile (94) has determined the fluorescence spectra of chlorophylls *a* and *b* in ether solution. The exciting radiation was supplied by a tungsten filament lamp. The *a* component showed two bands and the *b* component three bands in the region 6300–8200 Å. No observations were made at wave lengths below 6300 Å.

Kautsky and coworkers (49, 50) and Franck and Wood (36) have studied the effect of illumination time on the intensity of fluorescence in living leaves. In Kautsky's experiments the 3660 Å. line of mercury was used as the exciting source, while, in the experiments of Franck and Wood, a tungsten filament lamp with a blue filter was used to produce fluorescence. The results of these two series of investigations, while not identical, showed the same general type of behavior. Following a long period of darkness, the fluorescent intensity from an illuminated leaf is at first very low, but increases rapidly to a maximum after 2 to 5 sec. of illumination. The intensity then diminishes until a constant level is reached after about a minute. At a temperature of 35°C., Kautsky and Marx (50) found that this constant intensity was approximately two-thirds of the temporary maximum value, but at 0.1°C. the intensity remained constant at nearly the maximum value. In the presence of oxygen, the fluorescent intensity was reduced to about half the value observed in the absence of oxygen (49).

Franck and Levi (35) found that weak alcoholic or acetonic extracts of leaves, when irradiated in the presence of oxygen, showed a variation in fluorescent intensity similar to that found in leaves.

Kautsky concluded from his investigations that there is an intimate connection between the process of photosynthesis and the process of fluorescence. Earlier investigations (89) indicated that oxygen is necessary for photosynthesis. Consequently, Kautsky attributed the quenching of fluorescence by oxygen to the utilization of chlorophyll excitation energy in the process of photosynthesis. Kautsky and Hormuth (49) suggested that oxygen forms an addition compound with some substance in the chloroplast, and that this compound serves to transfer the chlorophyll excitation energy to carbonic acid, which is thereupon reduced to formaldehyde or carbohydrate.

Kautsky's interpretation is open to question from several points of view. In the first place, recent experiments by Gaffron (39), with *Chlorella*, indicate that oxygen is not essential for photosynthesis. Gaffron observed that when *Chlorella* was illuminated following 15 hr. in darkness in a nitrogen atmosphere, carbon dioxide consumption proceeded normally. However, oxygen production did not occur for some time, presumably because of oxidation of excess intracellular fermentation products.

Secondly, Kautsky used the 3660 Å. line of mercury to excite fluorescence. This wave length is relatively inefficient for photosynthesis (see page 818).

Thirdly, as Emerson (23) has pointed out, a plant exposed to high light intensity is using only a small fraction of the absorbed energy in the photosynthetic process. Consequently, changes in fluorescent intensity might occur quite independently of the photosynthetic process.

Franck and Wood (36), while not considering oxygen as necessary for photosynthesis, concluded that there is a close connection between the processes of photosynthesis and fluorescence. They interpreted the variation in fluorescent intensity as being due to the formation and disappearance of a strongly fluorescent radical.

According to the mechanism of Kautsky and Hormuth (49), it would appear that, at low light intensities, the percentage yield of fluorescence should increase with increasing intensity of the incident light, approaching a maximum value after the attainment of a maximum photosynthetic rate. If this type of relation could actually be established, it would constitute strong evidence for a connection between photosynthesis and fluorescence.

The relation between chlorophyll concentration and the maximum rate of photosynthesis

Emerson (22) and Fleischer (33) have studied the effect of varying chlorophyll concentration on the rate of photosynthesis in *Chlorella*. Emerson grew *Chlorella* in a nutrient solution containing glucose, and varied the chlorophyll concentration by varying the concentration of iron in the nutrient solution. Fleischer varied the chlorophyll concentration in three different ways. In some of his series the iron concentration was varied, while in other series the magnesium or nitrogen concentrations were varied. Except for samples deficient in magnesium, Emerson and Fleischer both found that, at high light intensity and abundant carbon dioxide concentration, the rate of photosynthesis per unit volume of cells was approximately proportional to the amount of chlorophyll. When chlorophyll deficiency was caused by insufficient magnesium, Fleischer found an abnormally low rate of photosynthesis, and consequently concluded that magnesium influences the process of photosynthesis in some way other than by its influence on chlorophyll production.

Emerson and Arnold (26) have studied the relation in *Chlorella* between chlorophyll content and the rate of photosynthesis in intermittent light of high intensity. In these experiments the chlorophyll content was varied by varying the light conditions under which the *Chlorella* was cultured. As in previous work (25), they used light flashes which lasted only about 10^{-5} sec., a period which is short compared with the duration of the dark or Blackman reaction (see page 827). Sufficient time was allowed between flashes for completion of the dark reaction, so that light saturation in their intermittent light experiments implied, not that the rate of the dark reaction was limiting, as it is in the case of saturation with continuous light, but that the photochemical mechanism was saturated. Under these conditions the maximum rate was again found to be approximately proportional to the chlorophyll concentration. Emerson and Arnold calculated the ratio between the total number of chlorophyll molecules present in the reaction vessel and the number of carbon dioxide molecules reduced per single light flash. Instead of finding a value of 1 (or of 3 or 4 or 5, as would be expected in case a series of three or four or five alternate photochemical and thermal reactions were required for the photosynthetic cycle), they found a value of approximately 2500. This figure represented the average for all chlorophyll concentrations; its value was apparently independent of chlorophyll concentration. In similar experiments Kohn (52) found that light saturation was reached when only about one chlorophyll molecule in a hundred absorbed one or more quanta in a single flash. Arnold and Kohn (6) have determined the minimum value of the ratio of chlorophyll molecules to carbon dioxide molecules reduced per flash for several different species in different divisions of the plant kingdom. They found the value to lie between 2000 and 4000 in all cases.

Emerson (23, 24) has suggested that carbon dioxide probably does not combine with chlorophyll prior to the photoreaction, and that the ratio of about 2500 probably represents the ratio between chlorophyll and some other internal factor, perhaps the substance which combines with carbon dioxide. However, according to this mechanism, one would expect a very low quantum efficiency, even with low intensity continuous light. The high efficiency values reported by Warburg and Negelein (86), or even those found by Manning, Stauffer, Duggar, and Daniels (55), would thus be very difficult to explain.

The photosynthetic unit

One way of reconciling the small yield of carbon dioxide reduced per flash with the relatively high quantum efficiencies observed at low light intensities is to assume that light absorbed by a large number of chlorophyll molecules can be made available to a single carbon dioxide molecule. This assumption implies (unless one postulates an extremely long life for excited chlorophyll) that, in the chloroplast, the chlorophyll molecules are distributed in the form of groups or units, each containing a large number of individual molecules. Arnold and Kohn (6), Gaffron and Wohl (40), and Weiss (88) have favored this interpretation. The postulated size of such a unit would depend upon the number of successive photochemical reactions which are required to reduce one carbon dioxide molecule, and also on the number of carbon dioxide molecules associated with each group. Weiss (88) has suggested that a single unit may have carbon dioxide molecules adsorbed on the surface, with one carbon dioxide molecule to each surface molecule of chlorophyll. Assuming four successive photoreactions, it would thus be necessary to have 500 or 600 molecules in the interior for each surface molecule of chlorophyll. Weiss calculated that, if such a unit were spherical, its radius should be of the order of 0.4μ. Globules of this general size have been observed in photographs of chloroplasts (44). However, it is difficult to conceive of energy transmission through a unit of this magnitude without enormous losses in the form of heat.

Gaffron and Wohl (40) obtained additional support for the existence of of a photosynthetic unit from approximate calculations in which the data of numerous investigators were used. They found that the maximum photosynthetic rate (light saturation) corresponded to the reduction of one carbon dioxide molecule by each chlorophyll molecule every 10 or 20 sec. This period is approximately 1000 times as long as the average time for the dark or Blackman reaction (25, 26). Assuming a single dark reaction in each cycle, this would indicate a unit of about 1000 chlorophyll molecules for each carbon dioxide molecule.

It has also been suggested (34, 91) that the existence of a photosynthetic unit would account for the absence of a long induction period at low light intensities. If a single chlorophyll molecule were obliged to absorb four or more quanta before oxygen could be liberated, a long induction period would be required at low light intensities. But, if a unit of 500 or 1000 chlorophyll molecules were available for the reduction of each carbon dioxide molecule, the necessary quanta would be absorbed within a second or two, even at the lowest intensities that have been used in studies of photosynthesis.

If the process of photosynthesis involves a series of photochemical reactions, any thermal decomposition of intermediate products would result in a lowering of the overall efficiency of the process. If one or more of these intermediate products were sufficiently unstable to decompose appreciably within a period of a minute or less, then a plant should be greatly benefited at low light intensities by the coöperation of more than one chlorophyll molecule in the reduction of a carbon dioxide molecule, since the time between successive photoreactions would be shortened in proportion to the number of chlorophyll molecules per unit.

As Gaffron and Wohl (40) have pointed out, a variation in the size of the photosynthetic unit might account for the phenomenon of light adaptation, by which plants of the same species may be conditioned to efficient use of either high or low light intensities. A plant accustomed to high intensities will often photosynthesize more rapidly in bright light than will one accustomed to low intensities, and *vice versa.* A large number of small units would permit more rapid photosynthesis in bright light, while, with weak light, large units would serve to minimize the possible losses due to decomposition of intermediates.

Thermal decomposition of intermediate products might account for the type of behavior shown at low light intensities by the species of purple bacteria which French (37) used in his measurements of quantum efficiency (see page 838). At low light intensities French's measurements indicated a decreasing efficiency as intensity decreased. If thermal decomposition of intermediates was responsible for this behavior, it would be expected that an increase in temperature should increase the rate of decomposition, and thus cause the diminished efficiency to occur at higher light intensities. This effect was actually observed by French (reference 37, figure 5). However, it should be remembered that the change in ΔH is small for the reaction studied by French. The only reason for assuming a series of photoreactions for the process is its apparent similarity to green plant photosynthesis.

Perhaps the strongest argument against the existence of a photosynthetic unit is the difficulty involved in picturing a model which would permit an efficient transfer of energy from every region where visible light could be absorbed to the point where it could be utilized for carbon dioxide reduction.

Franck and Herzfeld (34) considered that the fluorescence of chlorophyll in living plants is an indication of unimolecular dispersion. Since colloidal chlorophyll does not fluoresce *in vitro,* they argue that chlorophyll in units of 500 or more should not fluoresce in the chloroplast.

However, the very low intensity of fluorescence *in vivo* weakens the argument. Rabinowitch[18] has suggested that the weak chlorophyll fluorescence observed in living material may be emitted by a few "misplaced" chlorophyll molecules which may play no part in photosynthesis.

Wohl (91) has discussed in detail various arguments favoring the existence of a photosynthetic unit. He also has suggested several experiments with intermittent light which might add to our knowledge of the photoprocess involved in photosynthesis.

The existence of a photosynthetic unit has thus far been neither proved nor disproved. Its existence would offer an explanation for several different groups of experiments, but on the other hand, various arguments, largely based on physical grounds, can be offered against it.

The mechanism of photosynthesis

Several recent investigators have proposed kinetic mechanisms for the process of photosynthesis, e.g., Arnold (5), Baly (7), Briggs (15), Burk and Lineweaver (16), Franck and Herzfeld (34), and Smith (68). Of these, the mechanism of Franck and Herzfeld is the only one which includes a detailed consideration of the photochemical reactions which may be involved. Other investigators have suggested a variety of chemical mechanisms without going into detail regarding the kinetics of the process (Conant, Dietz, and Kamerling (20), Gaffron and Wohl (40), James (47), Kautsky and Hormuth (49), Stoll (75), van Niel (79)).

In most of these mechanisms it is assumed that the quantum efficiency for the photochemical reaction is 0.25, in accord with the observations of Warburg and Negelein (86). However, the low efficiency values found by recent investigators (see page 835) suggest that the value 0.25 may be too high.

It has also been generally assumed that the photosynthetic process includes a series of four successive photochemical steps, ΔH for a single step being limited to the energy supplied by a single quantum. In van Niel's mechanism, however, the four photochemical steps are assumed to be identical, resulting in each case in the formation of a hydrogen atom; the four hydrogen atoms then presumably bring about the reduction of carbon dioxide to formaldehyde. Van Niel's mechanism is represented by the following equations:

$$4[\text{Chlorophyll}\cdot H_2O + h\nu \rightarrow \text{Chlorophyll}\cdot OH + H] \qquad (1)$$

$$CO_2 + 4H \rightarrow (CH_2O) + H_2O \qquad (2)$$

$$\underline{2[2\text{Chlorophyll}\cdot OH + H_2A \rightarrow 2\text{Chlorophyll}\cdot H_2O + A]} \qquad (3)$$

$$CO_2 + 2H_2A + 4h\nu \rightarrow (CH_2O) + H_2O + 2A \qquad (V)$$

---

[18] Private communication.

For reaction 1 to be energetically possible, the chlorophyll·H_2O compound would have to be a more intimate compound of chlorophyll and water than in the case of an ordinary hydrate. An alternative way of writing reaction 1 would be

$$4[\text{Chlorophyll}\cdot H_2O + h\nu \rightarrow \text{Dehydrochlorophyll}\cdot H_2O + H]$$

the hydrogen atom thus being split from the chlorophyll portion of the hydrated molecule.

In reaction 3, H_2A would be water in the case of algae and higher plants, and hydrogen sulfide in the case of the green sulfur bacteria.

Without modification this series of reactions could not take place (except perhaps in bacteria) with a quantum efficiency as high as 0.25, since reaction 2 is exothermic to the extent of about 150,000 cal. The energy thus wasted would be nearly equivalent to the total energy supplied by four photons at 7000 Å. For $H_2A = H_2O$, reaction 3 would be endothermic. The necessary energy would presumably have to be supplied by additional photons, unless reactions 2 and 3 were considered to be coupled in some manner so that the excess energy from reaction 2 could be utilized for reaction 3.

The mechanism of Franck and Herzfeld (34) was designed to avoid the necessity of assuming a photosynthetic unit. They assumed, as did Stoll (75), that carbonic acid forms a complex with chlorophyll. This complex, in turn, was assumed to be combined with an organic molecule ROH, present in abundance. Franck and Herzfeld suggested that ROH may be a protein which forms the main body of the chloroplasts. The following equations represent the forward reactions postulated by Franck and Herzfeld. They state that the equations are suggested as a working hypothesis, not as a final solution.

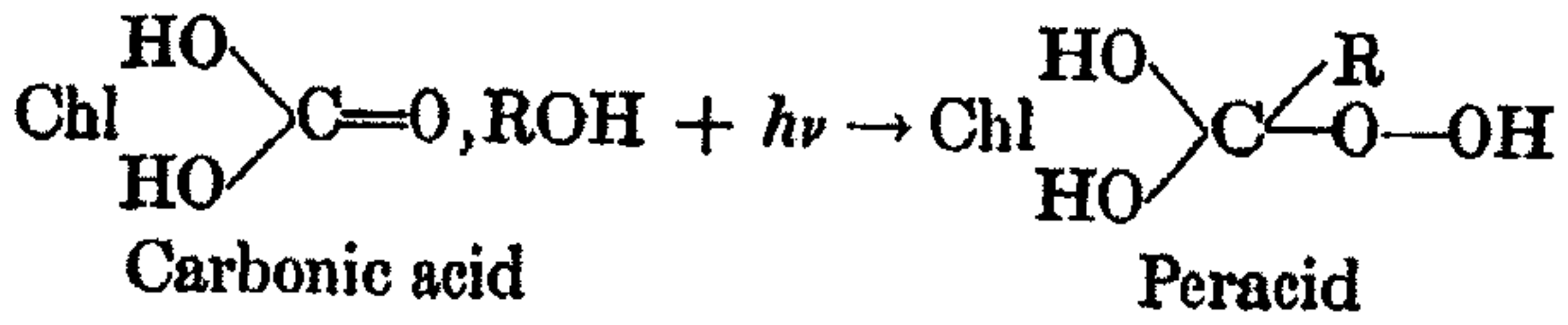

$$\mathrm{Chl}\begin{matrix}\mathrm{HO}\\ \mathrm{HO}\end{matrix}\!>\!C{=}O,\mathrm{ROH} + h\nu \rightarrow \mathrm{Chl}\begin{matrix}\mathrm{HO}\\ \mathrm{HO}\end{matrix}\!>\!C\!\begin{matrix}R\\ \diagup\end{matrix}\!\!O{-}OH \qquad (1)$$

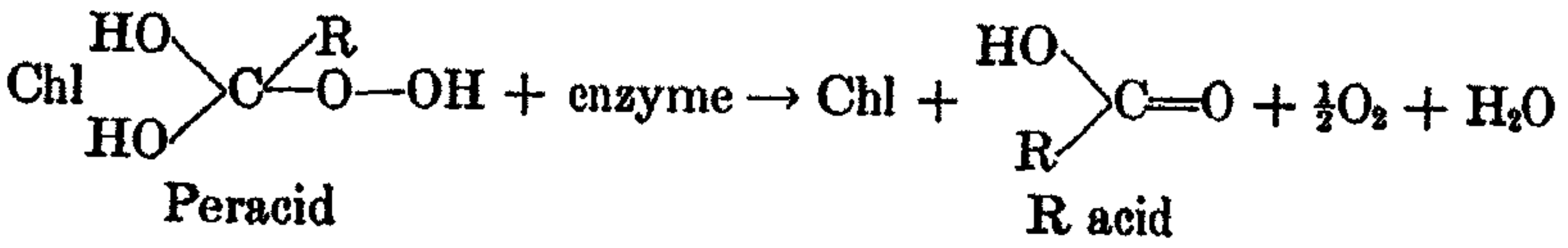

$$\mathrm{Chl}\begin{matrix}\mathrm{HO}\\ \mathrm{HO}\end{matrix}\!>\!C\!\begin{matrix}R\\ \diagup\end{matrix}\!\!O{-}OH + \text{enzyme} \rightarrow \mathrm{Chl} + \begin{matrix}\mathrm{HO}\\ R\end{matrix}\!>\!C{=}O + \tfrac{1}{2}O_2 + H_2O \qquad (2)$$

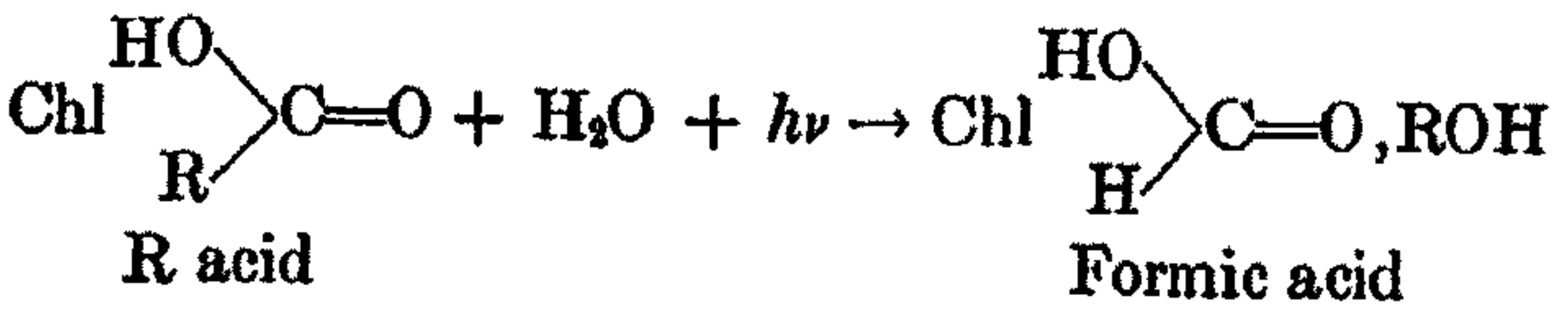

$$\mathrm{Chl}\begin{matrix}\mathrm{HO}\\ R\end{matrix}\!>\!C{=}O + H_2O + h\nu \rightarrow \mathrm{Chl}\begin{matrix}\mathrm{HO}\\ H\end{matrix}\!>\!C{=}O,\mathrm{ROH} \qquad (3)$$

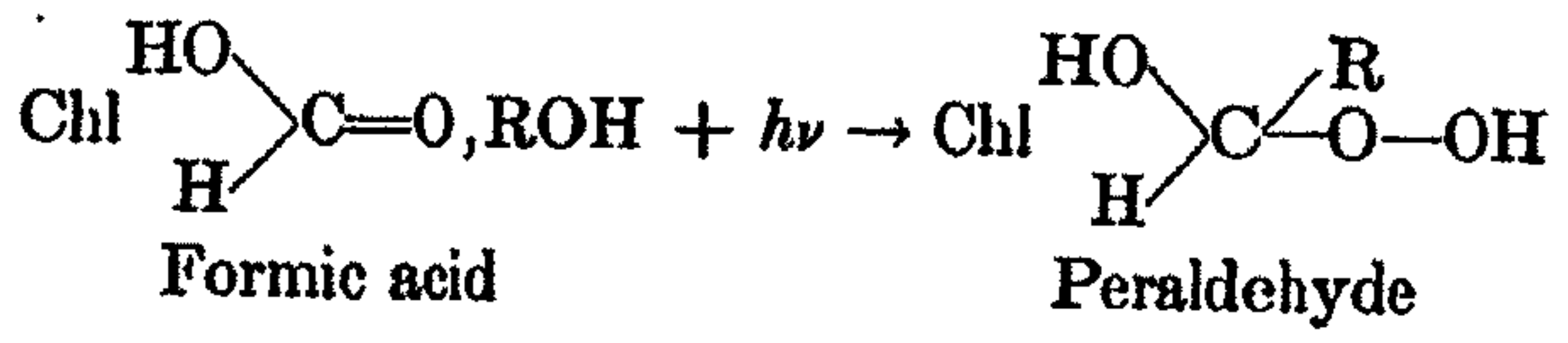

$$\mathrm{Chl}\begin{matrix}\mathrm{HO}\\ H\end{matrix}\!>\!C{=}O,\mathrm{ROH} + h\nu \rightarrow \mathrm{Chl}\begin{matrix}\mathrm{HO}\\ H\end{matrix}\!>\!C\!\begin{matrix}R\\ \diagup\end{matrix}\!\!O{-}OH \qquad (4)$$

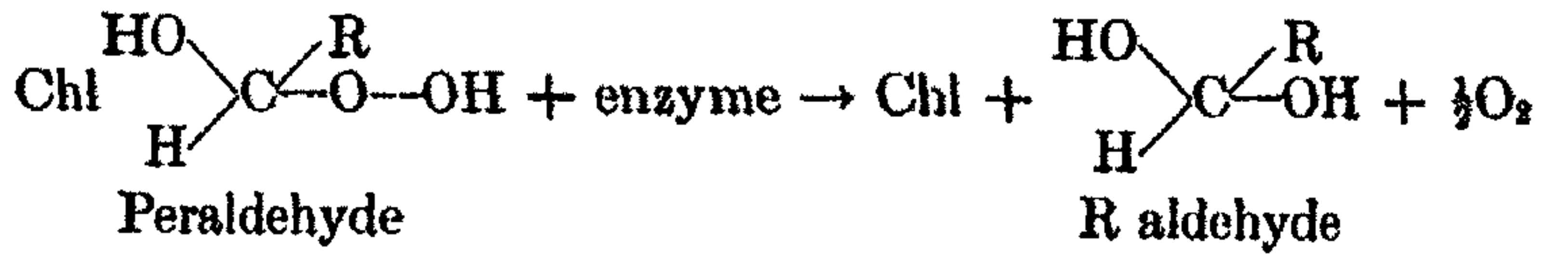

$$\text{Chl}\,\begin{matrix}\text{HO}\\ \text{H}\end{matrix}\!\!>\!\text{C}\!\begin{matrix}\text{R}\\ \end{matrix}\!\!-\text{O}-\text{OH} + \text{enzyme} \rightarrow \text{Chl} + \begin{matrix}\text{HO}\\ \text{H}\end{matrix}\!\!>\!\text{C}\!\begin{matrix}\text{R}\\ \end{matrix}\!\!-\text{OH} + \tfrac{1}{2}\text{O}_2 \quad (5)$$

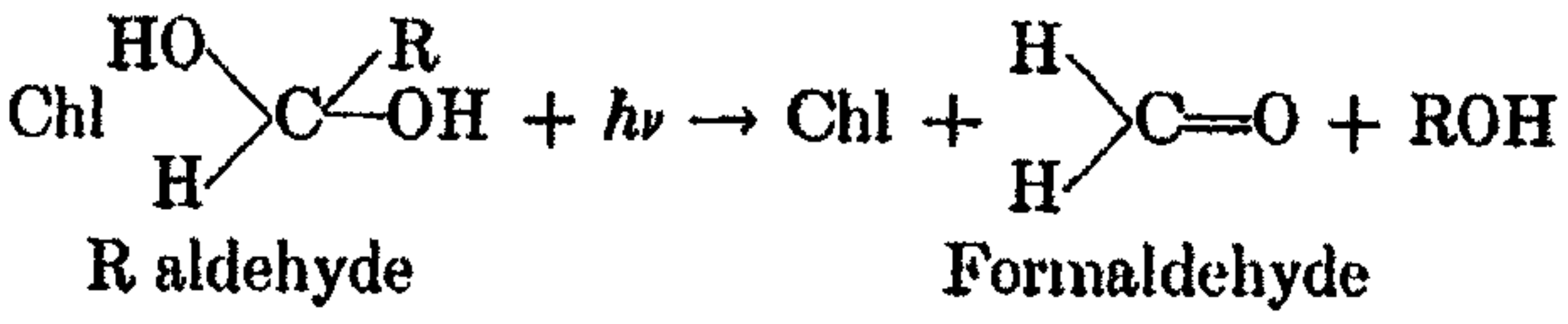

$$\text{Chl}\,\begin{matrix}\text{HO}\\ \text{H}\end{matrix}\!\!>\!\text{C}\!\begin{matrix}\text{R}\\ \end{matrix}\!\!-\text{OH} + h\nu \rightarrow \text{Chl} + \begin{matrix}\text{H}\\ \text{H}\end{matrix}\!\!>\!\text{C}=\text{O} + \text{ROH} \quad (6)$$

The two enzyme reactions, in which oxygen is evolved, constitute the temperature-sensitive or Blackman reaction.

According to Franck and Herzfeld, the calculated binding energy of —OH to —O— in the two peroxides is so weak that the —OH radical will be split off whenever the peracid or peraldehyde complexes absorb a photon. At low light intensities the probability of such an absorption would be negligible, because of the speed of the enzyme reactions. But, at intensities corresponding to light saturation in most leaves, they estimated this probability to be about $\frac{1}{10}$. According to their postulation, the photodecomposition of the permolecules into two radicals initiates chain reactions (back reactions in this case), each chain resulting in the decomposition of a large number of permolecules.

With these chains light saturation is thus reached at a much lower intensity than would be required if the rate were limited by the Blackman reactions. By assuming a sufficient chain length ($\sim 10^3$ at light saturation), saturation, both in flashing and in continuous light, can be explained without the assumption of a photosynthetic unit.

Franck and Herzfeld suggested that, after a long dark period, much of the chlorophyll may be attached to intermediate respiratory products, probably plant acids. Illumination could then cause photosynthesis, as in the case of chlorophyll-carbonic acid or chlorophyll-formic acid complexes. However, according to Franck and Herzfeld, photoöxidation of these plant acids, probably by a chain mechanism, should also take place to a large extent. Until the accumulated respiratory products were exhausted, this oxygen consumption would largely counterbalance the photosynthetic oxygen production, thus producing an induction period. Increased probability of oxidation at high light intensities would cause a more noticeable underproduction of oxygen at high intensities than at low intensities, in agreement with experimental results (53).

The kinetic equations derived by Franck and Herzfeld are in reasonable agreement with experimental facts. However, this cannot be considered as a criterion for the correctness of the mechanism, since equations derived by other investigators on the basis of various mechanisms are also in fairly good agreement with experimental results.

The reverse chain reactions of Franck and Herzfeld have been subjected to some criticism (91). Aside from doubts concerning this part of their mechanism, it is evident that to account for the high efficiencies found by Warburg and Negelein, the various forward reactions in the mechanism of Franck and Herzfeld would have to proceed with remarkable efficiency. Not only would the quantum efficiencies for each photoreaction have to be nearly unity, but the intermediate products would have to remain practically unchanged during the periods between the absorption of successive quanta by a single chlorophyll molecule. This period, according to calculations of Gaffron and Wohl (40), was about 10 min. in many of the experiments of Warburg and Negelein. But Franck and Herzfeld explained the induction period by assuming that, in the dark, a considerable fraction of the chlorophyll molecules become attached to intermediate respiratory products. The experiments of McAlister with wheat (53) indicated that 10 min. in the dark is sufficient to produce a noticeable induction period. Thus, in its present form, the mechanism of Franck and Herzfeld can hardly be reconciled with the results of Warburg and Negelein. It could much more easily account for the efficiencies found by Manning, Stauffer, Duggar, and Daniels (55). But, if the maximum quantum efficiency for photosynthesis is actually only 0.06 instead of 0.25, then there is no very good reason for choosing a mechanism involving four photoreactions, rather than one involving five or possibly more reactions.

In some respects it may be more desirable to postulate a mechanism involving only a single photoreaction, as in van Niel's mechanism (79). This result could also be obtained in a manner quite different from that suggested by van Niel. The following scheme indicates a possible mechanism of this type.

In the series of substances $A_1, A_2, \cdots A_{n-1}, A_n$, carbon dioxide or carbonic acid is represented by A_1 and formaldehyde or other product is represented by A_n, with the other symbols representing intermediate substances. Assuming for simplicity that there are three intermediates, the following series of changes might conceivably take place:

$$A_1 + A_5 \rightarrow 2A_3 \qquad (1)$$

$$2[A_3 + A_5 \rightarrow 2A_4] \qquad (2)$$

$$4[A_4 + h\nu \rightarrow A_5] \qquad (3)$$

The overall equation would then be $A_1 + 4h\nu \rightarrow A_5$. Water, oxygen, and other possible reactants are ignored in the above equations. Reactions 1 and 2 would presumably be enzyme reactions. The Blackman reaction might consist of one or more reactions like reaction 1 or 2, or it might be due to intermediate reactions not included in this or the following scheme.

To avoid postulating an enzyme reaction involving carbonic acid, one might use the following type of scheme:

$$4[A_1 + h\nu \rightarrow A_2] \tag{1'}$$

$$2[2A_2 \rightarrow A_1 + A_3] \tag{2'}$$

$$2A_3 \rightarrow A_1 + A_5 \tag{3'}$$

The sum of these reactions again gives the equation $A_1 + 4h\nu \rightarrow A_5$. Disproportionation reactions similar in principle to 2′ and 3′ are probably necessary in the production, by a plant, of such compounds as fats and oils, where presumably much of the energy comes from the oxidation of glucose.

If the maximum quantum efficiency is much lower than 0.25, many mechanisms of this type are possible, particularly ones involving more than three intermediate products.

With a mechanism of the type just proposed, a relatively high quantum efficiency could be maintained at very low light intensities without necessitating stable intermediate substances, such as would be necessary with a mechanism like that of Franck and Herzfeld.

Perhaps the principal value of this discussion has been to give an indication of how little actually is known concerning the chemistry of the photosynthetic process. When such entirely different mechanisms can possess even a small degree of plausibility, the need for further definite information becomes evident.

REFERENCES

(1) Albers, V. M., and Knorr, H. V.: Cold Spring Harbor Symposia Quant. Biol. **3**, 87 (1935).
(2) Albers, V. M., and Knorr, H. V.: Plant Physiol. **12**, 833 (1937).
(3) Arens, K.: Jahrb. wiss. Botan. **83**, 561 (1936).
(4) Arnold, W.: J. Gen. Physiol. **17**, 135 (1933).
(5) Arnold, W.: Cold Spring Harbor Symposia Quant. Biol. **3**, 124 (1935).
(6) Arnold, W., and Kohn, H. I.: J. Gen. Physiol. **18**, 109 (1934).
(7) Baly, E. C. C.: Proc. Roy. Soc. (London) **B117**, 218 (1935).
(8) Baly, E. C. C., Stephen, W. E., and Hood, N. R.: Proc. Roy. Soc. (London) **A116**, 212 (1927).
(9) Barcroft, J.: J. Physiol. **37**, 12 (1908).
(10) Barker, H. A.: Archiv Mikrobiol. **6**, 141 (1935).
(11) Beber, A. J., and Burr, G. O.: Paper read at Indianapolis meeting of American Society of Plant Physiologists (1937).
(12) Blackman, F. F.: Ann. Botany **19**, 281 (1905).
(13) Briggs, G. E.: Proc. Roy. Soc. (London) **B105**, 1 (1929).
(14) Briggs, G. E.: Proc. Roy. Soc. (London) **B113**, 1 (1933).
(15) Briggs, G. E.: Biol. Rev. Cambridge Phil. Soc. **10**, 460 (1935).
(16) Burk, D., and Lineweaver, H.: Cold Spring Harbor Symposia Quant. Biol. **3**, 165 (1935).

(17) Burns, G. R.: Am. J. Botany **24**, 257 (1937).
(18) Burns, G. R.: Am. J. Botany **25**, 166 (1938).
(19) Burr, G. O., and Miller, E. S.: Paper read at Indianapolis meeting of American Society of Plant Physiologists (1937).
(20) Conant, J. B., Dietz, E. M., and Kamerling, S. E.: Science **73**, 268 (1931).
(21) Craig, F. N., and Trelease, S. F.: Am. J. Botany **24**, 232 (1937).
(22) Emerson, R.: J. Gen. Physiol. **12**, 609 (1929).
(23) Emerson, R.: Ergeb. Enzymforsch. **5**, 305 (1936).
(24) Emerson, R.: Ann. Rev. Biochem. **6**, 535 (1937).
(25) Emerson, R., and Arnold, W.: J. Gen. Physiol. **15**, 391 (1932).
(26) Emerson, R., and Arnold, W.: J. Gen. Physiol. **16**, 191 (1932).
(27) Emerson, R., and Green, L.: J. Gen. Physiol. **17**, 817 (1934).
(28) Emerson, R., and Green, L.: Plant Physiol. **12**, 537 (1937).
(29) Emerson, R., and Green, L.: Plant Physiol. **13**, 157 (1938).
(30) Fischer, H.: Chem. Rev. **20**, 41 (1937).
(31) Fischer, H., and Breitner, S.: Ann. **522**, 151 (1936).
(32) Fischer, H., and Hasenkamp, J.: Ann. **515**, 148 (1935).
(33) Fleischer, W.: J. Gen. Physiol. **18**, 573 (1935).
(34) Franck, J., and Herzfeld, K. F.: J. Chem. Phys. **5**, 237 (1937).
(35) Franck, J., and Levi, H.: Z. physik. Chem. **B27**, 409 (1935).
(36) Franck, J., and Wood, R. W.: J. Chem. Phys. **4**, 551 (1936).
(37) French, C. S.: J. Gen. Physiol. **20**, 711 (1937).
(38) French, C. S.: J. Gen. Physiol. **21**, 71 (1937).
(39) Gaffron, H.: Biochem. Z. **280**, 337 (1935).
(40) Gaffron, H., and Wohl, K.: Naturwissenschaften **24**, 81, 103 (1936).
(41) Heinicke, A. J., and Hoffman, M. B.: Cornell Univ. Agr. Expt. Sta. Bull. **577** (1933).
(42) Hoover, W. H.: Smithsonian Misc. Collections **95**, No. 21 (1937).
(43) Hoover, W. H., Johnston, E. S., and Brackett, F. S.: Smithsonian Misc. Collections **87**, No. 16 (1933).
(44) Hubert, B.: Rec. trav. botan. néerland. **32**, 364 (1935).
(45) Inman, O. L.: Science **85**, 52 (1937).
(46) Inman, O. L., Rothemund, P., and Kettering, C. F.: in Biological Effects of Radiation, p. 1093. McGraw-Hill Book Co., Inc., New York (1936).
(47) James, W. O.: New Phytologist **33**, 8 (1934).
(48) Jenkin, P. M.: J. Marine Biol. Assoc. United Kingdom **22**, 301 (1937).
(49) Kautsky, H., and Hormuth, R.: Biochem. Z. **291**, 285 (1937).
(50) Kautsky, H., and Marx, A.: Biochem. Z. **290**, 248 (1937).
(51) Knorr, H. V., and Albers, V. M.: Cold Spring Harbor Symposia Quant. Biol. **3**, 98 (1935).
(52) Kohn, H. I.: Nature **137**, 706 (1936).
(53) McAlister, E. D.: Smithsonian Misc. Collections **95**, No. 24 (1937).
(54) Manning, W. M., Juday, C., and Wolf, M.: J. Am. Chem. Soc. **60**, 274 (1938).
(55) Manning, W. M., Stauffer, J. F., Duggar, B. M., and Daniels, F.: J. Am. Chem. Soc. **60**, 266 (1938).
(56) Maquenne, L., and Demoussy, E.: Compt. rend. **156**, 506 (1913).
(57) Meier, F. E.: Smithsonian Misc. Collections **95**, No. 2 (1936).
(58) Miller, E. C.: Plant Physiology. McGraw-Hill Book Co., Inc., New York (1931).
(59) Mitchell, J. W.: Botan. Gaz. **98**, 87 (1936).
(60) Nutman, F. J.: Ann. Botany [N.S.] **1**, 353 (1937).

(61) Osterhout, W. J. V., and Haas, A. R. C.: J. Gen. Physiol. **1**, 1 (1918).
(62) Petering, H. G., and Daniels, F.: In press.
(63) Porret, D., and Rabinowitch, E.: Nature **140**, 321 (1937).
(64) Pratt, R., and Trelease, S. F.: Am. J. Botany **25**, 133 (1938).
(65) Rabinowitch, E., and Weiss, J.: Proc. Roy. Soc. (London) **A162**, 251 (1937).
(66) Roelefson, P. A.: Thesis, Utrecht, 1935.
(67) Rothemund, P.: Cold Spring Harbor Symposia Quant. Biol. **3**, 71 (1935).
(68) Smith, E. L.: J. Gen. Physiol. **20**, 807 (1937).
(69) Smith, E. L.: J. Gen. Physiol. **21**, 151 (1937).
(70) Spoehr, H. A.: Photosynthesis. Chemical Catalog Co., Inc., New York (1926).
(71) Spoehr, H. A., and McGee, J. M.: Ind. Eng. Chem. **16**, 128 (1924).
(72) Spoehr, H. A., and Smith, J. H. C.: in Biological Effects of Radiation, p. 1015. McGraw-Hill Book Co. Inc., New York (1936).
(73) Steele, C. C.: Chem. Rev. **20**, 1 (1937).
(74) Stiles, W.: Photosynthesis. London (1925).
(75) Stoll, A.: Naturwissenschaften **24**, 53 (1936).
(76) Thomas, M. D., and Hill, G. R.: Plant Physiol. **12**, 285, 309 (1937).
(77) van den Honert, T. H.: Rec. trav. botan. néerland. **27**, 149 (1930).
(78) van der Paauw, F.: Rec. trav. botan. néerland. **29**, 497 (1932).
(79) van Niel, C. B.: Cold Spring Harbor Symposia Quant. Biol. **3**, 138 (1935).
(80) van Niel, C. B.: Archiv Mikrobiol. **7**, 323 (1936).
(81) Vermeulen, D., Wassink, E. C., and Reman, G. H.: Enzymologia **4**, 254 (1937).
(82) Warburg, O.: Biochem. Z. **100**, 230 (1919).
(83) Warburg, O.: Biochem. Z. **103**, 188 (1920).
(84) Warburg, O.: Über die Katalyschen Wirkungen der lebendigen Substanz. Berlin (1928).
(85) Warburg, O., and Negelein, E.: Z. physik. Chem. **102**, 236 (1922).
(86) Warburg, O., and Negelein, E.: Z. physik. Chem. **106**, 191 (1923).
(87) Warburg, O., and Uyesugi, T.: Biochem. Z. **146**, 486 (1924).
(88) Weiss, J.: J. Gen. Physiol. **20**, 501 (1937).
(89) Willstätter, R., and Stoll, A.: Untersuchungen über die Assimilation der Kohlensäure. Berlin (1918).
(90) Winterstein, A., and Stein, G.: Z. physiol. Chem. **220**, 263 (1933).
(91) Wohl, K.: Z. physik. Chem. **B37**, 209 (1937).
(92) Yabusoe, M.: Biochem. Z. **152**, 498 (1924).
(93) Zscheile, F. P., Jr.: Botan. Gaz. **95**, 529 (1934).
(94) Zscheile, F. P., Jr.: Protoplasma **22**, 513 (1935).

THE SORPTION OF OXYGEN BY SEVERAL METAL CHROMITES

J. C. W. FRAZER AND LLEWELLYN HEARD

Department of Chemistry, The Johns Hopkins University, Baltimore, Maryland

22-49

Received March 9, 1938

The study made by C. G. Albert (2) of the sorption of oxygen and of carbon monoxide by a copper chromite catalyst indicated that a similar study of the sorption of oxygen by several metal chromites might be of interest. The opinion that alternate oxidation and reduction of chromite catalysts tended to render them more active had been suggested by limited experience with some chromites, but it was not known whether chromites prepared by other methods would sorb greater or lesser quantities of oxygen. However, a very good basis for surface comparison was at hand, since Lory (3) had arrived at a figure of 4.11×10^{18} surface atoms of chromium per gram of a copper chromite catalyst, this value having been obtained by leaching chromic acid from the oxidized catalyst with boiling water and titrating with sodium thiosulfate.

APPARATUS AND TECHNIQUE

The apparatus and technique employed in making these measurements, as well as the preparation and purification of gases involved, were as described by Albert (2), with the exception that the volume measurements of the catalyst bulb were made, at the several temperatures, with tank nitrogen instead of helium, it having been determined that, as far as this purpose was concerned, no differences could be observed. An oxygen pressure of 350 mm. of mercury was likewise adopted. Sorption data were plotted in terms of cubic centimeters of oxygen sorbed per gram of catalyst versus time in minutes. From the rate isotherms so obtained, energies of activation associated with the sorption process were calculated.

THE CATALYSTS

The general scheme of preparing the catalysts consisted in obtaining a crystalline intermediate of the type $(NH_4)_2M(CrO_4)_2 \cdot 2NH_3$ (1) (where M is a bivalent metal), drying, decomposing thermally at as low a temperature as possible (200–300°C.), leaching with hot 6 *N* hydrochloric acid until no further test for metal ion could be obtained, washing, and drying.

While the use of leach-acid may have influenced the catalyst otherwise, the primary purpose was to dissolve any undecomposed material and any metal oxide present, since the oxide would have been variously subject to reduction by carbon monoxide with consequent inaccurate sorption results.

The chromites studied are regarded as insoluble in concentrated hydrochloric acid, although in their oxidized state, concerning which little beyond conjecture is available, chromic acid may be leached from them by water.

Chromites made in this manner take up water and other liquids. It was the practice, immediately upon sealing them into the system, to raise the temperature to 300°C. and then carefully to evacuate to 1–10 mm. of mercury. Under these conditions from 48 to 72 hours were required to dry them.

The object of using the crystal intermediate method was that uniformity of composition would always be found in pure crystals, giving rise to catalyst reproducibility.

TABLE 1

Conversion temperatures of carbon monoxide by chromites

CHROMITE	LOWEST CONVERSION TEMPERATURE	LOWEST TEMPERATURE OF COMPLETE CONVERSION
	°C.	°C.
$CuCr_2O_4$	85	185
$ZnCr_2O_4$	100	210
$CoCr_2O_4$	68	210
$NiCr_2O_4$	78	141
$BeCr_2O_4$	105	186

The catalysts employed were the chromites of copper, zinc, cobalt, nickel, and beryllium. Those of copper, zinc, and cobalt were prepared by the scheme of Briggs (1), but nickel chromite by the same method was so finely divided that it could not be leached with 6 *N* hydrochloric acid without being peptized and carried away in the leach-acid. Its preparation consisted in dissolving nickelous pyridino dichromate (4), $NiCr_2O_7 \cdot 4Py$, in concentrated ammonium hydroxide, removing the pyridine layer which separated, and crystallizing. This product required heating to redness before any appreciable decomposition could be observed. The second leaching failed to give a test for nickel. Beryllium chromite was prepared by the thermal decomposition of $(NH_4)_2Be(CrO_4)_2$. It was a fine gray powder.

For each catalyst the temperature at which conversion of carbon monoxide to carbon dioxide began, and at which it was complete and continuous, was determined in the apparatus described by Lory. These operations established the ranges within which, at 25°C. intervals, sorption measurements should be made. The lower and upper limits are shown in table 1.

Before sealing a catalyst into the system the sample was placed in a Pyrex carbon dioxide trap within an electric resistance furnace and, when the temperature had come to equilibrium at 200°C., a slow stream of tank oxygen was passed over it for 2 hours. The object was to oxidize the catalyst surface completely. After sealing into the system the chromite was reduced in an atmosphere of carbon monoxide prior to making each measurement.

EXPERIMENTAL RESULTS

The data of the sorption of oxygen by the several chromites employed are indicated graphically in figures 1 to 5, inclusive, while the calculated values of *E* are given in tables 2 to 5.

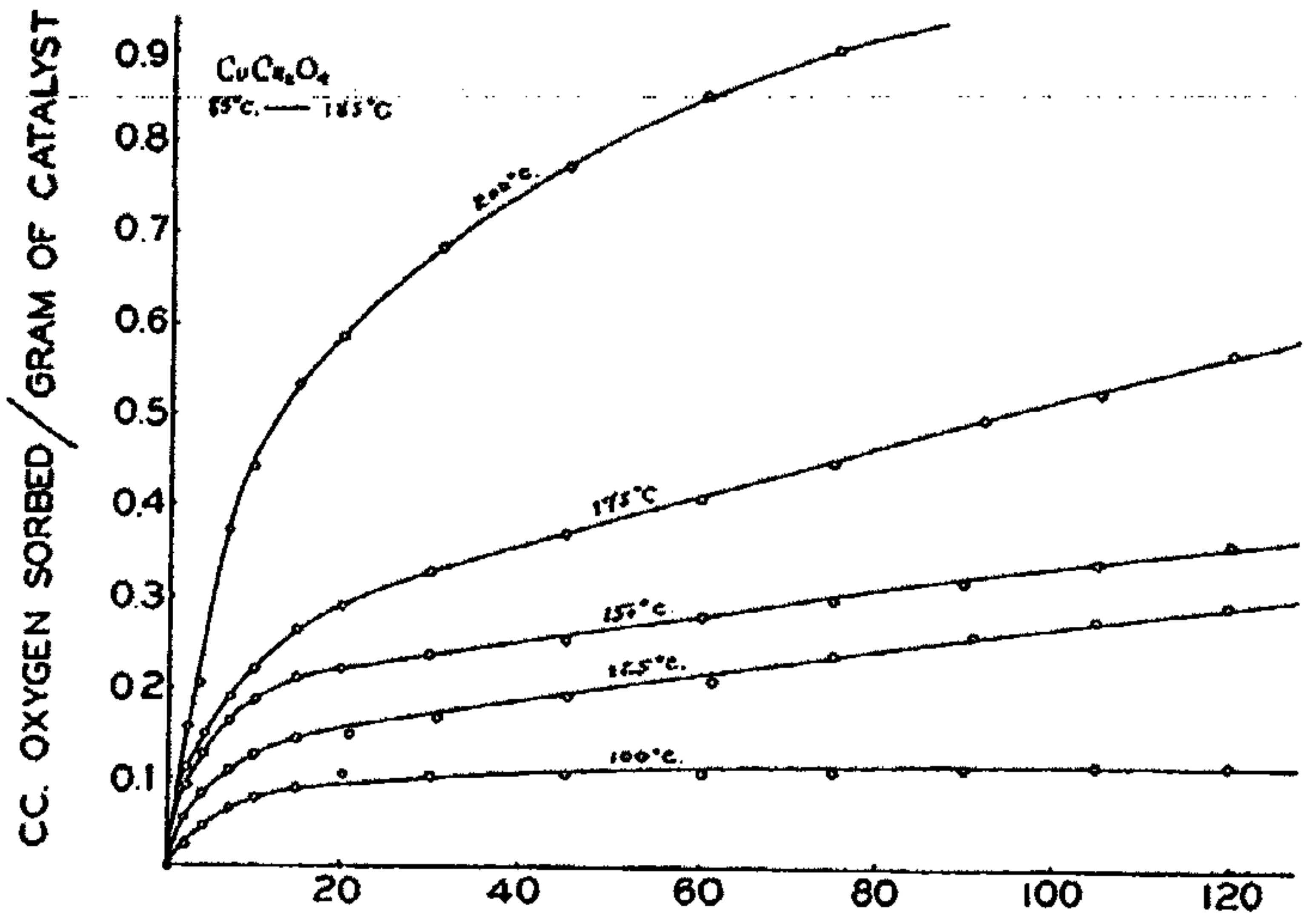

Fig. 1. Sorption of oxygen by copper chromite

It is interesting to note that while this sample of copper chromite sorbed approximately four times the amount of oxygen sorbed by Albert's catalyst, under the same conditions, the values for the energies of activation are in quite good agreement.

A sample of 5.1596 g. of this same batch of copper chromite was brought to 200°C. in a carbon dioxide trap, as indicated above, and a stream of tank oxygen was passed over it for 2 hours. The temperature rose at once to about 600°C., and then gradually fell during the next 10 to 15 minutes. At the end of the treatment the sample was leached with hot water until no further chromium could be found in a drop of the leach-water. It yielded 0.0815 g. of chromium, giving a figure of 1.84 × 10^{20} surface atoms of chromium per gram of catalyst, which, divided by Lory's figure, indicates an oxidizable or active surface 44.77 times greater than that shown

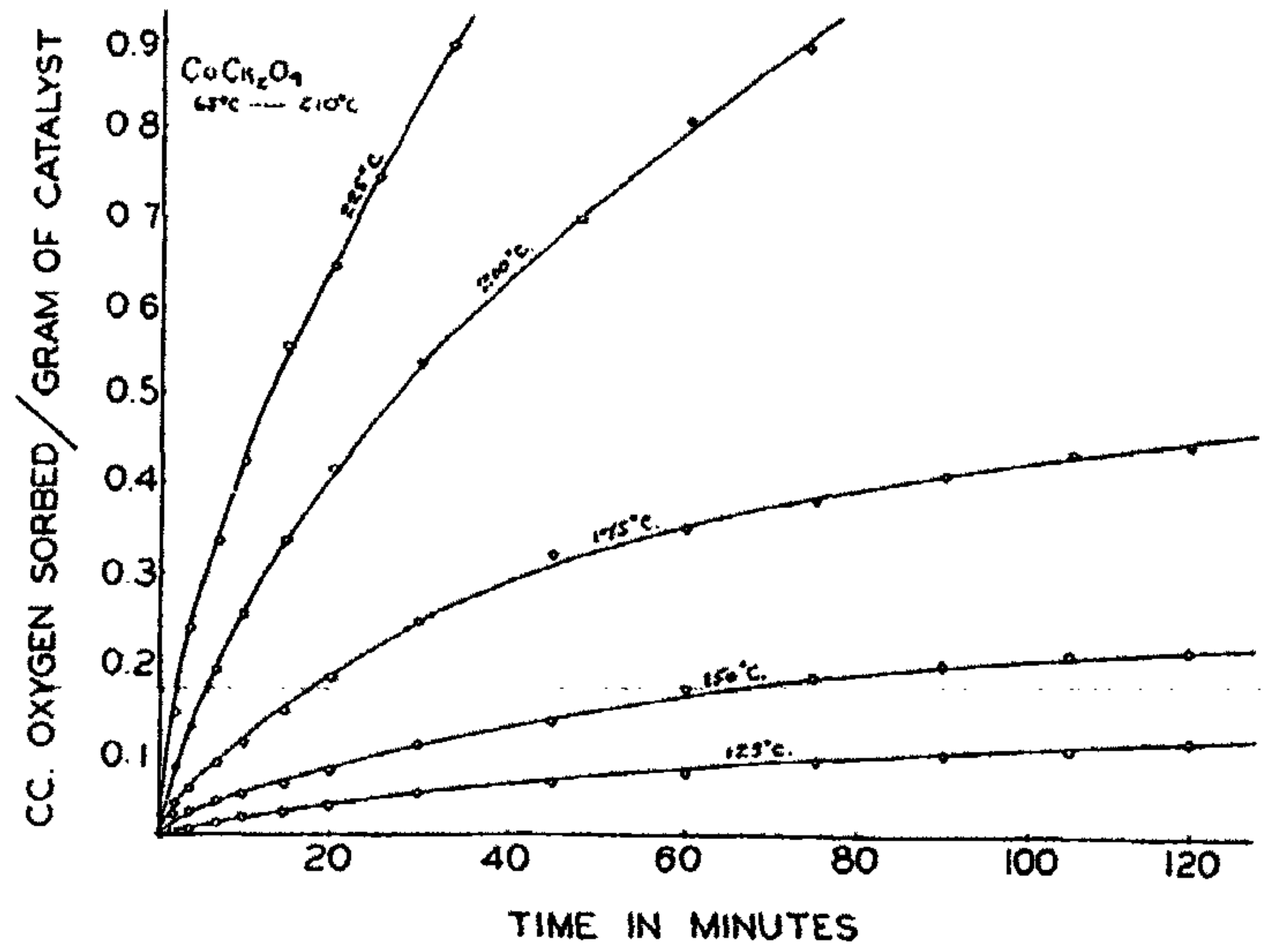

Fig. 2. Sorption of oxygen by cobalt chromite

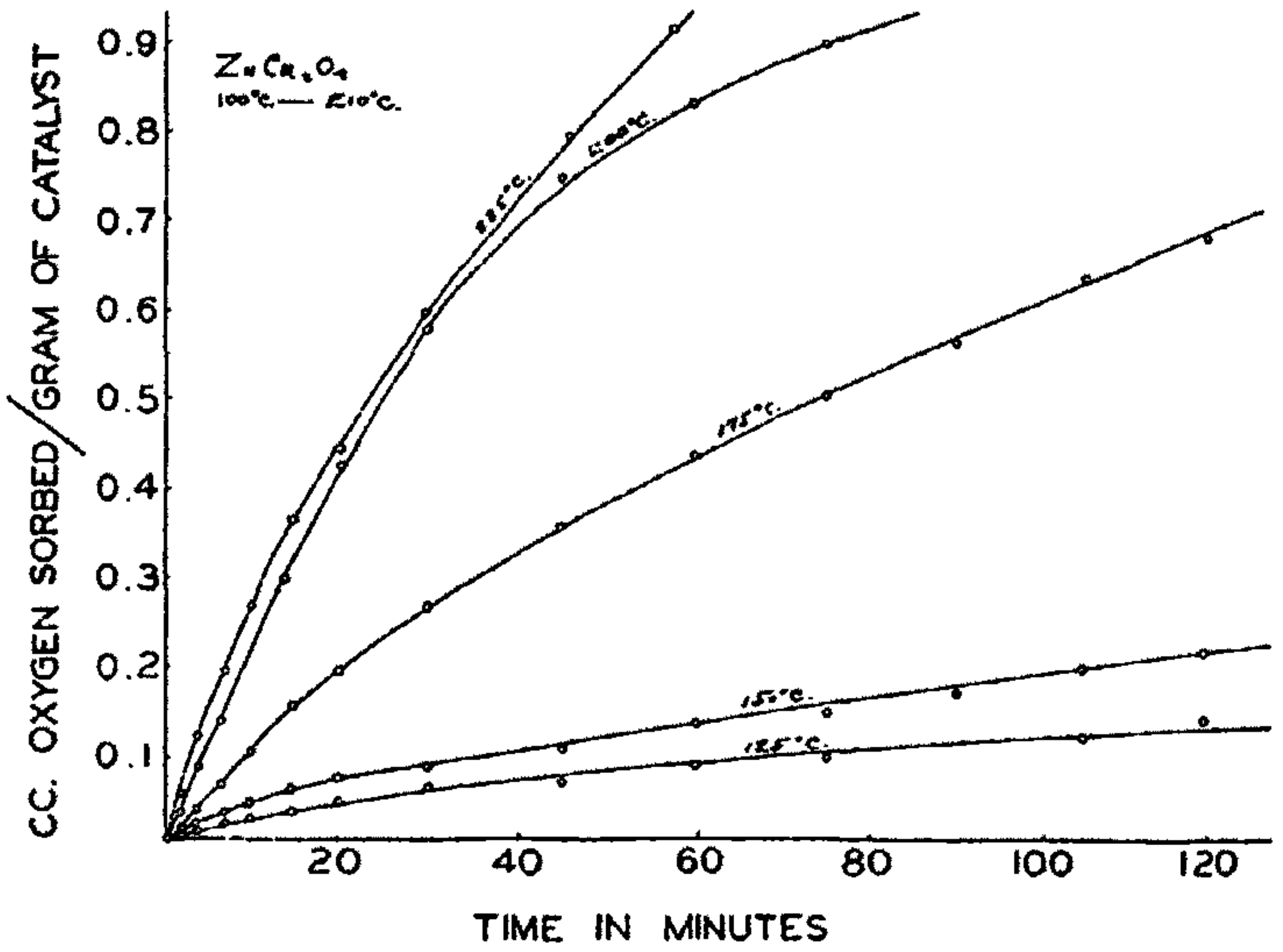

Fig. 3. Sorption of oxygen by zinc chromite

by Albert's catalyst. The apparent discrepancy between the amount of oxygen sorbed by the catalyst within the system at 200°C. and the enormity of the surface indicated by the leaching method is readily explained. The pressure maintained in the system was 350 mm. of mercury, whereas oxidation prior to leaching was carried out at atmospheric pressure. Thus more rapid oxidation accompanied by rapid increase in temperature produced in turn still greater oxidation, both sorption measurement and heat treatment being conducted over identical time intervals. Assuming the forma-

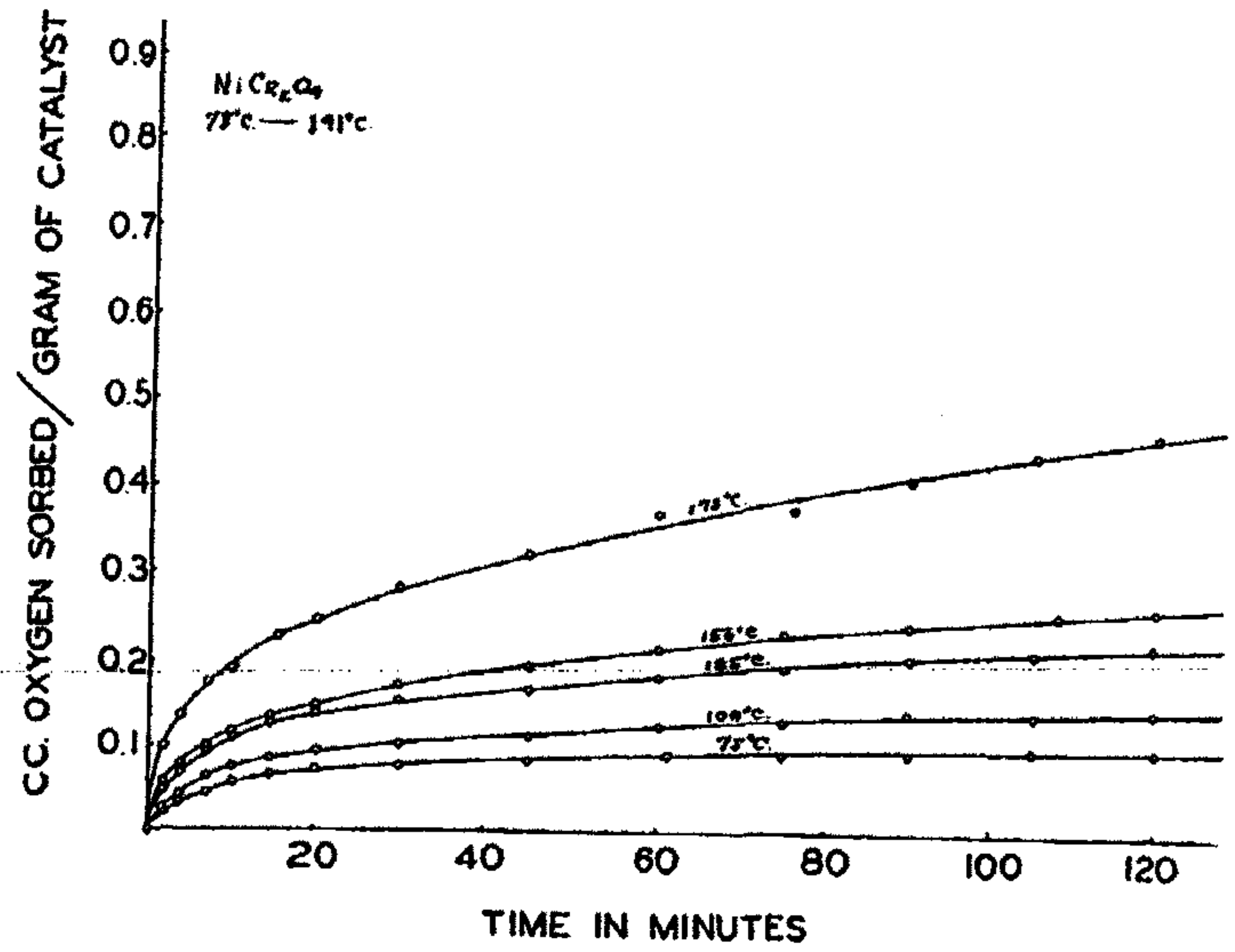

FIG. 4. Sorption of oxygen by nickel chromite

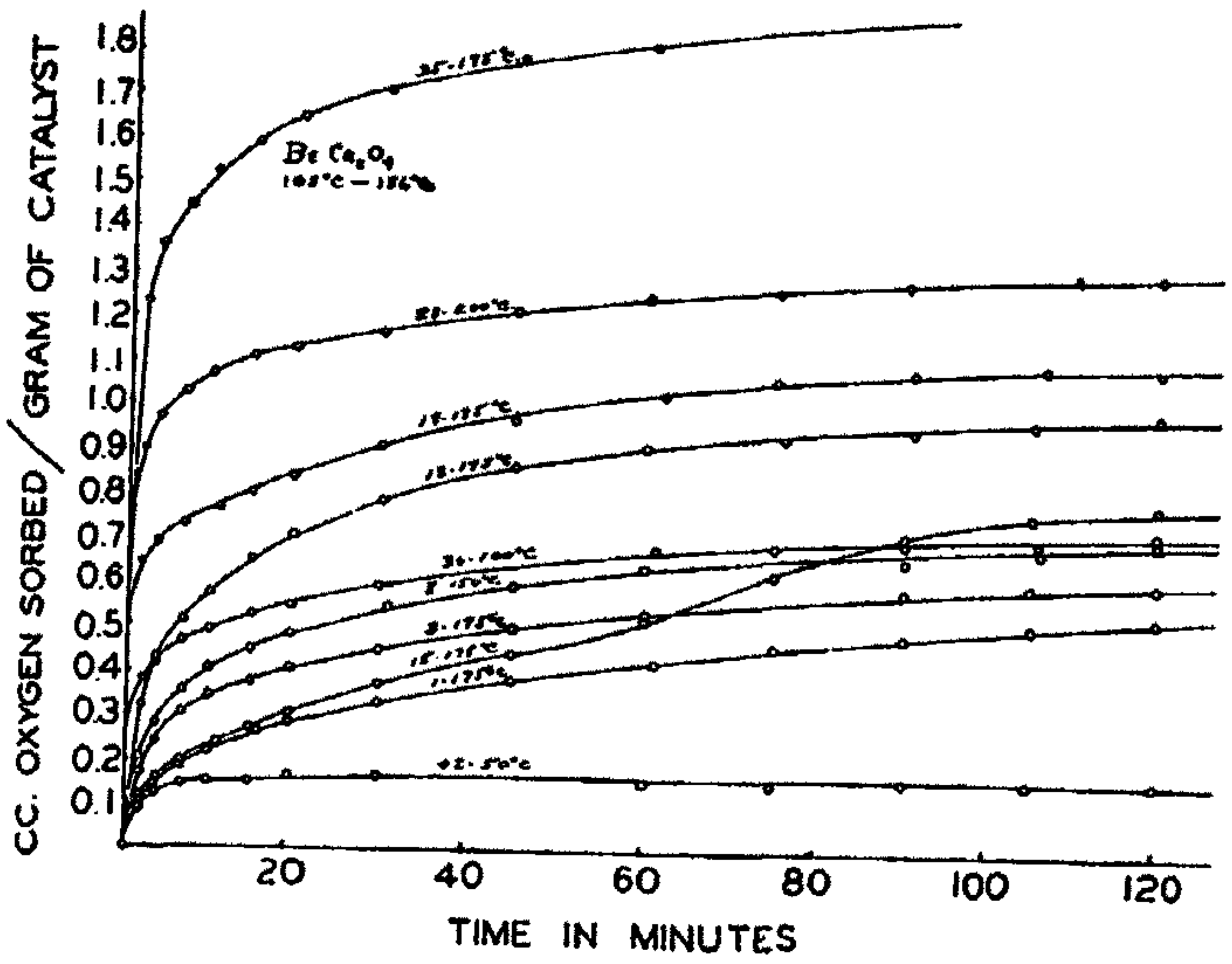

FIG. 5. Sorption of oxygen by beryllium chromite

TABLE 2

Activation energies of the sorption of oxygen by copper chromite

AMOUNT SORBED	*E* (IN KILOGRAM-CALORIES)						
	100-125°C.	100-150°C.	125-150°C.	125-175°C.	150-175°C.	150-200°C.	175-200°C.
cc.							
0.02	15.58	16.94					
0.04	12.63	13.58					
0.06	12.00	11.31					
0.08	12.07	10.87					
0.10	13.44	11.92					
0.14			12.55	8.78			
0.18			18.91	12.66			
0.22			16.41	13.22			
0.26			9.17	13.21			
0.30			6.32	12.08			
0.33					18.36	22.83	
0.36					15.85	22.99	
0.39							33.39
0.42							34.03
0.45							34.19
0.48							35.46
0.51							33.26
0.54							32.42
0.57							31.60

TABLE 3

Activation energies of the sorption of oxygen by cobalt chromite

AMOUNT SORBED	*E* (IN KILOGRAM-CALORIES)						
	125-150°C.	125-175°C.	150-175°C.	150-200°C.	175-200°C.	175-225°C.	200-225°C.
cc.							
0.02	16.08	14.36					
0.04	13.87	14.58					
0.06	13.80	15.19					
0.08	15.76	16.32					
0.10	17.72	17.11					
0.12			16.92	17.87			
0.14			16.93	17.95			
0.16			17.70	18.39			
0.18			19.20	19.14			
0.20			20.89	20.08			
0.24					19.32	17.22	
0.27					19.86	17.36	
0.30					20.39	17.25	
0.33					20.85	17.59	
0.36					22.06	17.79	
0.39					24.50	18.65	
0.42					25.24	19.60	
0.45					27.51	20.43	
0.50							14.34
0.55							14.53
0.60							14.38
0.65							14.33
0.70							14.34
0.75							14.48
0.80							14.65
0.85							15.05
0.90							15.52

TABLE 4

Activation energies of the sorption of oxygen by zinc chromite

AMOUNT SORBED	E (IN KILOGRAM-CALORIES)				
	125-150°C.	125-175°C.	150-175°C.	150-200°C.	175-200°C.
cc.					
0.02	7.07	8.32			
0.04	8.18	9.72			
0.06	10.59	12.32			
0.08	10.96	14.15			
0.10	11.15	15.09			
0.12	9.80	15.64			
0.14	9.09	14.65			
0.16			24.51	18.89	
0.18			24.94	19.48	
0.20			25.32	19.81	
0.22			25.39	19.93	
0.25					14.65
0.30					15.02
0.35					16.12
0.40					16.69
0.45					17.24
0.50					17.87
0.55					18.59
0.60					18.53
0.70					18.72

TABLE 5

Activation energies of the sorption of oxygen by nickel chromite

AMOUNT SORBED	E (IN KILOGRAM-CALORIES)						
	75-100°C.	75-125°C.	100-125°C.	100-150°C.	125-150°C.	125-175°C.	150-175°C.
cc.							
0.02	1.151	6.33					
0.04	3.378	5.93					
0.06	4.961	6.46					
0.08	11.03	10.17					
0.10	13.91	14.11					
0.12			16.14	9.92			
0.14			18.23	11.77			
0.16			14.51	10.70			
0.18					6.62	13.45	
0.20					7.00	14.12	
0.22					8.42	14.89	
0.24							23.27
0.26							23.54

tion of monomolecular layers in both the Lory and the present form of chromite, there is far from enough information to relate surface to oxygen sorbed over short time intervals.

DISCUSSION

Many of the metal chromites may be prepared through the Briggs' intermediate, and those so prepared have large surfaces as compared with the Lory catalyst.

The energies of activation of those chromites studied compare favorably with the values obtained for copper chromite by Albert.

Because of the peculiar action of beryllium chromite it was not possible to obtain any reliable energy values. The first sorption measurement was conducted at 175°C., and when an effort was made to duplicate the rate isotherm a curve revealing greater sorption resulted. A third run at the same temperature gave a curve lying still higher. Curves representing runs 1 and 3 are shown on the graph as 1-175 and 3-175. A run was then made at 100°C., and no oxygen appeared to be taken up. Half a dozen runs were next made, alternately, at 150°C. and 175°C. Each successive curve fell higher than the preceding one for the same temperature.

After run 13 had been made at 175°C., where sorption occurred to approximately twice the extent in run 1, it was decided that the catalyst might be brought to a condition of maximum sorption by oxidizing it at atmospheric pressure and at 200°C. This treatment caused it to lose temporarily some of its sorptive capacity, and the run which followed, at 175°C., gave a curve lying almost on top of curve 1. Thereafter its sorptive capacity began to increase again, curve 15 indicating this tendency.

Several runs were then made alternately at 175°C. and 200°C.; two of the results are shown in curves 19 and 23. After run 35, at 175°C., when beryllium chromite was sorbing about thirty times the amount of oxygen sorbed by Albert's catalyst and about five times that sorbed by the copper chromite sample used in these measurements, several runs were made at lower temperatures; finally, run 42 was made at 50°C. with the results shown in the graph. It may be remembered that run 4 was made at 100°C. without measurable sorption occurring.

This points to the already-proposed view that alternate oxidation and reduction of a chromite catalyst tends to increase its activity,—certainly in the case of beryllium chromite. It is not known whether more surface was being progressively activated or whether the particles of catalyst were breaking into more finely divided particles. In any event the apparent volume of the catalyst in the tube appeared to be unchanged.

After the beryllium chromite was removed from the system it was retested in the Lory apparatus. The temperature of initial conversion of carbon monoxide to carbon dioxide had fallen to 38°C., while the temperature of complete conversion had risen to 192°C.

REFERENCES

(1) Briggs, S. H. C.: J. Chem. Soc. **83**, 394 (1903).
(2) Frazer, J. C. W., and Albert, C. G.: J. Phys. Chem. **40**, 101-12 (1936).
(3) Lory, E. C.: J. Phys. Chem. **37**, 685-92 (1933).
(4) Parravano and Pasta: Gazz. chim. ital. **37**, II, 255 (1907).

NEW BOOKS

Crystal Chemistry. By CHARLES W. STILLWELL. 431 pp. New York: McGraw-Hill Book Company, Inc., 1938. Price: $4.50.

Crystal chemistry is a new branch of chemistry. The author, in his preface, defines it as follows: "Crystal chemistry is the study of (1) the laws governing the arrangement of atoms in solids and (2) the influence of the arrangement and electronic structure of the atoms upon the physical and chemical properties of the solid." It had its beginning only about ten years ago when Pauling and Goldschmidt, independently, began the correlation of the accumulated data and results of crystal structure analysis. The principles of crystal chemistry already make necessary a revision of some of the basic concepts of chemistry. Hence the importance of this new science to every chemist, both in research and teaching, is only too obvious.

The reviewer wishes to state immediately that the author has produced a very excellent book which can be most enthusiastically recommended. Many have probably read the author's splendid series of papers on this subject which appeared in the *Journal of Chemical Education* in 1936-37. These papers form the basis of parts of four chapters. The chapter titles are as follows: I, Introduction; II, The Sizes of Atoms and Ions; III, The Structures and Properties of the Elements: The Metallic State; IV, The Nature of Alloys; V, The Structures of Binary Compounds; VI, The Properties of Binary Compounds; VII, The Structures of Ternary Compounds; VIII, The Structures of the Silicates; IX, The Structures of Werner Compounds; X, Isomorphism, Mixed Crystals, Polymorphism; XI, The Structures of Organic Crystals; XII, Natural Fibers; XIII, Synthetic Fibers.

No space is devoted to discussion of the methods of crystal analysis. In the introduction the author first very briefly discusses a few fundamentals of crystallography. The remainder of the chapter is then spent in giving the reader a brief and suggestive sketch of crystal chemistry. In fact the author points out, in his preface, that the material of the introduction is intended for use in the introductory course in chemistry. The fundamentals outlined in the introduction are then developed in greater detail in the remainder of the book, making it as a whole very suitable for advanced courses.

The book contains an immense amount of data in the form of 122 tables. In addition there are 72 figures (charts, diagrams, photographs, etc.) which are almost without exception well chosen and well reproduced. The list of references is not exhaustive, but it is sufficiently complete to form a basis for a more detailed study of the subject. There appear to be very few errors of a factual nature, but several obvious typographical errors have crept in.

In conclusion, the reviewer again wishes to state that all chemists, and readers interested in chemistry, will find this an excellent and timely book.

HAROLD P. KLUG.

Grundzüge der Theorie ungesättigter und aromatischer Verbindungen. By E. HÜCKEL. 21 x 15 cm; 160 pp. Berlin: Verlag Chemie, G.m.b.H., 1938. Price: 6 RM.

This is a reprint of an article appearing in *Zeitschrift für Elektrochemie* (volume 43). The author attempts to explain with a minimum of mathematics the ideas on which the recent theories of "resonance" are based, and the principal results which have been obtained. One of his first points is that the analogy between "resonance" in molecules and resonance in the theory of forced oscillations is remote; he therefore prefers to use "mesomerism," a word originally suggested by Ingold.

The first half of the book explains briefly the pair and orbital methods of approximation to the energy of formation of polyatomic molecules, and applies them to ethylene and to benzene and other ring compounds. A chapter on free radicals follows, and some interesting speculations on di-radicals are mentioned. The subject matter of chapter V is the reactivity properties of various unsaturated and aromatic compounds. Very simple calculations, for example, give the most likely point of attachment of a first and then a second halogen atom to a number of unsaturated rings or conjugated chains. Other more complicated reactions are also considered. The last chapter gives a brief sketch of the theory of ring compounds in which one of the corner atoms is not carbon. Polar effects of unknown size here make the theory very uncertain.

In the opinion of the reviewer, several topics have been omitted which should have been included. One of the early chapters should have explained the difference between the valency state of carbon and the normal state, and hence lead up to an estimate of the energy of reorganization (Van Vleck's theory). This chapter, or another, should have given a brief account of the localized bonds. Another possible omission is that no estimate of the resistance of the ethylene molecule to twisting is made, although the most stable position is stated to be planar.

A further criticism is that no matter in what form comparisons of "calculated" and observed energies of formation of long series of aromatic and unsaturated molecules are presented, far too good an impression of the accuracy of the theory is given. What is being tested by these comparisons is not the theory, but the constancy of bond energies from molecule to molecule. When the molecule is mesomeric, as a matter of observation, some of the bonds gain slightly in stability, and the theory of mesomerism in its present form seems to offer a convenient semi-empirical method for estimating these gains. Unless this is made very clear to the general reader, he will get the impression that the theory is almost rigorously precise, whereas all that may be said at present is that apparently it gives precise results.

The book is recommended because those topics with which it deals are covered very well. Any later book on mesomerism will be able to make considerable use of the present work. It would seem desirable, however, that in a more extended account of the subject other important topics should be mentioned, such as the difference between the valency state of carbon and the normal state, localized bonds, and a more detailed statement of the resistance of molecules such as that of ethylene to twisting. More emphasis might also be laid on the semi-empirical character of some of the calculations of the present time.

W. G. PENNEY.

Duodecimal Arithmetic. By GEORGE S. TERRY. 407 pp. New York: Longmans, Green and Co., 1938. Price: $7.50.

It has often been pointed out that the operations of arithmetic would be simplified in many respects if our counting were based on some other number than ten. The base twelve, in particular, has important advantages in its divisibility by 2, 3, 4, and 6. One must be an enthusiast, nevertheless, in order to look hopefully toward widespread adoption of a new system of numeration for the purposes of school, commerce, and science. The author of *Duodecimal Arithmetic* is such an enthusiast, and has given as favorable a presentation of the case for the duodecimal system as can well be imagined.

The verbal argument is brief, temperate, and judicious. The fundamental arithmetical processes are explained and illustrated in a notation using the digits 0, 1, 2, ··· 9, together with the symbols X and E, or modifications of them, for the numbers ordinarily called ten and eleven. The equation 34 + 121 = 155, for example, becomes 2X + X1 = 10E. The introduction is followed by an extensive set of tables including powers and roots, reciprocals, logarithms, and the natural values and logarithms of trigonometric functions, largely to nine places of duodecimals, designed to facilitate an adequate trial of the notation for purposes of actual calculation. The text and tables, excellent in arrangement, convenient to the hand and agreeable to the eye, will be interesting and instructive to many students who examine them with less serious purpose than the ultimate reform of all arithmetic.

DUNHAM JACKSON.

Expresion de la Reaccion y Calculos Potenciometricos en la Determinacion del pH. By DOMINGO GIRIBALDO. 271 pp. Montevideo: Casa A Bareiro y Ramos, 1937.

This book is divided into three parts. In the first part, involving eight chapters, the reaction (pH) of aqueous solutions is discussed with emphasis on the expression pR = log H$^+$ − log OH$^-$. The dissociation and neutralization curves of ampholytes are described in detail. The second part (nine chapters) deals mainly with principles of potentiometry, the calculations involved, and the potentiometric determination of pH with the hydrogen, quinhydrone, and glass electrodes. The last part presents tables with explanatory notes which are useful in the calculations.

The book is quite up to date and is a good addition to the literature on this subject in the Spanish language.

I. M. KOLTHOFF.

Qualitative Analyse mit Hilfe von Tüpfelreaktionen. By FRITZ FEIGL. 3rd edition. 554 pp. Leipzig: Akademische Verlagsgesellschaft, 1938. Price: bound, 30 RM.

Feigl's book does not need a recommendation. The rapid appearance of the third edition after the second one (1935), with the English and Russian translations of the latter, shows without doubt that the book is universally considered a standard work. It occupies a unique place in qualitative analysis. It serves as a guide for further research in the development of new (mainly) organic reagents and tests and it contains a wealth of information regarding the identification and separation of inorganic and organic ions and molecules.

To the theoretical part have been added chapters on "fluorescence analysis and spot reactions" and "effect of substitutions by heavy groups on solubility." The practical part occupies about 400 pages and gives an extensive review of the detection of inorganic cations and anions, of systematic schemes of separation, of the detection of elements and reactive groups in organic compounds and of a number of organic substances. The last chapter deals with the application of spot tests to purity tests and detection of traces of various constituents in minerals, ores, alloys, etc. Finally, an extensive alphabetical table is given in which the reagents and sensitivities of the reactions of the various inorganic and organic components are summarized with references to pages in the text.

The book is a tribute to Feigl's pioneer work in the field. It is a sad coincidence that the publication of this third edition occurred at the time when the author with many other scholars was dismissed from the University of Vienna for racial or political reasons. The reviewer expresses the wish that chemists whose views and outlook are determined mainly by the search for truth will coöperate in finding a deserving position for the author which will enable him to continue his important researches in a truly scientific environment.

I. M. KOLTHOFF.

Numerical Problems in Advanced Physical Chemistry. By J. H. WOLFENDEN. 227 pp. London: Oxford Press, 1938. Price: $2.75.

The 133 problems which make up this list have been selected from the original literature to illustrate the principal divisions of physical chemistry. In the reviewer's opinion the selection has been made wisely and with remarkably little bias. The essential data of each problem are accompanied by a brief but valuable discussion of the immediate background of the subject. The usefulness of the book is greatly increased by the inclusion of references to the original literature, to specialized monographs, and to a number of the better known texts of physical chemistry. Answers to the problems are furnished at the end of the book.

Any independent student of general physical chemistry should find this book helpful and stimulating. In this country it will probably be used most extensively by candidates for the doctor's degree in reviewing their elementary physical chemistry in preparation for examination.

ROBERT LIVINGSTON.

Newer Methods of Volumetric Chemical Analysis. By E. BRENNECKE, N. H. FURMAN, K. STAMM, R. LANG, and K. FAJANS; WILHELM BÖTTGER, Editor. Translated by Ralph E. Oesper. 268 pp. New York: D. Van Nostrand Company, Inc., 1938. Price: $3.75.

This volume is the English translation of the second German edition of *Neuere massanalytische Methoden*, one of the series *Die chemische Analyse*. The book is a collection of discussions of recent developments in volumetric analysis embracing the following topics: elimination of the titration error in acidimetric and alkalimetric titrations, ceric sulfate as a volumetric oxidizing agent, alkaline permanganate solution as volumetric oxidizing agent, iodate and bromate methods (including Manchot's bromometric method), chromous solutions as volumetric reducing agents, oxidation-reduction indicators, and adsorption indicators for precipitation titrations. Comprehensive bibliographies are appended to each section. As stated by the editor in the preface, "These topics have been treated with two objectives in mind: (a) exposition of the theory underlying the new method, so that an insight may be gained into the reasons for the way in which the subject has been developed, and (b) the presentation, so far as possible, of an exact set of directions for the performance of particular analyses."

In reading this book one cannot but be struck by the important rôle played by physicochemical principles in the development of modern methods of chemical analysis. The topics treated do not exhaust the field and one might wish that other phases of the subject (for example, induced reactions) had been included.

The translation has been excellently done. A number of minor errors of typographical nature were noted. "Quinquevalent" has been spelled "quinquivalent." In the footnote on page 99, the journal reference should be "Z. angew. Chem.," not "Z. anorg. Chem."

E. B. SANDELL.

Photoelements and their Application. By BRUNO LANGE. Translated by Ancel St. John. New York: Reinhold Publishing Corp., 1938. Price: $5.50.

This book is the first covering the whole field of semiconduction photo cells. About 238 references are cited and commented upon.

The book is divided into two sections. The first deals with the development and properties of the photoelements and the second with the applications. The first section gives an integrated picture of the development and properties of what

Dr. Lange calls "photoelements", including "barrier-layer cells, photovoltaic cells, crystal cells, Becquerel cells, etc."

The brief historical development is followed by a review of the various theories concerning the semiconductor photoeffect. The Shottky (barrier film) and the Teichmann (field funnel) theories are correlated, the electrochemical theory discarded, and the electron diffusion theory, using an insulating layer, stressed. It seems unfortunate to the reviewer that the difference of the insulating layer and the barrier layer is stressed. Although the cuprous oxide front wall cell mentioned on page 73 does not show unipolar conductivity, both the German electrocell and the Weston phototronic cell do show unipolar conductivity. Both of these are front-wall selenium cells. The conclusion would seem that the idea of a barrier film cannot be dismissed so easily. In explaining the photo E.M.F. by electron concentration gradients only the concentration in the semiconductor and the insulating layer are considered, although there would be considerable electron concentration in the metal layer above it. It is this factor that the barrier layer has tried to explain.

The chapter on physical properties coördinates a vast amount of literature of the past few years. It will be very valuable to anyone desiring to review these when time for review is limited. The characteristics of the cell—photocurrent, photopotential, and cell resistance as related to intensity of illumination as well as to each other—are described and the curves given. The effect of temperature, wave length of incident light, polarized light, x-rays, cathode rays, and magnetic field are discussed, similarly the frequency relations and capacitive properties. The stability and fatigue values are clearly separated from each other. The effect of fatigue is eliminated in stability measurements by allowing a two-hour dark recovery period before measurement. Of interest to physicists may be the method applied in determining the work function and the threshold wave lengths by indirect measurements.

The first section of the book serves as an excellent bibliography up to 1935; however, a great deal of work has been done since that date and this is not covered by the translator.

The second section deals entirely with construction and applications. The details on construction are very incomplete and would offer little help to anyone interested in this art.

The description of applications is, however, very complete. The section is very similar to a manufacturer's publication, and as such stresses particularly the apparatus of the German companies. The section is, however, very readable and has many interesting suggestions for manufacturers or chemists interested in control instruments.

Exposure meters for photographic control (some semiautomatic on motion picture cameras), for copying, and for photomicrographic use are described. Transparency and density meters, micro- and spectro-photometers, reflection and gloss meters are common uses. Of great interest to the chemist is the accurate measurement by differential means of absorption of light in colorimetry. The use for analytical work of this type is rapidly growing. The application of photoelement cells is described for long distance transmission of circular or straight scales, for industrial cases where the position of the original instrument is fixed. Other applications include auxiliary control for balances, switching and signal devices, etc. In some of these cases the advantages of the photoelement as opposed to the photoelectric vacuum tube are pointed out.

In conclusion the author suggests uses in the fields of chemistry, physics, astronomy, bioclimatology, meteorology, oceanography, hydrography, medicine, and electrical engineering and also as a source of energy.

The latter half of the book is primarily an advertising medium and should be treated as such. The first half is an interesting integration of the knowledge and theory of the semiconductor photocell at the time the book was written.

JOHNSTONE S. MACKAY.

The Catalytic Action of Surfaces. By J. E. NYROP. Second edition. 103 pp. 20 x 27 cm. Copenhagen, Denmark: Levin and Munksgaard, 1937. Price: 10 Danish krone.

The thesis that the author attempts to develop and support by experimental and theoretical arguments is stated in the following two postulates: "Postulate A. In a chemical reaction furthered considerably by the presence of a surface the surface is at the temperature in question able to ionize those molecules among the reactants most difficult to ionize and the surface will cause a strong adsorption as ions formed are attracted by the surface. Postulate B. A surface able to ionize molecules of a gas or liquid and hence able to yield a strong adsorption produces an increased adsorption when the molecules are substituted by others having a lower ionization potential assuming that all other conditions are the same."

Since new points of view in catalysis are always welcome, this book with its eighty-three references and its partial summary of experimental work in catalysis will probably be found interesting to many readers. To all it should prove thought-provoking. However, in the reviewer's opinion, the book is unconvincing and in some respects carelessly written.

The attempted substantiation of the ideas of postulates A and B by presentation of catalytic data is frequently marred by an evident lack of critical judgment or a careless scrambling of experimental results. The following excerpt from page 23 will suffice as an illustration: "When hydrogenation of the (carbon) monoxide takes place on copper, methane is produced and, as the ionization energy of these products is between 13.7 and 15 volts, none of them take up the space of the surface zone preferentially. If three volumes of hydrogen and one volume of nitrogen pass over a surface of nickel or one of iron at certain temperatures and pressures ammonia is produced and the best result is obtained when the adsorption takes place in the proportion of 3:1. In accordance with technical results this takes place on iron."

To appraise this statement properly one must bear in mind that copper is ordinarily considered incapable of hydrogenating carbon monoxide to methane, that the ionization potentials of H_2O,CO,CH_4, and H_2 are 12.7, 14.1, 14.5, and 15.37 volts, respectively, and that the separate adsorption measurements for hydrogen and nitrogen on iron catalysts do not reveal a 3:1 ratio at any temperature at which the synthesis of ammonia takes place, as far as the reviewer has been able to ascertain. No source of information was cited in connection with the paragraph from which the above quotation was taken.

The mathematical formulations in chapter II are insufficiently explained to enable the reviewer to assess their value. They are entirely unconvincing in their present form. However, it seems that no amount of revision or clarification of this or other portions of the book so far discussed will establish the case that the author is attempting to support, unless the conclusions arrived at in chapter VII are sound. In this chapter on "Metals" the author takes upon himself the task of explaining how, for example, iron or nickel catalysts are able to ionize impinging molecules whose ionization potentials are as high as 17 or 18 volts. Final judgment in this connection will have to be left to the mathematical physicist.

P. H. EMMETT.

Hydrophobic Colloids. Symposium on the Dynamics of Hydrophobic Suspensions and Emulsions, held at Utrecht on the 5th and 6th of November, 1937, under the auspices of the Colloidchemistry Section of the Nederlandsche Chemische Vereeniging. 188 pp. Amsterdam: D. B. Centen's Uitg. Mij. N.C., 1938. New York: Nordemann Publishing Co., Inc., 1938. Price: $2.50.

From a social and propagandistic point of view large scientific gatherings concerned with many fields of work will always be called for. For clearly stating and actually promoting knowledge, meetings of smaller groups of specialists are more important, and they have become therefore more and more popular, for at them it is possible to restrict the number of lectures and to find time for thoroughly discussing the problem in question. An excellent example of this type of meeting is the one in review.

The lectures delivered at the Symposium treated mainly the stability of hydrophobic colloidal solutions and emulsions, the electrical properties of their particles, and the protecting and sensitizing action of hydrophilic colloids. The younger generation of colloidal chemists, more theoretically minded than the older one—Holland may claim to possess a very active and successful group—is right in trying to apply new theoretical conceptions, e.g., Debije-Hueckel's theory, to these problems. The discussion shows that this theory cannot explain in a simple and straightforward way the difficulties of the electrical double layer. Several speakers, representing fairly different points of view, acknowledged that even with poorly hydrated colloids the hydration of the ions, so strongly depending upon their size and charge, is most important and may be decisive for the distribution of the ions on the surface of the particles. This specific nature and hydration of the ions is a cardinal point not covered by Debije-Hueckel's theory. Perhaps the time has come when conceptions concerning hydration, as they are discussed by Bernal and Fowler (*Journal of Chemical Physics*, 1933), may be extended and applied to these colloidal systems.

H. Freundlich.

STUDIES OF THE MEASUREMENT OF THE ELECTRICAL CONDUCTIVITY OF SOLUTIONS AT DIFFERENT FREQUENCIES. VIII

Oscillograph Tests on Conductivity Cells

S. F. ACREE,[1] EDWARD BENNETT, G. H. GRAY, AND HAROLD GOLDBERG

Department of Electrical Engineering, University of Wisconsin, Madison, Wisconsin

Received March 9, 1938

I. INTRODUCTION

In collaborative work in 1915–16 at the University of Wisconsin, dealing with precision inductance and capacitance bridges and techniques for measuring the true electrolytic conductance and the "capacitance or condenser effect" exhibited at the electrodes of a conductivity cell at different frequencies, it was shown (13, 8, 14, 11; see also 16, 15, 17, 5, 6, 2, 10) by both bridge and oscillograph measurements at audio frequencies that, to a first approximation, cells with bright platinum electrodes have the electrical characteristics of a resistor, R, *in series* with a large capacitor, C, rather than the properties of a resistor *in parallel* with a capacitor. A second and closer approximation to the characteristics of the electrolytic cell is obtained by conceiving a high resistance leak, R_1, to be connected across the terminals of the series capacitor of the first approximation, as illustrated in figure 1.

The features of the conductivity cell recognized at that time as of importance for further study are schematically illustrated by the arrangement of resistors and capacitors in the "artificial cell" or "simulating network" of figure 2.

In figure 2 the heavy lines of the two capacitors C_1 and C_2 represent the leads and platinum electrodes of the cell, and the + and − signs at their surfaces indicate the charges on the metal. The + and − signs back of the lighter lines of the capacitors C_1 and C_2 indicate charges in the layers of electrolyte adjacent to the electrodes. These charges in the electrolyte are the result of ionic migration and of elastic displacements within the molecular structures of the solution. In very precise approximations, outside the scope of this article, there is probably associated with C_1 and C_2 also the relation of transient and steady-state capacitance phenomena

---

[1] Present address: National Bureau of Standards, Washington, D. C.

to (*a*) the mechanism and rate of reversible deposition and discharge of the ions of the solute and solvent (e.g., H^+ and OH^- of water), (*b*) the behavior of fresh and aged optically flat, smooth, rough, and spongy electrode surfaces, in connection with the reversible deposition and discharge of ions, and association, union, and recharge of atoms and radicals, (*c*) the reversible segregation and re-deposition of ionic and colloidal particles of the electrode material, alone and electrically associated with other ions, and giving rise to alteration of the electrode surfaces, (*d*) oxidation and reduction of the ions and moles of electrolytes and non-electrolytes in solution and on the electrodes, (*e*) the amount, fate, and electrical and chemical character of gases deposited on the electrodes, (*f*) the activities of the pore walls and solutes causing adsorption of the solute and solvent, (*g*) electrical phenomena associated with the polarity, viscosity, electrophoresis, and internal structure of the solvents and solutes, particularly in such cases as solutions of metallic sodium in liquid ammonia, and (*h*) the capacitance due to the solvent alone as differentiated from that arising from the solute, and allowance for both the measured capacitance and conductance found for the solvent when making the usual solvent corrections in studies of the conductance-capacitance properties of electrolytes.

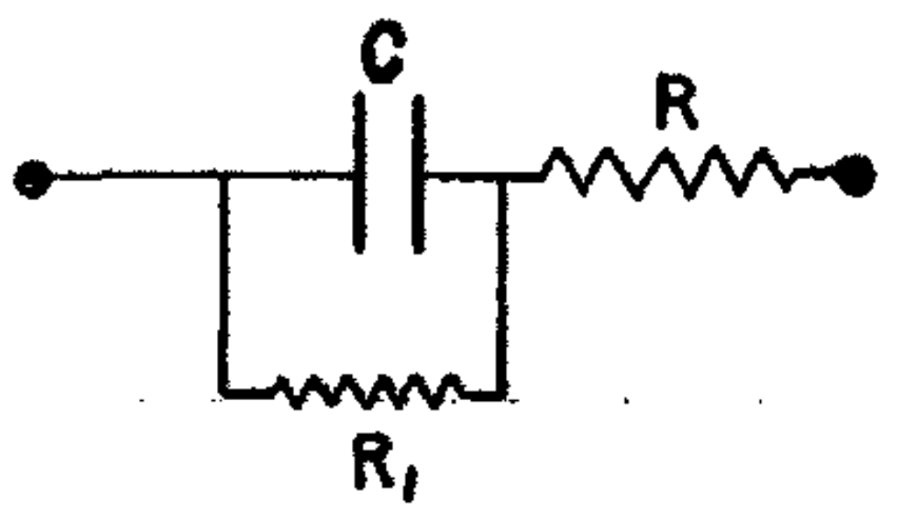

FIG. 1. Network simulating a conductivity cell. Second approximation to a conductivity cell.

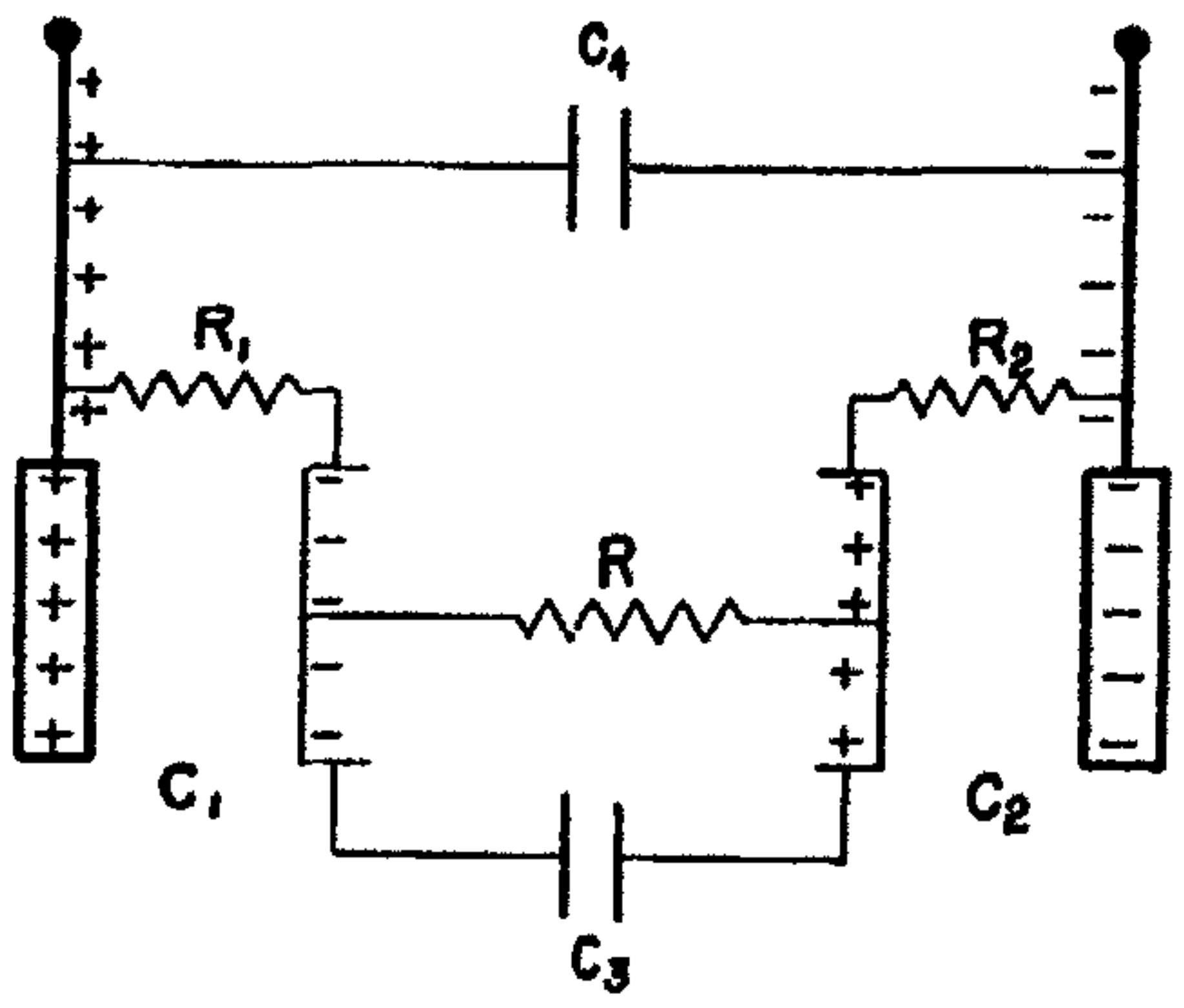

FIG. 2. Network simulating a conductivity cell. Third approximation to a conductivity cell.

The capacitances of C_1 and C_2 were shown to have different values depending upon the area, material, and surface character of each electrode, the degree of reversibility of the reactions at the two electrodes, and the types, mobilities, and activities of the solute ions. In the first approximation to the cell, the resultant capacitance of the two series capacitors C_1 and C_2 is treated as a single capacitance in series with the resistance R of the column of electrolyte between the electrodes.

The column of electrolyte between the electrodes may be thought of as made up of three portions: namely, the two layers of electrolyte each adjacent to one of the two electrodes, in which layers the concentration and composition of the electrolyte change throughout the current cycle, and the remaining portion of the column in which they do not change. It is readily seen that the actual resistance of the column of electrolyte varies throughout the current cycle. Moreover, its effective value averaged over the cycle will depend upon the frequency of the alternating current, since the lower the frequency, the greater will be the change in concentration in the electrode layers and the greater will be the depth of the layers which are affected by ionic migration. As the measuring frequency is made higher and higher, the changes in concentration over the cycle become less and less, and the measured resistance decreases and approaches the true ohmic resistance of an undisturbed column of electrolyte between the electrodes.

If a network simulating the electrolytic cell is to be made up of *fixed* resistances and capacitances, then the change with frequency of the measured resistance of the electrolytic cell can be closely (but not precisely) simulated by a network in which leaks R_1 and R_2 are connected in parallel with each of the capacitors C_1 and C_2 (or by a single leak, R_1 in figure 1, connected in parallel with the single capacitor whose capacitance is that of C_1 and C_2 in series). The ohmic resistances of the leaks R_1 and R_2 are high in comparison with the capacity reactances $1/(2\pi fC_1)$ and $1/(2\pi fC_2)$ of the respective capacitors. The electrical characteristics of such an arrangement are a third approximation to the characteristics of the actual cell.

To determine the additional elements which would have to be added to the simulating network of third-order approximation to make the network simulate the electrolytic cell with even greater precision, particularly at high frequencies, would require precision measurements over a wide range of frequencies. Undoubtedly a capacitor C_3 would be required in parallel with the resistance R to simulate better the effect of the elastic displacements within the molecular structures, and also a small capacitor C_4 between the cell terminals to represent the capacitance between cell leads.

In the earlier work these diagrams of the constitution of fixed element networks whose electrical characteristics were to simulate those of given electrolytic cells were deduced from bridge balances obtained on such cells after all transient terms had vanished from the measuring current and the alternating current had attained its "steady state". This question naturally arose: Will the transient currents which flow in these simulating networks when they are connected to and disconnected from the source of alternating current simulate the transient currents which flow in the electrolytic cells when they are subjected to similar switching operations? To answer this question, oscillograms were taken (1916) to show the wave forms of the potential across electrolytic cells and the current through the cells for a number of cycles after the cells were switched on to the source of alternating current at different points on the potential wave form. These earlier oscillograms have recently (1935) been supplemented by others, showing the fall of the potential of the cells after they have been disconnected from the source at different points on the current wave form.

As no actual oscillograms covering these new phases of the theory of the electrode reactions and their relations to conductivity measurements have apparently been available heretofore (7, 9, 4, 3)[2], this article is presented as a step in our attempts to secure a clear understanding of the fundamental nature of the electrode phenomena and to perfect methods for the accurate measurement of the ohmic resistance of electrolytic solutions.

II. EQUIVALENCE BETWEEN THE ELECTROMOTIVE FORCES OF POLARIZATION AND OF A SERIES CAPACITOR

When a small alternating electromotive force is impressed upon a conductivity cell containing an electrolyte between bright platinum electrodes, the cell is found by bridge and oscillograph measurements to have the characteristics, not of a pure ohmic resistance, but of an ohmic resistance connected *in series* with a capacitor.

The capacitor effect arises from the alternating electromotive force which is set up in the layers of electrolyte immediately adjacent to the electrodes as the result of changes during each cycle in the ionic concentration in these layers. For a sinusoidal current through the cell, this layer E.M.F. is a sinusoidal E.M.F. which is 90 degrees in advance of the current; as a first approximation it corresponds with the E.M.F. which would be observed across a capacitor connected in series with a pure ohmic resistance equal to the ohmic resistance of the column of electrolyte between the electrodes. However, this correspondence holds only as long as the measuring current densities are so low that the layer E.M.F. is below the E.M.F. of polarization of the cell. At current densities well above these values, the layer E.M.F. is neither directly proportional to the current nor sinusoidal in form.

In the case of electrolytic solutions of good conductivity measured between bright platinum electrodes at frequencies of 1000 cycles or less, the

---

[2] See Holler (1), who used exploratory electrodes near the cell electrodes for studying electrode potentials, as suggested by us in 1916 (12).

fictitious or equivalent capacitances C_1 and C_2 in *series* with the resistance of the column of electrolyte play a far more important part in the interpretation of measurements of the phase relations and the electrical impedance of the cell than do the capacitances C_3, paralleling the resistance R, and C_4 representing the capacitance between leads. Each of these four capacitances causes the sinusoidal current through the cell to lead the sinusoidal E.M.F. impressed upon the cell. But for some of our measurements the tangent of the angle of lead (at 1000 cycles per second) due to the series capacitance is about 45,000 times as great as the tangent of the angle due to the parallel capacitance.

That the interpretation of precision measurements on conductivity cells requires the consideration of this series capacitance effect (and the ionic phenomena to which it is due), as well as the parallel capacitance, was established by our earlier alternating current measurements at 250 to 4000 cycles per second with precision inductance and capacitance bridges to determine the relations concerning the true and apparent resistances, the equivalent series capacitance, the size, material, and surface condition of the electrodes, and the frequency and magnitude of the E.M.F. applied to the cell in the measurements.

This paper contains several sets of oscillograms which show the relations between the wave forms of an alternating current through a conductivity cell and that of the corresponding electromotive force across the cell for a number of cycles immediately following switching operations which close or open the circuit at different points on the wave form of the current. The oscillograms were taken with the first objective of determining the effect of the frequency and of the magnitude of the impressed electromotive force upon the apparent series capacitance of the cell and upon the wave shape of the current. A second objective was to determine whether the transient terms which occur in the current and the electromotive force across such a cell immediately after a switching operation which connects or disconnects a source of alternating electromotive force to the cell are, to a first approximation, identical in form with the transient terms which occur when identical switching operations are carried out upon a simulating network made up by connecting an appropriate resistor and capacitor in series. A third objective was to throw additional light on the nature of the "leak resistors" R_1 and R_2 of figure 2 by determining the rate of decrease of the cell E.M.F. when the cell is cut off from the source of current at the peak and zero points of the current, and is then allowed to discharge through resistors of different values.

III. METHOD AND APPARATUS

The oscillograms were obtained by means of a General Electric three-vibrator oscillograph with the circuit connections shown in figures 3 and 4. Referring to these figures: L and C represent an inductor and a capacitor of such values as to filter out all harmonics from the E.M.F. wave form of the 60-cycle circuit. T is a multi-tap auto-transformer by means of which the desired E.M.F. can be impressed upon the cell. S represents a switch which by means of a synchronous motor can be closed and subsequently opened at any desired points of the wave form of the impressed electromotive force. I represents the oscillograph vibrator which records the wave form of the current through the cell. In figure 4 the vibrator I records the total current taken by the cell and the vibrator E_c. The current taken by the vibrator E_c is only 3 to 8 per cent as great as that taken by the cell. E_c represents the vibrator which records the wave form of the E.M.F. impressed upon the cell. E_t represents the vibrator which records the wave form

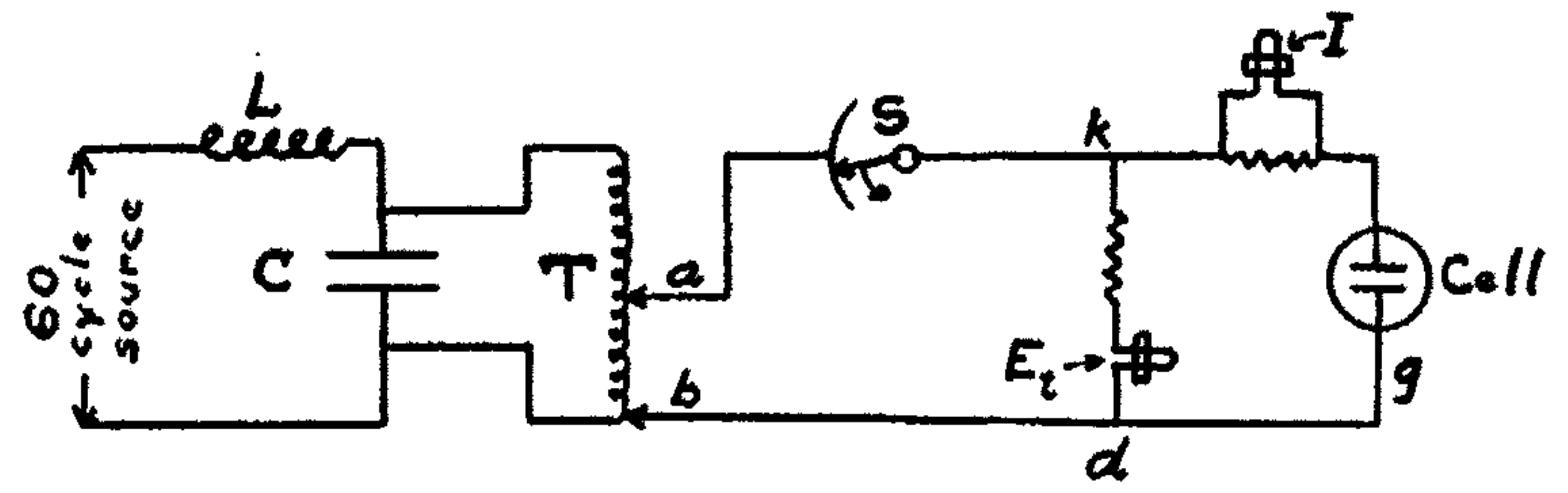

FIG. 3. Diagram of circuit for making oscillograms of wave forms of current and total impressed voltage. For the 240-cycle measurements wires a and b were connected to the secondary coil of the Vreeland oscillator.

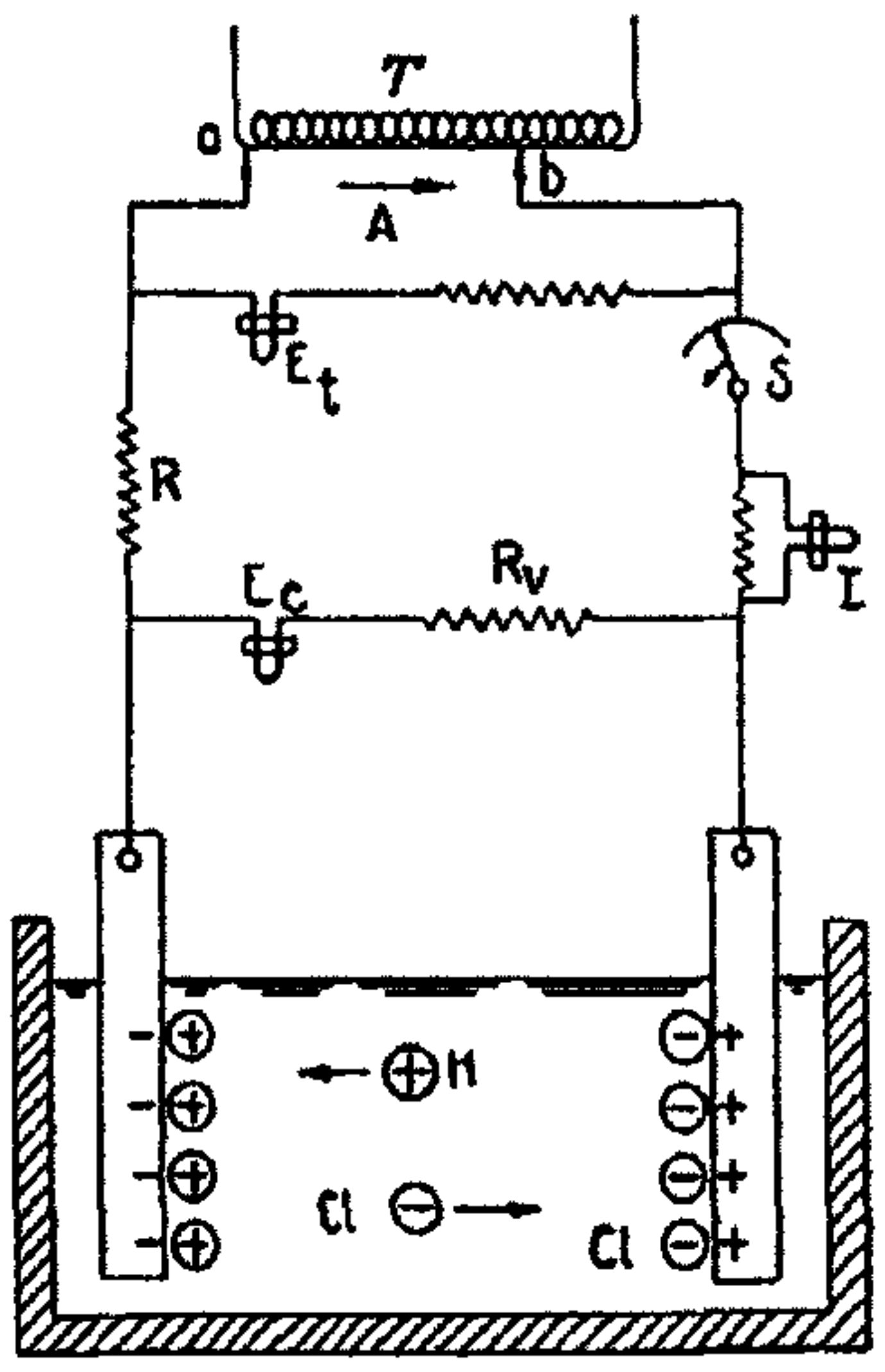

FIG. 4. Diagram of circuit for making oscillograms of wave forms of current, total impressed voltage, and E.M.F. impressed upon the conductivity cell. The signs on the electrodes indicate the charges on the electrodes. The condition is pictured for the end of the half-cycle in which the current has been flowing in the direction of the arrow A.

of the E.M.F. impressed across the series consisting of the cell and any resistance in series with the cell. In figure 4 a resistance, R, was inserted in series with the cell for the purpose of increasing the time-constant of the circuit. On the films the three wave forms referred to above are marked I, E_c, and E_t, respectively.

Suitable interconnections between the shutter mechanism of the oscillograph and the tripping mechanism of the motor-operated switch, S, were provided so that the following sequence of events occurred in the exposure of a film: (*1*) The shutter of the oscillograph opened, thereby exposing the film to the light from the vibrators of the oscillograph. Since the switch, S, remains open for an interval of about 2/100 of a second after the opening of the shutter, the vibrators trace on the film during this interval a short length (2 to 6 cm.) of the zero lines for current and voltage. (*2*) About 2/100 of a second after the opening of the oscillograph shutter, the trigger on the switch, S, is tripped and the synchronous motor then closes this switch at the selected point on the succeeding cycle of the E.M.F. E_t impressed upon the circuit. For some of the sets of films the switch, S, was set to close first as above and then after 7 cycles to open at predetermined points on the wave form of the current. (*3*) The shutter of the oscillograph is automatically closed after the drum on which the film is mounted has made one complete revolution.

The electrodes of the conductivity cells used in all these tests were concentric cylinders of bright platinum spaced approximately 1 mm. apart. For the oscillograms listed in tables 1, 2, and 3, the cylinders were each 5.1 cm. long and the inner cylinder had an outside diameter of 1.3 cm. For the oscillograms described in section VII, the corresponding dimensions were 7.7 cm. in length and 2.5 cm. in diameter. Three different solutions were used, as specified later, namely 0.2 *N* sodium chloride, 1 *N* sulfuric acid, and 1 *N* hydrochloric acid.

Two frequencies were used,—60 (or 61) and 240 cycles per second. The 240-cycle current was obtained from a Vreeland oscillator and the 60-cycle current from the local city service.

IV. FILM DATA FOR THE STEADY STATE:—EFFECT OF IMPRESSED VOLTAGE AND FREQUENCY

With the connections shown in figure 3, the voltage of the source was adjusted to the desired values and a series of oscillograms was taken with different impressed voltages and at the two frequencies, 61 and 240 cycles per second. For this series of films the solution in the cell was 0.2 *N* sodium chloride.

Figures 5, 6, 7, 8, and 9 (films 7, 8, 9, 10, and 11, respectively) are typical of this series. From these films the data compiled in tables 1 and 2 were obtained in the manner described below.

The magnitudes of the current and the voltage and the angle by which the current wave leads the voltage wave (designated as the phase angle) were obtained from measurements made on the films. The capacitance, the resistance, and the phase angle of the cell itself were then computed as follows:

Let E represent peak voltage (determined from oscillogram),
I represent peak current (determined from oscillogram),
θ represent the angle by which the sinusoidal current leads the sinusoidal voltage as measured on the oscillograms,
X_c represent the equivalent series capacitive reactance of circuit k-g-d (figure 3), and
R represent resistance of circuit k-g-d (figure 3).

Then

$$X_c/R = \tan\theta \tag{1}$$

The impedance Z of the circuit k-g-d (figure 3) is then

$$Z = E/I \tag{2}$$

and on the assumption that the capacitance of the cell is in series with its resistance,

$$R = Z\cos\theta \tag{3}$$

$$X_c = Z\sin\theta \tag{4}$$

The capacitance C of the cell in farads is

$$C = \frac{1}{2\pi f X_c} \tag{5}$$

The resistance of the cell itself (R_c) is found by subtracting from R the resistance of all parts of the circuit external to the cell between points k and d. The values of the external resistance and of the cell resistance are given in tables 1, 2, and 3 in the columns headed "External resistance" and "R_c", respectively.

The true phase angle θ_c of the cell is then

$$\theta_c = \text{arc tan } X_c/R_c \tag{6}$$

and the true voltage impressed on the cell is

$$E_c = I\sqrt{R_c^2 + X_c^2} \tag{7}$$

The values of the peak current, the peak voltage, and the phase angle of the cell were determined from measurements made on the last cycles recorded in the films. The transient terms in the current, the presence of which can be detected in the current during the first half-cycle, become of negligible magnitude within 1/60 of a second after the closing of the switch. These transient terms will be discussed later.

Tables 1 and 2 contain the results of the measurements made on the films.

V. DISCUSSION OF THE TABLES AND OF THE FILMS

No high degree of accuracy should be attached to the numerical values for the cell resistance and capacitance appearing in the tables. All these values were computed from measurements of rather short lengths. In some cases an error of 0.01 cm. in the measurement of an amplitude or phase angle would result in an error of 4 per cent in the computed values. The oscillograms were not taken with the idea of making precise determinations of the resistance and capacitance of the cell, but rather to examine the transient effects. The capacitance and resistance values are, however, of the same order as those found in our precision A.C. bridge measurements.

TABLE 1

Effect of impressed voltage on the characteristics of the cell containing 0.2 N sodium chloride

(Figure 3 connections)

FILMS	FREQUENCY	EXTERNAL RESISTANCE	LAST CYCLE			E_c	R_c	X_c	C	θ_c
			Peak volts	Peak amperes	Lead angle					
		ohms			*degrees*	*volts*	*ohms*	*ohms*	*μf*	*degrees*
7	61	0.102	0.665	1.48	42	0.565	0.233	0.301	8700	52
8	61	0.017	1.95	5.90	32	1.86	0.263	0.175	14900	33
9	61	0.017	3.33	10.5	25	3.17	0.270	0.134	19500	26
10	61	0.017	4.33	15.1	20	4.10	0.253	0.098	26700	21
11	61	0.017	7.70	31.2	13	6.90	0.214	0.056	46700	15

TABLE 2

Effect of frequency on the characteristics of the cell containing 0.2 N sodium chloride

(Figure 3 connections)

FILMS	FREQUENCY	EXTERNAL RESISTANCE	LAST CYCLE			E_c	R_c	X_c	C	θ_c
			Peak volts	Peak amperes	Lead angle					
		ohms			*degrees*	*volts*	*ohms*	*ohms*	*μf*	*degrees*
14	239	0.094	0.152	0.44	17	0.113	0.237	0.101	6600	23
15	240	0.103	0.805	2.30	20	0.589	0.226	0.120	5520	28
16	244	0.104	1.30	3.76	16.5	0.931	0.227	0.098	6670	23
17	61	0.094	0.165	0.31	45	0.146	0.282	0.376	6950	53
18	61	0.101	0.62	1.24	48	0.545	0.234	0.372	7020	58
19	61	0.104	1.29	2.70	43	1.10	0.246	0.327	8000	53

The tables indicate that the equivalent capacitance of the cell is approximately independent of the frequency and of the magnitude of the impressed E.M.F. if the latter is less than the E.M.F. of polarization of the cell. The equivalent capacitance of the cell increases with rise in the impressed E.M.F. above the E.M.F. of polarization and is roughly proportional to the rise. The results agree with our precise A.C. bridge measurements.

It should be recognized that this statement with reference to the equivalent capacitance at electromotive forces greater than the E.M.F. of polarization is a very loose one. The cell really has no *equivalent capacitance* for an impressed E.M.F. greater than the E.M.F. of polarization, because at these higher E.M.F.'s the oscillograms show that the cell no longer has the properties of a resistance connected in series with a capacitor. Compare, for example, the sine wave form of the current in figure 5 (film 7), which was taken at the impressed E.M.F. of 0.565 volt, with the distorted current wave forms of figures 6, 7, and 8 (films 8, 9, and 10), which were taken at 1.86, 3.17, and 4.1 volts, respectively. Film 8 (figure 6) is flattened on the left side of the *I* wave form with its peak shifted to the left, film 9 (figure 7) is flattened on top with its peak shifted downward, and film 10 (figure 8) is flattened on the right side with its peak shifted to the right. These differences are most easily observed by superimposing films 8, 9, and 10 (figures 6, 7, and 8). When the last cycle of film 10 (figure 8) was cut off, reversed, and superimposed on the preceding cycle a shift of the *I* peak to the right was clearly disclosed. This newly discovered "polarization peak-shift effect" must be associated with electrode reactions other than ion segregations and will be studied by scaling the heights and areas (and their differences) on both sides of the peaks of the wave forms to correlate these data with other polarization phenomena. For example, in film 10 (figure 8) the area of the portion of the current half-cycle lying to the right of the peak is roughly 10 per cent less than on the left. It is further noted in films 7 to 11 (figures 5 to 9) and in table 1 that with rise of the electrode potential E_c from 0.56 to 6.9 volts and of the apparent capacitance from 8700 to 46,700 microfarads, the transient terms decrease and the ratios of the heights of the peaks of the first and third current half-cycles are respectively about 0.77, 0.79, 0.86, 0.90, and 0.95. If the apparent electrode capacitance were constant above polarization voltage no such change should occur. A consideration of the phase relations between the current, the electromotive force expended in the resistance, and the electromotive force arising from changes in ion concentrations at the electrodes during

---

FIG. 5. Wave forms of applied voltage (E_t) and current (I) with 0.56 volt (E_c) across the cell. The current wave form was not distorted.

FIG. 6. Wave forms of applied voltage (E_t) and current (I) with 1.86 volts (E_c) across the cell. The current wave form was slightly distorted.

FIG. 7. Wave forms of applied voltage (E_t) and current (I) with 3.17 volts (E_c) across the cell. The current wave form was very much distorted.

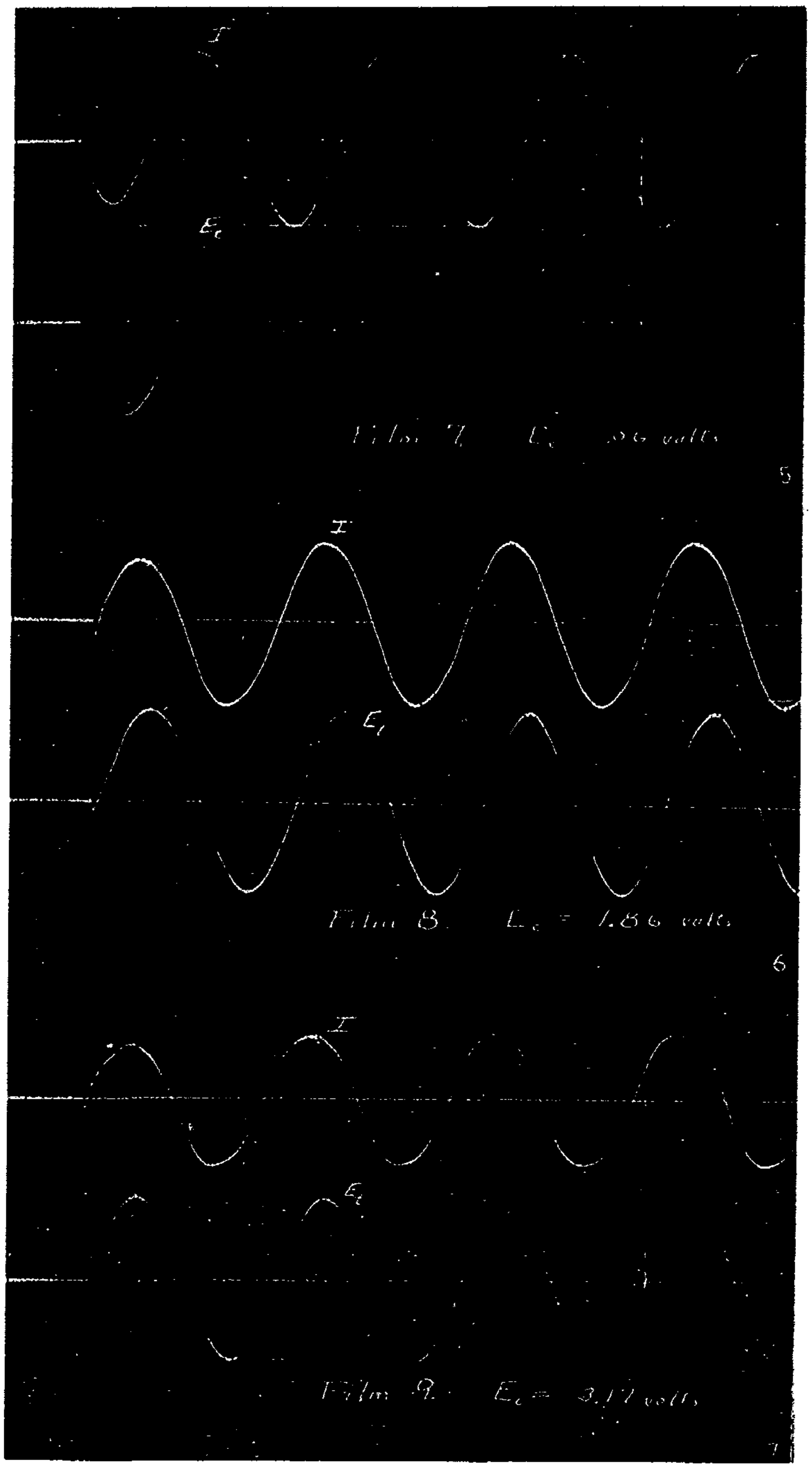
I
E_c
Film 7 E_c .56 volts
5
I
E_c
Film 8. E_c = 1.86 volts
6
I
E_c
Film 9. E_c = 3.17 volts
7

Figs. 5-7

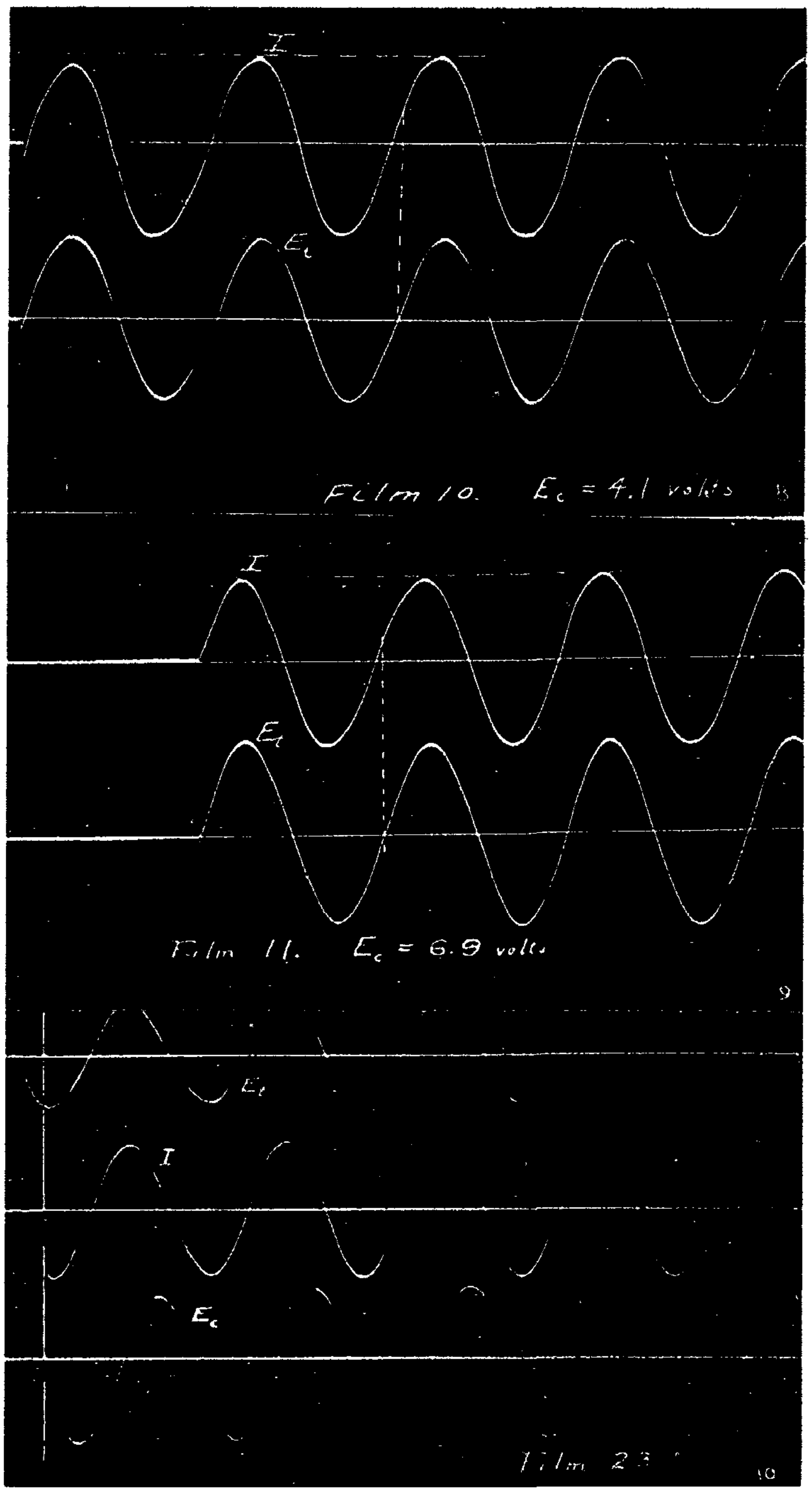
I
E_c
Film 10. E_c = 4.1 volts
8
I
E_c
Film 11. E_c = 6.9 volts
9
E_c
I
E_c
Film 23
10

Figs. 8-10

the cycle leads to the prediction of a flattening of the current wave form at voltages somewhat in excess of the E.M.F. of polarization, which may be seen most clearly in figure 7 (film 9). Under impressed electromotive forces greatly in excess of an E.M.F. of polarization, the current wave form will again approximate the sine wave form because of the fact that the E.M.F. expended in the resistance is many times the E.M.F. of polarization (see columns headed "R_c" and "X_c", table 1); therefore the latter will have little influence on the wave form of the current. This conclusion is borne out by a comparison of figures 7 and 9 (films 9 and 11) taken at 3.17 and 6.9 volts, respectively. In the latter film the distortion of the current wave form is not as marked as in the former. Film 7 (figure 5), taken at an impressed E.M.F. of 0.565 volt at 61 cycles, shows no distortion of the current wave form.

VI. TRANSIENT PHENOMENA IMMEDIATELY AFTER THE START OF AN ALTERNATING CURRENT THROUGH A CONDUCTIVITY CELL

The closing of the switch S in figure 3 suddenly impresses an alternating E.M.F. between the points k and d. This E.M.F. is recorded by the vibrator E_t while the current through the conductivity cell is recorded by the vibrator I. We may write the complete expression for the current which will flow through the cell under the impressed E.M.F. upon the assumption that the cell may be simulated by a capacitor having a capacitance of C farads in series with a resistor having a resistance R equal to the resistance R_c of the cell plus the resistance of the shunt and the current vibrator I.

If the equation for the impressed E.M.F. across k-g-d is

$$e_t = E \cos \omega(t - t_1) \tag{8}$$

the equation for the current, i, through the cell is

$$i = \frac{E}{\sqrt{R^2 + X^2}} \cos\left[\omega(t - t_1) + \text{arc tan}\,\frac{X}{R}\right] + \frac{E_d}{R} \exp\left(-\frac{t}{RC}\right) \tag{9}$$

in which time, t, is measured from the instant at which the switch closes, t_1 represents the interval from the instant of closing to the nearest positive peak of the impressed E.M.F., ω represents $2\pi f$, X represents $1/C\omega$, and

$$E_d = \frac{EX}{\sqrt{R^2 + X^2}} \sin\left[\omega t_1 - \text{arc tan}\,\frac{X}{R}\right] \tag{10}$$

FIG. 8. Wave forms of applied voltage (E_t) and current (I) at 60 cycles with 4.1 volt (E_c) across the cell. The current wave form was slightly distorted.

FIG. 9. Wave forms of applied voltage (E_t) and current (I) with 6.9 volts (E_c) across the cell. The current wave form was barely distorted.

FIG. 10. Wave forms of applied voltage (E_t), current (I), and E.M.F. (E_c) across the cell. When the switch was closed at peak E_t there was no noticeable transient effect in E_c.

The expression for the current contains two terms, the steady-state or sinusoidal term, and the transient or exponential term. The *damping constant* of the exponential term is ($-1/CR$), and its *time-constant* is CR. In any interval of time (after the closing of the switch) equal to the time-constant, or equal to CR seconds, the exponential term decreases to $1/\epsilon$th (36.8 per cent) of its initial value, and in an interval equal to 4.6 times the time-constant it decreases to 1 per cent of its initial value, or is negligibly small.

For the oscillograms taken with the figure 3 connections, of which films 7 to 11 are typical, the value of the time-constant was quite small, namely, 0.003 second or less. Consequently for these films the exponential term decreased to less than 1 per cent of its initial value in the first cycle after the closing of the switch. On the above set of films, the effect of the exponential term can be detected to best advantage in film 7 (figure 5). The low value of the first current peak on this film is due to the presence of the transient term.

In order to increase the time-constant of the transient term so that its value could be measured by scaling peak values over a number of cycles, the resistance of the circuit was now increased by inserting an additional resistance R of from 10.4 to 23.2 ohms, as shown in figure 4. Additional oscillograms were then taken upon the same conductivity cell as before, containing, however, 1 N sulfuric acid as the electrolyte. These oscillograms were all taken at a frequency of 60 cycles per second. Films 23, 24, and 25 (figures 10, 11, and 12) are typical. The data for these oscillograms are given in table 3.

The figure 4 network containing the conductivity cell is simulated to a first approximation by the artificial network shown in figure 13. In this figure the capacitance C and series resistance R_c replace the conductivity cell of figure 4, and the values assigned to C and R_c are to be computed by the method described for tables 1 and 2. These computed values are given in table 3.

The general equations for the current through the oscillograph vibrator I and for the electromotive force impressed on the cell, as measured by the vibrator E_c, have been derived in literal form. From these involved literal

FIG. 11. Wave forms of applied voltage (E_t), current (I), and E.M.F. (E_c) across the cell. When the switch was closed at zero E_t the large transient effect observed in E_c continued for more than 4 cycles.

FIG. 12. Wave forms of current (I) and E.M.F. (E_c) across the cell. When the switch was closed at zero E_t a large transient effect was observed in E_c with a drift to steady state in about 10 cycles (0.16 second).

FIG. 15. Wave forms of applied voltage (E_t), current (I), and E.M.F. (E_c) across the cell. When E_t and I in the steady state were cut off at zero values and there was ion segregation at the electrodes, E_c decreased very slowly (time-constant greater than 48 seconds) when the cell discharged (electrodes attached to amplifier).

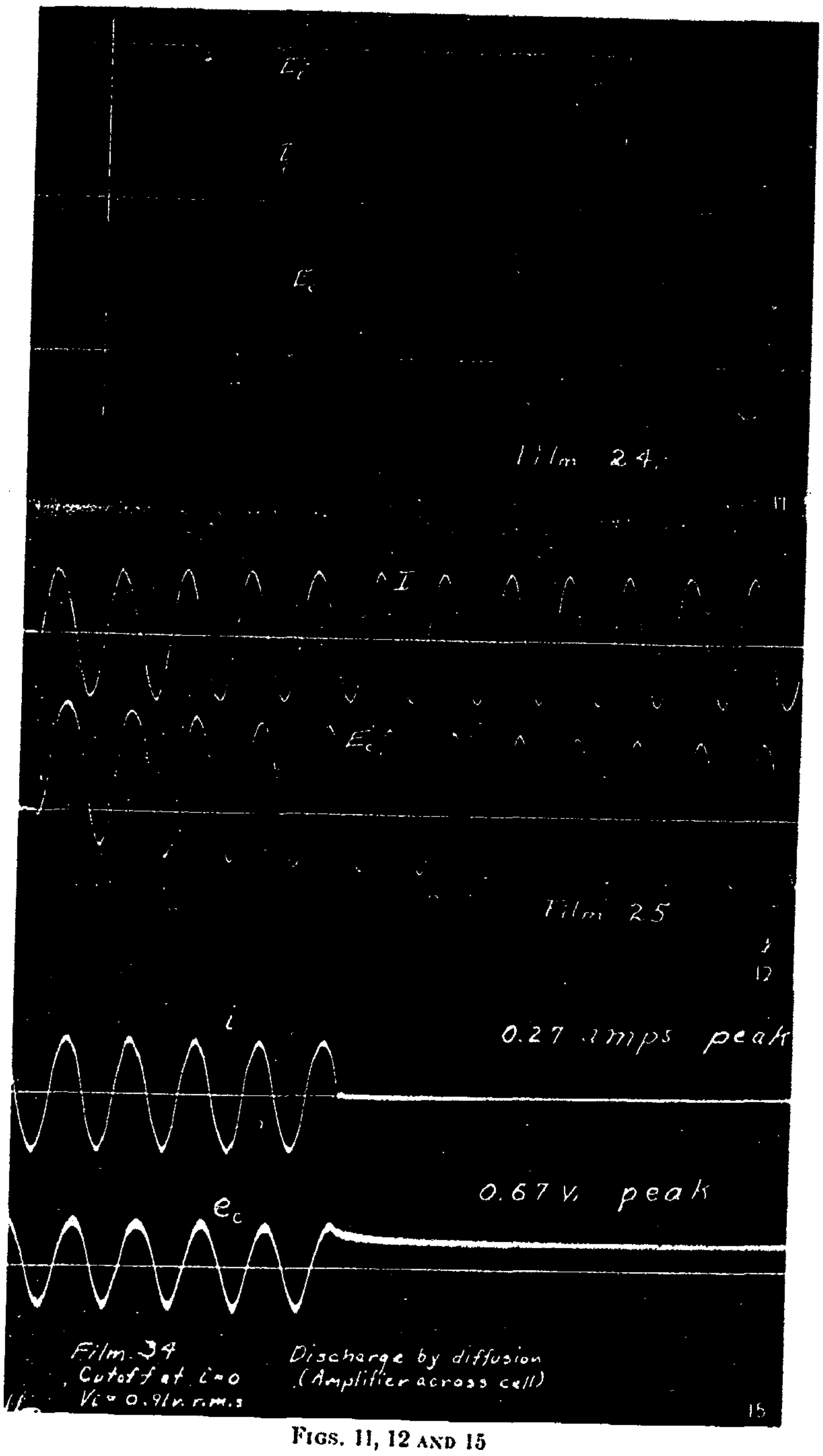

FIGS. 11, 12 AND 15

equations we have computed the numerical expressions for the current shown by the vibrator I and for the E.M.F. shown by the vibrator E_c for two cases; namely, (*a*) for the case in which the switch is closed at the zero of the E.M.F. across E_t, and (*b*) for the case in which the switch is closed at the peak of the E.M.F. across E_t.

If the switch is closed at the zero of the E.M.F. across E_t (as in figures 11 and 12) and if time is measured from the instant of closure of the switch S,

TABLE 3

Effect of transient terms on the characteristics of the cell containing 1 N sulfuric acid

(Figure 4 connections)

FILMS	FREQUENCY	EXTERNAL RESISTANCE	LAST CYCLE			E_c	R_c	X_c	C	θ_c
			Peak volts	Peak amperes	Lead angle					
		ohms				*volts*	*ohms*	*ohms*	*µf*	*degrees*
23	60	10.4		1.63		0.52	0.117	0.285	9300	60
24	60	23.2		1.6		0.48	0.118	0.279	9500	67
25	60	23.2		1.6		0.50	0.081	0.302	8800	75

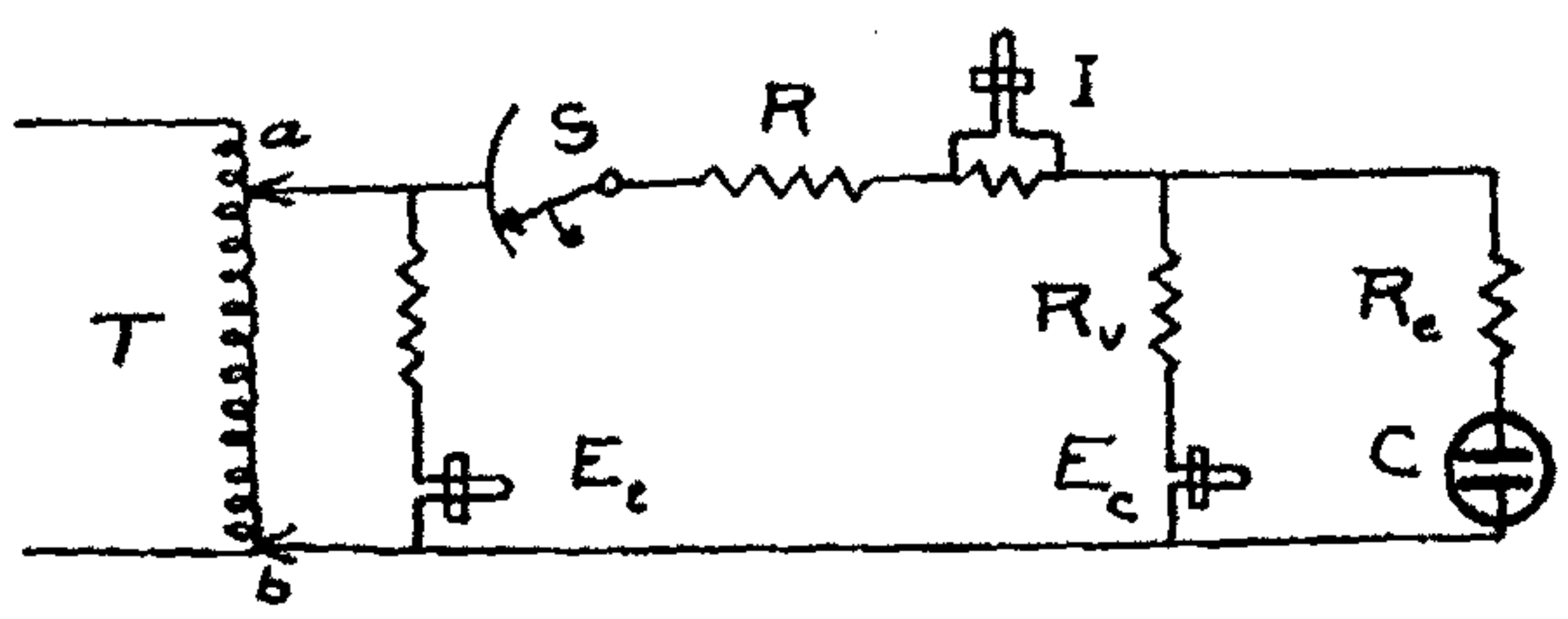

FIG. 13. Diagram of networks simulating figure 4

the equations for the figure 13 network used in obtaining film 24 (figure 11) are computed to be as follows:

For the total impressed E.M.F. as recorded by the vibrator E_t,

$$i = E_t \sin \omega t \tag{11a}$$

For the current as recorded by the vibrator I,

$$i = 0.01\ E_t\ [4.35 \sin (\omega t + 0.7°) + 0.0019 \exp (-at)] \tag{12a}$$

For the E.M.F. across the artificial cell as recorded by the vibrator E_c,

$$e_c = 0.01\ E_t\ [1.28 \sin (\omega t - 64.7°) + 1.16 \exp (-at)] \tag{13a}$$

The value of the damping constant, a, appearing in the exponential factor, $\exp(-at)$, is given by the expression

$$a = \frac{1}{C\left[R_c + \dfrac{RR_v}{R + R_v}\right]} \tag{14}$$

On the other hand, if the switch S is closed at the positive peak of the E.M.F. across E_t (as in figure 10) the corresponding equations for the figure 13 network used in obtaining film 23 (figure 10) are

$$e_t = E_2 \cos \omega t \tag{11b}$$

$$i = 0.01\, E_2[9.44 \cos (\omega t + 1.5°) + 0.013 \exp (-at)] \tag{12b}$$

$$e_c = 0.01\, E_2[2.98 \cos (\omega t - 59.4°) + 0.14 \exp (-at)] \tag{13b}$$

An examination of these equations will show that the insertion of the resistance R (having a value 70 to 200 times as great as the resistance R_c of the cell) has had the following effects: (*a*) The time-constants of the exponential terms as computed from equation 14 are found to be 0.049 second for film 23 (figure 10), 0.0688 second for film 24 (figure 11), and 0.0634 second for film 25 (figure 12). Within the limits of the experimental errors the value of the time-constant computed from equation 14 checks with the experimentally determined value obtained by scaling the peak values of the curve E_c of film 25 (figure 12). (*b*) An inspection of equations 12a and 12b for the current i shows that the insertion of the resistance R has reduced the initial value of the transient term in the current to less than 0.5 per cent of the peak values of the steady-state alternating current. This conclusion is supported by the films, since an examination of the current curves on films 23, 24, and 25 (figures 10, 11, and 12) shows that the magnitude of the exponential term is so slight that it cannot be detected. (*c*) An examination of the equations from which were derived 13a and 13b for the voltage e_c across the conductivity cell shows that the exponential term in e_c will be a maximum if the switch closes at the instant corresponding to the zero point of the steady-state current through the cell, and will be zero if the closure occurs at the instant corresponding to the peak of the steady-state current through the cell. For the circuit used in obtaining films 23, 24, and 25 (figures 10, 11, and 12), these instants correspond very closely to the zero point and the peak of the impressed E.M.F. e_t.

In the case of films 24 and 25 (figures 11 and 12), the switch S closed substantially at the zero of the impressed voltage e_t. The large effect of the exponential term on the voltage E_c across the cell is quite evident. In the case of film 23 (figure 10), the switch S closed slightly before the peak of impressed E.M.F. E_t. The exponential term in E_c can barely be detected on this film, and the observable effect is to be attributed to the fact that the switch closed some degrees before the peak of the E.M.F. E_t. These three films are in general agreement with the equations 13a and 13b.

The physical reason (see figure 14) for the extremely small magnitude of the transient terms in the case of film 23 (figure 10), is as follows: In the steady state of a cell carrying an alternating current, the difference in the concentrations of the positive and negative ions at each electrode (figure 14, A and E) is zero at the instant when the current has its maximum value and is a maximum (figure 14, D and F) at the instant when the current passes through the zero value. Consequently if the switch is closed at the instant when the current should have its maximum value, and if the inductance of the circuit is so low that the current can rise almost instantaneously to its normal peak value (as in film 23 (figure 10)), the cell attains practically at once (see below) the combination of values which characterizes the steady state, namely, peak value of impressed electromotive force (upon the entire circuit) in conjunction with peak value of current and zero difference of concentrations of positive and negative ions at the electrode. Under these conditions there will be no noticeable gradual drift from an initial combination of conditions to another corresponding to the steady state in the cell, and consequently there will be no appreciable transient terms in the electromotive force across the cell.

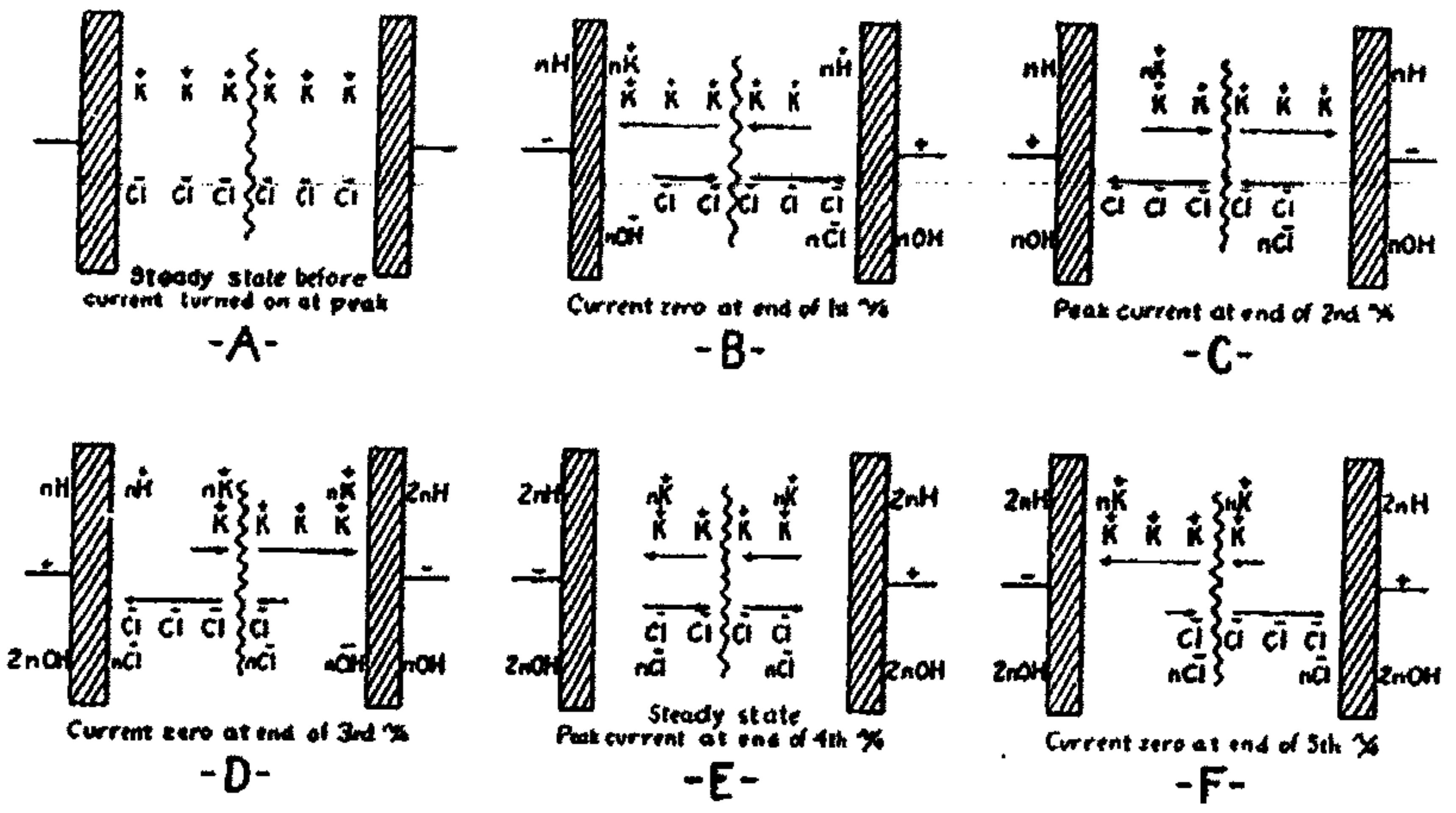

Steady state before current turned on at peak
-A-

Current zero at end of 1st ¼
-B-

Peak current at end of 2nd ¼
-C-

Current zero at end of 3rd ¼
-D-

Steady state
Peak current at end of 4th ¼
-E-

Current zero at end of 5th ¼
-F-

FIG. 14. Ion segregation and discharge at the electrodes during quarter-cycles

On the other hand, if the switch is closed at the zero point on the electromotive force wave form, at which in the steady state the current is zero and the difference in the concentrations of the two ions at the electrode is a maximum, then, during the *whole* of the succeeding half-cycle, the current will cause a change in concentration in one direction. In contrast to this, in the steady state, during the first half of the succeeding half-cycle (first quarter-cycle) following the point of zero current, the current reduces the difference in concentrations of the two ions from a maximum to zero, and then during the second half of the half-cycle builds up the difference in concentrations from zero to a maximum in the opposite sense.[3] Conse-

---

[3] It is planned to study the E.M.F. and capacitance at each electrode in relation to the transference numbers of the ions by means of A.C. potentiometer and oscillograph methods. For details of these phases see reference 13, pp. 2417, 2425, 2427, 2428, 2430.

quently, in the first half-cycle following the closing of the switch at the zero point of the impressed electromotive force wave corresponding in the steady state to zero current, the *difference* in ionic concentrations at the electrodes builds up to approximately *twice* its normal or steady-state maximum value, and the E.M.F. of polarization builds up to approximately twice its normal value. The drift from the relations pictured for the first half-cycle to the symmetrical steady-state relation arises from the fact that the unsymmetrical E.M.F. of polarization subtracts unsymmetrically from the impressed electromotive force during its succeeding positive and negative half-cycles. This results in a slight lack of symmetry in the current about the line of zero current. The lack of symmetry is such as to cause the cycle of concentration values to drift exponentially from the initial cycle, namely 0, p, $2p$, p, 0 to the steady-state cycle, namely $-p$, 0, $+p$, 0, $-p$.

The electrical and ionic phenomena in the first cycle after the closing of the switch at the exact peak of the impressed E.M.F. will receive attention, because in certain cases the electrode reactions may not be completely symmetrical and reversible. Figure 14 illustrates the changes in the electrode double layers of electrolytes like potassium chloride, whose ions have substantially the same mobilities. In the first quarter-cycle n layers of + and − ions are moved to, and discharged at, the cathode and anode, respectively, with attendant discharge of n H^+ and OH^- ions from water. Steady-state conditions of concentration and discharge of ions at the two electrodes are not reached at peak current at the end of the second quarter-cycle but are obtained at the peak of the fourth quarter-cycle. Hence very small transient effects may be found within the first cycle, with steady-state conditions thereafter, especially by use of the methods described in the next section.

VII. TRANSIENT PHENOMENA UPON DISCONNECTING THE ALTERNATING CURRENT SOURCE FROM THE CONDUCTIVITY CELL

The synchronous switch S of figure 13 was now arranged to close and then, after an interval of slightly less than 7 cycles, to open again. The set of oscillograms in figures 15, 16, 17, and 18 (films 34, 35, 43, and 44, respectively) was then taken (1935) to show the transient effects which follow the opening of the switch at the two extreme points on the wave form of the 60-cycle current through the cell—namely, at the peak and at the zero point of the current. For these oscillograms a 1 N hydrochloric acid solution was used in the cell.

Upon closing the synchronous switch S, the equivalent capacitance of the cell is supplied through the resistance R. For these oscillograms this resistance was reduced to 4.7 ohms; at this value the time-constant of the

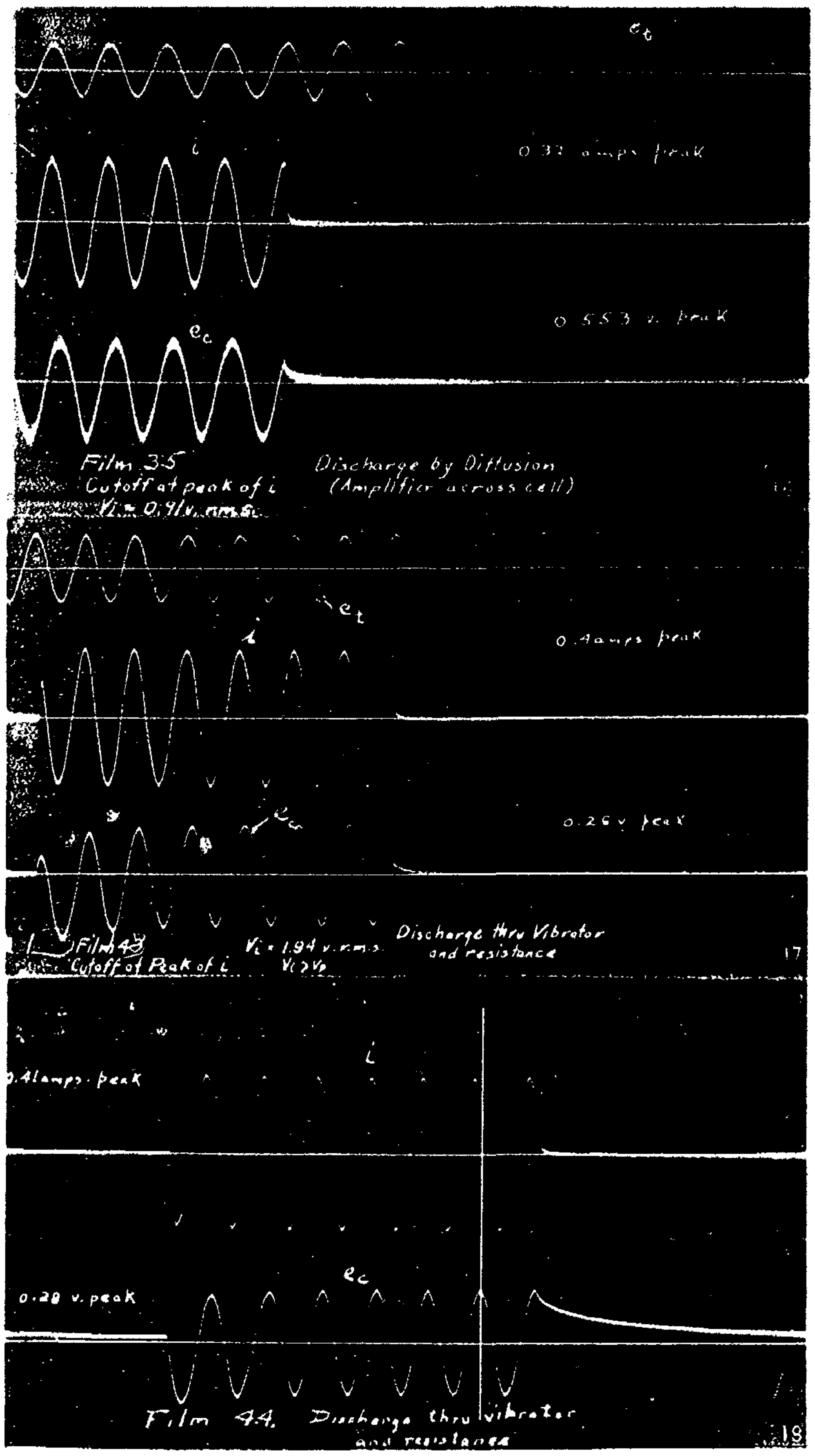
e_t
i
0.32 amps peak
e_c
0.553 v. peak
Film 35
Cutoff at peak of i
V_i = 0.91 v. r.m.s.
Discharge by Diffusion
(Amplifier across cell)
16
e_t
i
0.4 amps peak
e_c
0.26 v peak
Film 43
Cutoff of Peak of i
V_i = 1.94 v. r.m.s.
$V_i > V_p$
Discharge thru Vibrator
and resistance
17
i
0.41 amps. peak
e_c
0.28 v. peak
Film 44. Discharge thru vibrator
and resistance
18

FIGS. 16-18

circuit was roughly 1 period of the 60-cycle circuit. This means that the transient terms in the polarization E.M.F. associated with the closing of the switch all reduce to zero before the opening of the switch, which occurred 7 periods later.

After the opening of the switch S, the E_c 10.3-ohm voltage vibrator branch was left connected across the cell for films 43 and 44 (figures 17 and 18). For films 34 and 35 (figures 15 and 16) the 10.3-ohm voltage vibrator branch of figure 13 was replaced by a vacuum tube voltage amplifier, which supplied the vibrator E_c but represented an impedance in excess of 10,000 ohms to the discharge of the cell through it.

To aid in the interpretation of these films, figure 19 has been drawn. This figure shows the relations between a sinusoidal current (I) through a conductivity cell (or rather through a simulating network consisting of a series combination of a resistor and capacitor having a resistance and a capacitive reactance corresponding to those of the actual cell) and the three sinusoidal electromotive forces associated with the current: namely, the E.M.F. (E_r) equal to $R_c i$, which is impressed upon the resistance R_c of the column of electrolyte; the E.M.F. (E_x) impressed upon the capacitor, or counteracting the E.M.F. of polarization; and the E.M.F. (E_c) impressed across the terminals of the cell, which is the sum of E_r plus E_x.

The E.M.F., E_x, across the regions of polarization (or across the capacitor) is seen to lag the current by 90°, while the E.M.F. across the resistance of the cell is seen to be in phase with the current. Consequently when, as in films 43 and 35 (figures 17 and 16), the synchronous switch S interrupts the sinusoidal supply current at its peak value (the instant t_p in figure 19), the E.M.F., E_c, across the cell at once drops to zero. It does this because at this instant there is no segregation of ions at the electrodes, or the E.M.F. of polarization, E_x, is zero, and the E.M.F. of resistance across R_c drops to zero when the current drops to zero.

On the other hand when, as in films 44 and 34 (figures 18 and 15), the switch S interrupts the supply current at the zero point (the instant T_0 in

---

FIG. 16. Wave forms of applied voltage (E_t), current (I), and E.M.F. (E_c) across the cell. When E_t and I in the steady state were cut off at peak values and there was no ion segregation at the electrodes, E_c dropped at once to zero value (electrodes attached to amplifier).

FIG. 17. Wave forms of applied voltage (E_t), current (I), and E.M.F. (E_c) across the cell. When E_t and I in the steady state were cut off at peak values and there was no ion segregation at the electrodes, E_c dropped at once to zero value (electrodes attached to E_c vibrator, figures 4 and 13).

FIG. 18. Wave forms of applied voltage (E_t), current (I), and E.M.F. (E_c) across the cell. When E_t and I in the steady state were cut off at zero values and there was ion segregation at the electrodes, E_c dropped to 36.8 per cent in about 0.05 second when the cell discharged (electrodes attached to E_c vibrator in figures 4 and 13).

figure 19), the E.M.F., E_o, across the cell apparently[4] undergoes no abrupt or discontinuous change in value. At the instant t_0 the entire E.M.F. across the cell is associated with the segregation of ions indicated in figures 4 and 14 F. For the entire half-cycle preceding t_0, the migration of the hydrogen and chloride ions has been in the directions indicated by the arrows in figure 4, and the concentration of hydrogen ions adjacent to one electrode and of chloride ions adjacent to the other attains a maximum at the instant t_0. Upon the opening of S the two charged platinum electrodes start to discharge through the resistance of the branch containing the voltage vibrator E_o. As the charges on the platinum electrodes decrease, the hydrogen and chloride ions start to migrate in opposite directions to equalize the ionic concentrations at the face of the electrodes shown in figure 4. The rate at which the E.M.F. of the cell decreases to zero is inversely proportional to the sum of the ohmic resistances of the metallic discharge circuit connecting the platinum electrodes and the column of electrolyte between electrodes.

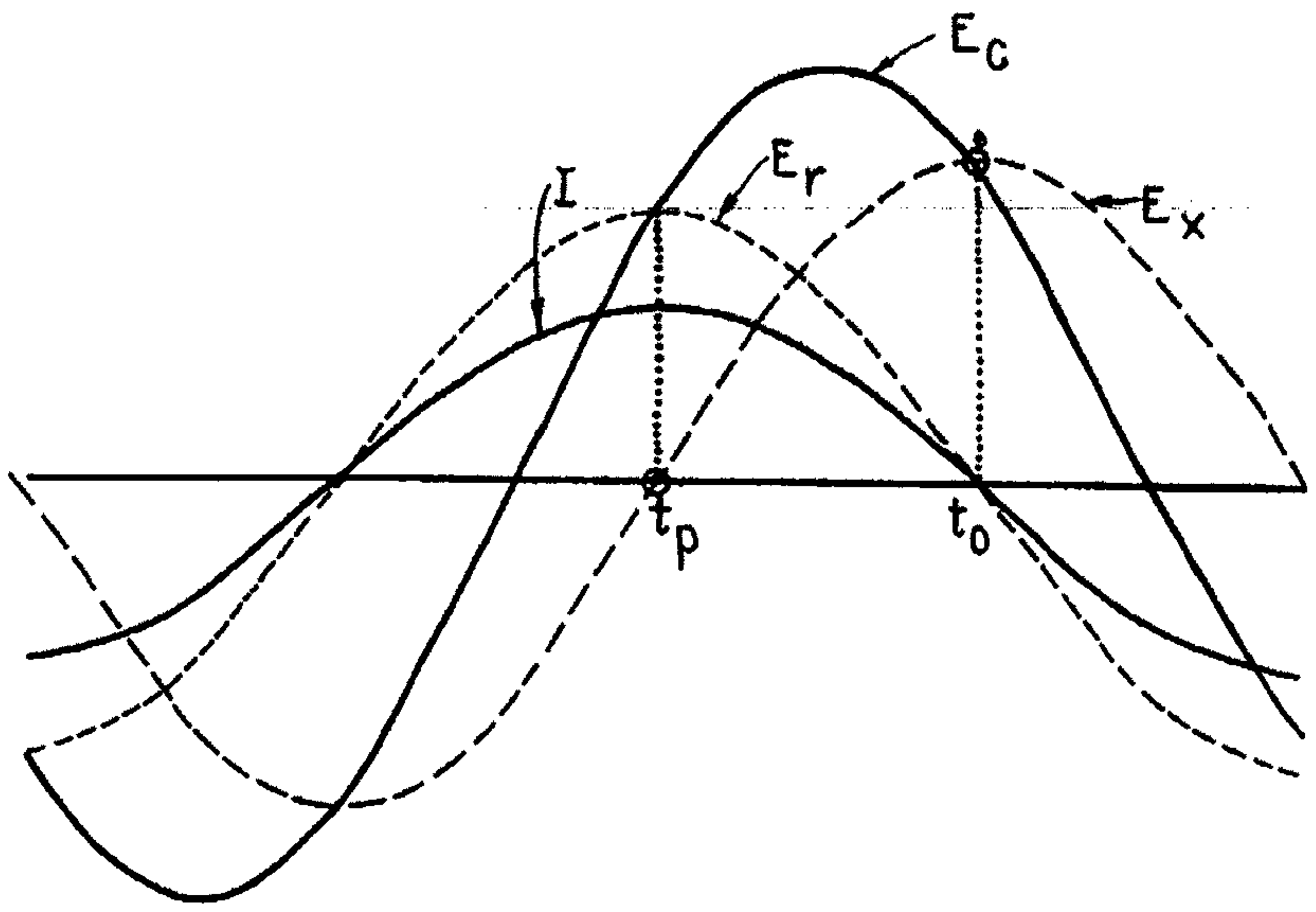

FIG. 19. The phase relations between a sinusoidal current through a conductivity cell and the associated electromotive forces. I, current through cell; E_r, E.M.F. impressed across resistance of column of electrolyte; E_x, E.M.F. impressed across surface films with abnormal concentration; E_c, total E.M.F. impressed on cell.

---

[4] Actually when the switch opens and the cell starts to discharge through the resistance R_o of the E_o vibrator branch, the voltage recorded by the vibrator abruptly drops to a new value which is equal to $R_r/(R_o + R_c)$ times the value before the opening of S. This drop is so small for films 44 and 34 that it cannot be detected.

An examination of film 44 (figure 18) shows that after the opening of the switch S the E.M.F. of the cell decreases to zero along an exponential curve. The resistance and equivalent capacitance of the cell with 1 *N* hydrochloric acid as computed from the steady-state relations recorded on the film are 0.45 ohm and 4800 microfarads, respectively. Using these figures the computed value of the time-constant for the discharge curve works out to be 0.052 second, or 3.1 periods of the 60 cycles per second current. This computed value of the time-constant agrees (within the limits of the rather large scaling errors) with the value of the time-constant found by scaling the discharge curve itself.

In the case of film 34 (figure 15) the vibrator showing the E.M.F. of the cell was actuated by a vacuum tube voltage amplifier which presented a resistance in excess of 10,000 ohms to the discharge of the cell. For these conditions the computed value of the time-constant exceeds 48 seconds, and there should be no appreciable decrease in the E.M.F. of the cell during the time of the exposure. An examination of the film shows a slight fall in the E_c voltage immediately following the opening of S, after which the voltage of the cell undergoes no further apparent decrease. The initial change does not represent an actual decrease in the voltage across the cell, but is caused by the faulty performance of the voltage amplifier. The spontaneous discharge of the cell is therefore rather slow.

The above discussion of films 34, 35, 43, and 44 (figures 15, 16, 17, and 18) and figure 19 was predicated on a phase difference of 90° for a perfect capacitor and resistor in series, and a lag of the E_c curves somewhat less than 90° behind the I curves. The E_c curves in the above films actually lag the I curves slightly less than 90°, and tables 1, 2, and 3 show that θ_c is somewhat less than 90°. It was pointed out above that a conductivity cell has imperfect or "leaking" capacitance. In view of the above facts, of the effects of the asymmetry, rotation, and inertia of the ions and of the friction (viscosity), relaxation forces, and electrophoresis in the solvent on the rapidity of attainment of maximum or true mobility for a given potential difference, of the varying distribution of the current and capacitance at the electrode surfaces as shown by Snow (18), of the backward pull and migration of the ions under electrostatic forces arising from segregation, as when the current approaches zero value, of the inertia of the vibrator oscillograph in contrast with the cathode ray type, and other factors, such as the electrode-chemical reactions differentiating a conductivity cell from figure 19, the data probably agree with theory within the errors inherent in recording and scaling the wave forms on these films.

Mr. W. H. Goss has begun work on the study of the series capacitance by using a highly insulated vacuum tube potentiometer and cathode ray oscillograph to measure the E.M.F. changes over microseconds to hours when cells are charged with direct currents from a primary cell or a capacitor below and above the polarization potential. The data show that plantinized electrodes require for discharge very short time periods to be measured with vibrator and cathode ray oscillographs. The results obtained to date harmonize with the present article.

VIII. DISCUSSION AND CONCLUSIONS

The oscillograms contained in this article have been obtained on two conductivity cells having large concentric cylinders of bright platinum spaced 1 mm. apart. Their dimensions lower the resistance of the column of electrolyte relative to the reactance of the *series* capacitance effects at the electrodes. This makes possible a better quantitative study of the relations. The conductivity of the solutions used was between 0.01 and 0.05 mho-cm.

It should be recognized that the scaling of the oscillograms for amplitudes and phase angles does not yield precise results. The errors of measurement (1 to 5 per cent) are large in comparison with those of our earlier precision A.C. bridge data on the cell. Our bridge measurements have shown that the simulating network comprising a resistor *in series* with a capacitor is only a first approximation to the actual cell, and that the second (and very precise) approximation is had by connecting a high resistance branch (leak) in parallel with the series capacitor (figure 1). The oscillograph method yields only a rough check of the first approximation, and can be expected to yield no data for a second approximation. With these limitations the following conclusions are drawn from the data.

1. Not only the steady-state relations but also the transient ones between the alternating current through a conductivity cell and the potential difference across its terminals have (within the limits of the large scaling errors) been shown to be identical with the relations between the current and the impressed E.M.F. which would be observed in a simulating network made by connecting an appropriate capacitor and a metallic resistor in series, provided the sum of the potential differences across the concentration layers does not exceed the E.M.F. of polarization of the solution.

2. The resistance of the column of electrolyte and the capacitive reactance of the equivalent series capacitor as computed by scaling the steady-state curves of current and impressed E.M.F. agree (within the limits discussed above) with the values computed from the transient curves.

3. Both the E.M.F. of ionic segregation (or the effect of the series capacitors C_1 and C_2 in the simulating network of figure 2) and the capacitance between electrodes and leads (the paralleling capacitors C_3 and C_4 of the network) cause the sinusoidal current through the cell to lead the sinusoidal E.M.F. impressed upon the cell. But for the cell and the 0.2 *N* sodium chloride solution used in this work, the angle of lead at

60 cycles per second due to the capacitance between electrodes (simulated by C_3 and C_4) is utterly insignificant, the computed angle of lead of the current being only 0.05 second of arc. On the other hand, at this same frequency the angle of lead due to the E.M.F. of ionic segregation (simulated by the series capacitors C_1 and C_2) is 58 degrees. Even at the audio frequency of 1000 cycles per second, the tangent of the angle of lead of the current due to the series capacitance effect is 44,000 times as great as that due to the parallel capacitance.

The capacitance of the simulating series capacitors C_1 and C_2, as determined from the measurements on the oscillograms, is approximately 7000 microfarads, while the capacitance of the simulating parallel capacitors C_3 and C_4, as computed from the dimensions of the cell, is approximately 1500 micromicrofarads. Because of the fact that the first of these capacitors is in series with the resistance of the column of electrolyte while the second is in parallel with the resistance, any direct comparison of the relative numerical values of the two capacitances is likely to be not only devoid of physical significance but also misleading. At a frequency of f cycles per second, the tangent of the angle of lead of the current due to a simulating capacitor of C_s farads in series with a resistor having R ohms resistance is $1/(2\pi f C_s R)$. On the other hand, the tangent of the angle of lead due to a capacitor of C_p farads in parallel with the same resistor of R ohms is $2\pi f C_p R$. From this it follows that to make the angle of lead infinitesimally small, a series capacitor C_s must be infinitely large, while a parallel capacitor C_p must be infinitesimally small.

4. The oscillograms show the departures from the sinusoidal shape of the current and electromotive force wave forms which occur when the E.M.F. of polarization of the cell is exceeded. Under an impressed E.M.F. greatly in excess of the polarization voltage, the current wave form again becomes approximately sinusoidal. This polarization peak-shift effect is associated with the greatly increased apparent capacitances and probably with electrode reactions other than ion segregation.

5. The oscillograms indicate that the value of the equivalent series capacitance of a given cell and solution is approximately independent of the measuring frequency at the two frequencies of 60 and 240 cycles, and is also independent of the value of the measuring E.M.F. and current provided the E.M.F. of polarization of the solution is not exceeded. With rise in the electrode potential E_c from 0.56 to 6.9 volts the apparent capacitance increases from 8700 to 46,700 microfarads, the transient terms decrease, and the peak value of the first current half-cycle approaches that for the steady state.

6. The preceding conclusions are consistent with the accurate data developed earlier by the use of precision bridges and sinusoidal currents at frequencies of 60 to 4000 cycles per second and extrapolation to infinite

frequency to obtain the true electrolytic conductances of solutions substantially free from the effects observed at high frequencies. It is suggested that in making the usual "solvent corrections" both the capacitance and conductance of the solvent be measured and used in interpretations of the conductance-capacitance properties of electrolytes.

The authors express their thanks to F. K. Harris of the National Bureau of Standards for suggestions in the arrangement of this article.

REFERENCES

(1) Holler, H. D.: Natl. Bur. Standards (U.S.), Sci. Papers **20**, 153 (1924-26), SP 504.
(2) Jones and coworkers: J. Am. Chem. Soc. **50**, 1049 (1928); **51**, 2407 (1929); **53**, 411, 1207 (1931); **55**, 1780 (1933), and later articles.
(3) LeBlanc, M.: Emf of Polarization from Oscillograms, Abhl. Bunsen-Ges. für ang. phys. Chem., No. 3 (1910).
(4) Miller and Gordon: J. Phys. Chem. **35**, 2785 (1931).
(5) Parker: J. Am. Chem. Soc. **45**, 1366 (1923).
(6) Parker and Parker: J. Am. Chem. Soc. **46**, 312 (1924).
(7) Reichenstein: Z. Elektrochem. **15**, 734, 913 (1909); **16**, 916 (1910); **17**, 85, 699 (1911); **18**, 850 (1912); **19**, 38, 518, 520 (1913).
(8) Robertson and Acree: Am. Chem. J. **49**, 501 (1913); J. Phys. Chem. **19**, 381 (1915).
(9) Rosebrugh and Miller: J. Phys. Chem. **14**, 816 (1910).
(10) Shedlovsky: J. Am. Chem. Soc. **52**, 1793 (1930); **54**, 1411 (1932).
(11) Taylor: Science **42**, 388 (1915).
(12) Taylor and Acree: J. Am. Chem. Soc. **38**, 2428 (1916).
(13) Taylor and Acree with Bennett: J. Am. Chem. Soc. **38**, 2397-8, 2405, 2408-9, 2411, 2416-17, 2423, 2427-8, 2430 (1916).
(14) Taylor and Curtis: Phys. Rev. **6**, 61 (1915).
(15) Washburn: J. Am. Chem. Soc. **38**, 2431 (1916).
(16) Washburn and Bell: J. Am. Chem. Soc. **35**, 177 (1913).
(17) Washburn and Parker: J. Am. Chem. Soc. **39**, 235 (1917).
(18) Snow, Chester: J. Research Natl. Bur. Standards **17**, 101 (1936), RP 905.

SURFACE VISCOSITY OF LONG-CHAIN ALCOHOL MONOLAYERS[1]

LYMAN FOURT AND W. D. HARKINS

George Herbert Jones Chemistry Laboratory, University of Chicago, Chicago, Illinois

Received July 1, 1938

INTRODUCTION

This work was undertaken with the purpose of providing a set of quantitative standards of surface viscosity, to clear the way for the more confident use of surface viscosity measurements in studies of molecular association and adsorption. Multivalent ions have very great effects on the viscosity and rigidity of fatty acid monolayers, and the interpretation that this is brought about by ionic bridges seems well supported. Films of macromolecules may show either great or very little shear resistance, and the adsorption of molecules beneath a film can sometimes be inferred from viscosity increases, as in the work of Langmuir, Schaefer, and Sobotka (4) with cholesterol and digitonin. The great desirability of more detailed knowledge of the relation of molecular structure to chemical reactivity and the special good fortune that the biological catalysts, the enzymes, are macromolecules makes it evident that a reliable method of interpreting viscosity in monolayers would be an important tool in the kit of the biophysicist. The underlying significance of surface viscosity may be seen from the fact that it is a measurable function related to the molecular binding energy within the plane of a monolayer, between molecules of specified orientation.

In order to simplify the problem as far as possible we have attempted to reduce the variables to two,—molecular length and orientation. As representatives of the two extreme types of molecular orientation, perpendicular and parallel to the surface, we have used the normal alcohols and the linear polymers of ω-hydroxydecanoic acid. The alcohols gave results of value for our purpose, but no viscosities large enough to measure could be obtained for the ω-hydroxydecanoic acid polymers. The alcohols have two special advantages as standards: (*1*) their force-area curves are simple, with two approximately straight lines, which indicates relative non-complexity of film structure; and (*2*) the effect of ions, etc., in the

---

[1] Presented at the Fifteenth Colloid Symposium, held at Cambridge, Massachusetts, June 9-11, 1938.

subphase should be less than on films with more reactive types of polar groups.

METHOD AND THEORY

The basic method is that used in the long series of studies of superficial viscosity dating back to Plateau (8) and in particular the work of Stables and Wilson in 1883 (10), Schütt in 1903 (9), Wilson and Ries in 1923 (13), Langmuir and Schaefer (3) in 1936 and 1937, and Myers and Harkins (6) in 1937. A circularly symmetrical body passes through the surface, and oscillates as a torsion pendulum about the vertical axis. The logarithmic decrement of the oscillations is proportional to the viscosity. Letting λ_{10} stand for the common logarithm of the ratio of successive amplitudes, and σ for the surface viscosity in C.G.S. units, we have

$$\sigma = \Delta\lambda_{10} \frac{2.3I}{2\pi P}\left(\frac{1}{a^2} - \frac{1}{b^2}\right) \qquad (1)$$

where I is the moment of inertia, P is the period, a is the radius of the oscillating body, and b the radius of the bounding vessel. The value of $\Delta\lambda_{10}$ gives the change of decrement between the clean surface and that covered by the film, that is, applies a correction for the water resistance on the assumption that all of the change in resistance is caused by the film. This may include in the viscosity ascribed to the film an effect of accompanying water, but this effect, if any, would be a monotonic function of the true film viscosity. The period remains practically constant throughout the compression of any alcohol thus far encountered. The slight increase found can be attributed in part to the damping itself, as well as to increase in the rotational inertia because of accompanying water. Rigid films, however, contribute to the elasticity of the oscillating system and thus shorten P. The outer radius, b, was always large with respect to the inner radius, and was taken as 12.5 cm., the distance to the three nearest points on the bounding rectangle. A film balance of the horizontal thrust type (Langmuir-Adam) was used for simultaneous force-area control. The trough was 1.9 cm. deep.

Myers and Harkins (6) employed a sharp edged ring to reduce the water resistance, and a fairly large diameter, 10 cm., to increase the film effect. The ring was placed so that its sharp edge just touched the surface. These experiments have been continued, using rings of 3-in. and 1-in. diameter. The comparative data on different substances we obtained by using a disc 1 in. in diameter, the same diameter as that used by Langmuir and Schaefer (3). This disc, the end of a brass cylinder, was lowered until it just touched the surface. Phosphor bronze wires served for suspensions. The whole system was enclosed in a box to eliminate drafts. Two air jets were arranged to start or brake oscillation in either direction. The parts in contact with the surface were always dipped in molten paraffin and allowed to drain freely while cooling, before each experiment.

Oberbeck in 1880 (7) and Fourt in 1937 (2) used an oscillating vane, instead of a circularly symmetrical system. Such a system has some distinct advantages in rigid films where slippage is a factor. From the damping of an oscillating vane of length l a surface viscosity may be computed

$$\sigma = \lambda_{10} \frac{4 \times 2.3 I}{P l^2} \tag{2}$$

on the assumption that the resistance arises from flow past the ends of the vane. Since this assumption is open to question, experimental comparisons with the ring and disc devices were made. The vane consisted of a microscope cover slip clamped between the halves of a slitted cylinder. It was cleaned with hot chromic acid and washed with water before each experiment, then put in place and lowered so that it just touched the surface.

The viscosity can also be computed from the torque required to maintain a uniform rotation. To do this we used the shaft of an electric clock motor for the upper suspension. The twist between the two ends of the torsion wire is measured by arranging two optical levers to throw spots of light from the moving suspension and from the rotating device onto the same scale. With the torsion constant, τ (dynes per radian), which is determined from oscillation trials, the torque can be obtained by timing the interval, t, between the passage of the two spots of light past a fixed mark. For true (Newtonian) viscosity, independent of the rate of shear, we have an equation in which the rate of rotation does not appear, although it must be constant. Here Δt is the change of interval caused by the film.

$$\sigma = \frac{\Delta t \tau}{4\pi} \left(\frac{1}{a^2} - \frac{1}{b^2} \right) \tag{3}$$

Anomalous viscosity or plasticity would cause a dependence on the rate of shear.

Although the experimental work with constant rotation is only preliminary, we have examined the theory because the interpretation of results with plastic films should be simpler for a method in which the rate of shear is constant, than for the oscillation methods in which the velocity is always changing. Moreover, of all the methods described here it seems the best adapted to the determination of the unique viscosity of the film without the effect of accompanying water. Hydrodynamic considerations indicate that absolute measurements of film viscosity could be obtained by using a device such as a hemisphere, to secure the condition that the vertical velocity gradient in the underlying fluid should be zero in the plane of the surface. This condition could be approached, but the increase in non-film resistance requires greater sensitivity in measurement, and meniscus and centrifugal effects and the superposition of oscillation upon rotation may be expected to reduce the degree of realization of the theoretical conditions. However, the idea is adaptable, at least in theory, to interfacial measurements, by aligning the interface with the equatorial plane of the sphere.

The choice of the parameter for molecular orientation was dictated by experimental circumstances. With small damping as many as ten oscillations may be required for a single determination of the decrement, and with the high degree of damping encountered in the plastic films, a series of decrements was needed for the comparison at constant rate of shear. Hence an interval of several minutes was usually required for a single measurement. For the results to have significance with respect to molecular properties, it is desirable that the film structure remain the same throughout the measuring interval. The lower alcohols, however, showed a distinct tendency to disappear from the film, by collapse or, more probably, solution. That is, the force-area curve is dependent on the rate of solution, the rate of compression, and the elapsed time. A plot obtained by the rapid compression of a film of tetradecyl alcohol is paralleled by the curve obtained after an interval during which viscosities were measured. The area per molecule, computed on the basis that all of the alcohol spread remains on the surface, is less; the type of force-area relations is the same, however, and, what is most important, the intersections of the two straight limbs of the force-area curves are at the same pressure. For this reason the surface pressure is taken as the parameter to indicate the molecular state and resultant film structure. The area per molecule for the molecules actually present in the monolayer is presumably the same for these substances, at a given pressure, in spite of the apparent change with time. In the experiments the pressure was held constant by manual adjustment of the area. The imperfection of this type of control is a major source of random error. However, of the substances used, tetradecyl alcohol is the only one rapidly soluble or expanded at the temperatures used in these experiments, which ranged from 21° to 26°C.

In the preliminary work for the comparison of different devices, cetyl alcohol purchased from the Eastman Kodak Co. was used. For the comparison of the different alcohols we were privileged to use the preparations of Dr. Jane D. Meyer, which were kindly furnished us by Dr. E. E. Reid. Redistilled ligroin was used as a solvent in spreading these films. The ω-hydroxydecanoic acid polymers were kindly furnished by Drs. W. H. Carothers, E. O. Kraemer, and F. J. van Atta of the du Pont Experimental Station. The polymers were dissolved in redistilled benzene. All of the alcohol films were spread on 0.01 N hydrochloric acid solution, made up in redistilled water.

RESULTS

All the alcohols from tetradecyl to heptadecyl showed viscosity relations of the same general type. The kink point of the force-area curve is likewise a singular point in viscosity. At all lower pressures the films behave as Newtonian fluids. At all higher pressures the films exhibit anomalous viscosity, that is, the apparent viscosity increases with decreasing rate of shear. Harkins and Myers (6) referred to this as plasticity, as did Wilson and Ries (13) for their adsorbed films. However, we use the term "plastic" merely as a convenient expression for anomalous viscosity, because our methods do not give us any measure of a yield point. Moreover, sensitive tests for rigidity, by means of the oscillating vane, observation of talc mobilities, and the behavior of floating strips of paper (Langmuir and Schaefer (3)) fail to give any evidence of rigidity.

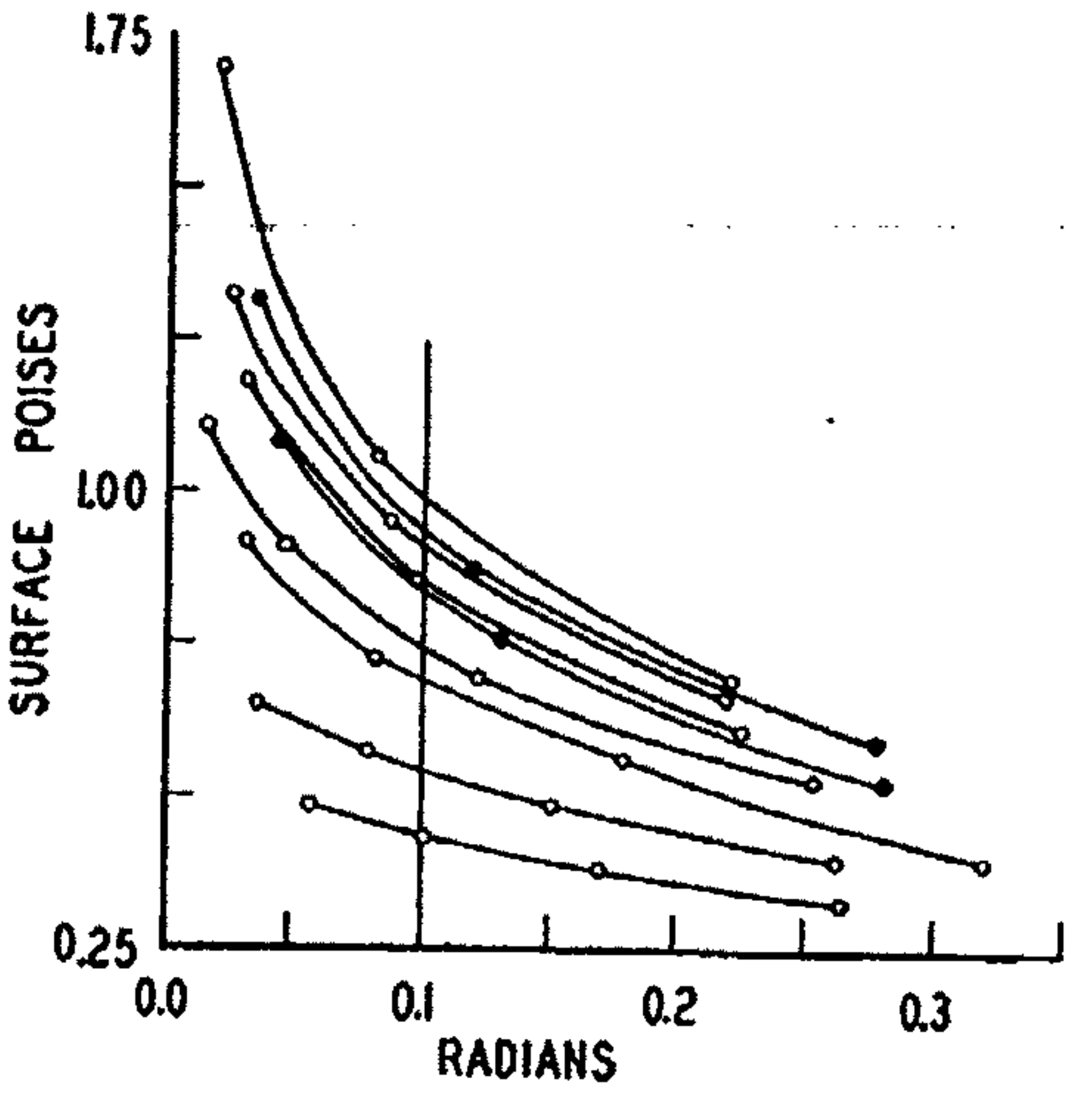

FIG. 1. Representative family of curves to show the dependence of viscosity on the rate of shear above the kink point pressure. Ordinate, apparent surface viscosity; abscissa, mean amplitude. The open circle curves are all at successively higher pressures and viscosities up to the viscosity maximum. The solid circles lie on curves for still higher pressures but decreasing viscosities.

The variation of apparent viscosity with rate of shear or amplitude, which is encountered above the kink point, has been treated by an empirical method designed to make the successive values in a given experiment comparable. To do this, the logarithmic decrement or the apparent viscosity was plotted against the sum of the amplitudes used in its computation. An example of the resulting families of curves is shown in figure 1. These curves do not cross each other, except for occasional irregularities, which shows that "greater than or less than" comparisons are justified. The values for the plastic films are those taken at a mean amplitude of 0.1 radian, but the greatest viscosities recorded in the plastic region were several-fold larger; the smallest was about half as large.

The transition at the kink point is very nearly free from hysteresis. Points taken by expanding a compressed film fall on the same curve, to the accuracy of this work, as those obtained by successive compressions. This type of experiment was tried with tetra-, hexa-, and hepta-decyl alcohols. It is not impossible that a more nearly instantaneous method of measurement might reveal a hysteresis or sluggishness obscured by the time required for a series of oscillations. In the steep part of the curve a second series of oscillations at a given pressure usually gives a higher apparent viscosity. With two films of tetradecyl alcohol, low values of the viscosity were obtained above the kink point. Although this may correspond to a metastable state, like a condition of undercooling or supersaturation, a comparatively large number of repeated experiments with this substance have not enabled us to specify the conditions under which this behavior may be observed.

TABLE 1

Dimensions of oscillation devices

TYPE	RADIUS OR LENGTH	MOMENT OF INERTIA	PERIOD IN CLEAN SURFACE	λ_{10} IN CLEAN SURFACE	APPARATUS CONSTANT $\div P$
	cm.	*g. cm.*^{2}	*sec.*		
Ring	5.00	2520	73.40	0.042	0.426
			10.88	0.0082	2.87
	3.91	695	33.68	0.034	0.476
	1.26	141	17.69	0.0051	1.88
Disc	1.26	127	16.88	0.0075	1.70
Vane	3.00	202	17.80	0.0030	14.6
	6.00	177	17.91	0.051	2.52

Except for octadecyl alcohol, the viscosity is Newtonian until well into the steep part of the transition curve. It is not a matter of the magnitude of the observed value of λ_{10}, since experiments with devices in which λ_{10} is large and the factor small agree with those used in the comparative work. Octadecyl alcohol differed in showing a slight plasticity below the kink point. This effect is small compared with the difference between check experiments on different films, but could be seen clearly in an individual experiment. Octadecyl alcohol has the further peculiarity that the curves which show the viscosity as a function of the amplitude, although they rise with decreasing amplitude, are nearly straight, in contrast to the considerable curvature found with the other alcohols.

The hexadecyl alcohol samples from the two sources (Eastman, and Meyer and Reid) gave nearly the same numerical values below the kink point, but above the kink point the Eastman sample showed values about half as large, though with a curve of similar shape. For a comparison of the different oscillation methods we may confine our attention to the values below the kink point. Table 1 shows the dimensions of the different systems used, the approximate value of λ_{10} for the clean surface, and the factor "apparatus constant ÷ P" by which the change in λ_{10} is multiplied to obtain σ.

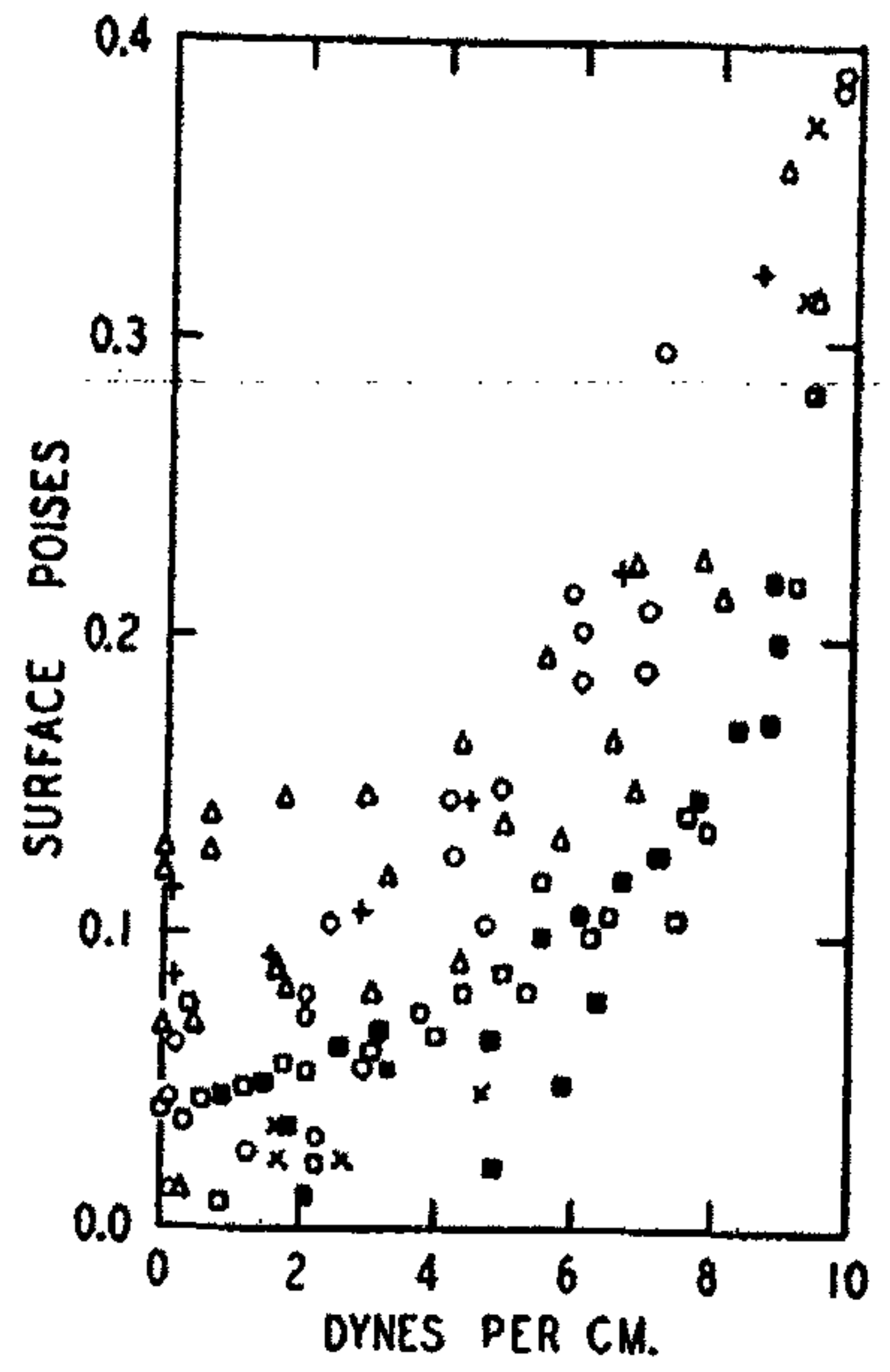

FIG. 2

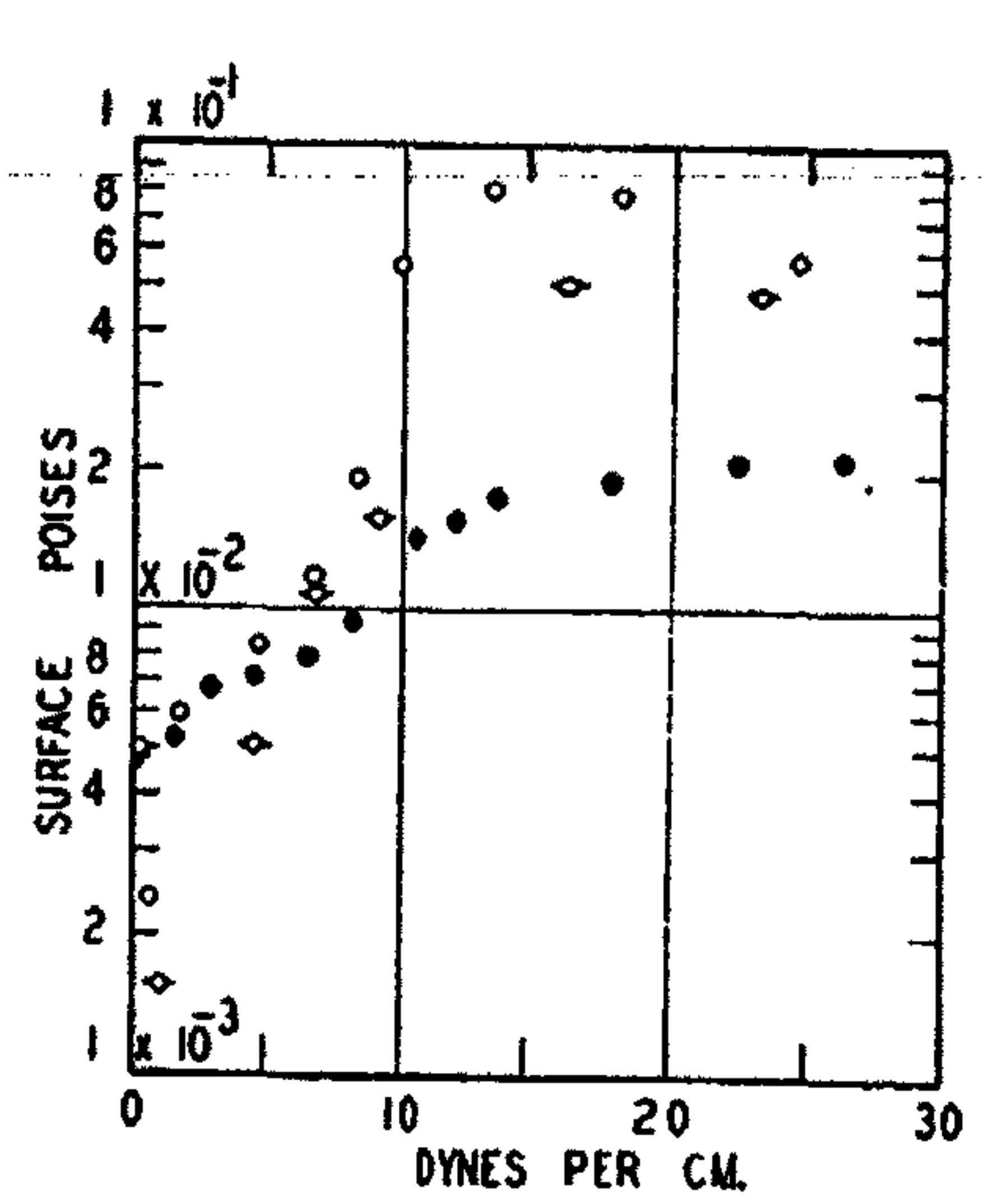

FIG. 3

FIG. 2. Surface viscosity of hexadecyl alcohol below the kink point, as measured by different devices. Ordinate, surface viscosity; abscissa, surface pressure. ○, 10-cm. ring; △, 3-in. ring; □, 1-in. ring; ■, 1-in. disc; +, 6-cm. vane; ×, 3-cm. vane.

FIG. 3. Surface viscosity of hexadecyl alcohol from constant rotation measurements. Ordinate, logarithm of viscosity; abscissa, surface pressure.

Figure 2 presents the results obtained with the different methods. Check experiments with each device show a range of values comparable to the difference between different devices; there is just a suggestion of a trend in that the largest values are obtained with the rings of largest diameter, and the smallest with those of smallest diameter. This may involve the approximation introduced by taking the half-width of the rectangular tray as an outer circular boundary. Most of the points with the 10-cm. ring were computed from the experiments of Myers (6). The values obtained with vanes 3 and 6 cm. long fall among the others. Above the kink point all of the devices give values similar in magnitude and in variation with pressure, the agreement being of the same order as that exhibited below the kink.

Figure 3 shows some preliminary results obtained for hexadecyl alcohol from the rotation of the 10-cm. and 3-in. rings, some with stopwatch timing and some by an automatic timing system. This apparatus could be adapted to automatic recording. Below the kink point these values are of the same order as those obtained by the oscillation methods, but are tenfold smaller above. The comparatively large angular velocity, 0.387 radian per second, compared with 0.0237, the average speed in oscillation at 0.1 radian, with $P = 16.88$ sec. is in the direction to account for this difference. The points were taken too far apart and the timing interval available was too coarse to do more than indicate the potentialities of the method.

The choice of apparatus for the work with different substances was somewhat arbitrary. The lower limit of viscosity measurable by any of the oscillation devices is about the same, as may be seen from the constancy of the product of "apparatus constant $\div P$" times unity in the place of the last significant figure of the clean surface λ_{10} (given in table 1). For this reason the work has been confined to a straightforward application of methods, such as would be desirable for exploratory experiments and routine testing. By an increased expenditure of time and a statistical analysis of the results any of these devices could be used to measure viscosities as low as 0.0002 surface poise.

The viscosities of the normal alcohols from C_{14} to C_{18} inclusive are shown in figure 4. The portions above and below the kink point are plotted on different arithmetic scales of viscosity, and the very high pressures are shown on a contracted scale. With increasing chain length, the kink points lie at increasingly higher pressures. The viscosities at low pressures are larger, the longer the chain. Below the kink point the viscosity of each alcohol increases with increasing pressure, and the more rapidly as this singular point is approached. The transition is more abrupt for the shorter chain.

Above the kink point the apparent viscosity of each alcohol tends to increase for a range of pressures, and finally, as collapse is approached, to fall off again. The scattering of values between different experiments on the same substance is more pronounced above than below the kink. Nevertheless, the trend of viscosity with chain length is clear: the longer the chain, the less the apparent viscosity. With respect to what we may call the degree of plasticity, the rate of change of apparent viscosity with amplitude, the trend is also reversed, octadecyl alcohol being the only one plastic below the kink point, and the least so above. No great degree of difference could be seen in the plasticity of the other alcohols, however.

The whole range of the viscosities of all of the alcohols can be shown on a single figure by plotting the viscosities on a logarithmic scale (figure 5). The range of values—nearly 10,000-fold—and the magnitude of the transition at the kink point is emphasized. Below the kink point the logarithm of the viscosity increases somewhat more rapidly than linearly with pressure.

The insert in figure 5 presents the mean values taken from the logarithmic plot, plotted against pressure expressed as fraction of the kink point pressure. This corresponding states graph facilitates comparison by omitting the crossing over with the reversal of order at the kink point. From this figure it is seen that below the kink point the viscosity increases with increasing chain length. Above the kink point pentadecyl alcohol is shown out of order; the fields of points represented by these median lines are so overlapping, though, for tetra-, penta-, and hexa-decyl alcohols, that only the general trend toward lower apparent viscosity with longer chain is significant.

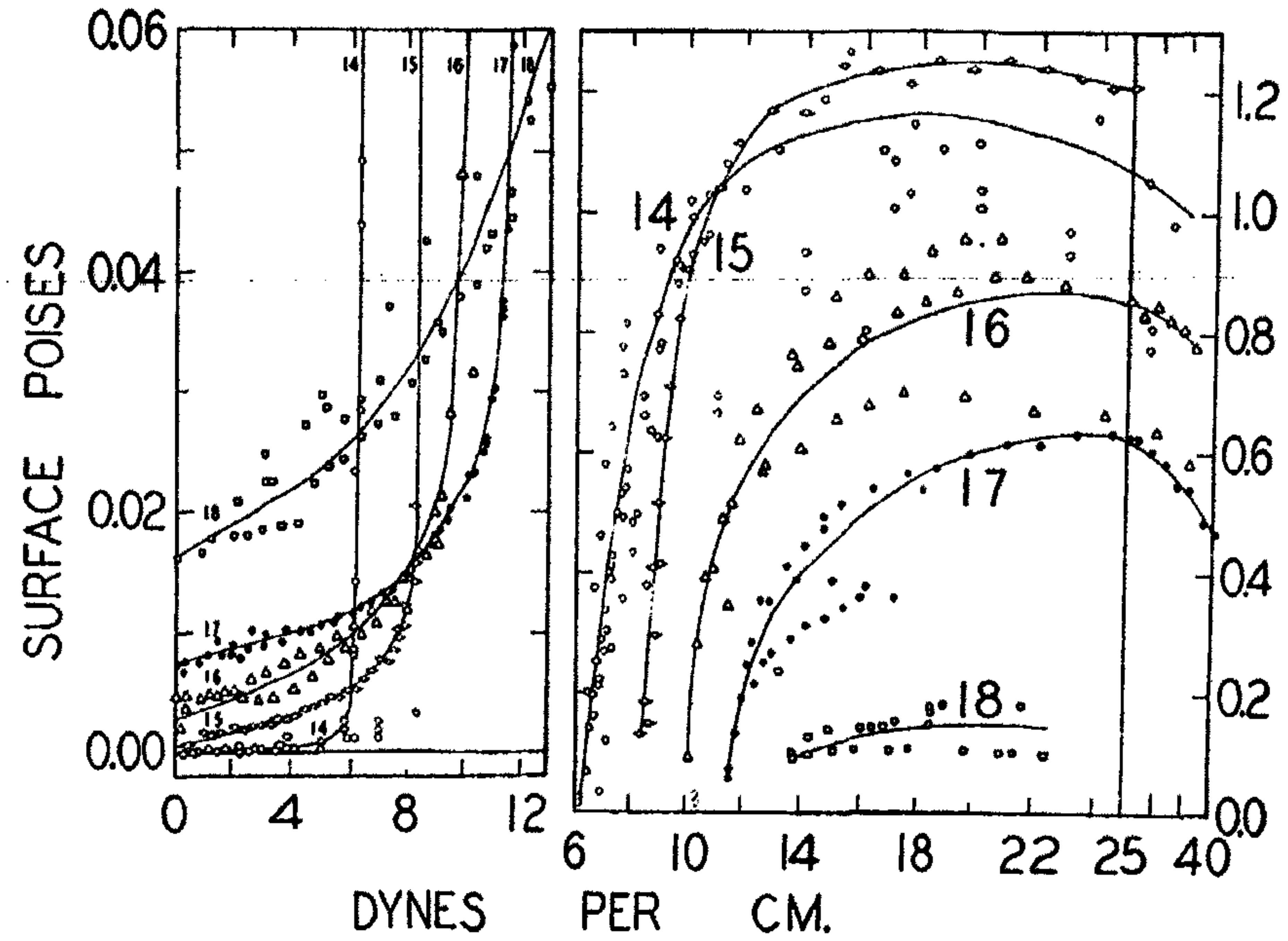

FIG. 4. Surface viscosities of the normal alcohols from C_{14} to C_{18}. Left-hand part, below the kink point; right-hand part, above the kink point, showing apparent viscosities at 0.1 radian mean amplitude. Ordinates, surface viscosity; abscissae, surface pressure. Pressures above 25 dynes per centimeter are shown on a reduced scale. On the low pressure side, the bottom of the plot represents −0.002 surface poise, to show that "negative viscosities" are not significant.

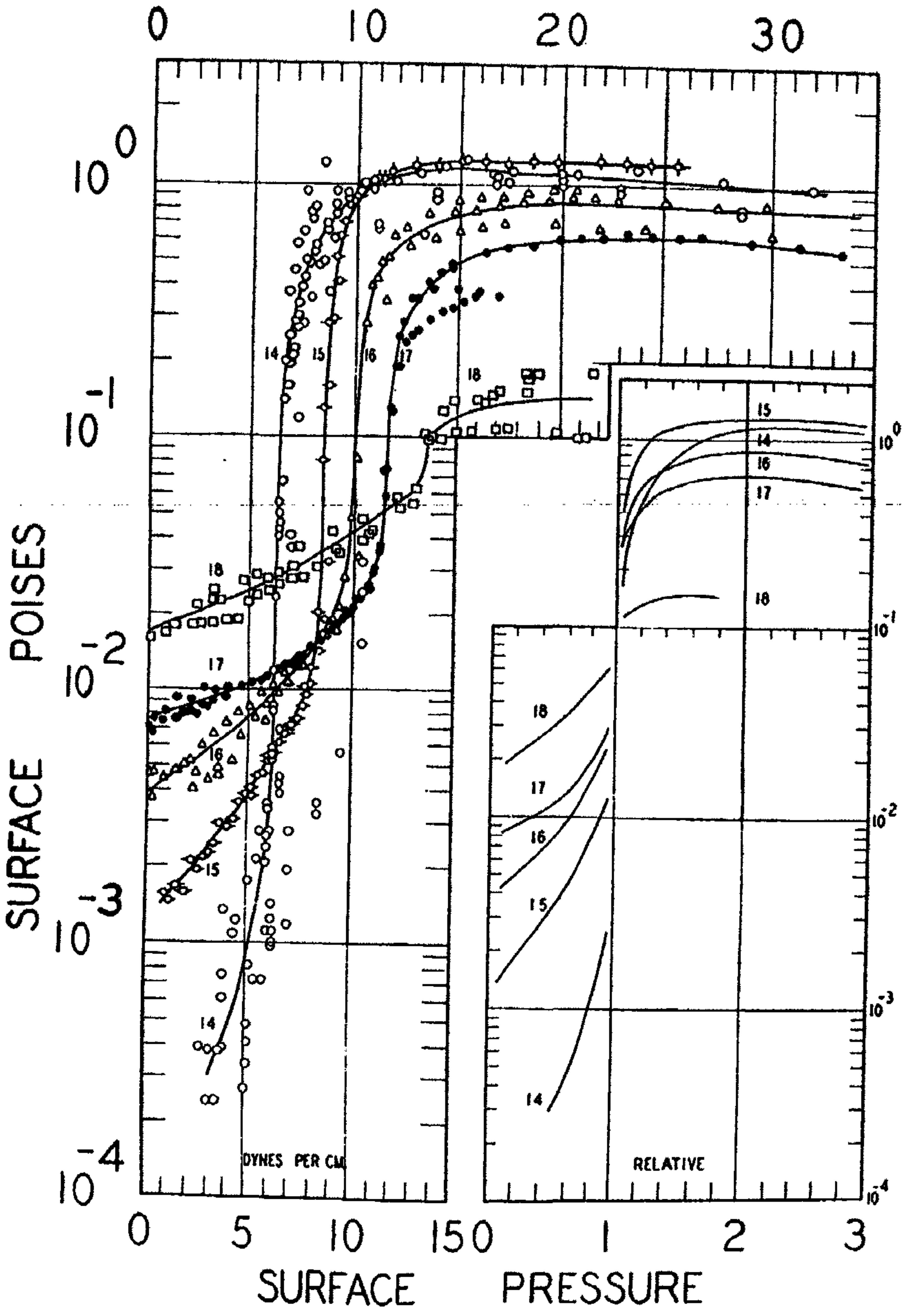

FIG. 5. Surface viscosity of the normal alcohols from C_{14} to C_{18}. Ordinate, logarithm of surface viscosity; abscissa, surface pressure. In the insert the surface pressure scale is in multiples of the mean kink point pressure.

Neither with respect to kink point pressures nor with respect to viscosities is there any alternation evident between odd and even numbers of carbon atoms in this series. This parallels the absence of alternation of melting point found by Meyer and Reid (5).

The mean values of the kink points for the different alcohols are given in table 2, which also shows the values reported by Adam and Dyer (1). The mean values given are the midpoints of the transition curves of viscosity shown in figure 5 and are accurate within 0.5 dyne. Within this limit they agree with the kink points determined from force–area measurements on the same samples in this laboratory.

The force–area curves of tetradecyl alcohol show a curved portion below 3 dynes pressure. This corresponds to the expanded type of film, which has too low a viscosity to measure, as may be seen in figure 5. All the other alcohols had measurable viscosities even at 0.1 dyne pressure, and these viscosities lie fairly well on the same smooth curve as those at higher pressures. At quite large areas, though with the film at practically zero pressure, one frequently observes a very small "negative viscosity," that is, a damping less than that of the original clean surface. This is, however, never much larger than the random fluctuation of the damping caused by the clean surface, and thus is hardly significant, as the arithmetic plot of figure 4 shows. This anomaly is less marked with the disc than with any of the rings. The C_{12} alcohol is quite soluble and has an entirely expanded force–area curve at room temperature. It showed no measurable viscosity.

TABLE 2

Transition pressures of the normal alcohols

ALCOHOL	PRESSURES, IN DYNES PER CENTIMETER	
	This work	Adam and Dyer
C_{14}	6.2	7.2
C_{15}	8.5	
C_{16}	10.0	9.2
C_{17}	11.6	
C_{18}	13.4	11.0
C_{20}		13.5

Likewise, we were unable to measure any viscosity for ω-hydroxydecanoic acid polymers of molecular weights 780 and 16,900, spread on 0.01 *N* hydrochloric acid or sodium hydroxide, or on sodium hydroxide to which a calcium salt had been added. Only on collapse and compression to a visible scum could a change in damping be obtained. Collapse occurs at comparatively low pressures, however (*ca.* 3 dynes per centimeter).

DISCUSSION

The relation of viscosity and of compressibility to the kink point is significantly different. To a close approximation, the two limbs of the force–area curve of the alcohols are straight lines, intersecting sharply, implying a discontinuity in compressibility. By contrast the change in viscosity, although large in magnitude and extreme in quality (reversal of relationship to molecular length), is continuous and spreads out on either side of the main transition.

Recent detailed studies of the region of the kink point for these substances, made in this laboratory by Dr. G. C. Nutting, show a previously unnoticed phenomenon; a slight increase in compressibility and an increased tendency of the pressure to fall off with time become evident just below the kink. This effect is found in a pressure range of about 0.5 dyne above and below the "kink" determined by the extrapolated curves.

TABLE 3

Computed bulk viscosities of the normal alcohols

ALCOHOL	FILM THICKNESS AT		MEAN SURFACE VISCOSITY		COMPUTED BULK VISCOSITY	
	21.6 Å.² per molecule	19.0 Å.² per molecule	Smallest	Maximum	Smallest	Maximum
	Å.	Å.	*surface poises*		*poises*	
C_{14}	19.9	22.7	0.0003	1.15	1.5×10^3	5.1×10^6
C_{15}	21.2	24.2	0.0015	1.25	0.7×10^4	5.2×10^6
C_{16}	22.5	25.7	0.0040	0.85	1.8×10^4	3.3×10^6
C_{17}	23.8	27.2	0.0075	0.62	3.2×10^4	2.3×10^6
C_{18}	25.1	28.7	0.0165	0.18	6.6×10^4	0.6×10^6

Adam's distinction between close-packed heads and close-packed chains was suggested by the force–area relations. Without making such a detailed picture as is implied by those phrases, we may speak of low and high pressure condensed films, and of a transition range.

The state of aggregation of the molecules in the structure predominating above the kink point must be left unsettled. Plasticity is a more convenient expression than anomalous viscosity, but it must be emphasized that a solid, in addition to phenomena of non-Newtonian deformation or flow, should show a yield point and especially the property of shear elasticity.

There is no necessity for an explanation of the decline of the apparent viscosity at the higher pressures in terms of film structure. For what they interpreted as a maximum strength phenomenon in monolayers, Talmud, Suchowolskaja, and Lubman (11) have postulated lessened intertwining of the more perfectly oriented chains and consequent more ready slippage under shearing stress. The viscosity maximum observed in the present experiments could also arise from an instability of the film with the approach of collapse. Under shearing stress molecules could yield by escaping from the plane of the film, the more readily the higher the pressure. These experiments offer no basis for choice.

A formal calculation of bulk viscosity may be made by dividing the surface viscosity by the vertical thickness of the films. If we take 21.6 Å². as the area per molecule at 0.1 dyne pressure for all the compounds, and 19 Å². as the area at the pressure of maximum viscosity, and use 0.82 as a round number for the density, the mean thickness of the monolayer can be computed for each alcohol. The corresponding ordinary viscosities are given in table 3.

When we consider that the viscosity of water at room temperature is 1×10^{-2} poises we see that the smallest values measured are from 10^4 to 10^6 times that, and that the maximum values are some 10^8-fold larger than for water. These might be regarded as excessively high values because of the participation of accompanying water, not taken into account in computing the film thickness. However, there is no reason apparent why more water should accompany one alcohol than another. This supports the idea that the differences found are really in the plane of the monolayer. Trouton and Andrews (12) found the viscosity of shoemaker's wax to be 5×10^6, of pitch around 10^{10}, and of soda glass 10^{13} poises. This would tend to show that there is nothing intrinsically unreasonable in the magnitudes of the maximum values encountered in this work.

SUMMARY

Methods based on the damping of oscillating rings, discs, and vanes by a surface film give values of the surface viscosity which agree well enough to indicate the usefulness of such methods. A continuous rotation device, although not yet refined to the same degree of usefulness, gives similar values. Theory indicates that such a device would possess advantages for use with plastic films, and that it could be adapted to give absolute values of surface and interfacial film viscosities, free from subphase effects.

The viscosity of expanded films of the normal alcohols is too low to measure by these means. Measurements were obtained on condensed films of the five alcohols from C_{14} to C_{18} inclusive. The low pressure linear part of the compression curve corresponds to low values of the surface viscosity, increasing more and more rapidly with increasing pressure. For this portion the longer the chain, the higher the viscosity. The high pressure linear part of the compression curve corresponds to high apparent viscosities, which are greater for lower rates of shear. These values, compared at a single average rate of shear, rise to a maximum as the pressure increases, then fall off with the approach of film collapse. Of the alcohols

examined, only octadecyl alcohol shows non-Newtonian viscosity below the kink point. The singular point or, as recent findings show, region of the force–area curves corresponds to the transition in viscosity.

REFERENCES

(1) Adam, N. K., and Dyer, J. W. W.: Proc. Roy. Soc. (London) **A106**, 694 (1924).

(2) Fourt, L.: Am. J. Physiol. **119**, 310 (1937).

(3) Langmuir, I.: Science **84**, 379 (1936).
Langmuir, I., and Schaefer, V. J.: J. Am. Chem. Soc. **59**, 2400 (1937).

(4) Langmuir, I., Schaefer, V. J., and Sobotka, H.: J. Am. Chem. Soc. **59**, 1751 (1937).

(5) Meyer, J. D., and Reid, E. E.: J. Am. Chem. Soc. **55**, 1574 (1933).

(6) Myers, R. J., and Harkins, W. D.: J. Chem. Phys. **5**, 601 (1937).

(7) Oberbeck, A.: Wied. Ann. **11**, 634 (1880).

(8) Plateau, J.: Phil. Mag. [4] **38**, 445 (1869).

(9) Schütt, K.: Ann. Physik [4] **13**, 712 (1904).

(10) Stables, W. H., and Wilson, A. E.: Phil. Mag. **15**, 406 (1883).

(11) Talmud, D. L., Suchowolskaja, S., and Lubman, N.: Z. physik. Chem. **A151**, 401 (1930).

(12) Trouton, F., and Andrews, E.: Phil. Mag. [6] **7**, 347 (1904).

(13) Wilson, R. E., and Ries, E. D.: Colloid Symposium Monograph **1**, 145 (1923).

THE VISCOSITY OF DILUTE SOLUTIONS OF LONG-CHAIN MOLECULES. I[1,2]

MAURICE L. HUGGINS

Kodak Research Laboratories, Rochester, New York

Received July 1, 1938

INTRODUCTION

This paper is a report of an attempt to develop a satisfactory theory, heretofore lacking, of the viscosity of dilute solutions of long-chain compounds.

For solutions or suspensions of *incompressible*, *spherical* particles which are *large* in comparison with the molecules of the solvent, Einstein (3, 4) has derived the relationship

$$\eta_{sp} = \frac{5}{2}\frac{v}{V} \tag{1}$$

For solutions or suspensions of particles consisting of spheres rigidly held together to form a rod-like molecule (the distance between sphere centers being twice the sphere diameter), Kuhn (15, 16) deduced the equation

$$\eta_{sp} = \frac{v}{V}\left(\frac{5}{2} + \frac{f_1^2}{16}\right) \tag{2}$$

In the derivation he assumed that the Brownian motion is large in comparison with the velocity gradient in the solution.

For ellipsoidal particles Eisenschitz (5, 6) derived the equation

$$\eta_{sp} = \frac{v}{V}\left(\frac{1.15f_2}{\pi \ln 2f_2}\right) \tag{3}$$

neglecting the Brownian motion, and

$$\eta_{sp} = \frac{v}{V}\left(\frac{f_2^2}{15\ln 2f_2 - \frac{45}{2}}\right) \tag{4}$$

for very long particles, with a large Brownian motion effect.

---

[1] Presented at the Fifteenth Colloid Symposium, held at Cambridge, Massachusetts, June 9-11, 1938. A preliminary report of this work was presented at the Ninety-fourth Meeting of the American Chemical Society, held at Rochester, New York, September, 1937.

[2] Contribution No. 647 from the Kodak Research Laboratories.

In these equations,

$$\eta_{sp} = \frac{\eta}{\eta_0} - 1$$

is the fractional increase in viscosity of the solution over that of the pure solvent, v/V is the volume of solute per unit volume of solution, f_1 is the ratio of the length of the rod-like molecule to the diameter of the spheres of which it is composed, and f_2 is the axial ratio of the ellipsoid.

Empirically Staudinger (26, 27, 28) showed that, for very dilute solutions of several types of long-chain compounds, the specific viscosity divided by the concentration in submoles ("Grundmole") per liter is approximately proportional to the number of *submolecules* ("Grundmoleküle", e.g., CH_2 groups in a paraffin chain) in the chain:

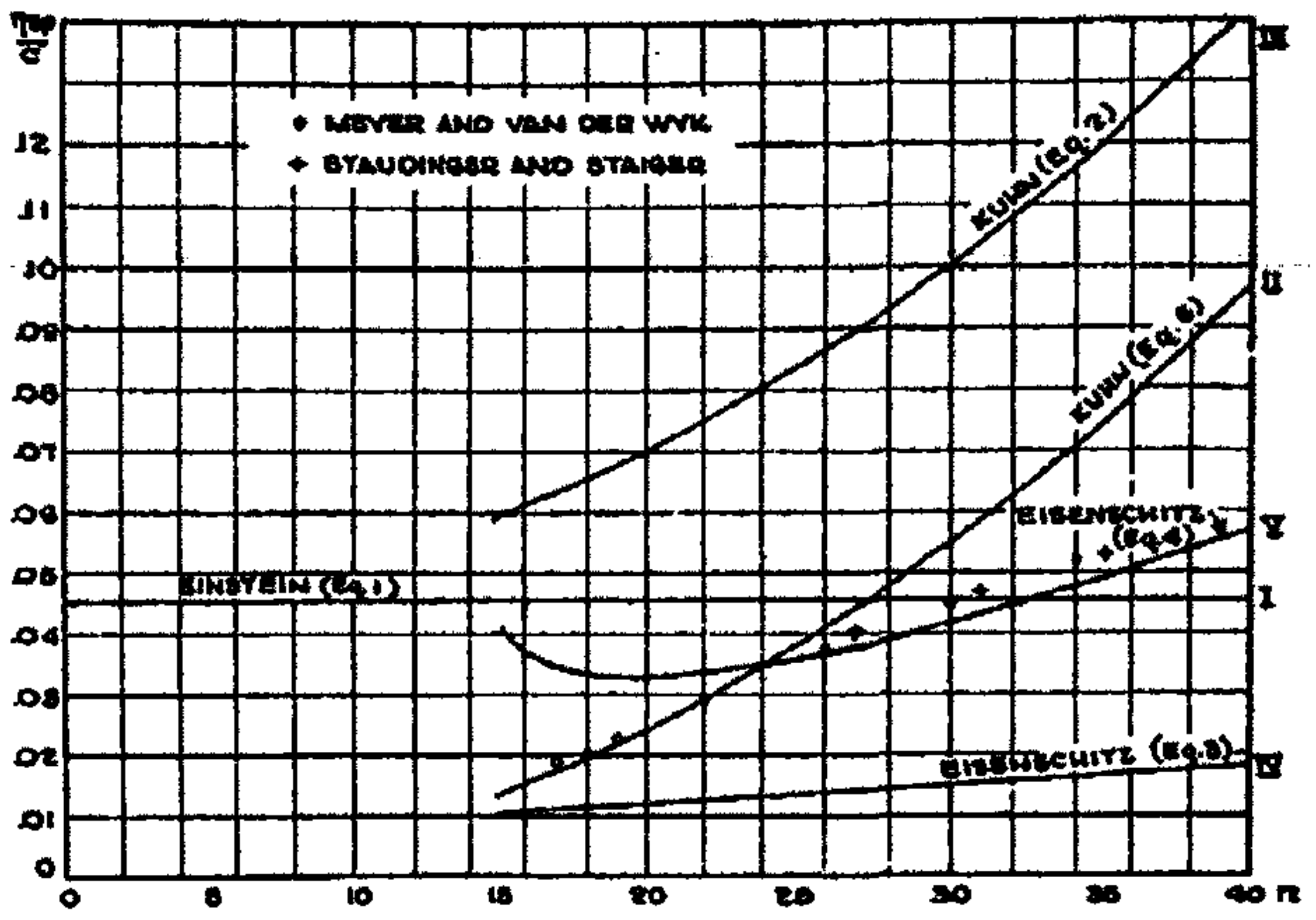

FIG. 1. Experimental and previous theoretical values of η_{sp}/c for dilute solutions of paraffins in carbon tetrachloride at 20°C.

$$\frac{\eta_{sp}}{c} = k_s n \tag{5}$$

This empirical relationship has been much used by Staudinger and others in deducing approximate average molecular weights of high polymers.

The experimental viscosity data of Meyer and van der Wyk (22) and of Staudinger and Staiger (28) for solutions of normal paraffins are compared with the theoretical values calculated from equations 1, 2, 3, and 4 in figure 1. Since, in the writer's opinion, the inclusion of an Einstein incompressibility term $\left(\frac{5}{2}\frac{v}{V}\right)$ in equation 2 for rod-like molecules is very questionable, a curve representing the equation

$$\eta_{sp} = \frac{v}{V}\left(\frac{f_1^2}{16}\right) \tag{6}$$

is also included in the figure.

It is evident that none of the theoretical curves is satisfactory. The experimental points lie approximately on a straight line, but (from Meyer and van der Wyk's data at least) not one that passes through the origin.

Aside from this comparison, there is considerable other evidence favoring the supposition that long-chain molecules, such as the paraffins, are very much kinked in solution, rather than straight. The rigidity of such kinked molecules is more questionable, although there is considerable evidence (10, 11, 12, 13, 14, 23, 24, 25; cf., however, 1) for the existence of potential energy humps of the order of magnitude of 3000 cal. (i.e., about 5 times *RT*) per mole tending to prevent rotation about each single bond in a paraffin chain. If so, intermolecular collisions will only very rarely have sufficient energy to produce rotation over these energy humps, but rotation through a few degrees will take place much more readily.

In view of the foregoing, a theoretical calculation of the viscosities of dilute solutions of rigid, randomly kinked chain molecules has been made, with some progress in extending the results to non-rigid, kinked chain molecules. Only an outline of the methods and results will be presented here; the details will be given in a later paper.

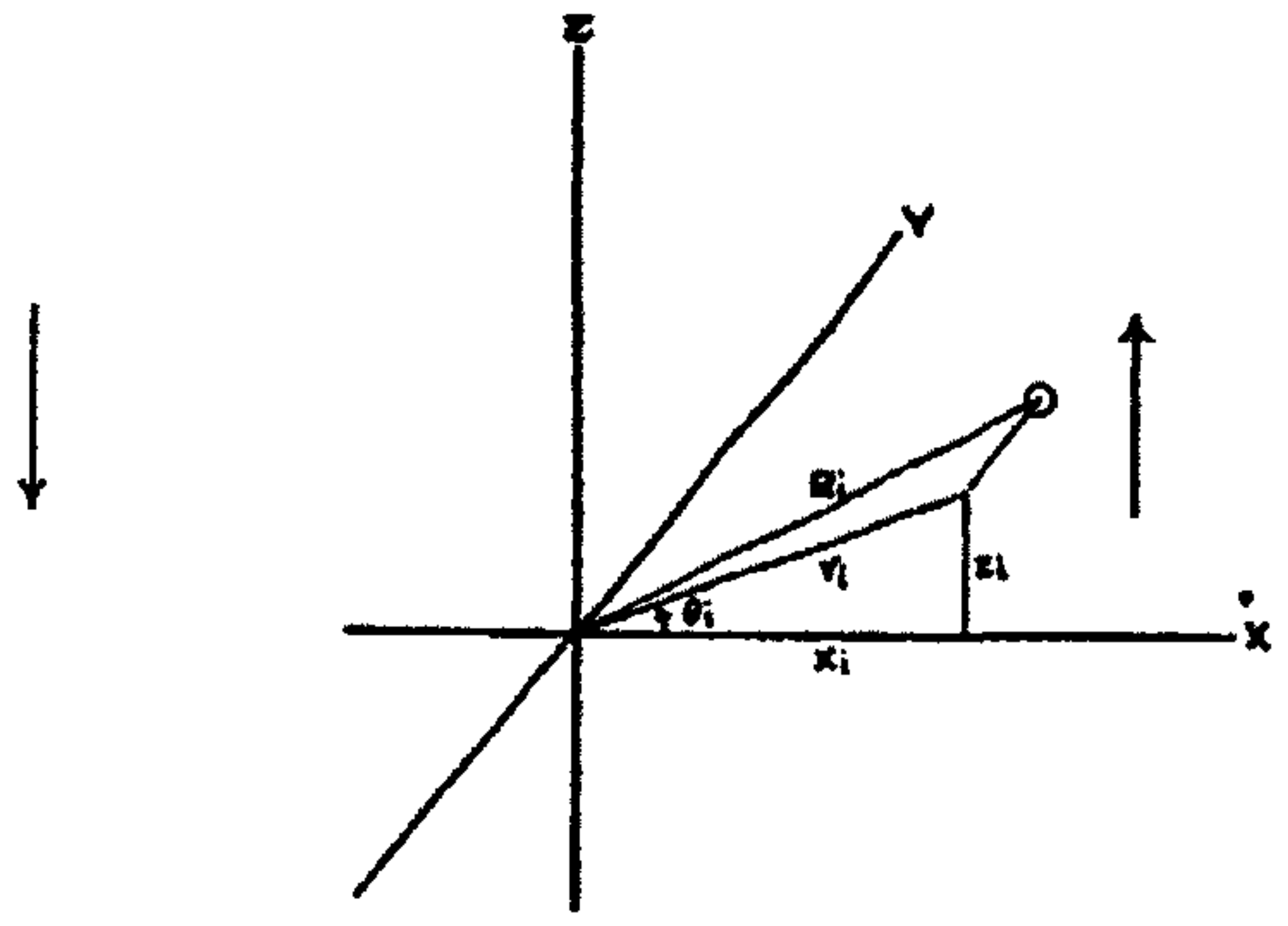

FIG. 2. Illustrating the orientation of reference axes, etc.

DERIVATION OF A GENERAL EQUATION FOR RIGID MOLECULES

We first consider a rigid molecule in dilute solution and, following an elaboration and extension of Kuhn's procedure (15, 16, 17), calculate the relation between the work done on this molecule by the solution as a function of the velocity gradient of the solution, the viscosity of the solution, and the coördinates of the atoms in the molecule.

The origin is taken at the center of moments of the molecule, with the axes so oriented that the surrounding liquid moves in the Z direction with a velocity, qx, which is proportional to x. The atoms are numbered 1, 2, 3 .... i .... n and their coördinates designated as x_i, y_i, z_i (see figure 2).

Because of the velocity gradient in the liquid, the molecules rotate about the Y-axis. We represent the length of the vector from the origin to the projection of the atom i onto the XZ plane by r_i and the angle measured counterclockwise from the X-axis to this vector by Θ_i.

The work expended on atom i in unit time is deduced to be

$$\epsilon_i = 6\pi\eta q^2 a_i \frac{[z_i^2(\Sigma a_i x_i^2)^2 + x_i^2(\Sigma a_i z_i^2)^2]}{(\Sigma a_i r_i^2)^2} \tag{7}$$

The work expended on all n atoms, if they all have the same radius a, is

$$\epsilon = 6\pi\eta q^2 a F_{xz} \tag{8}$$

where

$$F_{xz} = \frac{\Sigma x_i^2 \cdot \Sigma z_i^2}{\Sigma r_i^2} = \frac{\Sigma r_i^2 \cos^2\Theta_i \cdot \Sigma r_i^2 \sin^2\Theta_i}{\Sigma r_i^2} \tag{9}$$

From this is derived the relationship:

$$\frac{\eta_{sp}}{c} = \frac{6\pi Na\overline{F_{xz}}}{1000n\left(1 - \frac{6\pi Na\overline{F_{xz}}}{1000n}\,c\right)} \tag{10}$$

in which N is Avogadro's number and $\overline{F_{xz}}$ is the average of F_{xz} over all orientations.

It can be shown that, if

$$\frac{6\pi\eta aq(\Sigma r_i^2 \cos^2\Theta_i' - \Sigma r_i^2 \sin^2\Theta_i')}{kT}$$

is small compared to unity (k being the Boltzmann constant and T the absolute temperature), then

$$\overline{F_{xz}} = \frac{\Sigma\overline{R_i^2}}{12} + \frac{1}{3}\left[\frac{\Sigma R_i^2 \sin^2\Theta_i' \cdot \Sigma R_i^2 \cos^2\Theta_i'}{\Sigma R_i^2}\right]_{\text{ave.}} - \frac{1}{3}\left[\frac{(\Sigma R_i^2 \sin\Theta_i' \cos\Theta_i')^2}{\Sigma R_i^2}\right]_{\text{ave.}} \tag{11}$$

The angles Θ_i are constants, being measured relative to an arbitrary set of X- and Z-axes rotating with the molecule.

APPLICATION TO RIGID CHAIN MOLECULES

For linear rod-like molecules equation 11 reduces to

$$\overline{F_{xz}} = \frac{l^2(n^3 - n)}{144} \tag{12}$$

With large n and small concentrations, from equation 10,

$$\frac{\eta_{sp}}{c} \approx \frac{\pi N a l^2 n^2}{24000} \tag{13}$$

We next consider a rigid, randomly kinked, centrosymmetric chain molecule. For the average value of R_i^2 we make use of a relationship, derived by Eyring (7),

$$\overline{R_i^2} = l^2 B i \tag{14}$$

where

$$B = 1 + 2\left(\frac{i-1}{i}\right)\xi + 2\left(\frac{i-2}{i}\right)\xi^2 + 2\left(\frac{i-3}{i}\right)\xi^3 + \cdots + 2\xi^{i-1} \tag{15}$$

$$\xi = \cos\alpha \tag{16}$$

and α is the supplement of the angle included between adjacent bonds (see figure 3).

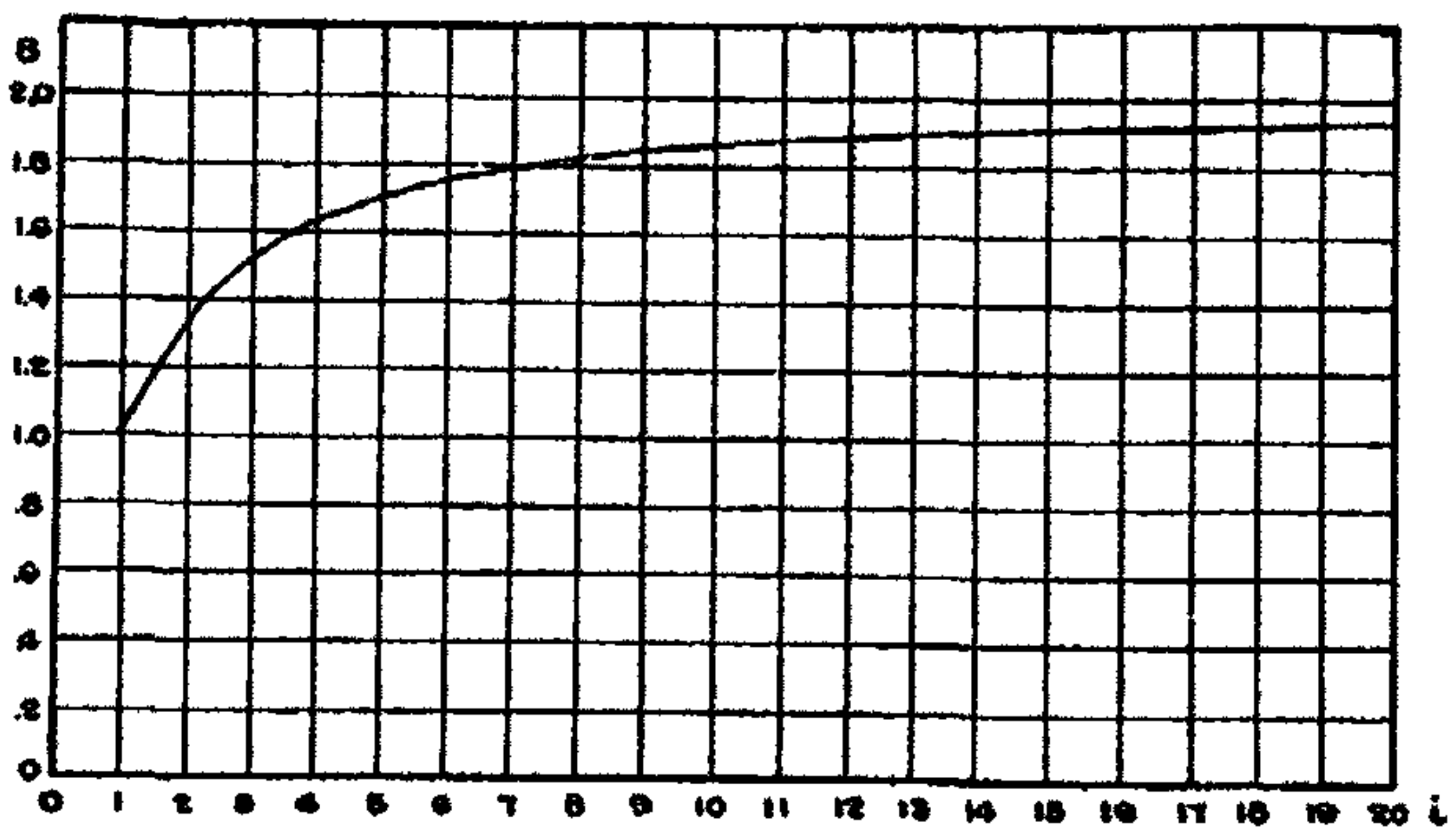

FIG. 3

By an extension of Kuhn's (18) statistical methods, it is possible to show that the average of the square of the distance of the i^{th} atom of the chain molecule from the straight line joining the origin (at the center of the molecule) to the end (m^{th}) atom is

$$\overline{S_i^2} = \frac{2}{3} B l^2 \left(i - \frac{i^2}{m}\right) \tag{17}$$

Also,

$$\overline{R_i^2 \sin^2 \Theta_i'} = \frac{3}{4}\overline{S_i^2} \tag{18}$$

$$\overline{R_i^2 \cos^2 \Theta_i'} = \overline{R_i^2} - \frac{3}{4}\overline{S_i^2} \tag{19}$$

Making the approximations

$$\left[\frac{\Sigma R_i^2 \sin^2 \Theta_i' \cdot \Sigma R_i^2 \cos^2 \Theta_i'}{\Sigma R_i^2}\right]_{\text{ave.}} \approx \frac{\overline{\Sigma R_i^2 \sin^2 \Theta_i} \cdot \overline{\Sigma R_i^2 \cos^2 \Theta_i}}{\overline{\Sigma R_i^2}} \tag{20}$$

$$\left[\frac{(\Sigma R_i^2 \sin \Theta_i' \cos \Theta_i')^2}{\Sigma R_i^2}\right]_{\text{ave.}} \approx 0 \tag{21}$$

and performing the summations, we obtain

$$\overline{F_{zz}} = 0.0324\beta B_\infty l^2 a(n^2 - 2n + 1) \tag{22}$$

$$B_\infty = \frac{1 + \xi}{1 - \xi} \tag{23}$$

in which β is a complicated function of n which approaches unity as n increases (see figure 4).

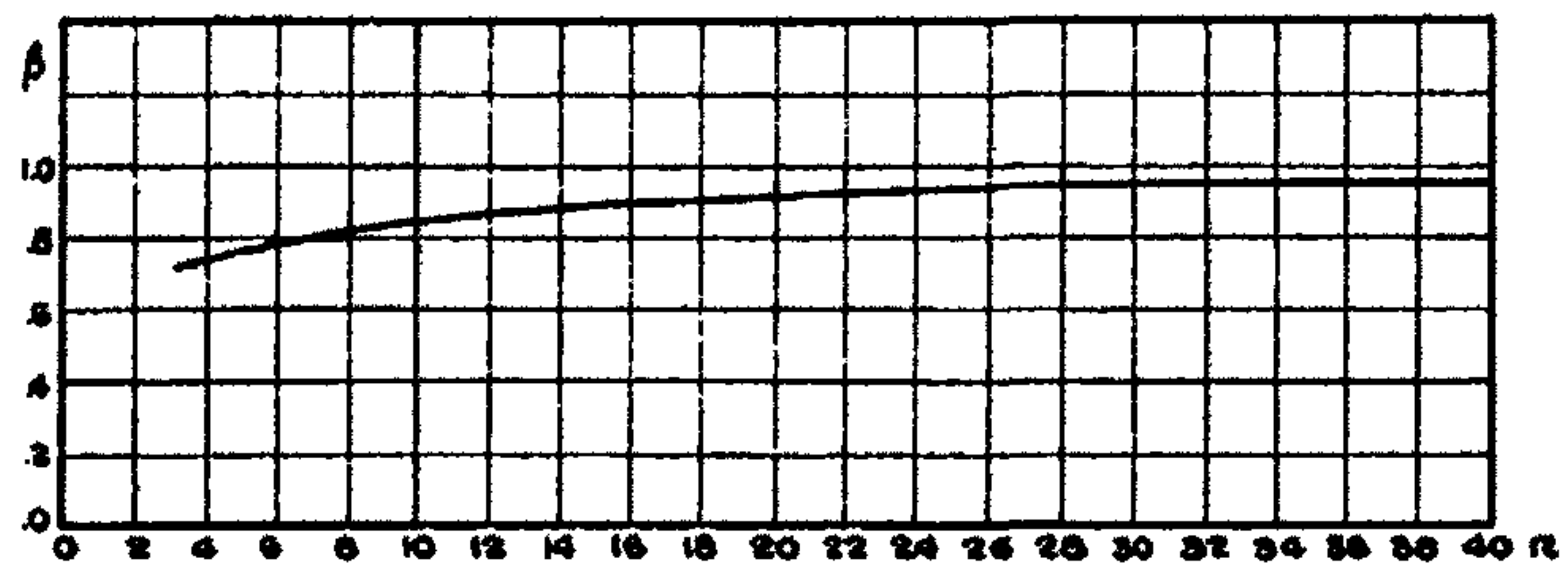

FIG. 4

By a complicated procedure, involving an analogy with a rod-like molecule bent in the middle, with all angles of bending equally probable, a factor of 4/5 has been calculated for the conversion of $\overline{F_{zz}}$ for randomly kinked *centrosymmetric* molecules to $\overline{F_{zz}}$ for otherwise similar molecules which do not necessarily have centers of symmetry. For this more general case, then,

$$\overline{F_{zz}} = 0.0259\beta B_\infty l^2 a(n^2 - 2n + 1) \tag{24}$$

$$\frac{\eta_{sp}}{c} = \frac{4.84 \times 10^{-4} N\beta B_\infty l^2 a(n - 2)}{1 - 4.84 \times 10^{-4} N\beta B_\infty l^2 a(n - 2)c} \tag{25}$$

For large values of n and small values of c equation 25 reduces to

$$\frac{\eta_{sp}}{c} = 4.84 \times 10^{-4} N B_\infty l^2 a n \tag{26}$$

We thus have a theoretical derivation of Staudinger's empirical viscosity law (26).

EXTENSION TO NON-RIGID CHAIN MOLECULES

An attempt has been made to determine the effect of introducing flexibility (resulting from free or restricted rotation about the bonds in the chain) into the molecular model. The problem is a complicated one, which will be dealt with in detail at another time. For the present a few comments will suffice.

In general, the viscosities should be nearly the same for flexible long-chain, kinked molecules as if they were rigid. The solvent exerts a stretching force for Θ_i between 0 and $\pi/2$ and between π and $3\pi/2$ and a compression force during the rest of the rotation. Tending to counteract this is the entropy change, which can be calculated approximately (2, 8, 9, 18, 19, 21). As a net result it can be shown that the η_{sp}/c values, as calculated for a rigid molecule, should be multiplied by a "flexibility factor," H, which varies with

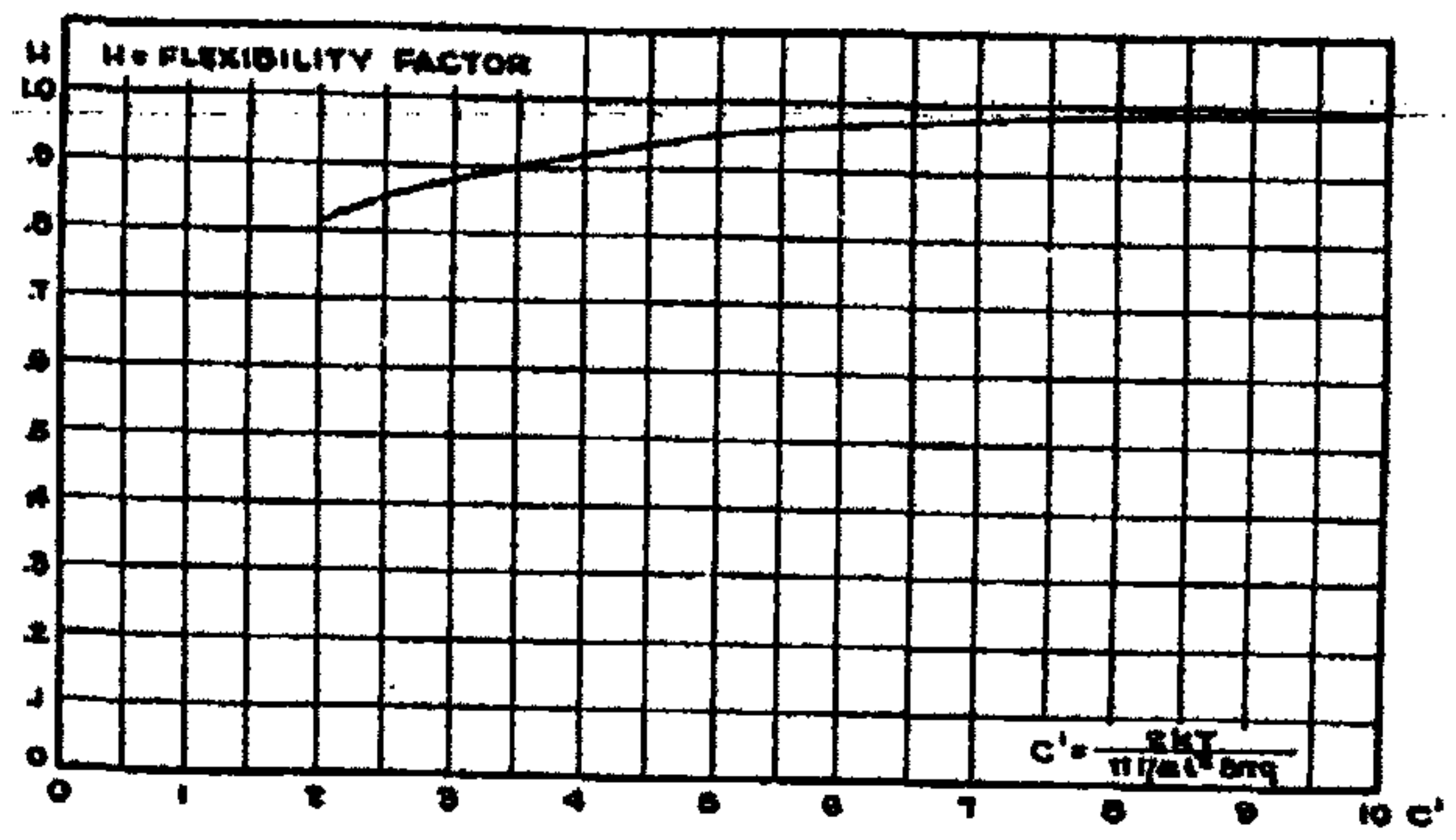

FIG. 5

$$C' = \frac{2kT}{\pi\eta a l^2 Bnq} \tag{27}$$

approximately as indicated in figure 5.

In addition, a small constant term should be added to η_{sp}/c to allow for rotation of units other than at the ends of the chain and a term of the form *const.*/n to cover rotation of the atoms and groups near the ends.

COMPARISON WITH EXPERIMENTAL DATA

The best experimental data now available for testing these theoretical results are for solutions of the paraffins (22, 28). We use equation 25 for rigid, randomly kinked molecules, rough calculations indicating that the corrections for flexibility would not make much difference in the result.

In agreement with x-ray and electron diffraction data we take

$$l = 1.54 \times 10^{-8} \text{ cm.} \tag{28}$$

and assume tetrahedral bond angles, hence

$$B_{\infty} = 2 \tag{29}$$

The effective radius, a, must be of the order of magnitude of 10^{-8} cm. Certain qualitative considerations suggest that it should approximately equal the radius of the sphere having the same surface area as the surface, per unit segment, of the molecule, considered as cylindrical. If this is assumed we calculate, from the density of liquid paraffins,

$$a = 1.28 \times 10^{-8} \text{ cm.} \tag{30}$$

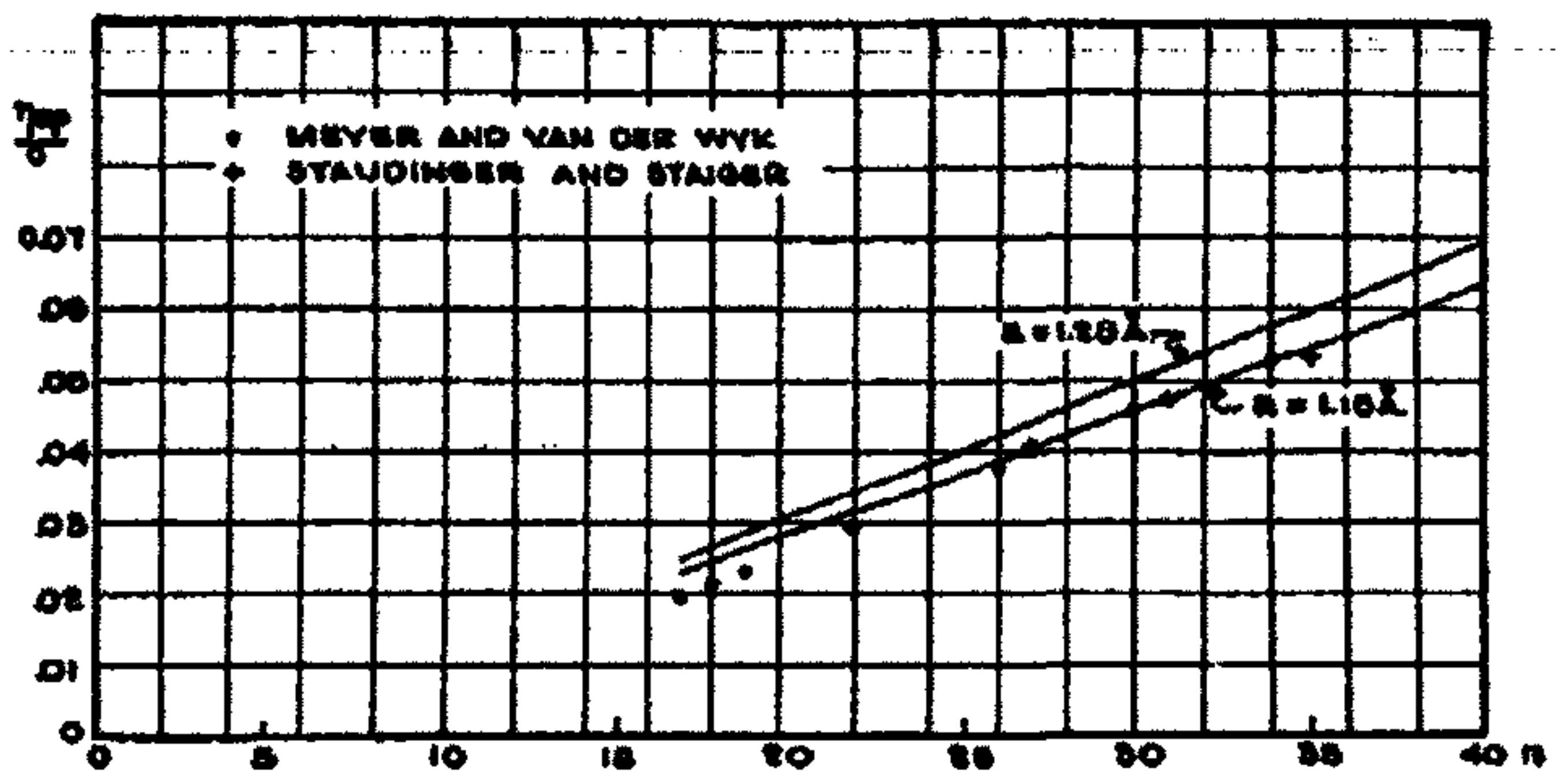

FIG. 6. Experimental and theoretical values (from equation 25) of η_{sp}/c for dilute solutions of paraffins in carbon tetrachloride at 20°C.

Substituting these values for l, B_{∞}, and a in equation 25 and reading β from figure 4, the values used in plotting the upper curve of figure 6 are obtained. If the slightly lower value, $a = 1.18 \times 10^{-8}$ cm., is used, the lower curve is obtained. The agreement is very satisfying, considering the method of estimating a and other approximations used in the derivation. The slope of the theoretical curve lies between that of the curve through Meyer and van der Wyk's values and that of the curve through Staudinger and Staiger's results.

Comparisons with experimental data for other series of compounds will be made at another time.

THE MCBAIN EXPERIMENTS

McBain and McBain (20) compared the velocities of fall through sucrose solutions of quartz fibers and quartz spheres of the same weight and volume, showing that the difference in frictional resistance to movement of these particles is by no means sufficient to account for the observed high viscosities of dilute solutions of long-chain compounds. They conclude, therefore, "that the chief factor is structural viscosity due to entanglement and local adherence of molecules and particles, effectively immobilizing a disproportionate amount of the solvent in comparison with the amount of the colloid itself."

It should be pointed out that the McBain experiments bear little or no relation to the problem, since in their experiments the velocity of one side of the particle relative to the surrounding liquid is the same as that of the other side. In any viscosity determination a velocity gradient is set up. As is shown in this paper (and has been shown previously by others), it follows from classical hydrodynamics that *because of this velocity gradient* frictional work is done on non-spherical particles by the liquid. This effect must exist, and the evidence presented here shows that its magnitude is such as to account practically quantitatively for the experimental data, at least for dilute solutions of paraffins.

SUMMARY

By an extension of Kuhn's hydrodynamical treatment a theoretical equation has been derived relating the specific viscosity of a solution to the coördinates and dimensions of the atoms in the solute molecules. Applied to rod-like molecules this equation leads to proportionality (with n large) between η_{sp}/c and n^2. Applied to randomly kinked chain molecules, it leads to proportionality between η_{sp}/c and n, the Staudinger relationship.

Theoretical expressions have been obtained for the proportionality constant and also for the deviations for small values of n. Using a reasonable value for the "effective radius" of the CH_2 group, without any arbitrary constants whatever, the experimental data for solutions of paraffins are quantitatively accounted for.

In conclusion, it is a pleasure to give acknowledgment to Miss Dorothy Owen, who performed a large part of the necessary calculations during the preparation of this paper.

REFERENCES

(1) Bartholomé, E., and Karweil, J.: Z. physik. Chem. **B39**, 1 (1938).
(2) Dostal, H.: Monatsh. **71**, 144 (1938).
(3) Einstein, A.: Ann. Physik [4] **17**, 549 (1905).
(4) Einstein, A.: Ann. Physik [4] **19**, 289 (1906).
(5) Eisenschitz, R.: Z. physik. Chem. **A158**, 78 (1931).
(6) Eisenschitz, R.: Z. physik. Chem. **A163**, 133 (1933).
(7) Eyring, H.: Phys. Rev. **39**, 746 (1932).
(8) Guth, E., and Mark, H.: Monatsh. **65**, 93 (1934).
(9) Guth, E., and Mark, H.: Z. Elektrochem. **43**, 683 (1937).
(10) Howard, J. B.: Phys. Rev. **51**, 53 (1937).
(11) Kemp, J. D., and Pitzer, K. S.: J. Chem. Phys. **4**, 749 (1936).

(12) Kemp, J. D., and Pitzer, K. S.: J. Am. Chem. Soc. **59**, 276 (1937).
(13) Kistiakowsky, G. B., and Nazmi, F.: J. Chem. Phys. **6**, 18 (1938).
(14) Kistiakowsky, G. B., and Wilson, E. B., Jr.: J. Am. Chem. Soc. **60**, 494 (1938).
(15) Kuhn, W.: Z. physik. Chem. **A161**, 1 (1932).
(16) Kuhn, W.: Z. physik. Chem. **A161**, 427 (1932).
(17) Kuhn, W.: Kolloid-Z. **62**, 269 (1933).
(18) Kuhn, W.: Kolloid-Z. **68**, 2 (1934).
(19) Kuhn, W.: Kolloid-Z. **76**, 258 (1936).
(20) McBain, J. W., and McBain, M. E. L.: J. Am. Chem. Soc. **59**, 342 (1937).
(21) Meyer, K. H., and Ferri, C.: Helv. Chim. Acta **18**, 570 (1935).
(22) Meyer, K. H., and van der Wyk, A.: Helv. Chim. Acta **18**, 1067 (1935).
(23) Pitzer, K. S.: J. Chem. Phys. **5**, 469 (1937).
(24) Pitzer, K. S.: J. Chem. Phys. **5**, 473 (1937).
(25) Schumann, S. C., and Aston, J. G.: J. Am. Chem. Soc. **60**, 985 (1938).
(26) Staudinger, H.: Die hochmolekularen organischen Verbindungen. Julius Springer, Berlin (1932).
(27) Staudinger, H.: Helv. Chim. Acta **19**, 204 (1936).
(28) Staudinger, H., and Staiger, F.: Ber. **68**, 707 (1935).

THE VISCOSITY OF CELLULOSE IN PHOSPHORIC ACID SOLUTIONS[1]

ALFRED J. STAMM AND WILBY E. COHEN[2]

Forest Products Laboratory,[3] Forest Service, U. S. Department of Agriculture, Madison, Wisconsin

93A-92

Received July 1, 1938

INTRODUCTION

Perhaps the best physical means of characterizing cellulose for industrial use is the determination of the viscosity of its solutions. Unfortunately, there are no true physical solvents for cellulose itself, although there are such solvents for cellulose derivatives. Cuprammonium solution perhaps comes the closest to being a true physical solvent, and it is for this reason that it is almost exclusively used in viscosity studies. Cuprammonium solution, however, is subject to several variations which may affect its solvent power and the nature of the cellulose dispersion: (*1*) the total copper ammonia complex concentration, (*2*) the relative proportions of copper and ammonia, (*3*) the portion of the copper (10) which exists as colloidal copper hydroxide, (*4*) the amount of sugar added to the solvent to stabilize the system, (*5*) the extent to which the ammonia is oxidized to nitrites in making the solvent, and (*6*) the extent to which the solvent is exposed to air in the preparation and study of the cellulose solutions. Because of these possible variations, it is not surprising that considerable difference of opinion has been expressed at recent chemical meetings as to the nature of the dispersion of cellulose in cuprammonium solvent. Farr (5) contends that the cellulose is not molecularly dispersed as many believe, but is broken down into elliptical particles similar to those which she obtained by treating cellulose with various acids (6, 7). In this case the particles, which do not deviate appreciably from spherical, would have but a slight effect upon the viscosity, as she contends. Farr believes that it is the solution of the pectic film of the cotton, rather than the cellulose itself, which is largely responsible for the viscosity (5).

---

[1] Presented at the Fifteenth Colloid Symposium, held at Cambridge, Massachusetts, June 9-11, 1938.

[2] Commonwealth Fellow, 1935-37, Division of Forest Products, Council for Scientific and Industrial Research, Melbourne, Australia.

[3] Maintained at Madison, Wisconsin, in coöperation with the University of Wisconsin.

Staudinger (12, 14), on the other hand, believes that cellulose in cuprammonium solvent is dispersed in the form of long macromolecular chains similar to many other polymeric materials, including cellulose derivatives in organic solvents. Staudinger's views are supported by a number of different investigators (8). It seemed highly probable to the authors that both Farr and Staudinger might be right, the difference resting on differences in the cuprammonium solvent used by each of the investigators. It thus seemed desirable to try to find a solvent for cellulose that was not subject to the foregoing variations. A preliminary survey indicated that concentrated phosphoric acid was the most promising solvent. It is true that this is a hydrolytic solvent, but hydrolysis takes place slowly enough to make possible viscosity measurements on the solutions after the cellulose has been in solution for different intervals of time. Extrapolation of the resulting relationship between viscosity and time to zero time gives the viscosity of the undegraded cellulose.

PREPARATION OF SOLUTIONS

A simple means of preparing cellulose solutions of known concentration in phosphoric acid was first sought. It was soon learned that undegraded cellulose cannot be completely dispersed in concentrated phosphoric acid without the use of some water. Apparently the cellulose must be swollen in water and the concentration of the acid built up gradually to get complete solution. This is in agreement with the findings of Ekenstam (3), who has recently claimed that cellulose forms an oxonium compound $(C_6H_{10}O_5 \cdot 2H_2O \cdot H_3PO_4)_n$, with two molecules of water and one of acid per glucose anhydride group, which is soluble in concentrated phosphoric acid.

The procedure finally adopted for preparing the solutions of known concentration was as follows: Accurately weigh 10 to 30 mg. of air-dry cellulose of known moisture content into a small agate mortar. Add 1 cc. of water and gently macerate with an agate pestle. Add phosphoric acid (85 to 100 per cent) drop by drop, working with the pestle between additions. When the swollen cellulose is almost completely dissolved, the acid may be added more rapidly. Wash the cellulose solution into a weighed beaker with concentrated phosphoric acid. Add phosphoric acid until the desired concentration of cellulose is obtained and weigh. Filter the solution through a No. 3 Jena fritted glass filter to remove any trace of foreign matter that might clog the viscometer. Remove air from the solution with a vacuum pump at room temperature. The preparation of the solution from the time the cellulose begins to dissolve to the time of complete removal of air generally takes from 20 to 30 min.

Solutions prepared in this way, even when the filtering step was omitted, were found to be practically void of microscopically visible particles, indicating that the cellulose is not dispersed as Farr elliptical particles (5, 6, 7).

VISCOSITY MEASUREMENTS

The viscosity measurements were made in a Bingham viscometer with a capillary bore of 0.0337 cm., a capillary length of 10.1 cm., and a bulb capacity between reading marks of 3.995 cc. The viscometer was securely clamped in place in a thermostatically controlled water bath held at 25°C. ± 0.002°. The applied air pressure was controlled with a reducing valve followed by one to four air-escape bubblers containing sulfuric acid, which were connected in series with each other and in parallel with the line to the viscometer. The air-pressure valve was set so that a constant but not too rapid rate of bubbling occurred through the bubblers. In this way the air pressure was controlled during a single measurement to 0.01 cm. of mercury, as was indicated by a mercury manometer that was read with a cathetometer. The readings could be reproduced in subsequent measurements to 0.03 cm. of mercury.

It would be practically impossible to prepare a phosphoric acid solution of exactly the same concentration as that serving as solvent for the cellulose. Fortunately, the viscosity of the solvent, which is required to calculate the specific viscosity of the cellulose, can be obtained by a simpler means (2). After completing the viscosity measurement on the solution, the solution can be heated in the viscometer to complete the hydrolysis of the cellulose to glucose and other final hydrolysis products. This avoids an extra cleaning and filling of the viscometer. Concentrations of hydrolysis products of 0.1 per cent and less will affect the viscosity of the phosphoric acid less than 0.25 per cent. If more accurate results are desired, the viscosity can be corrected for the presence of the hydrolysis products with an error of less than 10 per cent, using the Einstein viscosity equation (2).

Preliminary tests indicated that when the solutions of cellulose in phosphoric acid were heated in boiling water for half an hour or more to complete the hydrolysis, the solution developed a slight straw color and the viscosity of the solution after cooling to 25°C. increased for several days. Tests were made on solutions of 1 per cent glucose in phosphoric acid prepared in the same way as the cellulose solutions. The viscosity increased as much as 5 per cent in two days after heating to 100°C. for an hour. The change that occurs is so slow that the first viscosity value obtainable after cooling is but very slightly greater than the original viscosity before heating. Apparently the heating causes a caramelization which consists of a slow polymerization to chain molecules. This polymerization requires heat to initiate the reaction but is capable of continuing after cooling. When the solutions of glucose in phosphoric acid were not heated above 60°C. no discoloration resulted, nor was an increase in viscosity obtained. The solutions of cellulose in phosphoric acid were thus heated to 50° to 60°C. for several hours to insure complete hydrolysis and yet to avoid subsequent polymerization. Figure 1 shows the viscosity in terms of the applied pressure multiplied by the efflux time for phosphoric acid of different concentrations and hydrolyzed solutions of cellulose in phosphoric acid plotted against the acid concentration for two different applied pressures on the viscometer. The curves indicate that within experimental error the hydrolyzed solutions have the same viscosity as the solvent.

The measurements were made on a cotton linters alpha cellulose (99.6 per cent alpha) and a normal spruce sulfite pulp and the same after beating for 20 hr. in a rod mill. The concentrations used ranged from 0.000077 to 0.00099 g. per cubic centimeter (0.00048 to 0.0061 units of glucose anhydride per liter). The viscosity measurements were made at 30.9, 20.5, 10.3, and 3.4 cm. of mercury pressure on each of the solutions in the order given, a measurement from left to right and from right to left being made at each pressure. The average of these two times of efflux was used in the viscosity calculations. The mean time between starting the first measurement and ending the second was taken for calculating the time that the cellulose had been in solution. The agreement between the readings taken in the two directions was quite good when an interval of 2 min. was allowed between measurements for drainage of the viscous phosphoric acid,

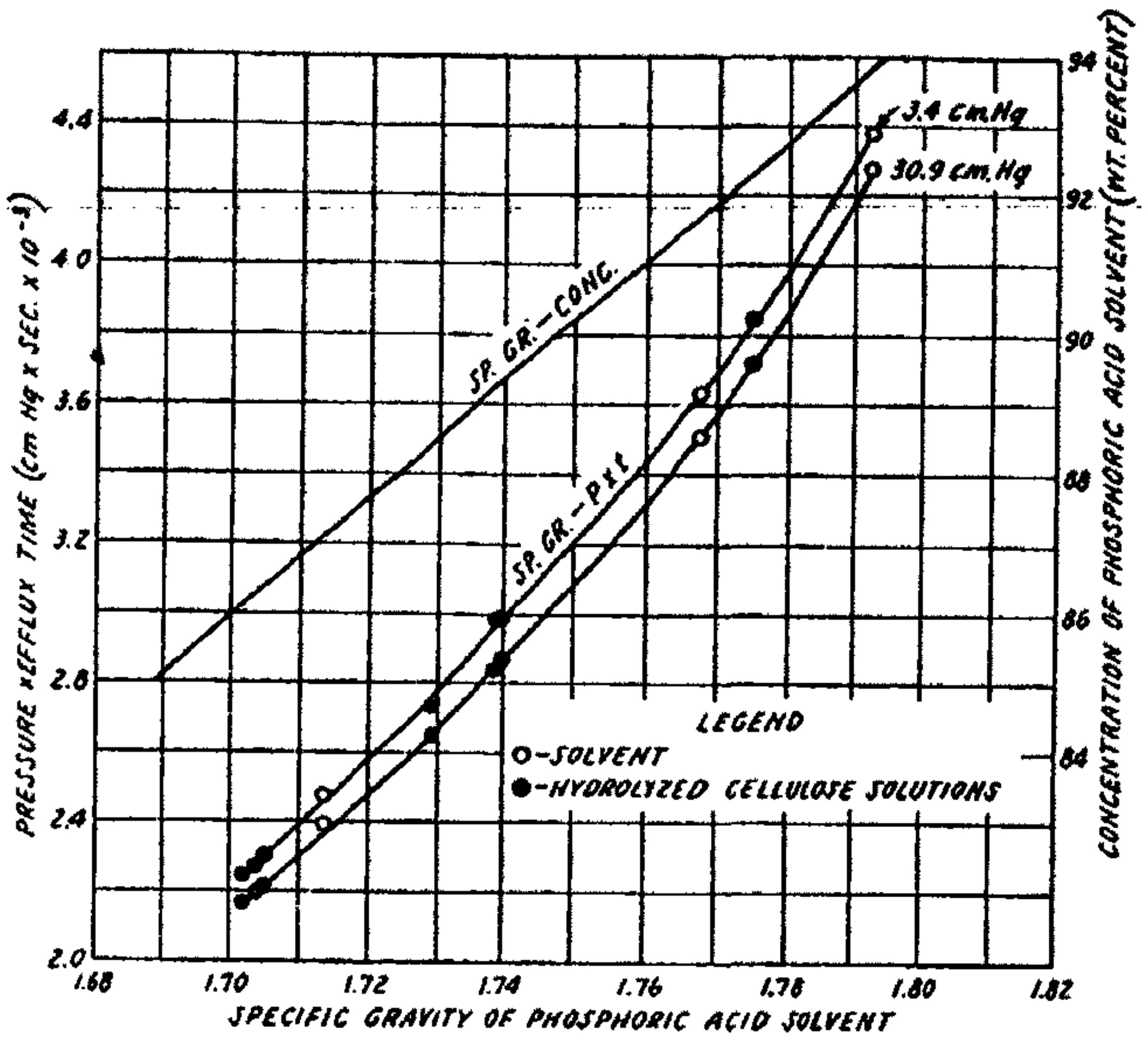

FIG. 1. Product of pressure and efflux time for phosphoric acid solutions of different specific gravity and concentration and the same containing hydrolyzed cellulose for two different applied pressures on the viscometer.

except for the initial readings where the viscosity was changing very rapidly with time. Although this short pause between measurements eliminates any difference in drainage between back and forth measurements at a single pressure, there is an unavoidable drainage difference between measurements made under different pressures.

Figure 2 gives the relationship between the product of the applied pressure and efflux time under different applied pressures plotted against the logarithm of the efflux time in seconds for completely hydrolyzed cellulose in 86.15 and 86.40 per cent phosphoric acid. When the efflux time is doubled the pressure-efflux time product is increased about 1.2 per cent.

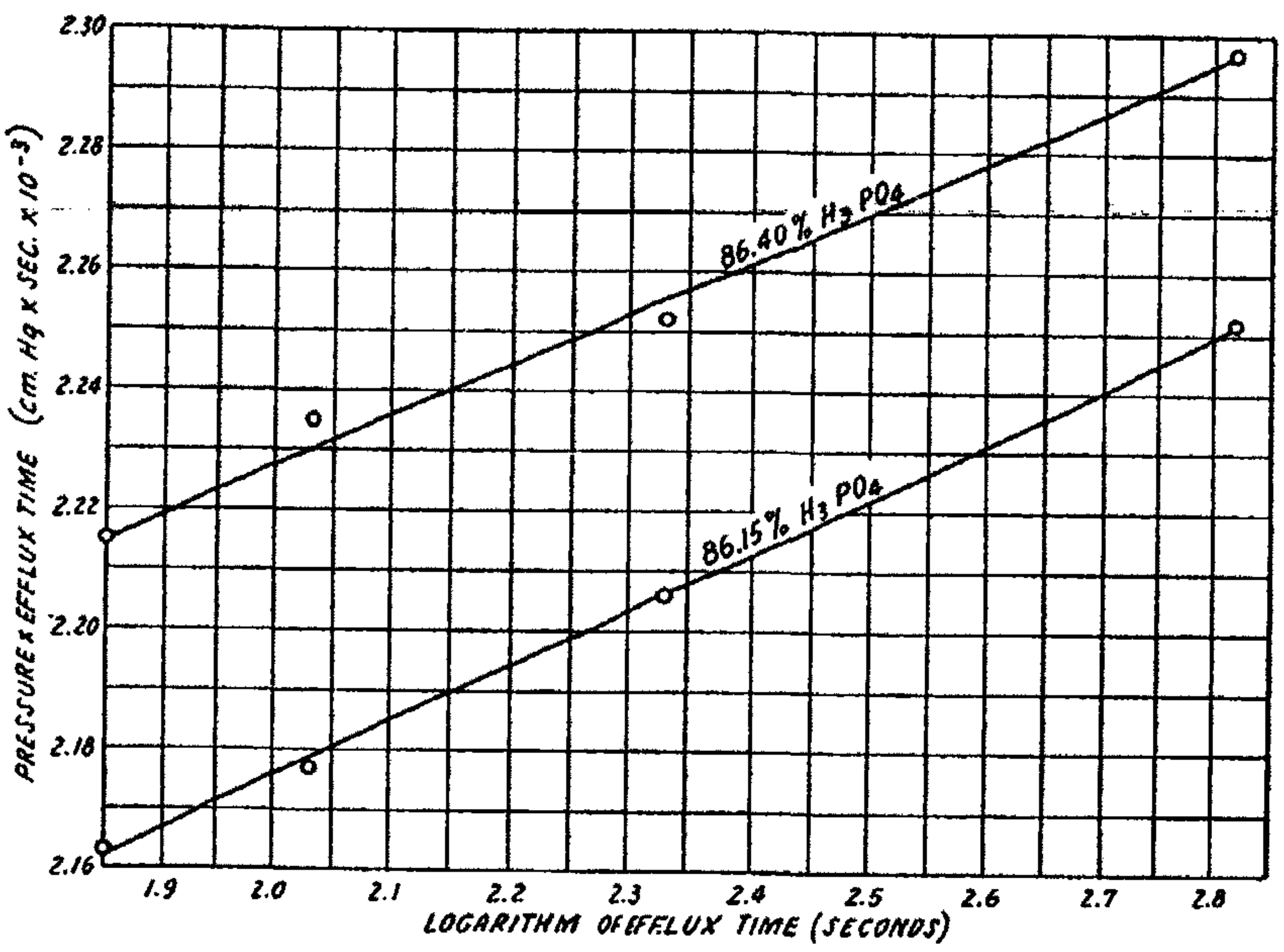

FIG. 2. Product of pressure and efflux time versus the logarithm of the efflux time for hydrolyzed cellulose solutions in two different concentrations of phosphoric acid.

The maximum time of efflux variation between the first measurement and the final hydrolyzed value for the most concentrated solution of cellulose used was 75 per cent. This would result in a viscosity error of 0.9 per cent, due to the drainage factor. In the case of solutions containing less than 0.0003 g. of cellulose per gram of acid, the error was less than 0.25 per cent. As the viscosity values of chief interest are those for the more dilute cellulose solutions, no attempt was made to make a drainage correction.

The specific viscosity η_{sp}(the increase in relative viscosity caused by the solute) per unit concentration in grams per cubic centimeter is plotted against the time the cellulose has been in solution in figures 3 and 4 for

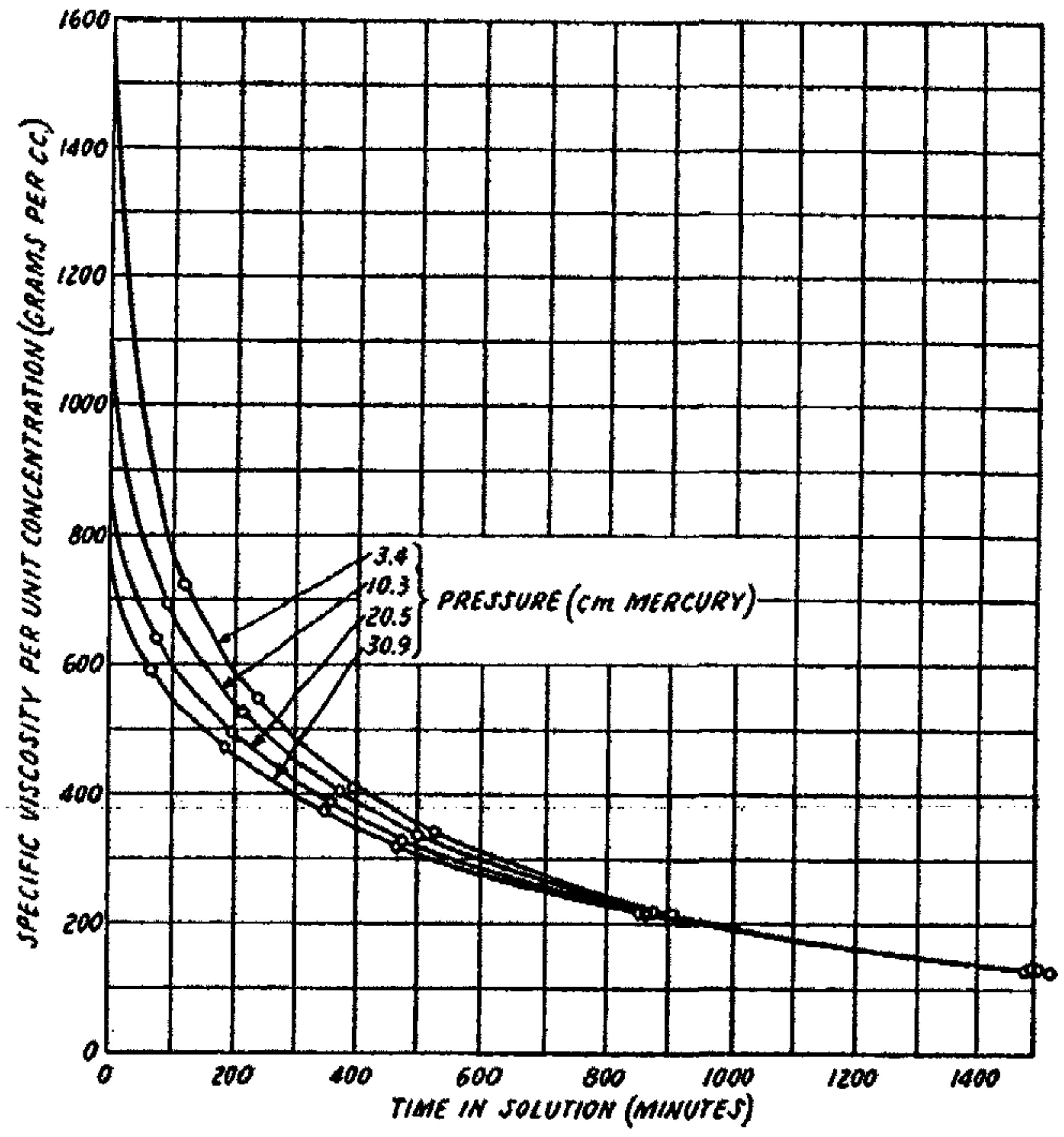

FIG. 3. Specific viscosity per unit concentration for a 0.000557 g. per cubic centimeter solution of unbeaten pulp in an 88.4 per cent phosphoric acid solution versus time in solution for different applied pressures on the viscometer.

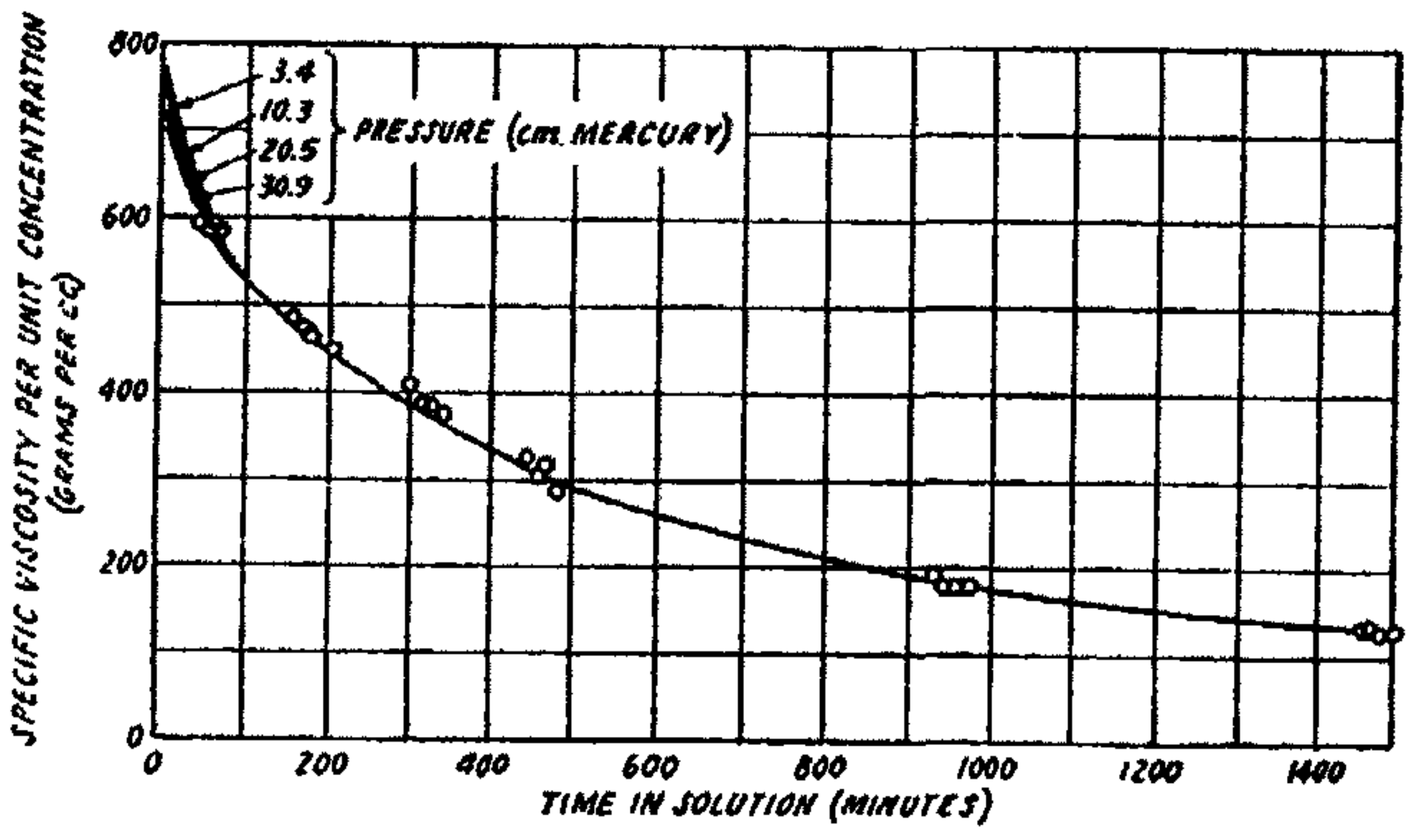

FIG. 4. Specific viscosity per unit concentration for a 0.0000979 g. per cubic centimeter solution of unbeaten pulp in an 89.4 per cent solution of phosphoric acid versus time in solution for different applied pressures on the viscometer.

unbeaten pulp solutions containing 0.000557 and 0.0000979 g. of pulp per cubic centimeter, respectively. The specific viscosity per unit concentration, η_{sp}/c, increases with a decrease in the applied pressure used in making the viscosity measurements for the higher η_{sp}/c values. The divergence of the η_{sp}/c values obtained at different applied pressures increases with an increase in the concentration of cellulose in solution. The apparent reason for this is that in concentrations sufficiently great for interference between the elongated cellulose molecules the interference is decreased with increasing velocity of shear, owing to the increased orientation of the molecular chains. This will be considered further in the next section.

MOLECULAR WEIGHT AND LIMITING CONCENTRATION OF CELLULOSE

The apparent molecular weights of the pulp in different concentrations, determined under different applied pressures and for different lengths of time that the cellulose has been in solution, were calculated from the data of figures 3 and 4 and the corresponding data for other concentrations of the unbeaten pulp, the beaten pulp, and the cotton linters alpha cellulose, using the relationship of Staudinger (12):

$$M = \frac{\eta_{sp}}{c}\frac{0.162}{K_m} \tag{1}$$

in which M is the molecular weight of the cellulose, η_{sp} is its specific viscosity, 0.162 is a factor to transpose the concentration c in grams per cubic centimeter to glucose anhydride units per liter, and K_m is the Staudinger proportionality constant. The constant K_m used in the following calculations is 11.8×10^{-4} at 25°C. This was obtained by a linear extrapolation of Ekenstam's (3) values, $K_m = 12.4 \times 10^{-4}$ at 20°C. and $K_m = 14.7 \times 10^{-4}$ at 0°C. Staudinger (13) gives a value for K_m of 18.0×10^{-4} at 20°C., which is larger. Further work on the molecular weight of cellulose in phosphoric acid solutions by other methods will have to be done before a more exact value for K_m can be obtained. Until then the actual molecular weight values can be considered only as approximate. The relative molecular weight values should be considerably more accurate, however, over the molecular weight range considered.

The apparent molecular weights of the undegraded celluloses (zero time in solution) for the different concentrations and different applied pressures are shown in figure 5 for the pulp and in figure 6 for the alpha cellulose. The apparent molecular weight varies but slightly with concentration over the range studied for the higher applied pressures on the viscometer, but increases appreciably with concentration for the lower pressures. The molecular weights of the beaten and the unbeaten pulp are identical within experimental error. Over the range studied (86 to 92 per cent) the concentration of phosphoric acid has no effect. The practical limiting concentration above which molecular interference appreciably affects the viscosity and the calculated molecular weight is thus dependent not only upon the molecular weight and the concentration of the cellulose solution,

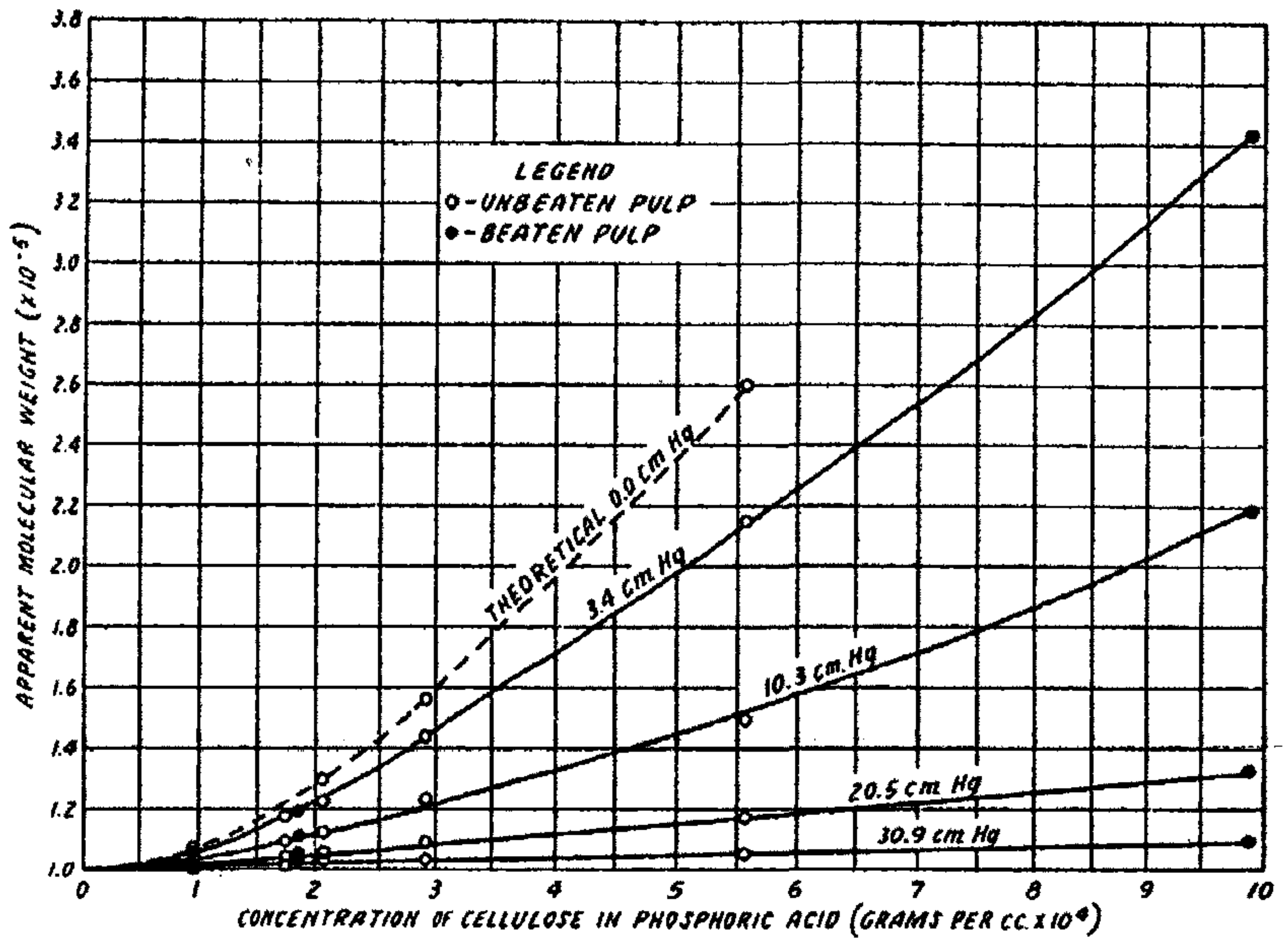

FIG. 5. Apparent molecular weight of beaten and unbeaten pulp versus the concentration of the pulp in phosphoric acid solution for different applied pressures on the viscometer.

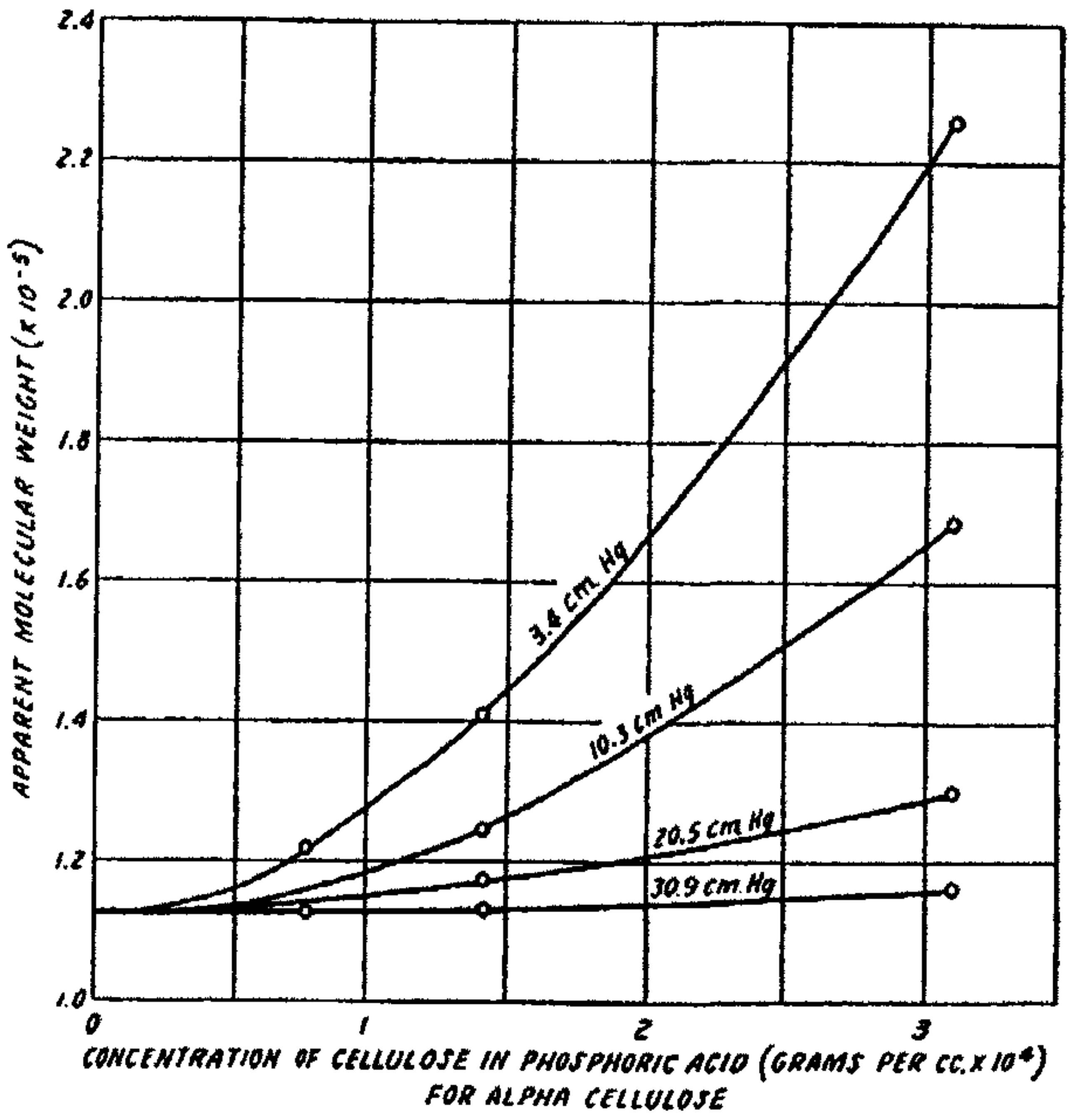

FIG. 6. Apparent molecular weight of cotton linters alpha cellulose versus the concentration of the cellulose in phosphoric acid solution for different applied pressures on the viscometer.

but also on the velocity of shear under which the measurements are made. The theoretical curve in figure 5 for the apparent molecular weights at the limiting value of zero applied pressure was obtained by plotting the apparent molecular weight against the applied pressure on the viscometer for different concentrations and extrapolating to zero pressure. The curves for the different applied pressures in figures 5 and 6 converge at a moisture content below 3 $\times$ 10^{-5} g. of cellulose per cubic centimeter. This limiting concentration can be more accurately estimated from figure 7, in which the limiting molecular weight values for the partially hydrolyzed pulps (corresponding to the points on curves of the type of figures 3 and 4 above which

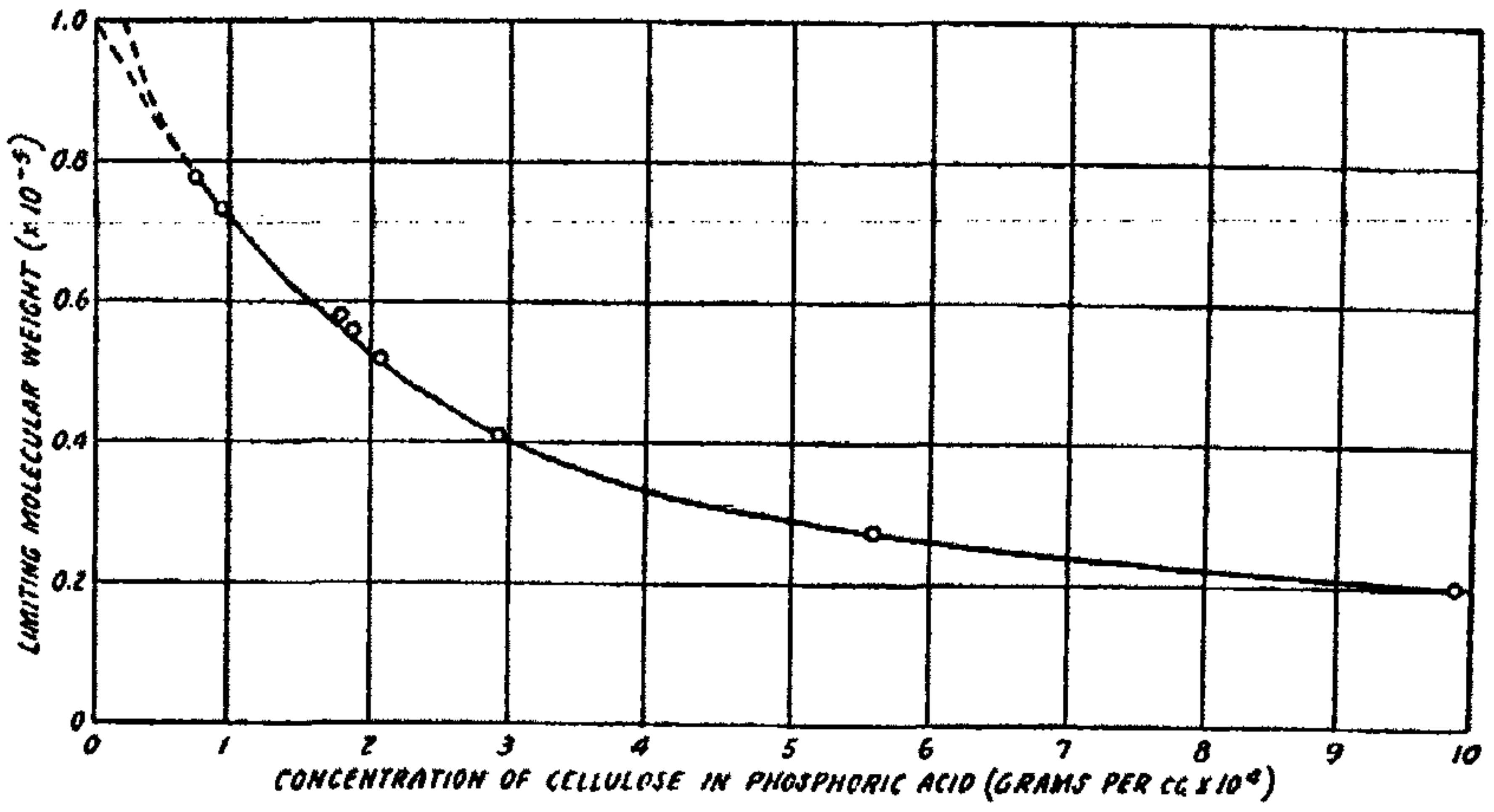

FIG. 7. Limiting molecular weights of partly hydrolyzed pulp above which the values are affected by the applied pressure on the viscometer versus the concentration of the pulp in phosphoric acid solution.

the η_{sp}/c values for different applied pressures diverge) are plotted against the pulp concentration. From this figure the limiting concentration appears to be less than 2 $\times$ 10^{-5} g. of cellulose per cubic centimeter for a molecular weight of 100,000.

This limiting concentration is practically equal to the theoretical value for packed spheres, calculated upon the assumption that the limiting volume of uninterfered motion of the elongated molecules is a sphere with the long axis of the molecule equal to the diameter. The pulp with a molecular weight M = 100,000 on a phosphoric acid-free and water-free basis, and M_1 = 183,000 on a hydrated and phosphated basis (4), has a degree of polymerization of 618, and a length, l, of 3180 Å. (5.15 Å. per glucose anhydride unit). The limiting concentration C on this basis is given by the equation

$$C = \frac{6M_1}{\pi l^3 A} \qquad (2)$$

in which A is the number of molecules in a gram molecule. This gives a value of 1.8×10^{-6} g. per cubic centimeter for the limiting concentration. A limiting concentration of the same order of magnitude is obtained on the basis of the limiting volume of uninterfered motion of elliptical molecules increasing, according to Onsager (9), as the square of the ratio of the major to the minor axis. This gives a limiting volume 1.5 times that obtained on the limiting sphere of action basis (11) and a limiting concentration 33 per cent less or 1.2×10^{-6} g. per cubic centimeter. Both of these values are within the range of accuracy of the experimental value.

The velocity of efflux under the different applied pressures was calculated from the viscometer dimensions and the theoretical time of efflux for the cellulose in solution for an infinitesimal length of time. These data indicate that over the concentration and applied pressure range used molecular weight values can be calculated with an accuracy of 5 to 10 per cent whenever the efflux velocity exceeds 10 to 12 cm. per second. Molecular weight values can thus be determined with a fair degree of accuracy at concentrations appreciably greater than the limiting concentration for velocities of shear approaching zero by increasing the velocity of shear sufficiently to reduce molecular interference as a result of molecular orientation. Because of this Staudinger (12) has been able to determine molecular weights of cellulose in concentrations of several tenths of a per cent.

HYDROLYSIS CONSTANT OF CELLULOSE

The viscosity measurements of cellulose dissolved in phosphoric acid furnish the data for calculating not only the molecular weight of cellulose but also the hydrolysis constant of cellulose. Ekenstam (4) has derived the following equation for calculating the hydrolysis constant:

$$K = \frac{1}{t} \ln \frac{1 - \frac{m}{M}}{1 - \frac{m}{M_t}} \qquad (3)$$

where t is the time, M the initial molecular weight, M_t the average molecular weight after time t, and m is the final molecular weight. When M and M_t are large compared to m this equation can be simplified to

$$K = \frac{m}{t}\left(\frac{M - M_t}{MM_t}\right) \qquad (4)$$

The molecular weight of the final hydrolysis product m dissolved in phosphoric acid is 240, according to Ekenstam (4). Table 1 gives the hydrolysis constant when t is expressed in minutes for the unbeaten pulp, beaten pulp, and cotton linters alpha cellulose calculated from equation 4, using

TABLE 1

Hydrolysis constants of cellulose dissolved in concentrated phosphoric acid at 25°C.

MATERIAL	CONCENTRATION		TIME IN SOLUTION	MOLECULAR WEIGHT	HYDROLYSIS CONSTANTS	
	Cellulose	H_3PO_4			Individual values $\times 10^6$	Average values 4 to 24 hr. $\times 10^6$
	grams per cc.	*per cent*	*hours*			
Unbeaten pulp	0.000557	89.3	0	105,500		
			2	72,000	8.83	
			3	65,100	7.84	
			4	59,600	7.30	
			6	50,600	6.85	
			8	43,200	6.83	
			10	37,400	6.90	
			12	33,200	6.89	
			16	26,900	6.93	
			20	22,600	6.96	
			24	19,200	7.10	6.97
	0.0000979	89.4	0	100,000		
			2	70,000	8.58	
			3	63,000	7.83	
			4	57,600	7.36	
			6	48,700	7.03	
			8	41,150	7.15	
			10	35,650	7.22	
			12	31,550	7.23	
			16	25,100	7.46	
			20	21,400	7.35	
			24	18,500	7.35	7.27
	0.000293	88.4	0	102,700		
			24	19,200		6.89
	0.000206	86.1	0	102,700		
			24	18,800		7.23
	0.000178	92.3	0	101,300		
			24	17,400		7.18
Beaten pulp	0.000989	86.4	0	109,600		
			24	21,550		6.77
	0.000188	86.1	0	102,700		
			24	18,900		7.07
Cotton linters alpha cellulose	0.000311	86.3	0	116,500		
			24	23,850		5.67
	0.000142	86.4	0	113,700		
			24	23,850		5.79
	0.0000766	86.3	0	113,000		
			24	23,300		5.58

Ekenstam's value for *m*. The individual hydrolysis constant values calculated for various intervals of time, from 0 to 24 hr., that the cellulose is in solution, are given for the two concentrations of unbeaten pulp shown in figures 3 and 4, together with the average value for 4 hr. through 24 hr. In the case of the other concentrations of unbeaten pulp, beaten pulp, and cotton linters alpha cellulose only the average values are given. The individual values for these solutions are similar to the individual values given in that they are constant within experimental error after the first 4 to 6 hr. Ekenstam (2, 4) obtained similar high initial values for some of his cellulose samples. The beaten and unbeaten pulps have the same hydrolysis constant within experimental error. The hydrolysis constants of the pulps are larger than for the cotton linters alpha cellulose, as would be expected, because they undoubtedly contain more readily hydrolyzable carbohydrates.

SUMMARY

Cellulose can be completely dissolved in concentrated phosphoric acid to form dilute solutions void of microscopically visible particles when the cellulose is first swollen in water and the acid concentration built up gradually. Viscosity measurements on these solutions after different times in solution and under different applied pressures were made. The viscosity of the solvent was shown to be equal to the viscosity of the dilute cellulose solutions after completely hydrolyzing for 1 hr. at 50° to 60°C. Hydrolysis at 100°C. initiates a slow polymerization of glucose dissolved in phosphoric acid which continues for days. The limiting concentration of cellulose above which molecular interference occurs when the viscosity measurements are made under a low rate of shear is about 2×10^{-5} g. per cubic centimeter. This is practically equal to the concentration in which spheres described about the long axis of the molecules are packed. When the viscosity is determined under higher rates of shear, higher concentrations can be used in molecular weight determinations because of the molecular orientation. The molecular weights of a highly beaten pulp and of the unbeaten pulp calculated from these data are both 100,000 on a water- and acid-free basis. The corresponding value for a cotton linters alpha cellulose is 113,000. Hydrolysis constants for cellulose in phosphoric acid calculated from these data are quite constant after the first 4 hr. in solution. The average hydrolysis constants for the pulp and for the cotton linters alpha cellulose are 7.05×10^{-6} and 5.68×10^{-6}, respectively, after the first 4 hr.

REFERENCES

(1) Einstein, A.: Kolloid-Z. **27**, 137 (1920).
(2) Ekenstam, A.: Svensk Kem. Tid. **46**, 157-67 (1934).
(3) Ekenstam, A.: Ber. **69B**, 549-52 (1936).

(4) EKENSTAM, A.: Ber. **69B**, 553-6 (1936).
(5) FARR, W. K.: Textile Research 7(2), 65-9 (1936).
(6) FARR, W. K.: J. Phys. Chem. **41**, 987-91 (1937).
(7) FARR, W. K., AND ECKERSON, S. H.: Contrib. Boyce Thompson Inst. **6**, 189-203 309-313 (1934).
(8) KRAEMER, E. O., AND LANSING, W. D.: J. Phys. Chem. **39**, 153-68 (1935).
(9) ONSAGER, L.: Phys. Rev. **40**, 1028 (1932).
(10) STAMM, A. J.: J. Phys. Chem. **35**, 659-60 (1931).
(11) STAMM, A. J.: U. S. Dept. Agr. Misc. Pub. No. 240 (1936).
(12) STAUDINGER, H.: Der Aufbau der hochmolekularen organischen Verbindungen Kautschuk und Cellulose im Sinne der Kekuleschen Strukturlehre. J. Springer, Berlin (1932).
(13) STAUDINGER, H., AND DAUMILLER, G.: Ber. **70B**, 2508-13 (1937).
(14) STAUDINGER, H., AND RITZENTHALER, B.: Ber. **68B**, 1225-33 (1935).

OPTICAL PROPERTIES OF SOLUTIONS OF TOBACCO MOSAIC VIRUS PROTEIN[1]

MAX A. LAUFFER

The Rockefeller Institute for Medical Research, Princeton, New Jersey

Received July 1, 1938

INTRODUCTION

Tobacco mosaic virus nucleoprotein was first obtained in crystalline form by chemical means by Stanley in 1935 (13), from the juice of Turkish tobacco plants infected with tobacco mosaic virus. All of the evidence available at present indicates that the active disease-causing agent is this nucleoprotein (14). The results of recent studies indicate that the virus nucleic acid closely resembles yeast nucleic acid, that it is in combination with protein, and that it is necessary for virus activity (1, 9). Because the virus protein has an extremely high molecular weight, a value in the millions (3, 7, 20), it is possible to obtain very superior preparations by differential centrifugation (20). The protein is insoluble at its isoelectric point and in 20 per cent ammonium sulfate solution. It crystallizes in small needle-shaped crystals, visible only with the microscope. Bernal and Fankuchen have studied the x-ray diffraction patterns of the virus protein in many states, and they concluded from their findings that these crystals are in the mesomorphic or paracrystalline state, rather than in the true crystalline state (2). These crystals are, nevertheless, definite solid objects, visible with the microscope, and, inasmuch as crystallinity of any kind is not an infallible criterion of protein purity, the crystallinity of the tobacco mosaic virus protein is probably not much less significant as a criterion of purity than that of other proteins.

DOUBLE REFRACTION OF FLOW

Takahashi and Rawlins (16) first showed that the juice from tobacco plants diseased with tobacco mosaic exhibited stream double refraction, and it has since been demonstrated that the solutions of the purified tobacco mosaic virus protein show the phenomenon to a marked degree (1, 8, 17). The question of the interpretation of this double refraction was recently considered in some detail, and it was concluded that the

---

[1] Presented at the Fifteenth Colloid Symposium, held at Cambridge, Massachusetts, June 9-11, 1938.

phenomenon was due in this case to the orientation of rod-like protein particles in the flowing stream (8). These rod-shaped particles may themselves be either optically isotropic or anisotropic. Wiener (19) has shown from theoretical considerations that a system composed of very small isotropic rods arranged parallel to each other in an isotropic medium of different refractive index is optically anisotropic. It behaves like a uniaxial crystal with the optic axis in the direction of orientation. The following equation, which represents the double refraction of such a system, may be derived from Wiener's considerations (8):

$$N_e^2 - N_0^2 = \frac{V_1 V_2 (N_1^2 - N_2^2)^2}{(V_1 + 1)N_2^2 + V_2 N_1^2} \qquad (1)$$

N_e and N_0 are the indices of refraction of extraordinary and ordinary rays, respectively, N_1 and N_2 the refractive indices of rods and medium respectively, and V_1 and V_2 their respective relative volumes. It is readily apparent from this equation that, if $N_1 = N_2$, one obtains no double refraction. If $(N_e - N_0)$ is plotted against N_2, a parabola is obtained with a minimum at the point $N_2 = N_1$. If rod-shaped particles are oriented in a medium with a refractive index equal to their own, the system should show no double refraction of this sort,—i.e., no morphic double refraction. Any double refraction shown by the system under such conditions must be the intrinsic double refraction of the particles themselves. This point was considered by Freundlich (4). Steubel (15) evaluated the intrinsic and morphic double refraction shown by cross-striated muscle by measuring the double refraction of the muscles immersed in various solvents of different refractive index. This method has been applied to stream double refraction by Signer (12) in his studies on polystyrene solutions.

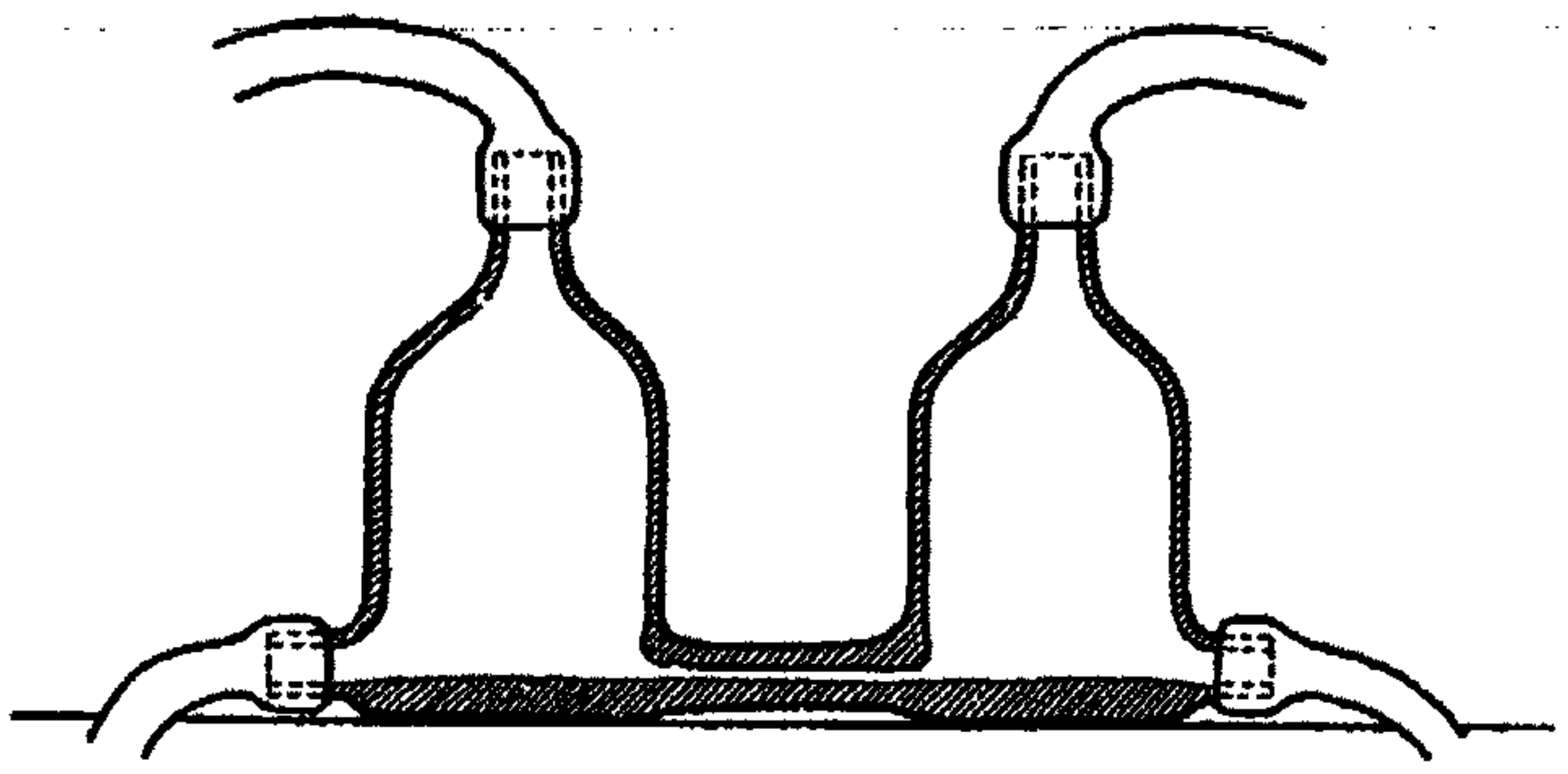

FIG. 1. Picture diagram of streaming cell

By measuring stream double refraction of tobacco mosaic virus protein in solvents of different refractive indices, such as various glycerol-water mixtures and aniline-glycerol-water mixtures, the effect of the refractive index of the medium on the double refraction of flow was determined. The apparatus used for this measurement consisted of a streaming cell and a polarizing microscope fitted with a photoelectric tube and a vacuum tube amplifying system, as described previously (8). The change in plate current caused by the flow of the liquid, as measured by galvanometer displacements in millimeters, was taken as a measure of stream double refraction. The streaming cell used in this case differed from that described in the original study. As may be seen in figure 1, it consisted of a glass capillary fused to two reservoirs, so arranged that all of the liquids studied could be made to flow at the same constant pressure. By this means the reduced rate of flow compensates for the increased viscosity of the less fluid solvents, and the mechanical force exerted on the suspended rods remains constant. It may be seen from table 1 and figure 2 that the double refraction of flow decreases greatly as the refractive index of the medium approaches 1.6, the approximate value of the refractive index of the tobacco mosaic virus protein. This value was calculated from the refractive index of a 1.78 per cent solution of the protein, $N_D^{25^\circ} = 1.33715$, and that of the solvent, $N_D^{25^\circ} = 1.33405$, using the equation presented by Wiener (19),

TABLE 1

Double refraction of flow of tobacco mosaic virus protein (1.08 mg. per cubic centimeter) in solvents of different compositions

	COMPOSITION OF SOLVENT IN VOLUME PER CENT			REFRACTIVE INDEX	STREAM DOUBLE REFRACTION EXPRESSED AS MILLIMETERS OF GALVANOMETER DEFLECTION
	Water	Glycerol	Aniline		
1	100	0	0	1.334	54
2	80	20	0	1.362	42
3	60	40	0	1.389	33
4	50	50	0	1.402	27
5	30	70	0	1.430	23
6	20	80	0	1.442	19
7	10	90	0	1.454	14
8	2	88	10	1.477	6.0
9	2	68	30	1.503	4.5
10	2	48	50	1.526	2.4
11	2	28	70	1.55	0

$$N_m^{2*} = \frac{(1 + V_1)N_1^2 + (1 - V_1)N_2^2}{(1 - V_1)N_1^2 + (1 + V_1)N_2^2} \times N_2^2 \qquad (2)$$

where N_m is the refractive index of the solution and the other symbols have the same meaning as in equation 1.

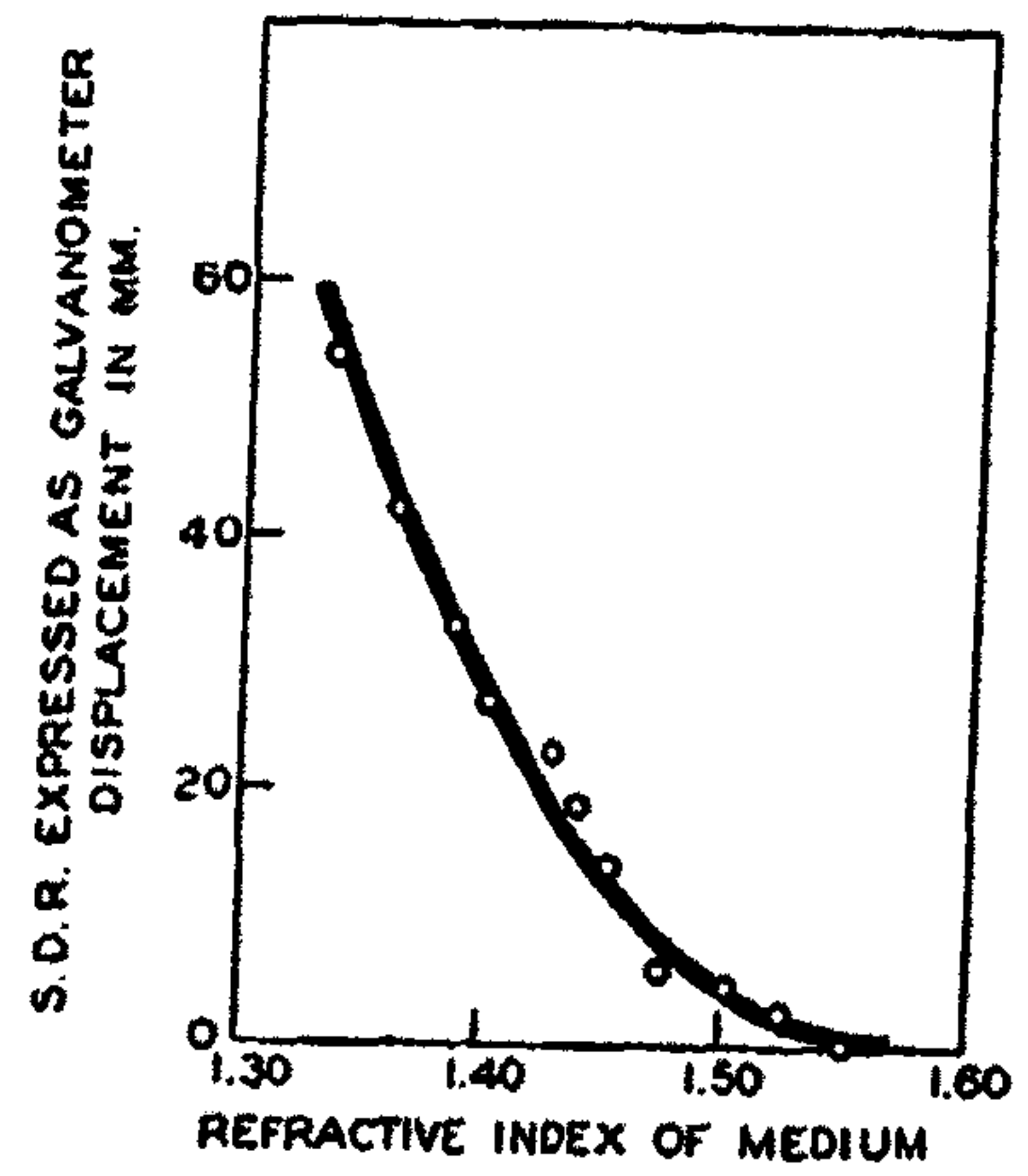

FIG. 2. The dependence of the stream double refraction of tobacco mosaic virus protein upon the refractive index of the solvent.

TABLE 2

The effect of various solvents on the activity of tobacco mosaic virus protein as measured by the half-leaf method on Phaseolus vulgaris

	1	2	3
Composition of solvent in volume per cent:			
Water	10	2	2
Glycerol	90	88	48
Aniline	0	10	50
Concentration of virus in contact with solvent	10 mg. per cc.	10 mg. per cc.	10 mg. per cc.
Time of contact with solvent	7 days	10 min.	10 min.
Concentration of virus in $M/10$ phosphate at time of inoculating	10^{-6} g. per cc.	10^{-7} g. per cc.	10^{-7} g. per cc.
Number of half-leaves inoculated	38	26	26
Average number of lesions per half-leaf ($\bar{X}$)	111.5	8.1	5.6
Average number of lesions per half-leaf for control at same concentration ($\bar{Y}$)	131.8	6.8	6.5
Standard error of $\bar{X} - \bar{Y} (SE_{\bar{x}-\bar{y}})$	9.52	0.89	0.90
$(\bar{X} - \bar{Y})/SE_{\bar{x}-\bar{y}}$	2.13	1.5	1.0

The control in each case was a sample of virus protein in water from the same batch as that exposed to the solvent under consideration. It was diluted directly from water solution. $(\bar{X} - \bar{Y})/SE_{\bar{x}-\bar{y}}$ is a test for the significance of the difference of the number of lesions per half-leaf shown by sample and corresponding blank. By convention, if this quantity exceeds 2.1, the difference is regarded as being due to factors other than experimental error. These results indicate that 1 week's contact with glycerol causes a slight decrease in virus activity, whereas 10 minutes' contact with the other solvents causes no significant change in virus activity.

In table 2 are presented the results of activity measurements made on virus protein samples which had been dissolved in the solvents employed in the present study for periods of time great enough to allow double refraction measurements to be made. It seen that no appreciable loss in activity results from this treatment. Since activity in the biological sense is a very sensitive measure of change in the protein molecule, it must be concluded that the reduction in double refraction of flow can not be attributed to denaturation or destruction of the protein by the solvents. This conclusion may be checked more directly for the case of the protein dissolved in glycerol-water solvents. It was found that, when solutions of the virus protein in 90 per cent glycerol were diluted with water, the double refraction per unit concentration of protein increased to the value obtained originally for a solvent of the same composition as that obtained upon dilution. This shows that the effect of the solvent is a reversible one, a necessary condition for an effect due to nothing but the refractive index of the solvent. In view of the facts that the property of stream double refraction shown by the virus protein is lost when the protein is dissolved in a medium whose refractive index is the same as that of the protein and that this effect seems not to be due to any change in the protein, it is evident that the double refraction of flow of the tobacco mosaic virus protein solutions is due largely, if not entirely, to the effect of the shape of the particles and scarcely, if at all, to the intrinsic double refraction of the particles themselves. This fact, as will be seen presently, is of great importance to those who are interested in the nature of plant viruses.

THE LIQUID CRYSTALLINE STATE

The liquid crystalline or paracrystalline state is encountered in many biological systems (5). As will be seen presently, relatively concentrated solutions of the tobacco mosaic virus protein afford an example of such systems, for they may exist in a state which can be described as two-component liquid crystalline. The jelly-like pellets obtained by ultracentrifuging solutions of the virus protein may be regarded as being very concentrated colloidal solutions. Figure 3 is a photomicrograph of a flattened section of the jelly-like material constituting a pellet of the ultracentrifuged tobacco mosaic virus protein, taken with a polarizing microscope. This picture resembles those obtained in a similar manner with substances known to be liquid crystalline or paracrystalline, for example, wetted bromophenanthrenesulfonic acid (11). Furthermore, the x-ray diffraction pattern shown by these pellets may be interpreted as being that of a paracrystalline material (2, 21). It would seem, then, that these jelly-like pellets are true examples of the paracrystalline state. As a result of his studies with a great number of organic compounds, Vorlander (18) has come to regard the ability to exist in the liquid crystalline state as being associated with materials having rod-shaped molecules. This generalization may be carried over from systems of one component to systems of two components, such as tobacco mosaic virus protein in water or bromophenathrenesulfonic acid in water. This paracrystallinity of the tobacco mosaic virus protein pellet, then, must be regarded as constituting additional evidence of the rod-like character of the tobacco mosaic virus protein.

FIG. 3

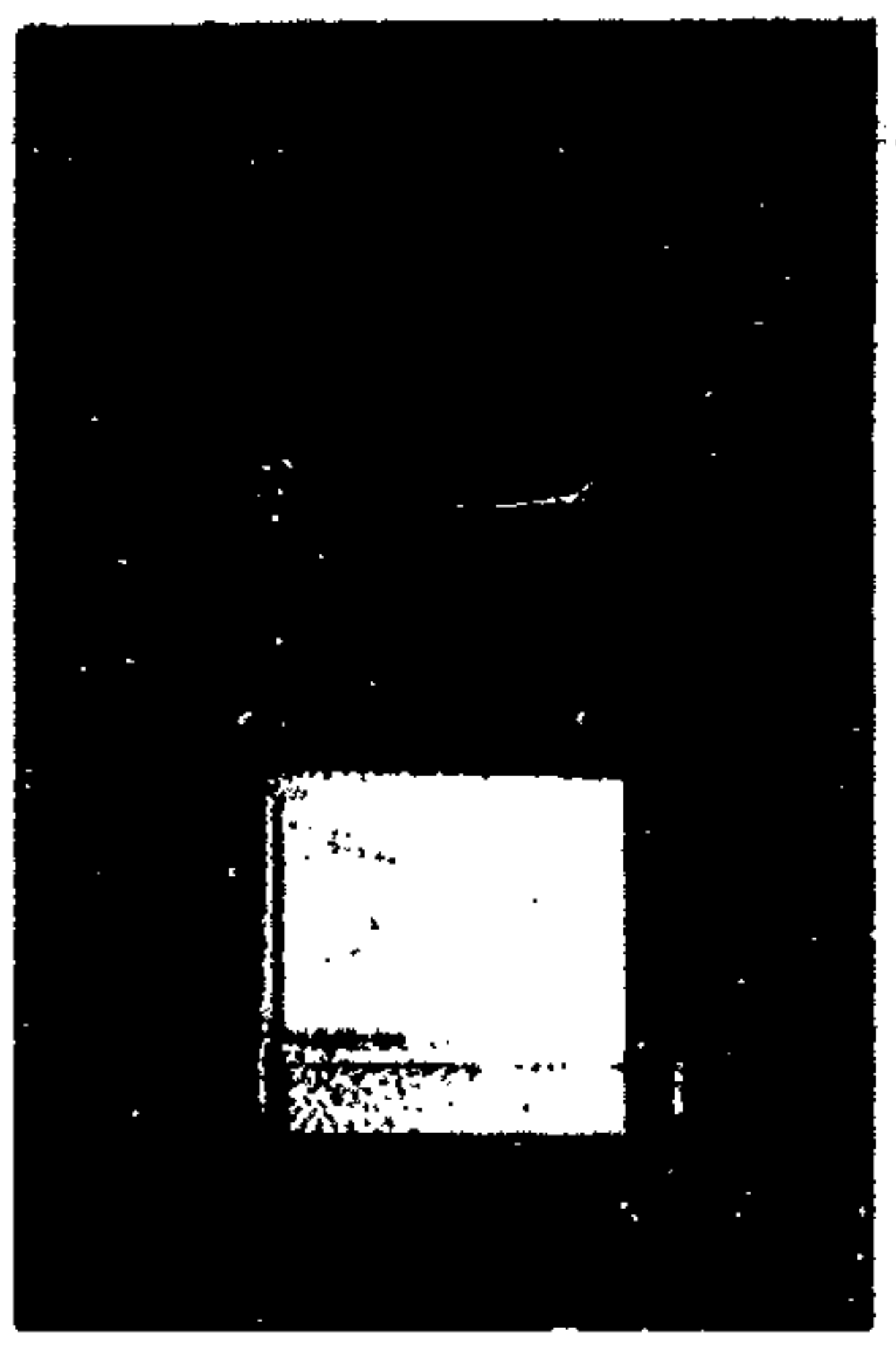

FIG. 4

FIG. 3. Photomicrograph of a flattened section of a tobacco mosaic virus protein pellet obtained by ultracentrifugation, taken with the aid of a polarizing microscope. × 135. (Photograph by J. A. Carlile.)

FIG. 4. A solution of tobacco mosaic virus protein following separation into two layers. Photographed between crossed Polaroid plates. (Photograph by J. A. Carlile.)

THE LAYERING PHENOMENON AND DEPOLARIZATION OF SCATTERED LIGHT

When relatively concentrated solutions of tobacco mosaic virus protein are allowed to stand, they separate into two layers, the bottom one of which is spontaneously birefringent or liquid crystalline (1, 8). Figure 4 is a picture of such a system, photographed between crossed Polaroid plates. Insofar as it is known, these two layers differ chemically only in that the concentration of protein is greater in the bottom layer (1). The light-scattering properties of these two layers differ considerably. The light scattered perpendicularly by a colloidal solution with a disperse phase consisting of very small isotropic spheres is completely polarized, with the electrical vector in the plane perpendicular to that defined by the incident beam and the direction of observations. However, if the disperse phase consists of very small anisotropic or asymmetrical particles, even though the incident light is polarized, the scattered light will be depolarized; that is, it will have electrical components in both the plane of incidence and that perpendicular to it. If the particles of the disperse phase are large and the incident light is unpolarized, there will be an apparent depolarization of the scattered light, even though the particles are spherical and isotropic (6). Figure 5 shows the horizontal and vertical components of the scattered light for both layers for incident beams vibrating hori-

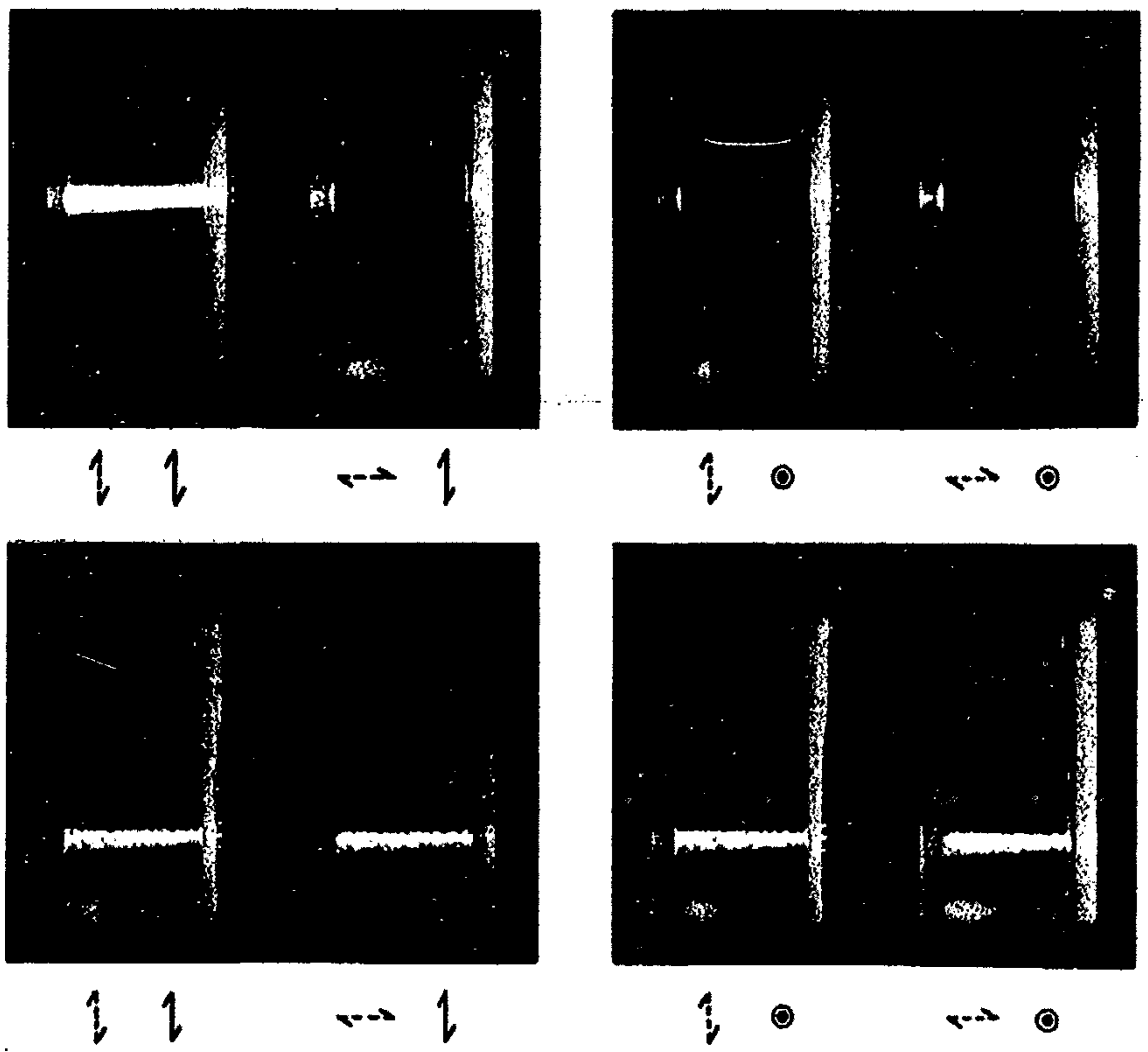

FIG. 5. The depolarization of the light scattered by the top and bottom layers (figure 4). The incident beam enters the cell at the right and leaves on the left. The solid symbols indicate the plane in which the electrical vector of the incident light is vibrating and the broken symbols represent the plane of vibration of the observed scattered light. The point enclosed by the circle is a symbol indicating that the vibrations are in a plane perpendicular to that of the paper. (Photographs by J. A. Carlile.)

zontally and for those vibrating vertically. The results for the top layer may be analyzed roughly by the method of Krishnan (6). The intensity of the scattered light is the sum of several terms: (*A*) a vertical component due to the size of the particles, (*B*) a horizontal component due to size, (*C*) a vertical component due to shape or anisotropy, and (*D*) a horizontal component due to shape or anisotropy.

In the case under consideration, when the incident light vibrates in the vertical plane, the vertical component of the scattered light is much greater than the horizontal component (figure 5, upper left). This light can be pictured as consisting of a relatively intense effect due to (*A*) as described above, no effect due to (*B*), a small horizontal component due to (*D*), and another small vertical component due to (*C*), which, on theoretical grounds, should be four-thirds as intense as the component due to (*D*). When the incident light vibrates in the horizontal plane, the scattered light consists of a relatively weak horizontal component and an essentially equal vertical component (figure 5, upper right). (*A*) and (*B*) may be thought to contribute little to the light scattering in this case, the vertical component being due largely to (*C*) and the horizontal component due largely to (*D*). In this case, on theoretical grounds, (*C*) should equal (*D*). These results show that the depolarization exhibited by the upper layer is due to anisotropy or asymmetry of the dispersed particles, rather than to size beyond the critical range. This conclusion is entirely in harmony with that drawn from the other observations discussed. In the bottom layer, on the other hand, scattered light is seen to be largely depolarized regardless of the condition of polarization of the incident light (figure 5, bottom). This is to be expected, because the bottom layer as a whole exhibits birefringence without extinction directions (8), and, therefore, the scattered light regardless of its state of polarization immediately after being scattered is largely depolarized while passing out through the solution.

An examination of figure 6, which is a photomicrograph of a droplet of the bottom layer material, taken with the aid of a polarizing microscope, reveals directly that this bottom layer is in the liquid crystalline or paracrystalline state. It has been visualized as consisting of "a three-dimensional mosaic of regions arranged at random to each other, but in each of which all the rod-shaped particles will lie approximately parallel" (1). We now know that these rod-shaped virus molecules or particles have very little or no intrinsic double refraction. The double refraction of the anisotropic region is, then, of the type discussed by Wiener,—a system consisting of small isotropic rods arranged parallel in an isotropic medium of different refractive index. These small doubly refracting volumes resemble to a considerable extent certain living cells known to exhibit double refraction, for example, the head of the sperm of the cuttlefish. This living cell probably contains nucleoprotein in the paracrystalline state (11). The question of whether plant virus protein particles should be regarded as being essentially living organisms or essentially unusual chemical individuals is not yet considered closed. It has been suggested by Rawlins and Takahashi (10) that the property of double refraction of flow and the related phenomenon of liquid crystallinity shown by plant virus nucleoproteins may indicate that these viruses are small living organisms composed of nucleoproteins in the paracrystalline state, analogous to the sperm heads just mentioned. The present finding, that these rod-shaped virus particles, or molecules, or organisms are in themselves either isotropic or nearly so, demonstrates that they are not the analogs of those living organisms exhibiting permanent double refraction. Rather they must be considered the analogs of one of the components of living organisms showing paracrystallinity, for example, the nucleoproteins found in the sperm head.

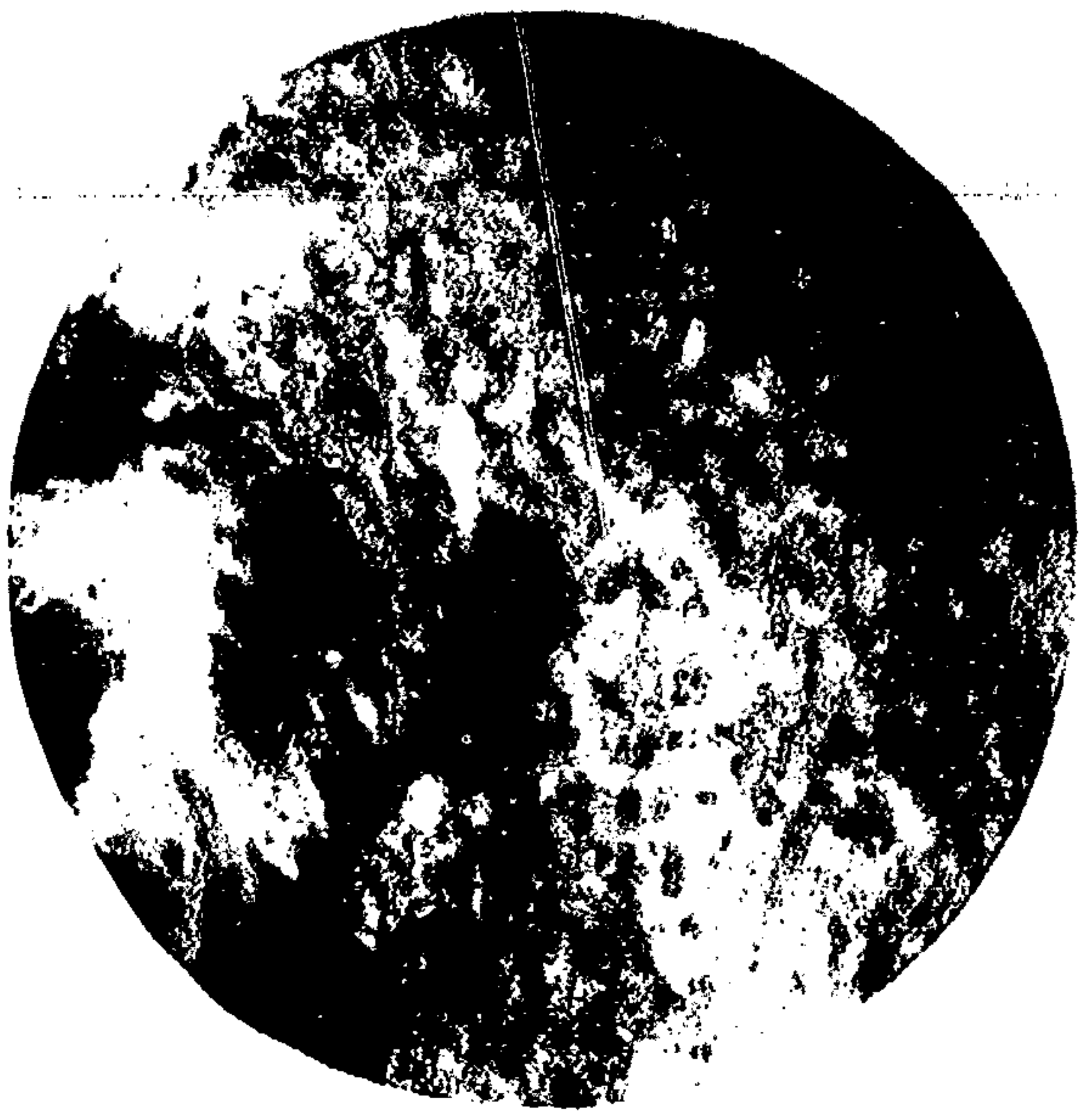

FIG. 6. Photomicrograph of droplet from the bottom layer (figure 4), taken with the aid of a polarizing microscope. × 135. (Photograph by J. A. Carlile.)

SUMMARY

The solutions of tobacco mosaic virus protein exhibit many interesting colloidal optical properties. It has been known for some time that dilute aqueous solutions of the virus protein exhibit double refraction of flow (1, 8, 17). It has now been shown that, when dissolved in liquids having a refractive index approaching that of the protein itself, little or no stream double refraction is obtained. Ultracentrifuged jelly-like pellets of the protein have properties characteristic of the liquid crystalline or paracrystalline state. As was shown by Bawden and Pirie (1) and confirmed in this laboratory (8), relatively concentrated solutions of the protein separate into two layers on standing, the bottom, more concentrated one being liquid crystalline. It was found in the present investigation that the Tyndall effect of the upper layer differs markedly from that of the lower layer. In the top layer the scattered light is depolarized to a small extent, whereas in the bottom layer the scattered light is very largely depolarized. All of these results are consistent with the conclusion that the tobacco mosaic virus protein particles or molecules are rod-shaped nucleoproteins having very little or no intrinsic double refraction. With respect to this latter property, the virus protein differs distinctly from the sperm cells of the cuttlefish and cells of other living organisms which have the property of double refraction or paracrystallinity.

REFERENCES

(1) Bawden and Pirie: Proc. Roy. Soc. (London) **B123,** 274 (1937).
(2) Bernal and Fankuchen: Nature **139,** 923 (1937).
(3) Eriksson-Quensel and Svedberg: J. Am. Chem. Soc. **58,** 1863 (1936).
(4) Freundlich: Colloid and Capillary Chemistry. Translated from 3rd German edition by H. S. Hatfield. E. P. Dutton and Co., New York (1926).
(5) Freundlich: J. Phys. Chem. **41,** 1151 (1937).
(6) Krishnan: Proc. Indian Acad. Sci. **1A,** 717 (1935).
(7) Lauffer: Science **87,** 469 (1938).
(8) Lauffer and Stanley: J. Biol. Chem. **123,** 507 (1938).
(9) Loring: J. Biol. Chem. **123** (Scientific Proceedings XXXII), lxxvi (1938).
(10) Rawlins and Takahashi: Science **87,** 255 (1938).
(11) Rinne: Trans. Faraday Soc. **29,** 1016 (1933).
(12) Signer: Trans. Faraday Soc. **32,** 313 (1936).
(13) Stanley: Science **81,** 644 (1935); Phytopathology **26,** 305 (1936).
(14) Stanley: J. Phys. Chem. **42,** 55 (1935); Ergeb. Physiol. biol. Chem. exptl. Pharmakol. **39,** 294 (1937).
(15) Steubel: Arch. ges. Physiol. (Pflügers) **201,** 129 (1933).
(16) Takahashi and Rawlins: Science **77,** 26, 284 (1933).
(17) Takahashi and Rawlins: Science **85,** 103 (1937).
(18) Vorlander: Trans. Faraday Soc. **29,** 899 (1933).
(19) Wiener: Abhandl. math.-phys. Klasse sächs. Akad. Wissenschaft (Leipzig) **32,** 507 (1912).
(20) Wyckoff, Biscoe, and Stanley: J. Biol. Chem. **117,** 57 (1937).
(21) Wyckoff and Corey: Science **84,** 513 (1936).

Les pages 946 à 950 se trouvent après la page 968

X-RAY DIFFRACTION STUDIES ON HEAVY-METAL FERROCYANIDE GELS[1]

HARRY B. WEISER, W. O. MILLIGAN, AND J. B. BATES

Department of Chemistry, The Rice Institute, Houston, Texas

Received July 14, 1938

Most heavy-metal ferrocyanides are so insoluble that they are thrown down in a highly gelatinous form on mixing even dilute solutions of metallic ion and ferrocyanide ion. The tendency of the gel to carry down ferrocyanide ion is so strong that the precipitation of the metal is incomplete on mixing equivalent amounts of metallic and ferrocyanide ions. This strong sorption is illustrated by the carrying down of potassium ferrocyanide, sodium ferrocyanide, and hydroferrocyanic acid during the precipitation of copper ferrocyanide (figure 1) (7, 11). Some of the heavy-metal ferrocyanide gels thrown down with excess ferrocyanide ion are assumed to be double salts such as $2Cu_2Fe(CN)_6 \cdot K_4Fe(CN)_6$. From the potassium ferrocyanide curve in figure 1, it might be argued that a definite double salt is formed having the formula $5Cu_2Fe(CN)_6 \cdot 2K_4Fe(CN)_6$, and that the upper portion of the curve represents the sorption of potassium ferrocyanide by the double salt. Although this is possible, the evidence is not sufficient to establish the existence of a definite double salt of this formula.

Attempts have been made to determine the composition of the precipitated ferrocyanide gels by electrometric (1, 8, 9) and conductometric (4, 5, 6) titration. The most recent work of this kind was done by Britton and Dodd (2), who made conductivity measurements at 25°C. on mixtures of heavy-metal salts and potassium ferrocyanide: first, in the form of direct conductometric titration of 125 cc. of 0.02 *M* salts with 0.1 *M* potassium ferrocyanide; and second, on similar mixtures of reactants which had stood in a thermostat until equilibrium was set up. In figure 2 are given the curves constructed from data corresponding to equilibrium conditions and the horizontal lines which represent the specific conductivity of potassium sulfate formed as a result of the equation:

$$2MSO_4 + (1 + x)K_4Fe(CN)_6 \rightarrow M_2Fe(CN)_6 \cdot xK_4Fe(CN)_6 + 2K_2SO_4$$

---

[1] Presented at the Fifteenth Colloid Symposium, held at Cambridge, Massachusetts, June 9–11, 1938.

The values of $x[= K_4Fe(CN)_6]$ deduced from the conductivity data, and from analysis of the precipitates formed in the presence of varying excess of potassium ferrocyanide, are summarized in table 1 (Britton and Dodd). The direct analysis of the precipitates is of little use in estimating the exact composition, since they are peptized before they can be washed free from entrained salt. Hence the values in the last column of table 1 represent only very rough approximations.

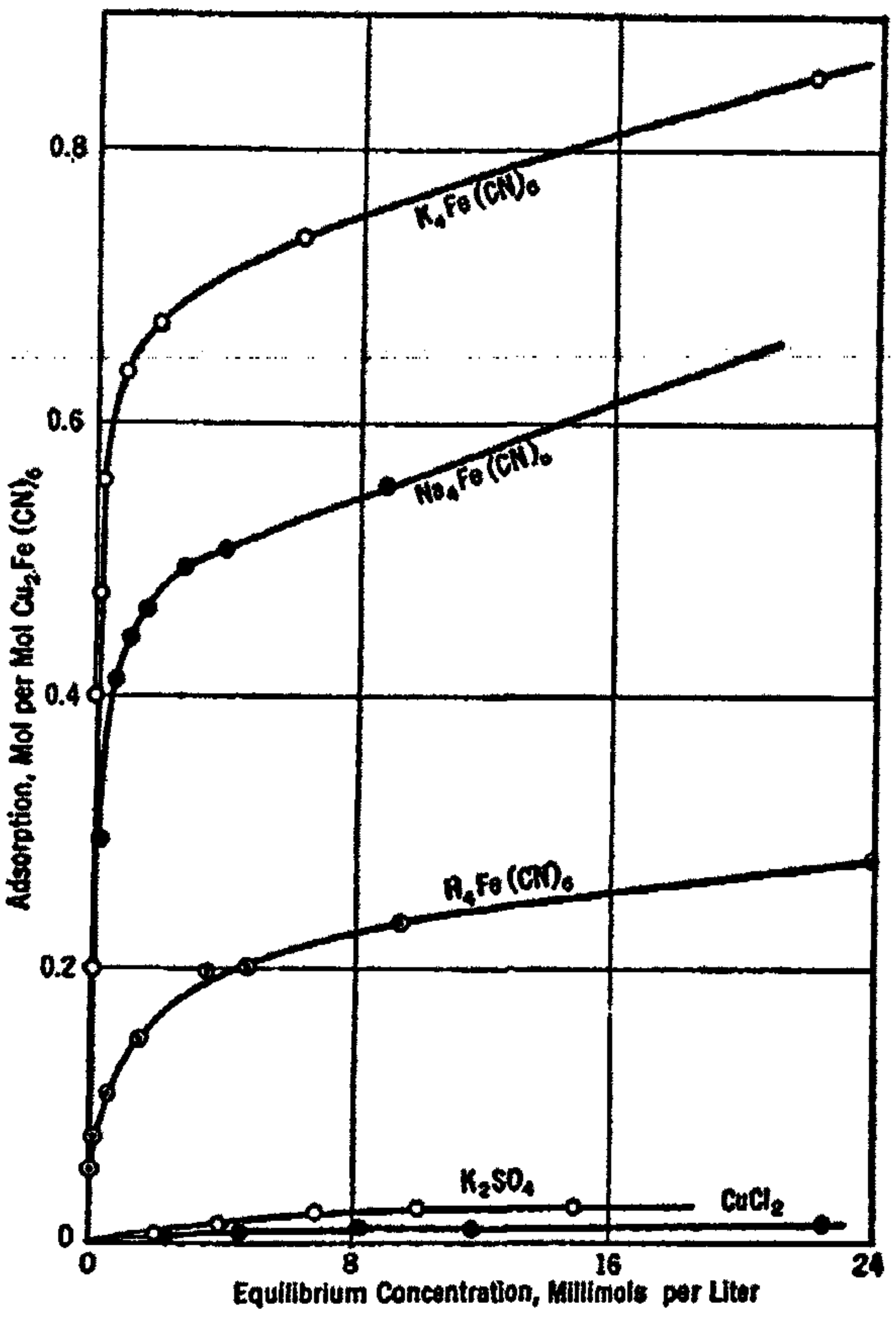

FIG. 1. Sorption of salts by copper ferrocyanide gel

Britton and Dodd recognize that the conductometric and analytical evidence given above is insufficient to decide whether the $M_2Fe(CN)_6$–$K_4Fe(CN)_6$ mixtures are definite double salts or sorption complexes. Moreover, since any highly gelatinous double salt that may form will sorb ferrocyanide, it is not possible from conductometric data to deduce the ratio of $M_2Fe(CN)_6$ to $K_4Fe(CN)_6$ in the alleged double salts.

Since Milligan (10) found that the gel of copper ferrocyanide is crystalline to x-rays, it seemed likely that the ferrocyanide gels of other metals

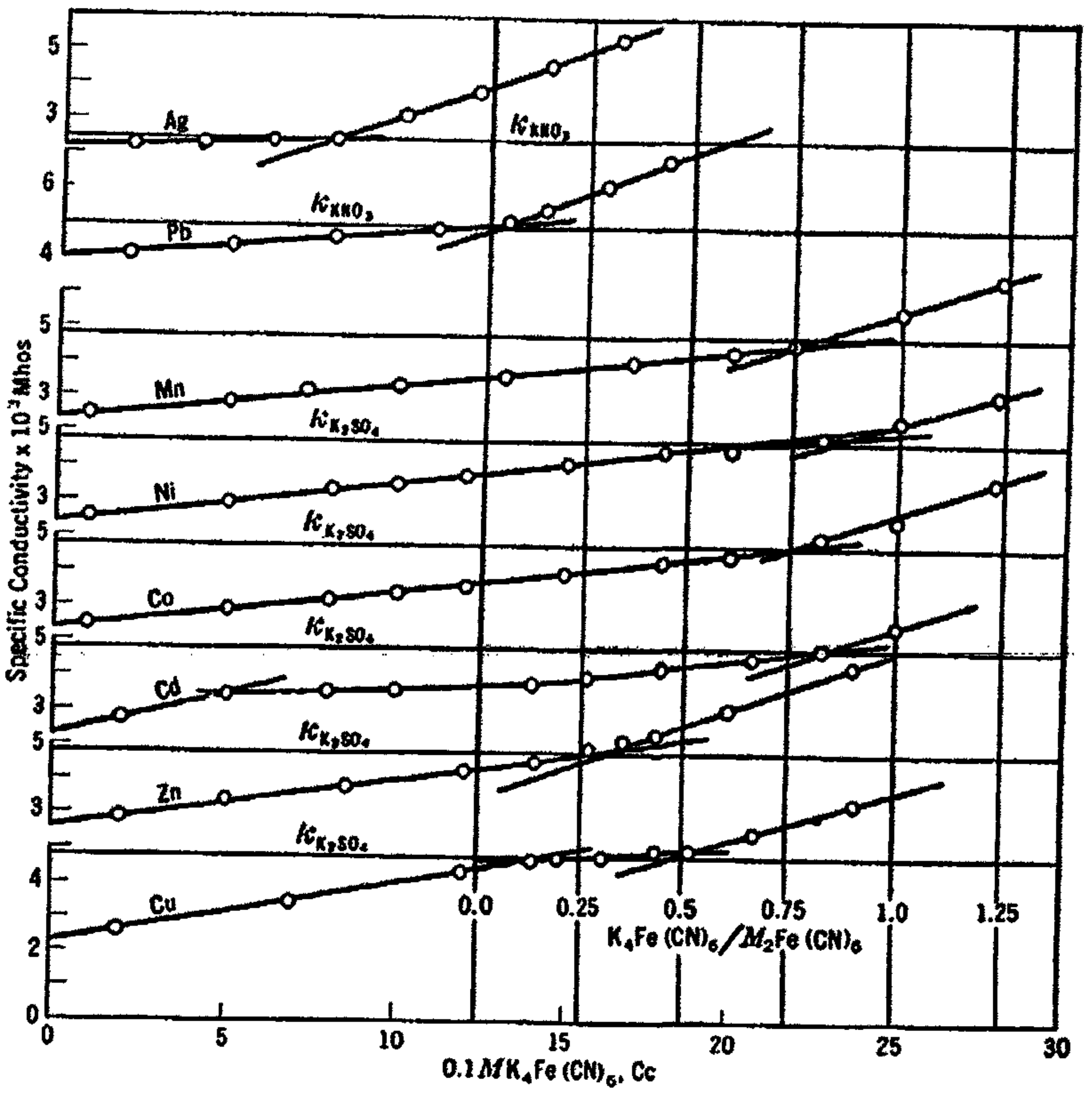

FIG. 2. Titration curves for ferrocyanide solution with various metallic salts (Britton and Dodd)

TABLE 1

Potassium ferrocyanide in ferrocyanide gels

x = moles of $K_4Fe(CN)_6$ per mole of $M_2Fe(CN)_6$

M	FROM CONDUCTIVITY MEASUREMENTS				FROM DIRECT ANALYSIS x
	First break		Second break		
	0.1 *M* $K_4Fe(CN)_6$	x	0.1 *M* $K_4Fe(CN)_6$	x	
	cc.		*cc.*		
Cu	14	0.12	18.7	0.52	0.52–0.71
Zn			16.4	0.31	0.71–0.78
Cd			23.0	0.84	0.59–0.90
Co			22.3	0.78	0.50–0.74
Ni	19.7	0.58	23.4	0.87	0.56–1.22
Mn			23.0	0.84	0.83–0.92
Pb	12.5	0.0			Very small
Ag	8.3	0.33			0.33

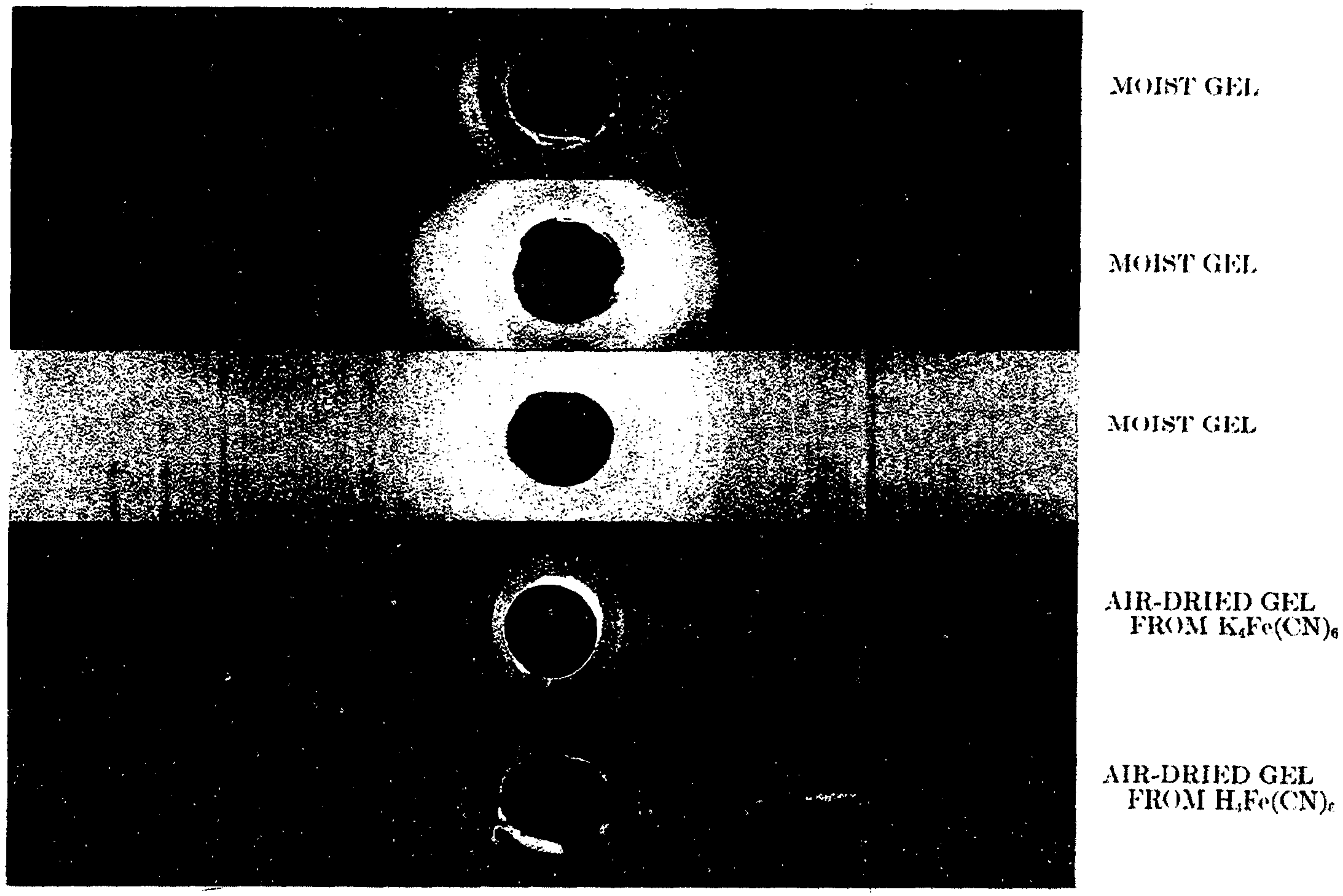

Fig. 3. X-ray diffraction patterns of copper ferrocyanide gels

would be crystalline. If so, the method of x-ray diffraction analysis should throw some light on the constitution of the gels formed under varying conditions. This paper gives a preliminary report of the results of the x-ray examination of the ferrocyanide gels of copper, cobalt, nickel, manganese, lead, zinc, cadmium, and silver.

EXPERIMENTAL

Copper ferrocyanide

In an investigation of the cause of the impermeability of the copper ferrocyanide membrane to ferrocyanide ion (11), it was concluded that the salt sorbs ferrocyanide ion strongly and irreversibly up to a composition of approximately 0.4 mole of potassium ferrocyanide per mole of copper ferrocyanide (figure 1). But, as already pointed out, the possibility of double salt formation can be neither proven nor ruled out by the results recorded in figure 1. A series of gels was therefore prepared by mixing varying amounts of cupric chloride and potassium ferrocyanide as given in table 2. The gels were centrifuged and the supernatant liquids analyzed for copper and ferrocyanide. The copper determinations were made by the standard iodometric procedure, while the ferrocyanide analyses were carried out by titrating with standardized potassium permanganate. It will be observed that the first three samples in the table contain but little excess potassium ferrocyanide.

TABLE 2

A series of copper ferrocyanide gels

SAMPLE NO.	SOLUTIONS MIXED					FINAL CONCENTRATION OF $CuCl_2$	AMOUNT OF $K_4Fe(CN)_6$ ADSORBED, MOLES PER MOLE OF $Cu_2Fe(CN)_6$
	$CuCl_2$		$K_4Fe(CN)_6$		H_2O		
	0.0874 *M*	0.0300 *M*	0.1173 *M*	0.0304 *M*			
	cc.	*cc.*	*cc.*	*cc.*	*cc.*	*millimoles*	*moles*
I	802.88		197.92		0	24.88	0.022
II		100.36		39.73	108.91	2.55	0.037
III		100.36		49.48	99.19	0.305	0.042
IV		100.36		54.50	94.17	0	0.117
V		100.36		59.34	89.33	0	0.224
VI		100.36		61.84	86.81	0	0.268
VII		100.36		64.36	84.31	0	0.319

A duplicate of sample I was washed, using a centrifuge, until the last washing was free of copper and ferrocyanide ions. This gel was air-dried and analyzed by a method similar to that of Hartung (3). The dry gel was dissolved in 6 *N* sodium hydroxide, and boiled until copper oxide was precipitated. The filtered and washed copper oxide was dissolved in nitric acid, excess acid removed, and the copper determined as given above. The filtrate was neutralized and ferrocyanide determined by titration with potassium permanganate. The sample was found to contain 41.53 per cent Cu, 24.42 per cent $Fe(CN)_6$, and 34.05 per cent H_2O (by difference); the mole ratio $Cu/Fe(CN)_6 = 1.962$.

The unwashed, moist gels obtained by centrifuging samples I to VII were placed in thin tubes of Lindemann glass for x-ray examination by means of the following procedure: The open end of the glass tube was thrust into a portion of the moist gel placed on a sheet of filter paper. The small quantity of gel obtained was moved toward the center of the glass tube by gentle suction, leaving about 4 to 5 mm. of empty tube below the gel. The Lindemann glass tube was then sealed off by means of a very small needle-point flame.

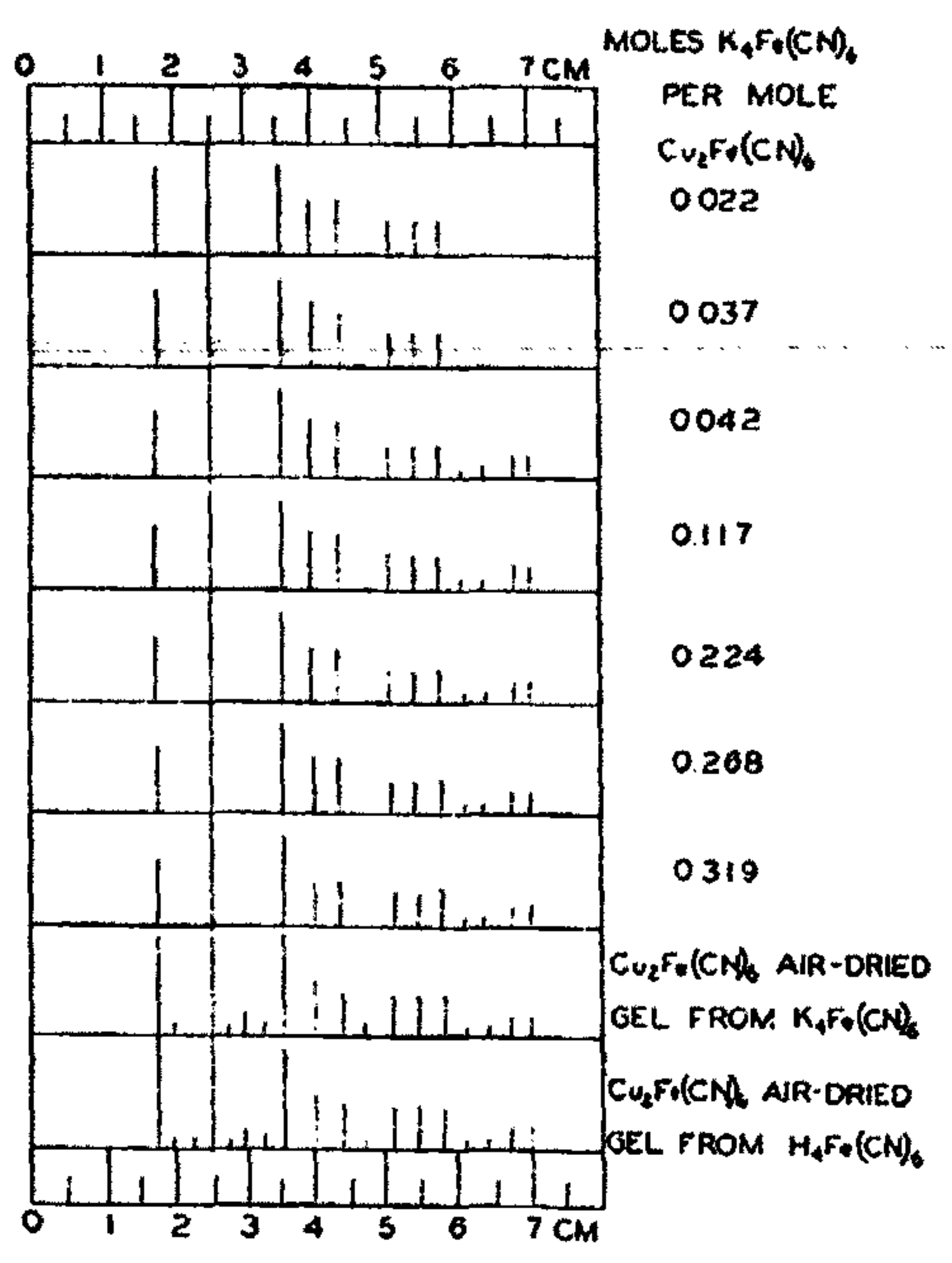

FIG. 4. Diagrams of the x-ray diffraction patterns of copper ferrocyanide gels containing varying amounts of sorbed potassium ferrocyanide.

The various gel samples were examined by x-ray diffraction methods, using Cu K_α x-radiation, in a camera 57.6 mm. in diameter, with an exposure time of 1 hr. The film was protected by aluminum foil from secondary radiation from the iron in the samples. Some typical patterns reproduced in figure 3 show the degree of crystallinity of the gels. The results with a series of gels of varying composition are represented diagrammatically in figure 4. For purposes of comparison the diagrams of practically pure copper ferrocyanide precipitated (*a*) with copper in excess and (*b*) with hydroferrocyanic acid in slight excess are included in the diagram. Since the several patterns are identical within the limits of accuracy of the observations, it would appear that the ferrocyanide carried down by copper ferrocyanide gel is not combined to form a definite double salt. There are three possibilities: (*1*) that the excess ferrocyanide is adsorbed on the surface of the highly dispersed crystals, (*2*) that the excess ferrocyanide is dissolved in the normal salt without causing sufficient change in the diffraction pattern to be detected, and (*3*) that both adsorption and solid solution are involved in the process. Since the crystals are so minute, x-ray diffraction patterns of the gels are not sufficiently sharp to enable one to detect minor differences in position or intensity of the bands. Until further information is available it seems advisable to use McBain's term "sorption" in referring to the phenomenon, which may involve both adsorption and a small amount of solid solution.

Other ferrocyanides

To prepare the other ferrocyanide gels investigated, 125-cc. portions of 0.02 *M* solutions of the several salts were added to varying amounts of 0.1 *M* potassium ferrocyanide (cf. Britton and Dodd (2)). Each ferrocyanide was precipitated (*1*) with one-half the theoretical amount required to react with the metal, (*2*) with an amount corresponding approximately to the break in Britton and Dodd's titration curve, and (*3*) with three times the theoretical amount. The gels were thrown down with the centrifuge and the x-ray diffraction patterns obtained as described above for copper ferrocyanide.

The ferrocyanides of cobalt, nickel, and manganese. The x-ray diffraction patterns of the several gels precipitated under varying conditions are shown diagrammatically in figure 5. With all three salts the diffraction patterns of the gels are the same irrespective of the $K_4Fe(CN)_6:2M_2SO_4$ ratio used in their preparation. This indicates that the potassium ferrocyanide carried down by the several gels is sorbed in an indefinite ratio and is not combined to give definite double salts. The breaks in the conductometric titration curves are therefore without significance in their relation to the possible formation of double salts. They may correspond approximately to the flat portion of the respective sorption isotherms.

A comparison of the diffraction patterns of the several ferrocyanides under consideration discloses that the positions of the lines are the same within the limits of the accuracy of measurement. The fairly sharp diffraction lines are in the same position, and the number and intensity of the lines are the same for the four salts, as nearly as can be estimated. This indicates that the salts are isomorphous, and have lattice constants that are nearly the same. This would be expected if the relatively large ferrocyanide anions were so arranged as to give spaces in which the smaller metallic ions are grouped. The fact that the ionic radii of the metallic ions under consideration are very nearly the same would account for the apparently small variations in lattice constants among the several salts.

Lead ferrocyanide. The lead salt gives a precipitate composed of relatively large crystals with a low sorbing power. The diffraction pattern shown in figure 5 is different from that of the other salts in the same figure. This would be expected in view of the much larger ionic radius of lead ion. The low sorption capacity accounts for the break in the conductometric titration curve at a point only a little above that corresponding to equivalent amounts of lead and ferrocyanide ions.

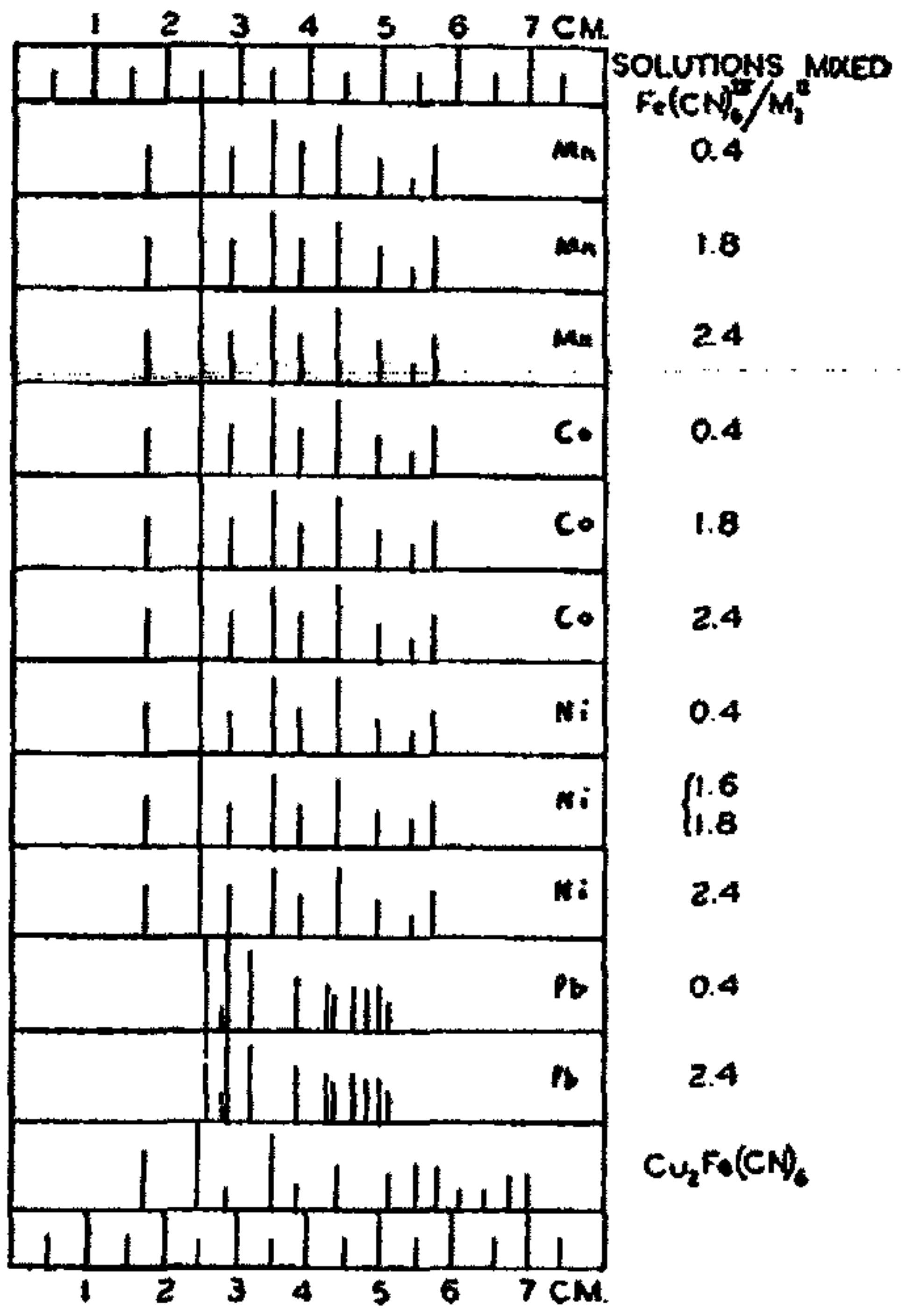

FIG. 5. Diagrams of the x-ray diffraction patterns of the ferrocyanide gels of cobalt, nickel, manganese, and lead.

The ferrocyanides of zinc, cadmium, and silver. The diffraction patterns of the ferrocyanides of zinc, cadmium, and silver are shown in diagrammatic form in figure 6. In contrast to the salts whose diffraction patterns are given in figure 5, the zinc, cadmium, and silver salts each give two patterns, depending on whether the gel is thrown down with metallic ion in excess or with ferrocyanide ion in excess. The two diffraction patterns for each of the three salts may correspond respectively to the normal salt and to a double salt with potassium ferrocyanide. It should be pointed out, however, that the possibility has not been excluded that the second pattern is due to a different crystalline modification or a different hydrate of the normal salt plus sorbed potassium ferrocyanide.

The composition of zinc ferrocyanide is of special importance, because zinc may be estimated volumetrically by titration with potassium ferrocyanide in neutral or acid solution. The following reaction is said to take place

$$2K_4Fe(CN)_6 + 3Zn^{++} \rightarrow K_2Zn_3[Fe(CN)_6]_2 + 6K^+$$

with the formation of a definite double salt. Referring to table 1 it will be seen that the observed equilibrium concentration of potassium ferrocyanide at the break in the curve is less than corresponds to the above formula, although in the rapid conductometric titration the break was observed at a point corresponding to the formula. This would seem to indicate that the precipitate is not a definite salt of the above composition, but is either zinc ferrocyanide with sorbed potassium ferrocyanide or a double salt containing less potassium ferrocyanide than the above, together with sorbed potassium ferrocyanide. To take care of possible variations in the composition of the precipitated gel and so to obtain accurate results in the estimation of zinc, it is essential not only that the conditions be rigidly controlled but also that they be exactly the same as in the standardization of the ferrocyanide solution against zinc.

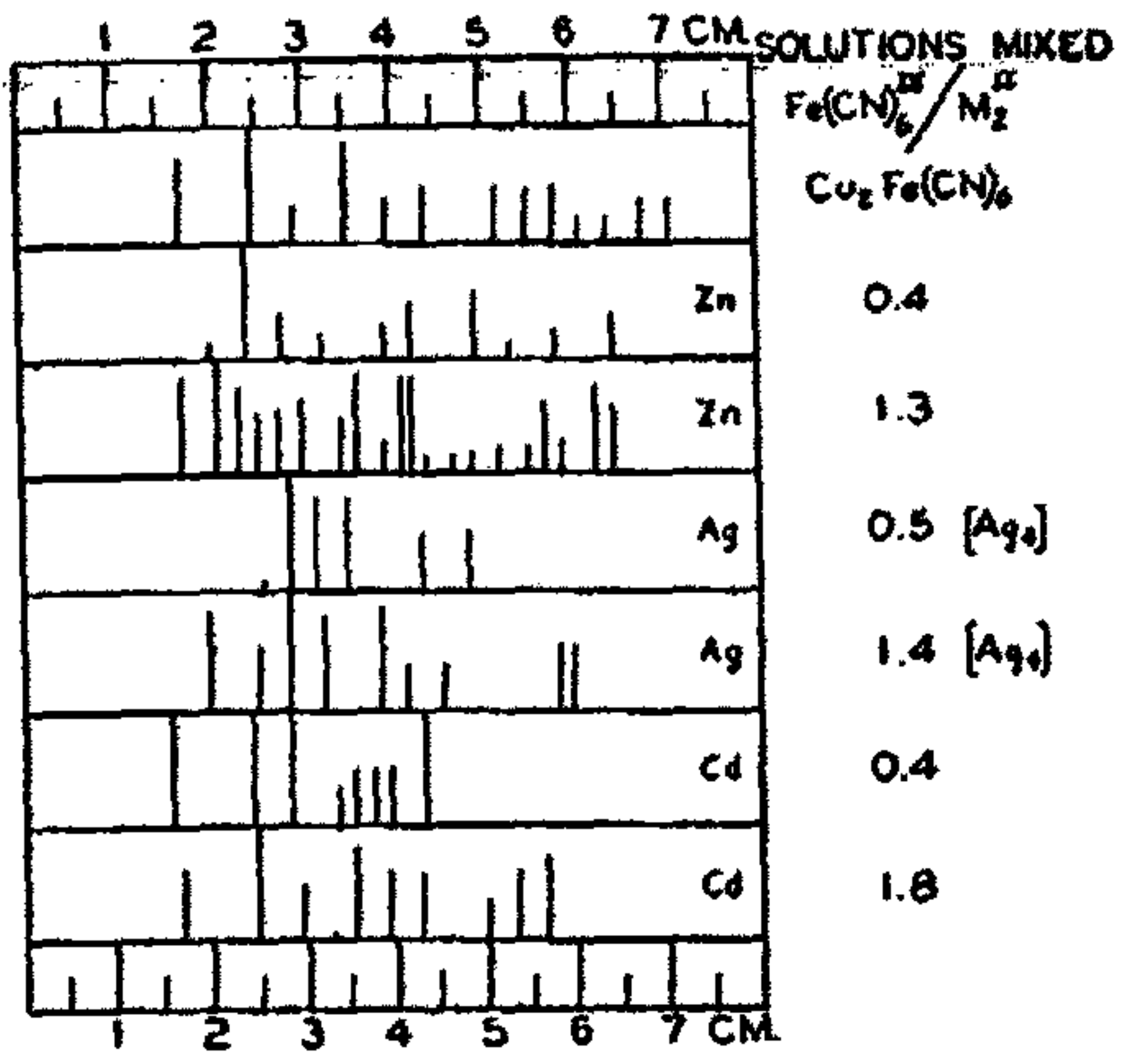

FIG. 6. Diagrams of the x-ray diffraction patterns of the ferrocyanide gels of zinc, cadmium, and silver.

Attention should be called to the fact that the diffraction pattern of the cadmium salt thrown down with ferrocyanide in excess is very similar to that of copper ferrocyanide. This suggests that the cadmium salt formed under these conditions is $Cd_2Fe(CN)_6$.

SUMMARY

The results of this investigation may be summarized as follows:

1. The gels of the heavy-metal ferrocyanides carry down alkali ferrocyanides strongly. It is not possible to determine by conductometric or potentiometric titration whether the gels adsorb the alkali ferrocyanide or whether double salts are formed.

2. Since the heavy-metal ferrocyanides are crystalline to x-rays, x-ray diffraction analysis of the moist gels throws some light on the constitution of the gels formed under varying conditions.

3. Copper ferrocyanide precipitated in the presence of excess copper is practically pure $Cu_2Fe(CN)_6$, which gives a distinctive x-radiogram. The gel thrown down with excess alkali ferrocyanide gives the same x-ray diffraction pattern as $Cu_2Fe(CN)_6$ even when it contains as much as 0.3 to 0.4 mole of $K_4Fe(CN)_6$ per mole of $Cu_2Fe(CN)_6$.

4. The alkali ferrocyanide carried down by copper ferrocyanide gel is not combined to form definite double salts. The excess ferrocyanide is adsorbed, for the most part, on the surface of the highly dispersed crystals of copper ferrocyanide. The possibility that a small amount of alkali ferrocyanide is dissolved in copper ferrocyanide has not been excluded. The phenomenon is therefore referred to as sorption.

5. The ferrocyanides of copper, cobalt, nickel, and manganese, but not of lead, are isomorphous, with lattice constants that are nearly the same. The crystals of lead ferrocyanide are relatively large and have a relatively low adsorption capacity for ferrocyanide ion.

6. The ferrocyanides of zinc, cadmium, and silver each give two distinct x-ray diffraction patterns, depending on whether the gel is thrown down with metal in excess or with potassium ferrocyanide in excess. The two diffraction patterns for each of the three salts may correspond respectively to the normal salt and to a double salt with potassium ferrocyanide. The similarity of the diffraction pattern of the cadmium ferrocyanide gel, thrown down with ferrocyanide in excess, to that of copper ferrocyanide suggests that the cadmium salt formed under these conditions is $Cd_2Fe(CN)_6$.

7. The breaks in the conductometric titration curves for metallic salts and alkali ferrocyanide are without significance in their relation to the possible formation of double salts. They may correspond approximately to the flat portion of the respective sorption isotherms.

REFERENCES

(1) Bichowsky: Ind. Eng. Chem. **9**, 668 (1917).
(2) Britton and Dodd: J. Chem. Soc. **1933**, 1543.
(3) Hartung: Trans. Faraday Soc. **15**, Pt. 3, 160 (1920).
(4) Cf. Ibarz and Feyto: Anales soc. españ. fís. quím. **34**, 823 (1936).
(5) Kolthoff: Z. anal. Chem. **62**, 209 (1923).
(6) Kolthoff and Verzijl: Rec. trav. chim. **43**, 394 (1924).
(7) Müller, Wegelen, and Kellerhoff: J. prakt. Chem. [2] **86**, 82 (1912).
(8) Treadwell and Chervet: Helv. Chim. Acta **5**, 633 (1922); **6**, 550 (1923).
(9) Treadwell and Weiss: Helv. Chim. Acta **2**, 680 (1919).
(10) Cf. Weiser: Inorganic Colloid Chemistry, Vol. III, p. 309. John Wiley and Sons, Inc., New York (1938).
(11) Weiser: J. Phys. Chem. **34**, 335 (1930).

A NEW ASPECT OF THE COLLOIDAL GOLD REACTIONS[1]

HANS M. CASSEL

Research Department, Colgate-Palmolive-Peet Company, Jersey City, New Jersey

Received July 1, 1938

THE BASIC IDEA

There is a general agreement about the rôle of the ζ-potential as a stabilizing factor. The ζ-potential is a measure of the repelling forces between neighboring particles, hence a sufficient reduction in potential leads to coagulation. But this is not the only possible way of explaining the collapse of colloidal dispersions; there must be another principle.[2] If the attractive forces are sufficiently increased the repulsion will be overcome, with coagulation as the result. Such an effect, indeed, should be expected if a "colloidal agent" condenses in the capillary interspaces between the particles during their collision.

In figure 1a two spherical particles are shown in a given volume containing under pressure P a gas which is adsorbed on the surface of the particles. Now suppose the two particles to be brought in contact. Immediately (figure 1b) the pressure must decrease, owing to capillary condensation taking place between the particles. In the case of very strong adsorption forces the pressure may become almost imperceptible. To establish the initial state by separating the particles, an energy of activation is required which might well exceed by far the work afforded by the ζ-potential. To distinguish this type of coagulation from that occurring in the absence of hydrophilic colloids we shall hereafter speak of "agglutination."

This process, of course, involves the consumption of agglutinin. Accordingly, a minimum concentration must be surpassed to start agglutination. On the other hand, when the interspaces are completely filled (figure 2) the consumption will reach a maximum, the value of which, naturally, depends on the geometrical conditions for tightest pack-

---

[1] Presented at the Fifteenth Colloid Symposium, held at Cambridge, Massachusetts, June 9-11, 1938.

[2] This subject was comprehensively discussed at the Symposium on Hydrophobic Colloids, held by the Nederlandsche Chemische Vereeniging at Utrecht, November, 1937. The contribution of F. Th. G. Overbeck dealt especially with the present problem. (Nordemann Publishing Co., New York (1938)).

ing. Thus it may appear as if a chemical compound of stoichiometric proportions had been formed. If the concentration is further increased, not agglutination but protection may result. This would require the vapor pressure of the single particle film to be smaller than that of coupled particles (see figure 3).

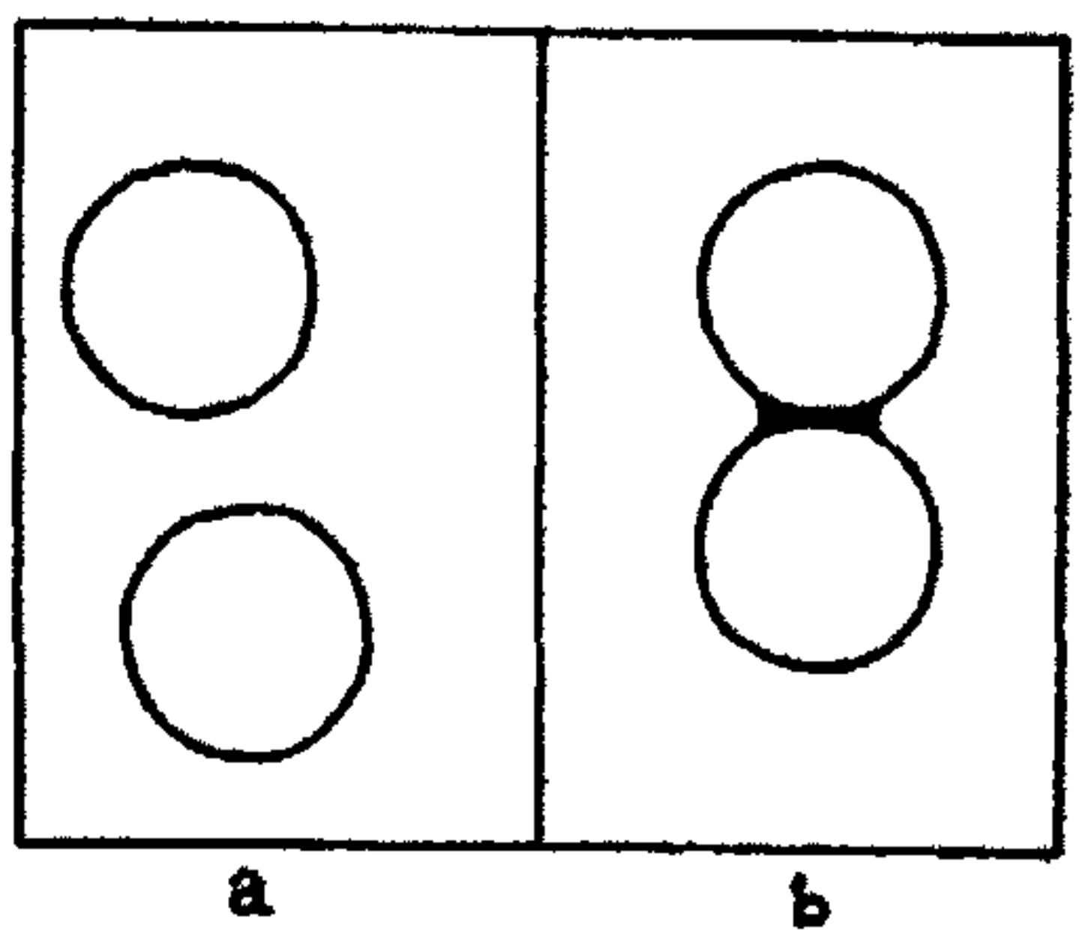

FIG. 1

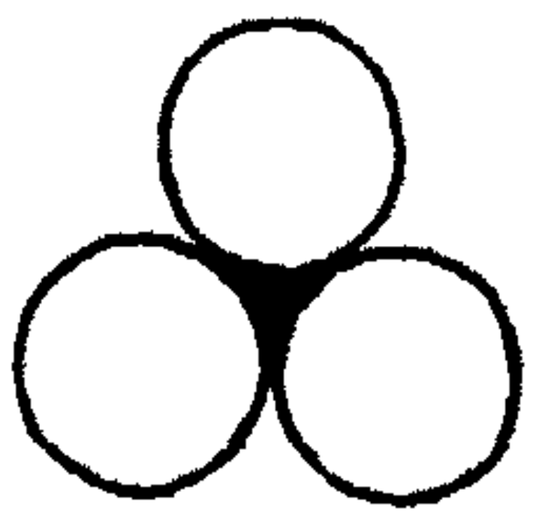

FIG. 2

FIG. 1. (a) Two spherical particles in a given volume containing under pressure P a gas which is adsorbed on the surface of the particles. (b) The two particles in contact; $p << P$.

FIG. 2. Apparent equivalence ratio = tightest packing

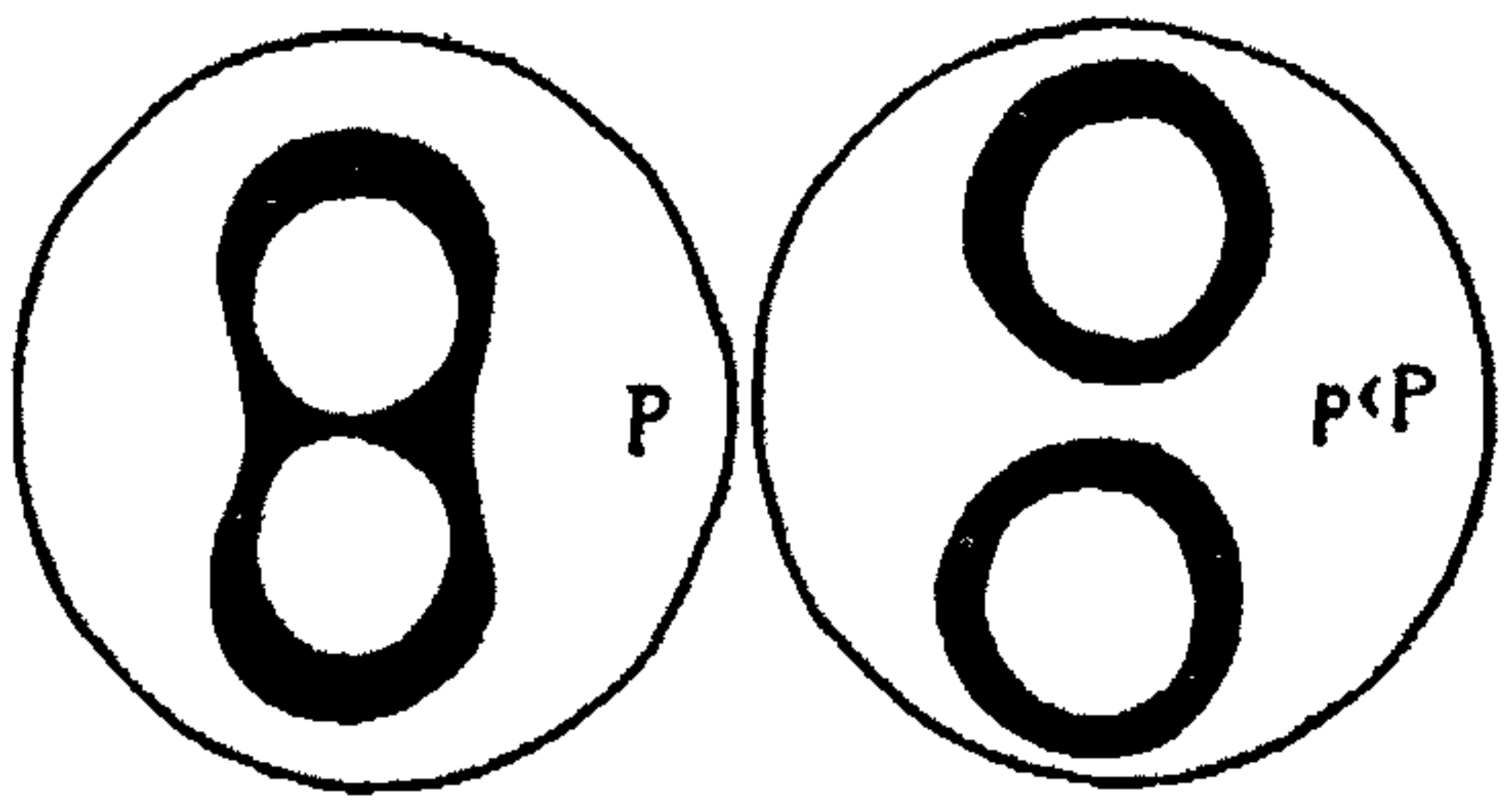

FIG. 3. Emulsification

DEVELOPMENT OF QUANTITATIVE RELATIONS

To define the conditions of capillary condensation, the relationship between the curvature of the adsorbing surfaces and the vapor pressures of the adsorbed films must be known. In the case of pure liquids the vapor pressure of smaller droplets is higher than that of larger ones. The contrary holds for concave menisci, according to the well known Gibbs-Thomson formula. However, we wish to know the vapor pressure of *films* adsorbed on curved surfaces.

Let us suppose that the film surrounding a spherical particle has, accidentally, the same vapor pressure as the adsorbent. Should we not expect the vapor pressure of the film to be exactly the same function of the curvature as that of the droplet? The thermodynamic treatment on the basis of Gibbs' Theory of Capillarity (3) confirms this expectation and leads to the conclusion (2) that the vapor pressure (thermodynamic potential) of the film-forming substance, for a given value of the interfacial density, Γ, either increases or decreases with increasing curvature. The decision as to what will happen depends on the sign of the term $\frac{\sigma}{2\Gamma/r - c}$, where σ is the interfacial tension, r the radius of the interface, and c is the concentration of the film substance in solution (mass per unit volume). When $2\Gamma > rc$ we have to deal with a tendency toward condensation in concavities, hence agglutination can be expected. On the other hand, when $2\Gamma < cr$ the tendency is to condense preferentially upon convex interfaces of smaller radii. Hence, emulsification and protection should be possible.

As shown in a previous publication this theory agrees with experiences in emulsification. Nothing seems to be in the way of applying this view to the reactions of hydrophilic sols with hydrophobic suspensoids in general, disregarding for a first approximation departures from the spherical symmetry of crystalline particles.

COMPARISON WITH EXPERIMENTAL FACTS

From the present standpoint the whole behavior of hydrophilic sols toward gold sols depends entirely on the individual shape of the adsorption isotherm. Unfortunately, not a single isotherm is known as yet, either on plane or on curved surfaces. Thus we have to make conjectures according to the known facts which consist chiefly in agglutination numbers (minimum amounts to produce "sensitization") and in protection numbers (minimum amounts to inhibit agglutination). In not a single case have the actual concentrations been determined!

Figure 4 shows two hypothetical adsorption isotherms drawn in a Γ–c diagram and representing the adsorption on a particle of radius r. The whole field is divided into two fields by the straight line $2\Gamma = rc$. Those parts of the isotherms rising above this discriminant line define a zone of possible agglutination, while those parts lying beneath the discriminant, where $2\Gamma < rc$, outline a zone of possible protection.

We read from the diagram that agglutination can occur at much lower concentrations than protection, which is in agreement with experiment. Furthermore, it becomes clear that no protection at all can be provided in case the adsorption is too strong (figure 5).

The addition of electrolyte will either increase or decrease the adsorption. The first, as a pre-stage of salting-out, seems generally to be the case in the determination of Zsigmondy's gold numbers. These conditions are supposed to be represented by the higher adsorption isotherm in figure 4. Here we see the protection zone for the particle size r considerably reduced. However, protection remains possible for larger sized particles, as illustrated by the discriminant r' having a steeper slope than r. This is the way the theory accounts for the characteristic feature of the gold sol reactions with hydrophilic sols, in that the disturbance of stability through electrolytes does not induce complete precipitation but ends in reëstablishing stable conditions for larger aggregates, in spite of the strong electrolytes present.

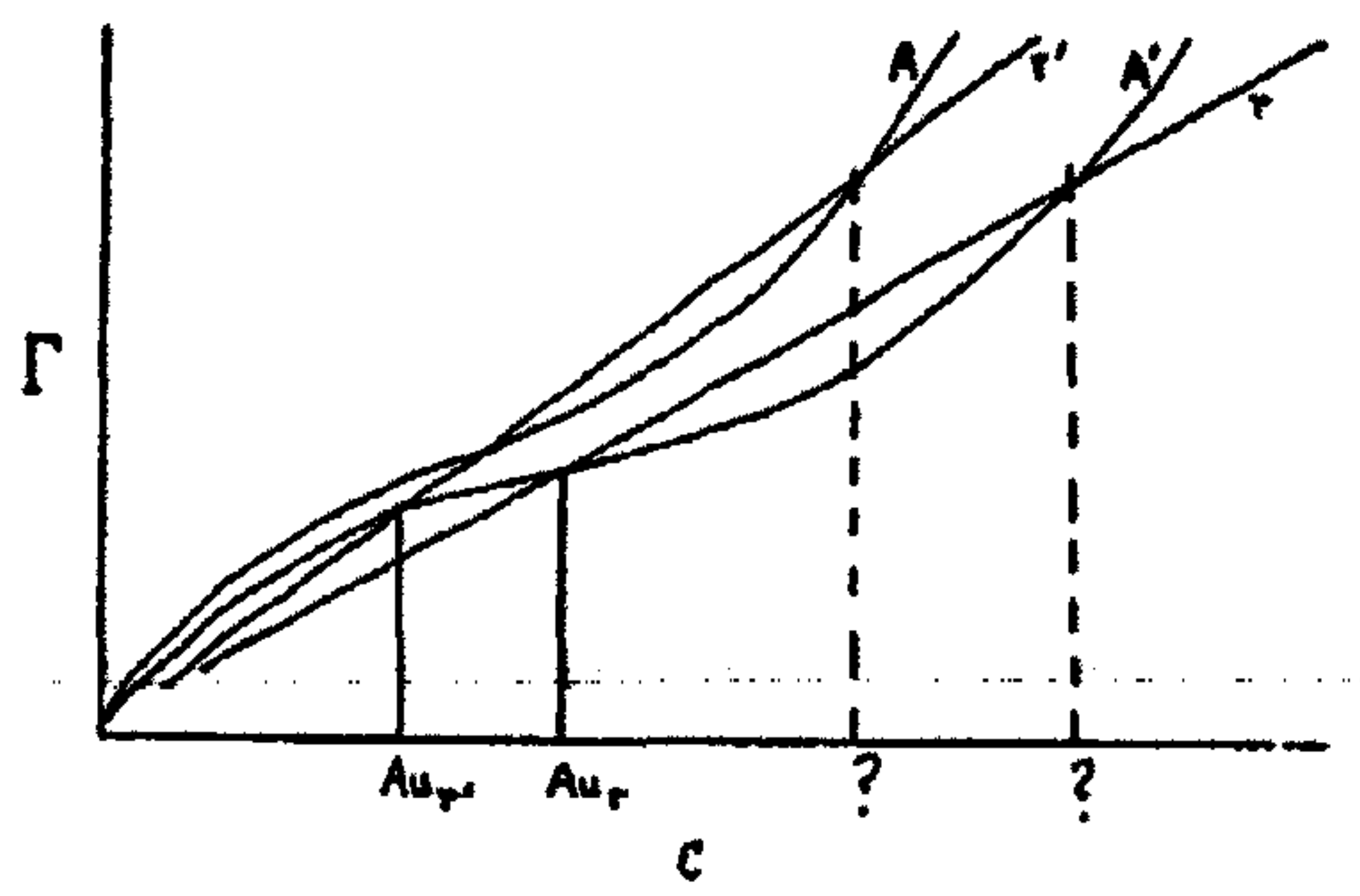

Fig. 4. The adsorption on a particle of radius r is shown in the presence and in the absence of electrolyte by curves A' and A, respectively. The straight lines r and r' represent the discriminants for particles of radii r and $r' > r$. Au_r and $\mathrm{Au}_{r'}$ indicate the corresponding gold number concentrations. The question marks indicate "upper gold numbers."

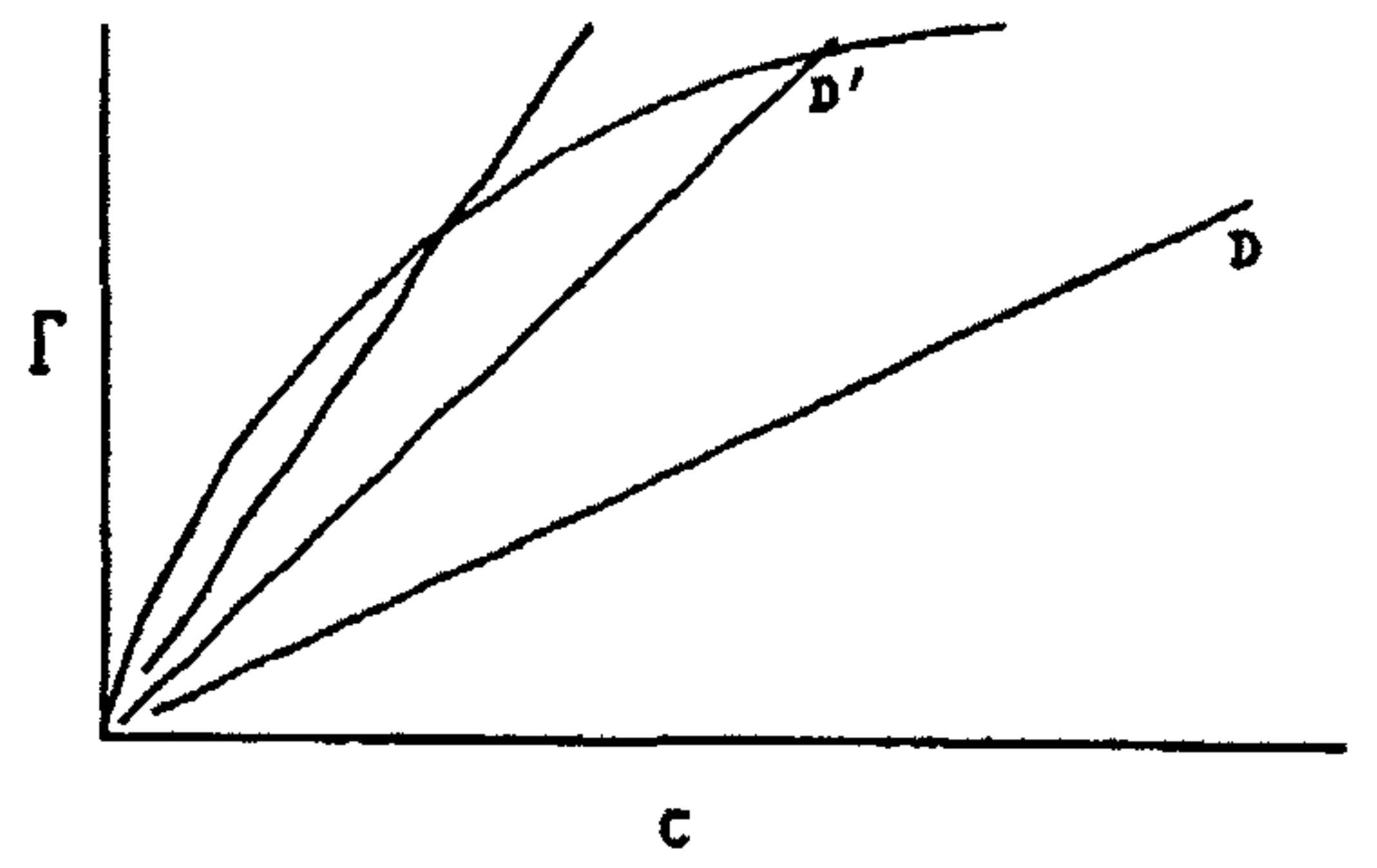

Fig. 5. This figure exemplifies strong adsorption where the discriminants even of rather large particles lie beneath the isotherm.

Zsigmondy's definition of the gold number implies the assumption that protection should always be enhanced by increasing the concentration of the colloids. However, while the chief concern has been to find out the best conditions for well-defined color changes, in actual practice this supposition has often been omitted. In violation of the original definition many so-called gold numbers were determined by the minimum amount of substance required to *produce* color changes instead of by those required to *prevent* them!

In any case caution is advisable in interpreting the presumably characteristic figures available in the literature, which may represent either the lower or the upper limit of the stability zone without apparent discrimination. Thus, for albumin, gum arabic, sodium oleate, and sodium laurate "upper gold numbers" are reported, as involuntarily demonstrated by the statement of Zsigmondy and Thiessen (4) that certain substances even at rather high concentrations do not effect any color changes, either spontaneously or on the addition of sodium chloride. These substances are those just mentioned!

From the present point of view such a behavior of hydrophilic sols can be foreseen. As already emphasized, the specificity of their reaction depends entirely on the shape of the adsorption isotherm. Let us imagine a type of curve which, up to rather high concentrations, always lies below the discriminant of the particle size chosen. Consequently, according to the theory, neither agglutination nor sensitization can be expected in the whole range of concentration limited by the "upper gold number." As a matter of fact, the gold numbers of the last-mentioned substances are representative of the higher values in Zsigmondy's classification.

There is one more argument in favor of the present view. If the low gold numbers correspond to the lower stability limit and the higher values to the upper limit they should be differently affected by changes in the size of the particles. It follows from the diagram (figure 4) that for discriminants of larger particles the protection zone is widened towards lower concentrations at the lower limit, but the opposite holds at the upper limit. Herewith it agrees that the gold numbers of soaps, dextrin, and albumin, which we recognized as "upper gold numbers," increase with increasing particle size, whereas the lower class colloids behave diametrically differently.

No one seems to have realized the possibility of gold numbers in the wider sense of the word, with the remarkable exception of such a critical observer as Wilhelm Biltz (1) who, studying the colloidal properties of dextrins, stated as early as in 1913 that two and more gold numbers may occur in different concentration ranges of the same substance.

So far as I can see, no contradictions are known to the present attempt to gain a unitarian aspect of the reactions between hydrophobic colloids and hydrophilic substances.

The results seem to encourage further experimental checking of the theory. If the present view is correct it should be promising to consider the behavior of gold sols as a prototype for certain antigen-antibody reactions.

In closing I wish to express my gratitude to Mr. Robert B. Colgate, Chairman of the Industrial Research Council, for his part in making this paper possible.

REFERENCES

(1) Biltz, W.: Z. physik. Chem. **83**, 695 (1913).
(2) Cassel, H. M.: J. Phys. Chem. **42**, 475 (1938).
(3) Gibbs, J. Willard: Collected Works, Vol. I, p. 219. Longmans, Green and Co., New York (1928).
(4) Zsigmondy, R., and Thiessen, P. A.: Das kolloide Gold. Kolloidforschung in Einzeldarstellungen. Akademische Verlagsgesellschaft, Leipzig (1925).

STUDIES ON GELATION AND FILM FORMATION OF COLLOIDAL CLAYS. I[1]

E. A. HAUSER AND D. S. LE BEAU[2]

Department of Chemical Engineering, Massachusetts Institute of Technology, Cambridge, Massachusetts

Received July 1, 1938

The mechanism which leads to the formation of gels is still a matter of considerable controversy. A critical review of the literature leaves the impression that the lack of a satisfactory and general explanation for this so common and important phenomenon lies not so much in its admitted complexity but in the fact that so far sufficient attention has not been paid to the gelation of simple systems, i.e., systems whose components are well defined and which permit actual observation of the changes which the system undergoes in its transition from sol to gel. Most of the theories are based on assumptions only, or are derived by indirect deductions.

For instance, the gelation of a gelatin sol upon cooling, or of rubber solutions in the presence of sulfur and accelerators, etc, is assumed to be the result of a felting together of long-chain molecules (8) and the formation of bridges and cross linkages between them. The solvent is held mechanically in the network formed or part of it may be immobilized by solvation.

The formation of silica gels is considered also today as the result of a chain-like arrangement of neighboring silicic acid molecules by condensation (splitting off of water) (6).

These assumptions have been so generally accepted that even the gelation of systems with microscopically or ultramicroscopically discernible particles has been considered to be caused primarily by a chain-like or pearl-string-like aggregation of these particles (10).

In the case of soap gels we frequently find a string-like aggregation of the highly disperse soap micelles on cooling the soap stock. However, such an arrangement cannot be essential for the gelation of soap, since gels can also be obtained without any such alignment and felting.

Although it cannot be denied that gelation is facilitated in many cases where the disperse phase consists of organic molecules joined, by primary

---

[1] Presented at the Fifteenth Colloid Symposium, held at Cambridge, Massachusetts, June 9-11, 1938.

[2] Present address: Dewey & Almy Chemical Co., Cambridge, Massachusetts.

valences, in chains of high molecular weight, or where condensation leads to chain-like aggregates, we have ample evidence that such a structure is not essential for an explanation of all types of gelation.

Extremely dilute and monodisperse colloidal clay sols[3] are excellent examples to disprove this general theory.

As a result of previous work pertaining to the production of monodisperse fractions of colloidal clays ranging in apparent average particle diameter from 14 to 180 mμ (5), it was found that the concentration of clay necessary to obtain a gel (system exhibiting yield point) decreases with decreasing particle size, and that gels with extremely low concentration ($<$ 0.1 per cent) of the disperse phase could be produced with the smallest particle size fractions. Very careful systematic ultramicroscopic studies of *freshly* prepared gels of concentrations not exceeding 0.1 per cent did not permit, contrary to previous assumptions, the detection of any ultramicroscopically visible specific alignment or grouping of the disperse phase. Results reported previously where grouping of particles had been observed were caused by excessive addition of electrolyte.

However, there might remain the possibility that invisible particles form the "missing links." Therefore a carefully prepared fraction of medium particle size, i.e., one from which all smaller particles had been carefully removed by repeated supercentrifugal fractionation, was selected for the present investigation to guarantee the absence of smaller, possibly undetectable particles. If such a fraction was studied in a slit-ultramicroscope (using an air-tight chamber), the particles were present in vivid Brownian motion. However, contrary to older observations carried out with unfractionated, or insufficiently fractionated, sols, only faint twinkling could be observed. This indicates that the particles in the selected fraction and concentration used are not excessively anisometric. This confirms the prevailing concept of the shape of the individual clay particle as deduced from x-ray diffraction analysis.

It is assumed that such a particle consists of layers of silicon and aluminum (the latter being replaceable by magnesium) bonded together by oxygen. Whereas the length and width of these sheets do not vary with the water content, the thickness shows very pronounced changes (1). There exists ample evidence that the difference in observed apparent particle sizes is due primarily to a different number of such layer units stacked up on each other and to a far smaller degree to any difference in the length or width of the atom sheets themselves.

Upon adding electrolyte to such a dilute fractionated sol, one observes a decrease in displacement of the particles due to Brownian motion, without being able to detect any alignment, grouping, or any specific structure. Upon reaching a certain concentration of electrolyte in the system, Brown-

---

[3] The term "colloidal clay" as used in this paper refers to montmorillonite, if not otherwise specifically stated.

ian motion ceases entirely. The individual particles may occasionally still show some rotation, but even so they remain fixed in their position (figure 1). At this stage the viscosity of the system has increased to a point where air bubbles do not rise any more. However, the slightest mechanical disturbance will immediately result in a revival of Brownian motion, which again comes to a standstill as soon as the outside influence stops (a *truly* thixotropic gel). Even if we assume that not all particles are visible when the system comes to a standstill—some might lie with their thinnest axis parallel to the direction of illumination—it seems highly improbable that all the optical voids should be filled with such invisible particles; moreover, such a configuration would have to be detectable by changing the azimuth. However, this is not the case.

It is theoretically impossible to determine the actual distance between reflection disks in an ultramicroscope. The only experimental statement which can be made is that the individual visible reflection disks are separated and that when a very narrow slit is used the probability that particles which do not happen to be in focus join the sharp reflection disks is negligible.

The disks might be caused by a group of primary particles, which is to be doubted. But even then such hypothetical groups would be separated from each other and exhibit no coherent structure, as postulated, for example, by the mechanical theory (7). This theory assumes that the individual particles actually touch each other in random arrangement, forming a skeleton comparable to a house of cards.

If only a slight excess of electrolyte is added, one observes the formation of "ultraflocks"[4] separated by narrow channels (figure 2). Although such a system will generally still be considered as a gel, and will not yet exhibit immediate syneresis, it is unquestionably present in a state of incipient coagulation. Further addition of electrolyte results in the formation of microscopic—and, finally, macroscopic—flocks. A *gel-like* system will persist as long as the flocks are sufficiently loose in structure, of microscopic size, and coherent. However, the above experiment demonstrates that *true gelation* is present prior to any sign of flocculation or agglomeration.

It is beyond the scope of this paper to discuss these experimental facts from a theoretical angle, yet it might be pointed out that we consider the formation of these gels to be caused by the particles taking up equilibrium positions in relation to each other. Since the overall attraction[5] between

---

[4] The term "ultraflock" should denote flocculation, which is visible only in the ultramicroscope.

[5] For the present discussion it is irrelevant if one considers only the disperse phase responsible for the development of these forces, or, in accordance with Wo. Ostwald (9), attaches at least equal importance to the composition of the dispersion medium and its ionic arrangement. A detailed theoretical discussion of these pertinent problems is in preparation.

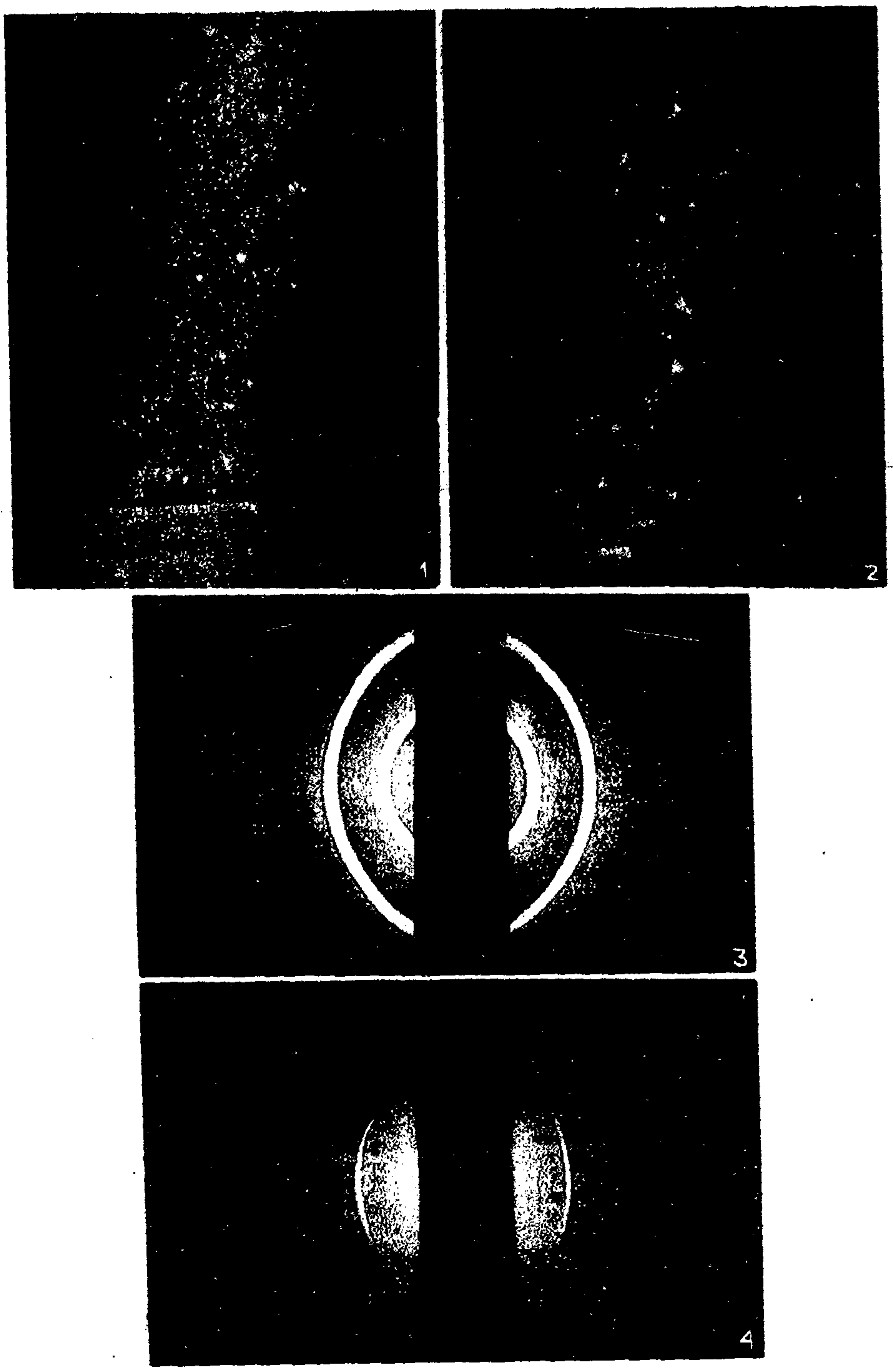

FIGS. 1-4

identical particles of equal size and shape in a given suspension must be considered as constant for every time differential and of sufficient magnitude in the colloidal range to cause permanent cohesion of the solid phase, if not counteracted by a repulsion force, it is the latter which becomes of predominant importance. Repulsion is composed of various factors, as, for example, the electric charge of the particle, the composition and nature of the ion arrangement in the dispersion medium, lyosorption or solvation, etc. Equilibrium will be reached as soon as the overall attraction is compensated by overall repulsion. That such a system exhibits a yield point finds its simple explanation in the fact that work must be done to move a particle out of its equilibrium position, i.e., to overcome the repelling force of the neighboring particles as well as their attraction, because of which they try to hold the particle in place. This theory is at variance with recent deductions based on the additive character of the London–van der Waals forces (4). The present theory considers repulsion as predominant, whereas the latter stresses the importance of attraction forces.

That dilute gels of hydrated clays like montmorillonite are not the result of any preferred structure or orientation is also demonstrated by a complete lack of alignment and the absence of tactoids or the like. On the contrary, the sols show orientation in polarized light only when in motion, but neither the sol at rest nor the gel is doubly refractive. On the basis of such a concept gelation must become more pronounced, the smaller the particles, because a system of a given volume can be considered the more volume-dispersed the more particles are available. Maximum gelation will exist if the particles are of uniform size and uniformly spaced (a system of random orientation but great regularity of distribution).

Still more striking is the evidence offered by the changes such gels undergo upon further drying. For example, if a sol is first converted into a gel by evaporation and the gel is spread on an appropriate support or deposited thereon directly from the sol state by centrifugal action, and then allowed to dry out completely, we observe with the aid of vertical dark-field illumination that the particles when forced closer together line up or actually snap into their new location, forming long, interlacing filaments or fiber bundles. The presence of separate reflection disks, as ob-

---

FIG. 1. Gel prepared from montmorillonite. Exposure time = 30 sec. Note the sharpness of the reflection disks. × 500.

FIG. 2. Ultraflocks formed upon the addition of a slight excess of electrolyte. × 500.

FIG. 3. X-ray of a film formed by drying the gel. Direction of x-rays vertical to the plane of the film.

FIG. 4. X-ray of a film formed by drying the gel. Direction of x-rays parallel to the plane of the film.

served in the sol and gel stage, gives way to continuous thread-like aggregations, which upon continued evaporation seemingly grow into larger crystals of highly anisometric shape. These filaments interweave and tie together by tridimensional cross-linkages, resulting in a coherent network or structure. *After complete desiccation an absolutely self-supporting film is obtained, which can be easily removed from its support as a coherent sheet.*

Such film production can be made absolutely continuous, starting with an appropriate sol by using the right type of filming machine. Another conceivable possibility is the production of fine threads by a combination spinning–drying process. Similar results have also been obtained with other clay minerals, vanadium pentoxide sols, etc. Depending on the particle size fractions used, films of varying degree of brittleness and flexibility are obtainable, the latter increasing with decreasing particle size. X-ray diagrams of such films,[6] taken vertical and parallel to its plane, reveal a typical Debye–Scherrer montmorillonite pattern in the former case, and a clear fiber pattern in the latter. This simply proves that all the particles have arranged themselves with the same crystallographic axis, parallel to the support (3) (figures 3 and 4).

The formed crystal threads are slightly doubly refractive.

The possibility of producing extremely thin, coherent, and self-supporting films without any binder and of high purity of the material offers a new method of studying the infrared absorption spectra of montmorillonite and other filming substances. Since these films can be produced from Na^+, Ca^{++}, or H^+, or any other adsorbed cation, further investigation should prove of great interest as to lattice configuration and especially water adsorption and absorption. So far distinct absorption bands have been observed at a reciprocal wave length of 3700 $cm.^{-1}$ due to free hydroxyl groups and between 3600–3200 $cm.^{-1}$ due to associated hydroxyl groups or adsorbed water. Whereas increasing temperature of drying the films reduces the second absorption band, the first remains practically unchanged[7] (2).

Films prepared from sodium bentonite swell and finally go into solution, if placed in water, whereas films of hydrogen bentonite resist very markedly and only show limited swelling. If sodium bentonite films are heated to white heat, they become water-resistant and decidedly stronger, the flexibility decreases, and they closely resemble mica in appearance and properties. If the films are subjected to high pressure they become transparent and much stronger. The translucency of the original film increases

---

[6] The x-ray diagrams were kindly taken by Professor B. E. Warren of the Department of Physics, Massachusetts Institute of Technology.

[7] Dr. Bowling Barnes of the American Cyanamid Co. was so kind as to determine the infrared absorption spectra.

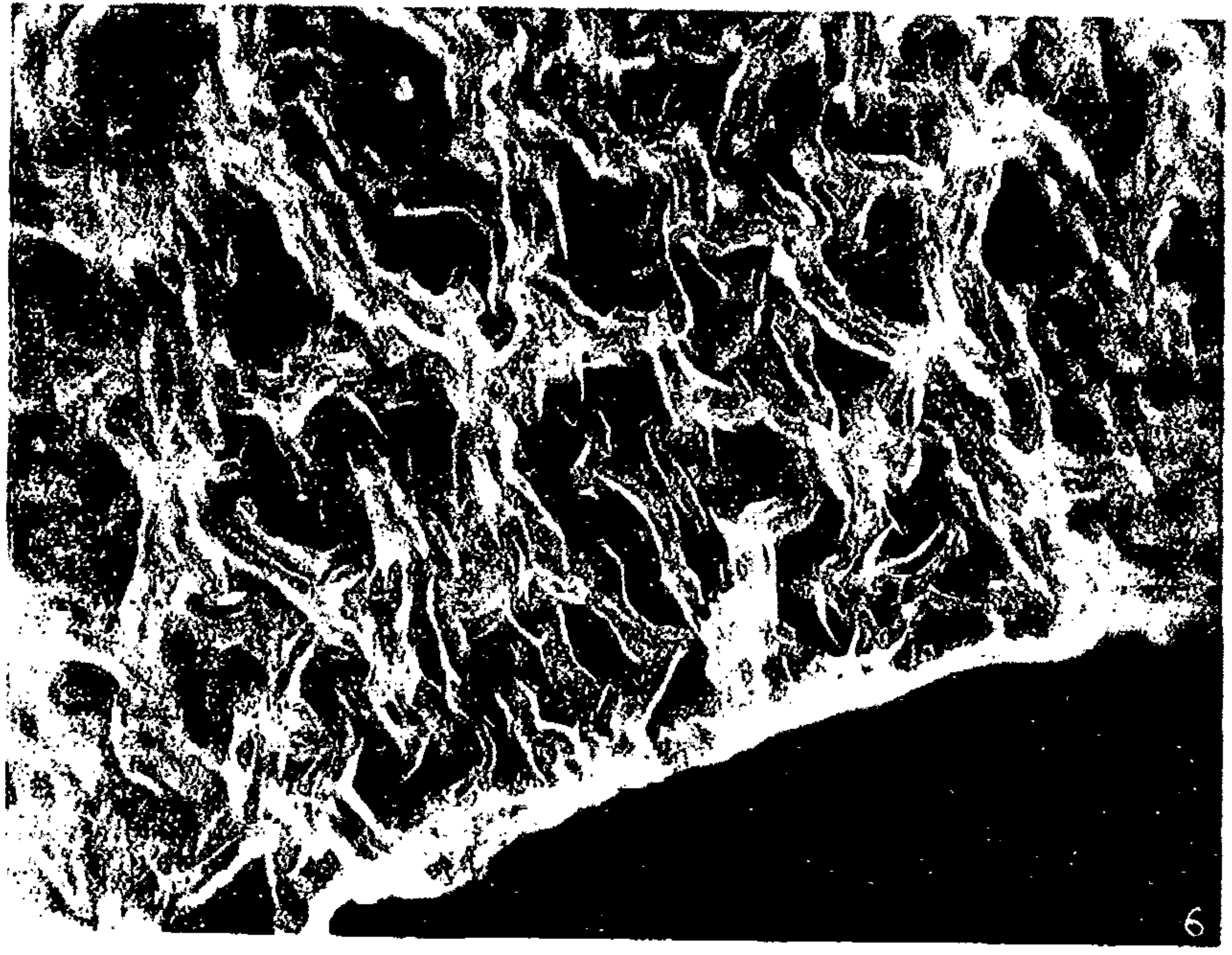

FIG. 5. Formation of crystal fiber bundles
FIG. 6. Structure after complete air-drying

with decreasing particle size and depends to some extent on the raw material used (aluminum silicate, magnesium silicate, iron content, etc.).

The structures which have been so far observed with dark-field microscopy are so numerous and complex that it has been impossible as yet to draw definite conclusions as to their significance for the formation of the film. However, it seems clear that high temperatures and pressure cause a drastic change in the basic crystal structure of the film (figures 5, 6, and 7).

The authors wish to have it understood that the discussion of the formation of self-supporting clay films is to be considered only as a brief summary of preliminary observations. A more detailed report will be published at a later date. The ability of inorganic particles to align and grow together to form the discussed networks or structures excludes the preexistence of a preferred arrangement in the gel. Even the slightest agglomeration in the gel, resulting in vacuolae, prevents the formation of continuous films. Furthermore, this phenomenon seems to offer a new insight into the possibility of crystal growth from colloidal dispersions instead of from true solutions and might be of special value for minerological and geological considerations. The work is being continued.

FIG. 7. Crystal formation after heating above 450°C.

In conclusion we should like to mention a peculiar phenomenon which was observed in the very finest fractions of bentonite. Besides the particles exhibiting regular Brownian motion, there exist particles which travel through the field of vision in a straight-line motion, like shooting stars, and then suddenly disappear. All tests[8] for living organisms (bacteria) were absolutely negative. At present the only plausible explanation for this peculiar phenomenon seems to be the possibility of point disintegration of submicrons, i.e., crystals, resulting in a recoil type of motion.[9] Further work is in progress.

SUMMARY

The most commonly accepted theories of gelation are discussed in connection with ultramicroscopic studies of the gelation of extremely dilute colloidal clay sols. A new concept for the transition from sol to gel is offered.

The formation of self-supporting coherent pure colloidal clay films of high flexibility has been observed, and the arrangement of the individual particles in chain aggregates is demonstrated. The possibility of crystal growth from colloidal dispersions and not from true solutions is considered.

X-ray and infrared absorption diagrams are discussed.

Attention is drawn to a peculiar rocket-like movement of particles found only in the finest colloidal clay fractions.

REFERENCES

(1) Bragg, W.: Proc. Roy. Inst. Great Brit. **30**, 39 (1938).
(2) Buswell, A. M., Krebs, Karl, and Rodebush, W. H.: J. Am. Chem. Soc. **59**, 2603 (1937).
(3) Clark, G. L., Grim, R. E., and Bradley, W. F.: Z. Krist. **96**, 322 (1937).
(4) Hamaker, C.: Symposium on Hydrophobic Colloids, p. 16, Utrecht (1937).
(5) Hauser, E. A., and Reed, C. E.: J. Phys. Chem. **40**, 1169 (1936); **41**, 911 (1937).
(6) Hurd, Charles B.: Sigma Xi Quarterly **26**, 28 (1938).
(7) Lewis, W. K., Squires, L., and Thompson, W. I.: Trans. Am. Inst. Mining Met. Engrs. **118**, 1 (1936).
(8) See, for example, Meyer, K. H., and Mark, H.: Der Aufbau der hochpolymeren organischen Naturstoffe, Leipzig (1930); Staudinger, H.: Die hochmolekularen organischen Verbindungen, Berlin (1932); Gerngross and Hermann: in Bechhold's Einführung in die Lehre von den Kolloiden, p. 145, Dresden (1934); Hauser, E. A., and Brown, J. R.: Ind. Eng. Chem., in press.
(9) Ostwald, Wo.: J. Phys. Chem. (November, 1938).
(10) Usher, Francis L.: Proc. Roy. Soc. (London) **A125**, 143 (1929).

---

[8] These tests were kindly carried out by Dr. M. W. Jennison of the Department of Biology, Massachusetts Institute of Technology.

[9] This suggestion was originally made by Dr. M. J. Buerger of the Department of Geology, Massachusetts Institute of Technology.

COMMUNICATIONS TO THE EDITOR

THE SOLUBILITY OF CALCIUM BICARBONATE[1]

The idea that passing carbon dioxide into a suspension of calcium carbonate solubilizes part of the salt as soluble calcium bicarbonate is so plausible that no one seems ever to have questioned it. Professor Bancroft reports that he can find no account of an experiment performed to determine whether calcium bicarbonate is in true solution. The point seemed worth considering, because there are natural streams of water which are green (apparently a structural green), yet every ordinary source of the color seems to be ruled out. If calcium bicarbonate were in colloidal suspension, this fact might account for the color.

Actually, there are three, not two, possible cases in this problem: (*1*) carbon dioxide might peptize calcium carbonate as such; (*2*) carbon dioxide might form calcium bicarbonate as a colloidal suspension; (*3*) carbon dioxide might form calcium bicarbonate in true solution. Accordingly, the following experiment in ultrafiltration was carried out.

Carbon dioxide was bubbled through a solution of c.p. calcium hydroxide for several hours. A collodion bag, previously tested for soundness with a Congo red sol, was filled with a portion of the suspension containing 26.8 mg. of calcium, calculated as calcium hydroxide, and immersed in distilled water. After standing overnight, the diffusate and the residue in the bag were analyzed for calcium by titration with hydrochloric acid. Any soluble calcium impurities in the original hydroxide would not interfere in this procedure; moreover, these were negligible in amount. The residue contained 6.2 mg., again calculated as calcium hydroxide, and the diffusate, 20.4 mg. This accounts for 26.6 mg., which differs negligibly from the amount introduced into the bag. The calcium which did not diffuse through seemed to be all in the form of calcium carbonate, since a precipitate settled to the bottom of the bag during the experiment.

The diffusate was examined with a Tyndall beam in direct comparison with an identical tube containing freshly drawn distilled water. The diffusate was optically empty, which made examination with an ultramicroscope unnecessary. Professor Mason of the microscopy staff supervised this examination.

Evaporation of a portion of the diffusate gave a residue which effervesced upon treatment with hydrochloric acid. The diffusate remained clear for several hours after the experiment, when it was discarded.

[1] Received June 13, 1938.

The diffusion experiment was repeated with bags which were dried for a longer time after preparation than the first one before being wetted, and which were soaked in distilled water a shorter time before use. (The first bag was dried for 10 min. and soaked for 12 hr.) This procedure should give smaller pores than the shorter drying period and/or a longer soaking period. Again the calcium diffused through the collodion membrane.

The conclusion is drawn that carbon dioxide converts the major portion of the calcium carbonate precipitated from a solution of calcium hydroxide into calcium bicarbonate, which is in true solution. Very reasonably, people have believed this all along, but it is satisfying to have experimental evidence to support the belief.

STEPHEN S. HUBARD.

Department of Chemistry
Cornell University
Ithaca, New York

THE STANDARD BATTERY (A CORRECTION)[1]

R. B. Elliott and G. A. Hulett in a previous article (J. Phys. Chem. **37**, 489 (1933)) have described the characteristics of standard batteries, but we find that the specifications given do not give a satisfactory electrolyte. The constancy of current and voltage of these batteries depends on maintaining the electrolyte within quite narrow limits. For the combination $Cd_{amg.}|CdSO_4$ $_{solution}$ $Hg_2SO_4|Hg$, Weston (U. S. patent 494,824, April, 1891) found that a cadmium sulfate ($CdSO_4 \cdot 8/3H_2O$) solution, saturated at 4°C., was satisfactory. This combination has a practically zero temperature coefficient of E.M.F. for all ordinary temperatures and furnishes a most satisfactory working standard of E.M.F. It is not an easy matter to make a saturated solution at 4°C., especially with $CdSO_4 \cdot 8/3H_2O$, which has an extraordinarily slow rate of solution. Solubility data show that a solution of $CdSO_4 \cdot 8/3H_2O$ saturated at 4°C. is 43.18 per cent $CdSO_4$ and 56.82 per cent H_2O, so that 100 g. or 100 cc. of water dissolves 112.75 g. of $CdSO_4 \cdot 8/3H_2O$. For the 30-cm. battery described (J. Phys. Chem. **37**, 492 (1933)) one needs 4 liters of water and 4.5 kg. of $CdSO_4 \cdot 8/3H_2O$. The best grade of commercial sulfate, or the cloudy crystals left over from recrystallizing the salt, are entirely satisfactory. Several hours stirring will be necessary to effect solution. Heating above 70°C. is not desirable. Four liters of water and 4.5 kg. of $CdSO_4 \cdot 8/3H_2O$ will give 5.3 liters of solution, and to this is added 25 cc. of C.P. sulfuric acid (density 1.84). This will give an acidity of 0.085 molar sulfuric acid,

---

[1] Received April 18, 1938.

which satisfactorily prevents hydrolysis of the mercurous sulfate and makes the cathode system a reversible equilibrium system.

The remaining specifications (J. Phys. Chem. **37**, 492 (1933)) are quite satisfactory. It may be well to append specifications for a battery made up in a 20-cm. diameter crystallizing dish. Such a battery will deliver 3 milliamperes without variations of more than 1.5 parts in a million, and two such batteries in series are quite satisfactory on a high-resistance potentiometer circuit. A 20-cm. crystallizing dish or flat-bottomed cylinder is satisfactory. The bottom of the dish is covered with mercury to a depth of about 5 mm., some 2 kg. being sufficient. The best grade of mercury is satisfactory, or used mercury may be shaken in a separatory funnel with 1:10 sulfuric acid (1.6 molar) and an excess of mercurous sulfate. Above this layer of mercury one adds the 2.6 liters of electrolyte made up by dissolving 2250 g. of a good grade of $CdSO_4 \cdot 8/3H_2O$ in 2 liters of water and adding 15 cc. of C.P. sulfuric acid (density 1.84). This gives a depth of some 8.5 cm. of electrolyte. The mercurous sulfate depolarizer is easily prepared chemically in a suitable flask or beaker by adding 50 cc. of sulfuric acid (density 1.84) to 500 cc. of water and in this dissolving 200 g. of C.P. mercuric sulfate. Sulfur dioxide is passed through this solution until the mercuric sulfate is reduced and the precipitate of mercurous sulfate begins to turn gray, owing to finely divided mercury. To this system one may add some mercury and stir overnight on a water bath to eliminate the very finely divided mercury due to surface tension effects and also to recrystallize some of the mercurous sulfate. This product is brought into a Büchner funnel, the acid is removed by filtration, and then the solid is washed twice with a minimum of the electrolyte. The cake of sulfate is freed from the filter paper and brought onto the mercury electrode in the electrolyte, where a uniform layer is easily obtained.

The cadmium amalgam anode should be about twice the area of the cathode and may be put into Petri dishes. It is prepared by melting together 110 g. of C.P. cadmium and 1000 g. of mercury; this is poured in equal portions into three 16-cm. Petri dishes. From a glass rod is made a low form of tripod that will hold a Petri dish about 1 cm. above the cathode; on this, separated by a glass triangle, the second Petri dish is placed, and the third on top of this. By suitably protected wires all three of these amalgams are connected with an anode binding post. This gives a total anode area of 603 $cm.^2$, which is quite satisfactory with the 314 $cm.^2$ cathode. The battery must be covered to prevent evaporation from the electrolyte; a glass plate is used and, if necessary, some vaseline.

The above unit is a satisfactory one and may be built up in series or parallel to meet any requirement. It will give a constancy of E.M.F.

or current quite unapproachable by any other combination. When not delivering a current it gives a most satisfactory working standard of E.M.F., but must be calibrated like any Weston cell.

G. A. HULETT.

Department of Chemistry
Princeton University
Princeton, New Jersey

CORRECTION

In the article entitled "Decomposition and Synthesis of Hydrogen Iodide by Alpha Particles" (J. Phys. Chem. **42**, 617 (1938)) the exponent $\frac{6}{7}$ in equation 4, page 624, should be $\frac{4}{5}$.

KEREN GILMORE BRATTAIN.

NEW BOOKS

Organic Chemistry. An Advanced Treatise. Vols. I and II. By HENRY GILMAN, *Editor-in-Chief.* 1890 pp. New York City: John Wiley and Sons, Inc., 1938. Price: $15.00 (complete).

This treatise has been prepared under the editorship of a board composed of Roger Adams, Homer Adkins, Hans Clarke, Carl Marvel, Frank Whitmore, and Henry Gilman, *Editor-in-Chief.* In addition, twenty-two contributors have shared in this undertaking.

The following sentences, taken from the preface, will make clear the general plan of this treatise. "There is a need for a general treatise of organic chemistry suitable for instruction at the graduate level. Such a book must focus attention upon new developments. At best, it can but serve the purpose of the moment and provide a point of departure for unceasing revision. The idea of a collaborative work by specialists in the several branches of the science was developed in 1934. Each author was asked to prepare a chapter dealing with a subject of particular interest to himself. It was hoped to obtain, in this way, an authoritative treatise which would cover most of the important phases of organic chemistry. . . . " "It is planned to revise both volumes at intervals, not only in order to bring the present material up to date, but also to permit the inclusion of new chapters to fill the more conspicuous gaps."

Volume I contains the following chapters: (1) Alicyclic Compounds and the Theory of Strain, by R. C. Fuson (51 pages). (2) Theory of the Structure and Reactions of Aromatic Compounds, by L. F. Fieser (98 pages). (3) Stereoisomerism, by R. L. Shriner, Roger Adams, and C. S. Marvel (256 pages). (4) Organometallic Compounds, by H. Gilman (83 pages). (5) Free Radicals, by W. E. Bachmann (53 pages). (6) Unsaturation and Conjugation, by C. F. H. Allen and A. H. Blatt (67 pages). (7) Open-chain Nitrogen Compounds, by C. D. Hurd (111 pages). (8) Molecular Rearrangements, by E. S. Wallis (82 pages). (9) Comparison of Chemical Reactivity, by H. Adkins (57 pages).

Again quoting from the preface, "For the sake of convenience in revising and expanding the book, the rapidly developing fields of natural products, relationship between physical properties and chemical constitution, valence and resonance have been grouped together in the second volume." Accordingly, Volume II contains the following chapters: (10) Natural Amino Acids, by H. T. Clarke (89 pages). (11) The Chemistry of the Pyrimidines, Purines, and Nucleic Acids, by Treat B. Johnson (70 pages). (12) Alkaloids, by Lyndon Small (96 pages). (13) The Anthocyanins and the Flavones, by Karl Paul Link (24 pages). (14) Carotenoids: The Polyene Pigments of Plants and Animals, by Marston Taylor Bogert (82 pages). (15) The Sterols, Bile Acids, and Related Compounds, by William H. Strain (179 pages). (16) Carbohydrates I, by M. L. Wolfrom (78 pages). (17) Carbohydrates II, by Albert L. Raymond (57 pages). (18) Carbohydrates III—Cellulose, by Emil Heuser (57 pages). (19) Modern Electronic Concepts of Valence, by John R. Johnson (61 pages). (20) Constitution and Physical Properties of Organic Compounds, by Wallace R. Brode and John A. Leermakers (117 pages). (21) Rotatory Dispersion, by P. A. Levene and Alexandre Rothen (67 pages). (22) The Significance of Resonance to the Nature of the Chemical Bond and the Structure of Molecules, by Linus Pauling (71 pages).

A glance at the chapter headings suffices to reveal the scope of this work. A more careful study of the individual chapters will further reveal that the individual authors have devoted considerable time and effort to their tasks. Each chapter opens with an outline and closes with a number of references.

This two-volume treatise should be in the personal library of every graduate student in chemistry.

W. M. Lauer.

Die Theorie der Komplexität und der Allotropie. By A. Smits. 22 x 16 cm.; xii + 372 pp.; 5 plates. Berlin: Verlag Chemie, 1938. Price: 19.50 RM.

Professor Smits in his book gives a full account of his theory of the complexity of the phases of a so-called simple substance (homogeneous allotropy), together with a detailed description of the experimental basis on which it is founded. The theoretical treatment is based on P,T,x diagrams and is illustrated by a number of clear and informative figures. The experimental work described includes a full discussion of the effects of intensive drying, and particular attention is devoted to sulfur trioxide, for which a large amount of experimental data is available. Other important systems are also discussed in sufficient detail to make the book a comprehensive monograph on its subject, which is one of considerable interest. The author has taken pains to make his account clear and understandable, and advanced students will be able to read the book with profit. Full references to literature are given, so that workers in cognate fields will be able to consult the original works. The book is very well produced and can be recommended to physical chemists.

J. R. Partington.

Der Smekal-Raman Effekt. Ergänzungsband, 1931–1937. By K. W. F. Kohlrausch. 15 x 22 cm.; ix and 288 pp. Berlin: Julius Springer, 1938. Price: 24 and 25.60 RM.

If testimony were needed for the industry of chemists and physicists, it is well supplied by this book.

The author states that some four thousand Raman spectra have been investigated, and approximately twelve hundred publications on the subject have appeared since the issue of his "parent" volume in 1931. Both the results themselves and the underlying development of theory are presented with completeness and with precision. In fact, readers of the original book will value the sense of balance which experience has brought about as knowledge has extended.

Perhaps the most valuable parts of these additional pages are those concerned with the optical model of the molecule, and with the "Polarizability theory" of Placzek. The advance in technique is well illustrated by the author's treatment of light sources and filters. In addition, there is a massive amount of tabular matter, admirably arranged.

Physical chemists will be grateful for this supplementary volume; with its help, the task of keeping up-to-date is considerably lightened.

F. I. G. Rawlins.

Kontinuierliche Spektren. By W. Finkelnburg. 24 x 18 cm.; xi and 368 pp. Berlin: Julius Springer, 1938. Price: 33 RM.

This scholarly work is undoubtedly a very valuable contribution to the study of continuous spectra. The author defines as continuous any spectrum not consisting of sharp lines. As a result of this a very wide ground requires to be covered.

This book is not only an admirable introduction to the whole broad field, it is also a complete report upon the present state of our knowledge of the subject. In the broader sense, the study of continua is rapidly acquiring more and more importance for physics, chemistry, engineering, and astronomy, and in order to meet the needs of such diverse possible readers, each chapter is preceded by a preliminary non-mathematical treatment. Summarizing chapters containing brief but complete surveys of the available experimental material are included.

The range covered is very wide and the treatment is thorough. A particularly clear and admirably concise section is that dealing with line widths, the many complex factors being clearly separated. Line broadening is treated as a limiting case of continua, a method of approach leading to important results. The contributions of the author himself in this field are well known.

The book contains much of interest to the chemist, since molecular continua naturally occupy the most important place. In that section which is effectively a report, detailed information is given about all the known diatomic and more complex molecular continua. Chapters upon the continuous spectra of liquids, solutions, and crystals are also included. Constant attention is given throughout to technical applications and to such varied aspects as photochemistry, flames, molecular dissociation, chemiluminescence, after-glows, etc.

The book closes with an extremely valuable list containing over seventeen hundred publications culled from practically every journal devoted to physics, chemistry, and astronomy.

Enough has been said to show that this treatise deserves a very warm welcome.

S. TOLANSKY.

Introduction to Physiological Chemistry. By MEYER BODANSKY. 4th edition. 14.5 x 23 cm.; 686 pp. New York; John Wiley and Sons, Inc., 1938. Price: $4.00.

The fourth edition of this valuable textbook has been brought up-to-date by inclusion of much new material. The generally lucid style has been maintained, and the relation of the science to practical medicine has been kept in mind without in general sacrificing scientific accuracy or rigorousness. The most attractive feature of the book is perhaps the fact that the physiological aspects of chemistry are constantly brought to the fore.

In places the author has, in the opinion of the reviewer, made somewhat too dogmatic assertions on the basis of a review of portions of the literature. It is perhaps inevitable that this would occur in such an ambitious undertaking. An example of this defect occurs on p. 168 where the author outlines in full an application of the Donnan membrane equilibrium theory to the mechanism of the secretion of hydrochloric acid by the gastric glands. He says, categorically, "The soundness of this theory has been confirmed experimentally by Donnan, who has shown that, under such circumstances, hydrochloric acid may actually be "secreted" across a membrane." No modern physiological investigator of gastric secretion subscribes to the view that concentrations of hydrochloric acid such as found in gastric juice could possibly be formed by such a process. The earlier investigator cited was unfortunately unaware of many of the facts in the situation, particularly of the concentrations in plasma and gastric juice of certain constituents. Later in his discussion Bodansky cites some of the evidence which, if critically interpreted, disproves Donnan's contentions.

The biochemistry of the sterols and other phenanthrenes is inadequately treated. For example, the digitalis group of glucosides is discussed under carbohydrates, and although empirical formulas are given for many of them, no reference is made there to their phenanthrene structure. This is certainly the most important aspect of their chemistry from a biological as well as chemical viewpoint. Since their aglucones have similar though less intense actions, it is obvious that the glucoside linkage is a minor point.

These critical details are not presented as serious defects, but to call attention to the fact that improvements are still possible. The mastery of any considerable portion of the subject matter in this book would represent a comprehensive grasp of modern physiological chemistry. The references to original and review literature are ample and well chosen. The index of 30 pages is very useful.

MAURICE B. VISSCHER.

Spectroscopy in Science and Industry. Proceedings of the Fifth Summer Conference on Spectroscopy and its Applications, Massachusetts Institute of Technology, Cambridge, Massachusetts. 134 pp.; 60 fig. New York: John Wiley and Sons, Inc., 1938.

Twenty-seven papers given at the 1937 conference have been collected in this volume in abbreviated form. They range in content from papers on physics, chemistry, metallurgy, biology, medicine, geology, and astronomy to papers on industry, in so far as these various fields use spectroscopy as a tool. Most of the leading American workers in applied spectroscopy are numbered among the authors. As Dr. George R. Harrison points out in the preface, the spectrograph is a tool whose use is rapidly increasing. Hence these conferences and also the present volume are very timely and should be of interest to many workers in scientific research, since they may learn that their own research may be furthered by application of spectrographic methods.

GEO. GLOCKLER.

The Elements of Quantum Mechanics. By SAUL DUSHMAN. 452 pp.; 82 fig. New York: John Wiley and Sons, Inc., 1938. Price: $5.00.

This volume arose from a series of lectures given by the author during the summer of 1932 at the Ohio State University. The notes prepared for these lectures appeared in a series of articles in the *Journal of Chemical Education* (1935 36) and have now been collected and arranged in book form. Dr. Dushman's chief aim is to discuss the latest views of atomic and molecular structure as described in the new quantum mechanics, in such a simple fashion that the average reader, who knows only calculus, can profit by a study of this book. He spares no effort in trying to make the mathematical development clear and understandable. However, in order to grasp the full significance of these newer concepts, it seems that a knowledge of differential equations and methods of solving them is quite necessary. Evidently Dr. Dushman feels the same way about this situation, for in the second chapter he deals in detail with some simple differential equations as, for example, the case of the vibrating string. This procedure serves as an introduction to the famous Schroedinger equation of wave mechanics.

The content of the book is the usual one in such a beginning treatise: the Schroedinger equation, potential barriers, linear oscillator, rigid rotator, the hydrogen atom, van der Waals forces, the perturbation theory, the helium atom, the hydrogen molecule and its rotational and vibrational states, valency bonds, activation and resonance energy and radiation theory. But even so it is always an advantage to study these newer ideas from different authors. A rewording of a given topic by another writer may make its meaning clear to a reader who may have failed to grasp the logic of the development as rendered in the first book studied. Each chapter has an ample list of literature references. This treatise is therefore a welcome addition to the literature of this important subject.

The printing of the many mathematical formulae of most intricate design is excellent, and the figures are executed in admirable fashion. The clarity of expression on the part of the author and the admirable work done by the publishers make this volume welcome also to those workers who already have some knowledge of the newer logic. It has been a distinct privilege and a matter of enjoyment to review this book.

GEO. GLOCKLER.

German for Chemists. By J. H. YOE AND A. BURGER. 537 pp. New York: Prentice-Hall Inc., 1938. Price: $4.50.

It has always been troublesome to find suitable reading material in teaching chemical German to students. This book supplies such material. It presupposes a good grounding in German grammar. The first part consists of practice in sentence structure, and both the German and the equivalent English sentences are given on opposite pages. Following this are sections of reading matter on inorganic chemistry (79 pages), organic chemistry (81 pages), analytical chemistry (61 pages), physical chemistry (62 pages), colloid chemistry (31 pages), chemical technology (64 pages), physiological chemistry (32 pages), and extracts from German books and magazines (32 pages).

The subject matter of each section, including the sentence structure matter, is progressive and is therefore an excellent review of the various fields of chemistry. The book is an excellent one and should find considerable use in teaching scientific German. Unless it is used not earlier than the third year in college it would not have the maximum value in teaching, because the student could not greatly benefit from sections dealing with material that is usually given in chemistry courses ordinarily taken during the last two years of college.

C. A. MANN.

Die Diffusionsanalyse am Blutplasmagel. By RUDOLF BUCHER. 123 pp.; 70 fig. 16 x 24 cm. Basel, Switzerland: Benno Schwabe and Co. Verlag, 1937. Price: 30 Swiss francs.

The author describes a method of transforming the blood plasma into a gel so that Liesegang rings can be obtained if a 5 per cent silver nitrate solution is allowed to diffuse into the potassium dichromate-impregnated gel. The method is applied to different physiological and pathological problems, so that the book is of interest both to colloid chemists and to physicians.

Colloid chemists find in this book one of the most important contributions to the problem of the Liesegang phenomenon made in recent years. The results are given in small type between pages 15 and 36. The author shows that the Liesegang phenomenon can be obtained in a quantitatively reproducible manner if certain experimental factors (e.g., temperature) are rigorously the same. Reproducibility means that the "Latenz Zone" (L. Z.) and the "Latenz Periode" (L. P.) have rather constant values if identical experiments are made with the same blood plasma. (L. Z. means the distance between the surface of the gel where the silver nitrate diffusion starts and the place where the first ring appears. L. P. is the time elapsing between the start of the diffusion and the appearance of the first ring.) This result removes much of the hazardous character inherent in the phenomenon up to now. Using a microtome the author carries out a topographical study of the gels formed. By this method he obtains very remarkable results with respect to the repartition of the crystalline precipitate of silver dichromate throughout the gel and to the size and number of the crystals inside and outside the Liesegang ring zones.

As far as the main purpose of the author is concerned, i.e., the attempt to use his method in physiology and pathology, a definite statement must be reserved until more experimental material has been collected. The data already given show that the method is sensitive for very small changes in chemical composition and the colloid chemical behavior of the blood plasma. L. Z. and L. P. are different for different animals. They differ noticeably if the blood has been taken from different parts of a body. They change with the age of the organism and even with very slight changes in conditions of life. Their statistical mean values are different for the two sexes, etc. This extreme sensitivity of the method is at the same time its strength and its weakness.

It is regrettable that the author writes in a rather circumstantial style and uses without necessity a number of unusual German words and certain colloid chemical expressions of vague meaning.

The book is very well printed and illustrated, and contains numerous colored lates of remarkable technical quality.

WILFRED HELLER.

Chemical Kinetics. By FARRINGTON DANIELS. 6 x 9 in.; 273 pp.; 41 fig. Ithaca, New York: Cornell University Press, 1938. Price: $3.25.

Although this book is based on lectures at Cornell University under the George Fisher Baker Non-resident Lectureship in Chemistry from February to June, 1935, it contains new developments in the field up to 1938. The object of the author has been to give the historical background as well as recent advances in chemical kinetics. In doing this he has followed the tradition of Baker Lectures by drawing illustrations from his own rich experiences in the laboratory.

The lectures have been addressed not only to experts but to students in all of the physical sciences. With this purpose in mind, experimental work has been stressed and mathematical discussion minimized. However, without employing it extensively Professor Daniels emphasizes repeatedly the use which is and can be made of mathematics in solving fundamental chemical problems.

The informal style of the book and the optimistic views of the author toward research are refreshing to the reader. Theoretical kineticists will profit from the review of many well-chosen experiments upon which modern theoretical developments are based. Research ideas abound throughout the book, and workers in other fields may see where chemical kinetics could help in solving their problems. To students and beginners in research this book will be especially inspiring. Unsolved research problems are so interspersed with seemingly equally difficult problems which have been worked out, that one is led to feel that the barriers to their ultimate solution are by no means insurmountable.

The first half of the book gives the elementary principles of kinetics as well as some details of experimental technique, while the second half is devoted to the use which may be made of such research tools as photochemistry, electrical activation, infrared spectroscopy, and isotopic tracers in this field.

F. E. BLACET.
W. A. NOYES, JR.

ELECTROLYTE COAGULATION AND COEFFICIENT OF ELECTROLYTE ACTIVITY[1]

WOLFGANG OSTWALD

University of Leipzig, Leipzig, Germany

Received July 1, 1938

I. INTRODUCTION

I believe that a colloid chemist, if asked today to explain the coagulation of a lyophobic hydrosol by electrolytes, will make a rather unhappy face. Most presumably, when explaining simple and well-investigated cases, as, for example, the flocculation of arsenic trisulfide sols with neutral salts, a conscientious colloid chemist will even voice a warning to the effect that this matter is not as simple as it looks.

We can summarize the most important steps in the theory of electrolyte coagulation of feebly solvated sols in abbreviated form by the following headings:

1. Neutralization of charge and equivalent ion exchange.
2. Critical potential.
3. Adsorption as the determining variable of coagulation.
4. The electrokinetic, and not the electrochemical, potential is determinative.
5. Density of charge instead of magnitude of charge.
6. Compression of the double layer.

The sequence of these headings corresponds approximately to the historical development of the theory. We all know that at least the first four assumptions mentioned are wrong. The electrokinetic potential or its reduction is also not determinative for coagulation, as we are finding more and more cases where the rate of electrophoretic migration increases just prior to coagulation (Tuorila, Lagemann, Kruyt and collaborators, Bull and Gortner, Mukherjee, and others). I have nothing to say against the last two assumptions. They may be right; however, they are insufficient. They, too, have so far been unable to give a fairly comprehensive quantitative theory of coagulation. The newest development of the theory, for example, that by the Dutch colleagues (Verwey, Hamaker, etc.), becomes continually more complicated and speculative.

---

[1] Presented at the Fifteenth Colloid Symposium, held at Cambridge, Massachusetts, June 9-11, 1938.

If a professor is obliged to discuss this unsatisfactory condition of the theory of coagulation for thirty or more years, in every term of the academic year, then it may easily happen that he becomes more and more impatient. Either he becomes resigned or he commences to curse. The latter course is in general more fruitful. Such mental discontent leads one to the experiment of disregarding for the time being the different approaches of the existing theory, or even to forget them entirely, and to consider the possibility of coming closer to the problem in a way entirely *different* from any so far used. Such radical doubts as to the suitability of the theoretical assumptions existing lead, for example, to the following considerations:

A sol is composed not only of a disperse part but also of its dispersion medium. So far, the properties of the disperse part, i.e., of the micelles, have always stood in the foreground of the theory. Their composition, magnitude of charge, their potential, their double layer and its changes, etc., were the center of the theories advanced. The rôle of the dispersion medium was of decidedly less importance. The dispersion medium was considered in the theory primarily as the carrier of the micelles and of the stabilizing and coagulating ions. Possibly the different evaluation of the rôles played by the disperse part and the dispersion medium is incorrect. Possibly we are going a step further when, contrary to prior methods, we put the properties of the dispersion medium in the foreground.

The dispersion medium of a hydrosol is without exception an electrolyte solution both in the condition of stability and in the condition of coagulation. Our concepts of the inner structure of an electrolyte solution are today somewhat at variance with those of the days of van't Hoff and Arrhenius. We assume that such a solution is *a priori* highly dissociated and that the ions in the solution medium are present in a statistic and kinetic type of ionic lattice. In a salt solution there exists, therefore, a certain segregation of the ions. The factor, i, in the concentration equation of van't Hoff and Arrhenius has today been substituted, following the procedure of G. N. Lewis, by the factor f, the coefficient of activity. Instead of referring to the ion concentration ic, we talk about the activity, $fc = a$, where f represents the coefficient of activity. We can either determine f thermodynamically or evaluate the coefficient theoretically, in accordance with the physical theory of Milner-Debye-Hückel. Just as the numerical factor of van't Hoff received the physical significance of the degree of dissociation, we can explain the coefficient of activity from a physical point of view, although it also was first introduced as a numerical factor only. It is a measure of the interionic attraction and therefore of the inner stability of the lattice. These ionic forces will be weaker, the more the value of f in extreme dilutions approaches unity.

From this standpoint a sol exhibits a certain resemblance to a mixed crystal, but of course only a statistical one. The comparatively giant micelles are built into the highly disperse ionic lattice. If we have a stable sol, the interionic forces will carry these micelles. If the sol is coagulated by dialysis, the interionic forces become too weak to carry the particles any longer. The mutual lattice is torn apart. If the sol coagulates by an increase in electrolyte concentration, a kind of "auto-cleansing" of the statistical ionic lattice takes place. The interionic forces become so large that they drive the micelles together and expel them. It is not the micelles which coagulate owing to mutual attraction; the dispersion medium coagulates the micelles by aggregation and expulsion from the ionic lattice.

This, unquestionably, is a different picture from the usual one. It is now my purpose to demonstrate to you that one can go a step further on this basis than has been done so far, and especially can one actually obtain *quantitative* related functions for coagulation.

II. THE COEFFICIENT OF ACTIVITY

In the following we shall consider only coagulation by typical neutral salts and discard, for example, flocculation by H^+ and OH^- ions or heavy-metal salts. Furthermore, we want to keep in mind that the flocculation values so far have been rather inaccurate data, owing to the difficulty of expressing a time reaction with a single figure. Finally, we shall restrict our discussion to truly lyophobic sols, in which the so-called "ion spreading" between ions of equal valency is experimentally negligible. We shall therefore select a specific type, for example, the negative arsenic trisulfide hydrosol.

According to the briefly sketched idea, it is the coefficient of activity itself and not the activity, the product of f and c, which is determinative. The coefficient of activity referring to *one* ion type, can, according to the physical theory for water at 18°C., be defined as

$$-\log f^+ = 0.5z_+^2\sqrt{u}$$

where z represents the valency and u the ionic strength. $u = 1/2(m_+ \cdot z_+^2 + m_- \cdot z_-^2)$, where m_+ = molality of the cation, z_+ the valency of the cation, m_- the molality of the anion, and z_- the valency of the anion. *Both* ions are therefore taken into consideration. The value of f^+ varies greatly with the value of both ions and with concentration, as can be seen in table 1.

In the first column the type of salt is given, in the second the value for the molality of the salt solution, which corresponds to a *constant* value for $f^+ = 0.70$. We find that, depending on the structure and the valence of the ions, the coefficient of activity of very different concentrations (molalities) corresponds to the same value for f^+, i.e., the same intensity of interionic forces. The relative figures in the last column will remind a colloid chemist vividly of the relative coagulation values for salts of different valencies. In these cases too, as is known, one needs decidedly smaller concentrations of polyvalent cations for coagulation, and here, too, the counter ions of the same valence have a certain, although decidedly smaller, influence on the coagulation value.

TABLE 1

TYPE OF SALT*	MOLALITY (m) AT $f^{+} = 0.70$	m (RELATIVE)
+ −		
1 - 1	0.096	100,000
1_2 - 2	0.068	70,800
1_3 - 3	0.050	52,000
1_4 - 4	0.042	43,800
2 - 1_2	0.0022	2,290
2 - 2	0.0017	1,770
3 - 1_3	0.00022	229
3_2 - 2_3	0.00017	177
3 - 3	0.000145	151
4 - 1_4	0.000040	42
6 - 1_6	0.000004	4

* The subscripts represent the number of ions present in a molecule.

TABLE 2

Arsenic trisulfide sols

(H. Schulze: J. prakt. Chem. 25, 431 (1882))

TYPE OF SALT	NUMBER OF SALTS	$m_{\pm}$ (MEAN VALUE)	f^{+}	$f^{\pm}$
1 - 1	11	0.109	0.69	0.69
1_2 - 2	5	0.0578	0.71	0.51
1_3 - 3	1	0.0375	0.73	0.39
1_4 - 4	1	0.0405	0.69	0.23
2 - 1_2	5	0.00172	0.72	0.85
2 - 2	6	0.00246(!)	0.63*	0.63
3 - 1_3	3	0.000176	0.72	0.89
3_2 - 2_3	1	0.000112	0.74	0.81

Mean value of f^{+} (with *) = 0.71 ± 0.03 (about 4 per cent).
Mean value of f^{+} (without *) = 0.70 ± 0.55 (about 8 per cent).

I have checked many hundreds of coagulation values to see whether there exists a quantitative relation between coefficient of activity and coagulation value. Tables 2, 3, 4, 5 and 6 give a few examples thereof.

In these tables m_k represents the coagulating molality. To eliminate the influence of the cation spreading, only the mean values for m_k of one valency class of ions were used in the calculation. Where more than one ion is present in the molecule, as, for example, in potassium sulfate, the molar coagulation concentration only refers as usual to *one* cation ($= 1/2\ K_2SO_4$).

TABLE 3

Arsenic trisulfide sols

TYPE OF SALT	NUMBER OF SALTS	m_k (MEAN VALUE)	f^+
(S. E. Linder and H. Picton: J. Chem. Soc. 67, 63 (1895))			
$1 - 1$	13	0.0954	**0.70**
$1_2 - 2$	4	0.0316	**0.78**
$2 - 1_2$	21	0.00128	**0.75**
$2 - 2$	7	0.00186(!)	**0.67***
$3 - 1_3$	2	0.000099	**0.78**
$3_2 - 2_3$	6	0.000112	**0.74**
(H. Freundlich: Z. physik. Chem. 44, 135 (1903))			
$1 - 1$	5	0.0502	**0.77**
$1_2 - 2$	1	0.0164	**0.83**
$2 - 1_2$	1	0.000672	**0.82**
$2 - 2$	7	0.000810	**0.77**
$3 - 1_3$	2	0.000093	**0.78**
$3_2 - 2_3$	1	0.000046	**0.82**

Mean value of $f^+ = 0.80 \pm 0.03$ (3.8 per cent).

TABLE 4

Antimony trisulfide sols

TYPE OF SALT	NUMBER OF SALTS	m_k (MEAN VALUE)	f^+
(H. Schulze: J. prakt. Chem. 27, 328 (1883))			
$1 - 1$	2	0.129	**0.66**
$1_2 - 2$	2	0.0732	**0.68**
$2 - 1_2$	4	0.00216	**0.69**
$2 - 2$	2	0.00402(!)	**0.63(!)**
$3 - 1_3$	1	0.000247	**0.67**
(A. Iwanitzkaja-Orlowa: Kolloid-Beihefte 18, 1 (1923))			
$1 - 1$	3	0.0293	**0.82**
$2 - 1_2$(chlorides)	4	0.000362	**0.86**
$2 - 1_2$(nitrates)	4	0.000475	**0.84**
$3 - 1_3$	3	0.000023	**0.88**

The tables, which could be increased in number by dozens, demonstrate that the coefficient of activity actually represents approximately the measure for the flocculation power of neutral salts in hydrophobic sols. *Electrolyte-containing dispersion media will flocculate at approximately the same value for the coefficient of activity of the dominating ions.* This is the first quantitative consequence of this new method of consideration.

TABLE 5

Influence of counter ions on arsenic trisulfide sols

(Wo. Pauli and E. Valkó)

AUTHOR	CONCENTRATION OF SOL IN GRAMS PER LITER	SALT	FORMULA WEIGHT IN EQUIVALENT MILLIMOLES PER LITER	$m_{\pm}$	f^{+}
Freundlich................	1.8	KCl	49.5	0.0495	**0.774**
		K_2SO_4	65.5	0.0328	**0.774**
		$K_4Fe(CN)_6$			
Ghosh and Dhar...........	3.7	KCl	85	0.085	**0.72**
		K_2SO_4	100	0.050	**0.73**
		$K_4Fe(CN)_6$	185	0.046	**0.68**
Weiser and Nicholas........	6.0	KCl	33.2	0.0332	**0.811**
		K_2SO_4	43.5	0.0218	**0.812**
		$K_4Fe(CN)_6$	71.2	0.0178	**0.791**

TABLE 6

Ferric oxide sols

TYPE OF SALT	NUMBER OF SALTS	$m_{\pm}$ (MEAN VALUE)	f^{-} (POSITIVE SOL)
(H. Freundlich: Z. physik. Chem. **44**, 135 (1903))			
1 - 1	5	0.01175	**0.88**
1_2 - 2	4	0.000296	**0.87**
2 - 2	2	0.00021	**0.88**
(H. Freundlich, Joachimsohn, and Ettisch: Z. physik. Chem. **141**, 249 (1929))			
1 - 1	1	0.013	**0.88**
1_2 - 2	1	0.00039	**0.86**
1_3 - 3	1	0.000031	**0.87**
1_4 - 4	1	0.000015	**0.80**

III. QUANTITATIVE RELATION BETWEEN COAGULATION VALUE AND VALENCE

If this relation stands, then automatically, or better, mathematically, a new quantitative formulation of the Schulze–Hardy valence rule results. The former mathematical formulations of this rule, as, for example, those of Whetham, Robertson, and also myself have already been found insufficient, for the reason that they did not consider the influence of the equally charged counter ions. From the relation f_k^+ = constant and the equation defining the coefficient of activity, we now obtain for the molecular flocculation power ($1/m_k$) the relation:

$$\frac{1}{m_k} = \frac{z_+^5(z_+ + z_-)}{2K}$$

TABLE 7

Arsenic trisulfide sols

TYPE OF SALT	$1/m \cdot n_+$ (RELATIVE)	$1/m \cdot n_+$ (MEAN VALUE; EXPERIMENTAL)
$1 - 1$	1	1
$1_2 - 2$	1.5	1.65
$1_3 - 3$	2.0	2.5
$1_4 - 4$	2.5	2.8
$2 - 1_2$	48	51
$2 - 2$	64	+47
$3 - 1_3$	486	573
$3_2 - 2_3$	608	938
$4 - 1_4$	2,560	1,720
$6 - 1_6$	27,216	14,050

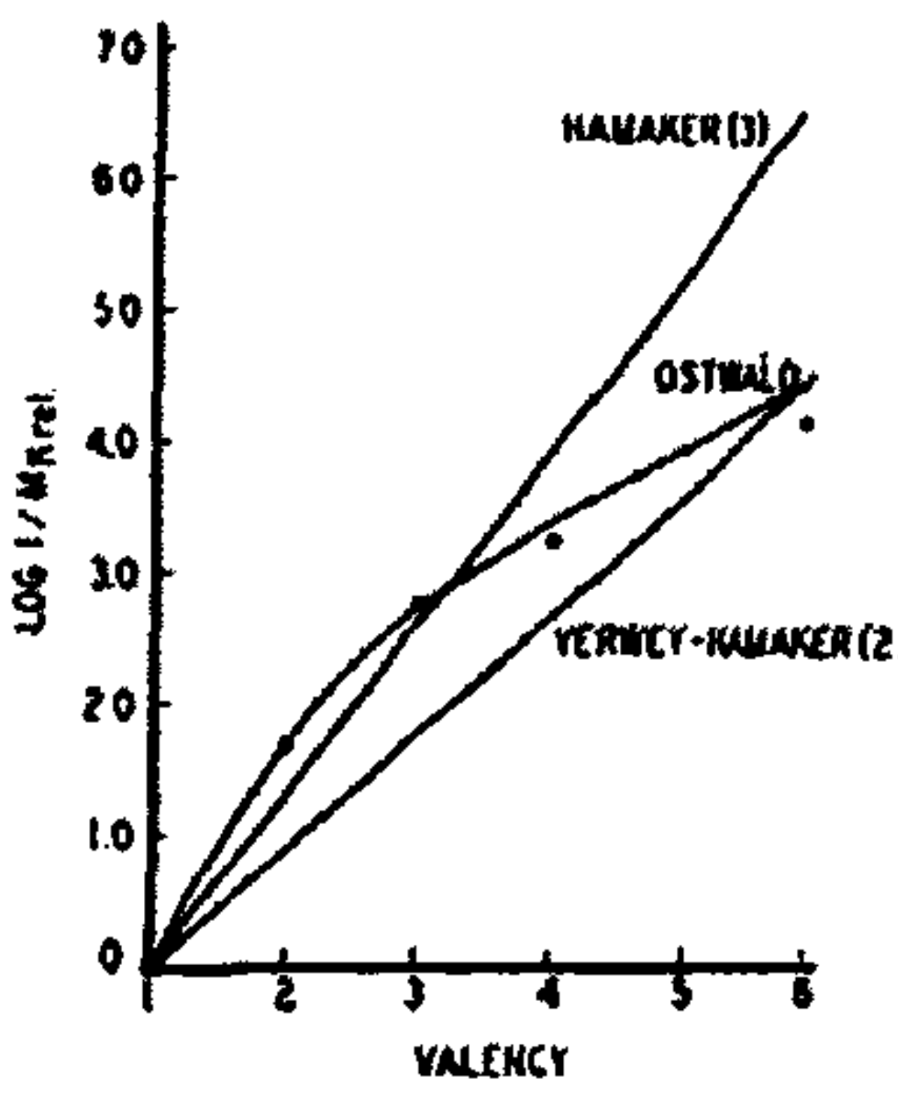

FIG. 1

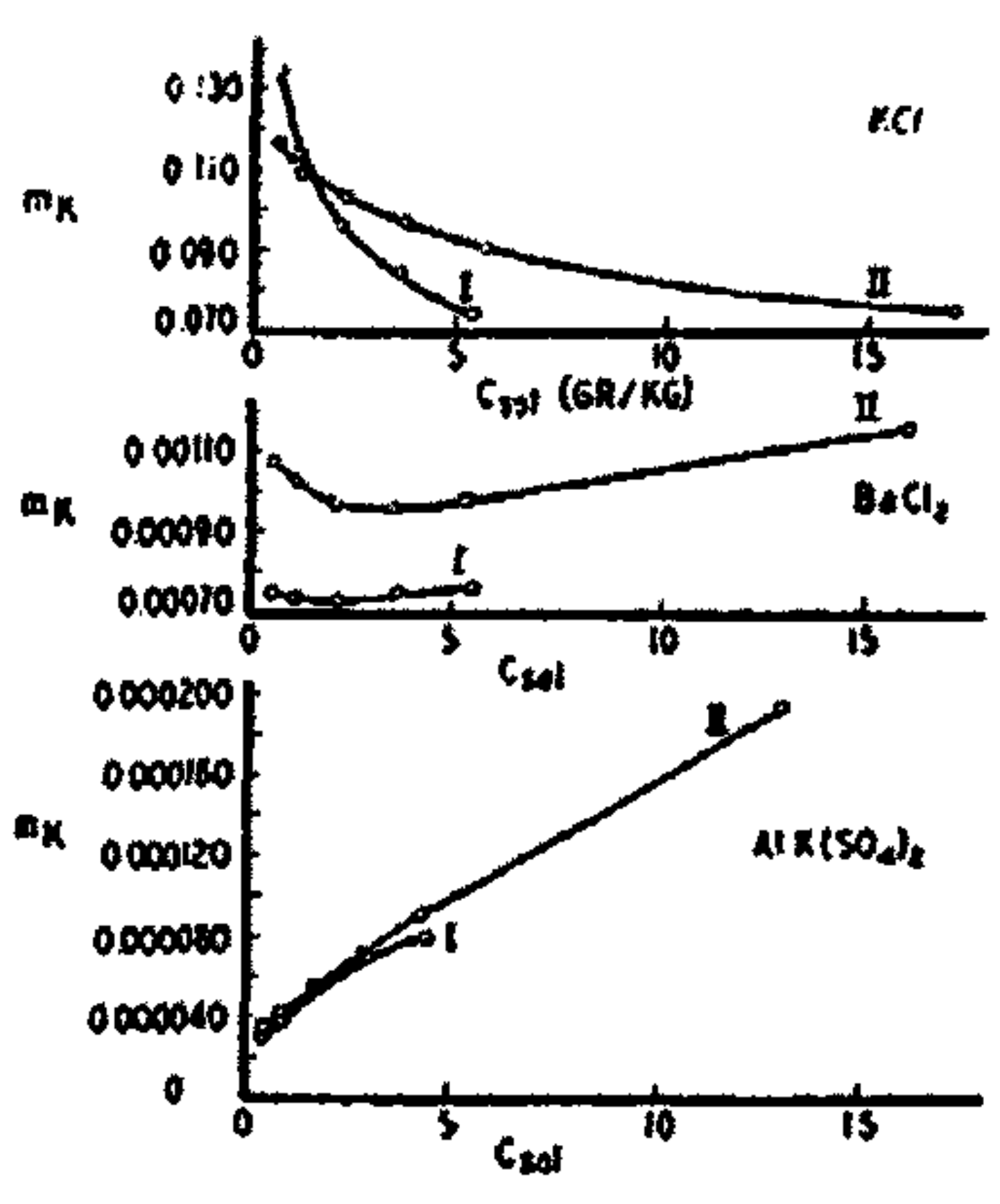

FIG. 2

FIG. 1. Relation between coagulation value and valence
FIG. 2. Effect of concentration of sol on the coagulation value

Here we only have one constant which is characteristic for the sol, whereas the numerical factor 2 = 1/0.50, the characteristic constant of the coefficient of activity equation for water at 18°C., is independent of the sol. We find that in this equation the valence of the counter ions is also considered.

Table 7 shows how closely the new formulation of the Schulze-Hardy rule corresponds to experiment. Mean values taken from the above tables on measurements of arsenic trisulfide sols have been used.

Recently, Verwey and Hamaker have also evaluated quantitative relations between coagulation value and valence, but in rather speculative ways. These results are graphically demonstrated in figure 1. The valence is given on the abscissa and on the ordinate the logarithm of $1/m_k$. The circles represent the experimental mean values of table 7 taken from work on arsenic trisulfide sols. One realizes that the relations as postulated by Verwey and Hamaker are principally in error, notwithstanding the many assumptions which had to be made *ad hoc*. The relation between the logarithm of the coagulating power and the valence cannot be represented by a straight line, as was done by Verwey and Hamaker, but only by a curved one, as it results directly, for example, from the theory of the coefficient of activity.

IV. THE EFFECT OF SOL CONCENTRATION ON THE COAGULATION VALUE

It is known that the concentration of the sol (C_{sol}) influences the coagulation value, and, according to the valence of the dominant ion, frequently in a different way. The most important case, the basis for the so-called Burton's rule, can be demonstrated by figure 2.

When dealing with a monovalent cation, the coagulation molality decreases with increasing sol concentration; in the case of trivalent or higher valent cations, it increases. Weiser and others have demonstrated that exceptions to this course are known, as, for example, with chromic hydroxide and ferric hydroxide sols. I do not intend to discuss in this paper the theory of these relations and should like to refer to a paper published elsewhere.[2] From an experimental point of view it should be pointed out that, according to recent investigations in my laboratory undertaken at extreme dilutions of the sols, all curves bend upward. In the case of infinitely dilute sols, one would therefore need infinitely concentrated salt solutions to obtain coagulation, an unquestionably obvious conclusion.

How will these curves look if we plot the coefficient of activity at the coagulation point against the sol concentration, instead of the coagulation molalities? Figure 3 gives a picture of this new method of graphical representation. First of all, we can place all curves in one coördinate system, and all curves approach each other with increasing sol concentration. Figures 4 and 5 give further examples.

We find that with increasing sol concentration the curves approach a

[2] Kolloid-Z. 80, 304 (1937).

common point. *The rule that the coefficient of activity is a constant in the case of coagulation will be more exact the more concentrated the sol.* As a result of very recent investigations, which have been undertaken with a

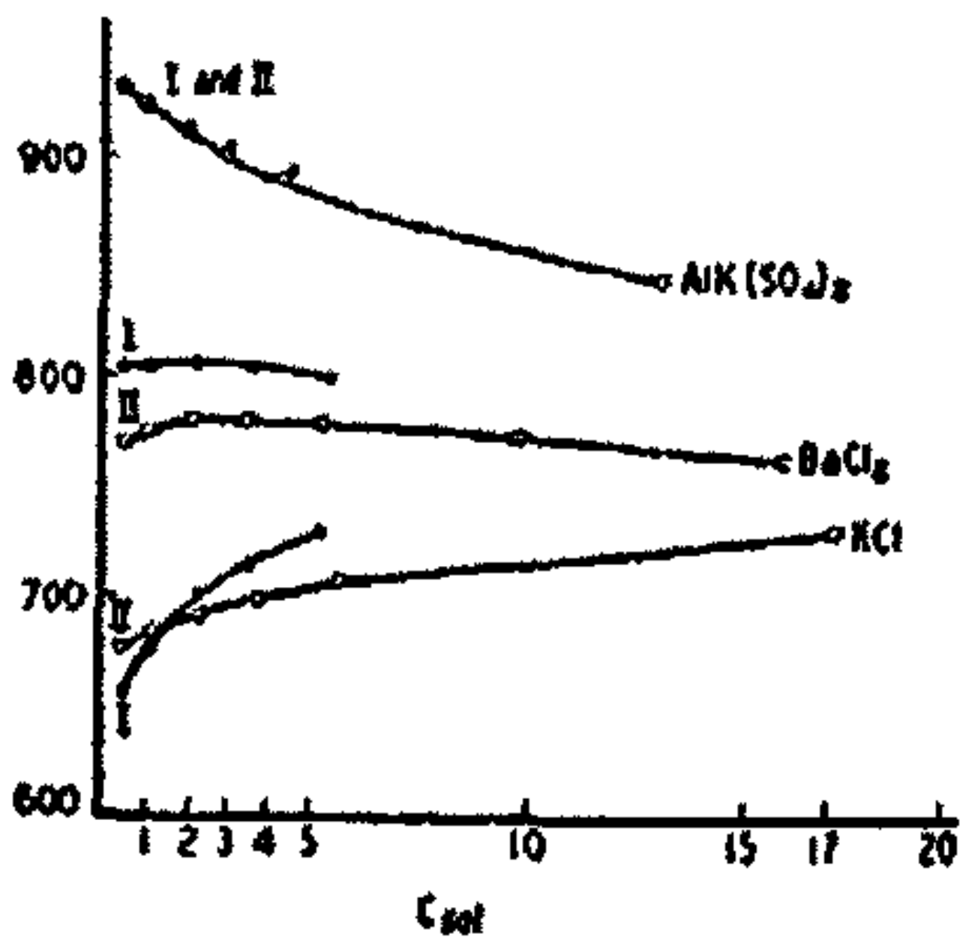

FIG. 3

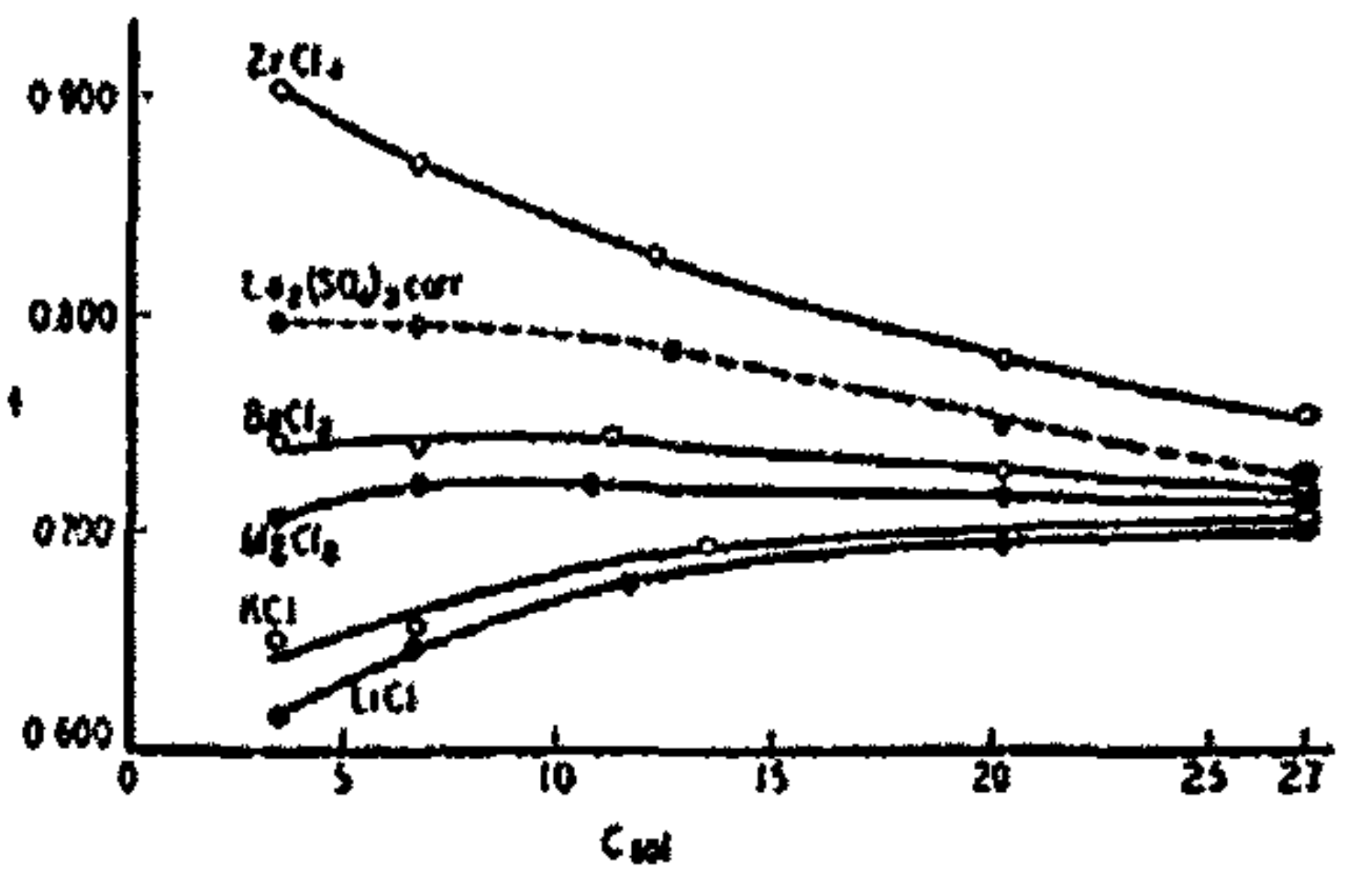

FIG. 4

FIG. 3. Plot of coefficient of activity at the coagulation point against sol concentration.

FIG. 4. Plot of coefficient of activity at the coagulation point against sol concentration.

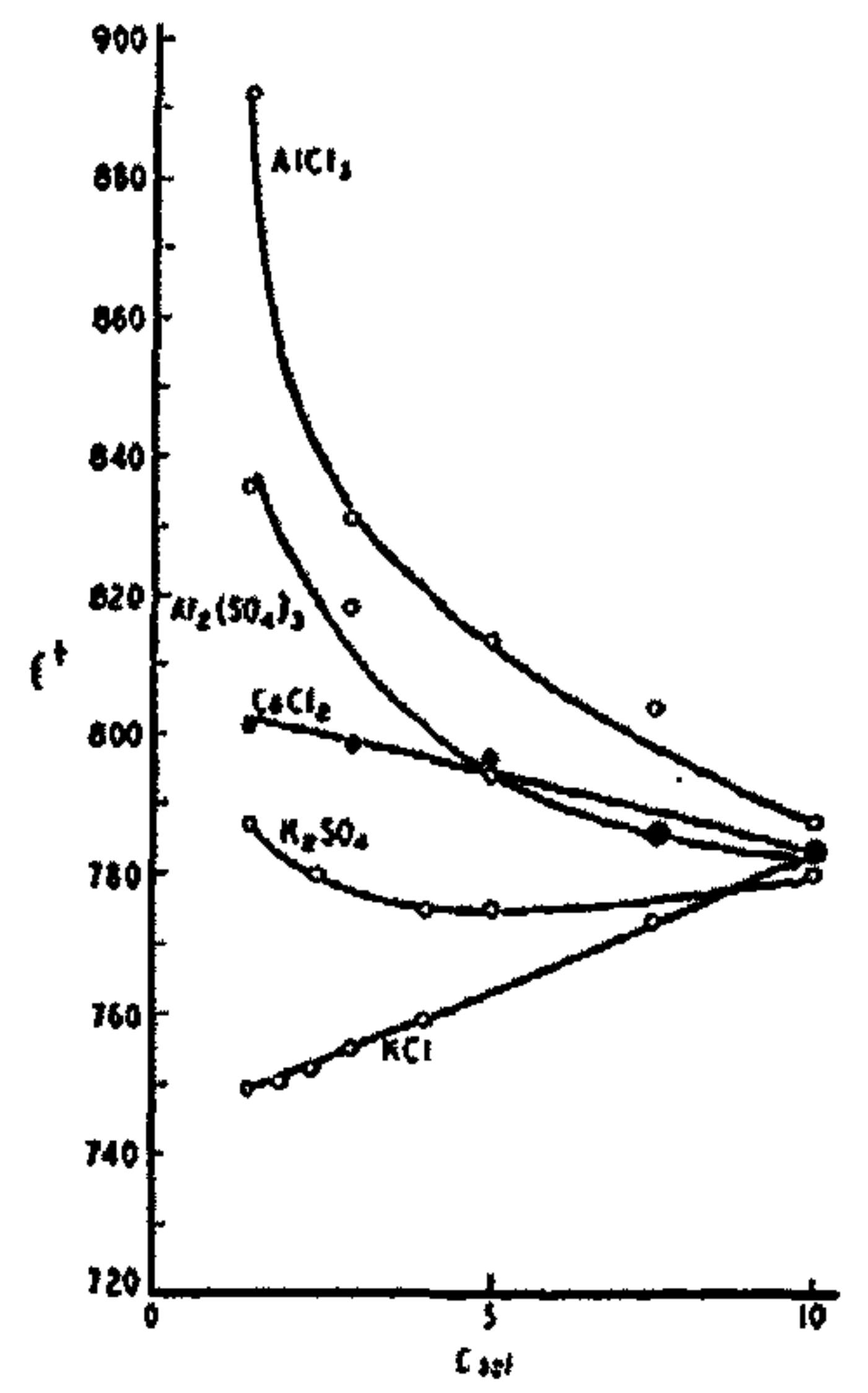

FIG. 5

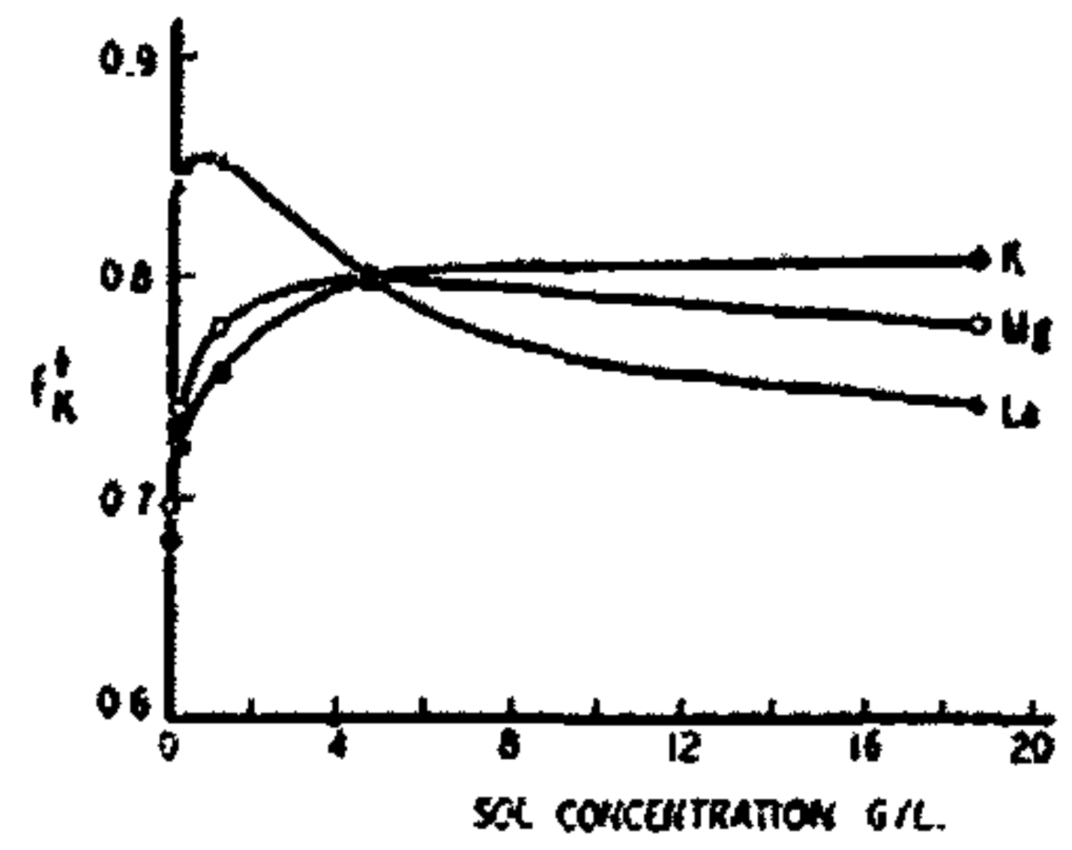

FIG. 6

FIG. 5. Plot of coefficient of activity at the coagulation point against sol concentration.

FIG. 6. Plot of coefficient of activity at the coagulation point against sol concentration for arsenic trisulfide sols. Appearance of "over optimal" sol concentration.

special technique for determining coagulation points, there seemed to exist "over optimal" sol concentrations, as is demonstrated in figure 6, using arsenic trisulfide sols. Admittedly, so far only one single case of this type has been found, so that it is premature to decide whether such an intersecting of the curves is a general rule.

V. PHENOMENON OF DOUBLE COAGULATION

Every colloid chemist is familiar with the phenomenon of double coagulation, or the so-called "irregular series" of coagulation. Table 8 represents a common example of a mastic sol. If one successively increases the concentration of a salt with polyvalent cations (negative sols), one obtains two zones of coagulation and three coagulation values: f_{k1}, f_{k2}, and f_{k3}. If one considers that every hydrosol needs a minimum ion concentration for its stability which cannot be reduced below a certain value without coagulation by dialysis, then we have a fourth value of coagulation, f_{k0}, whose molality is very low, or, in other words, whose coefficient of activity must be close to unity. This double coagulation is, as known, caused by reversal of charge of the sol, owing to a higher concentration of polyvalent ions.

TABLE 8

Coagulation values obtained in treating a gum mastic sol, concentration 0.688 g. per liter, with aluminum chloride

(Boutaric)

m	RESULTS	COAGULATION VALUES
0.0000040	Stable	
0.0000067	Stable	$f_{k1}^{+} = 0.936$
0.0000075	Coagulated in 3 min.	0.933
0.0000100	Coagulated instantly	**0.923**
0.0000125	Coagulated in 1 min.	
0.0000250	Coagulated in 5 min.	
0.0000300	Coagulated in 2 hr.	$f_{k2}^{-} = 0.995$
0.0000400	Stable	0.994
0.0000750	Stable	
0.000150	Coagulated in 2 hr.	
0.000310	Coagulated in 10 min.	
0.000620	Coagulated in 2 min.	$f_{k3}^{-} = 0.960$
0.00125	Coagulated instantly	**0.944**
0.00500	Coagulated instantly	
0.0200	Coagulated instantly	
0.0750	Coagulated instantly	

To the best of my knowledge, no one has ever brought up the question whether these four different molalities of coagulation happen to be related to each other in some quantitative way. Let us consider figure 7 for this purpose. As abscissa we have plotted the logarithm of molality, as ordinate the two individual coefficients of activity, f^{+} and f^{-}. We have

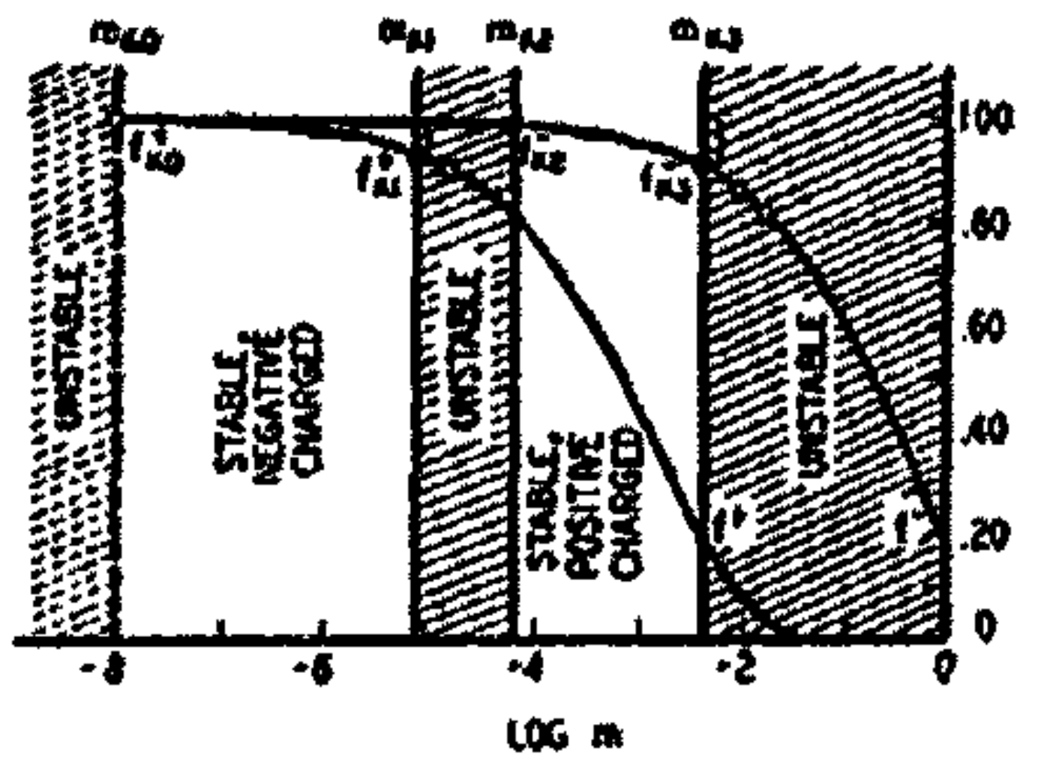

Fig. 7

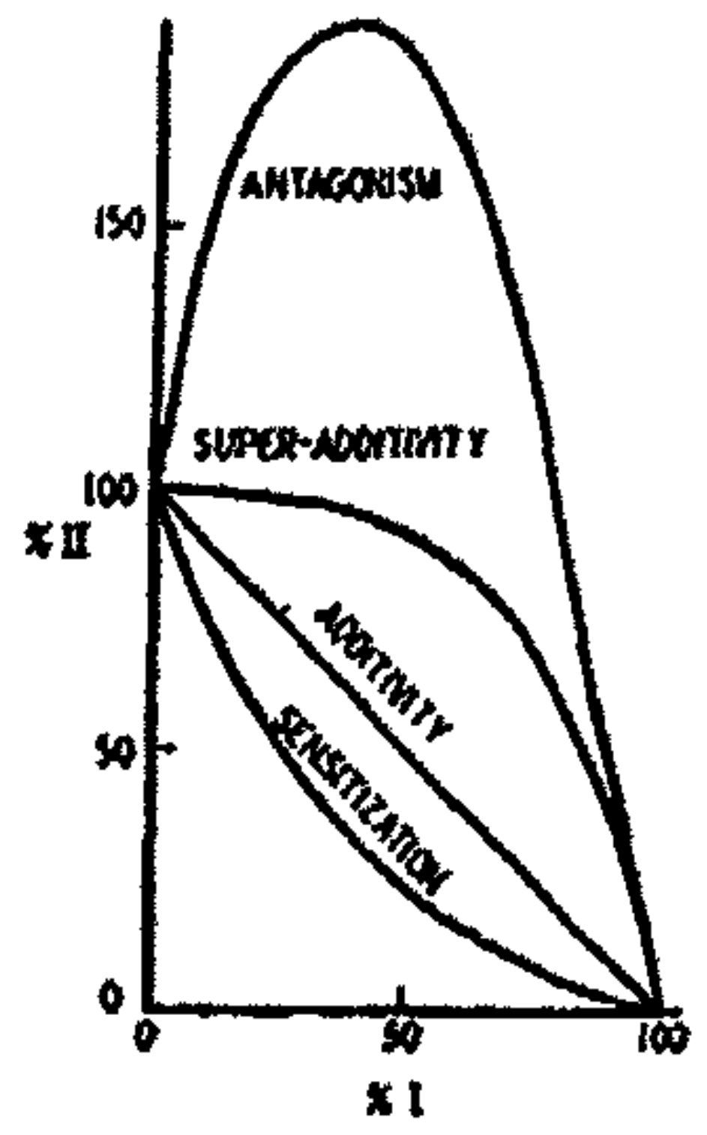

Fig. 8

Fig. 7. Plot of log of molality against f^+ and f^-
Fig. 8. Coagulation by salt mixtures

TABLE 9

Coagulation of a gum mastic sol

(Buxton, Teague, and Shaffer)

m	RESULTS	
	$FeCl_3$	
0.0000208	No coagulation	
0.0000557	No coagulation	
0.0000833	Coagulation	$f^+_{k1} = 0.79$; $f^-_{k2} = 0.985$
0.000163	No coagulation	
0.0333	Coagulation	$f^-_{k3} = 0.74$
	$Fe(NO_3)_3$	
0.0000333	No coagulation	
0.0000557	Coagulation	$f^+_{k1} = 0.83$
0.0000833	Coagulation	$f^-_{k2} = 0.985$
0.000166	No coagulation	
0.00833	Coagulation	$f^-_{k3} = 0.86$
	$AlCl_3$	
0.0000833	No coagulation	
0.000166	Coagulation	$f^+_{k1} = 0.72$
0.000333	Coagulation	$f^-_{k2} = 0.971$
0.000666	No coagulation	
0.0333	No coagulation	(0.74)
0.0833	Coagulation	$f^-_{k3} = 0.63$

two zones of stability and three zones of instability. The two S-curves demonstrate the changes of the two coefficients of activity with the logarithm of concentration. Let us consider the points where the S-curves intersect with the stability zones. We find that always two coagulation points belong together: f_{k0} and f_{k2} on one hand, and f_{k1} and f_{k3} on the other hand. Two of these points lie at the same height. That means nothing else but that at double coagulation the four coagulation values are quantitatively related to each other. *The value of the positive coefficient of activity at the coagulation point* of a negative sol equals the value of the negative coefficient of activity at the point of coagulation of the charge-reversed positive sol, etc.

TABLE 10

Formol gold, undialyzed, treated with aluminum chloride

(Fuchs and Pauli: Kolloid-Beihefte **21**, 412 (1925))

m	RESULT AFTER 24 HR.		
0.00002	No noticeable change		
0.00006 0.00007 0.00008	Violet, not completely coagulated Coagulated	m_{k1}	$f_{k1}^{+} =$ **0.822** = **0.809** = **0.797**
0.0003 to 0.002	Red-violet color to Red color	m_{k2}	$f_{k2}^{-} = 0.972$
0.003	Red		
0.018	Blue, coagulated	m_{k3}	$f_{k3}^{-} =$ **0.804**

$$-\log f^{+} = 4.5\sqrt{6m}; \ -\log f^{-} = 0.5\sqrt{2m}$$

TABLE 11

Formol gold sol

(Boutaric and Dupin)

SALT	m_{k1}	f_{k1}^{+}	m_{k2}	f_{k2}^{-}	m_{k3}	f_{k3}^{-}
$AlCl_3$	0.00000319	**0.956**	0.00026	0.977	0.00095	**0.951**
$ThCl_4$	0.00000758	**0.956**	0.000444	0.962	0.000823	**0.949**
$FeCl_3$	0.00000146	**0.911**	0.000243	0.975	0.001625	**0.937**

The last two figures have demonstrated that this coefficient of activity rule is supported by facts. The examples in tables 9, 10, and 11 might further substantiate this.

To be able to test the equality of f_{k0} and f_{k2} more accurate data in regard to the electrolyte content at dialytic flocculation are needed. From the available experimental values for f_{k2} one can deduce that these dialytic coagulation values must be, in full accord with experience, extremely small.

VI. COAGULATION BY SALT MIXTURES

A group of the most peculiar phenomena are found in the coagulation by salt mixtures. We place the coagulation value of a monovalent salt at 100 and also the coagulation value of a single trivalent salt. If we now examine the coagulating power·of mixtures of these two salts we very rarely obtain additivity. As figure 8 demonstrates, we find either sensitization, super-additivity, or antagonism. This latter effect is particularly striking. The coagulation molality of the mixtures can be many hundreds above the 100 per cent for the individual values. The reason for this anomaly is not yet clear. Might it be possible that the proposed theory would also give us some new ideas as to these phenomena?

Naturally one can also evaluate the coefficient of activity of salt mixtures. I am refraining from reproducing here the somewhat cumbersome formulas and prefer simply to give some actual examples. If we look at a mixture of equimolal solutions, we have, for example:

$$0.001\ m\ \mathrm{KCl};\ {}_{\mathrm{I}}f^{+} = 0.964$$

$$0.001\ m\ \mathrm{AlCl_3};\ {}_{\mathrm{II}}f^{+} = 0.449$$

$$0.001\ m\ \mathrm{KCl} + 0.001\ m\ \mathrm{AlCl_3};\ {}_{\mathrm{I+II}}f^{+} = \mathbf{0.709}$$

The coefficient of activity of the mixture therefore lies *between* the values for the individual coefficients.

If we now look at a mixture of both salts, of *unequal* molality but of *equal coefficient of activity*, we obtain the following figures:

$$0.0612\ m\ \mathrm{KCl};\ {}_{\mathrm{I}}f^{+} = 0.750$$

$$0.000126\ m\ \mathrm{AlCl_3};\ {}_{\mathrm{II}}f^{+} = 0.750$$

$$0.0612\ m\ \mathrm{KCl} + 0.000126\ m\ \mathrm{AlCl_3};\ {}_{\mathrm{I+II}}f^{+} = \mathbf{0.914}$$

In such a mixture we obtain a material increase of the joint coefficient of activity. According to the first-mentioned coefficient of activity rule, this means that when using such mixtures a much higher molality is necessary for coagulation than would correspond to additivity. The appearance of ion antagonism in such coagulation experiments is also contained in the new theory.

Figure 9 gives only one example from a large number of theoretical calculations available, namely, the combination of a monovalent salt with a polyvalent one. We can see that the antagonism becomes more pronounced the larger the valence difference between the two salts. In a mixture of two salts of the same valence no antagonism exists. These, as well as further theoretical postulates, are in full accord with experiment. Figures 10 and 11 give two examples of the attempt to evaluate experimental cases quantitatively by the new theory. That we have not obtained better agreement is due to the fact that the sols were too dilute, so that the first coefficient of activity rule could not be exactly fulfilled. Compare, for example, the differences in the f_k values in figure 10. Furthermore, the location as well as the height of the maximum are extremely sensitive towards minute variations of the proportions in the mixture.

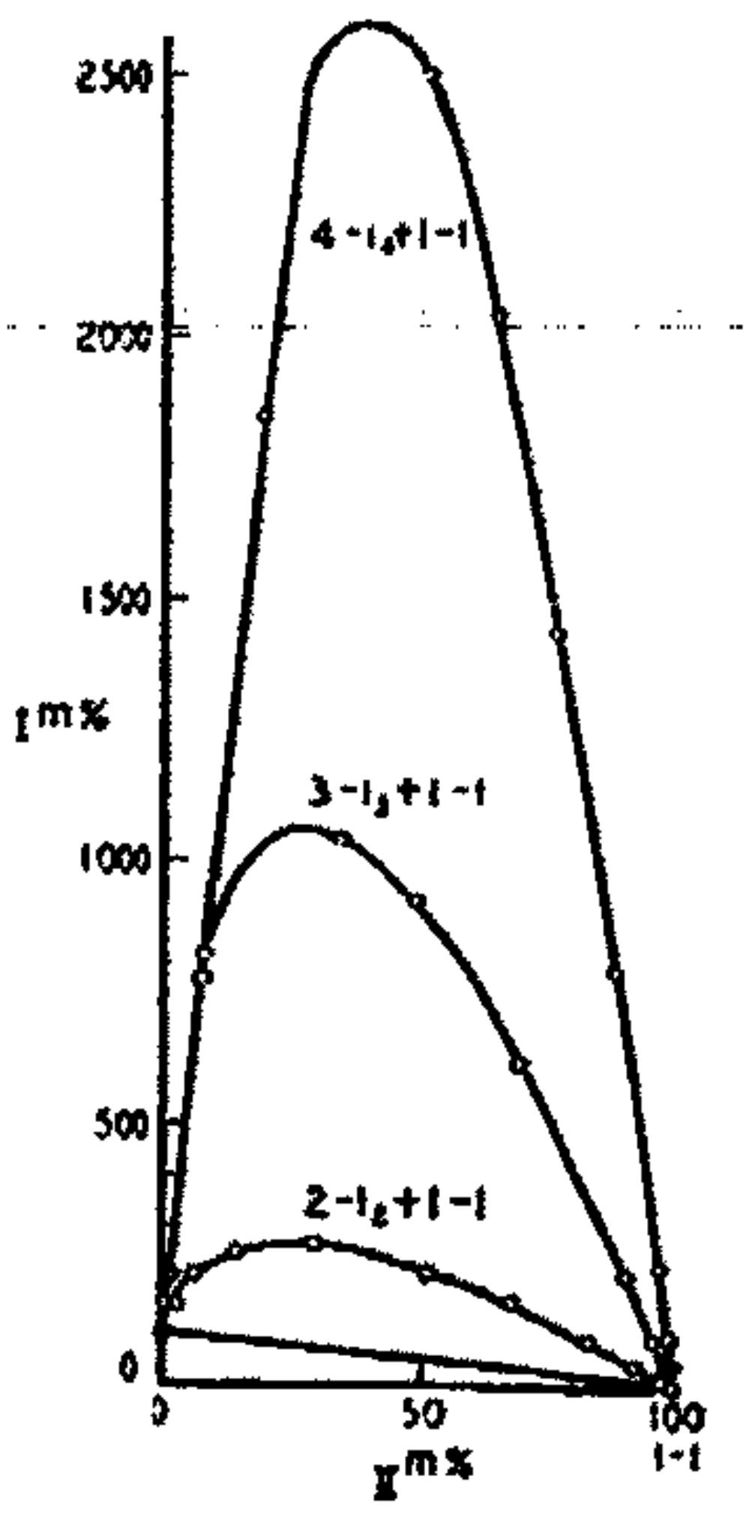

Fig. 9

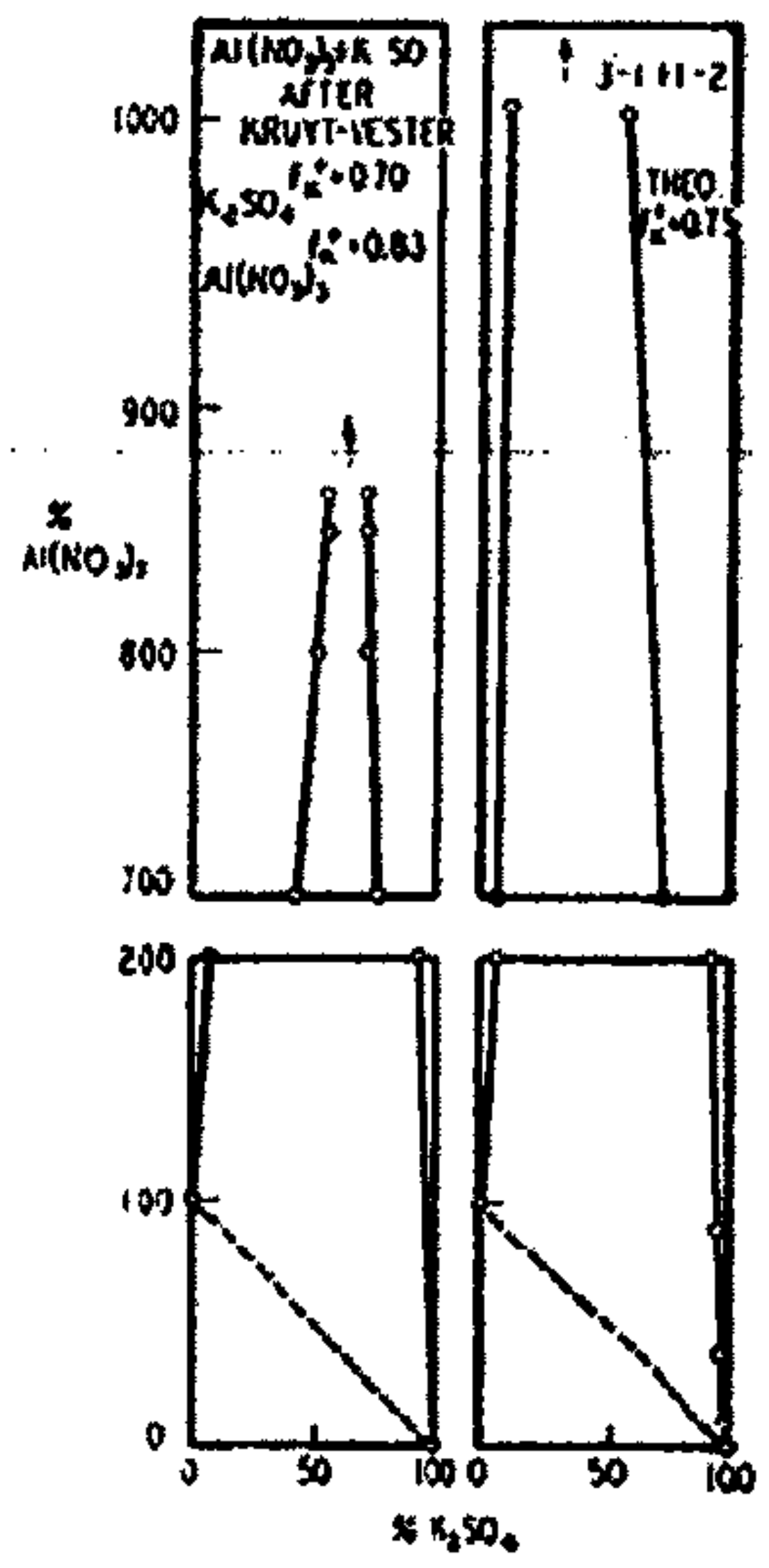

Fig. 10

Fig. 9. Coagulation by a monovalent salt combined with a polyvalent one.
Fig. 10. An example of the attempt to evaluate experimental cases quantitatively by the new theory.

Experimental errors in the fifth decimal point of the molality are clearly noticeable in the curves.

VII. THE EFFECT OF CHANGES IN SOLVENT AND TEMPERATURE

The equation defining the coefficient of activity as given above holds only for water at 18°C. If we change the nature of the solvent, for example, by the addition of alcohol or, if we coagulate at other temperatures, we must apply the extended equation for f^+ which is given by:

$$-\log f^+ = \frac{0.434e^2}{2DkT}\sqrt{\frac{1}{DT}}\cdot z_+^2\sqrt{\frac{1}{2}\sum m\cdot z^2}$$

where e = elementary electric charge, D = dielectric constant, T = absolute temperature, k = Boltzmann's constant, and the root content = ionic strength. As can be seen, the coefficient of activity is a multifunction of the dielectric constant and temperature. It may not be overlooked that D in itself already is a function of T.

If the proposed theory is correct, the coagulation molalities in the cases discussed must decrease with increasing temperature as well as with increasing addition of a solvent with lower D, for example, alcohol. Figure 12 reveals the decrease of m_k for the case in which f^+, the coefficient of activity at the point of coagulation, equals 0.75. This means that by the addition of ethanol the coagulation value can be reduced much more easily and much more markedly than by an increase in temperature. The curvature of the two curves is opposite.

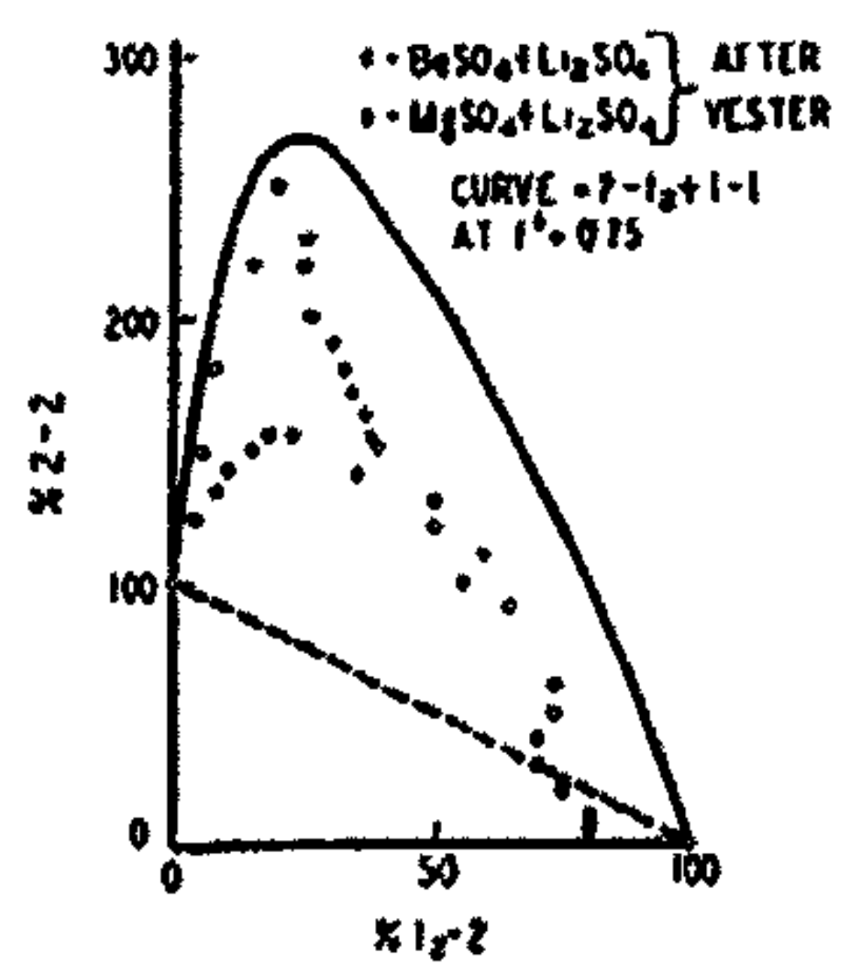

FIG. 11

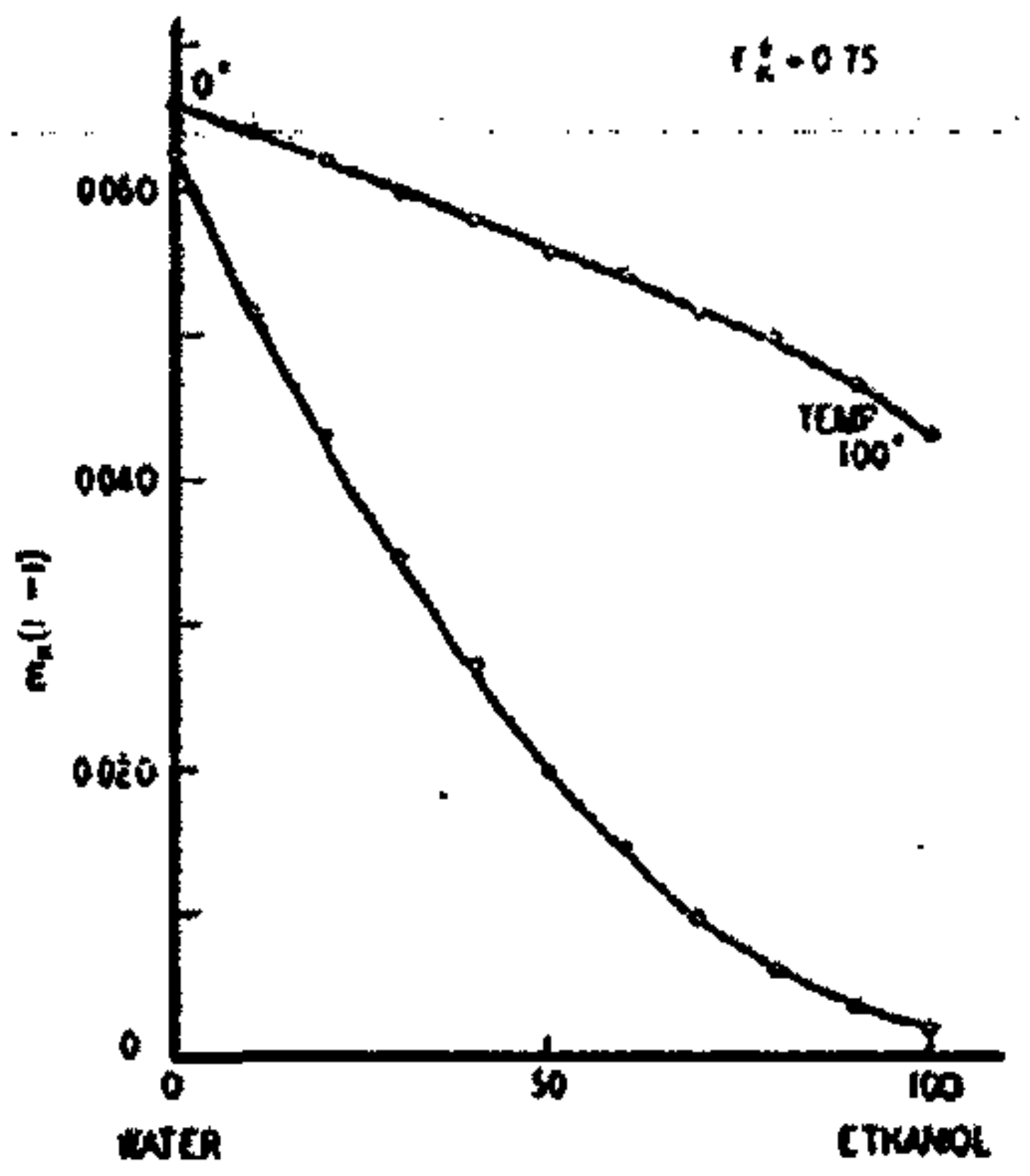

FIG. 12

FIG. 11. Another example of the attempt to evaluate experimental cases quantitatively by the new theory.

FIG. 12. Effect of ethanol and of temperature upon the coagulation of arsenic trisulfide sols by salts.

If this deduction is tested experimentally, one actually obtains (with normal and neutral salts) these two types of curves, as shown in figures 13 and 14, resulting from my own measurements on arsenic trisulfide sols.

Naturally one can also start with an ethanol or propanol sol, as, for example, Weiser and Mack (8) did, and change D by the addition of water, as can be seen on the right-hand side of figure 14. One obtains the same curves.

The theory also permits one to predict the magnitude of such a variation for the coagulation value when varying the temperature and the D of the solvent. For this purpose it is only necessary to introduce into the above formula, which contains D and T, the new values of D and T. Instead of the numerical factor 0.505 we will obtain other numerical factors. If the theory is correct the f_k^+ values must remain constant, notwithstanding variations in temperature and the nature of the solvent.

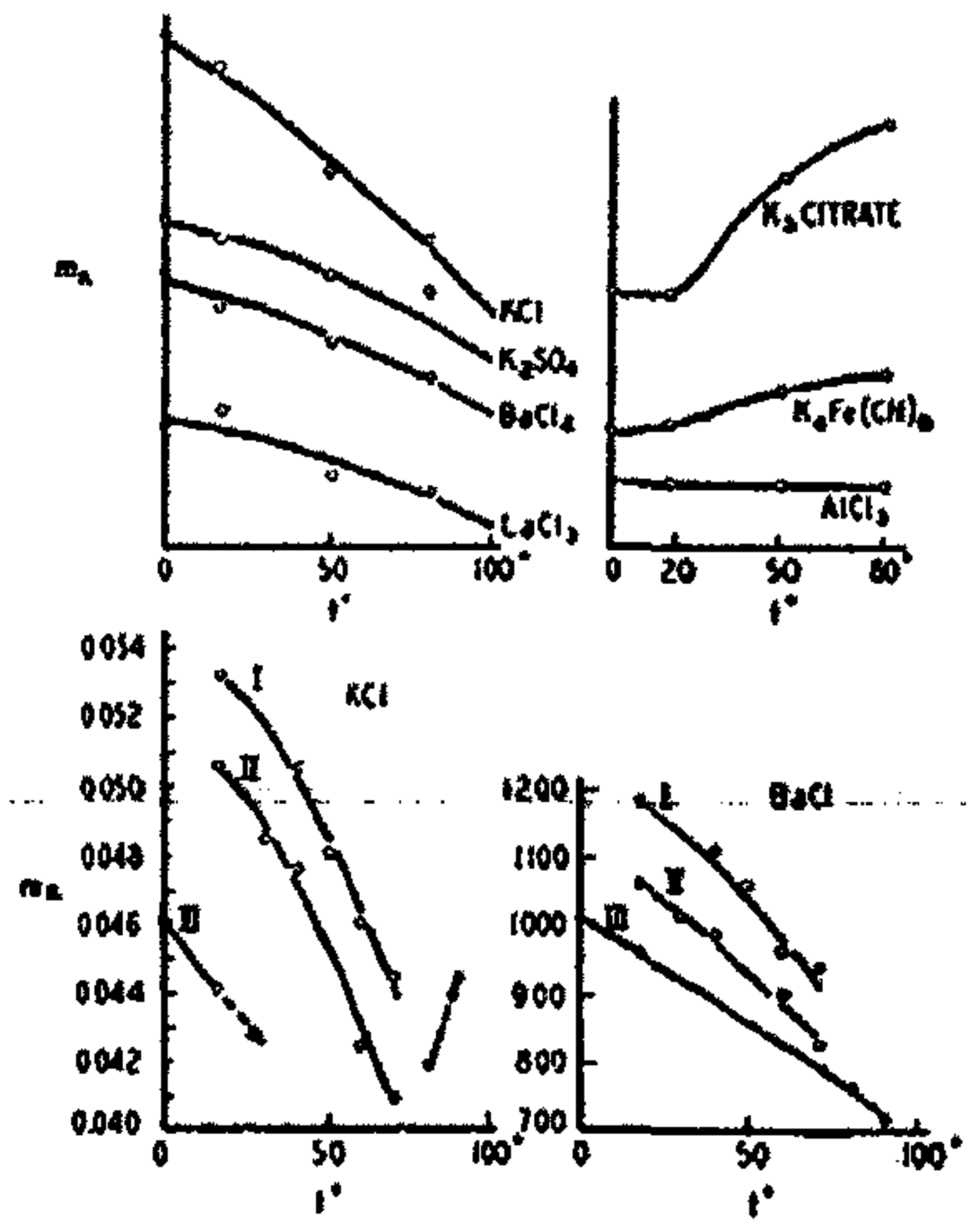

FIG. 13. Effect of temperature on the coagulation of arsenic trisulfide sols by salts

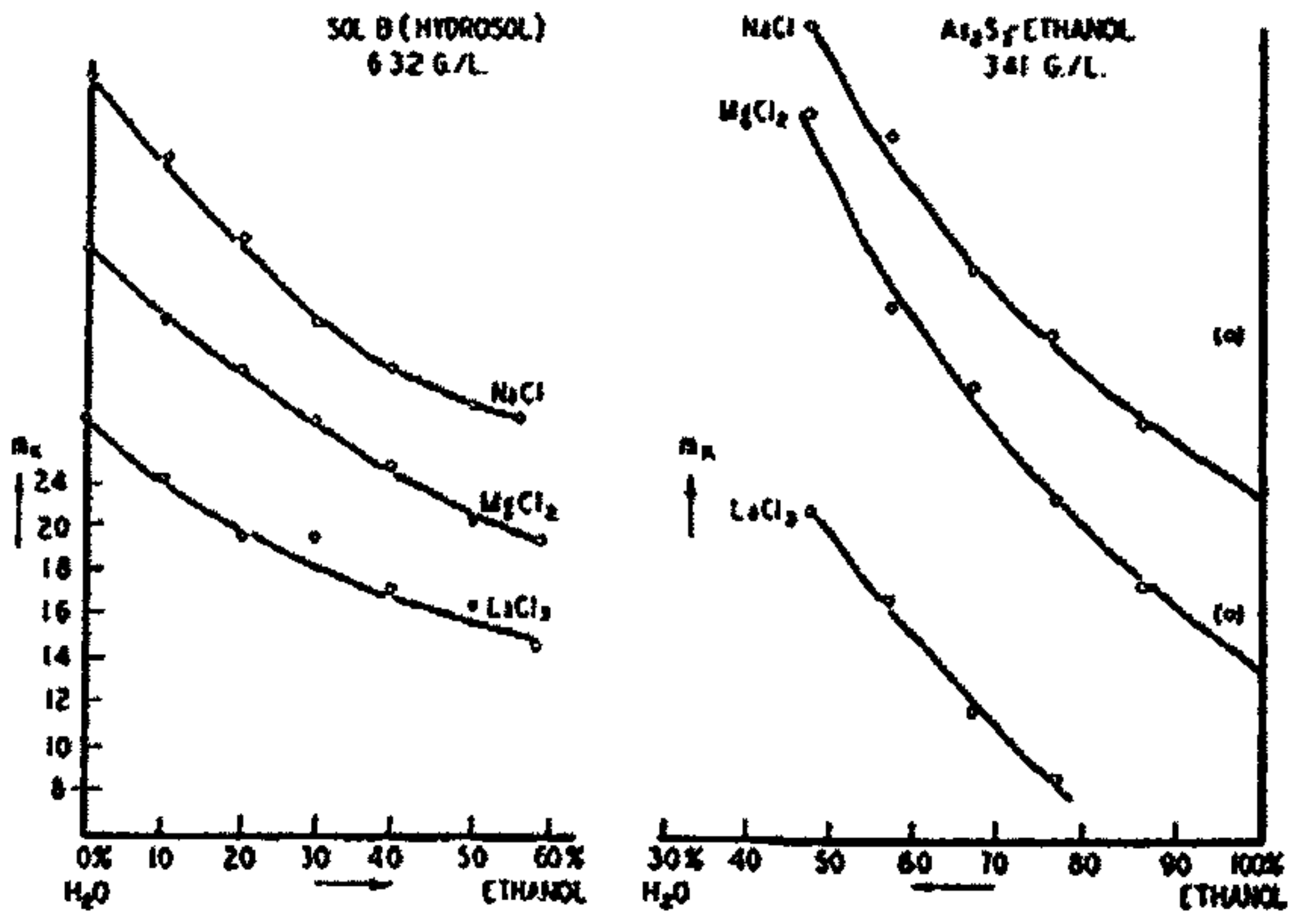

FIG. 14. Effect of ethanol on the coagulation of arsenic trisulfide sols by salts

Table 12 shows some figures taken from measurements on arsenic trisulfide sol. The measurements are not simple to perform, because, especially at higher temperatures, the sols themselves hydrolyze and it is therefore necessary to work very fast. However, the constancy of f_k^+ is, on the average, to be considered as very good.

The last tables, tables 13 to 16, show similar quantitative tests with changes of the dispersion medium. Table 13 refers to measurements by C. H. Sorum (5) on ferric oxide sols up to very high concentrations of alcohol. Table 14 shows propanol sols of mercuric sulfide, studied by Weiser and Mack (8), to which water had been added. Table 15 refers to my own measurements on arsenic trisulfide hydrosols. The constancy of

TABLE 12

Arsenic trisulfide sol B; f_k^+ values at varying temperatures

SALT		0°C.	18°C.	30°C.	40°C.	50°C.	60°C.	70°C.	80°C.	90°C.	MEAN VALUE
KCl	I		0.766		0.764	0.765	0.766	0.765			**0.765**
KCl	II		0.772	0.772	0.770	(0.779)	0.775	0.774			**0.773**
KCl	III	0.786	0.785						(0.767)	(0.755)	**(0.776)**
K_2SO_4	I		0.783	0.784	0.783	0.783	0.780	0.776			**0.781**
K_2SO_4	II	0.798							(0.767)	(0.755)	**(0.773)**
$BaCl_2$	I		0.761		0.762	0.763	0.764	0.764			**0.763**
$BaCl_2$	II		0.771	0.776	0.770	(0.779)	0.773	0.777			**0.773**
$BaCl_2$	III	0.785	0.780						0.780	0.780	**0.781**

TABLE 13

Experiments on ferric oxide sol

(C. H. Sorum)

SOL	ETHANOL	D	φ_D	m_k FOR NaCl	$_Df_k^+$
	per cent				
IIIa; 2.0 g. Fe_2O_3 per liter	0	80.4	0.500	0.022	**0.84**
	10.2	74.5	0.561	0.016	**0.85**
	20.4	68.7	0.632	0.012	**0.85**
	43.1	54.0	0.909	0.008	**0.83**
	54.9	47.4	1.102	0.007	**0.81**
IIIb; 4.0 g. Fe_2O_3 per liter	0	80.4	0.500	0.014	**0.87**
	10	74.6	0.562	0.011	**0.87**
	20	68.9	0.623	0.010	**0.87**
	40	56.1	0.857	0.008	**0.84**
	45	53.0	0.935	0.007	**0.835**
IIIc; 8.0 g. Fe_2O_3 per liter	0	80.4	0.500	0.014	**0.87**
	10	74.6	0.562	0.008	**0.88**
	20	68.9	0.623	0.007	**0.89**
	40	56.1	0.857	0.007	**0.85**
	45	53.0	0.935	0.006	**0.85**

TABLE 14

Mercuric sulfide-propanol sols

(H. B. Weiser and G. L. Mack)

PER CENT H_2O	D*
0	22.0
5	23.25
10	24.5
15	27.1
20	29.8
25	32.4
30	35.5
35	38.5
40	41.5
45	45.0

PER CENT H_2O	D	$\varphi_D \cdot z_+^2$	m_k	$_Df_k^+$
		LiCl		
0	22.0	3.50	0.0033	**0.63**
5	23.25	3.25	0.0037	**0.63**
15	27.1	2.56	0.0043	**0.68**
22	30.3	2.11	0.0064	**0.68**
25	32.4	1.96	0.0092	**0.65**
		$CaCl_2$		
0	22.0	24.3	0.0$_5$44	**0.89**
5	23.25	22.5	0.0$_5$70	**0.87**
10	24.5	20.6	0.0$_4$119	**0.85**
15	27.1	17.75	0.0$_4$19	**0.84**
20	29.8	15.3	0.0$_4$31	**0.82**
25	32.4	13.6	0.0$_4$52	**0.80**
30	35.5	11.85	0.0$_4$82	**0.78**
35	38.5	10.9	0.0$_3$13	**0.76**
40	41.5	9.35	0.0$_3$235	**0.74**
45	45.0	8.28	0.0$_3$335	**0.71**

* Own measurements.

TABLE 15

Influence of ethanol on coagulation of arsenic trisulfide hydrosols

ETHANOL	NaCl		$MgCl_2$		$LaCl_3$	
	m_k	$_Df_k^+$	m_k	$_Df_k^+$	m_k	$_Df_k^+$
			Sol A: 0.50 g. per liter			
per cent						
0	0.046	**0.779**	0.0$_3$75	**0.802**	0.0$_4$50	**0.836**
10	0.038	**0.791**	0.0$_3$50	**0.820**	0.0$_4$40	**0.837**
20	0.032	**0.779**	0.0$_3$50	**0.805**	0.0$_4$33	**0.838**
30	0.0254	**0.780**	0.0$_3$45	**0.795**	0.0$_4$31	**0.826**
40	0.0192	**0.783**	0.0$_3$325	**0.802**	(0.0$_4$31)	(0.801)
46.6	0.017	**0.777**				
47.6					(0.0$_4$31)	(0.780)
50				**0.798**		
			Sol B: 2.53 g. per liter			
0	0.0608	**0.751**	0.0$_3$90	**0.785**	0.0$_4$90	**0.784**
10	0.0517	**0.748**	0.0$_3$74	**0.786**	0.0$_4$76	**0.786**
20	0.0419	**0.751**	0.0$_3$62	**0.786**	0.0$_4$62	**0.785**
30	0.0321	**0.756**	0.0$_3$50	**0.785**	(0.0$_4$62)	(0.763)
40	0.0263	**0.751**	0.0$_3$39	**0.785**	(0.0$_4$50)	(0.755)
50	0.0220	**0.736**	0.0$_3$28	**0.787**	(0.0$_4$46)	(0.733)
56	0.0203	**0.738**				
57.38			0.0$_3$22	**0.786**		
58					(0.0$_4$36)	(**0.737**)

f_k^+ is unexpectedly good. Only the trivalent lanthanum chloride does not conform to the rule at higher alcohol concentrations. Table 16 demonstrates the influence of water on an ethanol sol. If one compares the figures in table 16 in horizontal order one again obtains an example for the correctness of the basic coefficient of activity rule (Ak — rule): f_k is approximately constant even if the valence of the coagulating salt is varied.

TABLE 16

Influence of water on coagulation of arsenic trisulfide-ethanol sols

Sol contains 1.7 g. arsenic trisulfide per liter

WATER	NaCl		$MgCl_2$		$LaCl_3$	
	m_k	$_Df_k^+$	m_k	$_Df_k^+$	m_k	$_Df_k^+$
per cent						
96	0.0045	**0.796**	$0.0_4 25$	**0.813**	($0.0_4 14$)	(0.610)
86.4	0.0025	**0.803**	$0.0_4 375$	**0.806**	($0.0_4 12$)	(0.720)
76.8	)0.0045(	**0.795**	$0.0_4 75$	**0.814**	$0.0_5 9$	**0.797**
67.2	0.0060	**0.806**	$0.0_3 125$	**0.806**	$0.0_4 17$	**0.808**
57.6	0.0090	**0.802**	$0.0_3 163$	**0.813**	$0.0_4 17$	**0.809**
48.0	0.0115	**0.794**	$0.0_3 250$	**0.802**	$0.0_4 23$	**0.808**

VIII. SUMMARY

Summing up, the tables and curves as given seem to demonstrate that the new idea proposed herein, namely, to place the properties of the dispersion medium in the focal point of the theory, is rather fruitful. Seemingly, the quantitative characteristics of the electrolytic dispersion medium and the coefficient of activity offer a tool which permits a quantitative control of a number of coagulation phenomena.

Let us return to our original question: What actually happens during the coagulation of a hydrophobic sol by neutral salts? We now might formulate the following reply: The coagulating forces seem to be the same as the interionic attraction forces between ions of the dispersion medium. This results from the fact that the coefficient of activity, the measure for these forces, also plays a predominant rôle in coagulation. Nevertheless, it might be wise to add that the entire mechanism even today is not as simple as the procedure actually looks.

The new theory is by no means contrary to the many attempts to evaluate the rôle played by the double layer between the disperse part and the dispersion medium. The only difference is that now the double layer is looked upon as an interposed apparatus of the dispersion medium, and not as the coagulating motor itself. The dispersion medium brings about coagulation and not the double layer. It is the arm that hits and not the cane.

REFERENCES

(1) **Buzágh, A. v.**: Kolloid-Z. **76**, 2 (1936); **79**, 156 (1937).

(2) **Hamaker, H. C.**: Hydrophobic Colloids (Symposium held at Utrecht, November, 1937), p. 16. D. B. Centen's Uitg. Mij. N. C., Amsterdam (1938).

(3) **Lederer, E. L.**: Kolloid-Z. **76**, 54 (1936).

(4) **Ostwald, Wo., and collaborators** (**H. Kokoros, K. Hoffmann, H. A. Wannow, and W. W. Stuart**): Kolloid-Z. **73**, 301 (1935); **75**, 297 (1936); **76**, 54, 159 (1936); **78**, 324 (1937); **79**, 49, 287 (1937); **80**, 186, 304 (1937); **81**, 48 (1937).

(5) **Sorum, C. H.**: Kolloid-Z. **58**, 314 (1931).

(6) **Verwey, E. J. W.**: Chem. Rev. **16**, 363 (1935). Hydrophobic Colloids (Symposium held at Utrecht, November, 1937), p. 58. D. B. Centen's Uitg. Mij. N. C., Amsterdam (1938).

(7) **Wannow, H. A., and Hoffmann, K.**: Kolloid-Z. **77**, 46 (1936); **80**, 294 (1937).

(8) **Weiser, H. B., and Mack, G. L.**: J. Phys. Chem. **28**, 1254 (1924).

BOUNDARY TENSION BY PENDANT DROPS[1]

J. M. ANDREAS, E. A. HAUSER, AND W. B. TUCKER

Department of Chemical Engineering, Massachusetts Institute of Technology, Cambridge, Massachusetts

Received July, 1, 1938

Boundary tension is a measure of the free energy of a fluid interface. The term is derived from the superficial analogy between the surface of a liquid and a stretched membrane. For, just as it has proven to be convenient to express the potential energy of a fluid mass in foot pounds per pound as a "head" in feet, it has been shown to be useful to speak of the free energy of a fluid surface in ergs per square centimeter as a "tension" in dynes per centimeter.

Surface tension is the boundary tension at an interface between a liquid and a gas or vapor, and interfacial tension is the boundary tension at a phase boundary between two incompletely miscible liquids.

Nearly all of the common specific properties of fluids, such as the density, boiling and freezing points, optical rotation, and thermal conductivity, are properties of the main body of the fluid. The boundary tension is the best known property of liquid *surfaces*. For this reason it is of outstanding importance in colloid chemistry, which frequently is called the chemistry and physics of surfaces and surface reactions. The usefulness of boundary tension measurements has been limited in the past by the great difficulty of making determinations with satisfactory speed, accuracy, and precision.

A great many procedures have been developed for the determination of boundary tension, of which the majority are just barely workable and are characterized by low precision and lack of versatility. Of seventeen methods listed by N. E. Dorsey (6) in 1926, only a few are in common use. These depend upon observing: (*a*) the behavior of a liquid in a capillary tube (24, 35, 46); (*b*) the force required to pull a wire ring or staple out of the liquid surface (29, 36); (*c*) the weight or volume of drops falling from a vertical tube of known size (15, 16); or (*d*) the maximum pressure required to form bubbles in a liquid from a tube of known size (47, 53). Each of these methods has serious limitations (1).

This lack of a generally satisfactory method of measurement suggested that it would be profitable to resurvey the field in search of some possi-

---

[1] Presented at the Fifteenth Colloid Symposium, held at Cambridge, Massachusetts, June 9-11, 1938.

bility which had been overlooked by the earlier workers and in the hope that a new method could be developed which would succeed where others had failed.

Previous work (8) had demonstrated that the method of pendant drops has a number of outstanding advantages over other methods. Outstanding from the colloid chemist's point of view is the fact that this method is a static one. Once the surface is formed, it is not subjected to any changes due to outside influence prior to or during the measurement. It is the only known method which permits an accurate study of changes in surface composition with time, a phenomenon of predominant importance in the study of various colloidal systems. Accordingly, the focus of our attention was on the design of apparatus and the development of methods with which its possibilities could be explored. In addition to this, an extensive series of measurements was made of typical liquid systems to show the range of usefulness of the new method and to show the sort of results which can be expected.

The method which was decided upon consists in suspending a small drop of the liquid to be tested from the end of a vertical tube which is mounted in a thermostat. The surface of the drop will be a surface of revolution whose shape and size can be determined by measurements made on a large photographic image obtained with a special camera built for the purpose. Since the equations determining the equilibrium of the drop are known, the boundary tension of the liquid can be calculated from a few simple measurements made on a photograph of a hanging drop.

This method has been undeservedly in disrepute for a number of years, because the first workers (11, 55) who attempted to employ it had no satisfactory pendant drop camera and used methods of calculation which were tedious and of low precision. These difficulties have now been overcome.

APPARATUS

The apparatus consists, essentially, of a light-source, a thermostat chamber, a set of drop-forming tips, and a precise camera having a fixed image distance and a telecentric lens system (figure 1).

Experience shows that monochromatic light gives slightly more satisfactory images than white light. It can conveniently be obtained by using a mercury arc lamp (GE, Type H-3, 85-watt, high pressure) and gelatin filter (Wratten No. 77-A) combination.

The drop hangs from a vertical, cylindrical tip in a glass cuvette inside the thermostat (figure 2). In this way the drop is maintained at all times in physical equilibrium with its surroundings. The inner chamber of the thermostat must be totally enclosed to prevent loss of liquid by evaporation, and it should be held to within ± 0.05° C. of the desired temperature, since solubilities, vapor pressures, and boundary tensions all change with temperature. Our thermostat was maintained to within ± 0.01° C. by a sensitive thermoregulator.

To guarantee such constant temperatures, water from a tank containing the thermoregulator was pumped through the thermostat at a rate of 30 gallons per minute. Vibrations set up by the pump were absorbed by flexible rubber hose connections between pump and thermostat. The thermostat was chromium-plated to minimize radiant heat transfer.

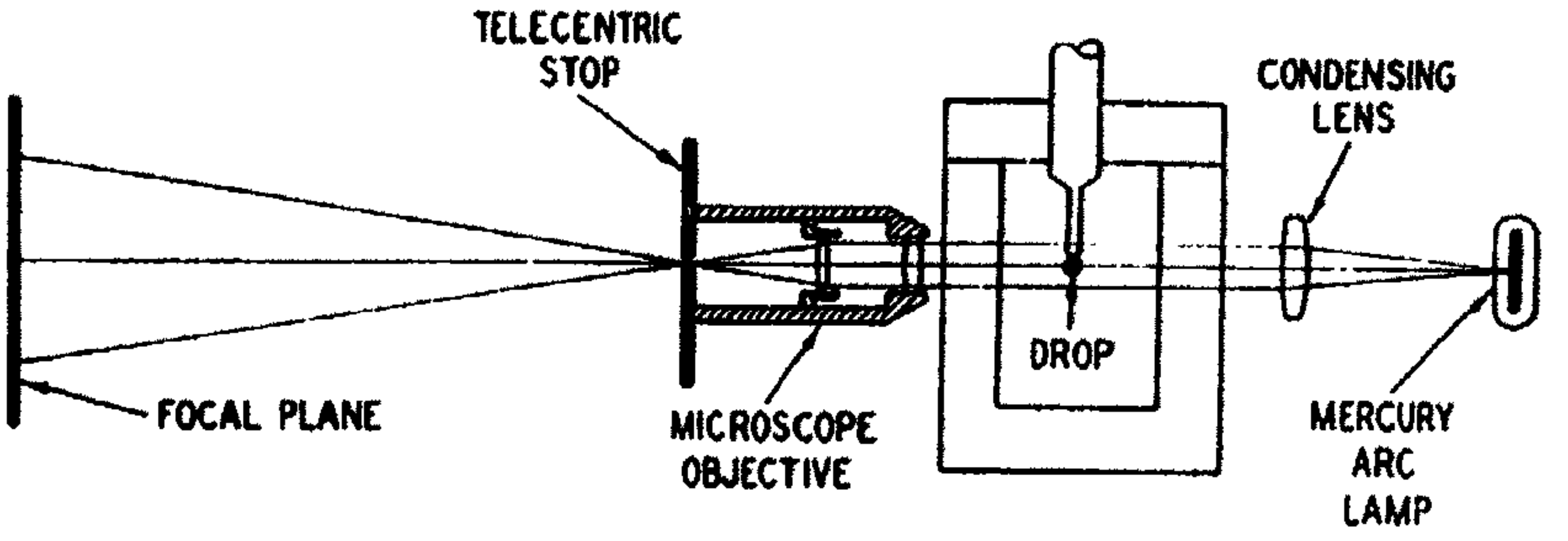

Fig. 1. The apparatus

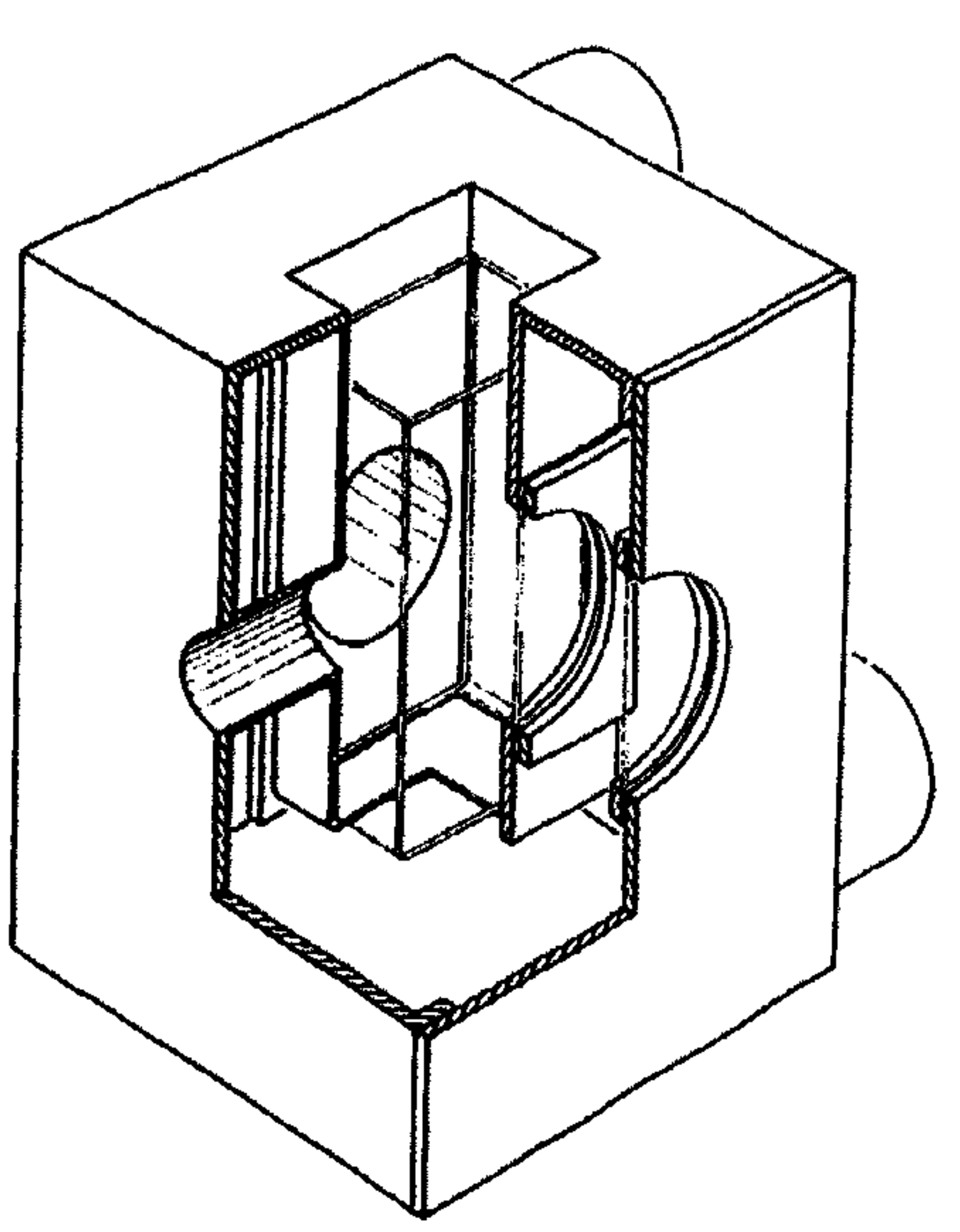

Fig. 2

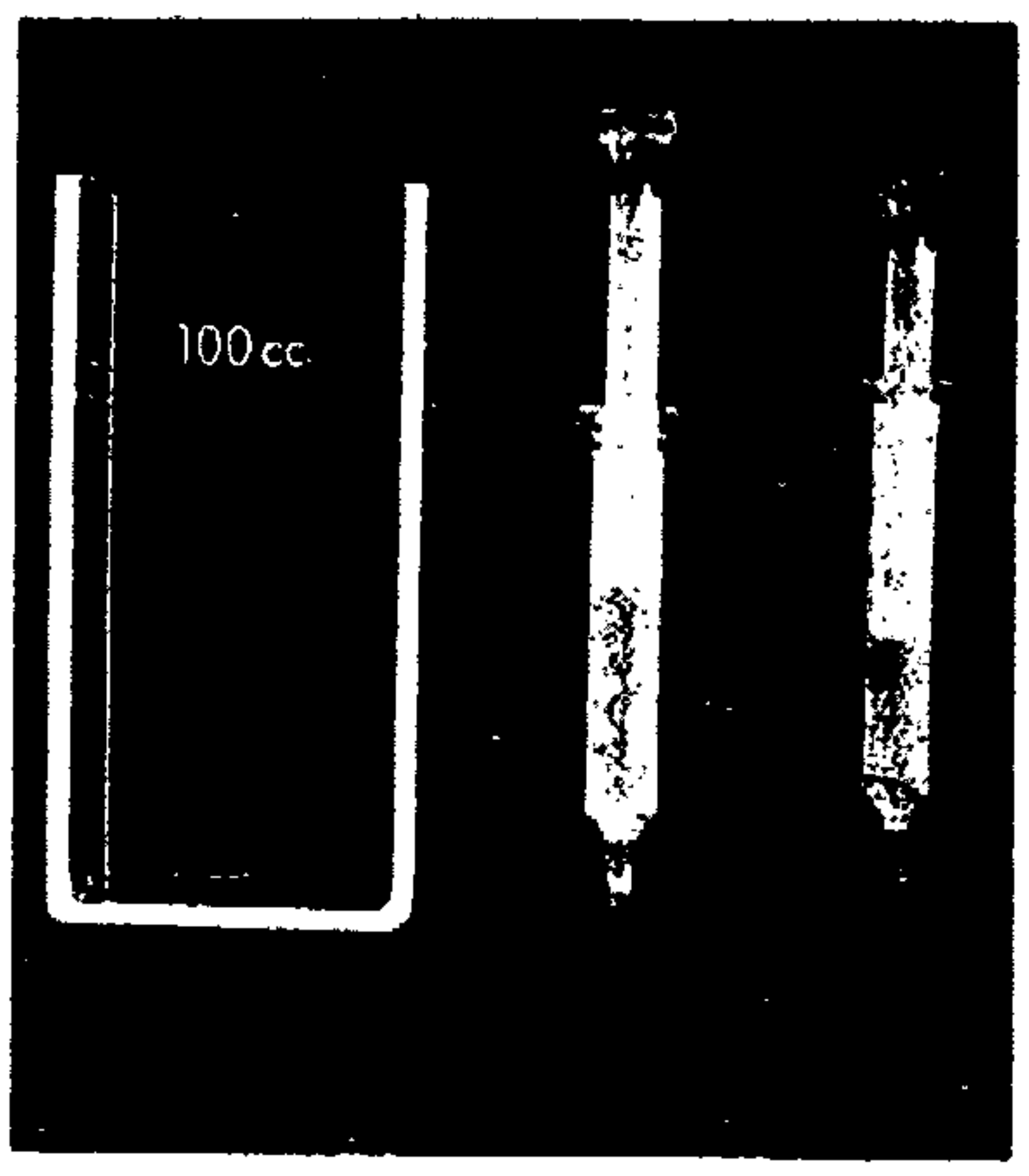

Fig. 3

Fig. 2. Thermostat containing cuvette

Fig. 3. Cuvette and drop-forming tip prepared from hypodermic syringe

Drop-forming tips for surface tension measurements can conveniently be made by welding short lengths of 2-mm. Pyrex tubing on standard 1.5-cc. hypodermic syringes (figure 3). It is desirable that the end of the tip be made from tubing having a circular cross section, and that the end be cut off perpendicular to the vertical axis. However, microscopic perfection is not essential, since the liquid surface tends to bridge over any minor irregularities. The measurements are made at points on the liquid surface which are remote from the end of the tip and where the influence of imperfections in the shape of the tip is normally negligible. Interfacial tension measurements require a set of tips of various diameters if the drops are always to have a convenient shape. Diameters ranging from 0.2 to 20.0 mm. may be required in exceptional cases. Rectangular cuvettes built of optically flat glass can be purchased from dealers in scientific apparatus.

The construction of a satisfactory camera is a matter of considerable experimental difficulty and determines to a large extent the success of the final results. The exact details of the design depend upon the method by which the image is to be measured and upon the precision which is required, but certain features must be incorporated in any case. It is essential for the drop to be photographed with rays of light which are parallel to the optical axis, if error due to perspective is to be avoided. We accomplished this by using standard microscope objectives of 48 or 24 mm. focal lengths which were equipped with telecentric stops. The camera should be built to make pictures on glass plates and to have an optical magnification of from 10 to 30 diameters.

CALCULATIONS

A. The method of the plane of inflection

The boundary tension can be computed directly from an analysis of the stresses in a static, pendant drop. The mathematical treatment is based on two fundamental equations. The first of these states that the pressure caused by the curvature of the surface is equal to the product of the boundary tension and the mean curvature.[2] The second says that, when the drop is in equilibrium, the vertical forces acting across any horizontal plane are balanced.

$$p = \gamma(1/R + 1/R') \qquad (1)$$

$$2\pi x\gamma \sin\phi = V\sigma g + \pi x^2 p \qquad (2)$$

where p = the pressure due to the curvature of the surface,
γ = the boundary tension,
R and R′ = the two principal radii of curvature,
x = the horizontal distance to the axis of the drop,
ϕ = the angle between the normal and the axis,
V = the volume of fluid hanging from the plane,
σ = the difference in density between the two fluids, and
g = the acceleration of gravity.

---

[2] This equation originated with Thomas Young (56) and Pierre Laplace (26). A simple derivation is given by N. K. Adam (reference 1, pp. 8–9).

These equations may be combined and solved for γ in a number of ways. A satisfactory method is to pass a horizontal plane through the drop at the level where the profile curve passes through a point of inflection (figure 4).

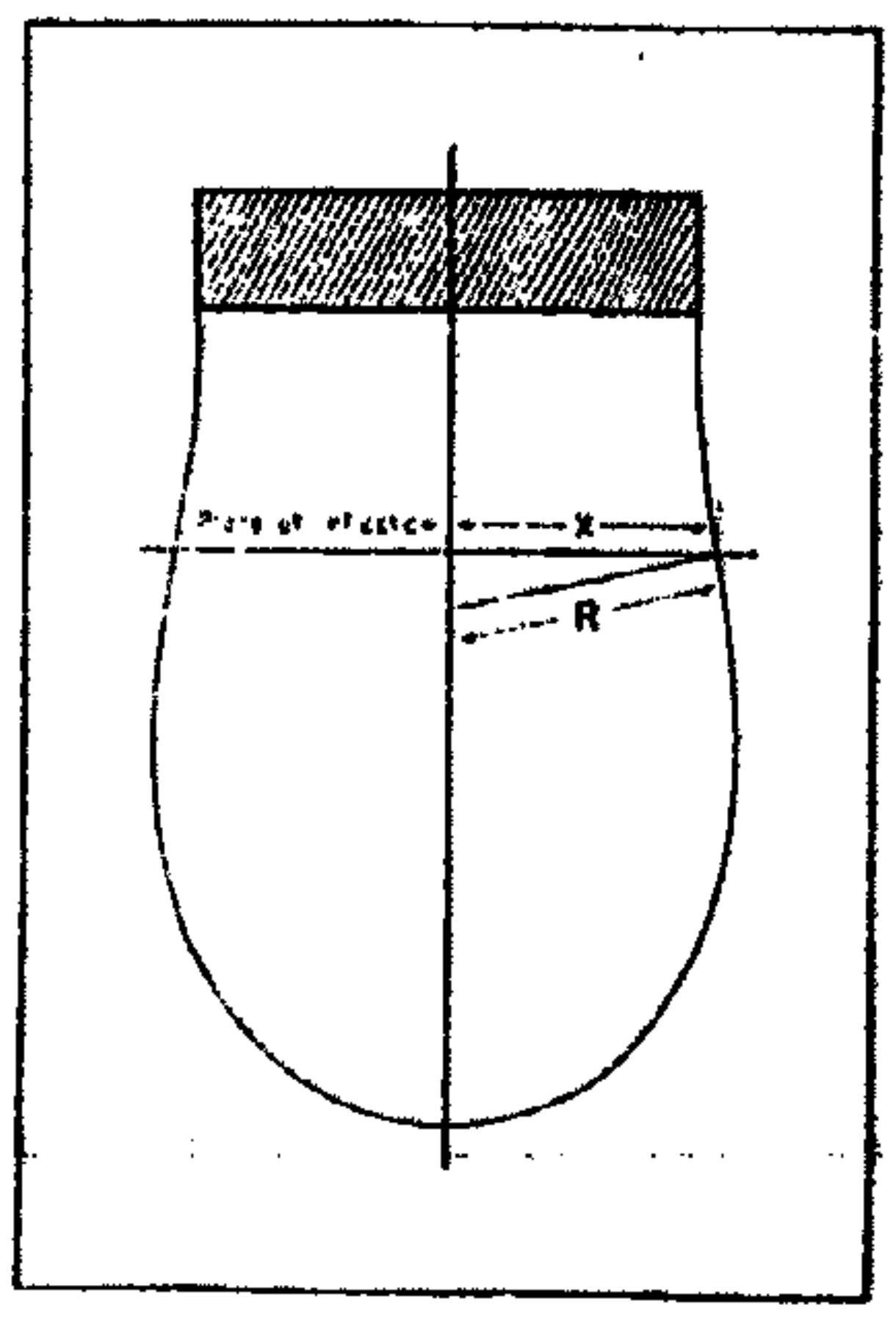

FIG. 4

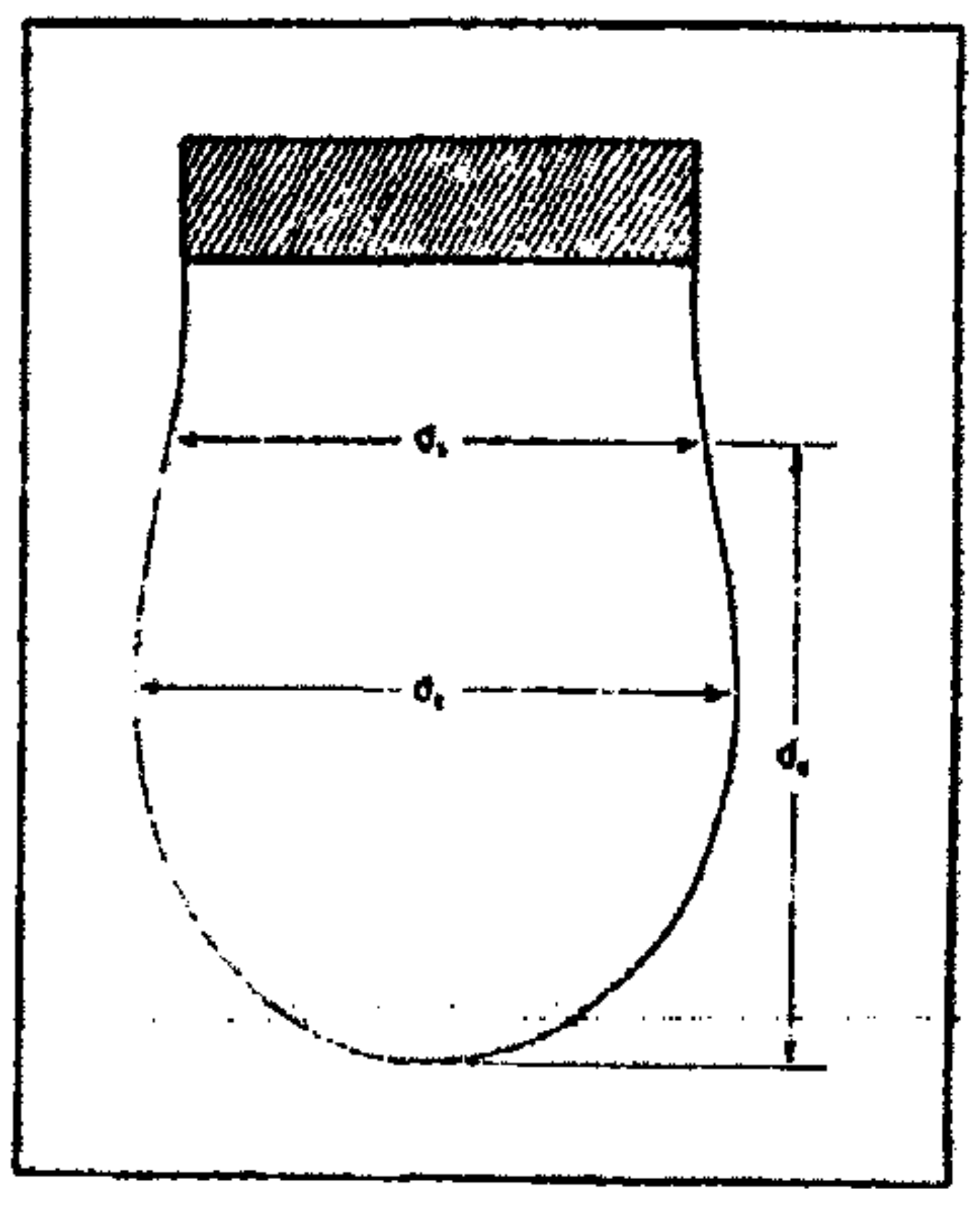

FIG. 5

FIG. 4. Method of the plane of inflection
FIG. 5. Method of the selected plane

The external radius of curvature, R', is infinite at the plane of inflection, and therefore equation 1 reduces to

$$p = \frac{\gamma}{R}$$

Substituting this value of p in equation 2, and solving for the boundary tension, γ, we obtain for this special case,

$$\gamma = \frac{V\sigma g}{2\pi x \sin \phi - \dfrac{\pi x^2}{R}}$$

and since

$$\sin \phi = \frac{x}{R}$$

$$\gamma = \frac{g}{\pi} \frac{V\sigma R}{x^2} \qquad (3)$$

This equation is mathematically exact, but its use is subject to two severe limitations: (*1*) It is necessary to locate the true plane of inflection. This is a difficult graphical problem. If a plane is used which is slightly above the true plane of inflection, the measured value of V will be too large and the measured value of x will be too small. If a plane is used which lies slightly below the true plane of inflection, the opposite will be true. In either case, a double error is introduced in the computed value of the boundary tension. (*2*) It is necessary to compute the volume of the drop from its profile. This is a tedious process which must either be done by graphical integration or with a special, very costly, planimeter. These practical difficulties limit the attainable precision of the "method of the plane of inflection" to about ± 2.0 per cent.

B. The method of a selected plane

A less direct method of attack leads to a more rapid and precise solution. It is first necessary to examine the differential equation of the surface of the drop.

If z is the vertical coördinate measured away from an origin placed at the point where the axis of rotation cuts the surface of the drop, and if b is the radius of curvature of the drop at the origin, the pressure due to the curvature is at any point equal to

$$p = \frac{2\gamma}{b} - g\sigma z \tag{4}$$

If equations 1 and 4 are combined, we obtain

$$\gamma(1/R' + 1/R) = \frac{2\gamma}{b} - g\sigma z$$

and the radii of curvature can be eliminated, since

$$R' = \frac{\left[1 + \left(\frac{dz}{dx}\right)^2\right]^{3/2}}{\frac{d^2z}{dx^2}}$$

and

$$R = \frac{x}{\sin\phi} = \frac{x\left[1 + \left(\frac{dz}{dx}\right)^2\right]^{1/2}}{\frac{dz}{dx}}$$

Then

$$\frac{\frac{d^2z}{dx^2}}{\left[1 + \left(\frac{dz}{dx}\right)^2\right]^{3/2}} + \frac{\frac{dz}{dx}}{x\left[1 + \left(\frac{dz}{dx}\right)^2\right]^{1/2}} = \frac{2}{b} - \frac{g\sigma z}{\gamma}$$

or

$$\frac{d^2z}{dx^2} + \frac{\frac{dz}{dx}}{x}\left[1 + \left(\frac{dz}{dx}\right)^2\right] = \left[\frac{2}{b} - \frac{g\sigma z}{\gamma}\right]\left[1 + \left(\frac{dz}{dx}\right)^2\right]^{3/2}$$

This is a second-order, second-degree differential equation whose integrated form is unknown. It can be reduced to the dimensionless form,

$$Z'' + \frac{Z'}{X}[1 + (Z')^2] = [2 - \beta Z][1 + (Z')^2]^{3/2} \tag{5}$$

if we set

$$\beta = \frac{g\sigma b^2}{\gamma} \tag{6}$$

and let $X = x/b$, $Z = z/b$, $Z' = dZ/dX$, and $Z'' = d^2Z/dX^2$, which is equivalent to using b as the unit of length.

This derivation follows that of Bashforth and Adams (1, 3), with the exception that the algebraic signs of σ and of β are defined so as to be positive for pendant drops.

The differential equation 5 is seen to contain *two* parameters β and b, whose values identify the particular drop represented by the equation.

By rearranging equation 6, it is possible to express the boundary tension as a function of the two parameters β and b and of the effective specific weight ($g\sigma$). No method is known by which either β or b can be determined precisely and quickly from a picture of a drop. We must therefore transform equation 6 to a form which uses parameters whose values can be measured easily and accurately.

The size of a drop is most conveniently gauged by measuring its diameter at the equator, and the shape can be described by giving the ratio of the diameters measured at two different horizontal planes. If one diameter is at the plane of the equator, and the other is taken at a distance from the end of the drop equal to the equatorial diameter (figure 5), the shape can be described by the ratio,

$$S = \frac{d_s}{d_e} \tag{7}$$

where d_e is the diameter at the equator, and d_s is the diameter at the arbitrarily selected plane.

Figure 6 shows the useful range of drop shapes and will illustrate the way in which the shape ratio, S, varies from drop to drop. This figure was made from actual silhouette photographs of pendant drops. The black spots in the center are images of the light source caused by the liquid drop acting as an imperfect lens.

It has been shown that the quantities β and S are functions of the drop shape. A third quantity which is a function of the drop shape is the ratio of the diameter at the equator to the radius of curvature at the origin, d_e/b. Accordingly, we can define a new quantity,

$$H = \beta \left(\frac{d_e}{b}\right)^2 \tag{8}$$

which will be a function of S.

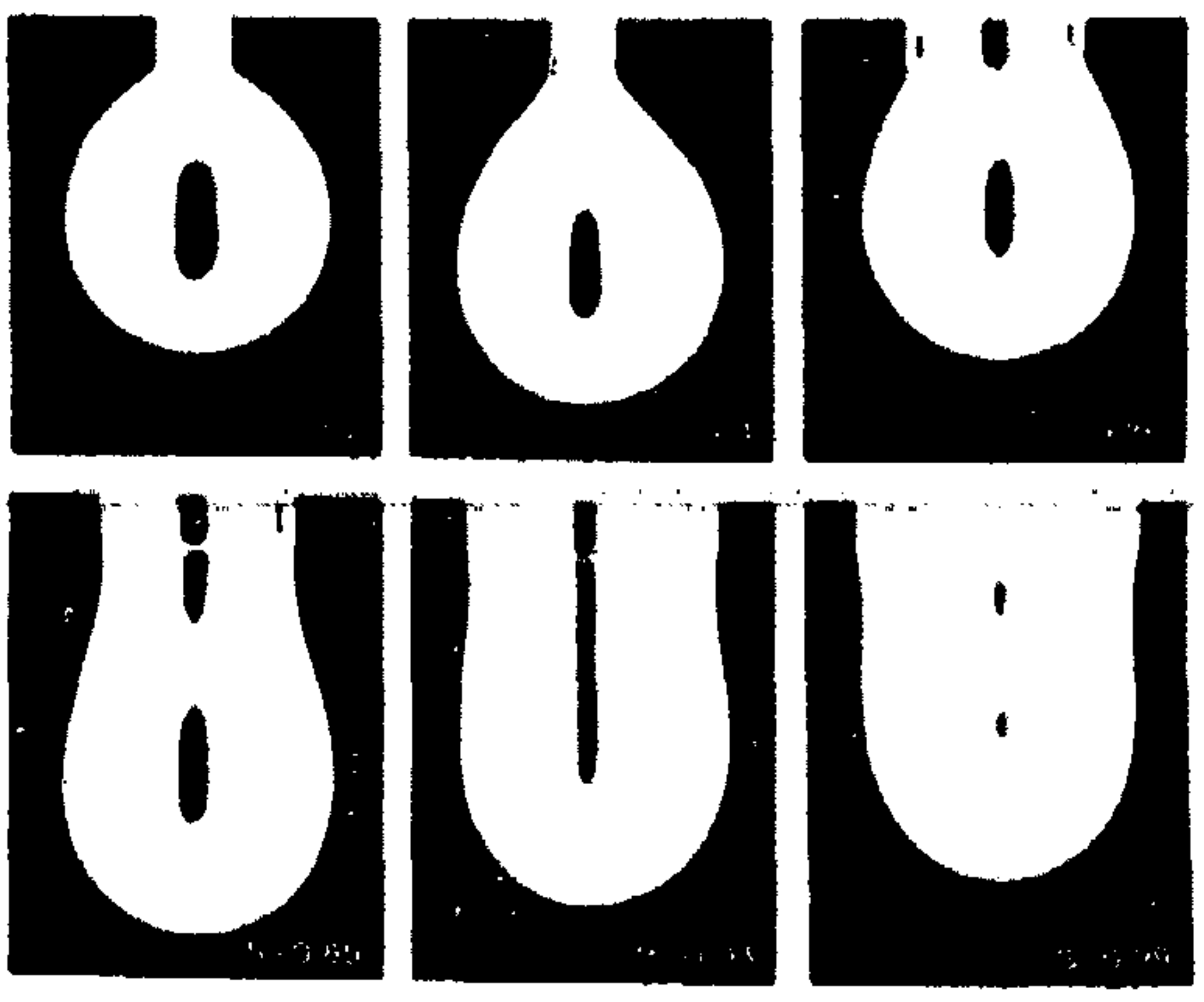

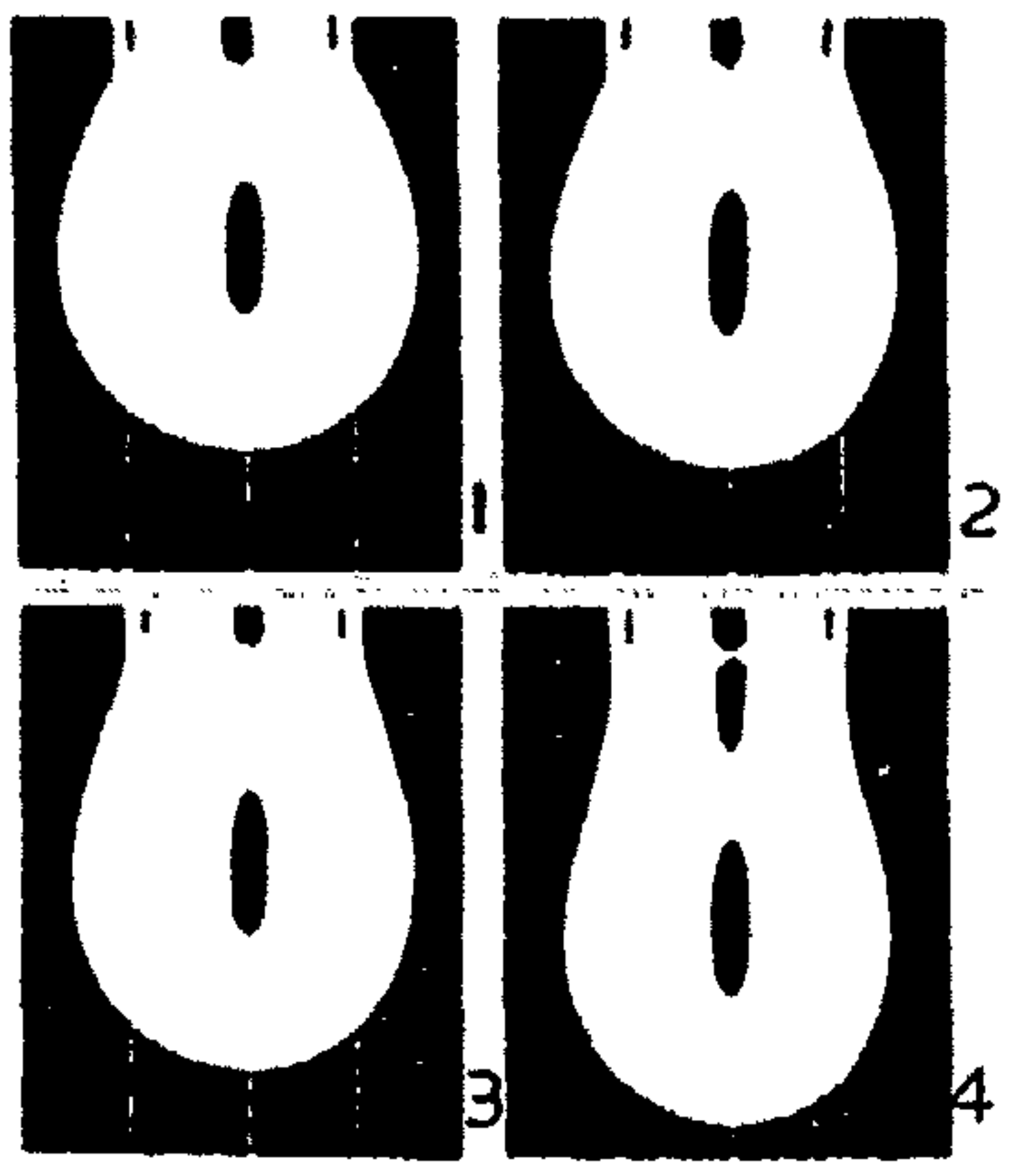

Fig. 6 Fig. 7

Fig. 6. Variation in the shape of pendant drops

Fig. 7. Change of shape of drop and surface tension with age. 0.025 per cent solution of sodium stearate in water at 25°C. (1) aged 10 sec., $S = 0.787$, $\gamma = 71.9$; (2) aged 60 sec., $S = 0.818$, $\gamma = 58.2$; (3) aged 120 sec., $S = 0.828$, $\gamma = 54.4$; (4) aged 1800 sec., $S = 0.849$, $\gamma = 39.2$.

Equation 6 can now be solved for γ, combined with equation 8, and used in conjunction with a table of values of H as a function of S to determine the value of the boundary tension from a photograph of a pendant drop (table 1).

$$\gamma = \frac{g\sigma b^2}{\beta} = \frac{g\sigma (d_e)^2}{\beta\left(\frac{d_e}{b}\right)^2} = \frac{g\sigma (d_e)^2}{H} \tag{9}$$

Equation 9 is exact and convenient. Its precision depends upon the accuracy with which the linear measurements can be made and upon the labor which is expended in preparing the table of values of H as a function of S.

It is theoretically possible for this function to be evaluated mathematically, but the calculations are very laborious and unsatisfactory.

TABLE 1

Arithmetic tabulation of H-S function for pendant drops

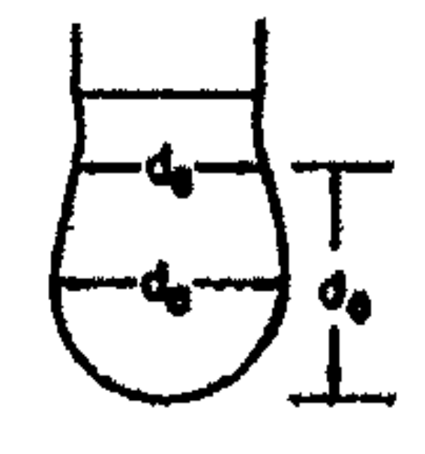

$S = \frac{d_s}{d_e}$ S vs. $1/H$ $\gamma = \frac{(\rho_1 - \rho_2)\, g d_e^2}{H}$

Interpolation is unwarranted

S	0	1	2	3	4	5	6	7	8	9
0.70	0.797	0.795	0.792	0.790	0.787	0.785	0.782	0.780	0.777	0.775
0.71	0.772	0.770	0.767	0.765	0.762	0.759	0.757	0.754	0.752	0.749
0.72	0.747	0.744	0.742	0.739	0.737	0.735	0.732	0.730	0.727	0.725
0.73	0.722	0.720	0.718	0.715	0.713	0.711	0.709	0.706	0.704	0.702
0.74	0.699	0.697	0.695	0.692	0.690	0.688	0.685	0.683	0.681	0.679
0.75	0.676	0.674	0.672	0.670	0.668	0.665	0.663	0.661	0.659	0.657
0.76	0.655	0.652	0.650	0.648	0.646	0.644	0.642	0.640	0.637	0.635
0.77	0.633	0.631	0.629	0.627	0.625	0.623	0.621	0.619	0.617	0.615
0.78	0.613	0.611	0.609	0.607	0.605	0.603	0.601	0.599	0.597	0.595
0.79	0.593	0.591	0.589	0.587	0.585	0.583	0.581	0.579	0.577	0.575
0.80	0.573	0.571	0.570	0.568	0.566	0.564	0.562	0.561	0.559	0.557
0.81	0.555	0.553	0.551	0.550	0.548	0.546	0.544	0.542	0.540	0.539
0.82	0.537	0.535	0.533	0.532	0.530	0.528	0.526	0.524	0.523	0.521
0.83	0.519	0.518	0.516	0.515	0.513	0.511	0.509	0.507	0.506	0.504
0.84	0.502	0.501	0.499	0.498	0.496	0.494	0.493	0.491	0.490	0.488
0.85	0.486	0.485	0.483	0.482	0.480	0.479	0.477	0.476	0.474	0.473
0.86	0.471	0.470	0.468	0.467	0.465	0.464	0.462	0.461	0.459	0.458
0.87	0.457	0.455	0.454	0.452	0.451	0.450	0.448	0.447	0.446	0.444
0.88	0.443	0.441	0.440	0.439	0.437	0.436	0.434	0.433	0.431	0.430
0.89	0.429	0.428	0.426	0.425	0.423	0.422	0.420	0.419	0.418	0.417
0.90	0.415	0.414	0.413	0.411	0.410	0.409	0.408	0.406	0.405	0.404
0.91	0.403	0.401	0.400	0.399	0.398	0.396	0.395	0.394	0.393	0.391
0.92	0.390	0.389	0.388	0.386	0.385	0.384	0.383	0.382	0.381	0.379
0.93	0.378	0.377	0.376	0.375	0.373	0.372	0.371	0.370	0.369	0.368
0.94	0.366	0.365	0.364	0.363	0.362	0.361	0.359	0.358	0.357	0.356
0.95	0.355	0.354	0 53	0.352	0.351	0.350	0.349	0.348	0.346	0.345
0.96	0.344	0.343	0.342	0.341	0.340	0.339	0.338	0.337	0.335	0.334
0.97	0.333	0.332	0.331	0.330	0.329	0.328	0.327	0.326	0.325	0.324
0.98	0.323	0.322	0.321	0.320	0.319	0.318	0.317	0.316	0.315	0.314
0.99	0.313	0.312	0.311	0.310	0.309	0.308	0.307	0.306	0.305	0.304
1.00	0.303									

Methods of solution which have been attempted are based upon the use of finite increments or of series. They tend to be least satisfactory in the regions which are most important (3, 30, 31, 32, 33). However, an empirical evaluation of the function is entirely feasible and adequate, and the function has been established to ± 0.2 per cent by measurements made on photographs of various sized drops of conductivity water having a known surface tension of 72.0 dynes per centimeter at 25°C. (table 1). The function has also been checked and found to be in agreement with the theoretical curves computed from the differential equation by Bashforth and Adams (3).

Experience shows that, if the linear dimensions of a drop can be measured with a probable error of not more than ± 0.1 per cent, this method will give values for the boundary tension which have an uncertainty of about ± 0.5 per cent. Measurement and calculation require about 10 min. per picture.[3]

EXPERIMENTAL APPLICATION

A number of boundary tension measurements were made on C.P. grade chemicals to obtain a comparison of the results obtainable by the method of pendant drops with results obtained by other methods and published in the literature. These results, given in abridged form in table 2, were calculated by the method of the selected plane, using table 1, which is based on the accepted value for the surface tension of water at 25°C. of 72.0 dynes per centimeter.

All of the pendant drop measurements reported in this table were made on surfaces 10 sec. old, while those given in the literature were made on surfaces whose age is not reported. It will be noted that the agreement between the two sets of surface tension data is good, since the surface tensions of pure, non-viscous liquids reach their ultimate equilibrium value very soon after the formation of a new surface. The agreement between the observed results and the published data on interfacial tension is less perfect, but these greater discrepancies are to be expected, since it is

---

[3] Sample calculation of the surface tension of a pendant drop by the method of the selected plane:

Carbon tetrachloride in air at 25.0°C.; surface 15 sec. old.

Density of CCl_4	1.585 g. per cm.^{3}
Density of air	0.001 g. per cm.^{3}
Effective density	1.584 g. per cm.^{3}
Diameter of drop at equator, d_e	0.228 cm.
Diameter of drop at selected plane, d_s	0.224 cm.

$$S = \frac{d_s}{d_e} = 0.224/0.228 = 0.982$$

From table 1, $1/H = 0.321$

$$\gamma = \frac{g\sigma(d_e)^2}{H} = (0.321)\ (980.4)\ (1.584)\ (0.228)^2$$

$$= 26.0 \text{ dynes per centimeter}$$

The International Critical Tables, Vol. IV, p. 447, give for the surface tension of carbon tetrachloride at 25°C. the value 26.15 ± 0.1 dynes per centimeter.

generally recognized that the published values for interfacial tensions are frequently of low precision. Several causes are responsible for this. After a study of the sources of error which disturb standard methods and because of the relative freedom of the method of pendant drops from these difficulties, the new values are presented with the belief that they represent the true interfacial tensions of the samples, as and when they were measured, within a probable error of not more than ± 1.0 per cent.

TABLE 2

Boundary tensions at 25°C.

BOUNDARY	TENSIONS IN DYNES PER CENTIMETER	
	Observed	In the literature
Benzene-air	28.1	28.4
Ethanol-air	21.9	21.9
Methanol-air	22.5	22.2
Toluene-air	27.7	27.8
Mercury-benzene	362.	355.
Mercury-water	369.	374.
Water-benzene	30.1	34.7
Water-carbon tetrachloride	43.8	44.5
Water-toluene	32.9	36.1

TABLE 3

Boundary tensions at 25°C.

BOUNDARY	TENSIONS IN DYNES PER CENTIMETER						AVERAGE VALUES
Ether-air	17.6	17.3	17.6	17.4	17.5	17.3	17.4
Ether-mercury	376.	389.	381.	380.	377.	375.	378.

TABLE 4

Boundary tensions at 25°C.

INTERFACE	TENSIONS IN DYNES PER CENTIMETER	
	Pendant down	Pendant up
Benzene-water	30.1	30.1
Carbon tetrachloride-water	43.8	43.9
Ether-water	11.2	10.9

The results in table 2 are the averages of six determinations, each of which was made by measuring a *different* liquid drop. In table 3 the complete set of six measurements for diethyl ether-air and for diethyl ether-mercury interfaces is given to show the consistency of a typical set of measurements.

It is not necessary for the fluid from which a drop is formed to wet the tip. For instance, drops of mercury can be suspended from a glass tip. The only difference is that in this case the drop will hang from the *inside* rather than from the *outside* of the glass tube. Drops may be supported by the tip in a number of ways. They may hang from the outer wall, from the outer rim, from the flat end, from the inner rim, or even from the inner wall of the tube. This does not in any way affect the applicability of the method or the precision of the results. It is necessary that the drop be supported in such a way that it is a solid of revolution, but the exact size, shape, or manner of support are determined by considerations of convenience alone.

Drops may be hung "pendant down," the heavier fluid inside the lighter, or "pendant up," the lighter fluid in the heavier. It will be seen from table 4 that the results are independent of whether the drops are hanging up or down.

SURFACE-ACTIVE SYSTEMS

If one or more of the components of a fluid system migrates into or out of an interface which is under observation, a change in the boundary tension with time can usually be detected. Likewise if some sort of surface structure is formed or if a chemical reaction is taking place at the interface, a similar change may be noted. If the boundary tension changes as the surface grows older, the surface is said to "age." Aging effects may cause the boundary tension of a fluid system to decrease to a small fraction of its initial value.

Data on the aging of aqueous solutions of sodium oleate and sodium stearate in contact with air and with mineral oil are illustrative of aging effects. The method of pendant drops is particularly suited to the determination of such data, since it makes it possible to obtain instantaneous determinations at any desired time intervals without disturbing the surface under observation.

Pendant drops of a solution containing a surface-active substance, such as sodium stearate, have a constant volume, but they exhibit a progressive change of shape with time due to the aging of their surfaces. This effect is shown in figure 7, which presents a series of photographs which were made in succession on a single drop.

Before presenting the results graphically, it will be well to examine typical data. In table 5, the results which were computed from two sets of pictures are given. Each set of values represents measurements made on a single drop, and the liquid hanging from the tip was completely replaced before the second drop was formed. In general, duplicate sets of measurements were made for each solution which was studied, and the curves of figures 8 and 9 were plotted from the averages of these values.

It will be noted that there is good agreement between the two runs, even though the surface tension was changing quite rapidly and small errors in timing can produce considerable scattering in the results.

TABLE 5

Surface tension at 25°C. of a 0.025 per cent solution of sodium stearate in water

(See figures 7 and 10)

AGE IN SECONDS	SURFACE TENSION IN DYNES PER CENTIMETER	
	First drop	Second drop
5	70.8	72.2
10	71.9	71.6
15	69.7	66.3
30	62.9	63.4
60	58.2	56.9
120	54.4	54.6
240	51.6	50.7
480	47.3	45.8
960	42.8	42.6
1800	39.2	39.1
3600	36.0	35.7

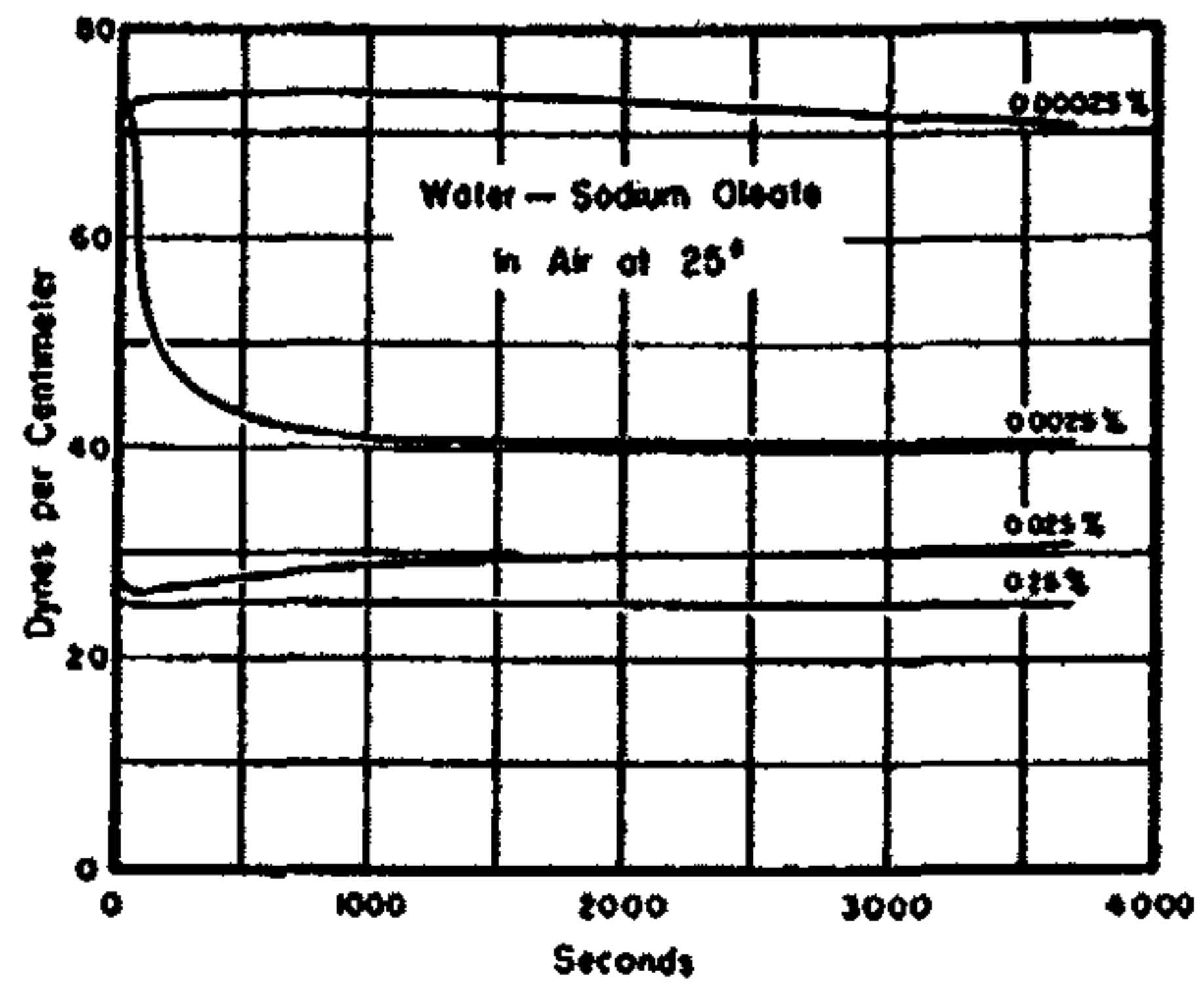

FIG. 8

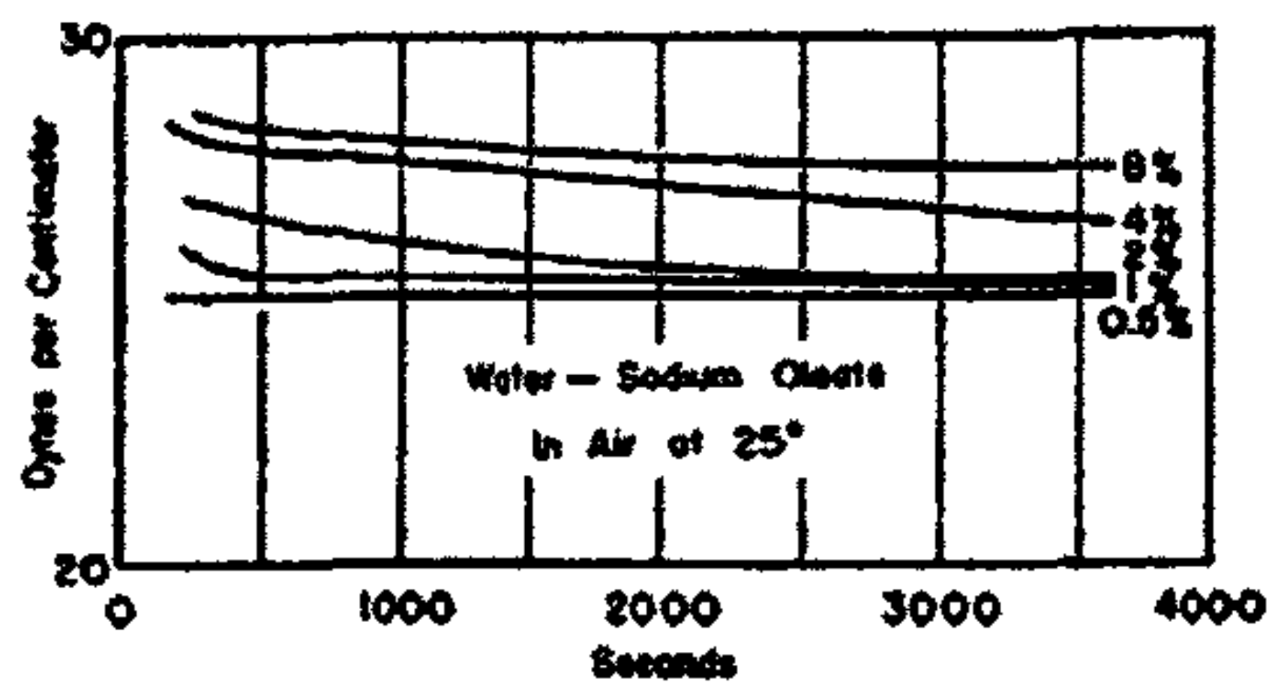

FIG. 9

FIG. 8. Change in surface tension of solutions of sodium oleate with time

FIG. 9. Change in surface tension of solutions of sodium oleate with time

Figure 8 shows the change, with time, of the surface tensions of solutions of sodium oleate. It will be noticed that extremely dilute solutions, 0.00025 or 0.0025 weight per cent, of this soap have an initial surface tension which is almost the same as that of pure water. During the first few seconds that the drop ages, the surface tension may increase. This is especially noticeable in the 0.00025 per cent curve, which rises rapidly, levels off, and then slowly decreases. It remains at a value of slightly more than 72 dynes per centimeter for the first 3000 sec. The second sample in the series, containing 0.0025 per cent of sodium oleate, shows this same initial increase above the surface tension of pure water. However, in this case the rise is very rapid, and within the first 15 sec. the surface tension starts to fall rapidly, having approximately reached an asymptote after about 1500 sec. Still more concentrated solutions, 0.025 and 0.25 per cent, show a decrease during the first few seconds, which is followed by a slow recovery. The 0.025 per cent solution seems to be approaching the same asymptote as the 0.0025 per cent solution, but it is approaching it from the lower side.

A minimum surface tension is observed for a solution containing 0.5 per cent sodium oleate and the aging curve for this solution is a horizontal straight line[4] (figure 9). More concentrated solutions have slightly higher surface tensions and all of them decrease with time, approaching the asymptote defined by the curve for the 0.5 per cent solution.

These results seem to indicate the existence of three different surface structures. One of these has a surface tension of about 74, the second has a surface tension of about 41, and the third has a surface tension of approximately 25 dynes per centimeter.

The explanation of these phenomena can undoubtedly be found in the concentration of soap in the interface resulting from surface activity. A freshly formed surface of a very dilute soap solution can be expected to have a surface tension very close to that of pure water, since the quantity of soap present in the new surface must be equal to the average throughout the drop. However, after a short interval of time has elapsed, enough soap will have collected in the interface to alter appreciably the boundary tension. As long as the concentration of soap in the interface remains sufficiently low, the molecules will exist in an ionized form, will behave as strong electrolytes, and will slightly raise the boundary tension. A further increase in the soap concentration will tend to change the soap molecules to an undissociated form and will cause a decrease in the boundary tension. Surface tensions greater than that of pure water may be explained by the presence of ionized soap.

The surface tension decreases rapidly as the concentration of soap in the interface increases, until a monomolecular or a colloidal film is formed. It is possible that the second type of surface is a structure of this kind.

Further concentration of soap in the interface increases the thickness of the film without greatly altering the surface tension. The minimum surface tension is probably reached when the film reaches an optimum colloidal thickness. A semi-solid "skin" is finally formed which gives

---

[4] J. W. McBain *et al.* (38) have previously mentioned the existence of such a minimum.

rise to (*a*) an apparent increase in boundary tension, and (*b*) a surface structure so different from the condition of homogeneous, isotropic liquids assumed in the simple theory of surface tension that the meaning and interpretation of the results become a matter of some uncertainty. Before these hypotheses can be established definitely, it will be necessary to examine many other dilute solutions.

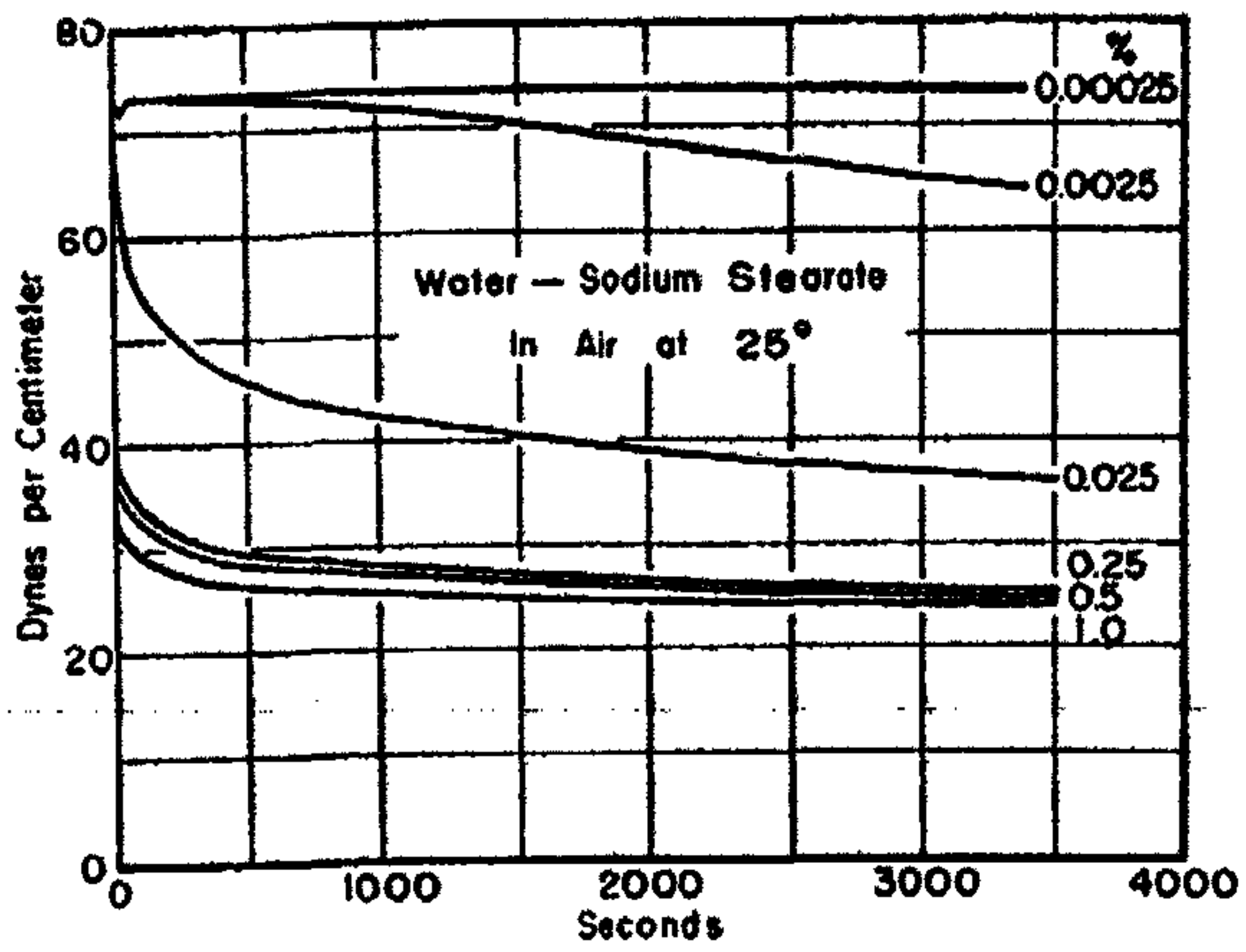

FIG. 10. Change in surface tension of solutions of sodium stearate with time

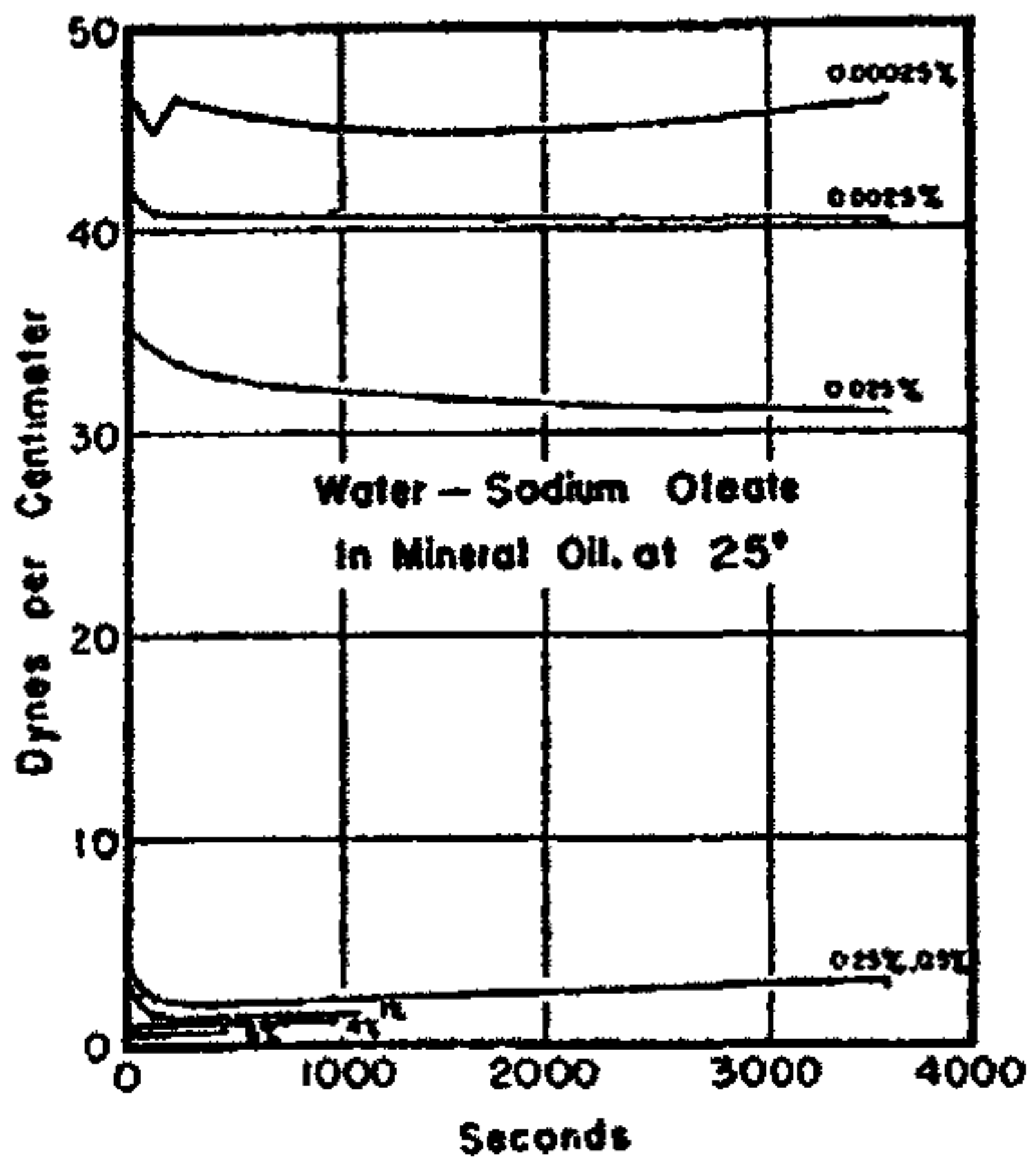

FIG. 11. Aging of the interface between aqueous solutions of sodium oleate and mineral oil

The curves for the aging of aqueous solutions of sodium stearate in air (figure 10) show a more uniform trend than do those for the oleate. As with sodium oleate, there appear to be at least two types of surface structure. More concentrated solutions could not be studied since they are semi-solid, anisotropic pastes.

Figure 11 shows the aging of the interface between several aqueous solutions of sodium oleate and mineral oil. The curves are qualitatively similar to those obtained for the aging of the same sodium oleate solutions in air, but it will be noted that the addition of a given amount of surface-active material causes a much greater percentage decrease in the interfacial tension than it does in the surface tension. For example, 1 per cent of sodium oleate reduces the equilibrium surface tension to 35 per cent, but it decreases the interfacial tension to 3 per cent of the no-soap value.

No concentration of sodium oleate was found which gives a minimum interfacial tension between the solution and the mineral oil. In this respect the interfacial tension results differ from the surface tension results, which show that a definite, minimum surface tension is obtained for solutions containing about 0.5 per cent of sodium oleate (38). This failure to find a minimum interfacial tension may be caused by the impossibility of examining sufficiently concentrated soap solutions.

The "break" in the 0.00025 per cent curve in figure 11 appears to be quite definite and to represent a real, sudden change in the surface of the drop. Similar effects have been observed in the aging of aqueous soap solutions in air. (Examine the 0.00025 per cent and 0.0025 per cent curves in figure 10.) The effect has only been observed with certain of the solutions, and, when it does occur, a second series of measurements always checks with the first. Unfortunately, the present data are too meager to throw much light on this curious effect. It is hoped that future work will reveal its cause.

SUMMARY

New work has demonstrated that the method of pendant drops provides a means for measuring either surface tension or interfacial tension which gives precise results under the most difficult conditions. The mathematical theory of the shape of static liquid drops is revised, and new methods are developed by which the boundary tension can be computed readily from a knowledge of the specific gravities of the liquids which are to be tested and from simple measurements made on a photograph which shows the silhouette of a hanging drop.

The construction of apparatus is discussed. With the equipment and empirical function now available, the method gives results which are comparable in speed and accuracy to the best obtainable by standard methods. With the present apparatus, the results have a probable error of about ± 0.5 per cent. The method is potentially capable of giving results accurate to ± 0.05 per cent. Future improvement depends upon a more precise determination of the mathematical function connecting drop shape with boundary tension and upon the construction of special, high-precision equipment.

The method has the following outstanding advantages: (*1*) It is sufficiently simple to be subjected to a complete mathematical analysis. (2) The results are independent of the angle of contact between the fluid interface and the apparatus. (*3*) The method is static and is therefore not influenced by viscosity effects. (*4*) Measurements are made instantaneously. (*5*) Successive measurements can be made of a given surface without disturbing it, thus permitting an accurate study of the aging of surfaces. (*6*) Boundary tensions of any magnitude can be observed. Values as great as 370 dynes and as small as 0.3 dyne per centimeter were measured with the present apparatus. (7) Either surface tension or interfacial tension can be measured in any system in which at least one fluid is transparent and the fluids are of unequal density. (*8*) Only small samples are required. One cubic centimeter of the internal phase is usually more than enough for several measurements. (*9*) The apparatus is adapted to simple temperature control. (*10*) The photographs on which the measurements are made serve as permanent records.

Typical measurements are presented which show that: (*1*) The results are in agreement with those determined by standard methods and published in the literature. (*2*) The method gives self-consistent results for the boundary tensions of a great variety of liquid systems, of which some have not been reported previously. (*3*) The presence of surface-active materials can have a tremendous effect on the boundary tension, and liquid-liquid interfaces are relatively more affected by surface-active materials than are liquid-gas interfaces. (*4*) Boundary tensions may either increase or decrease during the aging of an interface.

Preliminary suggestions as to the possible reasons for the observed phenomena are offered.

The results so far obtained justify the belief that the method of pendant drops will prove to be of special value in studying the boundary tensions of (*1*) viscous liquids, (*2*) surface-active solutions, (*3*) small samples of rare chemicals, and (*4*) systems in which the contact angle is not zero.

REFERENCES

(1) ADAM, N. K.: The Physics and Chemistry of Surfaces, 2nd edition. The Clarendon Press, Oxford (1938). (General.)

(2) ANDREAS, J. M.: Sc. D. Thesis, Massachusetts Institute of Technology, 1938. (Pendant drops.)

(3) BASHFORTH, F., AND ADAMS, J. C.: An Attempt to Test the Theories of Capillary Action. University Press, Cambridge, England (1883). (Pendant drops.)

(4) BOSANQUET, C. H.: Phil. Mag. [7] **5**, 296-301 (1928) (Capillary rise.)

(5) CLAYTON, W.: Theory of Emulsions. P. Blakiston's Son and Co., Philadelphia (1935). (General.)

(6) Dorsey, N. E.: Natl. Bur. Standard (U. S.), Sci. Papers **21**, 563-95 (1926). (General review and bibliography.)

(7) Dupré, A.: Théorie Mécanique de la Chaleur. Gauthier-Villars, Paris (1869). (Pendant drops.)

(8) Edgerton, H. E., Hauser, E. A., and Tucker, W. B.: J. Phys. Chem. **41**, 1017-28 (1937). (Falling drops.)

(9) Ernst, R. C., Watkins, C. H., and Ruwe, H. H.: J. Phys. Chem. **40**, 627-35 (1936). (Data.)

(10) Eversole, W. G., and Dedrick, D. S.: J. Phys. Chem. **37**, 1205-12 (1933). (Falling drops.)

(11) Ferguson, A.: Phil. Mag. [6] **23**, 417-30 (1912). (Pendant drops.)

(12) Ferguson, A.: Fifth Report on Colloid Chemistry. London (1923). (Review and bibliography.)

(13) Ferguson, A., and Kennedy, S. J.: Proc. Phys. Soc. (London) **44**, 511-20 (1932). (Modified capillary.)

(14) Freundlich, H.: Colloid and Capillary Chemistry. Dutton and Co., New York (1926). (General.)

(15) Harkins, W. D., and Brown, F. E.: J. Am. Chem. Soc. **38**, 246-53 (1916). (Falling drops.)

(16) Harkins, W. D., and Brown, F. E.: J. Am. Chem. Soc. **41**, 499-524 (1919). (Falling drops.)

(17) Harkins, W. D., and Gans, D. M.: J. Am. Chem. Soc. **52**, 2287-9 (1930). (Falling drops.)

(18) Harkins, W. D., and Humphrey, E. C.: J. Am. Chem. Soc. **38**, 228-36 (1916). (Falling drops.)

(19) Harkins, W. D., Young, T. F., and Cheng, L. H.: Science **64**, 333-6 (1926). (Ring.)

(20) Harkins, W. D., and Zollman, H.: J. Am. Chem. Soc. **48**, 69-80 (1926). (Aging.)

(21) Hauser, E. A.: Colloidal Phenomena. McGraw-Hill Book Co., Inc., New York (1939). (General.)

(22) Hauser, E. A., Edgerton, H. E., Holt, B. M., and Cox, J. T., Jr.: J. Phys. Chem. **40**, 973-88 (1936). (Falling drops and ring.)

(23) Hunter, R. F.: Chem. News **143**, 406-8 (1931). (Parachor.)

(24) Jones, G., and Ray, W. A.: J. Am. Chem. Soc. **59**, 187-98 (1937). (Modified capillary.)

(25) Kohlrausch, F.: Ann. Physik [4] **20**, 798-806 (1906). (Pendant drops.)

(26) Laplace, P. S.: Mécanique Céleste, supplement to the 10th book. France (1806). (Pendant drops.)

(27) Léauté, A.: Compt. rend. **201**, 41-3 (1935). (Capillary rise of viscous substances.)

(28) Lemarchands, M., and Convers, L.: J. chim. phys. **32**, 657-69 (1935). (Data.)

(29) Lenard, P.: Ann. Physik **74**, 381-404 (1924). (Staple.)

(30) Lohnstein, T.: Ann. Physik **54**, 713-23 (1895). (Pendant drops.)

(31) Lohnstein, T.: Ann. Physik **20**, 237-68 (1906). (Pendant drops.)

(32) Lohnstein, T.: Ann. Physik **20**, 606-18 (1906). (Pendant drops.)

(33) Lohnstein, T.: Ann. Physik **21**, 1030-48 (1906). (Pendant drops.)

(34) Lohnstein, T.: Ann. Physik **22**, 767-81 (1907). (Falling drops.)

(35) Mack, G. L., and Bartell, F. E.: J. Am. Chem. Soc. **54**, 936-42 (1932). (Double capillary.)

(36) Macy, R.: J. Chem. Education **12**, 573-6 (1935). (Ring.)

(37) Maxwell, J. C.: The Encyclopaedia Britannica, 9th edition (1875). (Summary on surface tension.)

(38) McBain, J. W., Ford, T. F., and Wilson, D. A.: Kolloid-Z. **78**, 1 (1937). (Aging.)

(39) Plateau, J. A. F.: Statique Expérimental et Théorétique des Liquides Soumis aux Seules Forces Moléculaires. Gauthier-Villars, Paris (1873). (Weightless liquids.)

(40) Porter, A. W.: Phil. Mag. [7] **7**, 624–30 (1929). (Pendant drops.)

(41) Porter, A. W.: Phil. Mag. [7] **8**, 180 (1929). (Pendant drops.)

(42) Reynolds, W. C.: J. Chem. Soc. **119**, 460–76 (1921). (Data.)

(43) Richards, T. W., and Carver, E. K.: J. Am. Chem. Soc. **43**, 827–47 (1921). (Capillary rise.)

(44) Rideal, E. K.: An Introduction to Surface Chemistry, 2nd edition. Cambridge University Press, London (1930). (General.)

(45) Speakman, J. C.: J. Chem. Soc. **1933**, 1449–53. (Complicated capillary.)

(46) Sugden, S.: J. Chem. Soc. **119**, 1483–92 (1921). (Capillary rise.)

(47) Sugden, S.: J. Chem. Soc. **121**, 858–66 (1922). (Maximum bubble pressure.)

(48) Sugden, S.: The Parachor and Valency. G. Routledge & Sons, London (1930). (Parachor.)

(49) Thompson, Sir Wm.: Nature **34**, 270–2, 290–4, 366–9 (1886). (Capillary rise.)

(50) Thompson, Sir Wm.: Popular Lectures and Addresses of Lord Kelvin, Vol. I, pp. 1–72. The Macmillan Co., New York (1889). (Capillary rise.)

(51) Tucker, W. B.: Sc. D. Thesis, Massachusetts Institute of Technology, 1938. (Pendant drops.)

(52) Verschaffelt, J. E.: Commun. Phys. Lab. Univ. Leiden **14**, No. 42e (1918). (Pendant drops.)

(53) Vickers, A. E. J., Sugden, J. A., and Bell, R. A.: J. Soc. Glass Tech. **18**, 224–5A (1933). (Maximum bubble pressure.)

(54) Willows, R. S., and Hatschek, E.: Surface Tension and Surface Energy. P. Blakiston's Son and Co., Philadelphia (1923). (General.)

(55) Worthington, A. M.: Proc. Roy. Soc. (London) **32**, 362 (1881). (Pendant drops.)

(56) Young, T.: Phil. Trans. **5**, 65–87 (1805). (General.)

CONVENTIONS AND ASSUMPTIONS IN THE INTERPRETATION OF EXPERIMENTAL DATA BY MEANS OF THE GIBBS ADSORPTION THEOREM[1]

PIERRE VAN RYSSELBERGHE

Department of Chemistry, Stanford University, California

Received July 1, 1938

I. INTRODUCTION

Various conventions used in the interpretation of surface tension data by means of the Gibbs adsorption theorem (4) have been discussed in a number of recent contributions, such as those of Guggenheim and Adam (5), Butler and Wightman (2), and Rice (8). We shall briefly recall the essential points of these methods. Let us consider a two-component, two-phase system, for instance, a binary solution and its mixed vapor, separated from each other by a plane interface. The Gibbs adsorption theorem (4) states that, when the inhomogeneous layer at the interface is in complete equilibrium with the liquid and the vapor phase at a given temperature,

$$d\sigma = -\Gamma_1 \, d\mu_1 - \Gamma_2 \, d\mu_2 \tag{1}$$

in which σ is the surface tension of the solution, μ_1 and μ_2 the molar chemical potentials of the two components, and Γ_1 and Γ_2 the surface excesses in moles per unit area. It has been demonstrated by Gibbs (4) that, when the mathematical dividing surface is plane, equation 1 is invariant in form with respect to a change in the position of this surface and $d\sigma$ has the same value for all positions of the surface. The surface excesses Γ_1 and Γ_2, on the contrary, depend on the position of the surface, but the expression $\Gamma_1 \frac{N_2}{N_1} - \Gamma_2$, in which N_1 and N_2 are the mole fractions of the bulk solution, is invariant with respect to a change in the position of the dividing surface, since, on account of the Gibbs-Duhem formula

$$N_1 \, d\mu_1 + N_2 \, d\mu_2 = 0 \tag{2}$$

---

[1] Presented at the Fifteenth Colloid Symposium, held at Cambridge, Massachusetts, June 9-11, 1938.

(in which the concentrations of both components in the vapor phase are neglected), formula 1 may be rewritten

$$d\sigma = \left(\Gamma_1 \frac{N_2}{N_1} - \Gamma_2\right) d\mu_2 \tag{3}$$

The two differentials $d\sigma$ and $d\mu_2$ being invariant, the expression

$$\Gamma_1 \frac{N_2}{N_1} - \Gamma_2$$

is also invariant. A special position of the mathematical dividing surface corresponds to what Gibbs has called the "surface of tension," for which certain equations have "the same form as if a membrane without rigidity and having a tension σ, uniform in all directions, existed at the dividing surface" (4, page 229). Defay (3) has established the conditions of mechanical equivalence between the real system with an inhomogeneous layer of finite thickness and the idealized system in which the two phases are separated by the surface of tension. These conditions are only of theoretical interest and cannot yield explicit information concerning the exact position of the surface of tension until the complete structure of the layer and the distribution of tensions are known. Let us note, however, that even in the case of plane interfaces, in spite of the invariance of σ, there is a definite surface of tension, determined, as shown by Defay (3), by conditions of equivalence of total torques. It is necessary, however, to have recourse to other dividing surfaces if one wishes to calculate values of Γ_1 and Γ_2 from which some information as to the structure of the layer can be derived.

It is customary to locate the dividing surface in such a manner that the surface excess Γ_1 of the solvent is equal to zero and to calculate the surface excess Γ_2 of the solute from the formula

$$\Gamma_2^{(1)} = -\frac{d\sigma}{d\mu_2} \tag{4}$$

which gives us a convenient and suggestive method of recording the results of surface tension measurements. If, however, one wishes more precise information concerning the inhomogeneous layer, it is preferable to put the dividing surface immediately underneath the layer. Since the concentrations in the vapor phase are neglected, the values of Γ_1 and Γ_2 represent the total amounts of components 1 and 2 present in a column of 1 cm.^{2} cross section on top of the homogeneous liquid. So far, we have only one equation to determine the unknowns Γ_1 and Γ_2, namely, the Gibbs theorem 3. We thus have to set up a second relationship between Γ_1 and Γ_2.

For instance, we may assume that the layer is one molecule thick and write

$$\Gamma_1 A_1 + \Gamma_2 A_2 = 1 \tag{5}$$

in which A_1 and A_2 are the areas per mole of each component. Guggenheim and Adam (5) and also Butler and Wightman (2) have shown, in the case of water–alcohol mixtures, that the simultaneous equations 3 and 5 yield reasonable values of Γ_1 and Γ_2 when plausible constant values of A_1 and A_2 are adopted and all other disturbing effects are neglected. The surface mole fraction $\Gamma_2/\Gamma_1 + \Gamma_2$ obtained by these authors is not steady and exhibits a slight maximum before increasing to the value 1 in pure alcohol. Guggenheim and Adam (5) ascribe this effect to a possible lack of constancy of the molar areas A_1 and A_2, while Butler and Wightman (2) suggest that the layer may not be truly monomolecular.

Various mixture rules for the surface tension of binary solutions have been used in the older work on the subject without any reference to the Gibbs adsorption theorem. For instance, Morgan and Griggs (6) and Morgan and Scarlett (7) use the mixture rule

$$\sigma = x\sigma_1 + (1 - x)\,\sigma_2 \tag{6}$$

in which σ_1 and σ_2 are the surface tensions of the pure liquids, and x and $1 - x$ the percentages by weight of the components in the bulk solution. No discussion of adsorption at the interface is presented, and the Gibbs theorem is not mentioned. Whatmough (9) used mixture rules of the same type, but took for x and $1 - x$ mole fractions, weight fractions, or volume fractions of the bulk solution, again without reference to the phenomenon of adsorption.

In this paper we wish to present and discuss the simplest possible mixture rule in which adsorption is taken into account, namely

$$\sigma = \frac{\Gamma_1\sigma_1 + \Gamma_2\sigma_2}{\Gamma_1 + \Gamma_2} \tag{7}$$

This formula is derived from the logical assumption that the Γ_1 and Γ_2 values actually responsible for the surface tension will contribute, as a first approximation, the portions

$$\frac{\Gamma_1}{\Gamma_1 + \Gamma_2} \cdot \sigma_1 \quad \text{and} \quad \frac{\Gamma_2}{\Gamma_1 + \Gamma_2} \cdot \sigma_2$$

to the total surface tension σ. The Gibbs theorem 3 and our formula 7 are simultaneous equations, the unknowns being Γ_1 and Γ_2.

II. DISCUSSION OF THE MIXTURE RULE AND OF THE GIBBS ADSORPTION THEOREM

The terms "positive adsorption" and "negative adsorption" of the solute at the surface of the solution are based upon the sign of $\Gamma_2^{(1)}$ of formula 4, which is obviously opposite to that of $d\sigma/d\mu_2$ or also opposite to that of $d\sigma/dN_2$, since $d\mu_2/dN_2$ is always positive. From formula 3, however, nothing can be said about the sign of Γ_2 until Γ_1 is known, or *vice versa*. Our mixture rule (equation 7) requires both Γ_1 and Γ_2 to be positive. We shall associate the terms "positive adsorption" and "negative adsorption," respectively, with the following two inequalities

$$\frac{\Gamma_2}{\Gamma_1 + \Gamma_2} > N_2 \qquad \frac{\Gamma_2}{\Gamma_1 + \Gamma_2} < N_2 \tag{8}$$

Formula 7 gives

$$\frac{\Gamma_2}{\Gamma_1} = \frac{\sigma_1 - \sigma}{\sigma - \sigma_2} \quad \text{and} \quad \frac{\Gamma_2}{\Gamma_1 + \Gamma_2} = \frac{\sigma_1 - \sigma}{\sigma_1 - \sigma_2} \tag{9}$$

Combining equations 3 and 7 we get

$$\frac{d\sigma}{d\mu_2} = \Gamma_2\left[\frac{\sigma - \sigma_2}{\sigma_1 - \sigma}\cdot\frac{N_2}{N_1} - 1\right] \tag{10}$$

Now, Γ_2 being positive, we have

$$\frac{\sigma - \sigma_2}{\sigma_1 - \sigma}\cdot\frac{N_2}{N_1} - 1 \gtrless 0 \quad \text{when} \quad \frac{d\sigma}{d\mu_2} \gtrless 0 \tag{11}$$

or also

$$\frac{\Gamma_2}{\Gamma_1 + \Gamma_2} = \frac{\sigma_1 - \sigma}{\sigma_1 - \sigma_2} \gtrless N_2 \quad \text{when} \quad \frac{d\sigma}{d\mu_2} \lessgtr 0 \tag{12}$$

Our mixture rule is, therefore, in agreement with the familiar interpretation of the Gibbs theorem based upon the convention $\Gamma_1 = 0$.

Figure 1 corresponds to positive adsorption of alcohol (component 2) at the surface of water–alcohol mixtures. The curve represents the surface tension plotted against the bulk mole fraction N_2; the straight line represents the surface tension plotted against the surface mole fraction $\Gamma_2/\Gamma_1 + \Gamma_2$. The analogy with phase rule diagrams is obvious. If the surface tension curve exhibits a minimum or a maximum at some particular composition (N_1^0, N_2^0) our mixture rule cannot be applied without modification. At the extremum we have

$$\frac{d\sigma}{d\mu_2} = \frac{d\sigma}{dN_2}\cdot\frac{dN_2}{d\mu_2} = 0 \tag{13}$$

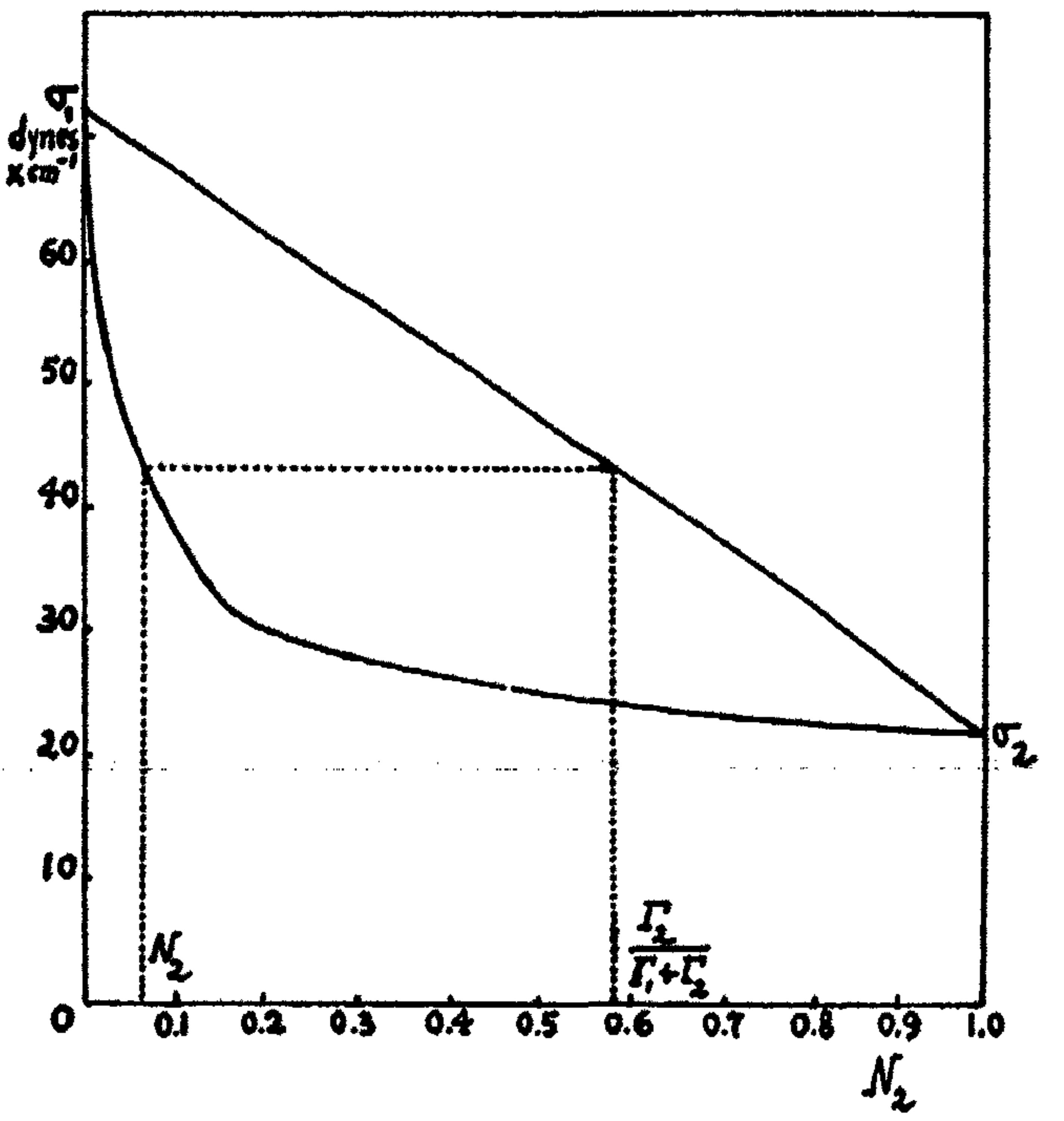

FIG. 1. Surface tension of water-alcohol mixtures plotted against bulk and surface mole fraction of alcohol

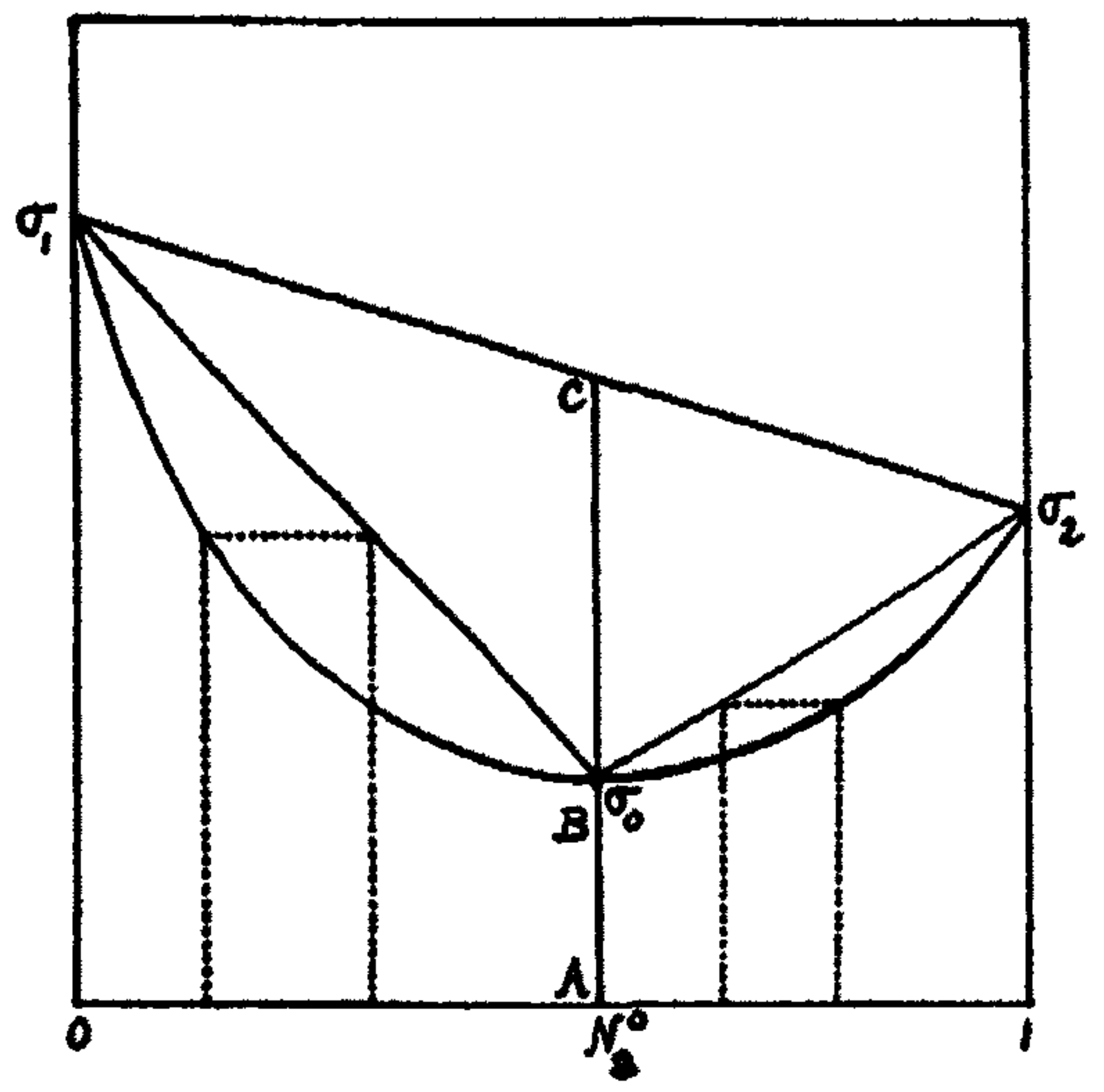

FIG. 2. Surface tension curve exhibiting a minimum

and, according to equation 3,

$$\frac{\Gamma_2^0}{\Gamma_1^0} = \frac{N_2^0}{N_1^0} \quad \text{or} \quad \frac{\Gamma_2^0}{\Gamma_1^0 + \Gamma_2^0} = N_2^0 \qquad (14)$$

In other words, the surface mole fraction and the bulk mole fraction are identical at the extremum. We should have, according to our mixture rule,

$$\sigma_0 = N_1^0\sigma_1 + N_2^0\sigma_2 \qquad (14)$$

which is impossible, since it would require the segments *AB* and *AC* of figure 2 to be equal. We can, however, overcome this difficulty by applying the mixture rule separately between σ_1 and σ_0 and between σ_0 and σ_2. We then have positive adsorption of the mixture N_2^0 between σ_1 and σ_0 and negative adsorption of this mixture between σ_0 and σ_2. The analogy with the boiling point diagram of an azeotropic mixture is obvious.

III. INTERPRETATION OF SURFACE TENSION DATA FOR WATER–ALCOHOL MIXTURES AND DESCRIPTION OF THE SURFACE LAYER

In order to test the plausibility and usefulness of our mixture rule we now present a new interpretation of the surface tension data of water–alcohol mixtures. The values of $d\sigma/d\mu_2$ are obtained from the paper of Guggenheim and Adam (5), where $-\ d\sigma/d\mu_2$ is called $\Gamma_2^{(1)}$, being the value of Γ_2 corresponding to the usual convention $\Gamma_1 = 0$. The values of σ are those of Bircumshaw (1). Similar values for both σ and $d\sigma/d\mu_2$ were obtained by Butler and Wightman (3). In table 1 we give, for a series of mole fractions N_2 of alcohol, the surface tension σ in dynes per centimeter, the derivative $d\sigma/d\mu_2$ in moles per cm.^{2}, the surface excesses Γ_1 and Γ_2 as calculated by means of our formulas 7 and 10, in moles per cm.^{2}, the surface mole fraction $\Gamma_2/\Gamma_1 + \Gamma_2$, and the area A_2 in cm.^{2} occupied by one mole of alcohol and calculated as indicated below. The temperature is 25°C.

Our values of Γ_1 and Γ_2 are of the right order of magnitude for a monomolecular layer. A comparison with those obtained by Guggenheim and Adam (5) from equation 5 shows that, while their values of Γ_2 increase with N_2, our values decrease, indicating that the area occupied per mole of alcohol increases with N_2. This area is constant in Guggenheim and Adam's calculations. Their values of Γ_1 decrease when N_2 increases and so do ours, but our Γ_1's are smaller, in agreement with the idea of an increasing area for the alcohol molecules, since the area of water molecules can probably be assumed constant and independent of possible changes of orientation, while the area occupied by alcohol molecules will vary considerably, the two extreme cases being molecules standing up on the surface and molecules lying flat on it. We have calculated the area occupied by one mole of alcohol at the various mole fractions N_2 by assuming the area A_1 for water to be 0.06×10^{10} cm.^{2} per mole, i.e., the second of the three values considered by Guggenheim and Adam (5). The results are reported in the last column of table 1. Extrapolating to $N_2 = 0$ we see that the limiting value of A_2 is in perfect agreement with the value 0.12×10^{10} cm.^{2} per mole adopted by Guggenheim and Adam (5) for molecules of alcohol oriented perpendicularly to the surface. Extrapolating to $N_2 = 1$ we find $A_2 = 0.45 \times 10^{10}$ cm.^{2} per mole, a result which would indicate that in pure alcohol most of the molecules are lying flat on the surface. The intermediate values of A_2 can be considered as giving a measure of the average orientation of alcohol molecules at the surface. It is of course true that, if orientation changes with concentration, the values of σ_2 in the mixture rule (7) also depend on concentration, but in an unknown manner. It is, however, probable that such a variation is small and that our interpretation of surface tension data is just as plausible as that based upon the initial assumption of a monomolecular layer and upon the corresponding formula (formula 5) in which the area A_2 is considered as constant. The mole fractions $\Gamma_2/\Gamma_1 + \Gamma_2$ reported in table 1 increase with N_2 in a continuous and steady manner, as is shown on figure 3 by the heavy curve I, while the dotted curve II represents the mole fractions obtained by Guggenheim and Adam (6) for $A_1 = 0.06 \times 10^{10}$. Similar results were obtained by these authors with $A_1 = 0.04 \times 10^{10}$ and 0.08×10^{10}, A_2 being 0.12×10^{10} in the three cases. It is interesting to note that our interpretation of the composition of the surface layer agrees with a suggestion made by Rice (8, page 573): "Now it might happen

TABLE 1

Surface tension and surface composition of water-alcohol mixtures

N_2	σ	$-\frac{d\sigma}{d\mu_2} \times 10^{10}$	$\Gamma_1 \times 10^{10}$	$\Gamma_2 \times 10^{10}$	$\frac{\Gamma_2}{\Gamma_1 + \Gamma_2}$	$A_2 \times 10^{-10}$
0	72.2	0.0	(16.7)	0	0	(0.12)
0.05	45.0	5.85	5.2	6.1	0.54	0.11
0.1	36.4	6.3	2.65	6.6	0.715	0.13
0.2	29.7	6.45	1.2	6.75	0.845	0.135
0.3	27.6	5.9	0.78	6.25	0.89	0.155
0.4	26.35	5.1	0.52	5.45	0.915	0.18
0.5	25.4	4.25	0.33	4.6	0.935	0.215
0.6	24.6	3.4	0.20	3.7	0.95	0.265
0.7	23.85	2.9	0.12	3.2	0.965	0.31
0.8	23.2	2.5	0.07	2.75	0.975	0.36
0.9	22.6	2.2	0.03	2.45	0.99	0.405
1.0	22.0	2.1	0.00	(2.2)	1.00	(0.45)

that with increasing concentration of alcohol, the more polar water molecules being replaced by weaker alcohol molecules, there would be a decrease in orientation with an increase in area occupied, caused by each alcohol molecule lying flat in the surface."

It is interesting to note that the distance between our dividing surface and that corresponding to $\Gamma_1 = 0$ varies from 1.09 Å. for $N_2 = 0.05$ to 0.16 Å. for $N_2 = 0.9$. A displacement of the dividing surface smaller than the thickness of a monomolecular layer has thus a profound influence on the values of Γ_1 and Γ_2. When the surface corresponding to $\Gamma_1 = 0$ is used we are unable to obtain any information regarding the amount of component 1 which, together with the amount Γ_2 of component 2, is responsible for the surface tension, while our mixture rule gives a first approximation for both Γ_1 and Γ_2.

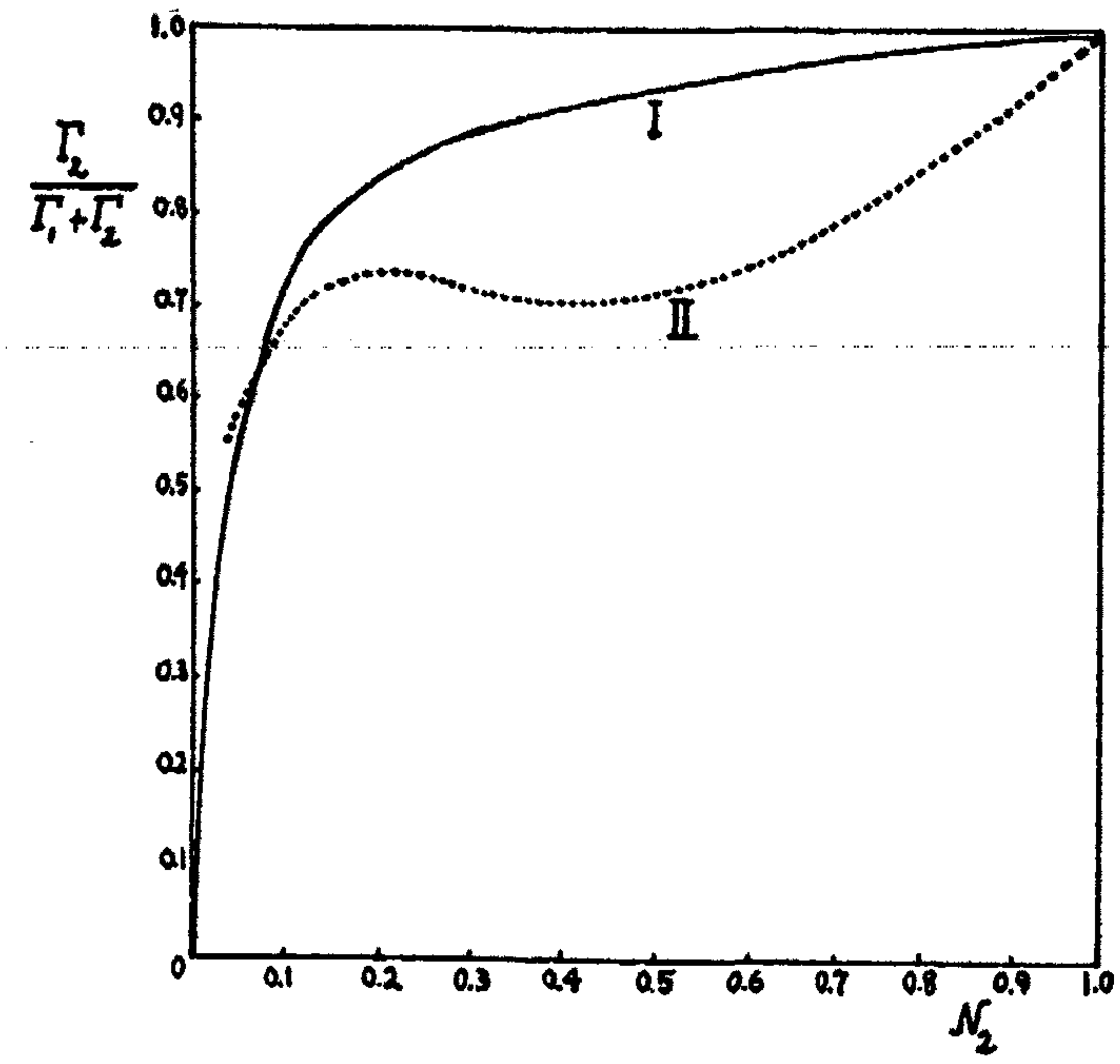

FIG. 3. Surface mole fraction of alcohol plotted against bulk mole fraction in water-alcohol mixtures

IV. SUMMARY

1. Conventions and assumptions in the interpretation of surface tension data of binary mixtures are briefly discussed. The concept of surface of tension is recalled.

2. A mixture rule for the surface tension of binary mixtures involving

the surface excesses of both components is proposed. This rule and the Gibbs adsorption theorem form a system of two simultaneous equations in which these surface excesses are the unknowns.

3. It is shown that the mixture rule agrees with the familiar concepts of positive and negative adsorption usually defined by means of the convention $\Gamma_1 = 0$. The case of surface tension curves with an extremum is discussed separately.

4. The method is applied to water-alcohol mixtures. The results show that the surface mole fraction of alcohol increases rapidly and steadily when the bulk mole fraction increases, that the surface excess of water decreases rapidly, that the surface excess of alcohol decreases after passing through a maximum near $N_2 = 0.2$. If the inhomogeneous layer is monomolecular, the alcohol molecules, oriented perpendicularly to the surface in very dilute solutions, lie flat on the surface in pure alcohol.

REFERENCES

(1) **Bircumshaw**, L. L.: J. Chem. Soc. **121**, 887 (1922).
(2) **Butler**, J. A. V., and **Wightman**, A.: J. Chem. Soc. **1932**, 2089.
(3) **Defay**, R.: Étude Thermodynamique de la Tension Superficielle, pp. 97–105, 150–151. Gauthier-Villars, Paris (1934).
(4) **Gibbs**, J. W.: Collected Works, Vol. I, pp. 219–331. Longmans, Green and Co., New York (1928).
(5) **Guggenheim**, E. A., and **Adam**, N. K.: Proc. Roy. Soc. (London) **A139**, 218 (1932).
(6) **Morgan**, J. L. R., and **Griggs**, M. A.: J. Am. Chem. Soc. **39**, 2261 (1917).
(7) **Morgan**, J. L. R., and **Scarlett**, A. J.: J. Am. Chem. Soc. **39**, 2275 (1917).
(8) **Rice**, J.: A Commentary on the Scientific Writings of J. W. Gibbs, Vol. I, pp. 505–708. Yale University Press, New Haven (1936).
(9) **Whatmough**, W. H.: Z. physik. Chem. **39**, 129 (1902).

STUDIES IN COLLOIDAL CLAYS. I[1]

E. A. HAUSER AND D. S. LE BEAU[2]

Department of Chemical Engineering, Massachusetts Institute of Technology, Cambridge, Massachusetts

918-110

Received July 1, 1938

Only in recent years has it been possible to produce for the purpose of further studies well-defined monodisperse fractions of colloidal clays by rational supercentrifugal separation (2, 3).

The lack of data concerning, primarily, clay sols of low concentration and varying particle sizes made highly desirable a closer study of *freshly* prepared natural suspensions of the clay mineral montmorillonite (the major constituent of bentonite) in concentrations from about 0.06 to 2 per cent by weight.

Of special interest was the question whether any signs of structure could be detected in such low concentrations and, if so, how these change with particle size of the suspension and also what effect certain pretreatments of the original suspensions, as, for instance, thermal concentration at different temperatures, would have on their properties. Changes due to the addition of electrolyte have not been considered in this investigation, but will be discussed separately in a later publication.

The particular bentonite used in this work was of the Wyoming type, mined by the American Colloid Co., Chicago, Illinois. (For further details as to location of the deposit, see reference 3.)

The analysis of the finest fraction of this bentonite gave the values in table 1.

The different particle size fractions were produced according to a method described by Hauser and Reed (2). Six fractions were obtained. The gels produced by supercentrifuging had about 10 per cent dry weight content. They were stored in the condition in which they were scraped from the liner of the centrifuge. The overflow of the finest and final fraction was collected and stored as a sol of 0.46 per cent dry weight. It will be referred to as fraction 7.

The following experiments were carried out with fraction 6 containing particles of an average apparent diameter of 14 mμ. Comparative studies

---

[1] Presented at the Fifteenth Colloid Symposium, held at Cambridge, Massachusetts, June 9-11, 1938.

[2] Present address: Dewey & Almy Chemical Co., Cambridge, Massachusetts.

were also made with fraction 4 (average apparent particle diameter = 28 mμ) and fraction 2 (average apparent particle diameter = 48 mμ) and fraction 7. (This sol contains only particles of an apparent diameter below 14 mμ.)

PREPARATION OF STANDARD SOLS

Sols varying in concentration from 0.06 to 2 per cent dry weight of bentonite were made up from fractions 6, 4, and 2, by careful dilution of the gels obtained by supercentrifuging with conductivity water, to approximately the desired concentrations. The exact concentrations of these dispersions of known apparent particle size were determined gravimetrically by evaporation to constant weight at 105°C.

TABLE 1

Composition of the bentonite

	per cent
Loss at 105°C.	6.20
SiO_2	58.88
Fe_2O_3	2.86
Al_2O_3, Mn_3O_4, P_2O_5	26.16
CaO	0.80
MgO	2.67
Na_2O/K_2O as Na_2O	2.13
SO_3	Not determined
	99.78

Finally, a dispersion of fraction 6 of only 0.077 per cent dry weight was produced for the purpose of studying the influence of temperature on property changes of sols obtained by concentration instead of dilution. This standard dispersion was reconcentrated by means of thermal evaporation at 75°C. and 95°C. to approximately the same concentrations as obtained by dilution of the original gels.

APPARENT SPECIFIC GRAVITY AT 25°C.

All determinations were carried out with a simple type of pycnometer, this having been found most suitable for the work. All precautions essential in obtaining accurate results as, for example, temperature control provided by a thermostat sensitive to ± 0.01°C., perfect cleanliness, freedom from air bubbles in the sols, etc., were carefully observed.

The apparent specific gravity was determined as follows:

$$W_s - W_B = W_W \qquad (1)$$

$$V_p - V_W = V_B \qquad (2)$$

$$\frac{W_B}{V_B} = \text{apparent specific gravity}$$

where W_s = weight of suspension in pycnometer (25°C.),
W_B = weight of bentonite present in W_s as known by dry weight determinations,
V_p = volume of pycnometer (at 25°C.),
V_W = volume of water in suspension (25°C.), and
V_B = apparent volume of bentonite in suspension

The apparent specific gravities of seven dispersions of fraction 6, all obtained by dilution varying in per cent dry weight from 0.067 to 1.939 are given in table 2.

It can be seen that, starting with the most dilute dispersion which gives a value slightly below the one generally recorded in literature for dry bentonite (2.6–2.7), there is a continuous increase in apparent specific gravity. It is more pronounced in the lower concentrations than in the higher ones. From concentrations above 1.5 per cent dry weight the apparent specific gravity approaches an asymptotic value. Since the specific gravity of a substance is determined by the term $\frac{\text{weight}}{\text{volume}}$, it should be a constant, independent of the amount (weight) of the substance used. The actual weight of the bentonite present in any of the dispersions studied being known, the only variable left is its apparent volume, since the determination of the volume of bentonite present in the suspension is an indirect one. The calculated values for the apparent volume turn out to be smaller than the volume as computed when using the dry specific gravity of bentonite. This can be explained by assuming that the amount of water present in the pycnometer when filled with the *suspension* is in excess of the theoretical amount needed to fill the pycnometer containing a known volume of bentonite. Therefore, the surplus of the water must be strongly adsorbed and compressed on to the surface of the bentonite particles.

TABLE 2

Apparent specific gravities (25°C.) of seven dispersions of fraction 6

CONCENTRATION IN PER CENT DRY WEIGHT	APPARENT SPECIFIC GRAVITY
0.067	2.580
0.152	2.714
0.368	2.773
0.710	2.796
1.146	2.845
1.506	2.860
1.643	2.861
1.939	2.861

As a further consequence of this deduction one would have to expect that the apparent specific gravity will decrease inversely with the particle size of the sols studied. Increasing particle size results in a decrease of available surface area of the disperse phase. The apparent specific gravities[3] for fractions 4 and 2, respectively, are recorded in tables 3 and 4 (figure 1).

As can be seen, fraction 4—although here, too, an increase in apparent specific gravity with increasing concentration is noticeable—does not reach the values of fraction 6. Fraction 2 in turn gives lower apparent specific gravities than fraction 4. However, up to a concentration of 2 per cent, none of these fractions approaches a constant value, as fraction 6 did. This can be explained by the presence, at a given concentration, of a smaller surface area available for adsorption in fraction 2 than in 4, and in fraction 4 than in fraction 6.

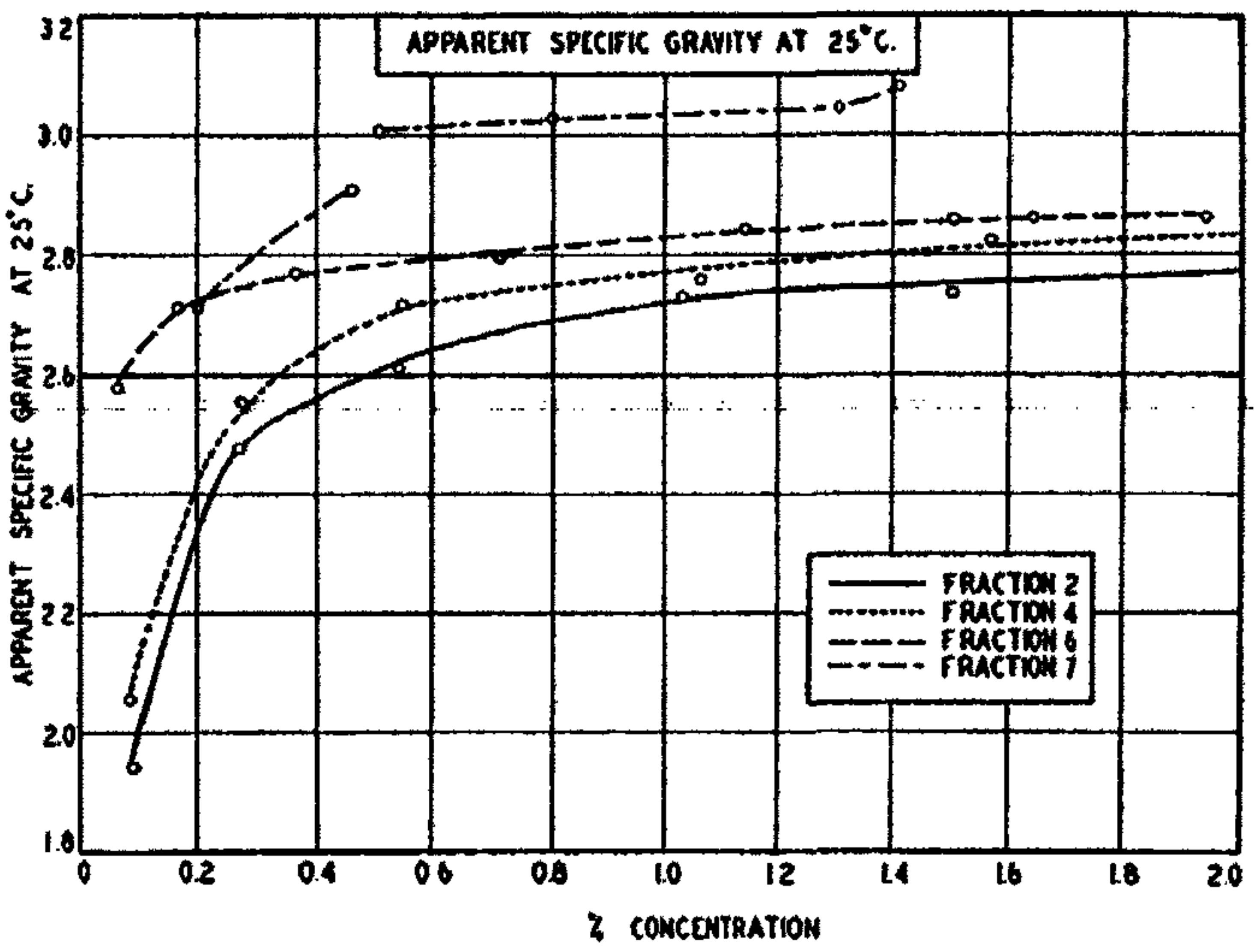

FIG. 1. Apparent specific gravities for fractions 2, 4, 6, and 7 at 25°C.

---

[3] For the determination of the apparent specific gravity, two pycnometers were always used. Each pycnometer was filled and weighed four different times. Each series consisted of four weighings, and the weights checked within 0.0002 g. The apparent specific gravities calculated from the average of each series were checked with a series using the second pycnometer. Even in the most dilute dispersions the differences in weight between the pycnometer filled with the suspension and the pycnometer filled with distilled water were never less than 0.0020 g. With this method the calculated maximum error in the most dilute suspension studied is ± 5 per cent. Therefore, given a value of 1.94 for the apparent specific gravity of the most dilute dispersion of fraction 2, the possible deviation can be between 1.84 and 2.04. With increasing concentration of the suspension the maximum possible error naturally decreases rapidly.

The figures shown in tables 3 and 4 demonstrate that the most dilute suspensions exhibit a value for the apparent specific gravity which is lower than the one generally accepted for dry bentonite. Similar results were found by van Bemmelen (5) when determining the apparent specific gravity of silica gel containing different amounts of water. Minima in apparent specific gravity could be found with silica gels having a maximum amount of water content, as well as with those containing a minimum amount of water, whereas in medium concentrations the apparent specific gravity rose.

Since only the range of very dilute suspensions has been studied in this investigation, no second minimum in apparent specific gravity can be expected. However, the asymptotic value obtained in higher concentrations of fraction 6 might point to this effect in case the concentration were further increased.

TABLE 3

Apparent specific gravities of fraction 4 at 25°C.

CONCENTRATION IN PER CENT DRY WEIGHT	APPARENT SPECIFIC GRAVITIES
0.086	2.054
0.273	2.544
0.548	2.718
1.063	2.762
1.573	2.827
2.033	2.842

TABLE 4

Apparent specific gravities of fraction 2 at 25°C.

CONCENTRATION IN PER CENT DRY WEIGHT	APPARENT SPECIFIC GRAVITIES
0.094	1.941
0.270	2.477
0.544	2.609
1.035	2.781
1.505	2.732
2.040	2.782

When the dilute suspension of fraction 6 was reconcentrated by evaporation at 75°C. (table 5) and the apparent specific gravities were determined, the increase in apparent specific gravity, especially in low concentrations, never reached the value of the untreated samples, although it was still observable. During thermal evaporation partial agglomeration of primary particles takes place. This has been confirmed by ultramicroscopic studies. Such agglomeration increases the effective particle size of the suspension as well as the apparent volume of the disperse phase, while the available active surface decreases. The stability of a sol which has been obtained by dilution from a stable gel will increase with increasing concentration of the disperse phase. Less agglomerates will form, i.e., more active surface will be available; moreover the available surface automatically increases with concentration. Therefore, the apparent specific gravity must increase.

Reconcentration of the dilute suspension of fraction 6 at 95°C. (table 6) shows a similar decrease in apparent specific gravity in lower concentrations (figure 2).

Fraction 7 is a sol containing, as previously mentioned, particles of an average particle size diameter below 14 mμ. Since its dry weight content was only 0.46 per cent, it was necessary to concentrate it by evaporation.

TABLE 5

Apparent specific gravities at 25°C. of fraction 6, reconcentrated at 75°C.

CONCENTRATION IN PER CENT DRY WEIGHT	APPARENT SPECIFIC GRAVITIES
0.153	2.460
0.306	2.682
0.512	
0.046	2.716
1.358	2.728

TABLE 6

Apparent specific gravities at 25°C. of fraction 6, reconcentrated at 95°C.

CONCENTRATION IN PER CENT DRY WEIGHT	APPARENT SPECIFIC GRAVITIES
0.283	2.617
0.583	2.695
1.118	2.744

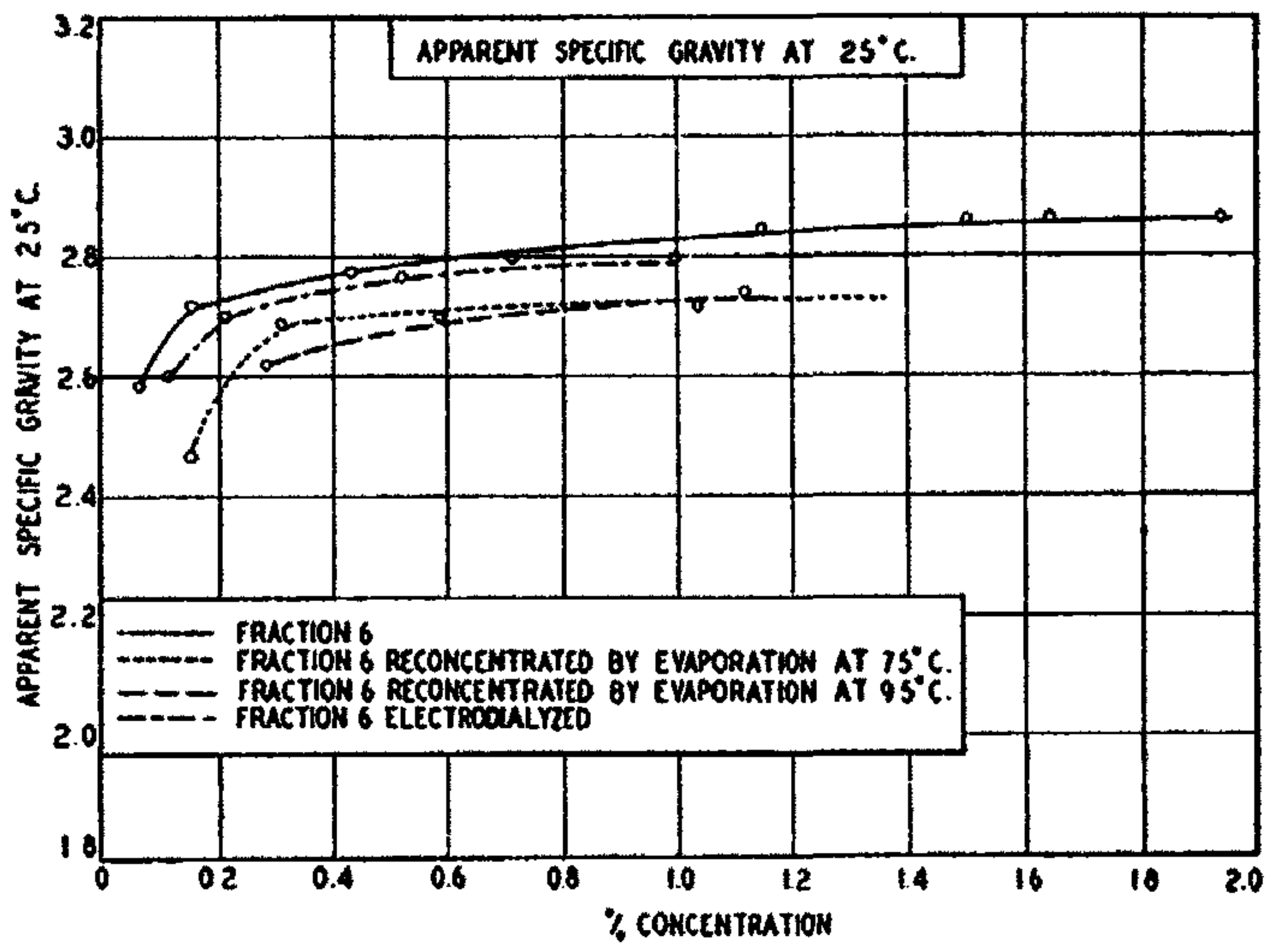

Fig. 2. Apparent specific gravities of fraction 6 at 25°C.

Only one dispersion was produced by dilution for the specific purpose of studying a concentration lower than 0.46 per cent. The results are given in table 7.

Here, too, an increase in apparent specific gravity with concentration can be found. As was to be expected with a system containing extremely fine particles, the original dispersion already has a higher apparent specific gravity than any of the fractions so far discussed. The sol obtained by dilution exhibits an apparent specific gravity corresponding to the one accepted for the dry material. This system is very dilute and the particles most probably are monoplates, so that neither appreciable interlamellar swelling nor adsorption can take place. However, the first of the series of reconcentrated dispersions (0.505 per cent) reveals a sudden and remarkable increase in apparent specific gravity. The apparent specific gravities are extremely high and are still rising at a concentration of 1.41 per cent. These sols also reveal a pronounced increase in viscosity and exhibit high yield values. These data substantiate the fact already established by Hauser and Reed (3) that the tendency to form gels increases with decreasing particle size. The formation of a strong thixotropic gel without the addition of electrolyte at a concentration of only 1.41 per cent dry weight is, to our knowledge, the lowest figure so far recorded. The above data, if viewed in the light of the previous discussion, indicate further that increased adsorption of the dispersing medium on the dispersed particles, as indicated by the abnormal increase in apparent specific gravities (formation of large water hulls), is a predominant factor in the gelation of colloidal clay suspensions of low concentration.

TABLE 7

Apparent specific gravities at 25°C. of fraction 7

CONCENTRATION IN PER CENT DRY WEIGHT	APPARENT SPECIFIC GRAVITIES
0.201*	2.710
0.460†	2.911
0.505‡	3.007
0.798‡	3.028
1.303‡	3.042
1.410‡	3.081

* Sol obtained by dilution of the original sol.

† Original sol.

‡ Original sol concentrated at 95°C.

DETERMINATIONS OF ABSOLUTE VISCOSITIES

A Hoeppler viscosimeter (4) was used, which permits a quick determination of absolute viscosities over a fairly large range. The method is based on the principle of a ball rolling down the wall of a glass tube inclined 10° from the vertical. The ball travels in a guided and predetermined eccentric position through the tube, so that uncontrollable wall effects and the influence of turbulent flow are avoided. The determinations of viscosity were carried out at 25°C. and 40°C.

In the very dilute sols up to 0.27 per cent dry weight only small differences in the viscosities of fractions 2 and 4 can be found. Fraction 6 (table 10) is slightly higher in viscosity than fractions 4 (table 9) and 2 (table 8), and fraction 7 again is slightly higher than fraction 6 (figure 3), With such low concentrations no great differences were to be expected. owing to the small number of particles present. With increasing concentration of fraction 2, the viscosity increases nearly proportionally. Only in the very high (above 2 per cent) concentrations studied does a slight deviation become noticeable.[4] Fractions 4 and 6 deviate rapidly

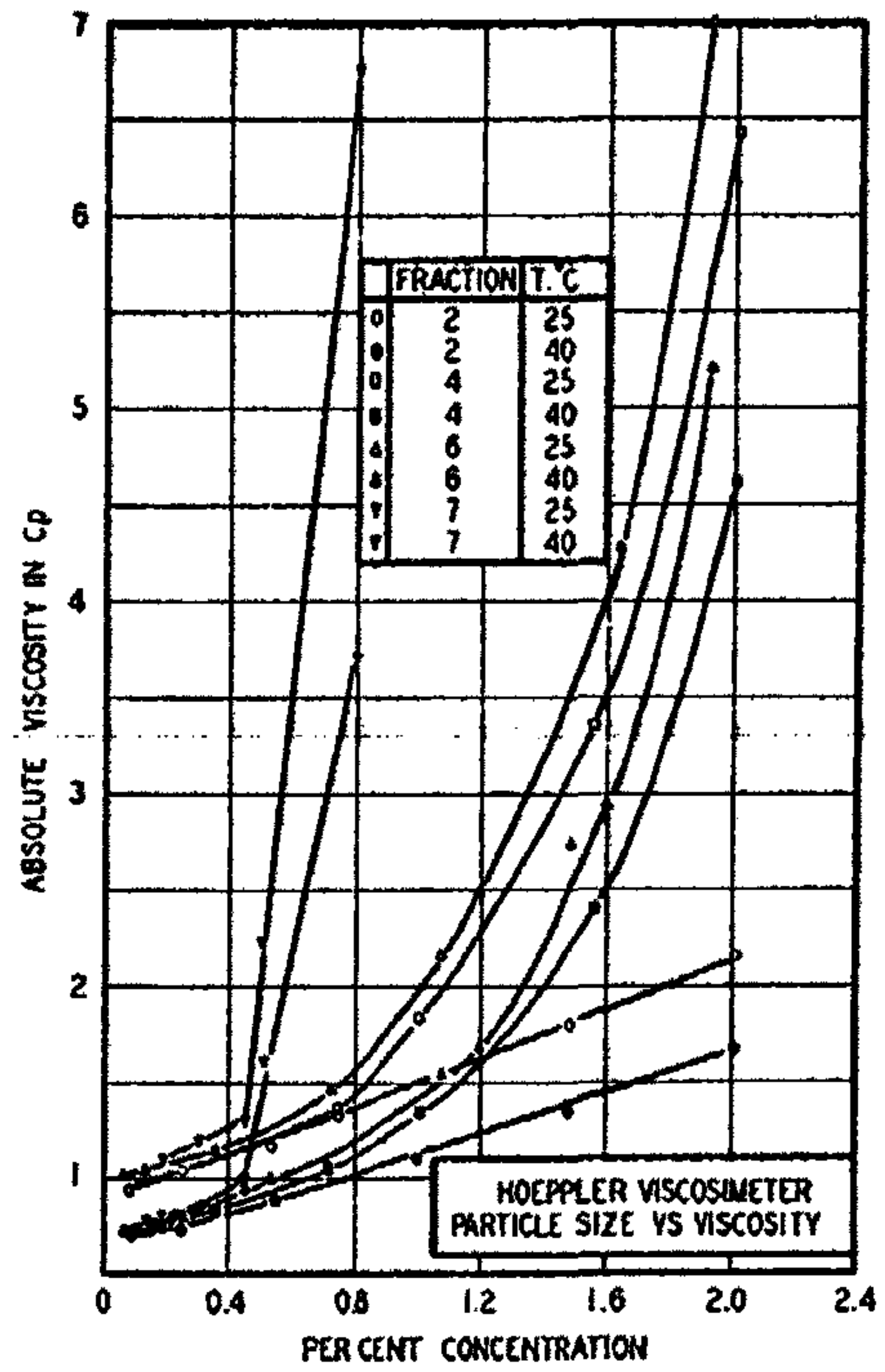

FIG. 3. Viscosities of fractions 2, 4, 6, and 7 at 25°C. and 40°C., determined in a Hoeppler viscosimeter.

TABLE 8

Viscosities of fraction 2

CONCENTRATION IN PER CENT DRY WEIGHT	C_p AT 25° C.	C_p AT 40° C.
0.094	0.956	0.696
0.270	1.065	0.735
0.544	1.154	0.884
1.035	1.368	1.092
1.505	1.795	1.338
2.040	2.163	1.684

TABLE 9

Viscosities of fraction 4

CONCENTRATION IN PER CENT DRY WEIGHT	C_p AT 25° C.	C_p AT 40° C.
0.086	0.968	0.717
0.273	1.065	0.790
0.348	1.312	0.934
1.063	1.840	1.356
1.573	3.360	2.411
2.033	6.428	4.609

---

[4] The scale used in the reproduced curve does not show this deviation.

from the curve of fraction 2 above a concentration of 0.27 per cent. The increase in viscosity becomes more and more pronounced. This can be easily explained by the following considerations. The amount of particles present in a given concentration of these three different sols increases with their decreasing apparent particle diameter. The particles in sol 4 are packed closer than in sol 2, and in sol 6 closer than in sol 4. Thus the resistance against shear will increase. On this basis it is quite evident that fraction 2, having the largest particles and the smallest overall surface, will begin to show a more rapid increase in viscosity only in concentrations very much higher than those of fractions 6 and 4.

TABLE 10

Viscosities of fraction 6

CONCENTRATION IN PER CENT DRY WEIGHT	C_p AT 25°C.	C_p AT 40°C.
0.067	1.002	0.715
0.152	1.048	0.777
0.368	1.137	0.806
0.710	1.469	1.056
1.085	2.187	1.505
1.203	2.429	1.690
1.506	3.929	2.724
1.643	4.271	2.946
1.939	7.117	5.212

TABLE 11

Viscosities of fraction 7

CONCENTRATION IN PER CENT DRY WEIGHT	C_p AT 25°C.	C_p AT 40°C.
0.201	1.085	0.744
0.460	1.308	0.931
0.505	2.253	1.600
0.798	6.751	3.698
1.302		
1.409		

TABLE 12

Viscosities of fraction 6 after evaporation at 75°C.

CONCENTRATION IN PER CENT DRY WEIGHT	C_p AT 25°C.	C_p AT 40°C.
0.153	1.038	0.756
0.306	1.093	0.805
1.045	1.892	1.376
1.358	2.473	1.703

TABLE 13

Viscosities of fraction 6 after evaporation at 95°C.

CONCENTRATION IN PER CENT DRY WEIGHT	C_p AT 25°C.	C_p AT 40°C.
0.283	1.093	0.791
0.582	1.350	0.956
1.177	2.116	1.489

The values obtained for the viscosity of the first two sols of fraction 7 (table 11) (the original sol and the one obtained therefrom by dilution) correspond to these considerations. The first sol of fraction 7 obtained by reconcentration shows a very sudden and enormous increase in viscosity, which could also be recorded for the second sol obtained by evaporation and which is in line with the extremely high apparent specific gravities recorded. These are the sols where, as previously mentioned, thixotropy could already be observed at concentrations as low as 1.4 per cent. If we

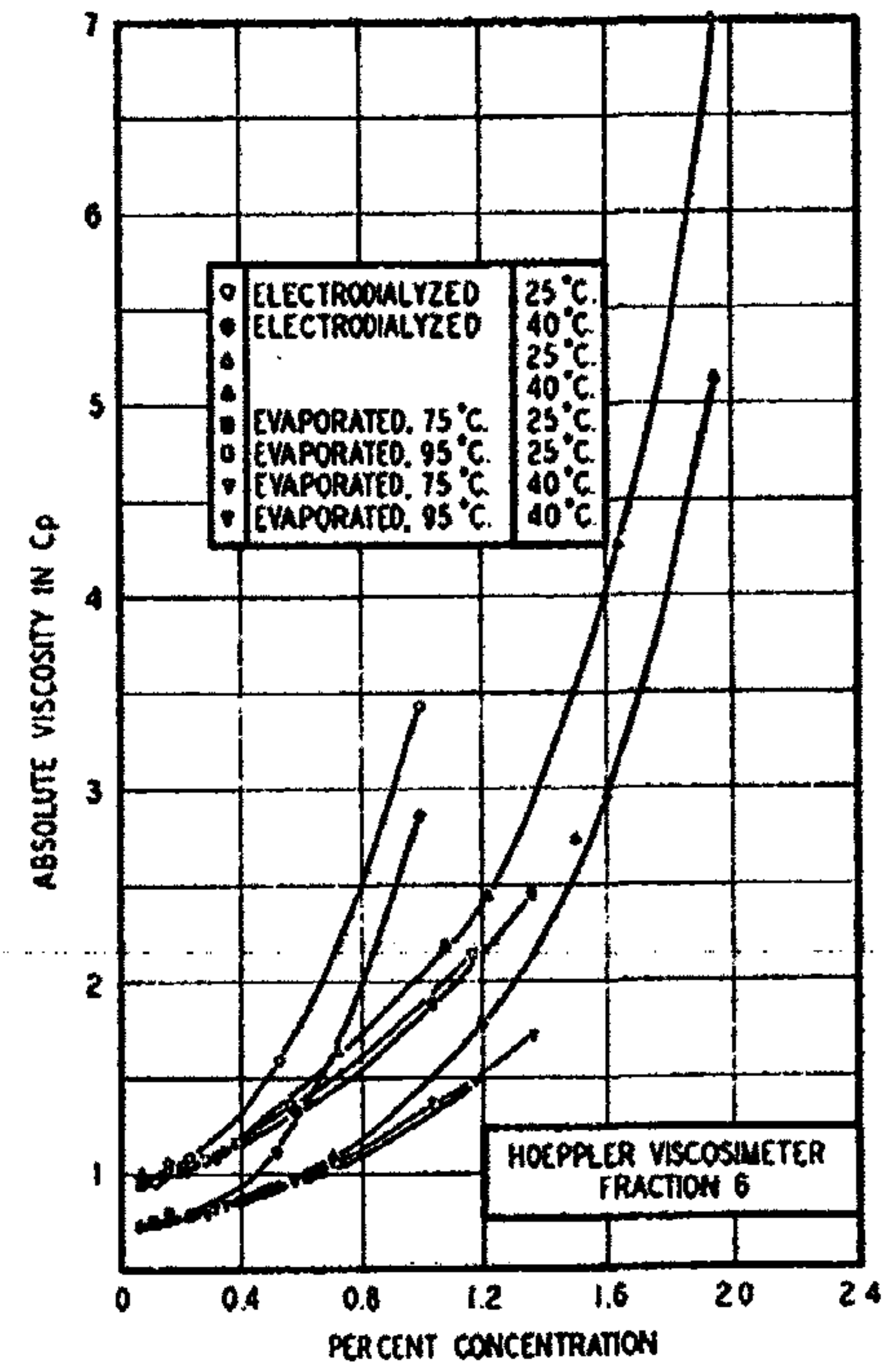

FIG. 4. Change in viscosity of fraction 6 after concentration, determined at 25°C. and at 40°C. in a Hoeppler viscosimeter.

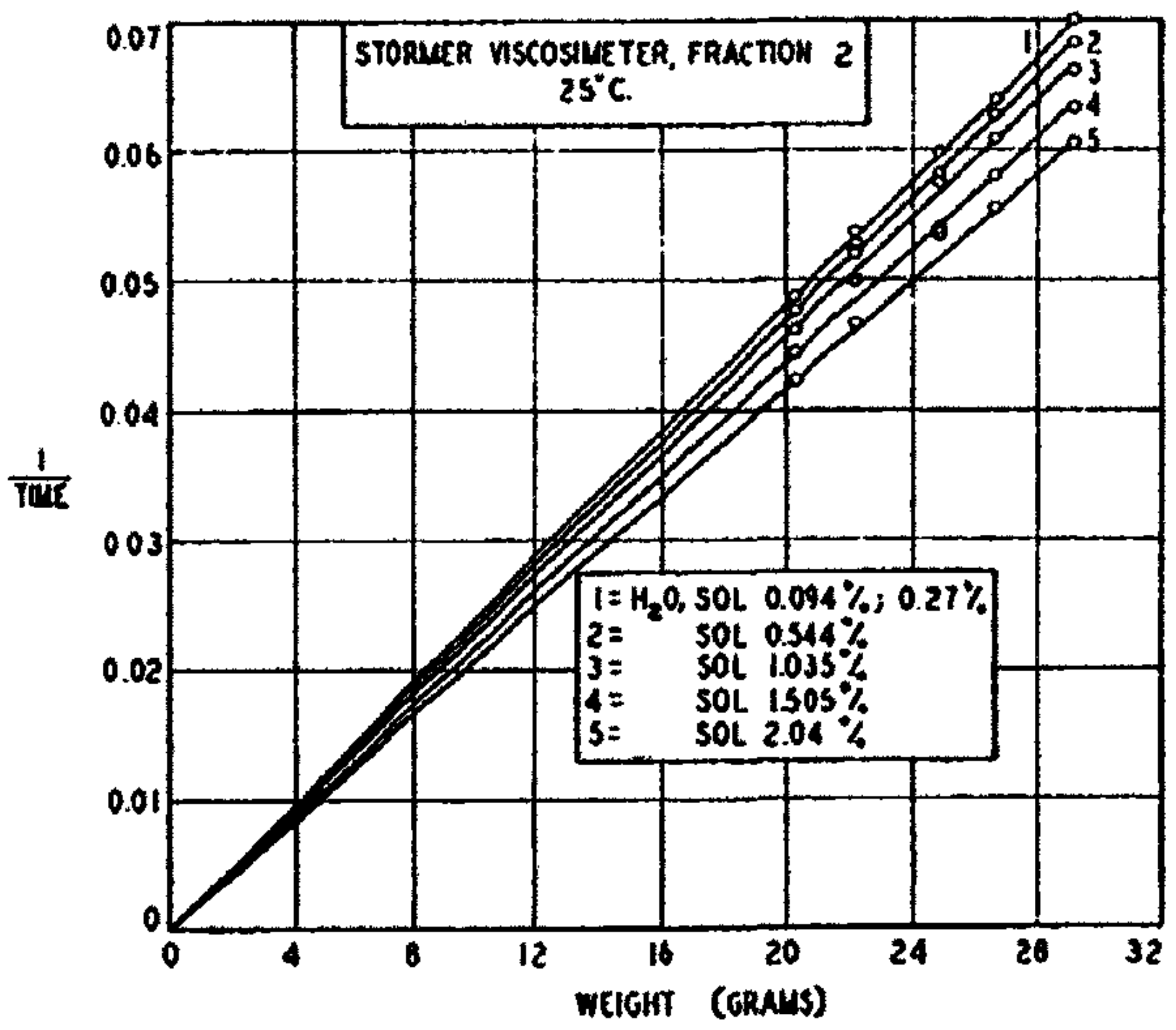

FIG. 5. Fraction 2 in a Stormer viscosimeter at 25°C.

assume that at a given concentration the thickness of the adsorbed water layer surrounding a particle would be the same if the apparent particle

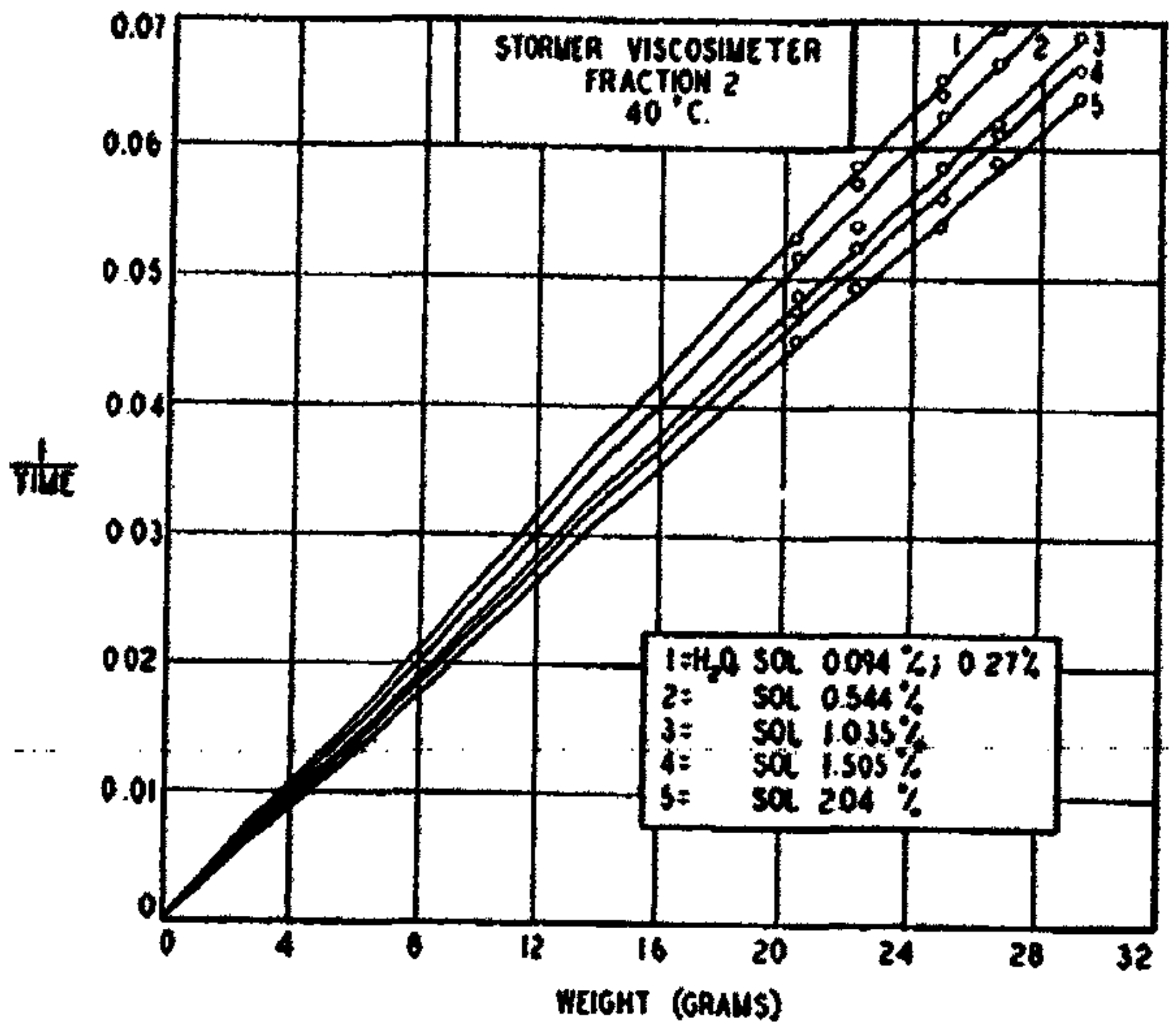

FIG. 6. Fraction 2 in a Stormer viscosimeter at 40°C.

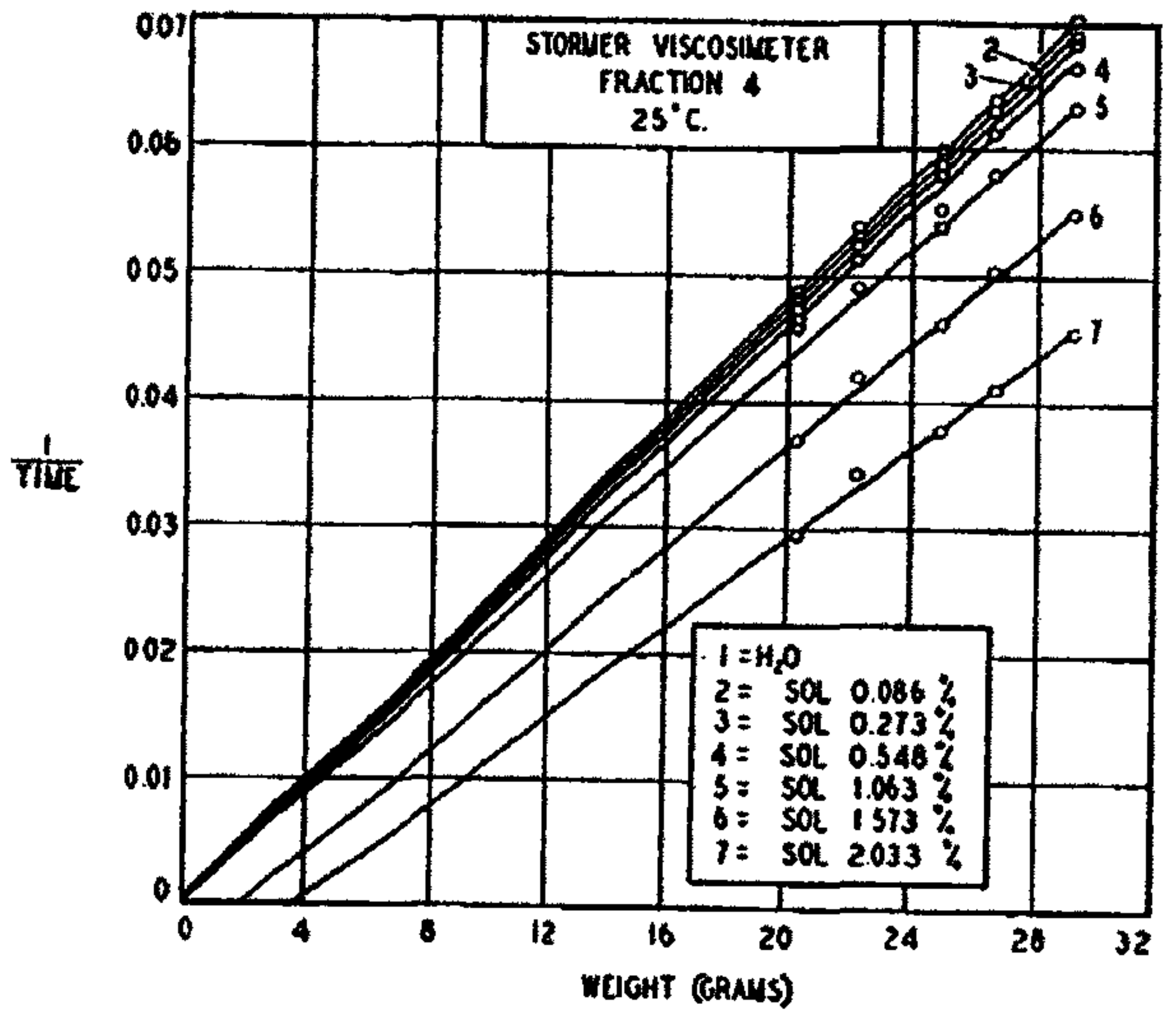

FIG. 7. Fraction 4 in a Stormer viscosimeter at 25°C.

diameter is 28 mμ, 14 mμ, or less, then the ratio of adsorbed water to particle will be greater the smaller the particle. Therefore comparatively more water will be immobilized in a sol of extremely fine particles than in one of greater particle size.

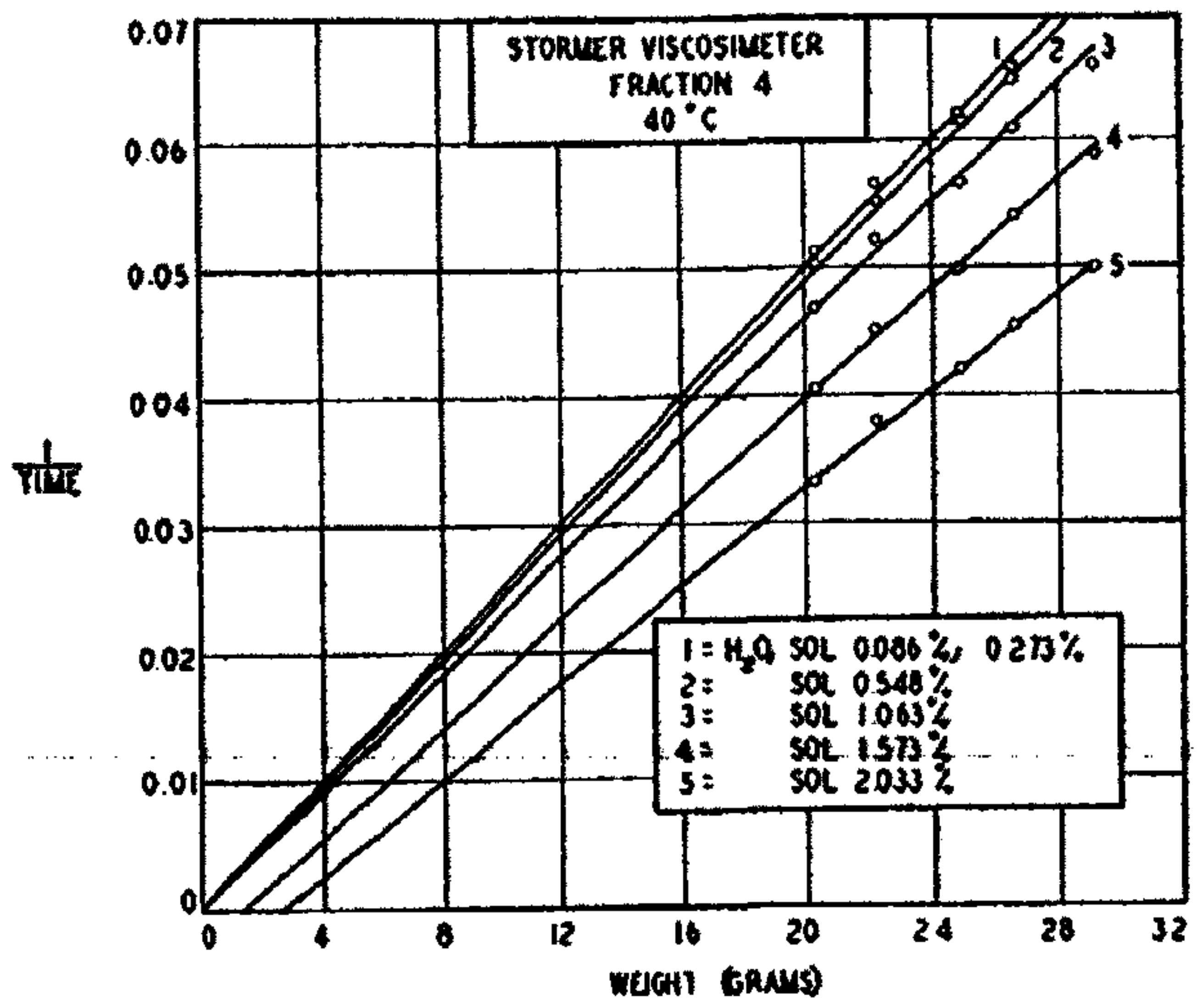

FIG. 8. Fraction 4 in a Stormer viscosimeter at 40°C.

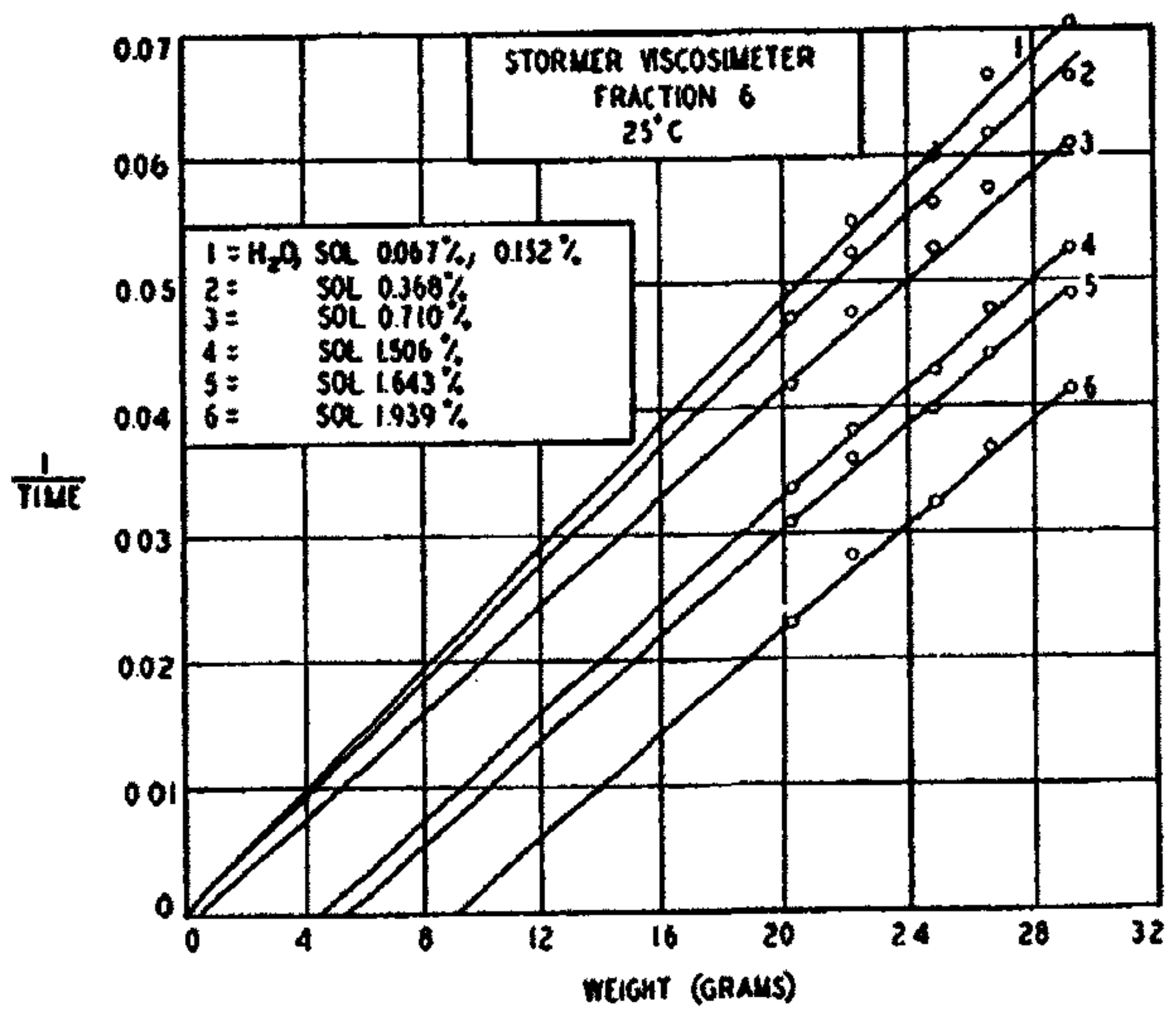

FIG. 9. Fraction 6 in a Stormer viscosimeter at 25°C.

The viscosity measurements in the Hoeppler viscosimeter for fractions 4, 6, and 7 were discontinued as soon as the first signs of "structural viscosity" could be detected, since in our opinion even the refined falling-ball method cannot give accurate and reproducible results in systems of such a nature.

The viscosities of fraction 6, reconcentrated at 75°C. and 95°C., show

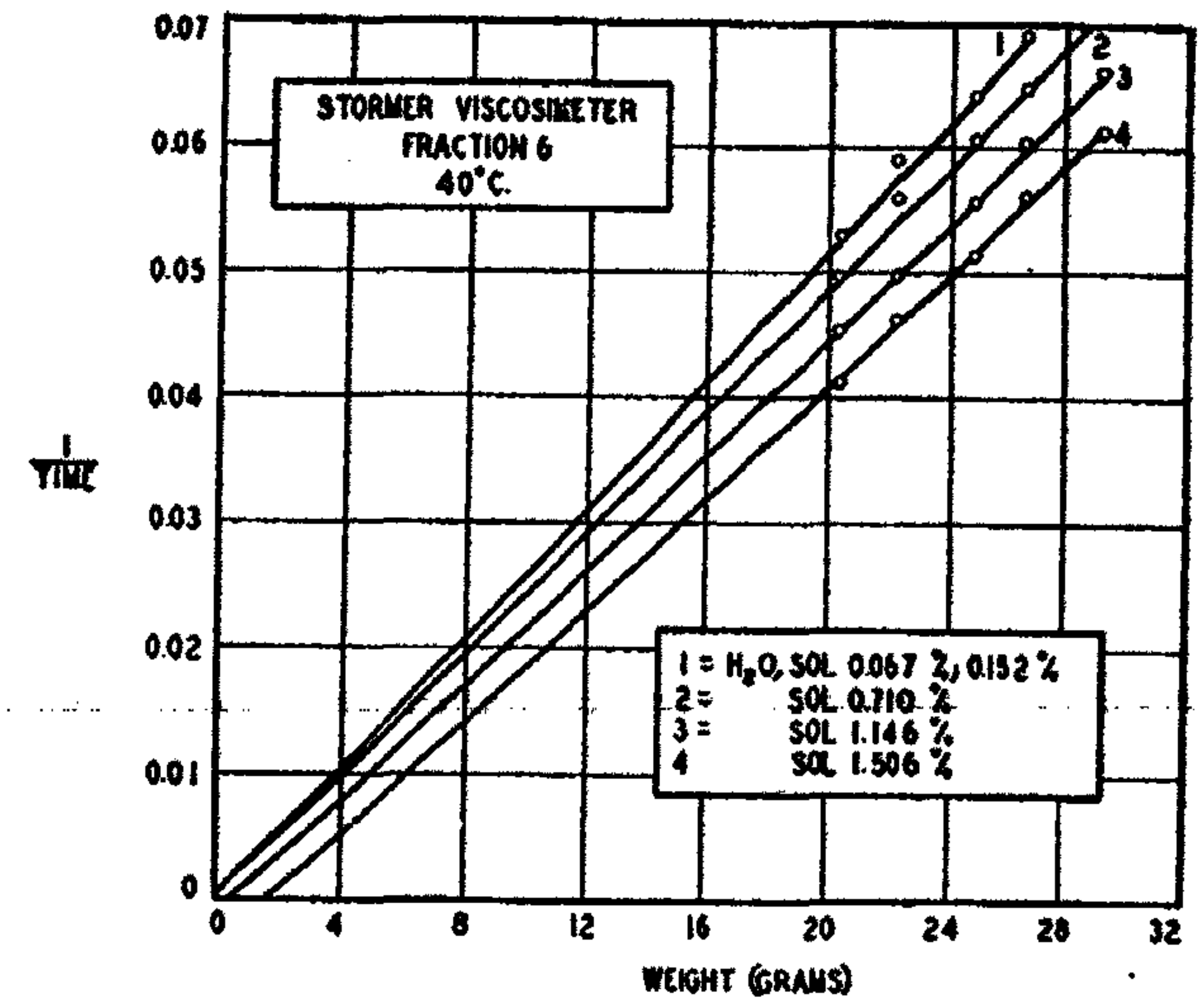

Fig. 10. Fraction 6 in a Stormer viscosimeter at 40°C.

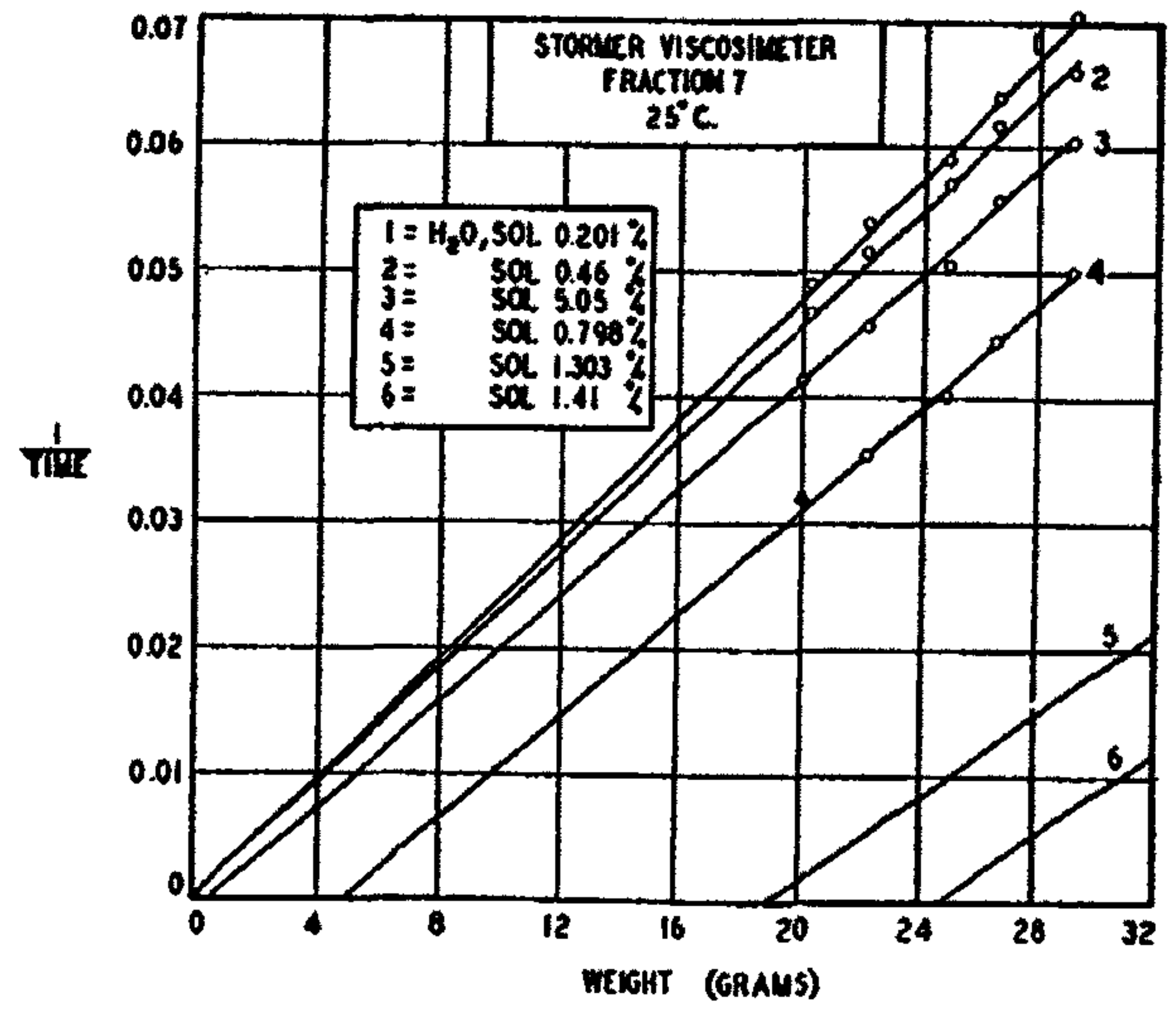

Fig. 11. Fraction 7 in a Stormer viscosimeter at 25°C.

very little change up to concentrations of 1.17 per cent (tables 12 and 13). In higher concentrations the viscosity does not rise to the same degree as the original (figure 4).

The determinations of absolute viscosity at 40°C. gave the results to be expected. A general decrease in viscosity is observed.

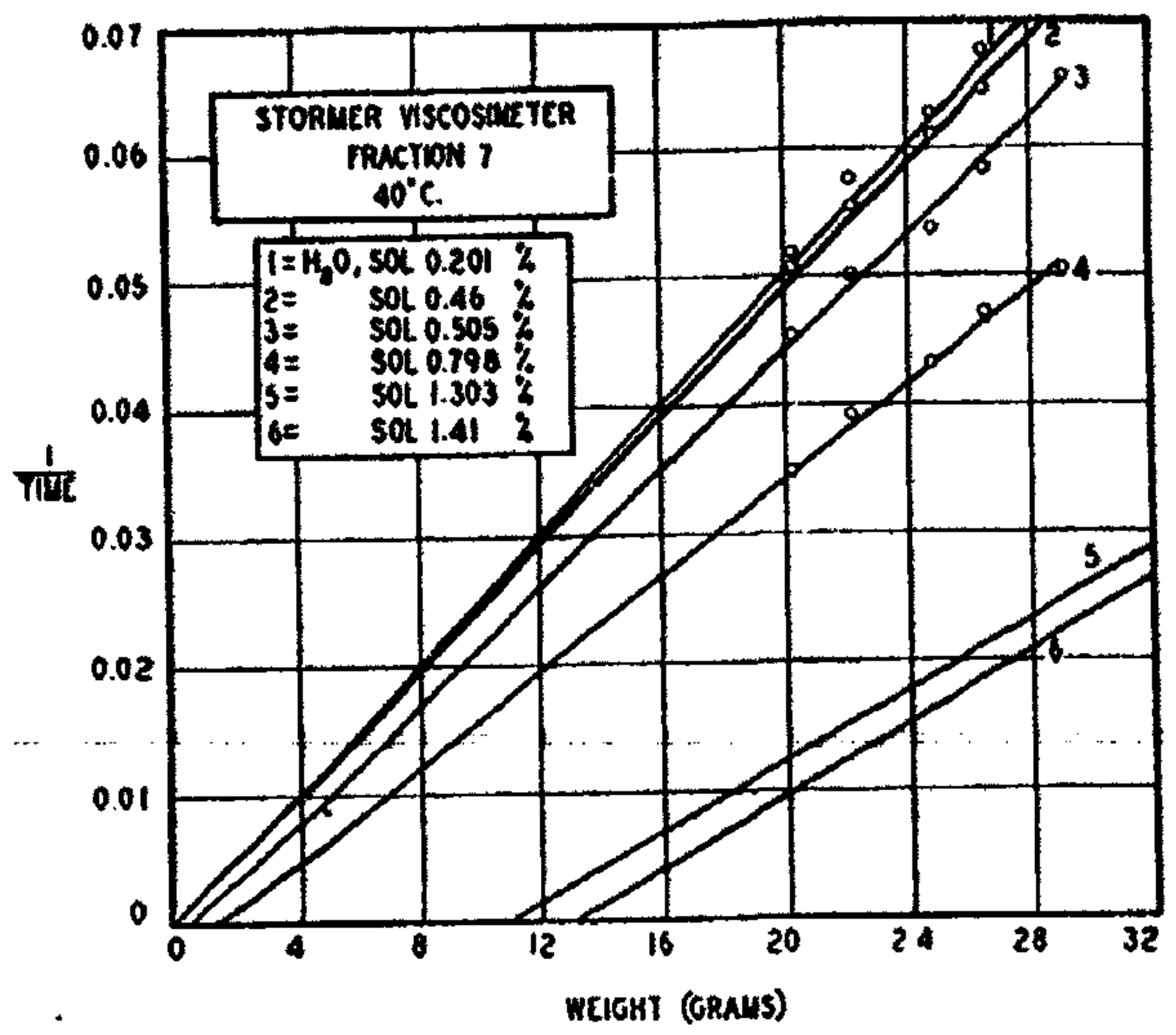

Fig. 12. Fraction 7 in a Stormer viscosimeter at 40°C.

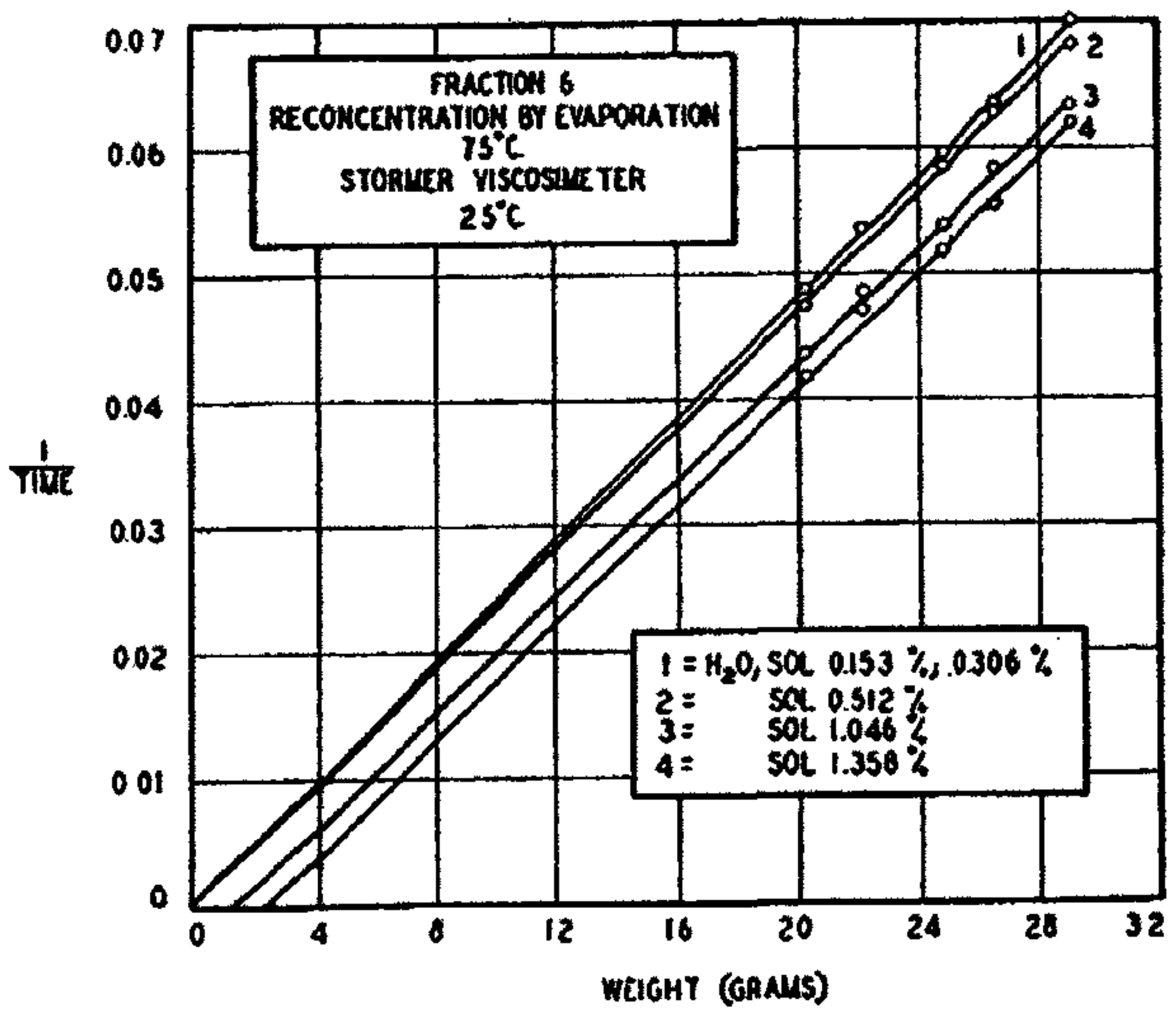

Fig. 13. Fraction 6, reconcentrated by evaporation at 75°C., in a Stormer viscosimeter at 25°C.

Since it is impossible to make any accurate statements as to the formation of a structure or the development of a yield point when using a falling-ball type of instrument, it was decided to study the different sols in a Stormer viscosimeter at 25°C. and 40°C.

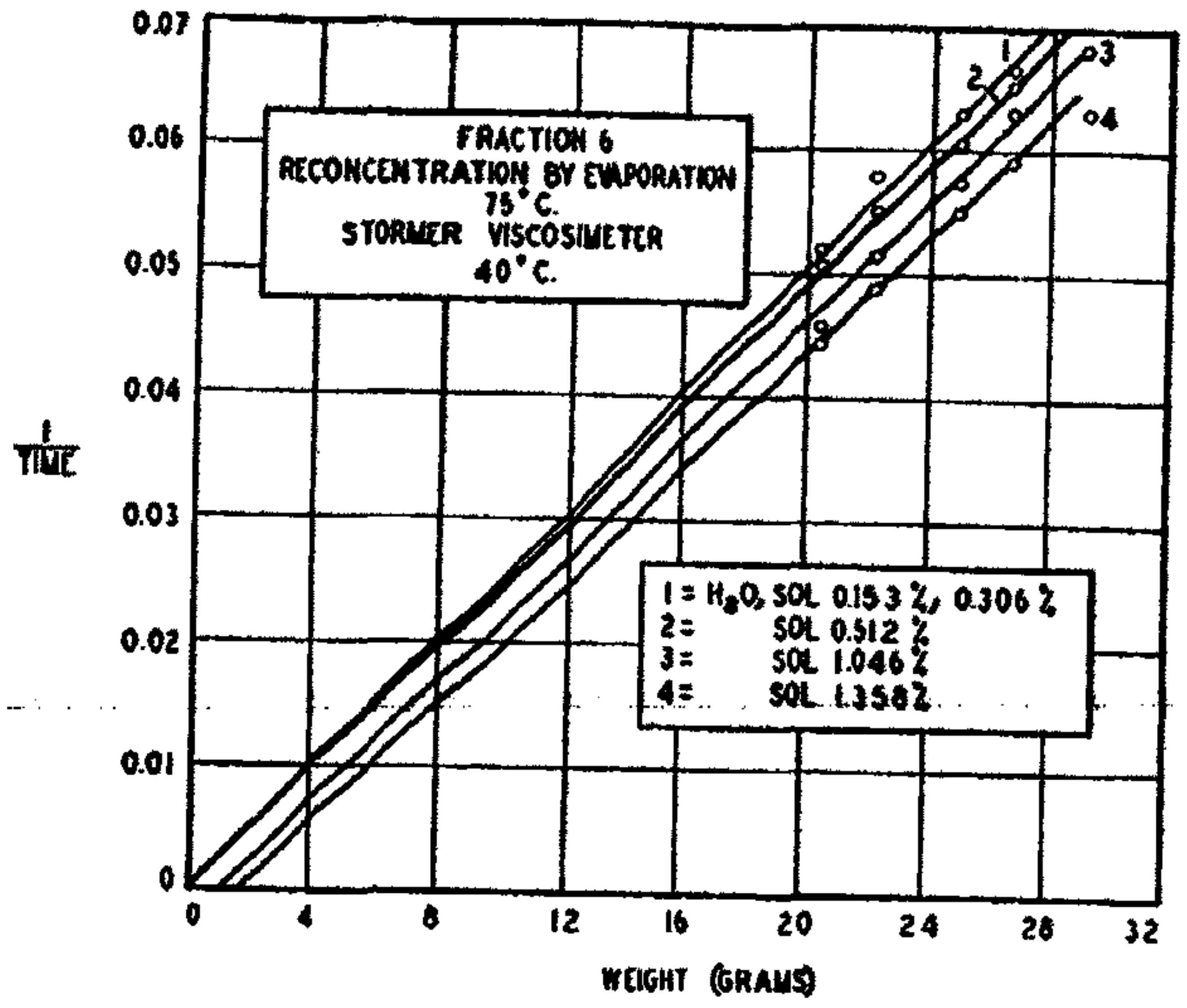

FIG. 14. Fraction 6, reconcentrated by evaporation at 75°C., in a Stormer viscosimeter at 40°C.

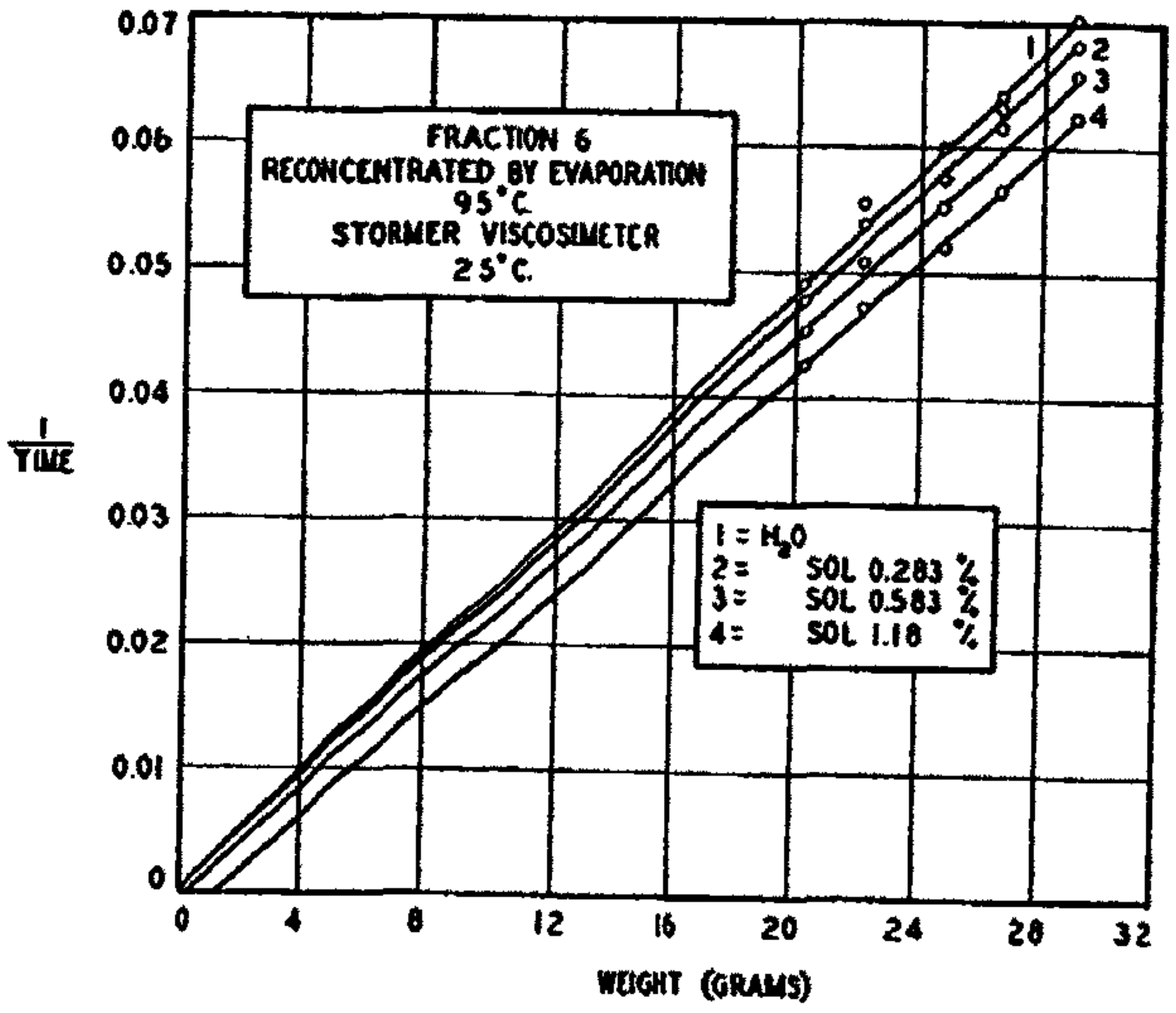

FIG. 15. Fraction 6, reconcentrated by evaporation at 95°C., in a Stormer viscosimeter at 25°C.

Fraction 2, which consists of the coarsest particles (average apparent particle diameter = 48 mμ), exhibits no yield point up to 2.04 per cent (figures 5 and 6). Fraction 4 (average apparent particle diameter = 28 mμ) reveals a noticeable yield point already at 1.5 per cent (figures 7 and 8), fraction 6 (average apparent particle diameter = 14 mμ) at 1 per cent (figures 9 and 10), and fraction 7 (average apparent particle diameter less than 14 mμ) at 0.5 per cent (figures 11 and 12). At 40°C. all the yield points decrease. The decrease becomes the more pronounced the smaller the particle sizes of the fractions studied. The yield points naturally increase with increasing concentration. No appreciable changes in yield points of fraction 6 have been found when reconcentrating the sols by evaporation (figures 13, 14, 15, 16).

The results of viscosity determinations have demonstrated that the viscosity follows the Einstein equation only for the coarsest fraction and in extreme dilutions. For the finer particles increasing deviations are observed. Yield points also increase with decreasing particle sizes and increasing concentration. The unexpectedly high viscosities at the concentrations studied cannot be accounted for by simple particle interference. In addition a high degree of solvation (adsorbed water hulls) is necessary to explain this fact satisfactorily.

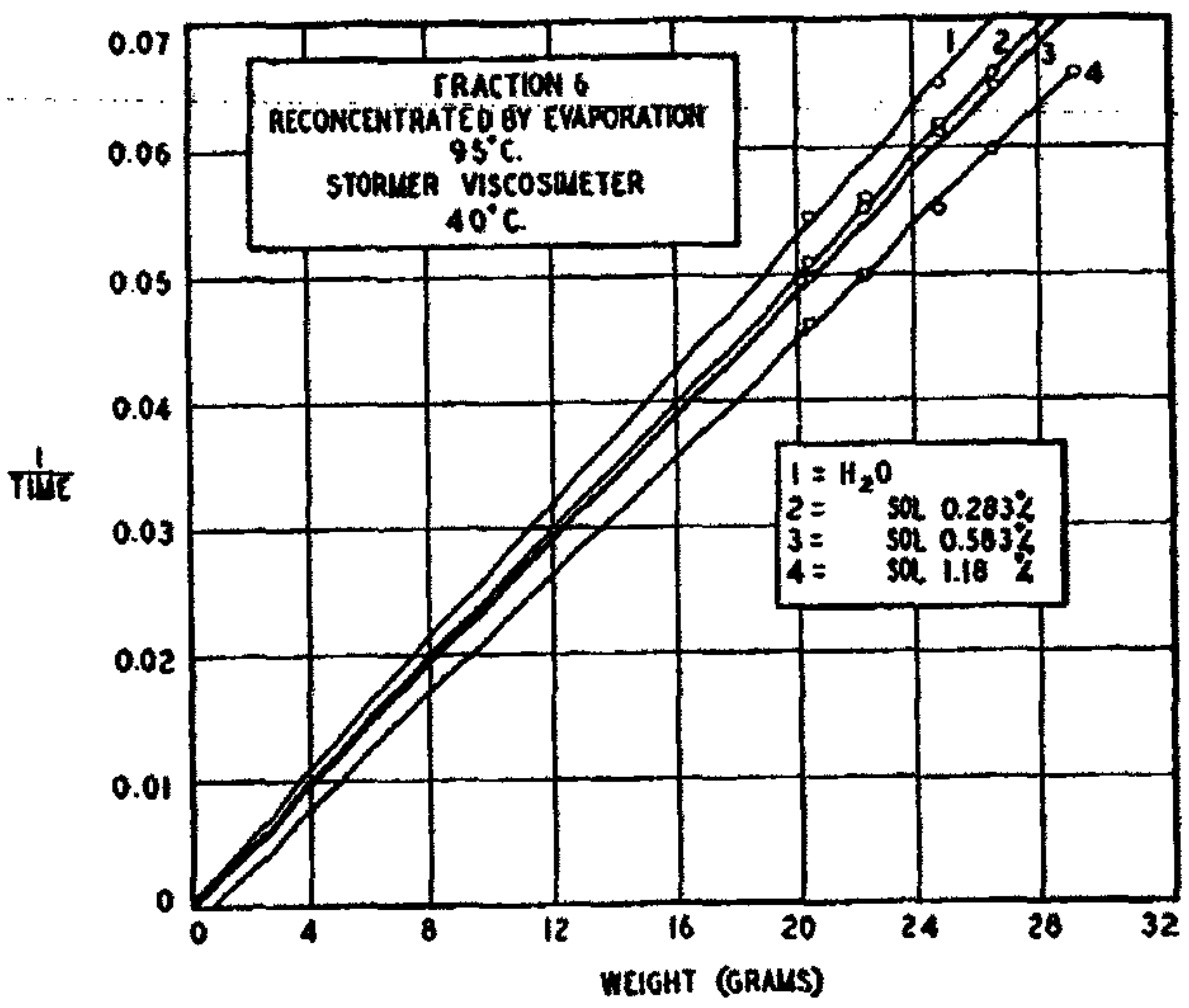

FIG. 16. Fraction 6, reconcentrated by evaporation at 95°C., in a Stormer viscosimeter at 40°C.

It seems only logical that such a bond will be weaker the higher the temperatures, thus causing a reduction in viscosity.

OPTICAL DENSITY

It finally was decided to examine the finest fractions for their light transmission, as it was hoped that such measurements might permit some insight as to the actual distribution of the particles in the sols. A Hardy color analyzer (1) was used for this purpose. All measurements were recorded with distilled water as a blank.

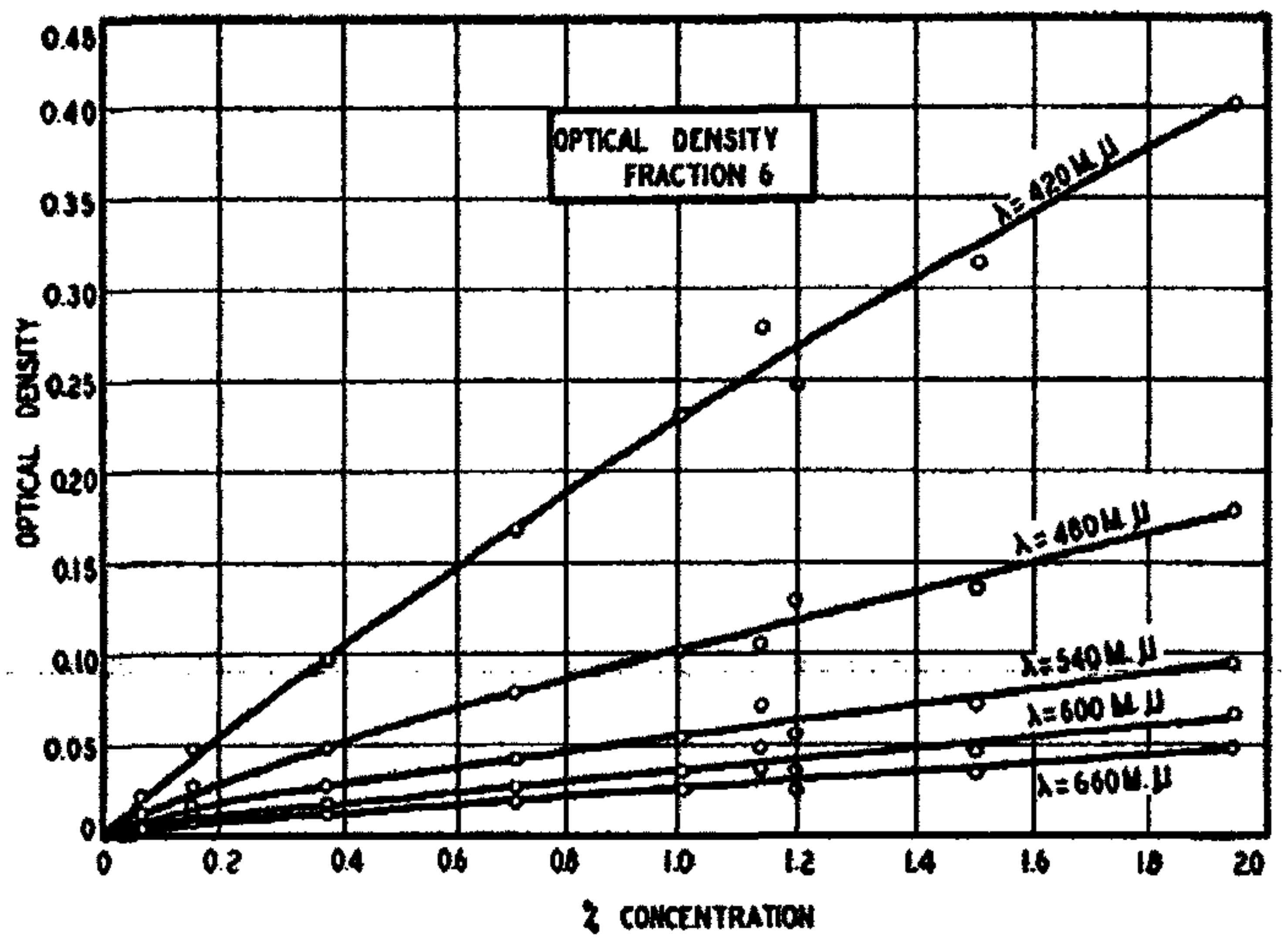

FIG. 17. Optical density of fraction 6

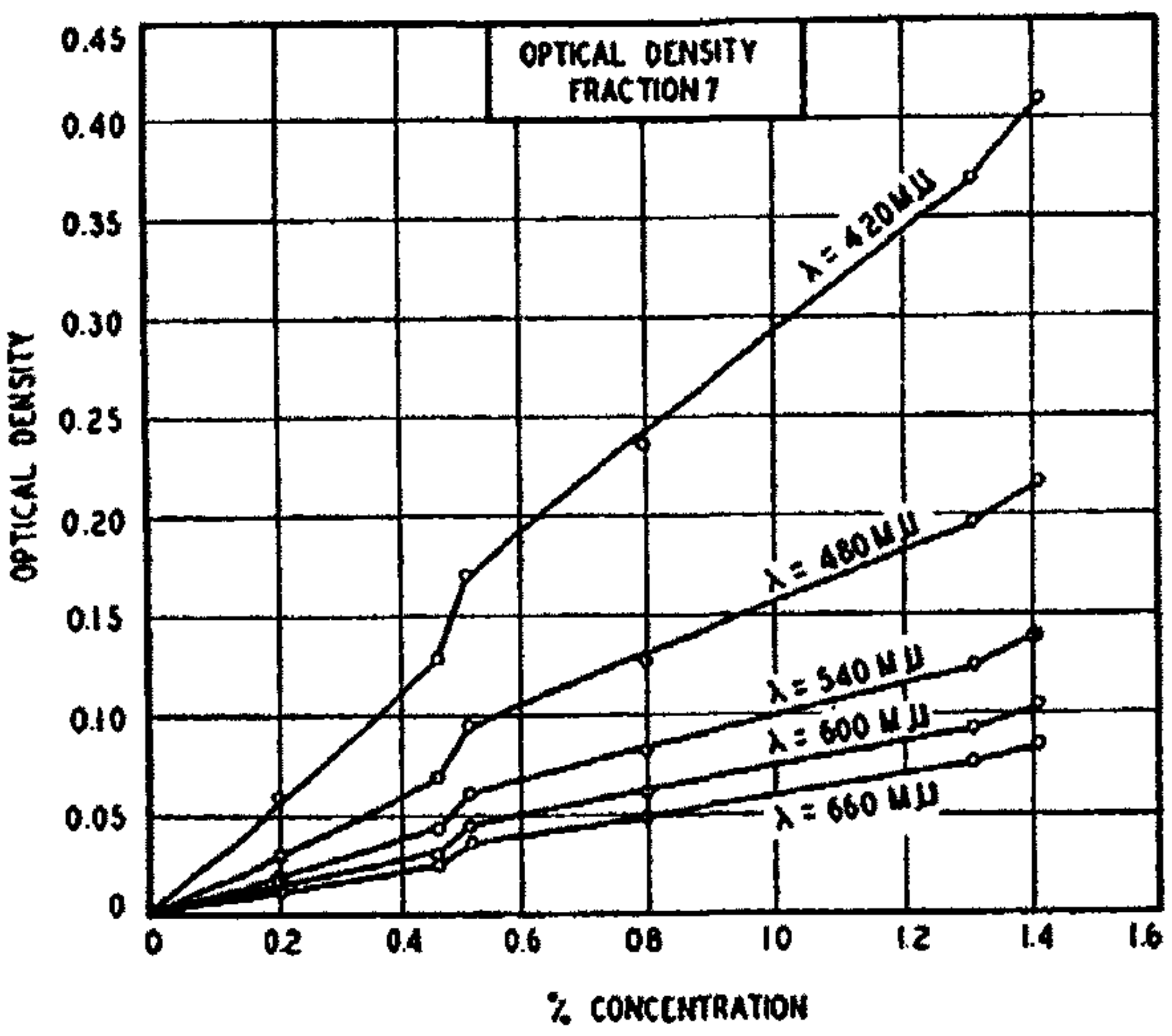

FIG. 18. Optical density of fraction 7

The curves for the optical density of fraction 6 show a very pronounced light absorption in the smaller wave lengths (figure 17). This simply proves that the sol contains a large number of small particles.

The curves for the optical density of fraction 7 (figure 18) are of interest as they show, when the sol is reconcentrated by evaporation, a sudden increase. These systems have a very marked tendency to form thixotropic gels when being cooled down. Although no final explanation for this phenomenon can yet be offered it seems highly probable that the particles, becoming more and more locked into equilibrium positions, cause an increased absorption or scattering. (Further work to clarify this effect is in progress.)

STREAM DOUBLE REFRACTION

Stream double refraction in fine clay fractions has already been reported by Hauser and Reed (*loc. cit.*). In the present study it was noticed in fraction 6 (average apparent particle diameter = 14 mμ), but seemed to be a function of the concentration of this fraction, since it became noticeable only in concentrations above 1 per cent. Below this concentration no stream double refraction could be noticed, even after prolonged storage. The part of fraction 6 which had been reconcentrated by evaporation at 75°C. and 95°C. also showed stream double refraction, but only from concentrations above 1.045 and 1.177 per cent, respectively. No stream double refraction could be observed in fraction 7, either at higher concentration or after long storage.

It seems that in these systems stream double refraction is detectable with the eye only if particles of a certain range and concentration are present, since with larger particle sizes this phenomenon again becomes less pronounced. However, even the finest fraction in extreme dilution will, if put into motion and placed between crossed nicols, exhibit strong double refraction, which proves that the slightest mechanical influence causes some orientation of the submicrons present in the system. This also proves that gelation is not a result of preferential orientation of particles.

SUMMARY

The apparent specific gravities of monodisperse montmorillonite fractions of extremely low concentrations and different particle sizes show an increase with decreasing particle size and increasing concentration. This is explained by the presence of strongly adsorbed water on the surface of the particles.

Absolute viscosity determinations of the same systems demonstrate an increase with decreasing particle size and increasing concentration. These results are in line with the changes in apparent specific gravity. The coarsest fractions show no yield point up to concentrations of 2 per cent. The finer fractions reveal an increase with decreasing particle size and increasing concentration. The yield point as well as the viscosity de-

creases with increasing temperature. Gelation seems to cause a sudden rise in optical density over all wave lengths.

Preliminary studies in stream double refraction indicate it to be a function of particle size and concentration. Orientation of the submicrons in a sol, if placed between crossed nicols, is detectable only if the system is put in motion.

REFERENCES

(1) Hardy, A. C.: J. Optical Soc. Am. **25,** 305 (1935).
(2) Hauser, E. A., and Reed, C. E.: J. Phys. Chem. **40,** 1169 (1936).
(3) Hauser, E. A., and Reed, C. E.: J. Phys. Chem. **41,** 911 (1937).
(4) Hoeppler, R.: Chem.-Ztg. **57,** 62 (1933); Z. tech. Physik **14,** 165 (1933).
(5) van Bemmelen, J. M.: Z. anorg. allgem. Chem. **18,** 98 (1898).

THE STRUCTURE OF THE SURFACES OF SOLUTIONS AS SHOWN BY THEIR RESISTANCE TO THE SPREADING OF INSOLUBLE FILMS[1]

T. FOSTER FORD[2] AND DONALD A. WILSON[3]

Department of Chemistry, Stanford University, California

Received July 1, 1938

Our knowledge of the surfaces of liquids has been derived mostly from the work of Langmuir and others on the phenomena presented by insoluble films on water. It has been commonly taken for granted that somewhat similar layers must exist upon the surfaces of solutions of all surface-active substances, even soluble substances. This assumption is based upon analogy, and upon the Gibbs prediction of positive adsorption with lowered surface tension. Elsewhere the authors have presented direct and indirect evidence for the existence of such soluble films (11, 10, 3, 4). This paper has to do with their direct quantitative study.

In these experiments the surfaces of solutions of hydrocinnamic acid, caprylic acid, and phenol are compressed by means of oleic acid "piston films," an adaptation of the recent method of Langmuir and Blodgett (1) for studying insoluble monolayers. Here the only films possible are those formed spontaneously by adsorption from the solutions themselves. The piston films are visibly retarded, and from curves showing compression against time, recorded by moving pictures, the properties of the soluble films compressed are deduced. These seem to be capable of existing in all the states of aggregation common to insoluble films. The actual amounts of solute in these soluble surface layers is found to agree quite closely with values for the absolute adsorption found by other experimental methods (4, 5, 6, 9), and with the adsorption predicted by the Gibbs equation.

THE EXPERIMENTAL METHOD

The apparatus used is shown in figure 1. It consists of a circular dish 25 cm. in diameter for containing the solution, in an air-tight glass box, with a capillary tube reaching to the center of the dish through which the

---

[1] Presented at the Fifteenth Colloid Symposium, held at Cambridge, Massachusetts, June 9-11, 1938.

[2] Present address: Shell Development Company, Emeryville, California.

[3] Present address: Department of Physiological Chemistry, School of Medicine, University of Pittsburgh, Pittsburgh, Pennsylvania.

oleic acid may be introduced beneath the surface of the solution when desired. The dish is a brass hoop, paraffin waxed, fitted over a glass disk beneath which is a film of paraffin wax colored with lamp black to aid visibility. The interior of the apparatus is thoroughly paraffined to prevent contamination. The motion picture camera, not shown in figure 1, was mounted directly above the spreading film. The temperature was 11°C. in all cases.

In each experiment dish and capillary were first thoroughly cleaned and rinsed with conductivity water. The solution was then put into the dish, the surface swept with paper strips, and the enclosure covered for the desired length of time. The spreading oil was introduced by trapping a droplet from an eye-dropper in a column of solution in the vertical part of the capillary tube outside the enclosure so that solution and spreading oil ran into the dish by gravity. Before introducing the spreading oil, the cover was lifted just long enough to dust the surface of the solution with talc. All the necessary data were taken from the motion picture record by projecting successive frames onto a screen.

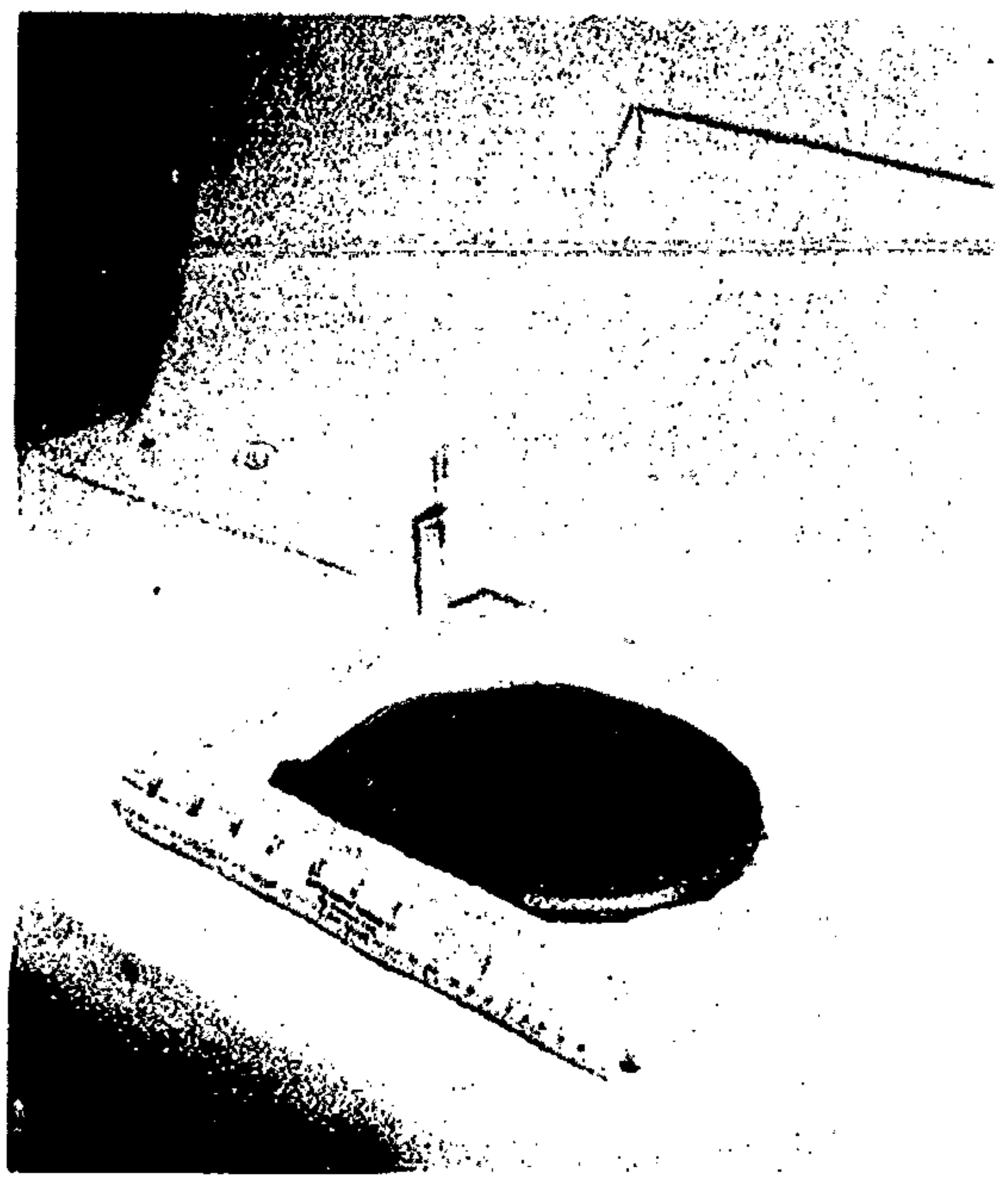

FIG. 1. The spreading-film apparatus

THE SPREADING OF OLEIC ACID ON WATER

The behavior of the oleic acid piston when compressing the surface of pure water is shown by the first compression curves in figures 3, 4, 5, and 6.

After a very short time the rate of spreading of the film in square centimeters per exposure is constant. That is, the area-time curve becomes a straight line, and, on water, it remains a straight line during the whole time of spreading. Evidently no sensible change in the retarding force due to water alone occurs as its free surface is reduced. Changes observed on solutions, then, must be due to the presence of solute films.

The rate of disentanglement

On water the area-time curve is linear over most of its length, and on solutions large linear segments are observed. This constant rate of increase of area of the piston film is probably determined by the rate of "disentanglement" of oleic acid molecules from a central globule of quite constant size. For solid nuclei of spreading Cary and Rideal (2) found the rate of spreading, or of disentanglement, to be proportional to the perimeter of the solid at the plane of contact with the water surface. For liquid globules also they consider it probable that solution occurs only at the circumference of contact.

Oleic acid droplets released beneath water surfaces seem to form first single lenses which then suddenly break up into many smaller ones. This behavior was noted by Cary and Rideal in studying the spreading of oleic acid over very large surfaces of water, and it explains the gradual increase in the spreading rate shown by their data, since there was an increase in the total perimeter of the reservoir. On some of our concentrated solutions, on which spreading was comparatively slow, an upward swing of the area-time curves similar to Cary and Rideal's is noted. In most cases, however, on the small areas studied by us the central globule evidently did not have time to break up. Its exact behavior fortunately has little bearing on the interpretation of our results. It may only be concluded that in the first part of the spreading on solutions the rate is dependent more on the nature of the reservoir than on the properties of the surface being compressed.

The terminal linear velocity

The data given here for both water and solutions show at the beginning of the spreading a constant linear velocity of the advancing edge. This must represent a terminal linear velocity. At this speed the resistance offered by the friction in the film and underneath the film, and by impact with chance obstructions ahead of the film, must equal the spreading pressure. This terminal velocity is observed only at first, because only then is the reservoir in effect infinite. As the film increases in area the rate of spreading quickly becomes limited by the rate of disentanglement.

THE RESULTS OF THE COMPRESSION OF SOLUBLE FILMS

Typical curves for the compression of soluble films by the oleic acid piston are shown in figure 2. The actual data obtained with various solutions of hydrocinnamic acid, caprylic acid, and phenol are recorded in figures 3, 4, 5, and 6. Many of the actual curves exhibit all of the characteristics formalized by the different segments in figure 2.

Terminal linear velocity

At the beginning of the compression the linear velocity of the advancing edge of the piston film is constant. This is the terminal velocity discussed above.

On a few of the more concentrated solutions the data suggest a slight acceleration of the linear velocity near the origin. Such an effect could result from the fountain-like manner in which the oleic acid is introduced into the surface, since a certain time should be required for the formation of a lens having a stable perimeter. The necessity of accelerating the talc particles used for reference may also be a factor. In most cases these effects are masked in our experiments by attainment of the terminal velocity in less than the 0.076 sec. elapsed between successive camera exposures.

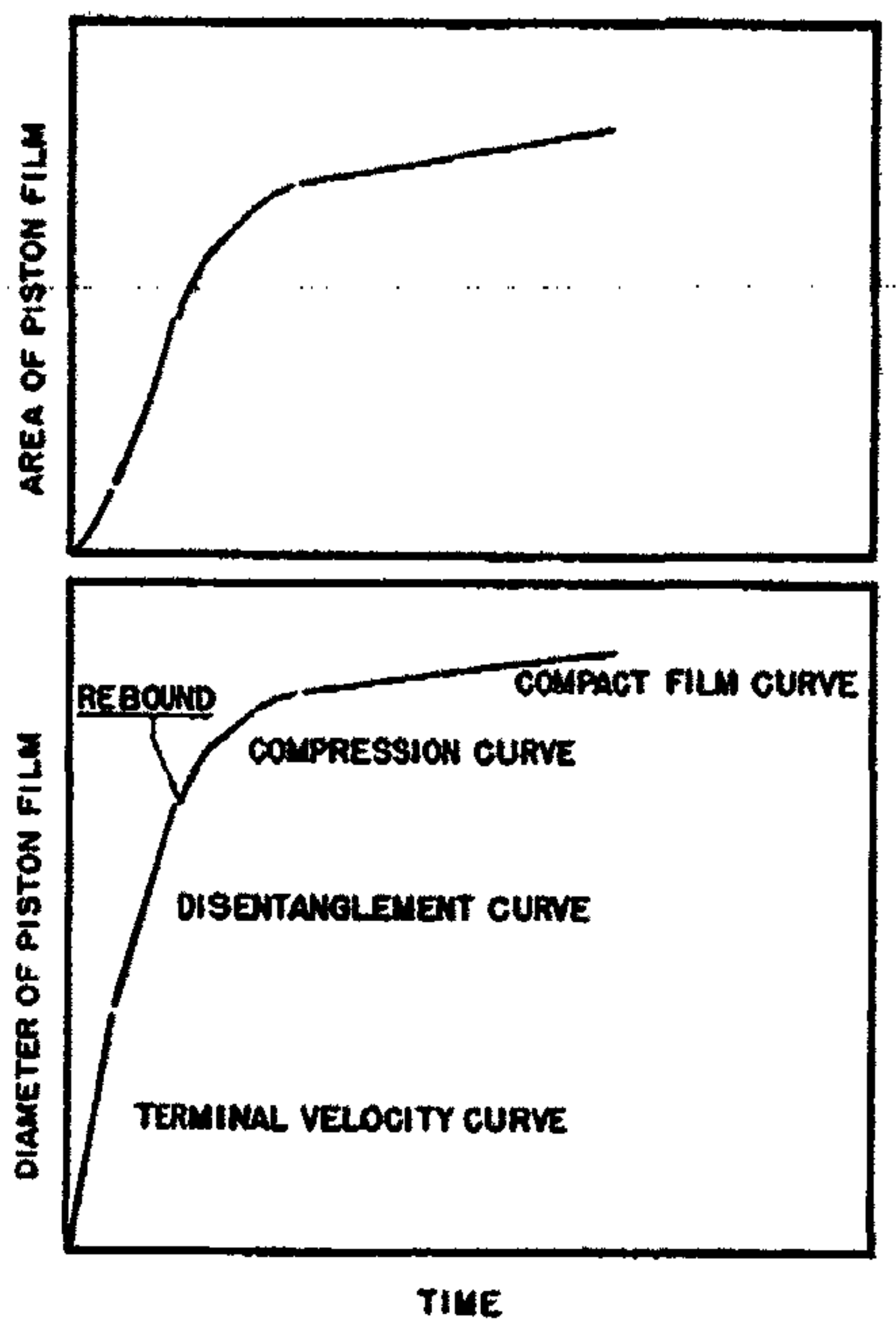

FIG. 2. Typical compression curves for soluble films

Disentanglement

On almost all of the compression curves for soluble films a point is reached beyond which the area-time curve rather than the diameter-time

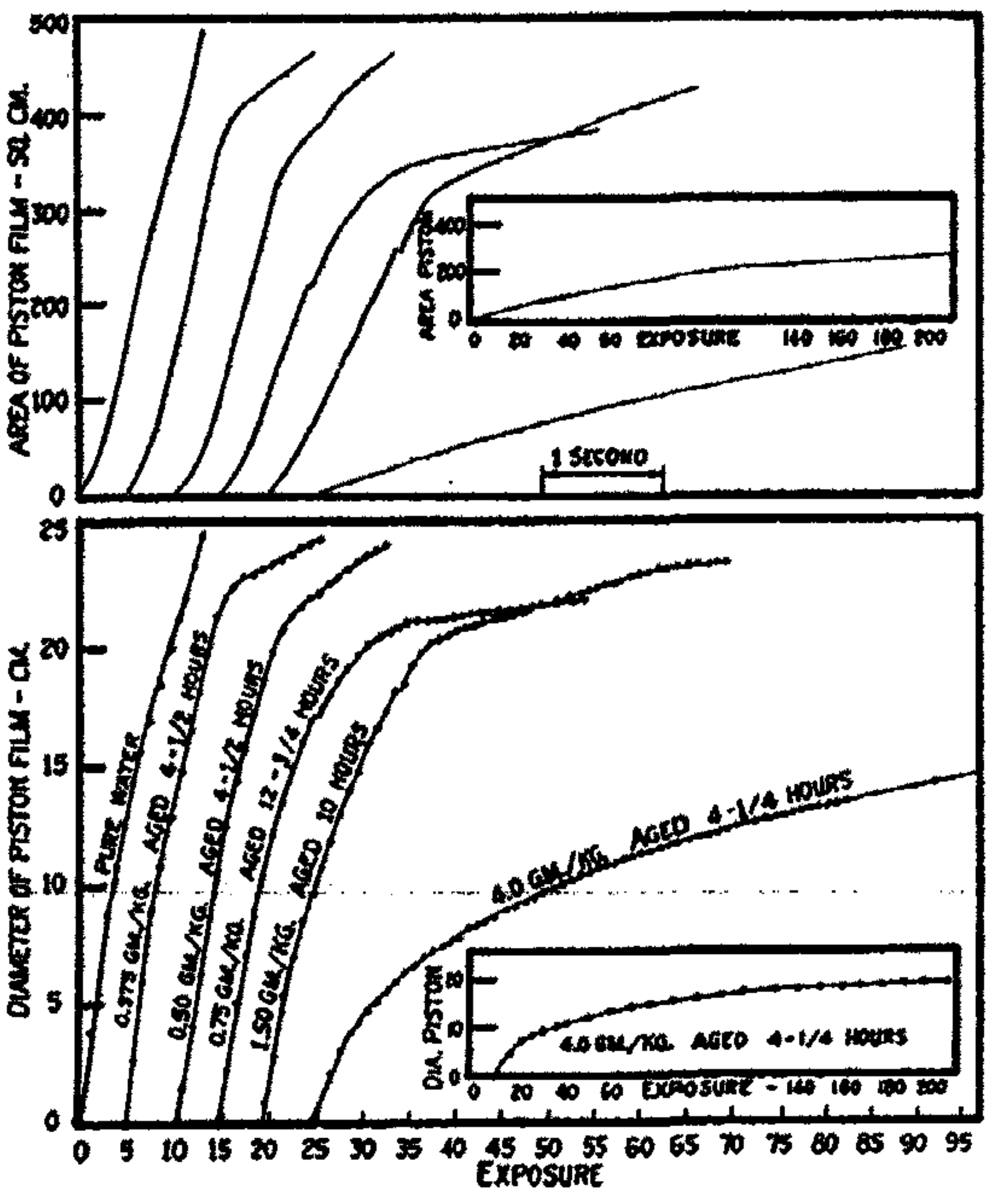

FIG. 3. Compression curves for aged surfaces of hydrocinnamic acid solutions

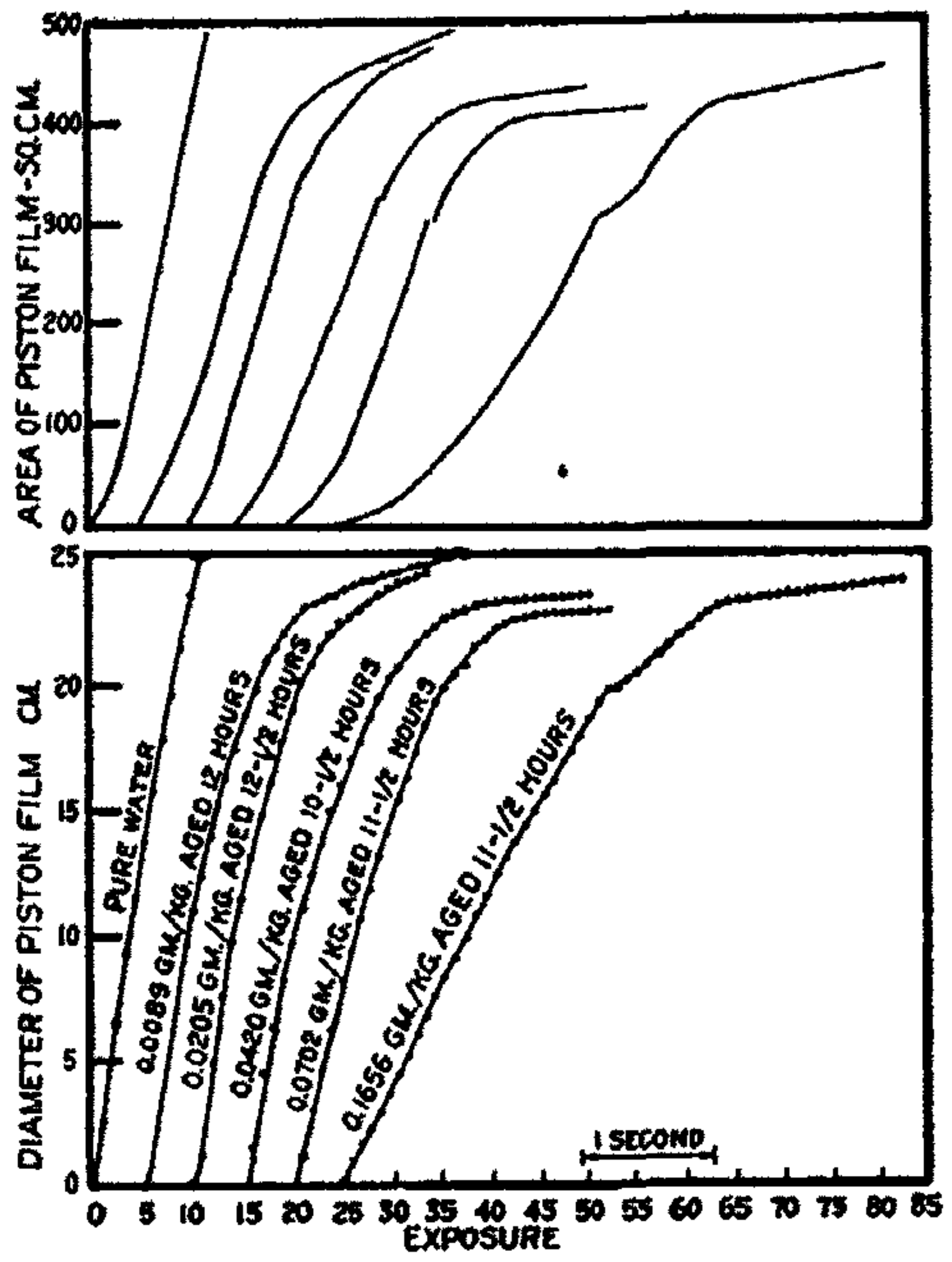

FIG. 4. Compression curves for aged surfaces of caprylic acid solutions

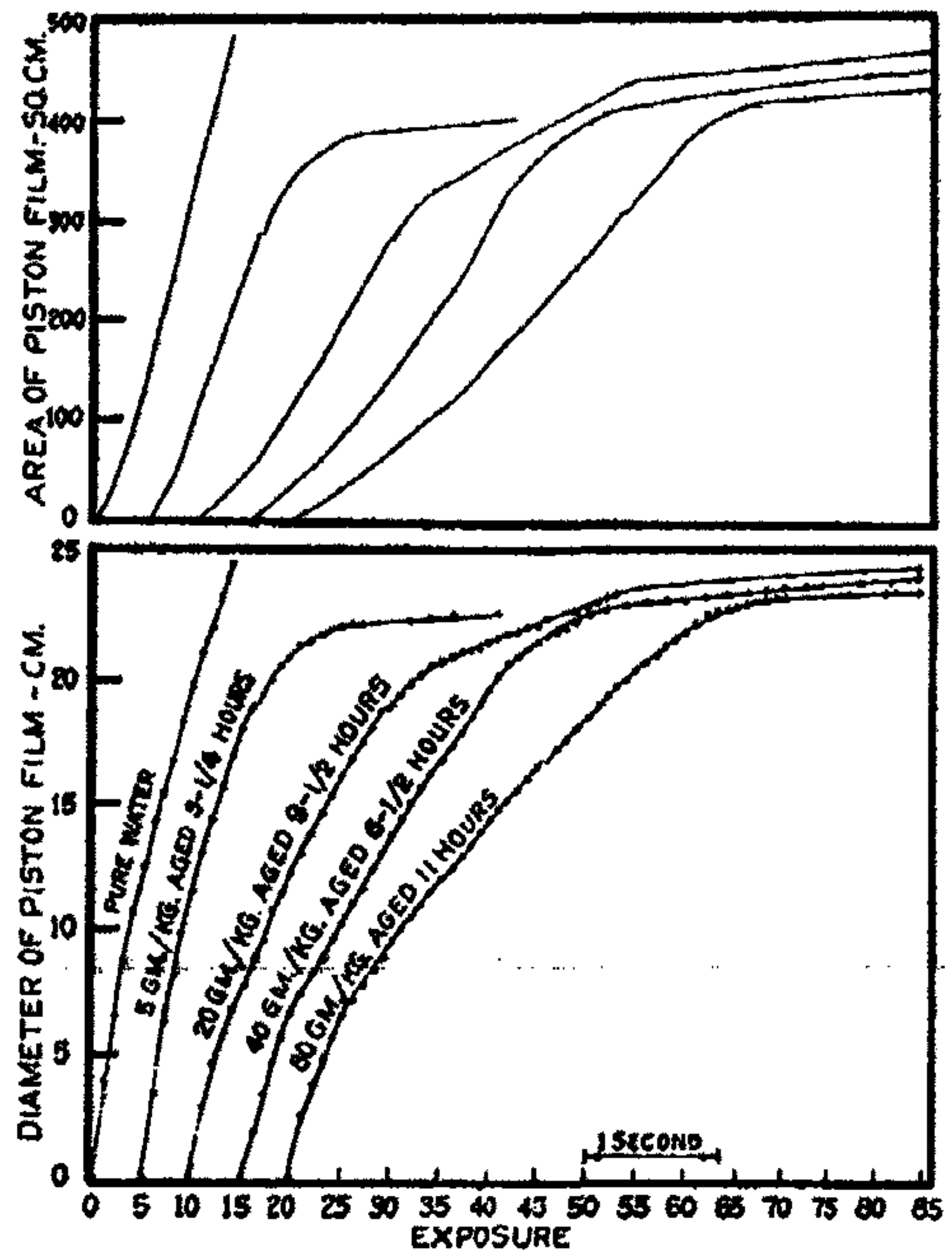

FIG. 5. Compression curves for aged surfaces of phenol solutions

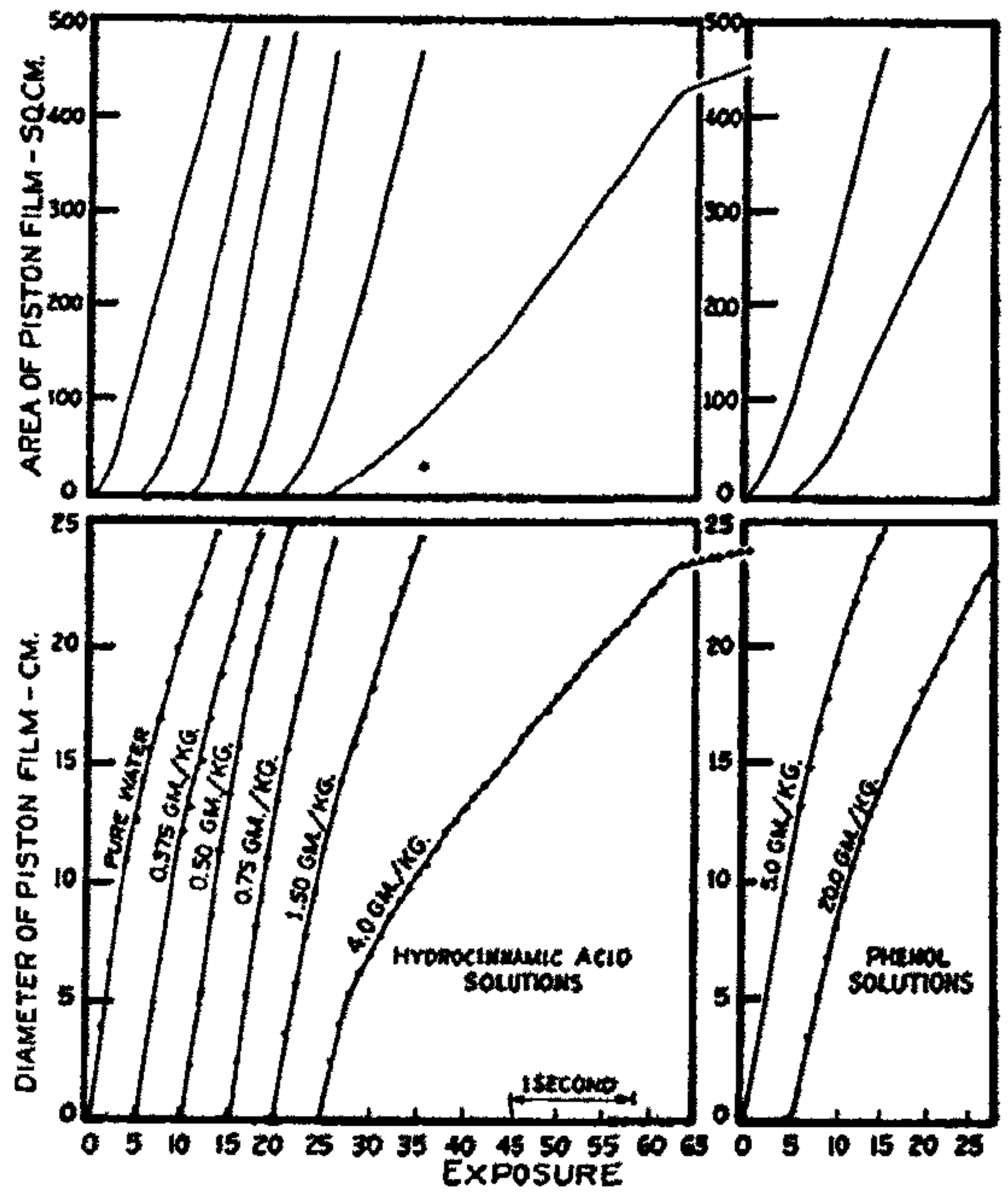

FIG. 6. Compression curves for freshly swept surfaces

curve becomes a straight line. It has been assumed that at this point the spreading rate becomes limited no longer by the terminal velocity but by the rate of disentanglement of molecules from the central globule.

If the rate of disentanglement is assumed to be proportional to a difference in spreading pressure between the piston film and the film compressed, then the soluble film must oppose the piston film with a constant pressure in the region where the area–time curve is linear. This portion of the curves, then, may be assumed to represent a transition from one surface phase to another. Presumably this change is from the two-dimensional gaseous state to a two-dimensional liquid state, a presumption confirmed by the nature of the subsequent changes.

If the central globule always had the same perimeter on the different solutions, then the slopes of the disentanglement curves should be expected to be the same on solutions of the same solute regardless of concentration if two-dimensional condensation were occurring, and on solutions of different solutes the slopes should be proportional to the two-dimensional vapor pressures of the solutes.

It seems probable, however, that the perimeter of the central globule should itself be a function of the initial opposing pressure, as well as of the vapor pressure, and the slopes of the disentanglement curves should tend to decrease with increasing concentrations of solutions, as observed.

Rebound compression of the piston film

Immediately after or during the period of disentanglement, most of the curves show a momentary break in the progress of the piston film. In slow motion the films seem actually to stand still for an instant. A possible explanation is that at this point the piston film, which has been in the so-called liquid expanded state, is opposed by a force sufficient to compress it to a more compact form. At the same time the soluble film may or may not be undergoing compression. When the piston film has been compacted, the normal compression of the soluble film proceeds.

From the existence of the "rebound" it is reasonable to suppose that until compression to this point the soluble film was in some state more expanded than that of the piston film. That the point of rebound coincides roughly with the departure of the area–time curve from linearity would confirm the presumption that this point marks the completion of a transition from the gaseous to the liquid state. Another alternative explanation, depending upon the momentum of the body of the liquid set in motion toward the walls of the containing vessel by the advancing film during the period of its fastest motion, has been mentioned elsewhere (7).

The change from liquid to compact films

The rounded portions of the curves, where neither the area nor the diameter is a linear function, apparently represent compression of the "liquid" films to compact films. The compression of the compact films, in which the rate of reduction in area is comparatively low and may be assumed to depend only on the rate of escape of molecules from the films, is represented by the final linear or approximately linear portions of the curves.

By extrapolating these final linear portions of the curves backward we presumably obtain the total areas that all of the molecules in the soluble films at any time would occupy if compressed into films as closely compacted as these curves represent. In table 1 these minimum compact film areas are compared to the actual areas of the films for the particular point where the disentanglement curves cease to be linear. The ratios are seen to agree very well with the ratios between the vertical and horizontal cross sections of the molecules, as calculated from x-ray data or as deduced by analogy with data for insoluble films. From the apparently real discrepancy in the case of caprylic acid it may be concluded that many of these molecules already are oriented in the uncompressed surfaces. The conclusion from these results is that in the transition from the liquid to compact films the essential change is in the "up-ending" of molecules in the surface.

TABLE 1

Ratios of horizontal cross sections, A_h, to vertical cross sections, A_v, of molecules as deduced from film experiments and as calculated from data from other sources

SOLUTION	CONCENTRATION	AGED	A_h/A_v (FILM EXPERIMENTS)	A_h/A_v (CALCULATED)
	grams per kilogram	*hours*		
Hydrocinnamic acid	0.375	4½	1.27	1.6
	0.5	4½	1.38	1.6
	0.75	12¾	1.60	1.6
	1.5	16	1.43	1.6
	4.0	4¾	1.56	1.6
Caprylic acid	0.0089	12	1.88	2.4
	0.0205	12½	1.89	2.4
	0.0420	10½	1.89	2.4
	0.0702	11½	1.95	2.4
	0.1656	11½	1.86	2.4
Phenol	5.0	3¼	1.7	1.4
	20.0	9½	1.2	1.4
	40.0	6½	2.0	1.4
	80.0	11	1.5	1.4

These results confirm the original presumption that, in the compression of soluble films as well of insoluble films, the transitions are from the two-dimensional gaseous state, to the liquid state, to a solid or compact film state.

Adsorption accounted for by the surface films

If extrapolating the compact film curves back to zero time gives the total areas which could have been occupied by all the molecules in the original soluble films, if compacted, then in each case the number of grams of solute originally present as a film per square centimeter of surface can be calculated by assuming that the area per molecule in the film is the same as the vertical cross-sectional area of the molecules as calculated from x-ray data. The results represent the amount of the Gibbs adsorption which is accounted for as existing in the surface as a film, in these cases. In table 2 these values are compared with the theoretical values of adsorption as calculated from surface tensions. The failure of the calculated adsorption to be wholly accounted for by the film measurements in every case might arise from a greater rate of escape of molecules from gas-

TABLE 2

Values of adsorption for hydrocinnamic acid, caprylic acid, and phenol solutions as obtained from the areas of the compact solute films at 11°C. and as calculated from surface tensions at ordinary temperatures

SOLUTION	CONCENTRATION	AGED	$\Gamma \times 10^9$ G. PER CM.^{2}	
			Extrapolated compact films	Calculated from surface tension data
	grams per kilogram	*hours*		
Hydrocinnamic acid	0.375	4½		1.7*
	0.5	4½		2.0*
	0.75	12¾	3.7	3.2*
	1.5	16	4.3	5.2*
	4.0	4¼	6.4	7.6*
Caprylic acid	0.0089	12		1.1†
	0.0205	12½		2.2†
	0.0420	10½	2.8	3.7†
	0.0702	11½	3.0	5.5†
	0.1656	11½	4.0	7.8†
Phenol	5	3¼	1.9	2.1‡ 2.0†
	20	9½	1.3	4.2‡ 4.2†
	40	6½	1.3	4.4‡ 4.3†
	80	11	1.3	4.4‡ 2.3†

* Bacon and Swain, unpublished results.

† D. A. Wilson, unpublished results.

‡ From data of Harkins and Grafton (J. Am. Chem. Soc. 47, 1329 (1925)).

eous and liquid films than from compact films, which would cause the areas of compact films found by back extrapolation to be lower than the true areas.

It can be concluded from these results that the adsorption predicted from the lowering of surface tension with increasing concentration is at least largely accounted for by the existence of a soluble film in the surface. By the microtome method and by interferometric methods it appears to have already been shown, at least for the case of hydrocinnamic acid (6, 9, 5), that the total amount of adsorption in a surface at equilibrium is in practical agreement with that predicted from the lowering of the surface tension. Apparently, then, the adsorption exists in the surface substantially as a soluble film, and there is here no evidence for a concentration gradient into the body of the solution at equilibrium.

THE COMPRESSION OF FRESHLY SWEPT SURFACES

Compression curves for freshly swept surfaces are shown in figure 6. Except on the most concentrated solutions, the behavior of the piston film is seen to be practically the same as on pure water. Each surface was carefully swept several times with paper strips, by the same procedure as used in cleaning all the surfaces before beginning an experiment. By "freshly swept" is meant that the time allowed for aging after sweeping was between 30 sec. and 2 min. From the results the conclusion might be drawn that the sweeping effectively removes any soluble as well as any insoluble film which may be on the surface, for the freshly swept surface appears to be almost identical with a pure water surface on dilute solutions and to carry only an attenuated gaseous film on concentrated solutions.

This result also is at least superficially in agreement with experiments by the microtome method (4, 6). There it was found that the absolute adsorption of hydrocinnamic acid reached the true equilibrium value only after about 12 hr., and that when only a few minutes were allowed with this apparatus the observed adsorption was much reduced. However, a film could appear in the surface almost instantaneously by denudation of the underlying layers of solution and the microtome would not detect it, because this apparatus removes an average sample, including both film and denuded layers (8).

The present experiments show either that there is no film on a freshly swept solution or that it is so readily displaced into the layers immediately beneath the surface as to offer no appreciable resistance to the motion of the oleic acid piston. It is difficult to believe that there is no film upon or in the surface, because the surface tensions of freshly formed droplets are found to be already greatly reduced, and it is indeed from drop-weight surface tensions that we calculate the theoretical values of the absolute adsorption which the microtome and other methods confirm. It seems possible, however, that in our experiments, where the surfaces were repeatedly swept with absorbent paper strips, the solute might have been almost completely removed from the surface layers by the sweeping, so that the spreading actually occurred, in effect, on greatly diluted surfaces. For formation of a film corresponding to the Gibbs adsorption on a 1.5 g. per kilogram hydrocinnamic acid solution total denudation to a depth of 3500 Å. would be necessary. This great depth of denudation might be used to support the alternative assumption that the film exists but is readily displaced, because in the layers immediately under the film there are no solute molecules tending to replace those escaping from it. These points should be settled by measurements of surface tensions on freshly swept solutions, which are now in progress in this laboratory.

SUMMARY

1. A new technique for the investigation of soluble films of positively adsorbed solutes upon the surfaces of their solutions has been developed.

2. Films of solute molecules have been shown to exist upon aged surfaces of solutions of caprylic acid, hydrocinnamic acid, and phenol, whereas the surfaces of freshly swept solutions seem more nearly to resemble water.

3. The analogy between these films of adsorbed solute molecules and two-dimensional insoluble films has been demonstrated.

4. The amount of solute in these soluble films is found to be of the same order of magnitude as predicted by the Gibbs theorem.

The authors wish to express their thanks to Professor J. W. McBain for the interest he has taken in this work.

REFERENCES

(1) Blodgett: J. Am. Chem. Soc. **57**, 1007 (1935).
(2) Cary and Rideal: Proc. Roy. Soc. (London) **A109**, 301 (1925).
(3) Ford: J. Phys. Chem. **40**, 835 (1936).
(4) Ford: Dissertation, Stanford University, 1936.
(5) Ford and McBain: J. Am. Chem. Soc. **58**, 378 (1936).
(6) McBain, Ford, and Mills: To be communicated.
(7) McBain, Ford, and Wilson: Kolloid-Z. **78**, 1 (1937).
(8) McBain and Humphreys: J. Phys. Chem. **36**, 300 (1932).
(9) McBain and Swain: Proc. Roy. Soc. (London) **A154**, 608 (1936).
(10) McBain and Wilson: J. Am. Chem. Soc. **58**, 379 (1936).
(11) Wilson and Ford: Nature **137**, 235 (1936).

OPAQUE ULTRACENTRIFUGES FOR DIRECT ANALYSIS[1,2]

JAMES W. McBAIN

Department of Chemistry, Stanford University, California

Received July 1, 1938

Upon a recent occasion Kraemer (6) stated that nowadays the first instrument which any colloid laboratory should acquire is an ultracentrifuge. This must have seemed to many listeners and readers a counsel of perfection unattainable without special financial resources. It is the purpose of this presentation before the Colloid Symposium to exhibit some of the inexpensive alternatives which are now available to any scientific laboratory that has only modest means, but yet is not satisfied with anything less than the highest degree of accuracy so far attained in this field.

The opaque ultracentrifuges[3] designed and developed by the author and his collaborators at Stanford University are all based on the direct air-driven spinning top of Henriot and Huguenard (5). They possess no optical system, and they are run at any desired constant temperature, in the open air (not *in vacuo*), the driving air being passed through a coil of copper pipe immersed in a thermostat. They run at 125,000 to 156,000 R.P.M. with an air pressure of 100 lb. per square inch, but lower pressures of air are usually employed. The steel must be protected with many thin coats of Bakelite lacquer, each baked on at 135°C.

With these simplest of means, both sedimentation velocity and sedimentation equilibrium are readily measurable with great accuracy. The sedimentation equilibrium of sucrose (9) yielded a molecular weight of 341 instead of the theoretical value 342. The sedimentation velocity of egg albumin (7) measured in rotor V (described below) gave $s_{20°} = 3.56 \times 10^{-13}$

---

[1] Presented at the Fifteenth Colloid Symposium held at Cambridge, Massachusetts, June 9-11, 1938.

[2] Transparent ultracentrifuges are not discussed here, but it may be mentioned that the original air-driven ultracentrifuge of McBain and O'Sullivan (J. Am. Chem. Soc. **57**, 780, 2631 (1938)) has been so improved that it is available for every purpose; for example, the sedimentation velocity of hemoglobin was found by A. H. Lewis to be $s_{20°} = 4.65 \times 10^{-13}$, in agreement with the value 4.63×10^{-13} published by Steinhart (J. Biol. Chem. **123**, 543 (1938)), rather than the previous value of 4.5×10^{-13} obtained at the University of Upsala.

[3] Eight different designs of these ultracentrifuges were exhibited at the Colloid Symposium, in addition to the transparent rotor of McBain and O'Sullivan. The external diameter of the rotors was usually 37 mm.

in good agreement with the definitive value 3.55×10^{-13} published by workers at the University of Upsala.

An ultracentrifuge avoids convection in the sedimenting liquid. This is achieved either by careful avoidance of temperature fluctuations and of vibration, or by allowing the sedimentation to take place within narrow radial spaces mechanically shielded from convection. With the direct air-drive we employ, the temperature is as constant and fixed as the thermostat.

I. PRIMITIVE ONE-PIECE ROTOR

We may begin with a reference to the very simplest hollow one-piece rotor with which many problems can be solved. The system may be immobilized by the use of a jelly or curd, the method introduced by McBain and Stuewer (8). This enables the sedimentation equilibrium of any substance present to be measured, but it is unsuitable for the measurement of sedimentation velocity except that of the jelly structure itself. With 0.3 per cent agar jelly it gave the same sedimentation rate (65×10^{-13}) as was given (63×10^{-13}) by the transparent ultracentrifuge of McBain and O'Sullivan. Swelling pressures of the jellies were also measured.[4] Soap curd was used in the sedimentation equilibrium of sucrose (9). Details and drawings of the one-piece top may be found in earlier articles (8, 9).

II. ROTOR WITH ANNULAR WASHERS FOR SEDIMENTATION EQUILIBRIUM

In this rotor, fully described by McBain and Tostado (9), the immobilized sedimenting liquid lies between horizontal annular washers spaced at uniform known distances apart by using alternately narrow and wide washers. Convection is permitted in the liquid in contact and in equilibrium with the innermost part of the sedimentation column. Analysis of this liquid before and after gives the molecular weight of any monodisperse substance, such as sucrose, or larger particles.

---

[4] Dilute agar jelly has been used in the National Institute for Medical Research, London (Schlesinger: Nature 138, 549 (1936); Schlesinger and Galloway: J. Hyg. 37, 445, 463 (1937)) to convert the Sharples Super-Centrifuge into a convectionless ultracentrifuge. Five cubic centimeters of virus solution gelatinized with dilute agar lines the closed bowl to a depth of 0.18 mm. Another 5 cc. is then added and the film is so thin that convection does not occur, thus allowing both rate and equilibrium to be measured. Virus of foot-and-mouth disease is measured after 3 min. An antibody required only 30 min. for sedimentation equilibrium. It is necessarily assumed that the agar jelly is of such concentration that it neither swells nor sediments. This, however, can be verified by direct experiment and adjusting the concentration of agar to the requisite value. Any influence of the agar on the absolute rate has to be tested by comparison in some other ultracentrifuge. Sedimentation equilibrium is of course unaffected (McBain: Science 87, 2250 (1938)).

III. ROTOR WITH ANNULAR WASHERS FOR SEDIMENTATION EQUILIBRIUM

This insertion in a rotor, designed by Tostado, is a modification of rotor II, permitting analysis of the liquid above and below the sedimenting column, especially for use in polydisperse systems. Here the annular washers are all alike and are merely piled loosely upon each other. They are kept centered by perforated buttresses or bosses on the container, as is shown in figure 1. The liquid from the middle and the exterior has to be withdrawn at approximately the same rate to avoid mixing. In using rotors II, III, IV, V, and VII the rotor is stopped before analysis, and experience shows that this is easily accomplished without mixing. With rotor VI the samples must be taken while running; in the case of rotor I this is merely a matter of optional convenience, using the technique described elsewhere (8, 9).

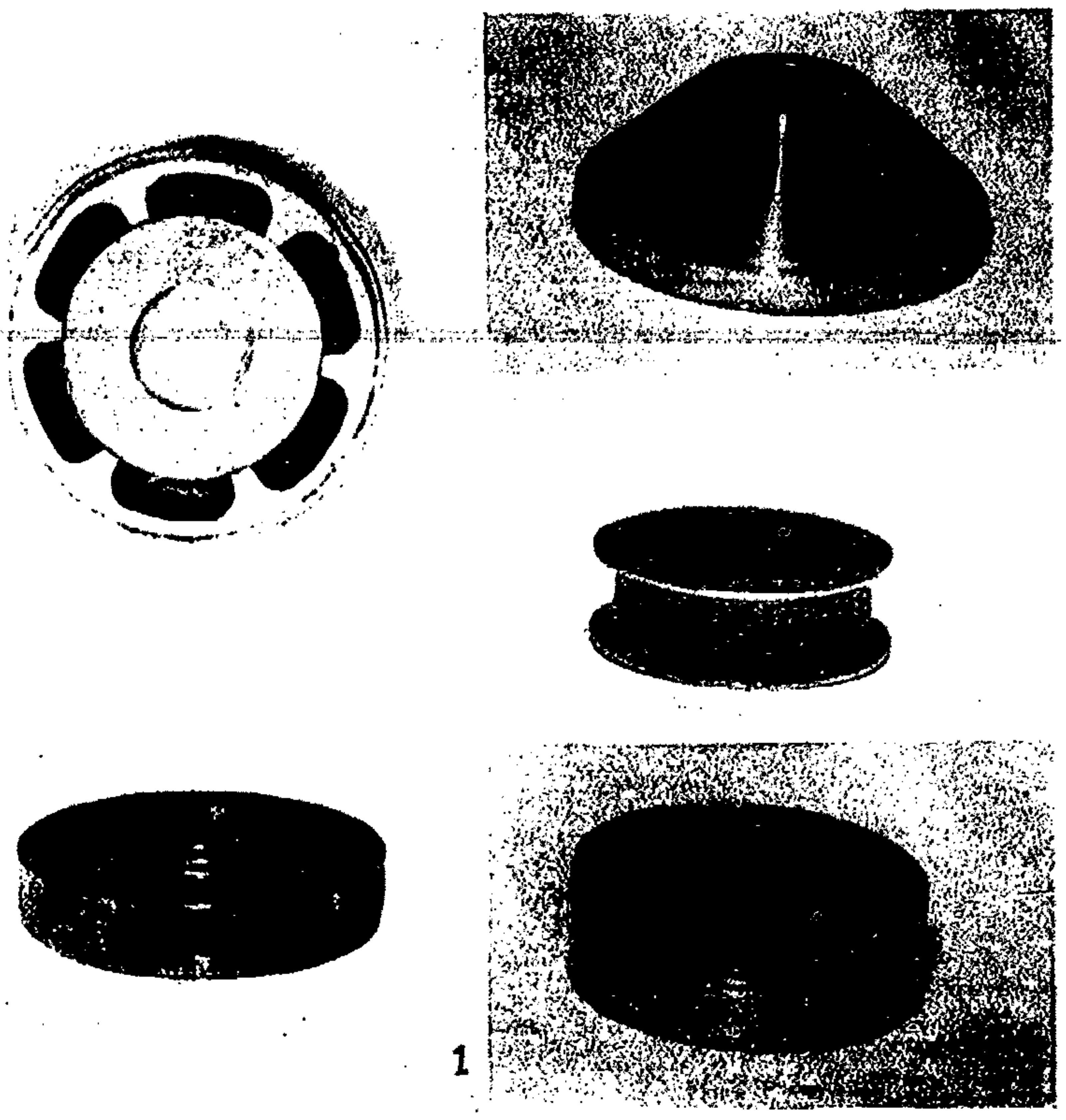

FIG. 1. Rotor with annular washers for sedimentation equilibrium
FIG. 2. Rotor for sedimentation velocity or equilibrium using solid circular discs

IV. CONCENTRIC BAFFLE RINGS FOR ANALYSES OF THE DIFFERENT FRACTIONS OF THE SEDIMENTATION COLUMN

In certain cases such as the soaps it is advisable to analyze all portions of the sedimenting column. The method suggested by my former collaborator, Dr. Tirey Foster Ford,[5] is to use concentric metal rings closely fitting and bored radially with numerous holes. Our own method, also exhibited, is to use instead concentric piles or nests of loosely piled washers, each pile being held as a unit by three vertical pins connecting the uppermost and lowermost washer of that set. This has the advantage of providing radial spaces for sedimentation.

V. ROTOR FOR SEDIMENTATION VELOCITY OR EQUILIBRIUM USING SOLID CIRCULAR DISCS

The simplest and for most purposes the best design (7) is that of McBain and Leyda (figure 2). The cells are ideally radial, consisting of a central pile of discs about 0.08 mm. thick, alternately wide and narrow, with a larger disc just fitting the container at top and bottom to keep them central. A vertical axial pin runs through the central solid pile of metal, holding it together. The sedimenting liquid is immobilized between the successive larger discs. Both the liquid outside the discs and that within them is analyzed. About 2.2 cc. of liquid has been employed.

Polydisperse systems require that runs be made at several speeds. There is also the advantage that every constituent may be analyzed for independently. Such opaque ultracentrifuges possess the further advantage over any transparent ultracentrifuge that the whole of the column of liquid from its upper surface outwards and from the very beginning of the sedimentation is available, without distortion, for exact measurement. Incidentally, the agreement of the measurements of sedimentation velocity made with this cell with those obtained by the McBain and O'Sullivan transparent ultracentrifuge and those of Svedberg shows that there is no wall effect upon velocity of sedimentation or diffusion where the spaces are as small as 0.08 mm., as would indeed be expected from hydrodynamic theory. The protein particles or molecules are 10,000 times smaller than the capillary spaces. Recently Svedberg and his collaborators (14) have been making effective use of a similar analytical method by putting a partition of filter paper in the middle of their transparent ultracentrifuge cell.

Attention is also directed to the design of the rotor by which a perfectly tight seal has invariably been obtained. The lower part of the rotor, ruggedly made of 4 UMA steel, has placed upon it in succession a narrow loose washer to cause slipping when assembling, a thin metal disc, a disc

---

[5] Present address: Shell Development Company, Emeryville, California.

of thin rubber or Pliofilm, or rubberized Cellophane, etc., and upon this the upper part of the rotor is directly screwed down. Its thinner longer annular wall bends outwards in the centrifugal field, engaging still more tightly in the lower piece. The rotor is assembled and opened upside down so as not to disturb the cell and its contents. Two small nicks are made in the periphery of the cell to enable the liquid to be withdrawn before taking out the cell if desired.

VI. ONE-PIECE STEEL ROTOR WITH WINDOW AND WITH SECTORIAL BAFFLES

When it is inconvenient to make a two-piece rotor, or where with a non-aqueous solvent a suitable seal cannot readily be found, the simplest one-piece rotor (as in I) may be used for sedimentation equilibrium (as in II) by simply inserting sectorial baffles (cut radially from annular washers) piled like open brickwork. For sedimentation velocity it is necessary first to place in the rotor a circular distributing disc. When platinum is used for this purpose the rotor must not be more than 20 mm. in diameter, since larger pieces of such pure soft metals as silver and platinum flow freely in the centrifugal field. In a two-piece rotor any strong metal or plastic may be used. A window must be left in the upper part of the two-piece rotor. The platinum disc is inserted in the one-piece 20-mm. rotor folded like an umbrella and then opened out. Through its center there is a smooth hole with upturned edges. Upon the distributing disc is piled the annular circle of sectorial baffles (figure 3).

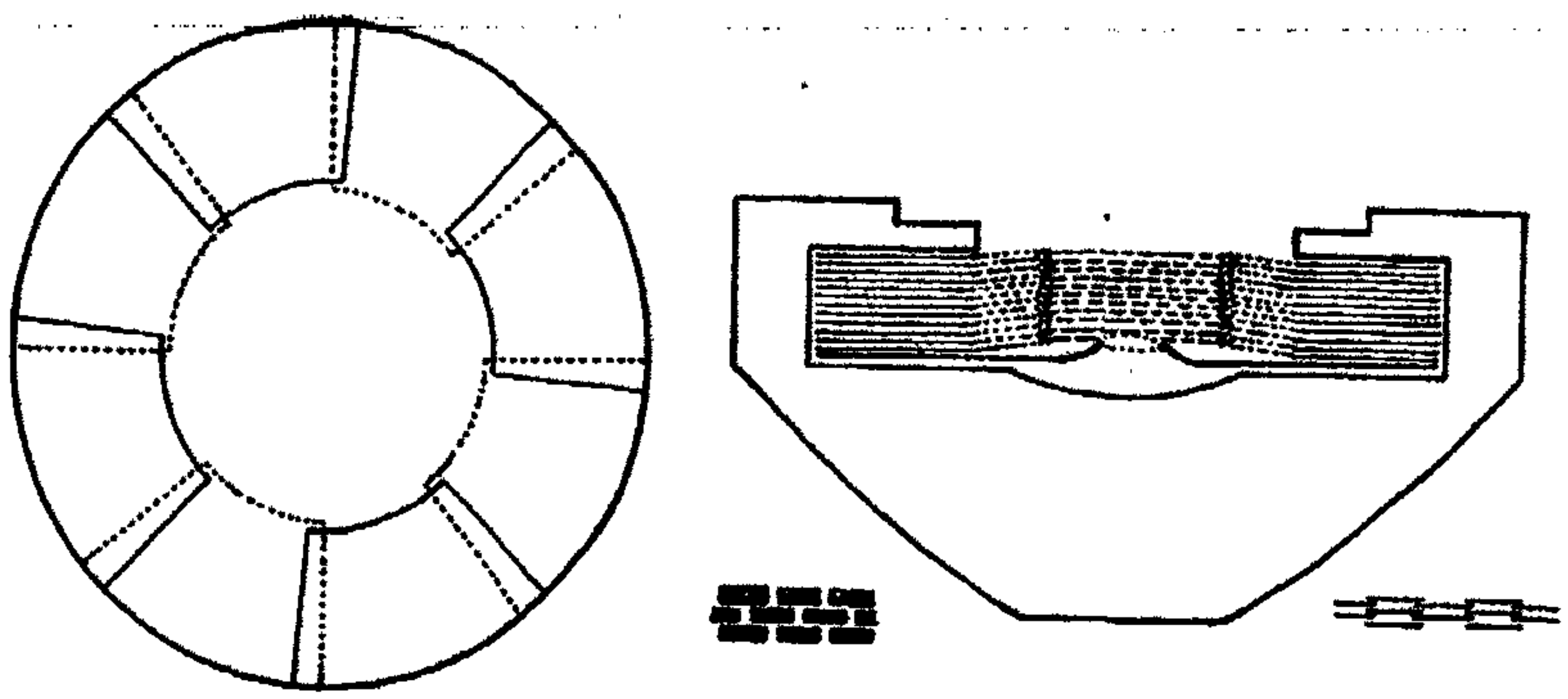
SECTORIAL BAFFLES, FROM ABOVE

COMPLETE ASSEMBLY

FIG. 3. One-piece steel rotor with window and with sectorial baffles

To make a measurement of sedimentation velocity, only sufficient liquid is put in to fill the spaces between the baffles. After the top has been spinning for a suitable time, the Cellophane window is opened with a flame or a razor (8, 9) without stopping the rotor. Then a heavy liquid such as carbon tetrachloride is inserted through the hole in the platinum, which instantly distributes it outside all the baffles, displacing an equal volume of liquid inwards. This is collected with a glass capillary scraping pipet. When a colored material is sedimenting, such as the respiratory protein of earthworm blood, no precautions whatever are taken except to stop when the pipet begins to collect some colored liquid. The sedimentation velocity obtained is naturally too large. In the case of earthworm blood such crude measurements (even with thick baffles) yield values of 80 to 90×10^{-13} instead of Svedberg's value of 61×10^{-13}. However, even an approximate analysis as by color, or color reaction etc., enables correction to be made to the actual distance the meniscus has sedimented, the total volume displaced being known from the carbon tetrachloride added. Method VI is far inferior to V when thick baffles with essentially liquid only between their edges are employed, but with thin baffles, as in II to V, placed just so as just to overlap, it is much improved and contains much more liquid.

VII. A LARGER ROTOR WITHIN INVERTED IMMERSED METAL TUBES FOR VELOCITY OR EQUILIBRIUM

This is a modification by a number of workers at Stanford University of the idea first employed by Elford and his collaborators (2, 3, 4, 13) and of the rotor of McIntosh and Selby (10, 11).

VIII. FORD'S MODIFICATION FOR GLASS CAPILLARY TUBES

The lower part of the rotor has a flat cylindrical depression upon its upper surface. In this rests a thin tray carrying two circular flanges through which holes are bored radially. Through these are placed glass capillary tubes closed at the outer end. The tray is held down by a broad-headed screw. This is suitable for velocity using Elford's method of observing the position of the boundary after the rotor is stopped, either by eye, using the color or scattered light or fluorescent light or cutting the tube in two for analysis, or by photography along with a series of tubes of different concentrations. This latter method has also been used by Dr. Ford for observing sedimentation equilibrium of hemolyzed beef blood.

IX. THE BECHHOLD–SCHLESINGER CONVECTIVE PROCEDURE

This method was originated (1, 12) in 1931. It encourages slow convection. Originally a commercial centrifuge was used. During the following years various quantitative and semiquantitative observations of its occurrence were made in the author's laboratory at Stanford, in that of Beams at Virginia, and also by Gratia in Belgium, using the simplest form of the one-piece hollow rotor I. Although admitting of quantitative results this is not an ultracentrifuge, and the periphery must be of, or lined with, some material which like filter paper holds all particles sedimented into it. McIntosh and Selby (10, 11) obtained quantitative results for the sedimentation velocity of bacteria, viruses, phages, and oxyhemoglobin, and also measured the actual specific gravity of the sedimenting particles. For example, McIntosh and Selby obtained a diameter of 56 Å. for oxyhemoglobin, identical with that quoted by Svedberg.

Where in the absence of convection the concentration of the homogeneous part of the liquid after time T would become proportional to $R(1 - e^{-KT})$, where R is the radius, Bechhold and Schlesinger have shown that with convection it will be proportional to $h(1 - e^{-\frac{R}{h} \cdot KT})$, where h is the inner radius of the sedimenting liquid. But after a given time in an ultracentrifuge, all the particles will have been centrifuged out, whereas in the centrifuge the concentration is asymptotically impoverished. Bechhold and Schlesinger show that therefore, if the centrifuging is greatly prolonged, the residual concentration of the convecting liquid becomes exceedingly sensitive to the size of the sedimenting particles, a change of twice the diameter soon making a difference of 10^6-fold in the concentration or as much more as is desired. This is valuable with virus or phage where the analysis may be good only to a single power of 10.

In conclusion, it may be noted that even the Bechhold-Schlesinger method may be used for distinguishing between monodisperse and multidisperse systems. It is easy to ascertain whether or not two substances are combined or associated with each other or sediment separately (as was done, for example, by Gratia in 1934).

It is evident that the problem of obtaining exact quantitative data on sedimentation velocity, sedimentation equilibrium, the actual density or the true partial specific volume has been completely solved by simple means within the reach of every scientific laboratory, and that the time is approaching for this to be a routine experiment in courses of physical or colloid chemistry.

SUMMARY

A number of simple and very inexpensive opaque rotors are now available with which measurements both of sedimentation equilibrium and of sedimentation velocity have been made with an accuracy at least as great as that obtainable with the best transparent ultracentrifuges.

REFERENCES

(1) Bechhold and Schlesinger: Biochem. Z. **236**, 392 (1931); Z. Hyg. Infektionskrankh. **112**, 668 (1931); **115**, 342, 354 (1933); Phytopathology **6**, 627 (1933).
(2) Elford: Brit. J. Exptl. Path. **17**, 399 (1936).
(3) Elford and Andrewes: Brit. J. Exptl. Path. **17**, 422 (1936).
(4) Elford and Galloway: Brit. J. Exptl. Path. **18**, 155 (1937).

(5) Henriot and Huguenard: Compt. rend. **180**, 1389 (1925); J. phys. radium **8**, 433 (1927).
(6) Kraemer: Ind. Eng. Chem., Anal. Ed. **10**, 128 (1938).
(7) McBain and Leyda: Nature **141**, 913 (1938); J. Am. Chem. Soc. **60** (1938), communicated.
(8) McBain and Stuewer: Kolloid-Z. **74**, 11 (1936).
(9) McBain and Tostado: Nature **139**, 1066 (1937); J. Am. Chem. Soc. **59**, 2489 (1937).
(10) McIntosh: J. Path. Bact. **41**, 215 (1935).
(11) McIntosh and Selby: Brit. J. Exptl. Path. **18**, 162–74 (1937).
(12) Schlesinger: Z. Hyg. Infektionskrankh. **114**, 161 (1932); Biochem. Z. **264**, 6–12 (1933); Kolloid-Z. **67**, 135 (1934); Biodynamica **1935**, 1.
(13) Tang, Elford, and Galloway: Brit. J. Exptl. Path. **18**, 269 (1937).
(14) Tiselius, Pedersen, and Svedberg: Nature **140**, 848 (1937); Ind. Eng. Chem., Anal. Ed. **10**, 116 (1938).

ULTRASONIC WAVES IN COLLOID CHEMISTRY[1]

KARL SOLLNER[2]

Department of Agronomy, New York State College of Agriculture, Cornell University, Ithaca, New York

Received July 14, 1938

The main phenomena of interest for the colloid chemist caused by ultrasonic waves (2, 6, 13, 14, 28) are so well known that they need not be considered extensively. Ultrasonics may cause all sorts of disintegration phenomena, e.g., the formation of emulsions and of fogs, and they may bring about coagulation. Although these facts have been well known for ten years, the underlying mechanisms have been obscure; accordingly several years ago we undertook their investigation. This paper gives a short account of the work.

The experimental technique described by Wood and Loomis (28) was used. Plates about 7 cm. in diameter and 1 cm. thick, cut from quartz crystal, are placed on a lead electrode and covered with a brass ring electrode. The whole system is immersed in transformer oil, an alternating field is applied, and the quartz, which is pronouncedly piezoelectric, starts vibrating. Since the electrical frequency is the same as the mechanical frequency of the quartz plate, the vibrations are so pronounced that the oil over the quartz is set into motion and a fountain of oil rises above it. Although the quartz discs used (11) had frequencies of about 200,000 cycles a second, it must be emphasized that the frequency employed is immaterial.

If a test tube containing water and mercury or water and an immiscible organic liquid is dipped into the oil fountain, emulsification occurs at once. Gray clouds of very fine mercury droplets are thrown into the water from the water-mercury interface, and white clouds of dispersed water or organic liquid, respectively, are produced where the two liquids meet; soon more or less concentrated emulsions are obtained. These emulsions do not show any special features. In non-protected systems under our standard conditions 6 g. of mercury per liter and 50 to 60 g. of benzene or similar substances are dispersed, when the equilibrium state is reached. This occurs under our experimental conditions in approximately 1 min. In the presence of suitable emulsifiers very high concentrations can be obtained.

---

[1] Presented at the Fifteenth Colloid Symposium, held at Cambridge, Massachusetts, June 9-11, 1938.

[2] New address: Department of Physiology, University of Minnesota, Minneapolis, Minnesota.

The size of the particles (5, 7, 28) varies somewhat with the metal dispersed and the medium of dispersion; low concentration and a fluid medium of dispersion favor a higher degree of dispersion, from a few tenths of a micron to several micra, although the truly colloidal fraction in many cases is rather small.

In 1929 Richards (20) emphasized the differences in the nature of the emulsification of mercury and in the dispersion of organic liquids in water. For liquid and molten metals the mechanism of dispersion, according to him, is as follows (4, 20): When brought into the oil fountain the violent transversal vibrations of the glass tube pump small quantities of water into the liquid metal; the water droplets rising in its interior reach the interface metal-water covered with a thin film of metal. When this film breaks, a cloud of minute metal droplets is thrown into the liquid. This process, as described for the macro-interface metal-water, obviously occurs also between the water droplets in the interior of the liquid metal, thus accentuating the effect.

Figure 1 demonstrates the whole mechanism rather convincingly. A low-melting alloy was irradiated with water and cooled down during the irradiation. Its sponge-like nature is apparent from its cross section and from its surface covered with little blisters. For a reason which may be understood later, it must be stressed that this dispersion of metals occurs equally well *in vacuo* or when high external pressure is applied.

Now let us turn our attention to the mechanism of emulsification in oil-water systems[3] (3), which was shown to hold quite generally, e.g., for the peptization of gels (12) or the formation of fogs (23) of organic or aqueous liquids, and for the dispersion of solids in liquids (25). The only exception is the formation of metal emulsions, discussed above.

The facts concerning emulsification in non-metallic systems, as described first by Newton Harvey (13), are as follows: Emulsification, i.e., disintegration, in general, occurs neither *in vacuo* nor when sufficiently high outside pressure is applied, the liquids in the latter case being gas-free or saturated with gas at a lower pressure only. This rule applies as well in the presence of even the best emulsifiers, where mere shaking may easily produce stable and fine-grained emulsions (3). At equilibrium pressure emulsification always occurs, provided this pressure is neither too high nor too low. The lower limit is much more sensitive in toluene-water systems, e.g., a gas pressure of at least 100 mm. of mercury is necessary.

---

[3] L. A. Chambers and M. Newton Gaines must be given credit for prior publication of an explanation of their experiments, similar to ours, on emulsification with low frequencies. This work (J. Cellular Comp. Physiol. 1, 451 (1932)) unfortunately did not come to our attention until after the whole series of our investigations on ultrasonics had been published.

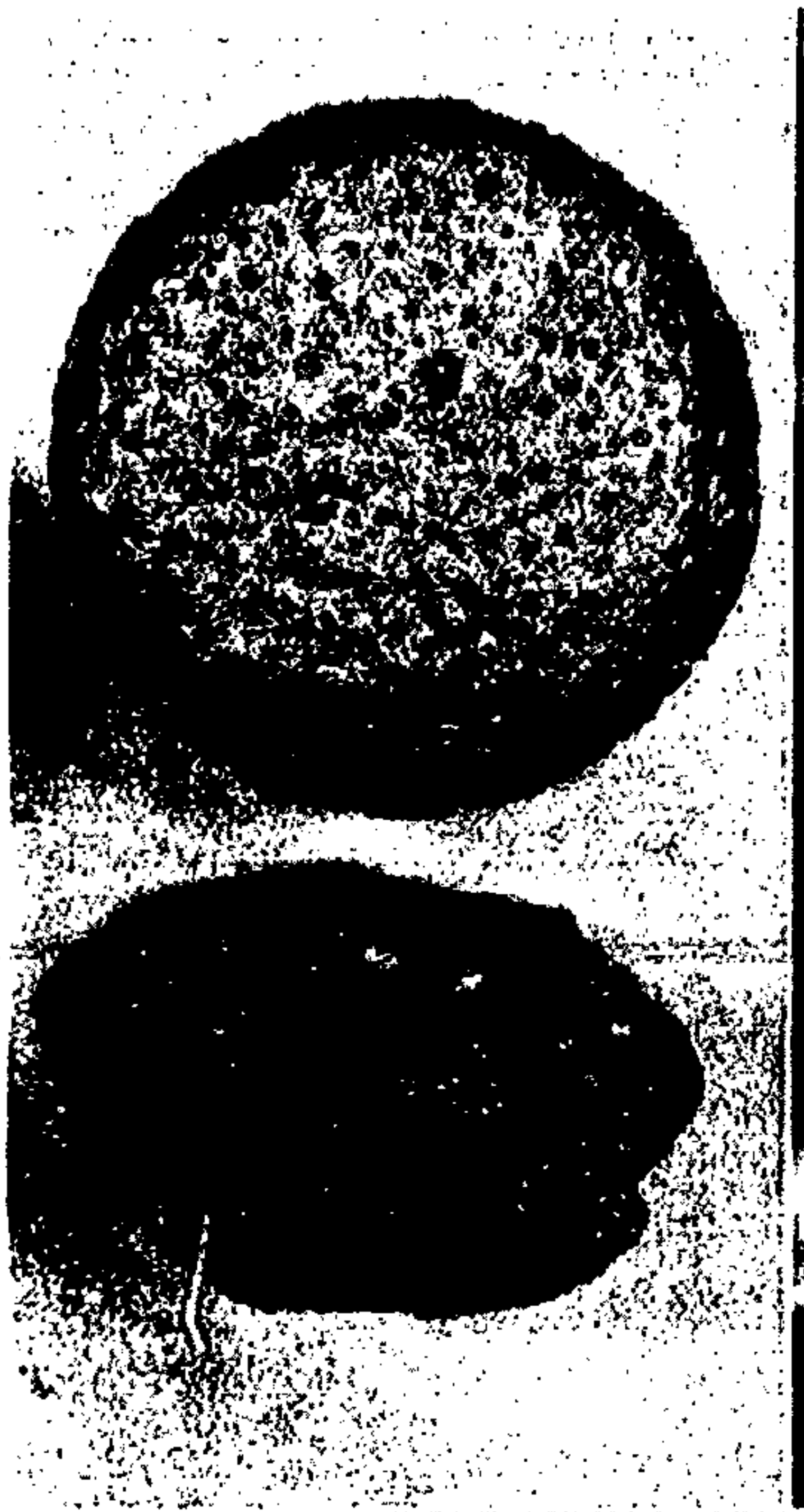

1

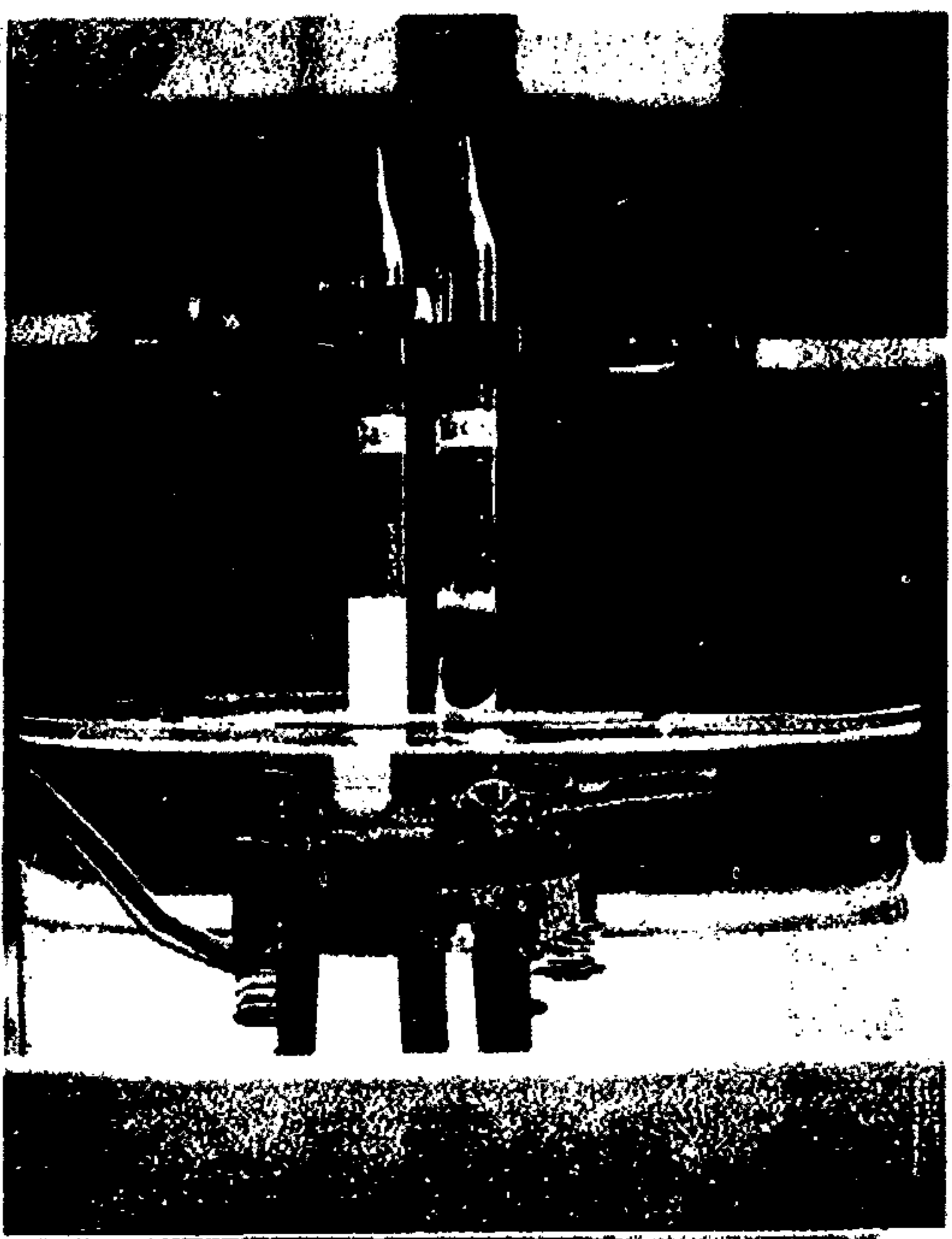

2

3

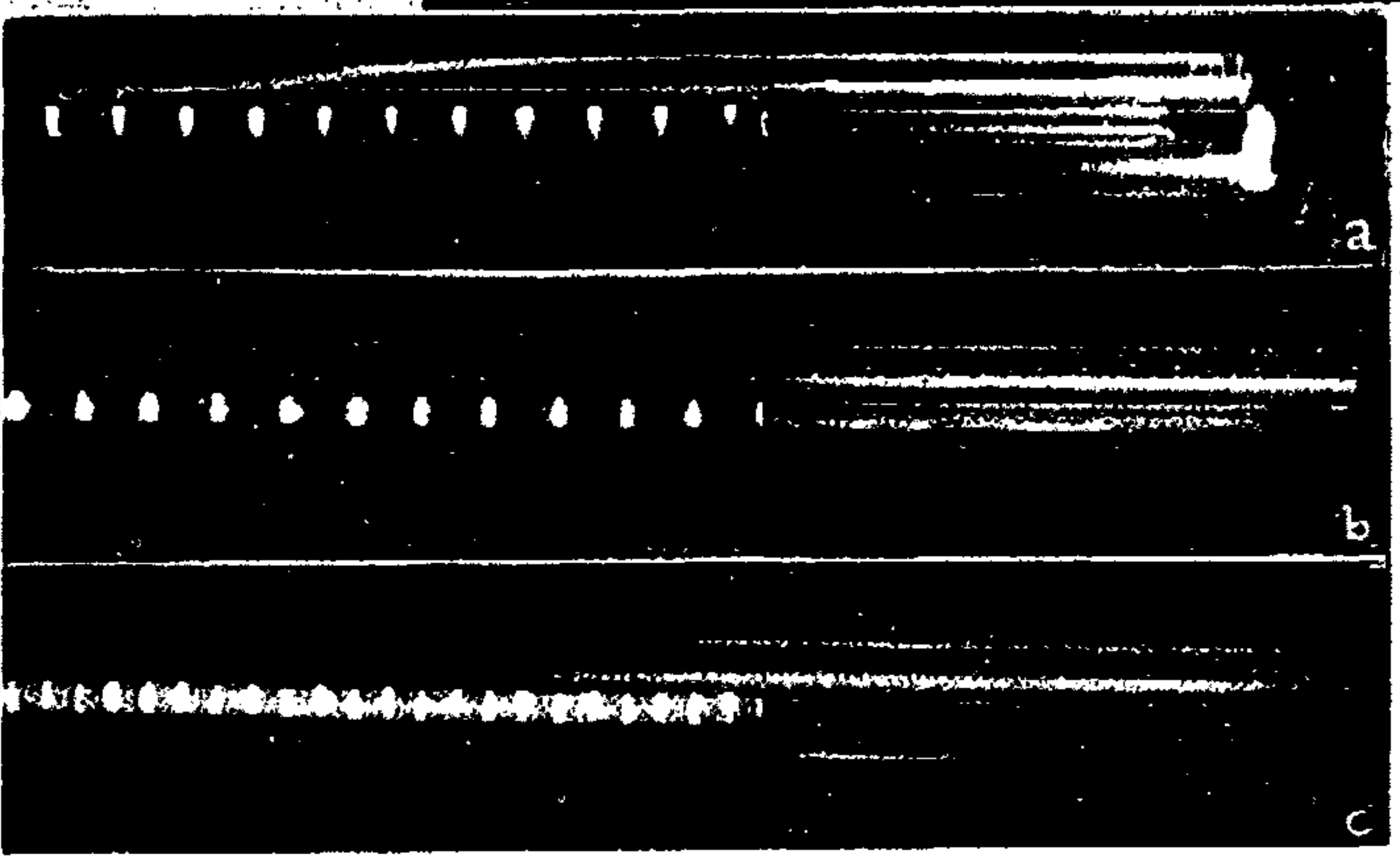

4

FIG. 1. Emulsification of a metal by ultrasonics. A low-melting alloy solidified during irradiation. About twice actual size.

FIG. 2. Emulsification by ultrasonics. The influence of the presence of a foreign gas upon emulsification. About one-third actual size.

FIG. 3. Coagulation of an emulsion by ultrasonics. About one-quarter actual size.

FIG. 4. Stationary wave patterns. (a) Toluene in water; (b) quartz in water; (c) toluene and quartz in water. About 1.5 times actual size.

How striking this difference is may be gathered from figure 2. The pressure experiments were performed in long test tubes. The column of the upper liquid is rather high, so that no saturation can occur in the critical region, the interface liquid–liquid, when an outside pressure is applied by means of a compressed gas.

How do the sound waves cause what at first sight appears to be such complicated phenomena, the effects being substantially the same whether performed at a few thousand or at millions of cycles a second (3)? A sound wave travelling through a liquid compresses and stretches it periodically. If the stretch is moderate and the irradiated liquid is free of gas, nothing spectacular occurs, but if the liquid is saturated with gas, gas bubbles appear, as was shown in detail by Boyle (6) and Newton Harvey (13) and their coworkers. What happens if the liquid is stretched unduly was described more than sixty years ago as a curiosity by Kundt and Lehmann (17) (working at low frequencies). They said: "While the whole system was vibrating violently the water close to the end of the vibrating rod turned turbid during the vibration. Since it was entirely free of air, these small bubbles causing the turbidity could only be due to the disruption of the water under the influence of the intense vibrations." When irradiating with ultrasonics (9, 24) in a long test tube containing a carefully degassed liquid, such as benzene, toluene, or slightly warmed water, zones of a slight and somewhat glittering opacity were always formed. Although no bubbles rose to the surface, a hissing noise was always heard.

Thus it is clearly indicated that the liquid disrupts under the stretch of sound waves, hence a high hydrostatic pressure prevents the whole phenomenon. If the same experiment is performed in a vacuum even at low energies, the liquid bubbles and boils but no hissing noise is heard. Under neither of these conditions does emulsification occur. Strong mechanical action by ultrasonics is always accompanied by the hissing noise, its loudness being so characteristic that it is used as an indicator of their efficiency. It is apparent that, although the formation of cavities does not give rise to destructive action, their disappearance, always connected with the hissing sound, does.

Lord Rayleigh (19) calculated the pressures which may occur when a vapor bubble collapses in a liquid and found that many thousands of atmospheres may be obtained locally in this way. The collapse of cavities at the rear of steamship propeller blades may cause the rapid destruction of the blades. In engineering the entire phenomenon, involving the formation of cavities and their vehement collapse due to outside pressure, is called "cavitation." This term will be used in this sense.

It may be easily demonstrated that the collapse of steam bubbles produces emulsification when occurring at the interface of two liquids. The collapse of the steam bubbles when accompanied by a rattling sound causes rapid emulsification (3). This method of emulsification is substantially different from the older one in which the vapor of an organic liquid is introduced into water, forming an emulsion on condensation.

We may safely conclude that the emulsification by ultrasonics is due to "cavitation" as defined above (3). This accounts for the fact that no emulsification occurs in a vacuum or when a high outside pressure is applied. In a vacuum cavities may be formed, but lack of outside pressure prevents their violent collapse. On the other hand, a sufficiently high pressure prevents the formation of cavities. The prevention of cavitation by applying an outside pressure is well known in engineering.

The influence of dissolved gases will not be discussed here in detail; one of their main functions is to act as weak spots when the liquid is stretched, thus promoting cavitation (3). Similarly, cavitation is favored at the interface water-oil, a fact promoting the dispersing action.

The influence of pressure and vacuum is not observed when dispersing liquid metals since, as already mentioned, their dispersion is not due to cavitation.

The dispersion of gels (10, 11, 12), e.g., rubber in benzene, or the liquefaction of thixotropic gels, is due to the same mechanism as emulsification in oil-water systems, occurring under exactly the same conditions. This is also true for the dispersion of solid bodies in liquids (25). An efficient dispersion of this kind has not as yet been observed with metallic or other substances of great cohesion, although oxide films, etc., may be easily removed by ultrasonics. On the other hand softer substances, especially of high cleavage (such as graphite or mica), may be readily dispersed. This process proceeds at a remarkably rapid rate when semicolloidal or microscopic suspensions, but not macrocrystals, are irradiated, colloidal solutions being readily obtained (25).

It can be demonstrated also that the formation of fog (23) by ultrasonics, as described by Wood and Loomis, is due to cavitation. A beaker or test tube containing a volatile liquid, such as benzene or toluene, is rapidly filled with a white cloud or fog when irradiated. With less volatile liquids it is necessary to use high energies or, more advantageously, to concentrate the energy by means of a special collector, a test tube drawn out at the middle to a thin-walled constriction. When brought into the oil fountain the constriction vibrates violently, and even liquids of a very viscous nature and of a high boiling point are dispersed into the air, if they are allowed to run down through the constriction. Air currents set up by the rectifying action (18) of the transversally vibrating collector transport the fog droplets away from it.

The very suggestive idea that one is dealing with evaporation on account of the great heat developed at the critical spot can readily be shown to be wrong. When an oil containing a non-volatile dyestuff is used, a colored cloud is formed around the collector, which proves that the dispersion is a direct one. Here, too, experiments at varying pressures show that cavitation causes the dispersion. On close inspection one may see how the surface becomes rippled at energies just sufficient to start fog formation. It looks as if the surface were hit from above,—indeed it is hit from above by the collapse of the cavities formed at the surface (23).

How active the interface liquid-gas is may also be seen from the following experiment: A strip of rubber partially dipped into benzene is, on irradiation, attacked most near the surface of the benzene, and may be eaten away entirely at this point, whereas its lower end, further away from the surface of the benzene, is practically free from attack.

We shall consider next the opposite of the phenomena discussed, the coagulating action of ultrasonics (21). Ultrasonics must be able to coagulate at a high speed, since a stationary state is soon reached in preparing an emulsion. It is easily demonstrated that this coagulation is not due to the streaming or stirring which is always observed during strong irradiation. Rapid coagulation occurs also at rather low energies where such a movement is never observed.

It may be shown that coagulation is due to the formation of stationary wave patterns,—Kundt's dust figures in liquids (21). When an emulsion is irradiated (the phenomenon is best seen in high columns of liquid), more whitish zones appear in the lower and middle part of the test tube, where the droplets of the emulsion accumulate. How such a test tube looks after a few minutes of irradiation may be seen from figure 3. Near the surface, where cavitation is strongest, the emulsion is not much affected, whereas in the lower parts all the dispersed material is accumulated. The process of coagulation may be observed microscopically (21). With low energies practically complete coagulation may be brought about, since the opposite process, emulsification, needs energies exceeding a rather well defined limiting value.

The coagulation of suspensions is quite analogous. In unstable systems, for instance quartz powder in organic liquids, it is very impressive. On slight irradiation the particles accumulate and stick to each other, thus forming big lumps which sink rapidly to the bottom of the tube; the whole liquid is free from particles after a few seconds.

To study the stationary wave patterns more closely, capillaries filled with an emulsion or suspension were used. They were closed at one end with picein, leaving a small air gap between the emulsion and the picein stopper, to prevent any appreciable movement of the liquid. When the oscillations are started the dispersed phase forms zones of accumulation which rapidly get very sharp; one has the impression of small disks standing upright in the capillary (figure 4). The distance between each two of the zones of accumulation can be calculated rather exactly from the sound velocity of the liquid and the known frequency of the oscillation.

In some cases the dispersed phase is collected in the nodes; in other cases in the loops. The main decisive factor—there must be some other ones too—seems to be the ratio of the specific gravities of the dispersed phase and the medium of dispersion. If the dispersed phase is lighter, it accumulates in the nodes; if it is heavier than the medium of dispersion, in the antinodes (16). This means that in the former case the meniscus becomes free from dispersed phase; in the latter case, there is a locus of accumulation (figure 4a, 4b). When a mixed system containing, e.g., dispersed toluene and quartz powder is irradiated the two dispersed phases separate and accumulate at their proper places, in the nodes and loops, respectively (figure 4c). Larger particles are much more readily collected; particles several micra in diameter accumulate practically instantaneously, whereas smaller particles, below 0.5μ or so in diameter, are hardly affected at moderate energies and the frequency employed.

The coagulating action of the ultrasonics is now easily understood: firstly, the particles are accumulated and, as one knows, the rate of spontaneous coagulation increases rapidly as the concentration increases; secondly, particles of different size migrate with different velocities towards the zones of accumulation, thus being liable to additional collisions, a kind of orthokinetic coagulation (26, 27); thirdly, the particles do not migrate only in one direction, their macroscopic movements merely being the result of the asymmetry of the oscillations which they perform according to their (different) size; this too causes a kind of orthokinetic coagulation.

Much very interesting work has been done by other investigators (1, 15) on the coagulation of fogs and smokes. There is considerable analogy with the coagulation in liquid systems, orthokinetic coagulation being particularly pronounced with such systems (22).

In conclusion, mention should be made of the orientation of anisometric, i.e., rod- and plate-like, particles by ultrasonics (8). When a very dilute suspension of finely ground mica or graphite is irradiated even with very weak energies, brilliantly glittering zones are observed at once in transmitted or reflected light, indicating an orientation of the (anisometric) particles, perpendicular to the axis of the tube, i.e., perpendicular to the flux of energy. In this experiment the energy applied may be so weak as to cause no appreciable accumulation even over long periods.

This orientation is found with all rod- and plate-like substances of macroscopic and microscopic dimensions; it was also found with some truly colloidal systems, e.g., vanadium pentoxide sols or ferric oxide sols containing anisometric particles, ultramicroscopic in all three dimensions. The orientation with these sols is studied most conveniently with polarized light, the orientation of the particles being in all cases perpendicular to the flux of energy; this interesting phenomenon undoubtedly needs further investigation.

REFERENCES

(1) Andrade: Trans. Faraday Soc. **32,** 1111 (1936).
(2) Bergmann: Der Ultraschall. VDI Verlag, Berlin (1937).
(3) Bondy and Söllner: Trans. Faraday Soc. **31,** 835 (1935).
(4) Bondy and Söllner: Trans. Faraday Soc. **31,** 843 (1935).
(5) Bondy and Söllner: Trans. Faraday Soc. **32,** 556 (1936).
(6) Boyle: Science Progress **23,** 75 (1928); (Gives further references).
(7) Bull and Söllner: Kolloid-Z. **60,** 263 (1932).
(8) Burger and Söllner: Trans. Faraday Soc. **32,** 1598 (1936).
(9) Chambers and Gaines: J. Cellular Comp. Physiol. **1,** 451 (1932).
(10) Freundlich, Rogowski, and Söllner: Z. physik. Chem. **A160,** 469 (1932).
(11) Freundlich, Rogowski, and Söllner: Kolloid-Beihefte **37,** 223 (1933).
(12) Freundlich and Söllner: Trans. Faraday Soc. **32,** 966 (1936).
(13) Harvey: Biol. Bull. **59,** 306 (1930) (further references given).
(14) Hiedemann: Ergeb. exakt. Naturw. **14,** 201–63 (1935).
(15) Hiedemann and coworkers: Trans. Faraday Soc. **32,** 1101 (1936); Kolloid-Z. **77,** 103, 168 (1936).
(16) King: Proc. Roy. Soc. (London) **147A,** 212 (1934).
(17) Kundt and Lehmann: Pogg. Ann. **153,** 1 (1874).
(18) Cf., e.g., Meissner: Physik. Z. **28,** 621 (1927); Naturwissenschaften **17,** 25 (1929).
(19) Lord Rayleigh: Phil. Mag. [6] **34,** 94 (1917).
(20) Richards: J. Am. Chem. Soc. **51,** 1724 (1929).
(21) Söllner and Bondy: Trans. Faraday Soc. **32,** 616 (1936).
(22) Söllner: Trans. Faraday Soc. **32,** 1119 (1936).
(23) Söllner: Trans. Faraday Soc. **32,** 1532 (1936).
(24) Söllner: Trans. Faraday Soc. **32,** 1537 (1936).
(25) Söllner: Trans. Faraday Soc., in press.
(26) Tuorila: Kolloid-Beihefte **24,** 1 (1927).
(27) Wiegner: J. Soc. Chem. Ind. **50,** 55 (1931).
(28) Wood and Loomis: Phil. Mag. [7] **4,** 417 (1927).

ADSORPTION AT CRYSTAL-SOLUTION INTERFACES. X

A Study of the Adsorption of Monoazo Dyes by Crystals of Potassium Sulfate during their Growth from Solution[1]

MERLE D. RIGTERINK and WESLEY G. FRANCE

Department of Chemistry, The Ohio State University, Columbus, Ohio

Received July 14, 1938

This paper is a continuation of previously reported studies made in this laboratory on the adsorption of foreign substances by growing crystals (1, 3, 5, 6, 7, 8, 10, 11, 15, 16). Attention has been focussed especially on one point which has received very little previous study,—the presence and distribution of polar groups in the foreign molecules. Only a few cases of closely related dyes where one was adsorbed and the other was not have been observed in the earlier work. Buckley (2) investigated a large number of closely related dyes but only a rather limited number which were isomeric; consequently he was unable to arrive at any general conclusions which would predict the behavior of a dye not previously investigated.

Fortunately samples of the members of two series of dyes which were admirably suited for such an investigation were obtained. These were originally prepared by Dr. Wallace R. Brode and two of his former students (4, 9) for spectroscopic investigations, and therefore are of a higher purity than the usual commercial products. These dyes were prepared by coupling aniline and the ortho-, meta-, and para-sulfonated anilines by the usual method of diazotization with a series of mono- and di-sulfonic acid derivatives of α- and β-naphthols and α- and β-naphthylamines. They will be referred to in the tables by abbreviations which are derived from the intermediates used in their preparation. These intermediates were as follows: aniline (A), ortho-sulfonated aniline (O), meta-sulfonated aniline (M), para-sulfonated aniline (P), α-naphthol (α-OH), β-naphthol (β-OH), α-naphthylamine (α-NH_2), and β-naphthylamine (β-NH_2). The numbers given in the tables after the abbreviations refer to the positions of the —SO_3Na groups attached to the naphthalene rings. The dyes which are starred in the tables possess the nucleus

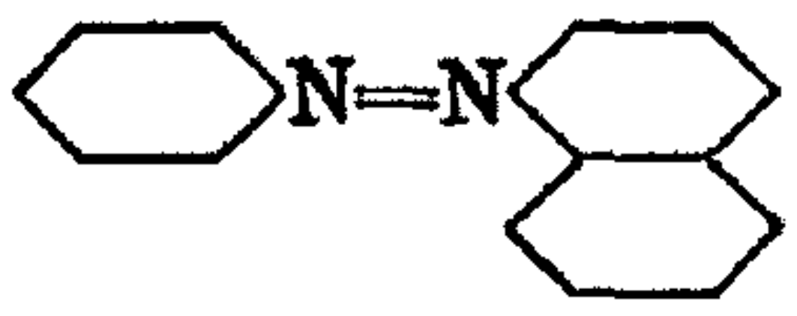

---

[1] Presented at the Fifteenth Colloid Symposium, held at Cambridge, Massachusetts, June 9-11, 1938.

while the others possess the nucleus

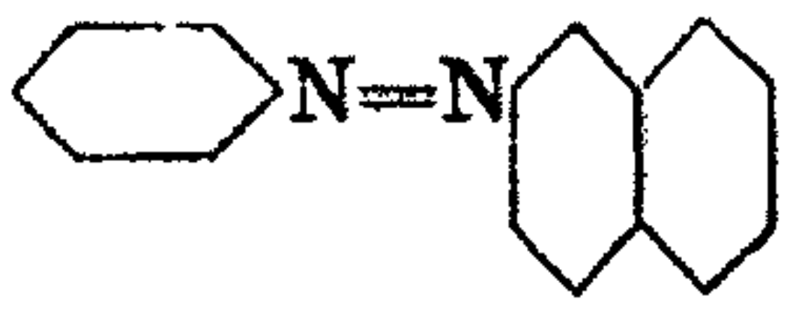

EXPERIMENTAL

Potassium sulfate was selected for this investigation, since preliminary experiments showed that it adsorbed a number of the dyes of these series. Qualitative experiments were made to determine which of the dyes were adsorbed, and therefore which should be chosen for further quantitative experiments. In 50 cc. of a saturated potassium sulfate solution was dissolved 0.005 ± 0.0005 g. of each dye. These solutions were then set aside in 50-cc. beakers, and slow evaporation allowed to take place at room temperature. The resultant crystals were examined for adsorption and habit modification.

For the quantitative experiments equal molar concentrations of dye rather than equal weight concentrations were used. A concentration of 2×10^{-5} moles of dye per 100 cc. of solution was chosen for this purpose, since for the majority of the dyes this is approximately equal to the 0.01 per cent concentration by weight used in all of the qualitative experiments. 1×10^{-4} mole of each dye was dissolved in 500 cc. of a saturated potassium sulfate solution. The resulting solution was filtered and set away in eight 100-cc. beakers to crystallize by slow evaporation at 30°C. ± 0.1° at constant humidity for 96 hr.

In those cases in which the dyes were slightly soluble the solutions were prepared by dissolving the dye in a hot saturated potassium sulfate solution and then allowing the mixture to stand at 30°C. for two days to allow the excess dye to precipitate out.

The crystals were removed after their growth, rinsed twice with distilled water, dried above an electric oven at a temperature of 50–60°C., and allowed to cool in a desiccator containing Drierite (anhydrous calcium sulfate). A portion of the crystals was then weighed, dissolved in water, and diluted to 100 cc. A standard solution with an approximately equal dye concentration was also prepared. The two solutions were then compared in a Leitz colorimeter with an average of ten readings taken as the colorimeter reading used in the calculation. From these data the number of moles of dye adsorbed, per mole of potassium sulfate that crystallized, was calculated.

RESULTS

The results obtained are summarized in tables 1, 2, 3, and 4. In the second determinations appearing in the tables a new crop of crystals was used for the analysis, and an equal concentration of the salt was used in the standard solutions.

In table 5 are given the results of quantitative measurements made of the amount of adsorption of P-β-OH-6 at a number of different concentrations. The results above concentrations of 3×10^{-6} moles of dye per 100 cc. of solution are not quite as accurate as the results at lower concentration, owing to the fact that it was difficult to induce crystallization at the higher concentrations of dye.

TABLE 1

Summary of effect of soluble acid dyes on potassium sulfate

DYE	PER CENT PURITY	MOLES OF DYE ADSORBED (PER MOLE OF K_2SO_4) $\times 10^3$			MODIFICATION
		First determination	Second determination	Average	
P-β-OH*	84.63	91	103	97	Types 1 and 2
M-β-OH-6*	71.25	87	94	90.5	Type 1
M-β-OH-7*	74.15	79	97	88	Type 1
P-β-OH-6*	66.40	49	50	49.5	Type 2
P-β-OH-6:8*		24	22	23	Type 1
O-β-OH-7*	98.87	14	13	13.5	Type 3
O-β-OH-6*	93.05	8.9	9.1	9.0	Type 3
P-β-OH-7*	61.25	4.3	4.0	4.25	Type 1
M-α-OH-3	54.61	3.7	3.5	3.6	Types 4 and 5
M-α-OH-4	77.87	1.9	1.7	1.8	Type 5
O-β-OH-3:6*	46.01	0.8	0.7	0.75	None
M-α-OH-3:8	68.28	<1.0			Type 5
O-α-OH-5	82.39	<1.0			None
O-α-OH-3:8	55.10	<1.0			Type 5
A-α-OH-3	90 25	0			None
A-β-OH-6*	62.75	0			None
A-β-OH-6:8*	89.99	0			None
P-α-OH-3	62.52	0			None
P-α-OH-4	62.20	0			None
P-α-OH-5	63.00	0			None
P-α-OH-3:8	96.66	0			None
M-α-OH-5	73.99	0			None
M-β-OH-6:8*	43.41	0			None
O-α-OH-4	93.86	0			None

The types of crystals referred to in the tables are as follows: *Type 1.* These consisted of very thin plates growing in several directions from a central axis. Often there were several of these very thin sheets growing close together and parallel to one another from the central axis, and then there would not be any more for an angle of about 45–60°, when another set of parallel sheets grew outward. The coloration in these crystals was very high and quite uniform throughout. This coloration, however, was produced by adsorption on the (111) and (110) faces only, as shown by a further experiment with the dye M-β-OH-7. When crystals of potassium sulfate were grown from solutions containing only one-fourth the concentration of dye used in the previous experiments, the dye could be seen strongly adsorbed on the above two faces, while the other faces were almost free of color. This adsorption produced small grooves down the edges of the crystals, but aside from this there was no modification of the habit.

Type 2. These also were quite highly and uniformly colored but grew in the form of needles, varying considerably in diameter and often growing in bunches with the needles running parallel to one another or sometimes individually forming a network on the bottom of the beaker. The adsorption in this case occurred mainly on the (110) plane, as shown by crystals of potassium sulfate grown in half the previous concentration of P-β-OH-6. There was also a very small amount of adsorption on the (010) planes. With these crystals the growth perpendicular to the (110) face was apparently decreased enough to make these faces the prominent ones, and thus the long diamond-shaped needles were produced.

TABLE 2

Summary of effect of acid dyes forming a saturated solution with potassium sulfate solution

DYE	PER CENT PURITY	SOLUBILITY	MOLES OF DYE ADSORBED (PER MOLE OF K_2SO_4) $\times 10^5$	MODIFICATION
M-α-OH*.	83.75	Slightly soluble	25	Types 3 and 4
P-α-OH*.	70.00	Nearly soluble	16	Types 3 and 4
M-β-OH-3:6*.	69.57	Slightly soluble	8.1	Type 3
A-α-OH-5.	53.13	Nearly soluble	7.9	Type 2
M-β-OH*.	88.00	Slightly soluble	2.6	Type 5
A-α-OH-4.	79.25	Slightly soluble	1.6	None
O-α-OH-3.	63.98	Nearly soluble	<1.0	None
A-α-OH-3:8.	58.16	Slightly soluble	0	None
A-β-OH*.		Insoluble	0	None
A-β-OH-7*.	83.00	Slightly soluble	0	None
O-α-OH*.	62.75	Slightly soluble	0	None
O-β-OH*.	49.00	Insoluble	0	None

Type 3. These were examples in which there was very pronounced twinning. Practically all of these twins were of the triplet variety, in which there was an incomplete interpenetration of the individuals. The deepest coloration seemed to be in the angles of these "three-rayed stars." The production of these twins is not readily explained, although it is presumably connected with the deposition of the dye. Twins in pure potassium sulfate

TABLE 3

Summary of effect of soluble basic dyes on potassium sulfate

DYE	PER CENT PURITY	MOLES OF DYE ADSORBED (PER MOLE OF K_2SO_4) × 10^5			MODIFICATION
		First determination	Second determination	Average	
M-α-NH$_2$-6*	94.50	83	83	83	Type 1
A-β-NH$_2$-7*	76.13	31	32	31.5	Type 2
P-α-NH$_2$-7*	94.10	24	22	23	Type 1
P-α-NH$_2$-2*	87.26	6.0	7.1	6 6	Very long needles; uneven adsorption
M-α-NH$_2$-2*	89.97	5.7	5.7	5.7	Type 4
O-α-NH$_2$-2*	97.28	3.5	4.1	3.8	Type 4
M-α-NH$_2$-8*	87.47	3.2	3.0	3.1	Type 4
M-β-NH$_2$-7*	71.80	2.8	2.4	2.6	Type 5
M-α-NH$_2$-7*	89.76	1.8	2.3	2.05	Type 4
M-α-NH$_2$-4	89.76	1.8	1.7	1.75	Type 5
A-α-NH$_2$-3	75.40	<1.0			None
A-α-NH$_2$-4	83.55	<1.0			None
P-β-NH$_2$-5*	61.40	<1.0			None
P-β-NH$_2$-6*	87.27	<1.0			None
P-β-NH$_2$-7*	83.56	<1.0			None
M-α-NH$_2$-3	88.64	<1.0			None
M-α-NH$_2$-5	91.06	<1.0			None
O-α-NH$_2$-6*	83.16	<1.0			None

DYE	PER CENT PURITY	MOLES OF DYE ADSORBED × 10^5	MODIFICATION
P-α-NH$_2$-3	71.28	0	None
P-α-NH$_2$-4	80.00	0	None
P-α-NH$_2$-5	91.55	0	None
M-β-NH$_2$-5*	90.58	0	None
M-β-NH$_2$-6*	90.99	0	None
O-α-NH$_2$*	93.12	0	None
O-α-NH$_2$-3	76.48	0	None
O-α-NH$_2$-4	87.37	0	None
O-α-NH$_2$-5	79.00	0	None
O-α-NH$_2$-7*	65.96	0	None
O-α-NH$_2$-8*	82.14	0	None
O-β-NH$_2$-5*	92.25	0	None
O-β-NH$_2$-6*	96.87	0	None
O-β-NH$_2$-7*	69.00	0	None

occur rather frequently on the (110) plane, although in such cases there is usually a complete interpenetration of the individuals.

Type 4. These were almost rectangular crystals, in which the dye was only adsorbed on the (110) planes, producing an hour-glass effect with parts of the crystal colorless and other parts of it colored. In this case the chief modification occurred on the (010) faces, making them the most prominent ones even though the adsorption occurred only on the (110) planes.

TABLE 4

Summary of effect of basic dyes forming a saturated solution with potassium sulfate solution

DYE	PER CENT PURITY	SOLUBILITY	MOLES OF DYE ADSORBED (PER MOLE OF K_2SO_4) $\times 10^5$	MODIFICATION
A-β-NH_2-6*	85.49	Slightly soluble	33	Type 2
P-β-NH_2*	88.83	Slightly soluble	22	Type 1
A-β-NH_2-5*	92.47	Slightly soluble	20	Type 1
P-α-NH_2*	84.59	Slightly soluble	15	Type 4
P-α-NH_2-8*		Nearly soluble	11	Type 1
M-β-NH_2	93.23	Nearly soluble	7.8	Types 1 and 2
P-α-NH_2-6*	90.78	Nearly soluble	7.4	None
A-α-NH_2-5	66.92	Nearly soluble	3.1	Type 5
M-α-NH_2*	96.34	Slightly soluble	1.4	None
A-α-NH_2*		Insoluble	0	None
A-α-NH_2-2*	87.16	Slightly soluble	0	None
A-α-NH_2-6	66.39	Nearly soluble	0	None
A-α-NH_2-7	92.88	Slightly soluble	0	None
A-α-NH_2-8	92.96	Slightly soluble	0	None
A-β-NH_2*		Insoluble	0	None
O-β-NH_2*	80.90	Slightly soluble	0	None

TABLE 5

Summary of adsorption of P-β-OH-6 *by potassium sulfate from solutions of various concentrations*

CONCENTRATION OF DYE MOLES PER 100 CC. $\times 10^4$	MOLES OF DYE ADSORBED (PER MOLE OF K_2SO_4) $\times 10^5$
1	9
2	50
3	108
4	167
5	171
6	174
8	257
10	232
12	273

Type 5. These were crystals that had little if any modification of habit, A striking feature was that they were approximately five to ten times larger than the crystals of potassium sulfate obtained from pure solutions under the same conditions. The small amount of adsorption did not seem to

be concentrated upon any one face, but there was a slight uniform tinge of color throughout.

As an aid in interpreting the data and to account for the fact that the adsorption generally occurred on the (110) and the (111) planes, scale models of both dye molecules (figure 1) and the potassium sulfate crystal were constructed (figure 2). The dimensions of the unit cell as determined by Ogg and Hopwood (13, 14) were used for this purpose. The hydrogen atoms in the dye molecule were assigned the dimensions of the atomic domain of hydrogen as calculated by Mack (12).

The potassium sulfate model (figure 2) clearly showed the (100) planes to be populated by mixtures of K^+ and SO_4^{--} ions, and the (110) and (111) planes to be predominantly K^+ or SO_4^{--} ions. The ionic grouping in the (110) and (111) planes should therefore result in these planes having strong adsorptive forces, and in the absence of interfering factors, such as steric hindrance, one would expect the adsorption to occur on the (111) and (110) planes in preference to the (100) plane. The collected data are in most instances in accord with this prediction.

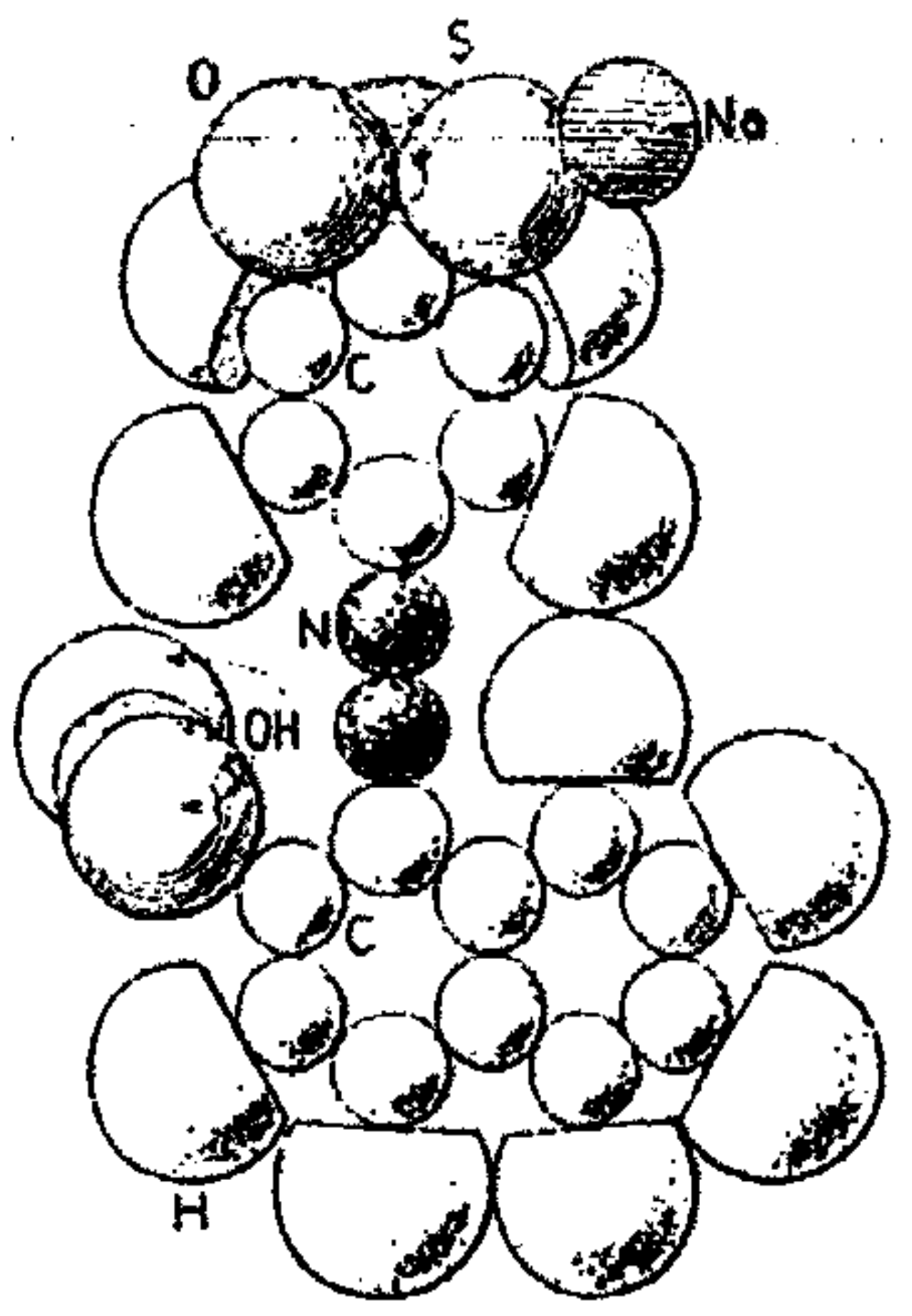

Fig. 1

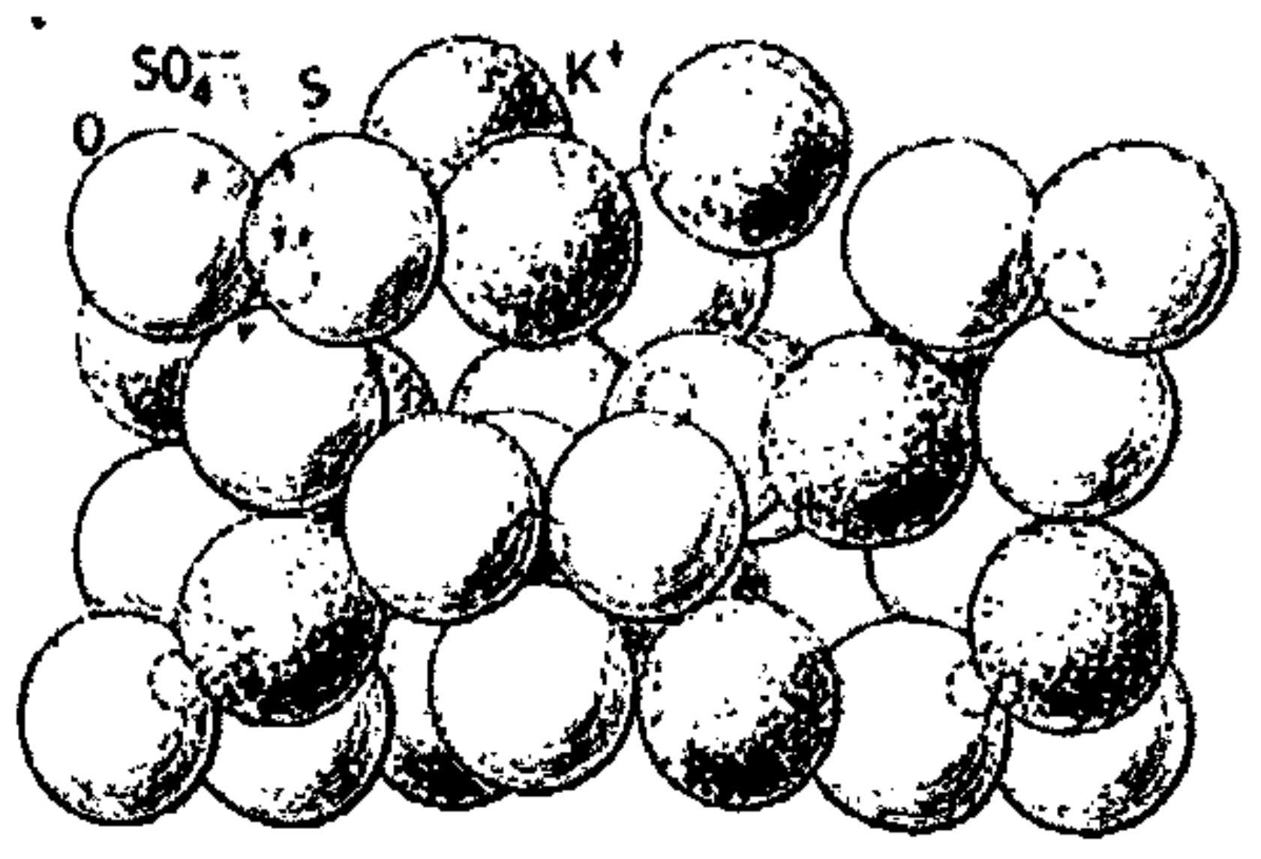

Fig. 2

Fig. 1. Model of dye P-β-OH
Fig. 2. Model of potassium sulfate. Side elevation (100) plane

The mode of attachment of the dye molecule is probably through the oxygen triangle possessed by the —SO_3Na group of the dye, as previously suggested by Buckley (2). The dyes ionize in solution giving a sodium ion and a large anion possessing a number of charges equal to the number of substituent —SO_3Na groups. The dye anion, therefore, has three oxygen atoms in an equilateral triangle attached to a sulfur atom exactly as in an SO_4^{--} ion, with the rest of the large dye molecule attached in place of the fourth oxygen. The —SO_3 group of the anion could, therefore, be drawn into the place ordinarily occupied by the SO_4^{--} ion, with the remainder of the large dye molecule left to obstruct further crystal growth.

A study of the tables brings out a number of interesting facts. For example, the presence of a benzene ring with no substituent groups appears to be detrimental. Also the presence of the $—SO_3Na$ group adjacent to the —N═N— group renders the dye less effective. This may be explained on the basis of steric hindrance. By means of the molecular dye models it was clearly evident that whenever the $—SO_3Na$ group is adjacent to the —N═N— group it is so protected by nearby hydrogen atoms that it cannot present the oxygen triangle to any given plane of the crystal even though the dye molecules are not linear. There are also some structural hindrances when the $—SO_3Na$ group is in the 1-, 4-, 5-, or 8-position in the naphthalene ring. Dyes containing the $—SO_3Na$ groups at these positions, therefore, would likewise not be very effective. This leaves only the meta and para positions in the benzene rings and the 6- and 7-positions in the naphthalene rings. The data in the tables bear out the conclusion that these would normally be the most effective positions for the $—SO_3Na$ groups.

A combined study of the tables of data and the formulas of the dyes reveals the fact that in general the dyes produced from the β-naphtholsulfonic acids are much more effective than those produced from the α-naphtholsulfonic acids. If $—NH_2$ groups are substituted for the —OH groups, however, the situation is exactly reversed. In this case the dyes formed from the α-naphthylaminesulfonic acids are much more effective than those formed from the β-naphthylaminesulfonic acids. This suggests that the dipole moment of the foreign molecule must be considered in the adsorption process. Thus, if attention for the moment is confined to the dyes which are starred in the tables (those possessing the

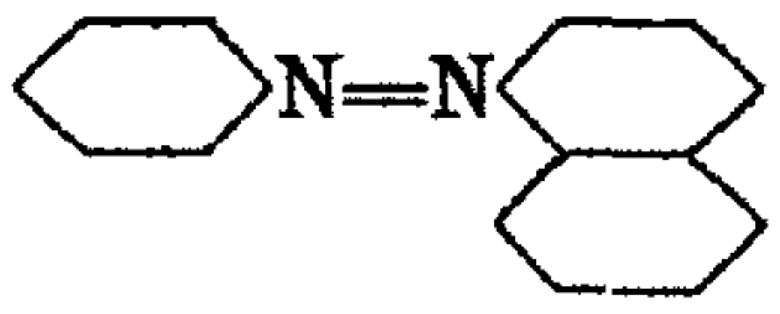

basic structure), the above facts simply mean that the most effective position for the —OH group is ortho to the —N═N— group, while the most effective position for the $—NH_2$ group is the para or 4-position in the naphthalene ring. Williams (17) gives -1.5 Debye units as the dipole moment of the —OH group and $+1.7$ Debye units for the dipole moment of the $—NH_2$ group. Therefore, assuming that the other groups remain in the same positions, the dipole moments of the dye molecules would be more nearly the same if the —OH group were ortho and the $—NH_2$ group para to the —N═N— group. This then suggests a plausible reason for the differences pointed out above.

The results of the quantitative measurements of the amount of adsorption of P-β-OH-6 at a number of concentrations is graphically shown in figure 3. The results are obviously in complete agreement with previous work (1, 3, 5, 6, 7, 8, 10, 11, 15, 16), in that there is a minimum concentration below which no adsorption takes place and above which the adsorption gives a typical adsorption curve. The adsorption can, therefore, be represented by the expression developed earlier (3):

$$a = kc^{1/n} - k'c^{-1/n'}$$

In other qualitative experiments it was shown that none of the dyes was adsorbed by potassium alum and none of the acid dyes by ammonium alum. The basic dyes were not investigated with the latter salt. Hydrochloric acid was found to increase the amount of adsorption of the dye P-β-OH-6 by potassium sulfate, and sodium hydroxide decreased the amount.

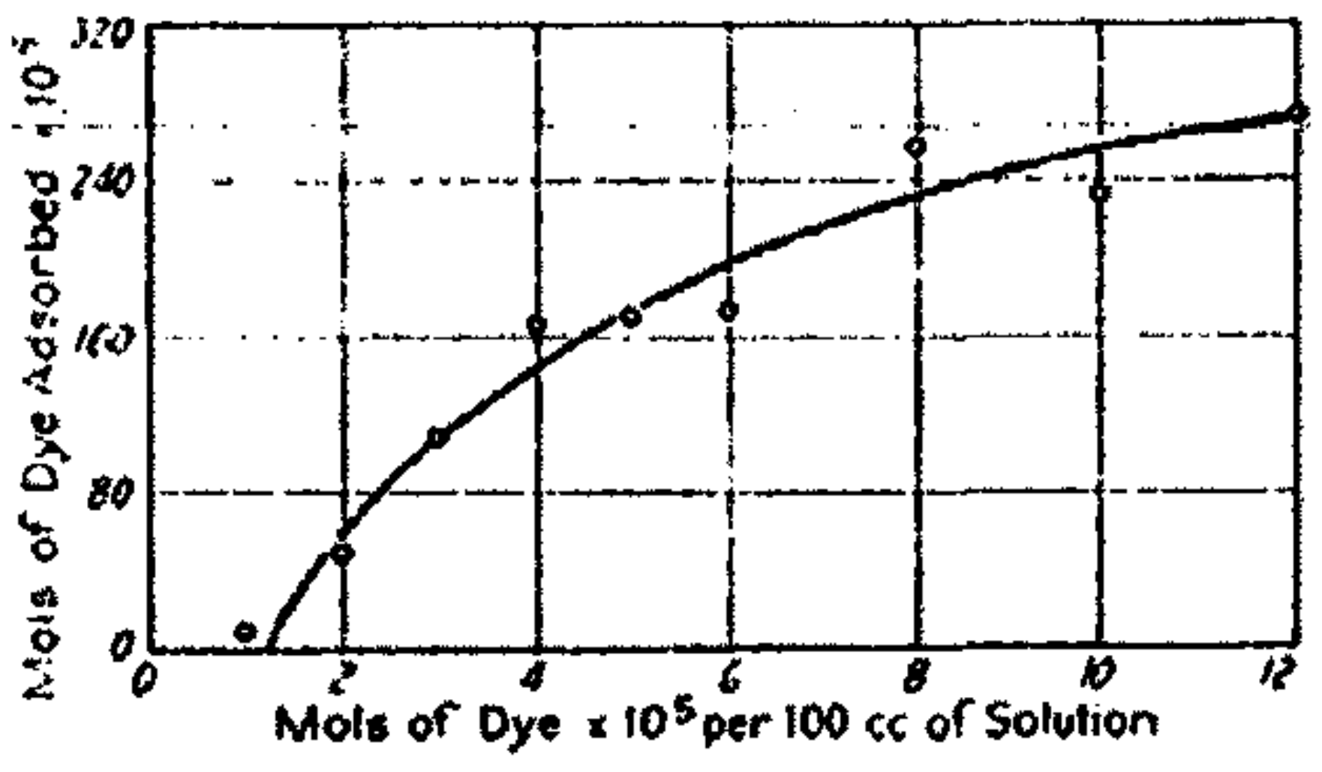

FIG. 3. Adsorption of P-β-OH-6

SUMMARY

1. The results obtained in this investigation have been found to be in harmony with the theory that adsorption by a growing crystal is dependent on (*1*) the residual valency force fields of the crystal faces, (*2*) the interionic distances within the faces, (*3*) the concentration of the foreign substance in the solution, and (*4*) the presence and distribution of polar groups in the foreign molecules. However, it may be only necessary for one of the substituent groups to fit into the ionic planes of the faces.

2. Adsorption of foreign substances is highly specific, with only a few crystalline substances adsorbing a given series of dyes.

3. Adsorption of foreign substances usually produces a habit modification, although the modification may be on faces other than those upon which the dye is adsorbed.

4. Twinning in crystals can be made very much more pronounced by the adsorption of some foreign substances. This suggests the possibility that twinning in general may be caused by the adsorption of a very minute amount of impurity at some favorable point during the growth of the crystal.

5. The mode of attachment of these monoazo dyes to crystals of potassium sulfate may be through the oxygen triangle of the —SO_3Na groups.

6. Dyes with the

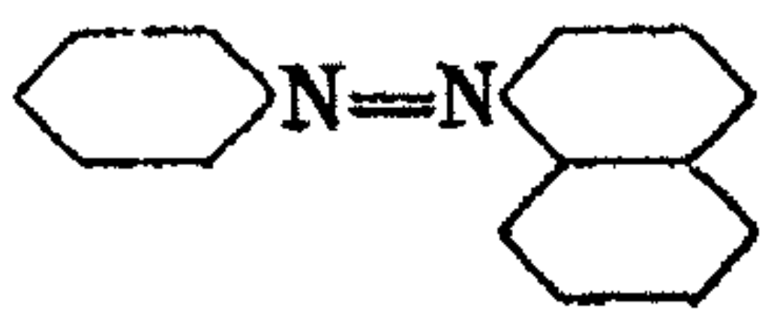

basic formula are much more strongly adsorbed than those possessing the

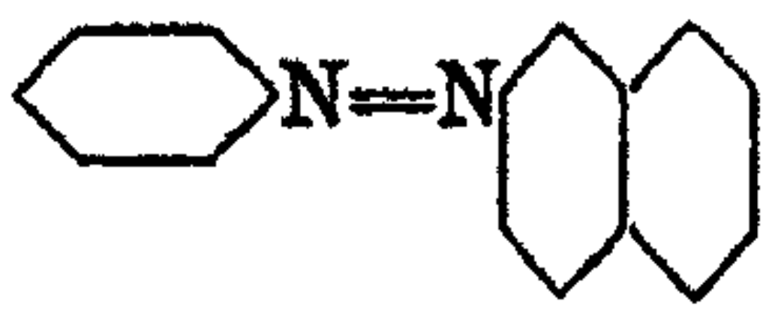

basic formula.

7. An "empty" benzene ring is detrimental to adsorption, as is a —SO_3Na group adjacent to the —N=N— group. The most active positions for the —SO_3Na groups are meta and para to the —N=N— group in the benzene ring and in the 6- and 7- positions in the naphthalene ring.

8. The change of an —OH group to an —NH_2 group has a profound effect on the adsorption in a manner which indicates that the dipole moment of the molecule is concerned.

9. The adsorption of the dye P-β-OH-6 followed the expression:

$$a = kc^{1/n} - k'c^{-1/n'}$$

The authors wish to take this opportunity to acknowledge their indebtedness to Dr. Wallace R. Brode and his former students, Dr. Marion E. Griffith and Dr. Dale R. Eberhart. All of the dyes used in this investigation were prepared by them, and they very generously supplied the samples which made this investigation possible. The purities of the dye given in the tables were also determined by them.

REFERENCES

(1) Bennett and France: J. Am. Ceram. Soc. **11**, 571 (1928).
(2) Buckley: Z. Krist. **85**, 58 (1933); **88**, 381 (1934).
(3) Davis and France: J. Phys. Chem. **40**, 81 (1936).
(4) Eberhart: Dissertation, The Ohio State University, 1935.
(5) Eckert and France: J. Am. Ceram. Soc. **10**, 579 (1927).
(6) Foote, Blake, and France: J. Phys. Chem. **34**, 2236 (1930).
(7) France: Colloid Symposium Monograph **3**, 317 (1925); **7**, 59 (1930).
(8) France and McBurney: J. Am. Chem. Soc. **46**, 540 (1924).
(9) Griffith: Dissertation, The Ohio State University, 1934.
(10) Keenen and France: J. Am. Ceram. Soc. **10**, 821 (1927).
(11) Lash and France: J. Phys. Chem. **34**, 724 (1930).
(12) Mack: J. Am. Chem. Soc. **54**, 2141 (1932).
(13) Ogg: Phil. Mag. **5**, 354 (1928); **9**, 665 (1930).
(14) Ogg and Hopwood: Phil. Mag. **32**, 518 (1916).
(15) Paine and France: J. Phys. Chem. **39**, 425 (1935).
(16) Weinland and France: J. Phys. Chem. **36**, 2832 (1932).
(17) Williams: J. Am. Chem. Soc. **52**, 2352 (1928).

EXPANSION PATTERNS OF PROTEIN MONOLAYERS ON WATER[1]

VINCENT J. SCHAEFER

Research Laboratory, General Electric Company, Schenectady, New York

Received July 14, 1938

When a monolayer of a protein is formed on a water surface, it exists as a homogeneous, insoluble, reversibly compressible (8, 6), two-dimensional structure with certain properties characteristic of the specific proteins.

Protein monolayers can be formed by a number of methods: for example, from a small amount of dried protein placed on the water surface (5), from a small amount of dissolved protein ejected from a micropipet inserted parallel and half submerged in the water surface (4), from drops of a solution placed on a flat plate dipped into the water, by dissolving the protein in the bulk substrate followed by subsequent stirring, or by spreading the protein on a strong salt solution followed by removal to another tray (7). As has been shown by many investigators, a protein spreads best at or near its isoelectric point.

Protein monolayers spread and deposited under low pressures show thicknesses ranging from 6 Å. to 18 Å., depending on the specific protein used. This paper will describe a very simple technique for rendering such films visible and will indicate the possibilities available for following changes in molecular structure, orientation, and other characteristics which are related to the fundamental properties of the native protein.

The apparatus required for studying expansion patterns is exceedingly simple. A shallow tray with flat edges, several barriers for cleaning the water surface, suitable illumination, and a few drops of indicator oil comprise the total necessary equipment.

Our trays are made of ½-in. angle brass fastened to a $\frac{1}{16}$-in. flat sheet of the same material, the joints being water-proofed and the inside covered with black Bakelite paint. A mixture of carbon black and paraffin applied hot will serve satisfactorily. The black background which emphasizes the contrasting intensities may also be obtained by using a sheet of cobalt glass or Bakelite in the bottom of the tray or by coating the outside of a glass tray with black paint.

---

[1] Presented at the Fifteenth Colloid Symposium, held at Cambridge, Massachusetts, June 9-11, 1938.

Dr. K. B. Blodgett has previously described the preparation of indicator oil (2). Automobile oil oxidized by prolonged heating is mixed with pure mineral oil. When placed on clean water this mixture spreads to form thin films of a definite thickness, depending on the amount of the oxidized material added. For observing expansion patterns a mixture which produces a thickness of about 1500 Å. and a first-order yellow film when viewed at 45° has proved to be very satisfactory.

Several lamps placed behind a sheet of opal glass (milk glass) provide a very fine source of diffuse illumination for viewing the patterns. Daylight interspersed by a sheet of translucent paper also works quite well.

FORMATION OF AN EXPANSION PATTERN

In order to illustrate what is meant by the expansion pattern of a protein, let us use a sample of pepsin. The important steps are illustrated in figure 1. Distilled water at equilibrium with the air at pH 5.8 is placed in the tray. The surface is cleaned by sweeping several times with barriers, and enough indicator oil is applied to cover three-quarters of the clean surface. A cleaned platinum wire transfers a small amount of pepsin in the form of powder to the center of the surface area. It spreads on the water, forming an invisible film whose advancing border will be seen as it drives the indicator oil ahead of it in radial directions. In the case of pepsin, this advancing film will be seen to present a smooth rounded concentric edge, of a radius equal to the distance from the point of application. The outline of the advancing boundary of the monolayer is often characteristic of specific proteins and will be referred to from time to time. Care should be observed that only enough protein is applied so that the remaining free surface is nearly covered with a monolayer.

After the monolayer is spread, barriers are used to push the surrounding indicator oil into intimate contact with the outer edge of the monolayer, care being taken that the monolayer is not subjected to any degree of pressure. This is controlled by stopping compression before any change in color of the indicator oil occurs. A perceptible change in color equals a pressure of $F = 1$ dyne per centimeter. After intimate contact is reached with the oil and the monolayer, a small drop of indicator oil is placed in the central portion, and will in the case of pepsin expand to produce a geometrical figure of a star-like form, with the indicator oil showing a peculiar gradation in color intensity, appearing thinner than normal at the monolayer boundary. If other portions of the monolayer are treated in a similar way, patterns identical in every respect will be observed, indicating that the film possesses a structure which is uniform throughout, showing no memory of the point of formation.

Because of their high compressibility, many proteins, if permitted, will spread on the water to build up pressures of more than 10 dynes per centimeter. Most proteins exhibit varied changes in expansion pattern as the surface pressure is increased. Egg albumin, for example, when subjected to a compression of 35 dynes in one direction will show a fibrous structure when expanded by a high-pressure indicator oil, while still under pressure, with the fibrous sheets oriented parallel to each other at right angles to the direction of compression. Such sheets may be lifted from the water surface as threads and when dried are nearly invisible.

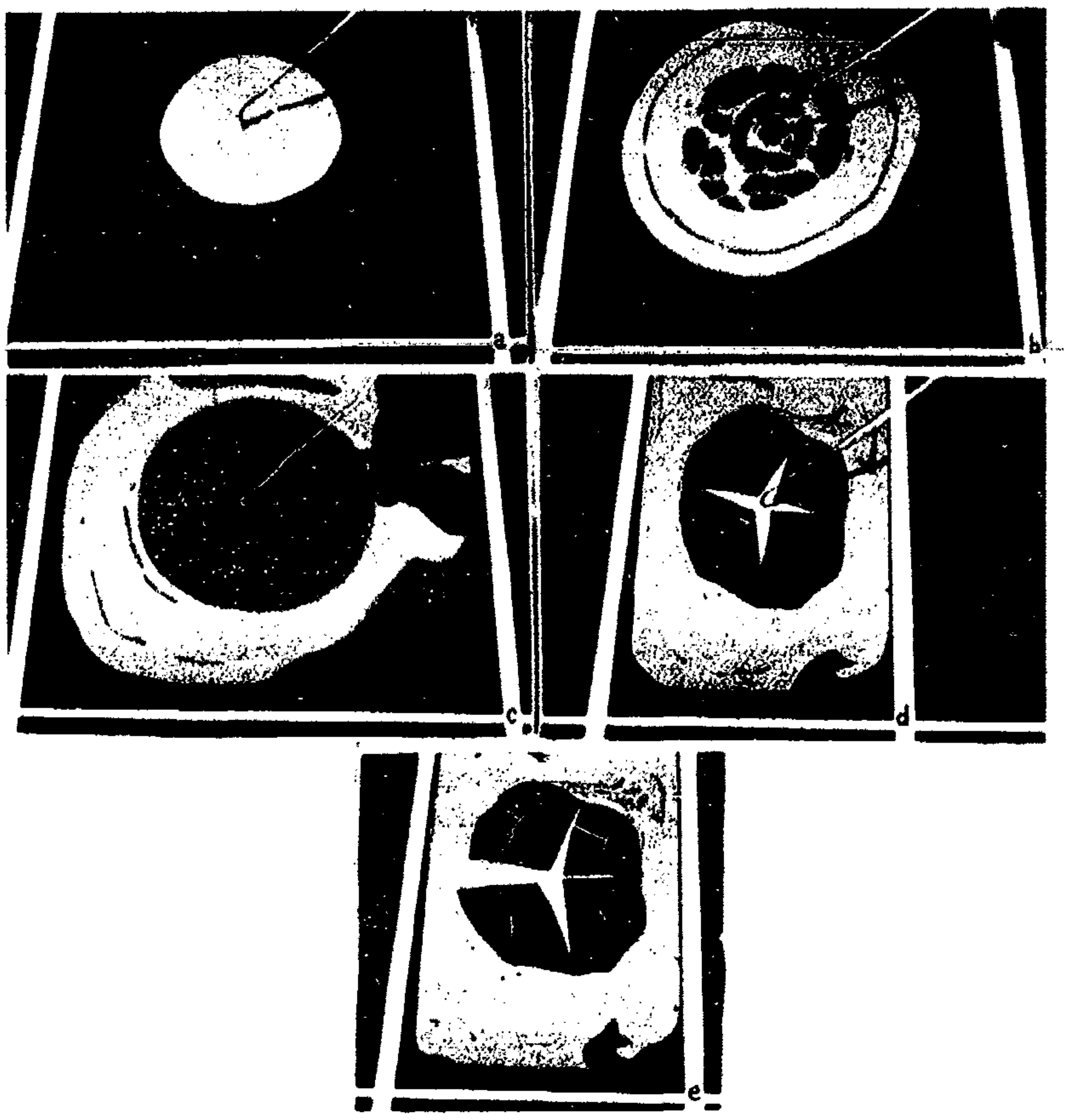

Fig. 1. Formation of expansion patterns. a, applying indicator oil; b, indicator oil spreading; c, applying protein monolayer; d, expanding monolayer; e, pepsin expansion pattern.

CLASSIFICATION OF EXPANSION PATTERNS

Expansion patterns of the proteins studied may be roughly divided into three general groupings of geometrical configuration. The terms "star-like," "rough circular," and "smooth circular" will serve to describe these three classes.

"Star-like" refers to patterns which expand at low pressure to produce figures related in configuration to a star. Although five-pointed stars are often formed, the number of points observed varies from three to six. Typical examples of these figures may be found with pepsinogen, tobacco seed globulin, and trypsinogen, illustrated in figure 2. In certain cases, particularly with pepsin and trypsinogen, the star form produced by the expansion of the indicator oil is further modified by a peculiar gradation in the color of the indicator oil, producing a thinning out of the oil film which under normal conditions is exceptionally uniform. The protein monolayers which produce expansion patterns of the star-like form are, in general, of the type described by Hughes and Rideal as a gel structure. It should be noted here, however, that the gel-like monolayers considered in this paper are formed spontaneously at very low pressures of the order of 0.5 to 1.0 dyne per centimeter and in general are found to be characteristic of the specific protein, regardless of the spreading method used. That higher pressure often produces a film of the gel type from a liquid monolayer may be observed if gliadin acetate is compressed to 15 dynes per centimeter. Under this compression this protein, which is very liquid under low pressure, shows a typical star-like expansion pattern.

While about half of the proteins studied show the general star-like expansion pattern, each one has its own modification of the general form. Aside from the question of pH and relation to the isoelectric point, there are other characteristics peculiar to the specific protein. Thus the advancing edge of the monolayer in the case of pepsin is smoothly circular, while with egg albumin it is very irregular, with the indicator oil forming peculiar wedge-like structures which divert the advancing edge of the monolayer to either side to produce the irregularity mentioned.

In the rough circular classification trypsin, papain, and wheat gliadin may be used as examples (figure 3). This form is characterized by an expansion pattern whose general form is circular, but when examined locally the edge exhibits a roughened appearance, the extent of irregularity being characteristic of the specific protein used. Thus trypsin produces a circular advancing edge but an internal slightly ragged outline, with the peculiar grading in indicator oil color observed with pepsin and trypsinogen. With wheat gliadin, on the other hand, both external and internal patterns are identical, the outline being very jagged.

The smooth circular form is characteristic of such proteins as zein, gelatin, and protamine (figure 4), and of films formed by proteins in an advanced stage of denaturation or by protein degradation products which still form monolayers.

EFFECT OF DENATURATION ON EXPANSION PATTERNS

Many investigators (1, 3, 9, 10) have shown that protein solutions, when subjected to treatment such as heating, ultraviolet radiation, and

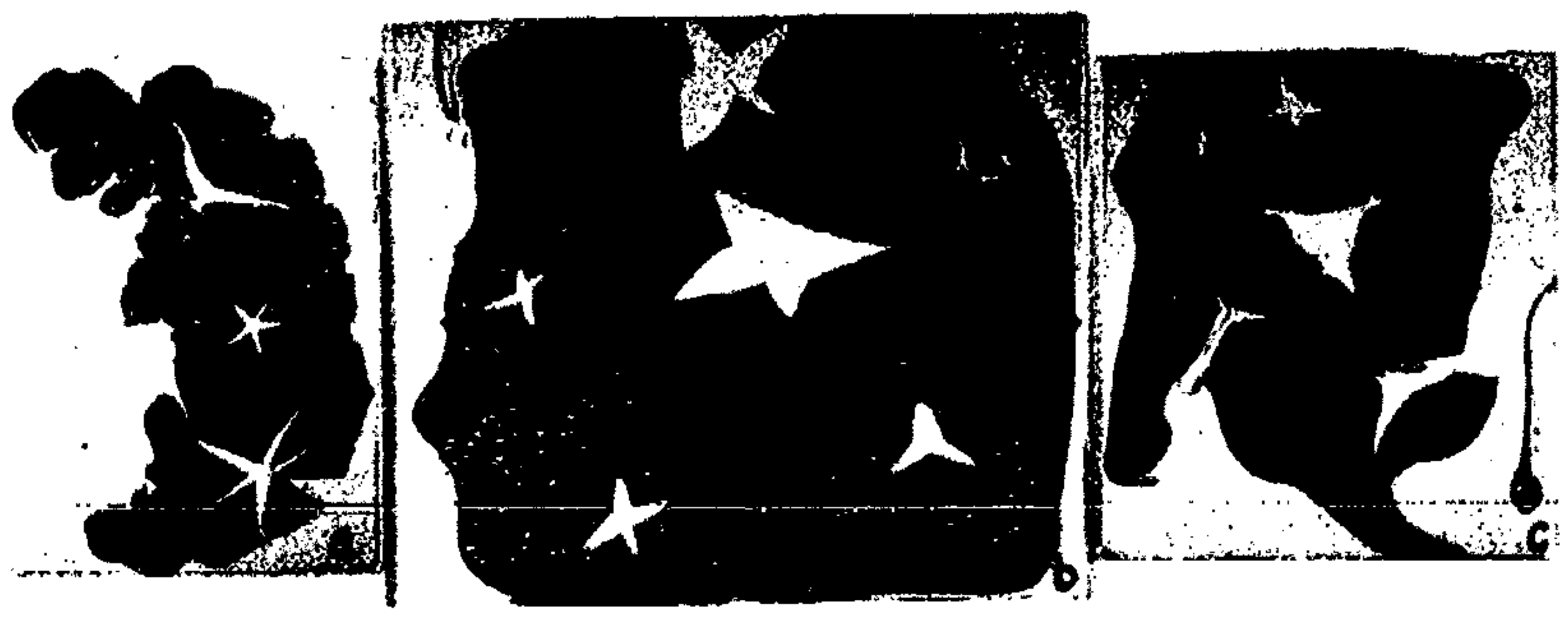

FIG. 2. Star-like expansion. a, pepsinogen; b, tobacco seed globulin; c, trypsinogen

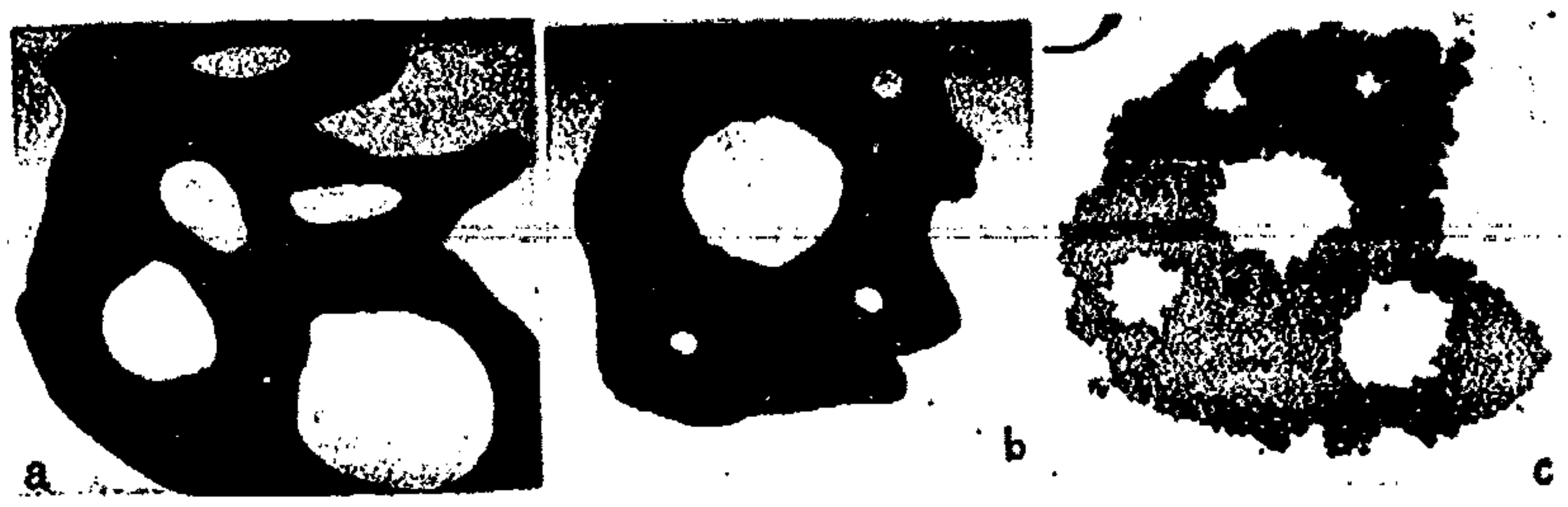

FIG. 3. Rough circular expansion. a, trypsin; b, papain; c, wheat gliadin

FIG. 4. Smooth circular expansion. a, gelatin; b, zein; c, protamine

FIG. 5. Effect of heat denaturation of pepsin. a, 2 min. at 65°C.; b, 5 min. at 65°C.; c, 7 min. at 65°C.; d, 25 min. at 65°C.

shaking, tend to alter the protein in such a way as to modify its native properties. In the case of pepsin this modification generally parallels loss in activity of its enzymatic properties. When 0.1 per cent solutions of pepsin are subjected to such denaturation processes, the loss of activity is strikingly demonstrated by the change in expansion pattern. In the case of pepsin the star-like pattern gives way to a circular form, the pattern showing a rapid transition, the first changes appearing before the loss of activity becomes readily detectable by the change in the power of pepsin to clot milk (6).

When a 0.1 per cent solution of pepsin (Lilly), held in a quartz tube 15 cm. from an ultraviolet lamp of 1.2 amperes and 145 volts, emitting wavelengths of 2536 Å. and up, was irradiated for 5 min., no change in activity or expansion pattern was found. When irradiated for 10 min., the pattern was completely changed, while the protein had lost but 4 per cent of its original activity. The pattern had become entirely circular after 15 min. with 25 per cent loss in activity, although the area which a given amount of protein covered remained about the same. After 30 min. of irradiation, the activity showed a 68 per cent loss, and now the actual area covered had decreased to less than half of that covered by the same amount of solution irradiated for 15 min.

The alteration in expansion pattern when a solution of pepsin is subjected to a vigorous shaking will now be considered. One hundred cubic centimeters of a 0.1 per cent pepsin solution in a half-liter bottle was placed in a machine which produces 400 movements a minute, the distance of travel for each stroke being 5 cm. Samples of the solution were withdrawn at definite time intervals, and the same amount of solution used for producing a monolayer on water.

The transition in expansion pattern showed a considerable change after only 1 min. of shaking, the alteration in pattern again shifting from the star-like to the circular form, as with the deactivation by ultraviolet irradiation. The ability of the pepsin to clot milk after 1 min. of shaking had decreased by more than 60 per cent. After 5 min. of shaking, the area of film produced showed about a 50 per cent decrease with the activity decreased by 83 per cent. After 10 min. of shaking the area of film had decreased still more, with the activity decreased by 88 per cent with no further change in expansion pattern.

When a solution of pepsin at pH 5.8 is subjected to an elevated temperature, it rapidly loses its enzymatic properties, which again is indicated by the change in pattern. A 0.1 per cent solution of pepsin was heated at 65°C. for definite periods of time; then it was chilled to room temperature and the expansion patterns observed. Heating for 2 min. failed to produce any apparent change in pattern, and activity measurements showed the pepsin retained its full power to clot milk. When heated for 3 min., however, the pattern indicated a slight change, and the milk-clotting test showed a 16 per cent decrease in activity. After 5 min. the activity had decreased 28 per cent, and the pattern changed to a very broad star form. After 10 min. the pattern was an irregular figure approaching a circle with a decrease in activity of 38 per cent; after 25 min. the pattern was a perfectly smooth circle, and the pepsin then showed a loss in activity of 62 per cent. The alterations in pattern and area due to the various types of denaturation are shown in figures 5 and 6.

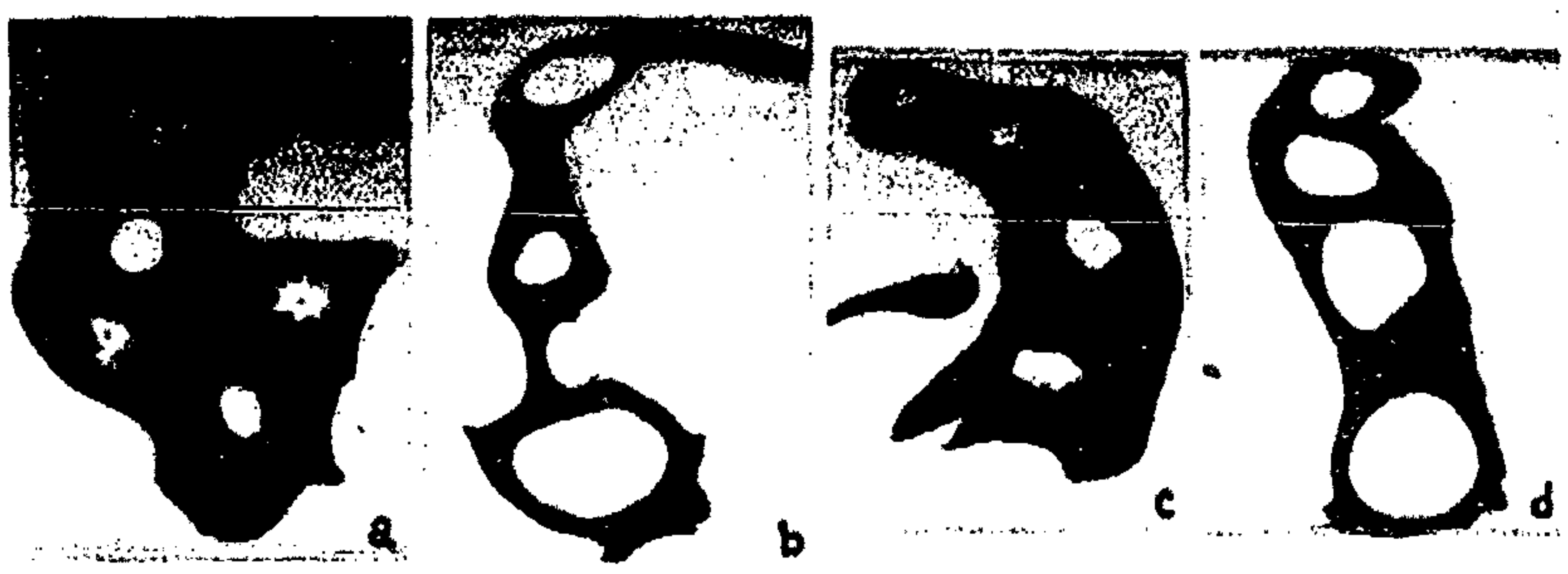

FIG. 6. Pepsin denaturation. a, irradiated with ultraviolet light for 10 min.; b, irradiated with ultraviolet light for 30 min.; c, shaken for 1 min.; d, shaken for 10 min.

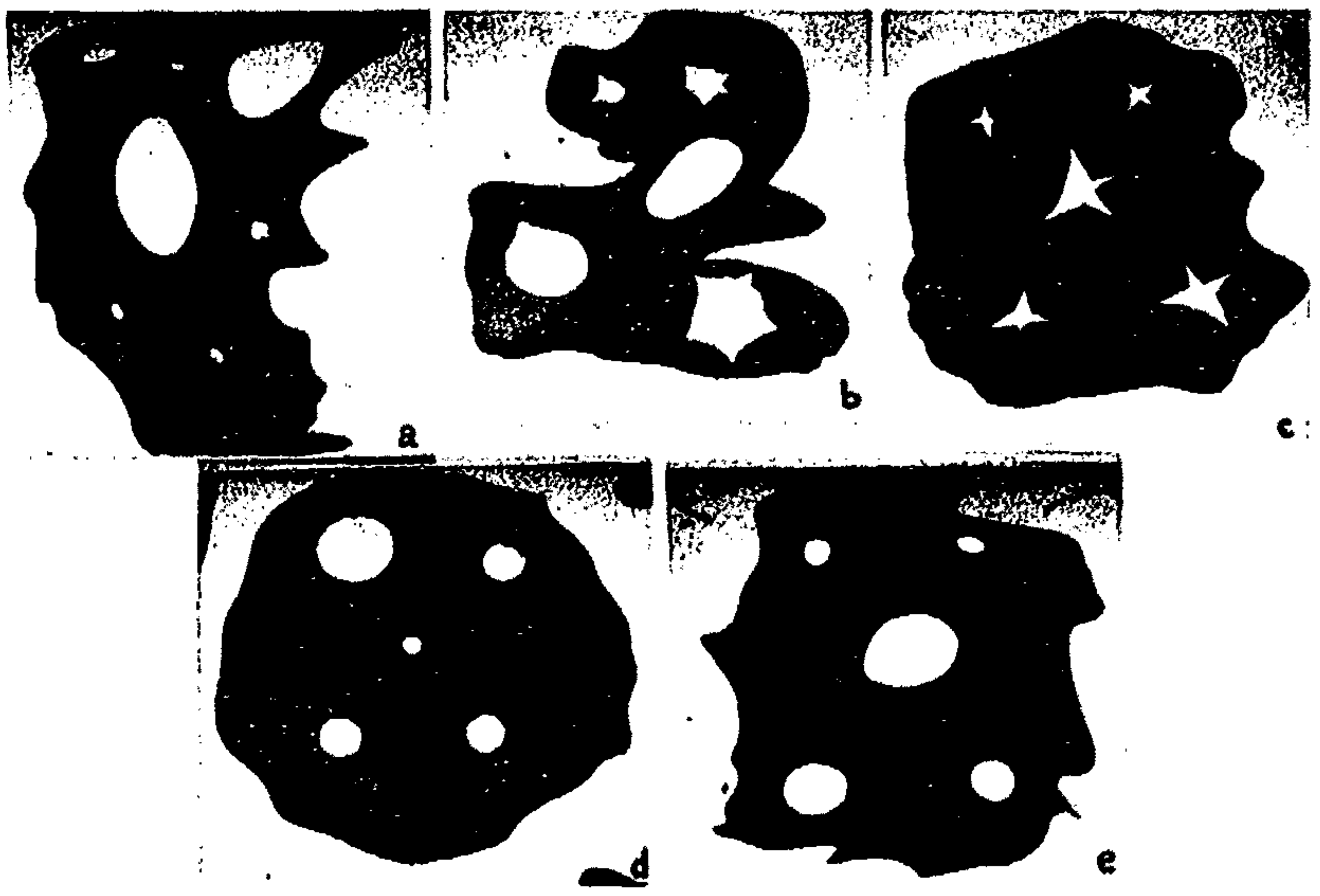

FIG. 7. Effect of dissolved salts on expansion patterns. a, insulin; b, insulin + 10^{-4} *M* zinc chloride; c, insulin + 10^{-4} *M* cupric chloride; d, gliadin acetate; e, gliadin acetate + 10^{-4} *M* cupric chloride.

Gorter (3) has shown that the addition of a very small amount of pepsin to solutions of proteins greatly increases their tendency to form monolayers. When a solution of egg albumin containing 10 mg. of the protein, partly coagulated by heating, was inoculated with 0.01 mg. of pepsin and the pH of the solution held at 4.6, the monolayer formed from a given amount of protein covered seven times the area of the control. The expansion pattern was of the smooth circular type, and gradually reverted to the star-like form as the film remained on the water. When the same procedure was followed with the pH of the inoculated solution held at 2.0, the area covered twice that of the control, showing a smooth circular expansion pattern which remained unchanged with time.

TABLE 1

General classification of expansion patterns

PROTEIN	PATTERN FORM AT F = 0.5 TO 1.0 DYNE PER CENTIMETER		
	Star-like	Rough circular	Smooth circular
Egg albumin	x		
Pepsin	x		
Pepsinogen	x		
Trypsin		x	
Trypsinogen	x		
Urease	x		
Edestin	x		
Tobacco seed globulin	x		
Tobacco mosaic virus*	x		
Wheat gliadin		x	
Gliadin acetate			x
Zein			x
Papain		x	
Casein			x
Protamine			x
Insulin			x
Protamine-insulin			x
Gelatin			x

* Formed on saturated ammonium sulfate solution.

EFFECT OF DISSOLVED SALTS ON EXPANSION PATTERNS

The expansion pattern of pure insulin when spread on distilled water at pH 5.8 was found to be circular in form. When a 10^{-4} molar solution of cupric chloride was added to the water, the expansion pattern of insulin spread in the same manner showed a major change, exhibiting the star-like pattern somewhat similar to pepsin. With the same concentration of zinc chloride a different form was found, showing much less molecular cohesion than was exhibited by insulin spread on water containing cupric ion.

In order to determine whether cupric ion might cause the same alteration in pattern with other proteins, gliadin acetate was spread on the cupric chloride solution which produced the striking change in the insulin pattern. No alteration in the normal circular pattern of gliadin acetate could be found. It would thus appear that the insulin molecule has reactive groups which readily combine in a specific manner with certain divalent ions to produce a definite change in the monolayer. These effects are shown in figure 7.

TABLE 2

Expansion patterns of proteins

PROTEIN	PATTERN FORM AT F = 0.5 TO 1.0 DYNE PER CENTIMETER		
	Star-like	Rough circular	Smooth circular
Pepsin	x		
Pepsin denatured by ultraviolet irradiation			x
Pepsin denatured by heat			x
Pepsin denatured by shaking			x
Insulin			x
Insulin + 10^{-4} *M* copper chloride	x		
Insulin + 10^{-4} *M* zinc chloride	x		
Gliadin acetate			x
Gliadin acetate + 10^{-4} *M* copper chloride			x
Wheat gliadin		x	
Wheat gliadin + 0.01 *N* acetic acid			x
Wheat gliadin + 0.01 *N* hydrochloric acid			x
Wheat gliadin + 0.01 *N* ammonium hydroxide		x	
Egg albumin	x		
Egg albumin + 0.01 *N* hydrochloric acid	x		
Egg albumin + 0.01 *N* ammonium hydroxide	x		

EFFECT OF pH ON EXPANSION PATTERN

Wheat gliadin spread in dry form on distilled water at pH 5.8 exhibited an expansion pattern of jagged outline, both internally and externally, and was very different from gliadin acetate, which produced a circular pattern in both respects. When the gliadin was spread on 0.01 *N* acetic acid (pH 3.4), the pattern was identical with that of the gliadin acetate. Since 0.01 *N* hydrochloric acid (pH 2.0) also produces a circular pattern, it is quite probable that the pH is a factor in producing the change in pattern. It should be noted, however, that a change in pH does not have the same result with a protein such as egg albumin, which retains its star-like pattern at pH 5.8, 3.4, 2.0, and 10.6 with only slight modifications. When the gliadin was spread on 0.01 *N* ammonium hydroxide (pH 10.6), it had a pattern nearly the same as that found at pH 5.8. Wheat gliadin dissolved in 70 per cent ethyl alcohol produced a monolayer identical with that of gliadin acetate in its pattern.

Table 1 is a general classification of observed expansion patterns of proteins spread on the cleaned surface of distilled water at pH 5.8. While it is realized that proteins spread best at or near their isoelectric points, it is significant that no change in the observed patterns could be found when special buffered solutions were used at the isoelectric points of specific proteins. The only difference was the greater area of monolayer formed for a given amount of protein when spread at the isoelectric point. This observation is due probably to the fact that the pH 5.8 is not very far from the isoelectric point of most of the proteins used.

Table 2 records a number of alterations in the expansion patterns of specific proteins by changes in the composition of the substrate solution or by alterations in the protein before spreading.

REFERENCES

(1) ANSON, M. L., AND MIRSKY, A. E.: J. Gen. Physiol. **13**, 121 (1930).
(2) BLODGETT, K. B.: J. Optical Soc. Am. **24**, 313 (1934).
(3) GORTER, E. K.: Trans. Faraday Soc. **33**, 1125 (1937).
(4) GORTER, E. K., AND GRENDEL, F.: Trans. Faraday Soc. **22**, 477 (1926).
(5) HUGHES, A. H., AND RIDEAL, E.: Proc. Roy. Soc. (London) **A137**, 62 (1932).
(6) LANGMUIR, I., AND SCHAEFER, V. J.: J. Am. Chem. Soc. **60**, 1351 (1938).
(7) LANGMUIR, I., AND SCHAEFER, V. J.: J. Am. Chem. Soc., to be published.
(8) LANGMUIR, I., SCHAEFER, V. J., AND WRINCH, D.: Science **85**, 76 (1937).
(9) NEURATH, H.: J. Phys. Chem. **40**, 361 (1936).
(10) PHILLIPI: On the Nature of Proteins; Thesis, Amsterdam, 1936.

THE SOLUTION OF INSOLUBLE DYES IN AQUEOUS DETERGENTS[1]

JAMES W. McBAIN AND TS-MING WOO[2]

Department of Chemistry, Stanford University, California

35-187

Received July 1, 1938

Our investigations have previously established that many colloidal solutions form spontaneously from their constituents, and that they are thermodynamically stable (9), like ordinary solutions, entering into true reversible equilibria both within the solution and in respect to other phases in contact with them.

We showed that, in the presence of stable colloid, other unstable or insoluble substances could likewise dissolve to form thermodynamically stable colloidal systems, comprising true reversible equilibria, the properties of the solutions being independent of previous history and determined solely by composition, temperature, and pressure (10, 11).

The present communication extends these observations to solutions of a water-insoluble dye, Yellow AB (benzeneazo-β-naphthylamine), in numerous detergents and mixtures thereof, in an homologous series of pure soaps, and in a pure hydrogen soap. All experiments are at 25.0°C., unless otherwise stated.

COLLOID STABILIZATION

The phenomenon described is that an aqueous detergent solution will take up a definite amount of dye, either from the solid dye itself or from a solution of the dye in an immiscible non-aqueous solvent, setting up a definite equilibrium, losing a portion of its dye to any less saturated non-aqueous solvent, and taking up more from a more nearly saturated non-aqueous solution. The chief non-aqueous solvents used were toluene and benzene. Freezing point measurements show that the dye exists as simple molecules in the benzene solution (molecular weight: theoretical value, 247; value found, 245). A detergent solution, which is originally clear in the ultramicroscope, on taking up dye is still clear in the microscope, but is full of particles visible in the ultramicroscope. In extremely dilute (a few ten-thousandths normal) solutions of a hydrogen soap, laurylsulfonic

---

[1] Presented at the Fifteenth Colloid Symposium, held at Cambridge, Massachusetts, June 9-11, 1938.

[2] Lever Brothers Company Soap Fellow.

acid, a small per cent of the particles are so large that they may be centrifuged out in a Swedish "angle" centrifuge. They pass through filter paper. Less dilute solutions are clear and transparent. They are still full of smaller particles, as shown by the ultramicroscope, but none can be centrifuged out. Interesting parallels are found in some of the observations of von Kúthy and Banga (6).

The dye is brought into aqueous solution by spontaneous colloid stabilization. Its amount increases with increasing concentration of the detergent or stabilizing colloid. However, it is a remarkable and distinctive fact that a given weight of detergent takes up more dye when it is most diluted. Thus, so far as our studies have gone, the protective solvent power of a definite amount of a stabilizing colloid is increased by addition of the non-solvent water. This distinguishes the formation of stabilized colloid from the typical cases of Neuberg's "hydrotropy" or increased solubility in water (3, 4, 6, 8, 13, 17), occurring in general without the presence or formation of any colloid.

Again the phenomenon of colloid stabilization is different from "protective action" or "peptization" of preëxisting particles in suspensions or gels.

THE FORMATION OF STABILIZED COLLOID DYE IN AQUEOUS LAURYLSULFONIC ACID

The especially pure laurylsulfonic acid, $C_{12}H_{25}SO_3H$, was prepared by Dr. Marie Louise Koenig by the method of Noller and Gordon (14).

The spontaneous colloid stabilization of Yellow AB in aqueous solutions of laurylsulfonic acid was determined in two series of experiments. In the first series a small weighed amount of solid dye was shaken with the aqueous detergent. The undissolved dye was filtered off in a Jena No. 4 sintered-glass Gooch crucible and the excess of undissolved dye weighed after washing and drying at 60°C. The filtrate was likewise analyzed by repeated extraction with purified benzene, from which the dissolved dye was recovered by evaporation, and weighed. The two analyses agreed.

A second series was carried out because of our fear lest some very fine particles of solid dye had passed through the filter. Solid dye was completely eliminated by the device of using only the solution in toluene. To 100 cc. of a saturated solution of the dye in toluene 10 cc. of toluene was added to obviate the possibility of solid dye separating. The aqueous solution was then exposed to the toluene layer, using the device previously described for determining dye numbers, when an extremely slow swirling motion was given to the system with no possibility of breaking up or mixing the layers. The results of the analyses by extraction and by the colorimeter were then multiplied by 11/10 to represent approximate saturation. No emulsified toluene was visible in the ultramicroscope either with or without dye. The Yellow AB contained 0.15 per cent by weight of a water-soluble sulfate and chloride. The data are given in table 1 and figure 1. The solubility of Yellow AB in pure water is so very slight that it is insufficient to color the water even faintly, far less to weigh or analyze. It should be noted that, since the molecular weight of the detergent (250.2) is so nearly that of the dye (247), the ratios in grams are equal to the ratios in molecules, as plotted in figure 1. Figure 1 emphasizes that in extreme dilution the detergent is most effective in bringing into stable colloidal solution almost half of its own weight of dye. This is

TABLE 1

The solubility of Yellow AB in aqueous laurylsulfonic acid at 25°C., in milligrams of dye per 100 cc. of solution

CONCENTRATION OF RSO_4H	FIRST SERIES			SECOND SERIES		
	Solubility		Grams of dye per gram of soap	Solubility		Grams of dye per gram of soap
	By weight	By extraction		By extraction	By color	
N_W	*mg.*	*mg.*	*grams*	*mg.*	*mg.*	*grams*
0.00052	6	5	0.4–0.5	5.5		0.42
0.00104	8	7	0.27–0.31	7.7		0.30
0.0052	24	23	0.18	24	23	0.18
0.0052	25	23	0.18			
0.0104	46	43	0.173	42	44	0.17
0.052	244	241	0.186	215	225	0.17
0.052	250	230	0.184			
0.104	640	650	0.245	671	638	0.251
0.52	2150	2130	0.165	1804	1919	0.143

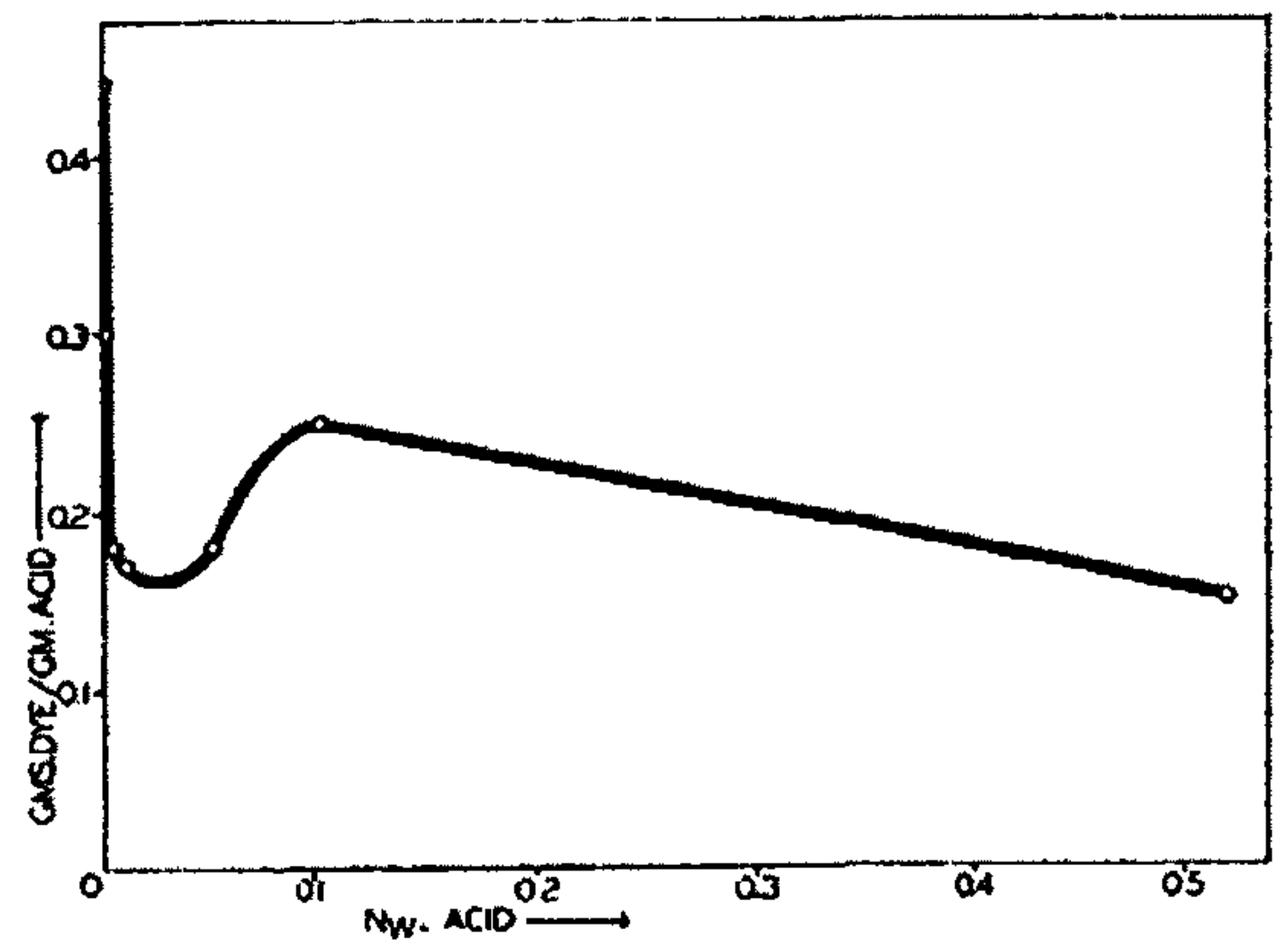

FIG. 1. Solubility of Yellow AB in laurylsulfonic acid, in grams of dye per gram of soap.

more remarkable because in extreme dilution most of the detergent itself is certainly not present in colloidal form, but is almost completely ionized. Its conductivity is slightly lowered by dissolving the dye. Hartley agrees that here the detergent is almost wholly ionized, but on the other hand he considers that the taking up of dye is "almost conclusive proof" of the presence of micelles and that the micelles are liquid. The increase in solvent power on dilution may be an important factor in rinsing.

The whole curve resembles the surface tension curve of aqueous laurylsulfonic acid, and the minimum occurs in the same low concentration in each case. The downward slope in the more concentrated solutions in figure 1 corresponds to the general behavior of very numerous detergents, following the purely empirical rule of McBain and Woo that the amount of dye stably dissolved is proportional only to the 2/3 power of the concentration of detergent.

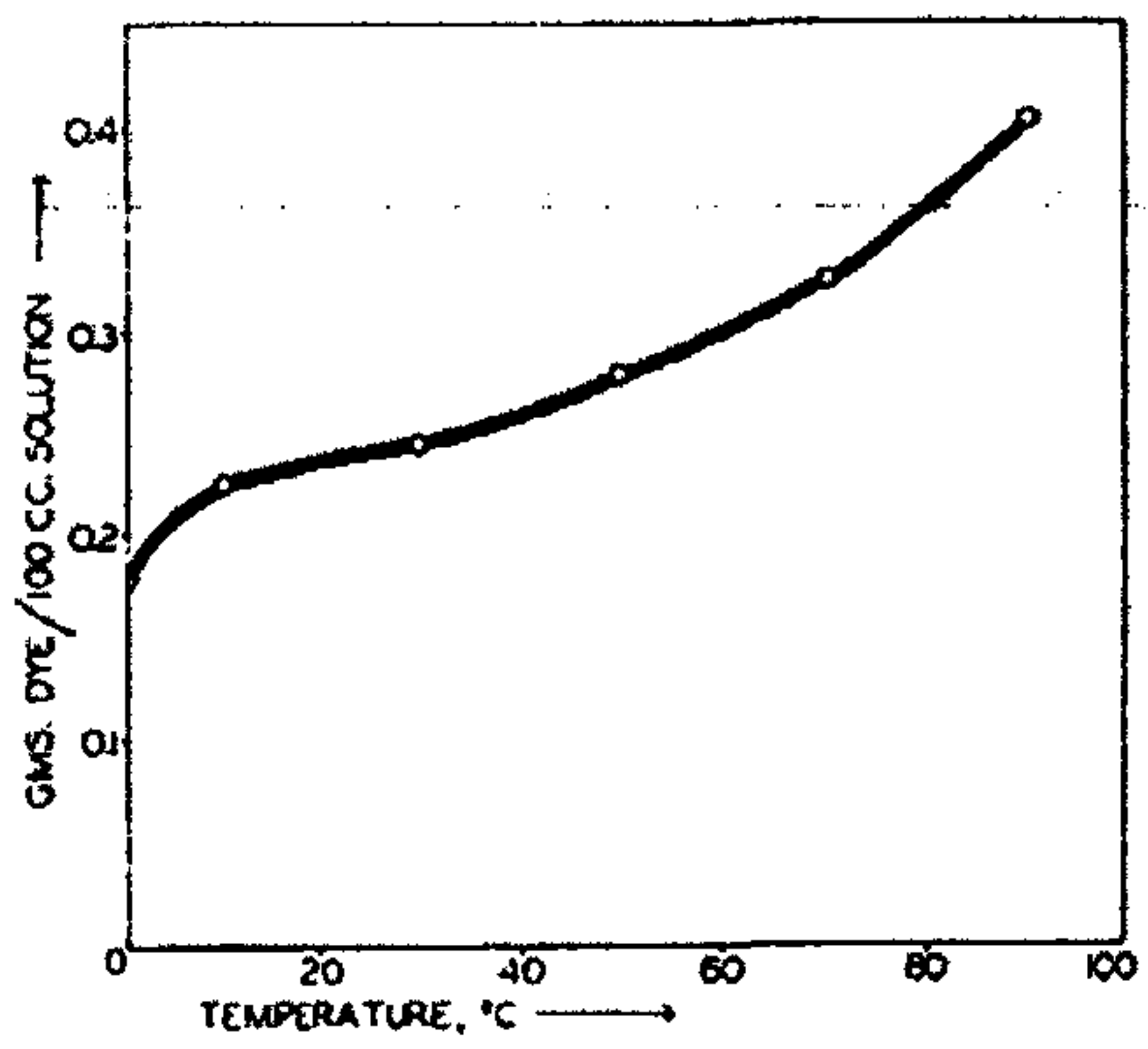

FIG. 2. Solubility of dye in 0.052 *N* laurylsulfonic acid, at temperatures from 0°C. to 90°C.

Likewise, the greatly increased solubility of Yellow AB when the temperature of 0.052 *N* laurylsulfonic acid is raised from 0°C. to 90°C. shows that the effect bears surprisingly little relation to the amount of colloid originally in the laurylsulfonic acid. This is largely colloidal at 0°C. and mostly crystalloidal at 90°C. The data are given in figure 2.

As regards other detergents, the solubility of Yellow AB in a 1 per cent, or 0.0226 *N*, solution of pure sodium sulfonate of dioctyl succinic ester (molecular weight 442) is 451 mg. per 100 cc. (determined by weight), 449 mg. (determined by extraction), or 0.45 of the weight of the detergent. Either in weight ratio or mole ratio this is much more than in laurylsulfonic acid of the same concentration. The commercial product, supposedly 99.6 per cent pure, twice gave a value of 449 mg. per 100 cc.

The solubility in 1 per cent "aliphatic ester sulfate" was 497.5 mg.

(determined by weight) and 496.1 (determined by extraction). That calculated from the empirical dye number formula is 496.1, showing the useful range of this merely empirical and certainly not general formula.

The solubility in a 0.0107 per cent solution of a commercial "75 per cent Turkey red oil" was 13.0 mg. (determined by weight), 12.8 mg. (determined by colorimeter), and 12.0 mg. (determined by extraction), which is much more than the weight of the Turkey red oil. (The dye number in this concentration, which is approximately only 0.0005 *N*, is at least 3.) A solution of twice this concentration dissolved 21.0 mg. (determined by weight), 21.0 mg. (determined by colorimeter), and 20.0 mg. (determined by extraction), about equal to the weight of the impure Turkey red oil. Without addition of water the solubility was 7.32 g., in 5 per cent solution it was 0.988 g., and in 1 per cent solution it was 0.291 g. (11), so that the proportionate weight of dye increases very greatly down to extreme dilution of the Turkey red oil.

The following solubilities were determined in 1 per cent aqueous solution: ethyl alcohol, 0.2 mg. (determined by weight), 0.3 mg. (determined by extraction); amyl alcohol, 0.0 mg. (determined by weight), no color; diethylene glycol, 0.1 mg. (determined by extraction), no color; glycerol, 0.0 mg. (determined by extraction), no color. These results are of exceptional interest when compared with the effect on dye numbers tabulated later.

The effect of the presence of 5 per cent Calgon in 1 per cent solution of the Turkey red oil is to change the solubility from 291 mg. to 18 mg. (determined by extraction). In 5 per cent Turkey red oil it is changed from 988 mg. to 296 mg. (determined by extraction). The solubility in 1 per cent Turkey red oil is raised from 291 mg. to 298 mg. by adding 0.2 per cent Calgon.

THE DYE NUMBERS OF THE HOMOLOGOUS SERIES OF SOAPS

Dye numbers are determined (11) by exposing a detergent solution to 2 cc. of toluene containing usually 40 mg. of Yellow AB, for at least 48 hr., avoiding all emulsification. They are expressed as 100*K*, where *K* is the constant from the equation

$$D_{\text{aq.}} = K \cdot D_{\text{tol.}}^{2/3} \cdot S_{\text{aq.}}^{2/3}$$

where *D* is the concentration of dye in the aqueous and toluene layers, respectively, and *S* is the concentration of the soap or other stabilizing colloid referred to the water present. Concentrations are in grams per 100 g. of solvent, except that for Yellow AB $D_{\text{tol.}}$ is expressed in grams per 100 cc. of toluene. The dye number so obtained is wholly independent of the previous history of the system and its components, provided that at least two days have been allowed for equilibrium to be established from either side. In every case the dye number is obtained by approaching equilibrium from both sides; in one experiment always dissolving the dye in the toluene first, and in the other dissolving it in the soap solution first

TABLE 2

Dye numbers, 100K, of the soaps (above C_8)

SOAP	DYE NUMBERS IN SOLUTIONS OF CONCENTRATIONS GIVEN				MEAN
	0.2 per cent	0.5 per cent	1 per cent	5 per cent	
Potassium nonylate, C_9	(0.38)	0.268	0.261	0.257	0.265
Potassium caprate, C_{10}	0.809	0.825	0.818	0.820	0.818
Potassium undecoate, C_{11}		2.68	2.69		2.68
Potassium laurate, C_{12}	3.58	3.59	3.57	3.55	3.57
Potassium myristate, C_{14}	3.83	3.80	3.84	3.71	3.79
Potassium palmitate, C_{16}	3.74				3.74
Sodium laurate		3.02	3.06		3.04
Potassium oleate			5.80		5.80
Sodium oleate			5.69	5.65	5.67
Sodium abietate			1.16	1.13	1.14
Sodium erucate	5.26				5.26

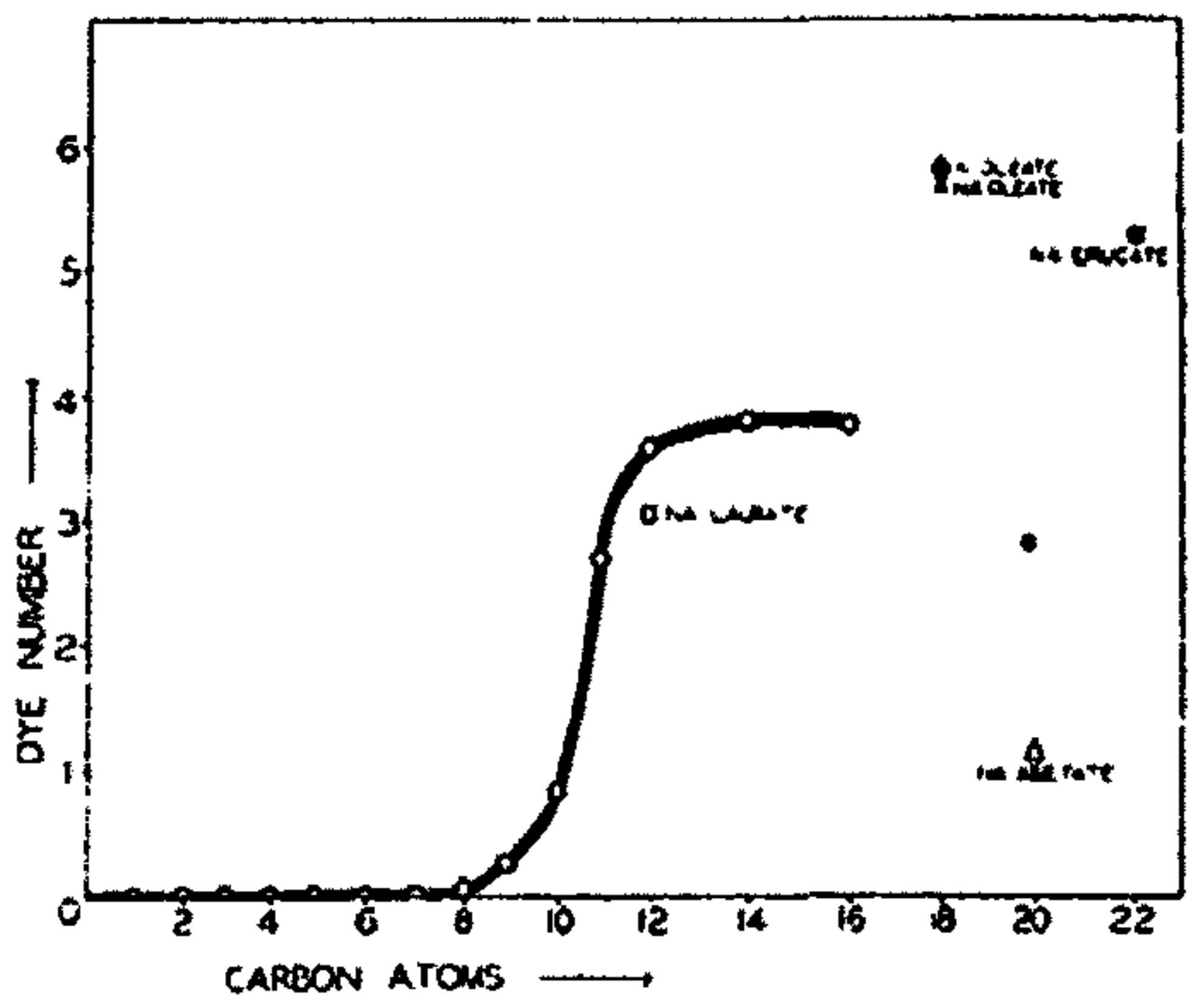

FIG. 3. Dye numbers of potassium salts of saturated fatty acids. □, sodium laurate; △, sodium abietate; ⊗, potassium oleate; ×, sodium oleate; ■, sodium erucate.

before exposing it to the other phase. The results almost always agreed within a few per cent, and the mean was taken to calculate the dye number. The dye number is 0 in the absence of stabilizing colloid. It is likewise 0 for an unstable hydrosol.

The dye number is 0 for the potassium salts of the fatty acids from the formate through the acetate, propionate, butyrate, valerate, and caproate to the heptylate inclusive, whether in 1 per cent or 5 per cent solution. Potassium octoate (caprylate) in 5 per cent solution gives a value 0.05, but for 1 per cent, 0.5 per cent, and 0.2 per cent solutions it is 0. The dye numbers for the higher soaps are given in table 2 and in figure 3. All these soaps and salts were prepared from Kahlbaum's and the Eastman Kodak Company's purest materials, except that the oleic acid was made by British Drug Houses by Lapworth's method; the sodium abietate was an especially pure specimen prepared by E. I. du Pont de Nemours and Company and preserved under alcohol; the decoic acid was made by Dr. S. Lepowsky, and the undecoic acid by Dr. C. R. Noller.

TABLE 3

Dye numbers of commercial soaps or those from technical ingredients

1 per cent solutions

SOAPS	DYE NUMBERS	SOAPS	DYE NUMBERS
Oleic acid soap	4.25	Flakes "A"	4.70
Palm oil soap	4.73	Flakes "B"	3.89
Tallow soap	8.50	Powder "A"	5.25
Olive oil soap	6.98	Powder "B"	3.28
Stearic acid soap	5.99	Powder "C"	3.54
Potassium coconut oil soap (dried)	4.80	Powder "D"	7.55

TABLE 4

Dye numbers of sulfonated oils

SULFONATED OILS	DYE NUMBERS		
	From 1 per cent solution	From 5 per cent solution	Mean
"75 per cent Turkey red oil"	6.22	5.96	6.09
"Sodium sulforicinoleate"	4.12	4.11	4.12
65 per cent sulfonated castor oil, of 8 per cent SO_3	6.06	5.88	5.97
82 per cent sulfonated castor oil, of 8 per cent SO_3	5.97	5.49	5.73
Equal mixture of last two	6.01	5.54	5.72
70 per cent sulfonated castor oil, of 4.3 per cent SO_3	4.40	4.60	4.50
Sulfonated castor oil "A"	2.39	2.39	2.39
Sulfonated castor oil "B"	2.17	2.07	2.12
Sulfonated castor oil "C"	6.03		6.03
"Highly sulfonated olive oil"	6.18	6.24	6.21
48 per cent sulfonated castor oil, of 32.5 per cent SO_3	5.16	5.14	5.15*

* Corrected for moisture of original, gives dye number 8.4.

For comparison with the pure chemicals in table 2, we have given in

TABLE 5

Effect of added substances upon dye numbers

SOLUTIONS USED	DYE NUMBERS
1 per cent potassium oleate	5.8
+ 1 per cent sodium chloride	3.05
+ 5 per cent sodium chloride	0
+ 1 per cent potassium carbonate	8.5
+ 0.1 per cent Calgon	6.0
+ 0.2 per cent Calgon	6.9
+ 0.5 per cent Calgon	5.2
+ 1 per cent Calgon	3.9
+ 5 per cent Calgon	0*
+ 0.2 per cent trisodium phosphate†	6.1
+ 1 per cent trisodium phosphate	6.9
+ 5 per cent trisodium phosphate	6.0
+ 5 per cent sodium metasilicate	3.9
+ 5 per cent sodium silicate (2.4)	7.0
+ 5 per cent sodium silicate (3.2)	7.0
+ 0.5 per cent gum tragacanth	5.2
1 per cent potassium laurate	3.57
+ 1 per cent sodium carbonate	4.20
1 per cent "75 per cent Turkey red oil"	6.1
+ 1 per cent sodium chloride	2.0
+ 5 per cent sodium chloride	0
+ 1 per cent sodium carbonate	8.5
+ 0.1 per cent Calgon	6.0
+ 0.2 per cent Calgon	6.9
+ 0.5 per cent Calgon	6.0
+ 1 per cent Calgon	4.2
+ 5 per cent Calgon	0*
+ 0.2 per cent trisodium phosphate	6.03
+ 1 per cent trisodium phosphate	5.94
+ 5 per cent trisodium phosphate	5.25
+ 5 per cent sodium metasilicate	6.1
+ 5 per cent sodium silicate (2.4)	8.6
+ 5 per cent sodium silicate (3.2)	10.6
+ 0.5 per cent gum tragacanth	6.0
5 per cent "75 per cent Turkey red oil"	6.0
+ 5 per cent diethylene glycol	9.0
+ 5 per cent glycerol	8.8
+ 1 per cent glycerol	8.5
+ 5 per cent ethyl alcohol	1.44
+ 5 per cent diethyl ether	0.92

* Salted out.

† $Na_3PO_4 \cdot 12H_2O$.

TABLE 5—*Concluded*

SOLUTION USED	DYE NUMBERS WHEN PER CENT OF SILICATE ADDED IS		
	5 per cent	1 per cent	0.2 per cent
1 per cent Turkey red oil (dye number = 6.1)			
+ silicate "S" (3.91)	10.51	6.84	6.08
+ silicate "O" (3.15)	10.5	6.81	6.01
+ silicate "N" (3.19)	10.6	6.84	6.03
+ silicate "K" (2.79)	6.1	6.08	6.01
+ silicate "U" (2.41)	8.5	6.01	6.00
+ silicate "C" (1.9)	6.0	6.87	5.99
+ metasilicate (1.0)	5.2	6.01	6.87

table 3 the dye numbers of five soaps made from single technical materails, kindly supplied by the National Oil Products Company, four commercial soap powders from different makers (one possibly containing a portion of synthetic detergent), two commercial soap flakes, and a potassium coconut oil soap supplied by the Davies-Young Soap Company.

THE DYE NUMBERS OF THE SULFONATED VEGETABLE OILS

In table 4 are listed the dye numbers of sulfonated oils, some of which, like sulfonated olive oil and sulfonated castor oil (Turkey red oil), have been known and used in the dye industry for nearly a century, but whose manufacture has in recent years been improved as regards control and degree of sulfonation. Our thanks are due to the many firms in this and other countries who kindly supplied or obtained for us these and our very varied assortment of detergents. A few were synthesized under the supervision of Dr. C. R. Noller at Stanford University. The dyes were given to us by the Calco Company. In table 4 degree of sulfonation appears to be a minor factor as compared with the dilution of the original material.

SOLUTIONS LACKING DYE NUMBER OR PROTECTIVE SOLVENT POWER

The following substances leave water a complete non-solvent for Yellow AB when they are added to the extent of 1 or 5 per cent, and their dye number is 0: sodium alginate (pure), sodium silicates (all), sodium hexametaphosphate (Calgon), trisodium phosphate, gum tragacanth, ethyl alcohol, amyl alcohol, diethylene glycol, glycerol, casein. It is all the more interesting that some of these substances enhance the dye numbers of Turkey red oil and of potassium oleate.

EFFECT OF ADDED SUBSTANCES UPON DYE NUMBERS

The experiments in table 5 were performed by adding various substances to solutions originally containing either 1 per cent of potassium oleate or 1 or 5 per cent of "75 per cent Turkey red oil." The effect of admixtures in enhancing the formation of stabilized colloid is noteworthy, even when some alone exhibit no dye numbers and have no hydrotropic actions in the dilutions considered. This is especially clear with such added substance as diethylene glycol and glycerol, as well as some of the sodium silicates. The addition of small quantities of Calgon is favorable, but large additions spoil the detergent.

TABLE 6

Dye numbers of synthetic electrolytic detergents

DETERGENTS	DYE NUMBERS		
	From 1 per cent solution	From 5 per cent solution	Mean
Trimethyldodecylammonium bromide (pure)	6.74	6.72	6.73
A technical cationic active detergent	2.07		2.07
A quaternary ammonium base	1.16	1.12	1.14
Another quaternary ammonium base	1.22	1.21	1.22
An imidazole compound	1.26	1.22	1.24
Sodium alkylated naphthalenesulfonate	3.28		3.28
Sodium monosulfonate of dioctyl succinate (pure)	8.15*		8.15*
+ 1 per cent glycerol	10.23		10.23
+ 1 per cent diethylene glycol	10.30		10.30
Sodium secondary-tetradecyl sulfate		1.47	1.47
Sodium secondary-octyl sulfate		0.13	0.13
Sodium secondary-heptadecyl sulfate	0.39	0.38	0.38
An Igepon product	6.85	6.92	6.89
Technical sodium oleyl sulfate	4.16	4.14	4.15
Technical sodium stenyl sulfate	9.74	9.81	9.78
Technical sodium lauryl sulfate	3.94	3.90	3.92
Technical sodium octyl sulfate	2.96	2.94	2.95
Sodium lauryl sulfate	5.06	5.18	5.12
Ammonium lauryl sulfate	5.93	6.04	5.99
Diethanolamine coconut oil dimethyl sulfate	3.89	3.65	3.8
A sulfated fatty alcohol	5.99	5.44	5.7
A technical alkyl sulfate powder	4.21		4.21

* Calculated from the solubility of the dye in 1 per cent solution (0.449 g. per 100 cc.) is 8.01; dye numbers with 1 per cent and toluene tend to give a higher result, and the experiment with 5 per cent is precluded by the complete emulsification of the toluene.

DYE NUMBERS OF SYNTHETIC DETERGENTS

The names given for the synthetic detergents listed in table 6 are those of the pure chemical or of the main constituent when thus stated and supplied by the maker. In many cases only an indication of the type of a commercial product can be given. The proportion of active material and of other materials in the technical preparations varies greatly and in many cases is unknown to us. Some of these data are included from a previous communication (11). Where the technical constituent is diluted or where it contains also salts or substances such as alcohol, the dye number suffers accordingly and the value recorded here is too low.

DETERGENTS THAT ARE NON-ELECTROLYTES

Colloid stabilization may be brought about by substances that are very different from the soaps or other salts, acids or bases, such as have been enumerated in the foregoing tables. It is of very great interest that detergent power is independent of both dissociation and hydrolysis, although both of these affect the electrolytic detergents. The non-electrolytic detergents cover the same range of dye numbers as the electrolytic ones. Table 7 lists a few of these.

TABLE 7

Dye numbers of non-electrolytic detergents

DETERGENTS	DYE NUMBERS		
	From 1 per cent solution	From 5 per cent solution	Mean
Nonyl glucoside (pure)	5.24		5.24
Synthetic non-electrolytic polymer	6.60	6.58	6.59
Another non-electrolytic polymer		7.33	7.33
Polyglycerol ester		4.15	4.15
Polyhydroxyether, technical		3.62	3.62
A polyether alcohol	1.81		1.81
Polyethylene glycol condensate (?)	5.97	5.29	5.63
Condensate of C_{18} alcohol and ethylene oxide	1.96		1.96
Another condensate or polymer	1.89		1.89
Diglycol laurate	5.63	5.63	5.63
Saponin Quillaia, Merck, purified	0.54	0.54	0.54
Diethanolamine fatty acid	4.21	3.53	3.9
Diethanolamine coconut oil	6.01	5.39	5.7
Another diethanolamine coconut oil	5.97	5.49	5.7
Diethanolamine oleic acid	3.86	3.66	3.8
Diethanolamine stearic acid	3.57	3.62	3.6

DISCUSSION

Considerations of space preclude any detailed discussion here. The newer trend of the results is quite clearly in the further direction of surmising that a stabilized particle, that is, an unstable particle merely coated with stabilizing agent, may possibly be stable as compared with the separate constituents of which it is composed. This has not yet been proven. However, in the cases here studied it seems probable that, especially in very dilute systems, there is comparatively little stabilizing agent as compared with the insoluble stabilized material. This would lead to the point of view that the molecules of dye associate statistically to particles whose formation is less and less probable as the size increases, but once formed are stabilized by the protective colloid. This presents the conception of a statistical equilibrium.

This paper deals only with proven true reversible equilibria, reached equally from both sides. It is thus distinguished from the experiments of Pickering (15), Bailey (1), Lester Smith (16), Hartley (5), and Lawrence (7), where the usual mechanisms for producing unstable von Weimarn types of sols and emulsions are not guarded against and in many cases are certainly operative; these have long been the usual methods of exceeding equilibrium concentrations.

The present results deal only with moderately dilute systems, and not with the exceedingly complex relations observed in concentrated systems illustrated by the phase rule diagrams of Booth (2) or of Weichherz (18), or with the very concentrated systems in which hydrotropy is so often studied (such as 75 to 250 per cent sulfosalicylic acid).

A detergent might almost be defined as a substance which achieves in very dilute solution a solvent action comparable to that of a highly concentrated organic solvent.

It must again be emphasized that the 2/3 power rule is valid only over a limited, moderately dilute range. It serves as a reminder that the proportion of dye to Turkey red oil is eighteen times greater in extreme dilution than in pure Turkey red oil itself. The solubility of an azobenzene dye was likewise found by Hartley and Miss Parsons to be fivefold more in a given amount of paraffin-chain salt present than in an equal weight of pure hexadecane. The facts here recorded for these numerous detergents do not accord with the interpretations suggested by Hartley (5) and Lawrence (7).

The 2/3 power rule for these detergents may, as shown by calculations of Dr. R. D. Vold and Dr. M. J. Vold, equally well be replaced by a formula based upon calculations of Meyer and van der Wyk (12), assuming that particles are built up stepwise, each step (the addition of one more molecule) involving the same energy, provided that it is further assumed that each particle, independent of size, has the same average power of stabilizing a molecule of dye within the detergent solution. This, like the original calculations of Meyer and van der Wyk, is an interesting opposite extreme from the views of Hartley and Lawrence.

It should be emphasized again that the dye numbers and the dye solubilities measure one, but only one, of the factors involved in detergent action. Further work is needed with systems including fabrics, where dye and detergent compete for the surface of the fabric as well as for each other.

SUMMARY

1. The spontaneous formation of stabilized colloid involving true reversible equilibrium has been further studied.

2. The colloid stabilization appears to be more closely related to the surface activity than to the colloidality of the detergent.

3. Dye numbers of many types of modern and synthetic detergents, including pure soaps and other compounds as well as commercial products, have been measured.

4. Detergents that are anion-active like soaps and sulfonates, cation-active like substituted ammonium derivatives, and, most interestingly, non-electrolytic detergents cover the same range of dye numbers.

5. Blends and mixtures, even with materials which possess zero dye number, such as silicates and phosphates, may noticeably enhance the dye numbers of detergents.

REFERENCES

(1) Bailey: J. Chem. Soc. **123**, 2579 (1923).
(2) Booth: Chemistry & Industry **56**, 1120 (1937).
(3) Freundlich and Krüger: Biochem. Z. **205**, 186 (1929).
(4) Hadjioloff: Naturwissenschaften **25**, 762 (1937).
(5) Hartley: Symposium on Wetting and Detergency, London (1937).
(6) Kúthy, A. von, and Banga: Biochem. Z. **230**, 458; **237**, 380 (1931); **244**, 317 (1932).
(7) Lawrence: Trans. Faraday Soc. **33**, 325, 815 (1937).
(8) Lindar: Naturwissenschaften **20**, 396 (1932).
(9) McBain: Kolloid-Z. **40**, 1-9 (1926); Colloid Symposium Monograph **4**, 7 (1926).
(10) McBain and McBain: J. Am. Chem. Soc. **58**, 2610 (1936).
(11) McBain and Woo: J. Am. Chem. Soc. **60**, 223 (1938).
(12) Meyer and van der Wyk: Helv. Chim. Acta **20**, 1313 (1937).
(13) Neuberg: Biochem. Z. **76**, 107 (1916).
(14) Noller and Gordon: J. Am. Chem. Soc. **55**, 1090-4 (1933).
(15) Pickering: J. Chem. Soc. **91**, 2001 (1907); **111**, 86 (1917).
(16) Smith: J. Phys. Chem. **36**, 1401, 1672, 2455 (1932).
(17) Verzár and Kúthy, A. von: Biochem. Z. **225**, 267 (1930).
(18) Weicherz: Kolloid-Z. **47**, 133; **49**, 158 (1929); **58**, 214; **60**, 192, 298 (1932).

THE MICROSCOPIC STRUCTURE OF PLANT CELL MEMBRANES IN RELATION TO THE MICELLAR HYPOTHESIS[1]

WANDA K. FARR

Cellulose Department, Chemical Foundation, Boyce Thompson Institute, Yonkers, New York

Received July 14, 1938

The invention of the compound microscope (7) by the Janssens in 1590 marked the opening of a new era in biological research. Before the close of the seventeenth century, the first important observations of the tissue structure of both plants and animals had been made by Hooke (13), von Leeuwenhoek (17), Grew (12), and Malpighii (20). During the eighteenth century there were few additions to the findings of these pioneers. The impetus to microscopic study which came with the nineteenth century was linked inextricably with marked improvements in the microscopes themselves (29).

Before 1820 the work of Mirbel (22), Treviranus (38), Link (18), and Rudolphi (31) had helped to create an active interest both in England and on the continent. The observations in the botanical laboratory of Schleiden (32) in Jena and in the zoological laboratory of Schwann (34) in Berlin were summarized in 1838 with the announcement that "All organized structures are composed of essentially similar units, namely cells." It is well known to those who are familiar with the development of the biological sciences that this recognition of the universal cellular structure of plants and animals was shared with other contemporary workers (30).

In the living plant cells there are visible two distinctly different parts: the delicate, more or less viscous protoplast, and the comparatively rigid cell membrane which surrounds it. The general organization and function of the protoplast presents problems of the greatest difficulty. Its appearance is constantly changing, and one hundred years ago but little was known of the cellular changes which accompany metabolic and reproductive processes. Cell membranes are more stable, and it is not surprising to find the earliest interest directed toward a more complete understanding of their microscopic structure and composition.

The chemical studies of Payen (27) demonstrated in 1842 that the

---

[1] Presented at the Fifteenth Colloid Symposium, held at Cambridge, Massachusetts, June 9-11, 1938.

membrane substance of cells from all parts of the plant kingdom, when purified from foreign deposits, exhibits the same composition in terms of relative proportions of carbon, hydrogen, and oxygen. He found also that it assumes a blue color in the presence of iodine and sulfuric acid. He named this membrane material "cellulose."

Concurrently the finer physical structure of certain plant cell membranes was described by von Mohl (23), Schleiden (33), Agardh (1), and others who had observed that they are made up of fine fibrils of uniform diameter. These fibrils, arranged in crossed spirals, have become familiar objects in the many published illustrations of the swollen membranes of cotton fibers (plate I, figure 2).

By means of the polarizing microscopes then available in many laboratories, it was learned that the cellulose membranes are doubly refractive (plate I, figure 1). It was for the purpose of explaining this particular phenomenon, and also the swelling behavior of both cell membranes and starch grains, that, in 1858, Carl von Nägeli (24, 25, 26) developed his well-known micellar hypothesis. The crystalline nature of both structures is indicated by their double refraction in polarized light. Nägeli was not able to see individual crystallites, the presence of which is indicated by this double refraction; therefore he stated that they are submicroscopic. In the dry membrane he believed these "micellae" to be nearly contiguous, to occupy almost all of the available space. The membranes, moistened with water or aqueous fluids, were supposed to take up capillary water upon the surfaces of the micellae, in such a way that the crystallites were separated from one another without losing their cohesive force. If the imbibed water were subsequently evaporated, the condition would be reversed and the original state of the dry material resumed.

Ambronn's (2, 3, 4) studies of the orientation of the crystalline cellulose in cell membranes appeared after a considerable lapse of time. His careful and extensive observations in polarized light have shown that the long axes of the crystallites are arranged parallel to the long axis of the fibril and not necessarily parallel to the long axis of the fiber itself. No finer subdivisions of the fibril were visible to him and he based his interpretations, therefore, upon the assumption that the fibrils are composed of crystalline micellae. His publications have furnished an abundance of data which are in excellent form to be correlated directly with results from the more recently developed method of crystalline analysis,—x-ray diffraction. Ambronn's revival of the micellar hypothesis has played an important part in the widespread use of this theory by x-ray chemists in the interpretation of the diffraction patterns of cell membrane materials.

These studies of orientation by means of polarized light and x-ray diffraction have been supplemented more recently by observations of fibril orientation in ordinary light (28). The high degree of correlation in the results obtained with the three methods has established Ambronn's original conclusions concerning orientation beyond any reasonable doubt. It must be kept clearly in mind, however, that in these studies of orientation the x-ray diffraction and polarized light analyses have furnished no direct evidence as to the size of the crystallite itself.

The exact form and size of the crystallite, as well as its behavior in the membrane, have been the source of controversy in many allied fields of research. Physiologists have been constantly reminded of the fact that a plant cell membrane made up entirely of submicroscopic crystalline micellae could not exhibit the observed swelling behavior. The enormous force involved in connection with the first intake of water into their carefully dried samples is of a much greater magnitude than is commonly associated with capillarity. These doubts have been augmented by the observance of the profound changes in cell membranes after treatment with reagents which could not be shown to have affected the cellulose itself. A cell membrane may thus lose all of its natural physical characteristics, be resolved into a fine white powder, and during the process the cellulose x-ray pattern shows no evidence of change except the transition from regular to random orientation (9, 10). In a discussion of the shortcomings of the micellar hypothesis from the viewpoint of the physiologist, Fischer in 1927 presented, in one sense, a real challenge to microscopists (11, pages 327 and 328): "This phenomenon of double refraction shows that such an inner structure must exist. This, however, may be a fallacy; we cannot prove the matter experimentally. We cannot produce such a body made up of diminutive parallel-arranged crystallites and then study with polarized light or x-rays a structure of which we, with full certainty, know that it has this microstructure, because we ourselves have produced it."

To many investigators employing microscopic technique, the physical nature of the cellulose crystallite of the cell membrane has never been a settled issue. In the presence of an accumulating mass of indirect evidence that the cellulose crystallites are in the form of submicroscopic micellae of varying dimensions, their efforts have been directed toward a possible physical disintegration of the cellulose fibril into visible units. Such units, fibrillar or otherwise, must not owe their existence to a chemical degradation of the cellulose. Degradation may be avoided by the use of reagents which do not affect the cellulose itself or, even more satisfactorily, by the dissection of fresh membranes from living plant cells by mechanical means alone.

Early in 1930 a new approach to the problem of fibril structure through dissections of fresh membranes and mild chemical treatments of dried membranes was made in our laboratory. We studied many types of living plant cells from various parts of the plant kingdom during the period of membrane formation. In 1932, by means of improved optical technique, we observed large numbers of uniform-sized ellipsoid particles in the cytoplasm of these living cells (8). They are remarkably stable physically, and, although diminutive in size (1.5 x 1.1 μ), lend themselves readily to both optical and microchemical analyses. They are definitely doubly refractive in polarized light; the refractive indices of the moist particles from the living cytoplasm of the cotton fiber are 1.565 lengthwise and 1.530 crosswise; they swell and turn blue in the presence of sulfuric acid and iodine; their combustion analysis yields the following results:

	Theoretical value	*Found*
Carbon, per cent	44.4	44.34; 44.30
Hydrogen, per cent	6.17	6.31; 6.29
		(no ash)

their x-ray diffraction pattern is that of native cellulose (35); and when treated with 18 per cent sodium hydroxide they give the pattern of mercerized cellulose. In other words, these ellipsoid particles show the characteristic properties of cellulose and were designated by us "cellulose particles."

Although separate and in short chains in the interior of the cell, the cellulose particles, during the period of wall formation, appear in the outer regions of the cytoplasm arranged end to end in orderly single rows (plate II, figure 1). The fibrils thus formed were removed from the living cells for more careful study. It then became clear that each particle in the fibril is coated with a viscous material which functions as a cementing material, holding the particles together to form the fibril and the fibrils, layer upon layer, to form the membrane lamellae.

Membranes of moist cotton fibers from the unopened boll can be disintegrated into fibrils and particles by mechanical treatment alone. The membranes of mature, dried fibers require treatment with weak chemical reagents to bring about a similar degree of membrane disintegration. As the reaction proceeds, the cementing material surrounding the particles is observed microscopically to swell and, in so doing, to push the particles farther apart. Long-continued treatment brings about the removal of the cementing material by the solvent. A short treatment leaves little visible evidence of physical effect upon the membrane. The more specific techniques of staining and viscosity (14, 21) measurements show us, however, that few, if any, of these treatments leave the cementing material unaltered. The significant fact is that membrane disintegration is thus brought about without any measurable indication of cellulose degradation. Physically and chemically the particles themselves show no evidence of alteration. The crystalline cellulose of the plant cell membrane is therefore in the form of diminutive ellipsoid cellulose particles whose behavior in the process of membrane formation we are able to follow with certainty (plate II, figure 2).

The difficulty of obtaining protoplasm from a cell as small in diameter as a cotton fiber, free from all membrane material, is obvious. A larger cell, the marine alga *Valonia ventricosa*, the diameter of which is often as great as 3 cm., is useful in this connection. Samples of protoplasm, carefully removed with a fine pipet, show the presence of cellulose particles and their arrangement in single rows to form the fibrils of the mature membrane (plate III, figure 1). The mature membrane of *Valonia* shows a variation in the orientation of these fibrils from 60° to 90°. In the samples from the protoplasm, the arrangement, as shown by the x-ray diagram, is random. In the mature membrane the correlation between the measurements of orientation as shown in the photomicrographs and upon the x-ray diffraction pattern is very close (plate III, figure 2).

These observations constitute, therefore, a visible representation of the two fundamental principles which led Nägeli to develop the micellar hypothesis: (*1*) the presence of crystalline material in the membrane, and (*2*) the evidence that the crystallites themselves were unaltered during the swelling of the membrane with either water or aqueous fluids. The crystalline material is present in the form of microscopic cellulose particles. During the swelling of the membrane these particles themselves do not react with the water. They are observed to be pushed apart, not through a direct capillary force of the entering fluid, but by the swelling reaction of the colloidal matrix which surrounds each individual particle. The more important difference in the theoretical and the observed conditions is therefore due to the presence of the cementing material, the nature of which enables us to explain the known swelling behavior of cell membranes in its various aspects.

A recently completed survey of nineteenth century contributions to the microscopic structure of plant cells has revealed the fact that many investigators saw and recorded the presence of microscopic particles in the cell membranes. A few of them described their behavior in the cytoplasm during fibril formation and deposition (table 1). The cellulose nature of the particles in the cytoplasm was not recognized. The closest approach to this recognition is indicated in the expressed belief of Wiesner (40, page 66) that they are changed into cellulose after they are deposited in the membrane. Both Strasburger and Wiesner believed that the "microsomes" and "dermatosomes" in the living cytoplasm were protein because they stain yellow with iodine. We now know that this is a surface reaction. The greater number of recorded observations of the formation of cellulose membranes from visible structural units occurred before 1850. The wave of interest in cellular reproduction then turned the activities of most microscopists from cell membranes to the intricacies of nuclear behavior. This type of study brought with it the new techniques of fixing, embedding, sectioning, and staining. The tissues which were actually observed were usually dead and either successfully or unsuccessfully embalmed. After 1890 many generations of students of cytology passed through their entire period of academic training with only the most casual contact with the techniques required for the study of living cells.

TABLE I

Early observations of microscopic particles in cell membranes

AUTHOR	DATE	MATERIAL	METHODS	CONCLUSIONS
Lyngbye (19).......	1819	Algae: *Gastridium ovale* (or *Halicystis ovalis*)	Microscopic	Minute "points" visible in cell membrane; drawing indicates arrangement of the granular structures described
Link (18)...........	1819	Algae: *Conferva annulina*	Microscopic	"Granula Minuta" in the membrane
Valentin (39)........	1837	Cell walls	Microscopic	Granules in cytoplasm build cross lines which later become spiral lines of cell membrane
Kützing (16)........	1843	Marine algae	Microscopic	Granules in cytoplasm; very nearly invisible; ellipsoid or spherical, seldom filamentous
Agardh (1)..........	1852	Algae	Microscopic	Granules (spheroids) in cytoplasm believed to be beginning of fibrils in cell membrane
Nägeli (24, 25, 26)..	1858 1863	Starch grains Cell walls	Microscopic Swelling phenomena	Submicroscopic crystalline micellae to explain double refraction and swelling phenomena
Strasburger (37)	1882	Cell walls	Microscopic	Microscopic protein "microsomes" in "Hautschicht" play important rôle in wall thickening
Wiesner (40)........	1886	Cell walls Fibrils	Microscopic	Cell walls composed of microscopic cellulose "dermatosomes"
Ambronn (2, 3, 4)..	1892 1925	Cell walls Fibers	Microscopic	Cellulose composed of submicroscopic anisotropic crystalline micellae in orderly arrangement within the fibril

We are now in a position to realize that the earlier workers had two of the most important requisites in the study of the microscopic structure of cell membranes,—namely, well made, properly mounted lenses and fresh, unstained material.

The recorded observations of membrane structure made by Lyngbye (19), a Danish clergyman, in 1819, are worthy of reproduction in this connection (plate IV). The plant, *Gastridium ovale*, which he describes was reclassified in 1901 under the name *Halicystis ovalis*. From the description in table 18 (plate IV, figure 2), which applies to his drawings of the entire plant and enlarged portions of it (plate IV, figure 1), we see that he wrote with assurance, "Particula frondis". In the more detailed description of the plant he says (plate IV, figure 3), "Substantia membranacea, non gelatinosa, sed pro tenuitate tenacissima, sub lente minutissime punctata." The photomicrograph made recently in our own laboratory of the membrane of this same plant has the essential characteristics of this drawing made almost one hundred twenty years earlier,—minute particles in random arrangement (plate IV, figure 4). The x-ray diffraction pattern corroborates this random arrangement and shows, in addition, that the cellulose particles are mercerized (36). A cross section of the membrane shown in plate V, figure 1, shows a degree of orientation produced through the deposition of successive layers of cellulose particles. The microscopic and x-ray results show here, also, a close correlation. The regularity of natural orientation in *Halicystis* is, however, not in the same category with that of *Valonia*. In *Halicystis* the cellulose particles do not form fibrils.

At the meeting of the Cellulose Division of the American Chemical Society in April, 1937, a series of microscopic analyses of plant cell membranes was presented by Bailey, Anderson, and Kerr. These papers now published (5, 6) constitute one of the few recent reports of microscopic evidence in support of the micellar hypothesis. They state that their cross sections of cotton fibers have large numbers of lamellae which, upon the basis of counts and measurements made after swelling, are said to have been as thin as 0.1 μ in the original state. This width is far below the size of the cellulose particle and, if their interpretations of their preparations were correct, it would be incompatible with the existence in the membrane of cellulose in the form of particles 1.1 μ in width.

Our own studies of cross sections of cotton fibers in both intermittent and continuous illumination have extended over a period of several years. In the course of that time we have learned how to section mature fibers from a boll, not yet at the stage of natural opening, without any form of infiltration and embedding, have found that only cross sections of 2 to 3 micra in thickness are suitable for studies of the lamellate structure, and have learned that uniform swelling throughout the section depends upon a straight cut exactly perpendicular to the fiber axis across a "position of extinction" (plate I, figure 3). All measurements, counts, and direct observations show that each lamella is made up of a single layer of cellulose particles. A thin layer of cementing material surrounds each particle and alternates with each lamella.

The number of lamellae in the variety of cotton which we use for experimental purposes (*Gossypium hirsutum*, Super Seven, Strain 4) varies from fiber to fiber, from 4 to 15. A cross section whose membrane width is 13 micra will contain, for instance, 10 to 12 lamellae. From recent series of cross-sectional studies, Dr. F. L. Barrows of our laboratory has found an average lamellar width of 1.09 μ in eight hundred thirty cross sections. Fibers from plants grown in continuous light—both sodium vapor and sodium vapor and mercury arc—show no differences in the lamellate structure of their walls from those grown under ordinary conditions in the greenhouse or the field.

Our microscopic results may be summarized graphically with the illustrations in plate VI. There are large variations in shape and width of cross sections of fibers from any given boll (figure 1). The thin cross sections are very delicate and must be swollen with the greatest care. As swelling proceeds, the shape of an oval section is retained and the lumen enlarges as the section enlarges (figure 2). The outer limiting membrane of the fiber which does not swell in cuprammonium hydroxide does not play a part in the swelling behavior of such a thin cross section. As swelling continues, the lamellae become visible (figures 3 and 4). Longer continued treatment with the reagent gelatinizes the cementing material, distorts the lamellate structure, and obscures the separated particles (figure 5). Further addition of cuprammonium hydroxide to the mount helps to remove the swollen cementing material and the disarranged particles are more clearly visible (figure 6).

This description of cross-sectional structure and swelling behavior has no points in common with that reported by Bailey, Anderson, and Kerr (5, 6). They state that the sections should be 10 to 15 micra thick; ours are 2 to 3 micra in thickness. Soon after swelling begins in cuprammonium hydroxide their sections turn inside out so that the outer part of the fiber occupies the former position of the lumen; we have observed no such phenomenon in the swelling of the thin cross sections. The outline of the cross section in their final stages of swelling is shown to be circular, and the diameter of the opening in the center of the section is very small in proportion to the diameter of the cross section itself; our cross sections retain their original outline during swelling and the lumen enlarges progressively as the swelling proceeds. In order either to stop the reaction with the cuprammonium solution or to assist in the reversion of the "growth rings" they exert pressure upon the swollen section; the slightest pressure upon our cross sections at any stage of swelling produces so much distortion that all of the original tissue structure is destroyed.

The preparation of cross sections of cotton fibers according to the procedures described by Kerr (15) has furnished an explanation of the discrepancies between their results and ours. In cross sections 10 to 15 micra in length the cuticle plays an important rôle during swelling with cuprammonium hydroxide. It is observed to behave in three different ways: (*1*) The cuticle is rolled back to the center of the section and the swollen structure in outline resembles a sheaf of wheat (plate VII, figures 1 and 2). (*2*) The cuticle constricts one end of the swelling section and the separating fibrils radiate out from the ring of cuticle as a center. This explains the presence of the cuticle in the center of their "cross section". It is not due, however, to the reversal of the inner and outer portions of a true cross section (plate VII, figures 1 and 3). (*3*) The cuticle splits in the center and a band of it constricts each end of the swelling fiber section. This produces a lantern-like structure. If these sections begin to swell with their long axes horizontal to the surface of the microscope slide, they quickly tip, upon the curve of their swollen side, to a perpendicular position. This motion evidently has been mistaken for a reversal of the inner and outer portions of a true cross section.

Two or more of these three types of swelling may appear in a single field in the microscope (plate VII, figure 1). Only rarely does one type alone occur. Type 3 is evidently the one selected by Kerr and Anderson to demonstrate the number of "growth rings" in the wall of the fiber. These authors show, however, only the final stage of swelling. When the intermediate stages are followed (plate VIII, figure 1), the crossed fibrils of the surface come clearly into view. If swelling continues without pressure, the section is disintegrated without the appearance of "growth rings" (plate VIII, figure 2). If, however, after the swelling is well begun, pressure is exerted upon the cover glass of the mount, the entire swollen mass is thrown into a series of concentric microscopic ridges with the round of cuticle in the center as a point of origin (plate IX, figure 1). If the lantern-like structure is turned upon its side, both rings of cuticle serve as points of origin and the pressure ridges extend along the side of the lantern (plate IX, figure 2). In plate V, figure 2, this same phenomenon, resulting from pressure upon the swollen membrane of *Halicystis*, perpendicular to its surface, is shown. By a comparison with figure 1 it can be seen that these pressure ridges have no relation to the true lamellae. This represents a microscopic phenomenon which we have found in many different gum-like substances. Gum tragacanth softened in water illustrates this point (plate X). A small mass of foreign material has served in this instance as a point of origin.

These so-called "growth rings" have, therefore, no relationship to the true lamellae of the cotton fiber wall. Their number and width have no bearing upon the size of the crystalline units of cellulose and do not constitute evidence against the existence of cellulose particles of the size which we have described.

Anderson and Kerr have also stated that the cellulose particles which we have identified in the cytoplasm of the young cotton fiber are really small plastids containing starch. It is necessary, therefore, that we call attention to the fact that starch is not present in the cotton fiber at any stage of development. Starch is present in the outer integument of the cotton seed during its early stages of development (plate XI, figures 1a and 2). After about 12 days from the date of flowering much of this starch is converted into sugar and used up as food for the developing fibers. The starch in the inner integument (plate XI, figure 1) remains until about the 25th day. It is then gradually converted into sugar, which is used in turn in the development of oil in the embryo. The mature cotton seed contains no starch.

It is scarcely necessary to state that the identification of starch and cellulose is one of the most specific and well-known microchemical differentiations of closely related plant materials. The cellulose particles in the young cotton fiber have two refractive indices (1.565 and 1.530); cotton starch grains have one refractive index (1.518), and the plastid has a refractive index of the order of magnitude of protoplasm itself, not exceeding 1.4. The cellulose particles are remarkably uniform in size; plastids with and without starch grains are noted for their lack of uniformity in size. Particles from the cytoplasm of both cotton fibers and *Valonia* (plate II, figure 1, and plate III, figure 1) give x-ray diffraction patterns of cellulose and not starch. A cell from the inner integument of the cotton seed, at higher magnifications, shows a direct visible comparison of the cellulose particles, which have been formed in the cytoplasm of the living cell and used to build up the membrane, with the starch grains which have remained in the interior of the cell (plate XI, figure 3).

SUMMARY

Microscopic research resulted in the realization in the early part of the nineteenth century that all organized plant and animal structures are composed of essentially similar units, namely cells. Before 1850 many of the microscopic properties of the plant cell membrane had been described. Its double refraction in polarized light indicated the presence of a crystalline compound. Its swelling behavior indicated that the crystallites themselves did not react with the swelling agent. Upon the assumption that the cellulose crystallites were invisible and that in the swollen state of the membrane the reagent had merely brought about a wider spacing of these separate individuals, Nägeli, in 1858, developed the hypothesis that the plant cell membrane is composed of submicroscopic units to which he gave the name "micellae".

The observed cellulose particles have all of the optical properties in polarized light originally attributed to the crystalline micellae and later ascribed to them in orientation studies, with the exception of size. They are approximately 1 micron in size and therefore microscopically visible, while the micellae were presumably microscopically invisible. Especially significant is the additional observation that the space between the crystallites is not vacant, as Nägeli had believed it to be, but is occupied by a colloidal material having physical and chemical properties very different from those of the crystalline cellulose particles. The presence of this colloidal matrix accounts for an adequate force, not considered in the micellar hypothesis, to explain the unique swelling behavior of plant cell membranes.

A survey of botanical literature reveals the fact that the formation and structure of plant cell membranes from visible structural units was observed independently by many investigators previous to 1890. The failure to recognize the cellulose nature of the particles in the cytoplasm has probably contributed to the obscurity of these data, although it is clear that Wiesner approached this recognition in 1886 from his expressed belief that they change into cellulose after they have been deposited in the membrane.

The remarkable uniformity in size, shape, physical properties, and chemical properties of the cellulose particles from all parts of the plant kingdom indicates that our immediate fields for research are in a more complete study of their different types of orientation and of the nature of the materials with which they are so intimately associated.

REFERENCES

(1) Agardh, J. G.: De cellula vegetabili fibrillis tenuissimis contexta. 11 pp. Typis Berlingianis, Lundae (1852).

(2) Ambronn, Hermann: Anleitung zur Benützung des Polarizations-mikroskops bei histologischen Untersuchungen. Leipzig (1892).

(3) Ambronn, H.: Kolloid-Z. Ergänzungband (Zsigmondy Festschrift) 36, 119-31 (1925).

(4) Ambronn, Hermann, and Frey, Albert: Das Polarisationsmikroskop. 194 pp. Akademische Verlagsgesellschaft, Leipzig (1926).

(5) Anderson, Donald B., and Kerr, Thomas: Ind. Eng. Chem. 30, 48-54 (1938).

(6) Bailey, I. W.: Ind. Eng. Chem. 30, 40-7 (1938).

(7) Borelli, Peter: De Vero Telescopii inventore. Appendix. Centuria observationum microscopicarum (1665).

(8) Farr, Wanda K., and Eckerson, Sophia H.: Contrib. Boyce Thompson Inst. 6, 189-203 (1934).

(9) Farr, Wanda K., and Eckerson, Sophia H.: Contrib. Boyce Thompson Inst. 6, 309-13 (1934).

(10) Farr, Wanda K., and Sisson, Wayne A.: Contrib. Boyce Thompson Inst. **6**, 315-21 (1934).

(11) Fischer, Hugo: Beitr. Biol. Pflanz. **15** (3), 327-56 (1927).

(12) Grew, N.: The Anatomy of Plants. London (1682).

(13) Hooke, R.: Micrographia. London (1665).

(14) Joyner, R. A.: J. Chem. Soc. **121**, 2395-409 (1922).

(15) Kerr, Thomas: Protoplasma **27**, 229-41 (1937).

(16) Kützing, T. F.: Phycologia generalis, p. 305 (1843).

(17) Leeuwenhoek, A. von: Brieven. Delft (1663).

(18) Link, H. F.: Grundlehren der Anatomie und Physiologie der Pflanzen (1807).

(19) Lyngbye, Hans Christiano: Tentamen Hydrophytologiae Danicae (1819).

(20) Malpighii, M.: Anatome Plantarum (1675).

(21) McBain, James W., and Scott, Daniel A.: Ind. Eng. Chem. **28**, 470-3 (1936).

(22) Mirbel, C. F.: Traité d'Anatomie et de Physiologie Végétales (1801).

(23) von Mohl, Hugo. Erläuterung und Vertheidigung meiner Ansicht von der Structur der Pflanzen-Substanz. (1836).

(24) Nägeli, Carl von: Die Stärkekörner. Morphologische, physiologische, chemisch-physicalische und systematisch-botanische Monographie. Zurich (1858).

(25) Nägeli, Carl von: Beitrage Wiss. Bot. **3**, 1-126 (1863).

(26) Nägeli, Carl von: Über den inneren Bau der vegetabilische Zellmembranen. Sitzber. Kgl. Bayer. Akad. Wiss. Munchen **1**, 282-326 (1864).

(27) Payen, A.: Mémoire sur les dévelopements des végétaux. Paris (1842).

(28) Preston, R. D., and Astbury, W. T.: Proc. Roy. Soc. (London) **122**, 76-97 (1937).

(29) Quekett, John: A Practical Treatise on the Use of the Microscope. London (1855).

(30) Rich, Arnold Rice: Bull. Johns Hopkins Hosp. **39**, 330-65 (1926).

(31) Rudolphi, Karl Asmund: Anatomie der Pflanzen (1807).

(32) Schleiden, M. J.: Beitrage zur Phytogenesis (1838).

(33) Schleiden, M. J.: Bemerkungen über Spiralbildungen in der Pflanzenzell. I. Flora **21**, 321-36; **22**, 337-53 (1839).

(34) Schwann, Theodor: Mikroskopische Untersuchungen über die Übereinstimmung in der Struktur und dem Wachsthume der Thiere und Pflanzen. (1839). (Announced in 1838.)

(35) Sisson, Wayne A.: Contrib. Boyce Thompson Inst. **8**, 389-400 (1937).

(36) Sisson, Wayne A.: Science **87**, 350 (1938).

(37) Strasburger, E.: Ueber den Bau und das Wachsthum der Zellhäute. Jena (1882).

(38) Treviranus, L. C.: Beyträge zur Pflanzenphysiologie (1811).

(39) Valentin, G.: Repertorium für Anatomie und Physiologie. Veit, Berlin (1837).

(40) Wiesner, Julius: Sitzber. Akad. Wiss. Wien. Math.-naturw. Klasse I, **93**, 17-80 (1886).

COMMUNICATION TO THE EDITOR

ATTEMPTS TO PREPARE GREEN GOLD SOLS[1]

In attempting to prepare red gold sols by the method suggested by Ostwald,[2] namely, reduction of gold chloride solution by tannic acid in the presence of potassium carbonate, repeated trials resulted in a sol of a definitely green color. Suspicion pointed to the tannic acid solution which had been on the side-shelf for a long period of time.[3] In order to check this point, the experiments were repeated with freshly made solutions of tannic acid, and again with samples of this substance which were (*1*) allowed to age naturally exposed to air and (*2*) artificially aged by being bubbled with air for periods of 48 hr. Uniformly the fresh solutions gave the red sol, but both the naturally and artificially aged samples gave the green sols.

TABLE 1

Precipitation experiments on sols

Sample dialyzed 24 hr.; 10 cc. of gold sol taken in each case; time elapsed after addition of electrolyte = 15 min.

ADDED ELECTROLYTE (1 cc.)	RED SOL	GREEN SOL
0.01 *N* sodium nitrate	Positive	Negative (slight)
0.1 *N* potassium chloride	Positive	Negative
1.0 *N* sulfuric acid	Slight	Negative

0.1 *N* sodium hydroxide caused immediate precipitation in both cases.

These green sols were relatively stable, some of them being preserved in sealed tubes for eight months without coagulation.

A number of precipitation experiments on samples of the red and green sols of comparable strengths was tried. A Tyndall light cone from a brilliant source of illumination was used as the criterion of precipitation. The results of these experiments are summarized in table 1. If the Tyndall effect is listed as positive, the sol had not completely precipitated, while a negative effect signifies that it was optically clear. These results are

---

[1] Received August 27, 1938.

[2] See Holmes, Laboratory Manual of Colloid Chemistry, p. 32. John Wiley and Sons, Inc., New York (1928).

[3] The reference cited in note 2 points out that tannin solutions have a great tendency to develop mold, and suggests the addition of chloroform to prevent it.

PLATE I[2]

FIG. 1. Cell membranes of *Spirogyra sp.* show the presence of crystalline material through their double refraction in polarized light (× 630).

FIG. 2. Spiral fibrils in the cell membrane of a cotton fiber (*Gossypium hirsutum*) in polarized light (× 900).

FIG. 3. Fibrils in the cell membrane of the cotton fiber are arranged parallel to the axis at intervals throughout its length and produce "extinction areas" in polarized light (× 900).

---

[2] Each plate (I to XI) has been reduced by one-quarter in reproduction.

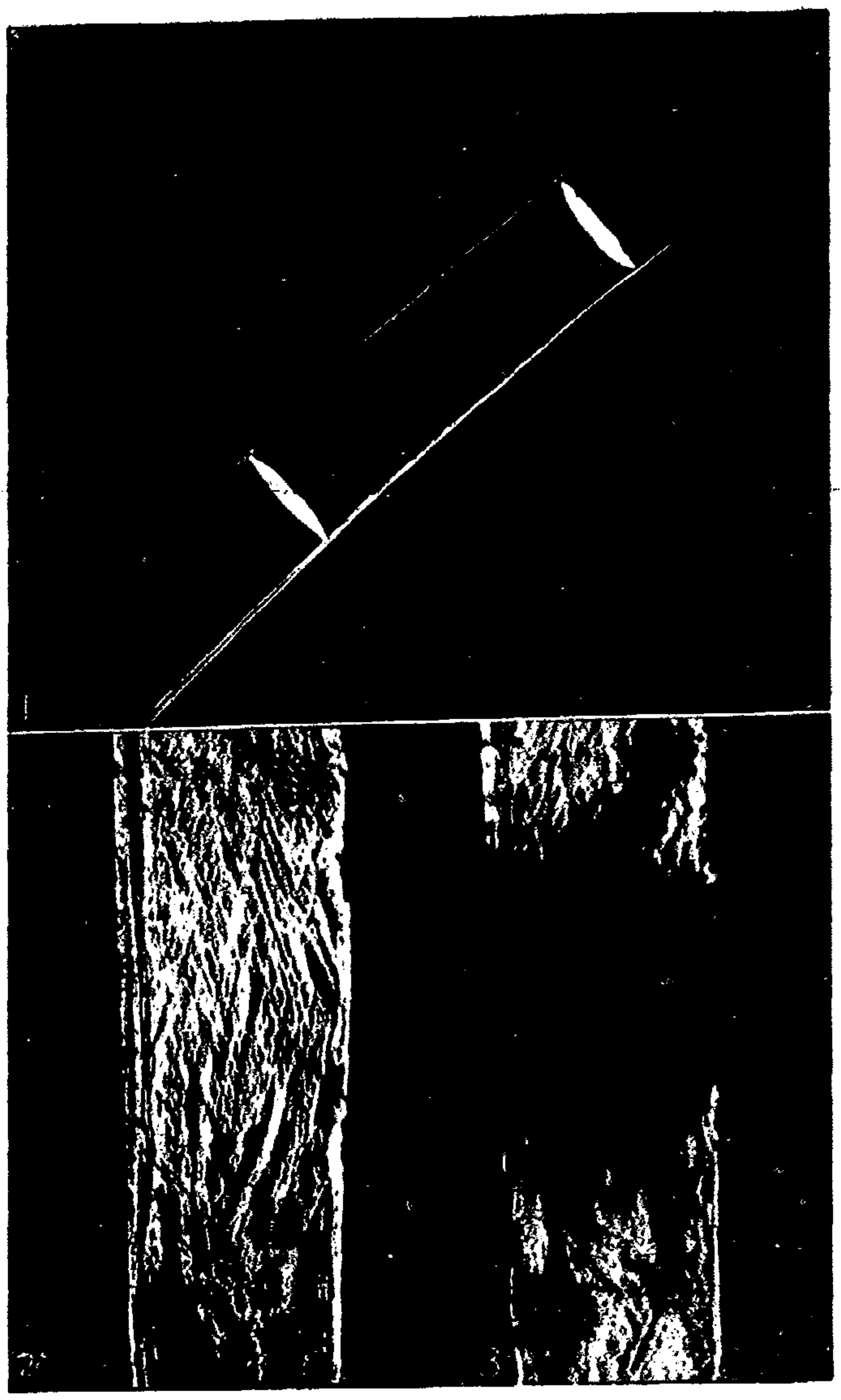

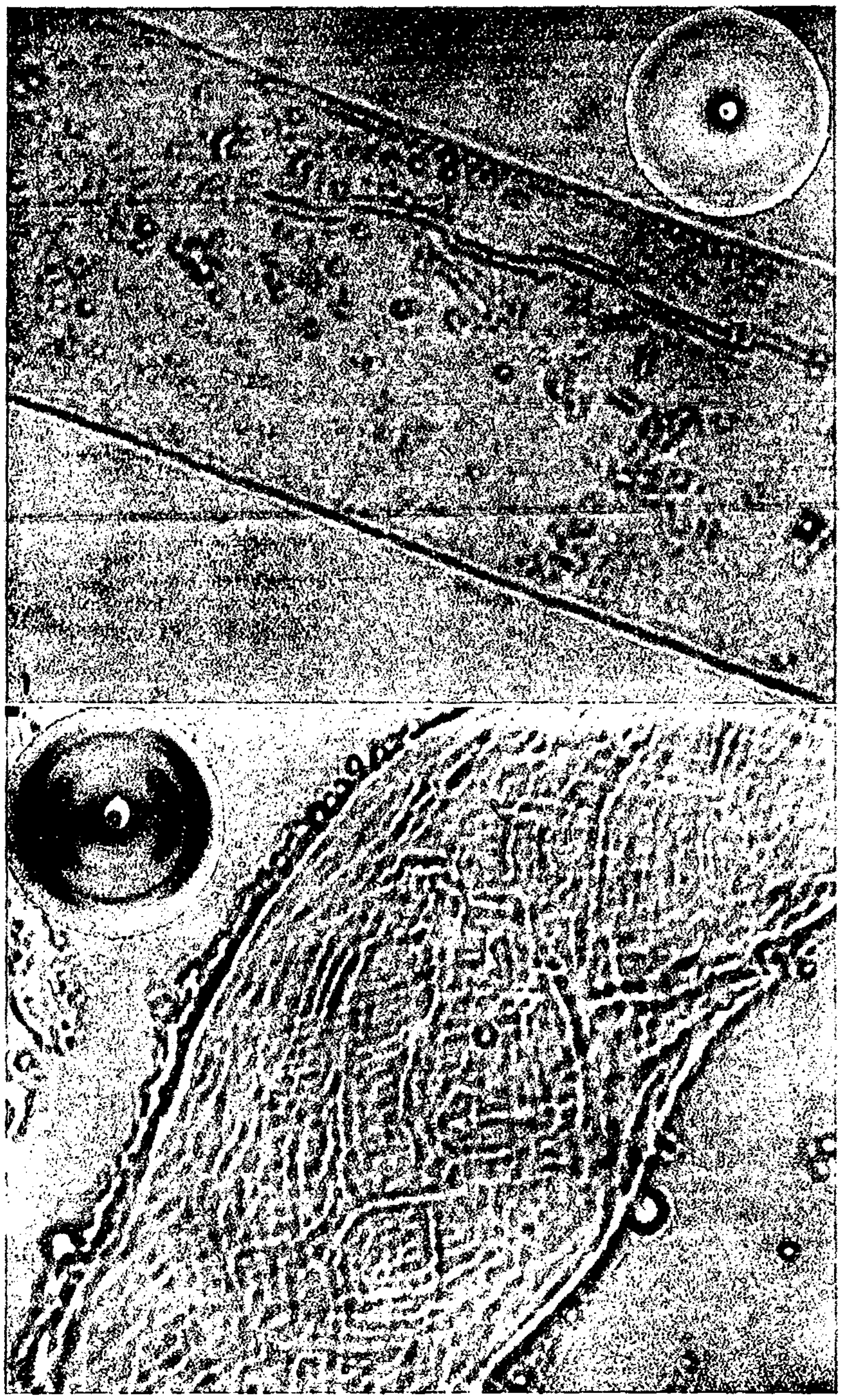

PLATE II

Fig. 1. Cellulose particles, separate and in short chains from the living cotton fiber produce an x-ray diffraction pattern of cellulose in random arrangement (× 1500).

Fig. 2. The cell membrane of a mature cotton fiber produces a diffraction pattern of more regularly oriented cellulose and disintegrates into fibrils and particles identical with those observed in the living cytoplasm (× 1380).

PLATE III

Fig. 1. Cellulose particles and fibrils from the cytoplasm of *Valonia ventricosa* and the x-ray diffraction pattern which they produce when freed from the associated cytoplasmic constituents (× 1380).

Fig. 2. Fibril orientation in the mature membrane of *Valonia ventricosa* is measured directly in the microscope and by means of the x-ray diffraction of the cellulose oriented parallel to the fibril axis (× 1350).


78°

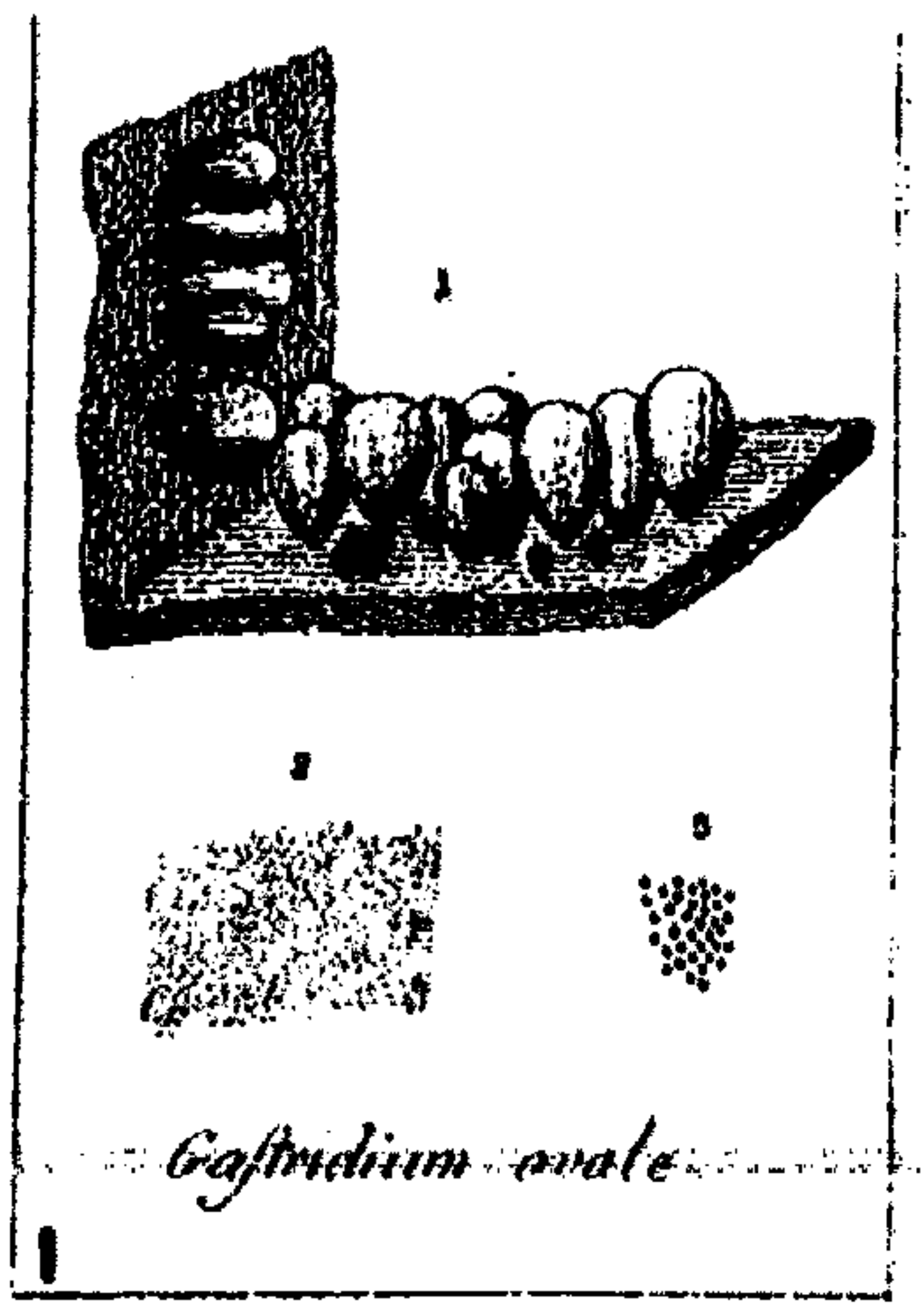

1

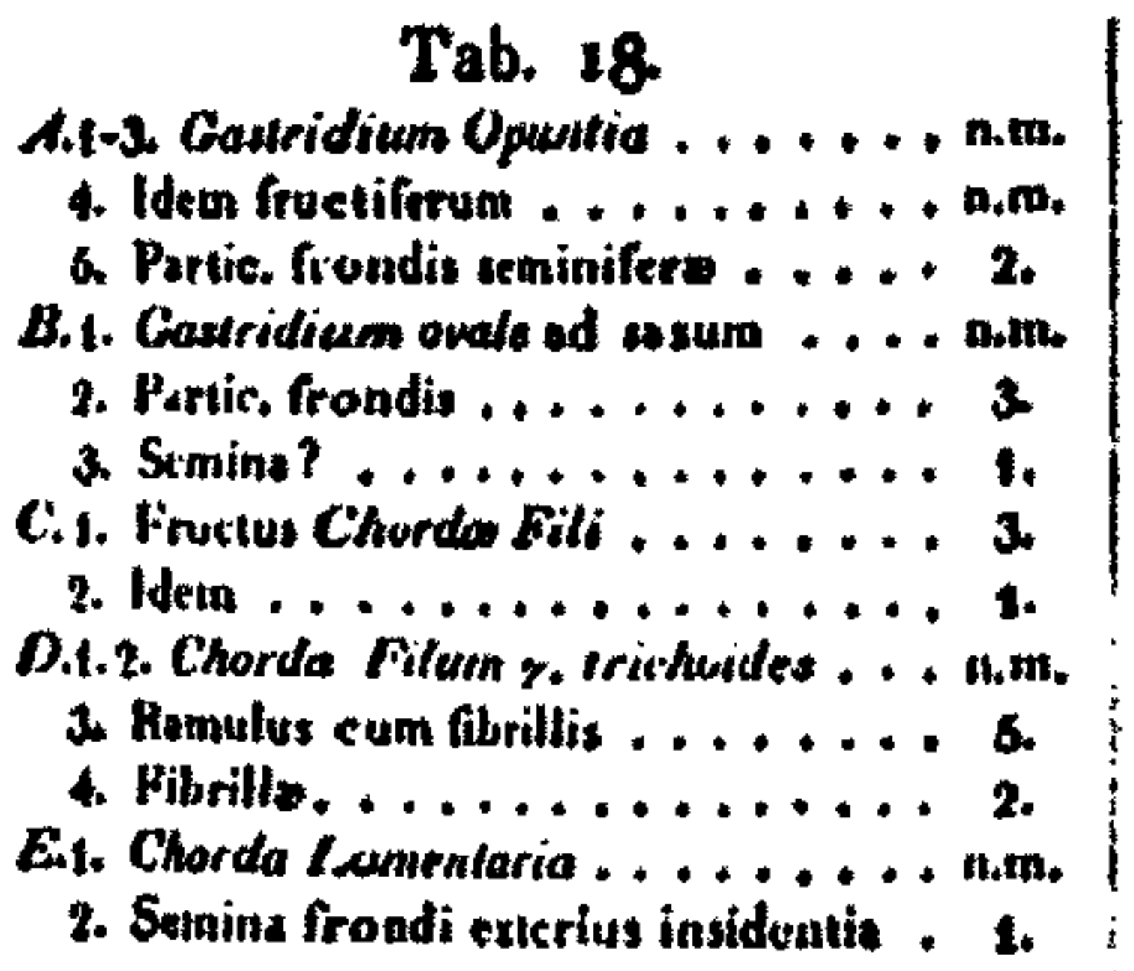

Tab. 18.

A. 1-3.	*Gastridium Opuntia*	n.m.
4.	Idem fructiferum	n.m.
6.	Partic. frondis seminiferæ	2.
B. 1.	*Gastridium ovale* ad saxum	n.m.
2.	Partic. frondis	3.
3.	Semina?	1.
C. 1.	Fructus *Chordæ Fili*	3.
2.	Idem	1.
D. 1.2.	*Chorda Filum γ. trichoides*	n.m.
3.	Ramulus cum fibrillis	6.
4.	Fibrillæ.	2.
E. 1.	*Chorda Lomentaria*	n.m.
2.	Semina frondi exterius insidentia	1.

2

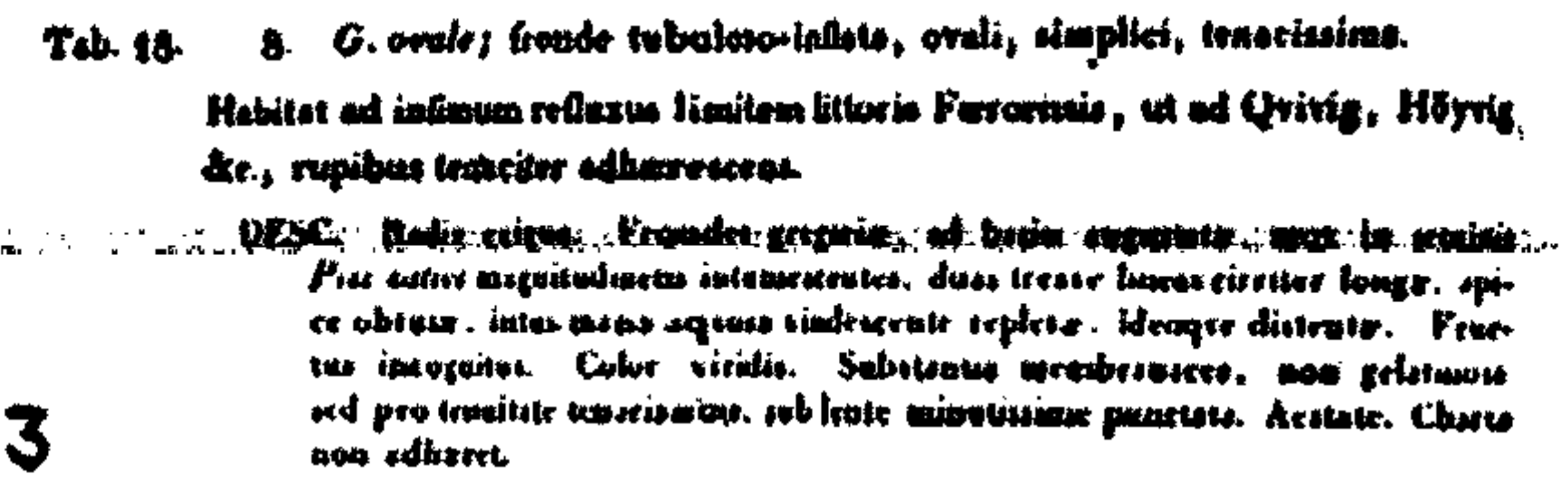

Tab. 18. 8. *G. ovale;* fronde tubuloso-inflata, ovali, simplici, tenacissima.

Habitat ad infimum refluxus limitem littoris Færoensis, ut ad Qvivig, Höyvig &c., rupibus tenaciter adhærescens.

DESC. Radix exigua. Frondes gregariæ, ad basin angustatæ, sunt in statu *Pisi sativi* magnitudinem intumescentes, duas treave lineas circiter longæ, apice obtusæ, intus massa aquosa viridescente repletæ, ideoque distentæ. Fructus incognitus. Color viridis. Substantia membranacea, non gelatinosa sed pro tenuitate tenacissima, sub lente minutissime punctata. Aestate. Chartæ non adhæret.

3

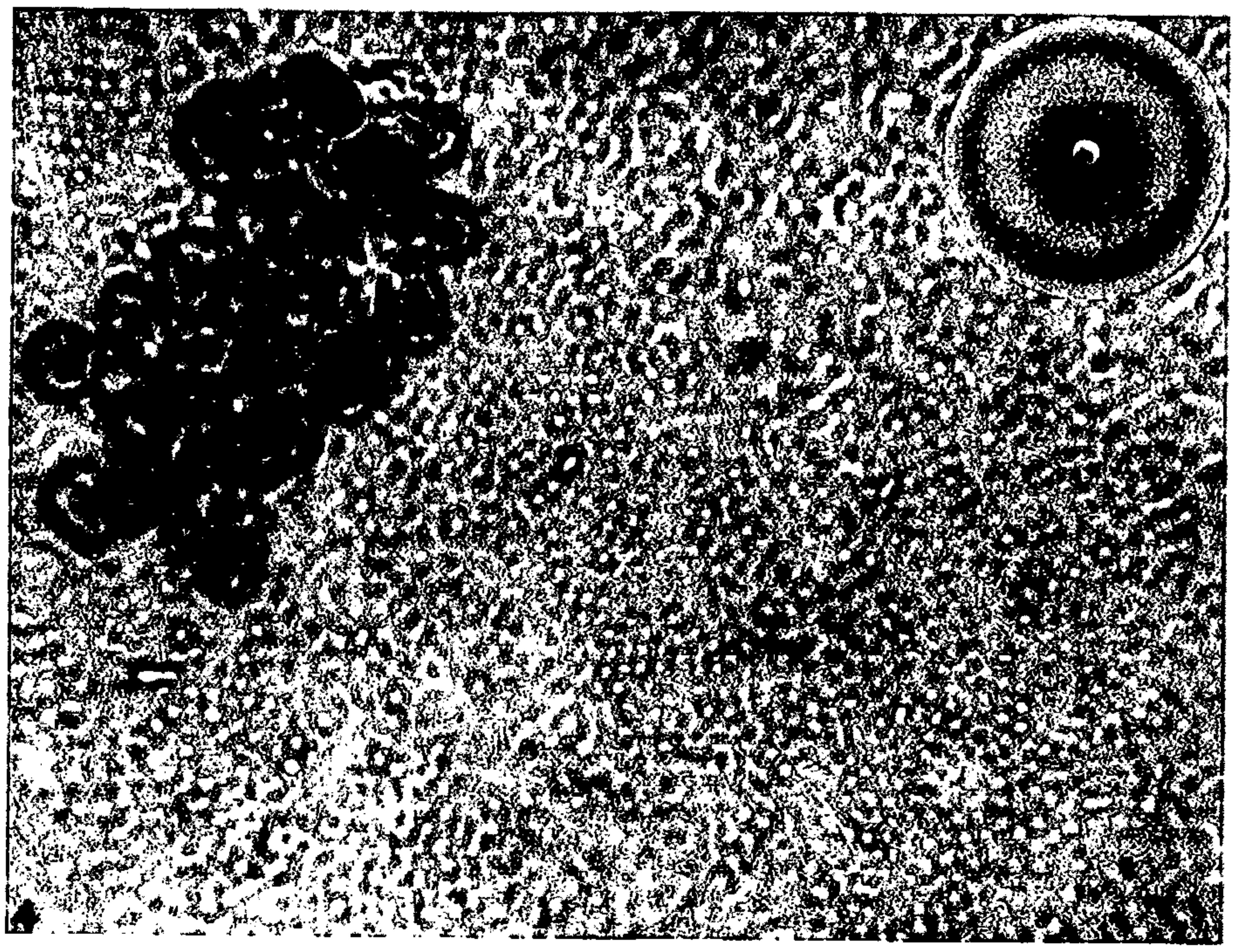

PLATE IV

Figs. 1, 2, and 3. Copies of a plate and text-descriptions from Lyngbye (1819). *Gastridium ovale* was renamed *Halicystis ovalis* in 1901.

Fig. 4. Cellulose particles in the inner layer of a membrane of *Halicystis ovalis* in random arrangement. A cluster of dark green plastids is attached to the membrane. The x-ray diagram of the untreated membrane with the beam perpendicular to the surface is that of mercerized cellulose in random arrangement (× 1400).

PLATE V

FIG. 1. A cross section of the membrane of *Halicystis ovalis* shows that single layers of cellulose particles make up the true lamellae (× 1120). The x-ray beam parallel to the surface produces a diffraction pattern of partially oriented, mercerized cellulose.

FIG. 2. Parallel ridges produced by pressure perpendicular to the surface upon the swollen membrane of *Halicystis* (× 1120).

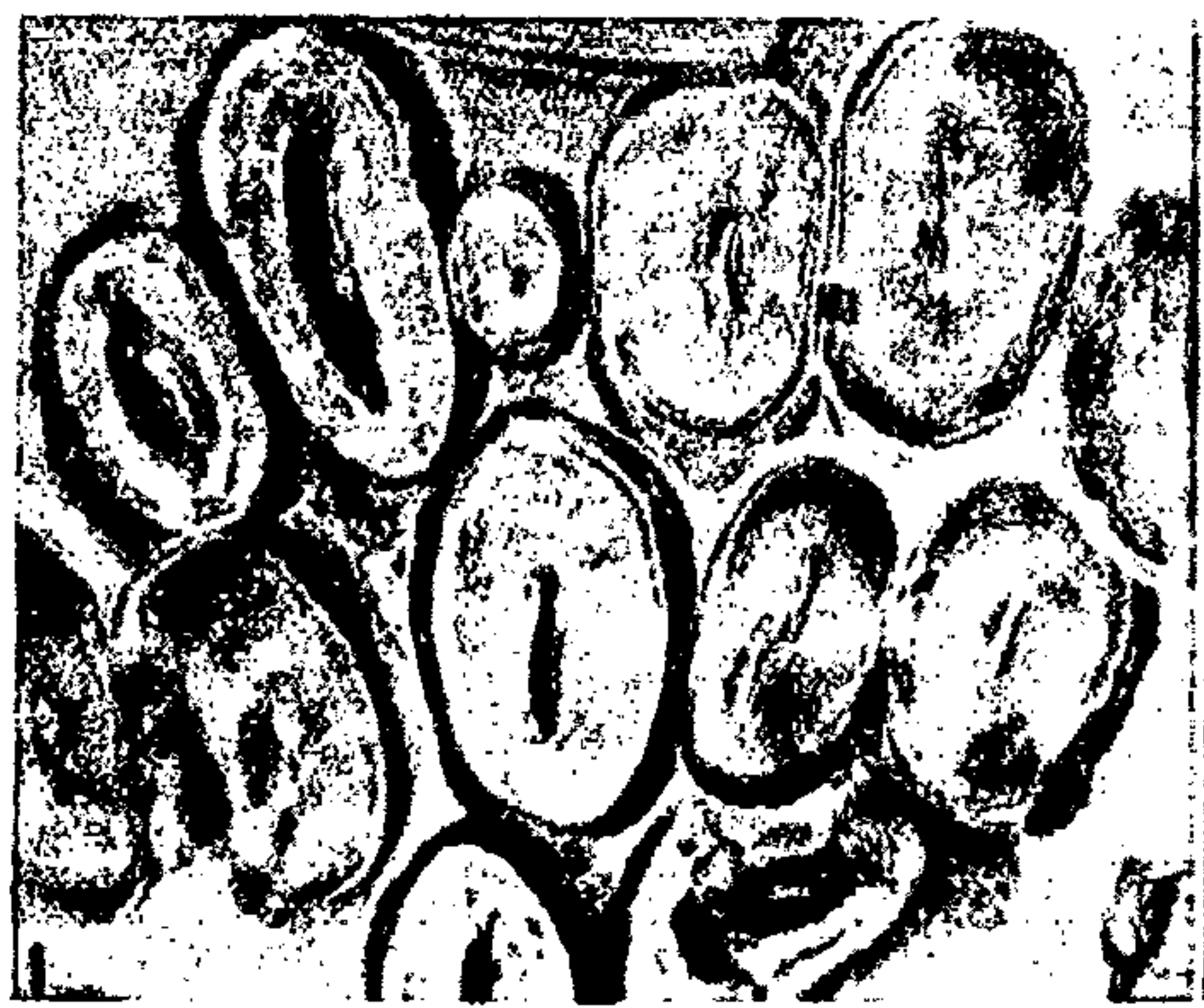
1


2

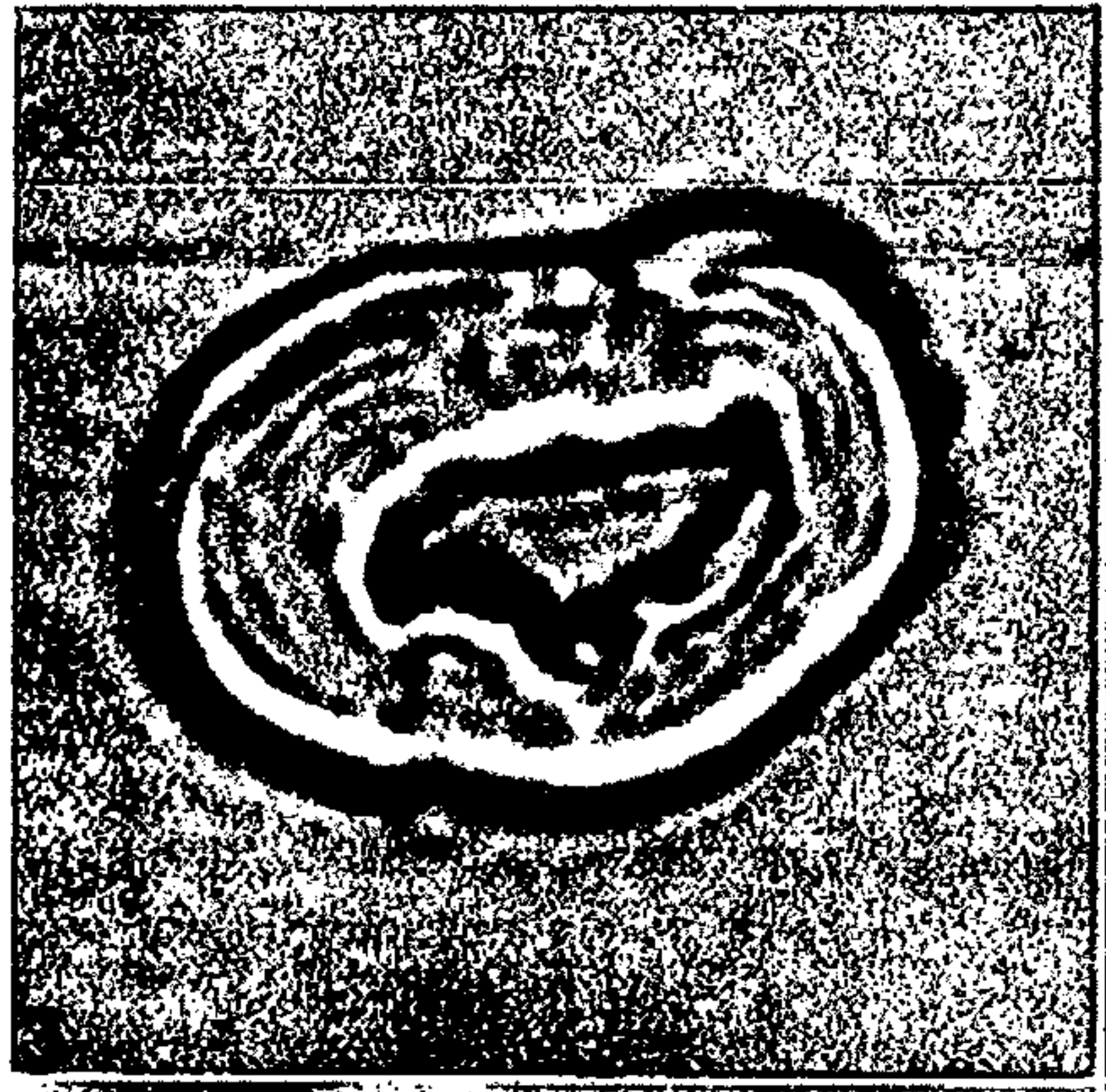

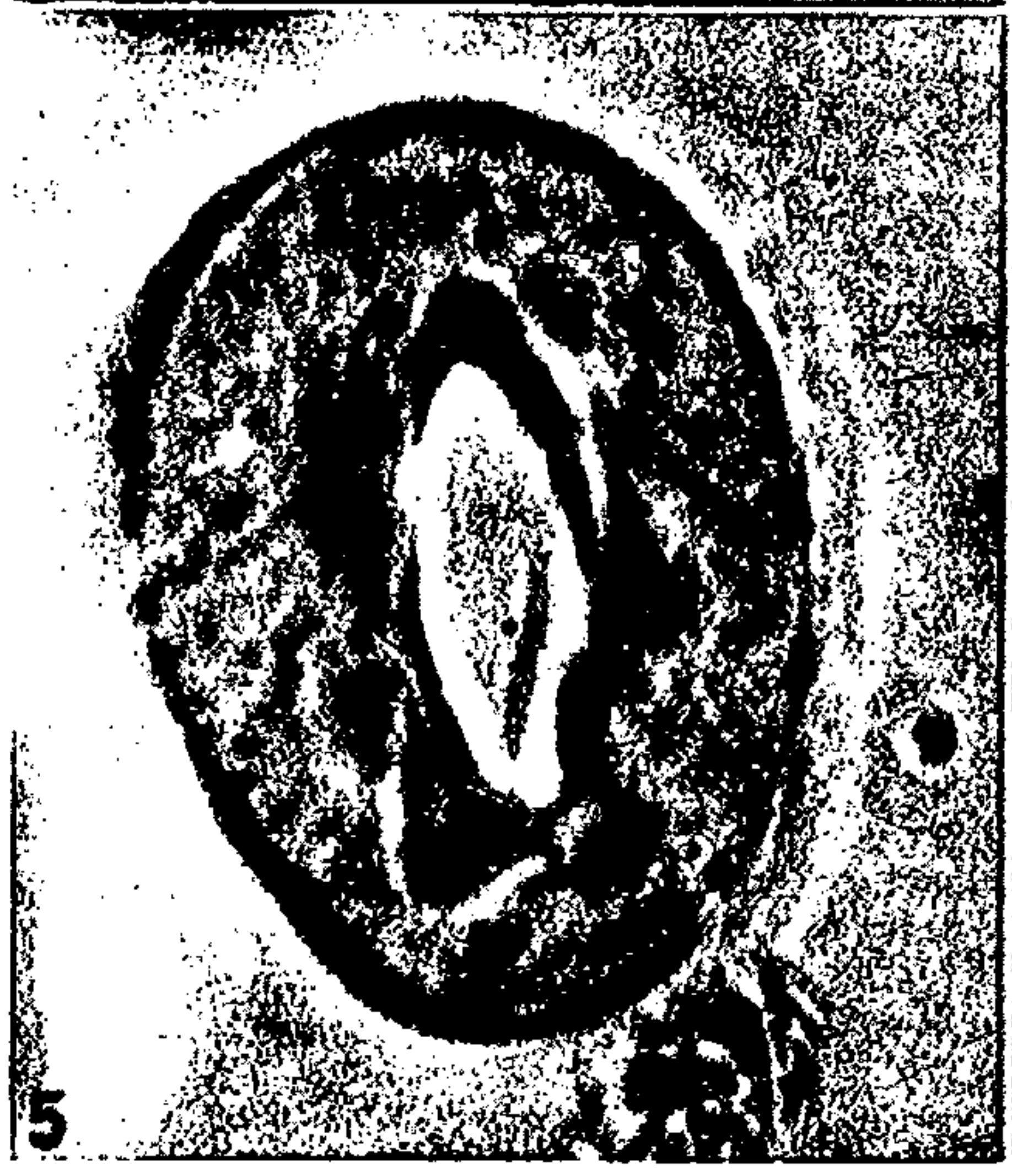
5

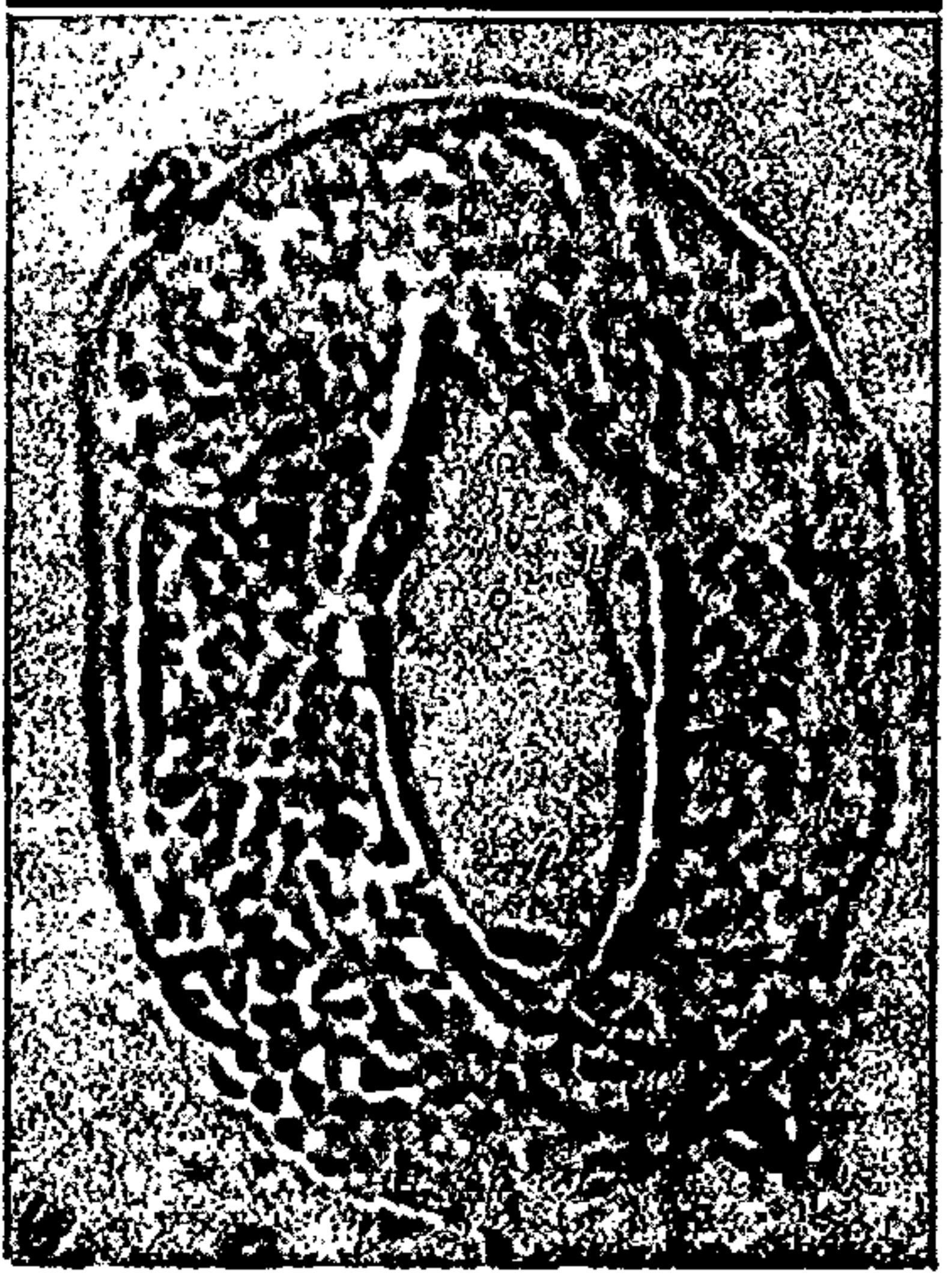
6

PLATE VI

FIG. 1. Cross sections of cotton fibers, 2 to 3 μ in thickness, show marked variations in size and shape (× 920).

FIG. 2. An early stage of swelling in cuprammonium hydroxide (× 920).

FIG. 3. A later stage of swelling of a section through a region where the fibrils are arranged at an angle with the fiber axis. The lamellae are visible but the swelling of the section is irregular (× 1600).

FIG. 4. A section across a region where the fibrils run parallel to the fiber axis. Swelling is more regular (× 1500).

FIG. 5. In a later stage the rapidly swelling cementing material distorts the lamellae and obscures the particles (× 1400).

FIG. 6. Continued washing with cuprammonium hydroxide carries away the swollen cementing material and the particles are more clearly visible (× 1300).

PLATE VII

FIG. 1. Early stages of swelling of thick cross sections (10 to 15 μ) of cotton fibers in cuprammonium hydroxide (× 1050). Two examples of type 1 and one of type 2 are shown.

FIG. 2. A late stage of swelling of type 1 (× 1030).

FIG. 3. A late stage of swelling of type 2 (× 1000).

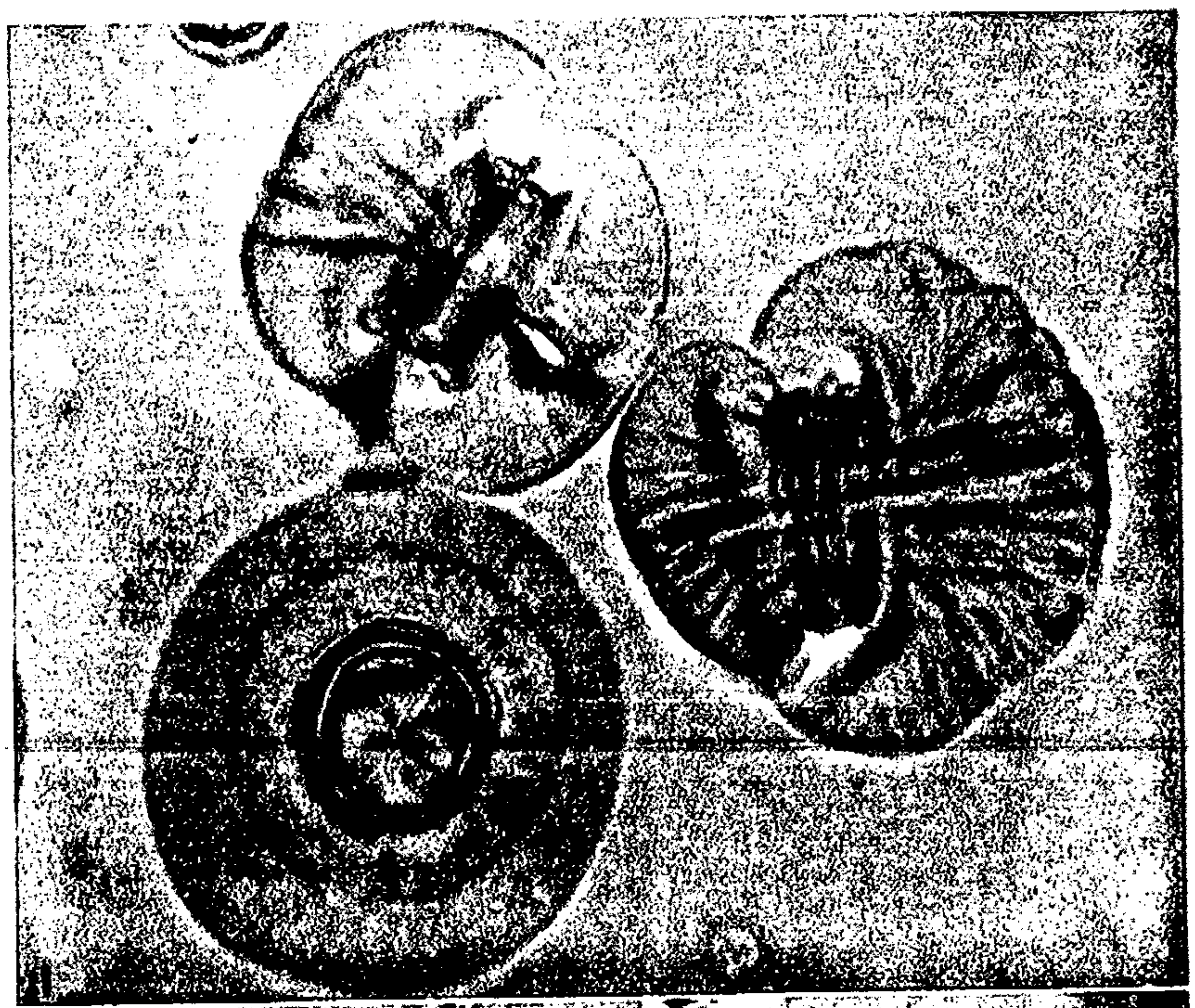

1

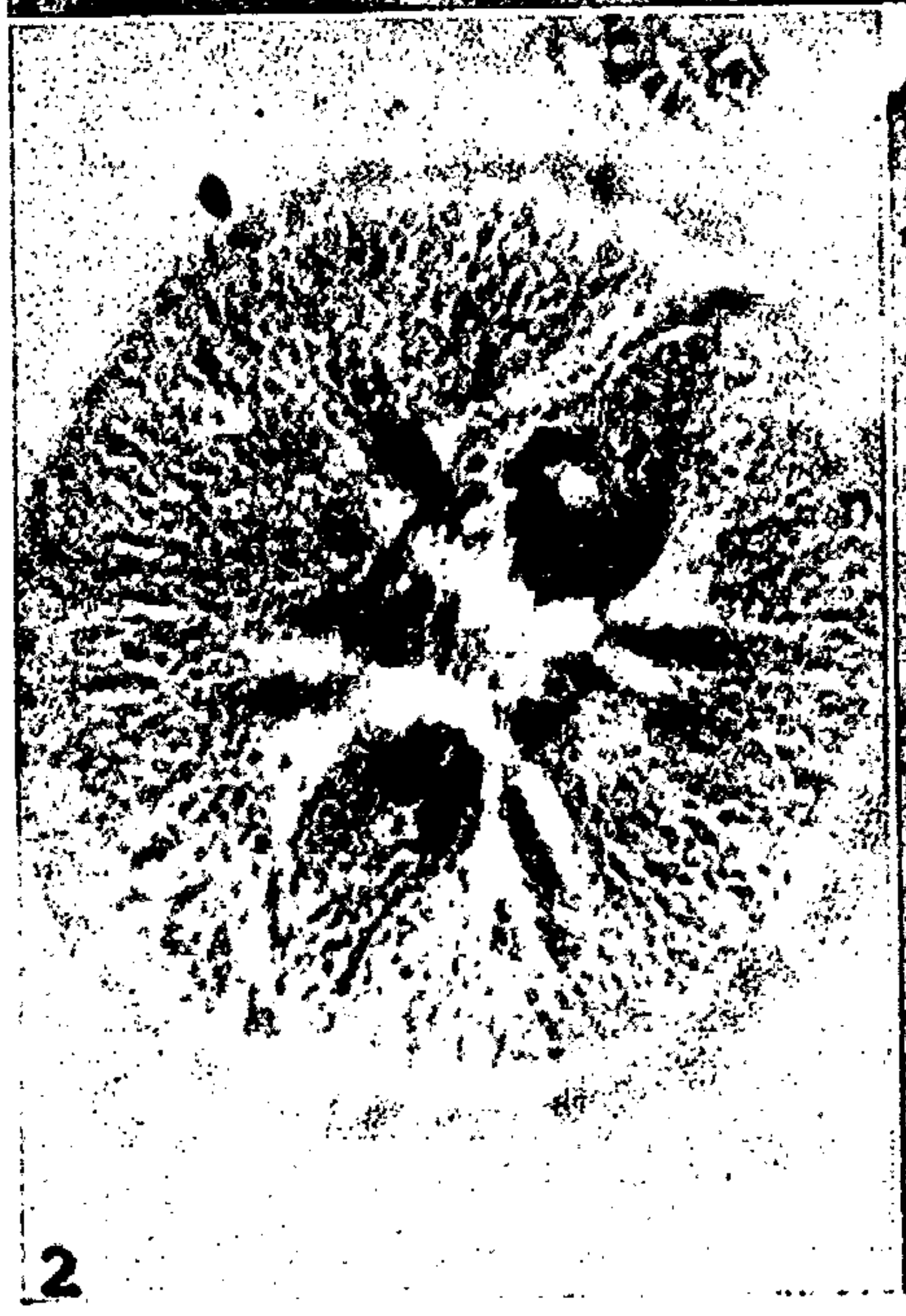

2

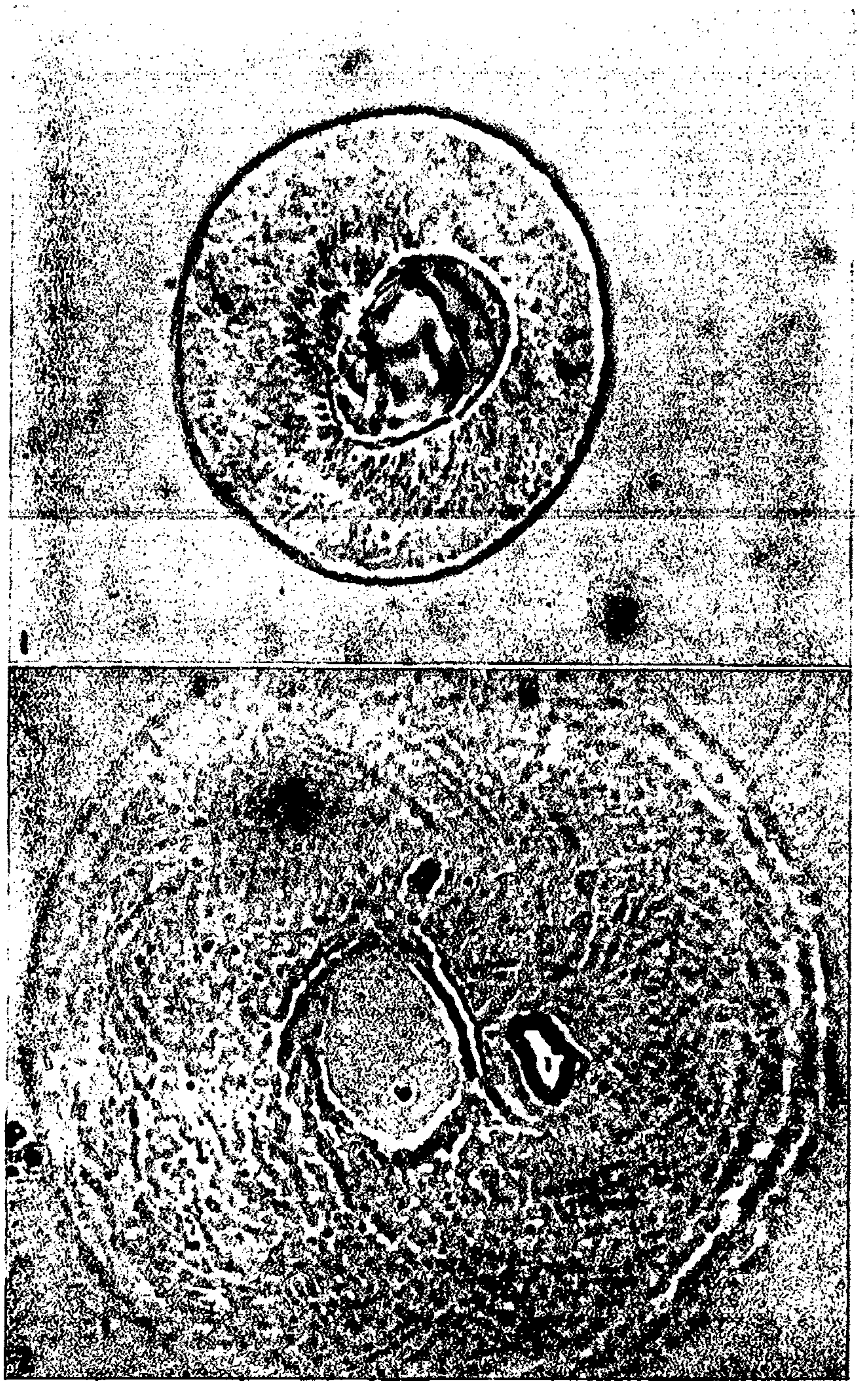

PLATE VIII

FIG. 1. An early stage of swelling of type 3. Crossed-spiral arrangement of fibrils upon surface of the lantern-like structure are visible (× 1050).

FIG. 2. A late stage of swelling of type 3. No "growth rings" are visible at any stage of swelling without pressure (× 1380); cf. plate IX, figure 1, for pressure artifacts.

PLATE IX

Fig. 1. The effect of pressure upon the cover slip during the swelling of type 3 is to produce a series of concentric "growth rings" with the central ring of cuticle as a point of origin (× 1100).

Fig. 2. When the lantern-like structure is turned upon its side, both rings of cuticle act as points of origin (× 700).

PLATE X

FIG. 1. Gum tragacanth swollen with water. Pressure upon the cover glass produces the parallel ridges radiating out from a small mass of foreign material as a point of origin (× 1200).

PLATE XI

FIG. 1. Polarized light. Cross section of cotton seed showing absence of starch in epidermal cells (a) from which fibers are formed and outer epidermis (c) of inner integument. Starch is present in cells of both outer (b) and inner (d) integument (× 743).

FIG. 2. Starch is absent in young fibers and epidermal cells from which they are formed. Starch grains are being formed in certain cells of the outer integument (× 1000).

FIG. 3. A cross section of cells from the inner integument shows large compound starch grains in the interior of the cells and cellulose particles in the membranes (× 1050).

COMMUNICATION TO THE EDITOR

ATTEMPTS TO PREPARE GREEN GOLD SOLS[1]

In attempting to prepare red gold sols by the method suggested by Ostwald,[2] namely, reduction of gold chloride solution by tannic acid in the presence of potassium carbonate, repeated trials resulted in a sol of a definitely green color. Suspicion pointed to the tannic acid solution which had been on the side-shelf for a long period of time.[3] In order to check this point, the experiments were repeated with freshly made solutions of tannic acid, and again with samples of this substance which were (*1*) allowed to age naturally exposed to air and (*2*) artificially aged by being bubbled with air for periods of 48 hr. Uniformly the fresh solutions gave the red sol, but both the naturally and artificially aged samples gave the green sols.

TABLE 1

Precipitation experiments on sols

Sample dialyzed 24 hr.; 10 cc. of gold sol taken in each case; time elapsed after addition of electrolyte = 15 min.

ADDED ELECTROLYTE (1 cc.)	RED SOL	GREEN SOL
0.01 *N* sodium nitrate	Positive	Negative (slight)
0.1 *N* potassium chloride	Positive	Negative
1.0 *N* sulfuric acid	Slight	Negative

0.1 *N* sodium hydroxide caused immediate precipitation in both cases.

These green sols were relatively stable, some of them being preserved in sealed tubes for eight months without coagulation.

A number of precipitation experiments on samples of the red and green sols of comparable strengths was tried. A Tyndall light cone from a brilliant source of illumination was used as the criterion of precipitation. The results of these experiments are summarized in table 1. If the Tyndall effect is listed as positive, the sol had not completely precipitated, while a negative effect signifies that it was optically clear. These results are

---

[1] Received August 27, 1938.

[2] See Holmes, Laboratory Manual of Colloid Chemistry, p. 32. John Wiley and Sons, Inc., New York (1928).

[3] The reference cited in note 2 points out that tannin solutions have a great tendency to develop mold, and suggests the addition of chloroform to prevent it.

typical of many different experiments with varying times and concentrations of added electrolytes, and were essentially the same whether the samples were previously dialyzed or not. In all cases the green gold sol precipitated more completely in a given time than the red.

Attempts were made to separate portions of the aged tannic acid by fractional dialysis. However, when each of these fractions was separately used for reducing gold chloride in a similar manner, green sols invariably resulted. In other words, our attempts to isolate the different possible oxidation products which might be responsible for the two kinds of sols were unsuccessful. Nevertheless, we feel that the experiments were of sufficient interest to justify their being recorded.

HAROLD B. FRIEDMAN.
J. JOE DAVIS, JR.

Department of Chemistry
Georgia School of Technology
Atlanta, Georgia

THE SYSTEM FERRIC OXIDE-SULFUR TRIOXIDE-WATER

F. W. KOERKER[1] AND H. N. CALDERWOOD[2]

Department of Chemistry, University of Wisconsin, Madison, Wisconsin

Received July 20, 1938

INTRODUCTION

Although the system ferric oxide–sulfur trioxide–water has been studied *in extenso* by many investigators (2), the literature reveals no data for temperatures below 18°C. This paper reports an extension of the study to 15°C., together with some observations on preliminary work at 10°C.

EXPERIMENTAL

Reagents

Analytical grade ferric sulfate and sulfuric acid were used throughout, their purity being determined before use by analysis. The ferric oxide was prepared by the method of Appleby and Wilkes (1). Specially purified distilled water was used for all dilutions.

As the work progressed, it was found that the preliminary mixing of reagents in the form of pastes permitted a closer estimation of the amounts necessary to obtain workable quantities of solid and liquid phases than did simply mixing the solids and liquids.

Method

Weighed samples in sealed glass bottles agitated in a constant-temperature bath for various lengths of time and allowed to settle there were filtered while still in the bath, using a fritted glass filter and the method of Campbell and Slotin (3), and were then analyzed. Disappearance of the liquid phase from the filter frequently required filtration for 6 hr., and even then the solids, although a friable cake, still contained varying amounts of the liquid phase. The minimum time which Appleby and Wilkes report as necessary to establish equilibrium was found applicable to only the basic and neutral regions at 15°C., much longer periods of time being necessary in the acid region. As the system approached the neutral region the liquid phase became deep red, but showed no Tyndall effect with the ultramicroscope until the system was definitely in the basic region.

---

[1] Present address: Dow Chemical Company, Midland, Michigan.

[2] Present address: 3105 Cross Street, Madison, Wisconsin.

The data obtained at 10°C. are compiled in table 1, while table 2 contains the results of the work at 15°C., also shown graphically in figure 1.

DISCUSSION OF RESULTS

The results obtained at 10°C. show that the solids from the acid region of the system were more acid in character than those obtained by Appleby and Wilkes at 18°C., and their composition indicates solid solutions of ferric sulfate with sulfuric acid rather than definite compounds. Such an occurrence is very probable, since the freezing points of sulfuric acid and its monohydrate ($H_2SO_4 \cdot H_2O$) are 10.49°C. and 8.62°C., respectively (4).

TABLE 1

Composition of the solutions, the corresponding residues, and the solid phases in the the system ferric oxide-sulfur trioxide-water at 10°C.

SOLUTION		RESIDUE		SOLID PHASES
Fe_2O_3	SO_3	Fe_2O_3	SO_3	
per cent	*per cent*	*per cent*	*per cent*	
2.76	4.12	20.09	30.00	Solid solution
7.32	12.59	29.20	25.80	
16.30	25.88	21.21	34.60	
2.23	16.19	8.38	29.80	$Fe_2O_3 \cdot 2.44SO_3 \cdot 8.65H_2O$
6.70	31.27	13.92	38.82	
0.00	37.23	11.54	38.26	Solid solution
0.05	43.95	8.54	43.90	
0.04	43.50	13.43	45.40	
0.04	45.00	9.61	54.15	
0.27	48.40	8.60	50.60	
0.41	50.10	10.53	53.70	
0.04	74.50	6.54	73.10	

The study at 15°C. shows that the compounds formed are analogous to those formed at 18°C. and 25°C. In the basic region at 15°C. the solid solutions appear to be less basic than those formed at higher temperatures, but are otherwise entirely similar to those reported for other temperatures and require no discussion beyond that available in the literature. Basic compounds appear to be absent from the system at 15°C., since the point *E*, an experimentally determined value, represents, within the limits of error, a compound having the composition of the neutral salt. Point *A*, determined by the method of Baskerville and Cameron, represents the octadecyl hydrate of the neutral salt. In the acid region equilibrium was established very slowly, and consequently the data are less reliable. At 15°C. the concentration of acid which renders iron insoluble is lower than the concen-

TABLE 2

Composition of the solutions, the corresponding residues, and the solid phases in the system ferric oxide–sulfur trioxide–water at 15°C.

SOLUTION		RESIDUE		SOLID PHASES	TIE LINE LOCUS*
Fe_2O_3	SO_3	Fe_2O_3	SO_3		
per cent	*per cent*	*per cent*	*per cent*		
12.46	16.60	32.70	14.17	Solid solutions	None
14.61	21.23	20.30	11.86		
15.70	23.05	24.40	35.75		
16.70	22.38	56.50	12.28		
16.63	24.00	42.50	31.88		
17.61	26.45	19.80	28.70		
16.10	25.40	21.24	34.45	$Fe_2O_3 \cdot 3SO_3 \cdot 18H_2O$	A
15.86	24.98	18.26	28.20		
14.47	26.15	18.05	28.60		
14.20	28.25	15.23	29.12		
10.30	30.90	13.65	35.41	$Fe_2O_3 \cdot 4.46SO_3 \cdot 19.2H_2O$?	C
7.25	32.31	16.99	42.82		
2.48	35.23	11.58	41.47		
0.80	36.40	11.01	41.80		
0.01	37.20	9.33	39.40		
3.59	30.60	13.02	39.96	$Fe_2O_3 \cdot 5.84SO_3 \cdot 30H_2O$?	D
0.77	34.80	11.12	41.70		
0.01	37.20	9.33	39.40		
13.18	32.84	23.68	41.32	$Fe_2O_3 \cdot 3.3SO_3 \cdot 10.3H_2O$	B
10.04	33.21	21.55	40.05		
2.48	35.23	11.58	41.47		
0.80	36.40	11.01	41.80		
0.01	37.20	9.33	39.40		
7.02	29.39	14.99	42.33	Supersaturated for	D
0.98	30.32	8.84	42.89	Unsaturated for	D
18.81	32.98	59.13	35.08	An irregular value	
14.09	33.80	24.62	39.06	Supersaturated for	B
17.11	31.01	40.12	47.47	Supersaturated for	A
18.75	31.94	38.60	37.41	Supersaturated for	A
15.65	42.27	23.92	42.09	Supersaturated for	B
17.75	31.85	43.06	44.03	Supersaturated for	A

* See figure 1 for the locations of these loci.

Analysis of the ferric sulfate: Fe_2O_3, 30.21 per cent; SO_3, 45.51 per cent.

trations necessary to produce insolubility at 18° and 25°C. In the present study the only rational formula indicated for the acid region is the one at point *D* in figure 1, and is approximately $Fe_2O_3 \cdot 6SO_3 \cdot 30H_2O$.

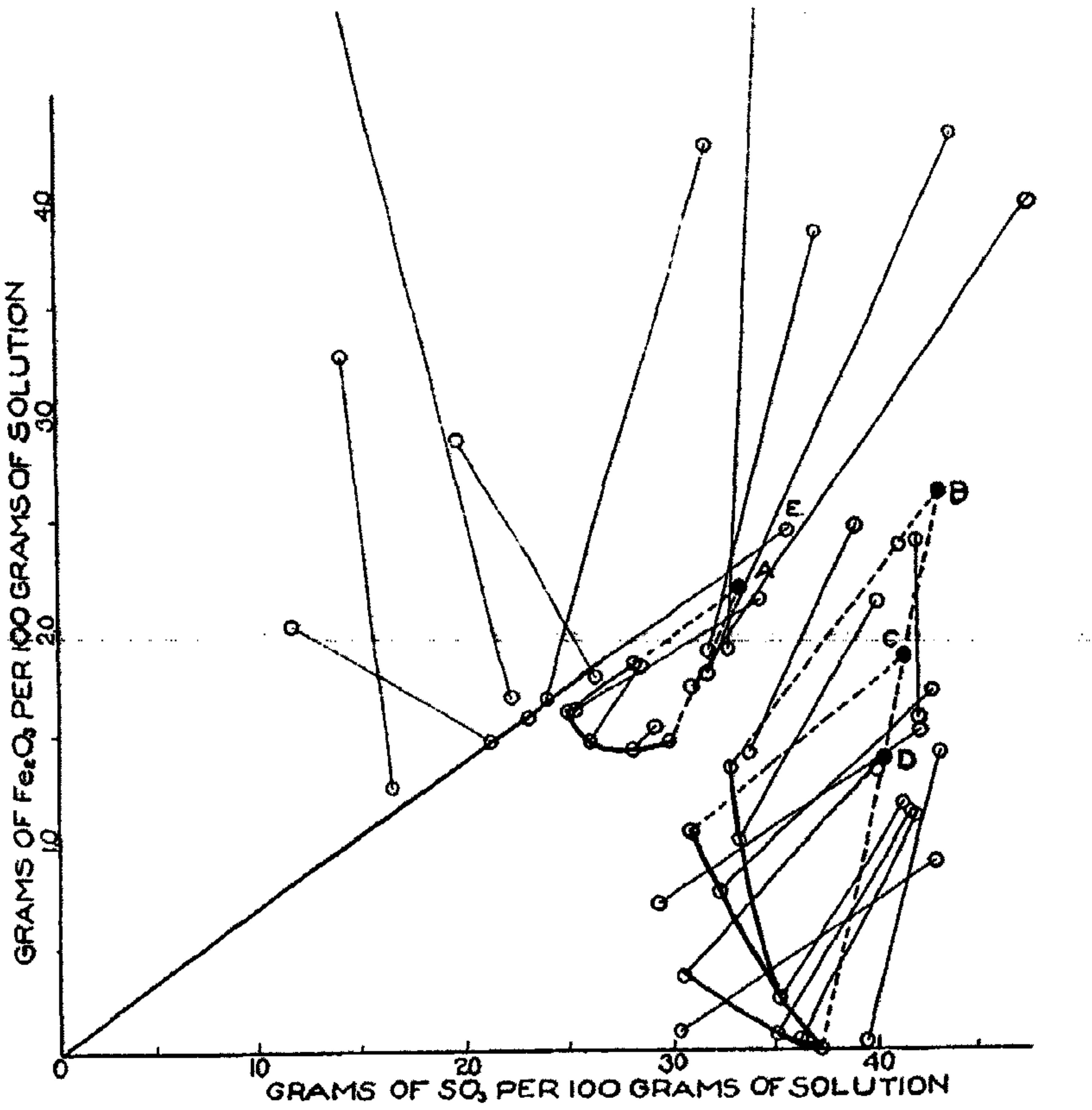

Fig. 1. Solubility curves, residues, tie lines, and solid phase in the system ferric oxide-sulfur trioxide-water at 15°C.

A, $Fe_2O_3 \cdot 3.0SO_3 \cdot 18.0H_2O$ B, $Fe_2O_3 \cdot 3.3SO_3 \cdot 10.3H_2O$
C, $Fe_2O_3 \cdot 4.46SO_3 \cdot 19.2H_2O$ D, $Fe_2O_3 \cdot 5.84SO_3 \cdot 30.0H_2O$
E, $Fe_2O_3 \cdot 2.93SO_3 \cdot 17.8H_2O$

SUMMARY

At 10°C., in the system ferric oxide-sulfur trioxide-water, the ferric sulfate and sulfuric acid appear to form solid solutions rather than acid salts when the concentration of sulfur trioxide exceeds 37 per cent. At 15°C. the system does not appear to form basic salts.

In the neutral region the salt formed appears to be the octadecyl hydrate.

In the acid region the information is too meager to justify definite statements, but the existence of a salt of the composition $Fe_2O_3 \cdot 6SO_3 \cdot 30H_2O$ is indicated.

The compounds formed at 15°C. appear to be more highly hydrated than those formed at 18° and 25°C.

Iron becomes insoluble in a lower concentration of sulfuric acid at 15°C. than at 18° or 25°C.

REFERENCES

(1) Appleby and Wilkes: J. Chem. Soc. **121**, 337 (1922).
(2) Baskerville and Cameron: J. Phys. Chem. **39**, 769 (1933).
(3) Campbell and Slotin: J. Am. Chem. Soc. **56**, 3961 (1933).
(4) International Critical Tables, Vol. I, p. 107. McGraw-Hill Book Co., Inc., New York (1926).

LODOCHNIKOV'S METHOD OF REPRESENTING POLYNARY SYSTEMS[1]

MERLE RANDALL AND BRUCE LONGTIN

Department of Chemistry, University of California, Berkeley, California

Received July 7, 1938

I. QUATERNARY SYSTEMS

A novel method of representing the phase relations in quarternary systems, using a two-dimensional diagram, has been described by Lodochnikov (1, 2, 3).[2,3] The method possesses certain obvious advantages and other serious disadvantages. One of the principal disadvantages is the difficulty with which the meaning of the diagrams may be visualized. In this paper we shall attempt to simplify Lodochnikov's presentation by showing the geometrical relationships that exist between his diagrams and familiar projections of tetrahedral phase models. As far as possible we shall use conventions and symbols which parallel American usage.

Lodochnikov's method

Lodochnikov's method consists essentially in representing each composition (N_1, N_2, N_3, N_4) of a single phase by two points in a triangular diagram. He uses the equilateral right triangle (OAB in figure 1) of Roozeboom (5). On the vertical axis he plots the mole fraction, N_3, of the component X_3.

Along the horizontal line $\overline{PR}$ at this height he lays off the distance $\overline{PS}$ from the vertical axis, equal to the mole fraction, N_2, of the component X_2. From the point Q, in which the diagonal side of the triangle intersects $\overline{PR}$, he lays off the distance $\overline{QT}$ in a negative direction, equal to the mole fraction, N_1, of the component X_1. Lodochnikov considers the line segment $\overline{ST}$ as a *vector* by which he represents the composition of the phase.

Since $\overline{QR} = \overline{RA} = N_3$, and the distance $\overline{OA} = \overline{PR}$ is taken as unity, the distance $\overline{ST}$ represents the mole fraction, N_4, of the fourth component, X_4, in the phase. The same property holds when the compositions are

---

[1] Clerical assistance of the Works Progress Administration of the United States Government is gratefully acknowledged. (OP-465-03-3-147)

[2] Reference 1 includes a lengthy review of methods of representing multicomponent systems.

[3] Reference 3 describes construction for five-, six- seven-, eight-, etc., component systems.

expressed in weight fractions (or in weight per cent if we take $\overline{OA}$ equal to 100 per cent).

Since $\overline{PT}$ is therefore equal to ($N_2 + N_4$), the two points which he plots have the coördinates ($X = N_2$, $Y = N_3$) and ($X' = N_2 + N_4$, $Y = N_3$) respectively. The diagram may be obtained directly by plotting two points with these coördinates.

Lodochnikov also proposed the use of an equilateral triangle, as shown in figure 2, but prefers the right triangle. While there are a number of reasons why the right triangle should be preferred (in addition to less expense for paper), the authors feel that the equilateral triangle is too firmly established in American usage to be replaced.

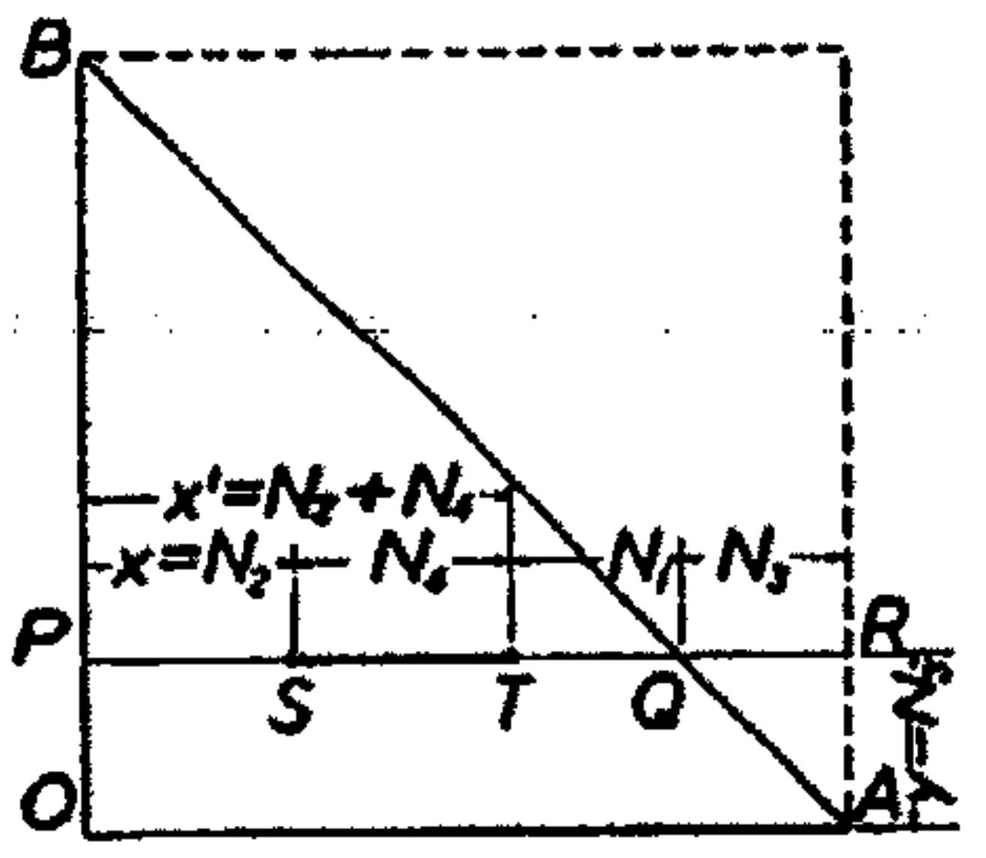

FIG. 1

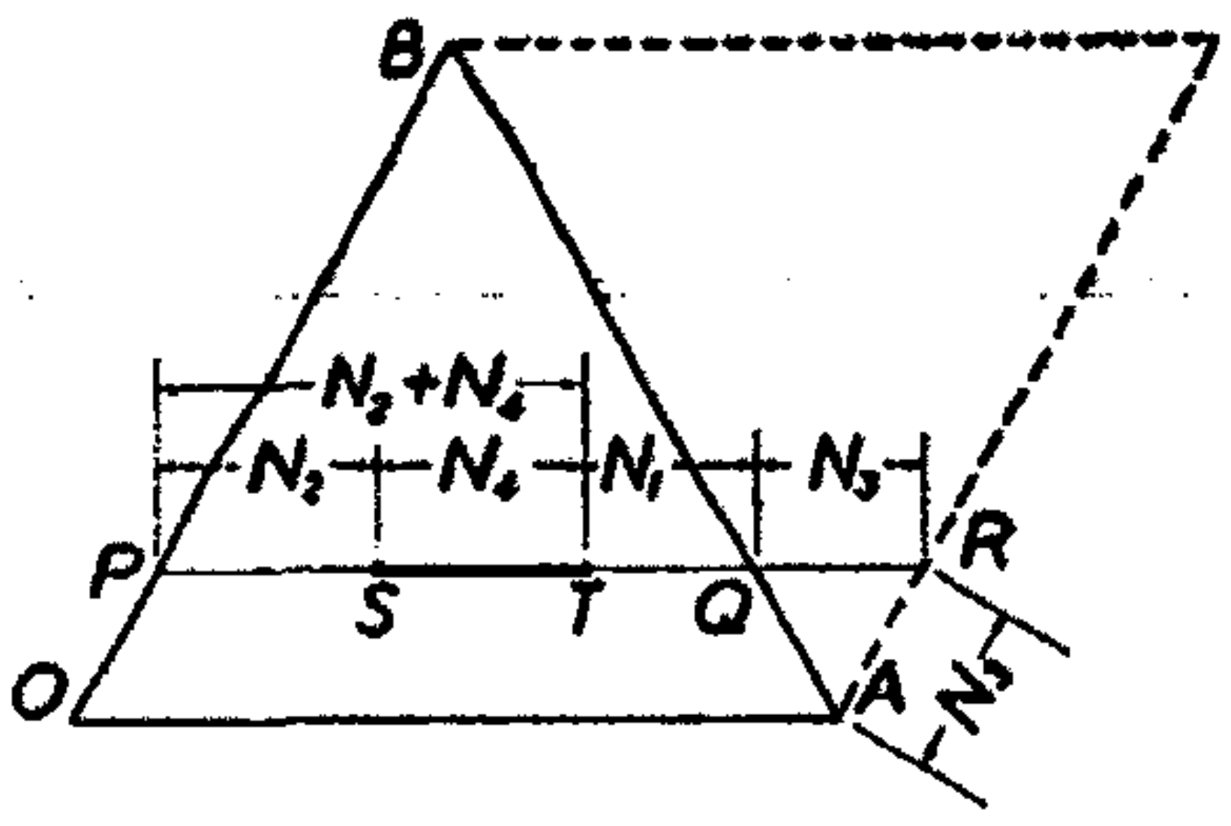

FIG. 2

FIG. 1. Lodochnikov's representation in Roozeboom's right triangle
FIG. 2. Lodochnikov's representation in Gibbs' equilateral triangle

Tetrahedral coördinates

It is customary to use a tetrahedral model or one of its projections in representing quarternary systems. Tetrahedral (as well as triangular) coördinates[4] were first proposed by the astronomer Möbius (4) in his geometric studies of the center of gravity. He showed that if we place the masses X_1, X_2, X_3, and X_4 at the vertices of a regular tetrahedron whose altitudes are unity, each of the perpendicular distances from the center of gravity to a face of the tetrahedron is equal to the ratio of the mass situated at the opposite vertex to the total masses. For instance in figure 3, if G is the center of gravity, then the perpendicular distance h_3 is equal to the ratio $X_3/(X_1 + X_2 + X_3 + X_4)$.

If we pass a plane through the center of gravity parallel to one of the faces of the tetrahedron, it cuts off equal intercepts on the three edges of the tetrahedron, which are proportional to the distance, h, between the center of gravity and the face. If we take the edges rather than the altitudes of the tetrahedron equal to unity, then these intercepts are equal to the particular mass ratio (e.g., to $X_3/(X_1 + X_2 + X_3 + X_4)$ in figure 3).

[4] Gibbs was well acquainted with the work of Möbius (4) and undoubtedly derived his concept of triangular and tetrahedral coördinates from this source.

If the masses which we locate at the vertices of the tetrahedron are each equal to the number of moles of one component in a phase, then the mass ratios involved (e.g., $X_3/(X_1 + X_2 + X_3 + X_4)$) are the mole fractions of the various components. Depending on the choice of the unit length we represent the mole fractions either by the distance of a representative point from each of the faces of the tetrahedron (Gibbs), or by the distances through the point parallel to the faces of the tetrahedron (Roozeboom). If the masses X_1, X_2, X_3, and X_4 are expressed in other than mole units we may represent weight fractions, weight per cents, or other composition units by these coördinates.

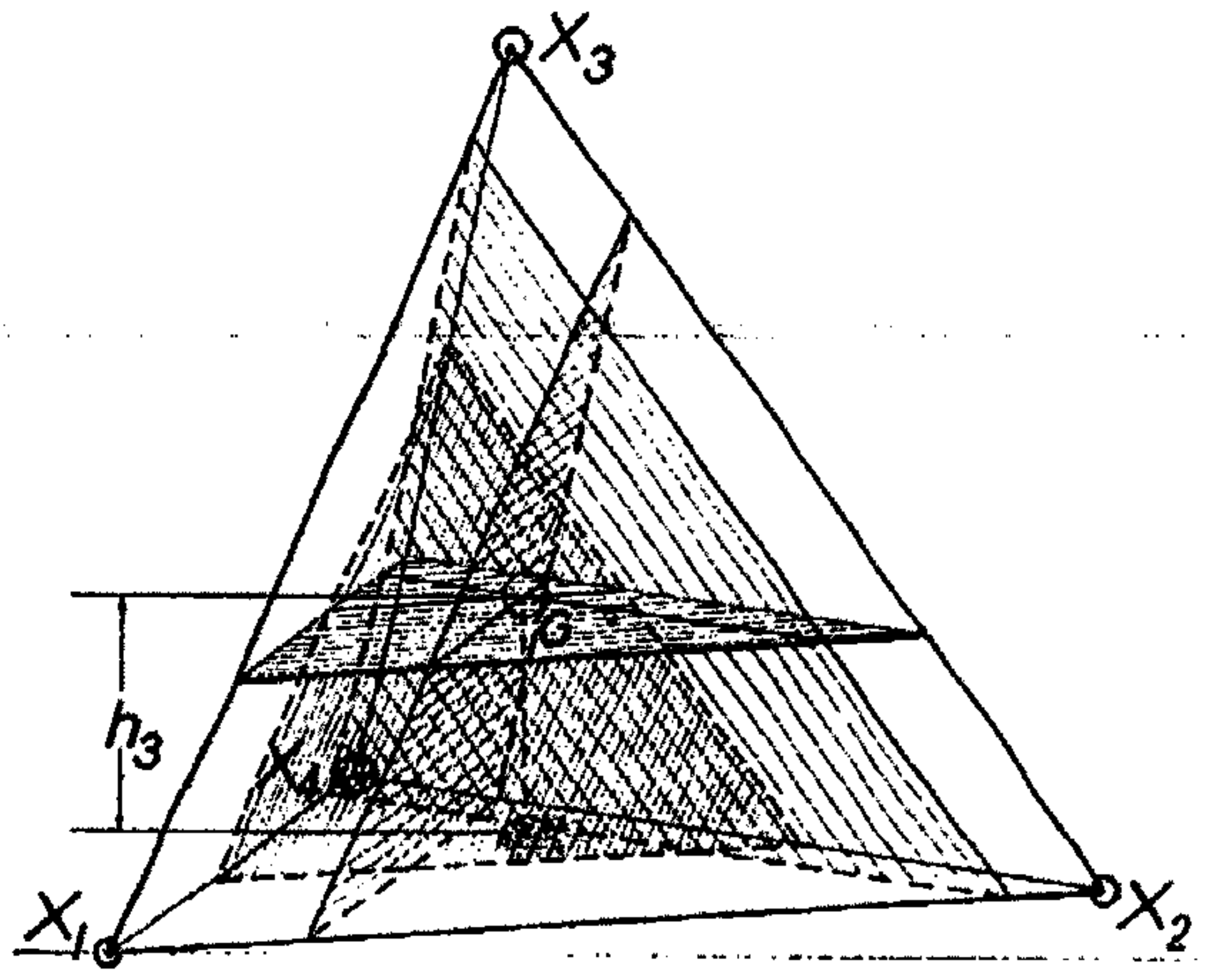

FIG. 3. Möbius' tetrahedral coördinates

Projections

In representing any solid model (e.g., $X_1X_2X_3X_4$ of figure 4) it is customary to use a plan and an elevation view. Actually it is only necessary to use any two independent projections.

Let us project the tetrahedral model by rays parallel to the edge $\overline{X_1X_4}$ (e.g., the ray $\overline{GG'}$ in figure 4). Since the edge $\overline{X_1X_4}$ lies in both the faces $X_1X_2X_4$ and $X_1X_3X_4$, each such ray is parallel to both of these faces. Hence the distance from any point on one of these rays (e.g., $\overline{G'''}$) to one of these two faces, measured parallel to one of the other edges (e.g., the distance $\overline{P'''G'''}$), is equal to the corresponding distance measured from G (e.g., $\overline{PG}$).

Let us use any plane parallel to $X_1X_2X_3$ as a projection plane. Then the face $X_1X_2X_3$ will project into an equilateral triangle $X_1'X_2'X_3'$ which is exactly congruent to the original triangle. Since the two vertices X_1 and X_4 lie on the same projection ray, the projected view of X_4 coincides with X_1', and the projected face $X_2'X_3'X_4'$ coincides with $X_1'X_2'X_3'$. The two faces $X_1X_3X_4$ and $X_1X_2X_4$ are seen edgewise, and appear as the straight lines $X_1'X_3'$ and $X_1'X_2'$, respectively.

The point G is projected as G'. In figure 4 the distance $\overline{P'G'}$ is measured parallel to $\overline{X_1'X_2'}$ and hence parallel to the edge $\overline{X_1X_2}$ of the tetrahedron. It is therefore equal to the mole fraction, N_2, of the component X_2 in the phase represented by point G. The distance $\overline{P'X_1'}$ is similarly equal to the mole fraction, N_3, of component X_3 in the phase represented by G. Hence in order to obtain this view by plotting from data, we merely consider the system as composed of the three components X_2, X_3, and a lumped component $(X_1 + X_4)$.

Similarly we may obtain a second view by projection onto any plane parallel to the same face, by rays parallel to the edge $\overline{X_2X_4}$. The view may be obtained from data by considering the system to consist of the three components X_1, X_3, and a lumped component $(X_2 + X_4)$. Of course, it is important to place the component X_3 at the top vertex of the triangle in each view, component X_1, whether alone or lumped with X_4, at the left, and X_2 at the right. In the second view the point G appears as a point G'' whose triangular coördinates are N_3 measured upwards and N_1 measured from the right side leftwards.

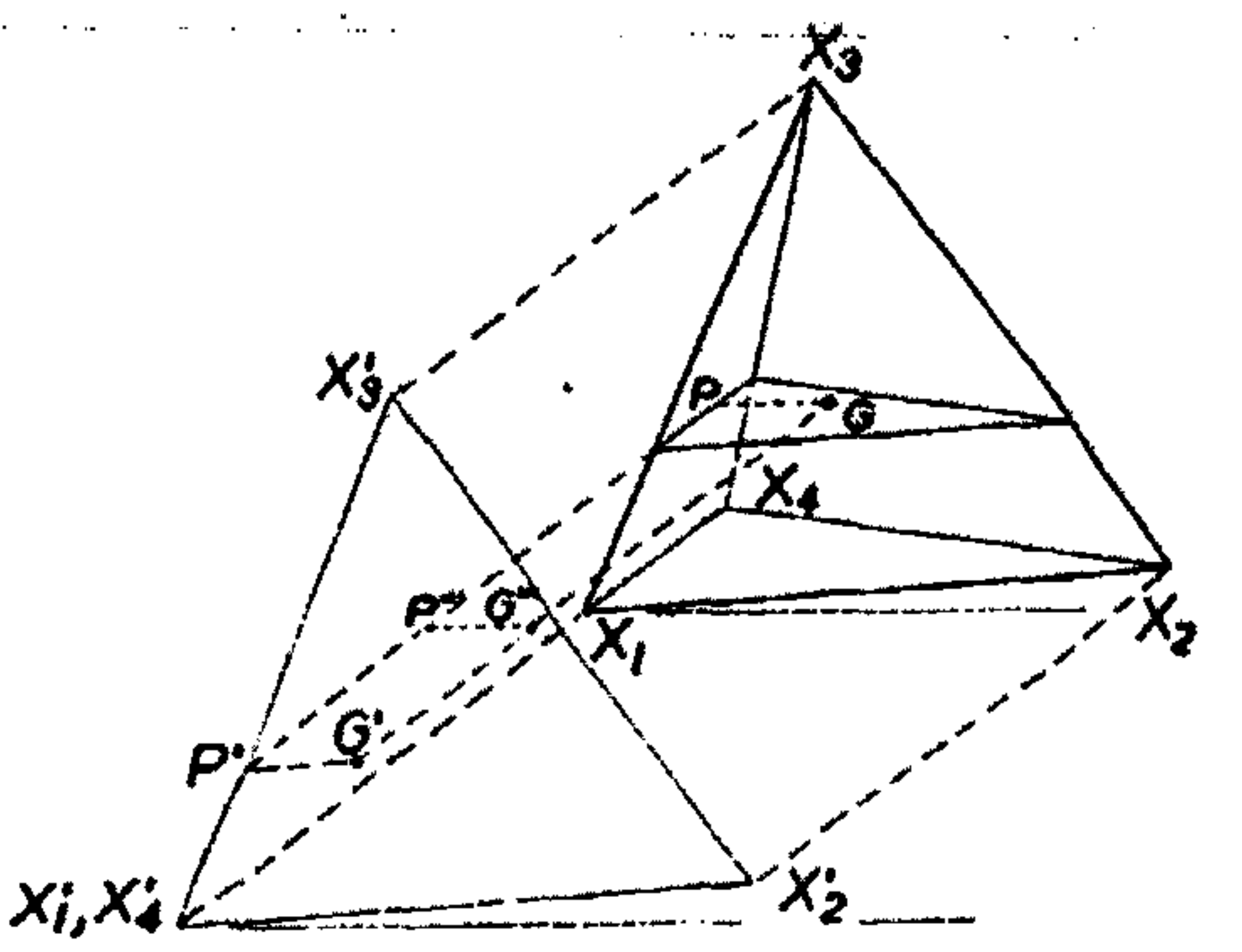

FIG. 4. Projection of Möbius' tetrahedron to obtain the left point of Lodochnikov's "vector"

The two views of the tetrahedron are shown in figure 5. They are the views we would obtain by looking at the tetrahedron from a great distance, first along the edge $\overline{X_1X_4}$, and then along $\overline{X_2X_4}$.[5] Since the point G does not lie in the front face of the tetrahedron, there will be parallax, so that the point appears to shift from G' to G'' in going from one viewpoint to the other. The amount of this parallax is exactly proportional to the

---

[5] Actually in looking at the tetrahedron in this way there will be a slight distortion so that the outline appears isosceles rather than equilateral. The parallel projection plane was used to avoid this distortion.

depth at which G lies behind the front face of the tetrahedron and is the length of Lodochnikov's "vector."

By comparison of these two views with figure 2 it is apparent that point G' is point S and G'' is T. Lodochnikov's representation may be obtained by superposing these two views. When Lodochnikov's method is of value, this superposition should be made, but ordinarily the superposition leads only to confusion. In any case it is better to keep in mind that his representation consists of two different views of a tetrahedron.

Use of the projections

In the tetrahedral model representing a particular system the important features are the equilibrium surfaces and their intersections, together with crystallization paths (i.e., intersections of planes with an equilibrium surface) and straight lines radiating from the point representing pure compounds. In the use of the model it is important to be able to locate intersections of straight lines with curved surfaces, with planes, and with other straight lines, and to pass a straight line through a given point.[6] In the projected views these problems become familiar problems in projective geometry, whose solutions may be found in any of a large number of texts on that subject. For this reason as well as others it is important to keep the two views of the tetrahedron in mind as separate projections.

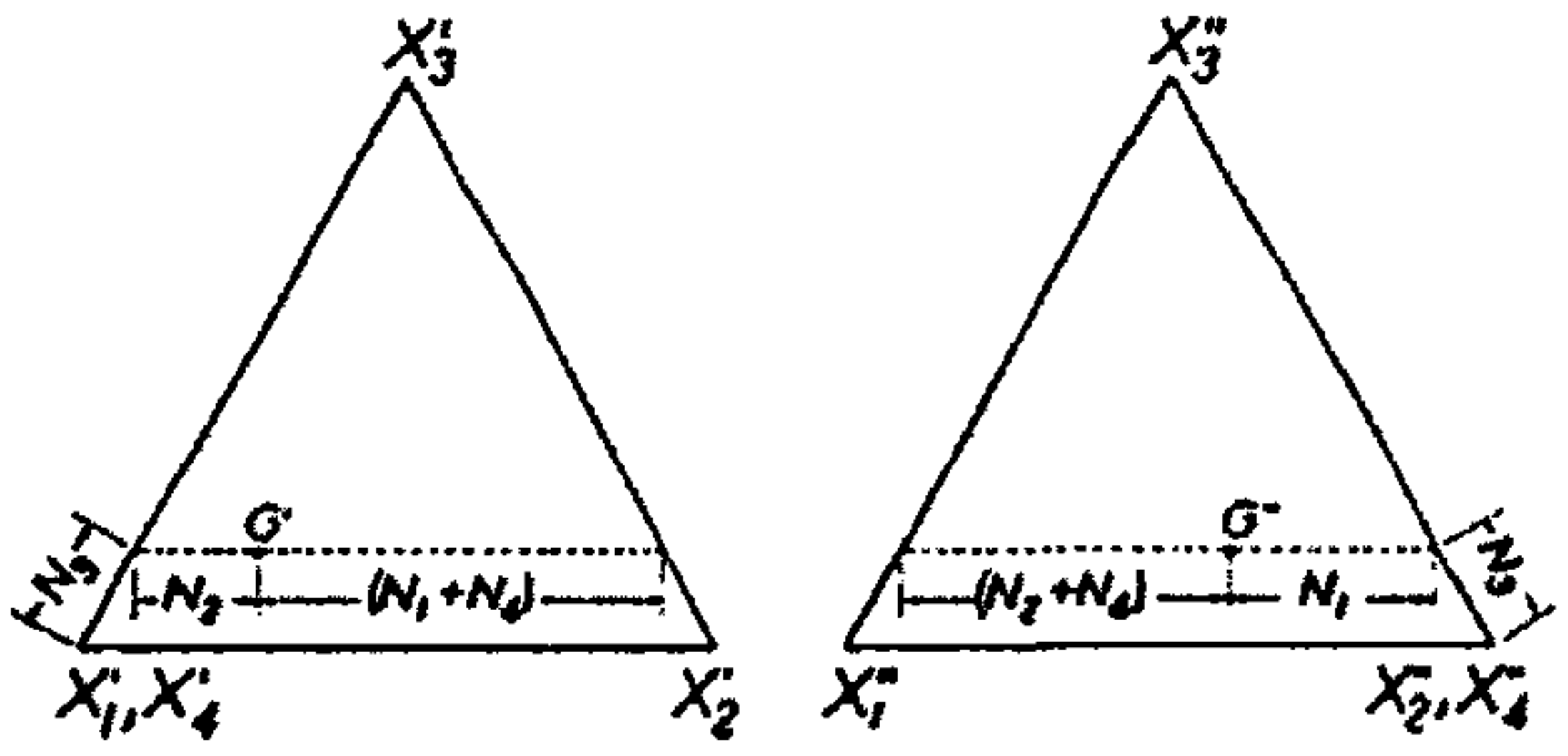

FIG. 5. Separated projections showing left and right ends of Lodochnikov's "vector"

Representation of a surface

In representing a surface projectively it is customary to draw some form of contour lines on the surface and represent them in the projection. In figures 6 and 7 we have illustrated the representation of a particular surface *ram* by three different means, using contour lines. Since the curve *ma* lies in the front face of the tetrahedron, it shows no parallax in the two views (figure 7), and hence in the superposed view of Lodochnikov (figure

---

[6] Lodochnikov demonstrated the methods of solving these problems on his diagram with some difficulty because he was "not well acquainted with the principles of projective geometry which were involved."

6b) appears as a single curve. None of the radial contours lies in the front face; hence each of them shows parallax and appears in Lodochnikov's view as two different curves which intersect on the curve *ma* (the only point on the contour which lies in the front face and shows no parallax is this intersection). The curve *pq*, which lies in a plane *parallel* to the front face, shows parallax, but no change in shape.

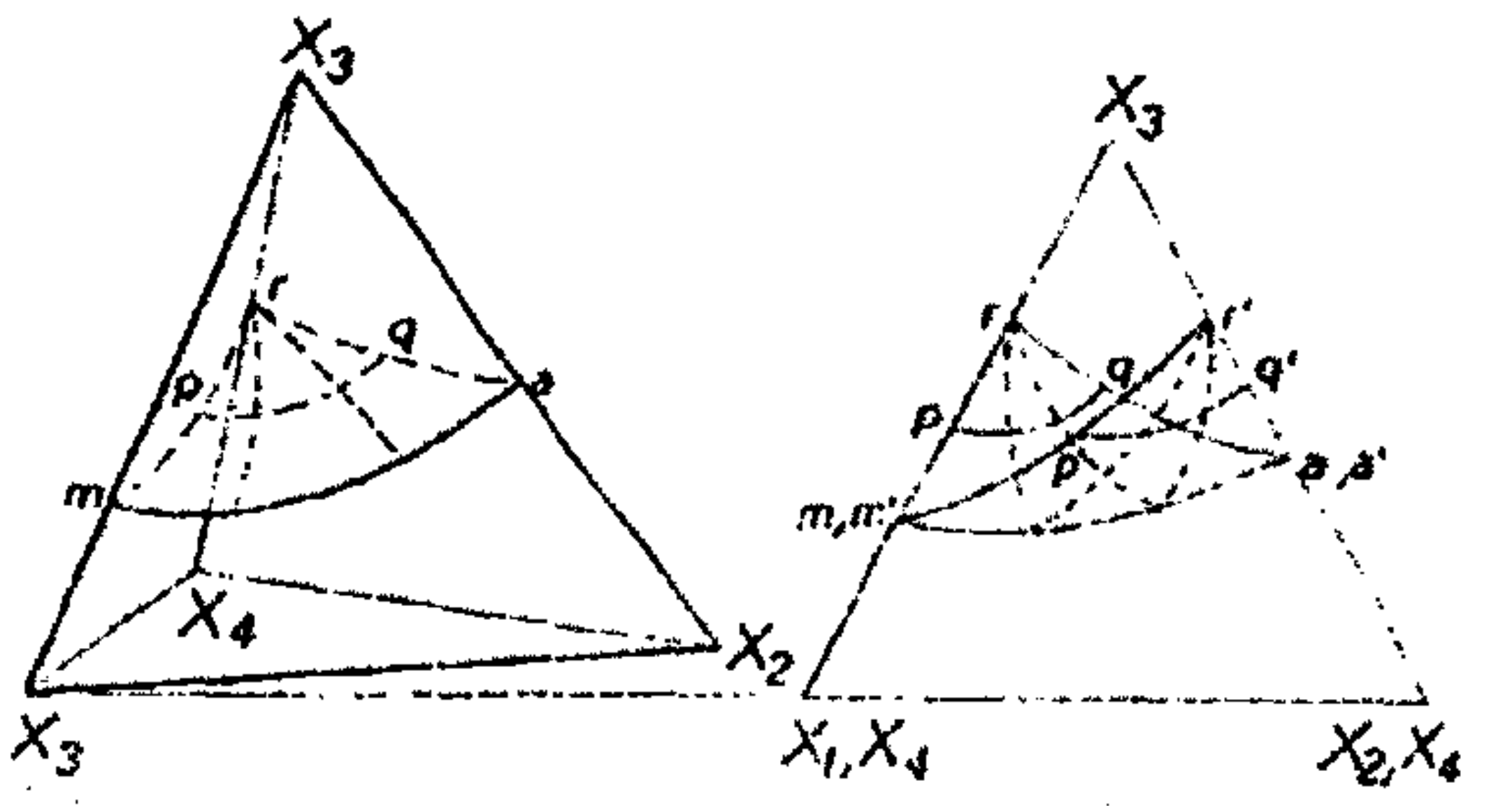

FIG. 6. Representation of a surface in a regular tetrahedron by (a) cabinet projection and (b) Lodochnikov's simultaneous projection.

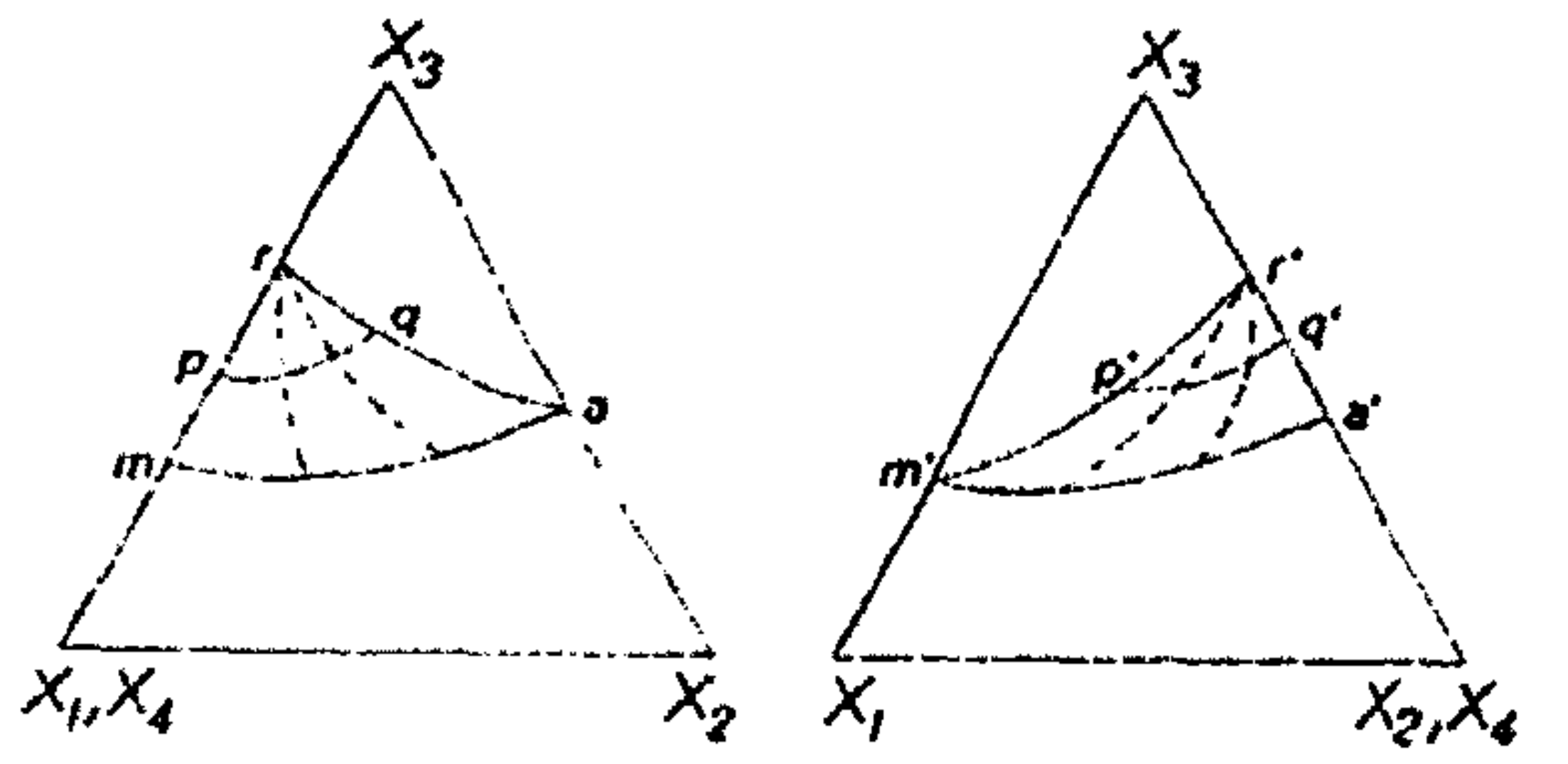

FIG. 7

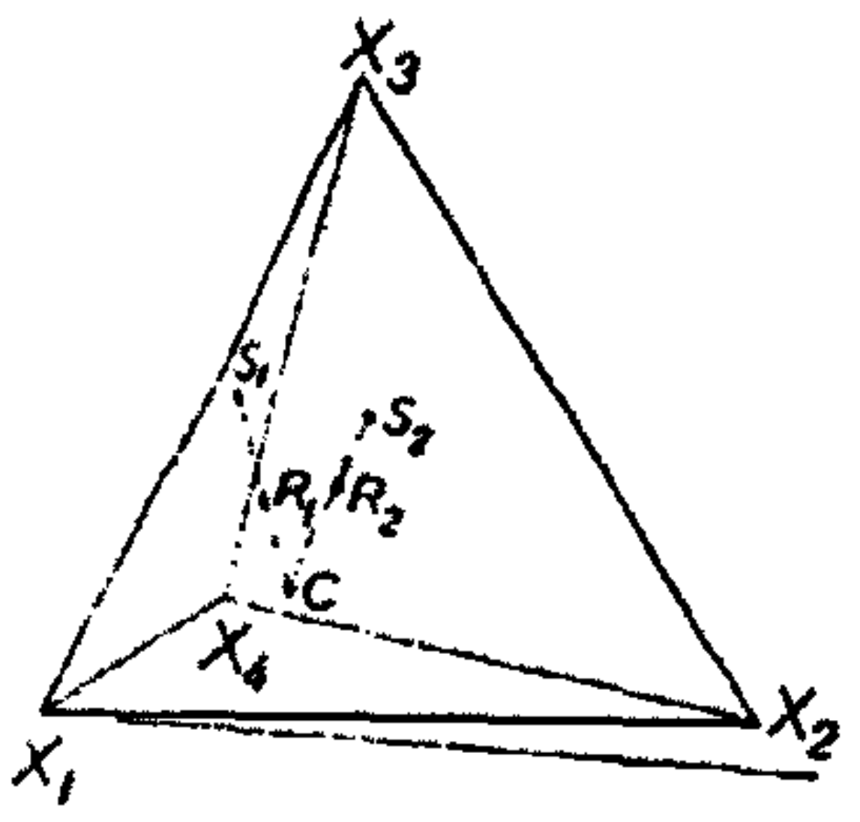

FIG. 8

FIG. 7. Representation of a surface in a regular tetrahedron by two separate projections

FIG. 8. Schreinemakers' method of residues

Center of gravity property

It is apparent from Möbius' derivation that two phases of different total amounts and compositions are represented by the centers of gravity of two different distributions of masses at the vertices of the tetrahedron. Furthermore, if we combine these two phases into a single phase, the combined phase is represented by the center of gravity of the combined masses.

It is an elementary principle of physics that the center of gravity of two or several distributed masses may be found by concentrating each of the distributed masses at its center of gravity and then locating the center of gravity of these concentrated masses. Hence we may represent both the composition and total amount of a phase by endowing the representative center of gravity in tetrahedral coördinates with a mass equal to the total amount of material present in the phase. When two phases are combined in any proportions, the two samples being combined are represented by two such mass points, and the combined phase by the total mass concentrated at their center of gravity. This property, which is quite well known, is useful in the graphical solution of material balance problems.

Schreinemakers' method of residues (*6*)

From two different solutions S_1 and S_2 (figure 8) we have obtained supposedly the same solid phase, C. In analyzing the product we may determine the compositions of the solutions accurately, but we can only obtain analyses for the composition of the solid, C, on residues R_1 and R_2 to which some of the solution adheres. Since R_1 is a combination of some of the solid phase C with some of the solution S_1, it is a center of gravity of the two points S_1 and C. Similarly, R_2 is the center of gravity of S_2 and C. Since the center of gravity of two mass points lies on the straight line joining them, point C must lie at the intersection of two straight lines, one through S_1 and R_1, and the other through S_2 and R_2.

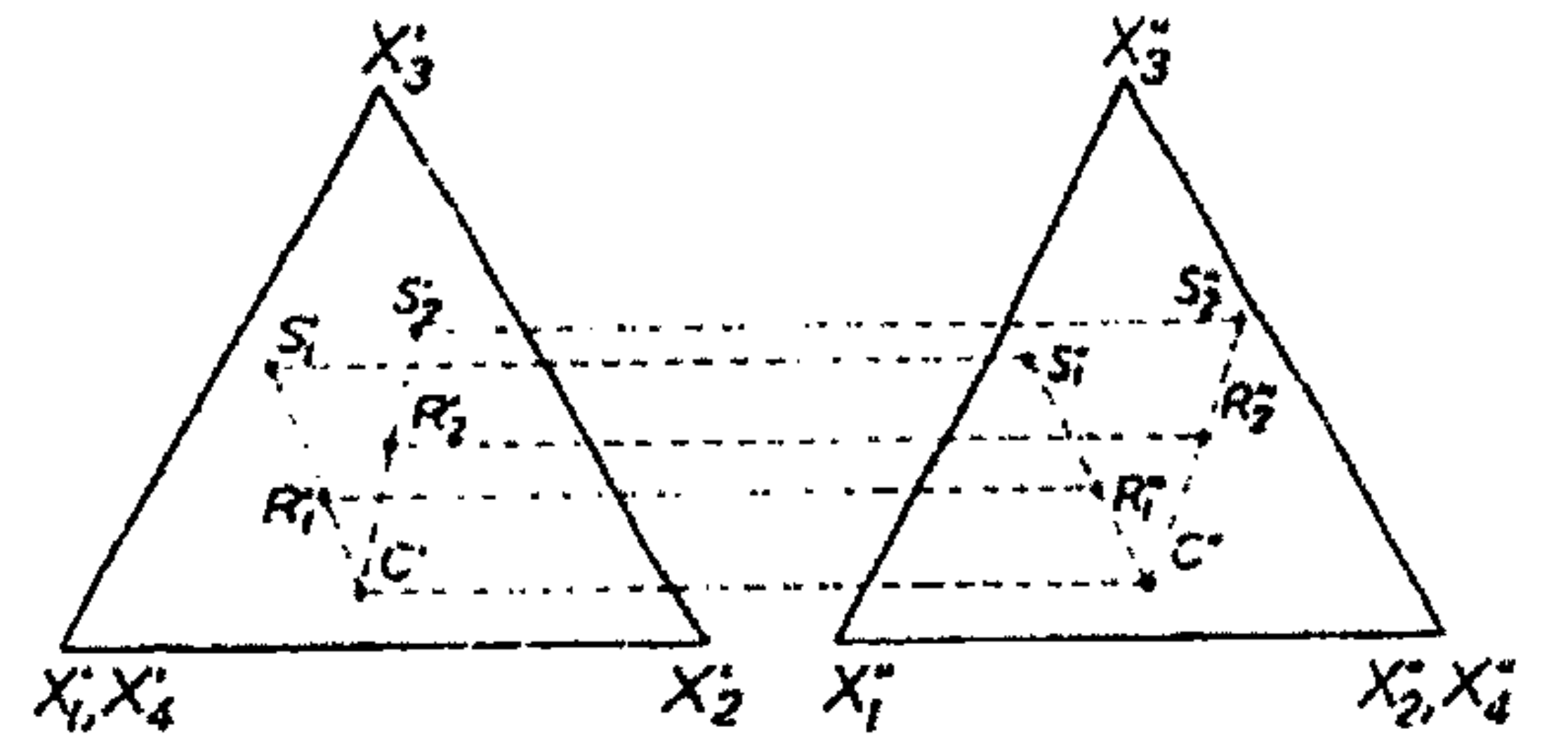

FIG. 9

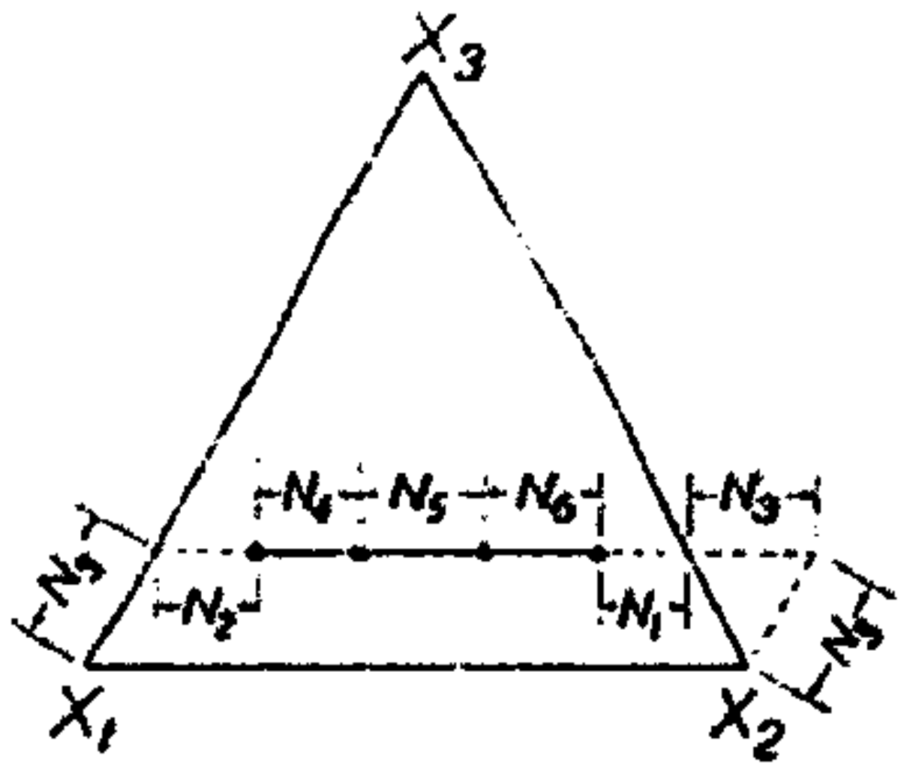

FIG. 10

FIG. 9. Schreinemakers' method of residues adapted to two-projection representation

FIG. 10. A representation of a six-component system

In our projections (figure 9) the location of the point C representing the unknown composition of the solid phase is a simple problem in projective geometry,—that of finding the intersection of two straight lines. In both views C will appear as the intersection of the lines $\overline{S_1R_1}$ and $\overline{S_2R_2}$. It is important to note that in both views each single point must appear at the same height, since the projection rays are both parallel to the base of the tetrahedron. If the two lines do not actually intersect in the solid model, there will be parallax between them, and the apparent intersection will shift vertically as well as horizontally in the two views. Such a behavior indicates either errors in analyzing or plotting the compositions, or that the solid phases were not actually the same in the two cases.

Other applications of the center of gravity property lead to other problems in projective geometry which are as readily solved as the two examples we have given. We intend to discuss some of these more in detail in subsequent papers.

II. POLYNARY SYSTEMS

It is possible to represent completely the composition of a *single* phase containing any number of components by means of triangular coördinates. This is accomplished by lumping the components in three groups and considering each group of components as a single lumped component. One such grouping will give a single point. We need a number of points to represent an m-dimensional model in two dimensions. Hence we shall need to regroup the components in a sufficiently large number of independent ways in order to represent completely the composition of the phase.

One such method is shown in figure 10. The three components X_1, X_2, and X_3 are always represented at the three corners of the triangle. For the first projection all of the remaining components are grouped with X_1, so that the principal coördinates are N_2 and N_3. Then we move component X_4, grouping it with X_2. The principle coördinates are now N_3 and $(N_2 + N_4)$. The point has shifted to the right a distance equal to the mole fraction, N_4, of the component which was shifted. We continue shifting components from the left to the right vertex of the triangle, and with each shift the representative point moves to the right an amount equal to the mole fraction of the component which was shifted. The mole fraction of each component may be read directly from the diagram by reading the distances between successive points.

It may be proved that in order to represent completely any m-dimensional model in n-dimensional space only (m/n) projected views are necessary. We have used four points in figure 10 to represent a point in a five-dimensional model, where we only needed 5/2 or two and one-half (i.e., three) points. Lodochnikov found a method of grouping the components which required a minimum number of points. The method which we present below is only a slight modification of his method.

Let us start with all of the components beyond X_3 grouped with X_1. Then each time we regroup one even-numbered component with X_2, we will simultaneously regroup an odd-numbered component with X_3. When we shift component X_4 over to the X_2 corner, we must simultaneously shift component X_5 over to the X_3 corner. The representative point moves parallel to the side $\overline{X_1X_2}$ a distance equal to the mole fraction N_4, and simultaneously a distance parallel to $\overline{X_1X_3}$ equal to the mole fraction N_5.

In this way the composition of a single phase is completely represented by a broken line. This broken line may be considered as made up of a number of vectors. The component of each vector parallel to $\overline{X_1X_2}$ represents the mole fraction of one of the even-numbered components of the phase, while the component parallel to $\overline{X_1X_3}$ represents the mole fraction of one of the odd-numbered components of the phase. The broken line always starts at the vertex, X_1, of the triangle. It may be shown that, in order for the mole fractions to total unity, it must end on the side opposite this vertex (i.e., $\overline{X_2X_3}$).

Problems involving the center of gravity property, such as Schreinemakers' method of residues, may be readily solved in this projection (figure 12). It is only necessary to recognize that the different points on a single broken line are different views of a single point in the m-dimensional model. The different views of the two lines $\overline{S_1R_1}$ and $\overline{S_2R_2}$ must each show them intersecting in a point which is one of the views of the point C.

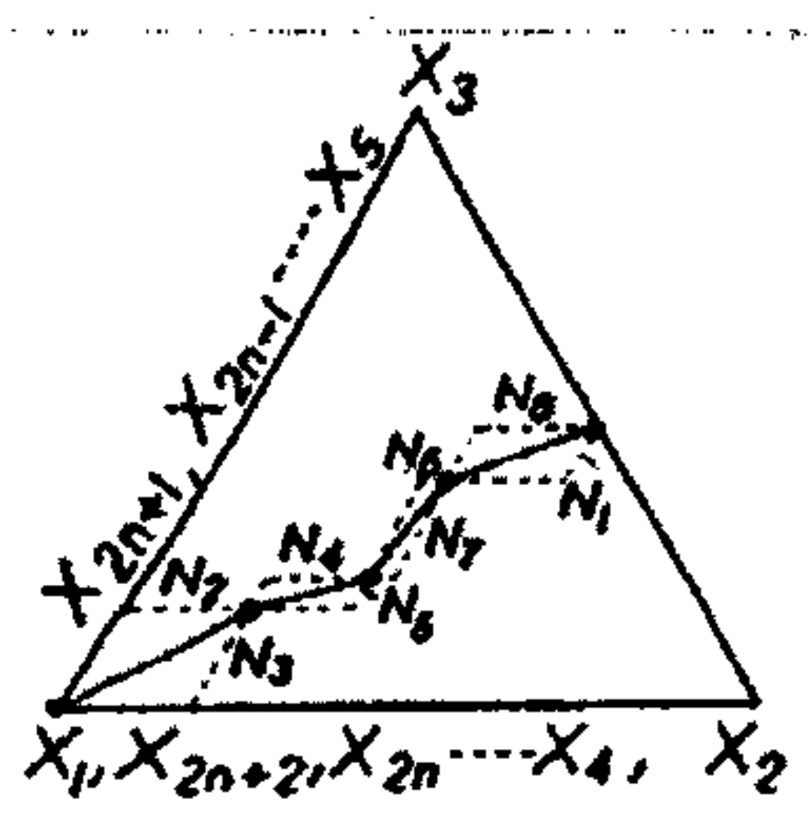

FIG. 11

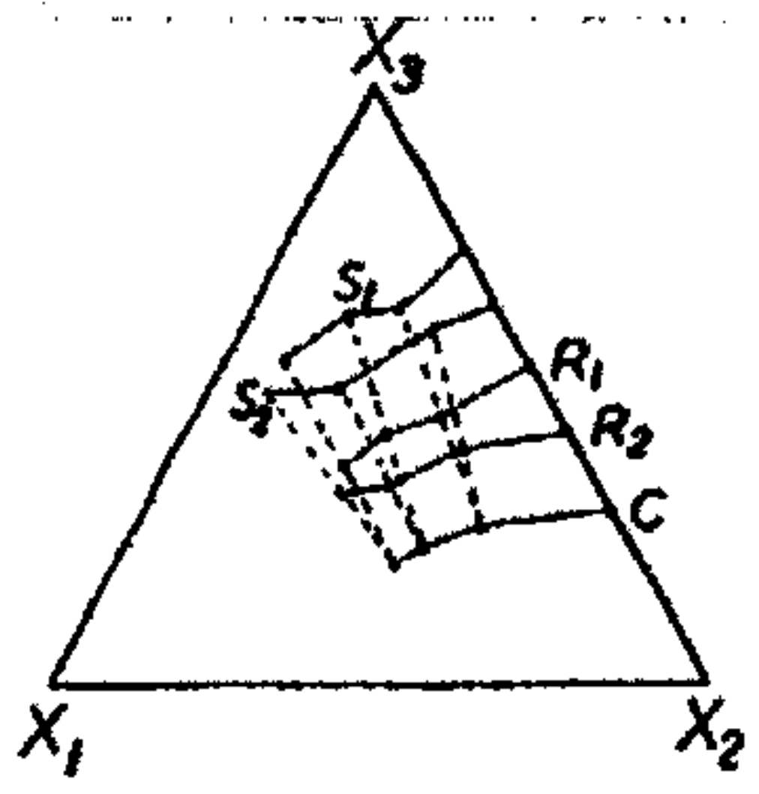

FIG. 12

FIG. 11. An eight-component phase in a multicomponent system by a modification of Lodochnikov's representation

FIG. 12. Schreinemakers' method of residues in an eight-component system

A false solution of the problem is to be detected by the ratio in which the lines $\overline{S_1R_1C}$ and $\overline{S_2R_2C}$ are divided by the point C in each view. If C is a true intersection, the ratio will be the same in all views. If not, this ratio will change.

This method of representing polynary systems offers no particular advantages in representing regions of more than two or at the most three degrees of freedom. It does permit us to represent completely any region in m dimensions which has no more than three degrees of freedom. However, in representing such regions by this method it becomes necessary to separate the different views of the m-dimensional model in order to avoid confusion.

SUMMARY

We have shown that Lodochnikov's method of representing systems is equivalent to two simultaneous projections upon one face of a tetrahedron. We have also simplified Lodochnikov's order of plotting to conform to

American usage of always plotting towards the position representing the pure component. In the solution of phase problems we have found it desirable to place each of the two or more simultaneous projections in separate triangles. We have also indicated the solution of a simple problem in polynary systems by the use of an extension of the projective principles which we have presented.

REFERENCES

(1) Lodochnikov, W.: Ann. inst. anal. phys.-chim. (U.S.S.R.) **2**, 255–351 (1924).
(2) Lodochnikov, W.: Z. anorg. allgem. Chem. **151**, 185–213 (1926).
(3) Lodochnikov, W.: Z. anorg. allgem. Chem. **169**, 177–245 (1928).
(4) Möbius: Der barycentrische Calcul, pp. 32–7. Barth, Leipzig (1827).
(5) Roozeboom: Z. physik. Chem. **12**, 359 (1893).
(6) Schreinemakers: Z. physik. Chem. **65**, 553 (1909).

THE VISCOSITY OF SOLS MADE FROM X-IRRADIATED APPLE PECTIN

C. H. DWIGHT AND H. KERSTEN

Department of Physics, University of Cincinnati, Cincinnati, Ohio

Received March 26, 1938

INTRODUCTION

In a previous paper (2) the authors described experiments upon the viscosity of sols which had been made from x-irradiated agar. It was concluded (*i*) that irradiation of dry agar by soft x-rays decreases the viscosity of the resulting sol, (*ii*) that there is no appreciable "recovery" of the dry agar from the effects of irradiation, at least within seventeen days, (*iii*) that the effect on the agar is not due to heat emanating from the target of the x-ray tube, and (*iv*) that irradiation of the dry agar slightly decreases the pH of the resulting sol. The present paper covers experiments upon apple pectin, with a view towards (*i*) the finding of an effect similar to that observed in the case of agar, when the sol is made up of an irradiated sample, (*ii*) the extension of the "recovery time," and (*iii*) showing that pH plays probably only a minor part in the experiments.

EXPERIMENTAL

As in the previous experiments, the x-rays were supplied by a copper target gas x-ray tube (1) operated at 37 peak kilovolts and 10 milliamperes. The window of the x-ray tube was made of thin aluminum and Cellophane, so that the most intense part of the radiation passing through it had a wave-length of 1.54 Å. Powdered apple pectin was irradiated in the cavity of a drop-culture slide, placed about 3 cm. from the focal spot of the x-ray tube. Each sample was irradiated for 3 hr., and, after having been irradiated, was mixed, and divided into several parts, each containing 0.12 g. These portions of the original sample were placed in flasks to which 20 cc. of buffer solution was added. pH concentrations from 1.76 to 6.95 were used. Control samples were made in exactly the same way, except that unirradiated pectin was used. In any one experiment three parts of a given sample, in buffers of as many different pH values, together with three controls, were employed.

In order to insure uniformity in the diffusion of the powder within the liquid, the six flasks were placed in a rocking frame operated by an electric motor. The flasks, frame, and motor were placed in an electrically heated oven, the temperature of which was kept at about 70°C. by a thermoregulator. A decrease in the density of the sol, due to evaporation while being heated, was prevented by closing the tops of the flasks with rubber caps. After agitation for 30 min. the motion was stopped, and the heater turned off. The flasks were then allowed to cool for 2 hr., in which time the sols were assumed to have reached room temperature and have "zero age."

A definite amount of each sol was pipetted into six separate Ostwald viscosity pipets, which were so arranged that suction or pressure could be applied singly or collectively to them by connecting the top "bus" tube to a small rotary pump or to the laboratory air compressor, respectively. Much greater convenience and dispatch were thus effected. After the experiment the viscosity pipets could be washed and dried simultaneously. The time of flow of the sol through the viscosimeters was observed with a stopwatch, and divided by the time of flow of distilled water at approximately the same temperature through the same viscosimeter. This quotient was taken as the "relative viscosity" of the particular sol. Check

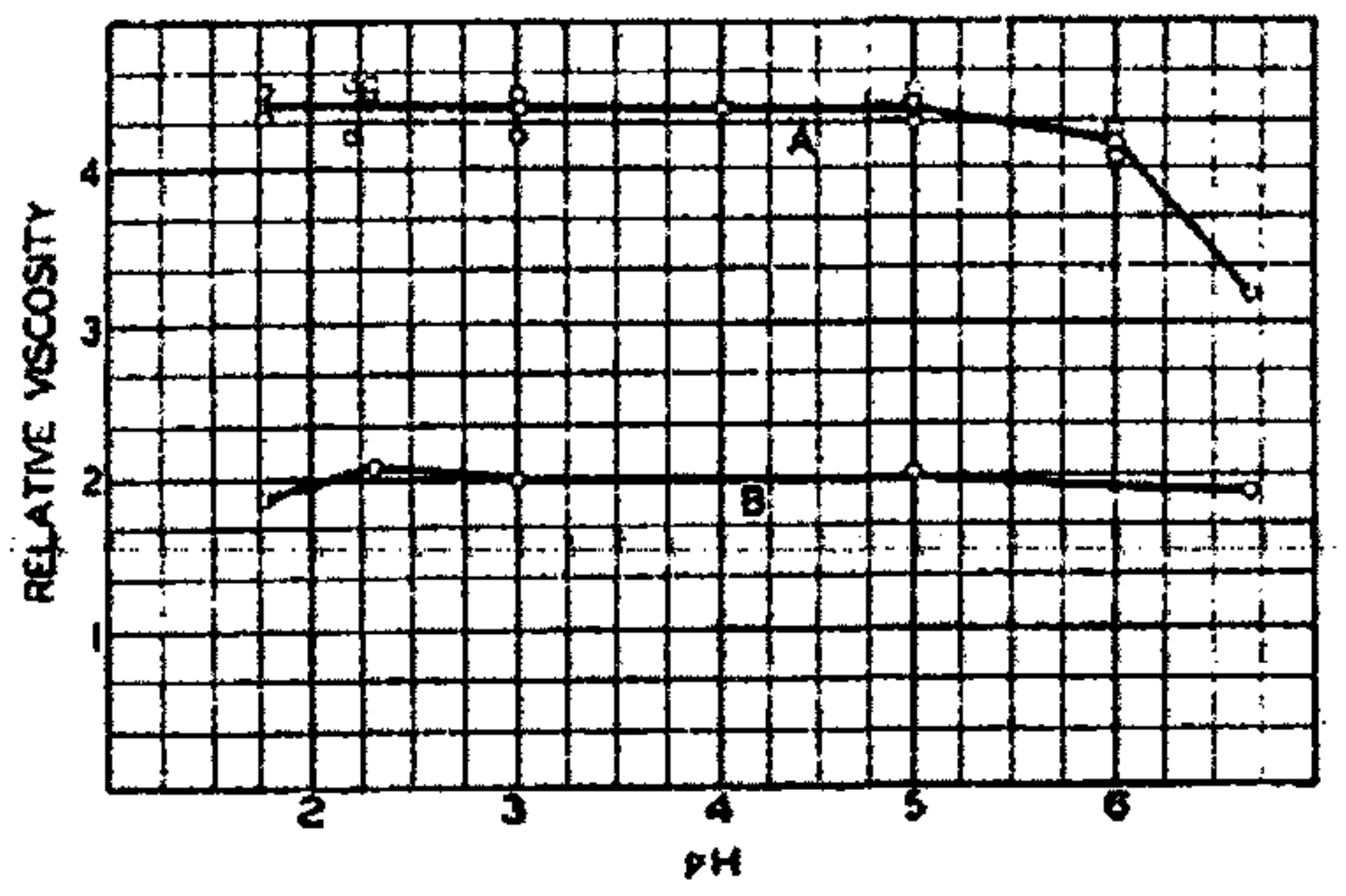

FIG. 1. Plot of relative viscosity of sol against pH. A, controls; B, irradiated powders. Sols of same age.

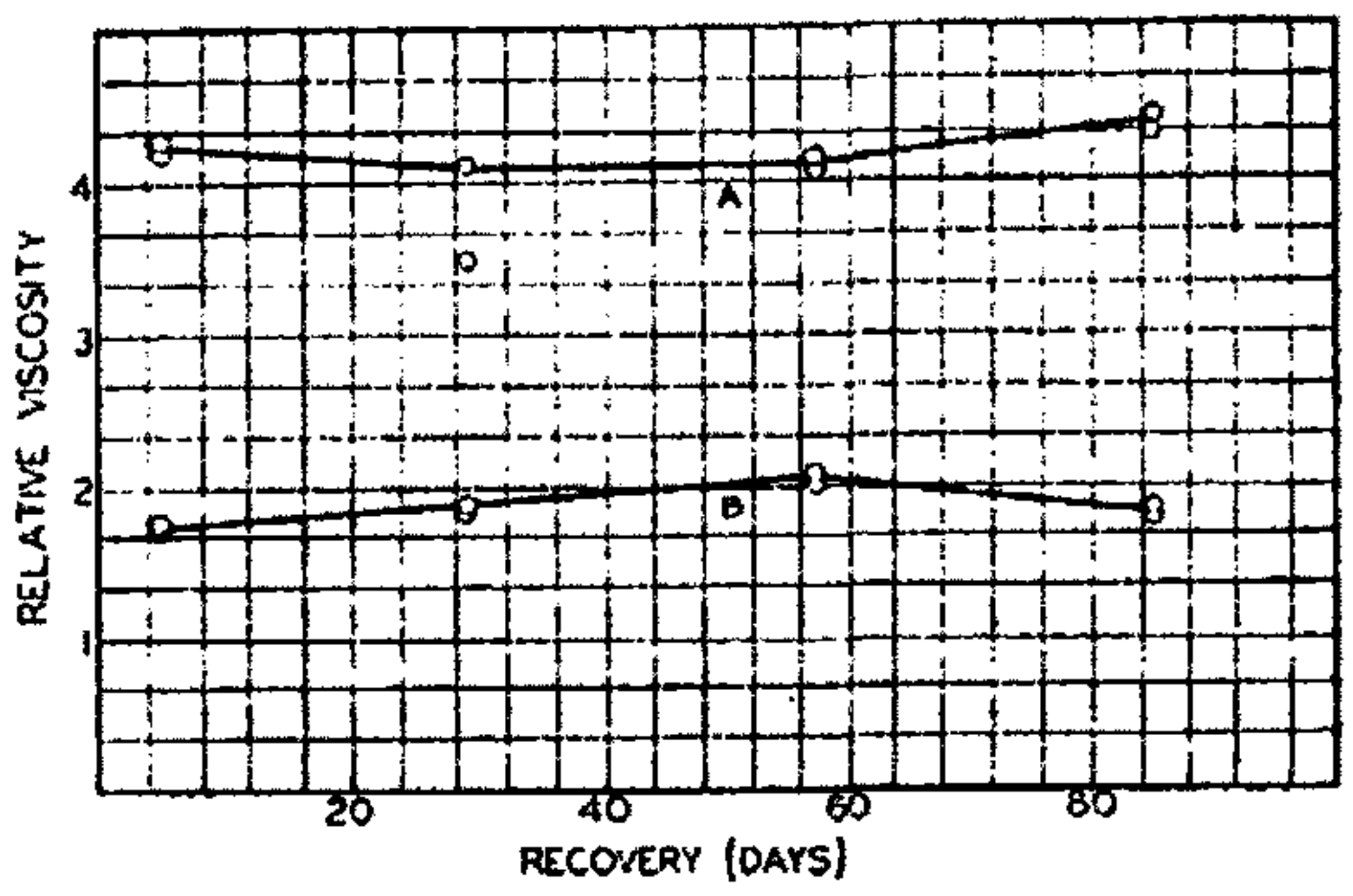

FIG. 2. Plot of relative viscosity against time for "recovery" of the pectin from the effects of irradiation. A, controls; B, irradiated powders. pH = 5.

readings were taken to show that within the time of the experiment there was little or no "age" effect in the sol.

The results obtained from these experiments are plotted in figure 1, which shows (*i*) that there is a marked difference between the controls (A) and the irradiated samples (B), (*ii*) that the effect of pH variation is unimportant, at least in comparison with (*i*), and (*iii*) that there is little effect due to the "age" of the sol, shown by the closeness of the points plotted at given pH values, throughout the time required for the experiment.

In order to investigate the possible "recovery" of the apple pectin powder from the effects of irradiation, a relatively large amount of the pectin was irradiated and then set aside in a bottle identical with that which contained the control. At the end of five days a sample (0.12 g., as previously) was run through a viscosity pipet, and the relative viscosity determined. A control was also run. This procedure was repeated at the end of twenty-nine, fifty-seven, and eighty-five days. In each case a pH of 5.0 was used for the sol. Figure 2 indicates that there is little recovery of the powder even after two and a half months.

CONCLUSIONS

1. As was the case with agar, irradiation of dry apple pectin powder by soft x-rays profoundly affects the viscosity of the resulting sol.
2. The effect of pH variation is not very important in comparison with the effects due to irradiation.
3. There is no appreciable recovery of the dry pectin powder from the irradiation, even after eighty-five days.

REFERENCES

(1) Kersten: Radiology **23**, 60–3 (1934).
(2) Kersten and Dwight: J. Phys. Chem. **41**, 687 (1937).

THE DIELECTRIC ABSORPTION AND DIELECTRIC CONSTANT OF SOLUTIONS OF ALIPHATIC AMINO ACIDS

HUGO FRICKE AND ADOLF PARTS

Walter B. James Laboratory for Biophysics, The Biological Laboratory, Cold Spring Harbor, Long Island, New York

Received July 20, 1938

Linhart (15) has reported a region of anomalous dispersion in solutions of glycine and certain other amino acids at wave lengths around 1 meter. The principal subject of this paper is a study of the dielectric absorption of solutions of some of the aliphatic amino acids on the long wave length side of this region. In the range of wave lengths used the dielectric constant is still practically constant. The values of dielectric absorption obtained by us are considerably smaller than would be expected from Linhart's measurements, and his conclusion that the relaxation time is that of a structure many times greater than the amino acid molecule is not confirmed by our work.

EXPERIMENTAL PROCEDURE

The method consists in balancing, in a resonance circuit, two identical microelectrolytic cells, one of which contains the amino acid solution and the other a solution of potassium chloride. The cells are balanced by changing the concentration of potassium chloride and by varying a parallel condenser. The experimental arrangement is shown in figure 1. The apparatus contains two interchangeable push-pull valve generators, G, one of which can be operated between 2.05 and 16.4 megacycles, and the other between 16.4 and 65.6 megacycles. The resonance circuit A contains the interchangeable inductance L, the variable condenser C, the micro condenser C_t and the electrolytic cell E. The electrolytic cell is inserted into the circuit at P_1 and P_2 by banana plugs and jacks. Part of the resonance circuit is surrounded by the tight grounded copper shield S, but C_t and E are placed outside the shield in order to make these units easily accessible. The axis of C is extended with a hard rubber rod which passes through the shield so that it is possible to vary C without opening the shield.

C_t contains two plates, 2.5 cm. in diameter. The capacity is varied by varying the distance between the plates, for which purpose one of the plates is mounted on a micrometer screw. In the position where C_t is usually used, its capacity can be read to an accuracy of $0.001\mu\mu f$.

A is tuned to resonance by varying C_t, which is actuated at a distance by a pulley and thread arrangement. The point of resonance and the intensity of the oscillating current are recorded by the tube voltmeter T.

By an arrangement not shown in figure 1, the cell and the microcondenser C_t can be introduced into one arm of a resistance-capacity bridge, allowing measurements to be made between 0.25 and 2048 kilocycles.

The generators were calibrated by means of a cathode ray oscillograph. An auxiliary oscillator was adjusted to a frequency of 2.05 megacycles by means of a wavemeter. Through an inductive coupling, this oscillator impressed an oscillating potential on one of the pairs of plates of the oscillograph, while the other pair of plates was connected to the resonance circuit at P_1 and P_2. With the resonance circuit kept tuned, frequencies of 2.05, 4.10, 8.19, and 16.4 megacycles were now established on one of the generators by the well-known method of producing certain types of stationary patterns on the oscillograph. This generator was thereafter used (at 16.4 megacycles) instead of the 2.05-megacycle oscillator for calibrating the other generator, which was used at 16.4, 32.8, and 65.6 megacycles.

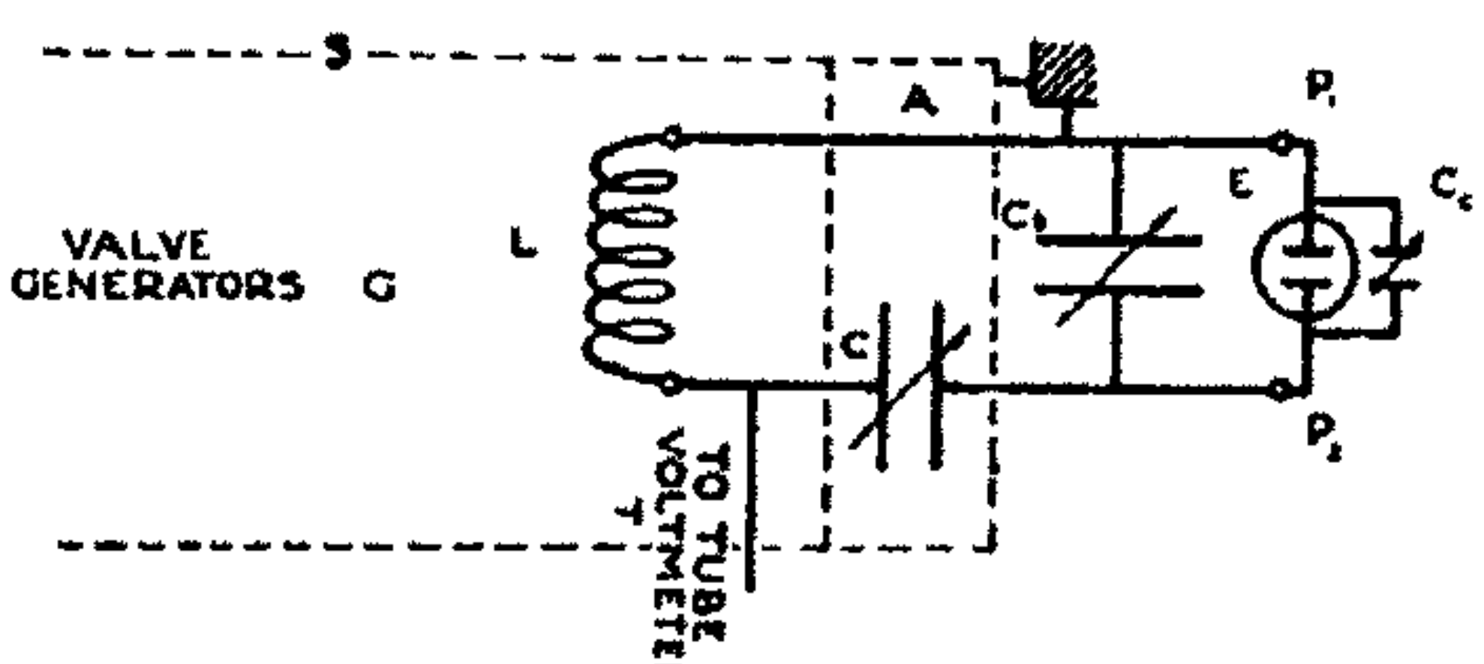

FIG. 1

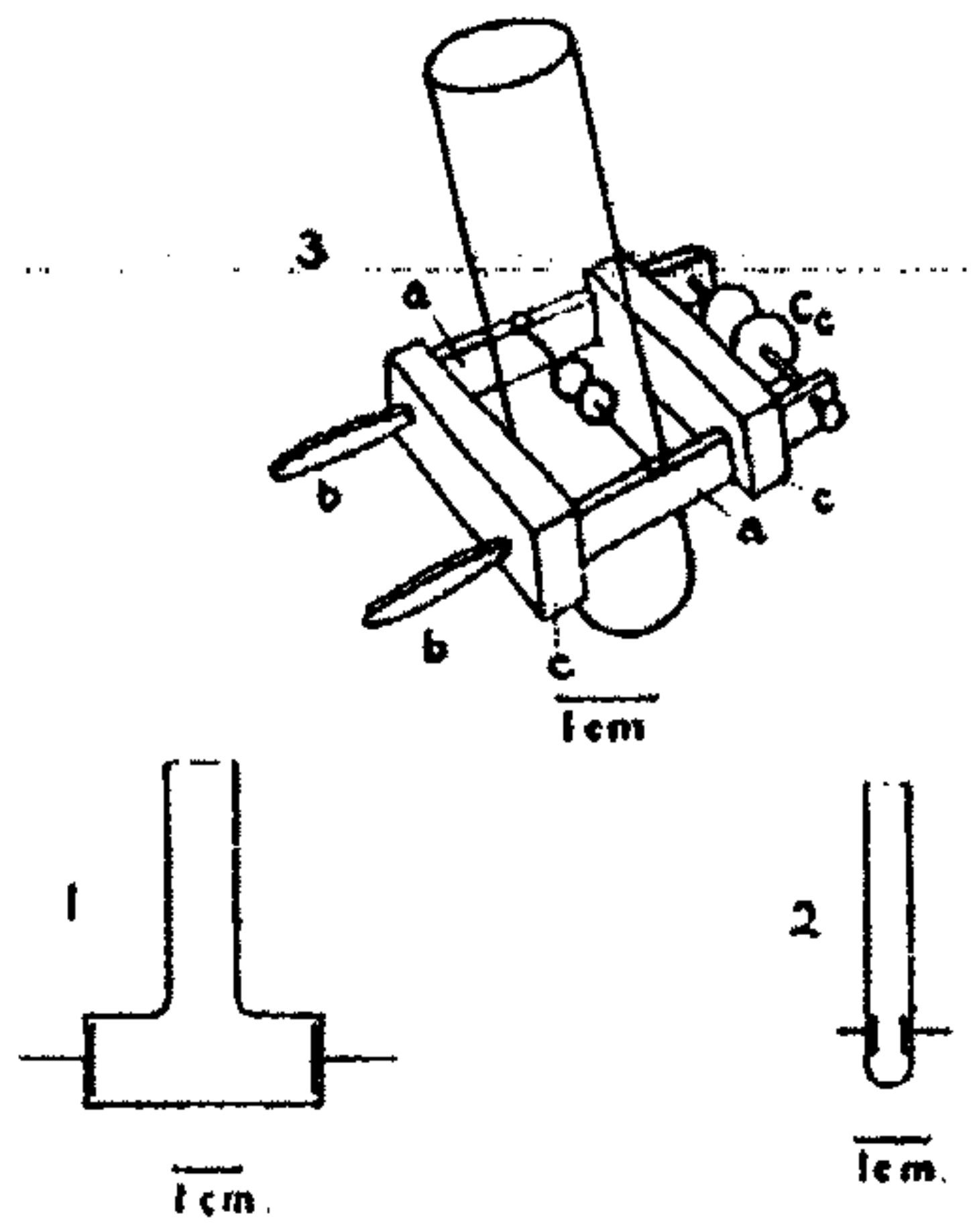

FIG. 2

FIG. 1. Diagram of resonance apparatus
FIG. 2. Electrolytic cells

The construction and mounting of the cells (No. 3) chiefly used in the present work are shown in figure 2. The cell has the form of a test tube 1.4 cm. in diameter. The electrodes are of platinum, 4.5 mm. in diameter and approximately 4 mm. apart. Connection through the glass is made by platinum wire 0.75 mm. in diameter and 6 mm. long. These wires connect to the brass rods (a) which carry the banana plugs (b). The whole unit is kept rigid by means of two narrow strips of Victron (c). This material has excellent dielectric properties, and tests showed that the presence of the strips introduced no appreciable damping in the circuit.

A small condenser, C_c, is placed across the cell, rigidly attached to the cell mounting. This condenser consists of a stationary plate and a movable plate, mounted on a small micrometer screw. The plates are 8 mm. in diameter, and the leads are 3 mm. in diameter. The condenser cannot be read directly with sufficient accuracy, but each time it is reset the change in its capacity is recorded by measurement at low frequency.

At the frequencies and conductances used in the present work, the influence of electrode polarization is negligible, even when blank electrodes are used. However, the electrodes of the cells were platinized in order to make it possible to use them at low frequencies also.

For the purpose of control, certain of the measurements were also made with two other types of cell (cells No. 1 and No. 2), shown in figure 2. The dimensions of these cells will be clear from the figure.

The measurements were made in a room kept at a constant temperature, which was 21.0°C. when not otherwise indicated.

In order to make a measurement on an amino acid solution the procedure is as follows: The condenser, C_c, on the cell with the potassium chloride solution, referred to as the K cell, is adjusted so that the capacities of the filled cells are nearly alike. C_c on the cell containing the amino acid solution (the A cell) is set at zero. The A cell is placed in the resonance circuit and the reading on the galvanometer of the tube voltmeter, at resonance, is recorded. The condition of resonance is established by varying C_t. The A cell is now replaced by the K cell, and the concentration of potassium chloride is changed until the reading on the tube voltmeter at resonance is the same as before. The low-frequency conductance of the potassium chloride solution is thereafter measured with the bridge. At the same time, the low-frequency conductance of the amino acid solution is also recorded, to make it possible to correct for slight changes in the conductance of this solution, caused by temperature fluctuation, etc. In actual practice the potassium chloride is adjusted twice, to give readings on the tube voltmeter which are slightly lower and slightly higher than the readings obtained for the amino acid solution. The low-frequency conductance of each of these two potassium chloride solutions is recorded, and by interpolation the low-frequency conductance of the potassium chloride solution which exactly balances the amino acid solution is obtained.

The difference in settings on C_t, with the amino acid solution and the potassium chloride solution, respectively, in the circuit, must not exceed a certain value, known from preliminary measurements. If the difference is too high, C_c is reset and the comparison repeated. In the range of frequencies used, the dielectric constant of the amino acid solution changes so little with frequency that we can use the same setting of C_c at all the different frequencies.

A typical resonance curve, *viz.*, readings on the tube voltmeter against readings on C_t obtained at 65.6 megacycles, is shown in figure 3. The curve was obtained at a conductance of 33×10^{-6} ohm^{-1}. The resonance curves are perfectly symmetrical, showing that there is no appreciable interference of the resonance circuit with the generating circuit.

The dielectric constant $\epsilon_a(\omega)$ and the conductivity $\kappa_a(\omega)$ of the amino acid solution are obtained from the equations:

$$\frac{10}{36\pi} \times \frac{\epsilon_a(\omega)}{k} = \Delta C + \frac{10}{36\pi} \times \frac{\epsilon_o(\omega)}{k} \tag{1}$$

$$\kappa_a(\omega) = \kappa_o(\omega) \tag{2}$$

$\epsilon_o(\omega)$ and $\kappa_o(\omega)$ are the dielectric constant and conductivity, respectively, of the potassium chloride solution at the frequency ω; k is the cell constant, defined on the basis of electric conductance measurements; ΔC is the difference in condenser readings (in $\mu\mu$f) when the K cell and the A cell are in the circuit.

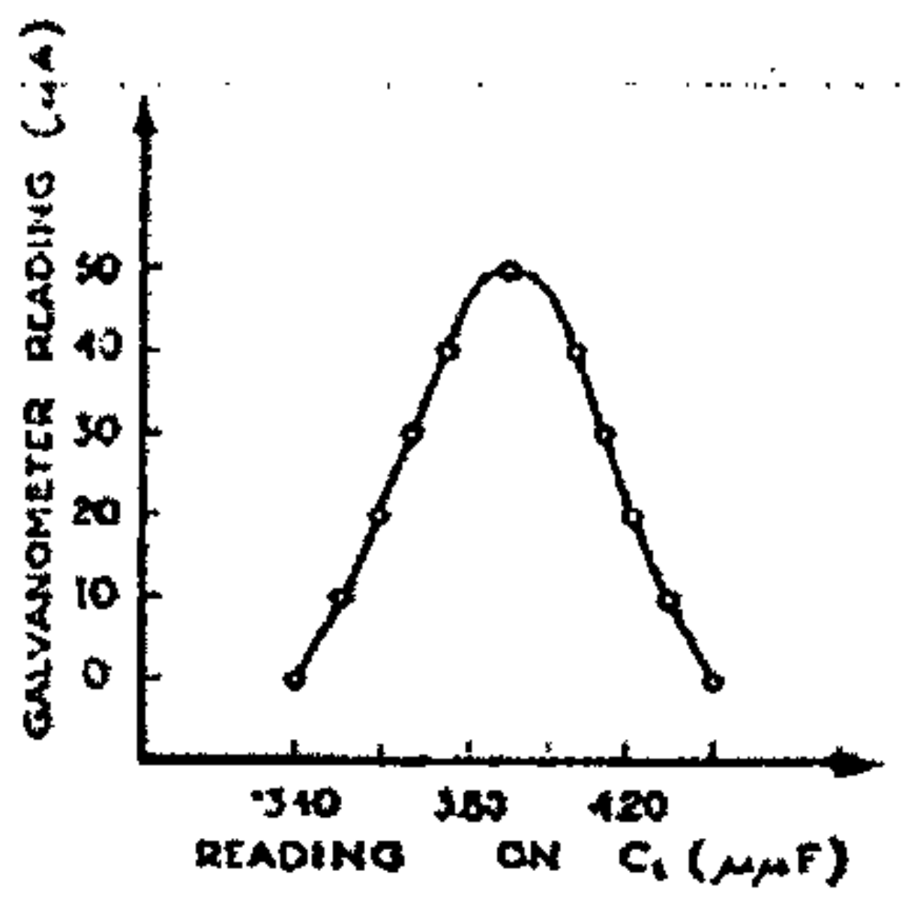

FIG. 3

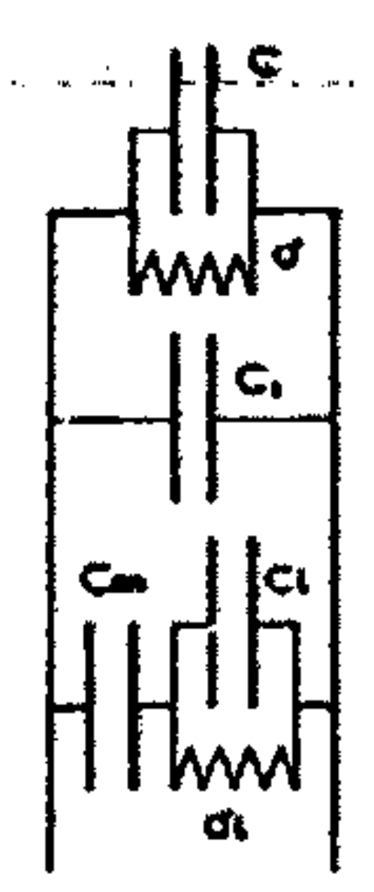

FIG. 4

FIG. 3. Resonance curve

FIG. 4. Diagrammatical representation of cell assemblage

Under the experimental conditions used, the dielectric constant of the potassium chloride solution can be taken as equal to that of water.

The electric conductance of the potassium chloride solution is derived from the ionic conduction and from the dielectric absorption of the solvent. At the concentrations used, the ionic conductance can be taken as independent of the frequency. We can therefore write

$$\kappa_o(\omega) = \kappa_o(o) + \kappa_o^d$$

where κ_o^d is the specific electric conductance of water due to its dielectric absorption. $\kappa_o(o)$ is the low-frequency specific electric conductance of the potassium chloride solution, obtained directly in the measurement. We introduce

$$\kappa_a^d = \kappa_a(\omega) - \kappa_a(o)$$

as the difference between the specific electric conductance of the amino acid solution at high and at low frequency, and we obtain:

$$\kappa_a^d - \kappa_o^d = \kappa_o(o) - \kappa_a(o) \tag{3}$$

DISCUSSION OF METHOD

The validity of equations 1 and 2 is based on the following assumptions: (*1*) The consumption of electric energy at the surface of the electrodes (electrode polarization) is negligible. (*2*) The inductance of the cell assembly can be neglected. (*3*) Electric energy flows to and from the fluid by way of the stray capacities which connect the different elements of area of the enveloping surface of the fluid with each other and with the leads to the cell. This flow of energy can be neglected in the comparison of the two cells.

That these requirements are met to a sufficient extent under the experimental conditions used is shown by various kinds of control measurements described below.

The influence of the stray capacities is comparatively small because of the high dielectric constant of the fluids investigated. The following considerations are presented for the purpose of elucidating the influence of this source of error. Although the cell assembly cannot be strictly represented by any simple network of conductances and capacities (inductance being neglected), for the present purpose we can use the representation shown in figure 4. In this diagram (C, σ) represents the admittance elements which solely involve the fluid.

$$C = \frac{10}{36\pi} \times \frac{\epsilon}{k}$$

$$\sigma = \frac{\kappa}{k}$$

C_l represents the admittance elements (capacities between the leads to the cell) which solely involve the dielectric (mainly air) surrounding the fluid and ($C_m C_i \sigma_i$) represents the admittance elements which involve partly the fluid and partly the dielectric. C_m is independent of the fluid and we can write

$$\sigma_i = \frac{\kappa}{k'}$$

$$C_i = \frac{10}{36\pi} \times \frac{\epsilon}{k'}$$

where k' is a constant dependent on the geometry of the cell assemblage. If we represent the complex admittance of the network $(C_m C_i \sigma_i)$ by

$$1/z = \sigma' + jC'\omega\ 10^{-12}$$

then we obtain

$$\sigma' = \frac{\sigma_i(1 + \alpha^2\omega^2)\left(\dfrac{C_y a}{\sigma_i(1 + \alpha^2\omega^2)}\right)^2}{1 + \left(\dfrac{C_y \omega}{\sigma_i(1 + \alpha^2\omega^2)}\right)^2}$$

$$C' = \frac{C_y}{1 + \left(\dfrac{C_y \omega}{\sigma_i(1 + \alpha^2\omega^2)}\right)^2}$$

$$\alpha = \frac{C_i}{\sigma_i} = \frac{10\epsilon}{36\pi\kappa} \times 10^{-12}$$

$$C_y = \frac{\dfrac{1 + \alpha^2\omega^2}{\alpha^2\omega^2} \times C_i C_m}{\dfrac{1 + \alpha^2\omega^2}{\alpha^2\omega^2}\,(C_i + C_m)} \times 10^{-12}$$

When the frequency is so high that

$$(\alpha\omega)^2 = \left(\frac{10\epsilon}{36\pi\kappa}\ 10^{-12}\omega\right)^2 \gg 1$$

we obtain

$$\sigma' = \sigma_i\left(\frac{C_m}{C_i + C_m}\right)^2$$

$$C' = \frac{C_m C_i}{C_m + C_i}$$

Because of the influence of $(C_m C_i \sigma_i)$, the values of the specific electric conductance and the dielectric constant of the amino acid solution calculated from equations 1 and 2 are too high by the amounts $\Delta\kappa_a$ and $\Delta\epsilon_a$, respectively:

$$\Delta\kappa_a = (\sigma'_{\epsilon=\epsilon_a} - \sigma'_{\epsilon=\epsilon_o})k$$

$$\Delta\epsilon_a = (C'_{\epsilon=\epsilon_a} - C'_{\epsilon=\epsilon_o}) \times \frac{36\pi}{10}\,k$$

$\Delta\kappa_a$ and $\Delta\epsilon_a$ are zero when the frequency is so low (or the electric conductance of the fluid so high) that

$$\left(\frac{10}{36\pi} \times \frac{\epsilon_o}{\kappa} \times 10^{-12}\omega\right)^2 \ll 1$$

and

$$\left(\frac{C_m \omega 10^{-12}}{\kappa} \times k'\right)^2 \ll 1$$

$\Delta\kappa_a$ and $\Delta\epsilon_a$ reach their highest values when the frequency is so high that

$$\left(\frac{10}{36\pi} \times \frac{\epsilon_v}{\kappa} \times 10^{-12}\omega\right)^2 \gg 1$$

This is the condition in our measurements. In this case and restricting ourselves to the case that

$$\frac{\epsilon_a - \epsilon_o}{\epsilon_o}$$

is smaller than, or of the order of, unity, we can write with sufficient accuracy

$$\frac{\Delta\epsilon_a}{\epsilon_a - \epsilon_o} = \frac{k}{k'} \times \left(\frac{C_m}{C_m + \frac{10}{36\pi}\frac{\epsilon_a}{k'}}\right)^2$$

$$\frac{\Delta\kappa_a}{\kappa_a} = \frac{10}{36\pi} \times \frac{k}{(k')^2} \times \frac{2C_m^2}{\left(C_m + \frac{10}{36\pi} \times \frac{\epsilon_a}{k'}\right)^3}(\epsilon_a - \epsilon_v)$$

$$= \frac{2\Delta\epsilon_a}{\epsilon_a - \epsilon_o} \times \frac{\frac{10}{36\pi} \times \frac{\epsilon_a - \epsilon_o}{k'}}{C_m + \frac{10}{36\pi} \times \frac{\epsilon_a}{k'}} < \frac{2\Delta\epsilon_a}{\epsilon_a}$$

Calibration measurements on cell No. 3 with fluids of known dielectric constant show that $\Delta\epsilon_a/\epsilon_a$ for the amino acid solutions studied is smaller than 0.5 per cent. Consequently the error introduced in our high-frequency conductance measurements with these cells, owing to the stray capacity of the cells, should not exceed 1 per cent.

CALIBRATION MEASUREMENTS

The value of k was determined by measuring the electric conductance of the cell at low frequency with solutions of potassium chloride of known concentration. The values of k for the cells used are given in table 3 (below).

These values were checked by measuring the capacity of the cell with fluids of known dielectric constant. These measurements serve essentially as a check on the error arising from the stray capacity. Alcohol, water, and mixtures of water and alcohol were used. The measurements were carried out with a capacity bridge at 0.5 and 2 megacycles. The cell was filled successively with the different fluids, and for each fluid the bridge was balanced by varying a condenser in parallel with the cell. Taking the dielectric constant (ϵ_o) of water as a standard of reference, the dielectric constant ($\epsilon_{obs.}$) of any other fluid is obtained from

$$\epsilon_{obs.} = \epsilon_o - \frac{36\pi k}{10} \times C$$

where C ($\mu\mu f$) is the difference in readings on the parallel condenser. The results of these measurements for cells No. 2 and No. 3 are shown in table 1. The dielectric constants of water, alcohol, and their mixtures were measured by Wyman (20) at frequencies between 21.5 and 41.0 megacycles, and by Åkerlöf (1) at a frequency of 2 megacycles. The results of these two investigators, which agree to within an accuracy better than 0.5 per cent, were averaged and the values are given in table 1. For the two mixtures of highest dielectric constant, the agreement between these values and those obtained by us with cell No. 3 is within the experimental error. For the fluids of lower dielectric constants our values are too low, as would be expected, owing to the influence of the stray capacities. Since the dielectric constant of the amino acid solutions is greater than that of water, in measuring these solutions the influence of the stray capacity would be smaller than it is in the case of the water-alcohol mixtures.

TABLE 1

Calibration of cells No. 3 and No. 2 by dielectric constant measurements on mixtures of water and alcohol

PER CENT ETHYL ALCOHOL (BY WEIGHT)	ϵ*	$\epsilon_{obs.}$	
		Cell No. 3	Cell No. 2
0	80.3		
10.3	74.4	74.4	73.9
26.2	64.9	65.0	63.6
67.0	41.8	39.7	37.3
99.7	25.1	22.1	19.2

* References 1 and 20.

It is important to note, with respect to the significance of these calibration measurements, that the electric conductance of all the calibrating fluids is sufficiently low so that the current transported through the cell by conductance is negligible at the frequencies used. The value of the power factor at 2 megacycles lies between 0.02 and 0.04.

Before any pair of cells was used, it was ascertained that the cells showed no difference when compared with potassium chloride solutions in both, at the different frequencies. This test was made with different concentrations of potassium chloride covering the range of electric conductance used in the work.

The effect on the measurements of transferring capacity from C_o to C_t was determined in a preliminary study. It is of interest to note, as bearing on the permissibility of using an external condenser, that a nearly inappreciable error would have been introduced in our conductance values for the amino acids if C_t had been used exclusively instead of C_o. The necessity for using C_o instead of C_t is chiefly to avoid errors in the dielectric constants.

EXPERIMENTAL RESULTS

The following amino acids were studied: glycine, *dl*-alanine, *dl*-α-aminobutyric acid, *dl*-α-aminocaproic acid, γ-aminobutyric acid, and ϵ-aminocaproic acid. The materials were obtained commercially, and most of them were purified by one or more recrystallizations from water–alcohol mixtures. The recrystallization caused a marked decrease in the conductance of the solutions, but no change could be seen in the values of ϵ_o and κ_a^d.

The electric conductance of these amino acid solutions remains constant, to within our experimental accuracy, for frequencies below 16 megacycles. At higher frequencies the conductance increases, the values of $\kappa_a^d - \kappa_o^d$ varying as the square of the frequency within the range of frequencies tested. No change in the dielectric constant with frequency could be established with certainty. For ϵ-aminocaproic acid a slight decrease was found at the highest frequency, but it was just at the limit of the experimental accuracy. The results of our measurements are shown in table 2. Several of the solutions were measured with cells No. 1 and No. 2, as well as with cell No. 3. The values of $(\epsilon_a - \epsilon_o)$ obtained with cells No. 1 and No. 2 are generally slightly higher than those obtained with cell No. 3, as would be expected, owing to the influence of the stray capacities. As regards the values of $(\kappa_a^d - \kappa_o^d)$, no difference between the cells could be seen. In table 3 are shown the results obtained with these cells for 1 molar glycine.

Hedestrand (13) found that the dielectric constant of solutions of glycine and alanine varies linearly with the molar concentration over a wide range of concentrations. For glycine this linear relation was established up to 2.5M. This result was confirmed later by Wyman and McMeekin (22). The present measurements show that the relationship is not strictly linear, but there is a slight decrease in slope with increasing concentration. The deviation from linearity seems to be somewhat more strongly pronounced in the longer chain molecules.

In comparing our values for $\frac{\epsilon_a - \epsilon_o}{C}$ with those obtained by earlier investigators (2, 7, 8, 10, 11, 12, 13, 15, 22) there is an uncertainty, owing to the difference in temperature used. If we assume that $\frac{\epsilon_a-\epsilon_o}{C}$ decreases 0.25 per cent for each degree Centigrade increase in temperature (22), then our

TABLE 2

Dielectric measurements on amino acids

AMINO ACID	MOLES PER LITER (C)	$(\epsilon_a-\epsilon_o)/C$	$\kappa_a^d-\kappa_o^d/C$			VISCOSITY (RELATIVE) η_l/η_0	MOLAL VOLUME		
							Φ_t*	Φ_d	Φ_e
Glycine	1.00	23.8	20.8	4.9	1.2	1.154	57.0	32.8	22.5
	2.00	23.6	24.5	6.0	1.5	1.362		33.3	
	2.70	23.4	26.1						
	3.00		27.4	6.7	1.6				
dl-Alanine	0.255	24.3	30.2			1.060	73.3	47.5	24.9
	0.941	23.9	33.8	8.7	2.8	1.286		45.4	
dl-α-Aminobutyric acid	0.332	25.0	39.3			1.104	89.6	56.6	
	0.927	24.3	46.5	10.9	3.3	1.401		53.9	
dl-α-Aminocaproic acid	0.077	24.1	60.0	15.0		1.05	122.2	84.0	
γ-Aminobutyric acid	0.202		85.0			1.072	89.6	70.3	
	0.927	50.3	114.0	28.0	6.4	1.44		73.4	
ϵ-Aminocaproic acid	0.196	86.8	234.0			1.110	122.2	118.0	
	0.775	86.5	326.0	82.0	19.5	1.529		120.0	
	1.00	84.8							
	1.50	83.2							
	2.00	80.1							

* Reference 3.

TABLE 3

Measurements on 1 M glycine with different electrolytic cells

CELL	k	$\epsilon_a-\epsilon_o$	$\kappa_a^d-\kappa_o^d$ (10^{-4}ohms^{-1}cm.$^{-1}$)		
			65.6 megacycles	32.8 megacycles	16.4 megacycles
No. 1	2.96	23.9	20.1	4.7	1.3
No. 2	3.59	25.3	21.4	4.7	1.1
No. 3	0.706	23.8	20.8	5.1	1.3

values of $\frac{\epsilon_a-\epsilon_o}{C}$ are slightly higher than those given by Hedestrand (13) and by Wyman and McMeekin (22), but considerably lower than those given by the other investigators. Wyman used wave lengths between 2 and 5 meters. He stated that he could see no dependence of the dielectric constant on wave length in this region. According to our dielectric loss measurements, at a wave length of 2 meters we should expect (compare below) the dielectric constant of the amino acids which we have studied to show a decrease from their long wave length values varying from a fraction of 1 per cent for glycine to a few per cent for ε-aminocaproic acid.

The curves representing $\kappa_a^d - \kappa_o^d$ as a function of concentration show increasing slope with increasing concentration. Our measurements at 65.6 megacycles are shown graphically in figure 5.

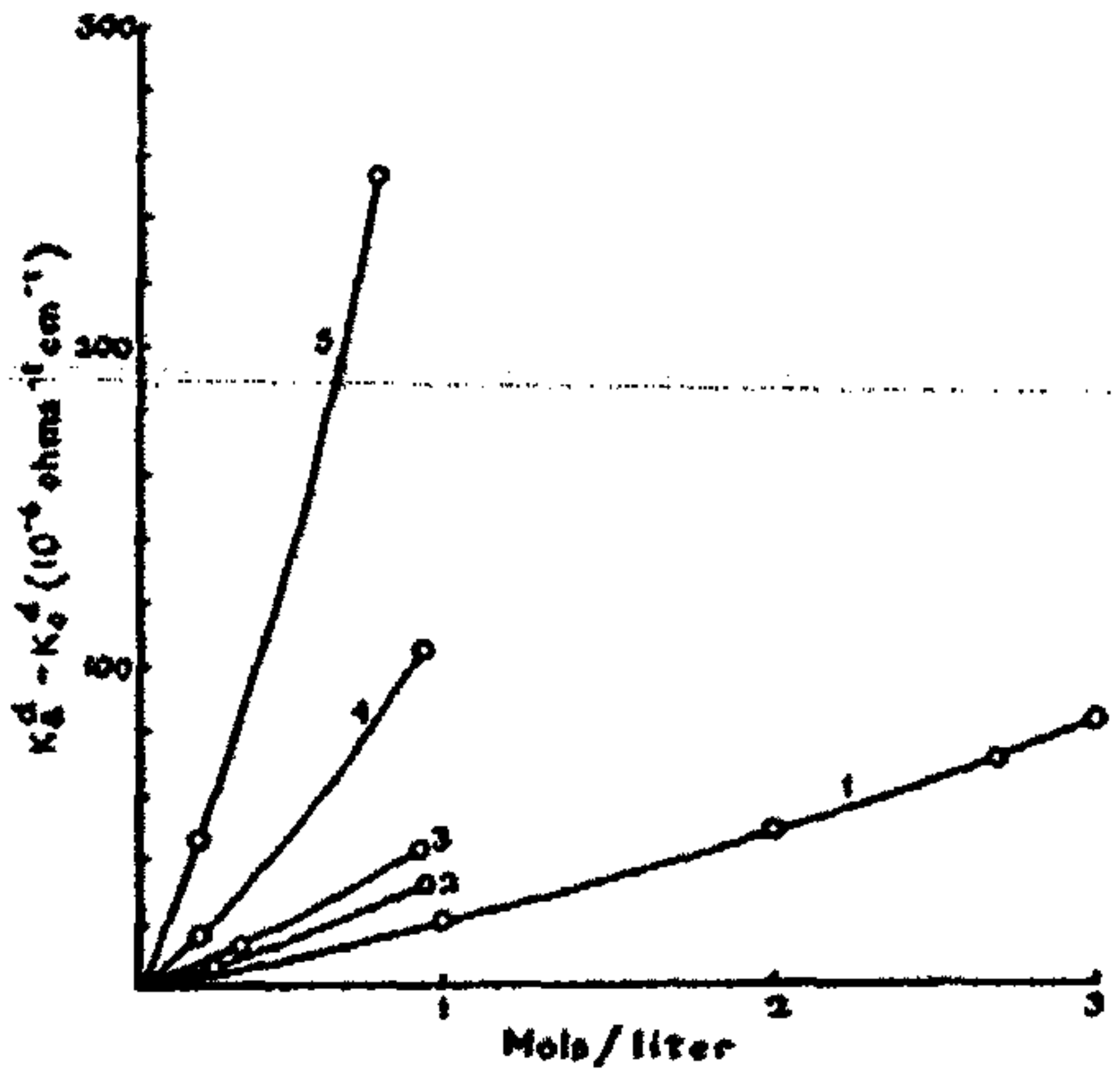

FIG. 5. $\kappa_a^d - \kappa_o^d \sim C$ for (1) glycine, (2) alanine, (3) α-aminobutyric acid, (4) γ-aminobutyric acid, (5) ε-aminocaproic acid. Frequency = 65.6 megacycles.

DISCUSSION

It is well known that Debye's theory (4) of dielectrics does not generally apply to fluid systems; in particular the theory fails when applied to systems of high dielectric constant. One reason for this lies in the assumption used for the relation of the polarizing electric force (F) to the external electric force (E), *viz.*

$$F = E + \frac{4\pi}{3}I$$

(I is the electric moment per unit volume). There is considerable indication that in fluids of high dielectric constant F is approximately independent of the polarization (cf. 16, 17, 21). It seems difficult to account for the near linearity of the relation of dielectric constant to concentration of the amino acid solutions on any other basis, and, as we shall now show, the observed relation of dielectric loss to concentration leads to the same conclusion.

If we assume that F is independent of the polarization, but otherwise follow the method of calculation used by Debye (4), we obtain (restricting ourselves to low frequencies):

$$\frac{(\kappa_a^d - \kappa_o^d) - \kappa_o^d \dfrac{\eta_1 - \eta_0}{\eta_0} + \rho\kappa_o^d \dfrac{\eta_1}{\eta_0}}{(\epsilon_a - \epsilon_o) + \rho(\epsilon_o - n^2)} = \frac{3\eta_1 V}{kT} \omega^2 \frac{10^{-11}}{36\pi} \tag{4}$$

η_1 and η_0 are the viscosities of the amino acid solution and water, respectively; $\rho = C\Phi/1000$ (C = moles per liter; Φ = molal volume of the amino acid); κ_o^d is the specific electric conductance of water resulting from its dielectric absorption (measurements of κ_o^d are recorded below); n is the refractive index of the amino acid (the value of n can be taken as equal to 1.5); V is the volume of the amino acid molecule; k is Boltzmann's constant; and T is the absolute temperature.

In order to test equation 4 we calculate V from this equation and ascertain whether or not the value is independent of the concentration of the amino acid. Since our measurements at 65.6 megacycles are considerably more accurate than those at the lower frequencies, these measurements are used exclusively.

The viscosity of solutions of glycine and alanine was measured by Hedestrand (14). The viscosity of solutions of the other amino acids does not appear to have been determined before, and this characteristic was therefore measured on most of our solutions. The results are shown in table 2.

From the value of V, calculated by means of equation 4, the molal volume $\Phi = 6.0 \times 10^{23}\ V$ is derived and this value is shown in table 2 under Φ_d. For some of the substances Φ_d decreases slightly with increasing concentration; for others the opposite is true. These variations may be due wholly to experimental errors.

We conclude that equation 4 satisfactorily represents the dependence of $\kappa_a^d - \kappa_o^d$ on concentration. We note that this signifies that the relation of dielectric loss to concentration would also have been linear, as is (to a close approximation) the relation of dielectric constant to concentration, if it were not that the viscosity of the solutions changed with concentration.

Under Φ_t we have shown in table 2 the molal volumes of the amino acids, as given by Cohn (3). The values of Φ_d are generally smaller than Φ_t.

It is of interest to compare the molal volumes obtained from the dielectric measurements with those obtained by using Stokes' law to account for the electric mobility of the ionized amino acid molecules (*viz.*, by taking $6\pi\eta a u = 1/300 \times 4.77 \times 10^{-10}$; $\Phi = (4\pi a^3)/3 \times 6.0 \times 10^{23}$; u = velocity of ion per volt centimeter). The mobilities of the glycine and alanine anions and cations were determined by Winkelblech (19), and the values Φ_c shown in table 2 were derived on the basis of his data. The mobilities of the anion and cation are different, and the two mobilities were averaged in carrying through the calculation. We note that Φ_c is still smaller than Φ_d.

The center of the region of anomalous dispersion associated with the amino acid molecule may be expected at the wave length

$$\lambda_m = 2\pi \times 3 \times 10^{10} \frac{(\kappa_a^d - \kappa_o^d) - \kappa_o^d \times \frac{\eta_1 - \eta_2}{\eta_0} + \rho\kappa_o^d \frac{\eta_1}{\eta_0}}{[\epsilon_a - \epsilon_o + \rho(\epsilon_o - n^2)]\omega^2} \times 36\pi \times 10^{11} \text{cm.}$$

For 1 *M* glycine we obtain $\lambda_m = 8.6$ cm.

The center of the region of anomalous dispersion found by Linhart (15) in solutions of glycine is at a considerably longer wave length. A peculiar circumstance is that he finds the region of anomalous dispersion to lie at about the same wave length for the different amino acids studied. It is difficult to reconcile these results with the results of the present work.

DIELECTRIC ABSORPTION OF WATER

For this measurement, cell No. 4 was constructed identical with cell No. 3, except that the electrodes were placed closer together. The value of *k* for this cell was 0.280. Cells No. 3 and No. 4 were balanced in the usual way, with dilute solutions of potassium chloride in both, at the different high frequencies. The balance was obtained by varying the concentration of potassium chloride in cell No. 3, while the solution in cell No. 4 was kept constant. We find that when the cells are balanced at a high frequency, the low-frequency electric conductance of the solution in cell No. 3 is higher than in cell No. 4. The reason for this is assumed to be the dielectric absorption of the water. The capacity difference between the cells remains constant at all the different frequencies. The results of a series of measurements are shown in table 4. The difference in capacity between the cells is shown under ΔC and the low-frequency electric conductance of the cells under σ_3 and σ_4, respectively.

TABLE 4

Dielectric absorption of water

FREQUENCY	ΔC $\mu\mu$f	$\sigma_4 \times 10^6$	$\sigma_3 \times 10^6$	$\kappa_o^d \times 10^6$
megacycles				
65.6	14.3	60.0	87.7	12.0
32.8	14.3	60.0	65.8	2.8
16.4	14.3	60.0	61.1	0.5

The dielectric constant of water calculated from

$$\epsilon = \frac{36\pi}{10}\Delta C$$

is $\epsilon = 80$ (temperature, 21.0°C.), which agrees well with the generally accepted value.

The specific electric conductance of water, κ_o^d, resulting from its dielectric absorption is obtained from

$$\kappa_o^d = \frac{\sigma_3 - \sigma_4}{(1/k_4) - (1/k_3)}$$

k_3 and k_4 being the values of k for the two cells. κ_o^d varies as the square of the frequency, within the experimental error. Measurement of the dielectric absorption of water was made by Schmelzer (18) at a frequency of 28.4 megacycles. His value for κ_o^d is given as lying between 1.4 and 2.0 $\times 10^{-6}$ ohm^{-1} cm.$^{-1}$ (at a temperature of 20°C.).

The wave length λ_m for the center of the region of anomalous dispersion of water may be calculated from

$$\lambda_m = 2\pi \times 3 \times 10^{10} \times \frac{36\pi\kappa_o^d}{(\epsilon_o - n^2)\omega^2} \times 10^{11}$$

n is the refractive index of water in the optical region, $n = 1.3$. If we use the value $\kappa_o^d = 12.0$ obtained at 65.6 megacycles, we derive $\lambda_m = 1.85$ cm. ± 10 per cent. Esau and Baz (9) found by direct observation $\lambda_m = 1.85$ cm. at a temperature of 19.0°C.

SUMMARY

Measurements, at frequencies up to 65.6 megacycles, are given of the dielectric absorption and dielectric constant of different concentrations of solutions of glycine, alanine, α-aminobutyric acid, α-aminocaproic acid, γ-aminobutyric acid, and ε-aminocaproic acid. The electrolytic cell containing the amino acid is balanced in a resonance circuit against a similar cell, containing a potassium chloride solution, and a parallel condenser. The errors of the method are discussed in some detail.

The relation of dielectric constant to molar concentration is approximately linear, showing a slight decrease in slope with increasing concentration. In the range of frequencies used, the dielectric absorption (represented by the equivalent electric conductance) increases as the square of the frequency. The relation of dielectric absorption to concentration shows increasing slope with increasing concentration in direct proportion to the change of the viscosity of the solutions with concentration. The results indicate that the relation of polarizing electric force to average electric force in the solutions is approximately independent of the degree of polarization. On this assumption and otherwise following Debye's theory of anomalous dispersion, values of the volume of the amino acid molecules are derived which are somewhat lower than the true volumes. The molecular volumes obtained from the dielectric measurements are closer to the true volumes than those obtained by using Stokes' law to calculate the electric conductance of the amino acid ions.

Measurements are also given of the viscosities of the solutions used and of the dielectric absorption of water.

We are indebted to Lillian Jacobson Tenzel, M.A., and Thomas T. Goldsmith, Jr., Ph.D., for making some of the measurements.

REFERENCES

(1) Åkerlöf, G.: J. Am. Chem. Soc. **54**, 4125 (1932).
(2) Blüh, O., and Kroczek, J.: Z. physik. Chem. **B27**, 270 (1934); **B28**, 908 (1934).
(3) Cohn, E. J., McMeekin, T. L., Edsall, J. T., and Blanchard, M. H.: J. Am. Chem. Soc. **56**, 784 (1934).
(4) Debye, P.: Polar Molecules. The Chemical Catalog Co., Inc., New York (1929).
(5) Debye, P.: Physik. Z. **36**, 100 (1935).
(6) Debye, P., and Ramm, W.: Ann. Physik **28**, 28 (1937).
(7) Devoto, G.: Gazz. chim. ital. **60**, 520 (1930).
(8) Devoto, G.: Gazz. chim. ital. **63**, 50 (1933).
(9) Esau, A., and Bäz, G.: Physik. Z. **38**, 774 (1937).
(10) Frankenthal, M.: Z. physik. Chem. **19**, 328 (1932); **21**, 310 (1933).
(11) Habedel, G.: Z. physik. Chem. **B33**, 83 (1936).
(12) Hausser, I.: Ber. Heidelberg Acad. **1935**.
(13) Hedestrand, G.: Z. physik. Chem. **135**, 36 (1928).
(14) Hedestrand, G.: Z. anorg. allgem. Chem. **124**, 153 (1922).
(15) Linhart, H.: Z. physik. Chem. **B38**, 23 (1937).
(16) Malsch, J.: Physik. Z. **33**, 383 (1932).
(17) Onsager, L.: J. Am. Chem. Soc. **58**, 1486 (1936).
(18) Schmelzer, C.: Ann. Physik **28**, 35 (1937).
(19) Winkelblech: Z. physik. Chem. **36**, 546 (1901).
(20) Wyman, J.: J. Am. Chem. Soc. **53**, 3292 (1931).
(21) Wyman, J.: J. Am. Chem. Soc. **58**, 1482 (1936).
(22) Wyman, J., and McMeekin, T. L.: J. Am. Chem. Soc. **55**, 908 (1933).

A PHOTOGRAPHIC METHOD FOR DETERMINING SMALL DIFFERENCES IN SPECIFIC VOLUME

ROBERT TAFT

Department of Chemistry, University of Kansas, Lawrence, Kansas

AND

LLOYD E. MALM

Department of Chemistry, Utah State Agricultural College, Logan, Utah

Received April 30, 1938

In a study of the electrical conductance of sols and gels of gelatin and of agar, it became necessary to determine whether there is an appreciable difference in the density, or specific volume, in the sol and gel state, i.e., whether or not any contraction or expansion in volume occurs when the solidification of the sol takes place.

A search of the literature gave very little information on this point, most authors tacitly assuming no change in specific volume during the gelation process. The usual methods of determining densities, especially of the material in the solid (gel) state are not satisfactory, because of the difficulty of removing and measuring the mass and volume of a given quantity of gel. Furthermore, we were primarily interested in detecting differences in density, rather than the actual density itself.

Our problem was solved by photographing a specimen of gelatin (or agar) sol in a suitable container before and after it had jelled. A comparison of the resulting negatives enabled us to determine that a slight contraction occurred in passing from the liquid state to the gel state. Further, the method permitted an approximate determination of the difference in density.

The actual procedure involved making a negative of the narrow neck of a 50-cc. pyknometer possessing a diameter of 3.7 mm., which contained the sol in question. To prevent changes in density occurring as a result of temperature difference, the pyknometer was placed in a constant-temperature bath provided with walls of plate glass. The negatives were made with a view camera of long bellows extension, fitted with a lens of 2″ focal length. With this arrangement the neck of the flask was projected on the negative at a magnification of 11 diameters. The camera was focussed on the meniscus of the sol, the field including also the defining mark on the neck of the capillary, as will be seen by an inspection of figure 1.

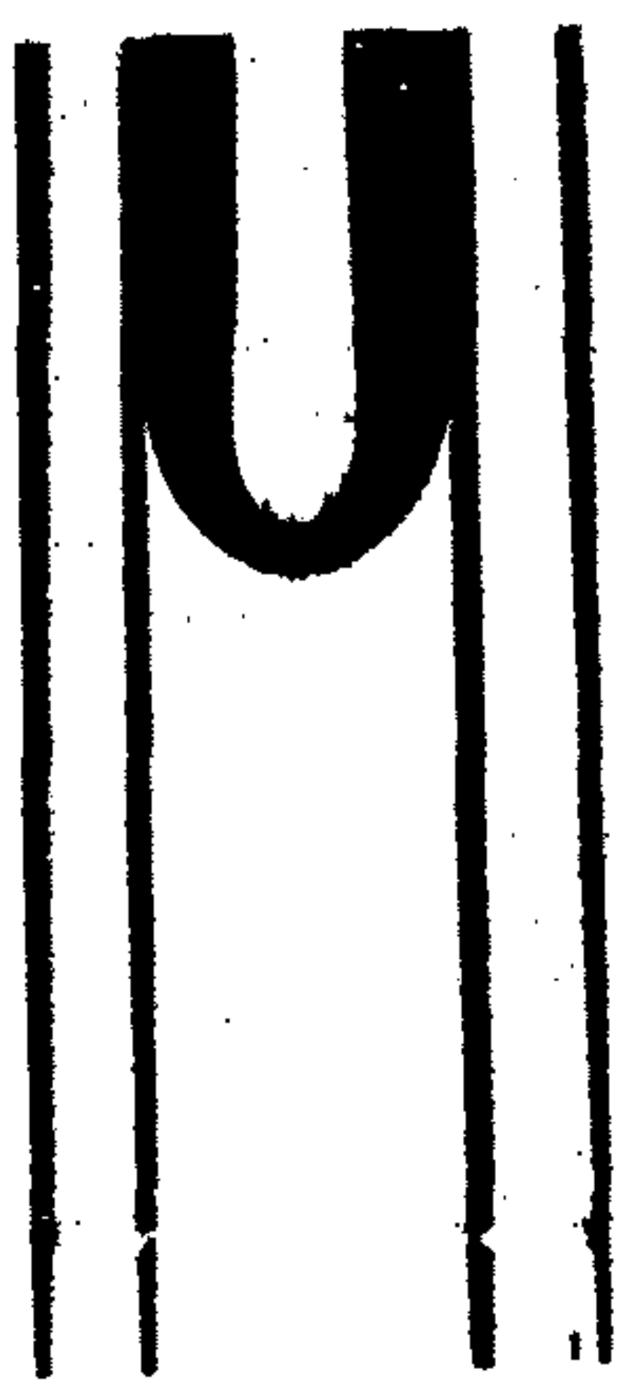

FIG. 1

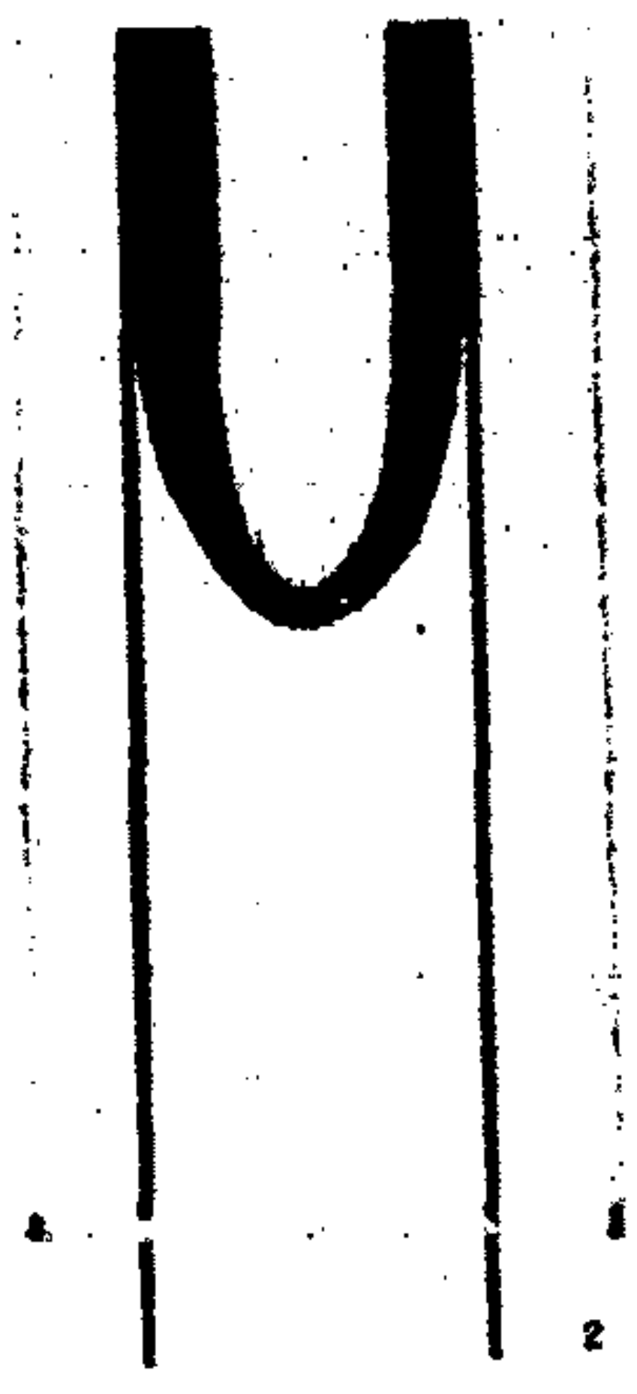

FIG. 2

FIG. 1. Capillary and meniscus (approximately times four). 7.80 per cent gelatin sol at 30°C.

FIG. 2. Capillary and meniscus (approximately times four). 7.80 per cent gelatin gel at 30°C.

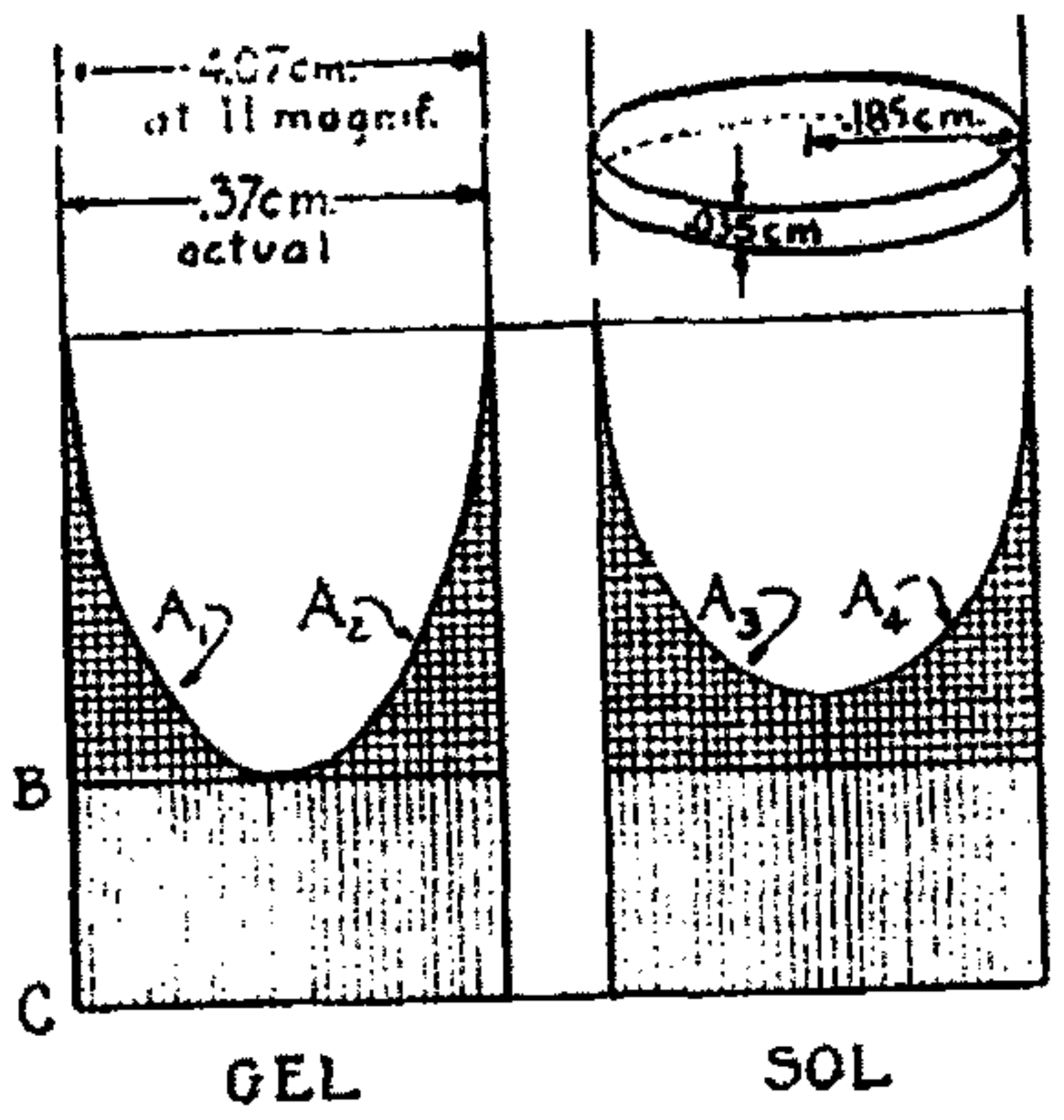

FIG. 3. Diagrammatic illustration of method employed in calculating density change. C corresponds to the defining mark on the capillary of the pyknometer; the areas A_1, A_2 and A_3, A_4 are so labeled for convenience in counting squares. $(A_3 + A_4) - (A_1 + A_2)$ gives the decrease in vertical cross-sectional area of the sol-gel transformation, measured from the bottom of the gel meniscus. This decrease in area can be converted into its corresponding volume decrease; if the total volume of the pyknometer is known, the percentage contraction can be computed.

Illustration of actual case (figures 1 and 2): $A_1 + A_2 = 225$ squares; $A_3 + A_4 = 324$ squares; the contraction is therefore 99 squares. Since, by measurement, 0.37 cm. was the linear equivalent of 32 squares (each square would thus have an equivalent side of 0.116 cm.), the decrease in volume was approximately a cylinder 0.37 cm. in diameter and 99/32 × 0.0116 cm. high. The volume decrease in cubic centimeters is therefore $(3.142)(0.37/2)^2(0.035) = 0.0038$ cc. The total volume of the pyknometer to B was found to be 50.071 cc. The contraction on gel formation was therefore $(0.004/50.071 + 0.012) \times 100 = 0.008$ per cent (0.012 cc. is the volume of sol above the line B).

The specimen under observation in figure 1 was a gelatin sol of 7.80 (weight) per cent gelatin and had a density of 1.0190 at 30°C., as determined by the usual pyknometric method. It was allowed to remain in the constant-temperature bath for an hour at 30°C., by which time it had set to a firm gel. It was then rephotographed, neither container nor camera having been changed from its original position. The print obtained from the second negative is shown in figure 2. A comparison of figures 1 and 2 shows that the meniscus in the gel state is very noticeably pointed; the meniscus in figure 1 shows the familiar form of all liquids. It is apparent that some contraction has occurred in passing from the liquid state to the gel state. To determine the extent of the contraction, the negatives of figures 1 and 2 were placed on squared paper; then the areas bounded by the meniscus, the walls of the capillary, and the defining mark on the wall of the capillary were carefully traced. From a comparison of these two tracings the change in volume was calculated. The actual method of calculation is shown in figure 3. For the case described it was found that 50 cc. of the liquid underwent a contraction of 0.004 cc.; or the density of the solid (the gel) was 0.008 per cent greater than that of the liquid.

It is recognized, of course, that such a determination is based on the assumption that the volume of the pyknometer is the same before and after gel formation. It is possible that gel formation contracted somewhat the volume of the container, owing to the cohesive forces between gel and glass. No cracks, or other evidences of strain, however, appeared between the glass walls and the gel.

In addition to the determination described in the present paper, other measurements were made, all showing that for gelatin and agar the density of the gel was always slightly greater than that of the liquid form at the same concentration and temperature.

SUPERSATURATION AND LIESEGANG RING FORMATION. I

ANDREW VAN HOOK[1]

Department of Chemistry, Lafayette College, Easton, Pennsylvania

Received April 9, 1938

The theory of Liesegang ring formation has been a highly controversial subject ever since the first attempt at an explanation by Wilhelm Ostwald in 1898. E. S. Hedges has summarized the situation up to 1932 (7). He mentions the four most prominent theories advanced to account for the mechanism of construction; while no one theory has been definitely established to the exclusion of the others, the supersaturation ideas of Wilhelm Ostwald (20), as modified by Wo. Ostwald (21) and applied by Hughes (8), seem to be most successful. Apparently the principal obstacle to the more general acceptance of this picture is the want of positive proof of the existence of supersaturation prior to ring formation, especially in view of the fact that rhythmic precipitation occurs in the presence of seeds of the material to be precipitated. Bolam and coworkers (1, 2, 22) have studied very carefully the cases of silver chromate and lead iodide in gelatin and agar in the absence of added seeds, and have definitely demonstrated that true supersaturation does occur in these systems. In the work to be described much of Bolam's work has been confirmed and extended to the case of added seeds. On the basis of the results obtained, a few generalizations regarding some other periodic actions are suggested.

EXPERIMENTAL

For observational purposes the usual Petri dish, test tube, microscope slide, and capillary technics were used. For quantitative measurements on the silver chromate system the silver electrode was used, and at times the limit of visible precipitation method, as described by Bolam *et al.* (1, 2, 22), was used. In some cases the concentrations were confirmed by analyzing for silver as the chloride and for chromate either colorimetrically or iodimetrically. Most of the experiments were conducted at room temperature; others at controlled temperatures. One batch of chloride- and phosphate-free gelatin, containing 11.1 per cent water, was used throughout the work.

[1] Present address: Department of Chemical Engineering, University of Idaho, Moscow, Idaho.

Crystal seeds were prepared either "externally" or "internally". In the former case the precipitation was conducted under conditions simulating those of the experiment to be performed, washing well, and storing under water. In the latter case an initial excess of inside electrolyte was precipitated directly by the addition of an equivalent amount of inoculant in relatively concentrated solution. The uniform dispersion of these crystal seeds was the most difficult condition to attain. In liquid media the smear (or less successfully, the capillary) technic was used. In the bulk experiments with gels, completely filled tubes were turned continuously end-over-end until gelation occurred.

RESULTS AND DISCUSSION

Many of Bolam's experiments establishing the fact that highly supersaturated solutions of silver chromate in gelatin exist were repeated, and the conclusions reached were the same. In a similar manner it was shown that supersaturated solutions of silver chromate are formed in water, in agar, and in bentonite suspensions.

(*1*) The solubility of silver chromate in water at 25°C., as determined by approach from both over- and under-saturation, is $1.0 \times 10^{-4}M$. Solutions of silver chromate, 2- to 2.5-fold supersaturated by metathesis, are quite stable, but do equilibrate to the saturation value under the influence of seeds. Several solutions of this strength were kept unaltered for days. At higher supersaturations, however, the stability decreases rapidly; at no time during this work was a solution fivefold or more supersaturated ever observed to have any appreciable permanence. The visibly delayed precipitation of silver chromate upon mixing silver nitrate and potassium chromate solutions is in line with these observations.

(*2*) Silver chromate seeds were shaken with 1 per cent agar solutions ($10^{-4}M$ in potassium nitrate, pH = 7.6) and kept at a temperature of 35°C. in order to maintain the medium fluid. After 3 hr. the concentration reached a constant of $1.05 \times 10^{-4}M$, as determined by the silver electrode. This compares favorably with the aqueous solubility of 1.2×10^{-4} (10). The solubility as determined by the limit of visible precipitation of equivalent amounts of potassium chromate and silver nitrate solutions after 48 hr. aging was $11 \times 10^{-4}M$. Some silver chromate seeds were added to one half of a 1 per cent agar solution $9 \times 10^{-4}M$ in silver chromate, while the second half remained clear. Both solutions were agitated frequently. The analytical results expressing the adjustment of these solutions are given in table 1. Apparently silver chromate in agar solutions supersaturates readily and adjusts slowly, even in the presence of seeds.

(3) Results of the same sort were obtained with silver chromate in 1 per cent bentonite suspensions at room temperature, although in this case

the initial degree of supersaturation was only from four- to six-fold and fell to the equilibrium value during ten days.

The adjustment of supersaturated solutions of silver chromate in 3 per cent gelatin is depicted in figure 1. Increasing the amount of seeding material accelerates the rate of adjustment of these solutions. A sixfold supersaturated, carefully filtered solution of silver chromate in 3 per cent gelatin at 35°C. was divided into twenty well-cleaned and steamed test tubes, and sealed with clean corks. Half of these were allowed to set upon cooling overnight to room temperature. At this time four of the liquid and five of the gelled samples had decreased more than 10 per cent of the initial silver concentration. A day later one additional sample from each set had materially decreased in concentration. The previously altered samples continued to decrease in concentration. Of the remaining five liquid and four gelled tubes, three of the former and two of the latter

TABLE 1

Adjustment of solutions of silver chromate

TIME	SILVER CHROMATE CONCENTRATION—NO SEEDS			SILVER CHROMATE CONCENTRATION—SEEDS (BY SILVER ELECTRODE)
	By silver electrode	By silver chloride	By chromate ion	
days	*M*	*M*	*M*	*M*
0	8.8×10^{-4}	6.5×10^{-4}	8.5×10^{-4}	8.8×10^{-4}
1	9.1			9.0
2	8.7	10.5	8.3	8.0
5	8.5			8.0
10	8.4			7.0
22	6.0	0.5	5.3	2.0

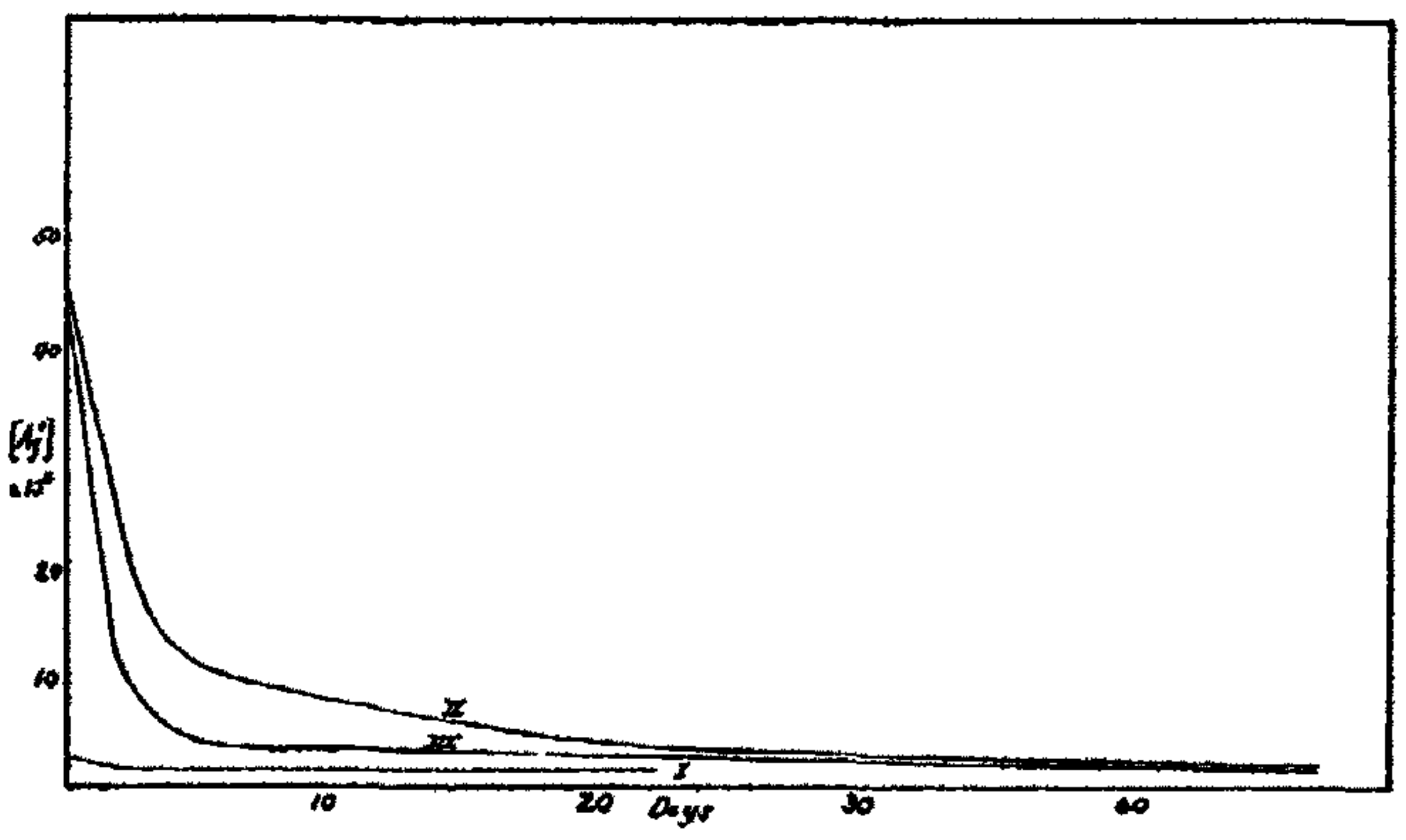

FIG. 1. Rate of adjustment of silver chromate in 3 per cent gelatin solutions after aging for 4 hr. I, saturated with excess solid. II, 44×10^{-4} *N* in silver nitrate and potassium chromate; no seeds. III, 44×10^{-4} *N* in silver nitrate and potassium chromate; seeds.

had decreased in concentration after one week, while the remaining one and two cases, respectively, persisted at their original concentrations for over two weeks. If the original supersaturation is less the persistence is greater, while the reverse is observed for higher concentrations. Seeding promotes the crystallization, and in no case was an original supersaturation retained for more than two days in the presence of seeds.

From numerous experiments representative supersolubilities of silver chromate in various media were calculated, and the results are presented in table 2. These are the values observed after 48 hr. aging, and are fairly reproducible under ordinary conditions. The values are not constant over long periods of time, but decrease as already described. The corresponding values of the supersolubility product, H, and the ordinary solubility product, $K_{sp.}$, are included. Corrections for the CrO_4^{--} - $Cr_2O_7^{--}$ equilibrium (11) were made when necessary. The solubility product of silver chromate is linear between 2.28×10^{-12} at 20°C. and 17.9×10^{-12} at 50°C. (10).

TABLE 2

Representative supersolubilities of silver chromate at room temperature

MEDIUM	METHOD	SILVER CONCENTRATION $\times 10^{-4}$	pH	$H \times 10^{-12}$	$K_{sp.} \times 10^{-12}$
		M			
Water	Silver electrode	2.5	7.2	7.8	0.5
	Limit of visible precipitation	11.0	6.4	670	
	Limit of visible precipitation	6.3	6.6	121	
	Limit of visible precipitation	4.5	7.0	52	
1 per cent agar	Limit of visible precipitation	11.0	6.5	670	
	Silver electrode	9.0	6.5	365	0.6
1 per cent bentonite	Silver electrode	5.0		62	
1 per cent gelatin	Silver electrode	15.0		1690	
3 per cent gelatin	Silver electrode	15.0	7.6	1690	
5 per cent gelatin	Silver electrode	18.0	7.8	2940	
	Silver electrode	20.0	6.4	4000	
	Limit of visible precipitation	4.4	5.0	44	4.5
	Limit of visible precipitation	3.9	6.0	29	
	Limit of visible precipitation	5.0	7.0	62	
	Limit of visible precipitation	22.0	7.6	5200	
	Limit of visible precipitation	14.0	7.8	1370	2.4
	Limit of visible precipitation	18.0	7.8	2940	1.3

The above results are strong confirmation of Bolam's conclusion that true supersaturation of silver chromate in gelatin does occur. The indications are that the phenomenon is general for the usual Liesegang ring materials and media, but it does not necessarily follow that supersaturation precedes rhythmic precipitation. Both direct and indirect evidence on this point was sought.

Direct method

Hughes (8), Lincoln and Hillyer (14), and Fricke and Suwelack (5) offer analytical results indicating that supersaturation occurs during the formation of a Liesegang ring in the silver chromate-gelatin, copper chromate-silica gel, and magnesium hydroxide-agar systems, respectively, but the conclusion is based on analysis for only one constituent ion, analysis of the clear spaces after ring formation, or involved calculation. It was thought that the conclusion would be more convincing if a locality which was about to have a band deposited were segregated and completely analyzed. Such a section can be accurately defined in space and time by the relationships (12):

$$\frac{h_n}{h_{n-1}} = \text{const.}$$

and

$$\frac{h_n}{\sqrt{t}} = \text{const.}$$

Absolutely clear slabs of gel which were about to have a band of silver chromate precipitated were removed from a 5 per cent gelatin gel containing initially 3.3 × 10^{-3} moles of potassium chromate per liter. It was ascertained from duplicate experiments that the slabs removed were at least five to eight previous to the last band which would have formed. The following analyses demonstrate irrevocably that the medium is highly supersaturated in silver chromate:

	No. 1	*No. 2*	*No. 3*	*No. 4*	*No. 5*
$[\mathrm{Ag}^+] \times 10^4$	24.8	60	58	61	42
$[\mathrm{CrO}_4^{--}] \times 10^3$	1.66	1.66	2.4	2.4	2.9
$H \times 10^{12}$	10,000	60,000	80,000	90,000	50,000

If a small amount of Cl^- is added to the gel before setting, the diffusion wave of Ag^+ ions is indicated by the faint van cloud of precipitated silver chloride. If this section is removed in whole or in part, analysis reveals it to be highly supersaturated in silver chromate.

Indirect method

The only requirement for a supersaturation theory of Liesegang ring formation to be compatible with the fact that rhythmic precipitation can occur in the presence of seeds is that the velocity of crystallization be slow compared to the rate of growth of rings. Even on this basis there should still be a limiting amount of seeding surface which will prevent ring formation, since the total crystallization depends, among other things, upon the abundance of crystallization centers. In some seeding experiments in water medium, H. W. Morse (18) found that, if the seed crystals are sufficiently close together, periodicity is completely prevented.

Seeds of various materials (silver chromate, lead iodide, lead chromate, mercurous chloride, ferric hydroxide, barium chromate, silver iodide, silver chloride, silver silicate, magnesium carbonate, and calcium carbonate) if present in sufficient amount inhibit the rhythmic precipitation of the same in various media (water, sugar syrups, gelatin, agar, silica gel, and bentonite gel). The same results obtain whether the seeds are prepared externally or internally. The smaller the seeds, the less the quantities required.

A given sample of seeds seems to be equally effective in preventing rhythmic precipitation in different media. For instance, 5.2 to 6.5 millimoles of potassium chromate per liter precipitated by the slow, dropwise addition of an equivalent amount of 0.25*N* silver nitrate in 3 and 5 per cent gelatin, 8 per cent bentonite gel, 1 per cent agar, or in water, in the presence of 16 millimoles per liter unprecipitated, were sufficient to arrest rhythmic precipitation upon inoculating with solid silver nitrate. Likewise 10 to 15 per cent of 0.09 mole of precipitated potassium iodide per liter, either internally or externally, was sufficient to prevent the further periodic precipitation of lead iodide in water, 1 per cent agar, and 8 per cent bentonite. The clarity of the rings was less, and their subsequent deformation and obscuration greater, the closer the amount of seeds to this limiting amount.

Bolam (1, 2) found that the major part of silver chromate in supersaturated solutions is present as a true crystalloid rather than as a protected colloid. The fact that the fraction precipitated are capable of preventing further rhythmic precipitation is independent of the medium and its concentration is more in keeping with Bolam's interpretation than the suggestion of many (see reference 7) that a colloid formation is involved in the deposition of a Liesegang ring. Specifically this uniform behavior makes improbable the suggestion of Notboom (19) and of Dhar and Chatterji (3) that nuclei may fail to release supersaturation because of an adsorbed immobilizing layer of gel. Ghosh (6) affirms the same from his experiments in water medium.

Repeated inoculation of a given gel with small crystals and dispersion of the rhythmically deposited precipitate also leads to the conclusion that there is a limiting concentration of seeds required to prevent banded precipitation. If the silver chromate seeds are prepared outside the test plate, it is only those crystals formed in slightly alkaline environment which prevent rhythmic construction. Seeds prepared in neutral or acid solution require an inordinate amount or even fail entirely to prevent the Liesegang phenomenon. When one realizes the complexity of the silver-chromate system this is in line with the fact that non-isomorphous seeds fail to prevent rhythmic precipitation while isomorphs do. For example: in gelatin medium approximately the same fraction of carbonate ion precipitated as either lead carbonate or barium carbonate (and sulfate precipitated as lead, strontium, or barium sulfate) prevents the further precipitation of either lead or barium (lead, strontium, or barium) in a periodic manner, whereas barium sulfate, silver chloride, and calcium oxalate (barium carbonate and silver chloride) seeds have no effect in concentrations of three to six equivalent times as much.

FIG. 2. Silver chromate in gelatin medium

A number of experiments concerning the precipitation of various materials in various media and in the presence of glass powder were performed. In general the same results as those reported by Wo. Ostwald (21) were obtained, namely, that rhythmic precipitation was not prevented. However, as the concentration of glass seeds is increased the rhythmic form of the precipitate becomes more indefinite, and in a few cases it was entirely absent. A single, rather novel result, depicted in figure 2, was obtained with silver chromate in gelatin medium. There is no indication from the diffusion laws, or from observation, that such a repetition of a series of bands will occur from a single inoculation in a homogeneous system. Such an occurrence would be possible in a heterogeneous system if the crystal seeds inhibiting ring formation were dispersed in a discontinuous manner. Mendhall and Mason (17) report that stratification of settling particles is possible when there is a lateral temperature gradient across the liquid, and it is very likely that this condition was realized during the uncontrolled settling of the specimen illustrated.

Careful microscopic observation during the process of ring growth, in the presence of a concentration of seeds below the critical amount, reveals that the development is more irregular and less definite than in their absence. In the immediate vicinity of a cluster of seeds, ring formation is completely inhibited, so that the formation is only partial. Subsequent alteration (formation of halos) and even complete obliteration are also pronounced.

APPLICATIONS

1. The difficulties of obtaining uniform dispersion of seeds, particularly in water medium, vitiate somewhat the quantitative results obtained. This non-uniform distribution must be either eliminated or evaluated before accurate quantitative results are realized. When this and the evaluation of the differential effects of various variables upon the competing processes of crystal growth and band formation are accomplished, another method for ascertaining the rate of growth of crystals from supersaturated solutions will be made available.

2. McMasters, Abbott, and Peters (16) suggest that there may be a common cause underlying the formation of Liesegang rings, rhythmic banding from melts, and rhythmic crystallization from solution. The picture favored above for Liesegang ring formation may be extended to the other two cases as follows: A melt supercools until the limit of stability is reached at a particular point. Crystallization ensues and spreads about this center. The process is partially adiabatic, so that as growth continues the local temperature rises until a condition is reached when there is an area immediately preceding the crystallization wave front that is no longer supercooled. This corresponds to the period of the rhythm, and the clear space must be traversed before crystallization begins anew. The subsequent alteration and crystallization of this molten section (4, 13, 9) will present a rhythmic appearance of the whole. The case of rhythmic crystallization from solution is explained in a similar manner, with supersaturation due to evaporation and exothermal crystallization being the active agents.

The blotchy appearance of such phenomena is in harmony with the above interpretation, and the common origin of Fick's law of diffusion and Fourier's treatment of flow of heat is reason for expecting that the three cases should exhibit a common rhythmic appearance.

3. Lloyd and Moravek (15) report that in addition to the usual two sets of rings formed in the silver nitrate-lead chromate system, there is formed at the air-gel interface a third, ribbon-like, brown set. Such iridescent sets were observed during this work, and they are thought to be secondary in origin as a result of surface tarnishing. They can be leached off readily with dilute nitric acid, and replaced, especially in an atmosphere rich in hydrogen sulfide. The first leachings test strongly for sulfide ion.

SUMMARY AND CONCLUSIONS

1. Silver chromate supersaturates readily in water, gelatin, agar, and bentonite suspension media. Representative values of the supersolubility constant for such solutions are given.

2. These supersaturated solutions return to equilibrium slowly, even in the presence of seeds.

3. The usual Liesegang ring materials supersaturate readily and adjust slowly, yet it does not necessarily follow that supersaturation precedes rhythmic precipitation. The indications that it does are as follows: (*a*) Direct analysis of sections about to have a Liesegang ring deposited discloses supersaturation of the above order. (*b*) There is a definite concentration of like or isomorphous seed crystals which prevents rhythmic precipitation. Smaller amounts are ineffective, because the rate of diffusion is high compared to the rate of crystal growth.

4. The compound to be precipitated as a Liesegang ring is present as a crystalloid and not as a complex colloid.

5. The point of view adopted suggests a new method for measuring the rate of growth of crystals from supersaturated solutions.

6. The mechanism of rhythmic crystallization from melts and from solutions is pictured in the same way as the Liesegang phenomenon.

REFERENCES

(1) Bolam, T. R.: Trans. Faraday Soc. **24**, 463 (1928); **26**, 133 (1930); **29**, 864 (1933).
(2) Bolam, T. R., and MacKenzie, M. R.: Trans. Faraday Soc. **22**, 151, 162 (1926).
(3) Dhar and Chatterji: J. Phys. Chem. **28**, 41 (1934).
(4) Dippy: J. Phys. Chem. **36**, 2354 (1932).
(5) Fricke and Suwelack: Z. physik. Chem. **124**, 359 (1926).
(6) Ghosh: J. Indian Chem. Soc. **7**, 509 (1930).
(7) Hedges, E. S.: Liesegang Rings. Longmans, Green and Co., London (1932).
(8) Hughes, E.: Biochem. J. **28**, 1086 (1934); Kolloid-Z. **71**, 100 (1935); **72**, 216 (1935).
(9) Hughes, E.: Nature **123**, 603 (1929).
(10) International Critical Tables, Vol. IV, p. 226. McGraw-Hill Book Co., Inc., New York (1928).

(11) International Critical Tables, Vol. VII, p. 287. McGraw-Hill Book Co., Inc., New York (1930).

(12) JABLCZYNSKI: Bull. soc. chim. [4] **33**, 1592 (1923).

(13) KUSTER: Kolloid-Z. **10**, 225 (1912).

(14) LINCOLN AND HILLYER: J. Phys. Chem. **40**, 645 (1936).

(15) LLOYD AND MORAVEK: J. Phys. Chem. **35**, 1512 (1931).

(16) McMASTERS, ABBOTT, AND PETERS: J. Am. Chem. Soc. **57**, 2504 (1935).

(17) MENDHALL AND MASON: Proc. Natl. Acad. Sci. U. S. **9**, 199 (1923).

(18) MORSE, H. W.: J. Phys. Chem. **34**, 1554 (1930).

(19) NOTBOOM: Kolloid-Z. **32**, 247 (1923).

(20) OSTWALD, WILHELM: Lehrbuch der allgemeinen Chemie, 2nd edition. Leipzig (1891).

(21) OSTWALD, WO.: Kolloid-Z. **36**, 380 (1935).

(22) WILLIAMS, A., AND McKENZIE, M. R.: J. Chem. Soc. **117**, 844 (1920).

SUPERSATURATION AND LIESEGANG RING FORMATION. II

ANDREW VAN HOOK[1]

Department of Chemistry, Lafayette College, Easton, Pennsylvania

Received July 20, 1938

It has been reiterated (12) that a supersaturation theory of Liesegang ring formation is compatible with the fact that rings are formed in the presence of crystal seeds of the material to be precipitated, if it is assumed that the rate of diffusion is rapid compared to the rate of crystal growth. There should then exist a critical concentration of seeds above which rhythmic precipitation will not occur. This has been observed (7, 12), and for particular conditions it is approximately independent of the medium. For concentrations below the critical the clarity and number of bands should increase as the seed concentration diminishes. This has been confirmed qualitatively, and it is with the quantitative aspects of this variation that this paper deals.

THEORETICAL

The classical case of strong silver nitrate diffusing into dilute potassium chromate may be taken as a model. In the usual experimental arrangement the source of silver nitrate is considered inexhaustible at the concentration of the saturated solution. Counterdiffusion of the weak potassium chromate solution will be neglected in the following simplified treatment.

By Fick's law the amount of silver nitrate diffusing regularly into a volume dx at a distance x from the origin is $D\frac{dc}{dx}$, where D is the diffusion constant. The amount leaving is

$$D\left(\frac{dc}{dx} - \frac{\partial \frac{dc}{dx}}{\partial x}\, dx\right)$$

or the amount accumulating is $D\left(\frac{d^2c}{dx^2}\right) dx$. This is potentially $\frac{D\left(\frac{d^2c}{dx^2}\right) dx}{2}$ moles of silver chromate, provided that the chromate-ion concentration is sufficient.

---

[1] Present address: Department of Chemical Engineering, University of Idaho, Moscow, Idaho.

If crystal seeds of surface s are dispersed uniformly throughout the medium, each one will grow at the rate of

$$\frac{\mathrm{d}w}{\mathrm{d}\theta} = ks[f(c-c_0)]$$

where $(c-c_0)$ is the supersaturation of silver chromate. The total growth will be $nks[f(c-c_0)]\mathrm{d}x$, where n is the seed density. The concentration of silver chromate, c, refers to a state of non-stable equilibrium, and therefore it is reasonable to interpret it in terms of an equivalent concentration of silver nitrate, i.e., potential silver chromate, generated by the incoming silver nitrate. This presumption amounts to neglecting the effect of the inner ion concentration on the rate of growth of the seeds, and seems appropriate in view of the incompletely known form of the rate of crystallization function, and also in view of the approximate experimental results obtained.

The limit of band formation will correspond to the condition when the rate of crystal growth equals the rate at which silver nitrate diffuses into the section: namely,

$$\frac{2nks}{D}\,[f(c - c_0] = \frac{\mathrm{d}^2c}{\mathrm{d}x^2}$$

That the Noyes-Whitney (10)-Nernst (9) theory of a unimolecular crystal growth is inadequate is evident from the work of Marc (6), who found that the order varies from unimolecularity to bimolecularity with decreasing temperature. Other workers (1, 2, 4, 5) also find a decided approximate nature for the first-order expression. Therefore, taking

$$f(c-c_0) = (c-c_0)^\alpha$$

empirically, the above equation may be solved by setting $(c-c_0)$ equal to y, and multiplying through by $2\mathrm{d}y/\mathrm{d}x$:

$$2\,\frac{\mathrm{d}y}{\mathrm{d}x}\cdot\frac{\mathrm{d}^2y}{\mathrm{d}x^2} = 2\left(\frac{2nks}{D}\right)y^\alpha\,\frac{\mathrm{d}y}{\mathrm{d}x}$$

Integrating:

$$\left(\frac{\mathrm{d}y}{\mathrm{d}x}\right)^2 = \frac{2}{\alpha+1}\left(\frac{2nks}{D}\right)y^{\alpha+1} + K_1$$

At $y = 0$, $c = c_0$, and $\mathrm{d}y/\mathrm{d}x = 0$, whence $K_1 = 0$, and

$$y^{-\left(\frac{\alpha+1}{2}\right)}\,\mathrm{d}y = \sqrt{\frac{2}{\alpha+1}\left(\frac{2nks}{D}\right)}\,\mathrm{d}x$$

Integrating again and evaluating the constant by means of the condition that c = a constant, B, at $x = 0$ gives the solution in the final form:

$$\left(\frac{1}{(c-c_0)^{\left(\frac{\alpha-1}{2}\right)}} - \frac{1}{(B-c_0)^{\left(\frac{\alpha-1}{2}\right)}}\right) = -\left(\frac{\alpha-1}{2}\right)\sqrt{\frac{2}{\alpha+1}\left(\frac{2nks}{D}\right)}\,x$$

If the criterion of Liesegang ring formation is taken as

$$C = \sqrt{\frac{\mathrm{H}}{[\mathrm{CrO_4^{--}}]}}$$

where H is the supersolubility product (3), then when everything but n is held constant, the extent of band formation will be given by $nx^2 =$ constant.

The foregoing analysis is admittedly crude, mainly because of considering the chromate-ion concentration constant and ignoring its counter-diffusion. This complication has been considered[2] and the correction is deemed unwarranted in view of the necessity of either transforming silver- and chromate-ion concentrations into un-ionized silver chromate concentration, or else expressing the crystal growth equation in terms of these two ion concentrations. Accurate information concerning these operations is not yet available.

EXPERIMENTAL

The relation, $nx^2 =$ constant, was tested with silver chromate in gelatin and in bentonite, lead iodide in agar, and magnesium hydroxide in agar systems. The usual capillary technic, with 1.5-mm. tubing, was utilized. Measurements of the extent of band formation were made to the nearest 0.1 mm. with an ordinary scale and magnifying glass, or to 0.01 mm. by means of a Gaertner micrometer microscope. In all rhythmic precipitation experiments there is a distance, immediately surrounding the point of inoculation, in which the precipitation is general. This "flushing-in" area, preceding the commencement of band formation, increases with the ratio of the concentrations of the reactants. The extent of band formation, x, was usually measured from the head of the series of bands, but since it was not always easy to identify this position (especially as the seed concentration increases), distances in such cases were measured to the point of inoculation and the results plotted in accordance with the modified equation:

$$n(x-a)^2 = \text{constant}$$

No appreciable difference in behavior was observed with seeds prepared and added in three different ways. For preliminary work seeds were precipitated "internally" (12). Externally precipitated seeds were prepared by bringing together the necessary reactants under conditions duplicating the experiment to be performed, and, after thorough mixing, the gel was allowed to set without agitation in a tall cylindrical vessel. Aliquot portions of a narrow horizontal slab were taken for seeding pur-

---

[2] Thanks are due Dr. R. Bailey of the Department of Mathematics of Lafayette College for assistance in this task.

poses. The third method consisted in precipitating the respective materials, washing, drying in an oven, and finally powdering. Graded portions were used, usually between 200 and 250 mesh in size.

Each batch of experiments was inoculated simultaneously with an excess of concentrated reactant. Observations on the extent of ring formation were made at various times, and for each set of conditions it was found that there was an optimum period of observation for best results. Beyond this time the rings became indefinite, distorted, and even totally obliterated, owing to secondary effects, while earlier the distance of ring formation was not sufficient for comparative purposes. The best time usually corresponded with the formation of 10 to 20 mm. of rings in a blank experiment.

RESULTS AND DISCUSSION

Representative results are presented in the following log-log plots (figures 1, 2, and 3). The points represent observed values, while the line is placed with a slope of -2 as expected from the equation:

$$\log n + 2 \log x = \text{constant}$$

In general the relation is approximately valid over a considerable portion of the entire range, although serious discrepancies exist. The more serious deviations at large values of n may be associated with the arbitrary assumption of ignoring the chromate-ion diffusion, while at the other extremity the generation and initial rapid growth of new nuclei may be the cause of the deviation.

That the presence of seeds does not seriously influence the fundamental diffusion nature of the Liesegang phenomenon is evident upon application of the Morse and Pierce (8) and Schleusner (11) relations: namely, $h_n/\sqrt{t_n} = \text{constant}, K$; and $h_n/h_{n-1} = \text{constant}, q$, respectively. h and t are the distance and time of appearance of a particular band. For 0.01 M potassium chromate in 5 per cent gelatin with (*a*) no seeds, (*b*) "internally" precipitated silver chromate seeds equivalent to 0.001 M potassium chromate, and (*c*) 0.0025 M seeds, the results shown in table 1 were obtained.

The rapid decrease in the values of k, as banding proceeds, for cases b and c is as expected. If the distance of the diffusion wave front (which is difficult to discern in case c) is employed for h, the values found for k are better:

Case	*Values of k*	*Average*
b	4.3; 4.4; 4.2; 4.0; 3.9	4.2
c	5.0; 4.3; 4.5; 4.1; 3.8	4.3

The slight decrease in these values over a distance well beyond that of usual observation indicates that the total diffusion during the time of

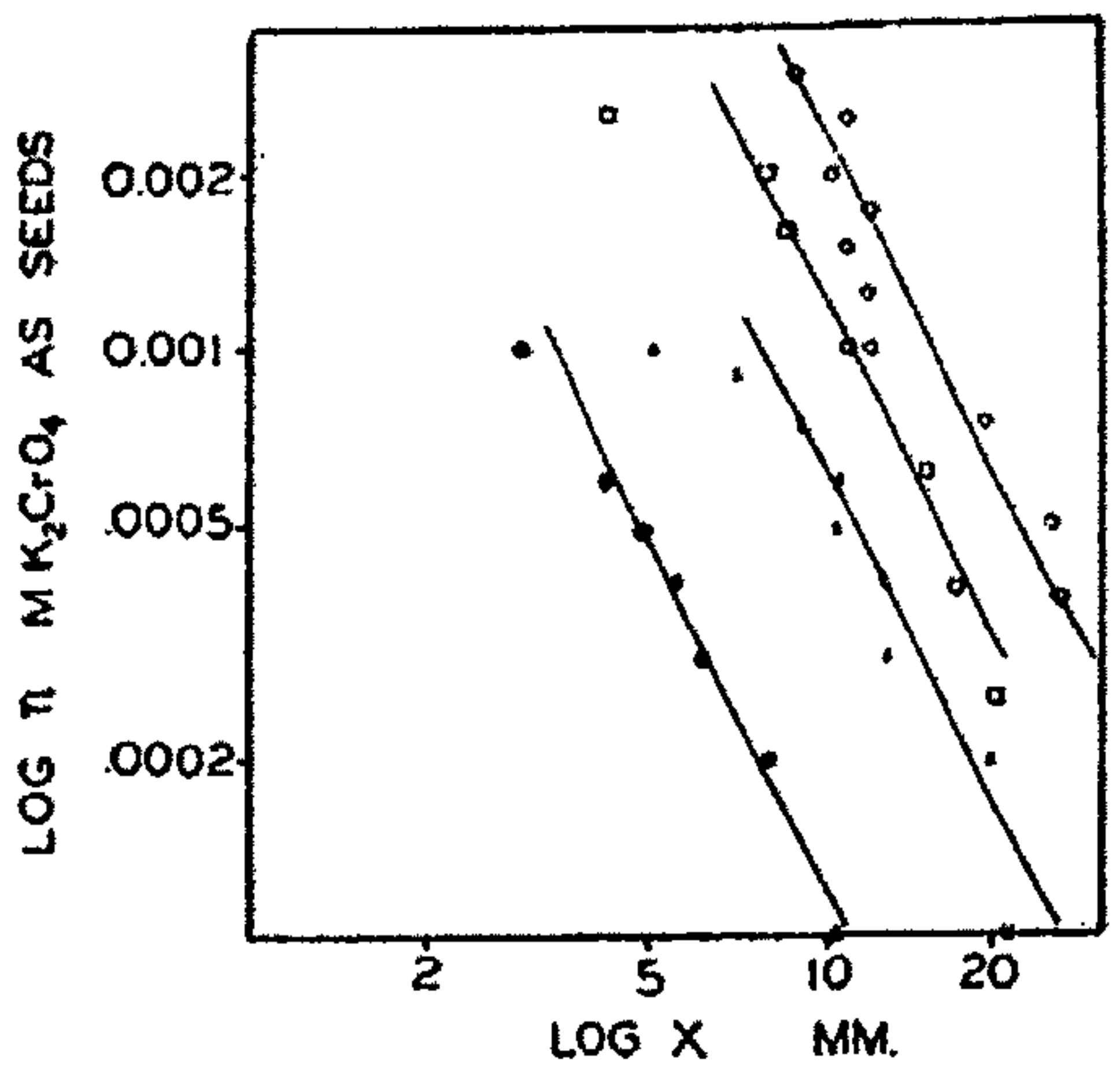

FIG. 1. 0.01 *M* potassium chromate in 5 per cent gelatin. Saturated silver nitrate. Seeds prepared as follows: □, "internally"; ○, "externally"; ×, dry; ●, "externally" in test tube experiment.

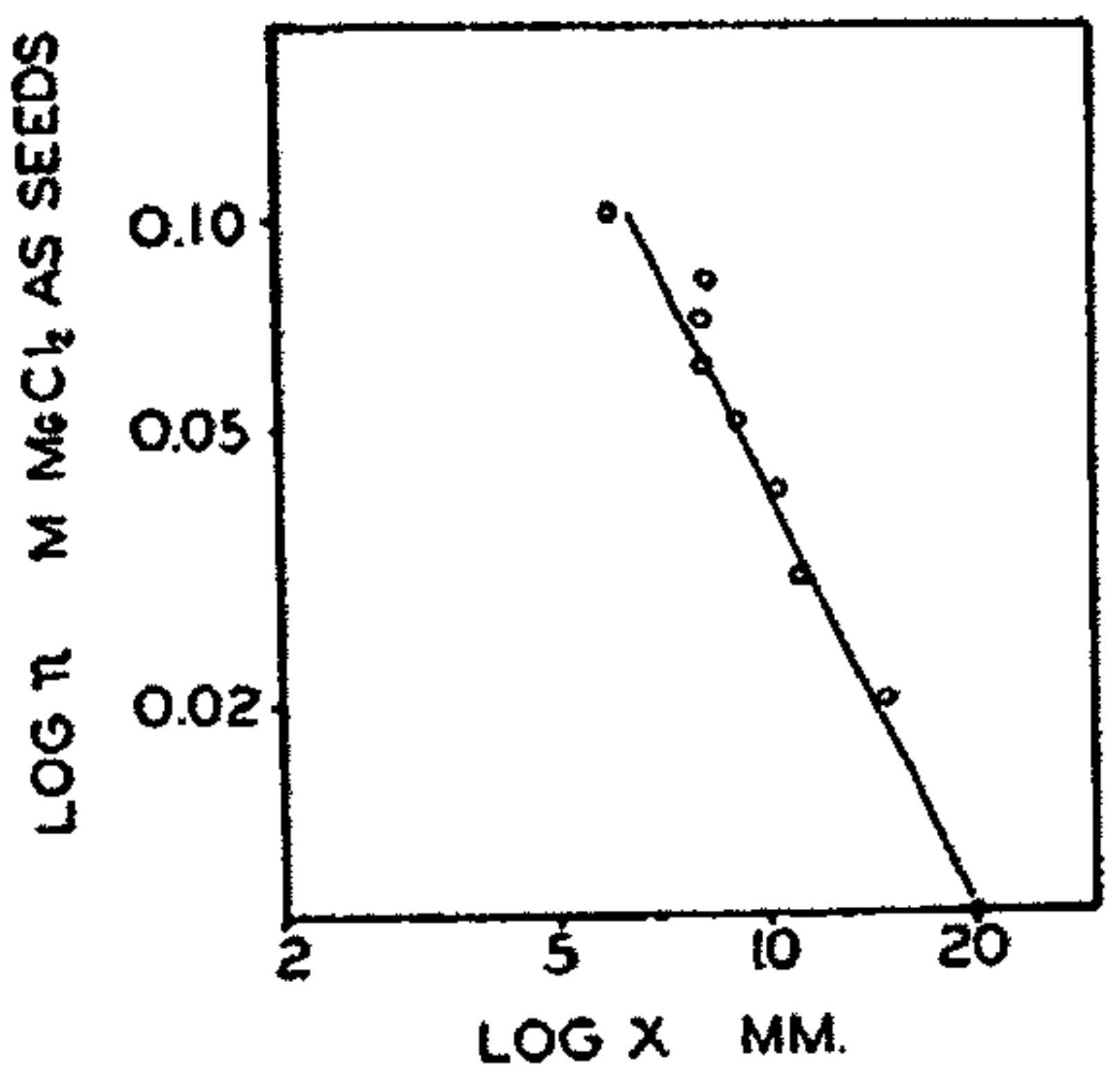

FIG. 2

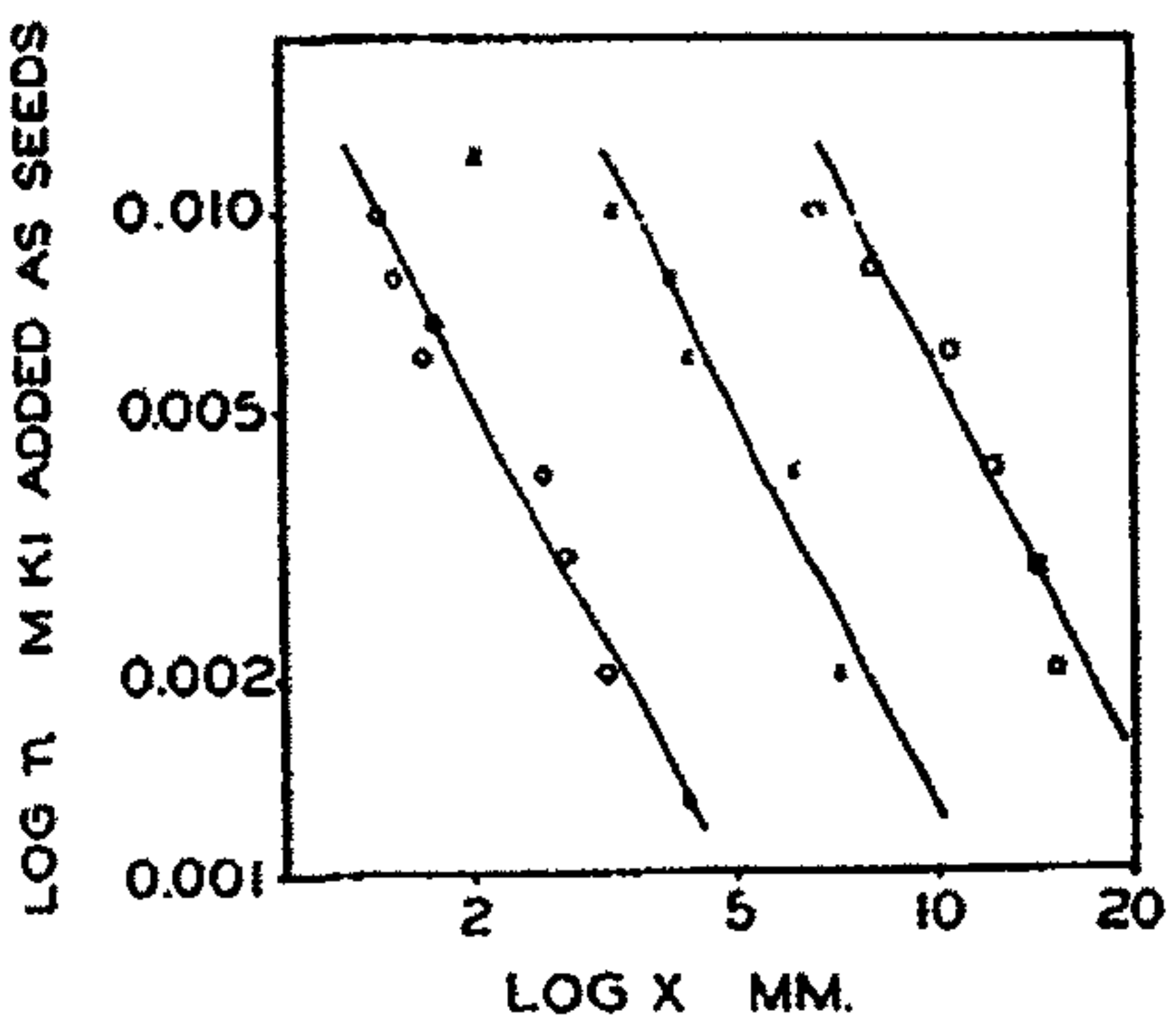

FIG. 3

FIG. 2. 1 *M* magnesium chloride in 1.5 per cent agar. 10 *M* ammonium hydroxide. Seeds prepared "externally".

FIG. 3. 0.1 *M* potassium iodide in 1.5 per cent agar. Half-saturated lead nitrate. Seeds prepared as follows: ○, "internally"; ×, "externally"; □, dry.

TABLE 1

Values of q and k

CONSTANTS	CASE	VALUES	AVERAGE
q	*a*	1.11; 1.08; 1.06; 1.11; 1.11; 1.10	1.10
	b	1.06; 1.12; 1.05; 1.07; 1.09; 1.08	1.08
	c	1.01; 1.05; 1.03; 1.06; 1.05; 1.04	1.04
K	*a*	4.49; 4.45; 4.55; 4.50	4.50
	b	4.2 ; 4.40; 4.2 ; 3.28	
	c	4.9 ; 4.51; 4.2 ; 2.4	

interest is little disturbed by the presence of seeds. That is, the number added is negligible compared to the number generated in the formation of a definite and distinct Liesegang band. Simultaneously with the above observations (extending over a distance of 30 to 50 mm. and up to 60 hr.), it was noted that the chromate-ion concentration remained undisturbed at a distance of only 2 to 5 mm. ahead of the diffusion wave front. In the capillaries used it would have been possible to detect visibly a variation of 10 to 15 per cent in concentration. This makes the early assumption of ignoring counterdiffusion of potassium chromate more agreeable.

According to the original complete expression, nsx^2 should be constant. Since s is proportional to the average size squared, then nL^2x^2 = constant; or if n is held constant, L and x should vary in an inverse manner. This was found to be only qualitatively true, x being less dependent on L than indicated.

SUMMARY AND CONCLUSIONS

The extent of Liesegang ring formation (x) in the presence of crystal seeds of the material precipitating is found to decrease rapidly as the number of nuclei (n) increases.

Over a limited range there is approximate confirmation of the expression nx^2 = constant. More exact information on the effect of ion concentrations on the rate of growth of slightly soluble substances is necessary for a more complete form of the above expression.

The initial presence of crystal seeds does not alter the fundamental diffusion nature of the Liesegang phenomenon.

REFERENCES

(1) Campbell, A. N., and Campbell, J. R.: Trans. Faraday Soc. **33**, 299 (1937).
(2) Gapon, E. N.: J. Russ. Phys. Chem. Soc. **61**, 1729, 2319 (1929).
(3) Hughes, E. B.: Kolloid-Z. **71**, 100 (1935); **72**, 216 (1935).
(4) Jenkins, J. D.: J. Am. Chem. Soc. **47**, 902 (1925).
(5) Kurbatov: Z. Krist. **77**, 164 (1931).
(6) Marc: Z. physik. Chem. **73**, 685 (1910).
(7) Morse, H. W.: J. Phys. Chem. **34**, 1554 (1930).
(8) Morse, H. W., and Pierce, G. W.: Z. physik. Chem. **45**, 589 (1903).
(9) Nernst, W.: Z. physik. Chem. **47**, 52 (1904).
(10) Noyes-Whitney: Z. physik. Chem. **23**, 688 (1897).
(11) Schleussner: Kolloid-Z. **34**, 338 (1924).
(12) van Hook, A.: J. Phys. Chem. **42**, 1191 (1938).

THE SURFACE TENSION-VISCOSITY RELATION

C. A. BUEHLER

Department of Chemistry, University of Tennessee, Knoxville, Tennessee

Received June 4, 1938

The surface tension and viscosity are two easily found physical constants which have been employed with some success in the determination of the structure of chemical compounds. Unlike many other physical properties, both appear in equations which, when applied to many organic compounds, give constant values regardless of the temperature. Because of this fact, a comparison of these equations becomes of interest in that it points out a relation between the surface tension and viscosity somewhat simpler than those (3, 4) previously advanced.

The surface tension appears in the well-known parachor equation in which P, the parachor, may be expressed, at temperatures removed from the boiling point, as

$$P = \frac{M\gamma^{\frac{1}{4}}}{D} \tag{1}$$

where M is the molecular weight, γ the surface tension, and D the density of the liquid. Recently Souders (5) has advanced a similar equation in which the viscosity appears:

$$I = \frac{M}{D}\left(\log_{10}(\log_{10}\eta) + 2.9\right) \tag{2}$$

Here I is the viscosity-constitutional constant and η is the viscosity. Since the data compiled in table 1 show that

$$1.2P = I$$

it follows from equations 1 and 2 that at the same temperature, since the densities are equal,

$$\gamma^{\frac{1}{4}} = \frac{\log_{10}(\log_{10}\eta) + 2.9}{1.2}$$

or

$$\log_{10}(\log_{10}\eta) = 1.2\gamma^{\frac{1}{4}} - 2.9$$

The compounds selected in table 1 are those for which the parachor is independent of the temperature. Alcohols, phenols, amines, and carboxylic acids, all of which exhibit an increase in parachor with a temperature rise, were intentionally omitted. The variations shown in I/P are doubtless due to inaccuracies in the physical constants involved, yet it is interesting to note that there seems to be a tendency for this constant to increase as the carbon chain lengthens.

TABLE 1

Parachor and viscosity-constitutional constants

COMPOUND	P	I*	I/P
Hexane	271.0†	340	1.25
Heptane	310.8†	393.5	1.27
Octane	350.7†	449	1.28
Decane	430.6†	561	1.30
Benzene	207.5‡	249.8	1.20
Toluene	246.5‡	296.2	1.20
Ethyl benzene	285.4‡	344.7	1.21
o-Xylene	283.3§	347	1.22
m-Xylene	284.5¶	343.5	1.21
p-Xylene	284.5¶	346.0	1.22
Naphthalene	312.5§	376.6	1.21
Methyl iodide	146.2†	170	1.16
Ethyl bromide	165.7†	198.5	1.20
Ethyl iodide	187.0†	225.5	1.21
Propyl chloride	190.4†	232	1.22
Propyl bromide	205.3†	250	1.22
Propyl iodide	226.0†	276.5	1.22
Isopropyl bromide	205.1§	257	1.25
Isobutyl chloride	228.4§	286	1.26
Isobutyl bromide	243.8§	303	1.24
Chlorobenzene	244.2¶	290.5	1.19
Bromobenzene	257.9¶	307.5	1.19
Ethyl ether	211.8§	257.0	1.21
Acetone	161.5§	191.5	1.19
Methyl ethyl ketone	199.5¶	241.5	1.21
Diethyl ketone	236.2§	288.5	1.22
Nitrobenzene	263.3§	308.5	1.17
m-Nitrotoluene	298.8§	358.9	1.20
Ethyl formate	177.7§	215.5	1.21
Methyl acetate	177.0§	211.5	1.19
Ethyl acetate	216.5‡	265.5	1.23
Propyl acetate	257.0‡	321.5	1.25
Mean			1.22

* Values are from reference 5. When a range is given, the intermediate value has been used.

† Values are from reference 2.

‡ Values are from reference 1.

§ Brit. Assoc. Advancement Sci. Rep. 1932, 265–83. When several values are given, a mean was used.

¶ Unpublished results of this laboratory.

REFERENCES

(1) **Buehler, C. A., Gardner, Thomas S., and Clemens, Milton L., Jr.**: J. Org. Chem. **2**, 167 (1937).
(2) **Desreux, V.**: Bull. soc. chim. Belg. **44**, 249 (1935).
(3) **Sharma, R. K.**: Quart. J. Indian Chem. Soc. **2**, 310 (1925).
(4) **Silverman, Daniel, and Roseveare, W. E.**: J. Am. Chem. Soc. **54**, 4460 (1932).
(5) **Souders, Mott, Jr.**: J. Am. Chem. Soc. **60**, 154 (1938).

THE SOLUBILITY OF NITROGEN AND ARGON IN SEA WATER[1]

NORRIS W. RAKESTRAW AND VICTOR M. EMMEL

Woods Hole Oceanographic Institution, Woods Hole, Massachusetts

Received April 30, 1938

INTRODUCTION

We recently described a method for the determination of dissolved nitrogen in sea water (4), in which the air is removed from the water sample *in vacuo* and the oxygen, nitrogen, and inert gas residue are measured separately. In making such determinations on actual sea water it is often necessary to compare the values obtained with the equilibrium solubility of nitrogen from the atmosphere. The only figures available for such comparison are those obtained by Fox (2, 3), which have never been seriously questioned. Using these for comparison, however, our analyses consistently indicated an unsaturated condition of water from nearly all sources, with respect to gaseous nitrogen. Believing this to be unlikely, and convinced of the accuracy of our own method, we undertook a redetermination of the solubility of nitrogen in sea water of different temperatures and chlorine contents, within the range ordinarily encountered.

Fox's method consisted in the measurement of the volume of "atmospheric nitrogen" absorbed by a fixed volume of water from a known total volume of the gas. This requires a correction for the argon content of the "atmospheric nitrogen," which can probably be made with sufficient accuracy for our purpose, even though the absorption coefficient of argon in sea water is not well known. But in addition to this, considering the use to which these figures are to be put, it would seem preferable to let the water come into complete equilibrium with the actual atmosphere, rather than with nitrogen alone, and to determine the dissolved nitrogen directly, assuming a constant composition of the atmosphere. The results of such a procedure, described below, are slightly lower than those of Fox (corrected for argon), but are more consistent with the nitrogen content which we find in sea water in nature.

Examining Fox's method more closely, we suspected that his systems might have been supersaturated. He saturated the water by vigorous shaking for several minutes, followed by only a short period of standing, until the pressure became constant. We have found that on shaking sea

---

[1] Contribution No. 175 from the Woods Hole Oceanographic Institution.

TABLE 1

Experimental data

CHLORINE CONTENT	SAMPLE*	EQUILIBRIUM TEMPERATURE	EQUILIBRIUM PRESSURE	MEASURED VOLUME		EQUILIBRIUM SOLUBILITY AT 760 MM. ATMOSPHERIC PRESSURE IN MILLILITERS PER 1000 ML. OF WATER	
				Nitrogen	Residue	Nitrogen	"Argon"
grams per kilogram		*°C.*	*mm.*	*ml.*	*ml.*	*ml.*	*ml.*
16.03	A	2.11	766.3	1.434		14.22	
	A	7.08	758.7	1.262	0.0356	12.68	0.352
	B	7.08	758.7	1.262	0.0346		
	A	12.15	767.0	1.160	0.0317	11.53	0.312
	B	12.15	767.0	1.162	0.0312		
	A	18.03	765.5	1.038	0.0289	10.33	0.288
	B	18.03	765.5	1.041	0.0290		
	A	25.05	764.0	0.925	0.0242	9.19	0.240
	B	25.05	764.0	0.920	0.0244		
18.00	A	2.11	767.0	1.394		13.81	
	A	7.08	758.7	1.283	0.0339	12.40	0.341
	B	7.08	758.7	1.234	0.0340		
	A	12.15	766.3	1.134	0.0301	11.27	0.303
	B	12.15	766.3	1.134	0.0309		
	A	18.03	768.5	1.016	0.0274	10.05	0.270
	B	18.03	767.7	1.015	0.0272		
	A	25.05	763.2	0.903	0.0237	9.00	0.236
	B	25.05	762.5	0.903	0.0236		
19.99	A	2.11	767.0	1.363		13.50	
	A	7.08	758.7	1.203	0.0338	12.08	0.332
	B	7.08	758.7	1.201	0.0324		
	A	12.15	766.3			10.95	0.296
	B	12.15	766.3	1.103	0.0298		
	A	18.03	764.7	0.991	0.0271	9.89	0.266
	B	18.03	764.7	0.997	0.0265		
	A	25.05	762.5	0.880	0.0226	8.81	0.227
	B	25.05	762.5	0.886	0.0230		

* Sample A was saturated with air at a temperature above the equilibrium temperature; sample B at a temperature below.

water with air and allowing to stand until the air bubbles are no longer visible, the nitrogen content is regularly about 2 per cent higher than the equilibrium value at that temperature. It has long been known that the surface water of the sea may be supersaturated with air, from the abnormal solubility of fine bubbles of foam. We are of course in no position to urge that the difference between our solubility values and those of Fox is entirely due to this.

METHOD

Samples of natural sea water containing approximately 16, 18, and 20 g. of chlorine per kilogram were prepared by dilution from the highest concentration. Duplicate portions, of about 250 ml., were placed in citrate bottles, one of these warmed to about 30°C. and the other cooled to about 8°C., and both shaken for 30 min. to saturate them with air. They were then placed in a thermostat at 25°C. for 18 hr. to come to equilibrium, open to the air, with occasional but not too vigorous agitation. Both samples were then analyzed for nitrogen. The same was done at temperatures of 18°, 12°, 7°, and 2°C., the duplicate portions being always saturated at temperatures above and below the final equilibrium temperature, except in the case of the lowest one, in which this was not possible. It may safely be assumed that complete equilibrium was reached in this latter instance also, in view of the satisfactory agreement of the two samples at all other temperatures.

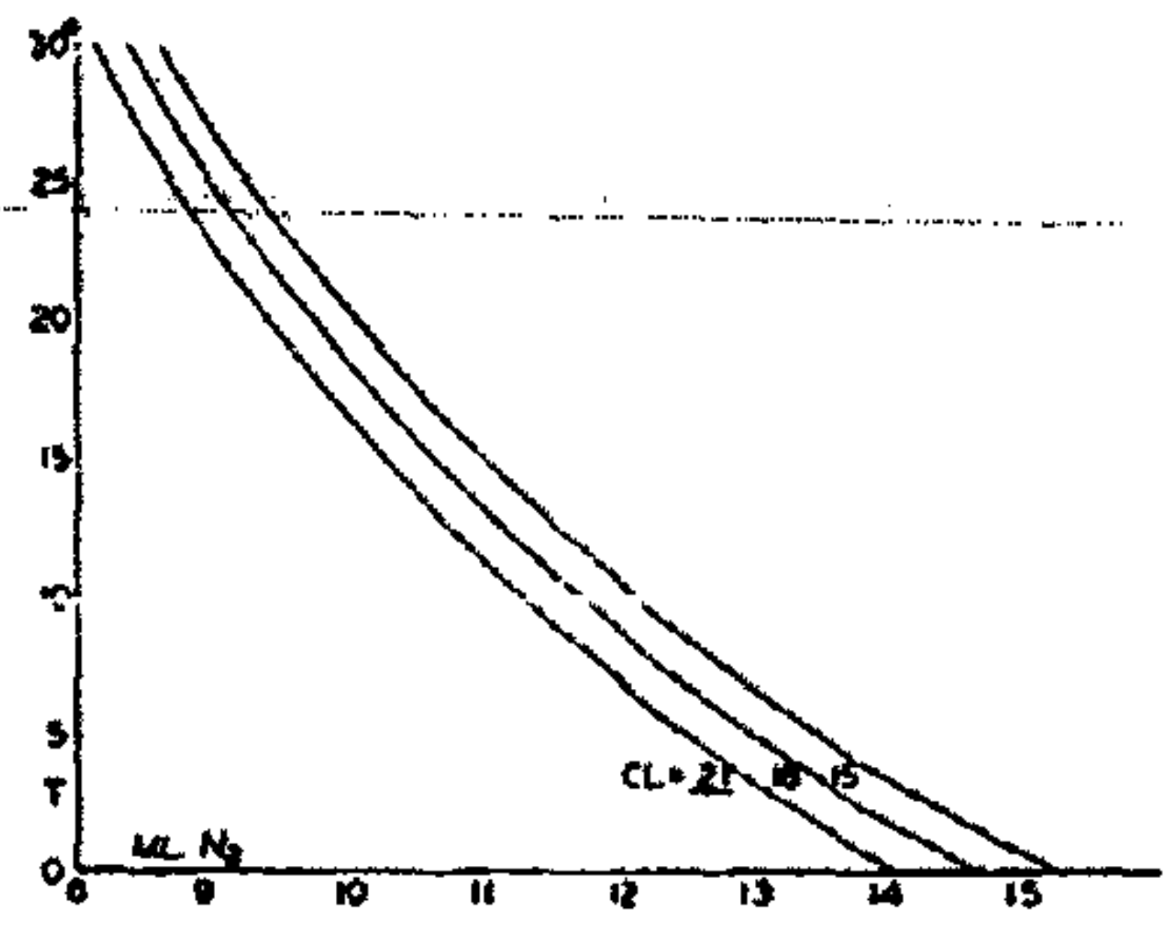

FIG. 1

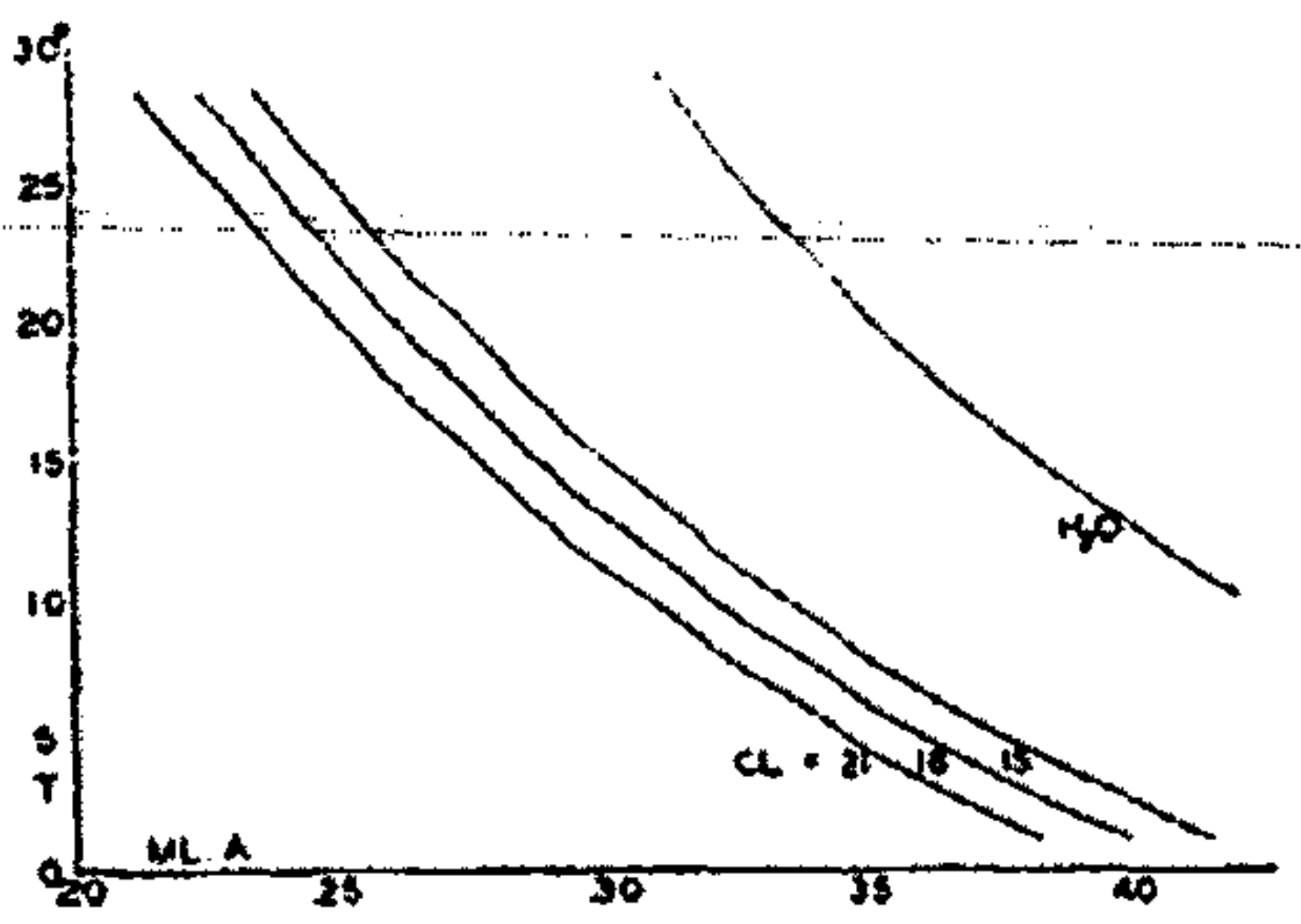

FIG. 2

FIG. 1. Solubility of nitrogen in sea water of different chlorine contents and temperatures. Solubility is expressed in milliliters of gas (at standard temperature and pressure) per liter of water, in equilibrium with air at 760 mm.

FIG. 2. Solubility of "argon" (total inert gas in atmosphere) in sea water of different chlorine contents and temperatures. Solubility is expressed in milliliters of gas (at standard temperature and pressure) per liter of water, in equilibrium with air at 760 mm. The curve for the solubility in pure water is taken from results of Estreicher (1).

The data are given in table 1. The barometric pressure is included, from which, in the last column, is calculated the equilibrium solubility in contact with a normal atmosphere of 760 mm.

It was thought worth while to measure the residual gas, after removal of carbon dioxide, oxygen, and nitrogen, and to include this as "argon," although these figures are of a distinctly lower order of accuracy. This crude fraction of inert gas will therefore be designated as argon, although obviously impure. These figures were obtained by measuring the pressure of the residual gas, when contained in the capillaries between the stopcocks

TABLE 2

Solubility of nitrogen in sea water

Expressed in milliliters (at standard temperature and pressure) per liter of water, from a normal atmosphere of 760 mm.

CHLORINE CONTENT	15	16	17	18	19	20	21
TEMPERATURE	SOLUBILITY						
°C.	*ml.*	*ml.*	*ml.*	*ml.*	*ml.*	*ml.*	*ml.*
0	15.22	15.02	14.82	14.61	14.40	14.21	14.01
1	14.81	14.61	14.42	14.23	14.04	13.85	13.66
2	14.43	14.24	14.06	13.88	13.69	13.51	13.33
3	14.07	13.89	13.72	13.54	13.36	13.19	13.01
4	13.73	13.56	13.40	13.24	13.06	12.89	12.72
5	13.43	13.26	13.10	12.94	12.78	12.62	12.45
6	13.14	12.98	12.82	12.67	12.51	12.35	12.19
7	12.88	12.72	12.56	12.41	12.26	12.10	11.95
8	12.62	12.47	12.32	12.17	12.02	11.87	11.71
9	12.38	12.23	12.08	11.94	11.79	11.64	11.49
10	12.15	12.00	11.86	11.71	11.56	11.42	11.27
11	11.92	11.78	11.63	11.49	11.34	11.20	11.06
12	11.69	11.56	11.42	11.28	11.13	10.99	10.85
13	11.47	11.34	11.21	11.07	10.93	10.79	10.65
14	11.25	11.13	10.99	10.86	10.73	10.59	10.45
15	11.04	10.92	10.79	10.66	10.53	10.39	10.26
16	10.83	10.72	10.59	10.47	10.34	10.21	10.08
17	10.63	10.52	10.40	10.28	10.15	10.03	9.91
18	10.44	10.33	10.21	10.10	9.98	9.86	9.74
19	10.26	10.15	10.03	9.92	9.81	9.69	9.58
20	10.08	9.98	9.87	9.76	9.65	9.54	9.43
21	9.91	9.82	9.71	9.61	9.50	9.39	9.28
22	9.75	9.66	9.56	9.46	9.35	9.24	9.14
23	9.60	9.51	9.41	9.31	9.20	9.10	9.00
24	9.45	9.36	9.26	9.16	9.06	8.96	8.86
25	9.30	9.21	9.11	9.02	8.92	8.82	8.73
26	9.16	9.07	8.97	8.88	8.79	8.60	8.60
27	9.02	8.94	8.84	8.75	8.66	8.56	8.47
28	8.89	8.84	8.72	8.62	8.53	8.44	8.35

1, 2, and 3 in the apparatus, shutting off the reservoir C, ordinarily used during the measurement of the oxygen and nitrogen.

Plotting the nitrogen and argon content against chlorine content, at different temperatures, gave a series of straight lines, from which points were taken for the construction of the curves in figures 1 and 2. From these curves tables 2 and 3 have been constructed.

TABLE 3

Solubility of "argon" in sea water

Expressed in milliliters (at standard temperature and pressure) per liter of water, from a normal atmosphere of 760 mm.

CHLORINE CONTENT............	15	16	17	18	19	20	21
TEMPERATURE	SOLUBILITY						
°C.	*ml.*	*ml.*	*ml.*	*ml.*	*ml.*	*ml.*	*ml.*
2	0.405	0.400	0.395	0.389	0.384	0.379	0.373
4	0.384	0.379	0.374	0.369	0.363	0.358	0.352
6	0.365	0.360	0.355	0.350	0.345	0.340	0.335
8	0.347	0.343	0.338	0.333	0.329	0.324	0.319
10	0.331	0.327	0.323	0.318	0.314	0.310	0.305
12	0.317	0.313	0.309	0.304	0.300	0.296	0.292
14	0.304	0.300	0.296	0.292	0.288	0.284	0.280
16	0.292	0.288	0.284	0.280	0.277	0.273	0.269
18	0.282	0.278	0.274	0.270	0.267	0.263	0.259
20	0.272	0.268	0.264	0.260	0.256	0.253	0.249
22	0.262	0.258	0.255	0.251	0.247	0.244	0.240
24	0.253	0.249	0.246	0.242	0.238	0.235	0.231
26	0.244	0.240	0.237	0.233	0.229	0.226	0.222
28	0.235	0.231	0.228	0.224	0.220	0.217	0.213

REFERENCES

(1) Estreicher, T.: Z. physik. Chem. 31, 176 (1899).

(2) Fox, C. J. J.: Publ. de circonstance. Cons. perm. internat. #41 (1907).

(3) Fox, C. J. J.: Trans. Faraday Soc. 5, 68 (1909).

(4) Rakestraw, N. W., and Emmel, V. M.: Ind. Eng. Chem., Anal. Ed. 9, 344 (1937).

THE OXIDATION-REDUCTION POTENTIALS OF UNSTABLE ORGANIC SYSTEMS[1]

A. E. CAMERON

Kodak Research Laboratories, Rochester, New York

Received April 9, 1938

The determination of the oxidation-reduction potential of a system requires that the two forms be present and in thermodynamic equilibrium under the conditions of the experiment. The rapidity with which the oxidized forms of most photographic developing agents are converted into other compounds, particularly in alkaline solution, makes direct measurements upon a mixture of reduced and oxidized forms uncertain. Fieser (5, 7, 8) introduced a method of making oxidation–reduction measurements upon such systems, based upon the experimental fact that the oxidized forms of many irreversible systems have a definite but short life in solution. When enough oxidizing solution is added to the reduced form of such a system to produce a half-oxidized mixture, and the readings of the observed potential of a noble metal electrode are plotted as a function of time, it is frequently possible to extrapolate to zero time and thus determine the potential of the mixture before alteration in the concentration of the oxidized form takes place.

This paper is the result of the application of Fieser's method to measurements upon certain organic systems of interest to photographic theory.

EXPERIMENTAL

The *p*-methylaminophenol sulfate used was the photographic product Elon, manufactured by the Eastman Kodak Co. This was given the purification treatment outlined by Schering (13) to eliminate any *p*-aminophenol present. A hot saturated solution of *p*-methylaminophenol sulfate in dilute acetic acid was treated with benzaldehyde, allowed to cool, the crystals filtered off, and a second crop of crystals thrown out by addition of acetone. Two recrystallizations were carried out from dilute sulfuric acid solution, with rejection of the first small crop of crystals formed in each case.

The monosulfonic acid of *p*-methylaminophenol was prepared by T. H. James of these laboratories by heating it with sulfuric acid for 8 hr. on a water bath and pouring it into water. No further purification

---

[1] Contribution No. 660 from the Kodak Research Laboratories.

was carried out, other than a thorough washing of the precipitate. The hydroquinone used was the photographic product manufactured by the Eastman Kodak Co., and the hydroxyhydroquinone was twice recrystallized before use.

All buffer salts used were of reagent quality from reliable manufacturers, as was the potassium ferricyanide used as oxidizing agent. For measurements in acid solutions it was found necessary to prepare potassium molybdicyanide. In this preparation the directions of Fieser (6) were followed. The oxidizing solutions were stored in dark glass bottles wrapped in opaque cloth.

The nitrogen used to maintain an inert atmosphere was taken from a commercial cylinder of compressed gas. Gas from the cylinder was passed through two towers of solid ammonium carbonate, and then through a tower of soda lime, leaving a definite partial pressure of ammonia in the gas. The mixture was passed through a quartz tube packed with platinized asbestos free from sulfur and heated to 450–500°C. Ammonia remaining after the reaction of ammonia and oxygen was removed with wash towers of 30 per cent sulfuric acid colored with bromophenol blue to indicate exhaustion, and acid spray and carbon dioxide were removed with a wash of 60 per cent potassium hydroxide. A bottle of a 0.1 per cent solution of reduced indigodisulfonate in the line indicated complete absence of oxygen, even at high rates of flow. It is important to insure saturation of the gas stream with ammonia, however. Exhaustion of any reagent was readily noted, and the line could be operated for long periods of time without attention.

Solutions of the compounds investigated were made up in 0.02 *M* concentration and stored in clear glass flasks in an atmosphere of hydrogen. The flasks were arranged so that the solutions could be delivered to water-jacketed, 10-ml. burets without destroying the protective atmosphere. The *p*-methylaminophenol and the monosulfonic acid both showed some sign of decomposition, even in acid solution. They gradually acquired a brownish-red coloration. This decomposition did not proceed to the point where a change in titer could be noted.

The reference half-cell and bridge employed in the pH determinations and in the oxidation–reduction potential measurements were 3.5 *N* in potassium chloride. This solution was prepared volumetrically at 20°C. This half-cell was assigned the value of 0.2502 volt against the normal hydrogen electrode at 20°C., and this value was used throughout the calculations.

APPARATUS

The essential parts of the apparatus are outlined in figure 1. A double-walled beaker, the top of which was flattened and ground plane, was fitted with a flanged glass cap, also ground plane, which carried a water seal for the stirrer, a glass electrode, and a neck in which could be inserted a stopper carrying the platinized electrodes, or blank platinum and gold electrodes. Lead-in tubes for the salt bridge and for the gas supply to a porous alundum bubble head were sealed through the cap. Three small necks on the cap permitted insertion of buret tips with pieces of small rubber tubing for gasketing. A thermometer mounted in this same cap permitted the determination of the temperature of the reaction mixture. Water was pumped through the jackets of the reaction vessel, the half-cell, and the burets from a 35-gallon thermostat operating at 20°C. ± 0.01°.

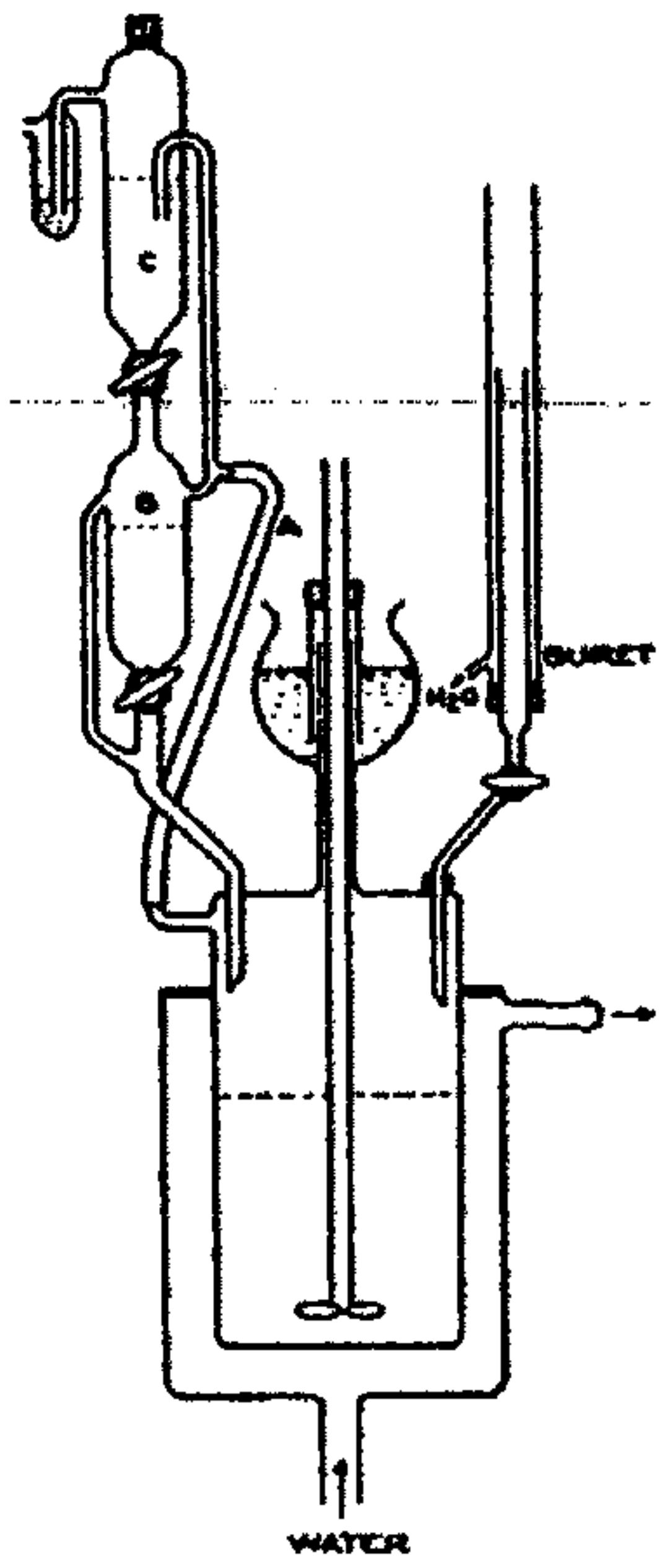

FIG. 1. The apparatus

The addition tube, shown in figure 1, made it possible to add the oxidizing solution rapidly and flush the vessel with buffer solution without admitting atmospheric oxygen. With the pinch clamp on the rubber tubing, A, nitrogen from the reaction vessel swept out compartment B, containing the oxidizing solution, and bubbled through the buffer solution in compartment C, before escaping to the air through the bubbler. When the clamp was removed from the tubing, nitrogen from the reaction vessel could replace the solutions when the lower and upper stopcocks were opened in succession. The stopcocks were both of large bore to permit 10 ml. of solution to be added in about 2 sec.

The experimental procedure followed consisted in adding 100 ml. of buffer solution, 0.2 *M* in buffering ion and with a sodium-ion concentration fixed by addition of sodium sulfate, as necessary, to the reaction vessel, and determining the pH with two hydrogen electrodes. The glass electrode was then read, and the hydrogen displaced with pure nitrogen with the substitution of blank platinum and gold electrodes for the platinized ones. The addition tube was set in place with the measured amount of oxidizing solution and buffer solution for flushing, and half an hour allowed for the sweeping out of hydrogen and air. Ten milliliters of reducing agent was then added from one of the jacketed burets. The lower stopcock of the addition tube was opened, and at the same time an electric timer was started which gave a single stroke on a bell at 15-sec. intervals.

TABLE 1

p-Methylaminophenol, 50 per cent oxidized, at 20°C.

pH	E'	pH	E'
	volts		*volts*
0.96	0.6869	8.57	0.1884
1.37	0.6574	9.14	0.1552
2.10	0.6182	9.32	0.1465
2.59	0.5919	9.52	0.1352
3.38	0.5402	9.81	0.1240
3.86	0.5122	9.93	0.1130
4.32	0.4762	10.33	0.0934
4.66	0.4463	10.36	0.0930
4.81	0.4309	10.47	0.0892
4.90	0.4301	10.75	0.0820
5.28	0.3960	10.81	0.0745
5.78	0.3574	10.85	0.0732
5.80	0.3582	11.02	0.0702
6.40	0.3220	11.30	0.0602
7.00	0.2820	11.35	0.0560
8.10	0.2202	11.69	0.0452
8.13	0.2135	11.97	0.0370
8.14	0.2132	12.18	0.0319
8.25	0.2040	13.03	0.0052
8.41	0.1990	13.60	−0.0118

The upper stopcock was then opened and the lower chamber flushed into the reaction vessel.

Readings were taken at 15-sec. intervals for 3 min. and at 1-min. intervals for 7 min. The glass electrode was then read again, and the pH of the solution as originally determined with the hydrogen electrode was corrected for any change in pH which had occurred. Readings were taken with a student-type potentiometer. The potential of the glass electrode was read with the same potentiometer, using a ballistic galvanometer and a 1 microfarad condenser as null point indicator.

Addition of the solutions raised the temperature of the reaction mixture slightly, but this effect could be disregarded, since in most cases the extrapolation to zero time was made from a graph which was a straight line up to 10 min.

The *p*-methylaminophenol and sulfonic acid solutions were standardized against the oxidizing solutions by discontinuous titrations, a run being made for each point on the titration curve. The hydroquinone solution was standardized by direct titration at a pH at which decomposition of the quinone did not interfere, and the hydroxyhydroquinone solution was standardized by rapid titration at pH 0.5, and by a discontinuous titration.

TABLE 2

p-Methylaminophenolsulfonic acid, 50 per cent oxidized, at 20°C.

pH	*E'*	pH	*E'*
	volts		*volts*
1.03	0.7323	5.59	0.4062
1.58	0.7000	6.62	0.3422
2.05	0.6729	7.05	0.3194
2.54	0.6414	8.44	0.2359
2.73	0.6224	9.21	0.1942
3.90	0.5389	9.77	0.1622
4.23	0.5102	10.31	0.1317
4.48	0.4902	10.70	0.1175
4.87	0.4585	11.39	0.0902
4.92	0.4542	11.45	0.0890
5.26	0.4229	11.81	0.0774

TABLE 3

Benzohydroquinone, 50 per cent oxidized, at 20°C.

pH	*E'*	pH	*E'*
	volts		*volts*
6.28	0.3342*	11.32	0.0957
6.33	0.3374	11.34	0.0945
7.03	0.2982	11.54	0.0874
7.17	0.2900	11.60	0.0888
8.01	0.2370	11.61	0.0872*
8.97	0.1844	11.85	0.0820
9.64	0.1469	12.00	0.0788
10.36	0.1209	12.30	0.0704
10.41	0.1189	12.36	0.0664*
10.43	0.1172	12.43	0.0664†
10.67	0.1104	12.55	0.0560*
10.86	0.1025	12.78	0.0370*
11.06	0.1022	12.81	0.0453
11.32	0.0916	13.01	0.0303*

* By addition of quinhydrone solution.

† By addition of quinone solution.

DATA

The data for *p*-methylaminophenol and *p*-methylaminophenolsulfonic acid are given in tables 1 and 2.

Table 3 contains the data obtained from an attempt to carry the measurements of the oxidation-reduction potential of the hydroquinone system up into the alkaline range where the quinone is unstable. The data, other than those specially marked, were obtained by the addition of sufficient ferricyanide solution to produce a half-oxidized mixture, or by selecting the midpoint of the titration with a ferricyanide solution in the lower pH range.

Attempts were made to investigate the oxidation-reduction potential of hydroxyhydroquinone over a considerable range of pH. The data for these measurements appear in table 4.

TABLE 4

Hydroxyhydroquinone, 50 per cent oxidized, at 20°C.

pH	E'	pH	E'
	volts		*volts*
0.50	0.5707	4.20	0.3310
1.26	0.5310	4.24	0.3490
2.30	0.4690	4.62	0.3217
2.76	0.4394	5.32	0.2542
3.40	0.3896	5.86	0.2102
3.58	0.3740	6.04	0.1840
3.76	0.3690	6.75	0.1255
3.87	0.3487	7.30	0.0802
4.06	0.3797		

DISCUSSION

The equilibrium between the oxidized and reduced forms of *p*-methylaminophenol may be formally represented by the following expression:

$$\text{Ox.} + 2\text{H}^+ \overset{2e}{\rightleftharpoons} \text{Red.}$$

The participation of hydrogen ions in the equilibrium and the possibilities of ionization of the secondary amino groups in both reduced and oxidized forms renders the system rather complicated. An expression which was derived and found to fit the experimental data with pleasing exactitude was the following:

$$E = E_0 - 0.029 \log_{10} S_R/S_O - 0.029\,\text{pH}$$

$$- 0.029 \log \frac{K_w + K_O[\text{H}^+]}{K_a K_w + K_w[\text{H}^+] + K_R[\text{H}^+]^2}$$

In this expression E_0 is a constant which is characteristic of the system, S_R and S_O are the total concentrations of reduced and oxidized forms, K_w is the ionization constant of water at 20°C., K_a is the acid ionization of the phenolic group in the reduced form, and K_O and K_R are the apparent basic ionization constants of the secondary amino groups in oxidized and reduced forms. The basic ionization constants are defined for the oxidized form by the expression:

$$K_O = \frac{[\text{Ox}^-]K_w}{[\text{Ox}][\text{H}^+]}$$

and by a similar expression for the reduced form. In [Ox] and [Red] are included the concentrations of both hydrated and unhydrated un-ionized forms.

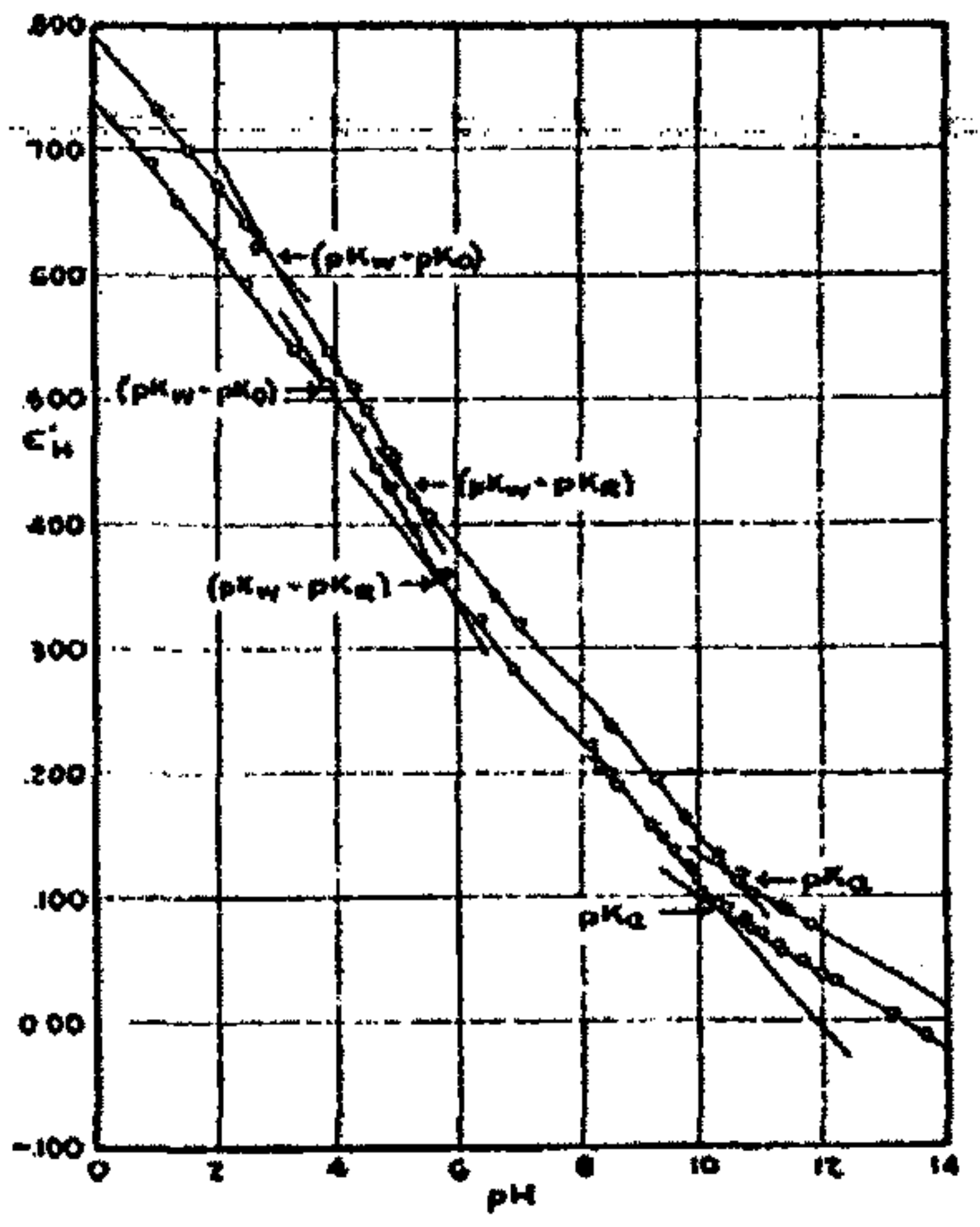

FIG. 2

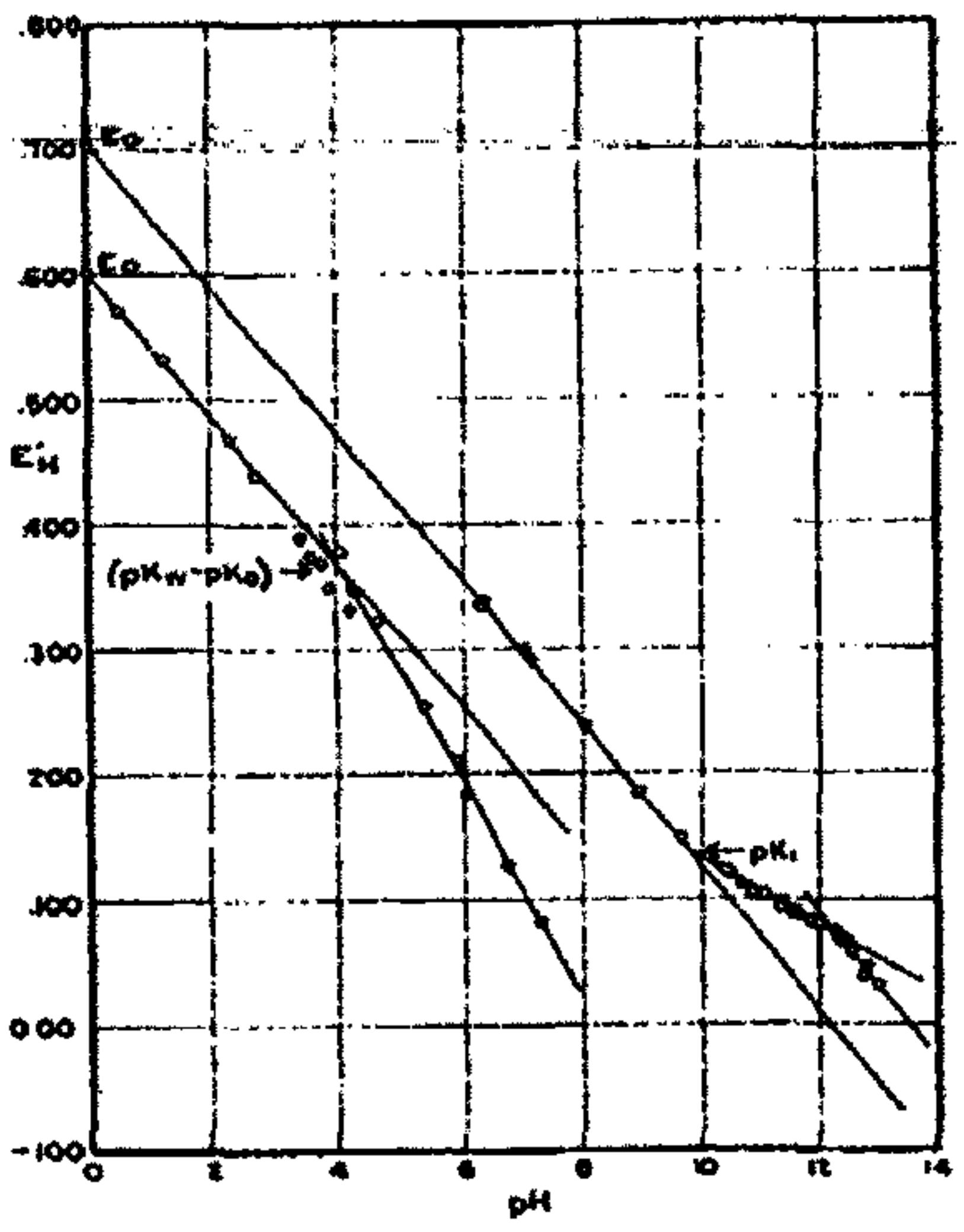

FIG. 3

FIG. 2. The oxidation-reduction potential of *p*-methylaminophenol (lower) and *p*-methylaminophenolsulfonic acid (upper) in equilibrium with their oxidants at 20°C.

FIG. 3. The oxidation-reduction potential of benzohydroquinone (upper) and hydroxyhydroquinone (lower) in equilibrium with their quinones at 20°C.

Figure 2 shows the graphs of the data for both systems. In these graphs the lines are drawn with theoretical slopes, and the constants given in table 5 were used in the calculations. It will be noted that the data fit the calculated lines with excellent regularity.

Data from other sources are included for purposes of comparison. Fieser found that, working in the presence of air, he was not able to carry the measurements above pH 8 before the rate of decomposition of the oxidized form became so rapid that extrapolation to zero time of the potential-time plot was impossible. In the present work it was found possible to carry the measurements into quite alkaline solutions before the decomposition became too rapid. In all measurements of both compounds, the graph of the potential against time was found to be a straight line for a considerable period. In some cases it remained a straight line up to 15 min. This indicated, since the drift was toward lower potentials, that the oxidized form was decreasing in concentration by a reaction whose rate was unimolecular.

The mechanism of this decomposition has been discussed by Fieser, but no direct data appear to be available. In the range of pH from the pK_0 of the two compounds up to pH 8.0, the decomposition leads to the formation of a purple compound. In lower ranges of pH the iminoquinone was yellow. The purple color appeared to develop as a function of time, indicating that it was due to a combination of the decomposition product of the iminoquinone with either the iminoquinone or the reduced form of the system. The combination with the iminoquinone appeared to be the more likely, for titration of the mixture with sodium sulfite, which removed the oxidized form as monosulfonate, gave an end point which coincided with the disappearance of the purple color. Furthermore, the titer decreased as a function of time; this agreed with the disappearance of the oxidized form.

TABLE 5

Constants used in the calculations

CONSTANTS	*p*-METHYLAMINOPHENOL		*p*-METHYLAMINOPHENOL-SULFONIC ACID
E'_{pH}	0.7402 volt		0.7920 volt
E_0	0.6888 volt	0.6877 volt (5)	0.7292 volt
K_O	6×10^{-11}	1×10^{-10} (5)	5.88×10^{-12}
K_R	3.54×10^{-9}	1×10^{-8} (5)	8.50×10^{-10}
K_a	4×10^{-11}	6.45×10^{-11} (14)	2.51×10^{-11}
K_w	6.16×10^{-15} (10)		6.16×10^{-15} (10)

The titration curves for these systems did not agree with the curve for a two-electron system. Fieser observed this and ascribed the deviation to the formation of meriquinone. The deviation found by the present writer was less than that observed by Fieser. The meriquinone formation will have no effect upon the measurements of potential at half oxidation unless the meriquinone is formed with other than a one-to-one ratio of oxidized and reduced forms.

The effect of the introduction of the sulfonic acid grouping was to shift all ionizations of the compound, so that it was now both a weaker acid and a weaker base. This shift occurred with an increase in the oxidation-reduction potential at any given pH.

Measurements upon the benzohydroquinone system were undertaken in the hope that measurements in the range in which quinone was unstable might make possible an estimation of the value of the second ionization constant of the reduced form. The potential of the hydroquinone-quinone system should be given by the following expression:

$$E = E_0 - 0.029(?) \log_{10} S_R/S_O + 0.029 \log_{10} (K_1K_2 + K_1[\mathrm{H}^+] + [\mathrm{H}^+]^2)$$

Inspection of this expression, when $S_R = S_O$, shows that the slope for the dependence of the oxidation-reduction potential upon pH should be 0.058 until the pK of the first ionization is reached, at which point the slope should become 0.029. When the pK of the second ionization is reached, the slope should become zero. Examination of the graph of the experimental data in figure 3 shows that the change at the pK of the first ionization occurs, but that at about the point where the pK of the second ionization should be, there is a change in slope back to the original 0.058. Furthermore, the slope between pH 9.8 and pH 12.3 is not the theoretical 0.029 but is 0.0261. This irregular slope indicates that in this region the potential is being determined by a mixture of two systems. At pH 12.3 the benzohydroquinone system must entirely disappear as far as any effect upon the potentials is concerned, for this change in slope would indicate that a group, common to both forms of the system, had now ionized in the oxidized form.

The disappearance of the quinone in the range of pH above 10 was accompanied by the formation of a deep orange-red coloration which faded more or less rapidly, depending upon the pH value, to a yellow. The drift of potentials was rapid, and above pH 11.5 more consistent results were obtained by extrapolating a graph of the antilogarithm of the potential as a function of time. This arbitrary extrapolation agreed closely with the best extrapolation that could be made from the graphs of potential as a function of time. Measurements in this region were made both by adding a ferricyanide solution to a hydroquinone solution and by adding a saturated aqueous solution of quinhydrone to the buffer.

The only system which it appeared might exist, even temporarily, in this region and which might show this behavior was the hydroxyhydroquinone system. The dismutation of quinone is said to occur in the following manner (2, 9, 12):

$$2\mathrm{C_6H_4O_2} \xrightarrow{\mathrm{H_2O}} \mathrm{C_6H_4(OH)_2} + \mathrm{C_6H_3(OH)O_2}$$

This reaction may then be followed by (11):

$$2\mathrm{C_6H_3(OH)O_2} \xrightarrow{\mathrm{H_2O}} \mathrm{C_6H_3(OH)_3} + \mathrm{C_6H_2(OH)_2O_2}$$

Hydroxyhydroquinone in equilibrium with hydroxyquinone might thus exist in the reaction mixture, although not necessarily in an equimolar mixture. Since this system is formed without participation of hydroquinone, an experiment was run in which a quinone solution was added to the buffer instead of a quinhydrone solution. The value of potential for this experiment (cf. table 3) checked perfectly with those obtained with quinhydrone, and the same color sequence appeared in the solution.

A measured quantity of acidified benzoquinone solution was reduced with hydrogen and colloidal palladium at pH 0.5 and titrated with potassium molybdicyanide solution in an inert atmosphere. The same quantity of quinone solution was then added to 0.1 *M* sodium hydroxide in an atmosphere of nitrogen, and after 30 min. the solution was acidified with sulfuric acid to a pH of 0.5 and titrated with molybdicyanide solution. The titration indicated that 9.2 per cent of a compound 0.100 volt more negative in oxidation-reduction potential than the benzohydroquinone system, and 67.7 per cent of hydroquinone had been formed from the quinone upon dismutation in alkaline solution.

TABLE 6

Constants determined for the two systems

CONSTANTS	BENZOHYDROQUINONE		HYDROXYHYDROQUINONE	
E_0	0.7049 volt	0.7029 volt (1)	0.6014 volt	0.5960 volt (3)
K_1	1.46×10^{-10}	1.33×10^{-10} (4) 1.75×10^{-10} (14)		
K_O			10×10^{-4}	

Measurements upon the hydroxyhydroquinone system were carried out, but in this case, also, the limiting factor was the stability of the quinone. The measurements shown in figure 3 indicate that a group in the oxidized form has a p*K* of approximately 4.0, for above this pH value the slope has changed from 0.058 to 0.087. Above this pH value the solution is orange-red in color, and below it, it is yellow. The quinone was not found to be stable in any solution used. As the solutions were made more and more alkaline, the dismutation of the quinone became more rapid, until above pH 7 the potential-time curves could not be extrapolated to zero time. The potentials showed an initial rise which was very rapid and which indicated formation of the hydroquinone from the quinone.

The constants determined for the two systems are given in table 6. No great significance is to be attached to the discrepancy in the value of E_0 for the benzohydroquinone system, for extreme precision was not being sought in this case. The chief interest in the investigation lay in the alkaline solutions.

Thus it appears from these investigations that the method introduced by Fieser is capable of extension and application to a great many organic systems ordinarily regarded as irreversible. The greatest success will be obtained with systems which do not give rise to the reduced form of an oxidation-reduction system upon decomposition of the oxidized form.

SUMMARY

1. The oxidation-reduction potentials of the systems arising from *p*-methylaminophenol and from its monosulfonic acid have been measured over a wide range of pH by the discontinuous titration method of Fieser.

2. Measurements have been attempted upon the benzoquinone system in alkaline solution and upon the hydroxyhydroquinone system, but such measurements were hampered by the production of the hydroquinones upon dismutation of the unstable quinones.

REFERENCES

(1) Biilmann, E.: Ann. chim. **16**, 109 (1921).
(2) Bogisch, A.: Phot. Korr. **37**, 273 (1900).
(3) Conant, J. B., and Fieser, L. A.: J. Am. Chem. Soc. **46**, 1858 (1924).
(4) von Euler, H., and Brunius, E.: Z. physik. Chem. **139**, 615 (1928).
(5) Fieser, L. F.: J. Am. Chem. Soc. **52**, 4915 (1930).
(6) Fieser, L. F.: J. Am. Chem. Soc. **52**, 5204 (1930).
(7) Fieser, L. F., and Fieser, M.: J. Am. Chem. Soc. **56**, 1565 (1934).
(8) Fieser, L. F., and Fieser, M.: J. Am. Chem. Soc. **57**, 491 (1935).
(9) Hesse, O.: Ann. **220**, 367 (1883).
(10) International Critical Tables, Vol. VI, p. 152. McGraw-Hill Book Co., Inc., New York (1929).
(11) Leubner, A.: Dissertation, Dresden, 1911.
(12) Scheid, B.: Ann. **218**, 227 (1883).
(13) Schering: German patent 208,434; Chem. Zentr. **1909**, I, 1367.
(14) Sheppard, S. E.: Trans. Am. Electrochem. Soc. **39**, 440 (1921).

CHEMICAL ACTION OF ALPHA PARTICLES FROM RADON ON AQUEOUS SOLUTIONS[1]

F. C. LANNING AND S. C. LIND

School of Chemistry, University of Minnesota, Minneapolis, Minnesota

Received April 2, 1938

INTRODUCTION

The action of radon on aqueous solutions has been relatively neglected. Theoretically, since alpha particles have no selective effect on the separate components of a mixture, one would expect that in dilute or moderately concentrated solutions the principal chemical effect would be exerted upon the solvent water.

It is well known that alpha particles decompose water into hydrogen and oxygen and form a little hydrogen peroxide. If a reducing agent such as hydrogen iodide be present in solution, the evolution of oxygen is suppressed and the equivalent amount of hydrogen iodide is oxidized to free iodine, hydrogen being liberated as gas. The converse case of the acceptance of hydrogen by an oxidizing agent present in solution with liberation of free oxygen has not been previously investigated, but is now demonstrated and quantitatively studied for aqueous solutions of iodine and of potassium permanganate.

Besides the theoretical interest pertaining to such reactions as just described, there is the practical problem of finding a convenient method of calibrating alpha-ray bulbs containing radon. By calibration is meant ascertaining how much ionization will be produced outside such a thin bulb per millicurie of radon contained. Various means of calculation or measurement have been employed. The calculation must assume the bulb to be a sphere of uniform wall thickness. Mund recently devised a very elegant method of making this calculation, but the present experiments show that the assumption of uniform wall thickness is sometimes so far from the truth as to render the application uncertain.

Evidently if one has a solution readily acted on by alpha particles to give a reaction of known yield per ion pair (M/N), it would only be necessary to dip the bulb containing radon into the solution for a suitable interval, titrate the amount of change, and calculate N.

It may be said at the outset that no solution was found capable of

---

[1] Submitted by F. C. Lanning to the Graduate School of the University of Minnesota in partial fulfillment of the requirements for the degree of Doctor of Philosophy.

yielding a result so simply. Complications, such as reverse reaction, made it necessary to measure the evolved gases also. This complicated the manipulation so that it was found simpler to calibrate the bulb in a separate experiment. A new method[2] was employed in decomposing gaseous ammonia and measuring the hydrogen and nitrogen left on freezing out the ammonia, which was used in such large excess that the back reaction was negligible.

Besides the employment of alpha-ray bulbs, the radon was also sometimes introduced directly into the water or the solution. As is well known, this method involves a knowledge of the distribution of radon between the liquid and gas phases and also the calculation of recombination of hydrogen and oxygen in the gas phase due to the radon then present. In this connection, it was found that when the neck separating the liquid and gas is narrow (so as to give a sharp demarcation of volumes), the distribution of radon according to the static distribution coefficient cannot be assumed. Apparently the evolved hydrogen and oxygen are carrying radon out through the neck faster than it can redissolve at the small surface, so that the equilibrium is displaced toward excess of radon in the gas phase, calling for a greater correction for back reaction, hence a high yield of the decomposition.

QUALITATIVE RESULTS

Aside from the decomposition of water brought about by radioactive salts dissolved in water, little has been done in the field of radiation of liquids. It is, of course, well known that the radiations produced by a radioactive salt dissolved in water produce decomposition of the water, yielding oxygen, an excess of hydrogen, and a small amount of hydrogen peroxide. In 1907 Cameron and Ramsay (2) studied the decomposition of water brought about by the radiation from radon dissolved in water. Their results indicate that the primary products of decomposition are hydrogen and oxygen in equal quantities and that a secondary reaction ensues with the formation of a small amount of hydrogen peroxide, so that the gas evolved contains a slight excess of hydrogen. They showed that the volume of gas produced was proportional to the amount of radon present in the water, also that the reaction was half completed in 3.8 days, which is approximately the half-life of radon.

Duane and Scheuer (3) showed that the hydrogen excess, amounting to as high as 36 per cent in the initial stage of the radiation, diminished steadily as the experiment proceeded. At very low temperature (183°C.) no excess hydrogen was formed. They concluded that the formation of hydrogen peroxide, and consequent hydrogen excess, was the result of the

[2] Kindly suggested by Dr. J. C. Jungers.

reaction of nascent oxygen on water. Their calculated values of $-M/N$, the number of molecules of water decomposed per ion pair formed, were between 0.86 and 1.05. Kernbaum (6) measured the amount of hydrogen peroxide formed in radon water solution and showed it to be equivalent to the hydrogen excess. He further showed that the diminishing hydrogen excess was due to establishment of equilibrium in the formation and decomposition of hydrogen peroxide. Lind (7) found that the rate of decomposition of potassium iodide in water, decomposed by means of radon dissolved in the solution, increased with the concentration. Potassium iodide in 2 normal sulfuric acid was decomposed still more rapidly. Nurnberger (9), by a direct method, found $-M/N$ for water to be between 0.7 and 0.9. $-M/N$ for the oxidation of ferrous sulfate, determined by both direct and indirect methods, increased with the concentration, but at higher concentration the $-M/N$ values (approximately 8) are too great to be accounted for by the action of liberated oxygen on ferrous sulfate to form ferric sulfate.

Qualitative experiments were conducted on aqueous solutions of hydrogen iodide, hydrogen bromide, iodine, and iodine in potassium iodide to determine their suitability for quantitative study, the first two as oxygen acceptors, the last two as hydrogen acceptors. The iodine solutions were studied to ascertain if hydrogen is accepted (resulting in synthesis of hydrogen iodide), since this would have an important bearing on the hydrogen iodide decomposition reaction. A 0.5 normal solution of hydrogen iodide in water was exposed to the radiations from radon confined in an alpha-ray bulb mounted on the ground-glass stopper so that it could be introduced into the liquid. Air above the solution was displaced by means of nitrogen. During the course of the reaction the solution was shaken greatly to dislodge any gas bubbles from the alpha ray and also to prevent the accumulation of decomposition products immediately next to the ionization source. After the lapse of a suitable interval of time the alpha-ray bulb was removed, and the solution was titrated with sodium thiosulfate.

By an arrangement similar to that given above for the decomposition of hydrogen iodide, it was shown that iodine, in aqueous solution, accepts hydrogen and is converted into hydrogen iodide. The following data were obtained:

Millicuries	140
Time of radiation, in hours	22
Ml. of 0.0241 N sodium thiosulfate	1.9
Ml. of 0.0335 N barium hydroxide	0.75

125 ml. of 0.00108 N iodine = 5.6 ml. of 0.0241 N sodium thiosulfate

Calculations:

(1) From the sodium thiosulfate titration:

$$\frac{5.6 - 2(1.9)0.024 \times 127.94}{1000} = 0.0055 \text{ g. of hydrogen iodide}$$

(2) From the barium hydroxide titration:

$$\frac{2 \times 0.75 \times 0.0335 \times 127.94}{1000} = 0.0064 \text{ g. of hydrogen iodide}$$

These results (although they do not agree exactly) indicate that there is at least some reaction between hydrogen from the primary decomposition of water and iodine in neutral solution with the formation of an equivalent amount of hydrogen iodide.

This experiment was next repeated with iodine in potassium iodide, to ascertain if iodine will combine to form hydrogen iodide. The results from four experiments showed no loss of iodine and no formation of hydrogen iodide. It was therefore concluded that there should be no back reaction in the decomposition of hydrogen iodide, since the iodine would, in all probability, exist in combination with hydrogen iodide as HI_3, as it does with potassium iodide as KI_3. Hydrogen iodide would, therefore, appear suitable for more extended study as oxygen acceptor. It should be noted that, in the results to be reported later in this reaction, the hydrogen iodide is 0.5 *N* (more than twice as concentrated as the potassium iodide in these preliminary experiments), and, further, that the iodine formed is always much less concentrated than the iodine used in the potassium iodide solutions.

QUANTITATIVE RESULTS

1. Decomposition of water and aqueous hydrobromic acid solutions by the direct method

The reactions were carried out in the apparatus shown in figure 1. B is the reaction vessel containing the solution. It is connected to the vessel *a* by means of a capillary tube of 3-mm. diameter. The volume of B = 56.0 cm.^{3} The vessel *a* during the experiment will contain evolved gases and radon in equilibrium with the radon in the solution. The vessel carries sealed-in tungsten electrodes for sparking evolved gases. The volume of the vessel, together with connecting capillary tubes to the manometer, is 4.29 cm.^{3} The liquid in B can be agitated by means of a glass-covered bead of soft iron actuated by an electromagnet. The procedure followed was to introduce the radon into the evacuated vessels, A and B, by means of the special device, D, which consists of a metal rod with an eye at the top through which the radon capsule was inserted. By turning the metal cup to which the rod is attached the capsule may be broken, allowing the radon to diffuse up into the reaction vessel, from G, through the connecting tubes and E. The course of the reaction was followed manometrically, by taking pressure readings at suitable intervals, both before and after sparking the evolved gases in the vessel A.

At the conclusion of the hydrogen bromide experiments, the liquid was withdrawn and analyzed for liberated bromine. Potassium iodide was added to the hydrogen bromide solution, and the liberated iodine was titrated with standard sodium thiosulfate solution. Calculations for both water and hydrogen bromide were made on the manometric data obtained.

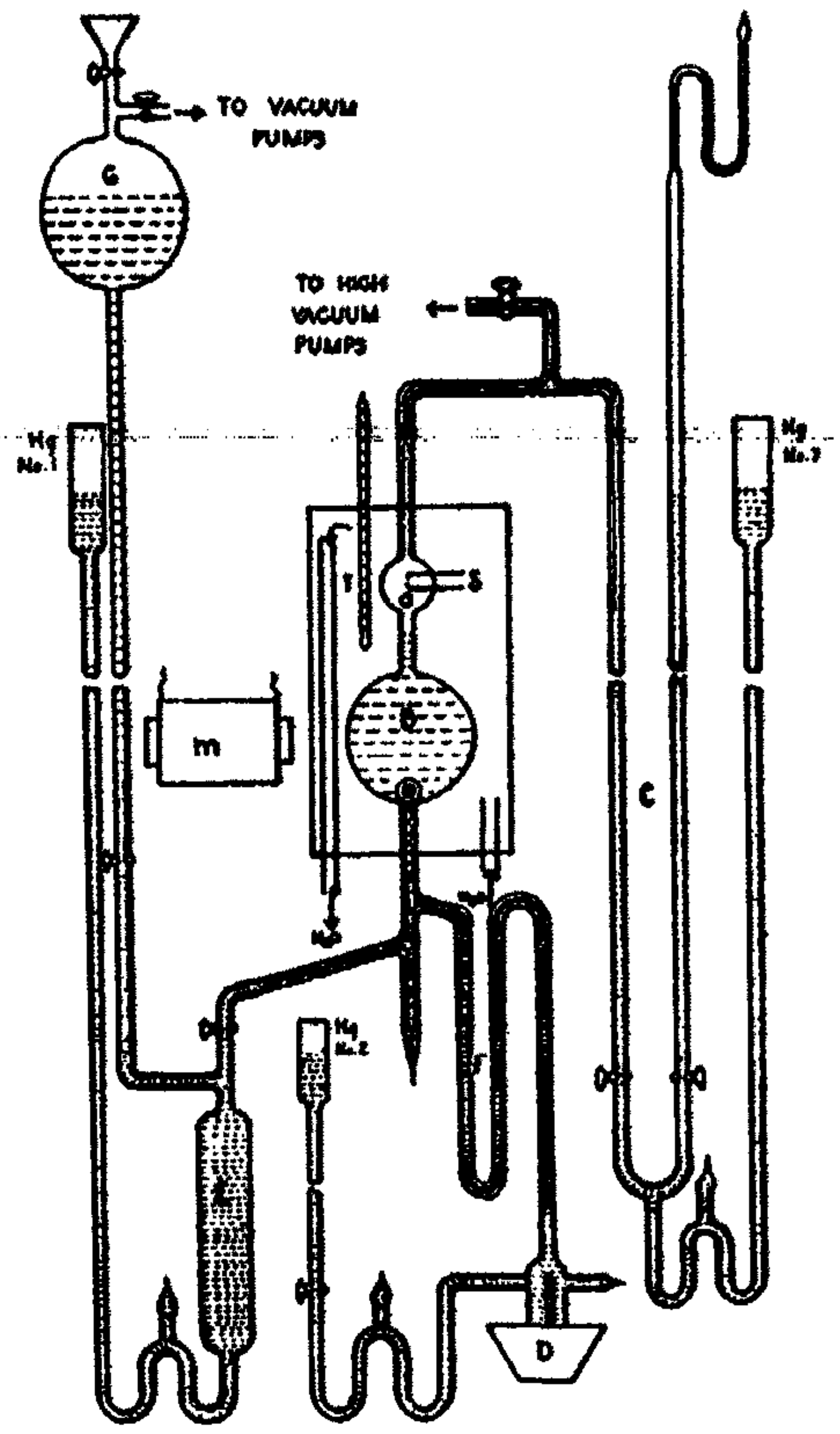

FIG. 1. Apparatus for the direct radiation of water and hydrobromic acid

Before calculations could be made it was necessary to determine the distribution of radon between the liquid and gas phases. The conditions under which these experiments were performed made it impossible to use the distribution coefficient of St. Meyer and Schweidler. In order to define the gas volume with sufficient accuracy to make possible suitable manometric measurements on the hydrogen and oxygen evolved, a small-bore tube, connecting vessels A and B, had to be used. The evolution of the hydrogen and oxygen in the liquid, and diffusion into the vessel above, not only prevented the prompt establishment of equilibrium of the radon between the gas and liquid phases, but also displaced the equilibrium toward the gas phase. This necessitated making actual measurements of radon distribution throughout the course of the experiment. This was

TABLE 1

Direct method for decomposition of water by radon

Experiment I: initial quantity of radon = 86.7 mc.; T = 13°C.

TIME	P_1*	P_2	V	M_1	M_2	N
hours	*cm.*	*cm.*				
9.5	3.52	0.71	0.249			
18.5	8.97	1.39	0.635			
25	12.89	2.22	0.912			
35	17.35	3.56	1.23			
45.5	22.34	5.2	1.58	0.95	0.093	1.69
59	27.79	7.25	1.97	1.95	0.212	3.78
70	32.53	8.88	2.30	2.84	0.299	5.23
82.5	36.46	10.35	2.58	3.60	0.389	6.17
90.5	39.07	11.34	2.805	4.20	0.442	7.03
105	43.02	12.85	3.085	4.97	0.534	8.08
117	47.14	14.58	3.388	5.79	0.610	9.10
130.5	50.45	16.07	3.62	6.40	0.687	10.06
139.5	51.80	16.50	3.725	6.69	0.737	10.68
161.5	57.60	18.86	4.13	7.80	0.853	12.38
185.5	62.32	20.97	4.47	8.70	0.956	13.48

PER CENT DISTRIBUTION OF RADON

Hours	Rw	Rg
36	40.7	59.3
61.5	40.8	59.2
106.0	38.6	61.4

$$M = 8.70 \times 10^{19} + 0.956 \times 10^{19}$$

$$M = 9.656 \times 10^{19}$$

$$-\frac{M}{N}(\mathrm{H_2O}) = \frac{9.656 \times 10^{19}}{13.48 \times 10^{19}} = 0.716$$

* P_1 = total pressure of hydrogen produced, in centimeters.

P_2 = total pressure of oxygen produced, in centimeters.

V = volume at standard conditions of hydrogen produced.

$M_1 \times 10^{19}$ = molecules of hydrogen in V.

$M_2 \times 10^{19}$ = molecules of water resynthesized.

$M \times 10^{19}$ = molecules of water decomposed = $M_1 + M_2$.

$N \times 10^{19}$ = number of ion pairs produced in water.

T = average temperature.

Volume of liquid in each case = 56.0 cc.

Rw = per cent of radon in the liquid phase.

Rg = per cent of radon in the gas phase.

done by x-ray comparison, using a Lind electroscope with heavy lead shielding first between A, then B, and the electroscope.

The data on the water and hydrobromic acid experiments are given in tables 1 and 2.

TABLE 2

Direct method for decomposition of hydrobromic acid by radon

Experiment III: radon in 0.397 N hydrobromic acid

TIME	P_1*	P_2	V	M_1	M_2	N
hours	*cm.*	*cm.*				
15	5.53	1.367	0.388	1.048	0.221	3.185
29	16.45	1.473	1.152	3.12	0.121	6.885
40	25.58	1.867	1.792	1.73	0.120	2.86
51	35.15	2.147	2.46	3.53	0.247	5.56
63	44.85	2.367	3.14	5.37	0.419	8.51
75	54.41	2.63	3.815	7.20	0.587	11.04
89	63.04	2.95	4.42	8.85	0.783	13.47

DISTRIBUTION OF RADON

Hours	Rw	Rg
16	41.2	55.8
69.5	50.2	49.8
88	48.9	51.1

$M = 8.85 \times 10^{19} + 0.783 \times 10^{19}$

$M = 9.633 \times 10^{19}$

$$\frac{M_{H_2}}{N_{H_2O}} = \frac{9.633 \times 10^{19}}{1.347 \times 10^{19}} = 0.716$$

	$-M_{HBr}/N_{H_2O}$
A. From titration of bromine liberated	1.155
B. From hydrogen liberated	1.187

$$\text{Per cent oxygen utilized} = \frac{1.155 \times 100}{2 \times 0.716} = 80.5.$$

---

* See footnote to table 1.

Calculations of M_{H_2}/N_{H_2O}:

$$M_{H_2} = M_1 + M_2$$

M_1 is the number of molecules of hydrogen produced as determined by the gas measurements. M_2 is the number of molecules of hydrogen resynthesized in the gas phase.

$$M_1 = \frac{V \times \text{Avogadro's number}}{22{,}400}$$

V is the volume (under standard conditions) of hydrogen produced.

$$M_2 = 5.34 \times 10^{13} \times 2.4 \times 10^4 \times mc. \times \bar{P} \times i \times \frac{P}{760} \times Y \times 3.85$$

In this expression *mc.* is the number of millicuries of radon decayed in the gas phase, $\bar{P}$ is the average path, in centimeters, that an alpha particle would travel, P is the average pressure, in millimeters, over the period calculated, i is the specific molecular ionization of the gas mixture referred to air as unity, Y is a factor to take into account the ionization produced by recoil atoms, and 3.85 represents the number of molecules of water produced per ion pair. $\bar{P}$ is equal to 0.61 times the radius of the sphere. The term i is calculated using the average pressures of hydrogen and oxygen during the period. Y is given by the expression $\frac{R + \alpha}{\alpha}$, in which R represents the ionization produced by recoil atoms and α the ionization produced by alpha particles.

The ionization N_{H_2O} is given by the following expression, in which α is the number of alpha particles per millicurie disintegrated, *mc.* is the number of millicuries of radon destroyed in the liquid, P_1 is the number of ion pairs produced per alpha particle, and KS is the molecular ionization of water (0.82).

$$N_{H_2O} = \alpha \times mc. \times P_1 \times KS$$

Calculation of $-M_{HBr}/N_{H_2O}$:

(1) from gas measurements: To obtain $-M_{HBr}$ from the gas measurements, it is necessary to correct only $M_1(H_2)$ for the unused oxygen and multiply by 2.

$$-M_{HBr} = 2\left[M_1 - \left(\frac{M_1 \times 2 \times \text{total cm. pressure of oxygen produced}}{\text{Total cm. pressure of hydrogen produced}}\right)\right]$$

(2) from titration: The titration was 23.1 cm.^{3} of 0.01483 N sodium thiosulfate.

$$-M_{HBr} = \frac{23.1 \times 0.01483 \times 6.06 \times 10^{23}}{1000} = 20.8 \times 10^{19}$$

$$N_{H_2O} = 18.01 \times 10^{19}$$

$$\frac{-M_{HBr}}{N_{H_2O}} = \frac{20.8 \times 10^{19}}{18.01 \times 10^{19}} = 1.155$$

Owing to the difficulties encountered in the measurements of distribution of radon between the liquid and the gas and in the calculation of the amount of recombination of the gases under the influence of the radon mixed with them, this direct method proved to be unsatisfactory. Since the use of an alpha-ray bulb eliminates both of these problems, the remainder of the work here reported was done by this indirect method. As will be pointed out later, it does require a careful calibration of the alpha-ray bulb.

2. Standardization of alpha-ray bulbs and determination of −M/N for water

The use of alpha-ray bulbs for the quantitative investigation of the effect of alpha particles on chemical reactions, particularly in aqueous solutions, possesses certain advantages as well as certain distinct disadvantages. In the first place, there is obviously no problem of the distribution of the radon. It remains always in the alpha-ray bulb and one needs only to measure the quantity of radon initially and, by means of the Kolowrat table, to calculate the quantity of radon which decays during the interval of the experiment. The alpha particles are completely absorbed by the solution before reaching the walls of the vessel, so that the average path travelled by the alpha particles from radon, radium A, and radium C in equilibrium with it need not be considered.

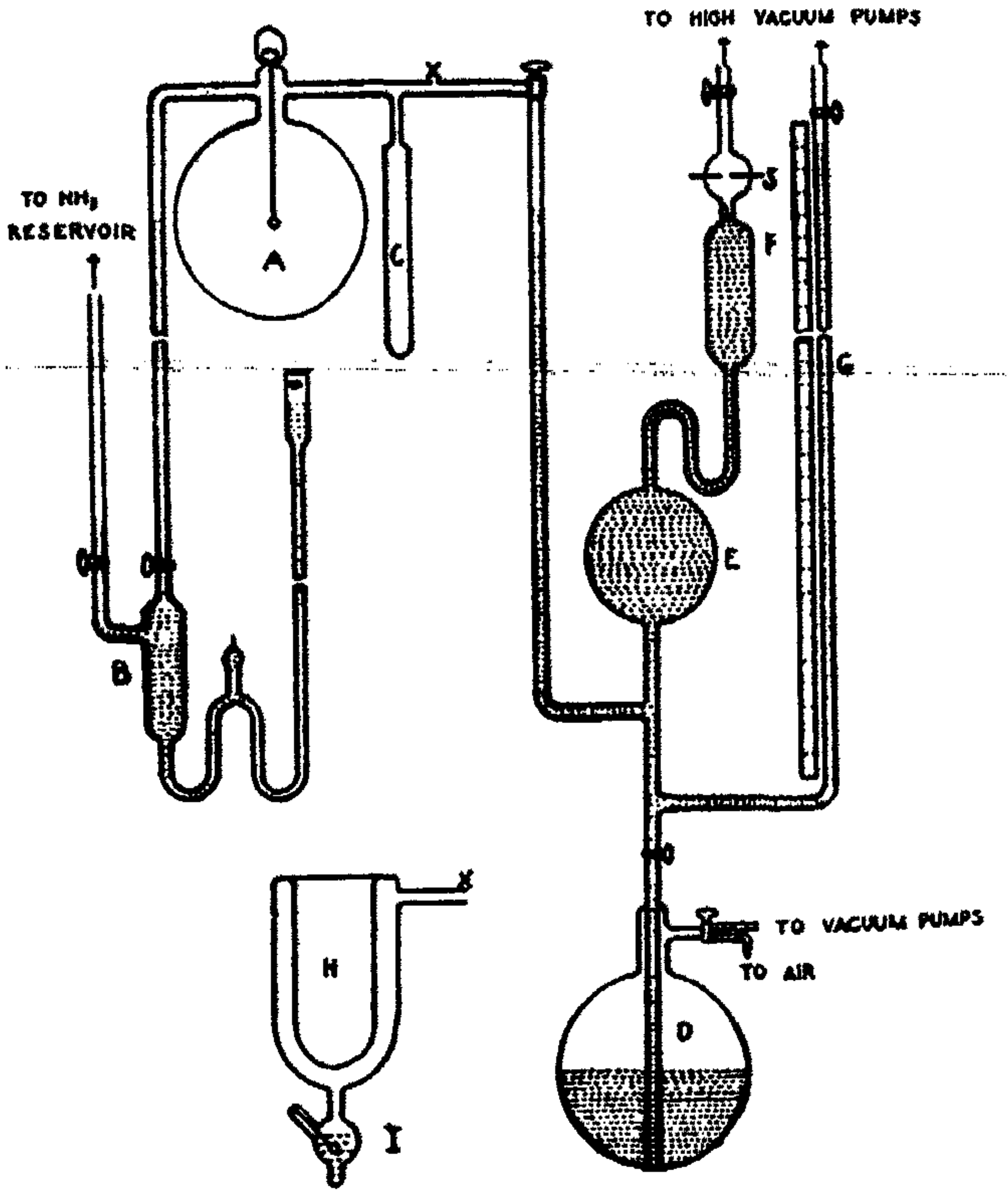

FIG. 2. Apparatus for the indirect radiation of ammonia, water, and potassium permanganate solutions

Mund (8) developed a method for the calculation of the efficiency of an alpha-ray bulb as an ionization source, from measurements of the diameter, wall thickness, and tip and stem corrections. Our investigation of the thickness of the walls of many alpha-ray bulbs, both by microscope and the interferometer, convinced us that the assumption of uniformity of wall thickness is not justified, and that the bulb must be calibrated by using it as an ionization source in a reaction whose ion yield is accurately known. The ammonia decomposition, suggested by Jungers, lends itself readily for this standardization. The apparatus used, together with that used for the potassium permanganate reduction, is shown in figure 2. The reaction vessel, A, in the center of which the alpha-ray bulb is suspended, is of sufficiently large diameter to insure complete absorption of all α-particles by the ammonia at the pressures used. At intervals the ammonia is frozen down in C and the gases, nitrogen and hydrogen, are pumped out and measured.

TABLE 3

Determination of $-M/N$ for water with a bulb standardized against ammonia decomposition

Initial quantity of radon = 125.9 mc.; T = 22°C.; h_1 (zero manometer reading) = 600; P_1 (pressure of ammonia) = 1.36 atm.

EXPERIMENT NO.	TIME ELAPSED FROM START	DURATION OF EACH EXPERIMENT	h MANOMETER READING	P PRESSURE OF GASES PRODUCED	mc. RADON DESTROYED IN EACH EXPERIMENT	P/mc.	$-M/N$
Standardization against ammonia							
	hours	*hours*	*mm.*	*mm.*	*mc.*	*mm.*	
1	10	10	645.0	45.0	9.09	4.95	0.868*
2	12 27	15	659.5	59.5	12.25	4.87	0.880
3	30 47.5	17.5	662.0	62.0	12.42	4.98	0.862
							Av. = 0.870
Radiation of water							
4	130 191	61	649	49	17.3	4.18	
After sparking..........			630	30			

* Calculations: (1) (4.18 × 1.023)/4.95 = 0.868; (2) (4.18 × 1.023)/4.87 = 0.880; (3) (4.18 × 1.023)/4.98 = 0.862.

The vessel, H, is a Dewar flask to which the small bulb, I, is attached. A side tube on I makes it possible to seal in the glass rod carrying the alpha-ray bulb which has been calibrated by the method just described. The whole is then sealed on to the Toepler pump and measuring apparatus at X.

In table 3 are given the data on three experiments on ammonia decomposition and one on water, all using the alpha-ray bulb containing, initially, 125.9 mc. of radon. The calculation of $-M/N$ for water, using a bulb calibrated in this manner, is as follows: Inspection of the decomposition equations

$$2NH_3 \rightarrow N_2 + 3H_2 \qquad (1)$$

$$2H_2O \rightarrow 2H_2 + O_2 \qquad (2)$$

shows that the total volume of gas evolved in reaction 1 is twice that of the hydrogen only, in reaction 2, per molecule decomposed. Comparison is made on this basis because of the fact that hydrogen is always in slight excess and more accurately represents the total reaction than the volume of oxygen or the mixture of hydrogen and oxygen. It happens that the molecular ionization of ammonia and that of water are the same, so that this factor (Bragg's *KS*) need not be taken.

Calculation

30 − 19.63 (V.P.) = 10.37 mm. of excess hydrogen
49 − 10.37 = pressure of the electrolytic mixture
2/3 (49 − 10.37) = 25.8 mm., pressure of hydrogen in the electrolytic mixture
25.8 + 10.37 = 36.17 mm., total hydrogen
36.17 × 2 = 72.34 mm., total pressure of hydrogen and nitrogen which would have been formed
17.3 mc. of radon decayed during the interval

$$\frac{72.34}{17.3} = 4.18 \text{ mm. per millicurie}$$

This value from the ammonia decomposition using the same bulb is 45.0/9.09 = 4.95. Thus 4.95:4.18 = 1.023:X, in which 1.023 is the value adopted, from the work of Jungers (5), for $-M/N$ for ammonia and X is the value of $-M/N$ for water. Thus $-M/N$ for water = 0.868. This value agrees well with those between 0.86 and 1.05, which were obtained by Duane and Scheuer (3).

Again, it should be pointed out that some resynthesis of water occurs within the bubbles clinging to the alpha-ray bulb, and, while it is impossible to estimate with any degree of accuracy the magnitude of the error which this introduces, it is safe to conclude that the true value of $-M/N$ for the decomposition of liquid water is very close to unity and that at least the net reaction is the decomposition of one molecule of water into hydrogen and nascent oxygen per ion pair.

In the two reactions now to be described, the alpha-ray bulbs used were calibrated by the water decomposition, measuring the volume of hydrogen evolved, assuming the value of $-M/N$ for water to be 0.87.

3. *Decomposition of hydrogen iodide*

In the preliminary studies it was shown that hydrogen iodide solutions, under the influence of radiations from radon, are decomposed with the liberation of iodine and hydrogen. The iodine may be conveniently titrated, and the hydrogen is readily measured manometrically. It was further shown that there is very probably no back reaction under the conditions of the experiments here reported. All the iodine formed has a high probability of forming I_3^-, which was proved to be stable under alpha radiation. The apparatus and method are essentially the same as that described for the hydrogen bromide decomposition, except that the radon is confined in an alpha-ray bulb located in the center of the reaction vessel, and thus no measurements on the distribution of radon are necessary. The alpha-ray bulb is calibrated against water, using the $-M/N$ value (for water) previously found by standardization against ammonia. The results are given in table 4.

TABLE 4

Determination of $-M_{HI}/N_{H_2O}$ with a bulb standardized against water

Experiment I: initial quantity of radon = 88 mc.; T = 32°C.

TIME ELAPSED FROM START	DURATION OF EACH EXPERIMENT	P_1 PRESSURE BEFORE SPARKING	P_2 PRESSURE AFTER SPARKING	P_{H_2} TOTAL PRESSURE OF HYDROGEN PRODUCED	*mc.* RADON DESTROYED	*P/mc.*
Standardization against water						
hours	*hours*	*mm.*	*mm.*	*mm.*	*mc.*	*mm.*
14	14	17.7	15.8			
24.5	24.5	35.85	26.35			
38	38	42.5	31.6			
50	50	56.7	40.45	69.04	27.3	2.53
Radiation of 0.5 *N* hydrogen iodide solution						
62	0					
96.5	34.5	38.05	38.05	41.09	14.97	2.74

	$-M_{HI}/N_{H_2O}$
From gas measurements $\left(\frac{2 \times 2.74 \times 0.87}{2.53}\right)$	1.88
From titration (5.0 − 0.2 = 4.8 ml. of 0.01538 *N* sodium thiosulfate)	1.87

As will be seen in table 4, there was no loss of pressure on sparking the gases. This indicates that all of the oxygen evolved for the primary decomposition of water is utilized in decomposing hydrogen iodide. The table also shows that the calculated $-M_{HI}/N_{H_2O}$ values from the hydrogen pressure measurements and for the titration of liberated iodine, respectively, agree closely. Note that this agreement is quite independent of the calibration against water also reported in table 4. The absolute value of $-M_{\mathrm{HI}}/N_{\mathrm{H_2O}}$ (1.88) does, of course, depend on this calibration and should, as indicated in the calculations given herewith, be twice that for $-M/N$ (H_2O). (This value for the ammonia decomposition comparison is 0.87.) That is, the value should be 1.74 if the theory of secondary utilization of oxygen is correct as indicated in the equations:

$$H_2O \longrightarrow H_2 + O$$

$$2HI + O \longrightarrow H_2O + I_2$$

The fact that it is somewhat higher is probably brought about because there is less recombination of hydrogen and oxygen in the gas bubbles formed on the alpha-ray bulb, since the oxygen is so promptly absorbed by hydrogen iodide, although there is undoubtedly some recombination in the bubbles even here. (Any oxygen actually in a bubble as it breaks away from the surface of the alpha-ray bulb is apparently completely absorbed before it escapes from the liquid.) It seems altogether probable, therefore, that the true values are:

$$\frac{-M}{N} \text{ (for } H_2O) = 1 \qquad \text{and} \qquad \frac{-M_{\mathrm{HI}}}{N_{\mathrm{H_2O}}} = 2$$

4. *Determination of* $-M_{\mathrm{KMnO_4}}/N_{\mathrm{H_2O}}$

The apparatus is the same as that used for ammonia and pure water, and is shown in figure 2, H and I being sealed on at X, as described previously. The potassium permanganate solution to be radiated is made by pipetting the desired quantity of a stock solution of aqueous potassium permanganate into water and adding the desired amount of aqueous C.P. sulfuric acid. The water used is conductivity water. A sample identical with that radiated is stored under vacuum until the end of the experiment and is then titrated in the same way as the radiated sample.

The procedure is to radiate a solution of potassium permanganate by means of an alpha-ray bulb (calibrated against water in the same apparatus). The evolved gases are measured before and after sparking. The solution is withdrawn and potassium iodide added, after which it is titrated with sodium thiosulfate. Results are shown in tables 5, 6, and 7. The calculation of $-M_{\mathrm{KMnO_4}}/N_{\mathrm{H_2O}}$ from the data given in table 5, having to do with the radiation of potassium permanganate, will now be given. The number of molecules of potassium permanganate which have been reduced is given by the following equation

$$-N_{\mathrm{KMnO_4}} = \frac{5.85 \times 0.01426 \times 6.06 \times 10^{23} \times 0.9377}{5 \times 1000} = 0.945 \times 10^{19}$$

TABLE 5

Determination of $-M_{KMnO_4}/N_{H_2O}$ *with a bulb standardized against water*

Experiment I: initial quantity of radon = 89.3 mc.; T = 26°C.

TIME ELAPSED FROM START	DURATION OF EACH EXPERIMENT	P_i PRESSURE BEFORE SPARKING	P_f PRESSURE AFTER SPARKING	P_{O_2} PRESSURE OF OXYGEN PRODUCED	*mc.* RADON DESTROYED	P_{O_2}/*mc.* PRESSURE OF OXYGEN PRODUCED PER MILLICURIE OF RADON DESTROYED
Standardization against water						
hours	*hours*	*mm.*	*mm.*	*mm.*	*mc.*	*mm.*
30	30	38	25.81	12.81	18.3	0.712
Radiation of 0.3 *N* potassium permanganate solution, normal in sulfuric acid						
48 149.5	0 101.5	71	68	62	33.1	1.875

TABLE 6

Determination of $-M_{KMnO_4}/N_{H_2O}$ *with a bulb standardized against water*

Experiments II and III: initial quantity of radon = 134.3 mc.; T = 23°C.

TIME ELAPSED FROM START	DURATION OF EACH EXPERIMENT	P_1 PRESSURE BEFORE SPARKING	P_2 PRESSURE AFTER SPARKING	P_{O_2} PRESSURE OF OXYGEN PRODUCED	*mc.* RADON DESTROYED	P_{O_2}/*mc.*	DIFFERENCE IN PERMANGANATE TITRATIONS
Standardization against water							
hours	*hours*	*mm.*	*mm.*	*mm.*	*mc.*	*mm.*	
22	22	56.8	31.9	19.12	20.45	0.934	
Radiation of 0.0848 *N* potassium permanganate, 1.25 *N* in sulfuric acid							
26 43	0 17	49.0	40.0	20.3	14.08	1.44	5.85 ml. of 0.01426 *N* sodium thiosulfate
Radiation of 0.371 *N* potassium permanganate, 1.25 *N* in sulfuric acid							
72 98	0 26	43.0	41.33	34.7	13.9	2.49	9 ml. of 0.01426 *N* sodium thiosulfate

TABLE 7

The values of $-M_{KMnO_4}/N_{H_2O}$ *obtained from the radiation of aqueous solutions of potassium permanganate containing sulfuric acid*

$KMnO_4$	H_2SO_4	$-M/N$ FROM TITRATION	$-M/N$ FROM GAS
N	*N*		
0.0848	1.25	0.516	0.536
0.3	1.0		0.907
0.37	1.27	0.864	0.922

in which 5.85 is the difference in volume of 0.01426 N sodium thiosulfate solution required by the unradiated and radiated solutions. 0.9377 is a correction term to take account of the time elapsing while the apparatus is being assembled, evacuated, etc. During this time the potassium permanganate is being acted upon, but the collection of gases cannot be started. The number of molecules of water decomposed in the water standardization is given by the following equation:

$$-M_{H_2O} = \frac{19.12 \times 17 \times 2 \times 6.06 \times 10^{23}}{760 \times 22{,}400} = 2.31 \times 10^{19}$$

Using the value $-M_{H_2O}/N_{H_2O} = 0.87$, found above by ammonia standardization,

$$N = \frac{2.31 \times 10^{19}}{0.87} = 2.65 \times 10^{19}$$

The number of millicuries of radon decayed for the production of this number of ion pairs was 20.45. For the 17-hr. interval during which potassium permanganate was being radiated, 14.08 mc. of radon decayed. Consequently, the corresponding number of ion pairs produced was

$$2.65 \times 10^{19} \times \frac{14.08}{20.45} = 1.83 \times 10^{19}.$$

Therefore,

$$\frac{-M_{KMnO_4}}{N_{H_2O}} = \frac{0.945 \times 10^{19}}{1.83 \times 10^{19}} = 0.516$$

$-M/N$ values for the other concentrations of potassium permanganate calculated in the same way are shown in table 7.

Discussion of potassium permanganate reaction

As will be seen, the value of $-M/N$ increases with the concentration. For the more concentrated solutions the value is approximately that found for water. If our previous conclusion that the true value for water is unity is correct, that should also be the value for $-M_{KMnO_4}/N_{H_2O}$ in the more concentrated solutions. This is 2.5 times as large as can be accounted for on the assumption that the entire primary reaction is

$$H_2O \rightarrow H_2 + O$$

and that potassium permanganate is reduced solely by hydrogen

$$MnO_4^- + 2.5\,H_2 + 3H^+ \rightarrow Mn^{++} + 4H_2O$$

It is obvious that some other reaction occurs which results in the reduction of potassium permanganate. The following series of equations accounts for the results in a fairly satisfactory manner:

1. *Primary reaction:*

$$5(H_2O)_2 + 5(E) \rightarrow 5H_2O_2 + 10H$$

2. *Secondary reactions:*

$$2MnO_4^- + 10H + 6H^+ \rightarrow 2Mn^{++} + 8H_2O$$

$$2MnO_4^- + 5H_2O_2 + 6H^+ \rightarrow 2Mn^{++} + 8H_2O + 5O_2$$

Thus there should be 0.8 as many potassium permanganate molecules decomposed as water molecules, by the primary reaction. In other words, $-M/N$ for potassium permanganate should be 0.8 of the value of $-M/N$ for water. Our experiments are not as close as desirable for upholding the theory, but are, nevertheless, within reason.

The low results for the more dilute solutions can be explained by less utilization of the hydrogen. The more dilute the solution, the less the probability of the hydrogen being used before it reaches the gas phase. This conclusion is justified by the results, as the excess hydrogen was larger in the case of the dilute solutions.

The assumption that the primary decomposition of water into hydrogen peroxide is made here, since it seems unlikely that if the decomposition were into hydrogen and oxygen, the oxygen would react quantitatively with water to form hydrogen peroxide, as would be necessary to explain the results. Further evidence for this conclusion is given in the section on mechanisms.

5. *Mechanisms*

Until the permanganate solutions were studied, all the effects produced in solution could be explained by the classical theory that water is decomposed directly into hydrogen and oxygen on being radiated by alpha particles. This theory is based on some results of Duane and Scheuer (3). They concluded that hydrogen peroxide was formed by the secondary reaction of nascent oxygen on water, and they based their conclusion on the experimental fact observed by them that the gases liberated at −183°C. under alpha radiation consisted wholly of electrolytic gas.

More recent work by Bonhoeffer and Reichardt (1) adds new light to this question and undermines the classical theory. They radiated water vapor at a temperature of 1000° to 1600°C. with ultraviolet light and obtained spectra for free hydroxyl. With this evidence, along with further considerations, they concluded that the mechanism for the decomposition of water under these conditions is given by the following equation:

$$2H_2O \rightarrow H_2 + 2OH$$

Two free hydroxyl groups obviously correspond to a dissociated hydrogen peroxide molecule. This leads to the conclusion that the decomposition of water in the liquid state produced hydrogen and hydrogen peroxide. Water in the liquid state is largely associated into $(H_2O)_2$ molecules. It is rather difficult to understand how one of the water molecules in the associated molecule could be influenced by the ionization without the other one being influenced, but it is easy to see how the two could be decomposed into hydrogen and hydrogen peroxide. *E*, in the equations, represents the energy necessary to produce one ion pair.

$$(H_2O)_2 + E \rightarrow H_2 + H_2O_2$$

Considering the evidence of Bonhoeffer and Reichardt (1), the necessity of using this mechanism for explaining the permanganate reaction and the fact that it is a logical one leads one to accept the above equation as being the true mechanism. The adoption of this new mechanism in no way affects the discussions and conclusions made from the classical theory as the net result is the same, since hydrogen peroxide is an unstable intermediate product. Probably some of that formed decomposes almost instantly.

$$H_2O_2 \rightarrow H_2O + O$$

The equation for the net result of water decomposition is then as follows:

$$H_2O + E \rightarrow H_2 + O$$

This is the same equation as is obtained by the classical theory.

Before considering the mechanisms for the hydrogen bromide and hydrogen iodide decompositions, the work of Harteck and Kopsch (4) on reactions with atomic oxygen should be mentioned. With electrically produced atomic oxygen they obtained spectra showing reactions between the oxygen and halogens.

$$HX + O \rightarrow OH + X$$

Thus we can conclude that the decomposition of the halogen acids can be due to both hydrogen peroxide and nascent oxygen liberated from the peroxide. The primary reaction, in the case of the hydrobromic acid, must be between it and hydrogen peroxide, and there must also be some reaction between it and nascent oxygen liberated from hydrogen peroxide.

$$H_2O_2 + 2HBr \rightarrow 2H_2O + Br_2 \qquad (1)$$

$$O + 2HBr \rightarrow H_2O + Br_2 \qquad (2)$$

Bromine reacts with water to form hydrobromic acid and hypobromous acid, which is unstable and decomposes to hydrobromic acid and oxygen.

$$Br_2 + H_2O \rightarrow HOBr + HBr$$

$$HOBr \rightarrow HBR + O$$

Then an equilibrium is set up, as shown in the following equation:

$$2HBr + O \rightleftarrows H_2O + Br_2$$

The per cent of oxygen utilized evidently depends on the concentrations and on the equilibrium constant, which depends on the temperature.

In the case of the hydriodic acid decomposition, the reaction goes to completion and the reactions taking place are as follows:

$$2HI + H_2O_2 \rightarrow 2H_2O + I_2 \qquad (1)$$

$$2HI + O \rightarrow H_2O + H_2 \qquad (2)$$

The first reaction is the chief one.

The permanganate decomposition requires two reactions to explain the production of 2.5 atoms of oxygen per permanganate molecule decomposed.

$$2MnO_4^- + 5H_2O_2 + 6H^+ \rightarrow 2Mn^{++} + 8H_2O + 5O_2$$

$$2MnO_4^- + 10H + 6H^+ \rightarrow 2Mn^{++} + 8H_2O$$

These reactions must also be equally probable to explain the results in the less dilute solutions. Furthermore, the reaction between the hydrogen peroxide and permanganate is assumed to take place before the hydrogen peroxide has a chance to decompose otherwise. The fact that the value of M_{KMnO_4}/N_{H_2O} drops for more dilute solutions is explained by the increased probability of hydrogen escaping from the solution before it takes part in the second reaction.

SUMMARY

A study has been made of alpha radiation of water and of certain aqueous solutions, with the following results:

1. Hydrogen iodide is decomposed into hydrogen and iodine; hydrogen bromide into hydrogen and bromine.
2. Iodine in pure water is shown to accept hydrogen and form hydrogen iodide.
3. Iodine in potassium iodide solutions is shown not to be a hydrogen acceptor.
4. Potassium permanganate solutions containing sulfuric acid are decomposed. Manganous sulfate is formed.
5. By the direct method, with the radon dissolved in water, the value of $-M/N$ for water was found to be 0.739; for hydrogen bromide, 1.187.
6. By the indirect method, with the radon in an alpha-ray bulb standardized by ammonia decomposition, the value of $-M/N$ for water was found to be 0.87.
7. It is concluded that the true value of $-M/N$ for water = 1. By the indirect method, $-M/N$ for hydrogen iodide = 1.86. If the true value of $-M/N$ for water is 1, the true value of $-M/N$ for hydrogen iodide is 2.

8. By the indirect method $-M/N$ for potassium permanganate is 0.516 in 0.0848 N potassium permanganate and 0.893 in 0.37 N potassium permanganate, each potassium permanganate solution being approximately normal in sulfuric acid.

9. The primary effect is the decomposition of water, and the effects on solutes are produced purely by secondary reactions instigated by the decomposition products of water.

10. The evidence seems to indicate that the primary effect is the decomposition of water into hydrogen peroxide and hydrogen:

$$(H_2O)_2 + E \rightarrow H_2 + H_2O_2$$

REFERENCES

(1) Bonhoeffer and Reichardt: Z. physik. Chem. **A139**, 75 (1928).
(2) Cameron, A. L., and Ramsay, Wm.: J. Chem. Soc. **91**, 193 (1907); **91**, 1266 (1907); **92**, 966 (1908).
(3) Duane, W., and Scheuer, O.: Le radium **10**, 33 (1913).
(4) Harteck and Kopsch: Z. physik. Chem. **B12**, 327 (1931).
(5) Jungers, J. C.: Bull. soc. chim. Belg. **41**, 389 (1932).
(6) Kernbaum, M.: Compt. rend. **148**, 705; Le radium **6**, 225 (1909).
(7) Lind, S. C.: Le radium **8**, 289 (1911).
(8) Mund, W.: Bull. soc. chim. Belg. **39**, 518 (1930).
(9) Nurnberger, C. E.: J. Phys. Chem. **38**, 47 (1934).

NEW BOOKS

Second Report on Viscosity and Plasticity. Prepared by the Committee for the Study of Viscosity of the Academy of Sciences at Amsterdam. vi + 287 pp. New York: Nordemann Publishing Company, Inc., 1938. Price: $7.50.

These *Reports on Viscosity and Plasticity* owe their origin to a suggestion of the International Council of Scientific Unions to found a committee for the purpose of "accumulating data on the use of instruments and methods developed in special branches of science, in order to make them known also in other branches." The choice of the problem made by the Dutch Academy appears to be particularly appropriate. Viscosity and plasticity are of paramount importance in many fields of work, for industrial and biological problems no less than for those of physics and chemistry, and our theoretical knowledge is poor. The use of the plastic properties of clay is one of the oldest of man's technical successes; the shards of pottery are the "leading fossil" by which the development of human culture is followed down to very early strata. Nevertheless how very little is known, from the point of theory, about plasticity, compared, for instance, to our knowledge of electrical machines, though the electromagnetic phenomena were discovered not much more than one hundred years ago. And as to viscosity, but recently Andrade first proposed a fairly promising theory correlating the viscosity of liquids with the mass and frequency of thermal vibrations of their molecules.

The first of these reports, published in 1935, contained the following chapters: I. Mechanical Considerations—Model Systems—Phenomenological Theories of Relaxation and Viscosity (by J. M. Burgers): II. Remarks in Connection with the Experimental Investigation of Flow Properties (by J. M. Burgers): III. Viscosity Measurements with Special Reference to their Application in Colloid Chemistry (by H. B. Bungenberg de Jong); IV. Viscosity and Plasticity from a Technical Point of View (by C. J. van Nieuwenburg); V. Plasticity of Crystalline Substances, in Particular of Metals (by W. G. Burgers and J. M. Burgers); VI. Viscosity Effects in the Living Protoplasm and in Muscles (by H. J. Jordan).

The second report contains: I. Introductory Remarks on Recent Investigations concerning the Structure of Liquids (by J. M. Burgers); II. Viscosity of Liquids in Connection with their Chemical and Physical Constitution (by F. M. Jaeger); III. On the Motion of Small Particles of Elongated Form, Suspended in a Viscous Liquid (by J. M. Burgers); IV. The Yield Value (by R. Houwink); V. Recent Plastometers (by C. J. van Nieuwenburg); VI. Technical Capillary Viscometers (by R. N. J. Saal).

The chapters by Burgers, Bungenberg de Jong, and Houwink are particularly suggestive for those interested in physical and colloid chemistry. The chapters of the last two authors cover a part of the viscous and plastic properties of colloidal systems, but not those of gels, which will probably be treated in a later report.

H. FREUNDLICH.

Dipole Moments. Their Measurement and Application in Chemistry. By R. J. W. LE FÈVRE. 10 x 16.5 cm.; 105 pp.; 28 diagrams. New York: Chemical Publishing Company of New York, Inc., 1938. Price: $1.50.

This little monograph covers the following range of topics: I. Dielectric Polarisation and the Calculation of Dipole Moments; II. Practical Methods for the Measurement of Dipole Moments; III. Solvent Effect in Dipole Moment Measurements; IV. Dipole Moments and Molecular Structure; V. Intramolecular Rotation and Flexibility of Molecules; VI. Some Anomalous Dipole Moments. It contains as well an abridged table of dipole moments.

As is evident from its size, the booklet does not undertake to be complete in detail nor to provide an exhaustive bibliography. It does give a useful condensed account of a subject which, after a dozen or more active years of study, is still attracting a good deal of interest. Particular attention is directed to fundamental theories, experimental methods, and interpretation of dipole moment data. Relations of the results to other fields of investigation are considered. The mathematical apparatus is reduced to a minimum. This clearly written monograph should prove of great interest and utility to those chemists who have found the more ambitious treatises too abstruse for their requirements.

The author deserves praise for the care with which he has done his work. The material is carefully organized and discussions are clear and attractively presented. The general appearance of the text is excellent. Perusal of this book should stimulate a more widespread interest in the subject.

J. W. WILLIAMS.

Mikroanalytische Nachweise anorganischer Ionen. By GERHARD KRAMER. 35 pp.; 8 plates. Leipzig: Akademische Verlagsgesellschaft, 1937. Price: 5.60 RM.

This booklet contains directions for carrying out crystal tests for the common metals and a few of the acid radicals. The reactions described are old classical ones which for the most part have stood the test of time. Some common forms of identification, such as zinc and cadmium mercuric thiocyanates and the "triple acetate" of sodium, are not mentioned. The sensitivity of the reactions is expressed, as is so often done, in terms of the absolute amount of the ion that can be detected in a drop of arbitrary size (in this case 0.03 ml.). It would seem to be better practice to base the expression for the sensitivity on the limiting concentration of the solution tested instead of on an absolute amount which has little real significance.

Forty-eight excellent photomicrographs are included in the work.

E. B. SANDELL.

An Introduction to Microchemical Methods for Senior Students of Chemistry. By CECIL L. WILSON. 196 pp.; 93 diagrams. New York: Chemical Publishing Company of New York, Inc., 1938. Price: $3.00.

A wide range of topics is included in this little volume. Among others, there are chapters on the compound microscope, the polarizing microscope, crystal tests, spot tests, inorganic qualitative analysis, inorganic gravimetric and volumetric analysis, the colorimeter, the nephelometer, organic operations, organic quantitative analysis, photomicrography, and the spectrograph. The book is hardly suitable for use as a text, because of the limited space that can be allowed so many different phases of the subject. The author himself says ". . . the work here described is only preliminary, and should be followed by the use of textbooks by recognized authorities in each branch . . ." The book serves a distinctly useful purpose in giving a general survey of a vast field, and it contains a surprising amount of information in a small space.

E. B. SANDELL.

Negative Ions. By H. S. W. MASSEY. 105 pp., 19 figs. Cambridge Physical Tracts. Cambridge, England: University Press, 1938. New York: The Macmillan Company, 1938.

This volume contains a very excellent discussion of negatively charged particles in respect to their occurrence, production, and behavior. The treatment covers both experimental results and theoretical considerations. The latter are carried out along the modern lines of wave mechanics. The book abounds with suggestions for further research and should be of greatest interest to workers in the field. However, all scientific workers, especially physicists and chemists, can readily bring their knowledge of this particular branch of atomic and molecular physics up-to-date by a perusal of this tract. The five chapters cover the following items: negative atomic ions; negative molecular ions; modes of formation of negative ions; detachment of electrons from negative ions; negative ions in the glow discharge and in the upper atmosphere.

Geo. Glockler.

Elementary Survey of Physics. By Arthur E. Haas and Ira M. Freeman. 203 pp.; 75 figs. New York: E. P. Dutton and Company, 1938. Price: $1.90.

This is a brief survey and compilation of physics which the authors suggest may be used to acquaint students, among them premedical students, with the whole field of physics. Its briefness has led to a number of naïve statements and generalizations, and the reviewer hopes that all premedical students will be required to complete a more comprehensive and detailed course than is given here. The essentials of physics are stated in the book, but it alone would give a very superficial knowledge of the field.

J. W. Buchta.

Spectrochemical Abstracts, 1933–1937. By F. Twyman. 24 x 15 cm.; 52 pp. London: Adam Hilger, Ltd., 1938. Price: 3/10.

This handy volume contains brief abstracts of the majority of papers dealing with spectrographic methods of chemical analysis that were published during the period stated. Some earlier papers are also included.

The sections comprise the following: I, a list of some two hundred papers arranged under authors' names; II, substances analyzed, with an indication of the methods used and some of the results obtained; III, apparatus; IV, methods; V, general; VI, books. Complete cross references are given. It is intended as a guide to the scattered literature for those who seek further information on their own problems. This purpose is usefully fulfilled. An attempt is made to indicate the relative value of the various papers, but this makes one wish for a more extended critical survey.

M. Milbourn.

Statistical Physics. By L. Landau and E. Lifshitz. Translated from the Russian by D. Shoenberg. viii + 234 pp. New York: Oxford University Press, 1938. Price: $6.00.

In this book the authors aim "to give a unified presentation of thermodynamics and classical statistics, based on the point of view associated with the name of Gibbs."

The first chapter introduces the concepts of probability, mean values, and statistical independence, while in the second chapter the entropy is defined statistically and the law of increasing entropy is formulated. The various thermodynamic functions are discussed in the third chapter, and the Gibbs distribution in the fourth. In the following chapter the thermodynamic functions are evaluated for a perfect gas, for a mixture of perfect gases, for an imperfect gas, and for a solid. Chapter VI is devoted to fluctuations and thermodynamic inequalities; it includes a discussion of the LeChatelier-Braun principle. Chapter VII introduces the chemical potential, and in chapter VIII phase equilibrium is studied. Chapter IX deals with solutions and includes a fairly extensive discussion of equilibrium curves. After a brief discussion of chemical reactions in chapter X, there is presented in chapter XI a valuable treatment of anisotropic bodies. Transition points (including Curie points) and order and disorder in solids and in solid solutions are treated in a clear manner. The book concludes with a brief discussion of surface phenomena, including adsorption, the formation of nuclei, and the growth of crystals.

This book is highly recommended to students, who will find in it an excellent treatment of the equilibrium properties of matter based on classical statistics.

F. H. MacDougall.

British Chemical Industry. By Sir Gilbert T. Morgan and David Doig Pratt. 372 pp. New York and Toronto: Longmans, Green and Company, 1938. Price: $6.25.

This book is a collection of public lectures delivered at the University College of Wales. It is not a textbook, but it can be used as such. Its contents have been strictly limited to the British practice of chemical manufacture. The subject matter is arranged under the raw materials, the availability of which from both domestic and foreign sources accounts for particular practices. Both the inorganic and organic industries are included in the sixteen chapters.

Each chapter begins with statements as to the availability of the raw materials. Most of the individual subjects have an historical sketch of a process of development which is both interesting and valuable. Reasons for using certain methods and applying changes in methods are given. Chemical reactions, conditions of operations, statistics, and numerous illustrations of equipment are included.

Though many of the subjects are treated at some length with considerable detail, others are passed over hurriedly. This is true of the organic processes. Further application of physical chemistry and the unit chemical engineering operations would have made this book more satisfactory for teaching purposes, but presumably that was not the intention of the authors.

This is a very interesting, informative, and valuable book. It contains many good illustrations. It is well written and is very readable.

Charles A. Mann.

Combustion, Flames and Explosions of Gases. By Bernard Lewis and Guenther von Elbe. 415 pp. Cambridge: University Press, 1938. New York: The Macmillan Company, 1938. Price: $5.50.

This monograph, which has been needed for a number of years, should be especially valuable to engineers interested in the more technical aspects of gaseous combustion and to students of the kinetics of gas reactions. To the former group it will serve as an introduction to the theoretical background of the subject and in addition will furnish a worthwhile correlation of the outstanding experimental results in terms of these theories. The latter group will find it valuable chiefly for its systematic and coördinated survey of the highly complex but interesting phenomena of flame propagation.

The four parts into which this book is divided are entitled, "Chemistry and Kinetics of the Reactions between Fuel Gases and Oxygen," "Propagation of Flames," "State of the Burnt Gas," and "Problems in Technical Combustion Processes." In addition, rather extensive tables of pertinent thermodynamic quantities, of limits of inflammability, and of flame temperatures are appended. The introductory chapter of the first section consists of a brief description of the theories of chain reactions, and is written largely from the viewpoint of Hinshelwood. In the two following chapters, the experimental results on the combustion of hydrogen and of hydrocarbons are interpreted in terms of these theories. This is followed by discussions of the emission spectra of the flame front and of the ignition of combustible mixtures by sparks. The second part, which in the reviewer's opinion is the most interesting section of the book, is devoted to a discussion of the propagation of flames under stationary, expanding, and detonating conditions. What might be called the thermodynamic properties of flames and of the products of combustion are discussed in the third part of the book. This section is introduced by a brief outline of the methods of obtaining the values of the thermodynamic functions of simple gases from spectoscopic data. The fourth part, which is only twenty-eight pages long, consists largely of an account of combustion processes occurring in internal-combustion engines.

The book is excellently printed and is well illustrated by a number of line drawings and half-tone reproductions of photographs.

ROBERT LIVINGSTON.

INDEX

AUTHOR INDEX

INDEX TO NEW BOOKS